MEIOTIC RECOMBINATION AND DNA REPAIR: NEW APPROACHES TO SOLVE OLD QUESTIONS IN MODEL AND NON-MODEL PLANT SPECIES

EDITED BY: Christophe Lambing, Mónica Pradillo, Kyuha Choi and Olivier Da Ines

PUBLISHED IN: Frontiers in Plant Science

frontiers Research Topics

frontiers

ISSN 1664-8714
ISBN 978-2-88974-604-0
DOI 10.3389/978-2-88974-604-0

About Frontiers

Frontiers is more than just an open-access publisher of scholarly articles: it is a pioneering approach to the world of academia, radically improving the way scholarly research is managed. The grand vision of Frontiers is a world where all people have an equal opportunity to seek, share and generate knowledge. Frontiers provides immediate and permanent online open access to all its publications, but this alone is not enough to realize our grand goals.

Frontiers Journal Series

The Frontiers Journal Series is a multi-tier and interdisciplinary set of open-access, online journals, promising a paradigm shift from the current review, selection and dissemination processes in academic publishing. All Frontiers journals are driven by researchers for researchers; therefore, they constitute a service to the scholarly community. At the same time, the Frontiers Journal Series operates on a revolutionary invention, the tiered publishing system, initially addressing specific communities of scholars, and gradually climbing up to broader public understanding, thus serving the interests of the lay society, too.

Dedication to Quality

Each Frontiers article is a landmark of the highest quality, thanks to genuinely collaborative interactions between authors and review editors, who include some of the world's best academicians. Research must be certified by peers before entering a stream of knowledge that may eventually reach the public - and shape society; therefore, Frontiers only applies the most rigorous and unbiased reviews.
Frontiers revolutionizes research publishing by freely delivering the most outstanding research, evaluated with no bias from both the academic and social point of view. By applying the most advanced information technologies, Frontiers is catapulting scholarly publishing into a new generation.

What are Frontiers Research Topics?

Frontiers Research Topics are very popular trademarks of the Frontiers Journals Series: they are collections of at least ten articles, all centered on a particular subject. With their unique mix of varied contributions from Original Research to Review Articles, Frontiers Research Topics unify the most influential researchers, the latest key findings and historical advances in a hot research area! Find out more on how to host your own Frontiers Research Topic or contribute to one as an author by contacting the Frontiers Editorial Office: frontiersin.org/about/contact

MEIOTIC RECOMBINATION AND DNA REPAIR: NEW APPROACHES TO SOLVE OLD QUESTIONS IN MODEL AND NON-MODEL PLANT SPECIES

Topic Editors:
Christophe Lambing, Rothamsted Research, United Kingdom
Mónica Pradillo, Complutense University of Madrid, Spain
Kyuha Choi, Pohang University of Science and Technology, South Korea
Olivier Da Ines, Université Clermont Auvergne, France

Citation: Lambing, C., Pradillo, M., Choi, K., Da Ines, O., eds. (2022). Meiotic Recombination and DNA Repair: New Approaches to Solve Old Questions in Model and Non-Model Plant Species. Lausanne: Frontiers Media SA.
doi: 10.3389/978-2-88974-604-0

Table of Contents

frontiers in Plant Science

EDITORIAL
published: 09 February 2022
doi: 10.3389/fpls.2022.841402

Editorial: Meiotic Recombination and DNA Repair: New Approaches to Solve Old Questions in Model and Non-model Plant Species

Olivier Da Ines[1], *Kyuha Choi*[2], *Mónica Pradillo*[3] *and Christophe Lambing*[4]*

[1] Institut Génétique Reproduction et Développement (iGReD), Université Clermont Auvergne, Centre National de la Recherche Scientifique (CNRS), Institut national de la santé et de la recherche médicale (INSERM), Clermont-Ferrand, France, [2] Department of Life Sciences, Pohang University of Science and Technology, Pohang, South Korea, [3] Department of Genetics, Faculty of Biology, Physiology and Microbiology, Universidad Complutense de Madrid, Madrid, Spain, [4] Rothamsted Research, Harpenden, United Kingdom

Keywords: meiosis, epigenetics, genome evolution, DNA double strand break, homologous recombination

Editorial on the Research Topic

Meiotic Recombination and DNA Repair: New Approaches to Solve Old Questions in Model and Non-model Plant Species

Accurate segregation of chromosomes at the first meiotic division relies upon the establishment of physical connections between homologous chromosomes, which with a few exceptions, are realized by crossover recombination. Recombination also reshuffles genetic information between homologs, and thus strongly influences genome evolution. At the molecular level, meiotic recombination is initiated by the programmed induction of DNA double strand breaks (DSBs) and their subsequent repair as a crossover (CO) or a non-crossover (NCO). However, COs are constrained and the majority of DSBs are repaired as NCOs in plants. Gutierrez Pinzon et al. provide a comprehensive overview of the most recent findings on the different steps controlling meiotic recombination, with an emphasis on the different anti-CO pathways. Notably, one of these, involving the RecQ4 helicase, has previously been shown to be active in Arabidopsis, rice, pea and tomato (Séguéla-Arnaud et al., 2015; Mieulet et al., 2018). Arrieta et al. extend this anti-CO role to the cereal barley. Through a suppressor screen of a CO-defective mutant, they show that mutating the *RecQ4* gene in Barley can increase meiotic recombination by nearly two-fold. The RecQ4 anti-CO pathway, initially discovered in Arabidopsis, appears thus largely conserved and translatable to cereals. Mechanisms of meiotic recombination are thus largely conserved across plant kingdom. Nevertheless specificities exist, as nicely illustrated by the characterization of the maize checkpoint clamp loader RAD17 by Zhang et al. RAD17 is not essential for meiotic DSB repair in Arabidopsis, while rice *Osrad17* mutants exhibit extensive meiotic chromosome fragmentation leading to male and female sterility (Hu et al., 2018). Here, Zhang et al., demonstrate that RAD17 is also essential for meiotic DSB repair in maize but, remarkably and contrary to rice, only in male meiosis. Thus, besides underlining the importance of studying various plant species, this work also points to important differences between male and female meiosis (highlighted by Gutierrez Pinzon et al.). New issues have also recently emerged at the forefront of research on meiotic recombination. First, considering the impact of global warming, understanding how temperature affects meiosis has become a major challenge and recent breakthroughs have been comprehensively described by Gutierrez Pinzon et al. Second, Dziegielewski and Ziolkowski present an extensive review of the knowledge around non-coding RNAs (ncRNAs) and their impact on plant meiosis. NcRNAs are key players in many biological processes, but their role in meiosis has remained elusive. An interesting proposal of Dziegielewski and Ziolkowski is that ncRNA pathways regulate meiosis through the

Edited and reviewed by:
Jean Molinier, UPR2357 Institut de biologie moléculaire des plantes (IBMP), France

***Correspondence:**
Christophe Lambing
christophe.lambing@rothamsted.ac.uk

Specialty section:
This article was submitted to Plant Cell Biology, a section of the journal Frontiers in Plant Science

Received: *22 December 2021*
Accepted: *17 January 2022*
Published: *09 February 2022*

Citation:
Da Ines O, Choi K, Pradillo M and Lambing C (2022) Editorial: Meiotic Recombination and DNA Repair: New Approaches to Solve Old Questions in Model and Non-model Plant Species. Front. Plant Sci. 13:841402. doi: 10.3389/fpls.2022.841402

controlled expression of meiosis-specific genes and this role may have evolved as a secondary effect of their primary function in the control of transposable elements in germ cells.

Visualization of meiotic chromosomes has been of major importance for our understanding of meiotic recombination and the dynamics of chromosome behavior. Sims et al. provide an overview of classical and advanced cytological sample preparation methods, and review the latest developments in microscopy techniques from epifluorescence, confocal laser scanning and super-resolution microscopies in Arabidopsis. The authors include representative STED (stimulated emission depletion)-based images of Arabidopsis meiotic proteins immunostained on chromosomes and suggest that nanoscale imaging will help in characterizing the fundamental processes of meiosis. Super-resolution microscopy has already provided us with novel insights into CO interference by determining the location, amount and intensity of the meiotic protein HEI10 E3 ligase in Arabidopsis (Capilla-Pérez et al., 2021; Morgan et al., 2021a). As an alternative approach of visualizing plant chromosomes, Prusicki et al. review technical aspects and applications of live imaging of meiosis in plants. The development of novel genomic approaches has also advanced our understanding of meiosis. For instance, Barr et al. develop an INTACT system to purify meiotic nuclei in a high-throughput manner in Arabidopsis and discover the importance of DNA demethylation in plant meiosis. The meiocyte INTACT system can be combined with single cell RNA sequencing (Nelms and Walbot, 2019) and other genomic approaches such as ATAC-seq, bisulfite-seq and ChIP-seq for mapping of meiotic chromatin features. Post-translational modifications also play crucial roles in the control of meiosis. Orr et al. highlight recent advances on the roles of ubiquitination in plant meiosis and overview various proteomic approaches for identifying substrates of ubiquitin E3 ligases which include BioID/TurboID-based proximity labeling. The proximity labeling and affinity purification–mass spectrometry can be adapted to generate a wide view of protein interactome during meiosis (Mair et al., 2019; Yang X. et al., 2021).

Along with powerful genetic screening of plant meiotic mutants, these advanced approaches have helped to confirm that COs are not evenly distributed along plant chromosomes. For instance, they are enriched in distal regions but also in interstitial regions that are at junctions with heterochromatin in Arabidopsis. In contrast, COs are almost exclusively restricted to distal regions in cereals. A correlation between CO distribution, transposon content and DNA methylation exists in plant species (Lambing et al., 2017). Raz et al. use Virus-Induced Gene Silencing to down-regulate the expression of genes coding for DNA methylases recombination proteins in tetraploid wheat and show that it is possible to influence the pattern of recombination using non-transgenic approaches. This technique has the potential to facilitate plant breeding by creating novel genetic diversity in regions normally deprived in meiotic recombination. However, in order to profoundly impact future breeding strategies, the control of meiotic recombination remains to be fully understood. Kuo et al. provide an overview on the factors known to be involved in CO distribution and hypothesize that the formation of COs near the telomere is a default position caused by the pairing of the telomeres prior to the initiation of recombination. Aguilar and Prieto extend this concept and review our current knowledge on the dynamics of the telomeres and sub-telomeres. The authors suggest that distal chromosome recognition could play an important role in the correct chromosome pairing in polyploid species. Since the telomeric repeats are highly conserved between plants species, the authors propose that the sub-telomeric regions, rather than the telomeres, may help differentiating homologous from homoeologous pairing. These new models of CO distribution and chromosome pairing will likely drive future experimental investigations. Kuo et al. further propose that a change in the composition of the chromosome axis between Arabidopsis and wheat could be a major contributor to the different patterns of recombination observed between the two species. In support to this model, Osman et al. perform a detailed analysis of meiotic recombination in hexaploid wheat and show that the chromosome axis and DSBs initiate first in distal regions before occurring in interstitial and proximal regions. The authors speculate that the sequential events of meiotic progression have an influence on the position of COs along the chromosomes, with the regions recombining first being more likely to form a CO while the regions recombining last rarely recombine. This recombination pattern is also influenced by an interfering signal that initiates at the CO sites and inhibits the formation of additional COs in adjacent regions. The formation of a CO involves the linkage between two chromatids from each of the two homologous chromosomes. It had remained unknown if interference can spread across the chromatids that are not directly involved in the CO. To answer this long-standing question, Sarens et al. develop a novel approach to quantify chromatin interference. The authors found that the interfering signal represses the formation of a second CO on the two chromatids of each chromosome and concluded that CO interference acts on the whole chromosome. In a separate study, Morgan et al. (2021b) showed that CO interference occurs along multiple connected axes to repress the formation of multivalent connections in tetraploid *Arabidopsis arenosa*.

One of the most important challenges in meiosis arises after whole genome duplication (WGD). The presence of more than two chromosome sets in the same meiosis may lead to the formation of univalents and multivalents during prophase I and subsequent chromosome mis-segregation during anaphase I. To face these problems, polyploids have developed strategies to control pairing preferences that result in diploid-like behavior during meiosis and disomic inheritance. Svačina et al. use allohexaploid bread wheat as a model to review molecular mechanisms and regulators involved in maintaining diploid-like pairing behavior in allopolyploids (polyploids resulted from the hybridization of related species). WGD is a prominent evolutionary process relevant for crop improvement. Indeed, many cultivated plants such as wheat, tobacco, potato, cotton, or sugarcane, among others, are polyploids. In addition, polyploids often display better tolerance to abiotic stresses (Van de Peer et al., 2021). Natural polyploids may emerge through several pathways, described in detail by Svačina et al., with the

generation of unreduced gametes being the more predominant. The production of these gametes, although highly influenced by the environment, also has a genetic basis (Van de Peer et al., 2017). The presence of mutations in certain genes may have contributed to polyploidisation, facilitating the formation of unreduced gametes by defects in either meiosis I or II. Recently, it has been reported that the function of the STRUCTURAL MAINTENANCE OF CHROMOSOME 5/6 (SMC5/6) complex is essential to ensure accurate gametophytic ploidy in Arabidopsis (Yang F. et al., 2021). Mutants defective for this complex generate unreduced gametes by recombination-independent mechanisms and produce triploid offspring. Yang et al. analyzed autotetraploid plants deficient for SMC5/6 and found even more drastic meiotic defects than in diploids, highlighting the importance of this complex in the maintenance of tetraploid genome stability. The meiotic function of other SMC complexes (cohesin, condensin) and associated cofactors, also involved in genome maintenance, is reviewed by Bolaños-Villegas. Besides polyploidy, holocentricity is another challenge to the proper progression of meiosis in the evolution of several plant species. Holocentric chromosomes possess multiple kinetochores dispersed along their length rather than a single region that functions as the centromere. As well as chromosome duplication, holocentric chromosomes evolved several times during plant evolution (Mandrioli and Manicardi, 2020). In plants, the presence of holocentric chromosomes is linked to inverted meiosis, a meiosis with a reverse order in which segregation of homologous chromosomes occurs during meiosis II. In an interesting review, Hofstatter et al. describe adaptations during meiosis in holocentric plants.

Overall, our Research Topic provides an in-depth overview of the latest developments in meiosis and will be of interest to a broad readership on meiosis, genome evolution and plant breeding.

AUTHOR CONTRIBUTIONS

All authors listed have made a substantial, direct, and intellectual contribution to the work and approved it for publication.

ACKNOWLEDGMENTS

OI acknowledges support by CNRS, INSERM and University Clermont Auvergne. KC acknowledges the support of National Research Foundation of Korea (NRF, NRF-2020R1A2C2007763). MP acknowledges the support of the Ministry of Science and Innovation of Spain (PID2020-118038GB-I00) and of the European Union (Marie Curie ITN, MEICOM 765212). CL acknowledges the support of the BBSRC grant-aided support as part of the Institute Strategic Program Designing Future Wheat Grant (BB/P016855/1).

REFERENCES

Capilla-Pérez, L., Durand, S., Hurel, A., Lian, Q., Chambon, A., Taochy, C., et al. (2021). The synaptonemal complex imposes crossover interference and heterochiasmy in Arabidopsis. *Proc. Natl. Acad. Sci. USA*. 118, 1–11. doi: 10.1073/pnas.2023613118

Hu, Q., Zhang, C., Xue, Z., Ma, L., Liu, W., Shen, Y., et al. (2018). OsRAD17 is required for meiotic double-strand break repair and plays a redundant role with OsZIP4 in synaptonemal complex assembly. *Front. Plant Sci.* 29, 1236. doi: 10.3389/fpls.2018.01236

Lambing, C., Franklin, F. C. H., and Wang, C.-J. R. (2017). Understanding and manipulating meiotic recombination in plants. *Plant Physiol*. 173, 1530–1542. doi: 10.1104/pp.16.01530

Mair, A., Xu, S. L., Branon, T. C., Ting, A. Y., and Bergmann, D. C. (2019). Proximity labeling of protein complexes and cell type specific organellar proteomes in Arabidopsis enabled by TurboID. *Elife.* 8, e47864. doi: 10.7554/eLife.47864

Mandrioli, M., and Manicardi, G. C. (2020). Holocentric chromosomes. *PLoS Genet.* 16, e1008918. doi: 10.1371/journal.pgen.1008918

Mieulet, D., Aubert, G., Bres, C., Klein, A., Droc, G., Vieille, E., et al. (2018). Unleashing meiotic crossovers in crops. *Nat. Plants.* 4, 1010–1016. doi: 10.1038/s41477-018-0311-x

Morgan, C., Fozard, J. A., Hartley, M., Henderson, I. R., Bomblies, K., and Howard, M. (2021a). Diffusion-mediated HEI10 coarsening can explain meiotic crossover positioning in Arabidopsis. *Nat. Commun.* 12, 4674. doi: 10.1038/s41467-021-24827-w

Morgan, C., White, M. A., Franklin, F. C. H., Zickler, D., Kleckner, N., and Bomblies, K. (2021b). Evolution of crossover interference enables stable autopolyploidy by ensuring pairwise partner connections in Arabidopsis arenosa. *Curr. Biol.* 31, 4713–4726. doi: 10.1016/j.cub.2021.08.028

Nelms, B., and Walbot, V. (2019). Defining the developmental program leading to meiosis in maize. *Science.* 364, 52–56. doi: 10.1126/science.aav6428

Séguéla-Arnaud, M., Crismani, W., Larchevêque, C., Mazel, J., Froger, N., Choinard, S., et al. (2015). Multiple mechanisms limit meiotic crossovers: TOP3α and two BLM homologs antagonize crossovers in parallel to FANCM. *Proc. Natl. Acad Sci. U S A.* 14, 4713–4718. doi: 10.1073/pnas.1423107112

Van de Peer, Y., Ashman, T. L., Soltis, P. S., and Soltis, D. E. (2021). Polyploidy: an evolutionary and ecological force in stressful times. *Plant Cell.* 33, 11–26. doi: 10.1093/plcell/koaa015

Van de Peer, Y., Mizrachi, E., and Marchal, K. (2017). The evolutionary significance of polyploidy. *Nat. Rev. Genet.* 18, 411–424. doi: 10.1038/nrg.2017.26

Yang, F., Fernández-Jiménez, N., Tučkov,á, M., Vrána, J., Cápal, P., Díaz, M., et al. (2021). Defects in meiotic chromosome segregation lead to unreduced male gametes in Arabidopsis SMC5/6 complex mutants. *Plant Cell.* 33, 3104–3119. doi: 10.1093/plcell/koab178

Yang, X., Wen, Z., Zhang, D., Li, Z., Li, D., Nagalakshmi, U., et al. (2021). Proximity labeling: an emerging tool for probing in planta molecular interactions. *Plant Commun.* 2, 100137. doi: 10.1016/j.xplc.2020.100137

Conflict of Interest: The authors declare that the research was conducted in the absence of any commercial or financial relationships that could be construed as a potential conflict of interest.

Publisher's Note: All claims expressed in this article are solely those of the authors and do not necessarily represent those of their affiliated organizations, or those of the publisher, the editors and the reviewers. Any product that may be evaluated in this article, or claim that may be made by its manufacturer, is not guaranteed or endorsed by the publisher.

frontiers in Plant Science

REVIEW
published: 09 July 2020
doi: 10.3389/fpls.2020.01056

Chromosome Pairing in Polyploid Grasses

Radim Svačina[1], *Pierre Sourdille*[2], *David Kopecký*[1] *and Jan Bartoš*[1]*

[1] Institute of Experimental Botany of the Czech Academy of Sciences, Centre of the Region Haná for Biotechnological and Agricultural Research, Olomouc, Czechia, [2] INRA, Génétique, Diversité, Ecophysiologie des Céréales, Clermont-Ferrand, France

Polyploids are species in which three or more sets of chromosomes coexist. Polyploidy frequently occurs in plants and plays a major role in their evolution. Based on their origin, polyploid species can be divided into two groups: autopolyploids and allopolyploids. The autopolyploids arise by multiplication of the chromosome sets from a single species, whereas allopolyploids emerge from the hybridization between distinct species followed or preceded by whole genome duplication, leading to the combination of divergent genomes. Having a polyploid constitution offers some fitness advantages, which could become evolutionarily successful. Nevertheless, polyploid species must develop mechanism(s) that control proper segregation of genetic material during meiosis, and hence, genome stability. Otherwise, the coexistence of more than two copies of the same or similar chromosome sets may lead to multivalent formation during the first meiotic division and subsequent production of aneuploid gametes. In this review, we aim to discuss the pathways leading to the formation of polyploids, the occurrence of polyploidy in the grass family (Poaceae), and mechanisms controlling chromosome associations during meiosis, with special emphasis on wheat.

Keywords: chromosome pairing, homoeologous pairing, meiosis, Poaceae, polyploidy

OPEN ACCESS

Edited by:
Mónica Pradillo, Complutense University of Madrid, Spain

Reviewed by:
Pilar Prieto, Spanish National Research Council, Spain
Tomás Naranjo, Complutense University of Madrid, Spain
Andrew Lloyd, Aberystwyth University, United Kingdom

***Correspondence:**
Jan Bartoš
bartos@ueb.cas.cz

Specialty section:
This article was submitted to Plant Cell Biology, a section of the journal Frontiers in Plant Science

Received: *27 April 2020*
Accepted: *26 June 2020*
Published: *09 July 2020*

Citation:
Svačina R, Sourdille P, Kopecký D and Bartoš J (2020) Chromosome Pairing in Polyploid Grasses. Front. Plant Sci. 11:1056. doi: 10.3389/fpls.2020.01056

INTRODUCTION

Poaceae (grasses) is a large family of monocotyledonous flowering plants that includes ~10,000 diverse species divided into 12 subfamilies, 51 tribes, and 80 subtribes (Soreng et al., 2015). This family includes the cereals, bamboos, as well as natural and cultivated grasses, and its members are found worldwide except in ice-covered areas. Their economic importance derives mainly from their utilization for food and feed production, but they also have ecological and aesthetic roles in ecosystems and for humanity. For example, maize (*Zea mays*), rice (*Oryza sativa*), and wheat (*Triticum aestivum*) together provide >50% of the calories consumed by all humans. Sugarcane (*Saccharum officinarum*) remains the major source of human-consumed sugar and is increasingly used for biofuel production. Ryegrasses (*Lolium* spp.), fescues (*Festuca* spp.), and bluegrasses (*Poa* spp.) are cultivated as fodder crops and for amenity purposes (i.e. sports, private and industrial lawns). Bamboos (Bambuseae) are used to construct elaborate scaffolds and the straws of cereals can serve as insulation in buildings or as raw material for paper production. All these uses make the Poaceae species a priority choice for enhancing both their quality (i.e., protein, lipid or sugar

contents; cooking-quality, and digestibility, among others) and quantity (yield of grain and straw, biomass production).

Besides their great economic importance, species of the Poaceae family also serve as excellent model organisms for evolutionary studies (Kellogg, 2001). According to the pollen fossil record, grasses arose 55–70 million years ago (MYA; Jacobs et al., 1999). With ever more sequenced genomes (for details see https://bioinformatics.psb.ugent.be/plaza/), a detailed investigation of the evolutionary fate of duplicated chromosomal blocks led to the proposition of an ancestral karyotype for grasses, one structured in seven protochromosomes that contained 16,464 protogenes (Murat et al., 2014). This ancestral genome then further evolved, through the fusion and fission of chromosomes, gene duplication events as well as deletions, and chromosomal inversions and translocations. Moreover, interspecific hybridization and polyploidization (whole genome duplication; WGD) are two other key mechanisms of speciation in the Poaceae. All these phenomena have contributed to the extensive genome diversity extant within the family, including its variability in basic chromosome numbers and a wide range of polyploidy levels (Keeler, 1998). In this review, we highlight the nature of polyploidy in grasses, using wheat as a model, with a special focus on chromosome pairing during meiosis.

POLYPLOIDY

Polyploidy plays a significant role in the evolution of higher plants, in that all angiosperms apparently underwent at least one round of WGD in their evolutionary history (Jiao et al., 2011). Polyploids can be categorized based on their origin. *Autopolyploids* possess three or more copies of the same chromosome set; by contrast, the multiple chromosome sets in *allopolyploids* are of different origin, due to the involvement of interspecific hybridization. Yet a strict boundary between these two categories is not always evident, such that a third (intermediate) group called segmental allopolyploidy is sometimes recognized in plants (Winterfeld et al., 2012). In general, autopolyploids often exhibit the formation of multivalents during meiosis and polysomic inheritance in their progeny. By contrast, allopolyploids with distant parental genomes usually exhibit formations of bivalents from homologous chromosomes (i.e., diploid-like pairing behavior), leading to disomic inheritance (Ramsey and Schemske, 1998). Nevertheless, allopolyploids sometimes carry chromosome sets that are not identical, but divergence of their sequence is insufficient to avoid the pairing of homoeologs (i.e., chromosomes originating from two related parental genomes with substantial homology); hence, they must employ an additional mechanism to ensure diploid-like behavior. Jauhar (2003) suggested that stable meiotic behavior and genome stability in allopolyploid species is achievable only after establishing a mechanism to ensure homologous chromosome recombination and segregation.

Autopolyploids

For a long time, autopolyploids were believed to suffer from various evolutionary disadvantages, leading to the conviction that autopolyploidy is rare in nature and often represents an evolutionary dead end (Clausen et al., 1945; Stebbins, 1971). This view, however, contrasts with their widespread utilization in crop production, for which many autopolyploids including potato, banana, watermelon, and sugarcane are of high economic importance. The proportion of autopolyploidy among plant species can only be debated so far, given that many autopolyploids have escaped recognition, being morphologically similar to their progenitors and concealed among common diploid taxa (Soltis et al., 2007). Recently, Barker et al. (2016) inferred that autopolyploids might be as frequent as allopolypoids among vascular plants. The Poaceae family contains many known autopolyploid species, such as *Andropogon gerardii*, a dominant grass of the tallgrass prairie (Keeler and Davis, 1999), several *Brachiaria* species (Gallo et al., 2007), the forage crop *Hordeum bulbosum* (Eilam et al., 2009), the sugarcane plant *S. spontaneum* (Wang et al., 2010), in addition to several *Avena* species (Ladizinsky, 1973).

Allopolyploids

Allopolyploids result from the hybridization of two more or less related species, such as *Psidium guineense* (Marques et al., 2016), wheat (*T. aestivum*) or the common oat (*Avena sativa*). Genomes inherited by allopolyploids vary in chromosomal homology, based on congeniality of parental species. In the case of hybridization between distantly related species, chromosomal homology can be low enough to not pair up during meiosis, frequently having different basic number of chromosomes. Conversely, allopolyploids that originated from the cross between closely related species carry chromosomes with much higher degree of homology. Accordingly, their homoeologous chromosomes have the potential to pair and recombine during meiosis (Ramsey and Schemske, 1998; Sun et al., 2017). Bread wheat is a typical example of an allopolyploid; it originated from two distinct interspecific hybridizations among three related diploid species that diverged 5–7 MYA (Marcussen et al., 2014). The first hybridization event occurred <0.82 MYA, between *T. urartu* and an as of yet unknown species from the *Sitopsis* section, closely related to *Aegilops speltoides*, which resulted in the development of a tetraploid species that further evolved into cultivated tetraploid wheat (*T. turgidum* ssp. *durum*; BBAA; Marcussen et al., 2014). The second hybridization took place more recently, between this newly developed tetraploid and *Ae. tauschii* (DD), resulting in hexaploid *T. aestivum* (2n = 6*x* = 42; BBAADD; Huang et al., 2002; Petersen et al., 2006; Marcussen et al., 2014). Similarly, oats (*Avena* spp.) also comprise diploid, tetraploid, and hexaploid species, either as auto- or allopolyploids. The allopolyploid oats behave diploid-like during meiosis despite having partial homology between their parental genomes (Thomas, 1992). Besides evolutionarily old allopolyploids, relativey recent allopolyploidazion events are evident in nature. For example, about 150 years ago, the two natural hybrids *Spartina* × *neyrautii* and *S.* × *townsendii* emerged through crosses between European *S. maritima* and *S. alternifolia*, the latter introduced from America. While the homoploid hybrid *S.* × *townsendii* is mostly sterile, chromosome doubling gave rise to the fertile allotetraploid

species *S. anglica* (Hubbard, 1968) which spread rapidly throughout salt marshes in Western Europe (Gray et al., 1990; Thompson et al., 1991; Baumel et al., 2001; Salmon et al., 2005). As such, the polyploidization found in *S. anglica* may represent a way by which interspecific hybridization can foster evolutionary success.

Pathways Leading to Polyploidy

There are several routes leading to the formation of a polyploid individual. The first way is *via* chromosome doubling because of non-disjunction during mitosis. However, this way is rarely observed under natural conditions and is usually achieved only by exposure to chemical agents (Ramsey and Schemske, 1998; Tamayo-Ordóñez et al., 2016; Pelé et al., 2018). The more likely mechanism operating is that through the generation of unreduced gametes. The frequency of their production usually varies from 0.1% to 2% (Kreiner et al., 2017; Pelé et al., 2018) but this increases in response to stress, such as drought, low or high temperatures, and physical damage (Mason et al., 2011; Pécrix et al., 2011; De Storme et al., 2012; Vanneste et al., 2014; Kreiner et al., 2017; Van de Peer et al., 2017). This fact indicates polyploid formation could accelerate in periods of intensive environmental disturbances and rapid changes (Soltis et al., 2007). Polyploidy can be achieved in a single step process by fusing two unreduced gametes, through a so-called triploid bridge, or *via* a pathway involving two steps (**Figure 1**). The triploid bridge is expected to more commonly occur than the one-step pathway, due to the low probability of fusion of two unreduced gametes in natural populations (Husband, 2004). The two-step pathway of allopolyploid formation first involves generation of a homoploid hybrid. Such an individual would either require a somatic doubling event, fusion of its two unreduced gametes, or involvement of the triploid bridge to restore its fertility (Mason and Pires, 2015). Alternatively, when the progenitors are autopolyploids, an allopolyploid can emerge immediately through the fusion of their standard (i.e., reduced) gametes (Pelé et al., 2018).

Polyploid species usually revert to a diploid state during evolution. The first part of this process, called *cytogenetic diploidization*, results in the formation of species, whose polyploid origin might be hidden by disomic inheritance and diploid-like meiosis. This step occurs rather rapidly after polyploid formation either by establishment of genetic control mechanism similar to Ph system in wheat (see below) or extensive chromosomal rearrangements. Over millions of years *genomic diploidization* continues. The content of the genes, which has doubled by polyloidization, is gradually returned towards one copy for each gene. For example, maize underwent an ancient WGD ~10 MYA. Since then, it has not only become cytogenetically diploid but also undergone extensive gene loss causing many genes to revert to a single-copy status in the genome (Renny-Byfield et al., 2017).

Advantages and Risks of Polyploidization

The question still stands: what is the main evolutionary advantage of polyploid formation in plants? While it may appear to have little impact on particular species (Meyers and Levin, 2006), it can also represent a significant evolutionary tool for improving possibilities of adaptation (Otto and Whitton, 2000). For example, gene redundancy offers an opportunity to better resist deleterious mutations and to diversify the extra copies of genes in subsequent evolution; in this way, new traits may be acquired without the adverse effects of losing the original genes' function (Ha et al., 2009). From comparative analysis of collinear genes in syntenic regions of wheat and its diploid relatives Akhunov et al. (2013) confirmed the increased gene diversification conferred by polyploidy. Besides gene redundancy, allopolyploids can also benefit from the advantages of heterosis immediately upon their formation (Osborn et al., 2003; Comai, 2005), which can foster a greater biomass and accelerated development. Similarly, autopolyploidy might result in higher biomass of plants (Stebbins, 1971) and seed size, the latter enabling a more rapid rate of early development, such as in *Triticum* and *Aegilops* species (Villar et al., 1998; von Well and Fossey, 1998). All these effects of polyploidization could contribute to faster colonization of new niches, including extreme habitats (Ehrendorfer, 1980). At the chromosomal level, the existence of extra chromosomal set(s) represents a significant fitness advantage for tolerating large rearrangements in the genome that would normally lead to fatal consequences in diploid progenitors.

Clearly then, polyploid species are evolutionarily successful. In many cases (e.g., *T. aestivum*) they can grow in broad geographical areas and occupy a range of habitats (Feldman and Levy, 2005; Dubcovsky and Dvorak, 2007) as well as colonize extreme environments, like *S. anglica* has done (Hubbard, 1968; Gray et al., 1990; Thompson et al., 1991; Baumel et al., 2001; Salmon et al., 2005). Van de Peer et al. (2009) argued the higher competitiveness of polyploids could be explained by an ability to produce more diverse phenotypes than diploid species. Finally, it is worth noting that many staple crops are in fact polyploid species, and humankind has been using artificial polyploidization techniques and wide hybridization as a tool for their breeding and crop improvement. The use of wild relatives to enhance crops dates back to the early 1940s but gained prominence during the 1970s and 1980s (Hajjar and Hodgkin, 2007). Specifically, allopolyploidization is implemented to widen the target species' genetic diversity or to introgress beneficial alleles from relatives into cultivated crops. For example, while the natural genetic diversity of elite sown material is significantly lower than that observed in its landraces, breeding programs have introduced new sources of diversity into wheat's cultivars. To date, novel alleles have been introgressed from more than 50 related species representing 13 genera, highlighting the importance of these alien introgressions for improved wheat breeding (Wulff and Moscou, 2014). Perhaps the most well-known case is the rye (*Secale cereale*) 1RS translocation that harbors genes involved in a plant's resistance to multiple diseases (*Pm8*/*Sr31*/*Lr26*/*Yr9*) and its yield enhancement. Other examples of introgressions include that of *Sr36*/*Pm6* from *T. timopheevii*, *Lr28* from *Ae. speltoides*, and *Pch1* and *Sr38*/*Lr37*/*Yr17* from *Ae. ventricosa*, which provided resistance to severe diseases such as

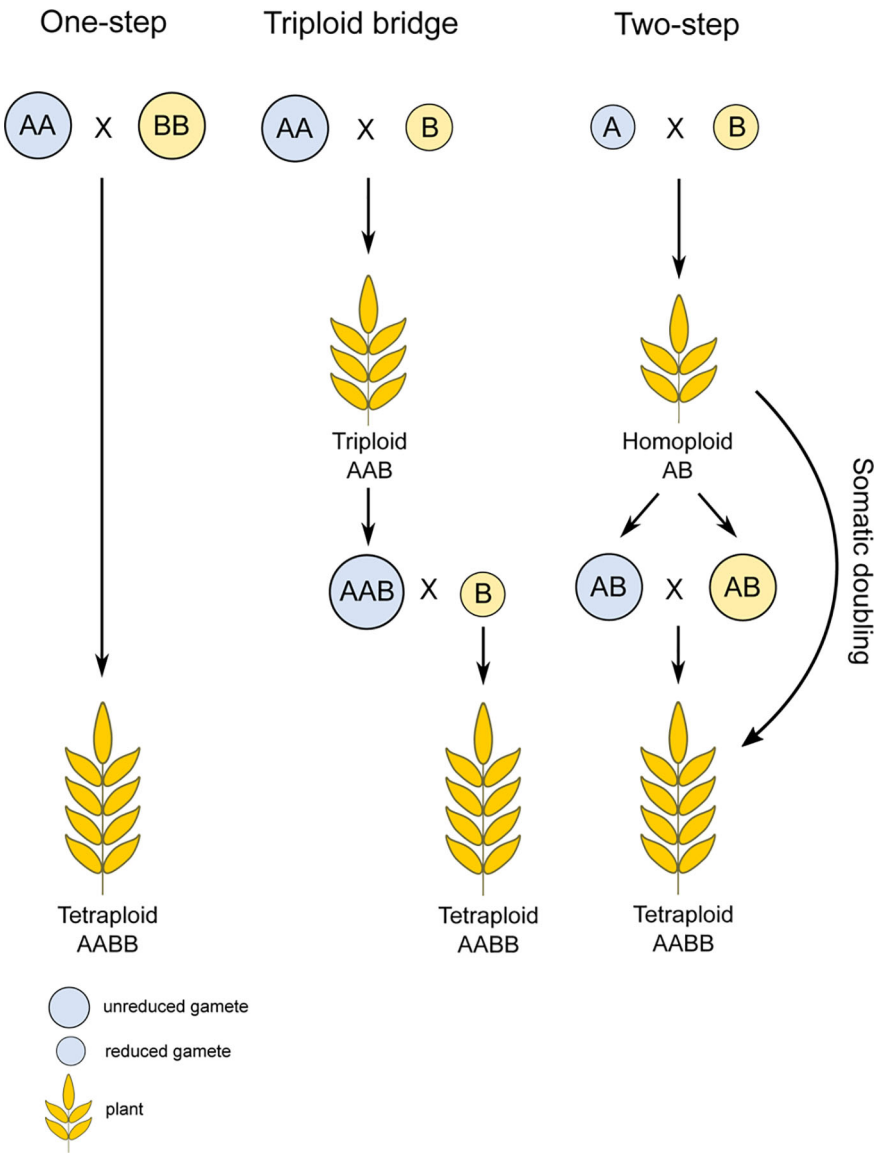

FIGURE 1 | Possible pathways of allopolyploid formation. Polyploidy can be achieved *via* multiple ways, most often through unreduced gamete formation and subsequent fertilization. In the case of the one-step pathway, two unreduced gametes merge, resulting directly in a polyploid species. Arguably, however, more steps are usually needed, where the reduced gamete merges with an unreduced gamete, forming a triploid bridge that requires an additional reduced gamete in subsequent generations. The final depicted option is the two-step pathway, through a homoploid hybrid, which needs a somatic doubling event or unreduced gamete formation to attain a polyploid state.

stem and leaf rust and powdery mildew. Some of these introgressions were implemented gobally in commercial lines; for example, the 1RS.1BL translocation now found in 10% of the world's genetic wheat diversity (Balfourier et al., 2019).

Nontheless, in addition to its positive impacts, polyploidy may have negative aspects. Perhaps the most obvious issue is the presence of more than one pairing partner in meiosis. Unless it is properly processed, it could result in multivalent formation and the production of aneuploid gametes, and thus, lower fertility or complete sterility (Ramsey and Schemske, 2002). Among the adaptive mechanisms described for autopolyploids, there is one based on a reduction in the number of cross-overs to one per chromosome pair, thereby ensuring only bivalents form from any two random homologs (Lloyd and Bomblies, 2016). This mechanism was observed in natural accessions of autotetraploid *Arabidopsis arenosa* (Carvalho et al., 2010; Pecinka et al., 2011; Yant et al., 2013; Pelé et al., 2018). By contrast, recognition of homologous chromosomes is critical for diploid-like pairing in allopolyploids. In allopolyploids containing distinct genomes, it is usually maintained by sequence variation between

homoeologous chromosomes. In allopolyploids containing closely-related genomes, homolog recognition seems to be genetically controlled (Jenczewski and Alix, 2004). However, some allopolyploid and homoploid hybrids do not necessarily display significantly reduced fecundity, despite the pairing of homoeologous chromosomes. In such case, aneuploidy, chromosome rearrangements, and the predominance of one of the parental genomes could be observed, as described for ×Festulolium hybrids (Kopecký et al., 2006). Hereon, we focus on mechanisms controlling chromosome pairing in some crops belonging to the grass family (Poaceae).

CONTROL OF CHROMOSOME PAIRING IN POLYPLOID GRASSES

Meiosis is a crucial process for sexual reproduction and gamete formation. It ensures reduction of genetic material to half resulting in restoration of normal chromosomal constitution in progeny. As noted above, some allopolyploids have evolved molecular mechanisms that govern homologous chromosome pairing. Such regulators were observed and identified in several species, including those of *Triticum*, *Avena*, and *Festuca*. The origin of the genes responsible for regulating chromosome pairing is not known yet, however. Nonetheles, several hypotheses explaining the possible emergence of such mechanisms have been proposed.

The first hypothesis works by presuming the presence of these pairing regulators in diploid progenitors (Waines, 1976; Jenczewski and Alix, 2004). In this model, a stable allopolyploid would emerge after a rare event, in which the appropriate combination of such genes is achieved (Waines, 1976). Indeed, several regulators acting as suppressors of homoeologous chromosome pairing were believed to exist in diploid relatives of allopolyploids, such as *Lolium* spp., *Hordeum vulgare* (Gupta and Fedak, 1985), *Hirschfeldia incana* (Eber et al., 1994), *Secale cereale* (Riley and Law, 1965), *Elytrigia elongata* (Dvorak, 1987), *Triticum monococcum* (Shang et al., 1989), and *Ae. tauschii* (Attia et al., 1979). In *Lolium*, the pairing suppressors were found present in some accessions of *L. multiflorum* and *L. perenne*, where they influenced the number of chiasmata during the first meiotic division of their homoploid hybrid. This chiasma reduction was accounted for exclusively by homoeologous pairing, as revealed by artificially tetraploidized hybrids (Evans and Aung, 1985; Jenczewski and Alix, 2004). Another example of how chromosome-pairing control is induced through a combination of genotypes or genes was found in rice. Generally, rice intersubspecific autotetraploid hybrids display meiotic instability such as chromosome lagging and the formation of univalents and trivalents (Cai et al., 2007). Yet two lines PMeS-1 and PMeS-2 were distinguished as being stable, presumably due to the presence of one or more active meiotic regulator *PMeS* (polyploid meiosis stability) genes (Cai et al., 2007). These two lines display regular meiotic behavior, with bivalents and quadrivalents. The existence of genetic chromosome pairing *PMeS* control was confirmed by the persistent meiotic stability of the two lines even after several generations (Xiong et al., 2019).

The second hypothesis posits that the regulators of chromosome pairing emerge during or immediately after the formation of polyploids, by a mutation or multiple, successive mutations (Riley and Law, 1965; McGuire and Dvořák, 1982). This can happen *via* conversion of a gene that promotes chromosome pairing in the diploid progenitor into a repressor in the polyploidy individual (Riley and Kempanna, 1963; Feldman, 1966b). This phenomenon was described in hexaploid wheat, where a mutation in a pairing promoter gene on the long arm of its chromosome 5D caused a reduction of homoeologous chromosome paring in several interspecific hybrids. Such mutations provide a more pronounced effect than does being 5D nullisomic, which suggests the mutation is antimorphic, changing the gene's function from pairing-promotion to suppression (Viegas et al., 1980). Those authors argued that this allele more likely arose from spontaneous mutation of a pairing-promoter known to be located on 5DL than from the transfer of *Ph1* from chromosome 5B.

The third hypothesis proposes that such regulators of chromosome pairing could be transferred *via* accessory B chromosomes (Riley et al., 1973; Sears, 1976). Early allopolyploid species would have depended on the presence of a B chromosome(s), until the gene was transferred to an A chromosome by translocation, with the subsequent loss of the B chromosome from the karyotype (Jenczewski and Alix, 2004). Many studies have investigated the role of B chromosomes in the repression of homoeologous pairing (Evans and Macefield, 1972; Evans and Macefield, 1973; Aung and Evans, 1985). It seems that one or more B chromosomes from a specific source could complement one copy of the aforementioned homoeologous-pairing suppressor into a functional complex. Evans and Aung (1986) found homoeologous pairing dramatically reduced in the hybrids of *F. arundinacea* × *L. perenne* carrying B chromosomes. Also, the average number of chromosome arms joined by chiasmata is reduced in the presence of B chromosomes in a diploid meadow fescue when compared to the control plants lacking B chromosomes (Kopecký et al., 2009). In the hybrids of *Ae. mutica* and *Ae. speltoides*, the B chromosomes can also complement a missing *Ph1* locus (Dover and Riley, 1972). Mechanisms controling chromosome pairing in allopolyploids seems to be specific among individual taxa, with very little known of the molecular pathways contributing to this phenomenon. In this respect, the best-elucidated molecular mechanism concerning the *Ph* genes is that of hexaploidy wheat (*T. aestivum*), which we describe in greater detail later on.

Apart from specific genetic systems to ensure proper chromosome pairing in particular species, various other (more general) genes are involved during process of meiosis that could increase the frequency of cross-overs between homologous chromosomes while suppressing them between homoeologs. Recently, Gonzalo et al. (2019) studied the effect of *MSH4* upon homo- and homoeologous cross-overs, by using the EMS (ethylmethanesulphonate) mutant population in *Brassica napus*. They discovered that, when the *MSH4* gene returns to a single

copy status, the frequency of homologous cross-overs remained at the same frequency, whereas that of homoeologous cross-overs decreased drastically compared with the presence of two functional copies of the gene. Gonzalo et al. (2019) also studied the copy numbers of other genes of the synapsis-initiation complex (SIC, or alternatively ZMM-pathway) vis-à-vis diploid relatives, deducing that the acquisition of additional copies of such genes through small-scale duplications is a rare event; an example its occurrence is *ZIP4* in wheat (Rey et al., 2017). Furthermore, the rapid reduction in the number of copies for ZMM genes in many species after whole genome duplication—namely for *MSH4*, *MSH5*, *MER3*, and *ZIP4*—supports the hypothesis that ensuring fewer copies of such genes could be a general process of meiotic stabilization (Lloyd et al., 2014; Gonzalo et al., 2019). Another study found no evidence for an increased loss of those genes after polyploidization in hexaploid wheat (including *MSH4*), in that most meiotic genes were retained in three homoeologous variants at similar expression levels (Lloyd et al., 2014). However, because wheat underwent its two hybridization events rather recently (Marcussen et al., 2014), the potential ZMM pathway gene reduction cannot be ruled out. Alternatively, the machinery established *via Ph* genes might have weakened the selective pressure for fewer copies of these genes.

Chromosome Pairing in Wheat

Allohexaploid bread wheat (*T. aestivum* L.; 2n = 6*x* = 42; BBAADD) can serve as a model plant for meiotic behavior analyses of allopolyploids. Despite the coexistence of three highly similar genomes, its meiotic behavior is strictly diploid-like, with 21 bivalents between homologous chromosomes forming in metaphase I of meiotic division. It has been known for more than 60 years that bread wheat developed genetic control of precise formation of homologous chiasmata, which is enforced by *Ph* (pairing homoeologous) genes (Sears and Okamoto, 1958; Riley and Chapman, 1958). The hexaploid nature of wheat allowed for the development of various aneuploid stocks, permitting the identification of several key genes involved in the regulation of meiosis (Sears and Okamoto, 1958; Sears, 1976; Sears, 1977; Sears, 1982; Sears, 1984).

It was proposed that premeiotic chromosome associations in interphase nucleus also play role in homolog recognition (Brown and Stack, 1968; Comings, 1968; Loidl, 1990; Aragón-Alcaide et al., 1997; Schwarzacher, 1997; Mikhailova et al., 1998; Martínez-Pérez et al., 1999). Nevertheless, different studies disagree in the extent and role of premeiotic chromosome associations, where they start and how long they last (Schwarzacher, 1997; Mikhailova et al., 1998; Martínez-Pérez et al., 1999). However, all these studies partially agree with Feldman (1966a), who suggested that *Ph1* controls spatial organization of chromosomes in premeiotic interphase nuclei. In wheat, the arrangement of chromosomes in interphase nuclei is done through distribution of centromeres and telomeres in opposite sides of nuclei into Rabl configuration (Fussell, 1987), whereas this configuration is being maintained in premeiotic cells (Naranjo, 2015). This organization plays a role in the recognition of homologs, as it reduces the homolog search and simplifies the subsequent alignment (Pernickova et al., 2019). The telomeres are then recruited to the nuclear envelope and form a telomere bouquet (Dawe, 1998; Harper et al., 2004), which is believed to be essential for homolog identification and initiation of synapsis (Bass et al., 2000; Scherthan, 2001; Bass, 2003; Harper et al., 2004; Scherthan, 2007). The molecular mechanisms driving these changes are, however, mostly unknown.

Formation of chiasmata in wheat is driven by both suppressors and promoters, of which several have already been identified. The most important gene regulating homologous chiasmata is *Ph1* (*Pairing homoeologous 1*), located on the long arm of chromosome 5B (Sears and Okamoto, 1958; Riley and Chapman, 1958). Another gene affecting chromosome behavior during meiosis, called *Ph2*, is located on the short arm of chromosome 3D but it exerts a weaker effect than does *Ph1* (Mello-Sampayo, 1971). The least effective regulator, *Ph3*, is located on the short arm of chromosome 3A (Driscoll, 1972; Mello-Sampayo and Canas, 1973). Similar effects of *Ph2* and *Ph3* genes and their location on the same chromosomes of different parental genomes suggest these two genes are probably paralogs. During metaphase I of meiosis, *ph* mutants typically display fewer ring bivalents (with two or more chiasmata) and more univalents, rod bivalents and multivalents when compared to the wild type (**Table 1**).

Pairing Homoeologous 1 (Ph1)

Among those genes controlling chiasmata formation during meiosis in wheat, *Ph1* has the strongest effect on ensuring the correct recognition of homologous chromosomes. Although the presence of this control element was discovered over 60 years ago, its molecular effect was uncovered in part only recently. Its existence was first proposed by Sears and Okamoto (1958) and Riley and Chapman (1958) in haploid lines of wheat lacking chromosome 5B, in which the formation of both bivalents and trivalents had been observed. This contrasted with the meiotic behavior of lines carrying a copy of 5B. Subsequent gene mapping was carried out using the *Ph1* mutant called *ph1b* (Sears, 1977), which helped to delimit the gene's location. Later

TABLE 1 | Comparison of chromosome associations in hexaploid and tetraploid wheat plants and particular *ph* mutants during metaphase I (Martínez et al., 2001a; Martínez et al., 2001b).

Genotype	Chromosome number	Univalents	Rod bivalents	Ring bivalents	Multivalents	Chiasmata per cell
Hexaploid WT	42	0.02	1.48	19.50	0.00	40.49
ph1b	42	2.76	4.76	14.5	0.77	38.57
ph2b	42	0.48	2.95	17.78	0.00	34.22
Tetraploid WT	28	0.04	0.34	13.64	0.00	27.62
ph1c	28	0.94	3.69	9.46	0.19	23.16

mapping, by Gill et al. (1993), used deletion lines to narrow down the genome region harboring the gene, which was cytogenetically estimated to be ~70 Mb. A more recent estimate of this deletion's length put its at 54.6 Mb (Gyawali et al., 2019). Countless studies have shown that when *Ph1* is missing, the chiasmata formation is no longer strictly diploid-like and chromosomes will form multivalents in more than 50% of pollen mother cells (Riley and Chapman, 1958; Riley, 1960). Work by Sánchez-Morán et al. (2001) confirmed that stark irregularities, such as aneuploidy and genomic rearrangements, are observable in lines lacking *Ph1*.

The *Ph1* locus is present in tetraploid wheat plants as well, such as *T. turgidum* subsp. *durum* (Dvorak et al., 1984) and *T. timopheevi* subsp. *timopheevi* (Feldman, 1966b). In the latter, a mutant for this particular gene was developed, called *ph1c*, having a similar phenotype as the hexaploid mutant *ph1b*, i.e., increased homoeologous chromosome chiasmata in metaphase I (Jauhar et al., 1999). In a comparative study assessing the effectiveness of *Ph1* gene in tetraploid and hexaploid wheat, Ozkan and Feldman (2001) crossed *Ae. peregrina* with hexaploid wheat and derivative lines, wherein chromosome 5B was replaced by its variant from tetraploid wheat (either from *T. turgidum* subsp. *dicoccoides* or *T. timopheevi* subsp. *Timopheevi*). With 5B from tetraploid wheat present, a higher frequency of homoeologous chromosome associations was observed in hybrids relative to the presence of endogenous 5B, indicating the tetraploid variant of *Ph1* gene might operate with lower effectiveness. Interestingly, once *Ph1* is introgressed from wheat into related species, its ability to modify chromosome bahavior is also preserved in the host genome (**Figures 2A, B**; Lukaszewski and Kopecký, 2010).

The *Ph1* regulator probably acts in multiple ways during meiosis. In early prophase I, it promotes the formation and subsequent correction of synapses (Holm, 1986; Martínez et al., 2001a), but later on, it affects the frequency of cross-over formation (Martín et al., 2014). Originally, the *Ph1* gene was thought to function as a suppressor of homoeologous synapses (Holm and Wang, 1988), but the current view is that it works primarily by promoting and stabilizing homologous synapses (Martín et al., 2017). During metaphase I in hexaploid wheat, ring bivalents are predominantly formed between homologous chromosomes, with some rod bivalents occurring in all meiocytes (Martín et al., 2014). In the *ph1b* mutant, only ~50% of meiocytes wil display similar meiotic behavior with increased frequency of rod bivalents; in the other half, variable numbers of multivalents and univalents were instead detected. This means that roughly half of the meiocytes display chiasmata only between homologous chromosomes (Martín et al., 2014). Similarly, other studies could not find homoeologous chiasmata in significant fractions of meiocytes in other *Ph1* mutants (Roberts et al., 1999; Al-Kaff et al., 2008; King et al., 2016). This suggests the promotion of homologous synapses is the main function of the *Ph1* gene, rather than suppression of homoeologous ones (Martín et al., 2017). This hypothesis is further supported by the higher occurrence of univalents in *ph1b* mutants than in the wild type or *ph2b* mutant (**Table 1**).

Griffiths et al. (2006) performed a screen for a *ph1*-like phenotype in the population of EMS mutants. Yet they failed to find an individual showing the full *ph1b*-like phenotype. This indicates the *Ph1* phenotype might not be under the control of a single gene. The *Ph1* locus was further narrowed down to a 2.5-Mb region on the long arm of the 5B chromosome (Griffiths et al., 2006), which contains a duplicated segment from chromosome 3B composed of a cluster of *Cdk2*-like kinases and methyl-transferase genes (Griffiths et al., 2006; Al-Kaff et al., 2008; Martín et al., 2017). The Cdk-like kinases in the locus show close homology to the mammalian Cdk2, which is essential for homologous chromosome recognition and recombination (Ortega et al., 2003; Viera et al., 2009). Two groups of researchers disagree on which of the genes located in this particular region is the one responsible for promotion of homologous chiasmata. Bhullar et al. (2014) proposed *C-Ph1* (RAFTIN1-like protein containing BURP domain) to be a putative *Ph1* gene, but deletion lines for *C-Ph1* locus failed to produce the same phenotype as the *ph1b* mutant (Al-Kaff et al., 2008). Moreover, the rice homolog and wheat paralog of this gene were already shown to be specific to tapetal cells (Jeon et al., 1999; Wang et al., 2003). The other group proposed a different candidate, a paralog of *ZIP4*. The encoded protein affects the homologous cross-overs in *Arabidopsis* and rice, supporting the assumption that this gene could be responsible for the *Ph1* phenotype (Chelysheva et al., 2007; Shen et al., 2012; Rey et al., 2017). Both EMS and CRISPR mutations for this gene (named *TaZIP4-B2)* promoted homoeologous cross-overs in hybrids between wheat and *Ae. variabilis* (Rey et al., 2017; Rey et al., 2018). But these hybrids did not show the same extent of multivalent formation or an increase in univalents as typically observed in hybrids between the *ph1b* mutant and *Ae. variabilis*. Nevertheless, these results do suggest the *TaZIP4-B2* plays an important role in the control of homoeologous pairing in wheat (Rey et al., 2017; Rey et al., 2018; Naranjo, 2019). The putative additional effector in this region has yet to be identified.

Pairing Homoeologous 2 (Ph2)

Another gene, called *Ph2*, has a weaker effect (than *Ph1*) on homologous chromosome pairing in wheat. That gene was assigned to chromosome 3D by Mello-Sampayo (1968; 1971) who observed multivalent formation in metaphase I in the absence of chromosome 3D in pentaploid hybrids between *T. aestivum* and *T. durum*, as well as in hybrids between *T. aestivum* and *Aegilops*. Two *Ph2* mutants were since developed; the X-ray-induced mutant *ph2a* carrying a large deletion (Sears, 1982), and the chemically-induced (EMS) mutant *ph2b* (Wall et al., 1971). Using both mutants, the *Ph2* phenotype was studied and the locus narrowed down, using synteny with rice, to a terminal 80 Mb of the short arm of chromosome 3D (Sutton et al., 2003). More recently, however, Svačina et al. (2020) showed that this deletion in the *ph2a* mutant is actually larger than expected, comprising about 125 Mb terminal part of the short arm of chromosome 3D.

The *Ph2* gene operates in a different way than does *Ph1* (Benavente et al., 1998; Martinez et al., 2001a). Both Martinez et al., (2001a) and Sánchez-Morán et al. (2001) evaluated the effect of its mutations in hexaploid wheat, finding no visible

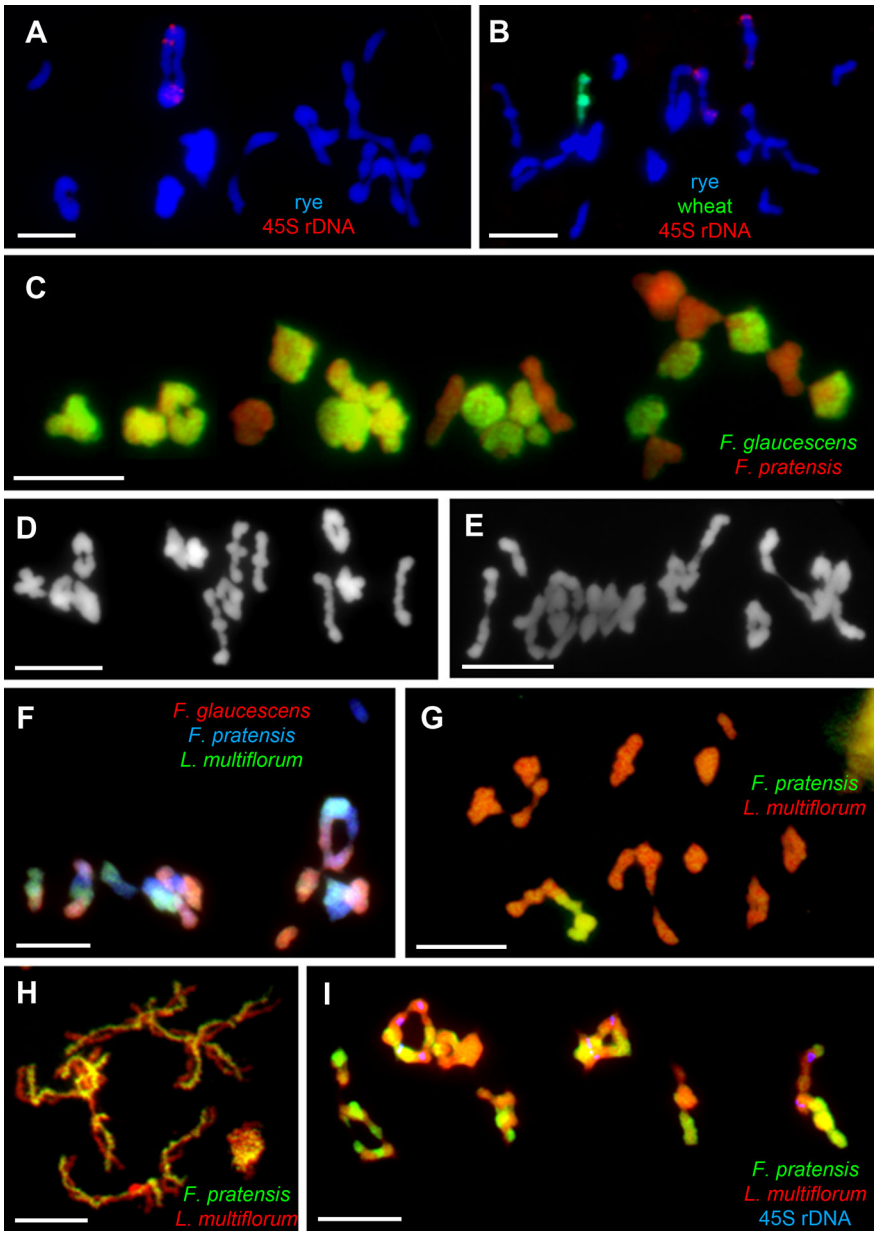

FIGURE 2 | Chromosome assocaitions in allo- and autopolyploids from the Poaceae family. Chromosome pairing in autotetraploid rye (2n = 4*x* = 28, RRRR) differs depending on the presence or absence of *Ph1* located on the introgressed 5BL chromosome arm of wheat. In **(A)**, trivalents and quadrivalents are commonly observed in the control line (2I+4II+2III+3IV), in **(B)**, multivalent chromosome formation is reduced in the line (6I+7II+2IV), where 5B and 5BL are introgressed. In both **(A, B)**, genomic DNA of *Triticum aestivum* was labeled with digoxigenin (green coloring), 45S rDNA was labeled with biotin (red), and genomic DNA of *Secale cereale* served as blocking DNA; all chromosomes counterstained with DAPI (blue). In **(C)**, the chromosome-pairing control system similar to that of *Ph1* found in allohexaploid *Festuca arundinacea* (2n = 6*x* = 42) hampers the associations of homeologous chromosomes and multivalent formation (21II). Genomic DNA of *F. glaucescens* was labeled with digoxigenin (green), while genomic DNA of *F. pratensis* was used as blocking DNA; all chromosomes were counterstained with DAPI (red pseudocolor). In **(D)**, the homoeolog suppressor was probably inherited from one of the progenitors, *F. glaucescens*, as this species also forms only bivalents during meiosis (14II). Conversely, in **(E)**, multivalent formation was detected in the autotetraploid form of the other progenitor, *F. pratensis* (2I+7II+3IV). The system is hemizygous-ineffective, thus allowing for promiscuous homeologous chromosome associations in tetraploid hybrids of *F. arundinacea* × *Lolium multiflorum*, where only one copy of the gene(s) is present **(F)**. Here, genomic DNA of *F. glaucescens* was labeled with biotin (red coloring) and that of *L. multiflorum* labeled with digoxigenin (green), while that of *F. pratensis* was used as blocking DNA; all chromosomes were counterstained with DAPI (blue). In **(G)**, homeologous chromosomes of *F. pratensis* and *L. multiflorum* pair freely in the substitution lines (1I+8II+1III+2IV) as well as in diploid *Festuca* × *Lolium* hybrids (7II), as seen in diplotene shown in **(H)**, due to the absence of any chromosome pairing system and the phylogenetic relationship of both genomes. Note many chiasmata between homeologous chromosomes. This results in frequent homeologous recombinations and massive chromosome rearrangements in successive generations **(I)**, as can be seen in the tetraploid *L. multiflorum* × *F. pratensis* cv. 'Sulino' (7IV). In panels **(G–I)**, genomic DNA of *F. pratensis* was labeled with digoxigenin (green coloring), while genomic DNA of *L. multiflorum* served as blocking DNA and all chromosomes were counterstained with DAPI (red pseudocolor).

influence upon homoeologous chiasmata when *Ph1* is present and *Ph2* absent, apart from a slight increase in univalent formations. Earlier, Sears (1977; 1982) had shown that in hybrids of wheat and closely related species, moderate frequency of homoeologous chiasmata happened in the absence of *Ph2* but in the presence of *Ph1*. In the case of wheat-rye hybrids lacking the *Ph2* locus, Prieto et al. (2005) also observed an intermediate number of homoeologous chiasmata; however, according to their GISH analysis, the chromosome associations only occur between wheat chromosomes, whereas wheat–rye associations were rare similarly to the wild-type hybrid. This contrasts with the *ph1b* mutant, for which some frequency of wheat–rye associations was detectable (refer to **Table 2**; Prieto et al., 2005). These findings suggest to us that *Ph2* plays a diminished functional role when homologous chromosomes are present (**Table 1**). Yet, in the absence of homologs, it may well suppress associations among homoeologous chromosomes. Furthermore, researchers discovered that *Ph2* has a different function to that of *Ph1* as it is not involved in recognition of homologous chromosomes but instead affects the progression of synapsis (Martinez et al., 2001a; Prieto et al., 2005). We should also not overlook possible cooperation between *Ph1* and *Ph2* in their modes of action, as suggested by the work of Boden et al. (2009).

The *ph2a* mutant has been exploited in trying to identify candidate genes underlying its phenotype. Many have been proposed, such as *TaMSH7*, the homolog of the *MSH6* DNA mismatch repair gene in yeast (Dong et al., 2002), in addition to the *WM5* (Thomas, 1997) and *WM1* gene family members (Ji and Langridge, 1994; Whitford, 2002). Sutton et al. (2003) used comparative genetics to further identify the putative genes involved in the *Ph2* phenotype; however, no clear candidate producing a mutant phenotype similar to the *ph2a* has been identified.

TABLE 2 | Number of chromosome-arm associations in metaphase I in haploid hybrids derived from the crossing of rye with euploid wheat (CS, 'Chinese Spring') and *ph1b* and *ph2b* mutants (Prieto et al., 2005).

Genotype Chromosome number	CS × rye 28	*ph2b* × rye 28	*ph1b* × rye 28
Wheat–wheat	0.48	1.68	7.14
Wheat–rye	0.08	0.08	0.59
Rye–rye	0.02	0.04	0.05
Total	0.58	1.80	7.78

Meiotic Behavior in Hybrids of *ph* Mutants and Wild-Type Wheat With Closely Related Species

The pairing of homoeologous chromosomes is mostly studied in haploids or interspecific hybrids, that is, in the absence of homologous chromosomes, the natural partners for pairing. The exent of chromosome associations during metaphase I of meiosis, in hybrids of wild-type hexaploid wheat or *ph2b* and *ph1b* mutants with various relatives, will differ based on the degree of homology between the genomes involved. The frequency of homoeologous chromosome chiasmata increases when there is a closer phylogenetic relationship of the parents. The fewest homoeologous associations were observed in the hybrids between hexaploid wheat and rye (**Table 3**; Naranjo et al., 1987; Naranjo et al., 1988). This can be explained by the fact that lineages towards wheat and rye split about 7 MYA while *Aegilops* diverged from wheat 2.5–5.0 MYA (Huang et al., 2002). Accordingly, the *Aegilops* chromosomes are more closely related to wheat chromosomes than those of rye. The highest frequency of homoeologous chromosome associations was observed in the hybrid of hexaploid wheat and *Ae. speltoides* (Maestra and Naranjo, 1998; **Table 3**); the latter is a species closely related to the donor of the B genome in wheat, and thus highly similar to one of the wheat genomes (Huang et al., 2002; Petersen et al., 2006). These observations suggest the *Ph* system's recognition of homologous chromosomes begins to fail with increasing homology between genomes in the hybrid, resulting in homoeologous chromosome chiasmata. Alternatively, there may exist genes that suppress or interfere with the *Ph* system in certain species used for hybridization with wheat (see below).

Homoeologous Chromosome Associations in the Presence of *Ph* Genes

Ph genes ensure that only homologous chromosome chiasmata occur in polyploid wheat during meiosis. However, the functioning of these genes can be suppressed in some hybrids, resulting in increased homoeologous chromosome associations; e.g., in hybrids of *T. aestivum* with *Ae. speltoides* or *Ae. mutica*

TABLE 3 | Associations of homoeologous chromosomes in metaphase I in various hybrids of wild-type wheat (WT) and *ph1b* and *ph2b* mutants with closely related plant species (Naranjo et al., 1987; Naranjo et al., 1988; Naranjo and Maestra, 1995; Maestra and Naranjo, 1997; Maestra and Naranjo, 1998).

Hybrid	Chromosome number	Univalents	Rod bivalents	Ring bivalents	Multivalents	Chiasmata percell
WT × rye	28	26.31	0.80	0.03	0.01	0.88
ph2b × rye	28	19.23	3.4	0.57	0.51	5.26
ph1b × rye	28	11.76	2.33	2.36	2.16	12.35
WT × *Ae. longissima*	28	24.55	1.59	0.06	0.05	1.81
ph2b × *Ae. longissima*	28	14.93	5.8	0.58	0.55	7.44
ph1b × *Ae. longissima*	28	3.48	4.4	2.99	2.86	18.28
WT × *Ae. sharonensis*	28	25.21	1.18	0.03	0.03	1.29
ph2b × *Ae. sharonensis*	28	10.16	5.58	1.42	1.13	11.17
ph1b × *Ae. sharonensis*	28	4.37	3.74	3.79	2.39	17.93
WT × *Ae. speltoides*	28	3.97	4.9	3.11	2.61	17.79
ph2b × *Ae. speltoides*	28	3.25	3.41	3.28	3.2	19.41
ph1b × *Ae. speltoides*	28	2.53	3.36	4.29	2.68	20.08

(Riley, 1960; Dover and Riley, 1972; Dvorak et al., 2006a). For the wheat × *Ae. speltoides* hybrid, Dvorak et al. (2006b) identified two suppressors on chromosomes 3S (*Su1-Ph1*) and 7S (*Su2-Ph1*) that affected homoeologous chromosome associations, varying from 7.0 to 16.4 chiasmata per cell. The *Su1-Ph1* was introgressed into both hexaploid and tetraploid wheat, opening new possibilities in inducing homoeologous chromosome recombinations for introgression into wheat (Li et al., 2017). This phenomenon can also be observed in lines where only a single chromosome was introgressed into the wheat background. In particular, the presence in wheat of chromosome 5U from *Ae. umbellulata* (Riley et al., 1973), or that of chromosome 5E from *Elytrigia elongata* (Dvorak, 1987), promotes homoeologous chromosome chiasmata with the formation of trivalents and bivalents in the haploids (ABD + 5U; ABD + 5E). This outcome suggests that introducing some alien chromosomes can suppress the functioning of *Ph* genes (Koo et al., 2017). Another case of homoeologous chromosome associations in the presence of *Ph* genes was reported on by Liu et al. (2011), who observed frequent recombination between $5M^g$ and 5D chromosomes in substitution lines containing $5M^g$ from *Ae. geniculata*. Later, Koo et al. (2017) used two different $5M^g$ chromosomes from different accessions in the wheat background and observed differential associations between $5M^g$ and 5D in both lines, for which chiasmata between $5M^g$ and 5D were detected in 6.7% and 21.7% of ensuing meiocytes. This might have been caused by the presence of genes located on the particular alien chromosome either actively promoting homoeologous chromosome chiasmata or repressing *Ph1*. Additionally, homoeologous associations probably occurred only between the $5M^g$ and 5D chromosome, as no multivalent was detected (Koo et al., 2017). In another example, homoeologous barley chromosomes fully associated in pairs in the presence of *Ph1* (Martín et al., 2017; Calderón et al., 2018). However, these homoeologous chromosomes did not cross-over, suggesting that *Ph1* does not prevent chromosome pairing between homoeologs, but supresses its recombination (Calderón et al., 2018).

In a natural population of the Chinese landrace of hexaploid wheat 'Kaixianluohanmai' (KL), another gene promoting homoeologous chiasmata in wheat–alien hybrids (presumably in presence of *Ph*) was posited (Luo et al., 1992). Meiosis is regular and normal in KL wheat by itself, as in other wheat landraces (Fan et al., 2019), but a moderate frequency of homoeologous chromosome associations occurs in hybrids of KL wheat with rye and *Aegilops variabilis* (similar as that between *ph1b* × rye and *ph2b* × rye hybrids) (**Table 4**; Luo et al., 1992; Liu et al., 1998; Liu et al., 2003; Xiang et al., 2005). In hybrids arising between KL wheat and *Psathyrostachys huashanica*, the frequency of homoeologous chromosome chiasmata even exceeded that of the *ph1b* × *P. huashanica* hybrid (Kang et al., 2008). This locus, named *phKL*, is most probably not allelic to either *Ph1* or *Ph2* (Liu et al., 2003; Hao et al., 2011). The analysis of monosomics did show that a locus on chromosome 6A in KL might be responsible for the *phKL* phenotype (Liu et al., 1997). However, using two mapping populations, Fan et al. (2019) recently identified a QTL locus possibly responsible for homoeologous associations on chromosome arm 3AL.

TABLE 4 | Chromosome associations in metaphase I in hybrids derived from crossings of rye with the wheat KL landrace, "Chinese Spring" (CS), and the Chinese Spring *ph1* (*CSph1b*) and *ph2* (*CSph2a*) mutants (Hao et al., 2011).

Genotype	Number of associations per cell			
	Rod	Ring	Multivalent	Chiasmata
KL × rye	4.73	0.20	0.11	5.40
CS*ph1b* × rye	4.85	1.87	0.47	9.53
CS*ph2a* × rye	1.74	0.00	0.02	1.78
CS × rye	0.54	0.00	0.00	0.54

Chromosome-Pairing Regulators in Other Poaceae Taxa

Bread wheat is undoubtedly the most studied and well-understood species concerning the mechanism of homologous chromosome recognition in the Poaceae family. Nonetheless, clues to the presence of similar machinery has been observed in other grass species, namely in *Avena* spp. (Ladizinsky, 1973), *Oryza* spp. (Cai et al., 2004), *Festuca* spp. (Jauhar, 1993), polyploid *Hordeum* spp. (Gupta and Fedak, 1985), or *Alopecurus* spp. (Murray et al., 1984). Several examples of chromosome associations in allo- and autopolyploids from the Poaceae family are shown in **Figure 2**.

The genus *Festuca* comprises over 500 species having a wide range of ploidy levels, from diploids to dodecaploids (Loureiro et al., 2007). Agriculturally most important are those species from the subgenus *Schedonorus* comprising broad-leaved fescues, the majority of which are polyploids, from tetraploids to decaploids (Kopecký et al., 2008b). Molecular and cytogenetic analyses have revealed that all these studied polyploid species arose from interspecific hybridization (Humphreys et al., 1995; Catalán and Olmstead, 2000; Hand et al., 2010; Ezquerro-López et al., 2017); hence, they are of allopolyploid origin. All these allopolyploid species—including the tetraploids *F. mairei*, *F. apennina*, and *F. glaucescens*, hexaploid *F. arundinacea*, and octoploids *F. arundinacea* subsp. *atlantigena* and decaploid *F. arundinacea* var. *letourneuxiana*—possess diploid-like pairing behavior during meiosis, with bivalent formation (reviewed in Jauhar, 1993). Jauhar (1975) had proposed the existence of a homoeologous-pairing suppressor in tall fescue (*F. arundinacea*, 2n = 6*x* = 42; FpFpFgFgFg'Fg') (**Figure 2C**). He found frequent multivalent formations in haploid plants of tall fescue (2n = 3*x* = 21) and speculated on the haplo-insufficiency or hemizygous-ineffectivity of the system: meaning that two copies of such gene(s) must be present for the induction of strict homologous pairing. This differentiates the fescues' system from *Ph1* of wheat and the regulator found in oats (Jauhar, 1993). Another difference is that *Ph1* can supress homeologous recombination and/or promote homologous ones, while the control system in tall fescue seems to be responsible for the formation of homologous bivalents. Colchicine-induced dodecaploid wheat was able to form quadrivalents composed of four homologous chromosomes, whereas only homologous

bivalents formed in the synthetically derived dodecaploid tall fescue plant (Jauhar, 1975).

Where the gene(s) underpinning diploid-like pairing system is located on one or more particular chromosomes or even subgenomes of tall fescue plants remains unknown. In tetraploid tall fescue (FpFpFgFg'), homoeologous chromosomes form chiasmata frequently; moreover, the frequent formation of quadrivalents was recorded in colchicine-induced autotetraploids of *F. pratensis* (**Figure 2E**; Kopecký et al., 2009). Thus, one of the subgenomes originating from *F. glaucescens* must harbor the responsible gene(s) (**Figure 2D**). In early work, Jauhar (1975) analyzed a set of monosomic lines of tall fescue and found one line with disrupted diploid-like behavior, probably due to an absence of the chromosome carrying the gene(s) for diploid-like pairing behavior. Unfortunately, this line was lost over time and so it cannot be further investigated. Later, Kleijer and Morel (1984) speculated that disruption of strictly homologous associations in a single plant is more likely to be only a consequence of normal variation among plants. The system may also interfere with other systems present in the genus, or in closely related genera. A high frequency of quadrivalents was observed in the tetraploid *Lolium multiflorum* × *F. arundinacea* hybrid (LmFpFgFg') (**Figure 2F**), which exceeded that of quadrivalents in tetraploid *F. arundinacea* (FpFpFgFg') (Kopecký et al., 2009).

The origin of the system in polyploid fescues is not known, but several scenarios are plausible. It could have developed in a currently unknown diploid species, which served as a progenitor of all recent polyploid species. Alternatively, such a system arose in an early-day polyploid (presumably an allotetraploid), since involved in the evolution of other allopolyploids. Support for both scenarios lies in the fact that the system in all species has the same (rare) attribute: haplo-insufficiency. The third possible scenario involves multiple origins of the system in different species during their evolutionary history. Or, the system is the outcome of two scenarios combined. It does seem that the systems found in various species are compatible in some hybrid combinations yet dysfunctional in others. Eizenga et al. (1990) found that multivalents were rare in the hybrids of tall fescue and giant fescue (*F. gigantea*). Similarly, hybrids of *F. mairei* × *F. glaucescens* show preferential formation of bivalents with a very low frequency of multivalents (nine quadrivalents and one trivalent among 200 PMCs [pollen mother cells]) (Malik and Thomas, 1967). By contrast, the hybrids of Continental and Mediterranean morphotypes of tall fescue all display high levels of multivalent formation (Kopecký et al., 2019), suggesting incompatibility of the two regulatory systems, or some epistatic effects. Therefore, we cannot unambiguously clarify if the system evolved once or twice (or even more times). However, if it did develop just once, the system diverged in different species during evolution to reach a level of incompatibility, as evinced from the analyses of interspecific hybrids.

The genus oat (*Avena* spp.) consists of diploid, tetraploid, and hexaploid species, including the important crop *A. sativa*. Polyploid oats include both auto- and allopolyploid forms, whose diploid-like behavior in meiosis is preserved despite partial homology between their genomes, suggesting the existence of a *Ph*-like system (Thomas, 1992). Oats comprise four cytologically distinct genomes (A, B, C, and D), however the genomes B and D occur only in polyploid taxa (Leggett and Thomas, 1995). Similar to wheat, the system found in tetraploid and hexaploid oats is hemizygous effective and haplo-sufficient, and susceptible to dosage effects and genetic repressibility. The locus that contains the gene(s) for meiotic regulation is likely localized to the A genome (Jauhar, 1977). Unfortunately, surpisingly little is known about the genes whose activity maintains homologous chromosome pairing in oats, apart from their existence being proven by increased associations among homoeologous chromosomes in some nulli-haploid *A. sativa* lines (Gauthier and McGuinnis, 1968).

POLYPLOIDY AND HOMOEOLOGOUS CHROMOSOME PAIRING IN PLANT BREEDING

Besides its key role in plant speciation, polyploidization and hybridization are popular tools in plant breeding. The most straightforward agronomical effect of polyploidy is an increased cell size, potentially resulting in larger organs, including fruits, roots, flowers, leaves, and seeds (Stebbins, 1950). Another frequent consequence of polyploidy is sterility, which generally has an agronomically negative effect; however, for seedless fruit production it can be a desirable trait, as in triploid seedless watermelon (Crow, 1994). The fixation of heterozygosity in allopolyploid species often leads to heterosis, resulting in higher vigor of the hybrids compared with their diploid progenitors, such as in hexaploid wheat *T. aestivum* (Sattler et al., 2016). Wide hybridization coupled to whole genome duplication is commonly used to merge beneficial inheritable traits from both parents, namely in the introgression of a chromosome segment carrying genes for a desirable trait from the wild relative to elite crop cultivars, or for simply widening the gene pool. One of the most promising artificially developed hybrids is Triticale, which originated from the crossing of wheat and rye with a subsequent chromosome doubling (Meister and Tjumjakoff, 1928).

One of the key components for the successful utilization of wide hybridization in plant breeding is the control of homoeologous chromosome associations. In countless studies, the *ph1b* mutant of wheat has been used to induce homoeologous chromosome recombinations between chromosomes of wheat and related species, for transferring desirable traits into the wheat genome (Marais et al., 2010; Niu et al., 2011; Ayala-Navarrete et al., 2013; Rey et al., 2015a; Rey et al., 2015b; Han et al., 2016; King et al., 2019). After the introgression of the chromosomal segment from a related species, it is necessary to immediately re-activate the *Ph1* gene to avoid risking the rapid elimination of the

segment. Nevertheless, some hybrids without meiotic regulation but with homoeologous chromosome pairing can be valuable also and remain relatively stable. Complementary attributes of ryegrasses (i.e., high yield and nutrition) and fescues (i.e., abiotic stress tolerance) can be combined in their hybrids called Festulolium. In last 50 years, many agriculturally successful cultivars have been released *via* several breeding programs (Ghesquière et al., 2010). To do this, the breeders often used tetraploid parents for the initial mating. Such F1 Festulolium hybrids are all allotetraploids and possess two sets of chromosomes from both parental species. One would presume that homologous chromosome associations would be the predominant mode of action due to variation in the DNA sequence. The repetitive elements from these two genera diverged sufficiently that it is now possible to distinguish chromosomes of *Festuca* from those of *Lolium* by genomic *in situ* hybridization (GISH) (Thomas et al., 1994). Yet, frequent formation of homoeologous chromosome chiasmata has been detected in F1 hybrids, as well as in monosomic and disomic substitution lines of *L. multiflorum* × *F. pratensis* (**Figures 2G, H**; Kopecký et al., 2008a). Such massive homoeologous associations and recombination leads to highly variable karyotypes differing from plant to plant (**Figure 2I**). An outcrossing mode of reproduction augments this variability within each population of hybrids over subsequent generations. Consequently, both high variability and heterosis ensue within the bred plant material. It is nevertheless possible to uniform the breeding material at a phenotypic level to the extent that it passes DUS tests for registration as a commercial cultivar. While the proportion of parental genomes was relatively stable in subsequent generations of three commercial hybrids (Kopecký et al., 2008a), substantial variability was found within populations of each generation of those cultivars.

Besides those amphiploid (or allotetraploid) cultivars, introgression breeding may also be used to develop Festulolium cultivars. Doing this involves at least one round of backcrossing of F1 hybrids with one of the parental species (usually *Lolium*), giving rise to plants similar to the parental species but with improved characteristics, such as frost tolerance or higher survivorship (reviewed in Kopecký et al., 2008b). Karyologically, these plants usually carry only one or few chromosome segments of *Festuca*. Such introgression lines are usually highly unstable and the introgressed segment(s) is/are often lost in subsequent generations (Kopecký et al., 2019). Accordingly, implementing any system capable of preventing associations of homoeologous chromosomes is arguably desirable to stabilize the genomic composition of hybrids. In amphiploids, immediate introgression of the system would be required to keep both parental subgenomes intact. To date, most cultivars have originated from the cross of *L. multiflorum* × *F. pratensis*, though none of the parents carry a homoeologous suppressor. Instead, tetraploid wild relatives, such as *F. glaucescens*, *F. apennina* and *F. mairei*, which possess a meiotic regulator hampering homoeologous pairing, should be considered for future crosses as they are known for their tolerance to biotic and abiotic stress, which might complement the high yield and nutrition traits of ryegrasses. In this respects, first attempts have been made and the cultivar of *L. multiflorum* × *F. glaucescens 'Lueur'* was registered in France (Ghesquière et al., 2010) and other similar cross combinations are used in breeding programs in both the UK and Czech Republic. Considering the haplo-insufficiency of the system found in polyploid fescues, evidently the F1 hybrids will possess some level of homoeologous associations. Still, it should be possible to select F2 plants that have two copies of the gene(s) of the system and then intercross them. Doing this should facilitate the stabilization of the hybrid genome in successive generations. For the corresponding introgression lines, the segment carrying the gene(s) of the system must be present among the introgressions. Thereafter, haploidization, followed by either spontaneous or induced chromosome doubling, should result in the establishment of plants having two copies of such gene(s) required for its/their functionality as the homoeologous pairing suppressor(s). Clearly, though, further investigation of chromosome behavior in fescues is necessary if we hope to foster genetically stable grass hybrids.

We envisage that with more knowledge of the mechanisms responsible for correct chromosome associations, the efficient employment of targeted interspecific hybridization techniques will become available in the near future. Perhaps the most challenging task is the developing and operating of an "OFF" and "ON" switch to control recombination of homoeologous chromosomes. It would be immensely helpful for breeders to switch "OFF" the system in wheat and other allopolyploids with an established and functional regulatory system for introgressing the specific segment from a wild relative. Once the segment is transferred, the switch to "ON" would then stabilize the segment and permit its proper transmission into successive generations. Similarly, introgression of the system into a hybrid (originally lacking the regulator) with desirable combinations of parental chromatin would assist in further stabilizing the hybrid genome composition. To conclude, additional research broadening our knowledge of the mechanisms governing meiotic chromosome behavior in allopolyploids is necessary to ensure further success in future breeding of grass plants.

AUTHOR CONTRIBUTIONS

RS, PS, DK, and JB wrote the manuscript.

FUNDING

This work was supported by the Czech Science Foundation (grant award 17-05341S) and the ERDF project "Plants as a tool for sustainable global development" (CZ.02.1.01/0.0/0.0/16_019/0000827).

REFERENCES

Akhunov, E. D., Sehgal, S., Liang, H., Wang, S., Akhunova, A. R., Kaur, G., et al. (2013). Comparative analysis of syntenic genes in grass genomes reveals accelerated rates of gene structure and coding sequence evolution in polyploid wheat. *Plant Physiol.* 161, 252–265. doi: 10.1104/pp.112.205161

Al-Kaff, N., Knight, E., Bertin, I., Foote, T., Hart, N., Griffiths, S., et al. (2008). Detailed dissection of the chromosomal region containing the ph1 locus in wheat *Triticum aestivum*: with deletion mutants and expression profiling. *Ann. Bot.* 101, 863–872. doi: 10.1093/aob/mcm252

Aragón-Alcaide, L., Reader, S., Beven, A., Shaw, P., Miller, T., and Moore, G. (1997). Association of homologous chromosomes during floral development. *Curr. Biol.* 7, 905–908. doi: 10.1016/S0960-9822(06)00383-6

Attia, T., Ekingen, H., and Röbbelen, G. (1979). Origin of 3D-suppressor of homoeologous pairing in hexaploid wheat. *Z. Pflanzenzüchtg* 83, 121–126.

Aung, T., and Evans, G. M. (1985). The potential for diploidizing *Lolium multiflorum* × *L. perenne* tetraploids. *Can. J. Genet. Cytol.* 27, 506–509. doi: 10.1139/g85-075

Ayala-Navarrete, L.II, Mechanicos, A. A., Gibson, J. M., Singh, D., Bariana, H. S., Fletcher, J., et al. (2013). The Pontin series of recombinant alien translocations in bread wheat: single translocations integrating combinations of Bdv2, Lr19 and Sr25 disease-resistance genes from *Thinopyrum intermedium* and *Th. ponticum*. *Theor. Appl. Genet.* 126, 2467–2475. doi: 10.1007/s00122-013-2147-0

Balfourier, F., Bouchet, S., Robert, S., DeOliveira, R., Rimbert, H., Kitt, J., et al. (2019). Worldwide phylogeography and history of wheat genetic diversity. *Sci. Adv.* 5 (5), eaav0536. doi: 10.1126/sciadv.aav0536

Barker, M. S., Arrigo, N., Baniaga, A. E., Li, Z., and Levin, D. A. (2016). On the relative abundance of autopolyploids and allopolyploids. *New Phytol.* 210, 391–398. doi: 10.1111/nph.13698

Bass, H. W., Riera-Lizarazu, O., Ananiev, E. V., Bordolo, S. J., Rines, H. W., Phillips, R. L., et al. (2000). Evidence for the coincident initiation of homologue pairing and synapsis during the telomere clustering (bouquet) stage of meiotic prophase. *J. Cell Sci.* 113, 1033–1042.

Bass, H. W. (2003). Telomere dynamics unique to meiotic prophase: formation and significance of the bouquet. *Cell. Mol. Life Sci.* 60, 2319–2324. doi: 10.1007/s00018-003-3312-4

Baumel, A., Ainouche, M. L., and Levasseur, J. E. (2001). Molecular investigations in populations of *Spartina anglica* C.E. Hubbard (Poaceae) invading coastal Brittany (France). *Mol. Ecol.* 10, 1689–1701. doi: 10.1046/j.1365-294X.2001.01299.x

Benavente, E., Orellana, J., and Fernández-Calvín, B. (1998). Comparative analysis of the meiotic effects of wheat *ph1b* and *ph2b* mutations in wheat×rye hybrids. *Theor. Appl. Genet.* 96, 1200–1204. doi: 10.1007/s001220050857

Bhullar, R., Nagarajan, R., Bennypaul, H., Sidhu, G. K., Sidhu, G., Rustgi, S., et al. (2014). Silencing of a metaphase I-specific gene results in a phenotype similar to that of the pairing homeologous 1 (Ph1) gene mutations. *Proc. Natl. Acad. Sci. U.S.A.* 111, 14187–14192. doi: 10.1073/pnas.1416241111

Boden, S. A., Langridge, P., Spangenberg, G., and Able, J. A. (2009). TaASY1 promotes homologous chromosome interactions and is affected by deletion of Ph1. *Plant J.* 57, 487–497. doi: 10.1111/j.1365-313X.2008.03701.x

Brown, W. V., and Stack, S. M. (1968). Somatic pairing as a regular preliminary to meiosis. *Bull. Torrey Bot. Club* 95, 369–378. doi: 10.2307/2483872

Cai, D. T., Chen, D. L., Chen, J. G., and Liu, Y. Q. (2004). A method of induction polyploidy rice with high frequency through tissue culture together with chemical agent induction. China Patent: ZL01133529.7.

Cai, D. T., Chen, J., Chen, D., Dai, B. C., Song, Z. J., Yang, Z. F., et al. (2007). The breeding of two polyploid rice lines with the characteristic of polyploid meiosis stability. *Sci. China Ser. C.* 50, 356–366. doi: 10.1007/s11427-007-0049-6

Calderón, M. C., Rey, M. D., Martín, A., and Prieto, P. (2018). Homoeologous Chromosomes From Two Hordeum Species Can Recognize and Associate During Meiosis in Wheat in the Presence of the *Ph1* Locus. *Front. Plant Sci.* 9, 585. doi: 10.3389/fpls.2018.00585

Carvalho, A., Delgado, M., Barão, A., Frescatada, M., Ribeiro, E., Pikaard, C. S., et al. (2010). Chromosome and DNA methylation dynamics during meiosis in the autotetraploid *Arabidopsis arenosa*. *Sex Plant Reprod.* 23, 29–37. doi: 10.1007/s00497-009-0115-2

Catalán, P., and Olmstead, R. G. (2000). Phylogenetic reconstruction of the genus *Brachypodium* P. Beauv. (*Poaceae*) from combined sequences of chloroplast *ndhF* gene and nuclear ITS. Pl. *Syst. Evol.* 220, 1–19. doi: 10.1007/BF00985367

Chelysheva, L., Gendrot, G., Vezon, D., Doutriaux, M. P., Mercier, R., and Grelon, M. (2007). *Zip4*/*Spo22* is required for class I CO formation but not for synapsis completion in *Arabidopsis thaliana*. *PloS Genet.* 3, e83. doi: 10.1371/journal.pgen.0030083

Clausen, J., Keck, D. D., and Hiesey, W. M. (1945). *Experimental studies on the nature of species, II. Plant evolution through amphiploidy and autopolyploidy, with examples from the Madiinae* (Washington, DC.: Carnegie Institute of Washington).

Comai, L. (2005). The advantages and disadvantages of being polyploid. *Nat. Rev. Genet.* 6, 836–846. doi: 10.1038/nrg1711

Comings, D. E. (1968). The rational for an ordered arrangement of chromatin in the prophase nucleus. *Am. J. Hum. Genet.* 20, 440–460.

Crow, J. F. (1994). Hitoshi Kihara, Japan's pioneer geneticist. *Genetics* 137, 891–894.

Dawe, R. K. (1998). Meiotic chromosome organization and segregation in plants. *Ann. Rev. Plant Physiol. Plant Mol. Biol.* 49, 371–395. doi: 10.1146/annurev.arplant.49.1.371

De Storme, N., Copenhaver, G. P., and Geelen, D. (2012). Production of diploid male gametes in *Arabidopsis* by cold-induced destabilization of postmeiotic radial microtubule arrays. *Plant Physiol.* 160, 1808–1826. doi: 10.1104/pp.112.208611

Dong, C., Whitford, R., and Langridge, P. (2002). A DNA mismatch repair gene links to the *Ph2* locus in wheat. *Genome* 45, 116–124. doi: 10.1139/g01-126

Dover, G. A., and Riley, R. (1972). Prevention of pairing of homoeologous meiotic chromosomes of wheat by an activity of supernumerary chromosomes of *Aegilops*. *Nature* 240, 159–161. doi: 10.1038/240159a0

Driscoll, C. J. (1972). Genetic suppression of homoeologous chromosome pairing in hexaploid wheat. *Can. J. Genet. Cytol.* 14 (1), 39–42. doi: 10.1139/g72-004

Dubcovsky, J., and Dvorak, J. (2007). Genome plasticity a key factor in the success of polyploid wheat under domestication. *Science* 316, 1862–1866. doi: 10.1126/science.1143986

Dvorak, J., Chen, K. C., and Giorgi, B. (1984). The C-banding pattern of a Ph-mutant of durum wheat. *Can. J. Genet. Cytol.* 26, 360–363. doi: 10.1139/g84-056

Dvorak, J., Akhunov, E. D., Akhunov, A. R., Deal, K. R., and Luo, M. C. (2006a). Molecular characterization of a diagnostic DNA marker for domesticated tetraploid wheat provides evidence for gene flow from wild tetraploid wheat to hexaploid wheat. *Mol. Biol. Evol.* 23, 1386–1396. doi: 10.1093/molbev/msl004

Dvorak, J., Deal, K. R., and Luo, M. C. (2006b). Discovery and mapping of wheat Ph1 suppressors. *Genetics* 174, 17–27. doi: 10.1534/genetics.106.058115

Dvorak, J. (1987). Chromosomal distribution of genes in diploid *Elytrigia elongata* that promote or suppress pairing of wheat homoeologous chromosomes. *Genome* 29, 34–40. doi: 10.1139/g87-006

Eber, F., Chèvre, A. M., Baranger, A., Vallée, P., Tanguy, X., and Renard, M. (1994). Spontaneous hybridization between a male-sterile oilseed rape and two weeds. *Theor. Appl. Genet.* 88, 362–368. doi: 10.1007/BF00223646

Ehrendorfer, F. (1980). ""Polyploidy and Distribution,"," in *Polyploidy. Basic Life Sciences*, vol. 13 . Ed. W. H. Lewis (Boston, MA: Springer), 45–60. doi: 10.1007/978-1-4613-3069-1_3

Eilam, T., Anikster, Y., Millet, E., Manisterski, J., and Feldman, M. (2009). Genome size in natural and synthetic autopolyploids and in a natural segmental allopolyploid of several *Triticeae* species. *Genome* 52, 275–285. doi: 10.1139/G09-004

Eizenga, G. C., Burner, D. M., and Buckner, R. C. (1990). Meiotic and isozymic analyses of tall fescue × giant fescue hybrids and amphiploids. *Plant Breed.* 104, 202–211. doi: 10.1111/j.1439-0523.1990.tb00424.x

Evans, G. M., and Aung, T. (1985). Identification of a diploidizing genotype of *Lolium multiflorum*. *Can. J. Genet. Cytol.* 27, 498–505. doi: 10.1139/g85-074

Evans, G. M., and Aung, T. (1986). The influence of the genotype of *Lolium perenne* on homoeologous chromosome association in hexaploid *Festuca arundinacea*. *Heredity* 56, 97–103. doi: 10.1038/hdy.1986.13

Evans, G. M., and Macefield, A. J. (1972). Suppression of homoeologous pairing by B chromosomes in a *Lolium* species hybrid. *Nat. New Biol.* 236, 110–111. doi: 10.1038/newbio236110a0

Evans, G. M., and Macefield, A. J. (1973). The effect of B chromosomes on homoeologous pairing in species hybrids. *Chromosoma* 41, 63–73. doi: 10.1007/BF00284074

Ezquerro-López, D., Kopecký, D., and Aramendía, L. (2017). Cytogenetic relationships within the Maghrebian clade of *Festuca* subgen. *Schedonorus* (*Poaceae*), using flow cytometry and FISH. *Anales del Jardín Botánico Madrid* 74, 1. doi: 10.3989/ajbm.2455

Fan, C., Luo, J., Zhang, S., Liu, M., Li, Q., Li, Y., et al. (2019). Genetic mapping of a major QTL promoting homoeologous chromosome pairing in a wheat landrace. *Theor. Appl. Genet.* 132, 2155–2166. doi: 10.1007/s00122-019-03344-x

Feldman, M., and Levy, A. (2005). Allopolyploidy – a shaping force in the evolution of wheat genomes. *Cytogenet. Genome. Res.* 109, 250–258. doi: 10.1159/000082407

Feldman, M. (1966a). The effect of chromosomes 5B, 5D and 5A on chromosomal pairing in *Triticum aestivum*. *Proc. Natl. Acad. Sci. U.S.A.* 55, 1447–1453. doi: 10.1073/pnas.55.6.1447

Feldman, M. (1966b). The mechanism regulating pairing in *Triticum timopheevii*. *Wheat Inf. Serv.* 21, 1–2.

Fussell, C. P. (1987). "The Rabl orientation: a prelude to synapsis," in *Meiosis*. Ed. P. B. Moens (Orlando: Academic Press), 275–299.

Gallo, P. H., Micheletti, P. L., Boldrini, K. R., Risso-Pascotto, C., Pagliarini, M. S., and do Valle, C. B. (2007). 2n Gamete formation in the genus *Brachiaria* (*Poaceae: Paniceae*). *Euphytica* 154, 255–260. doi: 10.1007/s10681-006-9294-1

Gauthier, F. M., and McGuinnis, R. C. (1968). The meiotic behaviour of a nulli-haploid plant in *Avena sativa* L. *Can. J. Genet. Cytol.* 10, 186–189. doi: 10.1139/g68-025

Ghesquière, M., Humphreys, M. W., and Zwierzykowski, Z. (2010). ""Festulolium," in Fodder Crops and Amenity Grasses," in *Handbook of Plant Breeding*, vol. 5 . Eds. B. Boller, U. Posselt and F. Veronesi (New York, NY: Springer), 288–311. doi: 10.1007/978-1-4419-0760-8_12

Gill, K. S., Gill, B. S., Endo, T. R., and Mukai, Y. (1993). Fine physical mapping of *Ph1*, a chromosome pairing regulator gene in polyploid wheat. *Genetics* 134, 1231–1236.

Gonzalo, A., Lucas, M., Charpentier, C., Sandmann, G., Lloyd, A., and Jenczewski, E. (2019). Reducing *MSH4* copy number prevents meiotic crossovers between non-homologous chromosomes in *Brassica napus*. *Nat. Commun.* 10, 2354. doi: 10.1038/s41467-019-10010-9

Gray, A. J., Benham, P. E. M., and Raybould, A. F. (1990). ""Spartina anglica — the evolutionary and ecological background,"," in *Spartina anglica — A Research Review*. Eds. A. J. Gray and P. E. M. Benham (London, UK: Institute of Terrestrial Ecology, Natural Environment Research Council), 5–10.

Griffiths, S., Sharp, R., Foote, T. N., Bertin, I., Wanous, M., Reader, S., et al. (2006). Molecular characterization of *Ph1* as a major chromosome pairing locus in polyploid wheat. *Nature* 439, 749–752. doi: 10.1038/nature04434

Gupta, P. K., and Fedak, G. (1985). Genetic control of meiotic chromosome pairing in polyploids in the genus *Hordeum*. *Can. J. Genet. Cytol.* 27, 515– 530. doi: 10.1139/g85-077

Gyawali, Y., Zhang, W., Chao, S., Xu, S., and Cai, X. (2019). Delimitation of wheat *ph1b* deletion and development of *ph1b*-specific DNA markers. *Theor. Appl. Genet.* 132, 195–204. doi: 10.1007/s00122-018-3207-2

Ha, M., Lu, J., Tian, L., Ramachandran, V., Kasschau, K. D., and Chapman, E. J. (2009). Small RNAs serve as a genetic buffer against genomic shock in *Arabidopsis* interspecific hybrids and allopolyploids. *Proc. Natl. Acad. Sci. U.S.A.* 106, 17835–17840. doi: 10.1073/pnas.0907003106

Hajjar, R., and Hodgkin, T. (2007). The use of wild relatives in crop improvement: a survey of developments over the last 20 years. *Euphytica* 156, 1–13. doi: 10.1007/s10681-007-9363-0

Han, C., Zhang, P., Ryan, P. R., Rathjen, T. M., Yan, Z., and Delhaize, E. (2016). Introgression of genes from bread wheat enhances the aluminium tolerance of durum wheat. *Theor. Appl. Genet.* 129, 729–739. doi: 10.1007/s00122-015-2661-3

Hand, M. L., Cogan, N. O., Stewart, A. V., and Forster, J. W. (2010). Evolutionary history of tall fescue morphotypes inferred from molecular phylogenetics of the *Lolium-Festuca* species complex. *BMC Evol. Biol.* 10, 303. doi: 10.1186/1471-2148-10-303

Hao, M., Luo, J. T., Yang, M., Zhang, L. Q., Yan, Z. H., Yuan, Z. W., et al. (2011). Comparison of homoeologous chromosome pairing between hybrids of wheat genotypes Chinese Spring *ph1b* and Kaixian-luohanmai with rye. *Genome* 54, 959–964. doi: 10.1139/g11-062

Harper, L., Golubovskaya, I., and Cande, W. Z. (2004). A bouquet of chromosomes. *J. Cell Sci.* 117, 4025–4032. doi: 10.1242/jcs.01363

Holm, P. B., and Wang, X. (1988). The effect of chromosome 5B on synapsis and chiasma formation in wheat, *Triticum aestivum* cv. *Chin. spring. Carls. Res. Communs.* 53, 191–208. doi: 10.1007/BF02907179

Holm, P. B. (1986). Chromosome pairing and chiasma formation in allohexaploid wheat, *Triticum aestivum* analyzed by spreading of meiotic nuclei. *Carlsberg. Res. Commun.* 51, 239. doi: 10.1007/BF02906837

Huang, S., Sirikhachornkit, A., Su, X., Faris, J., Gill, B., Haselkorn, R., et al. (2002). Genes encoding plastid acetyl-CoA carboxylase and 3-phosphoglycerate kinase of the *Triticum*/*Aegilops* complex and the evolutionary history of polyploid wheat. *Proc. Natl. Acad. Sci. U.S.A.* 99, 8133–8138. doi: 10.1073/pnas.072223799

Hubbard, J. C. E. (1968). *Grasses. 2nd edn* (London: Penguin Books).

Humphreys, M. W., Thomas, H. M., Morgan, W. G., Meredith, M. R., Harper, J. A., Thomas, A., et al. (1995). Discriminating the ancestral progenitors of hexaploid *Festuca arundinacea* using genomic in situ hybridization. *Heredity* 75, 171–174. doi: 10.1038/hdy.1995.120

Husband, B. C. (2004). The role of triploid hybrids in the evolutionary dynamics of mixed-ploidy populations. *Biol. J. Linn. Soc* 82, 537–546. doi: 10.1111/j.1095-8312.2004.00339.x

Jacobs, B. F., Kingston, J. D., and Jacobs, L. L. (1999). The origin of grass-dominated ecosystems. *Ann. Mo. Bot. Gard.* 86, 590–643. doi: 10.2307/2666186

Jauhar, P. P., Almouslem, A. B., Peterson, T. S., and Joppa, L. R. (1999). Inter- and intra-genomic chromosome pairing in haploids of durum wheat. *J. Hered.* 90, 437–445. doi: 10.1093/jhered/90.4.437

Jauhar, P. P. (1975). Genetic regulation of diploid-like chromosome pairing in the hexaploid species, *Festuca arundinacea* Schreb. and *F. rubra* L. (*Gramineae*). *Chromosoma* 52, 363–382. doi: 10.1007/BF00364020

Jauhar, P. P. (1977). Genetic regulation of diploid-like chromosome pairing in *Avena*. *Theor. Appl. Genet.* 49, 287–295. doi: 10.1007/BF00275135

Jauhar, P. P. (1993). *Cytogenetics of the Festuca-Lolium complex: relevance to breeding* (Berlin: Springer).

Jauhar, P. P. (2003). Formation of 2n gametes in durum wheat haploids: sexual polyploidization. *Euphytica* 133, 81–94. doi: 10.1023/A:1025692422665

Jenczewski, E., and Alix, K. (2004). From diploids to allopolyploids: the emergence of efficient pairing control genes in plants. *Crit. Rev. Plant Sci.* 23, 21–45. doi: 10.1080/07352680490273239

Jeon, J., Chung, Y., Lee, S., Yi, G., Oh, B., and An, G. (1999). Isolation and characterization of an anther-specific gene, RA8, from rice (*Oryza sativa* L.). *Plant Mol. Biol.* 39, 35–44. doi: 10.1023/A:1006157603096

Ji, L., and Langridge, P. (1994). An early meiosis cDNA clone from wheat. *Molec. Gen. Genet.* 243, 17–23. doi: 10.1007/BF00283871

Jiao, Y., Wickett, N., Ayyampalayam, S., Chanderbali, A. S., Landherr, L., Ralph, P. E., et al. (2011). Ancestral polyploidy in seed plants and angiosperms. *Nature* 473, 97–100. doi: 10.1038/nature09916

Kang, H. Y., Zhang, H. Q., Wang, Y., Jiang, Y., Yuan, H. J., and Zhou, Y. H. (2008). Comparative analysis of the homoeologous pairing effects of *phKL* gene in common wheat × *Psathyrostachys huashanica*. *Keng Cereal Res. Commun.* 36, 429–440. doi: 10.1556/CRC.36.2008.3.7

Keeler, K. H., and Davis, G. A. (1999). Comparison of common cytotypes of *Andropogon gerardii* (*Andropogoneae*: Poaceae). *Am. J. Bot.* 86, 974–979. doi: 10.2307/2656614

Keeler, K. H. (1998). "Population biology of intraspecific polyploidy in grasses," in *Population Biology of Grasses*. Ed. G. P. Cheplick (Cambridge, UK: Cambridge University Press), 183–206.

Kellogg, E. A. (2001). Evolutionary history of the grasses. *Plant Physiol.* 125, 1198–1205. doi: 10.1104/pp.125.3.1198

King, J., Grewal, S., Yang, C. Y., Hubbart, S., Scholefield, D., Ashling, S., et al. (2016). A step change in the transfer of interspecific variation into wheat from *Amblyopyrum muticum*. *Plant Biotech. J.* 15, 217–226. doi: 10.1111/pbi.1206

King, J., Newell, C., Grewal, S., Hubbart-Edwards, S., Yang, C. Y., Scholefield, D., et al. (2019). Development of stable homozygous wheat/*Amblyopyrum muticum* (*Aegilops mutica*) introgression lines and their cytogenetic and molecular characterization. *Front. Plant Sci.* 10, 34. doi: 10.3389/fpls.2019.00034

Kleijer, G., and Morel, P. (1984). Cytogenetic studies of crosses between *Lolium multiflorum* Lam. and *Festuca arundinacea* Schreb. II. The amphidiploids. *Z. Pflanzenzücht* 93, 23–42.

Koo, D., Liu, W., Friebe, B., and Gill, B. S. (2016). Homoeologous recombination in the presence of *Ph1* gene in wheat. *Chromosoma* 126, 531–540. doi: 10.1007/s00412-016-0622-5

Kopecký, D., Loureiro, J., Zwierzykowski, Z., Ghesquière, M., and Doležel, J. (2006). Genome constitution and evolution in *Lolium* × *Festuca* hybrid cultivars (Festulolium). *Theor. Appl. Genet.* 113, 731–742. doi: 10.1007/s00122-006-0341-z

Kopecký, D., Lukaszewski, A. J., and Doležel, J. (2008a). Meiotic behaviour of individual chromosomes of *Festuca pratensis* in tetraploid *Lolium multiflorum*. *Chromosome Res.* 16, 987. doi: 10.1007/s10577-008-1256-0

Kopecký, D., Lukaszewski, A. J., and Doležel, J. (2008b). Cytogenetics of Festulolium (*Festuca* x *Lolium* hybrids). *Cytogenet. Genome Res.* 120, 370–383. doi: 10.1159/000121086

Kopecký, D., Bartoš, J., Zwierzykowski, Z., and Doležel, J. (2009). Chromosome pairing of individual genomes in tall fescue (*Festuca arundinacea* Schreb.), its progenitors, and hybrids with Italian ryegrass (*Lolium multiflorum* Lam.). *Cytogenet. Genome Res.* 124, 170–178. doi: 10.1159/000207525

Kopecký, D., Talukder, S. K., Zwyrtková, J., Trammell, M., Doležel, J., and Saha, M. C. (2019). Inter-morphotype hybridization in tall fescue (*Festuca arundinacea* Schreb.): exploration of meiotic irregularities and potential for breeding. *Euphytica* 215, 97. doi: 10.1007/s10681-019-2419-0

Kreiner, J. M., Kron, P., and Husband, B. C. (2017). Evolutionary dynamics of unreduced gametes. *Trends Genet.* 33, 583–593. doi: 10.1016/j.tig.2017.06.009

Ladizinsky, G. (1973). Genetic control of bivalent pairing in the *Avena strigosa* polyploid complex. *Chromosoma* 42, 105–110. doi: 10.1007/BF00326334

Leggett, J. M., and Thomas, H. (1995). "Oat evolution and cytogenetics," in *The Oat Crop. World Crop Series*. Ed. R. W. Welch (Dordrecht, DE: Springer), 120–149. doi: 10.1007/978-94-011-0015-1_5

Li, H., Deal, K. R., Luo, M. C., Ji, W., Distelfeld, A., and Dvorak, J. (2017). Introgression of the *Aegilops speltoides Su1-Ph1* Suppressor into Wheat. *Front. Plant Sci.* 8, 2163. doi: 10.3389/fpls.2017.02163

Liu, D. C., Luo, M. C., Yang, J. L., Yen, C., Lan, X. J., and Yang, W. Y. (1997). Chromosome location of a new paring promoter in natural populations of common wheat. *Xi Nan Nong Ye Xue Bao* 10, 10–15. (in Chinese).

Liu, D. C., Luo, M. C., Yen, C., Yang, J. L., and Yang, W. Y. (1998). "The promotion of homoeologous pairing in hybrids of common wheat cv. Kaixianluohanmai with alien species," in *Proceedings of the 9th International Wheat Genetics Symposium*, vol. 4 . Ed. A. E. Slinkard (Saskatoon, CA: University Extension Press, University of Saskatchewan), 377–378.

Liu, D. C., Zheng, Y. L., Yan, Z. H., Zhou, Y. H., Wei, Y. M., and Lan, X. J. (2003). Combination of homoeologous pairing gene *phKL* and *Ph2*-deficiency in common wheat and its meiotic behaviors in hybrids with alien species. *Acta Bot. Sin.* 45, 1121–1128.

Liu, W., Rouse, M., Friebe, B., Jin, Y., Gill, B. S., and Pumphrey, M. O. (2011). Discovery and molecular mapping of a new gene conferring resistance to stem rust, *Sr53*, derived from *Aegilops geniculata* and characterization of spontaneous translocation stocks with reduced alien chromatin. *Chromosom Res.* 19, 669–682. doi: 10.1007/s10577-011-9226-3

Lloyd, A., and Bomblies, K. (2016). Meiosis in autopolyploid and allopolyploid *Arabidopsis*. *Curr. Opin. Plant Biol.* 30, 116–122. doi: 10.1016/j.pbi.2016.02.004

Lloyd, A., Ranoux, M., Vautrin, S., Glover, N. M., Fourment, J., Charif, D., et al. (2014). Meiotic gene evolution: can you teach a new dog new tricks? *Mol. Biol. Evol.* 31, 1724–1727. doi: 10.1093/molbev/msu119

Loidl, J. (1990). The initiation of meiotic chromosome pairing: the cytological view. *Genome* 33, 759–778. doi: 10.1139/g90-115

Loureiro, J., Kopecký, D., Castro, S., Santos, C., and Silveira, P. (2007). Flow cytometric and cytogenetic analyses of Iberian Peninsula *Festuca* spp. *Plant Syst. Evol.* 269, 89–105. doi: 10.1007/s00606-007-0564-8

Lukaszewski, A. J., and Kopecký, D. (2010). The *ph1* locus from wheat controls meiotic chromosome pairing in autotetraploid rye (*Secale cereale* L.). *Cytogenet. Genome Res.* 129, 117–123. doi: 10.1159/000314279

Luo, M. C., Yang, Z. L., Yen, C., and Yang, J. L. (1992). ""The cytogenetic investigation on F1 hybrid of Chinese wheat landrace,"," in *Exploration of Crop Breeding*. Eds. Z. L. Ren and J. H. Peng (Sichuan: Science and Technology Press), 169–176.

Maestra, B., and Naranjo, T. (1997). Homoeologous relationships of *Triticum sharonense* chromosomes to *T. aestivum*. *Theor. Appl. Genet.* 94, 657–663. doi: 10.1007/s001220050463

Maestra, B., and Naranjo, T. (1998). Homoeologous relationships of *Aegilops speltoides* chromosomes to bread wheat. *Theor. Appl. Genet.* 97, 181–186. doi: 10.1007/s001220050883

Malik, C. P., and Thomas, P. T. (1967). Cytological relationships and genome structure of some *Festuca* species. *Caryologia* 20, 1–39. doi: 10.1080/00087114.1967.10796244

Marais, G. F., Marais, A. S., Eksteen, A., and Pretorius, Z. A. (2010). Modification of the *Aegilops neglecta*-common wheat *Lr62*/*Yr42* translocation through allosyndetic pairing induction. *Crop Sci.* 49, 871–879. doi: 10.2135/cropsci2008.06.0317

Marcussen, T., Sandve, S. R., Heier, L., Spannagl, M., Pfeifer, M.IWGSC (2014). Ancient hybridizations among the ancestral genomes of bread wheat. *Science* 345, 6194. doi: 10.1126/science.1250092

Marques, A. M., Tuler, A. C., Carvalho, C. R., Carrijo, T. T., Ferreira, M. F., and Clarindo, W. R. (2016). Refinement of the karyological aspects of *Psidium guineense* (Swartz 1788): a comparison with *Psidium guajava* (Linnaeus 1753). *Comp. Cytogenet.* 10, 117–128. doi: 10.3897/CompCytogen.v10i1.6462

Martín, A. C., Shaw, P., Phillips, D., Reader, S., and Moore, G. (2014). Licensing *MLH1* sites for crossover during meiosis. *Nat. Commun.* 5, 1–5. doi: 10.1038/ncomms5580

Martín, A. C., Rey, M. D., Shaw, P., and Moore, G. (2017). Dual effect of the wheat *Ph1* locus on chromosome synapsis and crossover. *Chromosoma* 126, 669–680. doi: 10.1007/s00412-017-0630-0

Martínez, M., Cuñado, N., Carcelén, N., and Romero, C. (2001a). The *Ph1* and *Ph2* loci play different roles in the synaptic behaviour of hexaploid wheat *Triticum aestivum*. *Theor. Appl. Genet.* 103, 398–405. doi: 10.1007/s00122-001-0543-3

Martínez, M., Naranjo, T., Cuadrado, C., and Romero, C. (2001b). The synaptic behaviour of *Triticum turgidum* with variable doses of the *Ph1* locus. *Theor. Appl. Genet.* 102, 751–758. doi: 10.1007/s001220051706

Martínez-Pérez, E., Shaw, P., Reader, S., Aragón-Alcaide, L., Miller, T., Moore, G., et al. (1999). Homologous chromosome pairing in wheat. *J. Cell Sci.* 112, 1761–1769.

Mason, A. S., and Pires, J. C. (2015). Unreduced gametes: meiotic mishap or evolutionary mechanism? *Trends Genet.* 31, 5–10. doi: 10.1016/j.tig.2014.09.011

Mason, A. S., Nelson, M. N., Yan, G., and Cowling, W. A. (2011). Production of viable male unreduced gametes in *Brassica* interspecific hybrids is genotype specific and stimulated by cold temperatures. *BMC Plant Biol.* 11:, 103. doi: 10.1186/1471-2229-11-103

McGuire, P. E., and Dvořák, J. (1982). Genetic regulation of heterogenetic chromosome pairing in polyploid species of the genus Triticum sensu lato. *Can. J. Genet. Cytol.* 24, 57–82. doi: 10.1139/g82-007

Meister, N., and Tjumjakoff, N. A. (1928). Rye–wheat hybrids from reciprocal crosses. *J. Genet.* 20, 233–245. doi: 10.1007/BF02983142

Mello-Sampayo, T., and Canas, A. P. (1973). "Suppression of meiotic chromosome pairing in common wheat," in *Proceedings of the 4th International Wheat Genetics Symposium*. Eds. E. R. Sears and L. M. S. ER (Columbia, MI: Agricultural Experiment Station, College of Agriculture, University of Missouri), 703–713.

Mello-Sampayo, T. (1968). ""Homoeologous chromosome pairing in pentaploid hybrids of wheat,"," in *Third International Wheat Genetics Symposium*. Eds. K. W. Finlay and K. W. Shepherd (Canberra: Butterworth & Company), 179–184.

Mello-Sampayo, T. (1971). Genetic regulation of meiotic chromosome pairing by chromosome-3D of *Triticum aestivum*. *Nat. New Biol.* 230, 22. doi: 10.1038/newbio230022a0

Meyers, L. A., and Levin, D. A. (2006). On the abundance of polyploids in flowering plants. *Evolution* 60, 1198–1206. doi: 10.1111/j.0014-3820.2006.tb01198.x

Mikhailova, E. I., Naranjo, T., Shepherd, K., Wennekes-van, E. J., Heyting, C., and de Jong, H. (1998). The effect of the wheat *Ph1* locus on chromatin organisation and meiotic pairing analysed by genome painting. *Chromosoma* 107, 339–350. doi: 10.1007/s004120050316

Murat, F., Zhang, R., Guizard, S., Flores, R., Armero, A., Pont, C., et al. (2014). Shared subgenome dominance following polyploidization explains grass genome evolutionary plasticity from a seven protochromosome ancestor with 16K protogenes. *Genome Biol. Evol.* 6, 12–33. doi: 10.1093/gbe/evt200

Murray, B. G., Sieber, V. K., and Jackson, R. C. (1984). Further evidence for the presence of meiotic pairing control genes in *Alopecurus* L. *(Gramineae)*. *Genet.* 63, 13–20. doi: 10.1007/BF00137460

Naranjo, T., and Maestra, B. (1995). The effect of ph mutations on homoeologous pairing in hybrids of wheat with *Triticum longissimum*. *Theor. Appl. Genet.* 91, 1265–1270. doi: 10.1007/BF00220939

Naranjo, T., Roca, A., Goicoechea, P. G., and Giráldez, R. (1987). Arm homoeology of wheat and rye chromosomes. *Genome* 29, 873–882. doi: 10.1139/g87-149

Naranjo, T., Roca, A., Goicoechea, P. G., and Giráldez, R. (1988). "Chromosome structure of common wheat: genome reassignment of chromosomes 4A and 4B," in *Proceedings of the 7th International Wheat Genetics Symposium, eds*. Eds. T. E. Miller and R. M. D. Koebner (Cambridge, UK: Cambridge University), 115–120.

Naranjo, T. (2015). Contribution of Structural Chromosome Mutants to the Study of Meiosis in Plants. *Cytogenet. Genome Res.* 147, 55–69. doi: 10.1159/000442219

Naranjo, T. (2019). The effect of chromosome structure upon meiotic homologous and homoeologous recombinations in *Triticeae*. *Agronomy* 9, 552. doi: 10.3390/agronomy9090552

Niu, Z., Klindworth, D. L., Friesen, T. L., Chao, S., Jin, Y., Cai, X., et al. (2011). Targeted introgression of a wheat stem rust resistance gene by DNA marker-assisted chromosome engineering. *Genetics* 187, 1011–1021. doi: 10.1534/genetics.110.123588

Ortega, S., Prieto, I., Odajima, J., Martín, A., Dubus, P., Sotillo, R., et al. (2003). Cyclin-dependent kinase 2 is essential for meiosis but not for mitotic cell division in mice. *Nat. Genet.* 35, 25–31. doi: 10.1038/ng1232

Osborn, T. C., Pires, J. C., Birchler, J. A., Auger, D. L., Chen, Z. J., Lee, H. S., et al. (2003). Understanding mechanisms of novel gene expression in polyploids. *Trends Genet.* 19, 141–147. doi: 10.1016/S0168-9525(03)00015-5

Otto, S. P., and Whitton, J. (2000). Polyploid incidence and evolution. *Annu. Rev. Genet.* 34, 401–437. doi: 10.1146/annurev.genet.34.1.401

Ozkan, H., and Feldman, M. (2001). Genotypic variation in tetraploid wheat affecting homoeologous pairing in hybrids with *Aegilops peregrina*. *Genome* 44, 1000–1006. doi: 10.1139/g01-100

Pécrix, Y., Rallo, G., Folzer, H., Cigna, M., Gudin, S., and Le Bris, M. (2011). Polyploidization mechanisms: temperature environment can induce diploid gamete formation in *Rosa* sp. *J. Exp. Bot.* 62, 3587–3597. doi: 10.1093/jxb/err052

Pecinka, A., Fang, W., Rehmsmeier, M., Levy, A. A., and Scheid, O. M. (2011). Polyploidization increases meiotic recombination frequency in *Arabidopsis*. *BMC Biol.* 9, 24. doi: 10.1186/1741-7007-9-24

Pelé, A., Rousseau-Gueutin, M., and Chèvre, A. M. (2018). Speciation success of polyploid plants closely relates to the regulation of meiotic recombination. *Front. Plant Sci.* 9, 907. doi: 10.3389/fpls.2018.00907

Pernickova, K., Linc, G., Gaal, E., Kopecký, D., Šamajová, O., and Lukaszewski, A. (2019). Out-of-position telomeres in meiotic leptotene appear responsible for chiasmate pairing in an inversion heterozygote in wheat (*Triticum aestivum* L.). *Chromosoma* 128, 31–39. doi: 10.1007/s00412-018-0686-5

Petersen, G., Seberg, O., Yde, M., and Berthelsen, K. (2006). Phylogenetic relationships of *Triticum* and *Aegilops* and evidence for the origin of the A, B, and D genomes of common wheat (*Triticum aestivum*). *Mol. Phylogenet. Evol.* 39, 70–82. doi: 10.1016/j.ympev.2006.01.023

Prieto, P., Moore, G., and Reader, S. (2005). Control of conformation changes associated with homologue recognition during meiosis. *Theor. Appl. Genet.* 111, 505–510. doi: 10.1007/s00122-005-2040-6

Ramsey, J., and Schemske, D. W. (1998). Pathways, mechanisms, and rates of polyploid formation in flowering plants. *Annu. Rev. Ecol. Syst.* 29, 467–501. doi: 10.1146/annurev.ecolsys.29.1.467

Ramsey, J., and Schemske, D. W. (2002). Neopolyploidy in flowering plants. *Annu. Rev. Ecol. Syst.* 33, 589–639. doi: 10.1146/annurev.ecolsys.33.010802.150437

Renny-Byfield, S., Rodgers-Melnick, E., and Ross-Ibara, J. (2017). Gene fractionation and function in the ancient subgenomes of maize. *Mol. Biol. Evol.* 34, 1825–1832. doi: 10.1093/molbev/msx121

Rey, M. D., Calderón, M. C., and Prieto, P. (2015a). The use of the *ph1b* mutant to induce recombination between the chromosomes of wheat and barley. *Front. Plant Sci.* 6, 160. doi: 10.3389/fpls.2015.00160

Rey, M. D., Calderón, M. C., Rodrigo, M. J., Zacarías, L., Alós, E., and Prieto, P. (2015b). Novel Bread Wheat Lines Enriched in Carotenoids Carrying Hordeum chilense Chromosome Arms in the *ph1b* Background. *PloS One* 10 (8), e0134598. doi: 10.1371/journal.pone.0134598

Rey, M., Martín, A. C., Higgins, J., Swarbreck, D., Uauy, C., Shaw, P., et al. (2017). Exploiting the *ZIP4* homologue within the wheat *Ph1* locus has identified two lines exhibiting homoeologous crossover in wheat-wild relative hybrids. *Mol. Breed.* 37, 95. doi: 10.1007/s11032-017-0700-2

Rey, M. D., Martin, A. C., Smedley, M., Hayta, S., Harwood, W., Shaw, P., et al. (2018). Magnesium increases homoeologous crossover frequency during meiosis in *ZIP4* (*Ph1* gene) mutant wheat-wild relative hybrids. *Front. Plant Sci.* 9, 509. doi: 10.3389/fpls.2018.00509

Riley, R., and Chapman, V. (1958). Genetic control of the cytologically diploid behavior of hexaploid wheat. *Nature* 182, 713–715. . doi: 10.1038/182713a0

Riley, R., and Kempanna, C. (1963). The homoeologous nature of the non-homologous meiotic pairing in *Triticum aestivum* deficient for chromosome V. *Heredity* 18, 287–306. doi: 10.1038/hdy.1963.31

Riley, R., and Law, C. N. (1965). Genetic variation in chromosome pairing. *Adv. Genet.* 13, 57–114. doi: 10.1016/S0065-2660(08)60047-4

Riley, R., Chapman, V., and Miller, T. E. (1973). "The determination of meiotic chromosome pairing," in *Proceedings of the 4th International Wheat Genetics Symposium*. Eds. E. R. Sears and L. M. S. ER (Columbia, MI: Agricultural Experiment Station, College of Agriculture, University of Missouri), 731–738.

Riley, R. (1960). The diploidization of polyploid wheat. *Heredity* 15, 407–429. doi: 10.1038/hdy.1960.106

Roberts, M. A., Reader, S. M., Dalgliesh, C., Miller, T. E., Foote, T. N., Fish, L. J., et al. (1999). Induction and characterisation of the *Ph1* wheat mutants. *Genetics* 153, 1909–1918.

Salmon, A., Ainouche, M. L., and Wendel, J. F. (2005). Genetic and epigenetic consequences of recent hybridization and polyploidy in *Spartina* (Poaceae). *Mol. Ecol.* 14, 1163–1175. doi: 10.1111/j.1365-294X.2005.02488.x

Sánchez-Morán, E., Benavente, E., and Orellana, J. (2001). Analysis of karyotypic stability of homoeologous-pairing (*ph*) mutants in allopolyploid wheats. *Chromosoma* 110, 371–377 (2001). doi: 10.1007/s004120100156

Sattler, M. C., Carvalho, C. R., and Clarindo, W. R. (2016). The polyploidy and its key role in plant breeding. *Planta* 243, 281–296. doi: 10.1007/s00425-015-2450-x

Scherthan, H. (2001). A bouquet makes ends meet. *Nat. Rev. Mol. Cell Biol.* 2, 621–627. doi: 10.1038/35085086

Scherthan, H. (2007). Telomere attachment and clustering during meiosis. *Cell Mol. Life Sci.* 64, 117–124. doi: 10.1007/s00018-006-6463-2

Schwarzacher, T. (1997). Three stages of meiotic homologous chromosome pairing in wheat: cognition, alignment and synapsis. *Sex- Plant Reprod.* 10, 324–331. doi: 10.1007/s004970050106

Sears, E. R., and Okamoto, M. (1958). "Intergenomic chromosome relationship in hexaploid wheat," in *Proceedings of 10th International Congress of Genetics* (Toronto, CA: University of Toronto Press), 258–259.

Sears, E. R. (1976). Genetic control of chromosome pairing in wheat. *Annu. Rev. Genet.* 10, 31–51. doi: 10.1146/annurev.ge.10.120176.000335

Sears, E. R. (1977). An induced mutant with homoeologous pairing in common wheat. *Can. J. Genet. Cytol.* 19, 585–593. doi: 10.1139/g77-063

Sears, E. R. (1982). A wheat mutation conditioning an intermediate level of homoeologous chromosome pairing. *Can. J. Genet. Cytol.* 24, 715–719. doi: 10.1139/g82-076

Sears, E. R. (1984). "Mutations in wheat that raise the level of meiotic chromosome pairing," in *Gene Manipulation in Plant Improvement. Proc. 16th Stadler Genet. Symp*. Ed. J. P. Gustafson (New York, NY: Plenum Press), 295–300.

Shang, X. M., Jackson, R. C., NGuyen, H. T., and Huang, H. T. (1989). Chromosome pairing in the *Triticum monococcum* complex: evidence for pairing control genes. *Genome* 32, 213–226. doi: 10.1139/g89-432

Shen, Y., Tang, D., Wang, K., Wang, M., Huang, J., Luo, W., et al. (2012). *ZIP4* in homologous chromosome synapsis and crossover formation in rice meiosis. *J. Cell Sci.* 125, 2581–2591. doi: 10.1242/jcs.090993

Soltis, D. E., Soltis, P. S., Schemske, D. W., Hancock, J. F., Thompson, J. N., Husband, B. C., et al. (2007). Autopolyploidy in angiosperms: have we grossly underestimated the number of species? *Taxon* 56, 13–30. doi: 10.2307/25065732

Soreng, R. J., Peterson, P. M., Romaschenko, K., Davidse, G., Zuloaga, F. O., Judziewicz, E. J., et al. (2015). A worldwide phylogenetic classification of the Poaceae (Gramineae). *J. Syst. Evol.* 53, 117–137. doi: 10.1111/jse.12150

Stebbins, G. L. (1950). *Variation and Evolution in Plants* (New York: Columbia University Press).

Stebbins, G. L. (1971). *Chromosomal Evolution in Higher Plants* (London: Addison-Wesley).

Sun, Y., Wu, Y., Yang, C., Sun, S., Lin, X., Liu, L., et al. (2017). Segmental allotetraploidy generates extensive homoeologous expression rewiring and

phenotypic diversity at the population level in rice. *Mol. Ecol.* 26, 5451–5466. doi: 10.1111/mec.14297

Sutton, T., Whitford, R., Baumann, U., Dong, C. M., Able, J. A., and Langridge, P. (2003). The *Ph2* pairing homoeologous locus of wheat (*Triticum aestivum*): identification of candidate meiotic genes using a comparative genetics approach. *Plant J.* 36, 443–456. doi: 10.1046/j.1365-313X.2003.01891.x

Svačina, R., Karafiátová, M., Malurová, M., Serra, H., Vítek, D., Endo, T. R., et al. (2020). Development of deletion lines for chromosome 3D of bread wheat. *Front. Plant Sci.* 10, 1756. doi: 10.3389/fpls.2019.01756

Tamayo-Ordóñez, M. C., Espinosa-Barrera, L. A., Tamayo-Ordóñez, Y. J., Ayil-Gutiérrez, B., and Sánchez-Teyer, L. F. (2016). Advances and perspectives in the generation of polyploid plant species. *Euphytica* 209, 1–22. doi: 10.1007/s10681-016-1646-x

Thomas, H. M., Morgan, W. G., Meredith, M. R., Humphreys, M. W., and Leggett, J. M. (1994). Identification of parental and recombined chromosomes in hybrid derivatives of *Lolium multiflorum* × *Festuca pratensis* by genomic in situ hybridization. *Theor. Appl. Genet.* 88, 909–913. doi: 10.1007/BF00220795

Thomas, H. (1992). "Cytogenetics of Avena," in *Oat Science and Technology. Monograph 33, Agronomy Series*. Eds. H. G. Marshall and M. E. Sorrells (Madison, WI: ASA and CSSA), 473–507.

Thomas, S. W. (1997). Molecular studies of homologous chromosome pairing in *Triticum aestivum*. [dissertation]. [Adelaide]: University of Adelaide.

Thompson, J. D., McNeilly, T., and Gray, A. J. (1991). Population variation in *Spartina anglica* C.E. Hubbard. I. Evidence from a common garden experiment. *New Phytol.* 117, 115–128. doi: 10.1111/j.1469-8137.1991.tb00951.x

Van de Peer, Y., Maere, S., and Meyer, A. (2009). The evolutionary significance of ancient genome duplications. *Nat. Rev. Genet.* 10, 725–732. doi: 10.1038/nrg2600

Van de Peer, Y., Mizrachi, E., and Marchal, K. (2017). The evolutionary significance of polyploidy. *Nat. Rev. Genet.* 18, 411–424. doi: 10.1038/nrg.2017.26

Vanneste, K., Baele, G., Maere, S., and Van de Peer, Y. (2014). Analysis of 41 plant genomes supports a wave of successful genome duplications in association with the Cretaceous–Paleogene boundary. *Genome Res.* 24, 1334–1347. doi: 10.1101/gr.168997.113

Viegas, W. S., Mello-Sampayo, T., Feldman, M., and Avivi, L. (1980). Reduction of chromosome pairing by a spontaneous mutation on chromosomal arm 5DL of *Triticum aestivum*. *Can. J. Genet. Cytol.* 22, 569–575. doi: 10.1139/g80-062

Viera, A., Rufas, J. S., Martinez, I., Barbero, J. L., Ortega, S., and Suja, J. (2009). CDK2 is required for proper homologous pairing, recombination and sex-body formation during male meiosis. *J. Cell Sci.* 122, 2149–2159. doi: 10.1242/jcs.046706

Villar, R., Veneklaas, E. J., Jordano, P., and Lambers, H. (1998). Relative growth rate and biomass allocation in 20 *Aegilops* (Poaceae) species. *N. Phytol.* 140, 425–437. doi: 10.1046/j.1469-8137.1998.00286.x

von Well, E., and Fossey, A. (1998). A comparative investigation of seed germination, metabolism and seedling growth between two polyploid *Triticum* species. *Euphytica* 101, 83–89. doi: 10.1023/A:1018320230154

Waines, J. G. (1976). A model for the origin of diploidizing mechanisms in polyploid species. *Am. Nat.* 110, 415– 430. doi: 10.1086/283077

Wall, A. M., Riley, R., and Chapman, V. (1971). Wheat mutants permitting homoeologous meiotic chromosomes pairing. *Genet. Res.* 18, 311–328. doi: 10.1017/S0016672300012714

Wang, A., Xia, Q., Xie, W., Datla, R., and Selvaraj, G. (2003). The classical Ubisch bodies carry a sporophytically produced structural protein (RAFTIN) that is essential for pollen development. *Proc. Natl. Acad. Sci. U.S.A.* 100, 14487–14492. doi: 10.1073/pnas.2231254100

Wang, J., Roe, B., Macmil, S., Yu, Q., Murray, J. E., Tang, H., et al. (2010). Microcollinearity between autopolyploid sugarcane and diploid sorghum genomes. *BMC Genomics* 11, 261. doi: 10.1186/1471-2164-11-261

Whitford, R. (2002). From intimate chromosome associations to wild sex in wheat (*Triticum aestivum*). [dissertation]. [Adelaide]: University of Adelaide.

Winterfeld, G., Schneider, J., Perner, K., and Röser, M. (2012). Origin of highly polyploids: different pathways of auto- and allopolyploidy in 12–18*x* species of *Avenula* (Poaceae). *Int. J. Pl. Sci.* 173, 1–14. doi: 10.1086/664710

Wulff, B. B. H., and Moscou, M. J. (2014). Strategies for transferring resistance into wheat: from wide crosses to GM cassettes. *Front. Plant Sci.* 5, 692. doi: 10.3389/fpls.2014.00692

Xiang, Z. G., Liu, D. C., Zheng, Y. L., Zhang, L. Q., and Yan, Z. H. (2005). The effect of *phKL* gene on homoeologous pairing of wheat-alien hybrids is situated between gene mutants of *Ph1* and *Ph2*. *Hereditas* 27, 935–940.

Xiong, Y. G., Gan, L., Hu, Y. P., Sun, W. C., Zhou, X., Song, Z. J., et al. (2019). *OsMND1* regulates early meiosis and improves the seed set rate in polyploid rice. *Plant Growth Regul.* 87, 341–356. doi: 10.1007/s10725-019-00476-4

Yant, L., Hollister, J. D., Wright, K. M., Arnold, B. J., Higgins, J. D., Franklin, F. C. H., et al. (2013). Meiotic adaptation to genome duplication in *Arabidopsis arenosa*. *Curr. Biol.* 23, 2151–2156. doi: 10.1016/j.cub.2013.08.059

Conflict of Interest: The authors declare that the research was conducted in the absence of any commercial or financial relationships that could be construed as a potential conflict of interest.

frontiers in Plant Science

ORIGINAL RESEARCH
published: 04 February 2021
doi: 10.3389/fpls.2020.635139

Redistribution of Meiotic Crossovers Along Wheat Chromosomes by Virus-Induced Gene Silencing

Amir Raz[1,2], Tal Dahan-Meir[1], Cathy Melamed-Bessudo[1], Dena Leshkowitz[3] and Avraham A. Levy[1]**

[1] Department of Plant and Environmental Sciences, Weizmann Institute of Science, Rehovot, Israel, [2] Department of Plant Science, MIGAL Galilee Research Institute, Kiryat Shmona, Israel, [3] Bioinformatics Unit, Life Sciences Core Facilities, Weizmann Institute of Science, Rehovot, Israel

OPEN ACCESS

Edited by:
Christophe Lambing,
University of Cambridge,
United Kingdom

Reviewed by:
Pilar Prieto,
Institute for Sustainable Agriculture,
Spanish National Research Council,
Spain
James D. Higgins,
University of Leicester,
United Kingdom

***Correspondence:**
Avraham A. Levy
avi.levy@weizmann.ac.il
Amir Raz
amirr@migal.org.il

Specialty section:
This article was submitted to Plant Cell Biology, a section of the journal Frontiers in Plant Science

Received: 29 November 2020
Accepted: 31 December 2020
Published: 04 February 2021

Citation:
Raz A, Dahan-Meir T, Melamed-Bessudo C, Leshkowitz D and Levy AA (2021) Redistribution of Meiotic Crossovers Along Wheat Chromosomes by Virus-Induced Gene Silencing. Front. Plant Sci. 11:635139. doi: 10.3389/fpls.2020.635139

Meiotic recombination is the main driver of genetic diversity in wheat breeding. The rate and location of crossover (CO) events are regulated by genetic and epigenetic factors. In wheat, most COs occur in subtelomeric regions but are rare in centromeric and pericentric areas. The aim of this work was to increase COs in both "hot" and "cold" chromosomal locations. We used Virus-Induced gene Silencing (VIGS) to downregulate the expression of recombination-suppressing genes *XRCC2* and *FANCM* and of epigenetic maintenance genes *MET1* and *DDM1* during meiosis. VIGS suppresses genes in a dominant, transient and non-transgenic manner, which is convenient in wheat, a hard-to-transform polyploid. F1 hybrids of a cross between two tetraploid lines whose genome was fully sequenced (wild emmer and durum wheat), were infected with a VIGS vector ∼ 2 weeks before meiosis. Recombination was measured in F2 seedlings derived from F1-infected plants and non-infected controls. We found significant up and down-regulation of CO rates along subtelomeric regions as a result of silencing either *MET1*, *DDM1* or *XRCC2* during meiosis. In addition, we found up to 93% increase in COs in XRCC2-VIGS treatment in the pericentric regions of some chromosomes. Silencing *FANCM* showed no effect on CO. Overall, we show that CO distribution was affected by VIGS treatments rather than the total number of COs which did not change. We conclude that transient silencing of specific genes during meiosis can be used as a simple, fast and non-transgenic strategy to improve breeding abilities in specific chromosomal regions.

Keywords: VIGS, meiotic crossover, Met1, DDM1, XRCC2, FANCM, wheat

INTRODUCTION

During meiosis, homologous chromosomes pair and exchange DNA segments. This process, known as homologous recombination (HR), coupled with chromosome pairing, ensures proper segregation, and generates the genetic diversity among gametes. This is the main engine for crop improvement in sexually reproducing crops, hence, high recombination rates would improve breeding capabilities. However, in nature, recombination frequencies are restricted to a narrow

range of one to three recombination events per chromosome in each gamete [see (Mercier et al., 2015) for review].

The homologous recombination process starts with the formation of DNA double strand breaks (DSBs) by the SPO11 protein during Leptotene (Keeney et al., 1997). However, only a small portion of the breaks are resolved into crossovers (COs) events. For example in Maize about 20 COs events are resolved from around 500 DSBs in each meiocyte (He et al., 2017). Similarly, in tetraploid wheat about 2.3% of the DSBs resolved as CO events (Desjardins et al., 2020a). Hence, the way DSBs are being repaired is largely responsible for the frequency of COs events. CO formation involves creation and resolution of double Holliday junctions (Whitby, 2005; Gaskell et al., 2007). There are two distinct types of COs, type I and type II, which are outcomes of parallel pathways involving different complexes of proteins (Higgins et al., 2004; Chen et al., 2005; Mercier et al., 2005). Type I COs are subject to CO interference, a process that regulates the distribution of COs along the chromosome, preventing the formation of multiple CO in close proximity (Copenhaver, 2005; Mercier et al., 2005). This is the most prominent CO pathway in plants (Higgins et al., 2004; Hodzic et al., 2004; Wan et al., 2004; Guillon et al., 2005; Mercier et al., 2005; Lhuissier et al., 2007; Falque et al., 2009). Class II pathways which are Mus81-dependent are not subject to CO interference, they represent ∼10% of all CO events in plants and as with class I, class II pathways can also give rise to non-CO events through the resolution of Holliday-like junctions (Mercier et al., 2015). A recent study in tetraploid wheat reports on a ratio of 85% class I versus 15% class II events (Desjardins et al., 2020a). Another HR pathway that gives rise only to non-CO events is the synthesis-dependent strand annealing (SDSA) mechanism (Rubin and Levy, 1997; Allers and Lichten, 2001; Hunter and Kleckner, 2001; Börner et al., 2004). Research in *Arabidopsis* mutants led to the identification of three different pathways controlling recombination using either: *FANCM* (Crismani et al., 2012; Girard et al., 2014), *RECQ4A* and *RECQ4B* together with *TOP3α* and *RMI* (Séguéla-Arnaud et al., 2015, 2017), or *FIGL1* (Girard et al., 2015). An increase in CO rate by a factor of up to 3.6 was reported in the *fancm* mutant (Crismani et al., 2012) and a 1.5 and 6.2 fold increase in the *top3α* and *recq4a-recq4b* mutants, respectively (Hartung et al., 2007; Séguéla-Arnaud et al., 2015). In these experiments most of the additional COs were of the type II CO pathway. Furthermore, the *figl1 recq4* and *fancm recq4* double mutants showed about 10 fold increase in recombination rate reaching an unprecedented amount of 12 COs per *Arabidopsis* chromosome (Fernandes et al., 2018). Increase in COs events in *recq4* and *fancm* mutants was also found in different crops such as rice, tomato, pea, and turnip mustard (Blary et al., 2018; Mieulet et al., 2018; Fayos et al., 2019) suggesting that these genes serve as universal meiotic anti-CO genes which suppress mainly type II COs. Another anti-CO gene is the RAD51 paralog XRCC2. Serra et al. (2013) found a 50% increase in recombination rate in the *xrcc2 Arabidopsis* mutant compared to wild type.

Double strand breaks and crossovers are not uniformly distributed along the chromosome, instead, they tend to concentrate in hotspots (Mézard, 2006; Mézard et al., 2007; Pan et al., 2011; Smagulova et al., 2011). In wheat, most of the CO hotspots are found in the sub-telomeric regions while the centromeric and peri-centromeric regions which occupy large portions of the chromosome, show very low recombination rate (Avni et al., 2014; Choulet et al., 2014). What turns certain chromosomal regions as hotspots is not fully understood, however, mounting evidence suggest the involvement of epigenetic markers. For example H3 histone lysine 4 trimethylation (H3K4me3) and chromatin accessibility were found to correlates with DSB hotspots in yeast and mouse (Berchowitz et al., 2009; Borde and de Massy, 2013). In human and mouse, the key determinant for recombination hotspot – the PRDM9 protein – is a histone methyltransferase which target 13 bp long CCN repeat motif (Baudat et al., 2010; Myers et al., 2010). Although in plants a paralog for the *PRDM9* gene is still to be found, three short motives were found to be enriched in *Arabidopsis* and maize CO hotspots – CCN-repeat, CTT-repeat and A-rich motif (Shilo et al., 2015; He et al., 2017). Analysis of the epigenetic landscape around these motives in *Arabidopsis* and maize revealed a peak of H3K4me3, H3K27me3, and H2A.Z histone modification, as well as negative peak of nucleosome occupancy and CG methylation (Choi et al., 2013; Shilo et al., 2015; He et al., 2017). Since epigenetic markers may influence the occurrence of a CO, manipulating genes related to these markers may change the distribution or the rate of recombination events along the chromosome. In plants, maintenance of DNA methylation depends on the context where CG is methylated by *DNA METHYLTRANSFERASE 1 (MET1)* (Kankel et al., 2003), while CHG and CHH are methylated by *CHROMOMETHYLASE*s (*CMT2* and *CMT3*) (Lindroth, 2001). In addition, experiments in *Arabidopsis thaliana* showed that *DECREASE IN DNA METHYLATION 1* (*DDM1*) protein is involved in methylation maintenance of all cytosine contexts by releasing the wrapped DNA from the nucleosome (Lyons and Zilberman, 2017). Experiments in *Arabidopsis* showed that down regulating cytosine methylation through mutations in *DDM1* or *MET1*, correlates with an increase in the rate of CO in euchromatin but not in pericentromeric heterochromatin regions (Melamed-Bessudo and Levy, 2012; Mirouze et al., 2012; Choi et al., 2013). Underwood et al. (2018) showed that mutating the CHG DNA methyltransferase gene *CMT3* in *Arabidopsis*, led to increase in meiotic recombination rate even at the peri-centromeric regions.

Considering the above experiments, it seems possible to achieve recombination increments in wheat and maybe to affect CO localization, by mutating anti-CO and DNA methylation genes. Transformation and genome editing in wheat, as well as selection of homozygous and multiple mutants by TILLING is difficult and time-consuming with very low efficiency due to both its polyploid nature and the technically challenging transformation protocols. The most commonly used methods for cereal transformation is either *Agrobacterium*-infection or particle bombardment. Both methods rely on tissue culture procedures where the treated tissue (usually embryos) generates calli cells that can be regenerated into a transgenic plant. This procedure can take up to several month and transformation rates

are low. Moreover, the end product is a Genetically Modified Organism (GMO) which is not accepted by regulators in many countries. Recently, the lab of Caixia Gao greatly improved wheat transformation procedures, and managed to perform a knockout mutation in wheat by delivering components of the CRISPR-Cas9 system transiently using either Ribonucleotides-Proteins (RNPs) or mRNA (Zhang et al., 2016; Liang et al., 2017; Sánchez-León et al., 2018) which resulted in non-GMO mutants. However, the efficiency of this procedure is lower and the chances to mutate all alleles is even lower, thus it is labor intensive and not shortening the timescale. Simultaneous knock-out of all alleles of a specific gene in the same plant is possible. However, as the number of alleles increase in polyploid plants (as many as six alleles in bread wheat) the chance to obtain all the mutations in the same plant decreases, forcing at least one round of hybridization. Furthermore, knocking-out a gene is in many cases too drastic and leads to sterility, especially when targeting a housekeeping gene, as was shown in a *ddm1* knockout of tomato and maize plants (Corem et al., 2018; Fu et al., 2018). In cases like this, silencing approach such as microRNA or siRNA can be used. However, this still requires tissue culture transformation and results in GMO plants. Using a Virus Induced Gene Silencing (VIGS) system as a gene silencing method is an alternative to the traditional iRNA/siRNA cassettes. This system offers the advantages of fast and simple cloning stage followed by an easy and highly efficient infection. Another important feature of this method is a transient effect, which lasts 2 to 4 weeks, enabling the plant to grow normally at the end of the treatment. This was successfully used in wheat for both basic and applicative researches (Bennypaul et al., 2012; Lee et al., 2015). Moreover, VIGS treatment were successfully applied to manipulate meiotic-specific processes in wheat and *Arabidopsis* (Bhullar et al., 2014; Calvo-Baltanás et al., 2020; Desjardins et al., 2020b).

In this work, we used VIGS to silence meiotic anti-CO genes as well as DNA methylation genes during meiosis to study the effect of specific genes on meiotic recombination and to increase the rate of CO events in various regions of wheat chromosomes. The ability to manipulate COs is important for plant breeders, in particular in crosses with exotic germplasm, in which the CO rate is low, or when trying to break linkage between genes or bring new allelic variation to genes that are located in pericentromeric regions. VIGS offers the possibility to alter recombination rates without any genetic modification such as mutagenesis or transgenesis. We have tested the effect of *MET1, DDM1, XRCC2, RecQ4, and FANCM* genes on HR rates in tetraploid wheat in progeny of a fertile hybrid between wild emmer wheat, the direct progenitor of domesticated tetraploid wheat (WEW, var. Zavitan) and durum wheat (var. Svevo) where both parents have a well-characterized genome (Avni et al., 2017; Maccaferri et al., 2019; Zhu et al., 2019). We show that silencing of *MET1* and *DDM1* during meiosis led to redistribution of HR events in euchromatic regions while silencing of *XRCC2* resulted in redistribution of HR in both euchromatic and heterochromatic regions. Other genes tested had no effect on meiotic recombination.

MATERIALS AND METHODS

Plant Material

Seeds were germinated in a growth chamber for 4–5 weeks on a long day set up of 16 h of light and a temperature of 18°C at night and 20°C during the day. Plants were then moved to a greenhouse for the rest of the experiment and were grown under the same temperature regime. For hybrid formation, "Svevo" flowers were emasculated at heading stage and bagged for 4–5 days, followed by pollination with "Zavitan" fresh pollen. Spikes were kept bagged until seeds were fully developed.

VIGS Cloning and Propagation

All VIGS procedures were adapted from Lee et al. (2015) with minor changes. In short, a 250–400 bp segment was designed for each gene using the si-Fi (siRNA Finder)[1] software, based on the "Zavitan" WEW transcriptome. Anti-sense sequences were amplified from Zavitan genome using specific primers (**Supplementary Table 1**) and cloned into the BSMV RNAγ vector pCa-γbLIC (Yuan et al., 2011) via ligation-independent cloning (LIC) and transformed into *Agrobacterium tumefaciens* strain GV3103 as described (Lee et al., 2015). Four weeks old *Nicotiana benthamiana* leaves were co-infiltrated with a mix of *Agrobacterium tumefaciens* strains carrying BSMV RNAα, RNAβ, and RNAγ together in 1:1:1 ratio. Infected leaves were collected 5 days post infection and either stored at −80°C for later use or were used immediately for wheat infection. Non-infiltrated leaves were collected 8 days post infection to verify systemic infection ability of the virus. To that end, total RNA was purified using Nucleospin RNA Plant kit (MACHEREY-NAGEL) followed by cDNA synthesis with Verso cDNA synthesis kit (Thermo Fisher Scientific). Viral presence was verified using primers from the virus genome and the specific insert (**Supplementary Table 1**).

VIGS Infection

Nicotiana benthamiana infiltrated leaves were grounded under liquid nitrogen in 10 mM potassium phosphate pH 7.0 containing 2% w/v Celite© 545 AW (Sigma–Aldrich) in a ratio of 1.5 ml per 1 g of leaf tissue. Crude extracts were used to infect wheat leaves of 15 different spikes using two methods simultaneously: rubbing the leaf with two fingers and injecting the leaf with needle less syringe in two locations along the leaf. Time of infection was 2–3 weeks before meiosis, typically on the third or fourth leaf. Infected plants were sprayed with a mist of water and covered with plastic bags for the night. Plants were allowed to grow until spikes were dry and seeds were collected separately from each infected tiller.

qPCR

For analysis of *SPO11* expression, anthers from three different spikes were gently collected from 3 to 4 spikelets at the middle of the spike for each booting or maturation stage (**Figure 1**). For analysis of the VIGS effect, anthers from each of the 15 infected spikes were gently collected from 3 to 4 spikelets

[1] http://labtools.ipk-gatersleben.de/

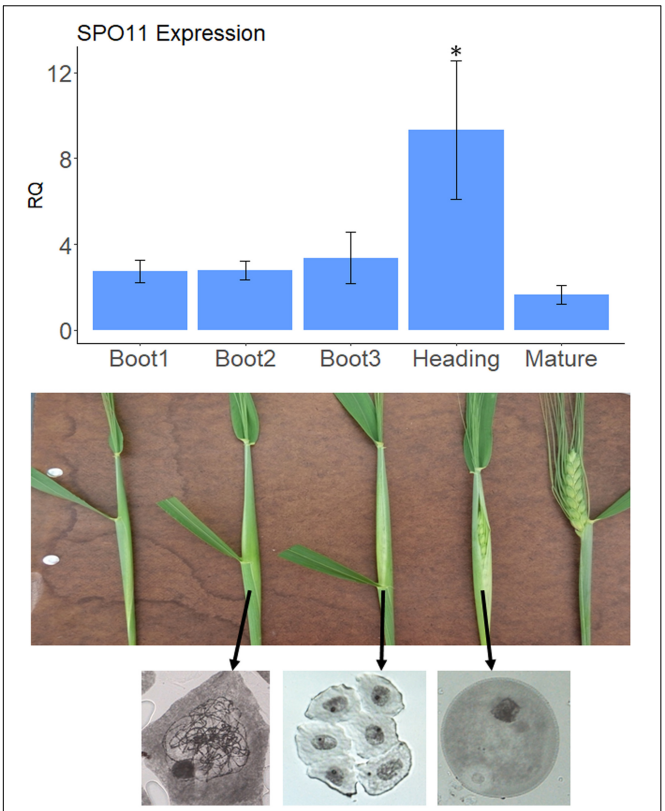

FIGURE 1 | *SPO11* expression at different developmental stages. The upper panel shows relative expression levels of *SPO11* as determined by qPCR, during five developmental stages of the spike, shown in the bottom panel for cv. Svevo. The reference gene was *Actin*. Bars represent SE, the number of replica, $N = 3$, Asterisk designate significant differences from the Mature stage ($p < 0.05$). The bottom panel shows meiotic stage analysis by Acetocarmine staining of male meiocytes taken from the middle spikeletes at different physiological stages. Arrows show origin of stained meiocyes. Left, zygotene; Middle, tetrad; Right, young pollen.

at the middle of the spike between boot2 and boot3 stages (**Figure 1**). Total RNA was purified using Nucleospin RNA Plant kit (MACHEREY-NAGEL) followed by cDNA synthesis with Verso© cDNA synthesis kit (Thermo Scientific). qPCR analysis was done in a StepOnePlus© real time system (Applied Biosystems). Each reaction contained 5 µl FAST Sybr (Applied Biosystems), 1 µl mixed primers (**Supplementary Table 2**) at 2 µM, and 2 µl of sample containing 40–50 ng cDNA. Relative expression was calculated using *Actin* as internal normalization gene (Bhullar et al., 2014). Note that alternative normalization genes for wheat meiosis (not used here) were recently reported and should be used in future works (Garrido et al., 2020).

Markers Design

In order to design simple PCR markers we aligned the sequence of chromosome 1A of "Svevo" and "Zavitan" and we screened for InDels (20–200 bp) which are easy to distinguish on a simple agarose electrophoresis gel. The InDels were detected by an in house developed pipeline that utilized public tools. Specially, initially alignment was done between Zavitan chromosome and the Svevo genome (160802_Svevo_v2_pseudomolecules.1.fasta) using the program NUCmer from MUMmer (version 3.23; parameters : -maxmatch -l 100 -c 500) (Kurtz et al., 2004). The output out.delta was analyzed with the program Assemblytics (parameter: 200)[2]. The bed output variants_between_alignments was filtered (using awk) to contain InDels that are between 20 and 200 bases long that align to chromosome 1A of Svevo. We found more than 2000 such InDels. Annotation of the InDel region was added using Homer script annotatePeaks.pl[3]. The 150 base sequence surrounding the InDel was extracted using bedtools getfasta[4]. In addition, to ensure that the certain sequence of Svevo does not have an homologous region in Svevo or and additional homologous region in Zavitan genome, blastn was run (version 2.5.0, parameters: -outfmt 7 -max_target_seqs 1) against the relevant genomes in which the InDel regions were masked by running bedtools program maskfasta.

We choose 12 deletions (in "Svevo" compared to "Zavitan") spreading all along the chromosome. Primers were carefully designed for chromosome-specific amplification, namely sequences of both "Zavitan" and "Svevo" chromosome 1A, but not of the homoeologous chromosome 1B nor from paralogous loci (**Supplementary Table 3**). DNA was purified from the first or second leaves of seedlings using Nucleospin DNA Plant© kit (MACHEREY-NAGEL). PCR reactions were done in 96 plates in total volume of 15 µl using Hy-Taq ready mix© (Hy-Labs, Israel) and products were analyzed by gel electrophoresis.

GBS Libraries Preparation and Analysis

Genotyping-By-Sequencing libraries were prepared following the protocol by Poland et al. (2012). Libraries were sequenced by Illumina NextSeq 550 mid-output using 150 base-pairs single-end kits. Reads were mapped to a "combined" genome containing the Zavitan WEW_v2.0 genome (Zhu et al., 2019) and the Svevo.v1 genome (Maccaferri et al., 2019) using *bwa-mem* (Li, 2013). Mapped reads were converted to binary alignment map (BAM) format and filtered for high quality (>30), uniquely mapped and perfect matched using SAMtools package (Li et al., 2009). Zavitan and Svevo-specific reads served to build each "combined" genome. We found an average of 32,000 to 64,000 markers per chromosome, namely parent-specific reads. Each pair of chromosomes was divided into identical number of ∼1 Mb bins and the number of filtered reads was calculated for each bin using BEDtools (Quinlan and Hall, 2010). For each pair of matching bins (from Zavitan and/or Svevo) the number of mapped reads was summed together. For each bin, the ratio between Zavitan reads and Svevo reads was calculated. Each bin was then re-calculated as the mean ratio of the surrounding 15 bins. A bin was genotyped as homozygous if the calculated ratio was higher than 0.9 (Zavitan) or lower than 0.1 (Svevo), otherwise it was considered as heterozygous. Bins with less than 10 reads were ignored. COs were assigned to regions where bins changed from one genotype to another. Double COs were ignored if the distance between them was less than 8 Mb for subtelomeric

[2]http://www.ncbi.nlm.nih.gov/pubmed/27318204
[3]http://homer.ucsd.edu/homer/ngs/annotation.html
[4]https://bedtools.readthedocs.io/en/latest/

regions or less than 70 Mb for pericentric regions. We applied this analysis on libraries of Zavitan and Svevo as well. Between 2 and 3% of the Bins were not consistent with parental genotypes and were removed from the progeny analysis.

Statistics

Data analysis and statistics were done in the R environment. In most cases, Wilcoxon test was used as significance test, except for recombination rate where the Chi square test was used.

Cytological Analysis

Staging of meiosis was done using contrast-phase microscopy: spikes were fixed in Carnoy's solution (3 ethanol: 2 chloroform: 1 glacial acetic acid) and anthers were squashed with Acetocarmine (Feldman, 1966).

RESULTS

Our goal was to silence genes that are putative suppressors of recombination during meiosis, when recombination between homologs occurs. Meiosis in wheat occurs during early booting stage. In order to determine the optimal stage to check for the silencing effect we sampled anthers from three different spikes at each booting stages as well as heading and mature spikes and checked the expression levels of *SPO11* as a meiotic marker. As shown in **Figure 1**, the level of expression of *SPO11* in anthers starts to increase already at Boot1 stage (in comparison with non-meiotic mature anthers) reaching the highest levels at heading, and going down after emergence of the spike (Mature stage). To be on the safe side we decided to sample anthers between Boot2 and Boot3 in order to test silencing of our target genes, considering also the fact that zygotene occurs during Boot2 stage as seen by chromosome staining (**Figure 1**).

Virus-Induced Gene Silencing of Recombination Suppressors

We have infected 15 tillers of F1 cv. Svevo x cv. Zavitan hybrid plants, with the recombinant BSMV (**Figure 2A**) 2 to 3 weeks before anthesis, usually on the third or fourth leaf, using both needle-less infiltration and the rubbing method (Lee et al., 2015). While designing the VIGS constructs, we carefully choose sequences that show high similarity between the two homoeologous allele as well as between the two parents of the hybrid. Accordingly, qPCR primers were designed from highly conserved sequences in the mRNA to match all four possible alleles. Thus, a lower expression level in the qPCR test reflects the total silencing effect of all four alleles of each gene. Anthers from three different spikelets, each from a different tiller, were sampled at Boot2 stage to measure expression levels of each gene by qPCR and assess the silencing effect. As shown in **Figure 2A** VIGS worked well on *MET1, DDM1, FANCM,* and *XRCC2* genes, reducing their expression level between 65 and 24% ($p < 0.05$) compared to WT plants (**Figure 2B**). The empty vector treatment showed some non-significant reduction in gene expression, possibly due to the stress effect of the virus infection. There was no significant reduction in expression of *RecQ4*, therefore we did not pursue further analyses with this gene which, originally, was a lead candidate (Mieulet et al., 2018).

Fertility in VIGS-Treated Plants

In order to check whether the silencing treatment of F1 cv. Svevo x cv. Zavitan hybrid plants had a deleterious effect on the gametes or the developing seeds, we counted the number of F2 seeds in the treated F1 spikes (**Supplementary Figure 1**). Silencing of *FANCM* or *DDM1* showed significant reduction in seeds number, reaching 5–7 seeds per spike compared to 19 seeds in the WT. The other treatments showed only mild, but non-significant reduction.

Crossover Rate in VIGS-Derived Seeds

To analyze recombination rate in the F2 progenies of F1 cv. Svevo x cv. Zavitan hybrid plants that underwent VIGS and of negative controls that were treated with an empty vector, we developed a series of InDel markers, that are easy to screen for, through a whole genome comparison of the "Zavitan" and "Svevo" genomes. We focused on chromosome 1A, where we choose 12 InDels markers along the chromosome. All markers have a 100–200 bp larger "Zavitan" product, so that a simple gel-electrophoresis was sufficient for genotyping. We selected three pairs of markers with genetic distance of 9 to 22 cM: one for each sub-telomeric region and another one spanning the pericentric region (**Figure 3A**). We used these three intervals to measure recombination rates. Progenies of F1 plants treated with MET1-VIGS as well as DDM1-VIGS showed increment in recombination of 76 and 94%, respectively, at the left arm in sub-telomeric region but not in the other intervals. XRCC2-VIGS progenies showed an increment of 82% in the right arm sub-telomeric region and, interestingly, a 57% increase in the pericentric region (**Figure 3B**). The treatment with FANCM-VIGS showed no significant changes in recombination. In order to check the total number of recombination events in chromosome 1A, we used 12 InDel markers along the chromosome to identify all events in each progeny. We found no overall increase of recombination events in any of the treatments (**Supplementary Figure 2**) but rather redistribution of crossover sites.

Genotyping by Sequencing (GBS)

To follow-up on the results of the markers analysis, we expanded the analysis to the whole genome with higher resolution (32,000 to 64,000 markers per chromosome) to better characterize the silencing effect on CO distribution. We choose to focus on the MET1-VIGS and XRCC2-VIGS treatment since these treatments showed significant changes in CO events and minor loss in seeds number. We used GBS-NGS approach (Poland et al., 2012) to genotype the same progenies populations used for the above low-resolution markers analysis. Reads were mapped to a combined "Zavitan"-"Svevo" genome and collapsed into ∼ 1 Mb bins (598 to 851 bins per chromosome). On average, we found 62.9 reads per bin while in the pericentric region we found 38.8 reads per bin and in the left and right subtelomeric regions the average reads count was 102.7 and 73.9, respectively. Bins were genotyped as homozygous when more than 90% of

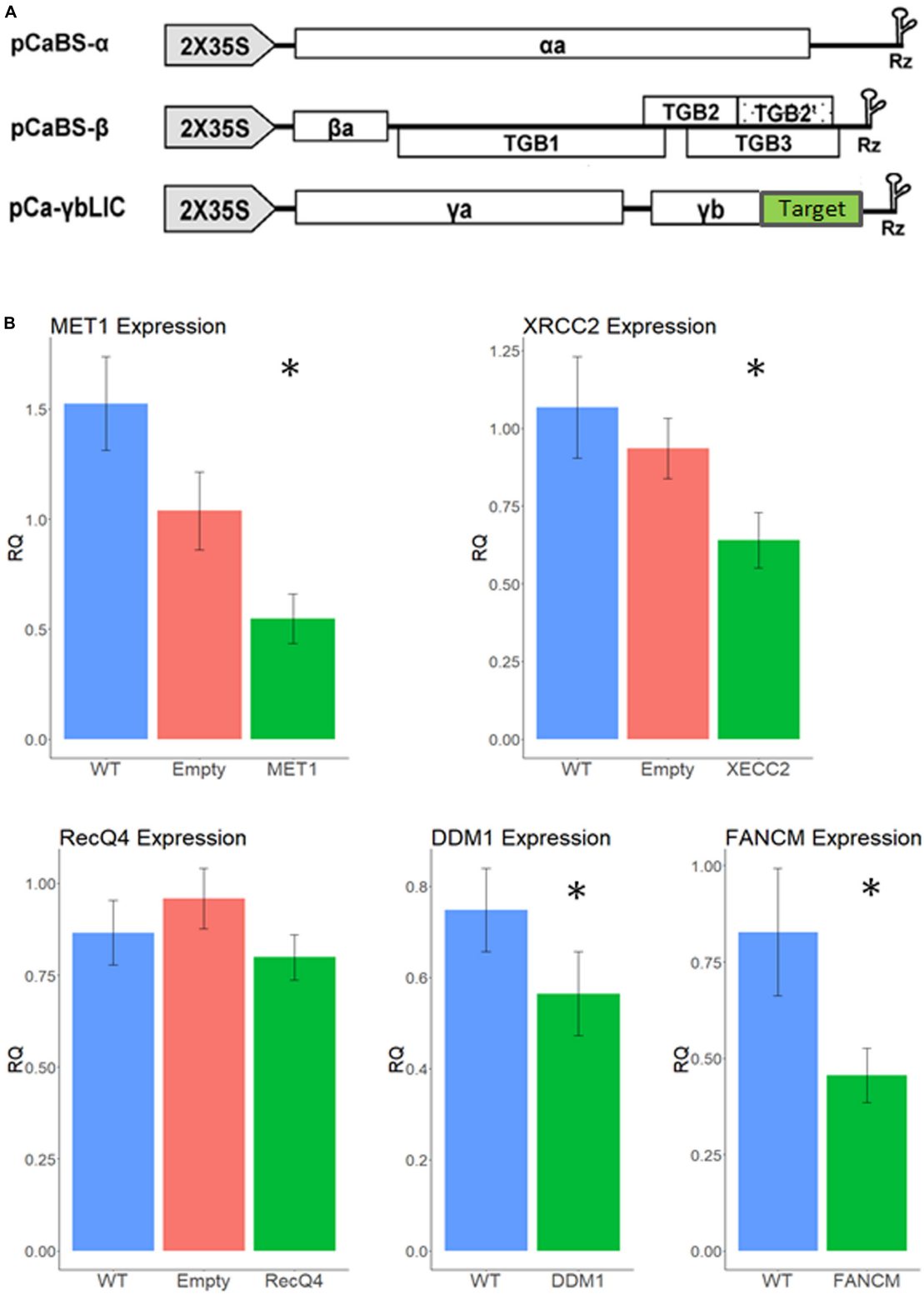

FIGURE 2 | Relative expression levels of recombination suppressor genes after infection with different VIGS treatments. **(A)** VIGS constructs. Each of the three BSMV sub-genomes was cloned into the pCass4-Rz binary vector under the 35S promoter. Target (green box) correspond to the gene of interest sequence (Adapted from Yuan et al., 2011). Vectors were introduced into *N. benthamiana* leaves for viral propagation and extracts from these leaves were used for wheat infection. **(B)** Silencing effect by VIGS treatments. Normalized relative expression is shown on the *Y* axis for each gene studied; WT, un-infected plants. Empty – infection with empty virus. Asterisk designate significant difference from WT ($p < 0.05$, $N = 15$). Error bars represent SE.

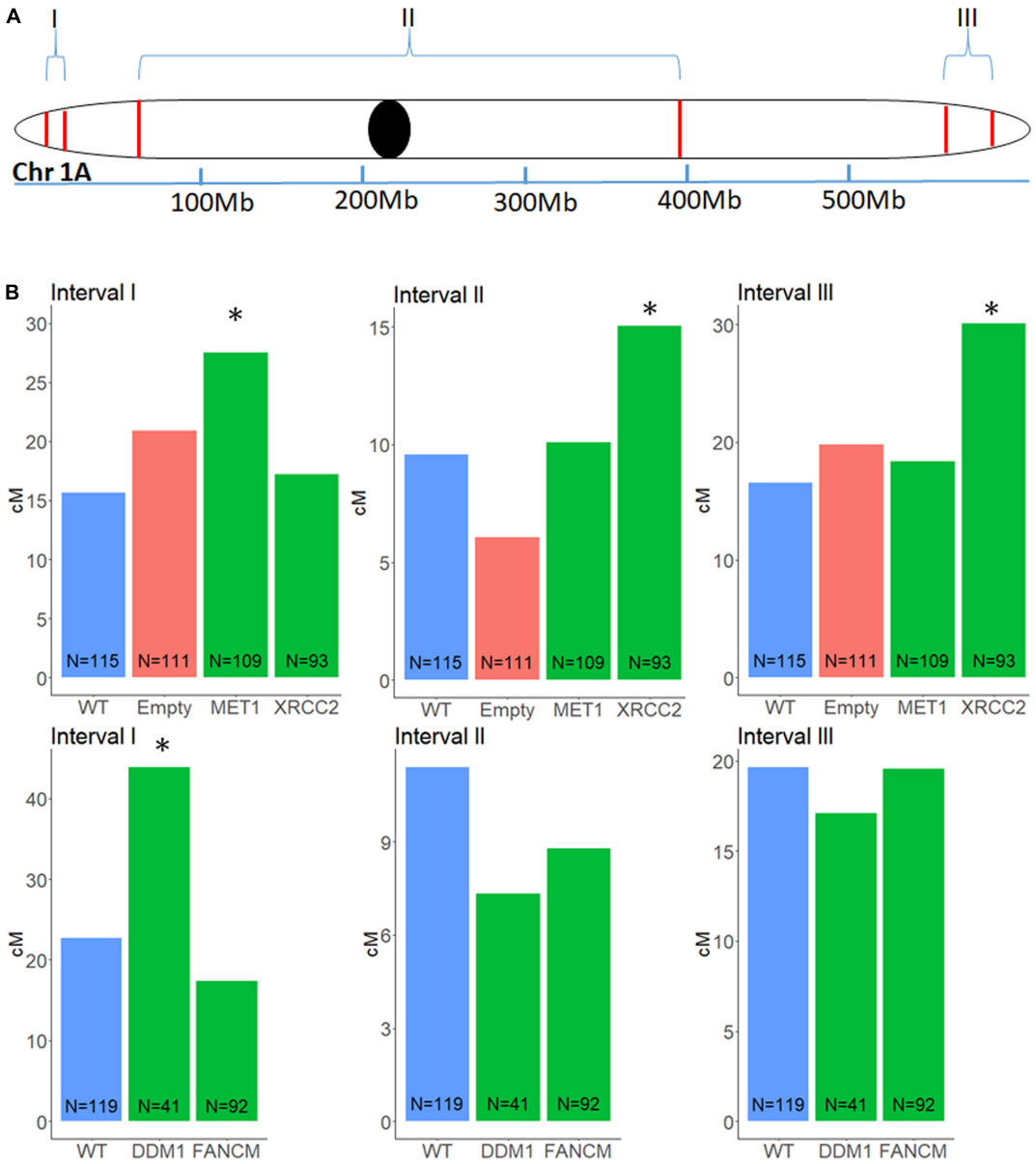

FIGURE 3 | Genetic distance in a F2 (Zavitan x Svevo) population, between three pairs of markers on chromosome 1A, after VIGS treatment of F1 plants. Markers were selected from a list of InDels between Zavitan and Svevo chromosomes. **(A)** Schematic map of the three intervals measured for changes in genetic distance. I, left arm sub-telomeric region; II, peri-centric region; III, right arm sub-telomeric region. **(B)** Effect of *VIGS* for *MET1*, *XRCC2*, *DDM1, FANCM* and their untreated WT F2 plants and empty vector control. locations of transition between genotypes correspond to a CO event. The number of plants in each population N, is marked at the base of the column. Asterisk designate significant difference from WT ($p < 0.05$).

its mapped reads belonged to one of the parents. COs were assigned to the junctions between adjacent bins differing in their genotype. To validate the consistency between the GBS analysis and the markers analysis, we computed the genetic distance of the three intervals in chromosome 1A and found high correlation between the GBS analysis and the markers results (**Supplementary Figure 3**). As in previous studies on Zavitan-Svevo hybrids (Avni et al., 2014), we found that most of the CO events were concentrated in hotspots at the subtelomeric regions while the pericentric regions showed a very low rate of recombination (**Figure 4**). Changes in CO rates following VIGS treatments, were observed in both the subtelomeric and pericentric regions. However, these changes did not show a consistent pattern of either increase or decrease in CO rates but rather a redistribution of the hotspots along the chromosome. Indeed, the total number of COs per chromosome was not affected by the treatment (**Supplementary Figure 4B**), however, there were several significant local effects in both pericentric and subtelomeric regions where CO rate was either increased or decreased at a specific locus compared to WT plants.

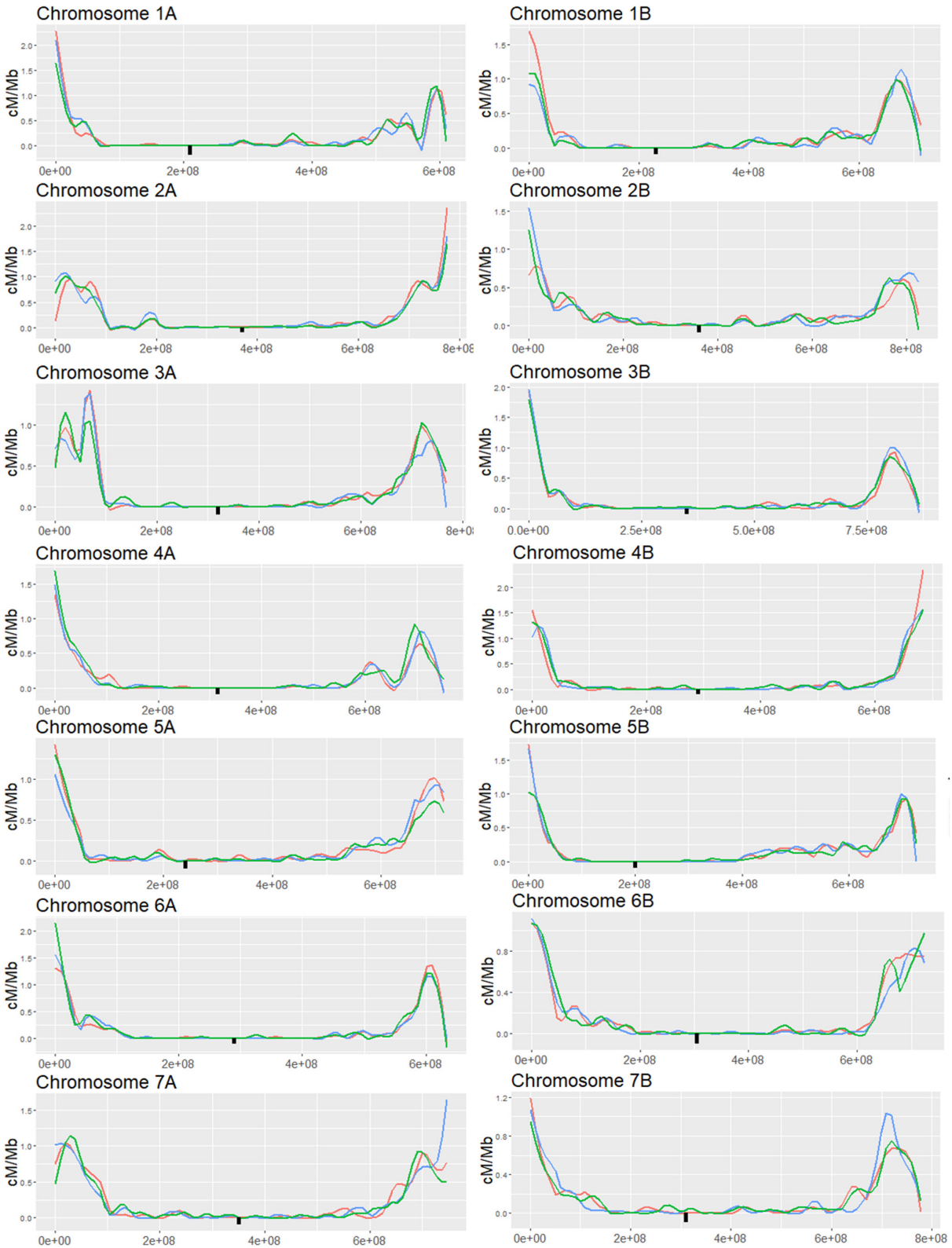

FIGURE 4 | Genome wide analysis of F2 (Zavitan x Svevo) populations derived from F1 plants which were treated by either MET1-VIGS or XRCC2-VIGS during meiosis or untreated (WT). COs were analyzed in F2 progenies by GBS method followed by NGS Illumina sequencing. Chromosomes were divided into 1 Mb bins which were genotyped according to the ratio of mapped reads. Genetic distance in centi-Morgans per mega base pairs (*Y* axis) is shown along each chromosome (*X*-axis represent bp in Zavitan chromosomes). Blue, WT control; Red, MET1-VIGS treatment; Green, XRCC2-VIGS treatment; Black square, centromere position.

Regions surrounding the centromere, which showed less than 0.1 cM/Mb in the untreated WT population were considered as pericentric. We summed all the CO events in each chromosome and checked whether either of the VIGS treatment led to a significant increased recombination rate in this area. Interestingly, silencing *XRCC2* led to a significant increase of between 51% and 136% in five of the chromosomes (**Figure 5A**). In addition, *MET1* silencing led to a significant increase of 44 to 93% in three of the chromosomes. As shown in examples of chromosomes 4B and 5B (**Figure 5B**), some of these increases are a result of COs which occurred in the close proximity of the centromere, whereas in the WT population we found virtually zero COs in these regions. On average, over all chromosomes, there was a significant enhancing effect on COs of 45 and 25% in pericentric regions when silencing *MET1* or *XRCC2,* respectively ($N = 14$, $p < 0.05$) (**Supplementary Figure 4A**), however, this was mostly due to effects originating from specific chromosome as shown in **Figure 5A**.

In subtelomeric areas, the VIGS effects were very variable and context-dependent. As shown in the examples of subtelomeric regions of chromosomes, 2A and 3A, local increase and decrease in CO events can be found in close proximity when comparing both VIGS treatment to the WT control in these regions (**Figure 6**).

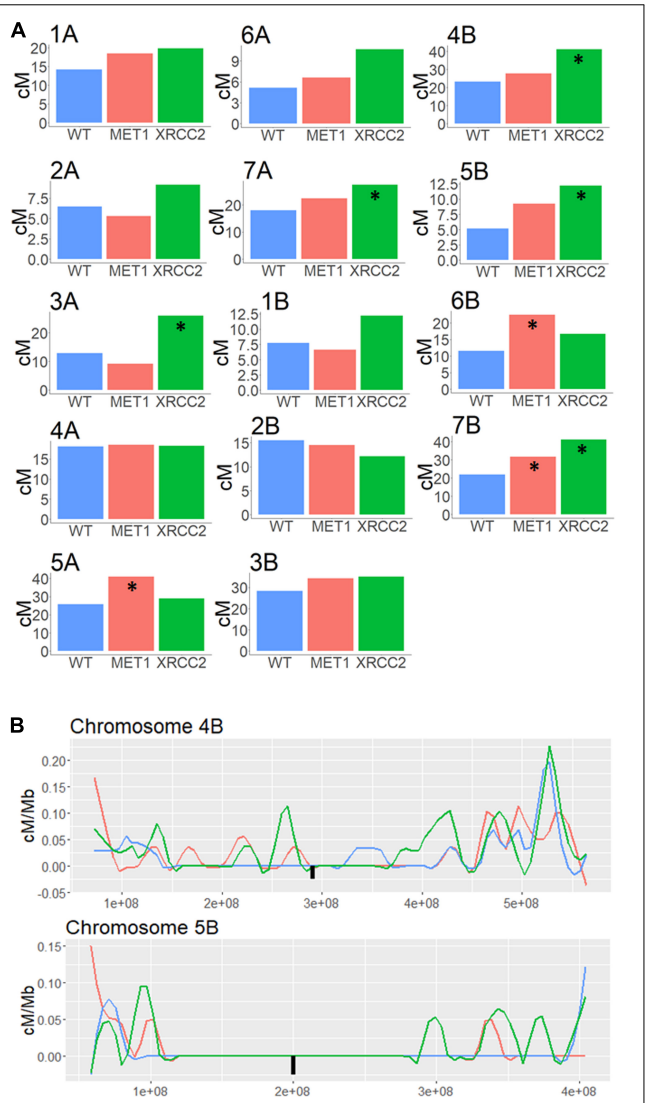

FIGURE 5 | Genetic distance analysis in Pericentric regions of F2 (Zavitan x Svevo) populations derived from F1 plants treated by either MET1-VIGS or XRCC2-VIGS during meiosis compared to untreated F1s (WT). **(A)** Genetic distance (centi-Morgans) of pericentric region in each chromosome. Asterisk marks treatments significantly different from untreated WT (chi-squared test, $p < 0.05$). **(B)** High resolution analysis of genetic distance (centi-Morgans/Mb) in pericentric regions of chromosome 4B and 5B in F2 (Zavitan x Svevo) populations derived from F1 plants treated by MET1-VIGS (Red, $N = 87$), XRCC2-VIGS (Green, $N = 82$) or untreated WT control (Blue, $N = 89$). The *X*-axis represent bp in Zavitan chromosomes. The Black square represents the centromere position.

DISCUSSION

In this work we have used the VIGS method developed by Lee et al. (2015) to silence various meiotic anti-CO and DNA methylation genes. By careful timing of the infection, we were able to reduce the transcripts levels of most of these genes in a transient manner at the stage spanning meiosis. A weakness of the VIGS method applied to meiosis is that it is not possible to accurately control and measure the degree of silencing in the meiotic cells. Likewise, it is not clear why a target like *RecQ4* was not silenced by VIGS in this experiment. Nevertheless, the benefits, as described below, compensate for this weakness. The transient nature of this method is advantageous over a stable gene silencing or knock out mutation for several reasons: it is non-transgenic and can be applied easily to any hybrid; it is transient so that if deleterious, the gene silencing effect is constrained in time; it is dominant and enables stacking of genes compared to the lengthy process of recessive mutations and double mutants production (especially important in polyploid hybrids); when affecting meiotic recombination its effect is transmitted to the next generation. For example, *MET1* and *DDM1* participate in the maintenance of DNA and chromatin methylation state and play a key role in maintenance of genome stability through suppressing of transposable elements (Ito and Kakutani, 2014; Paszkowski, 2015), thus permanent deficiencies in their activity may lead to a mutator effect and eventually to sterility. Moreover, even if not sterile, these mutants reduce plant fitness, and therefore once their effect has been achieved one has to "return" to wildtype to obtain a desired crop. Likewise, a full knockout of *DDM1* or *FANCM* might limit their use in breeding programs as suggested by the reduction in fertility observed by silencing.

Silencing DNA Methylation Genes

On the basis of studies showing increased recombination in *Arabidopsis* mutants (Melamed-Bessudo and Levy, 2012; Mirouze et al., 2012; Choi et al., 2013), we silenced *MET1* and *DDM1* genes during meiosis. In spite of the mild reduction in *DDM1* expression, we observed a drastic reduction in fertility of 74%, which may be a result of genome instability caused by enhanced activity of transposable elements. These findings are

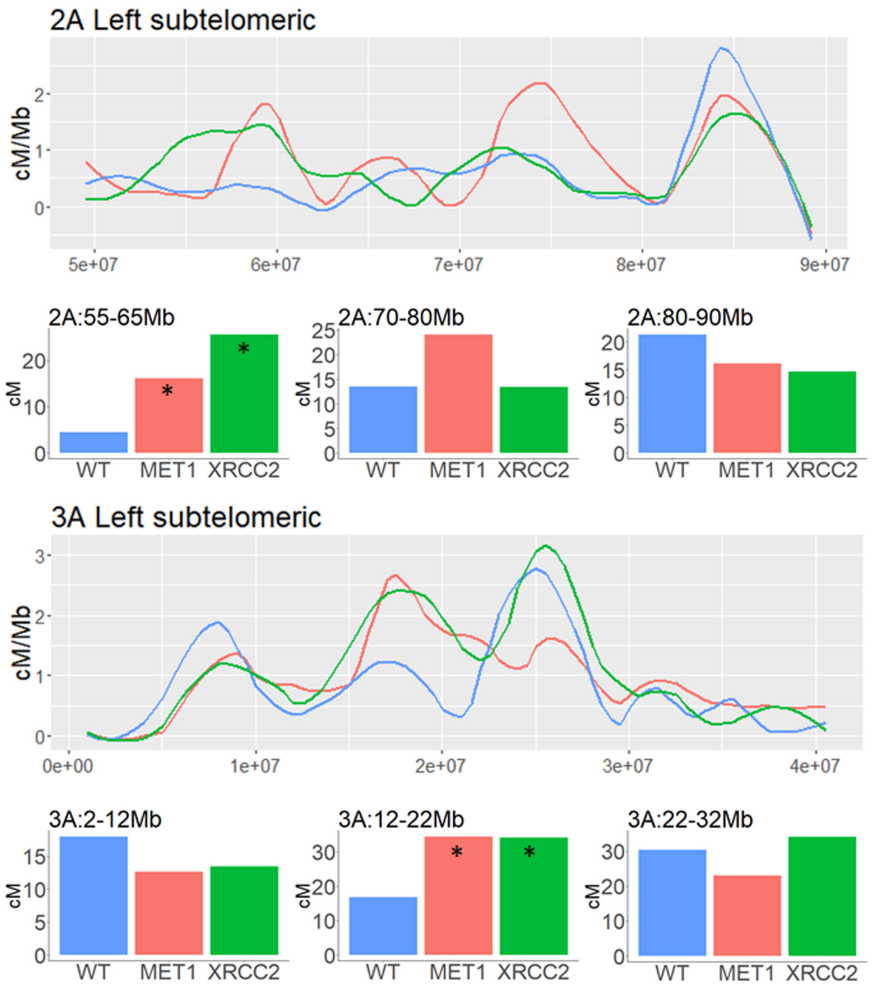

FIGURE 6 | Analysis of genetic distance in subtelomeric regions of three different chromosomes of F2 (Zavitan x Svevo) populations derived from F1 plants which were treated by either MET1-VIGS or XRCC2-VIGS during meiosis or untreated (WT). Lines show the Genetic distance in centi-Morgans per Mb along subtelomeric regions (*X*-axis represent bp in Zavitan chromosomes). Bars show the genetic distances in centi-Morgans in three 10 Mb intervals from each subtelomeric region. Asterisk indicate a significant difference from WT (chi-squared test, $p < 0.05$). Blue, WT control ($N = 89$); Red, MET1-VIGS treatment ($N = 87$); Green, XRCC2-VIGS treatment ($N = 82$).

in line with the sterility found in a *ddm1* tomato, maize and rice mutants (Corem et al., 2018; Fu et al., 2018). Silencing the wheat homologs of *DDM1* and *MET1*, led to a mix trend in the subtelomeric regions, where dramatic increase and decrease in COs were found in the same chromosome and in some cases in the same subtelomeric region, implying a change in hotspots strength rather than absolute change in recombination rates (**Figure 6**). Remarkably, increases in recombination tend to occur in a region that is already a hotspot in WT, suggesting that hot becomes hotter, and next to it, possibly due to genetic interference, a decrease in recombination is seen (**Figure 6**). Since the rate of COs in the pericentric area is so low, we assessed the genetic distance of the whole areas which span 291–568 Mb around the centromere. We found some strong enhancing effects in three chromosomes by MET-VIGS treatment (**Figure 5A**) but a milder average effect throughout the genome (**Supplementary Figure 4A**). Effects were stochastic in the pericentric region with new "lukewarm-spots" being formed but remaining 10–20 fold lower than hotspots in subtelomeric regions. It might be that regions which were completely silenced in WT plants became slightly more accessible when *MET1* was silenced. A report in *Arabidopsis*, by Underwood et al. (2018), showed that mutating the CHG DNA methyltransferase gene *CMT3* in *Arabidopsis*, led to increase in meiotic recombination rate in some peri-centromeric regions. Hence, it might be of interest to use VIGS to silence the wheat *CMT3* during meiosis. These results also highlight the efficacy of the approach in bypassing the expected lethality of these mutants in wheat.

Silencing Meiotic Anti CO Genes

In this study, we have applied VIGS to different anti-CO genes during meiosis. Unfortunately, the expression of the leading candidate genes, *RecQ4* homeologs, could not be reduced by VIGS. Silencing was achieved for *FANCM* and *XRCC2* but only

XRCC2 had significant effects on CO rates. A reduction in fertility was also found when silencing *FANCM* but no effects were observed on CO rate. Fernandes et al. (2018) reported that a *fancm* mutant has no effect on recombination in Col/Ler hybrid *Arabidopsis*, as opposed to the significant increase in recombination in the col parent reported by Crismani et al. (2012). Since our experiment was done on a hybrid of wild emmer and durum wheat, the lack of effect of FANCM-VIGS on CO might be due to either hybridity or to inter-species differences. The best results in all parameters were obtained when silencing the *XRCC2* gene. In this treatment, no significant reduction in fertility was found while increase in recombination was observed not only in sub-telomeric but also in the peri-centromeric region.

Genome-Wide

The total number of CO events along the chromosomes using the markers or the GBS analysis showed no differences between WT or VIGS treatments. This implies that the distribution rather than the amount of crossovers was affected as a result of the treatments. Nevertheless, if even a small proportion of the total COs were "moved" toward the pericentric region, or another cold region including genes of interest, VIGS may improve our ability to break linkages between genes or to introduce new allelic variation to pericentric regions.

CONCLUSION

In this work we examined a new way to enhance recombination events in progenies of a hybrid tetraploid wheat. We used the VIGS method to silence meiotic anti CO genes and DNA methylation genes during meiosis. We found a redistribution of recombination events in euchromatic and heterochromatic regions when *MET1*, *DDM1,* and *XRCC2* were silenced. Applying this method on more genes (such as *CMT3*) or silencing few genes in parallel as was done in *Arabidopsis* may further enhance meiotic recombination. We showed that this method can be used as a simple fast and non-GMO tool to modify the recombination landscape and enhance variation in certain regions for more efficient plant breeding.

DATA AVAILABILITY STATEMENT

The data presented in the study are deposit in the Sequence Read Archive (SRA) at https://www.ncbi.nlm.nih.gov/sra/, accession numbers PRJNA691681, PRJNA691573, and PRJNA691706.

AUTHOR CONTRIBUTIONS

AL and AR designed the research and wrote the manuscript. AR performed the research. DL did InDels analysis. TD-M helped with GBS calibration and data analysis. TD-M and CM-B helped with library preparation and NGS sequencing. All authors contributed to the article and approved the submitted version.

FUNDING

This research was supported by United States–Israel Binational Agricultural Research and Development Fund Grant US-4828-15 (to Wojciech P. Pawlowski and Avraham A. Levy) and also by the Sir Charles Clore Postdoctoral Fellowship for 2016–2017.

ACKNOWLEDGMENTS

We thank Asaf Distelfeld for providing Zavitan seeds and genomic data. We also thank Naomi Avivi-Ragolski for her help with wheat hybridization and to Prof. Moshe Feldman for his help with the cytological analysis.

SUPPLEMENTARY MATERIAL

The Supplementary Material for this article can be found online at: https://www.frontiersin.org/articles/10.3389/fpls.2020.635139/full#supplementary-material

REFERENCES

Allers, T., and Lichten, M. (2001). Differential timing and control of noncrossover and crossover recombination during meiosis. *Cell* 106, 47–57. doi: 10.1016/S0092-8674(01)00416-0

Avni, R., Nave, M., Barad, O., Baruch, K., Twardziok, S. O., Gundlach, H., et al. (2017). Wild emmer genome architecture and diversity elucidate wheat evolution and domestication. *Science* 357, 93–97. doi: 10.1126/science.aan0032

Avni, R., Nave, M., Eilam, T., Sela, H., Alekperov, C., Peleg, Z., et al. (2014). Ultra-dense genetic map of durum wheat × wild emmer wheat developed using the 90K iSelect SNP genotyping assay. *Mol. Breed.* 34, 1549–1562. doi: 10.1007/s11032-014-0176-2

Baudat, F., Buard, J., Grey, C., Fledel-Alon, A., Ober, C., Przeworski, M., et al. (2010). PRDM9 is a major determinant of meiotic recombination hotspots in humans and mice. *Science* 327, 836–840. doi: 10.1126/science.1183439

Bennypaul, H. S., Mutti, J. S., Rustgi, S., Kumar, N., Okubara, P. A., and Gill, K. S. (2012). Virus-induced gene silencing (VIGS) of genes expressed in root, leaf, and meiotic tissues of wheat. *Funct. Integr. Genomics* 12, 143–156. doi: 10.1007/s10142-011-0245-0

Berchowitz, L. E., Hanlon, S. E., Lieb, J. D., and Copenhaver, G. P. (2009). A positive but complex association between meiotic double-strand break hotspots and open chromatin in Saccharomyces cerevisiae. *Genome Res.* 19, 2245–2257. doi: 10.1101/gr.096297.109

Bhullar, R., Nagarajan, R., Bennypaul, H., Sidhu, G. K., Sidhu, G., Rustgi, S., et al. (2014). Silencing of a metaphase I-specific gene results in a phenotype similar to that of the Pairing homeologous 1 (Ph1) gene mutations. *Proc. Natl. Acad. Sci. U.S.A.* 111, 14187–14192. doi: 10.1073/pnas.1416241111

Blary, A., Gonzalo, A., Eber, F., Bérard, A., Bergès, H., Fourment, J., et al. (2018). FANCM limits meiotic crossovers in brassica crops. *Front. Plant Sci.* 9:368. doi: 10.3389/fpls.2018.00368

Borde, V., and de Massy, B. (2013). Programmed induction of DNA double strand breaks during meiosis: setting up communication between DNA and the chromosome structure. *Curr. Opin. Genet. Dev.* 23, 147–155. doi: 10.1016/j.gde.2012.12.002

Börner, G. V., Kleckner, N., and Hunter, N. (2004). Crossover/noncrossover differentiation, synaptonemal complex formation, and regulatory surveillance at the leptotene/zygotene transition of meiosis. *Cell* 117, 29–45. doi: 10.1016/s0092-8674(04)00292-2

Calvo-Baltanás, V., Wijnen, C. L., Yang, C., Lukhovitskaya, N., de Snoo, C. B., Hohenwarter, L., et al. (2020). Meiotic crossover reduction by virus-induced gene silencing enables the efficient generation of chromosome substitution lines and reverse breeding in *Arabidopsis thaliana*. *Plant J.* 104, 1437–1452. doi: 10.1111/tpj.14990

Chen, C., Zhang, W., Timofejeva, L., Gerardin, Y., and Ma, H. (2005). The *Arabidopsis* ROCK-N-ROLLERS gene encodes a homolog of the yeast ATP-dependent DNA helicase MER3 and is required for normal meiotic crossover formation. *Plant J.* 43, 321–334. doi: 10.1111/j.1365-313X.2005.02461.x

Choi, K., Zhao, X., Kelly, K. A., Venn, O., Higgins, J. D., Yelina, N. E., et al. (2013). *Arabidopsis* meiotic crossover hot spots overlap with H2A.Z nucleosomes at gene promoters. *Nat. Genet.* 45, 1327–1336. doi: 10.1038/ng.2766

Choulet, F., Alberti, A., Theil, S., Glover, N., Barbe, V., Daron, J., et al. (2014). Structural and functional partitioning of bread wheat chromosome 3B. *Science* 345:1249721. doi: 10.1126/science.1249721

Copenhaver, G. P. (2005). Plant genetics: when not to interfere. *Curr. Biol.* 15, 290–291. doi: 10.1016/j.cub.2005.04.007

Corem, S., Doron-Faigenboim, A., Jouffroy, O., Maumus, F., Arazi, T., and Bouché, N. (2018). Redistribution of CHH methylation and small interfering RNAs across the genome of tomato ddm1 mutants. *Plant Cell* 30, 1628–1644. doi: 10.1105/tpc.18.00167

Crismani, W., Girard, C., Froger, N., Pradillo, M., Santos, J. L., Chelysheva, L., et al. (2012). FANCM limits meiotic crossovers. *Science* 336, 1588–1590. doi: 10.1126/science.1220381

Desjardins, S., Kanyuka, K., and Higgins, J. D. (2020b). "A cytological analysis of wheat meiosis targeted by virus-induced gene silencing (VIGS)," in *Plant Meiosis Methods and Protocols*, eds M. Pradillo and S. Heckmann (New York, NY: Springer Nature), 319–330. doi: 10.1007/978-1-4939-9818-0_22

Desjardins, S. D., Ogle, D. E., Ayoub, M. A., Heckmann, S., Henderson, I. R., Edwards, K. J., et al. (2020a). MutS homologue 4 and MutS homologue 5 maintain the obligate crossover in wheat despite stepwise gene loss following polyploidization1[CC-BY]. *Plant Physiol.* 183, 1545–1558. doi: 10.1104/pp.20.00534

Falque, M., Anderson, L. K., Stack, S. M., Gauthier, F., and Martin, O. C. (2009). Two types of meiotic crossovers coexist in maize. *Plant Cell* 21, 3915–3925. doi: 10.1105/tpc.109.071514

Fayos, I., Mieulet, D., Petit, J., Meunier, A. C., Périn, C., Nicolas, A., et al. (2019). Engineering meiotic recombination pathways in rice. *Plant Biotechnol. J.* 17, 2062–2077. doi: 10.1111/pbi.13189

Feldman, M. (1966). The effect of chromosomes 5B, 5D, and 5A on chromosomal pairing in triticum aestivum. *Proc. Natl. Acad. Sci. U.S.A.* 55, 1447–1453. doi: 10.1073/PNAS.55.6.1447

Fernandes, J. B., Séguéla-Arnaud, M., Larchevêque, C., Lloyd, A. H., and Mercier, R. (2018). Unleashing meiotic crossovers in hybrid plants. *Proc. Natl. Acad. Sci. U.S.A.* 115, 2431–2436. doi: 10.1073/PNAS.1713078114

Fu, F.-F., Dawe, R. K., and Gent, J. I. (2018). Loss of RNA-directed DNA methylation in maize chromomethylase and DDM1-type nucleosome remodeler mutants. *Plant Cell* 30, 1617–1627. doi: 10.1105/tpc.18.00053

Garrido, J., Aguilar, M., and Prieto, P. (2020). Identification and validation of reference genes for RT-qPCR normalization in wheat meiosis. *Sci. Rep.* 10:2726. doi: 10.1038/s41598-020-59580-5

Gaskell, L. J., Osman, F., Gilbert, R. J., and Whitby, M. C. (2007). Mus81 cleavage of Holliday junctions: a failsafe for processing meiotic recombination intermediates? *EMBO J.* 26, 1891–1901. doi: 10.1038/sj.emboj.7601645

Girard, C., Chelysheva, L., Choinard, S., Froger, N., Macaisne, N., Lemhemdi, A., et al. (2015). AAA-ATPase FIDGETIN-LIKE 1 and helicase FANCM antagonize meiotic crossovers by distinct mechanisms. *PLoS Genet.* 11:e1005369. doi: 10.1371/journal.pgen.1005369

Girard, C., Crismani, W., Froger, N., Mazel, J., Lemhemdi, A., Horlow, C., et al. (2014). FANCM-associated proteins MHF1 and MHF2, but not the other Fanconi anemia factors, limit meiotic crossovers. *Nucleic Acids Res.* 42, 9087–9095. doi: 10.1093/nar/gku614

Guillon, H., Baudat, F., Grey, C., Liskay, R. M., and de Massy, B. (2005). Crossover and noncrossover pathways in mouse meiosis. *Mol. Cell* 20, 563–573. doi: 10.1016/j.molcel.2005.09.021

Hartung, F., Suer, S., and Puchta, H. (2007). Two closely related RecQ helicases have antagonistic roles in homologous recombination and DNA repair in *Arabidopsis thaliana*. *Proc. Natl. Acad. Sci. U.S.A.* 104, 18836–18841. doi: 10.1073/pnas.0705998104

He, Y., Wang, M., Dukowic-Schulze, S., Zhou, A., Tiang, C.-L., Shilo, S., et al. (2017). Genomic features shaping the landscape of meiotic double-strand-break hotspots in maize. *Proc. Natl. Acad. Sci. U.S.A.* 114, 12231–12236. doi: 10.1073/pnas.1713225114

Higgins, J. D., Armstrong, S. J., Franklin, F. C. H., and Jones, G. H. (2004). The *Arabidopsis* MutS homolog AtMSH4 functions at an early step in recombination: evidence for two classes of recombination in *Arabidopsis*. *Genes Dev.* 18, 2557–2570. doi: 10.1101/gad.317504

Hodzic, D. M., Yeater, D. B., Bengtsson, L., Otto, H., and Stahl, P. D. (2004). Sun2 is a novel mammalian inner nuclear membrane protein. *J. Biol. Chem.* 279, 25805–25812. doi: 10.1074/jbc.M313157200

Hunter, N., and Kleckner, N. (2001). The single-end invasion: an asymmetric intermediate at the double-strand break to double-holliday junction transition of meiotic recombination. *Cell* 106, 59–70. doi: 10.1016/s0092-8674(01)00430-5

Ito, H., and Kakutani, T. (2014). Control of transposable elements in *Arabidopsis thaliana*. *Chromosom. Res.* 22, 217–223. doi: 10.1007/s10577-014-9417-9

Kankel, M. W., Ramsey, D. E., Stokes, T. L., Flowers, S. K., Haag, J. R., Jeddeloh, J. A., et al. (2003). *Arabidopsis* MET1 cytosine methyltransferase mutants. *Genetics* 163, 1109–1122.

Keeney, S., Giroux, C. N., and Kleckner, N. (1997). Meiosis-specific DNA double-strand breaks are catalyzed by Spo11, a member of a widely conserved protein family. *Cell* 88, 375–384. doi: 10.1016/S0092-8674(00)81876-0

Kurtz, S., Phillippy, A., Delcher, A. L., Smoot, M., Shumway, M., Antonescu, C., et al. (2004). Versatile and open software for comparing large genomes. *Genome Biol.* 5:R12. doi: 10.1186/gb-2004-5-2-r12

Lee, W. S., Rudd, J. J., and Kanyuka, K. (2015). Virus induced gene silencing (VIGS) for functional analysis of wheat genes involved in Zymoseptoria tritici susceptibility and resistance. *Fungal Genet. Biol.* 79, 84–88. doi: 10.1016/j.fgb.2015.04.006

Lhuissier, F. G. P., Offenberg, H. H., Wittich, P. E., Vischer, N. O. E., and Heyting, C. (2007). The mismatch repair protein MLH1 marks a subset of strongly interfering crossovers in tomato. *Plant Cell* 19, 862–876. doi: 10.1105/tpc.106.049106

Li, H. (2013). Aligning sequence reads, clone sequences and assembly contigs with BWA-MEM. *arXiv* [Preprint]. Available online at: http://arxiv.org/abs/1303.3997 (accessed October 14, 2020),

Li, H., Handsaker, B., Wysoker, A., Fennell, T., Ruan, J., Homer, N., et al. (2009). The sequence Alignment/Map format and SAMtools. *Bioinformatics* 25, 2078–2079. doi: 10.1093/bioinformatics/btp352

Liang, Z., Chen, K., Li, T., Zhang, Y., Wang, Y., Zhao, Q., et al. (2017). Efficient DNA-free genome editing of bread wheat using CRISPR/Cas9 ribonucleoprotein complexes. *Nat. Commun.* 8:14261. doi: 10.1038/ncomms14261

Lindroth, A. M. (2001). Requirement of chromomethylase 3 for maintenance of Cpxpg methylation. *Science* 292, 2077–2080. doi: 10.1126/science.1059745

Lyons, D. B., and Zilberman, D. (2017). DDM1 and lsh remodelers allow methylation of DNA wrapped in nucleosomes. *Elife* 6:e30674. doi: 10.7554/eLife.30674

Maccaferri, M., Harris, N. S., Twardziok, S. O., Pasam, R. K., Gundlach, H., Spannagl, M., et al. (2019). Durum wheat genome highlights past domestication signatures and future improvement targets. *Nat. Genet.* 51, 885–895. doi: 10.1038/s41588-019-0381-3

Melamed-Bessudo, C., and Levy, A. A. (2012). Deficiency in DNA methylation increases meiotic crossover rates in euchromatic but not in heterochromatic regions in *Arabidopsis*. *Proc. Natl. Acad. Sci. U.S.A.* 109, E981–E988. doi: 10.1073/pnas.1120742109

Mercier, R., Jolivet, S., Vezon, D., Huppe, E., Chelysheva, L., Giovanni, M., et al. (2005). Two meiotic crossover classes cohabit in *Arabidopsis*: one is dependent on MER3, whereas the other one is not. *Curr. Biol.* 15, 692–701. doi: 10.1016/j.cub.2005.02.056

Mercier, R., Mézard, C., Jenczewski, E., Macaisne, N., and Grelon, M. (2015). The molecular biology of meiosis in plants. *Annu. Rev. Plant Biol.* 66, 297–327. doi: 10.1146/annurev-arplant-050213-035923

Mézard, C. (2006). Meiotic recombination hotspots in plants. *Biochem. Soc. Trans.* 34, 531–534. doi: 10.1042/BST0340531

Mézard, C., Vignard, J., Drouaud, J., and Mercier, R. (2007). The road to crossovers: plants have their say. *Trends Genet.* 23, 91–99. doi: 10.1016/j.tig.2006.12.007

Mieulet, D., Aubert, G., Bres, C., Klein, A., Droc, G., Vieille, E., et al. (2018). Unleashing meiotic crossovers in crops. *Nat. Plants* 4, 1010–1016. doi: 10.1038/s41477-018-0311-x

Mirouze, M., Lieberman-Lazarovich, M., Aversano, R., Bucher, E., Nicolet, J., Reinders, J., et al. (2012). Loss of DNA methylation affects the recombination landscape in *Arabidopsis*. *Proc. Natl. Acad. Sci. U.S.A.* 109, 5880–5885. doi: 10.1073/pnas.1120841109

Myers, S., Bowden, R., Tumian, A., Bontrop, R. E., Freeman, C., MacFie, T. S., et al. (2010). Drive against hotspot motifs in primates implicates the PRDM9 gene in meiotic recombination. *Science* 327, 876–879. doi: 10.1126/science.1182363

Pan, J., Sasaki, M., Kniewel, R., Murakami, H., Blitzblau, H. G., Tischfield, S. E., et al. (2011). A hierarchical combination of factors shapes the genome-wide topography of yeast meiotic recombination initiation. *Cell* 144, 719–731. doi: 10.1016/j.cell.2011.02.009

Paszkowski, J. (2015). ScienceDirect Controlled activation of retrotransposition for plant breeding. *Curr. Opin. Biotechnol.* 32, 200–206. doi: 10.1016/j.copbio.2015.01.003

Poland, J. A., Brown, P. J., Sorrells, M. E., and Jannink, J. L. (2012). Development of high-density genetic maps for barley and wheat using a novel two-enzyme genotyping-by-sequencing approach. *PLoS One* 7:e32253. doi: 10.1371/journal.pone.0032253

Quinlan, A. R., and Hall, I. M. (2010). BEDTools: a flexible suite of utilities for comparing genomic features. *Bioinforma. Appl. Note* 26, 841–842. doi: 10.1093/bioinformatics/btq033

Rubin, E., and Levy, A. A. (1997). Abortive gap repair: underlying mechanism for Ds Element formation. *Mol. Cell. Biol.* 17, 6294–6302. doi: 10.1128/mcb.17.11.6294

Sánchez-León, S., Gil-Humanes, J., Ozuna, C. V., Giménez, M. J., Sousa, C., Voytas, D. F., et al. (2018). Low-gluten, nontransgenic wheat engineered with CRISPR/Cas9. *Plant Biotechnol. J.* 16, 902–910. doi: 10.1111/pbi.12837

Séguéla-Arnaud, M., Choinard, S., Larchevêque, C., Girard, C., Froger, N., Crismani, W., et al. (2017). RMI1 and TOP3α limit meiotic CO formation through their C-terminal domains. *Nucleic Acids Res.* 45, 1860–1871. doi: 10.1093/nar/gkw1210

Séguéla-Arnaud, M., Crismani, W., Larchevêque, C., Mazel, J., Froger, N., Choinard, S., et al. (2015). Multiple mechanisms limit meiotic crossovers: TOP3α and two BLM homologs antagonize crossovers in parallel to FANCM. *Proc. Natl. Acad. Sci. U.S.A.* 112, 4713–4718. doi: 10.1073/pnas.1423107112

Serra, H., Da Ines, O., Degroote, F., Gallego, M. E., and White, C. I. (2013). Roles of XRCC2, RAD51B and RAD51D in RAD51-independent SSA recombination. *PLoS Genet.* 9:e1003971. doi: 10.1371/journal.pgen.1003971

Shilo, S., Melamed-Bessudo, C., Dorone, Y., Barkai, N., and Levy, A. A. (2015). DNA crossover motifs associated with epigenetic modifications delineate open chromatin regions in *Arabidopsis*. *Plant Cell* 27, 2427–2436. doi: 10.1105/tpc.15.00391

Smagulova, F., Gregoretti, I. V., Brick, K., Khil, P., Camerini-Otero, R. D., and Petukhova, G. V. (2011). Genome-wide analysis reveals novel molecular features of mouse recombination hotspots. *Nature* 472, 375–378. doi: 10.1038/nature09869

Underwood, C. J., Choi, K., Lambing, C., Zhao, X., Serra, H., Borges, F., et al. (2018). Epigenetic activation of meiotic recombination near *Arabidopsis thaliana* centromeres via loss of H3K9me2 and non-CG DNA methylation. *Genome Res.* 28, 519–531. doi: 10.1101/gr.227116.117

Wan, L., de los Santos, T., Zhang, C., Shokat, K., and Hollingsworth, N. M. (2004). Mek1 kinase activity functions downstream of RED1 in the regulation of meiotic double strand break repair in budding yeast. *Mol. Biol. Cell* 15, 11–23. doi: 10.1091/mbc.e03-07-0499

Whitby, M. C. (2005). Making crossovers during meiosis. *Biochem. Soc. Trans.* 33, 1451–1455. doi: 10.1042/BST0331451

Yuan, C., Li, C., Yan, L., Jackson, A. O., Liu, Z., Han, C., et al. (2011). A high throughput barley stripe mosaic virus vector for virus induced gene silencing in monocots and dicots. *PLoS One* 6:e26468. doi: 10.1371/journal.pone.0026468

Zhang, Y., Liang, Z., Zong, Y., Wang, Y., Liu, J., Chen, K., et al. (2016). Efficient and transgene-free genome editing in wheat through transient expression of CRISPR/Cas9 DNA or RNA. *Nat. Commun.* 7:12617. doi: 10.1038/ncomms12617

Zhu, T., Wang, L., Rodriguez, J. C., Deal, K. R., Avni, R., Distelfeld, A., et al. (2019). Improved genome sequence of wild emmer wheat zavitan with the aid of optical maps. *G3 (Bethesda)* 9, 619–624. doi: 10.1534/g3.118.200902

Conflict of Interest: The authors declare that the research was conducted in the absence of any commercial or financial relationships that could be construed as a potential conflict of interest.

frontiers in Plant Science

ORIGINAL RESEARCH
published: 12 February 2021
doi: 10.3389/fpls.2021.631323

Distal Bias of Meiotic Crossovers in Hexaploid Bread Wheat Reflects Spatio-Temporal Asymmetry of the Meiotic Program

Kim Osman[1]*, *Uthman Algopishi*[1], *James D. Higgins*[2], *Ian R. Henderson*[3], *Keith J. Edwards*[4], *F. Chris H. Franklin*[1] and *Eugenio Sanchez-Moran*[1]*

[1] School of Biosciences, University of Birmingham, Birmingham, United Kingdom, [2] Department of Genetics and Genome Biology, University of Leicester, Leicester, United Kingdom, [3] Department of Plant Sciences, University of Cambridge, Cambridge, United Kingdom, [4] School of Biological Sciences, University of Bristol, Bristol, United Kingdom

OPEN ACCESS

Edited by:
Mónica Pradillo, Complutense University of Madrid, Spain

Reviewed by:
Dylan Wyn Phillips, Aberystwyth University, United Kingdom
Pierre Sourdille, INRAE Clermont-Auvergne-Rhône-Alpes, France

***Correspondence:**
Kim Osman
k.osman@bham.ac.uk
Eugenio Sanchez-Moran
e.sanchezmoran@bham.ac.uk

Specialty section:
This article was submitted to Plant Cell Biology, a section of the journal Frontiers in Plant Science

Received: 19 November 2020
Accepted: 18 January 2021
Published: 12 February 2021

Citation:
Osman K, Algopishi U, Higgins JD, Henderson IR, Edwards KJ, Franklin FCH and Sanchez-Moran E (2021) Distal Bias of Meiotic Crossovers in Hexaploid Bread Wheat Reflects Spatio-Temporal Asymmetry of the Meiotic Program. Front. Plant Sci. 12:631323. doi: 10.3389/fpls.2021.631323

Meiotic recombination generates genetic variation and provides physical links between homologous chromosomes (crossovers) essential for accurate segregation. In cereals the distribution of crossovers, cytologically evident as chiasmata, is biased toward the distal regions of chromosomes. This creates a bottleneck for plant breeders in the development of varieties with improved agronomic traits, as genes situated in the interstitial and centromere proximal regions of chromosomes rarely recombine. Recent advances in wheat genomics and genome engineering combined with well-developed wheat cytogenetics offer new opportunities to manipulate recombination and unlock genetic variation. As a basis for these investigations we have carried out a detailed analysis of meiotic progression in hexaploid wheat (*Triticum aestivum*) using immunolocalization of chromosome axis, synaptonemal complex and recombination proteins. 5-Bromo-2′-deoxyuridine (BrdU) labeling was used to determine the chronology of key events in relation to DNA replication. Axis morphogenesis, synapsis and recombination initiation were found to be spatio-temporally coordinated, beginning in the gene-dense distal chromosomal regions and later occurring in the interstitial/proximal regions. Moreover, meiotic progression in the distal regions was coordinated with the conserved chromatin cycles that are a feature of meiosis. This mirroring of the chiasma bias was also evident in the distribution of the gene-associated histone marks, H3K4me3 and H3K27me3; the repeat-associated mark, H3K27me1; and H3K9me3. We believe that this study provides a cytogenetic framework for functional studies and ongoing initiatives to manipulate recombination in the wheat genome.

Keywords: ***Triticum aestivum*** **(bread wheat), meiosis, recombination, crossovers, distal bias, DNA double-strand breaks, immunolocalization**

INTRODUCTION

Utilizing the genetic variation that arises from meiotic recombination plays a pivotal role in crop improvement programs. Although substantial progress has been made in recent decades in the improvement of yield of major crops such as wheat, rice, and maize, the existential threat of climate change introduces additional demands for crops that are sufficiently robust to maintain

yield in the face of biotic and abiotic challenges (Halford et al., 2015). This is exacerbated by an increase in human population and individual wealth within many countries which places additional demands on food production (Hickey et al., 2019). Hexaploid wheat is the most widely grown cereal crop, currently accounting for 20% of the calories and protein consumed by humans and an important source of vitamins and micronutrients (Shewry, 2009). The recent establishment of a fully-annotated bread wheat reference genome and ensuing genomics resources promises to revolutionize functional studies and trait discovery for the improvement of crop varieties (IWGSC, 2018; Adamski et al., 2020). In order to fully benefit from the new technological developments and face future challenges a thorough understanding of the wheat meiotic recombination pathway will also be required.

Gamete formation in most sexually reproducing organisms is achieved through meiosis, a specialized form of cell-division in which S-phase is followed by two sequential rounds of nuclear division. During prophase I of meiosis homologous recombination (HR) between maternal and paternal chromosomes results in the reciprocal exchange of genetic information to form genetic crossovers (COs), which are manifested cytologically as chiasmata. CO formation gives rise to novel allelic combinations thereby generating genetic variation and is essential for accurate segregation of the homologous chromosomes (homologs) at the first meiotic division. A subsequent second division separates the sister chromatids to form haploid gametes.

Meiotic HR is initiated by the programmed formation of numerous DNA double-strand breaks (DSBs) catalyzed by the SPO11 complex supported by various accessory proteins (Lam and Keeney, 2014). In Arabidopsis, the SPO11 complex comprises two A subunits (SPO11-1 and SPO11-2) and two B subunits (MTOPVIB), forming a heteromeric complex (Stacey et al., 2006; Vrielynck et al., 2016). The genomic distribution of DSBs is non-random, preferentially forming in short regions referred to as DSB hotspots (Baudat and Nicolas, 1997; Smagulova et al., 2011; Choi et al., 2013). In Arabidopsis and maize meiotic DSB hotspots are associated with open chromatin, occurring in regions of low nucleosome density in gene promoters and specific classes of transposons, but differ from mammalian hotspots in their complex relationship with the open chromatin mark histone H3 lysine 4 tri-methyl (H3K4me3) (Choi et al., 2018). DSBs are resected by the MRX/N complex to reveal single-stranded DNA overhangs that are bound by RPA, followed by the strand invasion proteins RAD51 and DMC1 (Osman et al., 2011). To ensure that a proportion of the DSBs are repaired as CO products, the initial RAD51/DMC1 catalyzed strand-exchange stage is biased toward use of the homologous chromosome as the repair template (Schwacha and Kleckner, 1997). In plants, fewer than 10% of the DSBs are repaired as COs and the remainder as non-COs (Mercier et al., 2015). Repair is controlled such that a minimum of one, obligate, CO per homolog pair (bivalent) is formed (Jones and Franklin, 2006). Additional COs are subject to a patterning phenomenon known as CO interference, which results in COs being well-spaced along chromosomes (Jones and Franklin, 2006). In Arabidopsis, formation of these Class I COs, which amount to around 85% of total COs, requires the activities of the ZMM recombination proteins: Zip2/SHOC1, Zip3/HEI10, ZIP4, MSH4, MSH5, and MER3 (Higgins et al., 2004, 2008b; Mercier et al., 2005; Chelysheva et al., 2007, 2012; Macaisne et al., 2008, 2011). The remaining COs (Class II) are not sensitive to interference and in part, require the activity of MUS81 recombinase (Higgins et al., 2008a).

HR is accompanied by programmed remodeling of the meiotic chromosomes (Zickler and Kleckner, 1999). Following S-phase, pairs of sister chromatids are linked by cohesin proteins (Haering and Jessberger, 2012). At the onset of leptotene, the sister chromatids become organized into linear looped arrays that are conjoined at the loop bases by a proteinaceous axis that is elaborated along their length (Zickler and Kleckner, 1999). As leptotene transitions into zygotene, the homologs progressively align before coming into close apposition through the formation of the synaptonemal complex (SC) (Zickler and Kleckner, 1998). The SC has a tripartite structure comprising the chromosome axes, now referred to as lateral elements, cross-linked by overlapping transverse filament proteins (Page and Hawley, 2004). At pachytene the SC is fully polymerized along the length of the synapsed homologs. By diplotene CO formation is completed, the SC disassembles and the homologs become progressively condensed appearing at diakinesis as bivalents linked by one or more chiasmata. At metaphase I the bivalents align on the equator prior to the first meiotic division. Mutant analysis in a wide variety of organisms including plants has found that HR and meiotic chromosome remodeling are highly interdependent (Osman et al., 2011; Mercier et al., 2015).

One of the limitations in most crop species is that meiotic CO frequency is rather low, typically 1–3 COs per bivalent (Higgins et al., 2014). In addition, in many species CO distribution exhibits a tendency to localize in particular chromosomes regions, often favoring distal regions (Jones, 1984). This is particularly evident in cereals with large genomes, for example wheat and barley, where a strong distal CO bias limits their formation in interstitial and proximal chromosome regions amounting to 50–70% of the overall genome (Choulet et al., 2014; Higgins et al., 2014).

Studies in Arabidopsis have revealed that it is possible to significantly enhance the level of Class II COs through the mutation of anti-recombination genes, *FANCM*, *RECQ4,* and *FIGL1* (Crismani et al., 2012; Girard et al., 2015; Séguéla-Arnaud et al., 2015). In other work in Arabidopsis the meiotic E3 ligase, *HEI10*, has been found to regulate the level of Class I interfering COs (Chelysheva et al., 2012; Ziolkowski et al., 2017; Serra et al., 2018). When *HEI10* over-expression was combined with *recq4a* and *recq4b* mutations the combined number of Class I and Class II COs was boosted from an average of 7.5–31 in individual F_2 plants (Serra et al., 2018). Mutation of the recombination suppressor genes has been investigated in three crop species, rice (*Oryza sativa*), pea (*Pisum sativum*), and tomato (*Solanum lycopersicum*) where it was found that mutation of *recq4* increased COs by a factor of ∼3-fold (Mieulet et al., 2018). Whether a similar impact on CO frequency will occur in large genome crops such as wheat and barley remains to be determined. Also, the hyper-rec mutants exhibit some evidence

of reduced fertility and meiotic defects, which may prove more problematic in species with larger genomes (Fernandes et al., 2018). Furthermore, it appears that recombination-cold proximal/pericentromeric regions of chromosomes are relatively insensitive to the effects of hyper-rec mutants and *HEI10* overexpression (Serra et al., 2018).

Thus, despite substantial progress in manipulating meiotic CO frequency, effective application of these and other approaches such as targeting DSB sites will need refining if they are to be successfully employed in species such as wheat and barley, underlining the requirement for a detailed understanding of the meiotic pathway in these species. In a previous study we investigated meiotic progression in barley (Higgins et al., 2012). Unlike barley which is a diploid species, bread wheat, *Triticum aestivum,* is an allohexaploid, with 3 sub-genomes A, B, and D resulting from a double polyploidization process involving three related species (Sears, 1948). Despite being hexaploid, the presence of the *Ph1* locus enables bread wheat to behave as a diploid during meiosis by its influence on pairing of the homoeologous chromosomes and recombination (Riley and Chapman, 1958; Sears and Okamoto, 1958). The role of the *Ph1* locus has been studied extensively and was suggested to be two-fold. First, it was proposed that a cluster of Cdk2-like and S-adenosyl methionine-dependent methyltransferase (SAM-MTase) genes within the locus promote homologous chromosome pairing through an effect on chromatin structure and histone H1 phosphorylation and an associated change in the rate of pre-meiotic replication and subsequent synapsis (Greer et al., 2012; Rey and Prieto, 2014; Martín et al., 2017). Second, a paralog of the ZMM gene *ZIP4* within the *Ph1* region was reported to promote the maturation of late recombination complexes to form homologous COs (Martín et al., 2014, 2017; Rey et al., 2017). It now appears that the *ZIP4* paralogue may be responsible for most, if not all, of the *Ph1* effect (Rey et al., 2018). Apart from the analysis of *Ph1*, functional studies of wheat meiotic genes remain limited, with little over 10% of those described in other plant species (notably Arabidopsis, rice and maize), having been analyzed even to a limited degree (Da Ines et al., 2020). Nevertheless, the availability of TILLING populations and gene editing techniques is enabling progress as evidenced by recent analysis of *T. aestivum SPO11-2* and *T. turgidum MSH4/5* (Benyahya et al., 2020; Desjardins et al., 2020).

Here we present a detailed cytological overview of the meiotic program in Cadenza, a widely-used research variety with an EMS-induced TILLING mutant population (Rakszegi et al., 2010; Krasileva et al., 2017). We investigate how chromosome remodeling throughout prophase I is integrated with the recombination machinery and show that there is a spatio-temporal bias in the initiation and progression of recombination that mirrors the tendency of chiasmata/COs to occur in gene-dense distal regions of the chromosomes. We establish a time-frame for the duration of meiosis and confirm that wheat chromatin undergoes cycles of contraction and expansion during prophase I, as previously observed in barley and other species. Finally, we note and discuss interesting features of ASY1 and ZYP1 protein localization during the meiotic program. We believe this study will provide a reference framework for CO modification initiatives and functional studies of meiotic recombination for the benefit of crop improvement.

MATERIALS AND METHODS

Plant Material

T. aestivum cv. Cadenza was obtained from www.SeedStor.ac.uk. Plants were grown in a controlled environment with photoperiod 16 h, temperature 20°C and relative humidity 60%.

Antibody Production

AtHEI10 amino-acid residues 1–183 was expressed as a recombinant protein and purified from *E. coli.* Antibody was raised in rabbit (PTU/BS, Scottish National Blood Transfusion Service, now www.orygen.co.uk). Anti-TaCENH3 was raised in rabbit against a 19-residue peptide from the N-terminal of the protein [ARTKHPAVRKTKAPPKKQL-[C]-amide] conjugated to KLH (www.crbdiscovery.com).

Cytological Procedures

Meiotic chromosome spreads were prepared from anthers isolated at the required stage of meiosis. For chiasma counts anthers were fixed and slides prepared according to Howell and Armstrong (2013) with minor modifications: anthers were macerated in 70% acetic acid and incubated for 1 min on a 45°C hot-plate before fixing with 130 μl cold fixative (3 parts of absolute ethanol: 1 part of glacial acetic acid) and staining with 5 μg ml^{-1} 4′,6-diamidino-2-phenylindole (DAPI) in Vectashield (Vector Labs). For immunolocalization, slides were prepared as described for *Brassica oleracea* in Armstrong et al. (2002) with the following modifications: ∼20 anthers were digested in 20 μl enzyme mix (0.4% cytohelicase, 1.5% sucrose, 1% polyvinylpyrrolidone) in a cavity slide inside a humidified chamber at 37°C. After 4 min anthers were gently crushed to release pollen mother cells (PMCs), anther debris was quickly removed with a needle and digestion continued for a further 3 min. Up to 4 slides were prepared from each 20 μl digestion mix and PMCs were accurately staged using anti-AtASY1 and anti-AtZYP1 antibodies. Primary antibodies were used at the following dilutions: anti-AtASY1 rat, rabbit or guinea-pig, 1:500 (Armstrong et al., 2002); anti-AtZYP1 rabbit or guinea-pig, 1:500 (Higgins et al., 2005; Osman et al., 2018); anti-HsγH2A.X rabbit, 1:100 (Millipore); anti-AtDMC1 rabbit, 1:200 (Sanchez-Moran et al., 2007); anti-AtRAD51 rabbit, 1:200 (Mercier et al., 2003); anti-AtMSH4 rabbit, 1:200 (Higgins et al., 2004); anti-AtMSH5 rabbit, 1:200 (Higgins et al., 2008b); anti-AtHEI10 rabbit and HvHEI10 rabbit, 1:200 (see above and Lambing et al., 2015; Desjardins et al., 2020); anti-HvMLH3 rabbit, 1:200 (Phillips et al., 2013); anti-TaCENH3 rabbit, 1:200 (see above); H3K4me3, H3K27me1, H3K27me3, and H3K9me3 rabbit, according to the manufacturer's guidelines (Diagenode). For combined immunofluorescence and fluorescence *in situ* hybridization (FISH) of telomeric repeat sequences, slides were first prepared as for immunolocalization and the primary antibody applied (see above). After incubation and washing to remove unbound serum, the primary antibody was blocked with a secondary antibody-biotin conjugate at 1:100 in 1% bovine

serum albumin (BSA), in 1X phosphate buffered saline, 0.1% Triton X100 (PBST). Slides were incubated for 30 min at 37°C, washed 3 times with PBST and an Arabidopsis telomeric-repeat FISH probe labeled with digoxigenin (Armstrong et al., 2001) was applied as described in Armstrong (2013). Secondary antibodies were FITC (green), Alexa Fluor 350 (blue), Cy3 or Alexa Fluor 594 (red) conjugates (Sigma; Thermo Fisher). Nuclear size was determined according to Higgins et al. (2012) using NIS Elements software (Nikon).

Meiotic Time Course

Up to 0.5 ml BrdU (10 mM in 1X PBS, 0.1% Tween 20) was injected into the cavity above a developing wheat spike (taken as time 0). The spike was subsequently harvested at a defined time point and anthers of an appropriate size for meiosis were excised and fixed in 3:1 ethanol:acetic acid. Eight time points spanning the entire meiotic program were analyzed, each using a different spike/plant, and two replicates were analyzed for each. For each time-point, all stages of the meiotic program were assessed for BrdU labeling. Slides were prepared as for chiasma counts (see above), then made ready for immunolocalization by a modification of Chelysheva et al. (2010): slides were heated in 10 mM citrate buffer pH 6 in a 850 W microwave for 45 s (taking care not to let the buffer boil), then immediately transferred to PBST for 10 min. Standard immunolocalization (see above) was then used to detect ASY1/ZYP1 and incorporated BrdU (Armstrong et al., 2002). BrdU labeling reagent, mouse anti-BrdU antibody and anti-mouse Ig-fluorescein were from Roche.

Microscopy

Fluorescence microscopy was carried out using a Nikon Eclipse 90i microscope fitted with a Nikon DS-Qi1Mc camera. NIS Elements software (Nikon) was used to capture images as z-stacks with a 0.2 μM z-step and to carry out simple processing steps such as color balance adjustment and creation of composite images. For accuracy, chiasmata were interpreted and counted by examining all individual z-frames within a nucleus. Recombination foci were counted using single z-frames from the raw data files in order to clearly distinguish individual foci, confirm axis/SC-association and avoid the saturation of signal that can occur in composite images. All z-frames within a nucleus were counted - the count tool in NIS Elements was used to mark scored foci, thus preventing double counting when moving between frames. All in-focus foci (for the particular frame in question) were counted. Where necessary, the NIS Elements Gauss-Laplace sharpen tool was used to help resolve close-together foci. Any rare, aggregates of foci which could not be resolved at this level, were scored only once. An example image, with marked counted foci, is shown in **Supplementary Figure 1**.

Statistics

Nuclear size and recombination foci count differences were tested for significance using single-factor Anova.

RESULTS

Chiasmata Are Predominantly Distal in Hexaploid Wheat cv. Cadenza

A cytological analysis of chiasma frequency and distribution was carried out in pollen mother cells (PMCs) of Cadenza, a UK spring wheat variety which forms the background for an EMS-induced TILLING mutant population (Rakszegi et al., 2010; Krasileva et al., 2017). Despite having three related sub-genomes (A, B, and D), hexaploid wheat ($2n = 42$) behaves as a diploid during meiosis due to the presence of the *Ph1* locus (Riley and Chapman, 1958; Sears and Okamoto, 1958), the major regulator of homoeologue pairing and recombination which ensures that recombination is restricted to true homologs rather than homoeologues (equivalent chromosomes from the other sub-genomes). Thus, Cadenza usually forms 21 bivalents at metaphase I (**Figure 1A**). Chiasmata, the cytological manifestation of COs, were interpreted according to bivalent shape at metaphase I, allowing a determination of their relative position along chromosomes (Sybenga, 1975). The vast majority of bivalents (93%, $n = 1337$) were "ring" bivalents, with at least one chiasma in each chromosome arm, while "rod" bivalents possessed chiasmata in only one arm (**Figure 1B**). The mean number of chiasmata per PMC was 41.8 ± 0.28 ($n = 64$) (**Figure 1C**) and the majority (88%) were distal (near the telomeres) (**Figure 1B**). Of these 76% were classified as terminal, as they could not be visually resolved from the telomeres in the highly condensed metaphase I bivalents. The remaining 12% were classified as sub-terminal, as they were close to, but clearly distinguishable from, the chromosome ends (**Figure 1B**).

Chromosome Axis Formation and Synapsis Are Initially Polarized to the Distal Regions

During early prophase I, the telomeres of many species, including cereal grasses, cluster together and attach to the nuclear membrane in a highly conserved organization known as the "bouquet" (Chikashige et al., 1994). It was proposed that this configuration promotes initial contacts between homologous chromosomes, with subsequent alignment and synapsis facilitated by telomere-led movements driven by the cytoskeleton, although the functional significance of the bouquet is still a matter of debate (Zickler and Kleckner, 2016; Zeng et al., 2018).

Previous analysis of plant meiotic chromosomes using electron microscopy indicated that synapsis initiates in the distal chromosomal regions, close to the telomeres (Albini et al., 1984). More recently, immunolocalization using antibodies which recognize components of the meiotic chromosome axis and synaptonemal complex (SC) have enabled more detailed analysis of axis formation and synapsis in a range of plant species, including cereals (Golubovskaya et al., 2006; Mikhailova et al., 2006; Boden et al., 2009; Higgins et al., 2012; Khoo et al., 2012; Sepsi et al., 2017). For Cadenza, we combined immunofluorescence with fluorescence *in situ* hybridization (FISH) of telomeric repeat sequences to investigate

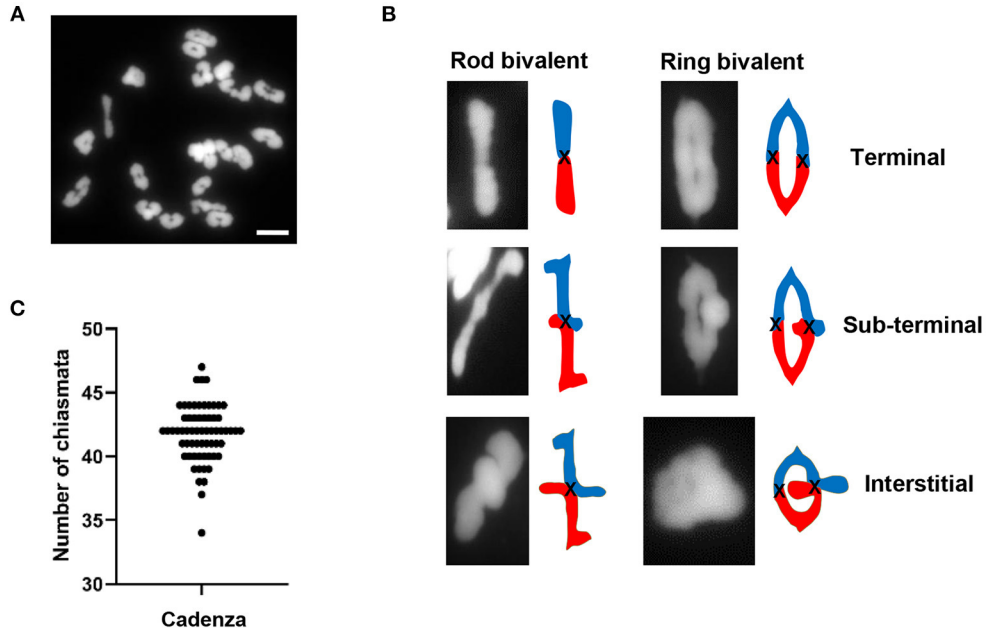

FIGURE 1 | Chiasma frequency of *T. aestivum* cv. Cadenza. **(A)** Chromosome spread of metaphase I PMC showing 21 DAPI-stained bivalents. **(B)** Bivalent shapes at metaphase I indicate number and position of chiasmata. **(C)** Number of chiasmata per PMC ($n = 64$). Bar = 10 μM.

axis morphogenesis and SC formation in conjunction with telomere dynamics.

The HORMA domain protein, ASY1, is a component of the meiotic chromosome axis essential for synapsis and wild type levels of COs (Caryl et al., 2000; Armstrong et al., 2002; Sanchez-Moran et al., 2007). In Arabidopsis and Brassica, ASY1 initially forms numerous foci throughout the nucleus in G2 (Armstrong et al., 2002; Sanchez-Moran et al., 2007). These then associate with the developing chromosome axis to form a linear signal along each pair of conjoined sister chromatids, which is characteristic of the leptotene sub-stage of prophase I. In PMCs of Cadenza, ASY1 also first appeared as weak foci throughout G2 nuclei (**Figure 2A**). At this stage, up to 84 widely dispersed telomeric FISH signals were observed (mean per nucleus = 69.4 ± 4.7; range = 49–84; $n = 9$), which tended to occupy one hemisphere of the nucleus. This is consistent with a pre-meiotic Rabl configuration of chromosomes, with telomeres and centromeres oriented to opposite hemispheres of the nucleus (Cowan et al., 2001; Sepsi et al., 2017). Telomere distribution then became more restricted, they began to cluster and ASY1 started to form short linear stretches around this region (**Figure 2B**). This was accompanied by an increase in ASY1 signal intensity in this region relative to the rest of the nucleus. As meiosis progressed, the number of telomere signals reduced as clustering continued, eventually forming the tight bouquet configuration which persisted during progressive linearization of the ASY1 signal throughout the more interstitial regions of the chromosomes (**Figure 2C**). By the time bouquet formation was complete, the ASY1 signal appeared highly enriched in the sub-telomeric (or distal) regions of chromosomes. This phenomenon was highly distinctive and could be used as a diagnostic marker for the bouquet region at this stage.

During zygotene, the SC forms between the aligned pairs of homologous chromosomes (Zickler and Kleckner, 1999; Page and Hawley, 2004). In Cadenza, development of the SC was monitored by immunolocalization of the transverse filament protein, ZYP1 (Higgins et al., 2005). In late leptotene, before any linear SC signal was observed, ZYP1 formed distinctive axis-associated foci distributed throughout the nucleus (mean no. of foci per nucleus = 83.9 ± 6.2; range = 28–128; $n = 20$). From now on, these will be referred to as "presynaptic" ZYP1 foci. They appeared after bouquet formation but before the ASY1 signal was completely continuous throughout the entire nucleus (**Figure 2D**) and dual localization with γH2A.X suggested they were located at a subset of DSB sites (see below and **Supplementary Figure 2**). At this stage the centromeric regions, marked by CENH3, were clustered in the opposite half of the nucleus to the distal regions and there was no particular colocalisation of the ZYP1 antibody with the centromeres (**Figure 2E** and **Supplementary Figure 3**). In early zygotene, ZYP1 began to form a linear signal in the distal regions. This signal continued to extend, coupled with the emergence of small foci and short stretches of ZYP1 in the interstitial regions, suggesting that SC formation initiates first in the sub-telomeric regions (**Figure 2F**). Later, some of the interstitial signals were observed to become more linear but by this time SC formation from the bouquet region was already well-established (**Figure 2G**). The telomere bouquet and the centromeres remained at opposite poles of the nucleus at least during the early stages of telomere-led synapsis

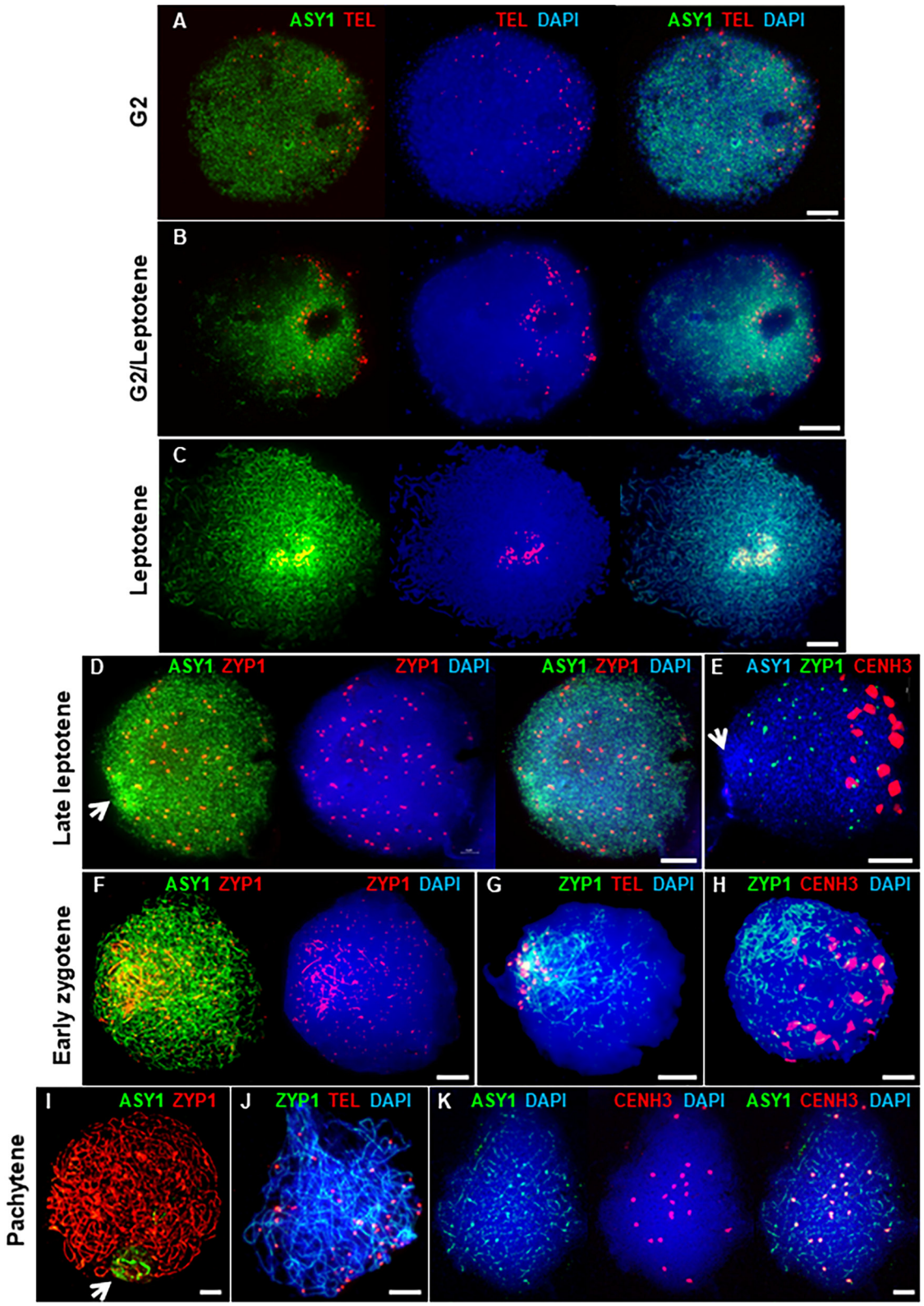

FIGURE 2 | Axis and SC development in Cadenza. **(A–C)** Early prophase I showing bouquet formation. **(A)** G2: ASY1 foci and individual telomeres are widely distributed. **(B)** G2/Leptotene: telomeres begin to cluster and ASY1 linearization and enrichment begins in surrounding region. **(C)** Leptotene: telomeres are

(Continued)

FIGURE 2 | tightly clustered and ASY1 continues to linearize, appearing highly enriched in the bouquet region. **(D–K)** Synaptic stages. **(D,E)** ZYP1 forms presynaptic foci throughout the nucleus. Arrows mark ASY1 signal enrichment in the bouquet region. **(F–H)** Initial stretches of SC form in the distal regions. **(I–K)** Full synapsis. **(I)** ZYP1 forms a linear signal throughout the nucleus and ASY1 signal intensity is reduced apart from in the nucleolar region (arrow). **(J)** By pachytene telomere pairs are widely distributed. **(K)** Residual ASY1 signal is weakly enriched in paired centromeric regions. DNA is stained with DAPI (blue). For clarity, some images are shown in several color combinations. Bar = 10 μM.

(**Figures 2G,H**). As synapsis progressed the linear ZYP1 signals gradually extended, replacing the intense ASY1 signal as the chromosome axes were remodeled (Lambing et al., 2015). By pachytene, the linear ZYP1 signal extended throughout the nucleus and very little intense ASY1 signal remained apart from near the nucleolus (**Figure 2I**), consistent with observations in Arabidopsis that the nucleolar organizing regions do not undergo synapsis (Sims et al., 2019). At this stage, paired telomeres were no longer in the tight bouquet organization but were again widely dispersed (**Figure 2J**). Interestingly, although ASY1 signal was very weak when chromosomes were fully synapsed at pachytene, it was clearly enriched at the 21 pairs of centromeres (**Figure 2K**).

In summary, axis formation and synapsis were spatially asynchronous, beginning in the sub-telomeric (distal) regions of chromosomes before progressing to the interstitial and centromere proximal regions. During prophase I, the distal regions may therefore be considered to be in advance of the interstitial and proximal regions at any given time. For simplicity, we have taken the onset of leptotene and zygotene to be the start of ASY1 and ZYP1 signal linearization in the distal regions, respectively, although it will be appreciated that the interstitial/proximal regions will be lagging with respect to these stages.

Chronology of Prophase I

To determine the chronology of the spatial asymmetry of axis formation and synapsis, we carried out an immunocytological time-course by monitoring ASY1 or ZYP1 localization in combination with 5-Bromo-2′-deoxyuridine (BrdU) labeling of replicating DNA in S-phase. BrdU delivery was based on a method developed for Arabidopsis (Armstrong et al., 2003) but involved direct injection of the growing plant as previously described for barley (Higgins et al., 2012; Ahn et al., 2020). BrdU was injected into the cavity above the developing spike (taken as Time 0 h) and followed by fixation of anthers at set time-points in order to determine the time taken from injection to landmark features of axis and SC development (as defined by ASY1 and ZYP1 localization, see above). For visualizing incorporated BrdU and ASY1/ZYP1 in PMCs we modified a previously described Arabidopsis immunolocalization protocol (Chelysheva et al., 2010). This enabled BrdU and ASY1/ZYP1 to be simultaneously labeled in fixed tissue chromosome spreads in one procedure. For each sample time, BrdU labeling of a subset of somatic anther nuclei provided a positive control for successful uptake into the anther, regardless of whether PMCs were labeled at that particular stage. For each time-point, we examined all meiotic stages in order to determine the latest meiotic stage to have incorporated BrdU, thus establishing a minimum time-frame for progression to that stage. For all time-points this assessment was based on observing a minimum of 20 BrdU labeled nuclei. For most time-points we also observed BrdU labeling of earlier stages (**Supplementary Table 1**). This variation was not surprising and could be due to several factors, including PMCs being at different stages of S-phase when exposed to BrdU, variation in the rate of meiotic progression between PMCs or differences in the time taken for BrdU to reach individual anthers. **Figure 3** shows the latest BrdU labeled stage for each time-point (see also **Supplementary Table 1**). ASY1 was detected as foci by 4 h after BrdU injection (**Figure 3A**) and by 7 h had begun to form short linear stretches and appear polarized (**Figure 3B**). By 16 h the characteristic region of highly enriched ASY1 signal indicative of the bouquet had formed (**Figure 3C**). ZYP1 foci were apparent by 21 h (**Figure 3D**) and between 21 and 24 h short stretches of SC began to form in the distal regions (**Figures 3E,F**). By 24 h, after the appearance of linear stretches of SC, the ZYP1 antibody also appeared to strongly mark several large structures at the opposite pole of the nucleus (**Figure 3F**). These were similar in appearance and distribution to the CENH3 signals in **Figures 2E,H** and were thought to be clustered centromeres. Marking of these structures by the ZYP1 antibody appeared transient; it was not observed at the pre-synaptic ZYP1 foci stage, prior to linear SC formation (**Figures 2D,E**, **3D** and **Supplementary Figure 3**), and became less obvious as synapsis progressed. Similar ZYP1 marking of the centromeric regions at specific stages of prophase I was reported in *T. aestivum* cv. Chinese Spring (Sepsi et al., 2017). As prophase I progressed, ZYP1 signal extension continued (**Figure 3G**) throughout the nucleus until full synapsis at pachytene and then was lost from chromosomes as they desynapsed at diplotene (by 40 h, **Figure 3H**). The subsequent division stages occurred rapidly, such that BrdU labeled tetrads were observed by 43 h (**Figure 3I**).

It was noticeable that during the initial stages of prophase I, the pattern of BrdU staining was consistent with it localizing to the distal regions of chromosomes, as marked by ASY1. Thus, when ASY1 foci appeared, distributed throughout the nucleus at 4 h (corresponding to the pre-bouquet stage when telomeres are widely dispersed, **Figure 2A**), BrdU localization was similarly widely distributed (**Figure 3A**). By 7 h, as ASY1 began to linearize and appear enriched within a restricted region of the nucleus (corresponding to the start of telomere clustering, **Figure 2B**), BrdU staining was similarly polarized (**Figure 3B**). Although not conclusive, this suggests that initial BrdU incorporation was in distal chromosome regions and implies that these chromosomal regions replicate first. By 16 h and in all subsequent stages ASY1 and BrdU staining were observed throughout the entire nucleus (**Figures 3C-I**), despite the bouquet configuration persisting until at least early zygotene (**Figures 2G**, **3G**). This suggests that by 16 h, replication of interstitial and proximal DNA had taken place.

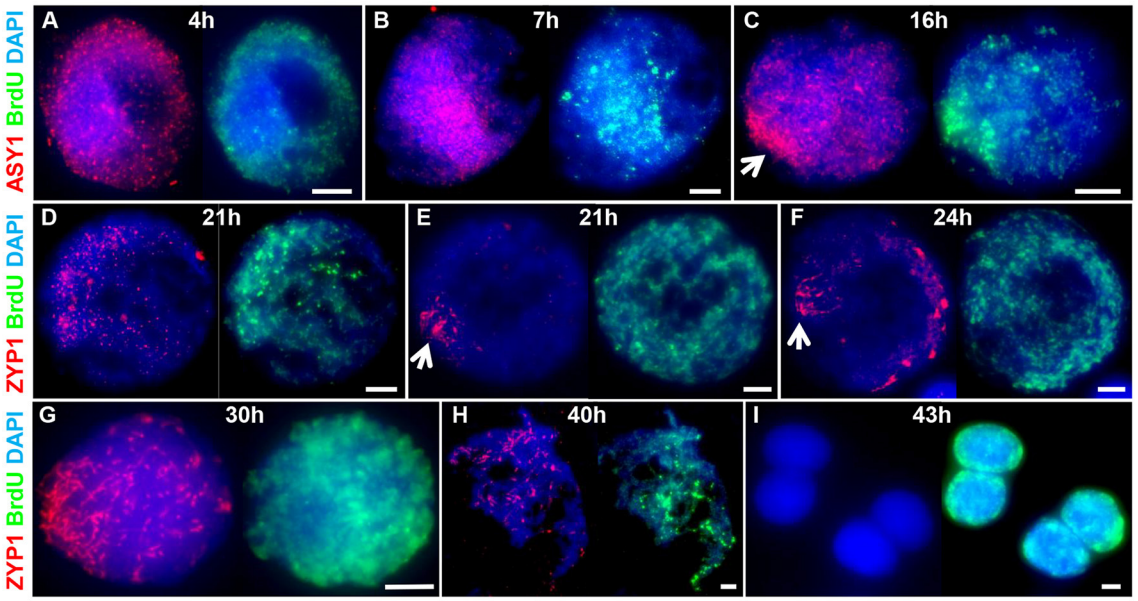

FIGURE 3 | A meiotic time-course of Cadenza. BrdU was incorporated into newly synthesized DNA during pre-meiotic S-phase and samples were taken at set time points following injection and assessed for BrdU labeling. ASY1 and ZYP1 were used to determine meiotic stage. **(A)** Labeled G2 nuclei with ASY1 foci were observed at 4 h; **(B)** the onset of leptotene and start of bouquet formation at 7 h (marked by ASY1 linear stretches and polarization); **(C)** tight bouquet formation by 16 h (marked by highly polarized ASY1 signal - arrow); **(D)** ZYP1 pre-synaptic foci by 21 h; **(E,F)** onset of zygotene (marked by polarized ZYP1 linear stretches, arrow) by 21–24 h; **(G)** progression of synapsis through 30 h; **(H)** diplotene (desynapsis) at 40 h and **(I)** tetrads by 43 h. Note ZYP1 staining of centromere clusters at opposite pole to SC extension in early zygotene **(F)**. DNA is stained with DAPI. For clarity, several color combinations of images are shown. Bar = 5 μM.

The meiotic time course is summarized in **Figure 7B** and shows that the minimum time for meiosis was 43 h. Leptotene occupied approximately 17 h with zygotene to diplotene taking 16 h. The remaining stages comprising diakinesis and the two meiotic divisions were completed relatively quickly, within 3 h.

Initiation and Progression of Recombination Is Distally Biased

In Arabidopsis recombination progression during prophase I can be monitored by immunolocalization of key recombination proteins on meiotic chromosome spreads (Osman et al., 2011). Many of the antibodies developed during the course of Arabidopsis research have been useful for the analysis of other flowering plants, including barley (Higgins et al., 2012). We therefore anticipated that they would be successful in hexaploid wheat, particularly as wheat co-expression analysis has suggested that homoeologues of most meiotic genes are highly conserved and have not undergone sub/neo-functionalization (Alabdullah et al., 2019). This proved to be the case, so unless otherwise stated, the recombination antibodies we used were raised against Arabidopsis proteins.

Meiotic recombination is initiated by the programmed formation of DSBs and is followed by the rapid phosphorylation of histone H2A.X around the break sites (Sanchez-Moran et al., 2007). We used an antibody specific to the phosphorylated form of HsH2A.X (γH2A.X) as a marker for DSBs in PMCs. γH2A.X foci were first observed enriched in one half of the nucleus in late G2, shortly after the appearance of ASY1 foci (between 4 and 7 h), and concomitant with the start of ASY1 signal linearization (**Figure 4A**). Subsequent bouquet formation confirmed that this region of enrichment corresponded to the distal chromosome regions where ASY1 linearization was most advanced; relatively few γH2A.X foci were observed in the more interstitial/proximal regions toward the nuclear periphery (**Figure 4B**). As ASY1 linearization progressed, the number of γH2A.X foci continued to increase, rising from a mean of 728 ± 63.1 per PMC (n = 15) around the time foci first appeared with up to 2,198 (mean = 1,651 ± 72.8, n =15) observed when ASY1 was fully linear in late leptotene/start of zygotene (**Figure 4H**). By this time foci were distributed throughout the nucleus (**Figure 4C**). These data are consistent with a study by Gardiner et al. (2019), which reported a mean of 2,133 DSBs per male meiosis at leptotene in hexaploid wheat.

Early stages of meiotic recombination are catalyzed by the coordinated activity of the strand exchange proteins, DMC1 and RAD51 (Neale and Keeney, 2006) and in Arabidopsis they are essential for CO formation and DSB repair, respectively (Couteau et al., 1999; Li et al., 2004). Wheat DMC1 foci localized to linear stretches of axis during leptotene as the ASY1 signal extended. Initial DMC1 localization was predominantly to the distal regions (marked by increased ASY1 staining) where axis development was most advanced; foci appeared in more interstitial/proximal regions at the opposite pole of the nucleus in late leptotene/early zygotene, when the ASY1 signal was linear throughout the nucleus (**Figures 4D,E**). Foci were counted in early-mid leptotene when they were first detected (mean

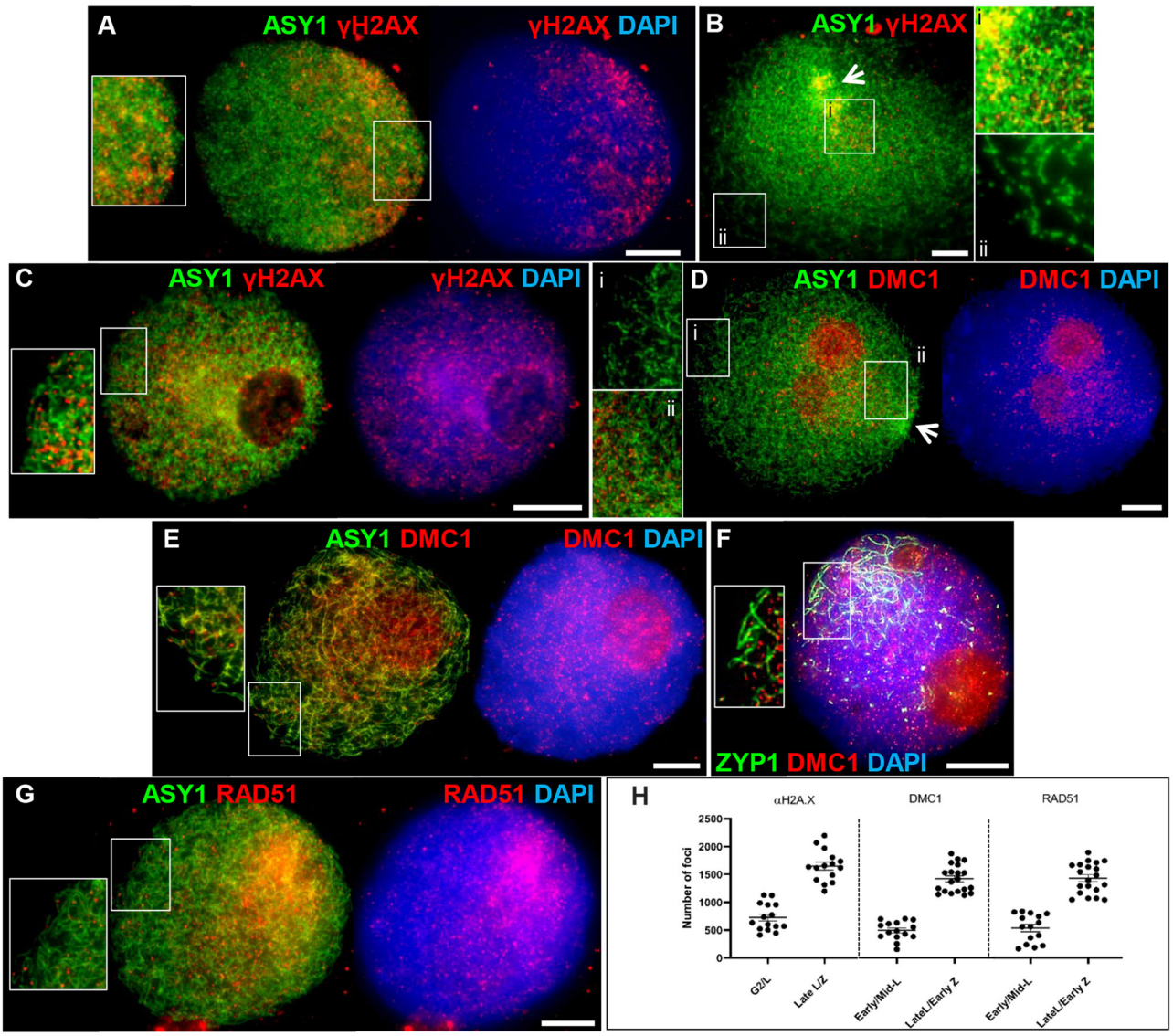

FIGURE 4 | Initiation of recombination in Cadenza. **(A)** Late G2; **(B,D)** early leptotene; **(C)** late leptotene; **(E–G)** early zygotene. Recombination proteins were initially observed in the distal regions [γH2A.X **(A,B)** and DMC1 **(D)**], later occurring throughout the nucleus [γH2A.X **(C)**; DMC1 **(E,F)** and RAD51 **(G)**]. ASY1 and ZYP1 mark the axis and SC, respectively. Note enrichment of ASY1 signal in the bouquet region in early leptotene **(B,D)** (arrows) and polarized early SC extension (single frame only shown, for clarity) **(F)**. DNA is stained with DAPI. For clarity, some images are shown in several color combinations. **(H)** γH2A.X, DMC1, and RAD51 foci were counted when they were first observed and when they occurred throughout the nucleus. Numbers per PMC are shown with mean and standard error (SE) bars. Bar = 10 μM.

per PMC = 494 ± 42.8, n = 15) and in late leptotene/early zygotene (maximum = 1,875, mean = 1,421 ± 55.0, n = 20), indicating an accumulation of foci as the chromosome axes progressively linearized (**Figure 4H**). For both counts, the large range reflects the highly dynamic nature of the process. Foci remained prominent throughout the nucleus during the early stages of zygotene where they marked early stretches of SC as the axes began to synapse (**Figure 4F**). During the later stages of prophase I foci numbers decreased (mid-late zygotene mean = 314 ± 68.3, n = 5) and signal was mostly gone by pachytene (**Supplementary Figure 4A**). These data are consistent with DMC1 counts reported for *T. aestivum* cv. Renan (Benyahya et al., 2020). The DMC1 antibody also prominently stained the nucleoli. This phenomenon has been observed in other plant species and for other antibodies and it has been suggested that the nucleolus may act as a reservoir for sequestering meiotic proteins, as it does for cell cycle proteins (Visintin and Amon, 2000; Jackson et al., 2006; Vignard et al., 2007; Higgins et al., 2012). Alternatively, non-specific staining of the nucleoli may be occurring due to its high protein content. RAD51 scored at similar stages to DMC1 showed similar loading dynamics (early-mid leptotene, mean = 537 ± 65.6, n = 15; late leptotene/early

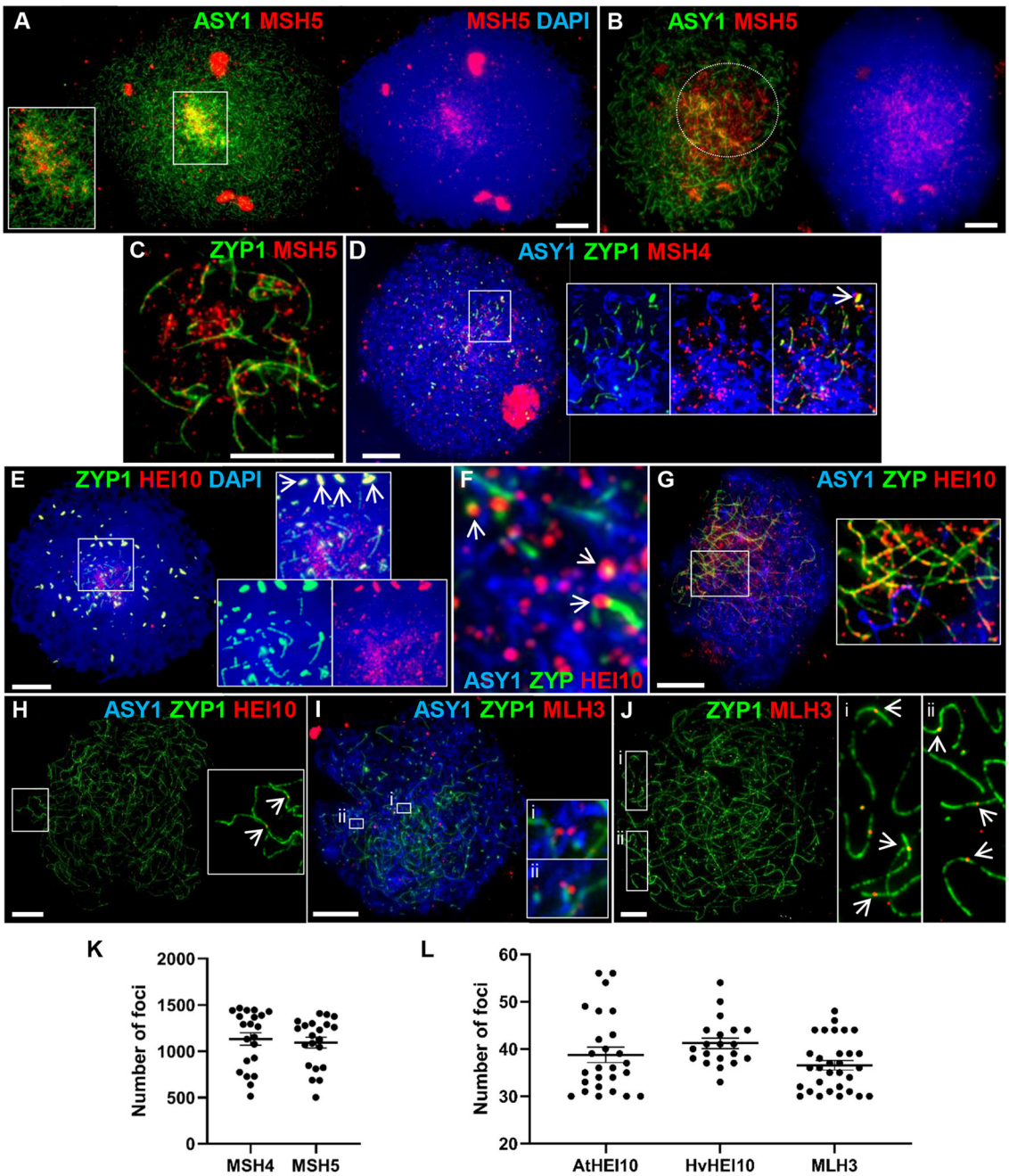

FIGURE 5 | Recombination progression in Cadenza showing MSH4/5, HEI10 and MLH3 localization. Axes and SC were marked by ASY1 and ZYP1, respectively. **(A)** Late leptotene: initial MSH5 foci were predominantly in distal regions, marked by higher intensity ASY1 signal. **(B)** Early zygotene: MSH5 localized throughout the nucleus but foci appeared more numerous in distal regions where ASY1 signal was depleted as chromosomes synapsed (marked by dotted circle). **(C)** Single frame detail of early zygotene nucleus showing localization of MSH5 foci to initial stretches of SC and to (unmarked) unsynapsed axes. **(D)** Start of zygotene: triple immunostaining showing MSH4 foci localized to unsynapsed axes, ZYP1 foci (inset, arrow) and early stretches of SC. **(E)** Start of zygotene showing numerous HEI10 foci surrounding initial stretches of SC in the distal regions and more prominent foci associated with SC ends (inset). HEI10 also colocalized with bright ZYP1 foci throughout the nucleus (main image and inset, arrows). **(F)** Detail of triple immunostained nucleus confirming HEI10 localization to unsynapsed axes and association of prominent foci with nascent SC (arrows). **(G)** Progression of zygotene showing HEI10 foci localized along the extending SC. Regularly spaced stretches of foci were observed along the SC and unsynapsed axes (inset). **(H)** Pachytene nucleus showing remaining HEI10 foci on SC. Inset shows two distal foci (arrows). **(I)** MLH3 localization in early zygotene. Insets show examples of foci pairs apparently flanking the axis or nascent SC. **(J)** At pachytene the number and position of prominent MLH3 foci was consistent with their marking CO sites. Insets show examples of near-distal foci (arrows). **(K)** MSH4 and MSH5 foci were counted as they accumulated in late leptotene/early zygotene. **(L)** Foci marked by the AtHEI10 or HvMLH3 antibodies were counted in late pachytene, foci marked by the HvHEI10 antibody were counted in late pachytene/diplotene. Numbers of foci per PMC are shown with mean and SE bars. Bar = 10 μM.

zygotene, maximum = 1,897, mean = 1,431 ± 61.2, $n = 20$; mid-late zygotene, mean = 259 ± 75.9, $n = 5$) (**Figures 4G,H** and **Supplementary Figure 4B**).

The meiosis-specific MutS homologs, MSH4 and MSH5, function as a heterodimer and bind and stabilize double Holliday Junction (dHJ) recombination intermediates (Snowden et al., 2004). In Arabidopsis and tetraploid wheat, MSH4 and MSH5 are essential for the formation of interference-sensitive Class I COs that account for ∼85% of COs (Higgins et al., 2004; Desjardins et al., 2020). In Cadenza MSH5 was first observed as foci along linear stretches of axis in late leptotene, as well as staining the nucleoli. As with DMC1 and RAD51, initial loading was predominantly distal where axis development was most advanced (**Figure 5A**). Foci rapidly increased in number and at early zygotene foci were present throughout the nucleus, yet still appeared more numerous in the distal regions where chromosomes began to synapse (evidenced by depletion in ASY1 signal) (**Figure 5B**). As well as localizing to unsynapsed axes, dual staining with ZYP1 at this stage confirmed that MSH5 localizes to early stretches of SC (**Figure 5C**). MSH4 also localized as foci during late leptotene/early zygotene where it marked unsynapsed linear axis, ZYP1 foci (see above) and nascent stretches of SC (**Figure 5D**). Staining of the nucleolus was also observed. Counts of MSH4 and MSH5 foci as they accumulated in late leptotene/early zygotene ranged from 513 to 1,465 (mean = 1,125) and 501 to 1,409 (mean = 1,096) per PMC, respectively ($n = 20$) (**Figure 5K**). From mid-zygotene onwards MSH4 and MSH5 foci gradually declined in number so that by pachytene only a few remained associated with the SC (MSH4 mean = 16 ± 2.0; MSH5 mean = 14 ± 3.1; $n = 6$) (**Supplementary Figures 5A,B**).

HEI10 is a member of the Zip3/HEI10 family of proteins thought to possess SUMO/ubiquitin E3 ligase activity (Chelysheva et al., 2012; Wang et al., 2012). Zip3/HEI10 marks Class I CO sites and in *A. thaliana* and *Sordaria macrospora* HEI10 foci at these sites have been shown to emerge from a much larger population of smaller axis-associated foci in early/mid prophase I (Chelysheva et al., 2012; De Muyt et al., 2014). In Cadenza HEI10 localization was investigated using antibodies against the Arabidopsis and barley proteins (Lambing et al., 2015; Desjardins et al., 2020). HEI10 was first detected in late leptotene where it colocalized with the presynaptic ZYP1 foci (see above) (**Supplementary Figure 6A**). Colocalization at bright ZYP1 foci was still apparent at the start of zygotene when the SC began to extend in the distal regions (**Figure 5E**). In addition, the ends of some of the linear ZYP1 stretches appeared to be associated with prominent HEI10 foci and numerous smaller HEI10 foci were observed in the chromatin immediately surrounding this region (**Figure 5E**). Triple localization of HEI10, ASY1, and ZYP1 at this stage indicated that HEI10 foci localize to unsynapsed axes (marked by ASY1) and confirmed the association of prominent HEI10 foci with nascent SC (**Figure 5F**). As the SC extended, HEI10 foci localized all along its length and stretches of regularly spaced foci could be observed on both unsynapsed axes and linear SC (**Figure 5G**). In late prophase I, HEI10 foci gradually became depleted from chromosomes leaving a sub-population of prominent foci. By pachytene, it was clear that many of the remaining foci were near to chromosome ends, consistent with marking CO sites (**Figure 5H**). In diplotene, foci marked by the AtHEI10 antibody quickly disappeared from chromosomes as they began to desynapse. However, foci marked by the HvHEI10 antibody remained detectable during early diplotene where they associated with residual stretches of ZYP1 staining (**Supplementary Figure 6B**). The mean number of prominent SC-associated foci per PMC at late pachytene was 38.8 ± 1.6 per PMC ($n = 26$) using the AtHEI10 antibody and 41.2 ± 1.1 ($n = 20$) with the HvHEI10 antibody (counted at late pachytene/diplotene) (**Figure 5L**).

The MutL homologs MLH1 and MLH3 act as a heterodimer to ensure that dHJs are resolved as COs rather than non-COs (Hunter and Borts, 1997; Wang et al., 1999; Cannavo et al., 2020; Kulkarni et al., 2020). Immunogold labeling has shown that the two proteins provide a reliable marker for Class I COs at pachytene (Moens et al., 2002; Lhuissier et al., 2007), and they have been routinely used for this purpose in a variety of organisms including plants (Jackson et al., 2006; Chelysheva et al., 2010; Phillips et al., 2013). We have investigated MLH3 localization in Cadenza using an antibody raised against the barley protein (Phillips et al., 2013). MLH3 foci are present in nuclei during the early stages of zygotene, but localization at this stage is not specific to the developing SC and many associate with the unsynapsed axis (**Figure 5I**). Interestingly, several examples of pairs of foci apparently flanking the axis or nascent SC were observed (**Figure 5I** detail). By pachytene, when the chromosomes were fully synapsed, localization of prominent MLH3 foci was largely confined to the linear SC signal (**Figure 5J**), with foci frequently located near the chromosome ends, consistent with marking CO sites (**Figure 5J** detail). The mean number of SC-associated MLH3 foci at pachytene was 36.6 ± 1.0 ($n = 31$) (**Figure 5L**), falling to 20.9 ± 2.6 ($n = 14$) as they became depleted from the chromosomes in early diplotene.

H3K4me3, H3K27me3 and H3K9me3 Histone Marks Are Enriched in the Distal Regions in Early Prophase I

In barley the spatio-temporal asymmetry of meiotic progression and eventual chiasma localization was potentially associated with the distal distribution of early-replicating euchromatin (Higgins et al., 2012). We were therefore interested in investigating the distribution of chromatin histone modifications in PMCs of Cadenza. H3K4me3, a marker of active genes, promotes recombination in budding yeast and has been shown to be associated with recombination sites in a range of other organisms, including plants (Borde et al., 2009; Liu et al., 2009; Choi et al., 2013; Shilo et al., 2015; Adam et al., 2018). In Cadenza H3K4me3 localized to chromatin throughout prophase I and in leptotene and early zygotene appeared enriched in the distal chromosome regions (**Figures 6A,B**). Distal enrichment was less obvious at pachytene when H3K4me3 was more widely distributed, often forming bands of increased signal intensity along chromosomes (**Figure 6C**). At this stage H3K4me3 staining was noticeably absent from bulbous regions of DAPI-stained chromatin, which were likely sites of heterochromatin

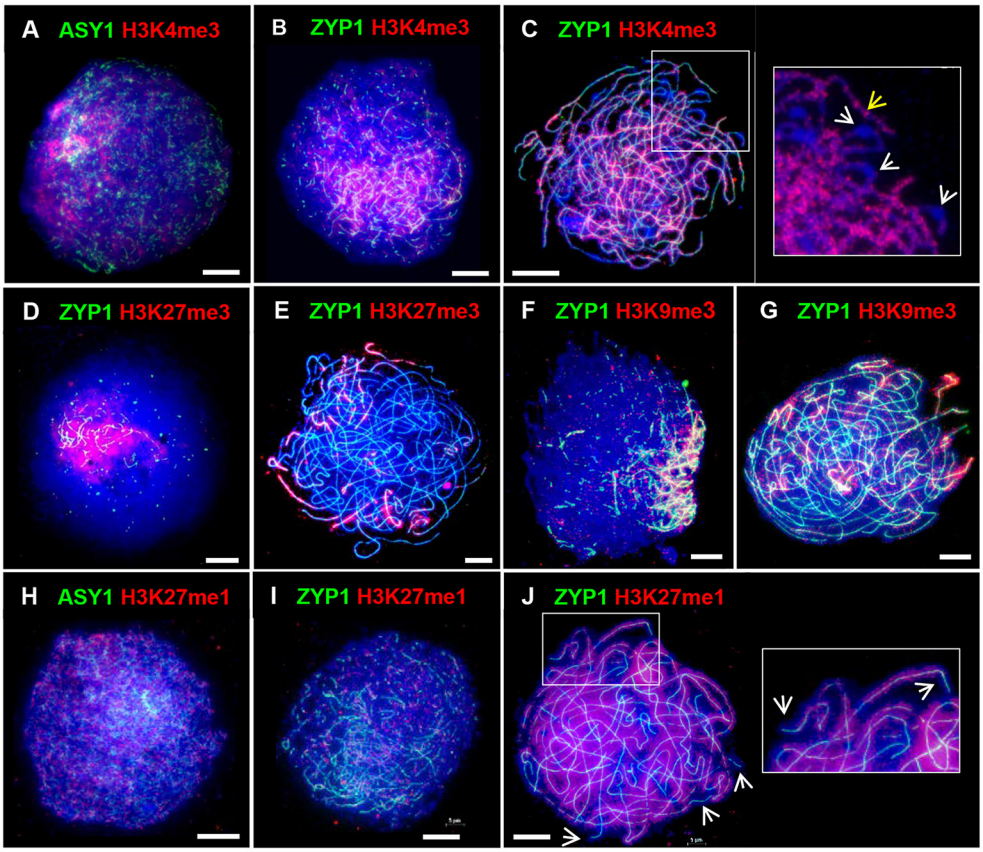

FIGURE 6 | Distribution of histone marks in Cadenza prophase I. ASY1 is used to mark the axes in leptotene; ZYP1 the SC from zygotene onwards. Gene-associated histone marks: **(A–C)** H3K4me3 at leptotene, early zygotene and pachytene, respectively - detail at pachytene shows discrete bands of H3K4me3 staining along chromosomes (yellow arrow) and likely paired centromeric regions devoid of staining (white arrows); **(D,E)** H3K27me3, a repressive mark, at early zygotene and pachytene, respectively; **(F,G)** H3K9me3 at early zygotene and pachytene, respectively. **(H–J)** H3K27me1, a marker of heterochromatin and TEs, at leptotene, zygotene and pachytene, respectively – detail and arrows at pachytene show absence of staining at chromosome ends. DNA is stained with DAPI (blue). Bar = 10 μM.

and paired centromeres (**Figure 6C**). H3K27me3 is associated with repression of gene transcription and marks facultative heterochromatin (Ramírez-González et al., 2018; Concia et al., 2020). This mark was highly enriched in distal regions during prophase I (**Figures 6D,E**), and in pachytene appeared to be preferentially marking chromosome ends (**Figure 6E**). Interestingly, H3K9me3 was also highly enriched in the distal regions in prophase I (**Figures 6F,G**). Although this is a marker of constitutive heterochromatin in mammals, in Arabidopsis it marks euchromatin and is reportedly associated with genes (Naumann et al., 2005; Roudier et al., 2011). Similar H3K9me3 distal enrichment was observed in barley PMCs in prophase I (Higgins et al., 2012). Finally, H3K27me1, a marker of heterochromatin and transposable elements (TEs) in plants, including wheat (Jacob and Michaels, 2009; Concia et al., 2020), showed generalized chromatin staining throughout the nucleus during prophase I (**Figures 6H–J**), and by pachytene it became evident that chromosomes were fairly evenly stained apart from near their ends (**Figure 6J**). In summary, the histone marks H3K4me3, H3K27me3, and H3K9me3 were enriched in the gene-rich distal regions in early prophase I.

Chromatin Exhibits Contraction/Expansion Cycles During Prophase I

A mechanical stress model of chromosome function has been developed based on the observation that eukaryotic mitotic and meiotic programs comprise global cycles of chromatin expansion and contraction (Kleckner et al., 2004). During meiotic prophase I, chromatin undergoes successive cycles which correlate with well-defined cytological stages and are proposed to coordinate four temporally distinct steps leading to CO formation: DSB formation; strand exchange; dHJ formation and dHJ resolution. Analysis of the meiotic program in barley showed that meiotic progression in the distal chromosome regions is coordinated with the expansion/contraction cycles (Higgins et al., 2012), so we were interested in whether a similar relationship exists in wheat. Cell walls of PMCs were digested so that nuclei occupied an in-solution envelope volume as determined by their chromatin state (Kleckner et al., 2004). As described in Higgins et al. (2012), changes in envelope volume were assessed by measuring the size of nuclei at specific stages, defined by ASY1 and ZYP1 localization patterns (**Figures 7A,B**). In early G2, when ASY1

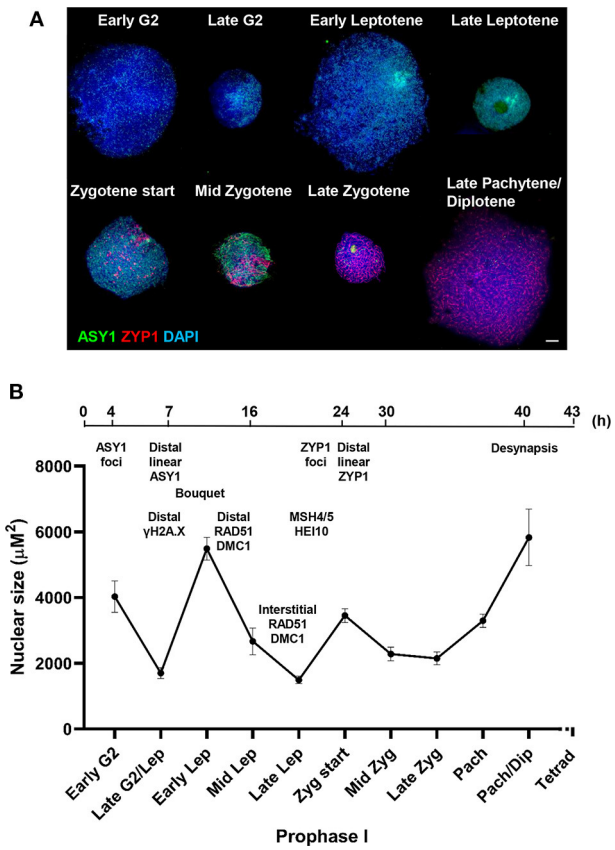

FIGURE 7 | Chromatin contraction/expansion cycles in Cadenza prophase I. **(A)** Immunolocalization of ASY1 (green) and ZYP1 (red) showing that initial distal meiotic events coincide with nuclear expansion phases. DNA is stained with DAPI (blue). Bar = 10 μM. **(B)** Mean nuclear size of PMCs at key stages of prophase I, as defined by ASY1 and ZYP1 staining. Bars represent standard error. A time-line of key events is included, based on cross-referencing ASY1/ZYP1 staining with a BrdU time course and refers to the "leading edge" of meiotic progression (i.e., not all PMCs within a sample may reach a particular stage in the time indicated). Times indicate hours after BrdU injection and the time-line is not to scale.

first appeared as weak foci, nuclei were relatively large (mean = 4,029 $\mu m^2 \pm 480.3$, $n = 12$). By late G2, when ASY1 began to exhibit loosely polarized signal enrichment and initiate short linear stretches, nuclear size had significantly reduced (mean = 1,703 $\mu m^2 \pm 161.3$, $n = 14$, $P < 0.0001$). However, by the time ASY1 linearization was clearly established in the distal regions in early leptotene, nuclear size had increased again (mean = 5,489 $\mu m^2 \pm 344.9$, $n = 41$, $P < 0.0001$). A second significant reduction in nuclear size had occurred by late leptotene when ASY1 signal was almost continuous (mean = 1,493 $\mu m^2 \pm 112.8$, $n = 16$, $P < 0.0001$). This was followed by an increase at the start of zygotene when linear stretches of ZYP1 staining began to appear in the distal regions (mean = 3,454 $\mu m^2 \pm 208.7$, $n = 26$, $P < 0.0001$). Nuclei had undergone a third significant contraction by mid-zygotene when SC polymerisation was ~50% complete (mean = 2,284 $\mu m^2 \pm 206.4$, $n = 20$, $P < 0.001$), remaining like this until full synapsis at the end of zygotene (mean = 2,150 $\mu m^2 \pm 191.9$, $n = 21$, $P = 0.64$). Finally, by late pachytene/early diplotene, when ZYP1 began to disappear from chromosomes, nuclei had increased in size again (mean = 5,831 $\mu m^2 \pm 861.2$, $n = 7$, $P < 0.0001$). These data therefore support the existence of chromatin contraction/expansion cycles in wheat similar to those in barley and other species (Kleckner et al., 2004; Higgins et al., 2012). Furthermore, as in barley, the timing of key events in the distal regions, such as RAD51/DMC1 localization, appear to coincide with periods of relative chromatin expansion.

DISCUSSION

Advances in wheat genomics and genome engineering present new opportunities to manipulate CO frequency and distribution to realize the potential of genetic variation for crop improvement (Adamski et al., 2020; Taagen et al., 2020). To provide a cytogenetic reference framework for CO modification initiatives and functional studies of meiotic recombination, we performed a detailed cytological analysis of recombination progression in the hexaploid spring wheat variety, Cadenza. We showed that there is a spatio-temporal bias in the initiation and progression of recombination that mirrors the tendency of chiasmata/COs to occur in the gene-dense distal regions of the chromosomes and is reflected in the distribution of gene-associated histone marks in the genome. We established a time-frame for the duration of meiosis and confirmed that wheat chromatin undergoes cycles of contraction and expansion during prophase I as previously observed in barley and other species (Kleckner et al., 2004; Higgins et al., 2012). During the course of this study, we also noted interesting aspects of ASY1 and ZYP1 protein localization during the meiotic program.

Chiasmata Occur Predominantly in Gene-Dense Distal Chromosomal Regions

Historically, the large chromosomes of wheat and other cereals have made them ideal candidates for cytogenetics studies so the tendency of chiasmata/COs to occur in the distal regions of chromosomes has long been known. More recently, wheat studies involving genetic mapping and whole-genome sequencing have provided fine-scale confirmation of this bias (Choulet et al., 2014; Darrier et al., 2017; Jordan et al., 2018; Gardiner et al., 2019). Formal quantification in Cadenza revealed a total mean chiasma frequency of 41.8 per PMC and confirmed that 88% of all chiasmata were in the terminal/sub-terminal regions of the chromosomes. Even so, the presence of chiasmata in the interstitial/proximal regions, albeit relatively infrequent, does at least support the feasibility of targeting COs to these regions. It would be interesting to carry out further analysis using genomic *in situ* hybridization (GISH) and chromosome-specific FISH probes to determine whether interstitial/proximal chiasmata favor particular sub-genomes, chromosomes or chromosome regions.

During early prophase I H3K4me3, a marker of euchromatin, and H3K27me3, a marker of facultative heterochromatin were enriched in the distal regions. H3K27me3 distal enrichment has

also been reported in wheat somatic nuclei (Concia et al., 2020; Liu et al., 2020). H3K9me3 also showed clear distal enrichment in prophase I, similar to its distribution in barley meiosis (Higgins et al., 2012). Although H3K9me3 marks constitutive heterochromatin in mammals, the dimethylated form is thought to be the major mark of heterochromatin in Arabidopsis (Jackson et al., 2004) and H3K9me3 is reportedly associated with euchromatin and genes (Naumann et al., 2005; Roudier et al., 2011; Xu and Jiang, 2020). The localization patterns of H3K4me3, H3K27me3, and H3K9me3 are therefore consistent with the high gene-density at distal regions previously reported by Choulet et al. (2014). On the other hand, distribution of H3K27me1, a marker of heterochromatin, was relatively homogeneous throughout most of the chromatin with the exception of the distal regions, where signal was absent. Thus, chiasmata/CO distribution broadly coincides with gene-rich DNA in Cadenza PMCs as it does in other organisms. However, in plants, any direct relationship between CO distribution and gene density or specific histone mark remains to be established. Despite the importance of gene density in influencing global distribution patterns of recombination, the factors that shape recombination are complex, involving multiple regulatory layers and fine-tuning at the local level (Dluzewska et al., 2018; Fayos et al., 2019). This is illustrated by fine-scale mapping of *A. thaliana* floral tissue which revealed a complex relationship between H3K4me3 levels and DSBs (Choi et al., 2018). Thus, H3K4me3 was enriched in proximity to SPO11-1-oligo hotspots at gene 5′ ends but hotspots also occurred at the 3′ end of genes where H3K4me3 was less abundant (Choi et al., 2018).

Chiasma frequency provides a cytological estimate of the total number of COs per nucleus while the recombination proteins HEI10 and MLH3 are markers of interference-sensitive (Class I) COs in late prophase I (Jackson et al., 2006; Chelysheva et al., 2012; Phillips et al., 2013). The proportion of Class I COs in hexaploid wheat is yet to be determined. However, in *A. thaliana*, rice (*Oryza sativa*), tomato (*Solanum lycopersicum*), oil seed rape (*Brassica napus*) and allotetraploid durum wheat (*Triticum turgidum subsp. durum*) they account for ∼85% of all COs suggesting that this proportion is widely conserved among plants (Higgins et al., 2004, 2008b; Luo et al., 2013; Anderson et al., 2014; Wang et al., 2016; Gonzalo et al., 2019; Desjardins et al., 2020). Assuming that 85% of COs are Class I in hexaploid wheat, we might expect them to account for ∼35.5 COs per PMC based on total chiasmata frequency. Our observed estimates of 36.6, 38.8, and 41.2 from the HvMLH3, AtHEI10, and HvHEI10 antibodies, respectively, therefore appear reasonable. The slightly higher estimates observed with the HEI10 antibodies may simply reflect the polarized nature of wheat prophase I progression whereby disappearance of "early" HEI10 foci from interstitial regions lags behind distal regions, thus emphasizing the need to score this marker as late in prophase I as possible. Alternatively, the possibility that HEI10 has additional roles in wheat cannot be ruled out. It should also be pointed out that chiasma counts may underestimate CO frequency due to COs which are very close together being difficult to resolve at the cytological level.

In addition to the MLH3 foci that marked COs at pachytene, we also observed pairs of foci flanking the axis and nascent stretches of SC during early zygotene. CO formation is dependent on the MutLγ complex, which comprises MLH3 and the MutL mismatch repair protein MLH1 (Cannavo et al., 2020; Kulkarni et al., 2020). MLH1 has also been implicated in the resolution of chromosome interlocks during zygotene (Storlazzi et al., 2010). Hence it is possible that the MutLγ complex itself has a role in interlock resolution and the pairs of MLH3 foci observed during early zygotene in wheat reflect this activity.

Recombination Initiation and Progression Exhibit a Spatio-Temporal Bias

In barley the spatio-temporal pattern of meiotic recombination is established during pre-meiotic S-phase whereby distal euchromatin-rich DNA regions are replicated first (0–4 h), followed by interstitial DNA (by 6 h) and finally proximal heterochromatin (by 13 h) (Higgins et al., 2012). Subsequent studies in budding yeast established a clear mechanistic link between the timing of DNA replication and downstream recombination initiation (Murakami and Keeney, 2014). In our study the distribution of early BrdU staining, particularly obvious during bouquet formation, is compelling evidence that DNA replication in the distal regions also occurs earlier than in interstitial/proximal regions in hexaploid wheat. Further support for this comes from an investigation of the dynamics of DNA replication in pre-meiosis and meiosis of *T. aestivum* cv. Chinese Spring using flow-cytometry which showed that replication in PMCs continues beyond the stage of bouquet formation and chromosome pairing in the distal regions (Rey and Prieto, 2014).

Immunolocalization of meiotic chromosome axis, SC and recombination proteins during early prophase I revealed a distal bias. Initial linearization of the ASY1 (axis) signal occurred predominantly, although not exclusively, in the sub-telomeric regions. Similarly subsequent SC extension, marked by linear ZYP1, also began in the distal regions. Sub-telomeric initiation of synapsis was previously described in *T. aestivum* cv. Chinese Spring (Sepsi et al., 2017). Here we have used BrdU labeling of DNA to determine a precise chronology for axis and SC development during prophase I. Dual localization of the recombination proteins with ASY1 and ZYP1 then allowed the initiation and progression of recombination to be indirectly anchored to the BrdU time-line. This confirmed that meiotic events in the distal regions preceded those in the interstitial/proximal regions by several hours and initiation of recombination, marked by γH2A.X foci, began in the distal regions before the meiotic axis was fully linear in the interstitial/proximal regions. As prophase I progressed this bias was maintained and the first appearances of RAD51, DMC1, MSH4/5, and HEI10 foci were similarly polarized.

At the leptotene/zygotene transition numerous DSBs were detected throughout the nucleus. At this stage up to 130 axis-associated ZYP1 foci were observed throughout the nucleus prior to the appearance of linear SC. Colocalization with γH2A.X, MSH4, and HEI10 suggested that the ZYP1 foci were located at a sub-set of recombination interactions raising the question

as to their significance. In budding yeast synapsis initiation sites correspond to CO designated recombination intermediates (Fung et al., 2004). However, in species with larger chromosomes, such as some fungi, plants, insects, and animals, in addition to SC nucleations which correspond to designated COs, there are additional SC nucleations at recombination sites that will not become COs (Zhang et al., 2014). For example, in *Sordaria macrosporum* there are 40 or so SC nucleations about half of which correspond to CO sites and in barley SC initiates at about 55 sites and CO estimates range from 13.6 to 22.7 (Li et al., 2010; Higgins et al., 2012; Phillips et al., 2013; Zhang et al., 2014). These additional SC nucleation sites are thought to aid efficient synapsis (Zickler and Kleckner, 1999). Studies in *S. macrosporum* have led to the proposal that in fungi, plants and mammals, a single round of interference acting on early recombination intermediates gives rise to an evenly patterned array of synapsis initiation sites, including the subset which are CO designated (Zhang et al., 2014). This may account for the ZYP1 foci in wheat. However, further study will be needed to determine if this is the case not least because SC extension is first apparent in the distal regions prior to other chromosomal regions. Also, as the SC polymerises during early zygotene the ZYP1 foci become less obvious with the emergence of short stretches of SC and smaller foci throughout the nuclear volume.

An alternative explanation for the pre-synaptic ZYP1 foci is suggested by a study of the role of the 26*S* proteasome in meiotic chromosome pairing and recombination in budding yeast (Ahuja et al., 2017). In early prophase I, prior to the DSB-induced homology search, non-homologous chromosomal interactions could become stabilized by the promiscuous association of SC proteins, including Zip1. Recruitment of the proteasome served to displace the SC proteins, restricting their localization to centromeres and allowing normal homologous pairing and a coordinated transition to SC assembly. Furthermore, proteolytic core and regulatory particles were recruited to the chromosomes by Zip1 and Zip3, in an evolutionarily conserved manner (Ahuja et al., 2017). It therefore seems possible that the presynaptic ZYP1 foci we observed in wheat represent similar promiscuous non-homologous interactions and even that ZYP1 (and possibly HEI10) has an analogous role to that in budding yeast in recruitment of the proteasome to chromosomes.

Factors Influencing Distal Bias of COs – Considerations

This study has revealed that the wheat meiotic program shares a number of similarities with barley meiosis: spatio-temporal asymmetry of axis and SC development and recombination initiation/progression; likely early-replicating distal euchromatin, nuclear contraction/expansion cycles at specific stages during prophase I and the overall duration of meiosis (minimum time to tetrad stage ∼43 h) (Higgins et al., 2012). The timing of specific events within the meiotic programs was also very similar: first appearance of ASY1 foci (by 4 h in both species); elongation of ASY1 signal to form short linear stretches (by 7 h in wheat, 6 h in barley), first linear stretches of SC in the distal regions (by 24 h in wheat, 25 h in barley) and desynapsis (by 40 h in wheat, 39 h in barley). This was perhaps surprising given that bread wheat is a hexaploid so has an overall genome size three times that of diploid barley (∼16.5 and ∼5.3 Gb, respectively). However, their chromosomes are of a similar physical size (IWGSC, 2018; https://www.barleygenome.org.uk). Our estimate of 43 h for the duration of meiosis in Cadenza was carried out under strictly controlled growth conditions, including a temperature of 20°C (see Materials and Methods for details) and is considerably longer than the 24 h previously reported for cv. Chinese Spring grown at 20°C (Bennett et al., 1971). This earlier study was carried out before the routine use of immunocytology to study meiosis and employed sampling methods and the use of tritiated thymidine to label DNA. Interestingly, in a later publication, the same author reported that at a temperature of 15°C the duration of meiosis in Chinese Spring was 43 h; identical to our Cadenza estimate (Bennett, 1977). It therefore remains to be established whether the observed differences in timing at the reported temperature of 20°C reflect genuine varietal differences or differing environmental conditions and/or methodology.

Studies in budding yeast indicate that the CO/NCO decision is made early in the meiotic program and likely precedes stable strand exchange (Bishop and Zickler, 2004; Börner et al., 2004). At early leptotene in wheat, DSBs and early recombination pathway proteins were predominantly detected in the distal euchromatic chromosome regions. At this stage some appeared elsewhere in the chromatin, albeit relatively infrequently before increasing in abundance as prophase I progressed. By late leptotene DSBs were present throughout the nucleus. Since COs are rare in interstitial/proximal regions it seems that generally these early "non-distal" DSBs do not progress to form COs. The reason for this is not fully clear. One possibility is that in the initial stages, the high levels of DSBs in the distal regions (relative to the non-distal), combined with telomere anchoring of the chromosomes to the nuclear membrane, may promote homolog engagement here before the more interstitial/proximal regions have received sufficient breaks to achieve this. Additionally, it is worth considering that centromere dynamics during prophase I may also influence stable homolog engagement. In early leptotene, as the axis begins to linearize and shortly before formation of the telomere bouquet, centromeres of cv. Chinese Spring cluster into ∼10 groups at the opposite pole of the nucleus (Sepsi et al., 2017). These clusters remain until early zygotene (this study, Sepsi et al., 2017). Coincident with the start of SC extension in the sub-telomeric regions, centromeres begin to be released from the clusters in a gradual, progressive manner with homologous centromeres released individually (and not necessarily from the same cluster) and it is suggested that this orderly release of centromeres may facilitate homologous pairing by restricting release to those undergoing pairing (Sepsi et al., 2017). This strategy would help to overcome the challenge of pairing large chromosomes whilst avoiding homoeologous pairing and minimizing the risk of chromosome interlocks. Based on this model, interstitial/proximal regions of chromosomes might be physically prevented from engaging with their homolog

until after their distal regions have synapsed. Interestingly, ZYP1 colocalizes with the centromeric clusters in early zygotene (this study, Sepsi et al., 2017). Presynaptic centromeric localization of the SC proteins Zip1 and C(3)G have also been observed in budding yeast and Drosophila, respectively, where they are required for centromeric associations (Tsubouchi and Roeder, 2005; Takeo et al., 2011; Tanneti et al., 2011), suggesting a possible role for ZYP1 in the regulation of wheat centromere dynamics (for detailed discussion see Sepsi et al., 2017).

A consequence of early homolog engagement in distal regions might be that CO designation is similarly spatially-biased and less likely to occur in interstitial/proximal regions as CO interference will disfavor COs in adjacent chromosomal regions. That said, analysis of the distribution of class I COs based on MLH3 foci along barley chromosomes 2H and 3H revealed respective mean inter-focus distances of 38.5 and 42.6% of total SC length but of these, 38 and 34%, respectively, were <20% apart (Phillips et al., 2013). This implies that CO interference may not entirely account for the deficit in interstitial/proximal COs in the grasses. In barley it has been proposed that the coordination of the appearance of the recombination foci on the chromosomes with the chromatin contraction/expansion cycles may be a contributory factor to the distal bias (Higgins et al., 2012). Chromatin organization is also likely important, indeed in barley MLH3 inter-focus distances were found to be increased across the centromeric regions suggesting an influence of the pericentromeric heterochromatin (Phillips et al., 2013). It seems possible that CO distribution is similarly influenced in wheat.

The relationship between the meiotic chromosome axis/SC and recombination is intimate and complex (Zickler and Kleckner, 1999). ASY1 has long been recognized as a key component in the coordination of these events in plant genomes (Caryl et al., 2000; Sanchez-Moran et al., 2007; Osman et al., 2011). ASY1 is a core axis component, necessary for wild type CO levels, which additionally acts in a dosage-dependent manner to influence the distribution of COs along chromosomes (Lambing et al., 2020b). Chromatin-immunoprecipitation (ChIP) revealed a gradient of ASY1 enrichment along *A. thaliana* chromosomes, increasing from the telomeres to the centromeres (Lambing et al., 2020b). Interestingly, *asy1*/+ heterozygotes maintained total CO numbers, but genome-wide mapping revealed that COs were redistributed toward the telomeres at the expense of the pericentromeres (Lambing et al., 2020b). Immunocytology of *asy1*/+ showed that although ASY1 appeared to form a continuous signal along chromosomes and full pairing and synapsis were achieved, ASY1 signal intensity in early prophase I was reduced by 21% compared to wild type (Lambing et al., 2020b). This led to the proposal that *A. thaliana* ASY1 antagonizes telomere-led recombination and promotes spaced CO formation along chromosomes via interference.

This interpretation of ASY1 function in Arabidopsis poses interesting questions regarding the distinctive distal enrichment of ASY1 signal we observed in early prophase I of wheat. It is possible that this feature reflects the more advanced state of axis development in the sub-telomeric regions of chromosomes at this stage, in addition to the chromosome ends being brought together by the formation of a more prominent bouquet in wheat (Martínez-Pérez et al., 1999; Armstrong et al., 2001). Interestingly, ASY1 ChIP-seq analysis of hexaploid wheat (Chinese Spring) revealed a similar pronounced distal enrichment toward the telomeres (Tock et al., submitted). Moreover, the ChIP-seq data also revealed a slight enrichment of ASY1 in the centromeric regions, consistent with our cytological observations of increased ASY1 signal intensity at paired centromeres in pachytene. It is therefore tempting to speculate that ASY1 dosage may influence CO distribution in wheat, as it does in Arabidopsis, although further investigation will be required to establish this. The complex interplay between the meiotic axis proteins, chromatin environment and recombination (Lambing et al., 2020a; Tock et al., submitted) promises to be an interesting area of future wheat research, especially given the contrasting chromatin and recombination landscapes in wheat compared to Arabidopsis.

In summary, this study involved a detailed cytological analysis of meiotic prophase I progression in the hexaploid wheat, Cadenza, providing insights into possible factors influencing the distal bias of COs. We believe it provides a useful framework for future functional studies and initiatives to manipulate recombination in wheat.

DATA AVAILABILITY STATEMENT

The original contributions presented in the study are included in the article/**Supplementary Material**, further inquiries can be directed to the corresponding author/s.

AUTHOR CONTRIBUTIONS

KO, JH, IH, KE, FCHF, and ESM designed the research. KO and UA performed the experiments. KO, UA, and ESM analyzed the data. KO and FCHF wrote the first draft of the manuscript. All authors contributed to the article and approved the submitted version.

FUNDING

This work was supported by the Biotechnology and Biological Sciences Research Council (BB/N002628/1 Releasing natural variation in bread wheat by modulating meiotic crossovers).

ACKNOWLEDGMENTS

We would like to thank Cristobal Uauy (John Innes Centre, UK) for useful discussions and advice on wheat genomics; Mark Winfield (University of Bristol, UK), Stuart Desjardins (University of Leicester, UK) and Wei Jiang (University of Cambridge, UK) for helpful discussions and support; Helen Harper as sLola project co-ordinator (University of Bristol, UK) and the sLola Steering Committee for guidance throughout the project. We are also grateful to Elaine Howell (University of Birmingham, UK) for critical reading of the manuscript; Steve

Price, Karen Staples and Andy Breckles (all at the University of Birmingham, UK) for technical and horticultural support; Stefan Heckmann and Andreas Houben for gifts of antibodies; Maria Cuacos and Yun-Jae Ahn for helpful discussions (all at IPK, Gatersleben, Germany).

SUPPLEMENTARY MATERIAL

The Supplementary Material for this article can be found online at: https://www.frontiersin.org/articles/10.3389/fpls.2021.631323/full#supplementary-material

REFERENCES

Adam, C., Guérois, R., Citarella, A., Verardi, L., Adolphe, F., Béneut, C., et al. (2018). The PHD finger protein Spp1 has distinct functions in the Set1 and the meiotic DSB formation complexes. *PLoS Genet* 14:e1007223. doi: 10.1371/journal.pgen.1007223

Adamski, N. M., Borrill, P., Brinton, J., Harrington, S. A., Marchal, C., Bentley, A. R., et al. (2020). A roadmap for gene functional characterisation in crops with large genomes: lessons from polyploid wheat. *Elife* 9:e55646. doi: 10.7554/eLife.55646

Ahn, Y. J., Cuacos, M., Ayoub, M. A., Kappermann, J., Houben, A., and Heckmann, S. (2020). In planta delivery of chemical compounds into barley meiocytes: EdU as compound example. *Methods Mol. Biol.* 2061, 381–402. doi: 10.1007/978-1-4939-9818-0_27

Ahuja, J. S., Sandhu, R., Mainpal, R., Lawson, C., Henley, H., Hunt, P. A., et al. (2017). Control of meiotic pairing and recombination by chromosomally tethered 26S proteasome. *Science* 355, 408–411. doi: 10.1126/science.aaf4778

Alabdullah, A. K., Borrill, P., Martin, A. C., Ramirez-Gonzalez, R. H., Hassani-Pak, K., Uauy, C., et al. (2019). A co-expression network in hexaploid wheat reveals mostly balanced expression and lack of significant gene loss of homeologous meiotic genes upon polyploidization. *Front. Plant Sci.* 10:1325. doi: 10.3389/fpls.2019.01325

Albini, S. M., Jones, G. H., and Wallace, B. M. (1984). A method for preparing two-dimensional surface-spreads of synaptonemal complexes from plant meiocytes for light and electron microscopy. *Exp. Cell Res.* 152, 280–285. doi: 10.1016/0014-4827(84)90255-6

Anderson, L. K., Lohmiller, L. D., Tang, X., Hammond, D. B., Javernick, L., Shearer, L., et al. (2014). Combined fluorescent and electron microscopic imaging unveils the specific properties of two classes of meiotic crossovers. *Proc. Natl. Acad. Sci. U. S. A.* 111, 13415–13420. doi: 10.1073/pnas.1406846111

Armstrong, S. (2013). "Spreading and fluorescence *in situ* hybridization of male and female meiocyte chromosomes from Arabidopsis thaliana for cytogenetical analysis," in *Plant Meiosis: Methods and Protocols*, eds W. P. Pawlowski, M. Grelon, and S. Armstrong (Totowa, NJ: Humana Press), 3–12.

Armstrong, S. J., Caryl, A. P., Jones, G. H., and Franklin, F. C. (2002). Asy1, a protein required for meiotic chromosome synapsis, localizes to axis-associated chromatin in Arabidopsis and Brassica. *J. Cell Sci.* 115, 3645–3655. doi: 10.1242/jcs.00048

Armstrong, S. J., Franklin, F. C., and Jones, G. H. (2001). Nucleolus-associated telomere clustering and pairing precede meiotic chromosome synapsis in Arabidopsis thaliana. *J. Cell Sci.* 114, 4207–4217.

Armstrong, S. J., Franklin, F. C. H., and Jones, G. H. (2003). A meiotic time-course for *Arabidopsis thaliana*. *Sexual Plant Reprod.* 16, 141–149. doi: 10.1007/s00497-003-0186-4

Baudat, F., and Nicolas, A. (1997). Clustering of meiotic double-strand breaks on yeast chromosome III. *Proc. Natl. Acad. Sci. U. S. A.* 94, 5213–5218. doi: 10.1073/pnas.94.10.5213

Bennett, M. D. (1977). The time and duration of meiosis. *Philos. Trans. R. Soc. Lond. B Biol. Sci.* 277, 201–226. doi: 10.1098/rstb.1977.0012

Bennett, M. D., Chapman, V., and Riley, R. (1971). The duration of meiosis in pollen mother cells of wheat, rye and Triticale. *Proc. R. Soc. Lond. B Biol. Sci.* 178, 259–275. doi: 10.1098/rspb.1971.0065

Benyahya, F., Nadaud, I., Da Ines, O., Rimbert, H., White, C., and Sourdille, P. (2020). SPO11.2 is essential for programmed double-strand break formation during meiosis in bread wheat (*Triticum aestivum* L.). *Plant J.* 104, 30–43. doi: 10.1111/tpj.14903

Bishop, D. K., and Zickler, D. (2004). Early decision; meiotic crossover interference prior to stable strand exchange and synapsis. *Cell* 117, 9–15. doi: 10.1016/S0092-8674(04)00297-1

Boden, S. A., Langridge, P., Spangenberg, G., and Able, J. A. (2009). TaASY1 promotes homologous chromosome interactions and is affected by deletion of Ph1. *Plant J.* 57, 487–497. doi: 10.1111/j.1365-313X.2008.03701.x

Borde, V., Robine, N., Lin, W., Bonfils, S., Géli, V., and Nicolas, A. (2009). Histone H3 lysine 4 trimethylation marks meiotic recombination initiation sites. *EMBO J.* 28, 99–111. doi: 10.1038/emboj.2008.257

Börner, G. V., Kleckner, N., and Hunter, N. (2004). Crossover/noncrossover differentiation, synaptonemal complex formation, and regulatory surveillance at the leptotene/zygotene transition of meiosis. *Cell* 117, 29–45. doi: 10.1016/S0092-8674(04)00292-2

Cannavo, E., Sanchez, A., Anand, R., Ranjha, L., Hugener, J., Adam, C., et al. (2020). Regulation of the MLH1-MLH3 endonuclease in meiosis. *Nature* 586, 618–622. doi: 10.1038/s41586-020-2592-2

Caryl, A. P., Armstrong, S. J., Jones, G. H., and Franklin, F. C. (2000). A homologue of the yeast HOP1 gene is inactivated in the Arabidopsis meiotic mutant asy1. *Chromosoma* 109, 62–71. doi: 10.1007/s004120050413

Chelysheva, L., Gendrot, G., Vezon, D., Doutriaux, M. P., Mercier, R., and Grelon, M. (2007). Zip4/Spo22 is required for class I CO formation but not for synapsis completion in *Arabidopsis thaliana*. *PLoS Genet.* 3:e83. doi: 10.1371/journal.pgen.0030083

Chelysheva, L., Grandont, L., Vrielynck, N., le Guin, S., Mercier, R., and Grelon, M. (2010). An easy protocol for studying chromatin and recombination protein dynamics during *Arabidopsis thaliana* meiosis: immunodetection of cohesins, histones and MLH1. *Cytogenet. Genome Res.* 129, 143–153. doi: 10.1159/000314096

Chelysheva, L., Vezon, D., Chambon, A., Gendrot, G., Pereira, L., Lemhemdi, A., et al. (2012). The Arabidopsis HEI10 is a new ZMM protein related to Zip3. *PLoS Genet.* 8:e1002799. doi: 10.1371/journal.pgen.1002799

Chikashige, Y., Ding, D. Q., Funabiki, H., Haraguchi, T., Mashiko, S., Yanagida, M., et al. (1994). Telomere-led premeiotic chromosome movement in fission yeast. *Science* 264, 270–273. doi: 10.1126/science.8146661

Choi, K., Zhao, X., Kelly, K. A., Venn, O., Higgins, J. D., Yelina, N. E., et al. (2013). Arabidopsis meiotic crossover hot spots overlap with H2A.Z nucleosomes at gene promoters. *Nat. Genet.* 45, 1327–1336. doi: 10.1038/ng.2766

Choi, K., Zhao, X., Tock, A. J., Lambing, C., Underwood, C. J., Hardcastle, T. J., et al. (2018). Nucleosomes and DNA methylation shape meiotic DSB frequency in *Arabidopsis thaliana* transposons and gene regulatory regions. *Genome Res.* 28, 532–546. doi: 10.1101/gr.225599.117

Choulet, F., Alberti, A., Theil, S., Glover, N., Barbe, V., Daron, J., et al. (2014). Structural and functional partitioning of bread wheat chromosome 3B. *Science* 345:1249721. doi: 10.1126/science.1249721

Concia, L., Veluchamy, A., Ramirez-Prado, J. S., Martin-Ramirez, A., Huang, Y., Perez, M., et al. (2020). Wheat chromatin architecture is organized in genome territories and transcription factories. *Genome Biol.* 21:104. doi: 10.1186/s13059-020-01998-1

Couteau, F., Belzile, F., Horlow, C., Grandjean, O., Vezon, D., and Doutriaux, M. P. (1999). Random chromosome segregation without meiotic arrest in both male and female meiocytes of a dmc1 mutant of Arabidopsis. *Plant Cell* 11, 1623–1634. doi: 10.1105/tpc.11.9.1623

Cowan, C. R., Carlton, P. M., and Cande, W. Z. (2001). The polar arrangement of telomeres in interphase and meiosis. Rabl organization and the bouquet. *Plant Physiol.* 125, 532–538. doi: 10.1104/pp.125.2.532

Crismani, W., Girard, C., Froger, N., Pradillo, M., Santos, J. L., Chelysheva, L., et al. (2012). FANCM limits meiotic crossovers. *Science* 336, 1588–1590. doi: 10.1126/science.1220381

Da Ines, O., Michard, R., Fayos, I., Bastianelli, G., Nicolas, A., Guiderdoni, E., et al. (2020). Bread Wheat TaSPO11-1 exhibits evolutionary conserved function in meiotic recombination across distant plant species. *Plant J.* 103, 2052–2068. doi: 10.1111/tpj.14882

Darrier, B., Rimbert, H., Balfourier, F., Pingault, L., Josselin, A. A., Servin, B., et al. (2017). High-resolution mapping of crossover events in the hexaploid wheat genome suggests a universal recombination mechanism. *Genetics* 206, 1373–1388. doi: 10.1534/genetics.116.196014

De Muyt, A., Zhang, L., Piolot, T., Kleckner, N., Espagne, E., and Zickler, D. (2014). E3 ligase Hei10: a multifaceted structure-based signaling molecule with roles within and beyond meiosis. *Genes Dev*. 28, 1111–1123. doi: 10.1101/gad.240408.114

Desjardins, S. D., Ogle, D. E., Ayoub, M. A., Heckmann, S., Henderson, I. R., Edwards, K. J., et al. (2020). MutS homologue 4 and MutS homologue 5 maintain the obligate crossover in wheat despite stepwise gene loss following polyploidization. *Plant Physiol*. 183, 1545–1558. doi: 10.1104/pp.20.00534

Dluzewska, J., Szymanska, M., and Ziolkowski, P. A. (2018). Where to cross over? Defining crossover sites in plants. *Front. Genet*. 9:609. doi: 10.3389/fgene.2018.00609

Fayos, I., Mieulet, D., Petit, J., Meunier, A. C., Périn, C., Nicolas, A., et al. (2019). Engineering meiotic recombination pathways in rice. *Plant Biotechnol. J*. 17, 2062–2077. doi: 10.1111/pbi.13189

Fernandes, J. B., Séguéla-Arnaud, M., Larchevêque, C., Lloyd, A. H., and Mercier, R. (2018). Unleashing meiotic crossovers in hybrid plants. *Proc. Natl. Acad. Sci. U. S. A*. 115, 2431–2436. doi: 10.1073/pnas.1713078114

Fung, J. C., Rockmill, B., Odell, M., and Roeder, G. S. (2004). Imposition of crossover interference through the nonrandom distribution of synapsis initiation complexes. *Cell* 116, 795–802. doi: 10.1016/S0092-8674(04)00249-1

Gardiner, L. J., Wingen, L. U., Bailey, P., Joynson, R., Brabbs, T., Wright, J., et al. (2019). Analysis of the recombination landscape of hexaploid bread wheat reveals genes controlling recombination and gene conversion frequency. *Genome Biol*. 20:69. doi: 10.1186/s13059-019-1675-6

Girard, C., Chelysheva, L., Choinard, S., Froger, N., Macaisne, N., Lemhemdi, A., et al. (2015). AAA-ATPase FIDGETIN-LIKE 1 and helicase FANCM antagonize meiotic crossovers by distinct mechanisms. *PLoS Genet*. 11:e1005369. doi: 10.1371/journal.pgen.1005369

Golubovskaya, I. N., Hamant, O., Timofejeva, L., Wang, C. J., Braun, D., Meeley, R., et al. (2006). Alleles of afd1 dissect REC8 functions during meiotic prophase I. *J. Cell Sci*. 119, 3306–3315. doi: 10.1242/jcs.03054

Gonzalo, A., Lucas, M. O., Charpentier, C., Sandmann, G., Lloyd, A., and Jenczewski, E. (2019). Reducing MSH4 copy number prevents meiotic crossovers between non-homologous chromosomes in *Brassica napus*. *Nat. Commun*. 10:2354. doi: 10.1038/s41467-019-10010-9

Greer, E., Martín, A. C., Pendle, A., Colas, I., Jones, A. M., Moore, G., et al. (2012). The Ph1 locus suppresses Cdk2-type activity during premeiosis and meiosis in wheat. *Plant Cell* 24, 152–162. doi: 10.1105/tpc.111.094771

Haering, C. H., and Jessberger, R. (2012). Cohesin in determining chromosome architecture. *Exp. Cell Res*. 318, 1386–1393. doi: 10.1016/j.yexcr.2012.03.016

Halford, N. G., Curtis, T. Y., Chen, Z., and Huang, J. (2015). Effects of abiotic stress and crop management on cereal grain composition: implications for food quality and safety. *J. Exp. Bot*. 66, 1145–1156. doi: 10.1093/jxb/eru473

Hickey, L. T. N., Hafeez, A., Robinson, H., Jackson, S. A., Leal-Bertioli, S. C. M., et al. (2019). Breeding crops to feed 10 billion. *Nat. Biotechnol*. 37, 744–754. doi: 10.1038/s41587-019-0152-9

Higgins, J. D., Armstrong, S. J., Franklin, F. C., and Jones, G. H. (2004). The Arabidopsis MutS homolog AtMSH4 functions at an early step in recombination: evidence for two classes of recombination in Arabidopsis. *Genes Dev*. 18, 2557–2570. doi: 10.1101/gad.317504

Higgins, J. D., Buckling, E. F., Franklin, F. C., and Jones, G. H. (2008a). Expression and functional analysis of AtMUS81 in Arabidopsis meiosis reveals a role in the second pathway of crossing-over. *Plant J*. 54, 152–162. doi: 10.1111/j.1365-313X.2008.03403.x

Higgins, J. D., Osman, K., Jones, G. H., and Franklin, F. C. (2014). Factors underlying restricted crossover localization in barley meiosis. *Annu. Rev. Genet*. 48, 29–47. doi: 10.1146/annurev-genet-120213-092509

Higgins, J. D., Perry, R. M., Barakate, A., Ramsay, L., Waugh, R., Halpin, C., et al. (2012). Spatiotemporal asymmetry of the meiotic program underlies the predominantly distal distribution of meiotic crossovers in barley. *Plant Cell* 24, 4096–4109. doi: 10.1105/tpc.112.102483

Higgins, J. D., Sanchez-Moran, E., Armstrong, S. J., Jones, G. H., and Franklin, F. C. (2005). The Arabidopsis synaptonemal complex protein ZYP1 is required for chromosome synapsis and normal fidelity of crossing over. *Genes Dev*. 19, 2488–2500. doi: 10.1101/gad.354705

Higgins, J. D., Vignard, J., Mercier, R., Pugh, A. G., Franklin, F. C., and Jones, G. H. (2008b). AtMSH5 partners AtMSH4 in the class I meiotic crossover pathway in *Arabidopsis thaliana*, but is not required for synapsis. *Plant J*. 55, 28–39. doi: 10.1111/j.1365-313X.2008.03470.x

Howell, E. C., and Armstrong, S. (2013). "Using sequential fluorescence and genomic *in situ* hybridization (FISH and GISH) to distinguish the A and C genomes in *Brassica napus*," in *Plant Meiosis: Methods and Protocols*, eds W. P. Pawlowski, M. Grelon and S. Armstrong (Totowa, NJ: Humana Press), 25–34.

Hunter, N., and Borts, R. H. (1997). Mlh1 is unique among mismatch repair proteins in its ability to promote crossing-over during meiosis. *Genes Dev*. 11, 1573–1582. doi: 10.1101/gad.11.12.1573

IWGSC (2018). Shifting the limits in wheat research and breeding using a fully annotated reference genome. *Science* 361:eaar7191. doi: 10.1126/science.aar7191

Jackson, J. P., Johnson, L., Jasencakova, Z., Zhang, X., PerezBurgos, L., Singh, P. B., et al. (2004). Dimethylation of histone H3 lysine 9 is a critical mark for DNA methylation and gene silencing in *Arabidopsis thaliana*. *Chromosoma* 112, 308–315. doi: 10.1007/s00412-004-0275-7

Jackson, N., Sanchez-Moran, E., Buckling, E., Armstrong, S. J., Jones, G. H., and Franklin, F. C. (2006). Reduced meiotic crossovers and delayed prophase I progression in AtMLH3-deficient Arabidopsis. *EMBO J*. 25, 1315–1323. doi: 10.1038/sj.emboj.7600992

Jacob, Y., and Michaels, S. D. (2009). H3K27me1 is E(z) in animals, but not in plants. *Epigenetics* 4, 366–369. doi: 10.4161/epi.4.6.9713

Jones, G. H. (1984). The control of chiasma distribution. *Symp. Soc. Exp. Biol*. 38, 293–320.

Jones, G. H., and Franklin, F. C. (2006). Meiotic crossing-over: obligation and interference. *Cell* 126, 246–248. doi: 10.1016/j.cell.2006.07.010

Jordan, K. W., Wang, S., He, F., Chao, S., Lun, Y., Paux, E., et al. (2018). The genetic architecture of genome-wide recombination rate variation in allopolyploid wheat revealed by nested association mapping. *Plant J*. 95, 1039–1054. doi: 10.1111/tpj.14009

Khoo, K. H., Able, A. J., and Able, J. A. (2012). The isolation and characterisation of the wheat molecular ZIPper I homologue, TaZYP1. *BMC Res. Notes* 5:106. doi: 10.1186/1756-0500-5-106

Kleckner, N., Zickler, D., Jones, G. H., Dekker, J., Padmore, R., Henle, J., et al. (2004). A mechanical basis for chromosome function. *Proc. Natl. Acad. Sci. U. S. A*. 101, 12592–12597. doi: 10.1073/pnas.0402724101

Krasileva, K. V., Vasquez-Gross, H. A., Howell, T., Bailey, P., Paraiso, F., Clissold, L., et al. (2017). Uncovering hidden variation in polyploid wheat. *Proc. Natl. Acad. Sci. U. S. A*. 114, E913–E921. doi: 10.1073/pnas.1619268114

Kulkarni, D. S., Owens, S. N., Honda, M., Ito, M., Yang, Y., Corrigan, M. W., et al. (2020). PCNA activates the MutLγ endonuclease to promote meiotic crossing over. *Nature* 586, 623–627. doi: 10.1038/s41586-020-2645-6

Lam, I., and Keeney, S. (2014). Mechanism and regulation of meiotic recombination initiation. *Cold Spring Harb. Perspect. Biol*. 7:a016634. doi: 10.1101/cshperspect.a016634

Lambing, C., Kuo, P. C., Tock, A. J., Topp, S. D., and Henderson, I. R. (2020b). ASY1 acts as a dosage-dependent antagonist of telomere-led recombination and mediates crossover interference in Arabidopsis. *Proc. Natl. Acad. Sci. U. S. A*. 117, 13647–13658. doi: 10.1073/pnas.1921055117

Lambing, C., Osman, K., Nuntasoontorn, K., West, A., Higgins, J. D., Copenhaver, G. P., et al. (2015). Arabidopsis PCH2 mediates meiotic chromosome remodeling and maturation of crossovers. *PLoS Genet*. 11:e1005372. doi: 10.1371/journal.pgen.1005372

Lambing, C., Tock, A. J., Topp, S. D., Choi, K., Kuo, P. C., Zhao, X., et al. (2020a). Interacting genomic landscapes of REC8-cohesin, chromatin, and meiotic recombination in arabidopsis. *Plant Cell* 32, 1218–1239. doi: 10.1105/tpc.19.00866

Lhuissier, F. G., Offenberg, H. H., Wittich, P. E., Vischer, N. O., and Heyting, C. (2007). The mismatch repair protein MLH1 marks a subset of strongly interfering crossovers in tomato. *Plant Cell* 19, 862–876. doi: 10.1105/tpc.106.049106

Li, H., Kilian, A., Zhou, M., Wenzl, P., Huttner, E., Mendham, N., et al. (2010). Construction of a high-density composite map and comparative mapping of

segregation distortion regions in barley. *Mol. Genet. Genom.* 284, 319–331. doi: 10.1007/s00438-010-0570-3

Li, W., Chen, C., Markmann-Mulisch, U., Timofejeva, L., Schmelzer, E., Ma, H., et al. (2004). The Arabidopsis AtRAD51 gene is dispensable for vegetative development but required for meiosis. *Proc. Natl. Acad. Sci. U. S. A.* 101, 10596–10601. doi: 10.1073/pnas.0404110101

Liu, S., Yeh, C.-T., Ji, T., Ying, K., Wu, H., Tang, H. M., et al. (2009). Mu transposon insertion sites and meiotic recombination events co-localize with epigenetic marks for open chromatin across the maize genome. *PLOS Genet.* 5:e1000733. doi: 10.1371/journal.pgen.1000733

Liu, Y., Yuan, J., Jia, G., Ye, W., Jeffrey Chen, Z., and Song, Q. (2020). Histone H3K27 dimethylation landscapes contribute to genome stability and genetic recombination during wheat polyploidization. *Plant J.* doi: 10.1111/tpj.15063. [Epub ahead of print].

Luo, Q., Tang, D., Wang, M., Luo, W., Zhang, L., Qin, B., et al. (2013). The role of OsMSH5 in crossover formation during rice meiosis. *Mol. Plant* 6, 729–742. doi: 10.1093/mp/sss145

Macaisne, N., Novatchkova, M., Peirera, L., Vezon, D., Jolivet, S., Froger, N., et al. (2008). SHOC1, an XPF endonuclease-related protein, is essential for the formation of class I meiotic crossovers. *Curr. Biol.* 18, 1432–1437. doi: 10.1016/j.cub.2008.08.041

Macaisne, N., Vignard, J., and Mercier, R. (2011). SHOC1 and PTD form an XPF-ERCC1-like complex that is required for formation of class I crossovers. *J. Cell Sci.* 124, 2687–2691. doi: 10.1242/jcs.088229

Martín, A. C., Rey, M. D., Shaw, P., and Moore, G. (2017). Dual effect of the wheat Ph1 locus on chromosome synapsis and crossover. *Chromosoma* 126, 669–680. doi: 10.1007/s00412-017-0630-0

Martín, A. C., Shaw, P., Phillips, D., Reader, S., and Moore, G. (2014). Licensing MLH1 sites for crossover during meiosis. *Nat. Commun.* 5:4580. doi: 10.1038/ncomms5580

Martínez-Pérez, E., Shaw, P., Reader, S., Aragón-Alcaide, L., Miller, T., and Moore, G. (1999). Homologous chromosome pairing in wheat. *J. Cell Sci.* 112 (Pt 11), 1761–1769.

Mercier, R., Armstrong, S. J., Horlow, C., Jackson, N. P., Makaroff, C. A., Vezon, D., et al. (2003). The meiotic protein SWI1 is required for axial element formation and recombination initiation in Arabidopsis. *Development* 130:3309. doi: 10.1242/dev.00550

Mercier, R., Jolivet, S., Vezon, D., Huppe, E., Chelysheva, L., Giovanni, M., et al. (2005). Two meiotic crossover classes cohabit in Arabidopsis: one is dependent on MER3, whereas the other one is not. *Curr. Biol.* 15, 692–701. doi: 10.1016/j.cub.2005.02.056

Mercier, R., Mézard, C., Jenczewski, E., Macaisne, N., and Grelon, M. (2015). The molecular biology of meiosis in plants. *Annu. Rev. Plant Biol.* 66, 297–327. doi: 10.1146/annurev-arplant-050213-035923

Mieulet, D., Aubert, G., Bres, C., Klein, A., Droc, G., Vieille, E., et al. (2018). Unleashing meiotic crossovers in crops. *Nat. Plants* 4, 1010–1016. doi: 10.1038/s41477-018-0311-x

Mikhailova, E. I., Phillips, D., Sosnikhina, S. P., Lovtsyus, A. V., Jones, R. N., and Jenkins, G. (2006). Molecular assembly of meiotic proteins Asy1 and Zyp1 and pairing promiscuity in rye (*Secale cereale* L.) and its synaptic mutant sy10. *Genetics* 174, 1247–1258. doi: 10.1534/genetics.106.064105

Moens, P. B., Kolas, N. K., Tarsounas, M., Marcon, E., Cohen, P. E., and Spyropoulos, B. (2002). The time course and chromosomal localization of recombination-related proteins at meiosis in the mouse are compatible with models that can resolve the early DNA-DNA interactions without reciprocal recombination. *J. Cell Sci.* 115, 1611–1622.

Murakami, H., and Keeney, S. (2014). Temporospatial coordination of meiotic DNA replication and recombination via DDK recruitment to replisomes. *Cell* 158, 861–873. doi: 10.1016/j.cell.2014.06.028

Naumann, K., Fischer, A., Hofmann, I., Krauss, V., Phalke, S., Irmler, K., et al. (2005). Pivotal role of AtSUVH2 in heterochromatic histone methylation and gene silencing in Arabidopsis. *EMBO J.* 24, 1418–1429. doi: 10.1038/sj.emboj.7600604

Neale, M. J., and Keeney, S. (2006). Clarifying the mechanics of DNA strand exchange in meiotic recombination. *Nature* 442, 153–158. doi: 10.1038/nature04885

Osman, K., Higgins, J. D., Sanchez-Moran, E., Armstrong, S. J., and Franklin, F. C. (2011). Pathways to meiotic recombination in Arabidopsis thaliana. *New Phytol.* 190, 523–544. doi: 10.1111/j.1469-8137.2011.03665.x

Osman, K., Yang, J., Roitinger, E., Lambing, C., Heckmann, S., Howell, E., et al. (2018). Affinity proteomics reveals extensive phosphorylation of the Brassica chromosome axis protein ASY1 and a network of associated proteins at prophase I of meiosis. *Plant J.* 93, 17–33. doi: 10.1111/tpj.13752

Page, S. L., and Hawley, R. S. (2004). The genetics and molecular biology of the synaptonemal complex. *Annu. Rev. Cell Dev. Biol.* 20, 525–558. doi: 10.1146/annurev.cellbio.19.111301.155141

Phillips, D., Wnetrzak, J., Nibau, C., Barakate, A., Ramsay, L., Wright, F., et al. (2013). Quantitative high resolution mapping of HvMLH3 foci in barley pachytene nuclei reveals a strong distal bias and weak interference. *J. Exp. Bot.* 64, 2139–2154. doi: 10.1093/jxb/ert079

Rakszegi, M., Kisgyörgy, B. N., Tearall, K., Shewry, P. R., Láng, L., Phillips, A., et al. (2010). Diversity of agronomic and morphological traits in a mutant population of bread wheat studied in the Healthgrain program. *Euphytica* 174, 409–421. doi: 10.1007/s10681-010-0149-4

Ramírez-González, R. H., Borrill, P., Lang, D., Harrington, S. A., Brinton, J., Venturini, L., et al. (2018). The transcriptional landscape of polyploid wheat. *Science* 361:eaar6089. doi: 10.1126/science.aar6089

Rey, M.-D., Martín, A. C., Smedley, M., Hayta, S., Harwood, W., Shaw, P., et al. (2018). Magnesium increases homoeologous crossover frequency during meiosis in ZIP4 (Ph1 gene) mutant wheat-wild relative hybrids. *Front. Plant Sci.* 9:509. doi: 10.3389/fpls.2018.00509

Rey, M. D., Martín, A. C., Higgins, J., Swarbreck, D., Uauy, C., Shaw, P., et al. (2017). Exploiting the ZIP4 homologue within the wheat Ph1 locus has identified two lines exhibiting homoeologous crossover in wheat-wild relative hybrids. *Mol. Breed* 37:95. doi: 10.1007/s11032-017-0700-2

Rey, M. D., and Prieto, P. (2014). Dynamics of DNA replication during premeiosis and early meiosis in wheat. *PLoS ONE* 9:e107714. doi: 10.1371/journal.pone.0107714

Riley, R., and Chapman, V. (1958). Genetic control of the cytologically diploid behaviour of hexaploid wheat. *Nature* 182, 713–715. doi: 10.1038/182713a0

Roudier, F., Ahmed, I., Bérard, C., Sarazin, A., Mary-Huard, T., Cortijo, S., et al. (2011). Integrative epigenomic mapping defines four main chromatin states in Arabidopsis. *EMBO J.* 30, 1928–1938. doi: 10.1038/emboj.2011.103

Sanchez-Moran, E., Santos, J. L., Jones, G. H., and Franklin, F. C. (2007). ASY1 mediates AtDMC1-dependent interhomolog recombination during meiosis in Arabidopsis. *Genes Dev.* 21, 2220–2233. doi: 10.1101/gad.439007

Schwacha, A., and Kleckner, N. (1997). Interhomolog bias during meiotic recombination: meiotic functions promote a highly differentiated interhomolog-only pathway. *Cell* 90, 1123–1135. doi: 10.1016/S0092-8674(00)80378-5

Sears, E. R. (1948). The cytology and genetics of the wheats and their relatives. *Adv. Genet.* 3b, 239–270. doi: 10.1016/S0065-2660(08)60470-8

Sears, E. R., and Okamoto, M. (1958). Intergenomic chromosome relationships in hexaploid wheat. *Proc. X Int. Congr. Genet. Montreal* 2, 258–259.

Séguéla-Arnaud, M., Crismani, W., Larchevêque, C., Mazel, J., Froger, N., Choinard, S., et al. (2015). Multiple mechanisms limit meiotic crossovers: TOP3α and two BLM homologs antagonize crossovers in parallel to FANCM. *Proc. Natl. Acad. Sci. U. S. A.* 112, 4713–4718. doi: 10.1073/pnas.1423107112

Sepsi, A., Higgins, J. D., Heslop-Harrison, J. S., and Schwarzacher, T. (2017). CENH3 morphogenesis reveals dynamic centromere associations during synaptonemal complex formation and the progression through male meiosis in hexaploid wheat. *Plant J.* 89, 235–249. doi: 10.1111/tpj.13379

Serra, H., Lambing, C., Griffin, C. H., Topp, S. D., Nageswaran, D. C., Underwood, C. J., et al. (2018). Massive crossover elevation via combination of HEI10 and recq4a recq4b during Arabidopsis meiosis. *Proc. Natl. Acad. Sci. U. S. A.* 115, 2437–2442. doi: 10.1073/pnas.1713071115

Shewry, P. R. (2009). Wheat. *J. Exp. Bot.* 60, 1537–1553. doi: 10.1093/jxb/erp058

Shilo, S., Melamed-Bessudo, C., Dorone, Y., Barkai, N., and Levy, A. A. (2015). DNA Crossover motifs associated with epigenetic modifications delineate open chromatin regions in Arabidopsis. *Plant Cell* 27:2427. doi: 10.1105/tpc.15.00391

Sims, J., Copenhaver, G. P., and Schlögelhofer, P. (2019). Meiotic DNA repair in the nucleolus employs a nonhomologous end-joining mechanism. *Plant Cell* 31, 2259–2275. doi: 10.1105/tpc.19.00367

Smagulova, F., Gregoretti, I. V., Brick, K., Khil, P., Camerini-Otero, R. D., and Petukhova, G. V. (2011). Genome-wide analysis reveals novel molecular features of mouse recombination hotspots. *Nature* 472, 375–378. doi: 10.1038/nature09869

Snowden, T., Acharya, S., Butz, C., Berardini, M., and Fishel, R. (2004). hMSH4-hMSH5 recognizes holliday junctions and forms a meiosis-specific sliding clamp that embraces homologous chromosomes. *Mol. Cell* 15, 437–451. doi: 10.1016/j.molcel.2004.06.040

Stacey, N. J., Kuromori, T., Azumi, Y., Roberts, G., Breuer, C., Wada, T., et al. (2006). Arabidopsis SPO11-2 functions with SPO11-1 in meiotic recombination. *Plant J.* 48, 206–216. doi: 10.1111/j.1365-313X.2006.02867.x

Storlazzi, A., Gargano, S., Ruprich-Robert, G., Falque, M., David, M., Kleckner, N., et al. (2010). Recombination proteins mediate meiotic spatial chromosome organization and pairing. *Cell* 141, 94–106. doi: 10.1016/j.cell.2010.02.041

Sybenga, J. (1975). *Meiotic Configurations*. Berlin: Springer.

Taagen, E., Bogdanove, A. J., and Sorrells, M. E. (2020). Counting on crossovers: controlled recombination for plant breeding. *Trends Plant Sci.* 25, 455–465. doi: 10.1016/j.tplants.2019.12.017

Takeo, S., Lake, C. M., Morais-de,-S.á, E., Sunkel, C. E., and Hawley, R. S. (2011). Synaptonemal complex-dependent centromeric clustering and the initiation of synapsis in Drosophila oocytes. *Curr. Biol.* 21, 1845–1851. doi: 10.1016/j.cub.2011.09.044

Tanneti, N. S., Landy, K., Joyce, E. F., and McKim, K. S. (2011). A pathway for synapsis initiation during zygotene in Drosophila oocytes. *Curr. Biol.* 21, 1852–1857. doi: 10.1016/j.cub.2011.10.005

Tsubouchi, T., and Roeder, G. S. (2005). A synaptonemal complex protein promotes homology-independent centromere coupling. *Science* 308, 870–873. doi: 10.1126/science.1108283

Vignard, J., Siwiec, T., Chelysheva, L., Vrielynck, N., Gonord, F., Armstrong, S. J., et al. (2007). The interplay of RecA-related proteins and the MND1-HOP2 complex during meiosis in *Arabidopsis thaliana*. *PLoS Genet.* 3, 1894–1906. doi: 10.1371/journal.pgen.0030176

Visintin, R., and Amon, A. (2000). The nucleolus: the magician's hat for cell cycle tricks. *Curr. Opin. Cell Biol.* 12:752. doi: 10.1016/S0955-0674(00)00165-4

Vrielynck, N., Chambon, A., Vezon, D., Pereira, L., Chelysheva, L., De Muyt, A., et al. (2016). A DNA topoisomerase VI-like complex initiates meiotic recombination. *Science* 351, 939–943. doi: 10.1126/science.aad5196

Wang, C., Wang, Y., Cheng, Z., Zhao, Z., Chen, J., Sheng, P., et al. (2016). The role of OsMSH4 in male and female gamete development in rice meiosis. *J. Exp. Bot.* 67, 1447–1459. doi: 10.1093/jxb/erv540

Wang, K., Wang, M., Tang, D., Shen, Y., Miao, C., Hu, Q., et al. (2012). The role of rice HEI10 in the formation of meiotic crossovers. *PLoS Genet.* 8:e1002809. doi: 10.1371/journal.pgen.1002809

Wang, T. F., Kleckner, N., and Hunter, N. (1999). Functional specificity of MutL homologs in yeast: evidence for three Mlh1-based heterocomplexes with distinct roles during meiosis in recombination and mismatch correction. *Proc. Natl. Acad. Sci. U. S. A.* 96, 13914–13919. doi: 10.1073/pnas.96.24.13914

Xu, L., and Jiang, H. (2020). Writing and reading histone H3 lysine 9 methylation in Arabidopsis. *Front. Plant Sci.* 11:452. doi: 10.3389/fpls.2020.00452

Zeng, X., Li, K., Yuan, R., Gao, H., Luo, J., Liu, F., et al. (2018). Nuclear envelope-associated chromosome dynamics during meiotic prophase I. *Front. Cell Dev. Biol.* 5:121. doi: 10.3389/fcell.2017.00121

Zhang, L., Espagne, E., de Muyt, A., Zickler, D., and Kleckner, N. E. (2014). Interference-mediated synaptonemal complex formation with embedded crossover designation. *Proc. Natl. Acad. Sci. U. S. A.* 111, E5059–5068. doi: 10.1073/pnas.1416411111

Zickler, D., and Kleckner, N. (1998). The leptotene-zygotene transition of meiosis. *Annu. Rev. Genet.* 32, 619–697. doi: 10.1146/annurev.genet.32.1.619

Zickler, D., and Kleckner, N. (1999). Meiotic chromosomes: integrating structure and function. *Annu. Rev. Genet.* 33, 603–754. doi: 10.1146/annurev.genet.33.1.603

Zickler, D., and Kleckner, N. (2016). A few of our favorite things: pairing, the bouquet, crossover interference and evolution of meiosis. *Semin. Cell Dev. Biol.* 54, 135–148. doi: 10.1016/j.semcdb.2016.02.024

Ziolkowski, P. A., Underwood, C. J., Lambing, C., Martinez-Garcia, M., Lawrence, E. J., Ziolkowska, L., et al. (2017). Natural variation and dosage of the HEI10 meiotic E3 ligase control Arabidopsis crossover recombination. *Genes Dev.* 31, 306–317. doi: 10.1101/gad.295501.116

Conflict of Interest: The authors declare that the research was conducted in the absence of any commercial or financial relationships that could be construed as a potential conflict of interest.

frontiers in Plant Science

ORIGINAL RESEARCH
published: 26 February 2021
doi: 10.3389/fpls.2021.626528

ZmRAD17 Is Required for Accurate Double-Strand Break Repair During Maize Male Meiosis

*Ting Zhang[1], Ju-Li Jing[1], Lei Liu[2] and Yan He[1]**

[1] Ministry of Education Key Laboratory of Crop Heterosis and Utilization, National Maize Improvement Center of China, College of Agronomy and Biotechnology, China Agricultural University, Beijing, China, [2] Beijing Key Lab of Plant Resource Research and Development, Beijing Technology and Business University, Beijing, China

RAD17, a replication factor C (RFC)-like DNA damage sensor protein, is involved in DNA checkpoint control and required for both meiosis and mitosis in yeast and mammals. In plant, the meiotic function of *RAD17* was only reported in rice so far. Here, we identified and characterized the *RAD17* homolog in maize. The *Zmrad17* mutants exhibited normal vegetative growth but male was partially sterile. In *Zmrad17* pollen mother cells, non-homologous chromosome entanglement and chromosome fragmentation were frequently observed. Immunofluorescence analysis manifested that DSB formation occurred as normal and the loading pattern of RAD51 signals was similar to wild-type at the early stage of prophase I in the mutants. The localization of the axial element ASY1 was normal, while the assembly of the central element ZYP1 was severely disrupted in *Zmrad17* meiocytes. Surprisingly, no obvious defect in female sterility was observed in *Zmrad17* mutants. Taken together, our results suggest that *ZmRAD17* is involved in DSB repair likely by promoting synaptonemal complex assembly in maize male meiosis. These phenomena highlight a high extent of divergence from its counterpart in rice, indicating that the *RAD17* dysfunction can result in a drastic dissimilarity in meiotic outcome in different plant species.

Keywords: maize, meiosis, DSB, HR, RAD17

OPEN ACCESS

Edited by:
Mónica Pradillo, Complutense University of Madrid, Spain

Reviewed by:
Piotr Andrzej Ziolkowski, Adam Mickiewicz University, Poland
Arnaud Ronceret, National Autonomous University of Mexico, Mexico

****Correspondence:***
Yan He
yh352@cau.edu.cn

Specialty section:
This article was submitted to Plant Cell Biology, a section of the journal Frontiers in Plant Science

Received: *06 November 2020*
Accepted: *09 February 2021*
Published: *26 February 2021*

Citation:
Zhang T, Jing J-L, Liu L and He Y (2021) ZmRAD17 Is Required for Accurate Double-Strand Break Repair During Maize Male Meiosis. Front. Plant Sci. 12:626528. doi: 10.3389/fpls.2021.626528

INTRODUCTION

In eukaryotes, meiosis is a key biological process for reproduction with one round of DNA replication followed by two successive cell divisions (meiosis I and II) to halve chromosome number (de Massy, 2013). During meiosis I, homologous pairing and synapsis promote crossover (CO) formation, guaranteeing the accurate segregation of homologous chromosomes (Mercier et al., 2015). Thus, this division is also called as reductional division (Ma, 2006). Subsequently, meiosis II (also called equational division) leads to sister chromatids separation (Zickler and Kleckner, 1999; Ma, 2006). The biological significances of meiosis are to maintain genome stability and boost the genetic diversity between offspring through homologous recombination (HR) (Zickler and Kleckner, 2015).

HR is initiated by the programmed formation of DNA double-strand breaks (DSBs), which are catalyzed by a topoisomerase-like protein SPO11 and several accessory proteins (Keeney et al., 1997; Lam and Keeney, 2015). DSB sites are further resected by a protein complex known as MRX/N (Mre11-Rad50-Xrs2/Nbs1) and Sae2/Com1/CtIP/Ctp1 (Lamarche et al., 2010; Wang et al., 2018),

generating replication protein A (RPA)-coated single-stranded DNA (ssDNA) overhangs (Mimitou and Symington, 2009). Then, RPA is replaced by the RecA recombinases RAD51 and DMC1 forming nucleoprotein filaments and promoting homology search and single strand invasion to produce recombination intermediates called as the displacement (D)-loop (Hunter and Kleckner, 2001; Cloud et al., 2012). Ultimately, the extended D-Loop gives rise to double Holliday Junction (dHJ), which is resolved into a minority of COs and large number of NCOs (Youds and Boulton, 2011; Pyatnitskaya et al., 2019).

RAD17, a replication factor C (RFC)-like protein, is required for responses to DNA damage, replication stress and DSB repair (Shinohara et al., 2003; Wang et al., 2003, 2006b; Budzowska et al., 2004). The mechanism of RAD17 has been well illustrated in several species, such as yeast and human cells. In general, RAD17 acts as the checkpoint clamp loader to recruit the 9-1-1 complex (RAD9/HUS1/RAD1) onto DSB sites to promote interhomolog recombination and crossover formation (Burtelow et al., 2001; Zou et al., 2001; Griffith et al., 2002; Parrilla-Castellar et al., 2004; Majka et al., 2004; Navadgi-Patil and Burgers, 2009; Liu, 2019). In human, RAD17 facilitates the MRE11-RAD50-NBS1 complex loading and regulates the response to DNA damage (Wang et al., 2014). RAD17 functions relatively comprehensive in yeast. In budding yeast, Rad24 (the homolog of RAD17) was not only necessary for Ddc1/Mec3/Rad17 (the homolog of Rad9/Hus1/Rad1, respectively) loading onto DSB sites, but also required for meiotic prophase arrest in *dmc1* mutant background (Lydall et al., 1996; Majka and Burgers, 2005).

In plant, the mutation in *AtRAD17* led to hypersensitivity to the DNA-damaging agent treatment, whereas mutant plants were fully fertile, suggesting that the *RAD17* may not play an important role in Arabidopsis meiosis (Heitzeberg et al., 2004). In contrast, the disruption in *OsRAD17* resulted in aberrant associations between non-homologous chromosomes, leading to massive chromosome entanglements and fragmentations, indicating that the *OsRAD17* is essential for meiotic DSB repair in rice (Hu et al., 2018). The marked dissimilarity of meiotic outcomes caused by the defective *RAD17* raises an intriguing question that whether the role of *RAD17* in meiosis is conserved across plant kingdom. In this study, we characterized the maize *ZmRAD17* using a reverse genetic approach. Our results demonstrate that *ZmRAD17* is required for accurate DSB repair only in male meiosis. We also show that the meiotic abnormalities in *Zmrad17* exhibit multifaced differences from its counterpart in rice, implying that although the roles of *RAD17* in DSB repair seem to be fundamentally conserved at least in grass species, the exactly operative manner of *RAD17* may vary in different plant organisms.

MATERIALS AND METHODS

Plant Materials

We obtained two *Zmrad17* mutants from the Maize EMS induced Mutant Database (MEMD)[1] (Lu et al., 2018). All plants were grown in field during the growing season or greenhouse under normal growth conditions. Primer sequences used in genotyping were listed in **Supplementary Table S1**.

Pollen Viability

Pollen grains were dissected out of fresh anthers during pollination stage and viability was assessed by 1% I_2-KI staining. Images of stained pollen grains were taken using a Leica EZ4 HD stereo microscope equipped with a Leica DM2000 LED illumination system (Leica, Solms, Germany).

Rapid Amplification of cDNA Ends (RACE) and Reverse Transcription Quantitative PCR (RT-qPCR) Analysis

Total mRNA was isolated from root, stem, leaf, developing meiotic ear (1-2cm in length), immature tassel, developing embryo and endosperm (16 days after pollination) of B73 plants with TRIzol (TIANGEN). cDNA synthesis was performed by TaKaRa kits according to manufacturer's instructions. The entire cDNA was cloned by RACE using the SMART RACE cDNA amplification kit (Clontech). RT-qPCR analysis was performed using the CFX Connect Real-Time PCR System (BIO-RAD). Primer sequences used in RT-qPCR were listed in **Supplementary Table S1**.

Preparation of Meiotic Chromosome Spreads

Immature tassels were fixed for 24 h in Carnoy's solution (ethanol: acetic acid = 3:1, v/v). Then, tassels were stored in 70% ethanol at 4°C. Anthers at meiotic stages were squashed in 45% (v/v) acetic acid solution. Slides with chromosomes were frozen in liquid nitrogen and then cover slips were removed immediately. The slides were dehydrated through an ethanol series (70/90/100%) for 5 min each once. Dried slides were stained with 4′,6-diamidino-2-phenylindole (DAPI) in an antifade solution (Vector). Images were captured using a Ci-S-FL microscope (Nikon, Tokyo) equipped with a DS-Qi2 Microscope Camera system.

Florescence *in situ* Hybridization (FISH)

The FISH analysis was performed according to protocols described previously (Richards and Ausube, 1988; Li and Arumuganathan, 2001; Wang et al., 2006a; Han et al., 2007; Cheng, 2013 6a). Two repetitive DNA elements, 5S rDNA repeats (pTa794) and the telomere-specific repeats (pAtT4), were used as probes (Richards and Ausube, 1988). Probes were labeled with digoxigenin by nick translation mix (Roche) and detected with anti-digoxigenin antibody (Vector). Chromosome images were captured under a Ci-S-FL fluorescence microscope (Nikon) equipped with a DS-Qi2 microscopy camera (Nikon, Tokyo, Japan).

Immunofluorescence Assay

Young anthers during meiotic stages were fixed in 4% (w/v) paraformaldehyde for 30 min at room temperature and stored in 1x Buffer A at 4°C. Immunofluorescence was performed

[1] www.elabcaas.cn/memd/

as previously described (Pawlowski et al., 2003; Cheng, 2013). The primary antibodies against ASY1, ZYP1, and γH2AX were prepared as described previously (Jing et al., 2019). Antibody against RAD51 was a gift from Wojtek Pawlowski's Lab at Cornell University. Fluorochrome-coupled secondary antibodies (ABclonal) were used for fluorescence detection. All primary and secondary antibodies were diluted at 1:100. Images of meiocytes were observed and captured using a Ci-S-FL microscope (Nikon) equipped with a DS-Qi2 microscopy camera (Nikon, Tokyo, Japan). The images were captured by software NIS-Elements and colored by the ImageJ software.

Chiasma Quantification

The number of chiasmata were quantified for meiocytes at diakinesis. The rod-, ring-and "∞"-shaped bivalents were scored as one chiasma and two, three chiasmata, respectively.

RESULTS

Identification of *ZmRAD17*

To identify a putative *RAD17* gene in maize, the full-length amino acid sequence of the rice *RAD17* was used as a query to search in the maize genome database[2] by BLASTp analysis. We identified only one candidate gene (*Zm00001d047946*) with the highest similarity to the rice *RAD17* (*LOC_Os03g13850*). Phylogeny analyses revealed that RAD17 homologs formed two distinct clades reflecting the divergence between monocot and dicot plants (**Figure 1A**). In addition, the multiple sequence alignment of ZmRAD17 amino acid with its orthologs indicated that the RAD17 proteins were conserved in the primary AAA-ATPase domains (**Figure 1B**). We then investigated the spatio-temporal expression pattern of *ZmRAD17* using RT-qPCR analyses. The result showed that *ZmRAD17* was highly expressed in the developing tassel, ear, and embryo, but weakly expressed in root, stem, leaf and endosperm (**Figure 1C**).

[2]https://maizegdb.org/

Characterization of *Zmrad17* Mutants

The full-length cDNA sequence of *ZmRAD17* was isolated by performing rapid amplification of cDNA ends (RACE). It contains 2,089 bp with an open reading frame of 1,851bp and consists of 12 exons and 11 introns (**Figure 2A**). To characterize biological functions of *ZmRAD17*, two independent stop codon mutants were obtained from the EMS induced Mutant Database (MEMD) in B73 background (Lu et al., 2018). By conducting locus-specific PCR amplification followed by Sanger sequencing, we confirmed that the stop codon mutation sites are located in the first exon (named as *Zmrad17-1*) and the eighth exon (named as *Zmrad17-2*) of *ZmRAD17*, respectively (**Figure 2A**). Both *Zmrad17* mutants exhibited normal vegetative growth, but partially male-sterile (**Figure 2B** and **Supplementary Figure S1A**). KI-I_2 staining displayed that unlike large, round and purple pollen grains of the wild-type (**Figure 2C** and **Supplementary Figure S1B**), a proportion of mutant pollen grains were empty, shrunken and unable to stain (**Figures 2D,E** and **Supplementary Figures S1C,D**). Surprisingly,

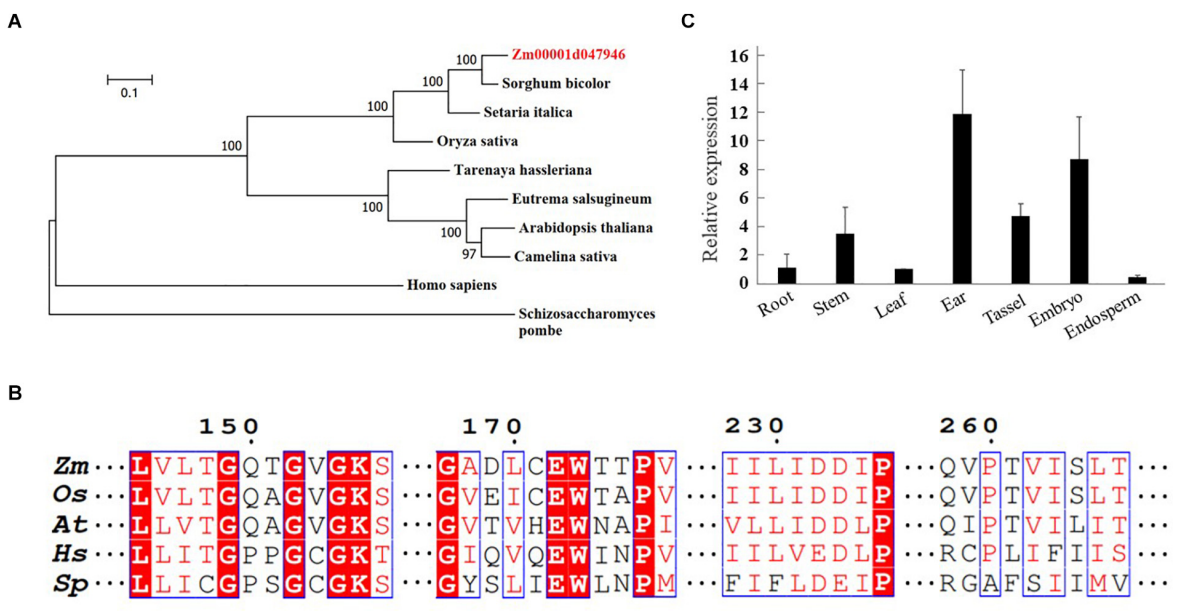

FIGURE 1 | Identification of ZmRAD17. **(A)** Phylogenetic analysis of RAD 17 proteins from representative dicotyledons, monocotyledons and mammal. The neighbor-joining method was used to construct an unrooted tree. **(B)** The conserved AAA-ATPase domain of RAD 17. Zea mays (Zm); Oryza sativa (Os); Arabidopsis thaliana (At); Schizosaccharomycespombe (Sp); Homo sapiens (Hs). **(C)** Tissue-specific expression analysis of ZmRAD 17 by RT-qPCR. The relative expression was calculated from the ratio of the expression in other tissues compared with leaf after normalizing by the ZmUBQ1 (Zm00001d010159) expression. Relative expression levels were mean values of three independent experiments with standard deviation.

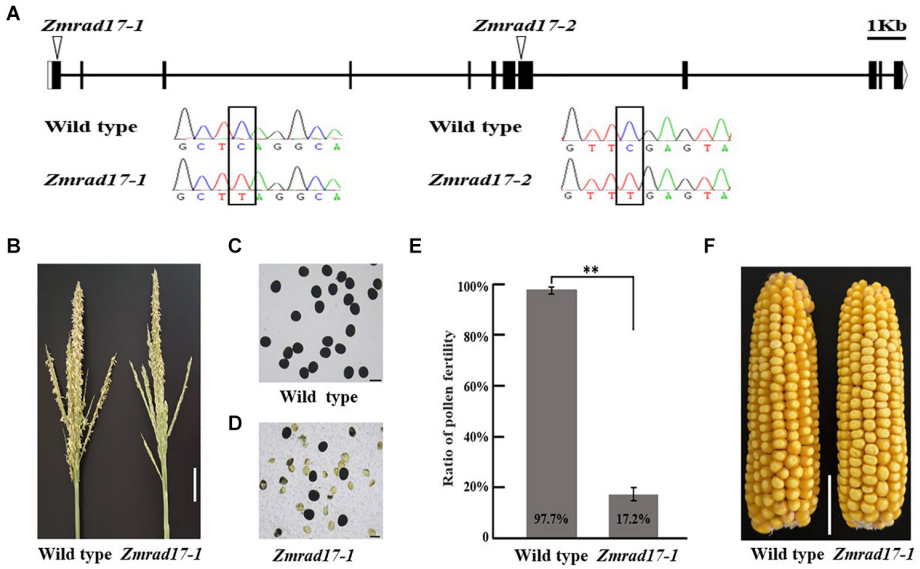

FIGURE 2 | Characterization of Zmrad17 mutant. **(A)** Gene structure of ZmRAD17. Mutation sites marked with triangles. Bars indicate exons and lines represent introns. Sequence analysis detected a single nucleotide substitute C in wild type to T in Zmrad17 mutants lead to premature translation termination. Bar = lkb. **(B)** Comparison of wild type tassel and Zmrad17-1 mutant tassel. Bar = 5 cm. **(C)** Pollen grains stained with I2-KI in wild type. Three biological and three technological replicates were used. Bar = 100 μm. **(D)** Pollen grains stained with I2-KI in Zmrad17-1. Three biological and three technological replicates were used. Bar = 100 μm. **(E)** Statistics analysis of pollen fertility in wild type and Zmrad17-1. Values are means ± *SD*. Double asterisks indicates the statistical significance at $p < 0.01$ using a two-tailed Student's *t*-test **(F)** Seed setting rate of wild type and Zmrad17-1 (homozygote) pollinated with wild type pollen. Bar = 3 cm.

when pollinated with pollen grains from wild-type plants, mutant ears exhibited a similar extent of seed setting (**Figure 2F** and **Supplementary Figure S1E**). These results indicate that the dysfunction of *ZmRAD17* causes effects on male reproductive development, but not on female.

Abnormal Meiotic Chromosome Behaviors in *Zmrad17* Mutants

To explore whether pollen abortion is resulted from the defect in male meiosis, chromosome behaviors were investigated in both wild-type and *Zmrad17* meiocytes at different stages by staining chromosome spreads with 4′,6-diamidino-2-phenylindole (DAPI). In the wild-type, chromosomes begun to condense and became visible as thin threads structures at leptotene (**Figure 3A**). Then, homologous chromosomes came close to each other and started to pair and synapsis at zygotene (**Figure 3B**). During pachytene, chromosomes were fully synapsed to form thick threads (**Figure 3C**). With chromosomes further condensed, 10 short, rod-like bivalents appeared to scatter in the nucleus at diakinesis (**Figure 3D**). Once entry into metaphase I, ten bivalents aligned on the equatorial plate in an orderly manner (**Figure 3E**). At anaphase I, homologous chromosomes separated equally and migrated toward the opposite poles (**Figure 3F**) forming dyad (**Figure 3G**). After the second meiotic division, the sister chromatids segregated and ultimately produced tetrad (**Figure 3H**).

In both of *Zmrad17* mutant meiocytes, chromosome behaviors were indistinguishable from the wild-type from leptotene to zygotene (**Figures 3I,J** and **Supplementary Figures S2A,B**). However, meiotic abnormalities started to be constantly observed at pachytene, showing abnormal chromosome associations between non-homologous chromosomes (**Figure 3K** and **Supplementary Figure S2C**). At diakinesis, although ten bivalents formed, aberrant bridges among bivalents were frequently observed in *Zmrad17* meiocytes (**Figure 3L**, $n = 37$; **Supplementary Figure S2D**). Despite all bivalents could be aligned on the equatorial plate during metaphase I, *Zmrad17* meiocytes exhibited abnormal bivalent aggregation (**Figure 3M** and **Supplementary Figure S2E**). At anaphase I, homologous chromosomes separated with obvious chromosome bridge and chromosome fragmentation (**Figure 3N** and **Supplementary Figure S2F**). Chromosome fragments were lagged and scattered randomly within the nucleus at telophase I (**Figure 3O** and **Supplementary Figure S2G**). The second meiotic division subsequently underwent and tetrad with micronuclei were formed (**Figure 3P** and **Supplementary Figure S3H**). These results suggest that the abnormal chromosome behaviors are responsible for the male sterility of *Zmrad17* mutants. Since *Zmrad17-1* and *Zmrad17-2* exhibited the same defect in the meiotic chromosome behaviors, all subsequent analyses were conducted using *Zmrad17-1* mutant as a representative of the *Zmrad17* dysfunction.

ZmRAD17 Is Not Required for DSB and CO Formation

To evaluate whether DSB formation is defective in *Zmrad17* mutant, we performed immunostaining with antibodies against

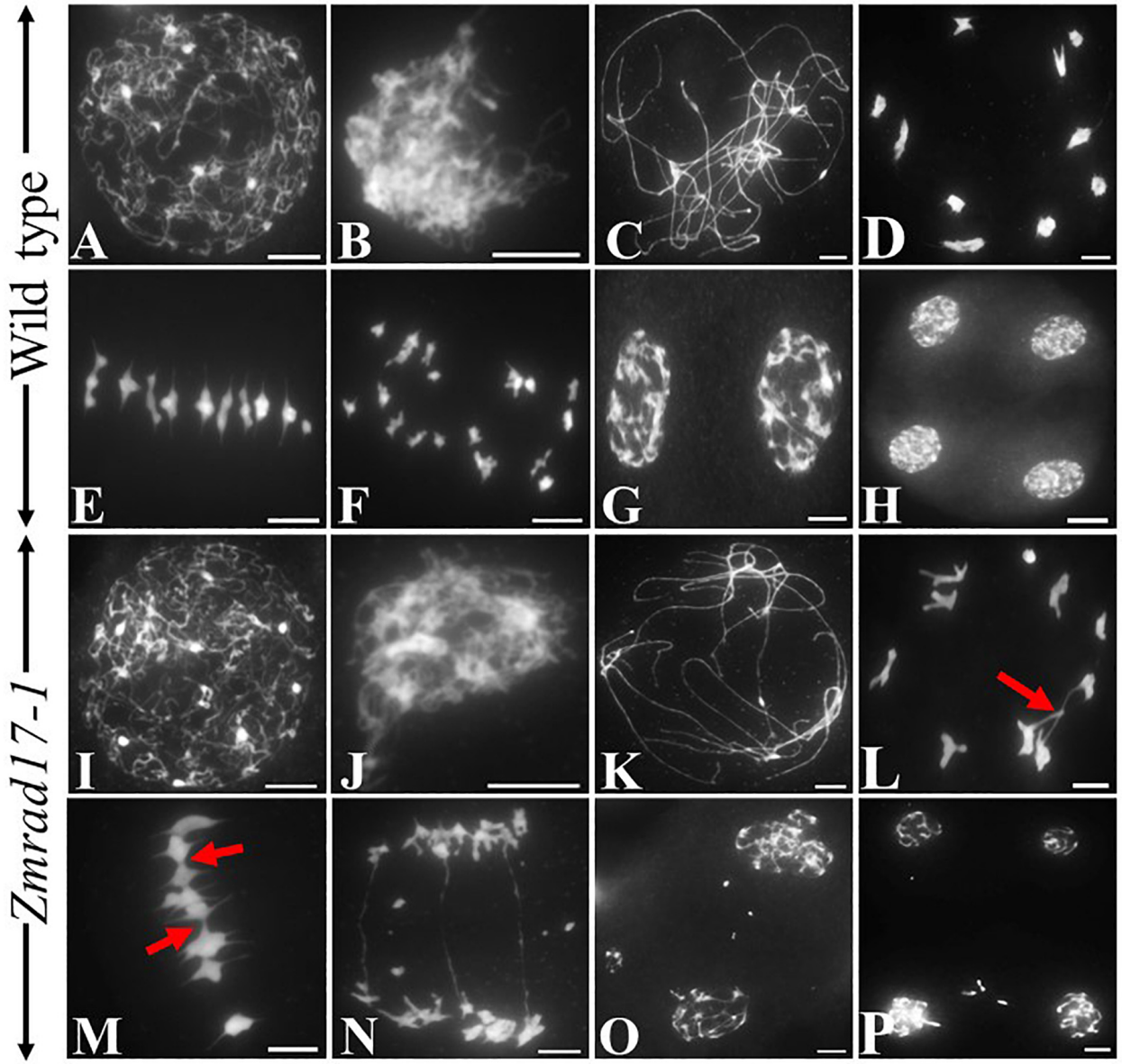

FIGURE 3 | The abnormal chromosome behaviors in Zmrad17-1 meiocytes. **(A–H)** Meiosis in the wild type. (I-P) Meiosis in the Zmrad17-1 mutant. **(A,I)** Leptotene; **(B,J)** Zygotene; **(C,K)** Pachytene; **(D,L)** Diakinesis; **(E,M)** Metaphase I; **(F,N)** Anaphase I; **(G,O)** Telophase I; **(H,P)** Tetrad. The red arrows pointed out the association between non-homologous chromosomes. Bars = 10 μm.

γH2AX and RAD51. γH2AX is a specific histone variant accumulating at damaged sites to promote DSB repair (Hunter et al., 2001; Dickey et al., 2009). Therefore, γH2AX is routinely used as a cytogenetic marker to detect the presence of DSB (Valdiglesias et al., 2013; Geric et al., 2014; Turinetto and Giachino, 2015). Our analysis revealed a substantial amount of dot-like γH2AX signals appeared in both wild-type (**Figure 4A**, n = 13) and mutant meiocytes at zygotene (**Figure 4B**, $n = 16$), suggesting that *ZmRAD17* is dispensable for DSB formation. The loading of RAD51 on chromosomes serves as an important marker to monitor HR-mediated DSB repair in many different organisms (Pawlowski et al., 2003). Constantly, we did not observe marked difference in the localization of RAD51 signals between wild-type (**Figure 4C**, $n = 24$) and *Zmrad17-1* meiocytes at zygotene (**Figure 4D**, $n = 35$), suggesting that *ZmRAD17* is not crucial for HR initiation. Moreover, the number of chiasmata were counted in both wild type and mutant meiocytes at diakinesis stage using a method described previously (Moran et al., 2001). We found that although aberrant associations among bivalents occurred in *Zmrad17-1* meiocytes, the number of chiasmata (**Supplementary Figure S3**) seemed comparable between wild type (17.08 ± 1.93, $n = 24$) and mutant

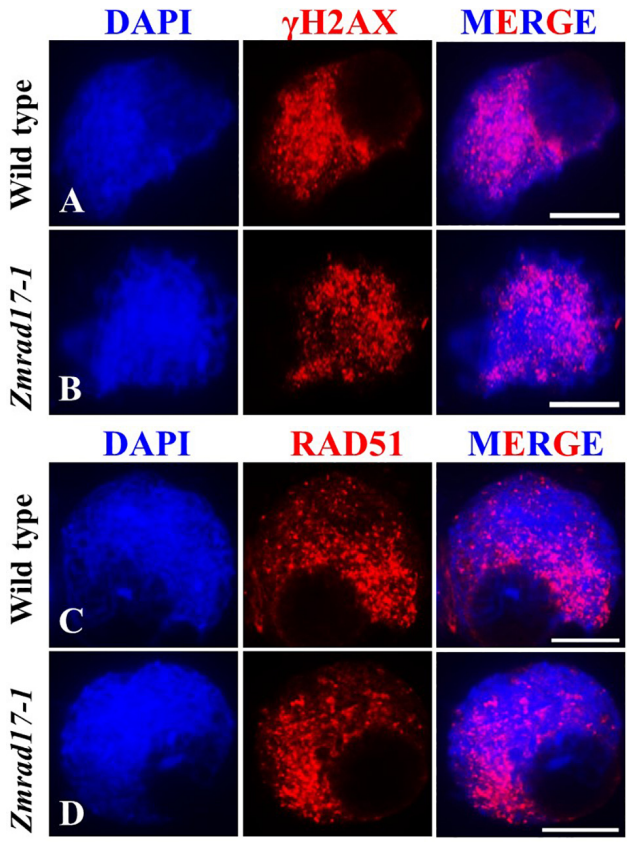

FIGURE 4 | ZmRAD17 is not required for DSB formation. **(A,B)** γH2AX foci in wild type **(A)** and Zmradl 7-1 meiocytes **(B)**. **(C,D)** RAD51 foci in wild type **(C)** and Zmrad17-1 meiocytes **(D)**. DAPI staining was used to indicate the chromosomes. Bars = 10 um.

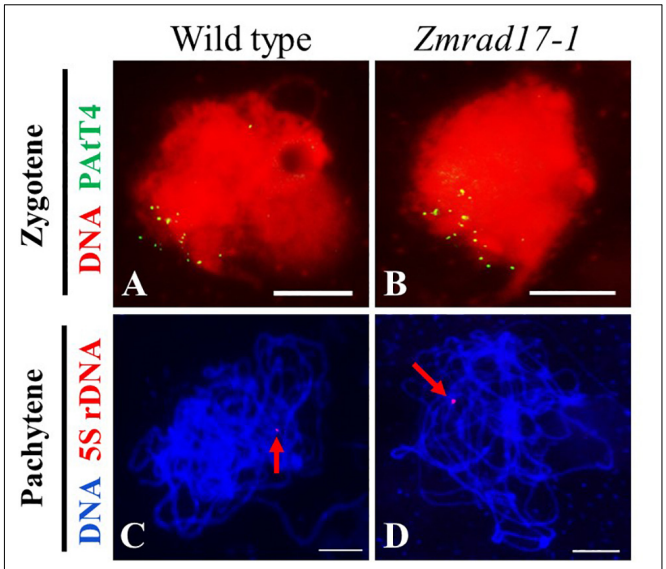

FIGURE 5 | ZmRAD17 is not required for telomere bouquet formation and homologous pairing. **(A,B)** FISH with the telomere-specific pAtT4 probe in the wild type **(A)**, Zmrad17-1 **(B)** meiocytes at zygotene. **(C,D)** FISH with the 5S rDNA the wild type **(C)** and Zmrad17-1 **(D)** meiocytes at pachytene. The red arrows pointed out the 5S rDNA signal. Bars = 10 um.

(17.11 ± 2.10, $n = 19$), implying that *ZmRAD17* is not critical for CO formation.

ZmRAD17 Is Dispensable for Telomere Bouquet Clustering and Homologous Pairing

Telomere bouquet clustering occurs specifically at early zygotene and is thought to be essential for homologous pairing and synapsis (Bass et al., 1997; Harper et al., 2004). To test whether telomere bouquet formation is affected in *Zmrad17-1*, we conducted FISH using a telomere specific probe (pAtT4) in both wild-type and *Zmrad17* meiocytes. The result displayed that nearly all of telomere signals were clustered and attached to the nuclear envelope in both wild-type (**Figure 5A**, $n = 12$) and *Zmrad17-1* (**Figure 5B**, $n = 24$) meiocytes at zygotene, indicating that *ZmRAD17* is not required for telomere bouquet formation.

The 5S ribosomal DNA (rDNA) is a tandemly repetitive sequence located on the long arm of chromosome 2 in maize and is often used to monitor homologous pairing (Li and Arumuganathan, 2001). To examine whether the disruption of *ZmRAD17* could impact the homologous chromosome pairing, FISH analysis using 5S rDNA as a probe was conducted. The results showed that only one 5S rDNA signal was constantly detected in both wild-type (**Figure 5C**, $n = 23$) and *Zmrad17-1* meiocytes (**Figure 5D**, $n = 37$) at pachytene, suggesting that *ZmRAD17* is not necessary for homologous pairing.

ZmRAD17 Is Indispensable for Synaptonemal Complex Assembly

The synaptonemal complex (SC) is a protein scaffold linking homologous chromosomes to promote meiotic crossover formation (Cahoon and Hawley, 2016). To inspect the installation behavior of the SC, we conducted immunolocalization using antibodies against ASY1 and ZYP1 in both wild-type and *Zmrad17-1* meiocytes. ASY1, the axial element (AE) component of SC, localizes at chromosome axis (Sanchez-Moran et al., 2007; Sanchez-Moran et al., 2008). In the wild-type, ASY1 loading appeared as continuous linear signals along entire chromosomes at zygotene (**Figure 6A**, $n = 10$). Similar pattern of ASY1 distribution was observed in *Zmrad17-1* at the same stage (**Figure 6B**, $n = 32$), indicating that *ZmRAD17* is not required for AE installation.

ZYP1 constitutes the central element (CE) of SC (Higgins et al., 2005; Golubovskaya et al., 2011). At pachytene, ZYP1 signals in wild-type meiocytes formed continuous linear signals along the whole length of synapsed chromosomes (**Figure 6C**, $n = 14$). In contrast, although 18.2% of *Zmrad17-1* meiocytes showed a similar ZYP1 staining as wild-type, the remaining 81.8% of meiocytes exhibited short stretches of ZYP1 signals in *Zmrad17-1* (**Figure 6D**, $n = 88$). Taken

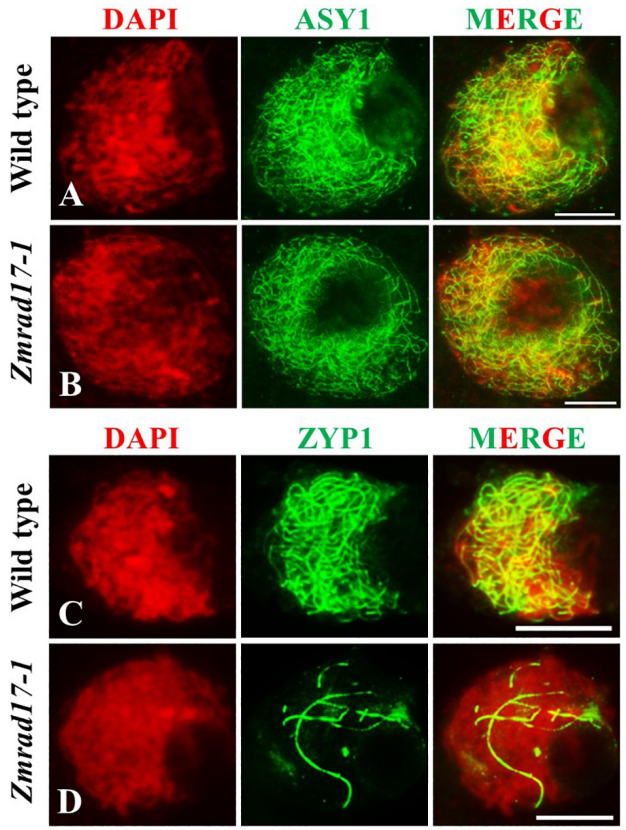

FIGURE 6 | Immunolocalization of ASY1 and ZYP1 antibodies on meiotic chromosomes in wild type and Zmrad17-1 meiocytes. ASY1 **(A)** and ZYP1 **(C)** in wild type meiocytes; ASY1 **(B)** and ZYP1 **(D)** in Zmrad17-1 meiocytes. DAPI staining was used to indicate the chromosomes. Bars = 10 μm.

together, these results indicate that *ZmRAD17* is indispensable for SC installation.

DISCUSSION

In yeast and mammals, it has been clarified that *RAD17* not only participates in mitosis, but also plays an important role in meiosis (Lydall et al., 1996; Grushcow et al., 1999; Shinohara et al., 2003; Budzowska et al., 2004). Deletion of *RAD24* in *S. cerevisiae* delayed DSB repair and resulted in abnormal recombination (Grushcow et al., 1999; Shinohara et al., 2003). In mouse, the mutation of *RAD17* caused embryonic lethality (Budzowska et al., 2004). In the model plant Arabidopsis, the defective *RAD17* was considered to have no strong effects on meiosis due to the normal fertility of both male and female, whereas the mutant displayed hypersensitive to DNA-damaging agents with the frequent presence of intrachromosomal HR during mitosis (Heitzeberg et al., 2004). In rice, the disruption of *RAD17* resulted in massive abnormal associations between non-homologous chromosomes, leading to enormous chromosome aggregations and fragments during male meiosis (Hu et al., 2018). In contrast, the loss-of-function of *RAD17* caused similar but much less severe effects on meiotic chromosome behaviors in maize, exemplified by subtle chromosome entanglement and fragmentation. Particularly, the unidirectional abnormality in male meiosis from the dysfunction of the maize *RAD17* seems strikingly different from rice, where both male and female were aborted (Hu et al., 2018). These findings highlight that although the participation of *RAD17* homologs in DSB repair is widely conserved, the precise effects of RAD17 on meiosis seem divergent among different organisms.

In budding yeast, the RAD24 (the homolog of RAD17) acts as the checkpoint clamp loader of the DNA damage response clamp 9-1-1 promoting assembly of synaptonemal complex and installation of ZMM proteins for CO formation (Shinohara et al., 2015; Crawford et al., 2018). In the *Zmrad17* mutant, the disturbed loading of ZYP1 protein supports the functional conservation of RAD17 in the SC installation between yeast and plant. In contrast, the SC formation seemed roughly normal in the *Osrad17* mutant, and the incomplete SC formation only occurred after combining *Osrad17* with mutation in ZMM proteins, such as ZIP4 or MSH5, implying that *OsRAD17* has to work cooperatively with ZMM proteins to promote homologous pairing and synapsis in rice (Hu et al., 2018). In this context, the redundancy between RAD17 and ZMM proteins in regulating the SC installation may not be critical in maize.

Chromosome fragmentation and entanglement are characteristic phenomena observed in mutants deficient in DSB repair machinery. Like the *Osrad17* mutants (Hu et al., 2018) and other related mutants such as *Zmcom1* (Wang et al., 2018), *Zmrad51c* (Jing et al., 2019), *Osxrcc3* (Zhang et al., 2015), *Atrad50* (Gallego et al., 2001; Bleuyard et al., 2004) and *Atmre11* (Samanic et al., 2013, 2016), the *Zmrad17* mutants showed the presence of chromosome fragmentation at prophase I. However, the severity of chromosome aberration seemed to be much less in *Zmrad17* when compared to the *Osrad17* mutants. A simple explanation for this discrepancy could be that other genes work redundantly with *ZmRAD17* in promoting accurate DSB repair. Alternatively, the other DSB repair pathway, such as classical non-homologous end-joining (C-NHEJ) (Shrivastav et al., 2008; Ceccaldi et al., 2016), which is routinely inhibited during meiotic DSB repair, could be active in the absence of the HR pathway (Hu et al., 2016). If this is true, such compensatory activity of C-NHEJ may vary between maize and rice. In this scenario, *ZmRAD17* might play a role in the DSB repair pathway choice, which has been suggested for the rice *OsRAD17* previously (Hu et al., 2018). Furthermore, as the CO formation appeared normal in the *Zmrad17* mutant, we propose that the repair of most DSBs by HR in *Zmrad17* is sufficient for the homologous recombination.

DATA AVAILABILITY STATEMENT

The original contributions presented in the study are included in the article/**Supplementary Material**, further inquiries can be directed to the corresponding author/s.

AUTHOR CONTRIBUTIONS

YH conceived and supervised the project. TZ, LL, and J-LJ conducted the experiments. TZ and YH prepared the manuscript. All authors read and approved the final manuscript.

FUNDING

This work was supported by grants from the National Natural Science Foundation of China (31970524) to YH.

ACKNOWLEDGMENTS

We thank all the members of our laboratories for helpful discussion and assistance during this research.

SUPPLEMENTARY MATERIAL

The Supplementary Material for this article can be found online at: https://www.frontiersin.org/articles/10.3389/fpls.2021.626528/full#supplementary-material

REFERENCES

Bass, H. W., Marshall, W. F., Sedat, J. W., Agard, D. A., and Cande, W. Z. (1997). Telomeres cluster de novo before the initiation of synapsis: a three-dimensional spatial analysis of telomere positions before and during meiotic prophase. *J. Cell Biol.* 137, 5–18. doi: 10.1083/jcb.137.1.5

Bleuyard, J. Y., Gallego, M. E., and White, C. I. (2004). Meiotic defects in the *Arabidopsis* rad50 mutant point to conservation of the MRX complex function in early stages of meiotic recombination. *Chromosoma* 113, 197–203. doi: 10.1007/s00412-004-0309-1

Budzowska, M., Jaspers, I., Essers, J., de Waard, H., van Drunen, E., Hanada, K., et al. (2004). Mutation of the mouse Rad17 gene leads to embryonic lethality and reveals a role in DNA damage-dependent recombination. *EMBO J.* 23, 3548–3558. doi: 10.1038/sj.emboj.7600353

Burtelow, M. A., Roos-Mattjus, P. M., Rauen, M., Babendure, J. R., and Karnitz, L. M. (2001). Reconstitution and molecular analysis of the hRad9-hHus1-hRad1 (9-1-1) DNA damage responsive checkpoint complex. *J. Biol. Chem.* 276, 25903–25909. doi: 10.1074/jbc.M102946200

Cahoon, C. K., and Hawley, R. S. (2016). Regulating the construction and demolition of the synaptonemal complex. *Nat. Struct. Mol. Biol.* 23, 369–377.

Ceccaldi, R., Rondinelli, B., and D'Andrea, A. D. (2016). Repair pathway choices and consequences at the double-strand break. *Trends. Cell Biol.* 26, 52–64. doi: 10.1016/j.tcb.2015.07.009

Cheng, Z. (2013). Analyzing meiotic chromosomes in rice. *Methods Mol. Biol.* 990, 125–134. doi: 10.1007/978-1-62703-333-6_13

Cloud, V., Chan, Y. L., Grubb, J., Budke, B., and Bishop, D. K. (2012). Rad51 is an accessory factor for Dmc1-mediated joint molecule formation during meiosis. *Science* 337, 1222–1225. doi: 10.1126/science.1219379

Crawford, M. R., Cooper, T. J., Marsolier-Kergoat, M.-C., Llorente, B., and Neale, M. J. (2018). Separable roles of the DNA damage response kinase Mec1ATR and its activator Rad24RAD17 within the regulation of meiotic recombination. *bioRxiv* [Preprint] doi: 10.1101/496182

de Massy, B. (2013). Initiation of meiotic recombination: how and where? Conservation and specificities among eukaryotes. *Annu. Rev. Genet.* 47, 563–599. doi: 10.1146/annurev-genet-110711-155423

Dickey, J. S., Redon, C. E., Nakamura, A. J., Baird, B. J., Sedelnikova, O. A., and Bonner, W. M. (2009). H2AX: functional roles and potential applications. *Chromosoma* 118, 683–692. doi: 10.1007/s00412-009-0234-4

Gallego, M. E., Jeanneau, M., Granier, F., Bouchez, D., Bechtold, N., and White, C. I. (2001). Disruption of the *Arabidopsis* RAD50 gene leads to plant sterility and MMS sensitivity. *Plant J.* 25, 31–41. doi: 10.1046/j.1365-313x.2001.00928.x

Geric, M., Gajski, G., and Garaj-Vrhovac, V. (2014). γ-H2AX as a biomarker for DNA double-strand breaks in ecotoxicology. *Ecotoxicol. Environ. Safe.* 105, 13–21. doi: 10.1016/j.ecoenv.2014.03.035

Golubovskaya, I. N., Wang, C. J. R., Timofejeva, L., and Cande, W. Z. (2011). Maize meiotic mutants with improper or non-homologous synapsis due to problems in pairing or synaptonemal complex formation. *J. Exp. Bot.* 62, 1533–1544. doi: 10.1093/jxb/erq292

Griffith, J. D., Lindsey-Boltz, L. A., and Sancar, A. (2002). Structures of the human Rad17-replication factor C and checkpoint Rad 9-1-1 complexes visualized by glycerol spray/low voltage microscopy. *J. Biol. Chem.* 277, 15233–15236. doi: 10.1074/jbc.C200129200

Grushcow, J. M., Holzen, T. M., Park, K. J., Weinert, T., Lichten, M., and Bishop, D. K. (1999). *Saccharomyces cerevisiae* checkpoint genes MEC1, RAD17 and RAD24 are required for normal meiotic recombination partner choice. *Genetics* 153, 607–620.

Han, F., Gao, Z., Yu, W., and Birchler, J. A. (2007). Minichromosome analysis of chromosome pairing, disjunction, and sister chromatid cohesion in maize. *Plant Cell* 19, 3853–3863. doi: 10.1105/tpc.107.055905

Harper, L., Golubovskaya, I., and Cande, W. Z. (2004). A bouquet of chromosomes. *J. Cell Sci.* 117, 4025–4032. doi: 10.1242/jcs.01363

Heitzeberg, F., Chen, I.-P., Hartung, F., Orel, N., Angelis, K. J., and Puchta, H. (2004). The Rad17 homologue of *Arabidopsis* is involved in theregulation of DNA damage repair and homologous recombination. *Plant J.* 38, 954–968. doi: 10.1111/j.1365-313X.2004.02097.x

Higgins, J. D., Sanchez-Moran, E., Armstrong, S. J., Jones, G. H., and Franklin, F. C. H. (2005). The *Arabidopsis* synaptonemal complex protein ZYP1 is required for chromosome synapsis and normal fidelity of crossing over. *Genes Dev.* 19, 2488–2500. doi: 10.1101/gad.354705

Hu, Q., Tang, D., Wang, H., Shen, Y., Chen, X., Ji, J., et al. (2016). The exonuclease homolog OsRAD1 promotes accurate meiotic double-strand break repair by suppressing nonhomologous end joining. *Plant physiol.* 172, 1105–1116. doi: 10.1104/pp.16.00831

Hu, Q., Zhang, C., Xue, Z., Ma, L., Liu, W., Shen, Y., et al. (2018). OsRAD17 is required for meiotic double-strand break repair and plays a redundant role with OsZIP4 in synaptonemal complex assembly. *Front. Plant Sci.* 9:1236. doi: 10.3389/fpls.2018.01236

Hunter, N., Börner, G. V., Lichten, M., and Kleckner, N. (2001). γ-H2AX illuminates meiosis. *Nat. Genet.* 27, 236–238. doi: 10.1038/85781

Hunter, N., and Kleckner, N. (2001). The single-end invasion: an asymmetric intermediate at the double-strand break to double-holliday junction transition of meiotic recombination. *Cell* 106, 59–70. doi: 10.1016/s0092-8674(01)00430-5

Jing, J., Zhang, T., Wang, Y., Cui, Z., and He, Y. (2019). ZmRAD51C is essential for double-strand break repair and homologous recombination in maize meiosis. *Int. J. Mol. Sci.* 20:5513. doi: 10.3390/ijms20215513

Keeney, S., Giroux, C. N., and Kleckner, N. (1997). Meiosis-specific DNA double-strand breaks are catalyzed by Spo11, a member of a widely conserved protein family. *Cell* 88, 375–384. doi: 10.1016/s0092-8674(00)81876-0

Lam, I., and Keeney, S. (2015). Mechanism and regulation of meiotic recombination initiation. *Cold Spring Harb. Perspect. Biol.* 7:a016634. doi: 10.1101/cshperspect.a016634

Lamarche, B. J., Orazio, N. I., and Weitzman, M. D. (2010). The MRN complex in double-strand break repair and telomere maintenance. *FEBS Lett.* 584, 3682–3695. doi: 10.1016/j.febslet.2010.07.029

Li, L., and Arumuganathan, K. (2001). Physical mapping of sorted chromosomes 45s and 5s rDNA on maize metaphase and by FISH. *Hereditas* 134, 141–145. doi: 10.1111/j.1601-5223.2001.00141.x

Liu, W. (2019). The structure of the checkpoint clamp 9-1-1 complex and clamp loader Rad24-RFC in *Saccharomyces cerevisiae*. *Biochem. Biophys. Res. Commun.* 515, 688–692. doi: 10.1016/j.bbrc.2019.05.138

Lu, X., Liu, J., Ren, W., Yang, Q., Chai, Z., Chen, R., et al. (2018). Gene-indexed mutations in maize. *Mol. Plant* 11, 496–504. doi: 10.1016/j.molp.2017.11.013

Lydall, D., Nikolsky, Y., Bishop, D. K., and Weinert, T. (1996). A meiotic recombination checkpoint controlled by mitotic checkpoint genes. *Nature* 383, 840–843. doi: 10.1038/383840a0

Ma, H. (2006). A molecular portrait of *Arabidopsis* meiosis. *Arabidopsis Book* 4:e0095. doi: 10.1199/tab.0095

Majka, J., and Burgers, P. M. (2005). Function of Rad17/Mec3/Ddc1 and its partial complexes in the DNA damage checkpoint. *DNA Repair* 4, 1189–1194. doi: 10.1016/j.dnarep.2005.07.008

Majka, J., Chung, B. Y., and Burgers, P. M. (2004). Requirement for ATP by the DNA damage checkpoint clamp loader. *J. Biol. Chem.* 279, 20921–20926. doi: 10.1074/jbc.M400898200

Mercier, R., Mezard, C., Jenczewski, E., Macaisne, N., and Grelon, M. (2015). The molecular biology of meiosis in plants. *Annu. Rev. Plant Biol.* 66, 297–327.

Mimitou, E. P., and Symington, L. S. (2009). DNA end resection: many nucleases make light work. *DNA Repair* 8, 983–995. doi: 10.1016/j.dnarep.2009.04.017

Moran, E. S., Armstrong, S. J., Santos, J. L., Franklin, F. C. H., and Jones, G. H. (2001). Chiasma formation in *Arabidopsis thaliana* accession Wassileskija and in two meiotic mutants. *Chromosom. Res.* 9, 121–128. doi: 10.1023/a:1009278902994

Navadgi-Patil, V. M., and Burgers, P. M. (2009). A tale of two tails: activation of DNA damage checkpoint kinase Mec1/ATR by the 9-1-1 clamp and by Dpb11/TopBP1. *DNA Repair* 8, 996–1003. doi: 10.1016/j.dnarep.2009.03.011

Parrilla-Castellar, E. R., Arlander, S. J., and Karnitz, L. (2004). Dial 9-1-1 for DNA damage: the Rad9-Hus1-Rad1 (9-1-1) clamp complex. *DNA Repair* 3, 1009–1014. doi: 10.1016/j.dnarep.2004.03.032

Pawlowski, W. P., Golubovskaya, I. N., and Cande, W. Z. (2003). Altered nuclear distribution of recombination protein RAD51 in maize mutants suggests the involvement of RAD51 in meiotic homology recognition. *Plant Cell* 15, 1807–1816. doi: 10.1105/tpc.012898

Pyatnitskaya, A., Borde, V., and De Muyt, A. (2019). Crossing and zipping: molecular duties of the ZMM proteins in meiosis. *Chromosoma* 128, 181–198. doi: 10.1007/s00412-019-00714-8

Richards, E. J., and Ausube, F. M. (1988). Isolation of a higher eukaryotic telomere from *Arabidopsis thaliana*. *Cell* 53, 127–136.

Samanic, I., Cvitanic, R., Simunic, J., and Puizina, J. (2016). *Arabidopsis thaliana*MRE11 is essential for activation of cell cycle arrest, transcriptional regulation and DNA repair upon the induction of double-stranded DNA breaks. *Plant Biol.* 18, 681–694. doi: 10.1111/plb.12453

Samanic, I., Simunic, J., Riha, K., and Puizina, J. (2013). Evidence for distinct functions of MRE11 in Arabidopsis meiosis. *PLoS One* 8:e78760.

Sanchez-Moran, E., Osman, K., Higgins, J. D., Pradillo, M., Cunado, N., Jones, G. H., et al. (2008). ASY1 coordinates early events in the plant meiotic recombination pathway. *Cytogenet. Genome Res.* 120, 302–312.

Sanchez-Moran, E., Santos, J. L., Jones, G. H., and Franklin, F. C. (2007). ASY1 mediates AtDMC1-dependent interhomolog recombination during meiosis in *Arabidopsis*. *Genes Dev.* 21, 2220–2233. doi: 10.1101/gad.439007

Shinohara, M., Hayashihara, K., Grubb, J. T., Bishop, D. K., and Shinohara, A. (2015). DNA damage response clamp 9-1-1 promotes assembly of ZMM proteins for formation of crossovers and synaptonemal complex. *J. Cell Sci.* 128, 1494–1506. doi: 10.1242/jcs.161554

Shinohara, M., Sakai, K., Ogawa, T., and Shinohara, A. (2003). The mitotic DNA damage checkpoint proteins Rad17 and Rad24 are required for repair of double-strand breaks during meiosis in yeast. *Genetics* 164, 855–865.

Shrivastav, M., De Haro, L. P., and Nickoloff, J. A. (2008). Regulation of DNA double-strand break repair pathway choice. *Cell Res.* 18, 134–147.

Turinetto, V., and Giachino, C. (2015). Multiple facets of histone variant H2AX: a DNA double-strand-break marker with several biological functions. *Nucleic Acids Res.* 43, 2489–2498. doi: 10.1093/nar/gkv061

Valdiglesias, V., Giunta, S., Fenech, M., Neri, M., and Bonassi, S. (2013). γH2AX as a marker of DNA double strand breaks and genomic instability in human population studies. *Mutat. Res.* 753, 24–40. doi: 10.1016/j.mrrev.2013.02.001

Wang, C. J., Harper, L., and Cande, W. Z. (2006a). High-resolution single-copy gene fluorescence in situ hybridization and its use in the construction of a cytogenetic map of maize chromosome 9. *Plant Cell* 18, 529–544.

Wang, Q., Goldstein, M., Alexander, P., Wakeman, T. P., Sun, T., Feng, J., et al. (2014). Rad17 recruits the MRE11-RAD50-NBS1 complex to regulate the cellular response to DNA double-strand breaks. *EMBO J.* 33, 862–877. doi: 10.1002/embj.201386064

Wang, X., Zou, L., Lu, T., Bao, S., Hurov, K. E., Hittelman, W. N., et al. (2006b). Rad17 phosphorylation is required for claspin recruitment and Chk1 activation in response to replication stress. *Mol. Cell* 23, 331–341.

Wang, X., Zou, L., Zheng, H., Wei, Q., Elledge, S. J., and Li, L. (2003). Genomic instability and endoreduplication triggered by RAD17 deletion. *Genes Dev.* 17, 965–970. doi: 10.1101/gad.1065103

Wang, Y., Jiang, L., Zhang, T., Jing, J., and He, Y. (2018). ZmCom1 is required for both mitotic and meiotic recombination in maize. *Front. Plant Sci.* 9:1005. doi: 10.3389/fpls.2018.01005

Youds, J. L., and Boulton, S. J. (2011). The choice in meiosis – defining the factors that influence crossover or non-crossover formation. *J. Cell Sci.* 124, 501–513. doi: 10.1242/jcs.074427

Zhang, B., Wang, M., Tang, D., Li, Y., Xu, M., Gu, M., et al. (2015). XRCC3 is essential for proper double-strand break repair and homologous recombination in rice meiosis. *J. Exp. Bot.* 66, 5713–5725.

Zickler, D., and Kleckner, N. (1999). Meiotic chromosomes: integrating structure and function. *Annu. Rev. Genet.* 33, 603–754. doi: 10.1146/annurev.genet.33.1.603

Zickler, D., and Kleckner, N. (2015). Recombination, pairing, and synapsis of homologs during meiosis. *Cold Spring Harb. Perspect. Biol.* 7:a016626.

Zou, L., Cortez, D., and Elledge, S. J. (2001). Regulation of ATR substrate selection-by Rad17-dependent loading of Rad9 complexes onto chromatin. *Gene. Dev.* 16, 198–208. doi: 10.1101/gad.950302

Conflict of Interest: The authors declare that the research was conducted in the absence of any commercial or financial relationships that could be construed as a potential conflict of interest.

frontiers in Plant Science

ORIGINAL RESEARCH
published: 04 March 2021
doi: 10.3389/fpls.2021.638051

Meiocyte Isolation by INTACT and Meiotic Transcriptome Analysis in *Arabidopsis*

*Lucia Barra[1†], Pasquale Termolino[1†], Riccardo Aiese Cigliano[2†], Gaetana Cremona[1], Rosa Paparo[1], Carmine Lanzillo[1], Maria Federica Consiglio[1] and Clara Conicella[1]**

[1] Institute of Biosciences and Bioresources, National Research Council of Italy, Portici, Italy, [2] Sequentia Biotech SL, Barcelona, Spain

Isolation of nuclei tagged in specific cell types (INTACT) is a method developed to isolate cell-type-specific nuclei that are tagged through *in vivo* biotin labeling of a nuclear targeting fusion (NTF) protein. In our work, INTACT was used to capture nuclei of meiocytes and to generate a meiotic transcriptome in *Arabidopsis*. Using the promoter of *AtDMC1* recombinase to label meiotic nuclei, we generated transgenic plants carrying *AtDMC1:NTF* along with biotin ligase enzyme (*BirA*) under the constitutive *ACTIN2* (*ACT2*) promoter. *AtDMC1*-driven expression of biotin-labeled *NTF* allowed us to collect nuclei of meiocytes by streptavidin-coated magnetic beads. The nuclear meiotic transcriptome was obtained by RNA-seq using low-quantity input RNA. Transcripts grouped into different categories according to their expression levels were investigated by gene ontology enrichment analysis (GOEA). The most enriched GO term "DNA demethylation" in mid/high-expression classes suggests that this biological process is particularly relevant to meiosis onset. The majority of genes with established roles in meiosis were distributed in the classes of mid/high and high expression. Meiotic transcriptome was compared with public available transcriptomes from other tissues in Arabidopsis. Bioinformatics analysis by expression network identified a core of more than 1,500 genes related to meiosis landmarks.

Keywords: meiosis, meiocyte, tagged nuclei, RNA-seq, meiotic transcriptome

OPEN ACCESS

Edited by:
Olivier Da Ines, Université Clermont Auvergne, France

Reviewed by:
Wei-Hua Tang, Shanghai Institutes for Biological Sciences (CAS), China
Josh T. Cuperus, University of Washington, United States

****Correspondence:***
Clara Conicella
conicell@unina.it

† These authors have contributed equally to this work and share first authorship

Specialty section:
This article was submitted to Plant Cell Biology, a section of the journal Frontiers in Plant Science

Received: *04 December 2020*
Accepted: *01 February 2021*
Published: *04 March 2021*

Citation:
Barra L, Termolino P, Aiese Cigliano R, Cremona G, Paparo R, Lanzillo C, Consiglio MF and Conicella C (2021) Meiocyte Isolation by INTACT and Meiotic Transcriptome Analysis in Arabidopsis. Front. Plant Sci. 12:638051. doi: 10.3389/fpls.2021.638051

INTRODUCTION

Meiosis is a complex process critical to sexual reproduction. In plants, meiosis appears to be influenced by environmental cues (reviewed in De Storme and Geelen, 2014; Si et al., 2015). Within this context, global climate change is expected to have an impact on crop production with consequences for food security (Parry et al., 1999). To face the new challenges, a fundamental understanding of meiosis is required in model, crop, and non-model plants (Lambing and Heckmann, 2018). Molecular knowledge of plant meiosis has primarily advanced through understanding the function of single genes involved in key steps being benefited by the conserved pathways across model species (reviewed in Mercier et al., 2015). Thereafter, transcriptome studies of specific cell types improved our understanding of the gene-expression landscape during meiosis (reviewed in Dubowic-Shulze and Chen, 2014). However, the isolation of plant meiocytes is challenging due to the difficulty in accessing the germline cells. Pollen mother cells and embryo

sac mother cells are enclosed by sporophytic tissues, i.e., anthers and ovules inside the flower buds. Over the last decade, different techniques were established for targeted isolation of meiocytes by micromanipulation (Chen et al., 2010; Libeau et al., 2011; Yang et al., 2011; Nelms and Walbot, 2019) and laser microdissection (Tang et al., 2010; Schmidt et al., 2011; Barra et al., 2012; Yuan et al., 2018).

An alternative method that achieves the isolation of nuclei tagged in specific cell types (INTACT) was developed by Deal and Henikoff (2011). INTACT overcomes the limitation of time-consuming manual dissection generally associated with contamination of undesired cells. Therefore, INTACT allows rapid and efficient nucleus isolation with the advantage of not requiring specialized and expensive equipment (Deal and Henikoff, 2010). INTACT is based on *in vivo* biotin labeling of a nuclear targeting fusion (NTF) protein which consists of three parts corresponding to (1) a unique target peptide of biotin ligase recognition (BLRP), (2) a domain from *Arabidopsis* RAN GTPASE ACTIVATING PROTEIN 1 (RanGAP1) for nuclear envelope localization (Rose and Meier, 2001), and (3) green fluorescent protein (GFP) for visualization. BLRP acts as a substrate for the BirA biotin ligase enzyme from *Escherichia coli* (Beckett et al., 1999). *BirA* and *NTF* need to be co-expressed in the same cell.

So far, INTACT has been used in combination with transcriptomic, epigenomic, and proteomic studies in different species including plants (Amin et al., 2014; Agrawal et al., 2019; Del Toro-De León and Köhler, 2019). However, in plants, a broad use of INTACT across different cell types remains challenging since it requires a cell-type marker and a method for genetic transformation for the species of interest. A peculiarity of INTACT is that it provides nuclear RNAs which could differ from cytosolic RNAs depending on the selective compartment enrichment of RNAs influenced by mechanisms such as nuclear retention and posttranscriptional regulation (Reynoso et al., 2018). For instance, the comparison between nuclear and total RNAs furnished additional insights into the transcriptome regulation in the early Arabidopsis embryo (Palovaara et al., 2017). In the future, INTACT could contribute to the elucidation of the transcriptome reorganization occurring in meiosis, particularly at the prophase I expression transitions that were recently defined in maize by single-cell RNA sequencing (Nelms and Walbot, 2019).

In this work, we applied the INTACT-based approach to obtain purified meiocyte nuclei from the total cell pool of floral bud in *Arabidopsis thaliana*. To label meiotic nuclei, we used the promoter of *AtDMC1* recombinase (Klimyuk and Jones, 1997; De Muyt et al., 2009). The AtDMC1-driven expression of biotin-labeled NTF allowed us to isolate meiocyte nuclei using streptavidin-coated magnetic beads. The meiotic nuclear transcriptome was obtained by RNA-seq and validated through analysis of the expression of known meiotic genes and the comparison with other tissues. Finally, expression network analysis was performed to find new candidate genes involved in the meiotic process.

MATERIALS AND METHODS

Plant Material, Transformation, and Growth Conditions

The transgenic line expressing *ACT2:BirA*, kindly given by Prof. R. Deal (Emory University, United States), and the reference ecotype Col-0 of *A. thaliana* (NASC stock N60000) were used in this work. The transgenic line was transformed by *Agrobacterium tumefaciens* (GV3101) according to floral dip method (Clough and Bent, 1998) to obtain plants carrying *DMC1:NTF* along with ACT2:BirA. About 1,500 seeds obtained after transformation were sterilized with 70% ethanol for 1 min., and bleach solution (10% commercial bleach and 0.05% Tween 20) for 10 min., finally washed with sterile water three times. Sterilized seeds were sown on a selective modified MS (Murashige and Skoog, 1962) medium containing hygromycin (50 mg/l) and 0.8% agar, kept for 2–3 days at 4°C, and germinated under long-day conditions (16 h light/8 h darkness) at 24°C. Seedlings transferred to pots were grown in a controlled growth chamber under long-day conditions. The A*DMC1:NTF/ACT2:BirA* double homozygous transgenic line (D.1) was selected from ten T_2 independent transformant lines. About 200 plants from the D.1 line were grown as above reported for subsequent experiments.

PCR and RT-qPCR

To confirm transgene insertion, PCR was conducted on the hygromycin resistance gene used as a selectable marker. Genomic DNA was extracted from leaf tissue of transgenic plants using the DNeasy Plant Mini Kit (Qiagen)[1] according to the manufacturer's instructions. PCR reactions were performed on genomic DNA using primers listed in **Supplementary Table 1**. RT-qPCR was performed to verify expression of target *BirA* gene under the constitutive promoter ACT2 in the floral buds. Total RNA from transgenic *ACT2:BirA* plants was extracted using RNeasy plant minikit (QIAGEN) following the manufacturer's instructions. mRNA was retrotranscribed to cDNA using Superscript III reverse transcriptase (Thermo Fisher Scientific, United States) and oligo dT(20) following the manufacturer's conditions, and relative expression was verified by real-time qPCR. The experiment was performed on a QIAGEN Rotorgene 6,000 qRT-PCR machine, using Power Sybr Green real time mix (Thermo Fisher Scientific, United States). The reaction conditions were as follows: one cycle at 95°C for 10 min, and 40 cycles of 95°C × 10″ denaturation and 60°C × 45″ annealing and extension. The melting curve was run to verify the specificity of the primers. The *ADENINE PHOSPHORIBOSYL TRANSFERASE 1* (*APT1*) gene was used as a housekeeping internal control. Target and housekeeping primers are listed in **Supplementary Table 2**.

Construct for INTACT, Nucleus Isolation, and Microscopy

The fusion gene *NTF* carried in the vector ADF8-NTF, kindly given by Prof. R. Deal (Emory University, United States),

[1]https://www.qiagen.com/

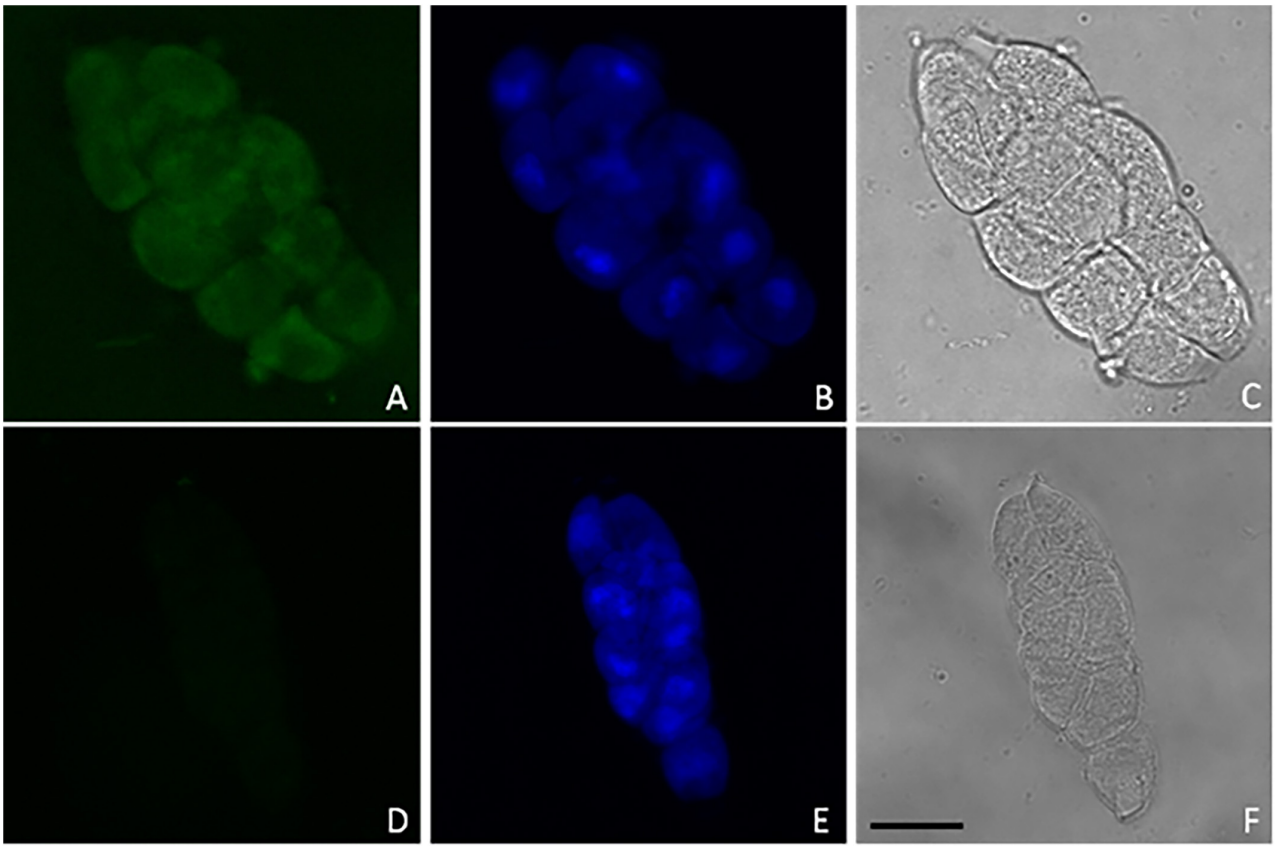

FIGURE 1 | Representative confocal images of GFP **(A,D)** and DAPI **(B,E)** fluorescence in male meiocytes along with phase contrast observations **(C,F)** from *AtDMC1:NTF/ACT2:BirA* line **(A–C)** and wild type **(D–F)**. Nuclei (blue) were stained by DAPI (10 μg/ml) to visualize DNA. Scale bar: 10 μm.

and the *AtDMC1* promoter carried in the vector SLJ7753, kindly given by Prof. J.D.G. Jones (The Sainsbury Laboratory, Norwich, United Kingdom), were amplified with specific primers carrying GATEWAY adapters. Subsequently, they were cloned into Gateway vectors pDONR/Zeo and pDONR/P4P1R, respectively (Thermo Fisher Scientific). Generated entry clones were recombined with multisite GATEWAY reaction into destination vector pH7m24GW,3[2], and the final expression clone, named pEXPR-DMC1-NTF, was generated. All gateway reactions were performed following the manufacturer's standard protocols. Primers used for vector construction are listed in **Supplementary Table 3**.

Flower buds of the size corresponding to male meiotic stage (Smyth et al., 1990) were collected, fixed with 1% formaldehyde solution, and stored at −80°C. Nuclei were purified from 1.5 g of frozen and homogenized tissue as described previously by Wang and Deal (2015) with some minor modifications. In particular, the tissue immersed in 40 ml of Nuclei Purification Buffer solution (NPBf) containing 20 mM MOPS (pH 7), 40 mM NaCl, 90 mM KCl, 2 mM EDTA, 0.5 mM EGTA, 0.5 mM spermidine, 0.2 mM spermine, 1% (v/v) formaldehyde was incubated in 50 ml tube under vacuum glass desiccator for 10 min., and vacuum release for 2 min. The procedure was repeated once. Then, glycine was added to a final concentration of 0.125 M under vacuum for 7 min. After NPBf solution elimination, the tissue was washed three times with water. Isolated nuclei were resuspended into RNAlater buffer, and RNA extraction was performed immediately.

Laser-scanning confocal microscopy imaging was performed using a confocal Zeiss LSM 510. Isolated nuclei were observed using a Florescence Microscope (Leitz Aristoplan).

RNA Extraction and Sequencing

Total RNA was extracted from three replicates of isolated nuclei using an RNeasy Extraction Mini Kit (Qiagen, see text footnote 1) according to the manufacturer's instructions. Isolated nuclei derived from the same population of inflorescences where the buds different from stage 9 (Smyth et al., 1990) had been manually dissected. Quantification was performed on a QUBIT fluorometer.

RNA sequencing was performed by IGA Technology Services Srl[3]. The libraries were produced using retrotranscribed cDNA previously amplified by Ovation Ultralow Library System V2 (NuGEN Technologies, Inc.). Library size and integrity were

[2]https://gateway.psb.ugent.be/search

[3]appliedgenomics.org

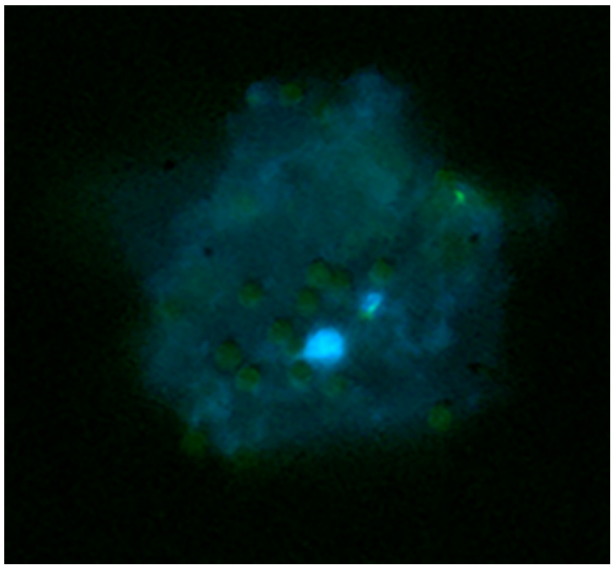

FIGURE 2 | Capture of biotinylated nuclei from meiocytes in the *AtDMC1:NTF/ACT2:BirA* line using streptavidin-coated magnetic beads. Nuclei (blue) stained with DAPI are surrounded by 2–8-μm spherical beads (pale green).

assessed using the Agilent Bioanalyzer (Santa Clara, CA) or Caliper GX (PerkinElmer, MA). Sequencing was performed by Illumina HiSeq 2,500 (Illumina, San Diego, CA) and 30-M paired-end reads (2 × 125) per replicate were generated.

Bioinformatics

Raw sequencing data (FASTQ files) were quality checked using the software FASTQC v0.11.5[4], then low-quality bases and adapter sequences were removed with the software BBDuk v35 (Bushnell et al., 2017) setting 35 bp as the minimum read length after trimming. The read length ranged from 35 to 125 bp after trimming. More than 98% of the final reads had a length of 125 bp since adapter contamination was very low. The trimmed reads were then mapped against the *A. thaliana* reference genome (Araport11) (Cheng et al., 2016) using STAR v2.7.3a with the option – alignEndsProtrude 100 DiscordantPair. The statistics from the mapping step were produced with Qualimap v2.2.1 (Okonechnikov et al., 2016). Kallisto v0.46.0 was used to obtain transcript expression quantification levels, as estimated counts and TPMs, which were then summarized as gene expression values using the R package "tximport" (Soneson et al., 2016).

The correlation analysis of the samples was performed using the R in-built function "cor," and the results were plotted with the function "corrplot." The classification of the gene classes and the saturation analysis were performed with the R package "NOISeq" (Tarazona et al., 2015). Genes were classified based on their average expression levels using the following criteria: "undetected" if the expression was 0 across all the replicates, "Low" if log2 average TPM $\leq$ 1.252, "Low_Mid" if log2 average TPM $>$ 1.252 and $\leq$ 2.207, "Mid_High" if log2 average TPM $>$ 2.207 and $\leq$ 4.169, and "High" if log2 average TPM $>$ 4.169. The abovementioned values correspond to the 25th, 50th, and 75th percentiles of the log2 average TPM distributions, respectively.

In order to compare the expression profile of the meiocytes against other datasets, TPM values from the following datasets were downloaded from EBI: E-GEOD-38612, E-GEOD-55866, and E-MTAB-4202 (**Supplementary Table 4**). In addition, gene expression profiles from pollen and tapetum cells were obtained from Loraine et al. (2013) and Li et al. (2017). When multiple replicates of the same tissue were available, an average was calculated. Similarly, when multiple developmental stages of the same tissue were available, the average was calculated. The only exception consisted of the tapetum datasets kept separate because the two available stages were highly different. Finally, a complete expression matrix was obtained by merging all the datasets and the ARSyN function from the NOISeq package was used to remove the batch effect. A PCA analysis was then performed with the in-built "prcomp" function in R and the results plotted with "ggplot2."

A gene expression network was generated using the expression matrix obtained after the ARSyN correction, following the Aracne algorithm implemented in the R package "parmigene" (Sales and Romualdi, 2011). Cytoscape v3.8.1 was then used to plot the network and select only the first neighbors of known meiotic genes in order to find new candidates. The gene ontology (GO) analysis of the obtained genes was then performed using the Cytoscape app named "BinGO" using the hypergeometric test as a statistical test and an FDR lower than 0.05 as threshold. All the heat maps were generated using Clustvis (Metsalu and Vilo, 2015).

Gene ontology enrichment analysis (GOEA) were performed using in-house scripts based on the method described in Tian et al. (2017) and setting a minimum FDR threshold of 0.05.

RESULTS

Generation of Transgenic Material and Isolation of Nuclei From Meiocytes Using INTACT in Arabidopsis

In order to isolate meiocyte nuclei by the INTACT method for RNA-seq analysis in Arabidopsis, we generated transgenic material carrying a *NTF* protein under the meiosis-specific *AtDMC1* promoter (Klimyuk and Jones, 1997) along with the biotinilase *BirA* under a constitutive *ACTIN2* (*ACT2*) promoter. The promoter of *ACT2* (At3g18780) was used by Deal and Henikoff (2011) to drive expression of *BirA* in root cell types (An et al., 1996). Following detection of *ACT2:BirA* expression in floral buds (not shown), we used the same transgenic line generated by Deal and Henikoff (2011) as starting material. In this line, we introduced the new construct carrying the *AtDMC1:NTF* expression cassette. Although *AtDMC1* (At3g22880) was expected to drive *NTF* expression in both male and female meiocytes (Klimyuk and Jones, 1997), we restricted

[4]https://www.bioinformatics.babraham.ac.uk/projects/fastqc/

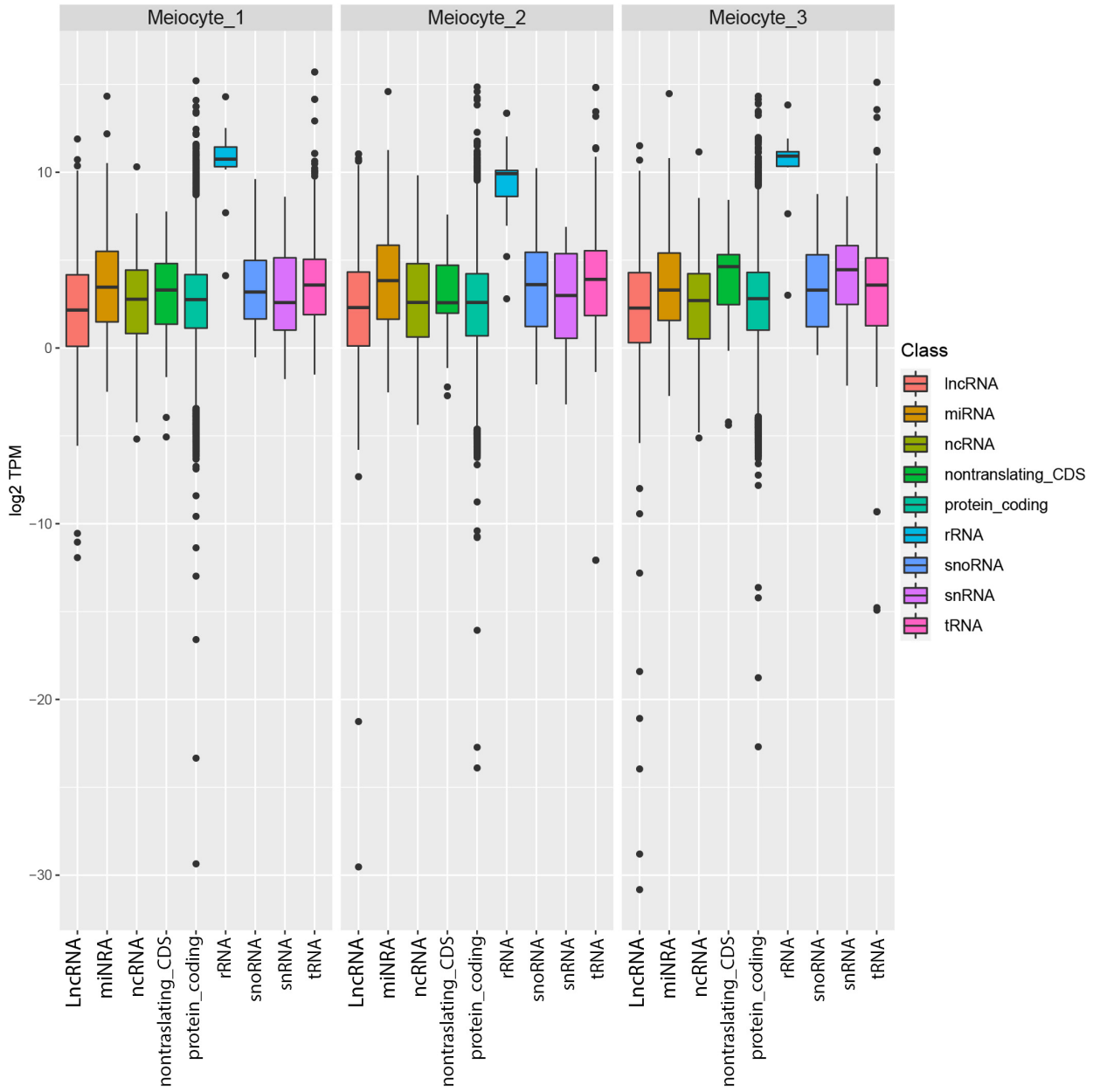

FIGURE 3 | Distribution of the expression levels of *Arabidopsis thaliana* genes in the meiocytes. Genes are divided in multiple biotypes according to the official annotation, and for each one the distribution of log2 TPM values is represented as box plots.

our confocal microscopy analysis to anthers and male meiocytes. Indeed, the flower buds were collected at a stage corresponding to male meiosis which occurs earlier than female meiosis (Schneitz et al., 1995). Confocal microscopic examination of the *AtDMC1*:*NTF/ACT2*:*BirA* line showed that *NTF* was expressed in the expected cell type. Indeed, we detected GFP-positive male meiocytes during prophase I stage, arguably before the nuclear envelope breakdown (NEBD; **Figure 1**). To purify labeled nuclei from meiocytes, we extracted total nuclei from whole inflorescences with buds at floral stage 9 (Smyth et al., 1990) in the *AtDMC1*:*NTF/ACT2*:*BirA* line. Then, the nuclei were incubated with streptavidin-coated magnetic beads according to INTACT protocols (Deal and Henikoff, 2011; Wang and Deal, 2015). After nucleus isolation, we used a fluorescence microscope to observe the complex DAPI-stained nuclei/beads (**Figure 2**).

RNA-seq From Isolated Nuclei of the Meiocytes

To obtain the meiotic nuclear transcriptome, RNA sequencing (RNA-seq) was performed downstream of INTACT. RNA extracted from isolated nuclei of meiocytes in three replicates

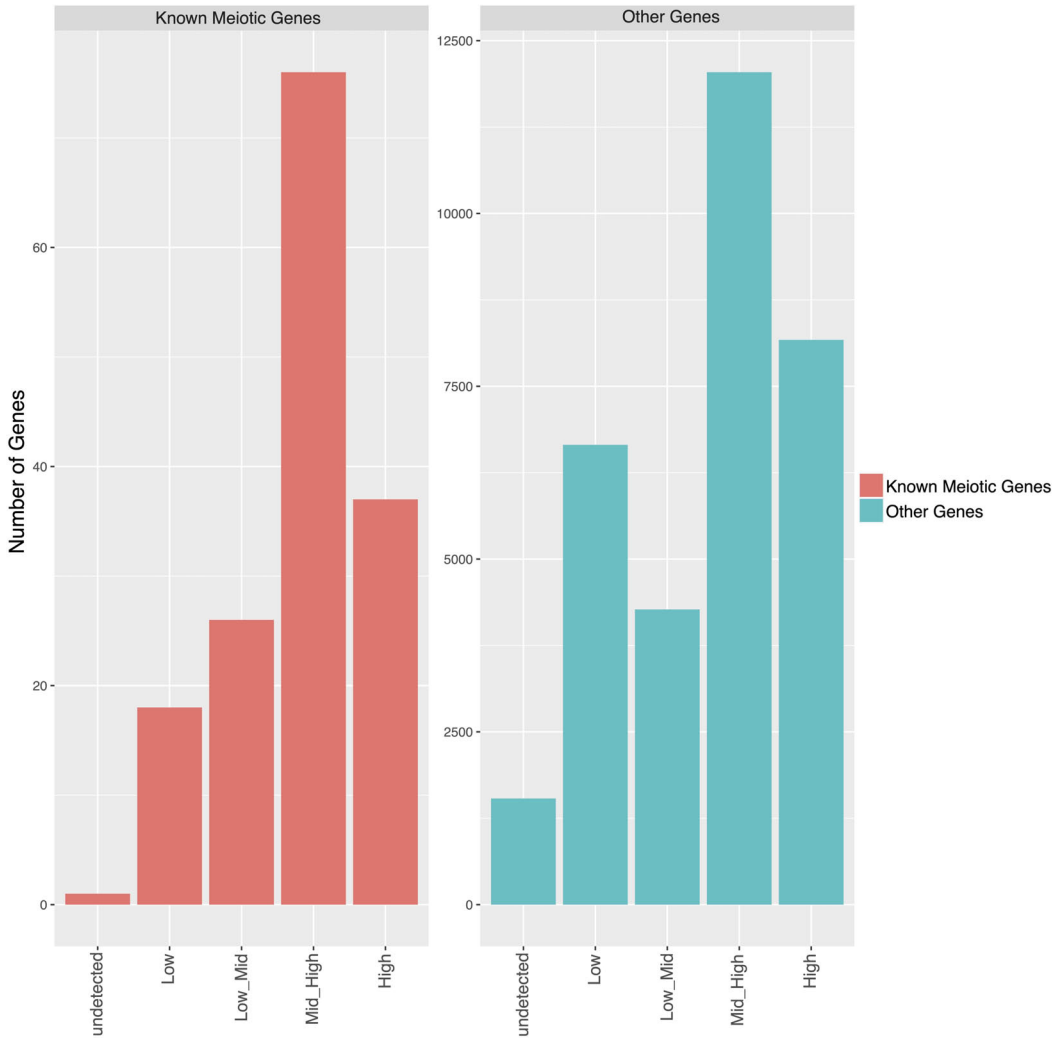

FIGURE 4 | Bar plot showing the number of genes classified in expression ranges in the meiotic cells. Genes were classified based on their average expression levels using the following criteria: "undetected" if the expression level was 0 in all the replicates, "Low" if log2 average TPM $\leq$ 1.252, "Low_Mid" if log2 average TPM $>$ 1.252 and $\leq$ 2.207, "Mid_High" if log2 average TPM $>$ 2.207 and $\leq$ 4.169, and "High" if log2 average TPM $>$ 4.169. Genes were divided into known meiotic genes (left) and other genes (right).

was sequenced by using the Illumina technology following an amplification step. Pearson's correlation coefficient indicated the reliability of the experiment (**Supplementary Figure 1**). After trimming, an average of 85,927,325 reads per replicate were obtained (**Supplementary Table 5**). About 77% of these reads were mapped onto the Arabidopsis genome (**Supplementary Table 6**). The percentages (calculated as average of the replicates) of the uniquely mapped reads located in known exons, introns, and intergenic regions are 38, 26, and 36%, respectively (**Supplementary Figure 2**). Given the high percentage of reads that mapped to multiple positions (**Supplementary Table 6**), the gene expression, measured as TPM (Transcript Per Million), was calculated by a specific algorithm (Kallisto) which is able to process multiple mapping reads (**Supplementary Table 7**). A frequency ranging between 75.2 and 81.3% of the genes (total no. 32,833) was detected across the replicates (**Supplementary Figure 3**). Transcript types of each replicate are summarized in **Figure 3** showing the distribution of expression profiles for the different gene classes. Ribosomal RNA appeared the most abundant class whereas lncRNA is the less expressed class. This result is consistent with a recent study in barley in which 65% of the downregulated DEGs were lncRNAs in leptotene/zygotene vs. pre-meiosis comparison (Barakate et al., 2020).

Transcripts were grouped into four classes according to their expression levels from low to high (**Supplementary Figure 4**). GOEA was performed to identify enriched (i.e., over-represented) GO terms associated with the different expression classes (**Supplementary Figures 5A–D**). The most enriched GO terms, such as "DNA demethylation" in the mid/high-expression class and "RNA stabilization" in the high expression class, suggest that these biological processes are particularly relevant to meiosis.

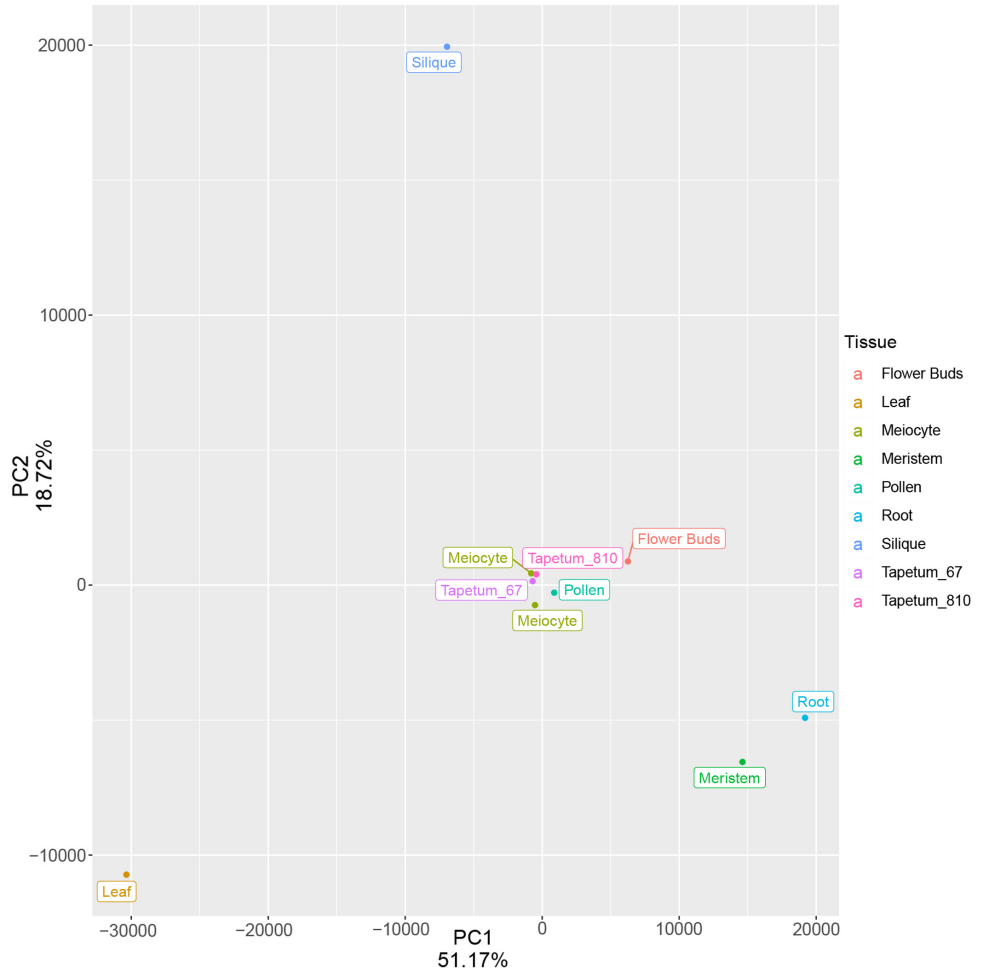

FIGURE 5 | Principal component analysis of meiocytes (current study) and multiple Arabidopsis tissues after batch correction of the TPM values. The variance associated with each PC is shown in the plot. Each point represents a tissue/cell type.

To assess the reliability of our results, we surveyed the genes with documented functions in Arabidopsis meiosis. A list of 197 meiotic genes was implemented using GO terms GO:0051321 (meiotic cell cycle) and GO:0140013 (meiotic nuclear division) (**Supplementary Table 8**). The majority of meiotic genes were distributed in the classes of mid/high and high expression while a small number were in the low-expression class (**Figure 4**). By comparison, this class was the third most represented for the total of transcripts (**Supplementary Figure 4**).

Transcriptome Comparison Between Male Meiocytes and Other Tissues

To further characterize our meiotic transcriptome, we compared it with publicly available transcriptomic data from other specific tissues and cell types of Arabidopsis. Initially, we planned to compare our RNA-seq data with those from male meiocytes isolated by micromanipulation in Arabidopsis (Chen et al., 2010; Yang et al., 2011) but, unfortunately, these datasets are not available.

Based on the low expression of *AtDMC1* (**Supplementary Figure 6**), we discarded replicate 1 in all the subsequent analyses. Principal component analysis (PCA) performed with meiocytes (current study), meristem, leaf, root, flower buds, tapetum (from two different developmental stages), pollen, and silique revealed that meiocytes clustered close to flower buds, as expected, but also to tapetum and pollen (**Figure 5**). We evaluated the expression profile of genes (list reported in **Supplementary Table 9**) considered to be specific for these two types of cells (Loraine et al., 2013; Li et al., 2017). The heat map revealed expression patterns specific for meiocytes, tapetum, and pollen (**Figure 6**). On the other hand, a hierarchical sample dendrogram showed that meiocyte sample groups together with tapetum 6–7 as well as pollen with tapetum 8–10 equivalent to a later stage.

Afterward, we assessed the overall gene expression of meiotic genes (list reported in **Supplementary Table 8**) and of the other transcripts in meiocytes and multiple tissues (**Figure 7**). The analysis revealed that the median expression value of meiotic genes was higher in isolated meiocytes when compared to the other tissues/cell types with the exception of floral bud

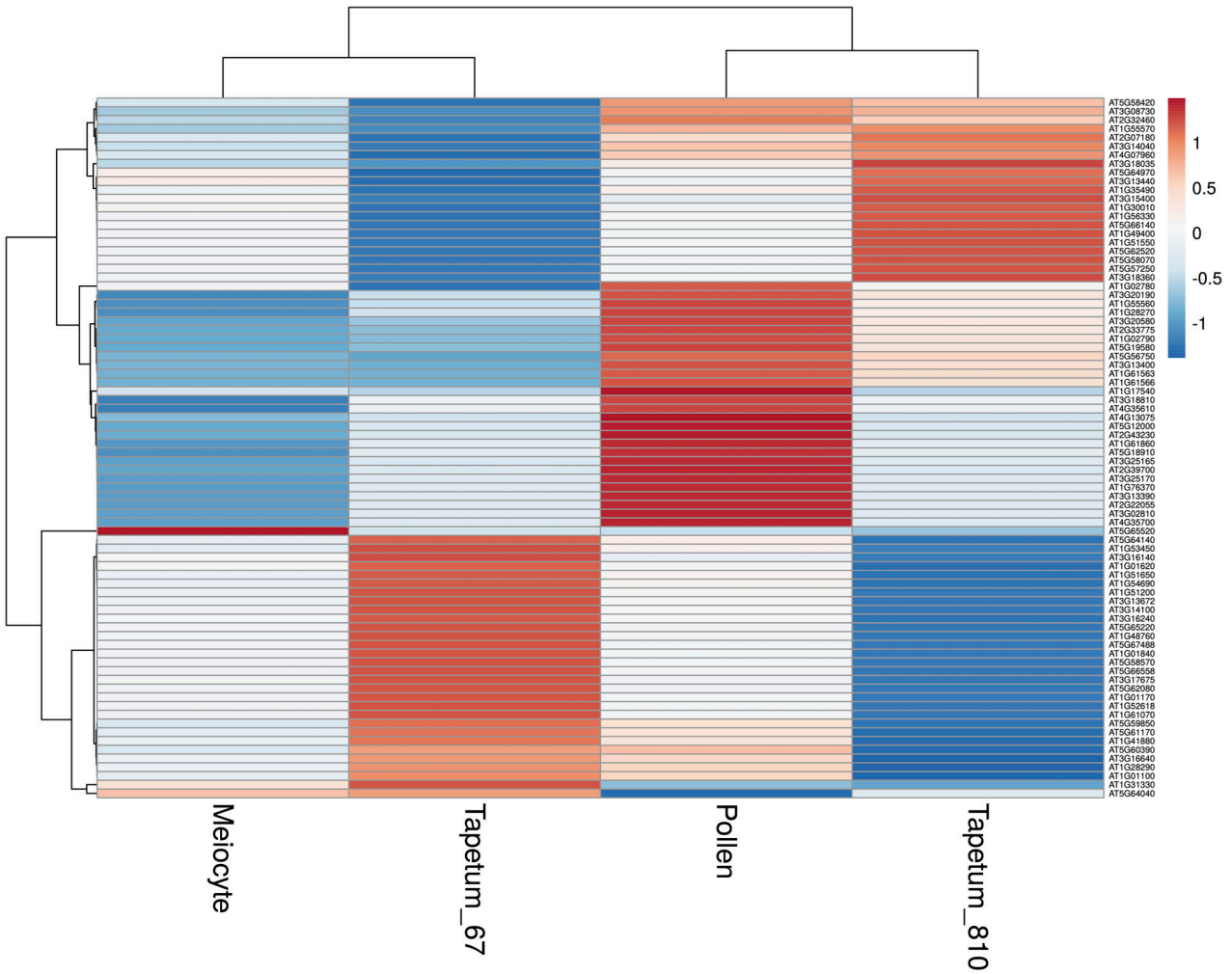

FIGURE 6 | Heat map showing the expression profile of genes considered to be pollen or tapetum specific. Each line represents a gene; the gradient of color was obtained after scaling of the TPM values and after batch correction of the expression data. The meiocyte data corresponds to the average of the two replicates. The genes and the samples are grouped applying a hierarchical clusterization on the Pearson correlation values as shown by the hierarchical tree on the left and on the top.

and meristem samples. This result is not surprising since the meiocytes are included in floral buds and they share cell-cycle genes with the meristem. The median expression value of the other transcripts was basically steady across the different tissues (**Figure 7**). Considering the meiotic gene expression fold changes between meiocytes and the other tissues/cell types, the heat map revealed a pattern in agreement with the above reported analysis (**Figure 8** and **Supplementary Table 10**).

Meiotic Gene Network

To identify new candidate genes with a meiotic function, we generated a gene expression network based on the genes known to be involved in meiosis (**Supplementary Table 8**). By selecting the first neighbors of the known meiotic genes, we found 1,503 genes with a total of 7,607 connections (**Figure 9** and **Supplementary Table 11**). The network is characterized by a very large cluster, thereby suggesting that the known meiotic genes and their neighbors are all highly connected as also indicated by an average degree of 4.95 connections. The most connected genes with 435 and 323 connections have a documented role in meiosis. In particular, FIDGETIN-LIKE-1 INTERACTING PROTEIN (FLIP, AT1G04650) forms a protein complex with FIDGETIN-LIKE-1 (FIGL1) that is conserved from Arabidopsis to human, and it regulates meiotic crossover formation via RAD51 and DMC1 (Fernandes et al., 2018). The other gene, *AXR1* (AT1G05180), is involved in the neddylation/rubylation protein modification pathway and TE methylation in meiocytes (Jahns et al., 2014; Christophorou et al., 2020). AXR1 plays a significant role in DNA repair (Martinez-Garcia et al., 2020). Collectively, this finding reinforces the reliability of the analysis performed in this study. New candidates which could play a role in meiosis are two transcription factors (TFs), AT1G06070 and AT1G02220, with 64 and 30 connections, respectively. These two genes belong to the bZIP and NAC TF families,

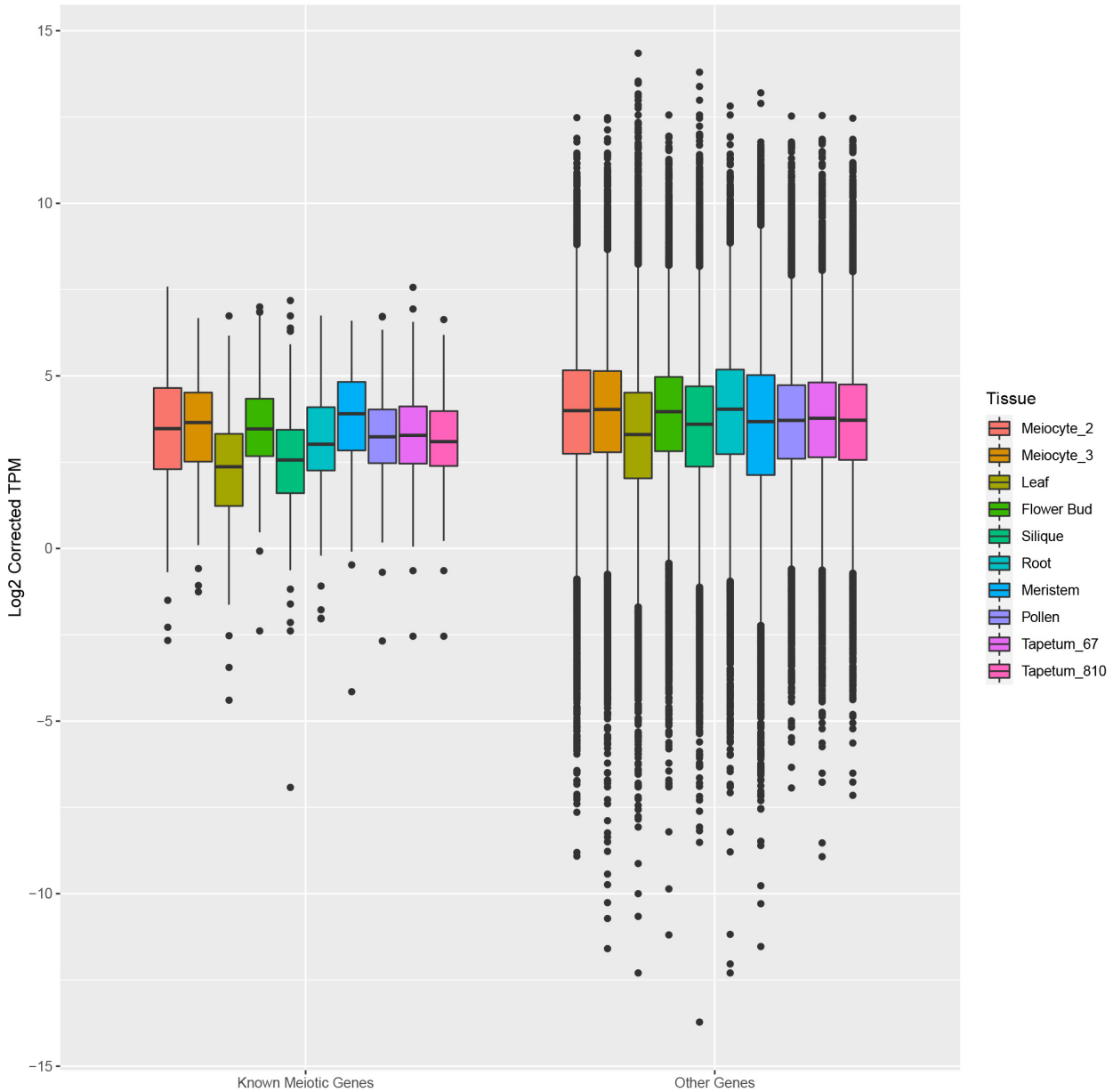

FIGURE 7 | Box plots showing the distribution of expression values of known meiotic genes (left) and other genes (right) in meiocytes (current study) and multiple Arabidopsis tissues. The box corresponds to the interquartile range (IQR), and the black line inside each box represents the median. The upper whisker extends from the hinge to the largest value no further than 1.5 * IQR from the hinge. The lower whisker extends from the hinge to the smallest value at most 1.5 * IQR of the hinge. Data beyond the end of the whiskers are called "outlying" points and are plotted individually.

and their function in meiosis has not been documented. Although with less connections than the genes reported above, AT1G04200, described as Dymeclin (DYM, Dyggve–Melchior–Clausen syndrome protein), is an interesting candidate for a possible meiotic function. Indeed, the mouse DYM homolog has a high expression in testis (Yue et al., 2014) and has a proved interaction with FANCD2, a component of the Fanconi anemia DNA repair pathway (Zhang et al., 2017).

A GO analysis performed using the genes identified by the network analysis revealed GO targets associated with meiotic processes and, particularly, to Meiosis I such as recombination, synapsis, chiasma assembly, and meiotic chromosome segregation (**Figure 10** and **Supplementary Table 12**).

DISCUSSION

In this work, we reported the application of the INTACT method in meiocyte isolation in *A. thaliana*. INTACT entails

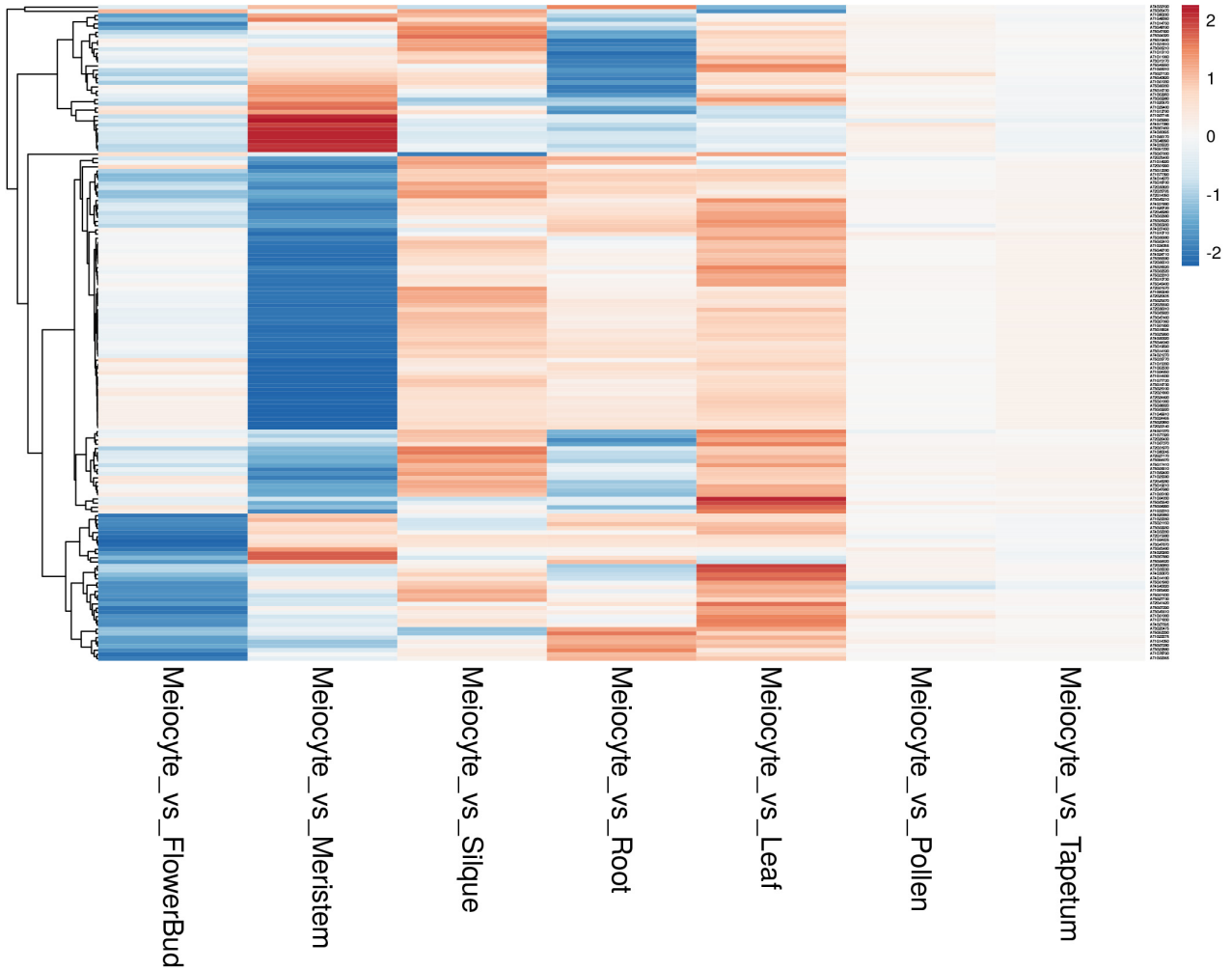

FIGURE 8 | Heat map showing the gene expression fold changes between meiocytes and multiple Arabidopsis tissues. Each line represents a gene; the gradient of color was obtained after scaling of the log2 fold changes and after batch correction of the expression data. The genes are grouped applying a hierarchical clustering on the Pearson correlation values as shown by the hierarchical tree on the left.

the use of a transgene that can be driven by spatially and/or temporally regulated promoters enabling the isolation of nuclei from specific cell types (Deal and Henikoff, 2010). In our experiment, because of a limited number of effective meiotically active promoters available, we employed the established *AtDMC1* promoter widely used in meiotic studies (Li et al., 2012). AtDMC1 is a recombinase involved in Double Strand Break (DSB) repair and expressed during early prophase I in both male and female meiotic cells in anthers and carpels, respectively (Klimyuk and Jones, 1997; De Muyt et al., 2009). However, AtDMC1 activity is not restricted only to meiotic cells. Indeed, AtDMC1 has been observed in embryonic cell culture (Doutriaux et al., 1998) and in young seedlings (Orel et al., 2003). On the other hand, *AtDMC1* was not expressed in the meiocyte's neighboring somatic cells (Klimyuk and Jones, 1997; Li et al., 2012). Our analysis has been restricted to male meiocytes collected from floral buds at a stage corresponding to microsporogenesis (Smyth et al., 1990). However, it cannot be excluded that female meiocytes also occur in our sample.

Isolation of nuclei tagged in specific cell types allowed us to obtain a nuclear meiotic transcriptome from meiocytes of *A. thaliana* based on RNA-seq data. On average, we detected the expression of about 25,000 genes corresponding to 76% of total genes. Similarly, approximately 22,000 and 24,000 genes were found to be expressed in Arabidopsis male meiocytes isolated in previous studies based on RNA-seq (Chen et al., 2010; Yang et al., 2011). Consistently, 60% or more of all genes in the genome were estimated to be expressed in rice and Arabidopsis male meiocytes (Schmidt et al., 2012). In Arabidopsis, the male meiotic transcriptome shows the largest overlap (approximately 67%) with tissues having cells in active division, including floral buds, anthers, and shoot apex (Yang et al., 2011). The number of reads in our RNA-seq experiment, and particularly the number of uniquely mapped reads, was higher in our study compared to that previously published (56 vs. 33%) (Yang et al., 2011). In addition,

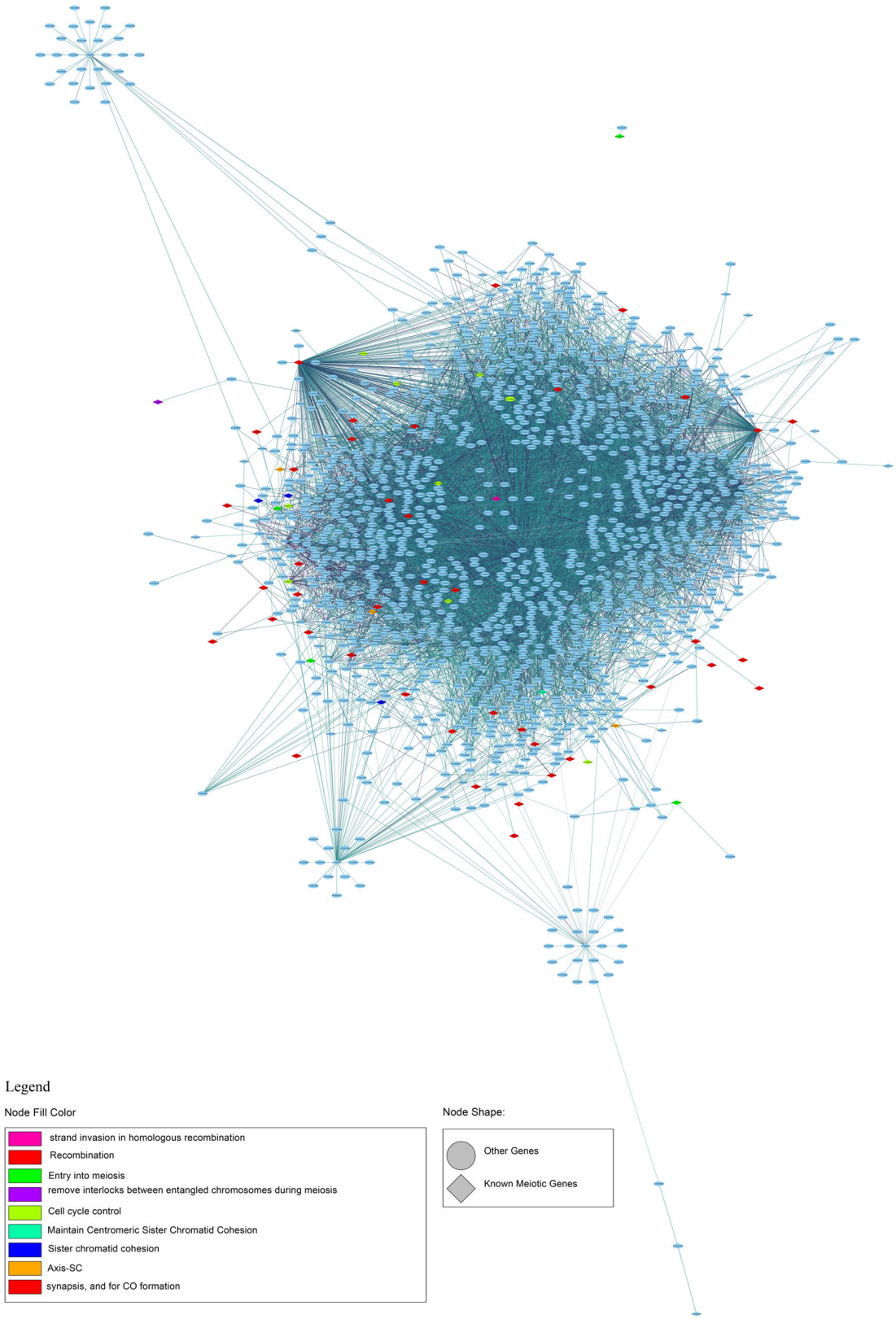

FIGURE 9 | First-neighbor meiotic gene network of co-expression. The legend shows the node fill colors associated with a different meiotic function and the node shape: rhomboidal shape for known meiotic gene and ellipsoidal shape for other genes.

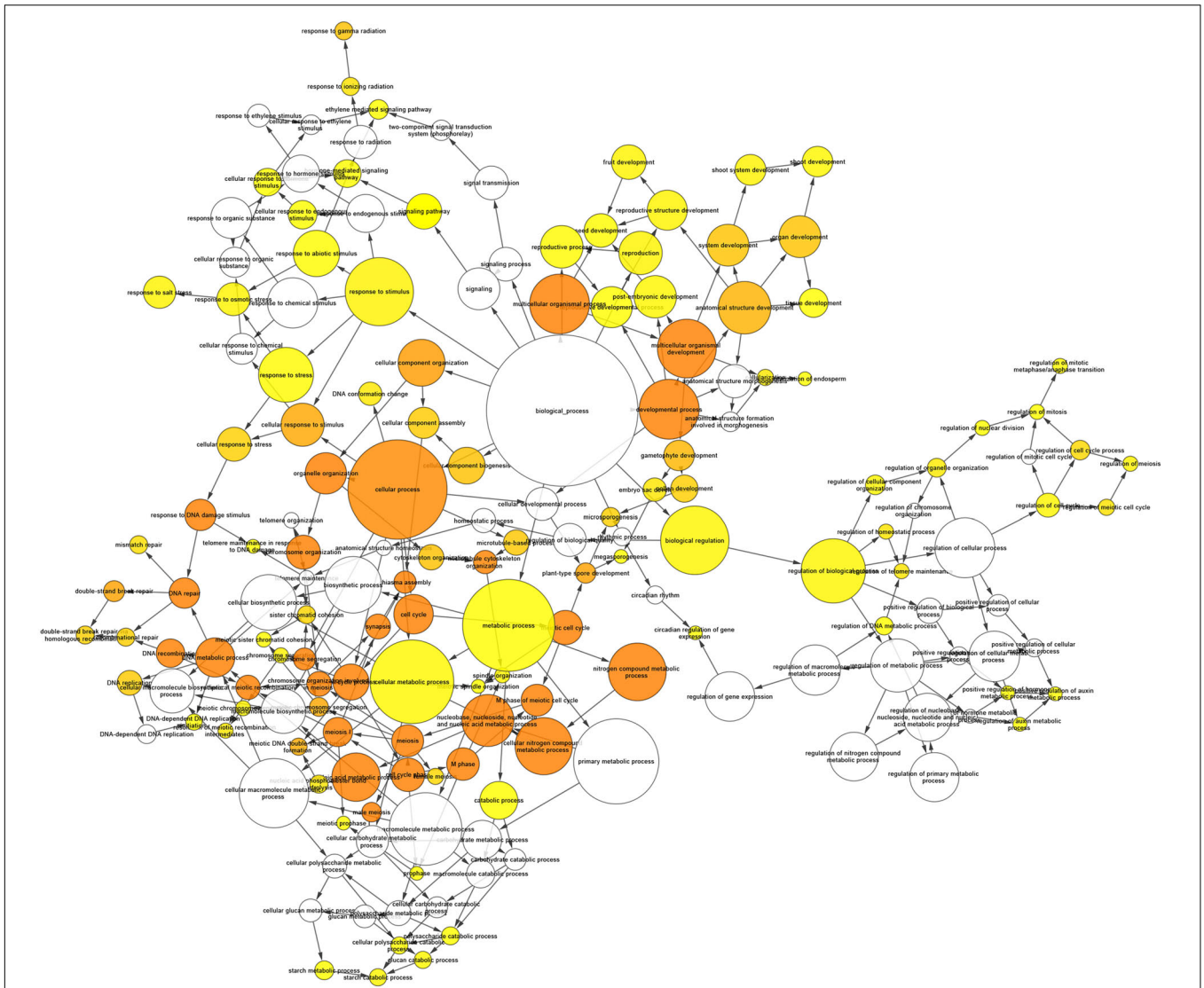

FIGURE 10 | Gene ontology (GO) Enrichment Network of the first neighbors of known meiotic genes obtained by Cytoscape's BinGO. Each node represents a GO category. The size of the node is proportional to the number of genes in the corresponding GO category. The color of the nodes from yellow to orange is associated with increasing level of significance in the enrichment while white nodes mean no significance.

we applied a specific algorithm (Kallisto) to multiple mapping reads (17% on average), thereby quantifying the expression of the genes more precisely. In our experiment, we observed an unexpected proportion of unmapped reads (23% on average) that was likely caused by the library preparation kit for RNA-seq using low-quantity input RNA. Indeed, a performance evaluation study of five methods evidenced that Ovation RNA-seq System V2 from NuGEN (the kit used in our study) generated fewer raw/mapped reads (Song et al., 2018).

Importantly, a distinct feature of our dataset compared to those reported in previous studies (Chen et al., 2010; Yang et al., 2011) is that INTACT provides RNAs occurring within the nucleoplasm. A strong correlation between nuclear RNA and total mRNA was reported in Arabidopsis embryo and endosperm (Palovaara et al., 2017; Del Toro-De León and Köhler, 2019). However, in our study, the comparison with total mRNAs from previous RNA-seq experiments in male meiocytes (Chen et al., 2010; Yang et al., 2011) was prevented due to the unavailability of latter datasets.

Meiosis involves two rounds of cell divisions and the nuclear envelope (NE) undergoes breakdown (NEBD) and reformation twice (Pradillo et al., 2019). In particular, the NEBD occurs at late prophases I and II. Since INTACT requires a NTF transgene which carries a domain for NE localization (Deal and Henikoff, 2010), INTACT does not operate during NEBD. On the other hand, the expression pattern and immunolocalization of AtDMC1 (Klimyuk and Jones, 1997; De Muyt et al., 2009) point out a potential early prophase I-specificity of AtDMC1. For these reasons, we expected the isolated meiocytes to provide a subset of meiotic genes enriched in processes related to early

prophase I substages. Apparently, however, the high number of transcripts and the fact that genes involved in later meiotic stages are expressed in our dataset seem to not support our expectations. For instance, the *AtPS1* (*Parallel Spindle 1*, AT1G34355) involved in the orientation of the spindles in Meiosis II (d'Erfurth et al., 2008) was present in the mid-high expression class in our dataset. This finding can be justified by different explanations. First, AtDMC1 could be expressed in other meiotic stages besides prophase I. Second, timing of the gene expression is not strictly associated with timing of the encoded protein function, as evidenced in maize prophase I (Nelms and Walbot, 2019). Finally, the transcriptional basis relevant for meiosis is already set up before its onset, as reported in rice and maize (Tang et al., 2010; Yuan et al., 2018). In the future, other prophase I-expressed genes could be used to build more INTACT lines. For this purpose, we suggest as candidates some meiosis-specific genes with established roles in prophase I identified in mid/high- and high-expression classes of our dataset (**Supplementary Table 13**). These genes exhibit a very low expression in the other tissues (leaf, root, meristem, flower bud, pollen, tapetum, and silique). In addition, they appear to be expressed also in maize at early prophase I as evidenced by the single-cell RNA-seq experiment (Nelms and Walbot, 2019).

The question whether all genes in meiotic transcriptome are essential for meiosis or whether the large number of transcripts is the result of a global de-repression of chromatin during meiosis remains to be answered (Lambing and Heckmann, 2018). Our study evidenced the prevalence of the biological process "DNA demethylation" when we considered the mid/highly expressed genes. Consistently, the upregulation of transposons (TEs) has been reported to be a prominent feature in Arabidopsis male meiocytes (Chen et al., 2010; Yang et al., 2011), and it supports the suggestion that DNA methylation decreases at meiosis onset (Kawashima and Berger, 2014). Methylome analysis showed that meiocytes have higher CG and CHG methylation but lower CHH methylation in comparison to somatic tissues (Walker et al., 2018). Therefore, it is likely that DNA demethylation engages the CHH context which, on the other hand, is interconnected with TEs. This view is reinforced by the methylome analysis of meiocytes in *axr1* mutant (Christophorou et al., 2020). Indeed, this mutation, which affects general DNA methylation in plants, showed a specific increase in meiocytes for CHH methylation in TEs. Remarkably, gene expression network analysis performed in our work identified *AXR1* as a relevant hub thereby confirming its important roles in meiosis (Jahns et al., 2014; Christophorou et al., 2020; Martinez-Garcia et al., 2020). Furthermore, DNA demethylation could have a profound influence on gene expression through TEs (Wang and Baulcombe, 2020). TEs can act *in cis* to affect expression of adjacent genes as observed in male meiocytes by Yang et al. (2011). Finally, our co-expression network revealed different gene modules related to meiosis as well as novel candidate genes with a potential meiotic role. The functional analysis of the candidate meiotic genes will contribute to our understanding of meiosis.

DATA AVAILABILITY STATEMENT

Raw sequencing data obtained by the INTACT experiment was deposited in the Sequence Read Archive (SRA) database of NCBI within the BioProject PRJNA668331.

AUTHOR CONTRIBUTIONS

LB and PT performed the experiments. PT designed the main experiments. RAC performed the bioinformatics analysis. GC performed the cytological analysis. RP and CL assisted with the experiments. PT, RAC, and GC contributed to the manuscript editing. CC conceived the study and wrote the grant. CC, LB, and FC wrote the manuscript. All authors contributed to the article and approved the submitted version.

FUNDING

This work was funded by the Epigenomics Flagship Project (EPIGEN) from the Italian Ministry of University and Research (MUR) and the National Research Council of Italy (CNR).

ACKNOWLEDGMENTS

The authors thank M. Rankenburg for proofreading and R. Nocerino for technical assistance in plant growth condition control.

SUPPLEMENTARY MATERIAL

The Supplementary Material for this article can be found online at: https://www.frontiersin.org/articles/10.3389/fpls.2021.638051/full#supplementary-material

REFERENCES

Agrawal, P., Chung, P., Heberlein, U., and Kent, C. (2019). Enabling cell-type-specific behavioral epigenetics in *Drosophila*: a modified high-yield INTACT method reveals the impact of social environment on the epigenetic landscape in dopaminergic neurons. *BMC Biol.* 17:30. doi: 10.1186/s12915-019-0646-4

Amin, N. M., Greco, T. M., Kuchenbrod, L. M., Rigney, M. M., Wallingford, J. B., et al. (2014). Proteomic profiling of cardiac tissue by isolation of nuclei tagged in specific cell types (INTACT). *Development* 141, 962–973. doi: 10.1242/dev.098327

An, Y.-Q., McDowell, J. M., Huang, S., McKinney, E. C., Chambliss, S., and Meagher, R. B. (1996). Strong, constitutive expression of the *Arabidopsis* ACT2/ACT8 actin subclass in vegetative tissues. *Plant J.* 10, 107–121. doi: 10.1046/j.1365-313x.1996.10010107.x

Barakate, A., Orr, J., Schreiber, M., Colas, I., Lewandowska, D., McCallum, N., et al. (2020). Time-resolved transcriptome of barley anthers and meiocytes reveals robust and largely stable gene expression changes at meiosis entry. *bioRxiv* [preprint] doi: 10.1101/2020.04.20.051425

Barra, L., Aiese-Cigliano, R., Cremona, G., De Luca, P., Zoppoli, P., Bressan, R. A., et al. (2012). Transcription profiling of laser microdissected microsporocytes

in an *Arabidopsis mutant* (Atmcc1) with enhanced histone acetylation. *J. Plant Biol.* 55, 281–289. doi: 10.1007/s12374-011-0268-z

Beckett, D., Kovaleva, E., and Schatz, P. J. (1999). A minimal peptide substrate in biotin holoenzyme synthetase-catalyzed biotinylation. *Protein Sci.* 8, 921–929. doi: 10.1110/ps.8.4.921

Bushnell, B., Rood, J., and Singer, E. (2017). BBMerge – Accurate paired shotgun read merging via overlap. *PLoS One* 12:e0185056. doi: 10.1371/journal.pone.0185056

Chen, C., Farmer, A., Langley, R., Mudge, J., Crow, J., May, G., et al. (2010). Meiosis-specific gene discovery in plants: RNA-Seq applied to isolated *Arabidopsis* male meiocytes. *BMC Plant Biol.* 10:280. doi: 10.1186/1471-2229-10-280

Cheng, C. Y., Krishnakumar, V., Chan, A. P., Thibaud-Nissen, F., Schobel, S., and Town, C. D. (2016). Araport11: a complete reannotation of the Arabidopsis thaliana reference genome. *Plant J.* 89, 789–804. doi: 10.1111/tpj.13415

Christophorou, N., She, W., Long, J., Hurel, A., Beaubiat, S., Idir, Y., et al. (2020). AXR1 affects DNA methylation independently of its role in regulating meiotic crossover localization. *PLoS Genet.* 16:e1008894. doi: 10.1371/journal.pgen.1008894

Clough, S. J., and Bent, A. F. (1998). Floral dip: a simplified method for agrobacterium-mediated transformation of *Arabidopsis thaliana*. *Plant J.* 16, 735–743. doi: 10.1046/j.1365-313x.1998.00343.x

De Muyt, A., Pereira, L., Vezon, D., Chelysheva, L., Gendrot, G., Chambon, A., et al. (2009). A high throughput genetic screen identifies new early meiotic recombination functions in *Arabidopsis thaliana*. *PLoS Genet.* 5:e1000654. doi: 10.1371/journal.pgen.1000654

De Storme, N., and Geelen, D. (2014). The impact of environmental stress on male reproductive development in plants: biological processes and molecular mechanisms. *Plant Cell Environ.* 37, 1–18. doi: 10.1111/pce.12142

Deal, R. B., and Henikoff, S. (2010). A simple method for gene expression and chromatin profiling of individual cell types within a tissue. *Dev. Cell* 18, 1030–1040. doi: 10.1016/j.devcel.2010.05.013

Deal, R. B., and Henikoff, S. (2011). The INTACT method for cell type-specific gene expression and chromatin profiling in *Arabidopsis thaliana*. *Nat. Protoc.* 6, 56–68. doi: 10.1038/nprot.2010.175

Del Toro-De León, G., and Köhler, C. (2019). Endosperm-specific transcriptome analysis by applying the INTACT system. *Plant Reprod.* 32, 55–61. doi: 10.1007/s00497-018-00356-3

d'Erfurth, I., Jolivet, S., Froger, N., Catrice, O., Novatchkova, M., Simon, M., et al. (2008). Mutations in AtPS1 (Arabidopsis thaliana parallel spindle 1) lead to the production of diploid pollen grains. *PLoS Genet.* 4:e1000274. doi: 10.1371/journal.pgen.1000274

Doutriaux, M. P., Couteau, F., Bergounioux, C., and White, C. (1998). Isolation and characterisation of the RAD51 and DMC1 homologs from *Arabidopsis thaliana*. *Mol. General Genet.* 257, 283–291. doi: 10.1007/s004380050649

Dubowic-Shulze, S., and Chen, C. (2014). The meiotic transcriptome architecture of plants. *Front. Plant Sci.* 5:220. doi: 10.3389/fpls.2014.00220

Fernandes, J. B., Duhamel, M., Seguéla-Arnaud, M., Froger, N., Girard, C., Choinard, S., et al. (2018). FIGL1 and its novel partner FLIP form a conserved complex that regulates homologous recombination. *PLoS Genet.* 14:e1007317. doi: 10.1371/journal.pgen.1007317

Jahns, M. T., Vezon, D., Chambon, A., Pereira, L., Falque, M., Martin, O. C., et al. (2014). Crossover localisation is regulated by the neddylation posttranslational regulatory pathway. *PLoS Biol.* 12:e1001930. doi: 10.1371/journal.pbio.1001930

Kawashima, T., and Berger, F. (2014). Epigenetic reprogramming in plant sexual reproduction. *Nat. Rev. Genet.* 15, 613–624. doi: 10.1038/nrg3685

Klimyuk, V. I., and Jones, J. D. (1997). AtDMC1, the *Arabidopsis homologue* of the yeast DMC1 gene: characterization, transposon-induced allelic variation and meiosis-associated expression. *Plant J.* 11, 1–14. doi: 10.1046/j.1365-313x.1997.11010001.x

Lambing, C., and Heckmann, S. (2018). Tackling plant meiosis: from model research to crop improvement. *Front. Plant Sci.* 9:829. doi: 10.3389/fpls.2018.00829

Li, D.-D., Xue, J.-S., Zhu, J., and Yang, Z.-N. (2017). Gene regulatory network for tapetum development in *Arabidopsis thaliana*. *Front. Plant Sci.* 8:1559. doi: 10.3389/fpls.2017.01559

Li, J., Farmer, A. D., Lindquist, I. E., Dukowic-Schulze, S., Mudge, J., Li, T., et al. (2012). Characterization of a set of novel meiotically-active promoters in *Arabidopsis*. *BMC Plant Biol.* 12:104. doi: 10.1186/1471-2229-12-104

Libeau, P., Durandet, M., Granier, F., Marquis, C., Berthome, R., Renou, J. P., et al. (2011). Gene expression profiling of *Arabidopsis meiocytes*. *Plant Biol.* 13, 784–793. doi: 10.1111/j.1438-8677.2010.00435.x

Loraine, A. E., McCormick, S., Estrada, A., Patel, K., and Qin, P. (2013). RNA-seq of Arabidopsis pollen uncovers novel transcription and alternative splicing. *Plant Physiol.* 162, 1092–1109. doi: 10.1104/pp.112.211441

Martinez-Garcia, M., Fernández-Jiménez, N., Santos, J. L., and Pradillo, M. (2020). Duplication and divergence: new insights into AXR1 and AXL functions in DNA repair and meiosis. *Sci. Rep.* 10:8860. doi: 10.1038/s41598-020-65734-2

Mercier, R., Mézard, C., Jenczewski, E., Macaisne, N., and Grelon, M. (2015). The molecular biology of meiosis in plants. *Annu. Rev. Plant Biol.* 66, 297–327. doi: 10.1146/annurev-arplant-050213-035923

Metsalu, T., and Vilo, J. (2015). ClustVis: a web tool for visualizing clustering of multivariate data using principal component analysis and heatmap. *Nucleic Acids Res.* 43, W566–W570. doi: 10.1093/nar/gkv468

Murashige, T., and Skoog, F. (1962). A revised medium for rapid growth and bio-assays with tobacco tissue cultures. *Physiol. Plantarum* 15, 473–497. doi: 10.1111/j.1399-3054.1962.tb08052.x

Nelms, B., and Walbot, V. (2019). Defining the developmental program leading to meiosis in maize. *Science* 364, 52–56. doi: 10.1126/science.aav6428

Okonechnikov, K., Conesa, A., and García-Alcalde, F. (2016). Qualimap 2: advanced multi-sample quality control for high-throughput sequencing data. *Bioinformatics* 32, 292–294. doi: 10.1093/bioinformatics/btv566

Orel, N., Kyryk, A., and Puchta, H. (2003). Different pathways of homologous recombination are used for the repair of double-strand breaks within tandemly arranged sequences in the plant genome. *Plant J.* 35, 604–612. doi: 10.1046/j.1365-313X.2003.01832.x

Palovaara, J., Saiga, S., Wendrich, J. R., Wout Hofland, N., Schayck, J. P., Hater, F., et al. (2017). Transcriptome dynamics revealed by a gene expression atlas of the early *Arabidopsis embryo*. *Nat. Plants* 3, 894–904. doi: 10.1038/s41477-017-0035-3

Parry, M., Rosenzweig, C., Iglesias, A., Fischer, G., and Livermore, M. (1999). Climate change and world food security: a new assessment. *Global Environ. Chang.* 9, S51–S67. doi: 10.1016/S0959-3780(99)00018-7

Pradillo, M., Evans, D., and Graumann, K. (2019). The nuclear envelope in higher plant mitosis and meiosis. *Nucleus* 10, 55–66. doi: 10.1080/19491034.2019.1587277

Reynoso, M. A., Pauluzzi, G. C., Kajala, K., Cabanlit, S., Velasco, J., Bazin, J., et al. (2018). Nuclear transcriptomes at high resolution using retooled INTACT. *Plant Physiol.* 176, 270–281. doi: 10.1104/pp.17.00688

Rose, A., and Meier, I. (2001). A domain unique to plant RanGAP is responsible for its targeting to the plant nuclear rim. *Proc. Natl. Acad. Sci. U S A.* 26, 15377–15382. doi: 10.1073/pnas.261459698

Sales, G., and Romualdi, C. (2011). Parmigene—a parallel R package for mutual information estimation and gene network reconstruction. *Bioinformatics* 13, 1876–1877. doi: 10.1093/bioinformatics/btr274

Schmidt, A., Schmid, M. W., and Grossniklaus, U. (2012). Analysis of plant germline development by high-throughput RNA profiling: technical advances and new insights. *Plant J.* 70, 18–29. doi: 10.1111/j.1365-313X.2012.04897

Schmidt, A., Wuest, S. E., Vijverberg, K., Baroux, C., Kleen, D., and Grossniklaus, U. (2011). Transcriptome analysis of the *Arabidopsis megaspore* mother cell uncovers the importance of RNA helicases for plant germline development. *PLoS Biol.* 9:e1001155. doi: 10.1371/journal.pbio.1001155

Schneitz, K., Hulskamp, M., and Pruitt, R. E. (1995). Wild type ovule development in *Arabidopsis thaliana* - a light microscope study of cleared whole mount tissue. *Plant J.* 7, 731–749. doi: 10.1046/j.1365-313X.1995.07050731.x

Si, W., Yuan, Y., Huang, J., Zhang, X., Zhang, Y., Zhang, Y., et al. (2015). Widely distributed hot and cold spots in meiotic recombination as shown by the sequencing of rice F2 plants. *New Phytol.* 206, 1491–1502. doi: 10.1111/nph.13319

Smyth, D. R., Bowman, J. L., and Meyerowitz, E. M. (1990). Early flower development in *Arabidopsis*. *Plant Cell* 8, 755–767. doi: 10.1105/tpc.2.8.755

Soneson, C., Love, M. I., and Robinson, M. D. (2016). Differential analyses for RNA-seq: transcript-level estimates improve gene-level inferences. *F1000 Research* 4, 1521–1531. doi: 10.12688/f1000research.7563.2

Song, Y., Milon, B., Ott, S., Zhao, X., Sadzewicz, L., Shetty, A., et al. (2018). A comparative analysis of library prep approaches for sequencing low input translatome samples. *BMC Genomics* 19:696. doi: 10.1186/s12864-018-5066-2

Tang, X., Zhang, Z. Y., Zhang, W. J., Zhao, X. M., Li, X., Zhang, D., et al. (2010). Global gene profiling of laser-captured pollen mother cells indicates molecular pathways and gene subfamilies involved in rice meiosis. *Plant Physiol.* 154, 1855–1870. doi: 10.1104/pp.110.161661

Tarazona, S., Furió-Tarí, P., Turrà, D., Di Pietro, A., Nueda, M. J., Ferrer, A., et al. (2015). Data quality aware analysis of differential expression in RNA-seq with NOISeq R/Bioc package. *Nucleic Acids Res.* 43:e140. doi: 10.1093/nar/gkv711

Tian, T., Liu, Y., Yan, H., You, Q., Yi, X., Du, Z., et al. (2017). AgriGO v2.0: a GO analysis toolkit for the agricultural community, 2017 update. *Nucleic Acids Res.* 45, W122–W129. doi: 10.1093/nar/gkx382

Walker, J., Gao, H., Zhang, J., Aldridge, B., Vickers, M., Higgins, J. D., et al. (2018). Sexual-lineage-specific DNA methylation regulates meiosis in *Arabidopsis*. *Nat. Genet.* 50, 130–137. doi: 10.1038/s41588-017-0008-5

Wang, D., and Deal, R. B. (2015). Epigenome profiling of specific plant cell types using a streamlined INTACT protocol and ChIP-seq. *Methods Mol. Biol.* 1284, 3–25. doi: 10.1007/978-1-4939-2444-8_1

Wang, Z., and Baulcombe, D. C. (2020). Transposon age and non-CG methylation. *Nat. Commun.* 11, 1221–1229. doi: 10.1038/s41467-020-14995-6

Yang, H., Pingli, Lu, P., Wang, Y., and Ma, H. (2011). The transcriptome landscape of *Arabidopsis* male meiocytes from high-throughput sequencing: the complexity and evolution of the meiotic process. *Plant J.* 65, 503–516. doi: 10.1111/j.1365-313X.2010.04439.x

Yuan, T. L., Huang, W. J., He, J., Zhang, D., and Tang, W. H. (2018). Stage-Specific gene profiling of germinal cells helps delineate the mitosis/meiosis transition. *Plant Physiol.* 176, 1610–1626. doi: 10.1104/pp.17.01483

Yue, F., Cheng, Y., Breschi, A., Vierstra, J., Wu, W., Ryba, T., et al. (2014). A comparative encyclopedia of DNA elements in the mouse genome. *Nature* 515, 355–364. doi: 10.1038/nature13992

Zhang, T., Du, W., Wilson, A. F., Namekawa, S. H., Andreassen, P.R., Meetei, A. R., et al. (2017). Fancd2 *in vivo* interaction network reveals a non-canonical role in mitochondrial function. *Sci. Rep.* 7, 45626–45636. doi: 10.1038/srep 45626

Conflict of Interest: RAC was employed by company Sequentia Biotech SL.

The remaining authors declare that the research was conducted in the absence of any commercial or financial relationships that could be construed as a potential conflict of interest.

frontiers in Plant Science

HYPOTHESIS AND THEORY
published: 09 March 2021
doi: 10.3389/fpls.2021.656691

The Role of Chromatid Interference in Determining Meiotic Crossover Patterns

Marie Sarens[1], *Gregory P. Copenhaver*[2] *and Nico De Storme*[1]*

[1] Laboratory for Plant Genetics and Crop Improvement, Division of Crop Biotechnics, Department of Biosystems, Katholieke Universiteit Leuven, Leuven, Belgium, [2] Department of Biology and the Integrative Program for Biological and Genome Sciences, University of North Carolina at Chapel Hill, Chapel Hill, NC, United States

Plants, like all sexually reproducing organisms, create genetic variability by reshuffling parental alleles during meiosis. Patterns of genetic variation in the resulting gametes are determined by the independent assortment of chromosomes in meiosis I and by the number and positioning of crossover (CO) events during meiotic recombination. On the chromosome level, spatial distribution of CO events is biased by multiple regulatory mechanisms, such as CO assurance, interference and homeostasis. However, little is known about how multiple COs are distributed among the four chromatids of a bivalent. Chromatid interference (CI) has been proposed as a regulatory mechanism that biases distribution of multiple COs toward specific chromatid partners, however, its existence has not been well-studied and its putative mechanistic basis remains undescribed. Here, we introduce a novel method to quantitatively express CI, and take advantage of available tetrad-based genotyping data from Arabidopsis and maize male meiosis to quantify CI effects on a genome-wide and chromosomal scale. Overall, our analyses reveal random involvement of sister chromatids in double CO events across paired chromosomes, indicating an absence of CI. However, on a genome-wide level, CI was found to vary with physical distance between COs, albeit with different effects in Arabidopsis and maize. While effects of CI are minor in Arabidopsis and maize, the novel methodology introduced here enables quantitative interpretation of CI both on a local and genome-wide scale, and thus provides a key tool to study CI with relevance for both plant genetics and crop breeding.

Keywords: chromatid interference, meiotic recombination, crossovers, *Arabidopsis thaliana*, genetic variation

OPEN ACCESS

Edited by:
Mónica Pradillo, Complutense University of Madrid, Spain

Reviewed by:
Christine Mezard, INRA UMR1318 Institut Jean Pierre Bourgin, France
Christophe Lambing, University of Cambridge, United Kingdom

***Correspondence:**
Nico De Storme
nico.destorme@kuleuven.be

Specialty section:
This article was submitted to Plant Cell Biology, a section of the journal Frontiers in Plant Science

Received: *21 January 2021*
Accepted: *15 February 2021*
Published: *09 March 2021*

Citation:
Sarens M, Copenhaver GP and De Storme N (2021) The Role of Chromatid Interference in Determining Meiotic Crossover Patterns. Front. Plant Sci. 12:656691. doi: 10.3389/fpls.2021.656691

INTRODUCTION

Meiosis is a specialized cell division that reduces ploidy by half and generates cells essential for sexual reproduction. It consists of a single round of pre-meiotic DNA replication, followed by two consecutive rounds of chromosome segregation, in which homologous chromosomes separate in meiosis I, and sister chromatids separate in meiosis II, to yield four daughter cells. Together with this ploidy reduction, meiosis also creates novel allelic combinations by reshuffling parental DNA through independent assortment and homologous recombination. Meiotic recombination occurs during prophase I and involves pairing and synapsis of homologous chromosomes, followed by the reciprocal exchange of genetic information via crossovers (COs), which are cytologically manifested as chiasmata (Janssens, 1909; Hunter, 2015).

Despite its complexity, key elements of meiotic recombination are conserved across eukaryotes. It is initiated by the programmed induction of double-strand breaks (DSBs) catalyzed by the conserved topoisomerase-like protein SPO11 together with several other associated proteins (Keeney et al., 1997; De Muyt et al., 2007, 2009; Vrielynck et al., 2016). Subsequent processing of DSBs by the MRN/X complex results in the formation of 3′ single-stranded DNA ends, which recognize and invade the homologous chromosome to enable DNA repair via the non-sister chromatid. This single-end invasion (SEI) is facilitated by the meiosis-specific recombinase DMC1 and RAD51, and results in the formation of a D-loop intermediate (Da Ines et al., 2013; Brown and Bishop, 2015). These SEI intermediates are unstable and frequently dissociate to be repaired by the synthesis-dependent strand annealing (SDSA) pathway to yield non-crossovers (McMahill et al., 2007). Some D-loops persist and are further processed by annealing to the 3′ single-stranded DNA end on the other side of the original break in a process called second-end capture. The resulting intermediate structure physically interlinks both homologs and after ligation of adjacent DNA ends goes on to form a double Holliday Junction (dHJ). Finally, endonucleases called resolvases cleave the dHJs and the primary product of this type of resolution are CO events, as evidenced in *Saccharomyces cerevisiae* (Allers and Lichten, 2001; Mercier et al., 2015; Wang and Copenhaver, 2018).

Most eukaryotes have an abundance of meiotic DSBs, but relatively few COs. Moreover, COs are non-uniformly distributed across the genome, with many organisms showing a preferential skewing of COs toward the (sub-)telomeric regions (Giraut et al., 2011; Li et al., 2015). Several regulatory phenomena have been found to influence CO distribution on the local, chromosomal and genome-wide scale, including CO assurance, homeostasis and interference (Berchowitz and Copenhaver, 2010; Wang et al., 2015; Wang and Copenhaver, 2018). In contrast, little is known about the regulation of CO distribution among the four chromatids of a paired chromosome set. Chromatid interference (CI) has been proposed as a mechanism that biases distribution of multiple COs within a meiotic bivalent toward specific chromatid partners (Zhao et al., 1995). When two COs occur on the same pair of homologous chromosomes, three different outcomes are possible (**Figure 1**): (A) both COs use the same non-sister chromatids, resulting in a two-strand double CO (2S-DCO); (B) COs share only one chromatid, resulting in a three-strand double CO (3S-DCO), as can be achieved in two different ways; or (C) COs use a different pair of non-sister chromatids, resulting in a four-strand double CO (4S-DCO). Typically, putative sister chromatid interactions are ignored because they are largely suppressed during meiosis (Schwacha and Kleckner, 1994). Depending on the type of DCOs that is favored in meiosis, different types of CI effects can be defined. In the absence of CI, chromatid partner participation in DCO events occurs randomly, resulting in a 1:2:1 ratio of 2S-, 3S-, and 4S-DCOs. Positive CI occurs when a CO between a pair of chromatids suppresses the occurrence of a second CO between the same two chromatids, resulting in a higher frequency of 4S-DCOs. In contrast, negative CI occurs when the same pair of chromatids is more likely to experience DCOs than what would be expected by a random distribution, resulting in an increased number of 2S-DCOs (Zhao et al., 1995).

The occurrence of CI would influence meiotic CO patterning and the genetic make-up of gametes, and would therefore have a major impact on genetic analyses such as linkage-based mapping and QTL assays. The construction of genetic maps and identification of QTLs relies on measuring the genetic distance between loci in mapping populations (e.g., F2, RIL, NIL, etc.) derived from crossing polymorphic parents. Genetic distance is determined by quantifying the frequency of recombinant genotypes between loci, and is expressed in centiMorgans (cM). Loci on different chromosomes segregate randomly in MI and yield equal fractions of recombinant and non-recombinant genotypes, resulting in a genetic distance of 50 cM. For loci on the same chromosome, however, recombinant genotypes can only result from intervening COs. Genetic map distances are therefore often simple calculations of CO frequency, although more nuanced formulas are available that account for the occurrence of DCOs, such as the Perkins (1949), Haldane (1919), and Kosambi (1944) functions. However, all these mapping functions assume a complete absence of CI and thus integrate a random 1:2:1 ratio of 2S:3S:4S DCOs as a core part of their derivation. This assumption, however, may lead to inaccuracies in the calculation of actual genetic distances. For example, negative CI will create relatively more 2S-DCOs and thus lower the odds of detecting double COs, particularly when loci are located far apart. As a result, negative CI can cause an underestimation of the actual genetic distance, even when calculated using approaches that account for DCOs. By comparison, positive CI results in relatively more 4S-DCOs and increases the odds of detecting DCOs, which can lead to an overestimation of the actual genetic distance. To investigate the significance of these biases and facilitate the development of mapping functions that incorporate the influence of CI, a quantitative measure of CI is needed.

Accurate quantification of CI requires genotypic information from all four meiotic products, referred to as "tetrad analysis." Many fungi retain their meiotic products in an ascus making tetrad data easy to obtain. Tetrad data is harder to gather from most multicellular organisms because their meiotic products do not remain attached in their meiotic configuration. Despite these difficulties, tetrad analysis has been achieved in several multicellular species, including plants, allowing analysis of CI. In Arabidopsis, mutations in the *QRT1* gene cause mature pollen grains to remain together in their original meiotic tetrad configuration (Preuss et al., 1994). Backcrossing single pollen tetrads from *qrt1* F1 plants from crosses between two polymorphic parents generates four progeny plants that can be analyzed to determine the genotype of the original tetrad (Copenhaver et al., 1998; Lu et al., 2012; Wijnker et al., 2013; Liu et al., 2018). Several plant species produce natural tetrads at the mature pollen stage (Copenhaver, 2005), but even in those that do not tetrad data can be obtained by isolating and genotyping individual microspores from single tetrads at the end of sporogenesis. The latter approach has been used to obtain high

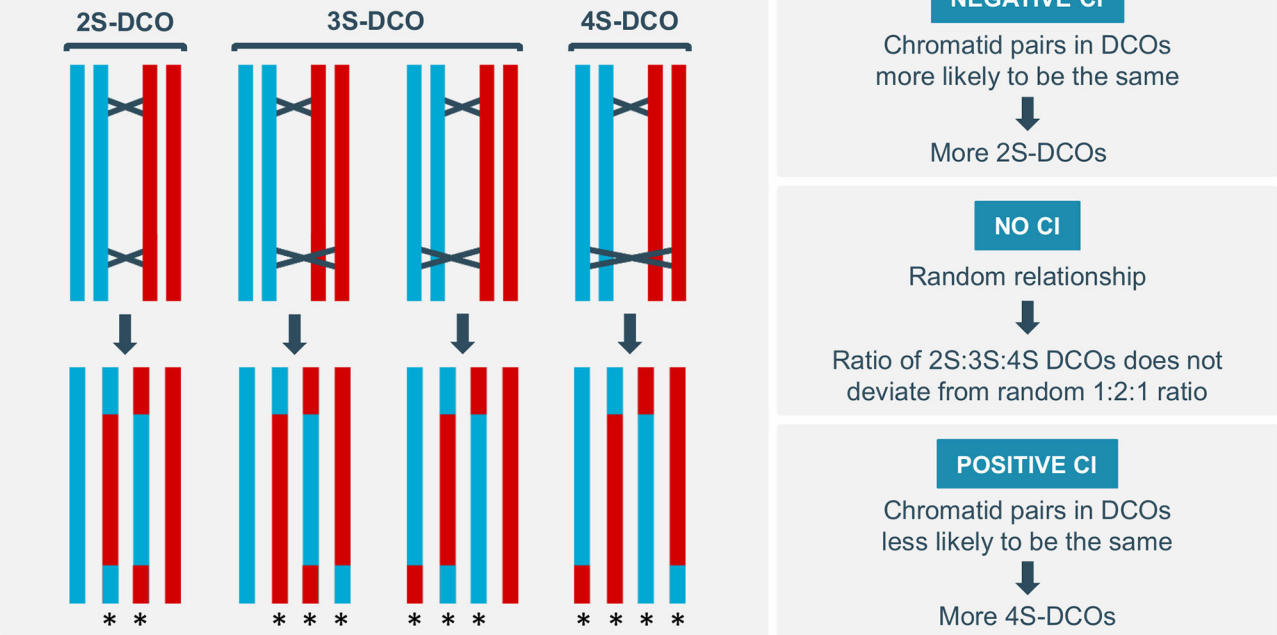

FIGURE 1 | Different types of double crossovers (DCOs) and chromatid interference (CI). DCOs can occur between the same pair of chromatids (two-strand or 2S-DCO), resulting in two recombinant and two parental chromosomes. DCOs can have only one chromatid in common (three-strand or 3S-DCO), resulting in three recombinant and one parental chromosome. DCOs can occur between different chromatids (four-strand or 4S-DCO), resulting in four recombinant chromosomes. If the 2S:3S:4S DCO ratio does not significantly deviate from the random 1:2:1 ratio, CI is absent. If there are relatively more 2S-DCOs, negative CI occurs; if there are relatively more 4S-DCOs, positive CI occurs. Recombinant chromosomes are indicated by an asterisk.

resolution CO data from maize male meioses (Li et al., 2015). In human oocytes, tetrad data has been obtained by isolating and sequencing the first and second polar bodies and the female pronucleus (Hou et al., 2013). In mouse, tetrad analysis has been performed for both male and female meiosis. In female mice this is achieved by microdissection of individual germinal vesicle-stage oocytes from F1 hybrids. In male mice, tetrad data was obtained by isolating late prophase I primary spermatocytes using flow cytometry (Cole et al., 2014).

CI has been examined in *Saccharomyces cerevisiae*, *Neurospora crassa*, *Aspergillus nidulans*, *Arabidopsis thaliana*, *Zea mays*, and humans (Lindegren and Lindegren, 1942; Strickland, 1957; Hawthorne and Mortimer, 1960; Zhao et al., 1995; Copenhaver et al., 1998; Chen et al., 2008; Hou et al., 2013; Li et al., 2015). These studies suggest weak or no CI with minor variation across eukaryotic phyla. In contrast, a recent study using *in situ* cytological probing of meiotic chromosomes provided direct evidence for strong positive CI (i.e., 64% 4S-DCOs instead of the expected 25%) in two interspecific hybrids, *Lolium multiflorum* × *Festuca pratensis* and *Allium cepa* × *A. roylei* (Ferreira et al., 2020). These findings are striking as they indicate that strong CI may occur in plant meiosis, and that this may be influenced by genetic background, and particularly hybrid status. Some studies have also examined the influence of the centromere on CI. In humans, weak negative CI is present within chromosome arms, but no CI effects are detected when the two COs are on the opposite sides of a centromere (Hou et al., 2013). In contrast, in maize, weak CI was observed for DCOs within one chromosome arm as well as for DCOs spanning the centromere (Li et al., 2015).

Prior CI analyses are limited to accepting or rejecting a fit to the expected 1:2:1 ratio and are mainly focused on genome-wide effects, leaving many questions unanswered, including: "If CI is present, does it show variation in strength across chromosomes?," "Is CI subject to chromosome-specific or location-specific effects?," "Does inter-CO distance influence CI and is there a link with CO interference?," and "Does CI differ between male and female meiosis?." In this study, we introduce a novel analytical framework for the quantitative interpretation of CI and apply this to tetrad-based genotyping data from Arabidopsis and maize male meiosis to unravel putative, yet unexplored CI effects.

ANALYSIS OF CHROMATID INTERFERENCE IN ARABIDOPSIS AND MAIZE MALE MEIOSIS

We quantified CI in Arabidopsis using previously acquired tetrad-based genotyping data of male meiosis (Copenhaver et al., 1998). This dataset contains PCR-based marker genotypes from 58 meiotic tetrads for chromosome 1, 3, and 5 and from 143 tetrads for chromosome 2 and 4 (see **Supplementary Data Sheet 1**). Additional information on the

number of markers used can be found in **Supplementary Table 1**. We measured CI in maize using tetrad-based genotyping data of male meioses provided by Li et al. (2015). This dataset consists of single-microspore sequencing data of 24 tetrads and provides high-resolution genotyping data of corresponding meiotic events with an average of 271,524 SNPs per tetrad. The corresponding Arabidopsis and maize datasets were used to identify all DCOs and to determine levels of CI. For Arabidopsis, the dataset contains a total of 843 COs, including 385 DCOs (**Table 1**). For maize, the dataset contains a total of 924 COs, and 684 DCOs (**Table 2**).

Novel Approach for Quantifying CI

Traditionally, CI is assessed by testing goodness-of-fit to the expected 1:2:1 ratio of 2S:3S:4S DCOs for individual genomic intervals (**Figure 1**). This method enables hypothesis testing for the presence or absence of CI but does not allow interpretation of the strength of CI when it is detected. Without a quantitative value for CI, it is difficult to compare different genomic intervals when trying to ascertain local variation, to interpret the impact of genetic or physical distance on CI, or to assess the putative effect of structural domains, such as the centromere. Additionally, the goodness-of-fit method does not allow easily interpretable graphical representations of putative CI dynamics and thus limits studies on the occurrence, relevance and regulation of CI.

To address this, we have developed a novel approach for CI analysis that relies on a quantitative parameter calculated from the number of DCO types in a specific genomic interval, and thus enables interpretation of both the strength and direction of CI in a local, chromosomal or genome-wide context. This is achieved by assigning discrete values to each DCO type within an interval and by calculating the mean CI value of all DCOs. The specific CI value for each DCO type is determined according to the following principle. If a chromatid participating in a first CO does not participate in the second CO of the DCO, it is assigned a value of 0.5. In the opposite case, if a chromatid participating in a first CO also participates in the second CO, it is assigned a value of −0.5. The CI value of a specific DCO type is hence obtained by the summed values assigned to the two non-sister chromatids involved in the first CO. Using this approach, 2S-DCOs are assigned a value of −1, 3S-DCOs are assigned a value of 0 and 4S-DCOs are assigned a value of 1. Averaging the assigned values of all DCOs within a specific genomic interval gives a mean CI value between −1 and 1, providing a quantitative measure for the strength and direction of CI. A mean CI value of −1 indicates complete negative CI (i.e., all DCOs are 2S type), a value of 1 indicates complete positive CI (i.e., all DCOs are 4S type), and a CI value of 0 indicates absence of CI.

Genome-Wide and Chromosome-Specific Levels of CI

We examined the presence and direction of CI for the complete genome and each chromosome using both the traditional ratio-based analysis and our novel quantitative analysis method (indicated as "CI value"). For Arabidopsis, the ratio of 2S:3S:4S DCOs for all five chromosomes does not deviate significantly from the random 1:2:1 distribution (**Table 1** and **Supplementary Table 2**), indicating absence of CI on a genome-wide and chromosome-specific scale, as was previously reported (Copenhaver et al., 1998). Consistent with this, quantitative determination of CI across the genome and for all individual chromosomes yields CI values that do not significantly differ from 0 (**Table 1** and **Supplementary Table 2**). These findings demonstrate that Arabidopsis male meiosis does not experience any bias toward a specific DCO type on a genome-wide or chromosome-specific level.

We also tested the hypothesis that the centromere influences CI. For this, DCOs were split into two groups: DCOs that occur on the same chromosome arm, and DCOs that span the centromere. On the genome-wide level, we detected a significant deviation from the 1:2:1 ratio for all DCOs occurring on the same chromosome arm (55:66:48, Chi-Square test of goodness-of-fit, $P = 0.013$). However, the corresponding CI value did not differ significantly from 0, indicating that this deviation is neutral (**Table 1** and **Supplementary Table 2**). For DCOs spanning the centromere, we observed a significant bias for chromosome 2 for both the ratio (12:29:4, Chi-Square test of goodness-of-fit, $P = 0.037$) and the CI value (−0.18, Wilcoxon signed rank test, $P = 0.024$), indicating presence of negative CI. However, after applying a multiple testing penalty using Bonferroni correction these deviations were no longer significant. All these results are based on PCR-based genotyping data, and it is possible that DCOs were undercounted, for example by missing terminally located COs for which no flanking markers were available. To address this, we examined two additional Arabidopsis datasets (Wijnker et al., 2013; Liu et al., 2018) that contain tetrad-based sequencing data from 22 male meiotic tetrads. Aalysis of CI using only these datasets is not informative because the number of DCOs is too low (**Supplementary Tables 3, 4**). However, merging these datasets with the marker-based genotyping dataset (Copenhaver et al., 1998) did not change prior results, with absence of significant deviations for all chromosomes (**Supplementary Table 5**), indicating that the marker-based data enables reliable interpretation of CI.

In maize, the genome-wide ratio of 2S:3S:4S DCOs does not deviate significantly from the null hypothesis of a 1:2:1 ratio (**Table 2** and **Supplementary Table 6**), indicating absence of CI. In line with this, quantitative analysis of CI yields a value that does not significantly differ from 0, confirming the results of the ratio-based method. Chromosome-specific analysis of the 2S:3S:4S DCO ratio shows a significant deviation from the random 1:2:1 ratio for chromosome 3 (15:52:11, Chi-Square test of goodness-of-fit, $P = 0.011$), but the corresponding CI value does not differ significantly from 0, indicating that this deviation is neutral and that CI is absent.

Genome-wide, DCOs on the same arm or spanning a centromere in maize do not show CI (**Table 2** and **Supplementary Table 6**). Chromosome-specific ratio-based analyses of CI for same-arm DCOs yield significant deviations from the 1:2:1 ratio for chromosome 3 and 6 (8:36:10 and 21:21:11, respectively, Chi-Square test of goodness-of-fit, $P = 0.046$ and $P = 0.048$, respectively), but for chromosome 3 no significant difference is observed for the CI value. Conversely, for same-arm DCOs on chromosome 6 a negative CI value (−0.19,

TABLE 1 | Analysis of chromatid interference (CI) in Arabidopsis male meiosis.

	Whole chromosome			Same arm			Different arm		
	Total DCOs	Observed 2S:3S:4S ratio (Expected ratio)	CI value	Total DCOs	Observed 2S:3S:4S ratio (Expected ratio)	CI value	Total DCOs	Observed 2S:3S:4S ratio (Expected ratio)	CI value
Chr1	101	33:44:24 (25.25:50.5:25.25)	−0.09	49	18:20:11 (12.25:24.5:12.25)	−0.14	52	15:24:13 (13:26:13)	−0.04
Chr2	98	24:52:22 (24.5:49:24.5)	−0.02	53	12:23:18 (13.25:26.5:13.25)	0.11	45	12:29:4 (*) (11.25:22.5:11.25)	−0.18 (*)
Chr3	66	20:33:13 (16.5:33:16.5)	−0.11	23	9:9:5 (5.75:11.5:5.75)	−0.17	43	11:24:8 (10.75:21.5:10.75)	−0.07
Chr4	69	20:28:21 (17.25:34.5:17.25)	0.01	30	12:9:9 (7.5:15:7.5)	−0.10	39	8:19:12 (9.75:19.5:9.75)	0.10
Chr5	51	15:21:15 (12.75:25.5:12.75)	0	14	4:5:5 (3.5:7:3.5)	0.07	37	11:16:10 (9.25:18.5:9.25)	−0.03
Total	385	112:178:95 (96.25:192.5:96.25)	−0.04	169	55:66:48 (*) (42.25:84.5:42.25)	−0.04	216	57:112:47 (54:108:54)	−0.05

CI is determined using both the 2S:3S:4S DCO ratio method and the novel quantitative analysis method (CI value). Results are shown for DCOs along the chromosomes, as well as for single-arm DCOs and for DCOs spanning a centromere. In the absence of CI, a random 2S:3S:4S DCO ratio of 1:2:1 and a CI value of 0 is expected. Deviations from the random 1:2:1 ratio were statistically analyzed using the Chi-Square test of goodness-of-fit (when total amount of DCOs ≥ 20) or using the exact multinomial test (when total amount of DCOs < 20). Deviations of the CI value were statistically tested using the Wilcoxon signed rank test. P-values of all statistical tests are provided in ***Supplementary Table 2****. Statistical tests were corrected via multiple penalty testing using Bonferroni correction (α = 0.008). Significant results before correcting are indicated with an asterisk. Results are based on PCR-based tetrad genotyping data (Copenhaver et al., 1998).*

Wilcoxon signed rank test, $P = 0.039$) is observed. For DCOs that span a centromere, we observe no significant deviation from the 1:2:1 ratio. For the CI value, significant deviations are observed for chromosome 2 and 3 (−0.25 for both, Wilcoxon signed rank test, $P = 0.021$), indicating negative CI. However, after applying a multiple testing penalty (Bonferroni correction) significant differences were no longer observed.

Effect of Inter-CO Distance on Chromatid Interference

To test the hypothesis that chromatid interference might vary depending on the distance between two adjacent COs we calculated the level of CI as a function of physical inter-CO distance (Mb) using the new CI quantification method (**Figures 2**, **3**). As marker-based genotyping data does not provide the precise location of recombination events, CO positions were estimated by averaging the genomic location of adjacent recombinant markers. To calculate the inter-CO distance of a DCO, the physical distance between the two COs was then determined and rounded to the closest Mb integer.

For Arabidopsis male meiosis, the genome-wide analysis indicates that CI increases as a function of inter-CO distance (**Figure 2**). As the presented averaged values are based on different numbers of DCOs, a weighted linear regression was performed. Although correlation is rather weak ($R^2 = 0.0058$), this analysis reveals a minor influence of inter-CO distance on CI, with negative CI values when inter-CO distances are <14 Mb and positive CI for inter-CO distances of more than 14 Mb. However, as the 95% confidence interval is rather broad and covers the zero baseline, the observed correlation is non-significant. A similar analysis was performed with the merged dataset containing both PCR-based and sequencing-based genotyping data (**Supplementary Figure 1**). This extended analysis revealed even lower correlation between CI and physical inter-CO distance with the mean CI value for all DCO distances amounting close to 0, further indicating that CI effects do not vary with inter-CO distance.

For maize, genome-wide results indicate positive CI when inter-CO distances are <60 Mb and negative CI when inter-CO distances are larger (**Figure 3**). However, considering the low correlation value ($R^2 = 0.0046$), observed effects are non-significant and more high-throughput genotyping data is required to validate these genome-wide trends and to assess for putative chromosome-specific variation.

DISCUSSION

Chromatid interference (CI), the mechanism that describes the bias of chromatid partner choice in multiple COs, is a poorly studied aspect of meiotic CO patterning. Generally, it is assumed that CI does not exist and that the choice of the specific sister chromatid involved in a CO event occurs randomly and independently of neighboring COs, leading to a balanced 1:2:1 ratio of 2S:3S:4S DCOs (Zhao et al., 1995; Teuscher et al., 2000). However, some studies have reported a bias of this 1:2:1 ratio, indicating the presence of CI, although often rather weak (Zhao et al., 1995; Hou et al., 2013; Li et al., 2015; Ferreira et al., 2020). As presence of CI has consequences for genetic mapping studies and specific breeding applications, more detailed studies are needed to unravel the actual occurrence and relevance of this rather elusive process. In order to facilitate this, we here introduce a novel approach for quantifying and representing

TABLE 2 | Analysis of chromatid interference (CI) in maize male meiosis.

	Whole chromosome			Same arm			Different arm		
	Total DCOs	**Observed 2S:3S:4S ratio (Expected ratio)**	**CI value**	**Total DCOs**	**Observed 2S:3S:4S ratio (Expected ratio)**	**CI value**	**Total DCOs**	**Observed 2S:3S:4S ratio (Expected ratio)**	**CI value**
Chr1	110	23:57:30 (27.5:55:27.5)	0.06	86	18:47:21 (21.5:43:21.5)	0.04	24	5:10:9 (6:12:6)	0.17
Chr2	83	17:47:19 (20.75:41.5:20.75)	0.02	59	10:31:18 (14.75:29.5:14.75)	0.14	24	7:16:1 (6:12:6)	−0.25 (*)
Chr3	78	15:52:11 (*) (19.5:39:19.5)	−0.05	54	8:36:10 (*) (13.5:27:13.5)	0.04	24	7:16:1 (6:12:6)	−0.25 (*)
Chr4	71	15:39:17 (17.75:35.5:17.75)	0.03	48	6:29:13 (12:24:12)	0.15	23	9:10:4 (5.75:11.5:5.75)	−0.22
Chr5	77	18:44:15 (19.25:38.5:19.25)	−0.04	53	12:34:7 (13.25:26.5:13.25)	−0.09	24	6:10:8 (6:12:6)	0.08
Chr6	64	23:25:16 (16:32:16)	−0.11	53	21:21:11 (*) (13.25:26.5:13.25)	−0.19 (*)	11	2:4:5 (2.75:5.5:2.75)	0.27
Chr7	56	14:25:17 (14:28:14)	0.05	32	8:13:11 (8:16:8)	0.09	24	6:12:6 (6:12:6)	0
Chr8	61	11:34:16 (15.25:30.5:15.25)	0.08	37	8:19:10 (9.25:18.5:9.25)	0.05	24	3:15:6 (6:12:6)	0.13
Chr9	43	12:21:10 (10.75:21.5:10.75)	−0.05	20	5:11:4 (5:10:5)	−0.05	23	7:10:6 (5.75:11.5:5.75)	−0.04
Chr10	41	12:22:7 (10.25:20.5:10.25)	−0.12	18	6:8:4 (4.5:9:4.5)	−0.11	23	6:14:3 (5.75:11.5:5.75)	−0.13
Total	684	160:366:158 (171:342:171)	−0.003	460	102:249:109 (101.5:203:101.5)	0.02	224	58:117:49 (56:112:56)	−0.04

Presence of CI is determined using both the 2S:3S:4S DCO ratio method and the novel quantitative analysis method (CI value). Results are shown for DCOs along the chromosomes, as well as for same-arm DCOs and DCOs that span a centromere. In case CI is absent, a DCO ratio of 1:2:1 and a CI value of 0 is expected. Deviations from the expected 1:2:1 ratio were statistically tested using a Chi-Square test of goodness-of-fit (when total number of DCOs ≥ 20) and via an exact multinomial test (when total number of DCOs < 20). Deviations of the CI value were statistically tested using the Wilcoxon signed rank test. P-values of all statistical tests are provided in ***Supplementary Table 6****. Statistical tests were corrected via multiple penalty testing using Bonferroni correction (α = 0.0045). Significant results before correcting are indicated with an asterisk. Results are based on genotyping data from Li et al. (2015).*

CI, and demonstrate its applicability by reassessing the role of CI in meiotic CO patterning in plants by using available tetrad genotyping data from Arabidopsis and maize.

CI is traditionally assessed by testing whether the ratio of 2S:3S:4S DCOs deviates from the expected 1:2:1 ratio (Copenhaver et al., 1998; Hou et al., 2013; Li et al., 2015; Liu et al., 2018; Ferreira et al., 2020). However, this method only verifies the presence or absence of CI, and does not provide straightforward information about its strength or direction. We here extend this basic analysis by introducing a new approach to quantitatively measure CI, enabling the assessment of both the strength and direction of CI. This new approach provides a single quantitative measure of CI for each genomic region, ranging from short intervals to whole chromosomes, and therefore strongly facilitates data interpretation and comparative analysis of CI. This new methodology could be useful in a broad range of studies that are focused on CO patterning, such as those aimed at describing the meiotic CO landscape and resulting genetic variation, as well as those aimed at elucidating the genetic basis and molecular mechanism(s) underlying CI.

Using both the ratio-based method and the CI value, we re-analyzed available tetrad-based genotyping data of Arabidopsis (Copenhaver et al., 1998; Wijnker et al., 2013; Liu et al., 2018) and maize (Li et al., 2015). Our results provide no evidence for genome-wide or chromosome-specific effects of CI in both species. Similarly, no common significant deviations were observed when assessing the effect of the centromere, indicating that the physical peculiarities of the centromere do not restrict or impose biases toward chromatid partner choice in DCO events. For maize, using the same data, Li et al. (2015) reported significant CI for DCOs occurring on the same chromosome arm and DCOs spanning the centromere. However, these conclusions were based on boot-strapping analysis which is different from the Chi-Square test of goodness-of-fit used in this analysis. Strikingly, for both Arabidopsis chromosome 2 and maize chromosomes 2 and 3 a tendency toward negative CI has been observed for DCOs that span the centromere (CI values of −0.20 and −0.25, respectively). These deviations indicate for the potential occurrence of chromosome-specific signatures, either structural or regulatory, that impose a directed CI effect on COs that occur on a different side of the centromere. However, whether these observed CO biases reflect actual CI effects, and if so, by which molecular mechanism(s) this is imposed remains to be further investigated. Overall, our findings are in line with

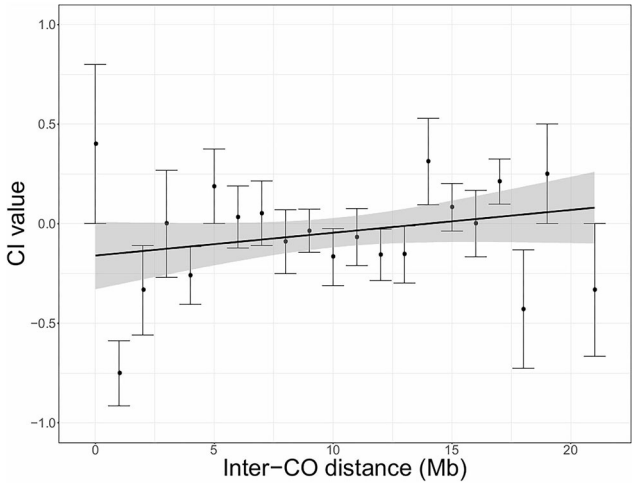

FIGURE 2 | Chromatid interference (CI) in function of physical distance (Mb) between adjacent COs (inter-CO distance) in Arabidopsis male meiosis. Linear regression is performed with the total number of DCOs per inter-CO distance as weighted factors. Gray shaded areas indicate the 95% confidence interval for the regression line. Intercept = −0.1598; Slope = 0.0115; $R^2 = 0.0058$. Results are based on PCR-based tetrad genotyping data (Copenhaver et al., 1998).

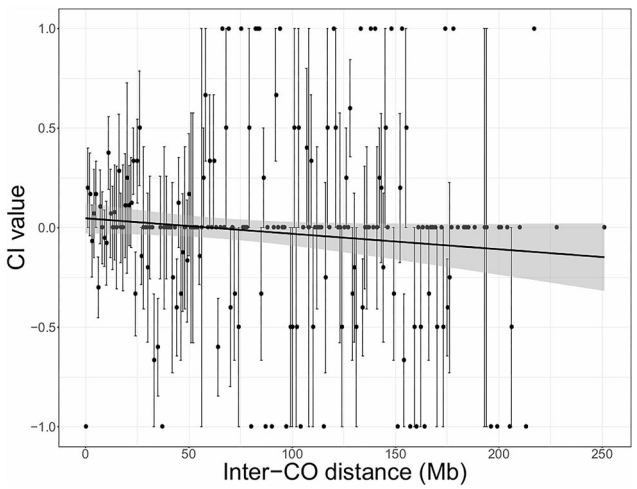

FIGURE 3 | Chromatid interference (CI) in function of physical distance (Mb) between adjacent COs (inter-CO distance) in maize male meiosis. Linear regression is performed with the total number of DCOs per inter-CO distance as weighted factors. Gray shaded areas indicate the 95% confidence interval for the regression line. Intercept = 0.04733; Slope = −0.00078; $R^2 = 0.0046$. Results are based on sequencing-based tetrad genotyping data (Li et al., 2015).

most previous studies, reporting no or only weak presence of CI in different species (Zhao et al., 1995; Copenhaver et al., 1998; Chen et al., 2008; Hou et al., 2013; Li et al., 2015). Interestingly, a recent study reported presence of strong positive CI in two interspecific plant hybrids, *Lolium multiflorum* × *Festuca pratensis* and *Allium cepa* × *A. roylei* (Ferreira et al., 2020). This is the first study that demonstrates a clear bias in the specific configuration of DCOs, and thus provides strong and unambiguous evidence that CI may occur in plant meiosis. However, it is important to note that CI in these grass and Allium species was observed in hybrid genotypes that result from interspecific or -genic hybridization, and thus relates to COs that occur between homeologous chromosomes with putative impact of genomic heterozygosity, structural chromosome variation or differential DNA compaction. As a consequence, it is not clear yet whether these findings can be extrapolated to non-hybrid or intraspecific hybrid genotypes that exhibit regular homology and sufficient compatibility between both parental genomes.

Using the new CI quantification methodology, we also assessed whether CI depends on the physical distance between COs. Due to the general absence of CI on a chromosome-wide level, this question has remained unaddressed in previous studies. However, it may still be possible that there is a bias toward specific sister chromatids when COs occur in close proximity to each other, whereas this may be antagonized by DCOs in which COs are distantly positioned from each other. For both Arabidopsis and maize, we observed variation in CI depending on physical inter-CO distance. For Arabidopsis, there was a tendency toward negative CI when participating COs are closely located to each other and toward positive CI when inter-CO distance becomes larger. In maize, we observed the opposite trend. However, as observed effects were only minor and lacked significant correlation, further investigation using more extended datasets is needed to validate the putative effect of inter-CO distance on CI.

Apart from being influenced by physical inter-CO distance, CI may also exhibit regional/local variation due to specific determinants that act *in cis* (e.g., chromatin status, sister chromatid cohesion, etc.). Such local effects have not yet been analyzed in any species due to lack of dedicated methodology, sufficient data and/or saturated genotyping data. By using our new methodology and applying it for the analysis of large datasets of highly saturated genotyping profiles, local effects of CI on CO patterning may be uncovered and characterized. However, similar as for the traditional ratio-based method, our approach still relies on tetrad-based genotyping data, as information on a large number of DCOs is required to perform reliable data interpretation, and this is in spite of several scientific advances often laborious and time consuming, or in some species even impossible to obtain. Therefore, it remains challenging to study local variation of CI effects, as well other aspects of CI, such as sex-specific differences (i.e., male vs. female meiosis) and temporal dynamics during plant aging and development.

DATA AVAILABILITY STATEMENT

Publicly available datasets were analyzed in this study. This data can be found here: data from Li et al. (2015) is available at https://www.nature.com/articles/ncomms7648#Sec21; data from Wijnker et al. (2013) is available at https://elifesciences.org/articles/01426/figures#files; data from Liu et al. (2018) is available at https://gattaca.nju.edu.cn/pub_data.html; data from Copenhaver et al. (1998) is provided as **Supplementary Material**.

AUTHOR CONTRIBUTIONS

NDS, GC, and MS contributed to the main conceptual ideas and manuscript outline. MS performed the data analysis and wrote the manuscript with inputs, corrections, and critical feedback from the other authors. All authors contributed to the article and approved the submitted version.

FUNDING

This work was supported by the Research Foundation Flanders (FWO) via a Ph.D. aspirant fellowship granted to MS (Grant number: 1168720N); GC was supported by a grant from the US National Science Foundation (IOS-1844264).

ACKNOWLEDGMENTS

The authors thank Peter Goos (KU Leuven) for helpful comments and advise on statistical data interpretation.

SUPPLEMENTARY MATERIAL

The Supplementary Material for this article can be found online at: https://www.frontiersin.org/articles/10.3389/fpls.2021.656691/full#supplementary-material

REFERENCES

Allers, T., and Lichten, M. (2001). Differential timing and control of noncrossover and crossover recombination during meiosis. *Cell* 106, 47–57. doi: 10.1016/S0092-8674(01)00416-0

Berchowitz, L., and Copenhaver, G. (2010). Genetic interference: dont stand so close to me. *Curr. Genomics* 11, 91–102. doi: 10.2174/138920210790886835

Brown, M. S., and Bishop, D. K. (2015). DNA strand exchange and RecA homologs. *Cold Spring Harb. Perspect.* 7:a016659. doi: 10.1101/cshperspect.a016659

Chen, S. Y., Tsubouchi, T., Rockmill, B., Sandler, J. S., Richards, D. R., Vader, G., et al. (2008). Global analysis of the meiotic crossover landscape. *Dev. Cell* 15, 401–415. doi: 10.1016/j.devcel.2008.07.006

Cole, F., Baudat, F., Grey, C., Keeney, S., De Massy, B., and Jasin, M. (2014). Mouse tetrad analysis provides insights into recombination mechanisms and hotspot evolutionary dynamics. *Nat. Genet.* 46, 1072–1080. doi: 10.1038/ng.3068

Copenhaver, G. P. (2005). A compendium of plant species producing pollen tetrads. *J. North Carolina Acad. Sci.* 121, 17–35. Available online at: https://www.jstor.org/stable/24336002

Copenhaver, G. P., Browne, W. E., and Preuss, D. (1998). Assaying genome-wide recombination and centromere functions with Arabidopsis tetrads. *Proc. Natl. Acad. Sci. U. S. A.* 95, 247–252. doi: 10.1073/pnas.95.1.247

Da Ines, O., Degroote, F., Goubely, C., Amiard, S., Gallego, M. E., and White, C. I. (2013). Meiotic recombination in Arabidopsis is catalysed by DMC1, with RAD51 playing a supporting role. *PLoS Genet.* 9:e1003787. doi: 10.1371/journal.pgen.1003787

De Muyt, A., Pereira, L., Vezon, D., Chelysheva, L., Gendrot, G., Chambon, A., et al. (2009). A high throughput genetic screen identifies new early meiotic recombination functions in Arabidopsis thaliana. *PLoS Genet.* 5:e1000654. doi: 10.1371/journal.pgen.1000654

De Muyt, A., Vezon, D., Gendrot, G., Gallois, J. L., Stevens, R., and Grelon, M. (2007). AtPRD1 is required for meiotic double strand break formation in Arabidopsis thaliana. *EMBO J.* 26, 4126–4137. doi: 10.1038/sj.emboj.7601815

Ferreira, M. T. M., Glombik, M., Pernichkova, K., Duchoslav, M., Scholten, O., Karafiatova, M., et al. (2020). Direct evidence for crossover and chromatid interference in meiosis of two plant hybrids (Lolium Multiflorum x Festuca Pratensis And Allium Cepa x A. Roylei). *J. Exp. Bot.* 72, 254–267 doi: 10.1093/jxb/eraa455

Giraut, L., Falque, M., Drouaud, J., Pereira, L., Martin, O. C., and Mézard, C. (2011). Genome-wide crossover distribution in Arabidopsis thaliana meiosis reveals sex-specific patterns along chromosomes. *PLoS Genet.* 7:e1002354. doi: 10.1371/journal.pgen.1002354

Haldane, J. B. S. (1919). The combination of linkage values, and the calculation of distances between the loci of linked factors. *J. Genet.* 8, 299–309.

Hawthorne, D. C., and Mortimer, R. K. (1960). Chromosome mapping in Saccharomyces: centromere-linked genes. *Genetics* 45, 1085–1110. doi: 10.1093/genetics/45.8.1085

Hou, Y., Fan, W., Yan, L., Li, R., Lian, Y., Huang, J., et al. (2013). Genome analyses of single human oocytes. *Cell* 155, 1492–1506. doi: 10.1016/j.cell.2013.11.040

Hunter, N. (2015). Meiotic recombination: the essence of heredity. *Cold Spring Harb. Perspect. Biol.* 7:a016618. doi: 10.1101/cshperspect.a016618

Janssens, F. A. (1909). La Thorie de la Chiasmatypie. Nouvelle interprétation des cinèses de maturation. *Cellule* 25, 389–411.

Keeney, S., Giroux, C. N., and Kleckner, N. (1997). Meiosis-specific DNA double-strand breaks are catalyzed by Spo11, a member of a widely conserved protein family. *Cell* 88, 375–384. doi: 10.1016/S0092-8674(00)81876-0

Kosambi, D. D. (1944). The estimation of map distances from recombination values. *Ann. Eugen* 12, 172–175. doi: 10.1111/j.1469-1809.1943.tb02321.x

Li, X., Li, L., and Yan, J. (2015). Dissecting meiotic recombination based on tetrad analysis by single-microspore sequencing in maize. *Nat. Commun.* 6:6648. doi: 10.1038/ncomms7648

Lindegren, C. C., and Lindegren, G. (1942). Locally specific patterns of chromatid and chromosome interference in neurospora. *Genetics* 27, 1–24.

Liu, H., Huang, J., Sun, X., Li, J., Hu, Y., Yu, L., et al. (2018). Tetrad analysis in plants and fungi finds large differences in gene conversion rates but no GC bias. *Nat. Ecol. Evol.* 2, 164–173. doi: 10.1038/s41559-017-0372-7

Lu, P., Han, X., Qi, J., Yang, J., Wijeratne, A. J., Li, T., et al. (2012). Analysis of Arabidopsis genome-wide variations before and after meiosis and meiotic recombination by resequencing. *Genome Res.* 22, 508–518. doi: 10.1101/gr.127522.111

McMahill, M. S., Sham, C. W., and Bishop, D. K. (2007). Synthesis-dependent strand annealing in meiosis. *PLoS Biol.* 5:e299. doi: 10.1371/journal.pbio.0050299

Mercier, R., Mézard, C., Jenczewski, E., Macaisne, N., and Grelon, M. (2015). The molecular biology of meiosis in plants. *Annu. Rev. Plant Biol.* 66, 297–327. doi: 10.1146/annurev-arplant-050213-035923

Perkins, D. D. (1949). Biochemical mutants in the smut fungus ustilago maydis. *Genetics* 34, 607–626.

Preuss, D., Rhee, S. Y., and Davis, R. W. (1994). Tetrad analysis possible in Arabidopsis with mutation of the QUARTET (QRT) genes. *Science* 264, 1458–1460. doi: 10.1126/science.8197459

Schwacha, A., and Kleckner, N. (1994). Identification of joint molecules that form frequently between homologs but rarely between sister chromatids during yeast meiosis. *Cell* 76, 51–63. doi: 10.1016/0092-8674(94)90172-4

Strickland, W. N. (1957). An analysis of interference in Aspergillus nidulans. *Proc. R. Soc. London Ser. B Biol. Sci.* 149, 82–101. doi: 10.1098/rspb.1958.0053

Teuscher, F., Brockmann, G. A., Rudolph, P. E., Swalve, H. H., and Guiard, V. (2000). Models for chromatid interference with applications to recombination data. *Genetics* 156, 1449–1460. doi: 10.1093/genetics/156.3.1449

Vrielynck, N., Chambon, A., Vezon, D., Pereira, L., Chelysheva, L., De Muyt, A., et al. (2016). A DNA topoisomerase VI – like complex initiates. *Science* 351, 939–944. doi: 10.1126/science.aad5196

Wang, S., Zickler, D., Kleckner, N., and Zhang, L. (2015). Meiotic crossover patterns: obligatory crossover, interference and homeostasis in a single process. *Cell Cycle* 14, 305–314. doi: 10.4161/15384101.2014.991185

Wang, Y., and Copenhaver, G. P. (2018). Meiotic recombination: mixing it up in plants. *Annu. Rev. Plant Biol.* 69, 577–609. doi: 10.1146/annurev-arplant-042817-040431

Wijnker, E., James, G. V., Ding, J., Becker, F., Klasen, J. R., Rawat, V., et al. (2013). The genomic landscape of meiotic crossovers and gene conversions in Arabidopsis thaliana. *Elife* 2013:e01426. doi: 10.7554/eLife.01426.020

Zhao, H., McPeek, M. S., and Speed, T. P. (1995). Statistical analysis of chromatid interference. *Genetics* 139, 1057–1065. doi: 10.1093/genetics/139.2.1057

Conflict of Interest: The authors declare that the research was conducted in the absence of any commercial or financial relationships that could be construed as a potential conflict of interest.

frontiers in Plant Science

REVIEW
published: 31 March 2021
doi: 10.3389/fpls.2021.659558

The Role of Structural Maintenance of Chromosomes Complexes in Meiosis and Genome Maintenance: Translating Biomedical and Model Plant Research Into Crop Breeding Opportunities

Pablo Bolaños-Villegas[1,2]*

[1]Fabio Baudrit Agricultural Research Station, University of Costa Rica, Alajuela, Costa Rica, [2]Lankester Botanical Garden, University of Costa Rica, Cartago, Costa Rica

OPEN ACCESS

Edited by:
Mónica Pradillo, Complutense University of Madrid, Spain

Reviewed by:
Veit Schubert, Leibniz Institute of Plant Genetics and Crop Plant Research (IPK), Germany
Stefanie Dukowic-Schulze, University of Regensburg, Germany

***Correspondence:**
Pablo Bolaños-Villegas
pablo.bolanosvillegas@ucr.ac.cr

Specialty section:
This article was submitted to Plant Cell Biology, a section of the journal Frontiers in Plant Science

Received: *27 January 2021*
Accepted: *15 March 2021*
Published: *31 March 2021*

Citation:
Bolaños-Villegas P (2021) The Role of Structural Maintenance of Chromosomes Complexes in Meiosis and Genome Maintenance: Translating Biomedical and Model Plant Research Into Crop Breeding Opportunities. Front. Plant Sci. 12:659558. doi: 10.3389/fpls.2021.659558

Cohesin is a multi-unit protein complex from the structural maintenance of chromosomes (SMC) family, required for holding sister chromatids together during mitosis and meiosis. In yeast, the cohesin complex entraps sister DNAs within tripartite rings created by pairwise interactions between the central ring units SMC1 and SMC3 and subunits such as the α-kleisin SCC1 (REC8/SYN1 in meiosis). The complex is an indispensable regulator of meiotic recombination in eukaryotes. In *Arabidopsis* and maize, the SMC1/SMC3 heterodimer is a key determinant of meiosis. In *Arabidopsis*, several kleisin proteins are also essential: SYN1/REC8 is meiosis-specific and is essential for double-strand break repair, whereas AtSCC2 is a subunit of the cohesin SCC2/SCC4 loading complex that is important for synapsis and segregation. Other important meiotic subunits are the cohesin EXTRA SPINDLE POLES (AESP1) separase, the acetylase ESTABLISHMENT OF COHESION 1/CHROMOSOME TRANSMISSION FIDELITY 7 (ECO1/CTF7), the cohesion release factor WINGS APART-LIKE PROTEIN 1 (WAPL) in *Arabidopsis* (AtWAPL1/AtWAPL2), and the WAPL antagonist AtSWITCH1/DYAD (AtSWI1). Other important complexes are the SMC5/SMC6 complex, which is required for homologous DNA recombination during the S-phase and for proper meiotic synapsis, and the condensin complexes, featuring SMC2/SMC4 that regulate proper clustering of rDNA arrays during interphase. Meiotic recombination is the key to enrich desirable traits in commercial plant breeding. In this review, I highlight critical advances in understanding plant chromatid cohesion in the model plant *Arabidopsis* and crop plants and suggest how manipulation of crossover formation during meiosis, somatic DNA repair and chromosome folding may facilitate transmission of desirable alleles, tolerance to radiation, and enhanced transcription of alleles that regulate sexual development. I hope that these findings highlight opportunities for crop breeding.

Keywords: meiosis, structural maintenance of chromosomes, cohesin, DNA recombination, food security, stress tolerance

INTRODUCTION

Our species faces a vexing problem. In the past, agricultural production kept pace with a growing population. However, by the year 2050, crop production will no longer meet demand. Increased consumption of meat and dairy in the developing world is worsened by biofuel production, depletion of water resources, and global warming. Thus, breeding of new varieties is key to boosting yields and matching future demand (Scheben and Edwards, 2018).

Global warming is often mentioned because of its negative effect on rainfall, but anthropogenic climate change is also believed to progressively suppress cloud formation, thus increasing exposure to UVB radiation (320–290 nm; Diffey, 2002; Lindfors and Arola, 2008; Schneider et al., 2019). The Food and Agriculture Organization of the United Nations has well-documented the reduced crop yield and total dry weight resulting from enhanced exposure to UVB radiation in the field for crops such as rice (*Oryza sativa* L., Poaceae), soybean (*Glycine max* L., Fabaceae), corn (*Zea mays* L., Poaceae), potatoes (*Solanum tuberosum* L., Solanaceae), pea (*Pisum sativum* L., Fabaceae), and sugar cane (*Saccharum officinarum* L., Poaceae; Krupa and Jäger, 2006). Exposure to a high dose of UVB radiation in C3 and C4 species exacerbates sensitivity to drought by reducing leaf conductance, water use efficiency, and leaf area. It also decreases floral yield, fruit set, and fruit yield (Krupa and Jäger, 2006). When combined with increased atmospheric CO_2, UVB radiation worsens crop performance (Wijewardana et al., 2016). Depletion of atmospheric ozone (O_3) and the anthropogenic release of atmospheric aerosols such as nitrogen oxides can also alter surface UV flux by their distribution in the atmospheric column (Erickson et al., 2015), which adds a layer of complexity to an already difficult scenario of climate instability.

In plants, the two major products of UVB damage are cyclobutene pyrimidine dimers and pyrimidine pyrimidone photoproducts, which are mostly repaired by cyclobutene pyrimidine dimers and 6–4 photolyases (Sakamoto, 2019). Also, extensive evidence indicates that nucleotide excision repair plays an important role in removing damage caused by UV radiation (Nisa et al., 2019; Sakamoto, 2019). However, UV radiation is also toxic because it distorts the template structure of DNA and prevents replication (Kim et al., 2019; Sakamoto, 2019). In turn, these stalled replication sites create fragile single-strand regions that easily lead to highly toxic double-strand breaks (DSBs; Nisa et al., 2019; Sakamoto, 2019). DSBs are repaired by translesion synthesis with the help of a translesion synthesis polymerase or by template switch and homologous recombination. The latter process relies on PROLIFERATING CELL NUCLEAR ANTIGEN (PCNA) polyubiquitination, the combined action of RAD51 and BRCA1 (Kim et al., 2019; Nisa et al., 2019; Sakamoto, 2019) and activity of the cohesin complex (Bolaños-Villegas et al., 2013).

Another serious genotoxic stress that affects output in crops such as rice and barley is the soil content of aluminum (Al; Awasthi et al., 2017; Jaskowiak et al., 2018), especially in acidic soils such as in India (Awasthi et al., 2017). In such soils (pH < 5.5), Al solubilizes into the phytotoxic species Al^{3+} from non-toxic silicates and oxides (Awasthi et al., 2017; Sjögren and Larsen, 2017). In flooded fields, the presence of Al^{3+} leads to an increase in soluble Fe^{2+} content, also leading to iron toxicity (Awasthi et al., 2017). The most severe symptoms of Al toxicity are rapid inhibition of root elongation caused by damage in cells at the root apex and reduction in crop yield by 20–40% (Panhwar et al., 2015; Awasthi et al., 2017). In barley roots, exposure to Al^{3+} causes the formation of micronuclei and apoptosis (Jaskowiak et al., 2018). Flow cytometry also revealed a delay in cell division, as evidenced by an increase in frequency of cells in the G2/M phase (Jaskowiak et al., 2018). Exposure to Al^{3+} in *Arabidopsis* causes roots to undergo DNA damage that requires homologous recombination and the expression of the cohesin subunit *SYN2* (Sjögren and Larsen, 2017).

The goal of this review is to summarize evidence related to the plant cohesin complex involved in genome maintenance and meiosis. The summary aims to help breeding elite cultivars that will be better adapted to cope with marginal environmental conditions and climate change (Panhwar et al., 2015; Shen et al., 2015), whose crop yields will be high enough to cope with population growth (Gerland et al., 2014), and that may transmit and receive valuable wild alleles efficiently (Dempewolf et al., 2017). The overall aim is to guarantee food security. Of particular interest in modern agriculture is the control of crossover (CO) formation during meiosis, because the low frequency and uneven patterning of COs has traditionally required breeders to work with large populations over many generations to produce desirable haplotypes (Taagen et al., 2020). Fortunately, genome sequencing and advanced genome editing by CRISPR-Cas9 in rice (Li et al., 2020) and maize (Zhang et al., 2020) may enable the translation of knowledge obtained in humans, yeast and *Arabidopsis thaliana*.

ASSEMBLY OF EUKARYOTIC COHESION AND STRUCTURAL MAINTENANCE OF CHROMOSOMES COMPLEXES

Cohesin is an evolutionarily conserved protein complex, believed to assemble as a tripartite ring, that wraps around DNA and modulates its topology (Muñoz et al., 2019). It has a broad range of functions that affect the organization of the eukaryotic genome. The functions include somatic repair of DNA DSBs, regulation of pericentromeric recombination during meiosis I, regulation of transcription, and establishment of sister chromatid cohesion (Fernandes et al., 2019; Muñoz et al., 2019). Biochemical and genetic evidence with baker's yeast suggest that the canonical cohesin complex contains two structural maintenance of chromosomes (SMC) proteins, SMC1 and SMC3; one α-kleisin subunit named SCC1/RAD21 (mitotic) or REC8/SYN1 (meiotic; Beckouët et al., 2016; Hsieh et al., 2020); and two additional HEAT repeat-containing subunits named SCC3 and PRECOCIOUS DISSOCIATON OF SISTERS 5 (PDS5; Liu et al., 2020). The two SMC proteins assemble as antiparallel coiled coils 50 nm long, with two key features: (1) a hinge domain at one end (N-terminal) and (2) an ABC-like ATPase domain (C-terminal) at the head (Beckouët et al., 2016).

Cohesin stably prevents the sister chromatids from DNA replication until anaphase (G2 to M phases; Elbatsh et al., 2016). In human cells, the loader complex MAU2-NIPBL (SCC2/SCC4 in yeast) loads DNA into the cohesin complex, whereas the activity of the antagonist WINGS APART LIKE (WAPL) releases cohesin from DNA (Faramarz et al., 2020) by opening an exit gate located between SMC3 and the N-terminus of the SCC1 α-kleisin (Elbatsh et al., 2016; Haarhuis et al., 2017). Loading of cohesin by the SCC2/SCC4 loader complex involves stimulation of ATP hydrolysis by the SMC1/SMC3 ATPase domain, which is required for the stable association of cohesin with chromatin (Elbatsh et al., 2016).

Cohesin may also dissociate from chromatin at anaphase by cleavage of the SCC1 α-kleisin by the separase (ESP), whereas at other stages of the cell cycle, the release of cohesin is mediated by WAPL and the HEAT-repeat subunit PDS5 (Dauban et al., 2020). Repression of cohesion release is enforced during replication by acetylation of two conserved lysine residues within the ATP-ase domain of SMC3, an action performed by ECO1 and assisted by PDS5 (see **Table 1**; Yang et al., 2019; Dauban et al., 2020). This process stabilizes the entrapment of DNA by cohesin and establishes sister chromatid cohesion throughout the G2 to M phases until cleavage of SCC1 by the separase and deacetylation of SMC3 by HOS1 (Dauban et al., 2020; see **Figure 1**).

According to the multi-state asymmetric ATPase cycle, the three known SMC complexes – cohesin SMC1/SMC3, condensin SMC2/SMC4, and SMC5/SMC6 complexes – have a ground state known as the nucleotide-free state, in which only one SMC head can bind to an ATP molecule. Upon binding of the first ATP molecule to the P-loop of the RecA lobe, the glutamine residue in the Q-loop changes its position and establishes hydrogen bonds with γ-phosphate and with an Mg^{2+} ion. As a result, the helical lobe tilts by 15°, repositions a tyrosine-lysine pair within the W-loop and causes dissociation of PDS5 from SMC1 (its SMC4 counterpart is YCS4; Hassler et al., 2019). Binding of a second ATP molecule causes the formation of a quasi-symmetric SMC1/SMC3 (or SMC2/SMC4) head dimer with both RecA active sites occupied by ATP molecules and induces the coiled-coils of SMC1 (or SMC2) to spread apart and dissociate from the SCC1 kleisin (BRN1 in the yeast condensin complex). This model implies that the structural transitions in SMC complexes are governed by nucleotide release, as observed in other ABC-type ATPases. It hints at the existence of directionality in the translocation of the SMC holocomplexes along the DNA double helix (Hassler et al., 2019). In plants, these results should be validated to develop a better understanding of the torsion of the W-loop of SMC1 and how it controls the dissociation of cofactors such as PDS5 during plant meiosis, for instance. Such validation might also open avenues for engineering changes in the rate of ATP-hydrolysis to cope with faster structural transitions under chronic DNA damage stress (see **Table 1**).

ENGINEERING OF COHESION, SUPERCOILING, AND CELL CYCLE PROGRESSION

During DNA replication in yeast, instead of entrapping just one DNA molecule, cohesin holds together two sister DNAs (Liu et al., 2020). Experimental evidence in yeast strain W303 suggests that this might be achieved in two ways: (1) the replisome is able to replicate through cohesin rings or (2) cohesin transiently loses contact with DNA and is reloaded behind the replication fork. In addition to the essential ECO1 acetyltransferase, several other non-essential replisome components contribute to the establishment of sister chromatid cohesion, such as the downstream Ctf18-replication factor-C (Ctf18-RFC) complex. Ctf18-RFC is a member of the RFC group, which are complexes of pentameric AAA^+ ATPases that load and unload PCNA sliding clamps and function as DNA-replication checkpoint factors. PCNA is involved in a wide array of DNA functions, mostly as a processivity factor for DNA polymerases but also as a docking platform for other proteins, possibly including ECO1. Yeast cells lacking the Ctf18 subunit show impaired SMC3 acetylation (K112 and K113) as well as cohesion defects. Notably while these defects are reversed by deletion of the PCNA unloader ELG1-RFC, the DNA replication checkpoint response only worsens (Liu et al., 2020). In *Arabidopsis*, *CTF18* may have a role in the establishment of cohesion and plant growth but not in somatic DNA repair (Takahashi et al., 2010). New alleles may need to be developed by CRISPR-Cas9 to fully characterize the function of *CTF18* in plants. The maize *SMC3* homolog has been successfully characterized with genome editing by CRISPR-Cas9 (Zhang et al., 2020). The homolog fulfills a crucial role during the establishment of centromeric pairing during meiosis and sister chromatid cohesion during mitosis (in root tips; Zhang et al., 2020). So, maize might be amenable to the study of SMC3 acetylation dynamics during meiosis and mitosis and perhaps lead to the discovery of novel phenotypes.

In yeast, a mechanism that links DNA replication and SMC3 acetylation has been characterized (Liu et al., 2020). CTF18 works upstream of SMC3 acetylation by facilitating loading of PCNA onto the leading strand, where it can face ECO1/CTF7 during the late stages of DNA replication, possibly by stimulating interaction at the PCNA interacting peptide (PIP) box of ECO1/CTF7 (QxxLxxFF; Moldovan et al., 2006; Liu et al., 2020). As a result, ECO1/CTF7 becomes well-placed behind the replication fork, where it can better acetylate freshly deposited cohesin, which causes both sister DNA molecules to become embraced by cohesin (see **Table 1**; Liu et al., 2020; see **Figure 1**). The cohesion defects present in yeast *ctf18* cells can be overcome by the *wapl* allele (Liu et al., 2020; **Table 1**), a result also observed in *Arabidopsis ctf7/wapl* mutants (De et al., 2016). Hence, in plants, weak *wapl* alleles may facilitate cohesion under replicative stress, although fertility may be compromised (De et al., 2016). Fusion of the PIP box to the PCNA also restores growth in the presence of $ECO1^{-pip}$ (Liu et al., 2020). Comparison of DNA repair efficiencies and plant growth in *wapl* mutants and plants engineered to carry new PCNA-ECO1 modules may be an interesting research topic in plants exposed to chronic DNA damage, including crops exposed to high doses of UVB radiation such as high-altitude maize (Rius et al., 2016) or plants grown in the aluminum-rich, acidic soils of most developing countries (Chen et al., 2019b).

TABLE 1 | Selection of cohesin/SMC genes and cofactors with potential for inclusion in breeding initiatives in major crops.

SMC gene and associated factors	Functional features in the literature and public databases[1,2]	Locus ID as determined by TAIR, NCBI, and the Human Genome Organization (HUGO)[5]	Presumed homologs of interest (rice and maize) retrieved from databases[3,4,6] by the respective coding sequences (CDS)	Likely agricultural use
Arabidopsis HORMA-domain protein *ASYNAPTIC 1* (*ASY1*)	Distribution of COs along meiotic chromosomes in a REC8/SYN1 dependent manner	*At1g67370*	*Os09g32930*, *GRMZM2G035996*	Knockdown alleles may reduce linkage drag in major crops
Human cohesin interacting factors *BRG1*/*SMARCA4* and *ARID2* (SWI/SNF subunits)	Cohesin-mediated repression of transcriptional activity, genome maintenance	*HGNC:6597* and *HGNC:196528*	*Os05g05230*, *GRMZM2G102625*, *Os07g33860*, *GRMZM2G009412*	Promotion of seed longevity, intentional induction of inversions and translocations
Human ATP-dependent DNA helicase *DEAD/H-box helicase 11* (*DDX11*)	Synthetically lethal with human *ECO1* homolog *ESCO2* (*HGNC:27230*) and epistatic to human *WAPL* (*HGNC:23293*). Promotes cohesion in arms and centromeres during replication, probably by promotion of SMC3 acetylation, and enhanced stability of replication forks	*HGNC:1663*	*Os05g13300*, *GRMZM2G100067*	Promotion of replication fork stability. May constitute an important layer of genome maintenance under stress across all eukaryotes
Arabidopsis N-acetylase *ECO1/CTF7*	Acetylation of the ATP-ase domain of SMC proteins, establishment of cohesion, homology-dependent DNA repair. Its function is antagonized by *WAPL*	*At4g31400*	*Os05g31230*, *GRMZM2G100067*; and *Os04g42120*, *GRMZM2G075145*	Prevention of large-scale rearrangements, targeted manipulation of chromosome folding during MSUC and MSCI in meiocytes of papaya, gene expression.
Yeast chromatin-remodeling ATPase *ISW1*/*YBR245C*	Cohesin-dependent processes such as DNA repair and transcription in promoters	*SGD:S000000449*	*Os03g22900*, *GRMZM2G469162*	May stabilize transcription under stress across eukaryotic organisms
Cohesin subunit *PRECOCIOUS DISSOCIATION OF SISTERS 5* (*PDS5A/E*)	Cohesion-promoting cofactor; has a role in fork protection and stable DNA replication	*At5g47690*, *At1g77600*, *At4g31880*, *At1g80810*, and *At1g15940*	For *PDS5A*: *Os06g17840*, *GRMZM2G010637*	May stabilize DNA replication under stress, may be a target for the manipulation of DNA looping and chromosome folding during MSUC and MSCI in meiocytes of papaya
Arabidopsis SCC2	Initial CO formation during meiosis, 3D-chromosome folding, loading of cohesin complexes, chromosome looping and DNA repair	*At5g15540*	*Os07g01940*, *GRMZM2G132504*, *Carica papaya evm.model. supercontig_2744.1*	Promotion of crossover resolution, targeted manipulation of chromosome folding during MSUC and MSCI in meiocytes of papaya
Arabidopsis SCC3	Regulates release of α-kleisins. Regulates meiotic orientation of kinetochores in *Arabidopsis*, and may have a role in the prevention of large-scale rearrangements during replication, dimerization of cohesin, and chromosome looping	*At2g47980*	*Os05g09620*, *GRMZM2G131443*	May prevent chromosomal rearrangements during replication, in plants, it may provide a valuable layer of genome maintenance under stress
Maize *SCC4/DEK15*	Mitotic chromosome segregation, endosperm and embryo formation, transcriptional regulation of kernel development in maize	*GRMZM2G079796*	*Os04g28010*	Promotion of embryo and endosperm development
Arabidopsis condensin subunit *STRUCTURAL MAINTENANCE OF CHROMOSOMES 4* (*SMC4*)	Silencing of pericentromeric TEs, DNA methylation, transcription of genes related to translesion synthesis, male gamete development, tolerance to Boron toxicity	*At5g48600*	*Os05g41750*, *GRMZM2G416501*	May lead to enhanced tolerance to exogenous DNA damage, and improved genome maintenance in crops

(Continued)

TABLE 1 | Continued

SMC gene and associated factors	Functional features in the literature and public databases[1,2]	Locus ID as determined by TAIR, NCBI, and the Human Genome Organization (HUGO)[5]	Presumed homologs of interest (rice and maize) retrieved from databases[3,4,6] by the respective coding sequences (CDS)	Likely agricultural use
Arabidopsis EXTRA SPINDLE POLES (*AESP1*), Separase	Cleavage of the REC8/SYN1 α-kleisin during anaphase I and anaphase II, allowing disjunction of homologs and sister centromeres, respectively. Proper assembly of radial microtubule system after telophase II, embryo development, cellularization of the endosperm, and vesicle trafficking	*At4g22970*	*Os02g53120*, *GRMZM2G300624*	Promotion of crossovers resolution and proper tetrad formation. May facilitate breeding of fertile cultivars in major crops
Arabidopsis SWITCH1/DYAD (*SWI1*)	Sister chromatid cohesion and meiotic chromosome organization, assembly of the chromosome axis	*At5g51330*	Known as *AMEIOTIC* (*OsAM1*) in rice: *Os03g44760*, and *AMEIOTIC* (*AM1*) in maize (possibly *GRMZM5G883855*)	May facilitate the identification of new alternative meiotic α-kleisins in crops
Arabidopsis WINGS APART-LIKE PROTEIN 1 (*WAPL1/2*)	Release of meiotic α-kleisin REC8/SYN1 during prophase I. Cohesin removal by WAPL is required to complete DNA synthesis under conditions of persistent DNA replication stress. Regulates chromosome folding	*At1g11060* and *At1g61030*	*Os10g35380*, *GRMZM2G034276*; *Os10g35380*, *GRMZM2G034276*	New alleles may facilitate DNA replication under persistent damage. May confer tolerance to chronic DNA damage in crops

MSUC, meiotic silencing of unsynapsed chromatin; MSCI, meiotic sex chromosome inactivation; TE, transposable elements.
[1]*Database consulted was The Arabidopsis Information Resource (TAIR): https://www.arabidopsis.org/.*
[2]*Database consulted was National Center for Biotechnology Information (NCBI): https://www.ncbi.nlm.nih.gov/.*
[3]*Database consulted was Phytozome v12.1: https://phytozome.jgi.doe.gov/pz/portal.html.*
[4]*Database consulted was Maize GDB: https://www.maizegdb.org/.*
[5]*Database consulted was the Human Genome Organization (HUGO): http://www.hugo-international.org/.*
[6]*Database consulted was the Rice Genome Annotation Project: http://rice.plantbiology.msu.edu/cgi-bin/gbrowse/rice/.*

PATHWAYS TO ACHIEVE ROBUST TRANSCRIPTION DURING PLANT MITOSIS AND MEIOSIS: NEW ROLES FOR COHESINS AND SMC5/SMC6 COMPLEXES

In addition to its role in establishing sister chromatid cohesion, the cohesin complex is also believed to mediate transcription, and it is recruited to sites of DNA DSBs to promote repair during the S and G2 phases of the cell cycle (Dorsett and Ström, 2012; Meisenberg et al., 2019). In response to a DNA DSB, eukaryotic cells usually respond by repressing transcriptional activity in neighboring chromatin. This pathway depends on the ATAXIA-TELANGIECTASIA MUTATED (ATM) kinase and involves the activity of chromatin remodeling complexes of the SWItch/sucrose non-fermentable (SWI/SNF) family that ubiquitylate H2AK119 at sites of damage. Recently, cohesin was found required for the activity of SWI/SNF complexes after DNA damage, mainly at centromeres. Repression of transcription by subunits BRG1 and ARID2 of the mammalian PBAF complex (a SWI/SNF complex; see **Table 1**) contributed to genome stability by preventing the formation of large-scale rearrangements during the S, G1, and G2 phases in the prostate cancer cell line LNCaP (Meisenberg et al., 2019). This novel function may not depend on the presence of a sister chromatid and may operate differently from non-homologous end joining or homologous repair. Cohesin may loop DNA in areas flanking the break to reorganize the chromosome. This situation may prevent transcription and remove the broken DNA end from the vicinity of other actively transcribed genes to prevent misrepair (Meisenberg et al., 2019). Notably, subunit SA2 (SCC3) and ECO1 are crucial for this process (see **Table 1**), but WAPL is dispensable (Meisenberg et al., 2019), which suggests that in human cells, SA2/SCC3 is a true tumor suppressor gene. In yeast, the activity of SCC3 is required for the release of the mitotic α-kleisin SCC1 (known as SYN2 and SYN4 in *Arabidopsis*), while during meiosis in *Arabidopsis*, the activity of *Arabidopsis* SCC3 is essential for the proper orientation of kinetochores (Chelysheva et al., 2005; Yuan et al., 2014; Beckouët et al., 2016). Further research could investigate whether SCC3 might also have a role in preventing rearrangements during the mitotic and meiotic S-phase.

To our knowledge, this SWI/SNF and SCC3-mediated mechanism of preventing large-scale re-arrangements has not been characterized in *A. thaliana* or in crops such as rice or maize and might constitute an entirely new system of DNA

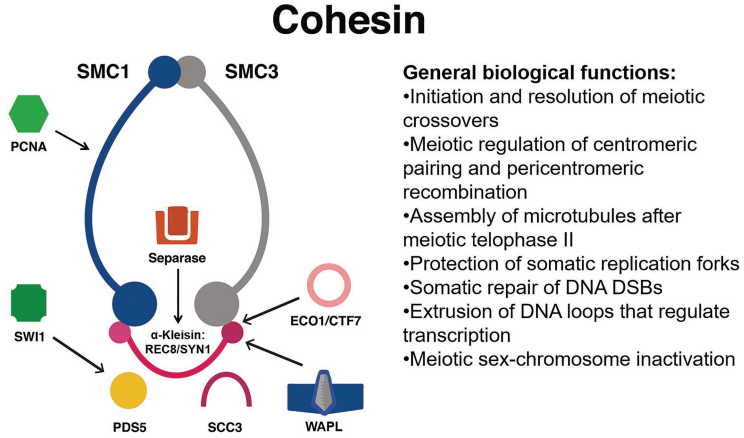

FIGURE 1 | Simplified interaction network between the eukaryotic structural maintenance of chromosomes (SMC) cohesin complex and its functional partners. The plant cohesin complex is proposed to be a ring that stably entraps DNA molecules and facilitates meiotic recombination, centromeric pairing, protection of replication forks, extrusion of chromatin loops, and inactivation of sex chromosomes. These processes are facilitated by locking and unlocking of the ring *via* the simultaneous activity of promoters of cohesion ECO1/CTF7, PDS5, and SWITCH1 (SWI1). Other particularly important factors are PCNA, which facilitates DNA repair and operates as a docking platform for ECO1/CTF7, and cohesin dissociating factors that facilitate dislodging or degradation of the kleisin such as Separase and SCC3 or competitors of PDS5 such as WAPL. Not shown: CTF18. ECO1/CTF7, ESTABLISHMENT OF COHESION 1/CHROMOSOME TRANSMISSSION FIDELITY 7, a N-terminal acetyltransferase; DSB, double-strand break; PCNA, PROLIFERATING CELL NUCLEAR ANTIGEN; PDS5, PRECOCIOUS DISSOCIATION OF SISTERS, a HEAT-repeat protein; REC8, RECOMBINATION PROTEIN 8, a meiotic α-kleisin also known as SYNAPTIC 1 and often abbreviated as REC8/SYN1. The yeast mitotic α-kleisin is known as SCC1, SISTER CHROMATID COHESIN 1, which in the Arabidopsis genome is represented by two *bona fide* orthologs known as SYN2 and SYN4; although a fourth α-kleisin unique to plants called SYN3 is important for both meiosis and mitosis. WAPL, WINGS APART LIKE, a cohesin dissociation factor.

repair that may lead to far-reaching discoveries in plant developmental biology and plant breeding. For instance, genome maintenance is crucial for seed longevity (Waterworth et al., 2019), so this topic seems promising in plant breeding and plant science because it may allow for the engineering of ultra-long seed storage.

Coincidentally, the activity of the SMC5/SMC6 complex is crucial for successful maintenance of the genome during interphase in cancer (HCT116) and immortalized non-cancer cells (RPE1; Venegas et al., 2020). DNA damage is increased in cells deficient in SMC5/SMC6 function that are stained with the DNA damage marker γ-H2AX, which suggests that SMC5/SMC6 is required for proper homologous recombination. Also during the S-phase, activity of the SMC5/SMC6 complex is required to prevent fragmentation of chromosomes later on during anaphase (Venegas et al., 2020). This second requirement might be linked to the role of the SMC5/SMC6 subunit NON-SMC ELEMENT2 (NSE2) during SUMOylation of topoisomerase IIα (Venegas et al., 2020). In general, the activity of the SMC5/SMC6 complex could be a target for plant breeding, specifically for selecting seed longevity and smooth endosperm proliferation. The *Arabidopsis* genome contains one SMC5 and two SMC6 homologs (SMC6A/B) as well as two γ-kleisins, NON-SMC ELEMENT4 A/B (NSE4A/B), and five other NSE subunits (see **Figure 2**). Their combined activity is required for proper seed development and for efficient homologous recombination in somatic tissues (Watanabe et al., 2009; Díaz et al., 2019; Zelkowski et al., 2019). Functional characterization of NSE4A/B indicates that their activity is required for pollen development, tolerance to the radiomimetic agent Bleomycin, proper chromosome segregation during meiosis, and proper assembly of the synaptonemal complex (Hesse et al., 2019; Zelkowski et al., 2019). The association between the SMC5/SMC6 complex, topoisomerase IIα, and prevention of mitotic chromosome fragmentation has not been functionally characterized in crops.

THE ROLE OF SMC COMPLEXES IN DNA REPAIR: OPPORTUNITIES FOR ENGINEERING TOLERANCE TO DNA DAMAGE

In humans, chronic DNA replication stress is a source of generalized DNA damage and a hallmark of cancer (Macheret and Halazonetis, 2015; Minchell et al., 2020), but in plants, little is known about the impact of chronic DNA replication stress or chronic DNA damage. Work in *Arabidopsis* suggests that a low dose of gamma radiation (2000 μGy h^{-1} for 54 days) is enough to reduce plant growth by 50% (Vandenhove et al., 2010). Exposure to a high dose (200 Gy) at the early reproduction stage (33 days after sowing) led to a robust increase in the expression of genes for homologous DNA repair, such as *PROLIFERATING CELL NUCLEAR ANTIGEN 1/2* (*PCNA1/2*, At1g07370, and At2g29570) and *POLY(ADP-RIBOSE) POLYMERASE 2* (*PARP2*, At4g02390; Kim et al., 2007). In *P. sativum*, seedlings irradiated with 0.4–10 Gy showed reduced

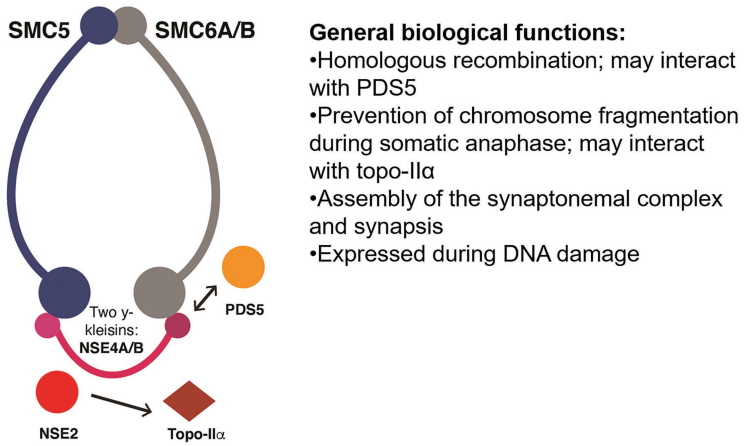

FIGURE 2 | Simplified functional interaction network of the SMC5/SMC6 complex in genome maintenance, homologous recombination, and meiosis. These SMC complexes interact with PDS5 during homologous recombination and have an especially important role during meiotic synapsis as well as somatic chromosome segregation. These complexes may also be required for proper somatic DNA repair *via* the SUMOylation of topoisomerase IIα by associated protein NSE2. NSE proteins have a wide variety of functions that affect pollen development and homologous DNA repair. Topo-IIα, topoisomerase-IIα.

pod set by 20–40%, but with >10 Gy, they were no longer able to flower. At all doses, male meiotic tetrad formation was defective, as evidenced by the formation of micronuclei at a rate of 10%. All F_2 plants from irradiated F_1 individuals showed reduced pod set and a significant formation of meiotic micronuclei (Zaka et al., 2004). Evidence in yeast suggests that DNA damage related to DNA replication is prevalent within genomic contexts that are not conducive to normal progression of the replication fork. Structures that block free rotation of DNA also cause accumulation of topological stress and exceed the relaxation activity of topoisomerases. Impaired progression of the replication fork caused by topological stress may lead to fork reversal, to stabilize an arrested fork, or to fork rotation that transforms overwinding ahead of the fork into precatenates behind the replication fork and thus allow elongation without intervention by topoisomerases (Minchell et al., 2020). Thus, further study is needed to understand how to facilitate replication while reducing topological stress and damage, possibly as a strategy to assist plant growth at critical moments such as during cotyledon emergence and seed ripening.

Work in budding yeast indicates that centromeres, telomeres, long terminal repeat sites, replication origins, and rDNA repeats consistently accumulate DNA damage, as seen by enrichment of γ-H2AX on ChIP-chip experiments (Szilard et al., 2010). In budding yeast, the cohesin complex promotes genome stability following replication stress, especially during the S phase when it is preferentially loaded onto centromeres and rDNA sites (Frattini et al., 2017; Minchell et al., 2020). However, paradoxically, the cohesin complex could also represent a large barrier to the diffusion of topological stress by preventing free rotation of DNA (Minchell et al., 2020). In fact, depletion of SCC1 in topoisomerase IIα-depleted yeast cells (strain W303-1a) suppresses the accumulation of γ-H2AX across centromeres and rDNA sites, whereas depletion of ECO1/CTF7 partially reduces γ-H2AX accumulation in centromeres. Surprisingly, depletion of the condensin SMC2 subunit reduces the abundance of the γ-H2AX mark in rDNA, which suggests that both SMC holocomplexes affect the accumulation of DNA damage following topological stress, perhaps as a mechanism to prevent ectopic recombination in rDNA sites and maintains the bi-orientation of centromeres stress (Minchell et al., 2020). In fact, use of the yeast mini-chromosomes YCp50 and YRp21 has shown that inactivation of *SMC2* leads to increased formation of DNA knots generated by the activity of topoisomerase IIα, possibly by affecting condensin-mediated loop extrusion (Dyson et al., 2021; see **Table 1**). This type of work has not been validated in plants, but double or triple mutants might be obtained in *Arabidopsis*. If so, the impact of increased topological stress in centromeres during replication could be determined by characterizing alleles that might make the process more robust during plant meiosis and mitosis.

In human cells, the super family 2 (SF2) helicase DEAD/H-box helicase 11 (DDX11, named Chl1 in budding yeast) is synthetically lethal with ESCO2, and knockdown of WAPL partially restored cohesion defects in DDX11-deficient cells (see **Table 1**). In humans, loss of DDX11 activity causes the cohesion syndrome Warsaw Breakage syndrome, whereas loss of ESCO2 causes Roberts syndrome. DDX11 interacts with several replication factors, such as PCNA, the 5'-flap endonuclease Flap Structure-Specific Endonuclease 1 (FEN1), the fork protection complex subunit Timeless, and CTF4, which links the activity of the Minichromosome Maintenance Protein Complex (MCM) helicase with DNA polymerases (Faramarz et al., 2020). DDX11 is believed to specialize in resolving DNA structures such as forked duplexes, 5′-flap duplexes, and anti-parallel G-quadruplexes, therefore, promoting replication fork

progression (Faramarz et al., 2020). DDX11 may promote the establishment of cohesion in three ways: (1) subtle promotion of SMC3 acetylation, (2) promotion of cohesin activity by facilitating second-strand capture, and (3) enhanced overall replication fork stability (see **Figure 3**). Rescue of cohesion in *DDX1*-deficient cells by knockdown of *WAPL* suggests that the helicase may facilitate chromatid cohesion in arms and centromeres (Faramarz et al., 2020). Once again, promotion of cohesion occurs in *ddx1* and *wapl* mutants could be tested in *Arabidopsis* or in crops such as rice and maize, as well as whether this genetic interaction may protect against chronic DNA damage (see **Table 1**).

In budding yeast, a strong link has also been observed between the establishment of cohesion, replicative stress during the S-phase, and nuclease activity by the Mre11-Rad50-Xrs2/Nbs1 (MRX/N) complex. Several other factors may participate as well, such as the histone remodelers Chd1 and Isw1. Collapse of replication forks and replication resumption requires extensive processing of stalled forks by DNA helicases, endo- and exonucleases, and recombinases. Of great importance for this process is the activity of the MRX/N complex, which is known for its role in repair of DSBs. At DNA DSBs, the endo- and exonuclease catalytic activity of MRE11 generates gaps seen as short single-strand DNAs that are then extended by the Exo1 nuclease or the Sgs1 complex. Under replication stress conditions, the MRX/N complex facilitates repair *via* recombination of damaged forks by resecting available nascent DNA strands. In budding yeast, the MRX/N complex promotes recruitment of cohesin to stalled forks to facilitate sister-chromatid recombination required for fork restart (Delamarre et al., 2020; see **Figure 3**). The exact mechanism by which the complex promotes the loading of cohesin to stalled forks is currently unknown (Delamarre et al., 2020), and their precise role in establishing cohesion in plants is ignored. In *Arabidopsis*, *mre11* mutants show chromosomal fragmentation during mitosis and meiosis and do not exhibit synapsis during meiosis. Plants are small, misshapen, and sterile (Puizina et al., 2004). Facilitating fork restart under active transcription might prove valuable to guarantee and boost growth in quickly developing tissues and organs such as flowers, fruits, and grains. Novel gain-of-function alleles may need to be developed in *Arabidopsis* and crops.

In yeast, the DSB processing activity of the MRX complex leads to the formation of excess single-strand DNA coated with replication protein A (RPA), which triggers the recruitment of the Mec1 kinase (ATAXIA-TELANGIECTASIA AND RAD3-RELATED, ATR in *Arabidopsis*; Bourbousse et al., 2018; Delamarre et al., 2020). In *Arabidopsis*, analysis of γ-H2AX foci in *mre11* and *rad50* mutants suggested that DNA damage signaling in these plants is ATR-dependent,

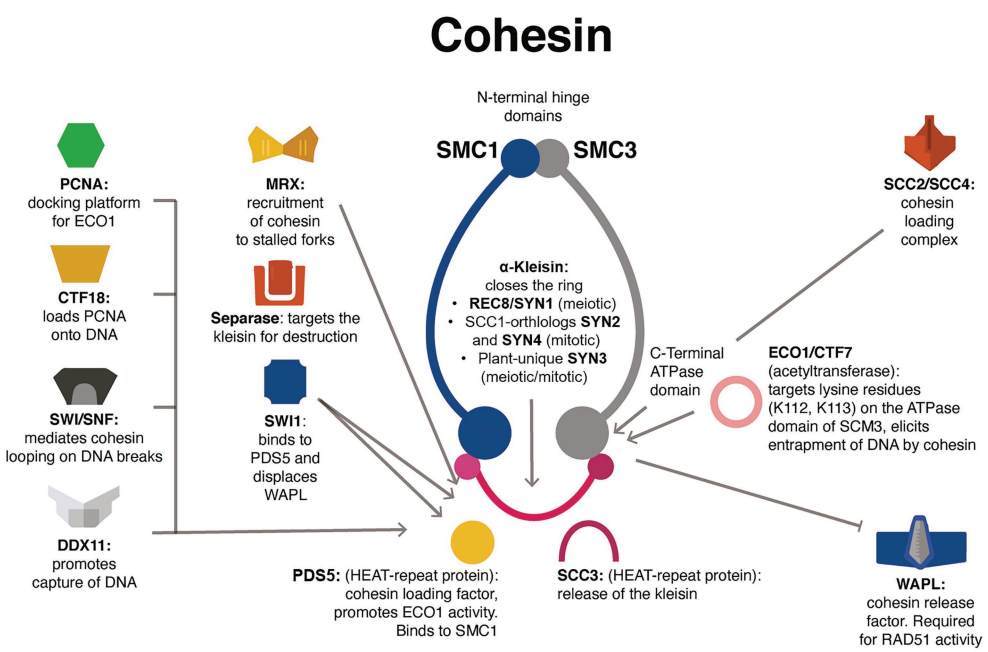

FIGURE 3 | Proposed simplified functional network between the plant cohesin complex and associated genome-maintenance factors. The cohesin complex performs a wide repertoire of functions including homologous recombination during meiosis and mitosis. The complex is loaded onto chromatin by SCC2/SCC4; it is stably locked onto chromatids by ECO1/CTF7, an acetyltransferase that targets lysine residues on the ATPase domains of SMC3 (and possibly SMC1); and entrapment of DNA is promoted by factors such as PDS5 and SWI1 and antagonized by WAPL and SCC3, which may target the meiotic α-kleisin REC8/SYN1 or the mitotic α-kleisin SCC1, which in *Arabidopsis* is represented by orthologs SYN2 and SYN4, while SYN3 is unique to plants and is both meiotic and miotic. The Separase (ESP1 in *Arabidopsis*) also targets kleisins for degradation. Several other factors promote its function, such as PCNA during homologous recombination; CTF18, which might promote its loading onto DNA; DDX11, which might promote capture of DNA; SWItch/sucrose non-fermentable (SWI/SNF) complexes that promote cohesin-mediated looping on DNA breaks; and the MRX complex that promotes recruitment of cohesin on replication forks that stall. Characterization of these processes in plants may facilitate the understanding of meiosis, DNA repair, and genome organization.

may facilitate recombination at stalled or collapsed replication forks, and may affect processes such as telomere maintenance, cell cycle regulation, and cell proliferation in roots (Amiard et al., 2010). In fact, in *Arabidopsis*, the ATM and ATR kinases are involved in targeting the master regulator of the DNA damage response, the SUPPRESSOR OF GAMMA RESPONSE 1 (SOG1) transcription factor, which then controls the expression of SMC5/SMC6, SYN2, SCC2, ASY3, and NSE4A (Yoshiyama et al., 2014; Bourbousse et al., 2018). This pathway regulates responses to Al^{3+} toxicity and DNA damage in roots of *Arabidopsis*. RAD51-dependent, homology-mediated repair is involved in these responses to Al^{3+} (Chen et al., 2019b). Further study could determine whether MRX/N complexes in conjunction with cohesin and other SMC complexes control tolerance to DNA damage by Al^{3+} in crops such as rice.

In humans, removal of cohesin by WAPL-and PDS5-dependent cohesin is important for fork protection and smooth DNA replication (Benedict et al., 2020). Tightly regulated cohesin loading and unloading occurs under conditions of DNA replication stress, characterized by stalling replication forks that frequently collapse and cause DNA DSBs (Benedict et al., 2020). In human cancer cells, a decrease in sister chromatid cohesion is a common trait resulting from oncogenic pathway activation and DNA replication stress (Benedict et al., 2020). Moreover, in the absence of *WAPL* or *PDS5B*, mouse embryonic fibroblasts with inactivation of *Retinoblastoma* (*Rb*; TKO-Bcl2-p53KO) and deprived of mitogens fail to repair DSBs at collapsed replication forks, which leads to reduced proliferation and increased apoptosis (see **Table 1**; Benedict et al., 2020). Increased cohesin removal by WAPL in human HAP1 cells is required to complete DNA synthesis under conditions of persistent DNA replication stress, probably by allowing RAD51-dependent repair of forks. This condition may also cause premature loss of sister chromatid cohesion during mitosis (Benedict et al., 2020). Whether overexpression of *WAPL* in *Arabidopsis* or crops may confer enhanced tolerance to DNA damage by UVB or Al^{3+} is unclear.

COHESINS, CHROMOSOME FOLDING, AND MEIOTIC SILENCING OF UNSYNAPSED CHROMATIN: ENGINEERING SEX DETERMINATION IN CROPS

In yeast, the interplay between cohesin, ECO1, PDS5, and WAPL is complex, and the processes regulated by this interplay may also extend into chromosome folding, a process that is associated with condensin-dependent formation of loops that then facilitate folding of mitotic chromosomes into compact structures (Dauban et al., 2020). However, cohesin rings organize DNA within chromatids *via* a loop extrusion process, in which small loops are captured and enlarged into large Mb-sized structures that contribute to long-range gene regulation during interphase, not compaction. This process also segments interphase chromosomes into topologically associating domains (TADs; Dauban et al., 2020). TADs also exist in *Nipponbare* rice and cover about one quarter of the genome. The boundaries feature (1) CG and CHG methylation; (2) euchromatic histone marks H3K4me2/3, H3K9ac, H3K36me3, and H3K12ac; and (3) active expression; and (4) are enriched with a GC-rich motif that is recognized by transcription factors of the TEOSINTE BRANCHED 1, CYCLOIDEA, PCF1 family (Liu et al., 2017a). The length of cohesin-mediated loops is considered to depend on the residence time of cohesin in DNA and a poorly understood extrusion driving force, perhaps related to SCC2-mediated ATP-hydrolysis (see **Table 1**), pushing of cohesin along the DNA by RNA polymerases or the frequency of cohesin injection. Hi-C maps of mitotic chromosomes from yeast cells (strain W303) depleted in CDC45 (which reach mitosis without replication) suggest that the establishment of loops is independent of sister chromatid cohesion. Inactivation of WAPL and PDS5 activity in mammalian cells abolish cohesin turnover and lead to an increase in loop length (see **Figure 4**). In yeast, the activity of ECO1 inhibits the loop translocation process that extends DNA loops. Moreover, depletion of ECO1 in yeast *wpl1Δ* cells promotes long intra-chromosomal contacts identical to those observed in PDS5-depleted cells. Hence, in yeast, PDS5 may recruit both ECO1 and WAPL to cohesin and the length of loops may be regulated by two independent pathways controlled by ECO1 and WAPL (see **Table 1**; see **Figure 4**; Dauban et al., 2020).

In mammals, deposition of chromosome axis proteins is required for meiotic silencing of unsynapsed chromatin (MSUC), the process whereby unsynapsed chromosomal regions in the Y chromosome undergo transcriptional inactivation during prophase I. This process constitutes a meiotic checkpoint activated in response to the presence of partially or completely unsynapsed regions such as extra chromosomes or chromosomal translocations and triggers epigenetic silencing. A related process is meiotic sex chromosome inactivation (MSCI), whereby transcriptional silencing of the X and Y chromosomes occurs during prophase I (see **Figure 4**). Usually, DSBs generated in leptotene are repaired during zygotene *via* homology search, but for sex chromosomes, large portions do not synapse, and thus DSB markers (such as RPA and RAD51) accumulate along their axes. The presence of such markers induces the ATM/ATR pathway to trigger two rounds of histone H2AX phosphorylation (γ-H2AX) deposition that coats both the X and Y chromosomes. The presence of γ-H2AX is followed by the accumulation of repressive histone marks such as H3K9me3/2, H2A ubiquitylation, H3K27m1/3, H3K9ac, and H4K16ac and the absence of active RNA polymerase II (Waters and Ruiz-Herrera, 2020). By Hi-C analysis in mice germ cells, MSCI was linked to 3D higher-order chromatin remodeling, which features reduced loading of meiotic cohesin α-kleisins REC8 and RAD21 Cohesin Complex Component Like 1 (RAD21L) and the organization of sexual chromosomes into TADs (see **Figure 4**). Sex chromosomes feature few and large loops and significant clustering of cohesins into

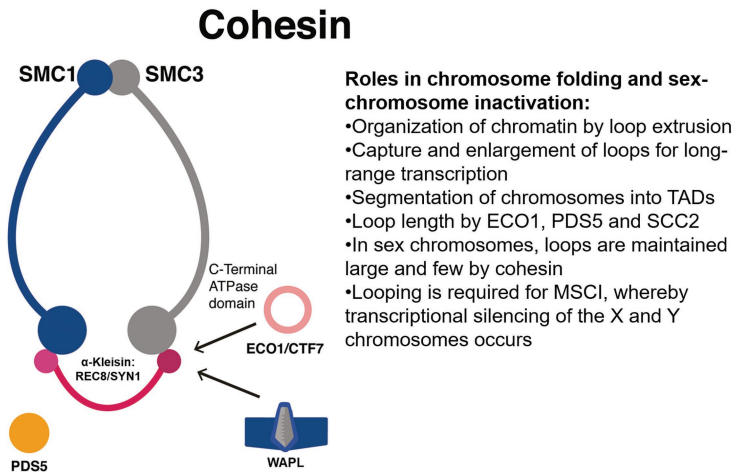

FIGURE 4 | Proposed roles for the SMC cohesin complexes in meiotic silencing of unsynapsed chromatin in sex chromosomes. Cohesin has roles in the organization of chromatin into loops that regulate expression and in sex chromosomes, may enforce silencing. ECO1/CTF7, N-terminal acetyltransferase ESTABLISHMENT OF COHESION 1/CHROMOSOME TRANSMISSSION FIDELITY 7; MSCI, meiotic sex chromosome inactivation; PDS5, HEAT-repeat protein PRECOCIOUS DISSOCIATION OF SISTERS; TADs, topologically associating domains; WAPL, cohesin dissociation factor WINGS APART LIKE.

the promoter regions of highly expressed genes most probably located in DNA loops out of the axes (Vara et al., 2019; see **Figure 4**).

In mice, MSCI is essential for avoiding ectopic expression of male "pachytene-lethal" genes (also known as "executioner" genes). These are Y-linked genes that encode zinc finger transcription factors, which, when expressed, induce pachytene arrest (Waters and Ruiz-Herrera, 2020). Notably, the tropical crop and emerging model system *Carica papaya* Linn features a sex chromosome system but with two slightly different Y chromosomes: Y for males and Y^h for hermaphrodites (Liao et al., 2017; Lee et al., 2018). Papaya has three sex types: female (XX), male (XY), and hermaphrodite (XY^h), males being rare because the trait is usually lethal (Chen et al., 2019a). The hermaphrodite-specific region of the Y^h chromosome (HSY) is 8.1 Mb long and the X chromosome is 3.5 Mb long (Liao et al., 2017) and heavily methylated (Zhang et al., 2008). Papaya is an important source of vitamin A, vitamin C, potassium, folate, niacin, thiamine, riboflavin, iron, and calcium. Clearly, suppression of recombination and degeneration of the Y chromosome occurs (Zhang et al., 2008; Charlesworth, 2017). Therefore, Hi-C could be used with papaya meiocytes to determine whether MSUC and MSCI occur and whether cohesins and especially PDS5 are important for such processes. Such research may help clarify how sex is determined in papaya, perhaps by differential loading of cohesins in DNA loops or by differential activity of ECO1 and WAPL. This type of work may allow for the deliberate engineering and breeding of constitutively hermaphrodite cultivars, the most agriculturally desirable (Lee et al., 2018; see **Table 1**). Constitutively hermaphrodite papaya cultivars are known to occur occasionally in farms. One example is the all-hermaphrodite progeny of BH*-TSS No. 7, an inbred line derived from the rare X chromosome mutant *S*, which may contain a recessive lethal allele, ml, on the X chromosome (Chen et al., 2019a).

THE ROLE OF ECO1 COMPLEMENTATION GROUP IN MITOSIS AND MEIOSIS: OPPORTUNITIES FOR PLANT BREEDING

In yeast, from the S-phase onward, cohesin stably holds together the sister chromatids. For this, cohesin must be protected from removal by WAPL. Protection is provided by the ECO1 acetyltransferase, which performs this task by targeting the SMC3 subunit at two highly conserved lysines on the outside of its ATPase domain, and as a result, locks cohesin and makes it resistant to WAPL (see **Table 1**; Elbatsh et al., 2016).

A genetic screen of about 500 *eco-1* mutants in haploid yeast strain W303 allowed for the identification of a complementation group that had no identifiable mutations in *WAPL*, *SMC3*, *SCC3*, and *PDS5* (Elbatsh et al., 2016). The SMC1 mutation L1129V, located in the signature motif, is an integral part of the ATP binding pocket, and D1164E is part of the D-loop, a motif required for the hydrolysis reaction and the proper orientation of another loop, the P loop, which is required for proper nucleotide binding (Elbatsh et al., 2016; Hassler et al., 2019). Although these mutations in SMC1 allow for binding to DNA in the absence of ECO1 and confer cohesion and viability, scanning force microscopy results suggest the mutants are unable to hydrolyze ATP, and the overall amount of cohesin is reduced by 30%. The analogous SMC3 mutation L1126V partially supports viability, whereas the SMC3 mutation D1161E is lethal. The SMC1 mutation L1129V shows impairment in the opening of the

cohesin exit gate due to failure to properly orientate the ATPase for hydrolysis (Elbatsh et al., 2016). This mechanism seems to be conserved in human cells (HCT116 *p53*$^{-/-}$) cells (Elbatsh et al., 2016), but has not been studied in plants. In yeast (strain W303), the acetylation of the ATPase heads by ECO1 is believed to occur preferentially during a conformation called the J mode (SMC1-S161/SMC3-K160), which allows for better entrapment of sister DNAs and is characteristic of cohesion (Chapard et al., 2019). Hence, mutations within the D loop of SMC1 (L1129V and D1164E) and in the J compartment need to be isolated in *Arabidopsis* to determine the corresponding phenotypes. Most likely, these might correspond to weak alleles.

In yeast, ECO1 has been proposed to interact physically with PCNA through the PIP box (also known as the QxxL motif). Introducing the alternate sequence AxxA causes cohesion defects (Moldovan et al., 2006). Fusion of the PIP box directly to the PCNA restores cell growth, sister chromatid cohesion, and SMC3 acetylation in yeast strain W303. Therefore, a possible explanation is that ECO1 is placed close to the PCNA during the late stages of DNA replication to function during the establishment of cohesion. A proposed mechanism is that the CTF18-RFC complex may operate upstream of this process by loading the PCNA at DNA replication forks, away from sites of active replication, possibly in a post-replicative manner (Liu et al., 2020). In yeast, the role of the PIP box during the establishment of cohesion has been thoroughly characterized, especially the role of post-translational modifications such as SUMOylation (Moldovan et al., 2006), and performing similar studies in plants might be scientifically relevant.

In yeast (YSD17 and several other haploid strains) and human cells (HeLa, 293 T), self-interaction of the cohesin subunits SCC1/RAD21 and SCC3 causes cohesin to dimerize in the S phase and monomerize in mitosis (see **Table 1**). Also, deletion of the deacetylase HOS1 (which erases SMC3 acetylation) or the ECO1 antagonist WAPL1 could increase cohesin dimer levels by 20%, whereas depletion of ECO1 had the opposite effect. Dimerization of SMC complexes (cohesin and condensin) is considered as a key for DNA loop formation (Shi et al., 2020), so ECO1/CTF7 appears indispensable for high-order chromosome structure and gene expression (see **Table 1**).

In *Arabidopsis*, *ECO1/CTF7* regulates tolerance to DNA damage, pairing at zygotene, proper segregation of meiotic and mitotic chromosomes at anaphase, tapetum integrity, mitotic cell cycle progression, somatic DNA repair, root development, pollen mitosis, seed development, and chromatin condensation (Bolaños-Villegas et al., 2013), in a manner that is epistatic to *WAPL1/2* (De et al., 2016). However, we have no biochemical information regarding its interaction with SMC3, SCC3, and PDS5 or the PCNA, and its role in CO formation is ignored as well. Rice has two *ECO1/CTF7* homologs that might be essential for the proper acetylation of SMC3 (K105 and K106) during meiosis. Thus, genome editing by CRISPR-Cas9 may facilitate the retrieval of suitable mutant alleles (Li et al., 2018).

Five homologs of *Arabidopsis PDS5* have been characterized. In the *Atpds5a/Atpds5b/Atpds5c/Atpds5e* mutant, the impact on meiosis is restricted to a minor reduction in chiasmata formation in chromosome 1, but the *Atpds5a/Atpds5b/Atpds5c* mutant shows significantly impaired somatic homologous repair after exposure of seedlings to Bleomycin (5 μg/ml), as observed with the *IC9* recombination reporter, in which the recombinant sectors appear blue after *GUS* staining. Double, triple, and quadruple mutants are also sensitive to γ-radiation (150–450 Gy) and the cross-linking agent mitomycin C. The authors indicated that this phenotype is similar to that reported for *Arabidopsis SMC6*, which may suggest a functional relationship between PDS5 and the SMC5/SMC6 complex (Pradillo et al., 2015).

In conclusion, the activity of *ECO1/CTF7* and its interacting partners PDS5 and WAPL is required for overall plant development, including meiosis, mitotic DNA repair, and most likely gene expression. It may be necessary to isolate mutants in crops to identify novel phenotypes relevant to plant breeding and perhaps determine whether these genes behave as a narrow complementation group as reported in yeast (Elbatsh et al., 2016).

ENGINEERING SYSTEMS REDUNDANCY: COMPLEMENTARY ROLES OF COHESIN AND CONDENSIN IN PLANT GENOME ORGANIZATION, SILENCING OF TRANSPOSONS, AND TOLERANCE TO DNA DAMAGE

Eukaryotes have three sets of canonical SMC protein complexes (Municio et al., 2021): (1) the cohesin complex composed of the core proteins SMC1 and SMC3, mentioned previously, mostly involved in sister chromatid cohesion; (2) the SMC5/SCM6 complex, which is mostly linked to DNA repair and recombination; and (3) the condensin complex, which is composed of core units SMC2 and SMC4 and is required for chromosome condensation and segregation (Sakamoto et al., 2019).

In *A. thaliana*, condensin is further divided into complexes I and II (Sakamoto et al., 2019). The plant condensin complex I consists of core units SMC2/SMC4, γ-kleisin (CAP)-H, β-kleisin (CAP)-H2, and HEAT repeat-containing proteins CAP-G and CAP-D2. However, the association of SMC2/SMC4 with CAP-H2 (β-kleisin), CAP-G2, and CAP-D3 form condensin II (Sakamoto et al., 2019; Municio et al., 2021), a complex that may be required for tolerance to DSBs caused by the radiomimetic agent zeocin for tolerance to boron (Sakamoto et al., 2011; see **Figure 5**). In *Arabidopsis*, defects in the function of *SMC2* (2 genes) or *SMC4* (3 genes) affect segregation of mitotic and meiotic chromosomes (Sakamoto et al., 2019). Also, defects in *Arabidopsis SMC4* (At5g48600, also known as *AtCAP-C*) cause deregulation in the expression of centromeric and pericentric transposable elements (such as *COPIA*), reduced CG methylation, and chromocenter decondensation (see **Table 1**), phenotypes reminiscent of those reported for *ECO1/CTF7* mutants (Bolaños-Villegas and Jauh, 2015; De et al., 2016) and

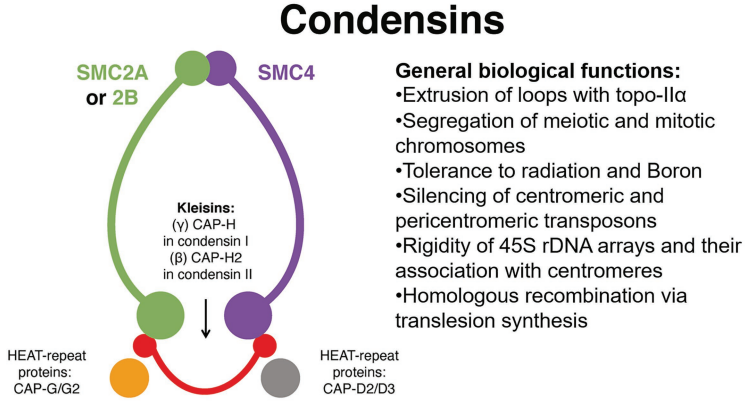

FIGURE 5 | Simplified functional network for SMC condensin complexes during genome maintenance and organization. The plant condensin complexes are versatile and regulate a wide range of processes including chromatin loop extrusion, chromosome segregation, silencing of centromeric transposable elements, organization of 45S ribosomal DNA arrays, and homologous recombination that affect pollen and embryo development. Much of this activity is facilitated by HEAT-repeat proteins CAP-G/G2 and CAP-D2/D3. Topo-IIα, topoisomerase-IIα.

perhaps suggesting a regulatory link between SMC4 acetylation and maintenance of the genome.

The *Arabidopsis* condensin II complex is also required for genome integrity and for pollen and embryo development (Schubert et al., 2013; Sakamoto et al., 2019; Municio et al., 2021). A combined spatial analysis of the localization of the 180-bp centromeric repeat and the 5S and 45S rDNA probes was performed in the *Arabidopsis cap-h2-2*, *cap-g2-1*, and *cap-d3-1* mutants (see **Figure 5**). Results indicated disassociation of the rDNA arrays from the centromeres, thus suggesting that direct binding of condensin II to rDNA array regions is necessary for their association with centromeres in *A. thaliana* (Sakamoto et al., 2019). However, cytological analysis of *Arabidopsis cap-d3* interphase nuclei indicated specific clustering of 45 rDNA sites, so CAP-D3 might localize in euchromatic loops and somehow determine the rigidity needed to maintain separation of chromocenters (Municio et al., 2021) In any case, an analysis of 3D chromatin organization by Hi-C may help clarify the distribution pattern of condensin II during interphase and its role in the clustering of rDNA arrays during interphase (Sakamoto et al., 2019). Evidence also indicates that SMC4/condensin is required for repression of a wide range of methylated genes subject to conditional expression (Wang et al., 2017). Gene examples are embryo and pollen vegetative cell-specific *GAMETE EXPRESSED-PROTEIN 1* (*GEX1, At5g5590*; Alandete-Saez et al., 2011), pollen tube-expressed *POLYMERASE DELTA 4* (*POLD4*, *At1g09815*; Wang et al., 2008), radiation-response factors such as *GAMMA-IRRADIATION AND MITOMYCIN C INDUCED 1* (*GMI1*, *At5g24280*; Böhmdorfer et al., 2011), and translesion-synthesis/homologous recombination factor *RECQ3* (*At4g35740*; Kobbe et al., 2009). Thus, breeding for condensin alleles may confer resistance to mitotic DNA damage caused by UVB and Al^{3+} and boost allele reshuffling *via* homologous recombination. Also because of the crucial role played by condensin in genome organization, these alleles may contribute to advance our knowledge in processes such as the regulation of MSUC and MSCI in crops.

OPPORTUNITIES FOR ENGINEERING MODIFIED CROSSOVER FORMATION DURING MEIOSIS WITH COHESINS, CONDENSINS, AND HORMAD PROTEINS

During meiosis, the reciprocal exchange of DNA between homologous chromosomes enables the reshuffling of parental genetic information and the transfer of the recombined material to the progeny (de Maagd et al., 2020). The formation of DSBs by the topoisomerase SPORULATION-DEFICIENT 11 (SPO11) is crucial for the initiation of synapsis between homologous chromosomes and CO formation (Esposito and Esposito, 1969; Ning et al., 2020). Then the MRX/N complex generates 3' single-strand DNAs at DSB sites that allow the recombinases RAD51 and DMC1 to bind to the single-strand DNA overhangs to promote search of homology and pairing. The subsequent simultaneous assembly of the multi-layered chromosome axis and synaptonemal complex by the α-kleisin REC8/SYN1, the coiled-coil proteins ASY3 and ASY4, the HORMA-domain protein ASY1 and transverse filament protein ZYP1 catalyze the successful synapsis of homologous chromosomes and the formation of COs (Ning et al., 2020). Thus, meiotic CO formation is an important target in crop breeding (de Maagd et al., 2020), especially because in modern crops, successive rounds of selection have reduced their genetic variation, leaving them with less allelic diversity than their wild relatives, called the "domestication bottleneck" (Dempewolf et al., 2017).

Meiosis starts with the formation of many DNA DSBs, most of which are repaired in non-CO events and do not result in recombinant chromosomes. In plants, only one to three DSBs per chromosome are processed into actual COs

(de Maagd et al., 2020), and most of these COs exhibit interference, the phenomenon that prevents multiple COs from occurring in close proximity along each chromosome pair (Lambing et al., 2020b). In *Arabidopsis*, type I COs are sensitive to interference and are associated with the activity of the ZMM class of proteins, including mutS homolog 4 (MSH4), a meiotic-specific reciprocal-recombination factor. However, type II COs are insensitive to interference and are the product of the activity of MMS and UV sensitive 81 (MUS81), a restriction endonuclease (Taagen et al., 2020; Wang et al., 2020). At least three independent pathways suppressing CO formation have been identified in *Arabidopsis* (Taagen et al., 2020), featuring the activity of (1) RECQ4, a homolog of the human Bloom syndrome helicase (BLM) that forms the BTR complex along with TOP3α and RECQ MEDIATED INSTABILITY 1 (RMI1) and unwinds recombination intermediates to suppress class I COs; (2) FANCM, a DEAD/DEAH box RNA helicase, that is a direct DNA-binding cofactor along with MHF1 and MHF2, may unwind recombination intermediates, limits class II COs, and promotes synthesis-dependent strand annealing (SDSA); and finally (3) FIDGETIN-LIKE 1 (FIGL1), a Holliday junction resolvase, that forms a complex with FIDGETIN-LIKE 1 INTERACTING PROTEIN (FLIP), suppresses RAD51 and DMC1 recombination activity, and constrains strand invasion (Séguéla-Arnaud et al., 2017; Taagen et al., 2020).

Arabidopsis has a single *SCC2* homolog, and homozygous knockout alleles are embryonic-lethal. However, use of the non-lethal *Atscc2-5* allele revealed that during meiosis, *SCC2* participates in chromosomal axis formation, pairing of homologous chromosomes, synapsis, and recombination upstream of MSH4 and MUS81 (see **Table 1**). Genetic analyses also suggested that *SSC2* is epistatic to RAD51 during DSB formation, participates in the same pathway as *REC8*/*SYN1* and *WAPL1/2*, and is required for efficient CO resolution. Results from plant pull-down assays suggest that the N-terminus of AtSCC2 interacts with AtSCC4 *in vivo*, but knockdown of *AtSCC4* during meiosis does not cause any obvious meiotic defects, which suggests a divergence in the roles played by SCC2/SCC4 during mitosis and meiosis. For instance, in maize, *SCC4* is called *DEK15* (*Zm00001d052197*/*GRMZM2G079796*) and the corresponding *dek15*/*scc4* EMS-mutants do not show any obvious defects during meiosis. However, mitosis in endosperm and embryos is defective, with precocious sister chromatid separation, misaligned chromosomes, lagging chromosomes, and micronuclei. These mutants develop kernels with only 40% of the weight observed in the W22 reference line, with few and small starch grains in endosperm, and the embryos are arrested in development and die after 18 days (He et al., 2019). Notably, *DEK15* is required for proper expression of genes for the starch biosynthetic pathway, such as *Shrunken2*, *Starch synthase I* (*SSI*), and *SSIIa* (He et al., 2019), a finding of great agricultural importance.

The likely answer for the functional divergence between plant SCC2 and SCC4 may lie in the presence of a plant-specific homeodomain (with a C4-H-C3 amino acid motif) that is found only in SCC2, which is believed to mediate binding to histones and be required for meiotic function but not vegetative growth (Wang et al., 2020). Thus, in plants, only the activity of SCC2 is required for key meiotic processes such as CO resolution, a process of huge relevance for plant breeders.

Accurate and faithful transmission of chromosomes into the gametes relies on the establishment of COs between paternal and maternal homologous chromosomes during prophase I, just prior to first meiotic division, when COs, together with sister chromatid cohesion, guarantee proper chromosome orientation on the meiotic spindle. Meiotic chromosome modeling requires the assembly of axial elements that include meiosis-specific subunits of cohesin such as the meiotic α-kleisin REC8/SYN1 (Castellano-Pozo et al., 2020). In *Arabidopsis*, REC8/SYN1 is associated with regions of high nucleosome occupancy; histone methylation at H3K4 (expressed genes), H3K27 (silent genes), and H3K9 (silent transposons); as well as suppression of meiotic DSBs and COs (Lambing et al., 2020b). It may be a mechanism to guarantee that repeat-rich regions do not undergo meiotic recombination, in that these are highly susceptible to nonallelic COs that may threaten genome stability (Shahid, 2020).

In addition to its primary role in establishing sister chromatid cohesion, meiotic cohesin loading promotes the recruitment of HORMA-domain proteins (HORMADs) to the axial elements, so that chromosomes can initiate meiotic recombination *via* the formation of DNA DSBs and to undergo pairing of homologous chromosomes. Homolog pairing features the assembly of the synaptonemal complex (SC), a ladder-like structure that bridges the axial elements of aligned homologs. This process, known as synapsis, stabilizes homolog interactions and is essential to ensure that a subset of DSBs become CO-designated sites during the pachytene stage of meiotic prophase, which is defined by full synapsis. Thus, the processes leading to CO formation require the presence of meiosis-specific chromosome structures built over a cohesin scaffold (Castellano-Pozo et al., 2020).

In addition to the REC8/SYN1 α-kleisin, major components of the plant meiotic chromosome axis include the HORMAD protein ASY1 and the coiled-coil proteins ASY3 and ASY4 (Lambing et al., 2020a). In this primary configuration, coaligned chromatin loops project laterally from the axis, but at late prophase I, the axis is remodeled by the simultaneous depletion of HORMAD proteins and the loading of transverse filament SC proteins, including ZYP1a and ZYP1b (Lambing et al., 2020a). Recent work that combines chromatin immunolocalization techniques with tetrad analysis and immunostaining suggests that the *Arabidopsis* ASY1 protein is enriched in the centromeres, it antagonizes telomere-led recombination and it promotes spaced CO formation along the chromosomes *via* CO interference (see **Table 1**), during which a set of pro-CO factors act to protect interhomolog strand invasion events from antirecombination pathways (Lambing et al., 2020a). This finding hints at the possibility of reducing ASY1 activity to modify CO distribution in the genome and reduce linkage drag in major crops, which is major problem during the introgression of valuable alleles (Lambing et al., 2020a). For instance, results

Genes	Target Crops	Predicted Result of Novel Alleles
ASY1	All	Reduction of linkage drag, accelerated plant breeding
CTF18/PCNA/WAPL/PDS5 /ECO1/SCC3	Rice and maize	Enhanced cohesion during replicative stress. Tolerance to chronic DNA damage caused by UVB or Aluminum
BRG1 and *ARID2* (SWI/SNF), *SCC3* and *ECO1*	All	Prevention of large-scale rearrangements, ultra-long seed storage
DDX11	All	Promotion of cohesion and stability of replication fork during chronic DNA damage
ESP1	All	Promotion of crossover resolution, promotion of embryo development, accelerated breeding
ISW1/YBR245C	All	Promotion of cohesion and stability of replication fork during chronic DNA damage
MRX/N complex	Rice	Tolerance to soil Aluminum via the ATM/ATR-response to DNA damage
SCC2	All	Reduction of linkage drag, accelerated plant breeding
SCC4/DEK15	Maize	Enhanced crop yield
SMC2	All	Tolerance to topological stress during DNA replication, tolerance to chronic DNA damage
SMC4, CAP-H2, CAP-G2, and *CAP-D3*	All	Tolerance to chronic DNA damage caused by UVB, may contribute to meiotic sex chromosome inactivation (MSCI)
SMC5, SMC6A/B, NSE4A/B, five other *NSE* genes, *PDS5*	Rice and Maize	Enhanced pollen development, enhanced meiotic synapsis and enhanced mitosis during exposure to UVB and soil Aluminum
SWITCH1/DYAD (SWI1)/AMEIOTIC	All	May facilitate identification of alternative meiotic α-kleisins with high processivity
REC8/SYN1	Rice	Breeding of apomictic rice, novel alleles may facilitate ASY1-dependent formation of COs under heat-stress
REC8/SYN1 and *WAPL*		Enhanced formation of COs, accelerated plant breeding
WAPL/PDS5/ECO1, perhaps *SMC4*	Rice	Changes in chromosome looping, unknown response to DNA damage
WAPL/PDS5/ECO1/REC8/ SCC2	Papaya	Deregulated meiotic silencing of unsynapsed chromatin (MSUC) and meiotic sex chromosome inactivation (MSCI), breeding of constitutively hermaphrodite papaya cultivars

FIGURE 6 | Suggested agricultural targeting of genes involved in SMC-regulated processes. In major crops such as rice and maize, it might be possible to stabilize transcription and homologous recombination under chronic stress caused by UVB radiation and soil aluminum, and in the case of papaya, it might be possible to manipulate sex chromosome silencing to breed all hermaphrodite progenies. Illustrative images were obtained from Google Images and Wikipedia (CC BY-SA 2.0 and CC BY-SA 4.0).

from modeling with R suggest that when a quantitative trait locus is within a region that is normally CO-poor, boosting the recombination rate may decrease the linkage drag nearly 10-fold after the foreground selection and may improve the return to the recurrent parent (Falque and Martin, 2020). In *Arabidopsis*, high temperature during meiosis (36–38°C, 24 h) reduces SPO11-dependent DSB formation, as observed by labeling with γ-H2AX, formation of DMC1 foci, recruitment of ASY4 to the chromosome axis during zygotene, and recruitment of ASY1 to the SC (during zygotene as well). Although heat treatment does not affect the distribution and abundance of REC8/SYN1 in chromosomes during zygotene and pachytene (Ning et al., 2020), loading of ASY1 is not defective in *syn* mutants exposed to heat, which suggests that the presence of REC8/SYN1 disturbs the proper loading of ASY1 during high temperatures (Ning et al., 2020). The biochemical nature of this interaction during heat has not been determined, but if it were optimized, it might allow the adaptation of crops to high temperatures.

EFFICIENT TRANSMISSION OF NEW ALLELES: BOOSTING CO FORMATION WITH MEIOTIC COHESINS

During meiosis in mouse oocytes, mutual recombination between parental homologous chromosomes creates chiasmata, the physical linkages that bind bivalents during

meiosis I (Silva et al., 2020). Cell cycle-dependent cleavage of the meiotic α-kleisin protein REC8/SYN1 that is present on the chromosome arms allows segregation of homologous chromosomes during anaphase I. Then during meiosis II, proteolytic cleavage of REC8/SYN1 at the centromeres by the Cys-protease separase (ESP1) allows centromeres to segregate from one another in the metaphase to anaphase transition (see **Table 1**; Yang et al., 2009, 2019; Hsieh et al., 2020). In general, the meiotic cohesin complex may regulate recombination and topology. In comparison to the mitotic α-kleisin SCC1, loading of meiotic α-kleisin REC8/SYN1 leads to early firing of replication origins and fast progression of replication forks, perhaps as a mechanism to facilitate passage from the G1 to the S phase (Hsieh et al., 2020). These results suggest that directed evolution in plant α-kleisins might optimize replication during meiosis, and perhaps may lead to the discovery of (a) heat-tolerant REC8/SYN1 alleles better able to load ASY1 or (b) discovery of useful, weak or loss-of function *REC8*/*SYN1* alleles. For instance, in *Kitaake* rice, an *rec8* allele is combined with the alleles *osd1* (*OSD1*, *OMISSION OF SECOND DIVISION*; regulation of cell cycle progression) and *pair1* (*PAIR1*, *HOMOLOGOUS PAIRING ABERRATION IN RICE MEIOSIS1*, control of DSB formation) to induce the apomictic-like and commercially valuable phenotype known as *Mitosis instead of Meiosis* (*MiMe*, *Osrec8*/*Ososd1*/*Ospair1*; Khanday et al., 2019). In this way, hybrid vigor (e.g., heterosis) can be fixed and maintained in the genotype of clonal progenies (Wang, 2020).

Cohesin is actively released from DNA by the separase protease (Silva et al., 2020), which targets the α-kleisin REC8/SYN1 (Faramarz et al., 2020). In yeast, before the metaphase-to-anaphase transition, the securin protein (the corresponding *Arabidopsis* orthologs are PATRONUS1/2) inhibits the protease activity of the separase. Then at the onset of anaphase, securin is itself degraded by the anaphase-promoting complex/cyclosome (APC/C), thus freeing the separase (Yang et al., 2009; Cromer et al., 2019). Cleavage of the REC8/SYN1 α-kleisin along chromosome arms at anaphase I by the separase allows for resolution of chiasmata, formed as a result of homologous chromosome recombination and the faithful segregation of homologous chromosomes (Yang et al., 2009; Silva et al., 2020). However, centromeric cohesion is protected by the conserved SUGOSHIN (SGO1/2 in *Arabidopsis*) family of proteins until anaphase II, when separase-mediated cleavage of REC8/SYN1 facilitates the separation of sister chromatids (Yang et al., 2009; Cromer et al., 2013). In *Arabidopsis*, the AESP1 separase regulates a wide range of important developmental processes such as meiotic chromosome segregation, tetrad formation, embryo development up to the globular stage, cellularization of the endosperm, proper assembly of the radial microtubule system after telophase II, and even N-acetylation of proteins required for vesicle trafficking such as the H^+ and V-ATPases (Yang et al., 2009; Liu et al., 2017b; see **Table 1**). However, separase homologs have not been characterized in major crops, and this gap may be limiting our understanding of chiasmata resolution, among many other processes of great agricultural relevance.

In eukaryotic organisms such as budding yeast and *Arabidopsis*, ample evidence indicates that WAPL is involved in the release of cohesin from meiotic chromosomes and its activity is essential for normal meiosis, especially for the release of REC8/SYN1 during prophase I (De et al., 2016; Silva et al., 2020). In mouse oocytes, deletion of *WAPL* leads to the formation of aberrant chiasmata-like structures, not because of an increase in CO formation but because of an increase in DNA damage, as observed by an increase in γ-H2AX foci, presumably linked to retention of the kleisin and increased rigidity, leading to inefficient homologous repair and formation of chromosome bridges. Structural analysis by Hi-C revealed that loss of *WAPL* during meiosis also leads to the formation of chromatin loops within loops (Silva et al., 2020), a phenotype not yet reported in *Arabidopsis*. Formation of aberrant chiasmata has not been documented in *Arabidopsis wapl* mutants either.

Perhaps we must consider how cohesin is loaded onto chromatin in the first place. Work in budding yeast suggests that during the G1 phase, proper loading of cohesin onto chromosomes depends on the remodeling structure of chromatin (RSC) chromatin remodeler, a member of the SWI/SNF family of ATPases (Tsukiyama et al., 1999; Muñoz et al., 2020). The RSC complex consists of 19 subunits, is enriched in centromeres, and is believed to function as a chromatin receptor that allows direct recruitment of SCC2/SCC4 on broad nucleosome-free-regions, which are probably remodeled by RSC *via* nucleosome eviction or DNA translocation. These nucleosome-free regions usually correspond to promoters where the cohesin loader is normally found (Muñoz et al., 2020). Other chromatin remodelers known to act as cohesin loaders in humans such as Imitation Switch 1 (ISW1) and Chromo-ATPase/helicase-DNA-binding domain (CHD1) support cell proliferation, so the SCC2/SCC4 module may be somehow promiscuous and may become functional in the proximity of alternative chromatin remodelers during cohesin-dependent processes such as DNA repair (Stokes et al., 1996; Tsukiyama et al., 1999; Muñoz et al., 2020; see **Table 1**). Further research could determine whether alternative meiotic chromatin remodelers exist in plants and identify the corresponding phenotypes.

In *Arabidopsis*, thorough work has helped uncover a meiotic antagonist of WAPL that may operate during prophase I by binding to PDS5 and displacing PDS5 from WAPL. This antagonist is the SWITCH1/DYAD protein (SWI1), a protein of unknown biochemical function and whose actual *modus operandi* is also ignored. The phenotype of the *swi-1* mutant features failure to assemble the chromosome axis and to establish sister chromatid cohesion. The biochemical evidence (GST pull-down assay in *Escherichia coli* and bimolecular fluorescence complementation in tobacco) indicates that SWI1 strongly interacts with the N-terminus of PDS5A, specifically the N-terminal 300 amino acids, but is also able to interact strongly with PDS5C/E and mildly with PDS5B/D, that is, all PDS5 proteins in *Arabidopsis*. WAPL was also found to bind to the N-terminus of PDS5A, which suggests the existence of a potentially antagonistic entanglement that was confirmed by a competitive binding assay in tobacco leaf cells, in which WAPL was displaced from PDS5 by SWI1. The APC is believed

to target SWI1 for degradation from zygotene onward, as suggested by prolonged chromatin residency and reduced fertility in *SWI1* mutants with mutation of five tentative D-boxes. Of note, in the *rec8* mutants, the SWI1-GFP signal is retained, which suggests that SWI1 may interact with yet unidentified meiotic cohesin complexes with alternative α-kleisins and that *swi1* mutants might show an increase in the formation of multiple female meiocytes, thus suggesting a role in the specification of meiocyte identity (see **Table 1**; Yang et al., 2019). The *Arabidopsis SWITCH1/DYAD* gene has homologs in rice and maize, called *AMEIOTIC1* (Pawlowski et al., 2009; Che et al., 2011; Yang et al., 2019), which indicates the possibility of validating these phenotypes in these crops.

CONCLUSION

Biomedical research in yeast and mammalian cohesin and condensin complexes and their respective regulators has contributed significantly to our understanding of the processes they affect, namely genome maintenance, meiotic recombination, CO formation, and regulation of high-order chromatin structure in chromosomes. Research in the model plant *A. thaliana* and crops has also pushed the boundaries of our knowledge and facilitated charting the way to applied plant breeding by providing clear mutant phenotypes and solid genetic evidence (de Maagd et al., 2020). Translation of basic research into crop breeding may speed the screening and retrieval of valuable alleles for tolerance to DNA damage by UVB and aluminum exposure (for a summary see **Figure 6**). It may help in manipulating CO frequency and distribution for enhanced transmission of key traits, both wild and mutant, at a time when climate change and population growth threaten food security (Gerland et al., 2014; Zhao et al., 2017; Lambing et al., 2020b; see **Figure 6**). Efficient genome-editing methods by CRISP-Cas9 have been developed for crops (Qi, 2019), so we may finally be able to perform detailed genetic, cytological, and biochemical characterization of SMCs in maize and rice. In conclusion, a better understanding of the establishment of cohesion and genome organization in crops may contribute to increases in yield under less-than-ideal environmental conditions.

AUTHOR CONTRIBUTIONS

The author confirms being the sole contributor of this work and has approved it for publication.

FUNDING

This work was funded by grant CO244 by the Vicerrectoría de Investigación, Universidad de Costa Rica.

ACKNOWLEDGMENTS

I would like to thank Vicerrectoría de Investigación at the University of Costa Rica for kind financial support and payment of publishing fees, Christopher A. Makaroff at Miami University (Oxford, OH, United States) for helpful suggestions on the text, Laura Smales at BioMedEditing (Toronto, Canada) for English editing, and Ernesto Bolaños-Villegas for designing and editing of the figures. I would also like to thank the American Society of Plant Biologists and TWAS/UNESCO for encouragement, guidance, and professional support.

REFERENCES

Alandete-Saez, M., Ron, M., Leiboff, S., and McCormick, S. (2011). *Arabidopsis thaliana* GEX1 has dual functions in gametophyte development and early embryogenesis. *Plant J.* 68, 620–632. doi: 10.1111/j.1365-313X.2011.04713.x

Amiard, S., Charbonnel, C., Allain, E., Depeiges, A., White, C. I., and Gallego, M. E. (2010). Distinct roles of the ATR kinase and the Mre11-Rad50-Nbs1 complex in the maintenance of chromosomal stability in Arabidopsis. *Plant Cell* 22, 3020–3033. doi: 10.1105/tpc.110.078527

Awasthi, J. P., Saha, B., Regon, P., Sahoo, S., Chowra, U., Pradhan, A., et al. (2017). Morpho-physiological analysis of tolerance to aluminum toxicity in rice varieties of north East India. *PLoS One* 12:e0176357. doi: 10.1371/journal.pone.0176357

Beckouët, F., Srinivasan, M., Roig, M. B., Chan, K. L., Scheinost, J. C., Batty, P., et al. (2016). Releasing activity disengages cohesin's Smc3/Scc1 interface in a process blocked by acetylation. *Mol. Cell* 61, 563–574. doi: 10.1016/j.molcel.2016.01.026

Benedict, B., van Schie, J. J. M., Oostra, A. B., Balk, J. A., Wolthuis, R. M. F., Te Riele, H., et al. (2020). WAPL-dependent repair of damaged DNA replication forks underlies oncogene-induced loss of sister chromatid cohesion. *Dev. Cell* 52, 683–698.e7. doi: 10.1016/j.devcel.2020.01.024

Böhmdorfer, G., Schleiffer, A., Brunmeir, R., Ferscha, S., Nizhynska, V., Kozák, J., et al. (2011). GMI1, a structural-maintenance-of-chromosomes-hinge domain-containing protein, is involved in somatic homologous recombination in *Arabidopsis*. *Plant J.* 67, 420–433. doi: 10.1111/j.1365-313X.2011.04604.x

Bolaños-Villegas, P., and Jauh, G.-Y. (2015). Reduced activity of *Arabidopsis* chromosome-cohesion regulator gene CTF7/ECO1 alters cytosine methylation status and retrotransposon expression. *Plant Signal. Behav.* 10:e1013794. doi: 10.1080/15592324.2015.1013794

Bolaños-Villegas, P., Yang, X., Wang, H. J., Juan, C. T., Chuang, M. H., Makaroff, C. A., et al. (2013). Arabidopsis CHROMOSOME TRANSMISSION FIDELITY 7 (AtCTF7/ECO1) is required for DNA repair, mitosis and meiosis. *Plant J.* 75, 927–940. doi: 10.1111/tpj.12261

Bourbousse, C., Vegesna, N., and Law, J. A. (2018). SOG1 activator and MYB3R repressors regulate a complex DNA damage network in Arabidopsis. *Proc. Natl. Acad. Sci. U. S. A.* 115, E12453–E12462. doi: 10.1073/pnas.1810582115

Castellano-Pozo, M., Pacheco, S., Sioutas, G., Jaso-Tamame, A. L., Dore, M. H., Karimi, M. M., et al. (2020). Surveillance of cohesin-supported chromosome structure controls meiotic progression. *Nat. Commun.* 11:4345. doi: 10.1038/s41467-020-18219-9

Chapard, C., Jones, R., van Oepen, T., Scheinost, J. C., and Nasmyth, K. (2019). Sister DNA entrapment between juxtaposed Smc heads and kleisin of the cohesin complex. *Mol. Cell* 75, 224–237. doi: 10.1016/j.molcel.2019.05.023

Charlesworth, D. (2017). Evolution of recombination rates between sex chromosomes. *Philos. Trans. R. Soc. B Biol. Sci.* 372:20160456. doi: 10.1098/rstb.2016.0456

Che, L., Tang, D., Wang, K., Wang, M., Zhu, K., Yu, H., et al. (2011). OsAM1 is required for leptotene-zygotene transition in rice. *Cell Res.* 21, 654–665. doi: 10.1038/cr.2011.7

Chelysheva, L., Diallo, S., Vezon, D., Gendrot, G., Vrielynck, N., Belcram, K., et al. (2005). AtREC8 and AtSCC3 are essential to the monopolar orientation

of the kinetochores during meiosis. *J. Cell Sci.* 118, 4621–4632. doi: 10.1242/jcs.02583

Chen, P., Sjögren, C. A., Larsen, P. B., and Schnittger, A. (2019b). A multi-level response to DNA damage induced by aluminium. *Plant J.* 98, 479–491. doi: 10.1111/tpj.14231

Chen, J. R., Urasaki, N., Matsumura, H., Chen, I. C., Lee, M. J., Chang, H. J., et al. (2019a). Dissecting the all-hermaphrodite phenomenon of a rare X chromosome mutant in papaya (*Carica papaya* L.). *Mol. Breed.* 39:14. doi: 10.1007/s11032-018-0918-7

Cromer, L., Jolivet, S., Horlow, C., Chelysheva, L., Heyman, J., De Jaeger, G., et al. (2013). Centromeric cohesion is protected twice at meiosis, by SHUGOSHINs at anaphase I and by PATRONUS at interkinesis. *Curr. Biol.* 23, 2090–2099. doi: 10.1016/j.cub.2013.08.036

Cromer, L., Jolivet, S., Singh, D. K., Berthier, F., De Winne, N., De Jaeger, G., et al. (2019). Patronus is the elusive plant securin, preventing chromosome separation by antagonizing separase. *Proc. Natl. Acad. Sci.* 116, 16018–16027. doi: 10.1073/pnas.1906237116

Dauban, L., Montagne, R., Thierry, A., Lazar-Stefanita, L., Bastié, N., Gadal, O., et al. (2020). Regulation of cohesin-mediated chromosome folding by Eco1 and other partners. *Mol. Cell* 77, 1279–1293.e4. doi: 10.1016/j.molcel.2020.01.019

De, K., Bolaños-Villegas, P., Mitra, S., Yang, X., Homan, G., Jauh, G.-Y., et al. (2016). The opposing actions of arabidopsis CHROMOSOME TRANSMISSION FIDELITY7 and WINGS APART-LIKE1 and 2 differ in mitotic and meiotic cells. *Plant Cell* 28, 521–536. doi: 10.1105/tpc.15.00781

de Maagd, R. A., Loonen, A., Chouaref, J., Pelé, A., Meijer-Dekens, F., Fransz, P., et al. (2020). CRISPR/Cas inactivation of RECQ4 increases homeologous crossovers in an interspecific tomato hybrid. *Plant Biotechnol. J.* 18, 805–813. doi: 10.1111/pbi.13248

Delamarre, A., Barthe, A., de la Roche Saint-André, C., Luciano, P., Forey, R., Padioleau, I., et al. (2020). MRX increases chromatin accessibility at stalled replication forks to promote nascent DNA resection and cohesin loading. *Mol. Cell* 77, 395–410.e3. doi: 10.1016/j.molcel.2019.10.029

Dempewolf, H., Baute, G., Anderson, J., Kilian, B., Smith, C., and Guarino, L. (2017). Past and future use of wild relatives in crop breeding. *Crop Sci.* 57, 1070–1082. doi: 10.2135/cropsci2016.10.0885

Díaz, M., Pečinková, P., Nowicka, A., Baroux, C., Sakamoto, T., Gandha, P. Y., et al. (2019). The SMC5/6 complex subunit NSE4A is involved in DNA damage repair and seed development. *Plant Cell* 31, 1579–1597. doi: 10.1105/tpc.18.00043

Diffey, B. L. (2002). Sources and measurement of ultraviolet radiation. *Methods* 28, 4–13. doi: 10.1016/S1046-2023(02)00204-9

Dorsett, D., and Ström, L. (2012). The ancient and evolving roles of cohesin in gene expression and DNA repair. *Curr. Biol.* 22, R240–R250. doi: 10.1016/j.cub.2012.02.046

Dyson, S., Segura, J., Martínez-García, B., Valdés, A., and Roca, J. (2021). Condensin minimizes topoisomerase II-mediated entanglements of DNA *in vivo*. *EMBO J.* 40:e105393. doi: 10.15252/embj.2020105393

Elbatsh, A. M. O., Haarhuis, J. H. I., Petela, N., Chapard, C., Fish, A., Celie, P. H., et al. (2016). Cohesin releases DNA through asymmetric ATPase-driven ring opening. *Mol. Cell* 61, 575–588. doi: 10.1016/j.molcel.2016.01.025

Erickson, D. J., Sulzberger, B., Zepp, R. G., and Austin, A. T. (2015). Effects of stratospheric ozone depletion, solar UV radiation, and climate change on biogeochemical cycling: interactions and feedbacks. *Photochem. Photobiol. Sci.* 14, 127–148. doi: 10.1039/C4PP90036G

Esposito, M. S., and Esposito, R. E. (1969). The genetic control of sporulation in Saccharomyces. I. the isolation of temperature-sensitive sporulation-deficient mutants. *Genetics* 61, 79–89. doi: 10.1093/genetics/61.1.79

Falque, M., and Martin, O. C. (2020). Enhancing backcross programs through increased recombination. bioRxiv [Preprint]. doi: 10.1101/2020.05.05.078287

Faramarz, A., Balk, J. A., van Schie, J. J. M., Oostra, A. B., Ghandour, C. A., Rooimans, M. A., et al. (2020). Non-redundant roles in sister chromatid cohesion of the DNA helicase DDX11 and the SMC3 acetyl transferases ESCO1 and ESCO2. *PLoS One* 15:e0220348. doi: 10.1371/journal.pone.0220348

Fernandes, J. B., Wlodzimierz, P., and Henderson, I. R. (2019). Meiotic recombination within plant centromeres. *Curr. Opin. Plant Biol.* 48, 26–35. doi: 10.1016/j.pbi.2019.02.008

Frattini, C., Villa-Hernández, S., Pellicanò, G., Jossen, R., Katou, Y., Shirahige, K., et al. (2017). Cohesin ubiquitylation and mobilization facilitate stalled replication fork dynamics. *Mol. Cell* 68, 758–772. doi: 10.1016/j.molcel.2017.10.012

Gerland, P., Raftery, A. E., Ševčíková, H., Li, N., Gu, D., Spoorenberg, T., et al. (2014). World population stabilization unlikely this century. *Science* 346, 234–237. doi: 10.1126/science.1257469

Haarhuis, J. H. I., van der Weide, R. H., Blomen, V. A., Yáñez-Cuna, J. O., Amendola, M., van Ruiten, M. S., et al. (2017). The cohesin release factor WAPL restricts chromatin loop extension. *Cell* 169, 693–707.e14. doi: 10.1016/j.cell.2017.04.013

Hassler, M., Shaltiel, I. A., Kschonsak, M., Simon, B., Merkel, F., Thärichen, L., et al. (2019). Structural basis of an asymmetric condensin ATPase cycle. *Mol. Cell* 74, 1175–1188.e9. doi: 10.1016/j.molcel.2019.03.037

He, Y., Wang, J., Qi, W., and Song, R. (2019). Maize Dek15 encodes the cohesin-loading complex subunit scc4 and is essential for chromosome segregation and kernel development. *Plant Cell* 31, 465–485. doi: 10.1105/tpc.18.00921

Hesse, S., Zelkowski, M., Mikhailova, E. I., Keijzer, C. J., Houben, A., and Schubert, V. (2019). Ultrastructure and dynamics of synaptonemal complex components during meiotic pairing and synapsis of standard (A) and accessory (B) rye chromosomes. *Front. Plant Sci.* 10:773. doi: 10.3389/fpls.2019.00773

Hsieh, Y. Y. P., Makrantoni, V., Robertson, D., Marston, A. L., and Murray, A. W. (2020). Evolutionary repair: changes in multiple functional modules allow meiotic cohesin to support mitosis. *PLoS Biol.* 18:e3000635. doi: 10.1371/journal.pbio.3000635

Jaskowiak, J., Tkaczyk, O., Slota, M., Kwasniewska, J., and Szarejko, I. (2018). Analysis of aluminum toxicity in *Hordeum vulgare* roots with an emphasis on DNA integrity and cell cycle. *PLoS One* 13:e0193156. doi: 10.1371/journal.pone.0193156

Khanday, I., Skinner, D., Yang, B., Mercier, R., and Sundaresan, V. (2019). A male-expressed rice embryogenic trigger redirected for asexual propagation through seeds. *Nature* 565, 91–95. doi: 10.1038/s41586-018-0785-8

Kim, J. H., Ryu, T. H., Lee, S. S., Lee, S., and Chung, B. Y. (2019). Ionizing radiation manifesting DNA damage response in plants: an overview of DNA damage signaling and repair mechanisms in plants. *Plant Sci.* 27, 44–53. doi: 10.1016/j.plantsci.2018.10.013

Kim, J. H., Yu, R. M., Kim, J. S., Oh, M. H., Lee, J. W., and Byung, Y. C. (2007). Transcriptomic profile of *Arabidopsis* rosette leaves during the reproductive stage after exposure to ionizing radiation. *Radiat. Res.* 168, 267–280. doi: 10.1667/RR0963.1

Kobbe, D., Blanck, S., Focke, M., and Puchta, H. (2009). Biochemical characterization of AtRECQ3 reveals significant differences relative to other RecQ helicases. *Plant Physiol.* 151, 1658–1666. doi: 10.1104/pp.109.144709

Krupa, S. V., and Jäger, H.-J. (2006). "Adverse effects of elevated levels of ultraviolet (UV)-B radiation and ozone (O_3) on grop growth and productivity" in *Global climate change and agricultural production. Direct and indirect effects of changing hydrological, pedological and plant physiological processes*. eds. F. Bazzaz and W. Sombroek (Chichester: Food and Agriculture Organization Of The United Nations and John Wiley & Sons).

Lambing, C., Kuo, P. C., Tock, A. J., Topp, S. D., and Henderson, I. R. (2020a). ASY1 acts as a dosage-dependent antagonist of telomere-led recombination and mediates crossover interference in Arabidopsis. *Proc. Natl. Acad. Sci. U. S. A.* 117, 13647–13658. doi: 10.1073/pnas.1921055117

Lambing, C., Tock, A. J., Topp, S. D., Choi, K., Kuo, P. C., Zhao, X., et al. (2020b). Interacting genomic landscapes of REC8-cohesin, chromatin, and meiotic recombination in Arabidopsis. *Plant Cell* 32, 1218–1239. doi: 10.1105/tpc.19.00866

Lee, C. Y., Lin, H. J., Viswanath, K. K., Lin, C. P., Chang, B. C. H., Chiu, P. H., et al. (2018). The development of functional mapping by three sex-related loci on the third whorl of different sex types of *Carica papaya* L. *PLoS One* 13:e0194605. doi: 10.1371/journal.pone.0194605

Li, X., Ye, J., Ma, H., and Lu, P. (2018). Proteomic analysis of lysine acetylation provides strong evidence for involvement of acetylated proteins in plant meiosis and tapetum function. *Plant J.* 93, 142–154. doi: 10.1111/tpj.13766

Li, C., Zhang, R., Meng, X., Chen, S., Zong, Y., Lu, C., et al. (2020). Targeted, random mutagenesis of plant genes with dual cytosine and adenine base. *Nat. Biotechnol.* 38, 875–882. doi: 10.1038/s41587-019-0393-7

Liao, Z., Yu, Q., and Ming, R. (2017). Development of male-specific markers and identification of sex reversal mutants in papaya. *Euphytica* 213:53. doi: 10.1007/s10681-016-1806-z

Lindfors, A., and Arola, A. (2008). On the wavelength-dependent attenuation of UV radiation by clouds. *Geophys. Res. Lett.* 35:L05806. doi: 10.1029/2007GL032571

Liu, H. W., Bouchoux, C., Panarotto, M., Kakui, Y., Patel, H., and Uhlmann, F. (2020). Division of labor between PCNA loaders in DNA replication and sister chromatid cohesion establishment. *Mol. Cell* 78, 725–738.e4. doi: 10.1016/j.molcel.2020.03.017

Liu, C., Cheng, Y., Wang, J., and Weigel, D. (2017a). Prominent topologically associated domains differentiate global chromatin packing in rice from *Arabidopsis*. *Nat. Plants* 3, 742–748. doi: 10.1038/s41477-017-0005-9

Liu, C., Stael, S., Gevaert, K., Van Breusegem, F., Bozhkov, P. V., and Moschou, P. N. (2017b). The proteolytic landscape of an *Arabidopsis* separase-deficient mutant reveals novel substrates associated with plant development. bioRxiv [Preprint], 140962, 1–24. doi: 10.1101/140962

Macheret, M., and Halazonetis, T. D. (2015). DNA replication stress as a hallmark of cancer. *Annu. Rev. Pathol. Mech. Dis.* 10, 425–448. doi: 10.1146/annurev-pathol-012414-040424

Meisenberg, C., Pinder, S. I., Hopkins, S. R., Wooller, S. K., Benstead-Hume, G., Pearl, F. M. G., et al. (2019). Repression of transcription at DNA breaks requires cohesin throughout interphase and prevents genome instability. *Mol. Cell* 73, 212–223.e7. doi: 10.1016/j.molcel.2018.11.001

Minchell, N. E., Keszthelyi, A., and Baxter, J. (2020). Cohesin causes replicative DNA damage by trapping DNA topological stress. *Mol. Cell* 78, 739–751.e8. doi: 10.1016/j.molcel.2020.03.013

Moldovan, G. L., Pfander, B., and Jentsch, S. (2006). PCNA controls establishment of sister chromatid cohesion during S phase. *Mol. Cell* 23, 723–732. doi: 10.1016/j.molcel.2006.07.007

Municio, C., Antosz, W., Grasser, K. D., Kornobis, E., Van Bel, M., Eguinoa, I., et al. (2021). The Arabidopsis condensin CAP-D subunits arrange interphase chromatin. *New Phytol.* doi: 10.1111/nph.17221 [Epub ahead of print]

Muñoz, S., Minamino, M., Casas-Delucchi, C. S., Patel, H., and Uhlmann, F. (2019). A role for chromatin remodeling in cohesin loading onto chromosomes. *Mol. Cell* 74, 664–673.e5. doi: 10.1016/j.molcel.2019.02.027

Muñoz, S., Passarelli, F., and Uhlmann, F. (2020). Conserved roles of chromatin remodellers in cohesin loading onto chromatin. *Curr. Genet.* 77, 1–21. doi: 10.1007/s00294-020-01075-x

Ning, Y., Liu, Q., Wang, C., Qin, E., Wu, Z., Wang, M., et al. (2020). Heat stress interferes with formation of double-strand breaks and homology synapsis in *Arabidopsis thaliana*. bioRxiv [Preprint]. doi: 10.1101/2020.10.02.324269

Nisa, M. U., Huang, Y., Benhamed, M., and Raynaud, C. (2019). The plant DNA damage response: signaling pathways leading to growth inhibition and putative role in response to stress conditions. *Front. Plant Sci.* 10:653. doi: 10.3389/fpls.2019.00653

Panhwar, Q. A., Naher, U. A., Radziah, O., Shamshuddin, J., and Razi, I. M. (2015). Eliminating aluminum toxicity in an acid sulfate soil for rice cultivation using plant growth promoting bacteria. *Molecules* 20, 3628–3646. doi: 10.3390/molecules20033628

Pawlowski, W., Wang, C., Golubovskaya, I. N., Szymaniak, J. M., Shi, L., Hamant, O., et al. (2009). Maize AMEIOTIC1 is essential for multiple early meiotic processes and likely required for the initiation of meiosis. *Proc. Natl. Acad. Sci. U. S. A.* 106, 3603–3608. doi: 10.1073/pnas.0810115106

Pradillo, M., Knoll, A., Oliver, C., Varas, J., Corredor, E., Puchta, H., et al. (2015). Involvement of the cohesin cofactor PDS5 (SPO76) during meiosis and DNA repair in *Arabidopsis thaliana*. *Front. Plant Sci.* 6:1034. doi: 10.3389/fpls.2015.01034

Puizina, J., Siroky, J., Mokros, P., Schweizer, D., and Riha, K. (2004). Mre11 deficiency in Arabidopsis is associated with chromosomal instability in somatic cells and Spo11-dependent genome fragmentation during meiosis. *Plant Cell* 16, 1968–1978. doi: 10.1105/tpc.104.022749

Qi, Y. (ed.) (2019). "Plant genome editing with CRISPR systems" in *Methods in protocols* (New York: Humana Press).

Rius, S. P., Emiliani, J., and Casati, P. (2016). P1 epigenetic regulation in leaves of high altitude maize landraces: effect of UV-B radiation. *Front. Plant Sci.* 7:523. doi: 10.3389/fpls.2016.00523

Sakamoto, A. N. (2019). Translesion synthesis in plants: ultraviolet resistance and beyond. *Front. Plant Sci.* 10:1208. doi: 10.3389/fpls.2019.01208

Sakamoto, T., Inui, Y. T., Uraguchi, S., Yoshizumi, T., Matsunaga, S., Mastui, M., et al. (2011). Condensin II alleviates DNA damage and is essential for tolerance of boron overload stress in *Arabidopsis*. *Plant Cell* 23, 3533–3546. doi: 10.1105/tpc.111.086314

Sakamoto, T., Sugiyama, T., Yamashita, T., and Matsunaga, S. (2019). Plant condensin II is required for the correct spatial relationship between centromeres and rDNA arrays. *Nucleus* 10, 116–125. doi: 10.1080/19491034.2019.1616507

Scheben, A., and Edwards, D. (2018). Towards a more predictable plant breeding pipeline with CRISPR/Cas-induced allelic series to optimize quantitative and qualitative traits. *Curr. Opin. Plant Biol.* 45, 218–225. doi: 10.1016/j.pbi.2018.04.013

Schneider, T., Kaul, C. M., and Pressel, K. G. (2019). Possible climate transitions from breakup of stratocumulus decks under greenhouse warming. *Nat. Geosci.* 12, 163–167. doi: 10.1038/s41561-019-0310-1

Schubert, V., Lermontova, I., and Schubert, I. (2013). The Arabidopsis CAP-D proteins are required for correct chromatin organisation, growth and fertility. *Chromosoma* 122, 517–533. doi: 10.1007/s00412-013-0424-y

Séguéla-Arnaud, M., Choinard, S., Larchevêque, C., Girard, C., Froger, N., Crismani, W., et al. (2017). RMI1 and TOP3α limit meiotic CO formation through their C-terminal domains. *Nucleic Acids Res.* 45, 1860–1871. doi: 10.1093/nar/gkw1210

Shahid, S. (2020). The rules of attachment: Rec8 cohesin connects chromatin architecture and recombination machinery in meiosis. *Plant Cell* 32, 808–829. doi: 10.1105/tpc.20.00094

Shen, X., Dong, Z., and Chen, Y. (2015). Drought and UV-B radiation effect on photosynthesis and antioxidant parameters in soybean and maize. *Acta Physiol. Plant.* 37:25. doi: 10.1007/s11738-015-1778-y

Shi, D., Zhao, S., Zuo, M. Q., Zhang, J., Hou, W., Dong, M. Q., et al. (2020). The acetyltransferase Eco1 elicits cohesin dimerization during S phase. *J. Biol. Chem.* 295, 7554–7565. doi: 10.1074/jbc.RA120.013102

Silva, M. C. C., Powell, S., Ladstätter, S., Gassler, J., Stocsits, R., Tedeschi, A., et al. (2020). Wapl releases Scc1-cohesin and regulates chromosome structure and segregation in mouse oocytes. *J. Cell Biol.* 219:e201906100. doi: 10.1083/jcb.201906100

Sjögren, C. A., and Larsen, P. B. (2017). SUV2, which encodes an ATR-related cell cycle checkpoint and putative plant ATRIP, is required for aluminium-dependent root growth inhibition in Arabidopsis. *Plant Cell Environ.* 40, 1849–1860. doi: 10.1111/pce.12992

Stokes, D. G., Tartof, K. D., and Perry, R. P. (1996). CHD1 is concentrated in interbands and puffed regions of Drosophila polytene chromosomes. *Proc. Natl. Acad. Sci. U. S. A.* 93, 7137–7142. doi: 10.1073/pnas.93.14.7137

Szilard, R. K., Jacques, P. T., Laramée, L., Cheng, B., Galicia, S., Bataille, A. R., et al. (2010). Systematic identification of fragile sites via genome-wide location analysis of γ-H2AX. *Nat. Struct. Mol. Biol.* 17, 299–305. doi: 10.1038/nsmb.1754

Taagen, E., Bogdanove, A. J., and Sorrells, M. E. (2020). Counting on crossovers: controlled recombination for plant breeding. *Trends Plant Sci.* 25, 455–465. doi: 10.1016/j.tplants.2019.12.017

Takahashi, N., Quimbaya, M., Schubert, V., Lammens, T., Vandepoele, K., Schubert, I., et al. (2010). The MCM-binding protein ETG1 aids sister chromatid cohesion required for postreplicative homologous recombination repair. *PLoS Genet.* 6:e1000817. doi: 10.1371/journal.pgen.1000817

Tsukiyama, T., Palmer, J., Landel, C. C., Shiloach, J., and Wu, C. (1999). Characterization of the imitation switch subfamily of ATP-dependent chromatin-remodeling factors in *Saccharomyces cerevisiae*. *Genes Dev.* 13, 686–697. doi: 10.1101/gad.13.6.686

Vandenhove, H., Vanhoudt, N., Cuypers, A., van Hees, M., Wannijn, J., and Horemans, N. (2010). Life-cycle chronic gamma exposure of *Arabidopsis thaliana* induces growth effects but no discernable effects on oxidative stress pathways. *Plant Physiol. Biochem.* 48, 778–786. doi: 10.1016/j.plaphy.2010.06.006

Vara, C., Paytuví-Gallart, A., Cuartero, Y., Le Dily, F., Garcia, F., Salvà-Castro, J., et al. (2019). Three-dimensional genomic structure and cohesin occupancy correlate with transcriptional activity during spermatogenesis. *Cell Rep.* 28, 352–367. doi: 10.1016/j.celrep.2019.06.037

Venegas, A. B., Natsume, T., Kanemaki, M., and Hickson, I. D. (2020). Inducible degradation of the human SMC5/6 complex reveals an essential role only during interphase. *Cell Rep.* 31:107533. doi: 10.1016/j.celrep.2020.107533

Wang, K. (2020). Fixation of hybrid vigor in rice: synthetic apomixis generated by genome editing. *aBIOTECH* 1, 15–20. doi: 10.1007/s42994-019-00001-1

Wang, J., Blevins, T., Podicheti, R., Haag, J. R., Tan, E. H., Wang, F., et al. (2017). Mutation of Arabidopsis SMC4 identifies condensin as a corepressor

of pericentromeric transposons and conditionally expressed genes. *Genes Dev.* 31, 1601–1614. doi: 10.1101/gad.301499.117

Wang, H., Xu, W., Sun, Y., Lian, Q., Wang, C., Yu, C., et al. (2020). The cohesin loader SCC2 contains a PHD finger that is required for meiosis in land plants. *PLoS Genet.* 16:e1008849. doi: 10.1371/journal.pgen.1008849

Wang, Y., Zhang, W. Z., Song, L. F., Zou, J. J., Su, Z., and Wu, W. H. (2008). Transcriptome analyses show changes in gene expression to accompany pollen germination and tube growth in Arabidopsis. *Plant Physiol.* 148, 1201–1211. doi: 10.1104/pp.108.126375

Watanabe, K., Pacher, M., Dukowic, S., Schubert, V., Puchta, H., and Schubert, I. (2009). The STRUCTURAL MAINTENANCE OF CHROMOSOMES 5/6 complex promotes sister chromatid alignment and homologous recombination after DNA damage in *Arabidopsis thaliana*. *Plant Cell* 21, 2688–2699. doi: 10.1105/tpc.108.060525

Waters, P. D., and Ruiz-Herrera, A. (2020). Meiotic executioner genes protect the Y from extinction. *Trends Genet.* 36, 728–738. doi: 10.1016/j.tig.2020.06.008

Waterworth, W. M., Bray, C. M., and West, C. E. (2019). Seeds and the art of genome maintenance. *Front. Plant Sci.* 10:706. doi: 10.3389/fpls.2019.00706

Wijewardana, C., Henry, W. B., Gao, W., and Reddy, K. R. (2016). Interactive effects on CO_2, drought, and ultraviolet-B radiation on maize growth and development. *J. Photochem. Photobiol. B Biol.* 160, 198–209. doi: 10.1016/j.jphotobiol.2016.04.004

Yang, X., Boateng, K. A., Strittmatter, L., Burgess, R., and Makaroff, C. A. (2009). Arabidopsis separase functions beyond the removal of sister chromatid cohesion during meiosis. *Plant Physiol.* 151, 323–333. doi: 10.1104/pp.109.140699

Yang, C., Hamamura, Y., Sofroni, K., Böwer, F., Stolze, S. C., Nakagami, H., et al. (2019). SWITCH 1/DYAD is a WINGS APART-LIKE antagonist that maintains sister chromatid cohesion in meiosis. *Nat. Commun.* 10:1755. doi: 10.1038/s41467-019-09759-w

Yoshiyama, K. O., Kimura, S., Maki, H., Britt, A. B., and Umeda, M. (2014). The role of SOG1, a plant-specific transcriptional regulator, in the DNA damage response. *Plant Signal. Behav.* 9, 1–8. doi: 10.4161/psb.28889

Yuan, L., Yang, X., Auman, D., and Makaroff, C. A. (2014). Expression of epitope-tagged SYN3 cohesin proteins can disrupt meiosis in Arabidopsis. *J. Genet. Genom.* 41, 153–164. doi: 10.1016/j.jgg.2013.11.006

Zaka, R., Chenal, C., and Misset, M. (2004). Effects of low doses of short-term gamma irradiation on growth and development through two generations of *Pisum sativum*. *Sci. Total Environ.* 320, 121–129. doi: 10.1016/j.scitotenv.2003.08.010

Zelkowski, M., Zelkowska, K., Conrad, U., Hesse, S., Lermontova, I., Marzec, M., et al. (2019). Arabidopsis NSE4 proteins act in somatic nuclei and meiosis to ensure plant viability and fertility. *Front. Plant Sci.* 10:774. doi: 10.3389/fpls.2019.00774

Zhang, J., Feng, C., Su, H., Liu, Y., Liu, Y., and Han, F. (2020). The cohesin complex subunit ZmSMC3 participates in meiotic centromere pairing in maize. *Plant Cell* 32, 1323–1336. doi: 10.1105/tpc.19.00834

Zhang, W., Wang, X., Yu, Q., Ming, R., and Jiang, J. (2008). DNA methylation and heterochromatinization in the male-specific region of the primitive Y chromosome of papaya. *Genome Res.* 18, 1938–1943. doi: 10.1101/gr.078808.108

Zhao, C., Liu, B., Piao, S., Wang, X., Lobell, D. B., Huang, Y., et al. (2017). Temperature increase reduces global yields of major crops in four independent estimates. *Proc. Natl. Acad. Sci.* 114, 9326–9331. doi: 10.1073/pnas.1701762114

Conflict of Interest: The author declares that the research was conducted in the absence of any commercial or financial relationships that could be construed as a potential conflict of interest.

frontiers in Plant Science

REVIEW
published: 07 April 2021
doi: 10.3389/fpls.2021.667314

Ubiquitination in Plant Meiosis: Recent Advances and High Throughput Methods

Jamie N. Orr[1], Robbie Waugh[1,2,3] and Isabelle Colas[1]**

[1] Cell and Molecular Sciences, The James Hutton Institute, Dundee, United Kingdom, [2] School of Life Sciences, University of Dundee, Dundee, United Kingdom, [3] School of Agriculture and Wine, University of Adelaide, Adelaide, SA, Australia

Meiosis is a specialized cell division which is essential to sexual reproduction. The success of this highly ordered process involves the timely activation, interaction, movement, and removal of many proteins. Ubiquitination is an extraordinarily diverse post-translational modification with a regulatory role in almost all cellular processes. During meiosis, ubiquitin localizes to chromatin and the expression of genes related to ubiquitination appears to be enhanced. This may be due to extensive protein turnover mediated by proteasomal degradation. However, degradation is not the only substrate fate conferred by ubiquitination which may also mediate, for example, the activation of key transcription factors. In plant meiosis, the specific roles of several components of the ubiquitination cascade—particularly SCF complex proteins, the APC/C, and HEI10—have been partially characterized indicating diverse roles in chromosome segregation, recombination, and synapsis. Nonetheless, these components remain comparatively poorly understood to their counterparts in other processes and in other eukaryotes. In this review, we present an overview of our understanding of the role of ubiquitination in plant meiosis, highlighting recent advances, remaining challenges, and high throughput methods which may be used to overcome them.

Keywords: meiosis, ubiquitin, plant, HEI10, APC/C, SCF

OPEN ACCESS

Edited by:
Christophe Lambing, University of Cambridge, United Kingdom

Reviewed by:
Marina Martinez-Garcia, Harvard Medical School, United States
Stefan Heckmann, Leibniz Institute of Plant Genetics and Crop Plant Research (IPK), Germany

****Correspondence:***
Jamie N. Orr
jamie.orr@hutton.ac.uk
Isabelle Colas
isabelle.colas@hutton.ac.uk

Specialty section:
This article was submitted to Plant Cell Biology, a section of the journal Frontiers in Plant Science

Received: *12 February 2021*
Accepted: *15 March 2021*
Published: *07 April 2021*

Citation:
Orr JN, Waugh R and Colas I (2021) Ubiquitination in Plant Meiosis: Recent Advances and High Throughput Methods. Front. Plant Sci. 12:667314. doi: 10.3389/fpls.2021.667314

INTRODUCTION

Meiosis

Meiosis is the production of haploid gametes through one round of DNA replication followed by two successive rounds of cell division. Meiotic recombination is the foundation of plant breeding efforts—essential to global food security—which seek to increase yield, drought tolerance, or resistance to pathogens in response to pressures on the food system such as global warming and a growing population. During the first meiotic division, replicated parental chromosomes—consisting of sister chromatids bound together by a ring-like complex called cohesin—condense, form homologous pairs, and are linked by a specialized tripartite protein structure called the synaptonemal complex (SC). Pairing is facilitated by the formation of double strand breaks (DSBs) in looped chromatin fibers, universally catalyzed by the conserved topoisomerase Spo11 (Bergerat et al., 1997; Keeney et al., 1997; Grelon et al., 2001), in conjunction with several other protein subgroups (Cole et al., 2010). DSB formation begins the process of meiotic recombination which is a result of their repair following partial 5′–3′ degradation (resection) of one strand of DNA at

both sides of the break, yielding 3′-ended single stranded DNA (Osman et al., 2011; Mercier et al., 2015; Wang and Copenhaver, 2018; Pyatnitskaya et al., 2019). DSBs may be resolved as class I or class II crossovers (COs) or as non-crossovers (NCOs); NCOs being much more common than COs (Franklin et al., 1999; Copenhaver et al., 2002; Mercier et al., 2005). Considerable progress has been made in dissecting the timing, movement, and proteins which are involved in meiotic division, and their effects on recombination. The critical function of post-translational modifications (PTMs) in the regulation of meiotic division and recombination in eukaryotes is well-established (Sawada et al., 2014). One of the most abundant PTMs of proteins is ubiquitination, the covalent attachment of the 76 amino acid protein ubiquitin to target proteins (Ciehanover et al., 1978; Swatek and Komander, 2016). Ubiquitination regulates almost all cellular processes (Dye and Schulman, 2007). During meiosis, chromosome axes show extensive ubiquitination (Rao et al., 2017; Li Y. et al., 2018), while specific ubiquitin cascade interactions are required for key processes such as homologous recombination (Ward et al., 2007; Chelysheva et al., 2012; Wang et al., 2012) and chromosome segregation (Wang et al., 2013; Jonak et al., 2017; Kernan et al., 2018; Yamano, 2019).

Ubiquitination

Ubiquitin shows remarkable conservation in the evolutionary history of eukaryotes, while the ubiquitination cascade has undergone massive expansion, resulting in one of the most versatile protein PTMs (Dye and Schulman, 2007; Zuin et al., 2014). This versatility derives from the ability of ubiquitin to form linked chains (polyubiquitination) *via* attachment of its C-terminal di-glycine motif (GG) to another ubiquitin protein at one of seven lysine (K6, K11, K27, K29, K33, K48, and K63) residues or to an N terminal methionine residue (M1) (Kulathu and Komander, 2012; López-Mosqueda and Dikic, 2014). In addition to polyubiquitination, proteins can be mono- or multi-monoubiquitinylated with unlinked ubiquitin (Emmerich and Cohen, 2015). Ubiquitin chains can be extended by a single linkage type or by multiple linkage types which may be formed at multiple residues on the same ubiquitin molecule forming a branched chain (**Figure 1**; Swatek and Komander, 2016). Ubiquitin can also be directly modified—in addition to the attachment of further ubiquitin to generate chains—by acetylation, phosphorylation, and attachment of ubiquitin-like modifiers (Swatek and Komander, 2016).

The canonical function of protein ubiquitination is to target the substrate for degradation by the proteasome, first described by Ciehanover et al. (1978). However, ubiquitin chain topology can confer specific substrate fates other than proteasomal degradation including recruitment of binding partners (Huang and D'Andrea, 2010), activation (Xu et al., 2009), or nuclear uptake (Plafker et al., 2004). Ubiquitination of a target protein is a tightly controlled cascade of ubiquitin activation, conjugation, and ligation involving three enzymes of increasing abundance and specificity—E1 activating enzymes, E2 conjugating enzymes, and E3 ligases (Dye and Schulman, 2007). E1 ubiquitin activating enzymes hydrolyze ATP forming an AMP-ubiquitin intermediate (Hatfield et al., 1997). The E1 enzyme then displaces AMP to form a thioester linkage to ubiquitin between an internal cysteine residue in the E1 and the carboxyterminal glycine of ubiquitin (Hatfield et al., 1997). The ubiquitin thioester bond is then transferred from the E1 activating enzyme to a cysteine residue in the ubiquitin conjugating (UBC) domain of an E2 conjugating enzyme (Ramadan et al., 2015). E3 ligases recruit ubiquitin conjugated E2s and target substrate proteins, conferring substrate specificity to the ubiquitination cascade (Iconomou and Saunders, 2016). E3 ligases can be divided into really interesting new gene (RING)/U-box, RING-in-between-RING (RBR), and homologous to E6AP C-terminus (HECT) domain containing groups (Dove et al., 2016). RING domain E3 ligases are the most abundant, binding both the substrate and E2-ubiquitin to catalyze the transfer of ubiquitin from E2 to the substrate protein (Dove et al., 2016). HECT E3s accept the transfer of the E2-thioester linkage forming an E3-ubiquitin intermediate before transferring ubiquitin to the substrate protein (Metzger et al., 2012). RBR E3 ligases are the least common and are characterized by the ordered appearance of a RING1 domain with a canonical structure, an in-between RING (IBR) domain, and a RING2 domain with a non-canonical RING structure (Dove et al., 2016). Although RBR E3s contain an E2-binding RING domain, they form a HECT-like E3-ubiquitin intermediate before transfer of ubiquitin to the substrate protein (Dove et al., 2016). The RING E3 ubiquitin ligases can be further subdivided into single and multi-subunit proteins (Iconomou and Saunders, 2016). An additional class of enzymes—E4 ubiquitin ligases—can extend shorter ubiquitin chains generated by E3 ligases (Hoppe, 2005). This can alter the fate of ubiquitinated protein from activation or transport to proteasomal degradation (Hoppe, 2005). Ubiquitination of substrate proteins by E3 and E4 ligases can also be trimmed or removed by deubiquitinating enzymes (DUBs), cysteine or metalloproteases which hydrolyze the bond between the modified protein and the C-terminal glycine of ubiquitin (Komander et al., 2009). Trimming or removal of ubiquitin can similarly alter substrate fate. The balance of E3/E4 and DUB activity can allow for fine tuning of protein activity as has been recently demonstrated in the acquisition of systemic acquired resistance in *Arabidopsis* (Huang et al., 2014; Skelly et al., 2019).

Ubiquitination seems to play an enhanced role in meiotic processes in all plants and higher eukaryotes. Transcriptome dynamics and characterization of a limited number of ligases indicates significant and varied roles for the ubiquitination cascade in plant meiosis which we are only beginning to explain. Although the identification of E3 substrate specificity is notoriously difficult, a number of tools are now available which may enable higher resolution characterization of such proteins, their target substrates, the types of ubiquitin chain linkages they build, and the roll of specific ubiquitination chain conformations in meiotic processes (Emmerich and Cohen, 2015; Iconomou and Saunders, 2016). Here we discuss recent developments in our understanding of ubiquitin—and ubiquitin like modifiers—in plant meiosis, with an emphasis on what is currently known about the role of specific E3 ubiquitin ligases and their substrates. Recent advances in mass spectrometry based molecular methods

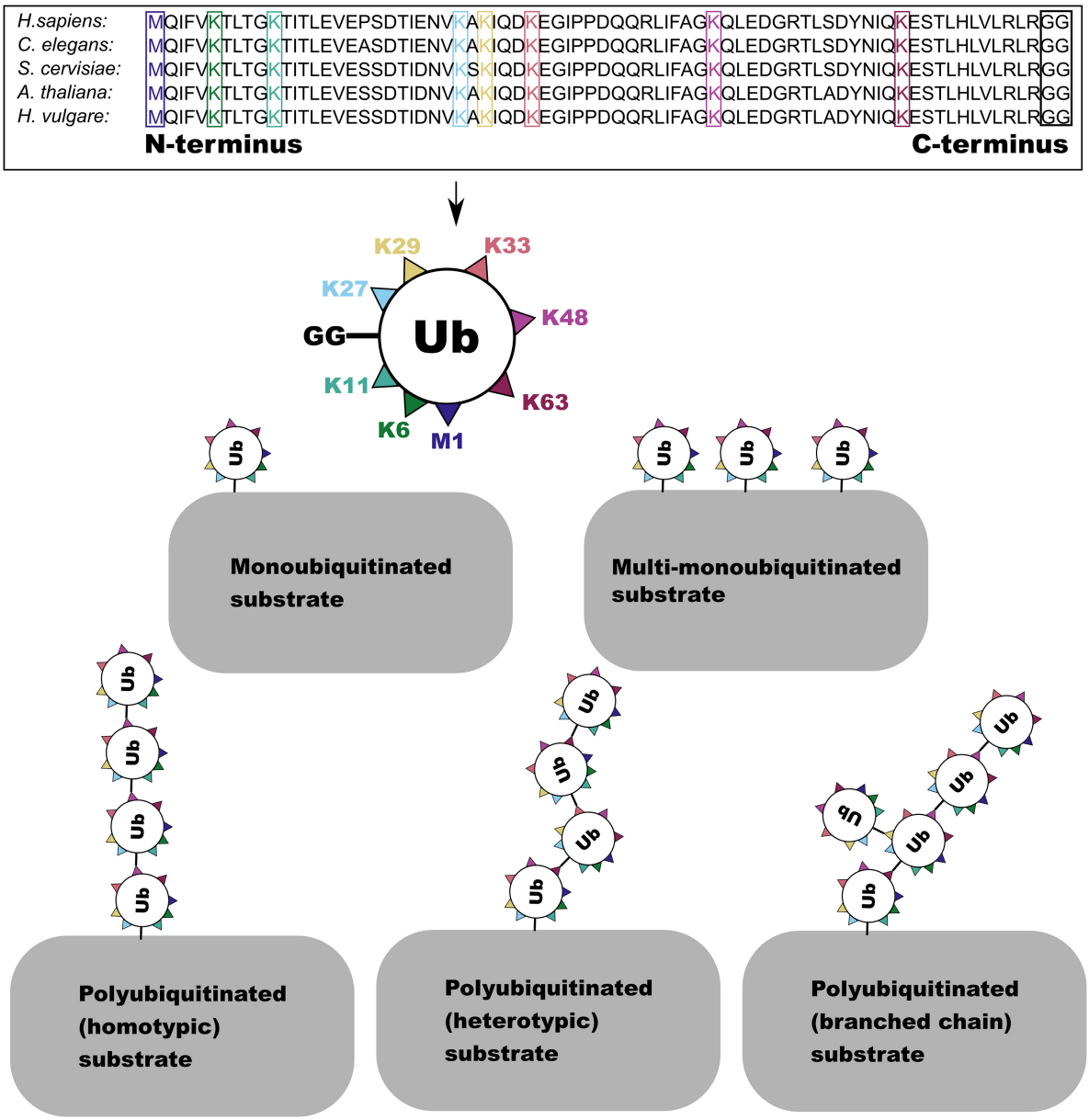

FIGURE 1 | The amino acid sequence of the ubiquitin monomer is highly conserved across eukaryotes. Here the one N terminal methionine (M) and seven lysine (K) residues in the sequence which are able to form linkages with the C-terminal GG residue (boxed in black) are highlighted. This enables the formation of several forms of ubiquitin and polyubiquitin conjugate.

of identifying these interactions are also discussed in the context of their application to plant meiotic tissues.

TRANSCRIPTOME DYNAMICS CONSISTENTLY INDICATE AN ENHANCED ROLE FOR UBIQUITINATION IN PLANT MEIOSIS

Enrichment of ubiquitin-proteasome system components is a common theme in plant meiotic transcriptome dynamics. In *Arabidopsis*, Yang et al. (2011) found that five of 17 Pfam domains significantly enriched in male meiocytes were related to ubiquitination. This was also reflected in the significant enrichment of the ubiquitination GO term (Yang et al., 2011). In our recent analysis of the barley anther meiotic transcriptome (BAnTr) dynamics we report significantly enriched expression of 71 potential E3 ligase genes in meiocytes, and differential expression of 166 putative E3 ligase genes before, during, or after prophase I in anthers (Barakate et al., 2021). Two genes orthologous to a *Drosophila melanogaster* seven *in absentia* (SINA) E3 ligase recently implicated in regulation of

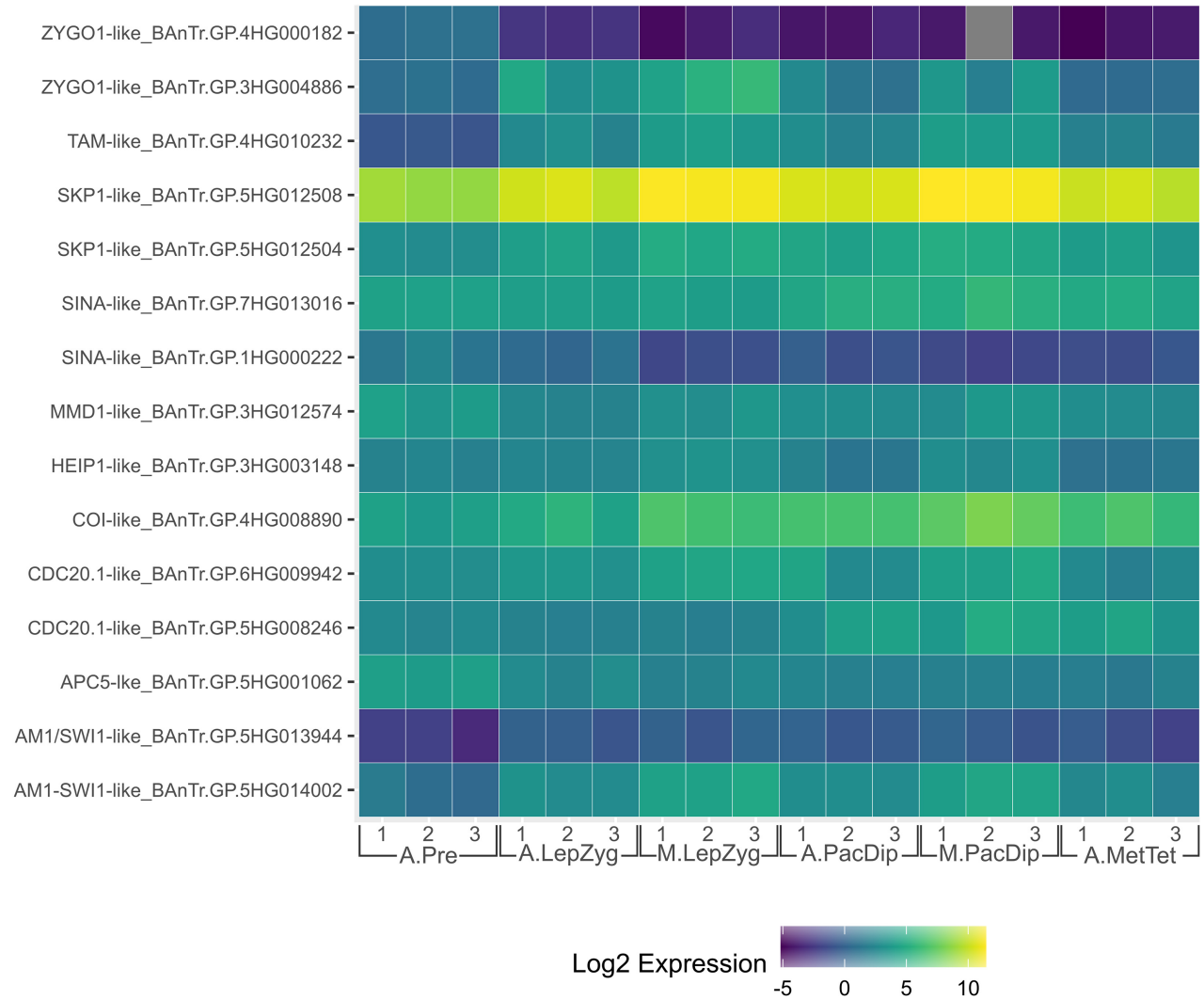

FIGURE 2 | Heat map of expression of genes orthologous to those discussed in this review in the Barley Anther and Meiocyte Transcriptome (BAnTr) dataset. Three replicates each of anthers at pre-meiosis (A.Pre); anthers at leptotene–zygotene stages (A.LepZyg); meiocytes at leptotene–zygotene stages (M.LepZyg); anthers at pachytene–diplotene stages (A.PacDip); meiocytes at pachytene–diplotene stages (M.PacDip); and anthers at metaphase–tetrad stages (A.MetTet).

both assembly and disassembly of the SC (CG9949; Hughes et al., 2019), showed significant differential expression in barley prophase I (**Figure 2**). A further thirteen genes orthologous to E3 ligases or interactors with known roles in meiosis (discussed below) were present in the list of BAnTr differentially expressed genes (**Figure 2**).

In maize, Yuan et al. (2018) reported that 39 genes preferentially expressed in pollen mother cells (PMCs) and 5 genes preferentially expressed in early PMCs (ePMCs) were E3 ubiquitin ligase components, including 18 F-box proteins in PMCs. F-box proteins confer substrate specificity as part of the multi-subunit SKP1-cullin_F-box (SCF) complex E3 ligases (Mocciaro and Rape, 2012), discussed in detail below. F-box proteins also appear to be enriched in rice meiotic tissues where Tang et al. (2010) identified 18 PMC enriched F-box-like genes. Interestingly, there is little crossover between these genes with only one of the PMC enriched F-box proteins in rice orthologous to those reported in maize. Further, this one rice F-box gene (**Figure 3**, highlighted in orange) is part of an expanded group of F-box-like genes in cereals which includes four of the 18 from maize but is far from the most similar rice ortholog to these four maize genes (**Figure 3**, highlighted in blue). This rice gene (Os04g0193300; F-box119) has no described role in replication or division but variants have been implicated in broad spectrum resistance to brown planthopper, an insect pest (Kamolsukyeunyong et al., 2019). This is the only characterization of any of the PMC preferentially expressed F-box genes in rice. Of the maize F-box genes, Zm00001d042833 (GRMZM2G125411; *ZmCOI1a*) is one of four maize orthologs of *CORONATINE INSENSITIVE (COI)-1* (An et al., 2018). The COI-1 protein is responsible for targeting the SCF complex to JAZMONATE ZIM-DOMIAIN 1, which binds

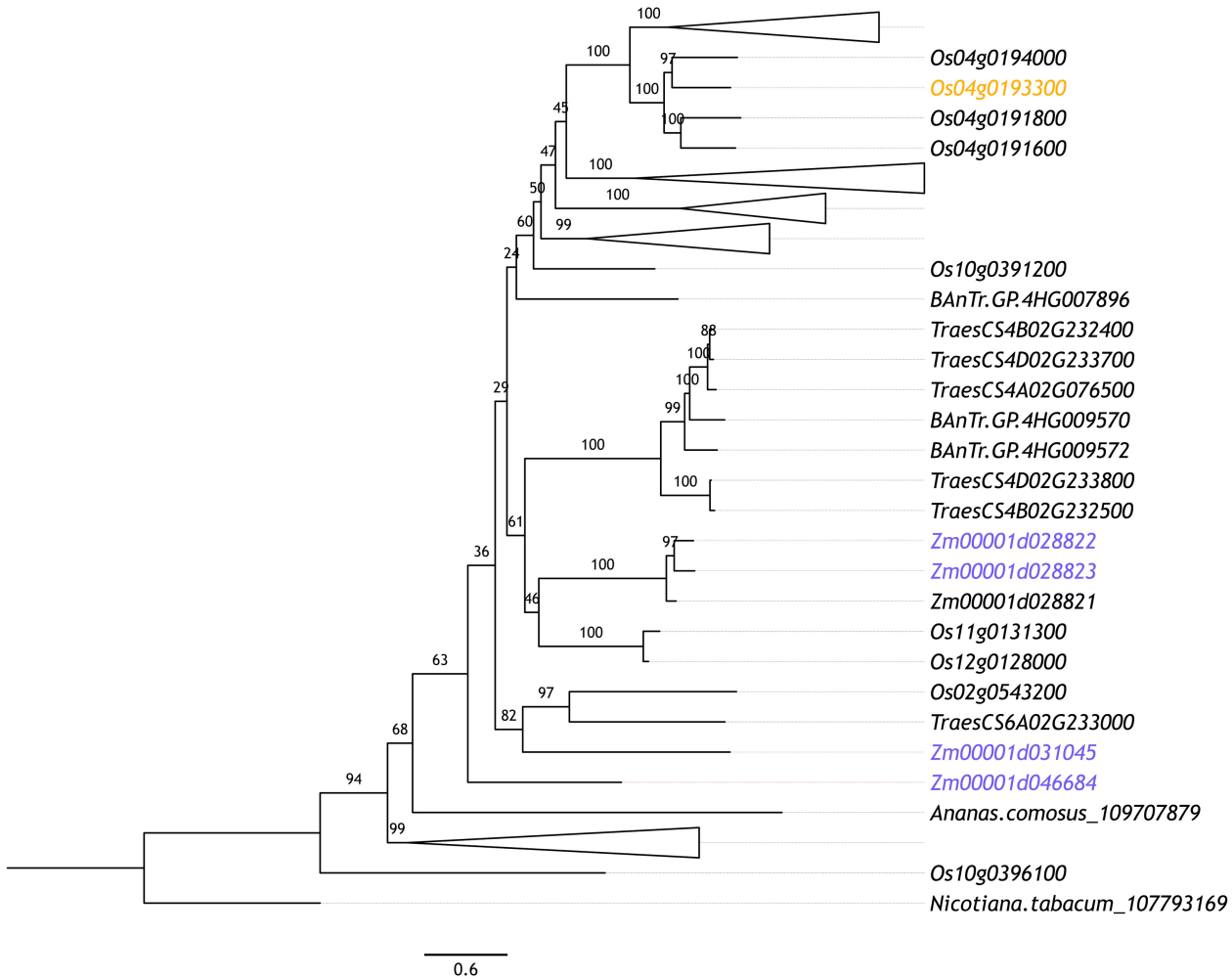

FIGURE 3 | Maximum likelihood phylogenetic tree of orthologous maize and rice F-box genes whose expression is indicated to be up-regulated in PMCs according to Yuan et al. (2018) (highlighted in blue) and Tang et al. (2010) (highlighted in orange), respectively. Orthologous sequences were identified from tobacco (*Nicotiana tabacum*), rice (*Oryza sativa*), maize (*Zea mays*), pineapple (*Ananas comosus*), and Barley (*Hordeum vulgare*) Anther and Meiocyte Transcriptome (BAnTr) dataset using OrthoFinder (v.2.3.3; Emms and Kelly, 2015). The longest orthologous sequences from each species were aligned using MAFFT (v7.266; Katoh and Standley, 2013). Alignments were refined using Gblocks (v0.91b; Castresana, 2000). Maximum likelihood phylogeny was computed using IQ-TREE (v1.6.9; Nguyen et al., 2014) with ultrafast bootstrapping (n = 1,000). The resultant phylogeny was plotted using FigTree (v1.4.3). Branches are labeled with bootstrap support.

to MYC transcription factors, repressing jasmonate responses (Thines et al., 2007; Yuan et al., 2018). In *Arabidopsis*, COI1 is required for male fertility (Xie et al., 1998). This is also true of its orthologs in maize which can rescue the infertility of *Arabidopsis* homozygous *coi1* mutants (An et al., 2018). Hence, COI1 enrichment in maize PMCs likely reflects increased jasmonate signaling pathway activity at the onset of meiosis. None of the 18 rice and maize F-box-like genes are orthologous to the F-box genes with characterized roles in plant meiosis, discussed below.

Taken together, these studies hint at the importance of ubiquitination to the regulation of plant meiosis. However, despite the vast number of ubiquitination related genes displaying differential expression in early meiosis, very few have been characterized. Currently, our understanding of the role of ubiquitination in this pathway is largely limited to a few extensively studied components: the SCF complex; the anaphase-promoting complex or cyclosome (APC/C); and human enhancer of invasion 10 (HEI10).

SCF COMPLEX E3s

SCF RING E3 ubiquitin ligase complexes consist of a conserved modular format where an E2 binding Ring-box protein (RBX) is linked *via* a cullin (CUL1) scaffolding protein to an S-phase kinase-associated adaptor protein (SKP) which in turn binds a substrate recognition F-Box protein (**Figure 4**; Mocciaro and Rape, 2012). F-box proteins are the most varied group in this complex and are the most significant determinant of substrate

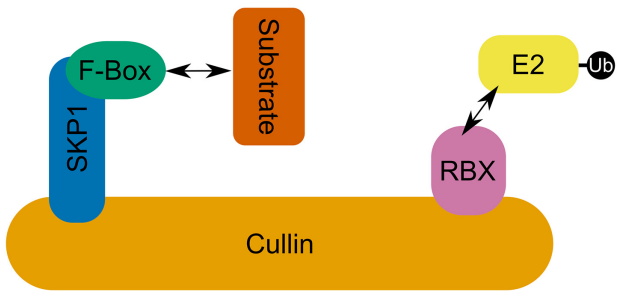

FIGURE 4 | The SCF complex in which an E2 interacting RBX domain containing protein is linked via a Cullin to SKP1 which binds an F-box domain containing protein facilitating SCF complex-substrate interactions.

specificity (Mocciaro and Rape, 2012). In fact, the F-box protein superfamily is one of the largest and most diverse in plants, although there is dramatic inter- and intra-specific variation in their number that is seemingly untethered to habitat or evolutionary history (Hua et al., 2011). *Arabidopsis* encodes 21 SKP1-like (ASK) proteins (Risseeuw et al., 2003). Among these, ASK1 and ASK2 are the most similar to SKP1 genes in yeast and humans—sharing 75% amino acid identity—and are able to interact with the same F-box proteins (Gagne et al., 2002; Kong et al., 2004). ASK1 is essential for *Arabidopsis* male fertility and synapsis (Yang et al., 1999; Wang and Yang, 2006). Transposon mutagenesis of ASK1 results in very stable association of homologous chromosomes which fail to separate at male anaphase I and remain associated at anaphase II despite normal spindle formation (Yang et al., 1999). ASK1 is also essential for the release of chromatin from the nucleolus which maintains a central location in mutants, failing to migrate to the nuclear periphery (Yang et al., 2006). Further, ASK1 appears to repress recombination as heterozygous ASK1/*ask1-1* plants demonstrate a recombination frequency approximately 2.6-fold greater than that of the wild type ASK1/ASK1 homolog (Wang and Yang, 2006). Despite the similarity of ASK1 and ASK2, *ask2* mutants are indistinguishable from wild type plants, showing no developmental defects (Liu et al., 2004). However, both ASK1 and ASK2 proteins are required for defective embryogenesis suggesting that they are in fact functionally redundant (Liu et al., 2004). The severity of the *ask1* single mutant in male meiosis seems to derive from the fact that while ASK1 is expressed in early prophase I anthers, ASK2 is not (Wang and Yang, 2006); while in developing embryos both ASK1 and ASK2 are expressed, allowing ASK2 to compensate for *ask1* mutants (Liu et al., 2004). Analysis of various ASK genes highlights diverse and overlapping expression patterns in organs and tissues as well as specific F-box interactions (Marrocco et al., 2003; Risseeuw et al., 2003; Takahashi et al., 2004; Dezfulian et al., 2012). Expression of wheat SKP1-like gene TSK1 in *Arabidopsis ask1-1/ask1-1* mutants was capable of partially rescuing of the sterile phenotype (Li et al., 2006). Recent evidence in mice—which along with humans and yeast possess only one *SKP1* gene—shows that SKP1 localizes specifically to the lateral element of the SC in spermatocytes where synapsis is complete (Guan et al., 2020). Further, germ cell specific inactivation of SKP1 in mouse testis led to the accumulation of HORMADs on the SC in pachytene and diplotene stages (Guan et al., 2020). Proteins of the HORMAD family regulate formation of DSBs and COs and their PCH2/TRIP13 mediated removal is involved in

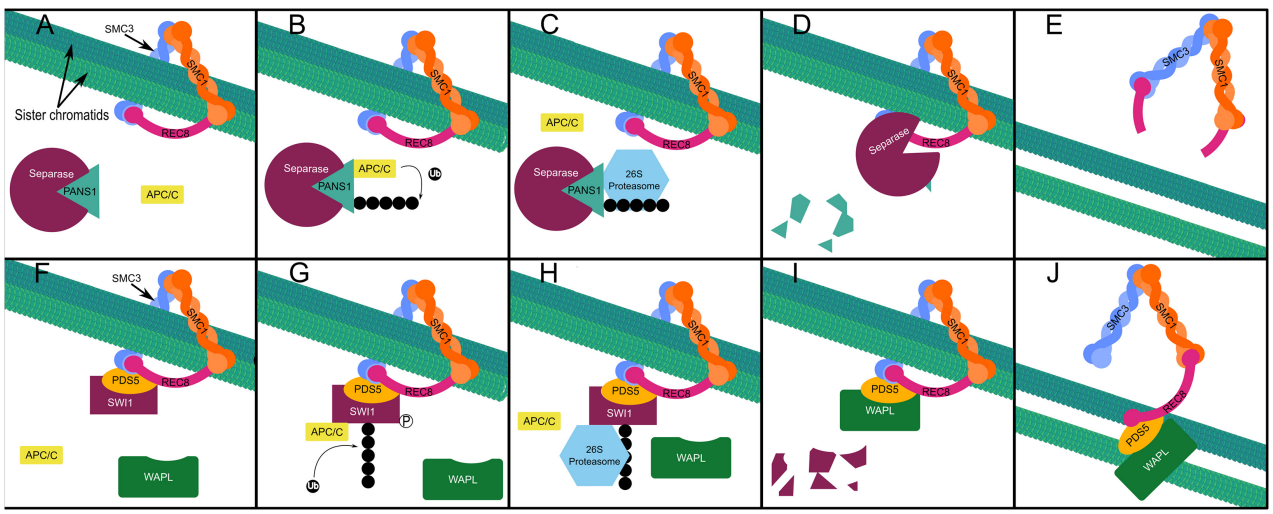

FIGURE 5 | Proteolytic cohesin removal **(A–E)**. Separase is inhibited by PANS1 protecting REC8 from proteolytic cleavage at chromosome arms preceding anaphase I and at the centromere preceding anaphase II redundantly and in parallel with SGO (A), APC/C mediated ubiquitination of PANS1 **(B)**, triggers its proteasomal degradation **(C,D)**, freeing separase **(D)** to cleave Rec8, the kleisin subunit of the cohesin ring, allowing sister chromatid separation in anaphase II **(E)**. Non-proteolytic (prophase pathway) cohesin removal **(F–J)**. SWI1 associates with cohesin beginning at interphase and inhibits the interaction of WAPL with PDS5 **(F)**. Phosphorylation of SWI1 enables APC/C mediated ubiquitination **(G)**. Proteasomal degradation of ubiquitinated SWI1 **(H–I)**, enables WAPL to interact with PDS5 **(I)**, triggering non-proteolytic "opening" of the cohesin ring complex and sister chromatid release from the onset of zygotene stage to the end of pachytene stage in prophase I **(J)**.

the coordination of SC assembly (Lambing et al., 2015; Vader, 2015). Recently, West et al. (2019) identified HORMAD-binding closure motifs in both mammalian and plant lateral element proteins SYCP2 and ASY3, indicating significant overlap in the mechanistic principle of meiotic chromosome axis assembly in eukaryotes. Guan et al. (2020) also showed that SKP1 depletion in mouse spermatocytes led to a concomitant decrease in TRIP13 abundance, speculating that SKP1 may be involved in stabilizing TRIP13. Given the conservation of SKP1-like protein sequence and apparent role in meiosis across eukaryotes (McLoud and Yang, 2012), it is tempting to speculate a common role for SCF complex mediated regulation of TRIP13/PCH2 in SC formation. However, as SKP1-like proteins may interact with multiple F-box proteins, phenotypic observations of SKP1-like protein meiotic mutants are likely to reflect multiple SCF E3 ligase complexes. Consequently, discovery and biochemical characterization of meiotic F-box proteins is a crucial step in continuing to unravel the role of SCF complexes in meiosis.

In rice, an F-Box protein called MEIOTIC F-BOX (MOF)—which interacts with rice SK1 ortholog OSK1—has been shown to be involved in the formation of the telomere bouquet, homologous chromosome pairing, synapsis, and DSB repair (He et al., 2016). MOF is highly expressed during meiosis and is active in leptotene to pachytene stage (He et al., 2016). *mof* mutants are completely male sterile, exhibiting arrested meiocyte development at late prophase I where chromosomes aggregate into a chromosome mass and degrade (He et al., 2016). Cytology of *mof* mutant meiocytes indicates severe disruption of SC formation and a lack of telomere clustering (He et al., 2016). Further, although phosphorylated H2AX foci appear normal at zygotene stage, indicating normal DSB formation, these foci are not reduced in number at pachytene stage, indicating that DSBs are not repaired (He et al., 2016). Immunolocalization showed that more than half of MOF foci colocalize with phosphorylated H2AX, and one third with COM1 and RAD51 indicating localization around DSB repair sites (He et al., 2016). A second rice F-Box protein, zygotene1 (ZYGO1), also interacts with OSK1 and has a putative role in meiosis (Zhang et al., 2017). Unlike *mof* and *ask1-1* mutants *zygo1* mutants are both male and female sterile (Zhang et al., 2017). ZYGO1 appears to regulate the formation of the telomere bouquet which does not form in the *zygo1* mutant (Zhang et al., 2017). *zygo1* mutants also demonstrate aberrant SC assembly with mutant SC length being 78.7% smaller than that of the wild type (Zhang et al., 2017). Further, although DSB and early recombination element installation is normal there is a significant reduction in cross-over (CO) formation (Zhang et al., 2017). In *Arabidopsis*, a plant specific F-box protein called COP9 signalosome interacting F_box Kelch 1 (CFK1), one of two highly similar CFK proteins in *Arabidopsis,* is also capable of forming an SCF complex (SCF^{CFK1}; Franciosini et al., 2013). Recently, Chen et al. (2020) demonstrated that SCF^{CFK1} interacts directly with domains rearranged methyltransferase 2 (DRM2) which catalyzes CHH methylation of euchromatin—predominantly transposable elements (TEs)—guided by 24nt siRNAs through the small RNA-directed DNA methylation (RdDM) pathway (Matzke and Mosher, 2014). In meiosis, silencing of TEs *via* methylation is essential to ensuring genetic integrity in progeny (Hsieh et al., 2016; Walker et al., 2018). Overexpression of CFK also led to a small decrease in CHH type methylation and a subsequent significant increase in expression of four hypomethylated TEs and genic regions (Chen et al., 2020). Despite this, no change in the total amount of ubiquitin-DRM2 ligation was observed between WT and *cfk1* null mutant lines (Chen et al., 2020).

THE ANAPHASE-PROMOTING COMPLEX

The APC/C, like the SCF complex, is a multi-subunit E3 ligase with core cullin (APC2) and RING domain containing (APC11) subunits (Eloy et al., 2015). However, the APC/C complex is much more complex, comprising at least 11 subunits (Eloy et al., 2015). Human APC/C interacts with ubiquitin conjugating E2 S (UBE2S), the only known E2 ubiquitin conjugating enzyme involved in specific K11-linked chain assembly (Wickliffe et al., 2011; Min et al., 2015). Homotypic K11 chains have been shown to prevent association with the mammalian proteasome (Grice et al., 2015). However, human APC/C interacts with both UBE2C and UBE2S forming heterotypic chains of branched K48 and K11 linkage types which leads to faster substrate proteasomal degradation than homotypic K11 or K48 chains alone (Meyer and Rape, 2014; Grice et al., 2015; Min et al., 2015). In *Saccharomyces cerevisiae*, the APC/C assembles K48 chains on its substrates in conjunction with ubiquitin conjugating E2 1 (Ubc1) and rapidly monoubiquitinates substrates in conjunction with Ubc4 (Rodrigo-Brenni and Morgan, 2007). Unfortunately, little is known about such atypical ubiquitin chain linkages in plants (Walsh and Sadanandom, 2014). *Arabidopsis* UBE2S ortholog UBC22 may be able to form K11 linked chains in conjunction with the APC/C but this remains to be experimentally validated (Wang et al., 2016). Substrate recognition by the APC/C is reliant on the presence of one or more of four conserved motifs: destruction box (D-box), KEN-box, GxEN-box, and A-box (Glotzer et al., 1991; Pfleger and Kirschner, 2000; Littlepage and Ruderman, 2002; Castro et al., 2003). In plants the function of only D-box and KEN-box motifs in APC/C mediated proteasomal degradation is validated (Eloy et al., 2015).

The APC/C is critical for both male and female meiosis in *Arabidopsis* (Zheng et al., 2011; Wang et al., 2013). Activation and substrate specificity of the APC/C is determined by the related co-factors Cell Division Cycle 20 (CDC20) and Cell Cycle Switch Protein 52 (CCS52). There are five CDC20-like genes in *Arabidopsis,* of which two (AtCDC20.1 and AtCDC20.2) are expressed and functionally redundant in mitosis (Kevei et al., 2011). CDC20.1—which interacts with APC/C subunits APC3, APC8, and APC10 (Kevei et al., 2011; Qiao et al., 2016)—is essential to proper chromosomal segregation (Niu et al., 2015). Similarly, AtAPC8 has been shown to be involved in chromosome alignment, chromosomal segregation, and microtubule organization (Xu et al., 2019). In recent years, considerable progress has been made in understanding the precise role and substrate specificity of APC/C in chromosomal segregation at anaphase I and II in *Arabidopsis*.

Sister chromatid cohesion during the first meiotic division is maintained in part by Shugoshin (SGO), which recruits protein phosphatase 2A (PP2A) to dephosphorylate the meiotic kleisin subunit of cohesin—REC8—protecting it from cleavage by the evolutionarily conserved protease separase (Kitajima et al., 2004; Cromer et al., 2019). Degradation of SGO1 in yeast is triggered by ubiquitination by the APC/C at anaphase II, allowing sister chromatid segregation (Jonak et al., 2017). In *Arabidopsis*, PATRONUS1 (PANS1) acts independently and in parallel to SGO to prevent premature cleavage of centromeric cohesin at anaphase I (Cromer et al., 2019). PANS1 occupies the active site of separase until its proteasomal degradation frees separase to cleave REC8 (**Figures 5A–E**; Cromer et al., 2019). Abolishing the interaction of PANS1 with the APC/C also prevented homologous chromosome separation at anaphase I, indicating that some degradation of PANS1 is required prior to anaphase I to allow separase mediated removal of cohesin at chromosome arms (Cromer et al., 2019). A separate non-proteolytic pathway results in the removal of approximately 90% of cohesin is from chromosomes in late prophase I (Yang et al., 2019). Non-proteolytic cohesin removal by Wings Apart-Like (WAPL) occurs from the onset of zygotene stage to the end of pachytene stage (**Figures 5F–J**; Yang et al., 2019). Switch 1 (SWI1) binds to precocious dissociation of sister 5 (PDS5), a cohesin accessory protein which assists in the acetylation of the SMC3 subunit, preventing interaction of PDS5 with WAPL in early prophase I (**Figure 5F**; Yang et al., 2019). In zygotene stage, SWI1 is phosphorylated allowing its ubiquitination by the APC/C—interacting *via* five D-box domains—and subsequent proteasomal degradation (**Figures 5G–I**; Yang et al., 2019). This allows WAPL interaction with PDS5 resulting in dissociation of the kleisin subunit from SMC3, "opening" the cohesin ring and allowing it to dissociate from chromatin (**Figure 5J**; Yang et al., 2019). While non-proteolytic cohesin removal mediated by WAPL is essential for homologous chromosome segregation at anaphase I (Yang et al., 2019), in the absence of both SGO and PANS1 there is complete loss of cohesion at metaphase I, indicating that PANS1 and SGO also protect chromosome arm cohesin from separase (Cromer et al., 2019).

SWI1 possesses sequence similarity of approximately 30% with maize and rice ameiotic 1 (AM1), required for very many early meiotic processes including sister chromatid cohesion in maize (Pawlowski et al., 2009; Che et al., 2011). Interestingly, PANS1 is well conserved in dicots but not in monocots (Cromer et al., 2013). It has been hypothesized that the rice salt sensitivity1 (RSS1) gene represents a monocot PANS1 ortholog based on: positionally limited sequence similarity; shared N-terminal KEN and D-box domain architecture facilitating APC/C interaction; shared salt sensitivity of knockout mutants; and apparent meristematic cell cycle regulation by RSS1 (Ogawa et al., 2011; Cromer et al., 2013, 2019). However, defects in meiotic segregation have not been demonstrated in *rss1* mutants, which are both viable and fertile (Ogawa et al., 2011). Cromer et al. (2019) highlight the presence of an uncharacterized RSS1 paralog, possibly possessing redundant function, which could explain the lack of *rss1* infertility. Yeast two-hybrid assays appear to show interactions between PDS5A and AM1 (Yang et al., 2019) supporting the hypothesis that AM1 performs the same functional role to SWI1. However, as with the role of RSS1 or its paralog in chromosomal segregation, this remains to be experimentally validated.

Oscillation in cyclin dependant kinase (CDK) activity dictates the timing and directionality of the cell cycle in both meiosis and mitosis (Coudreuse and Nurse, 2010). CDKs and cyclins form complexes to drive DNA replication and cell division events through phosphorylation of substrates such as DMC1, REC8, and SPO11 (Wijnker and Schnittger, 2013). The amount and type of cyclin available to form cyclin-CDK complexes regulates their activity and substrate specificity (Pines, 1995; Harashima and Schnittger, 2012). The APC/C regulates CDK activity by targeting cyclins for degradation and is in turn regulated by several activator and inhibitory proteins (Bolanos-Villegas et al., 2018). Dysregulation of the APC/C through disruption of these proteins can result in premature termination of meiosis following the first division or failure to terminate leading to entry into a third cycle of division (Cromer et al., 2012). Consequently, the regulation by and of the APC/C at this stage is fundamental to meiosis.

Initiation of each meiotic division is reliant on CDK activity rising to cross a threshold—peaking at metaphase I and II—as APC/C activity is reduced (Wijnker and Schnittger, 2013). In *Arabidopsis,* loss of function of either of the cyclins ommission of second division (OSD1) or tardy asynchronus meiosis (TAM) results in premature exit from meiosis following the first division (D'Erfurth et al., 2010). Further, loss of function in both TAM and OSD1 leads to meiotic exit following prophase I without entry into the first division, producing tetraploid spores and gametes (D'Erfurth et al., 2010). OSD1 interacts directly with the APC/C activating subunits CDC20.1, CDC20.5, CCS52A1, CCS52A2, and CCS52B through its conserved D-BOX and MR-tail domains to inhibit APC/C activation (Iwata et al., 2011; Cromer et al., 2012). In between the first and second division CDK activity drops below the threshold which triggers the initiation of division as APC/C mediated proteasomal destruction of cyclins increases (Wijnker and Schnittger, 2013). APC/C activity must then drop to trigger spindle disassembly and to allow CDK activity to rise back above this threshold to initiate the second meiotic division (Wijnker and Schnittger, 2013). However, should APC/C activity rise too much between the first and second division this leads to the separation of sister chromatids and premature termination of meiosis as is observed in the OSD1 mutant (Azumi et al., 2002; D'Erfurth et al., 2010; Wijnker and Schnittger, 2013). Therefore, OSD1 functions to partially inhibit activation of the APC/C to allow CDK activity to fall to a level sufficient for spindle disassembly while preventing sister chromatid segregation (Cromer et al., 2012). OSD1 is not conserved in mammals or yeast although, as the APC/C activators are highly conserved, expression of OSD1 in mouse oocytes leads to arrested development at metaphase I (Cromer et al., 2012). TAM forms an active complex with CDKA;1, the major cell cycle CDK in *Arabidopsis* (Cromer et al., 2012; Nowack et al., 2012). CDKA;1 has been shown to regulate meiotic progression, sister chromatid cohesion, chromosome axis formation, the number and position of COs, and microtubule organization (Wijnker et al., 2019; Yang et al., 2019; Sofroni et al., 2020). CDKA;1-TAM

complexes appear to control formation of the new cell wall between separated nuclei during division but not the meiotic spindle (Prusicki et al., 2019; Sofroni et al., 2020). Further, CDKA;1-TAM is proposed to inhibit the APC/C component three division mutant 1 (TDM1) at meiosis I (Cifuentes et al., 2016). *Arabidopsis* meiocytes carrying null mutant *tdm1* fail to exit meiosis, indicating that TDM1 modifies APC/C activity and/or specificity to trigger a reduction in CDK activity necessary for meiotic exit (Cifuentes et al., 2016). As TAM is expressed only in meiosis I and TDM1 is expressed throughout both meiosis I and II, premature exit from meiosis in *tam* mutants may be explained by the loss of CDKA;1-TAM inhibition of APC/C-TDM1 activity at metaphase I (Bulankova et al., 2010; Cifuentes et al., 2016).

HEI10

HEI10 is an E3 ubiquitin ligase which is part of a family of structurally and functionally related proteins sharing an N-terminal RING domain (Chelysheva et al., 2012). Another notable member of this family is the ZMM protein ZIP3/RNF212 (Chelysheva et al., 2012). Plants and fungi encode only HEI10 (Chelysheva et al., 2012), whereas budding yeast, *Drosophila,* and *C. elegans* encode only ZIP3/RNF212 (Agarwal and Roeder, 2000; Jantsch et al., 2004), and vertebrates encode both (Qiao et al., 2014; de Muyt et al., 2014). In mice, HEI10 and RNF212 are not redundant but both cooperative and antagonistic (Qiao et al., 2014; Rao et al., 2017). The apparently divergent functions of HEI10 and ZIP3/RNF2121 in vertebrates is largely attributed their respective ubiquitin and small ubiquitin-like modifier (SUMO) ligase activity (Qiao et al., 2014; Rao et al., 2017). SUMOylation operates *via* a similar E1, E2, and E3 cascade as ubiquitination; but, unlike ubiquitin ligases, SUMO ligases are non-essential to substrate SUMOylation, and SUMO itself may bind non-covalently to proteins (Bernier-Villamor et al., 2002; Lin et al., 2006). In mice, both HEI10 and RNF212 have SUMO E3 ligase activity (Strong and Schimenti, 2010; Rao et al., 2017). However, RNF212 appears to act primarily as a SUMO ligase, which antagonizes the rate of HEI10 mediated substrate ubiquitination and destruction (Qiao et al., 2014; Rao et al., 2017). In contrast, HEI10 directly antagonizes RNF212 by promoting its proteasomal degradation (Qiao et al., 2014). However, both HEI10 and RNF212 are absolutely required for class I CO formation in mammals, which constitute 80–90% of total crossovers (Ward et al., 2007; Reynolds et al., 2013). In fact, the absolute requirement for HEI10 or ZIP3/RNF212 orthologs for class I CO formation is conserved in *Arabidopsis* (Chelysheva et al., 2012; Ziolkowski et al., 2017), *C. elegans* (Jantsch et al., 2004), *Sordaria* (de Muyt et al., 2014), and rice (Wang et al., 2012). In mouse spermatocytes, SUMO, ubiquitin, and the proteasome localize to the chromosome axes at zygotene stage (Rao et al., 2017). Chemical inhibition of ubiquitin activation, SUMO conjugation, and proteasomal degradation each led to a dramatic increase in SC central element proteins SYCP3 and SYP2 and defective synapsis (Rao et al., 2017). Further, ubiquitin and SUMO appeared interdependent, where inhibition of SUMO conjugation reduced association of both ubiquitin and the proteasome at chromosome axes; while SUMO accumulated on the axes when ubiquitin activation was inhibited; and both SUMO and ubiquitin accumulated when the proteasome was inhibited (Rao et al., 2017). However, while ubiquitin promotes proteasomal degradation of RAD51 and DMC1, SUMO appears to negatively regulate their rate of turnover (Rao et al., 2017). In contrast, inhibition of SUMO leads to the accumulation of HEI10 indicating negative regulation of HEI10 accumulation (Rao et al., 2017). As in mice, both ubiquitin and SUMO have been shown to localize to the chromosome axes in rice and *Arabidopsis* respectively (Li Y. et al., 2018; Lambing and Heckmann, 2018).

In addition to RNF212, several HEI10 substrate proteins in mammals have been identified. Mammalian HEI10, like the APC/C, regulates CDK dependant cell cycle progression by targeting B type cyclins for degradation (Singh et al., 2007; Ward et al., 2007). HEI10 also appears to mediate degradation of the RecA-related recombinase RAD51, but not DMC1, in mouse spermatocytes as well as ZMM proteins—which associate with and stabilize homologous recombination intermediates— MutSγ (Msh4-Msh5), MER3, and TEX11 (Reynolds et al., 2013; Qiao et al., 2014; Rao et al., 2017). However, in a recent analysis of MutSγ component Msh4 in yeast, which possesses only ZIP3, He et al. (2020) demonstrated that Msh4 was a target of the 20S proteosome, independent of ubiquitination, and could be stabilized by phosphorylation. Rao et al. (2017) hypothesize that, in mammals, the antagonistic activities of RNF212 and HEI10 determine the fate of recombination intermediates: where predominant RNF212 mediated SUMOylation of ZMM proteins in a minority of strand exchange intermediates results in class I crossover formation; while predominant HEI10 mediated ubiquitination of ZMMs results in formation of NCOs. In yeast and *C. elegans,* ZIP3 appears to act exclusively as a SUMO E3 ligase (Cheng et al., 2006; Bhalla et al., 2008). In the fungus *Sordaria macrospora,* HEI10 was shown to positively regulate SUMO localization to the SC *via* its RING domain (de Muyt et al., 2014).

In *Arabidopsis,* HEI10 appears as ∼100–200 foci in leptotene to early pachytene stage (Chelysheva et al., 2012). In late pachytene stage HEI10 foci dramatically reduce in number by ∼90% co-localizing with MLH1 (Chelysheva et al., 2012), which is involved in late recombination and class I crossover maturation (Hunter and Borts, 1997). Despite appearing as foci in early meiotic prophase I meiotic defects are not apparent until diakinesis in *hei10* mutants, corresponding to the disappearance of HEI10 foci in the wild type (Chelysheva et al., 2012). In addition to being required for their formation, in *Arabidopsis* HEI10 promotes class I COs in a dose dependant manner (Ziolkowski et al., 2017; Serra et al., 2018). Increasing the copy number of HEI10 in *Arabidopsis* was sufficient to more than double DSB resolution as COs (Ziolkowski et al., 2017). Further, increased HEI10 expression also increases crossover coincidence, indicating that HEI10 also plays a role in crossover interference (Serra et al., 2018). In rice, HEI10 was shown to be capable of forming multi-protein complexes with ZMM proteins ZIP4, PTD, SHOC1, and MSH5 (Zhang J. et al., 2019). Additionally, OsHEI10, OsZIP4, OsSHOC1, and OsPTD displayed variable

interdependence in loading to the chromosome axis (Zhang J. et al., 2019). Li Y. et al. (2018) identified a plant specific protein called HEI10 interaction protein (HEIP1), which colocalizes with HEI10 on crossover sites from late pachytene to diplotene stage and is also required for class I CO formation. In addition to its interaction with HEI10, HEIP1 interacts directly with ZMM proteins ZIP4 and MSH5 (Li Y. et al., 2018). Further, loading of HEIP1 on chromosome axes was dependant on both HEI10 and ZIP4 (Li Y. et al., 2018). Chang et al. (2019) described a highly similar meiotic phenotype in their description of aberrant gametogenesis 1 (OsAGG1), which is synonymous with HEIP1. This work confirmed the essential role of OsAGG1/HEIP1 in class I CO formation as well as its interaction with HEI10, ZIP4, and MSH5 (Chang et al., 2019). However, Chang et al. (2019) also characterized four conserved N-terminal motifs which were essential to its function and interaction with characterized ZMMs.

UBIQUITIN-LIKE MODIFIERS

Related to ubiquitin (RUB) is another small peptide post-translational protein modifier in plants. In animals and fission yeast this modifier is known as neuronal precursor cell expressed developmentaly down-regulated 8 (NEDD8). The covalent attachment of this modifier to proteins is called rubylation or neddylation and is mediated by a cascade which— like sumoylation and ubiquitination—is dependent on specific RUB activating (E1), conjugating (E2), and ligating (E3) enzymes (**Table 1**). Jahns et al. (2014) demonstrated that *Arabidopsis* auxin resistant 1 (AXR1)—one half of the RUB E1 activating enzyme heterodimer (Leyser et al., 1993)—was involved in distribution of class I COs but not their number. Recently, Christophorou et al. (2020) expanded on this work to demonstrate a regulatory role for AXR1 in pericentromeric and transposable element methylation. Further, AXR1 deficient mutants exhibit enhanced sensitivity to DNA damage and significant down-regulation of HEI10, TOPII, and MLH3 (Martinez-Garcia et al., 2020). However, AXR1 acts upstream of E2 conjugating and E3 ligating enzymes, meaning that AXR1 mutant phenotypes might reflect defects in several distinct pathways. Indeed, the role of AXR1—and, by extension, rubylation—in regulating DNA methylation is not coupled to its role in determining CO distribution (Christophorou et al., 2020). Instead, CO abnormalities in *axr1* mutants are likely a product of aberrant synapsis due to a failure of ZYP1 to polymerize fully (Jahns et al., 2014). Disruption of CUL4 expression leads to a similar meiotic phenotype to *axr1* mutants indicating that the *axr1* meiotic phenotype might reflect perturbed CUl4 rubylation mediated by RBX1 which acts as both an E3 in the rubylation cascade and as part of SCF and cullin ring ligase 4 (CRL) ubiquitin E3 complexes (Jahns et al., 2014). In *C. elegans,* mutants of the CRL4 components CUL4 and DDB-1 also display aberrant synapsis with SYP-1, the ZYP1 equivalent, failing to polymerize normally, forming large polycomplexes (Brockway et al., 2014; Alleva et al., 2019). Interestingly, RBX1 mutants showed no defects in synapsis (Alleva et al., 2019). However, the role of CUL4 in SC formation does not appear to be universal as *cul4A* knockout mutants synapse fully in mouse spermatocytes (Kopanja et al., 2011; Yin et al., 2011). The meiotic substrates of CRL4 have yet to be identified, hindering the development of a molecular mechanistic model of its interaction in SC formation and DNA repair. Like SKP1, AXR1 appears to have undergone gene duplication in plants; however, unlike ASK2, AXR1-LIKE (AXL), sharing 80% amino acid identity with AXR1, was shown not to possess redundant function with AXR1 in meiosis, although it did also display a role in DNA damage repair (Martinez-Garcia et al., 2020).

TABLE 1 | Comparison of the number of identified E1, E2, and E3 enzymes in the ubiquitination, rubylation, and sumoylation cascade in *Arabidopsis* and processes they are known to regulate in meiosis.

	E1	E2	E3	Described regulation in plant meiosis
Ubiquitination	2	37	>1,300	Synapsis, DSB repair, chromosomal segregation, microtubule organization, DNA methylation, formation of telomere bouquet
Rubylation	1	1	1	CO distribution, synapsis, DNA methylation, transcription
Sumoylation	1	1	3	DSB repair, chromosome segregation, transcription

Methyl methanesulfonate sensitivity gene21 (MMS21)/high ploidy 2 (HPY2) is a conserved SUMO E3 ligase, one of three identified in *Arabidopsis* (Roy and Sadanandom, 2021), which interacts with structural maintenance of chromosome (SMC) 5 as part of the SMC5/6 complex (Liu et al., 2014; Yuan et al., 2014). Plants expressing mutant *mms21*-1 exhibited severe semi-sterility, with only 22% of the WT seed set (Liu et al., 2014). This phenotype was linked to defects in both male and female gametogenesis (Liu et al., 2014). In *mms21-1* mutant anthers, fragmented chromosomes and chromosome bridges between bivalents were observed in anaphase I, while in anaphase II sister chromatids did not segregate normally (Liu et al., 2014). Further, transcript abundance was significantly altered in *mms21-1* mutant flower buds, with *SPO11-1*, *RAD51*, *RBR*, condensin, cohesin, *SWI1*, SMC5/6 complex, and SMC-like genes showing up-regulation in the mutant; while expression of both *ASY1* and ZYP1a was reduced (Liu et al., 2014). Yuan et al. (2014) demonstrated hypersensitivity of *mms21* mutants to DNA damage, and the apparent involvement of this SUMO ligase in DSB repair by homologous recombination, indicating that unrepaired DSBs may explain the aberrant chromosome observed in *mms21-1* mutants (Liu et al., 2014). The N terminus of AtMMS21 interacts directly with the dimerization domain containing C terminus of DPa—which forms transcription factor complexes with E2F—resulting in its SUMOylation (Liu et al., 2016). The interaction of AtMMS21 with DPa abrogates its interaction with E2F and disrupts the nuclear translocation of E2Fa/DPa (Liu et al., 2016). E2Fa is one of three canonical E2Fs in *Arabidopsis* which play an essential but redundant role in both male and female gametogenesis, particularly pollen mitosis and

megaspore mother cell to archesporial cell transition respectively (Yao et al., 2018).

METHODS FOR IDENTIFYING E3 UBIQUITIN LIGASE SUBSTRATES

The difficulty of identifying E3 ligase-substrate interactions is thoroughly outlined by Iconomou and Saunders (2016). In brief, the highly dynamic nature of ubiquitination and rapid degradation of many substrates presents a very brief window in which to capture the interaction between ligase and substrate (Iconomou and Saunders, 2016). Additionally, the extraordinary diversity of substrate fates and the complicated redundancy this diversity entails confounds the inference of cause and effect in mutation and knockdown studies (Iconomou and Saunders, 2016). Although putative meiotic substrates of the APC/C (PANS1 and SWI1) and SCF^{CFK1} (DRM2) have been recently identified in *Arabidopsis* (Cromer et al., 2019; Chen et al., 2020; Yang et al., 2020), it's not yet clear that these interactions are conserved in other plant species nor whether they represent only a fraction of the total proteins targeted by these E3 ligase complexes. Putative substrates of SCF^{ZYGO1}, SCF^{MOF}—even HEI10—remain to be identified and/or substantiated in plants (He et al., 2016; Zhang et al., 2017; Ziolkowski et al., 2017; Li Y. et al., 2018; Chang et al., 2019; Zhang J. et al., 2019). Generally, meiotic E3 ligase-substrate interactions are poorly characterized, particularly in plants. For comparison, the well characterized human F-box proteins β-TrCP1 and 2, which are involved in regulation of mitotic progression as part of an SCF complex, have upwards of 50 characterized substrates (Mavrommati et al., 2018; Rayner et al., 2019).

Interaction of PANS1 with the APC/C^{CDC20} and of CFK1 with DRM2 was demonstrated using bimolecular fluorescence (BiFC) and yeast two-hybrid (Y2H) assays (Cromer et al., 2013; Chen et al., 2020) with later corroboration of the APC/C^{CDC20}- PANS1 interaction *via* PANS1 pulldown and mass spectrometry and disruption of the PANS1 D and KEN-box domains (Cromer et al., 2019). Evidence for APC/C mediated degradation of SWI1 is remarkably thorough, shown *in vitro* by persistence of SWI1 lacking all five D-box motifs (2 canonical RxxLxxxxN motifs; three motifs with the minimally required RxxL) far beyond prophase I meiocytes and into tetrads (Yang et al., 2019). This was further supported by persistence of purified C-terminal SWI1 in a cell free system with: inhibition of the proteasome; abolition of SWI1 phosphorylation sites; and CDK inhibition (Yang et al., 2019). For each of these supported interactions researchers worked backwards from the characterization of a target protein to the identification of an E3 ligase responsible for mediating its degradation. Given the apparently enhanced role of ubiquitination in regulating meiosis (Tang et al., 2010; Yang et al., 2011; Yuan et al., 2018; Barakate et al., 2021), working in the opposite direction, from E3 ligase to substrates, may present an opportunity to uncover novel meiotic proteins and mechanics by identifying the substrates of ligases whose involvement in meiosis is known or implicated. The inherent challenges of this approach may be partly overcome with a growing retinue of mass spectrometry based proteomic methods.

A common method for identifying candidate E3 ligase substrates is to compare the total complement of ubiquitinated proteins in wild type cells with cells overexpressing the ligase or in which ligase function is perturbed. One method of collecting this profile is overexpression of hexa-histidine tagged ubiquitin (His_6-Ub) followed by Ni-NTA pulldown (Beers and Callis, 1993; Saracco et al., 2009). This approach was first demonstrated by recovery of polyubiquitinated proteins with Ni^{2+} ion affinity chromatography after addition of purified His_6-Ub to a wheat germ lysate. It was later demonstrated that His_6-Ub could replace wild-type ubiquitin expression in yeast and that His_6-Ub modified to prevent polyubiquitin chain formation could be expressed in *Arabidopsis* to improve recovery of ubiquitinated proteins (Ling et al., 2000). Song et al. (2011) adapted this approach to the identification of substrates by parallel overexpression of an E3 ligase (BRCA1) and His_6-Ub followed by mass spectrometry to identify proteins which incorporated more His_6-Ub upon E3 overexpression. A similar approach was used to capture the first SUMOylome in *Arabidopsis,* consisting of 357 putative targets (Miller et al., 2010). However, modification and/or overexpression of ubiquitin might result in atypical substrate ubiquitination (Hjerpe et al., 2009). An alternative method relies on immunoprecipitation of the characteristic di-glycine (di-gly) residue which is left attached to ubiquitinated substrate lysine residues following trypsin digestion (Xu et al., 2010). This allows enrichment of ubiquitinated proteins without potential interference from modification of ubiquitin (Xu et al., 2010). However, proteins modified by ubiquitin-like proteins SUMO and RUB/NEDD8 also leave the characteristic di-gly residue following trypsin digestion (Xu et al., 2010). Akimov et al. (2018) generated an antibody which recognizes the 13 C-terminal amino acids of ubiquitin which are retained on ubiquitinated peptides following LysC digestion. This enables ubiquitin-specific peptide enrichment in a similar manner to di-gly enrichment (Akimov et al., 2018). As Iconomou and Saunders (2016) highlight, the amount of input lysate required for di-gly enrichment may be prohibitive in some systems. Yet, with improvements in mass spectrometry van der Wal et al. (2018) reported significant overlap in identified peptides whether using 4 or 40 mg of input to each trypsin digest. Di-gly affinity purification has recently been used to profile ubiquitination during maize seed de-etiolation, using 5 mg of leaf derived protein per sample (Wang et al., 2019). Zhu et al. (2020) used di-gly affinity purification to profile the meiotic ubiquitinome in young rice panicles, identifying 916 unique proteins with approximately 100 mg of protein as input. Rose et al. (2016) reported coupling of di-gly enrichment with isobaric tagging and fractionation using a high-pH reversed-phase spin cartridge to enable multiplexed quantification of ubiquitinated peptides with only 1 mg of lysate from each of ten cell culture samples or from 7 mg of tissue culture. Isobaric tagging—labeling of peptides with unique chemical groups of identical mass, allowing peptide samples to be combined in a single MS run (Ross et al., 2004)—allows a reduction in the amount of peptide input required for capture

by immunoprecipitation and reduces missing values in MS data output (Rose et al., 2016). However, isobaric tagging of peptide samples inhibits di-gly pulldown because chemical tagging of the di-gly remnant prevents interaction of the di-gly antibody and remnant motif (Rose et al., 2016). Isobaric tagging of di-gly captured peptides following elution from the antibody circumvented this problem (Rose et al., 2016). Udeshi et al. (2020) developed a similar di-gly antibody capture based method which they termed UbiFast. The main distinction between these two methods is the stage at which the isobaric tandem mass tag (TMT) is used to label the peptides (Rose et al., 2016; Udeshi et al., 2020). The UbiFast approach hypothesized that by labeling the di-gly captured peptides while still bound to the antibody instead of after elution would lead to improved yield (Udeshi et al., 2020). Indeed, in a head-to-head comparison on-antibody isobaric tagging led to an increase in the relative yield of di-gly peptides of 35.5% (Udeshi et al., 2020). This enabled quantification of more than 11000 peptides from only 0.5 mg of tumor tissue per sample (Udeshi et al., 2020). Recently, Hansen et al. (2021) coupled di-gly proteomics with tandem mass spectrometry operating in the data-independent acquisition (DIA) mode. DIA mode tandem mass spectrometry results in unbiased fragmentation of all ionized compounds in a sample based on relatively wide mass to charge windows (m/z), recording ion mass spectra irrespective of peptide precursor ion detection (Ludwig et al., 2018). Using this approach 89,650 di-gly sites were detected representing the deepest di-gly proteome to date (Hansen et al., 2021).

Yet another approach to global ubiquitome profiling is the use of tagged tandem ubiquitin binding entities (TUBEs) to capture polyubiquitinated proteins from lysates (Hjerpe et al., 2009). TUBEs are constructed from affinity tagged tandem repeats of ubiquitin associated (UBA) domains from ubiquilin 1 and human HR23A (Hjerpe et al., 2009). Four tandem UBA domains are included based on the hypothesis that at a ubiquitin chain length of at least four is required for proteasomal degradation (Thrower et al., 2000; Hjerpe et al., 2009). Each UBA domain retains independent capacity to bind ubiquitin but in tandem dissociation of ubiquitinated proteins is reduced 1,000-fold compared to equivalent single UBA domains (Hjerpe et al., 2009). Further, TUBEs do not bind NEDD8/RUB or SUMOylated protein and the association of polyubiquitinated proteins to TUBEs protects them from DUBs and proteasomal degradations at an equivalent level to specific inhibitors (Hjerpe et al., 2009). TUBE capture was first adapted to the identification of ubiquitinated peptides using mass-spectrometry by Shi et al. (2011). Yoshida et al. (2015) generated a trypsin resistant (TR)-TUBE by substituting three arginine residues for alanine residues in tandem repeated ubiquilin 1 UBA domains. Combining expression of TR-TUBEs with subsequent di-gly enrichment significantly reduced the proportion of identified peptides which did not contain the di-gly residue when compared to di-gly alone (Yoshida et al., 2015). All of these methods allow for the enrichment of ubiquitinated proteins from whole protein extracts (**Figure 6**). However, for the identification of specific E3 ligase substrates where there is redundancy in ligase-substrate interactions and/or low substrate abundance they may not be suitable. An alternative approach which circumvents this issue is to introduce E3 ligase specific traps or labeling.

Tan et al. (2013) devised the parallel adapter capture (PAC) method which combined parallel affinity purification of HA-tagged E3 ligases expressed in cells which were untreated or were treated with either a proteasomal inhibitor or cullin ring ligase (CRL) inhibitor. This approach then combined mass-spectrometry with the Comparative Proteomics Analysis Software Suite (CompASS) to identify high confidence interacting proteins by comparison of average peptide spectral matches, a proxy for abundance, across treatments (Tan et al., 2013). By design, this approach does not specifically capture E3 ligase substrates but all proteins with which an E3 ligase might interact (Tan et al., 2013). Additionally, substrates not targeted for degradation by the ligase are unlikely to be influenced by the inhibitor treatment. Further, this approach is still confounded by the weak and transient nature of ligase-substrate interactions. Several solutions to this have been developed. Mark et al. (2016) developed ligase-traps which combined a common affinity (FLAG) tag with a UBA domain to increase the affinity of the modified ligase for its substrates, improving recovery of interacting proteins (**Figure 7A**). To improve recovery of ligase substrates rather than all interactors Mark et al. (2016) combined expression of their UBA-FLAG tagged E3 ligase with His_6-Ub, allowing initial immunoprecipitation under native conditions followed by Ni^{2+} ion chromatography under denaturing conditions. An important consideration for this technique is the preference of UBA domains for ubiquitin chain linkage types; Rad23 has a fourfold preference for lys48 chains over lys68 (Mark et al., 2016). An alternative to the dual expression of modified ligase and ubiquitin to specifically recover substrates is ubiquitin-activated interaction traps (UBAITs) in which an affinity tagged E3 ligase is C-terminally tagged with ubiquitin through a flexible linker (**Figure 7B**; O'Connor et al., 2015). The attached ubiquitin can interact with E1 and E2 enzymes, the attached E3 facilitating recognition of its substrates and covalent attachment of the C-terminal ubiquitin to the target (O'Connor et al., 2015). The length of this linker can affect the efficiency of capture with longer linkers (up to 5xGGSG) proving more efficient at capture (O'Connor et al., 2015).

An approach which combines ligase-substate trapping with TUBE and di-gly was recently developed by Watanabe et al. (2020). This approach replaces the UBA-FLAG tagged E3 ligase proposed by Mark et al. (2016) with a TUBE-FLAG tag, further increasing the affinity of the ligase for its substrate and protecting the substrate from degradation (**Figure 7A**) (Watanabe et al., 2020). The addition of di-gly enrichment following anti-FLAG immunoprecipitation and trypsin digest of lysates lead to a dramatic increase in efficiency of putative substrate capture (Watanabe et al., 2020). Watanabe et al. (2020) also highlighted that attachment of the TUBE bait tag to the N or C terminal of the ligase affected the efficiency of capture in a ligase dependant manner. In *Arabidopsis*, Durand et al. (2016) and Lee et al. (2018) expressed affinity tagged RING and F-box proteins respectively which retained their ability to interact with substrates but lacked the ability to ligate ubiquitin. These substrate trapping approaches all rely on the ability to express modified proteins

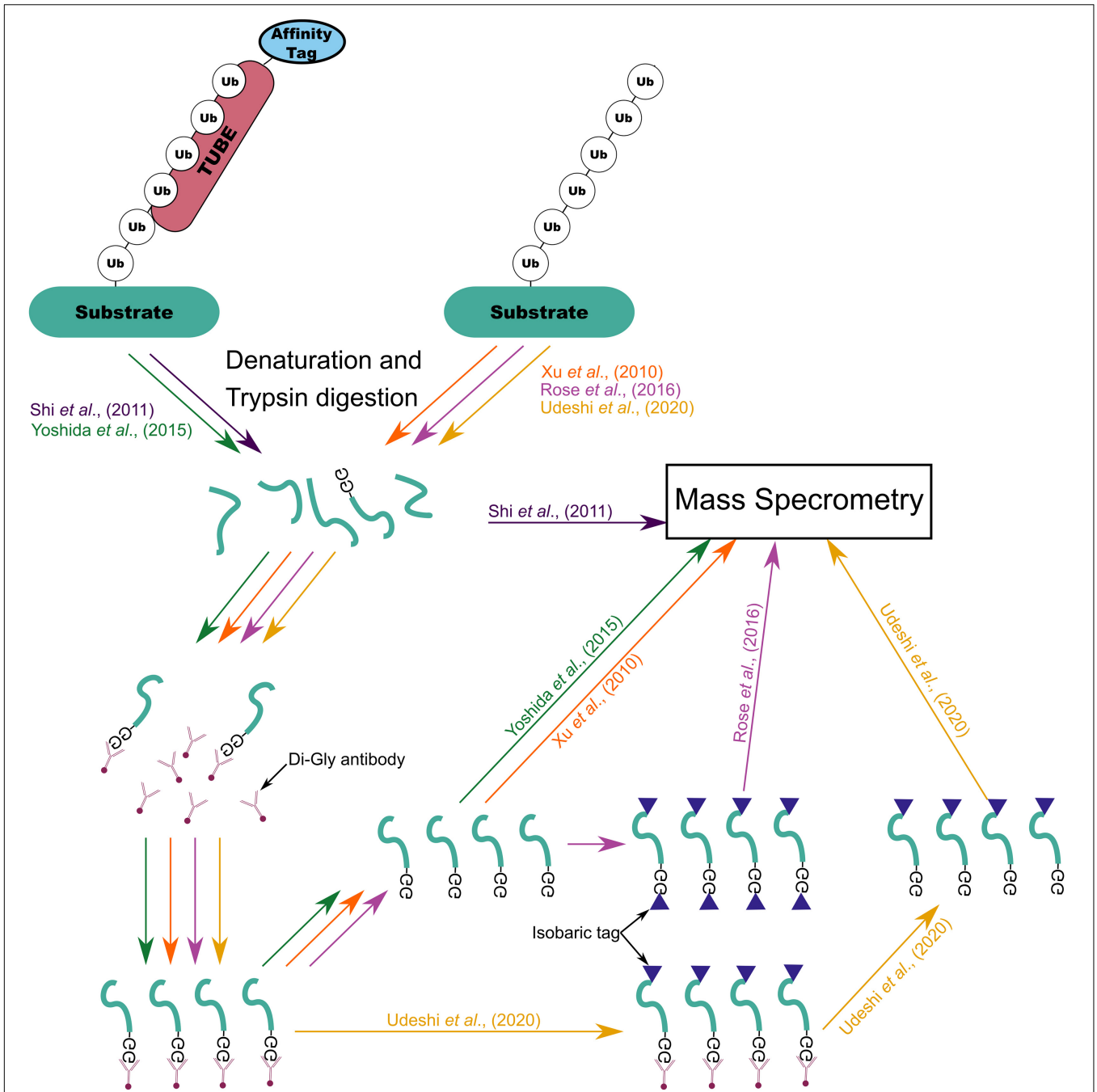

FIGURE 6 | Summary of mass-spectrometry based ubiquitylome profiling workflows from Xu et al. (2010), Shi et al. (2011), Yoshida et al. (2015), Rose et al. (2016), and Udeshi et al. (2020).

in a system of interest which may be prohibitive. In addition, as with His_6-Ub, modification or overexpression of substrates might generate non-native interactions. However, by specifically targeting E3 ligase substrates they offer a way to dramatically limit the depth of proteomic profiling required to identify putative substrates. Further, because they do not rely on assessing the stability of substrates, they can be more effective in identifying redundant and non-degradative interactions.

Another general approach, developed by Roux et al. (2012), which is not selective for specific substrates, is proximity-dependant biotin labeling (BioID), in which a protein of interest is fused to a mutant form of *E. coli* biotin conjugating enzyme BirA (BirA*) which is defective in self-association and DNA binding (**Figure 7C**). BirA* can activate biotin, generating biotinoyl-AMP, but its affinity for the activated substrate is two orders of magnitude lower than wild type

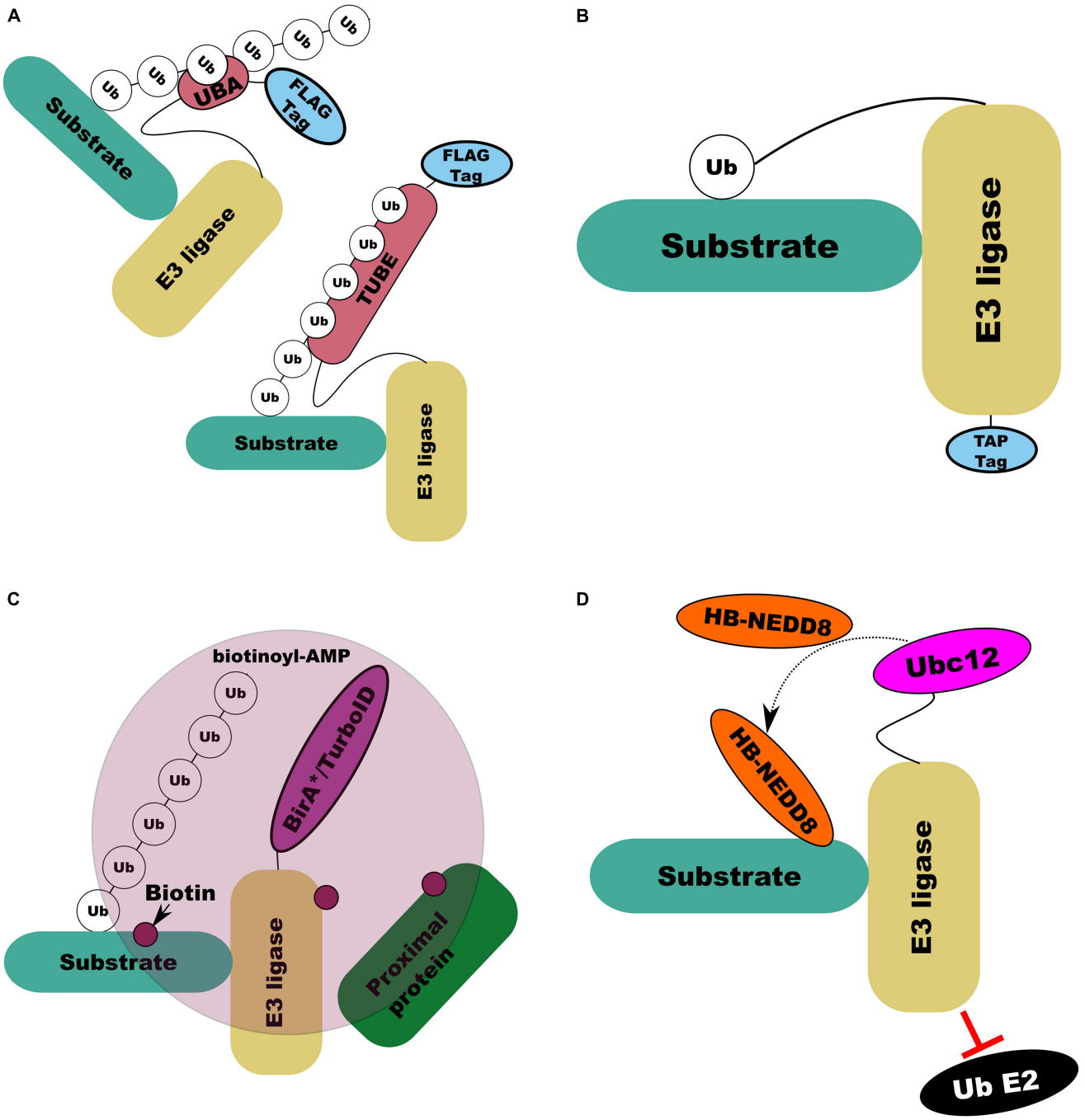

FIGURE 7 | Illustrations of E3 ligase substrate capture and labeling methods. **(A)** UBA (top left) and tandem UBA (TUBE; bottom right) capture by increasing the affinity of the E3 ligase modified with the UBA or TUBE domain for its ubiquitinated substrates. **(B)** UBAIT capture forming a covalent E3-substrate complex through C-terminal modification of the E3 itself with ubiquitin *via* a flexible linker. **(C)** BioID/TurboID based proximity labeling in which modified BirA enzyme conjugated to an E3 ligase of interest results in biotin labeling of interacting and associated proteins by creating a pool of reactive biotinoyl-AMP. **(D)** NEDDylator capture, in which an E3 ligase with E2 ubiquitin interaction domain disrupted to prevent substrate ubiquitination is fused to NEDD8 conjugating E2 (Ubc12). With co-expression of his-biotin (HB) tagged NEDD8 this enables HB-NEDD8 tagging of E3 ligase substrates.

BirA, allowing biotinoyl-AMP to interact with nearby amines, covalently modifying proteins near to the modified peptide with biotin which can then be purified with streptavidin (Roux et al., 2012). Coyaud et al. (2015) deployed BioID to characterize over 50 putative interactors for β-TrCP. However, the lengthy (16–24 h) incubation at high temperature (37°C) required for efficient BioID labeling is not optimal for *in vivo* proximity labeling in plants (Zhang Y. et al., 2019). Branon et al. (2018) engineered

BirA to produce promiscuous mutants capable of proximity labeling with biotin in only 10 min which they called TurboID and miniTurbo. Zhang Y. et al. (2019) deployed TurboID to determine the interactions of an immune receptor in *Nicotiana benthamiana*, demonstrating that TurboID at room temperature was significantly more efficient than BioID at 37°C. Recently, Wu et al. (2020) replicated this approach to identify specific E3 ligase interactions through expression of TurboID-tagged E3 ligases SNIPER1 and SNIPER2 in *N. benthamiana*. A similar proximity labeling approach has been developed by Zhuang et al. (2013) in which histidine-biotin (HB) tagged (Tagwerker et al., 2006) NEDD8/RUB E2 equivalent enzyme (Ubc12) (**Figure 7D**) is linked to a RING E3 ligase of interest with its RING domain removed to prevent its interaction with ubiquitin E2 conjugating enzymes. Expression of this construct *in vivo* or its addition to cell lysate leads to stable, covalent labeling of E3 ligase targets with RUB/NEDD8 which can be purified by both Ni^{2+} ion and streptavidin chromatography (Zhuang et al., 2013).

The difficulty of investigating E3-substrate interactions in plant meiosis is further compounded by the challenge of capturing enough meiotic cells at the right time. Plant meiotic cells are scarce and are embedded in complex tissues comprised largely of vegetative cells. In barley, meiocytes account for only 10% of cells in the developing anther (Lewandowska et al., 2019). A common strategy to overcome this is to collect meiotic tissues in bulk. This approach—while time consuming—has produced many valuable large scale meiotic transcriptomic and proteomic data sets. Several *Arabidopsis* studies have used this approach despite that *Arabidopsis* meiocytes have a diameter of only about 5 microns (Yang et al., 2011; Chen and Retzel, 2013). Similar methods have been developed in maize, wheat, and brassica (Greer et al., 2012; Khoo et al., 2012; Dukowic-Schulze et al., 2014; Osman et al., 2018). In rice, collection of approximately 10,000 anthers between PMCs to microspores allowed profiling of both the proteome (Collado-Romero et al., 2014; Ye et al., 2015) and acetylated proteins (Li X. et al., 2018). Non-destructive methods of approximating meiotic stage, such as by anther length (Arrieta et al., 2020), can reduce the labor intensity of such methods. The transient nature of E3-substrate interactions and ordered progression of meiosis might require isolation of meiotic tissue at a precise stage of development. Bulk collection of meiotic tissue can introduce variation in even carefully staged samples which may obscure small or rapid changes. Further, development of meiocytes within the same anther may not be fully synchronized but it is possible to overcome this issue by introducing further staging steps such as cytological analysis (Shunmugam et al., 2018; Barakate et al., 2021). Recently, Lewandowska et al. (2019) developed a micro-proteomic workflow, allowing identification of ∼2,800 and 4,000 proteins from precisely staged single and paired barley anthers. The amount of ubiquitinated compared to non-ubiquitinated protein at any one time is low (Hristova et al., 2020). As such comparative ubiquitylomics is outside the reach of micro-proteomics at the time of writing. However, as direct substrate capture methods do not require deep profiling they could be applied to smaller samples such as fewer anthers or isolated meiocytes, increasing the practicality of highly accurate staging.

OUTLOOK

While identification of the E3 ligases and their substrates involved in meiosis in plants remains a substantial undertaking, there are related processes worthy of exploration. In humans, the E3/E4 ligase UBE4A has been shown to be required for optimal DSB repair through fine adjustment of both K48 and K63-linked ubiquitin chain lengths in protein complexes involved in DSB repair (Baranes-Bachar et al., 2018). In the *C. elegans* germ line, the E4 ubiquitin ligase ubiquitin fusion degradation-2 (UFD-2) ensures the timely removal of RAD-51 from DSB sites and is involved in regulating the apoptotic response in the germ line when meiotic recombination intermediates or DSBs persist in late pachytene stage (Ackermann et al., 2016). An *Arabidopsis* ortholog of UFD-2, UBE4/Mutant, SNC1-Enhancing 3 (MUSE3), is known to be involved in the tight regulation of immune receptor degradation (Huang et al., 2014; Skelly et al., 2019). It is possible that, in addition to its role in the immune response, it might also play a role in regulation of DSB repair in plants. More broadly, it is possible that, given the complex temporal and spatial organization of meiotic processes, some meiotic ubiquitination events may operate in a "dimmer switch" rather than binary on/off manner as has been observed in other processes (Skelly et al., 2019). The essential reversing component to such a system are the DUBs (Skelly et al., 2019). Meiotic transcriptomes in both barley (Barakate et al., 2021) and *Arabidopsis* (Yang et al., 2011) point to enrichment of DUBs during male meiosis. The highly homologous ubiquitin specific proteases (UBPs) UBP3 and UBP4 have been shown to regulate pollen development at various stages in *Arabidopsis* (Doelling et al., 2007). Enrichment of DUBs in Barley anthers at pachytene–diplotene stages was driven by four ovarian tumor domain (OTU) proteases (Barakate et al., 2021), unfortunately these are presently poorly characterized in plants (March and Farrona, 2018). DUBs are fewer in number and exhibit less specificity than E3 ligases (Li et al., 2020); however, similar approaches can be deployed in characterizing their substrates (Sowa et al., 2009).

AUTHOR CONTRIBUTIONS

JO led manuscript preparation. RW and IC contributed to manuscript revision, read, and approved the submitted version. All authors contributed to the article and approved the submitted version.

FUNDING

This work was funded by the European Research Council (ERC Shuffle Project ID: 669182), Biotechnology and Biological Sciences Research Council (BB/T008636/1), and by the Scottish Government's Rural and Environment Science and Analytical Services Division work programme Theme 2 WP2.1 RD1 and RD2.

REFERENCES

Ackermann, L., Schell, M., Pokrzywa, W., Kevei, E., Gartner, A., Schumacher, B., et al. (2016). E4 ligase-specific ubiquitination hubs coordinate DNA double-strand-break repair and apoptosis. *Nat. Struct. Mol. Biol.* 23, 995–1002. doi: 10.1038/nsmb.3296

Agarwal, S., and Roeder, G. S. (2000). Zip3 provides a link between recombination enzymes and synaptonemal complex proteins. *Cell* 102, 245–255. doi: 10.1016/S0092-8674(00)00029-5

Akimov, V., Barrio-Hernandez, I., Hansen, S. V. F., Hallenborg, P., Pedersen, A. K., Bekker-Jensen, D. B., et al. (2018). UbiSite approach for comprehensive mapping of lysine and N-terminal ubiquitination sites. *Nat. Struct. Mol. Biol.* 25, 631–640. doi: 10.1038/s41594-018-0084-y

Alleva, B., Clausen, S., Koury, E., Hefel, A., and Smolikove, S. (2019). CRL4 regulates recombination and synaptonemal complex aggregation in the *Caenorhabditis elegans* germline. *PLoS Genet.* 15:e1008486. doi: 10.1371/journal.pgen.1008486

An, L., Ahmad, R. M., Ren, H., Qin, J., and Yan, Y. (2018). Jasmonate signal receptor gene family ZmCOIs restore male fertility and defense response of *Arabidopsis* mutant coi1-1. *J. Plant Growth Regul.* 38, 479–493. doi: 10.1007/s00344-018-9863-2

Arrieta, M., Colas, I., Macaulay, M., Waugh, R., and Ramsay, L. (2020). "A modular tray growth system for barley," in *Plant Meiosis, Methods in Molecular Biology*, Vol. 2061, eds M. Pradillo and S. Heckmann (New York, NY: Humana Press), 367–379. doi: 10.1007/978-1-4939-9818-0_26

Azumi, Y., Liu, D., Zhao, D., Li, W., Wang, G., Hu, Y., et al. (2002). Homolog interaction during meiotic prophase I in *Arabidopsis* requires the SOLO DANCERS gene encoding a novel cyclin-like protein. *EMBO J.* 21, 3081–3095. doi: 10.1093/emboj/cdf285

Barakate, A., Orr, J., Schreiber, M., Colas, I., Lewandowska, D., Mccallum, N., et al. (2021). Barley anther and meiocyte transcriptome dynamics in meiotic prophase I. *Front. Plant Sci.* 11:619404. doi: 10.3389/fpls.2020.619404

Baranes-Bachar, K., Levy-Barda, A., Oehler, J., Reid, D. A., Soria-Bretones, I., Voss, T. C., et al. (2018). The ubiquitin E3/E4 Ligase UBE4A adjusts protein ubiquitylation and accumulation at sites of DNA damage, facilitating double-strand break repair. *Mol. Cell* 69, 866–878. doi: 10.1016/j.molcel.2018.02.002

Beers, E., and Callis, J. (1993). Utility of polyhistidine-tagged ubiquitin in the purification of ubiquitin-protein conjugates and as an affinity ligand for the purification of ubiquitin-specific hydrolases. *J. Biol. Chem.* 268, 21645–21649.

Bergerat, A., De Massy, B., Gadelle, D., Varoutas, P.-C., Nicolas, A., and Forterre, P. (1997). An atypical topoisomerase II from archaea with implications for meiotic recombination. *Nature* 386, 414–417. doi: 10.1038/386414a0

Bernier-Villamor, V., Sampson, D. A., Matunis, M. J., and Lima, C. D. (2002). Structural basis for E2-mediated SUMO conjugation revealed by a complex between ubiquitin-conjugating enzyme Ubc9 and RanGAP1. *Cell* 108, 345–356. doi: 10.1016/S0092-8674(02)00630-X

Bhalla, N., Wynne, D. J., Jantsch, V., and Dernburg, A. F. (2008). ZHP-3 acts at crossovers to couple meiotic recombination with synaptonemal complex disassembly and bivalent formation in *C. elegans*. *PLoS Genet.* 4:e1000235. doi: 10.1371/journal.pgen.1000235

Bolanos-Villegas, P., Xu, W., Martinez-Garcia, M., Pradillo, M., and Wang, Y. (2018). Insights Into the role of ubiquitination in meiosis: fertility, adaptation and plant breeding. *Arabidopsis Book* 16:e0187. doi: 10.1199/tab.0187

Branon, T. C., Bosch, J. A., Sanchez, A. D., Udeshi, N. D., Svinkina, T., Carr, S. A., et al. (2018). Efficient proximity labeling in living cells and organisms with TurboID. *Nat. Biotechnol.* 36, 880–887. doi: 10.1038/nbt.4201

Brockway, H., Balukoff, N., Dean, M., Alleva, B., and Smolikove, S. (2014). The CSN/COP9 signalosome regulates synaptonemal complex assembly during meiotic prophase I of *Caenorhabditis elegans*. *PLoS Genet.* 10:e1004757. doi: 10.1371/journal.pgen.1004757

Bulankova, P., Riehs-Kearnan, N., Nowack, M. K., Schnittger, A., and Riha, K. (2010). Meiotic progression in *Arabidopsis* is governed by complex regulatory interactions between SMG7, TDM1, and the meiosis I-specific cyclin TAM. *Plant Cell* 22, 3791–3803. doi: 10.1105/tpc.110.078378

Castresana, J. (2000). Selection of conserved blocks from multiple alignments for their use in phylogenetic analysis. *Mol. Biol. Evol.* 17, 540–552. doi: 10.1093/oxfordjournals.molbev.a026334

Castro, A., Vigneron, S., Bernis, C., Labbé, J.-C., and Lorca, T. (2003). Xkid is degraded in a D-box, KEN-box, and A-box-independent pathway. *Mol. Cell. Biol.* 23, 4126–4138. doi: 10.1128/mcb.23.12.4126-4138.2003

Chang, Z., Xu, C., Huang, X., Yan, W., Qiu, S., Yuan, S., et al. (2019). The plant-specific ABERRANT GAMETOGENESIS 1 gene is essential for meiosis in rice. *J. Exp. Bot.* 71, 204–218. doi: 10.1093/jxb/erz441

Che, L., Tang, D., Wang, K., Wang, M., Zhu, K., Yu, H., et al. (2011). OsAM1 is required for leptotene-zygotene transition in rice. *Cell Res.* 21, 654–665. doi: 10.1038/cr.2011.7

Chelysheva, L., Vezon, D., Chambon, A., Gendrot, G., Pereira, L., Lemhemdi, A., et al. (2012). The *Arabidopsis* HEI10 is a new ZMM protein related to Zip3. *PLoS Genet.* 8:e1002799. doi: 10.1371/journal.pgen.1002799

Chen, C., and Retzel, E. F. (2013). "Analyzing the meiotic transcriptome using isolated meiocytes of *Arabidopsis thaliana*," in *Plant Meiosis*, eds W. Pawlowski, M. Grelon, S. Armstrong (Totowa, NJ: Humana Press), 203–213. doi: 10.1007/978-1-62703-333-6_20

Chen, J., Liu, J., Jiang, J., Qian, S., Song, J., Kabara, R., et al. (2020). F-box protein CFK1 interacts with and degrades *de novo* DNA methyltransferase in *Arabidopsis*. *New Phytol.* 229, 3303–3317. doi: 10.1111/nph.17103

Cheng, C. H., Lo, Y. H., Liang, S. S., Ti, S. C., Lin, F. M., Yeh, C. H., et al. (2006). SUMO modifications control assembly of synaptonemal complex and polycomplex in meiosis of *Saccharomyces cerevisiae*. *Genes Dev.* 20, 2067–2081. doi: 10.1101/gad.1430406

Christophorou, N., She, W., Long, J., Hurel, A., Beaubiat, S., Idir, Y., et al. (2020). AXR1 affects DNA methylation independently of its role in regulating meiotic crossover localization. *PLoS Genet.* 16:e1008894. doi: 10.1371/journal.pgen.1008894

Ciehanover, A., Hod, Y., and Hershko, A. (1978). A heat-stable polypeptide component of an ATP-dependent proteolytic system from reticulocytes. *Biochem. Biophys. Res. Commun.* 81, 1100–1105. doi: 10.1016/0006-291X(78)91249-4

Cifuentes, M., Jolivet, S., Cromer, L., Harashima, H., Bulankova, P., Renne, C., et al. (2016). TDM1 regulation determines the number of meiotic divisions. *PLoS Genet.* 12:e1005856. doi: 10.1371/journal.pgen.1005856

Cole, F., Keeney, S., and Jasin, M. (2010). Evolutionary conservation of meiotic DSB proteins: more than just Spo11. *Genes Dev.* 24, 1201–1207. doi: 10.1101/gad.1944710

Collado-Romero, M., Alós, E., and Prieto, P. (2014). Unravelling the proteomic profile of rice meiocytes during early meiosis. *Front. Plant Sci.* 5:356. doi: 10.3389/fpls.2014.00356

Copenhaver, G., Housworth, E., and Stahl, F. (2002). Crossover interference in *Arabidopsis*. *Genetics* 160, 1631–1639.

Coudreuse, D., and Nurse, P. (2010). Driving the cell cycle with a minimal CDK control network. *Nature* 468, 1074–1079. doi: 10.1038/nature09543

Coyaud, E., Mis, M., Laurent, E. M., Dunham, W. H., Couzens, A. L., Robitaille, M., et al. (2015). BioID-based identification of Skp Cullin F-box (SCF)beta-TrCP1/2 E3 ligase substrates. *Mol. Cell. Proteomics* 14, 1781–1795. doi: 10.1074/mcp.M114.045658

Cromer, L., Heyman, J., Touati, S., Harashima, H., Araou, E., Girard, C., et al. (2012). OSD1 promotes meiotic progression via APC/C inhibition and forms a regulatory network with TDM and CYCA1;2/TAM. *PLoS Genet.* 8:e1002865. doi: 10.1371/journal.pgen.1002865

Cromer, L., Jolivet, S., Horlow, C., Chelysheva, L., Heyman, J., De Jaeger, G., et al. (2013). Centromeric cohesion is protected twice at meiosis, by SHUGOSHINs at anaphase I and by PATRONUS at interkinesis. *Curr. Biol.* 23, 2090–2099. doi: 10.1016/j.cub.2013.08.036

Cromer, L., Jolivet, S., Singh, D. K., Berthier, F., De Winne, N., De Jaeger, G., et al. (2019). Patronus is the elusive plant securin, preventing chromosome separation by antagonizing separase. *Proc. Natl. Acad. Sci. U.S.A.* 116, 16018–16027. doi: 10.1073/pnas.1906237116

de Muyt, A., Zhang, L., Piolot, T., Kleckner, N., Espagne, E., and Zickler, D. (2014). E3 ligase Hei10: a multifaceted structure-based signaling molecule with roles within and beyond meiosis. *Genes Dev.* 28, 1111–1123. doi: 10.1101/gad.240408.114

D'Erfurth, I., Cromer, L., Jolivet, S., Girard, C., Horlow, C., Sun, Y., et al. (2010). The cyclin-A CYCA1;2/TAM is required for the meiosis I to meiosis II transition and cooperates with OSD1 for the prophase to first meiotic division transition. *PLoS Genet.* 6:e1000989. doi: 10.1371/journal.pgen.1000989

Dezfulian, M. H., Soulliere, D. M., Dhaliwal, R. K., Sareen, M., and Crosby, W. L. (2012). The SKP1-like gene family of *Arabidopsis* exhibits a high degree of differential gene expression and gene product interaction during development. *PLoS One* 7:e50984. doi: 10.1371/journal.pone.0050984

Doelling, J. H., Phillips, A. R., Soyler-Ogretim, G., Wise, J., Chandler, J., Callis, J., et al. (2007). The ubiquitin-specific protease subfamily UBP3/UBP4 is essential for pollen development and transmission in *Arabidopsis*. *Plant Physiol.* 145, 801–813. doi: 10.1104/pp.106.095323

Dove, K. K., Stieglitz, B., Duncan, E. D., Rittinger, K., and Klevit, R. E. (2016). Molecular insights into RBR E3 ligase ubiquitin transfer mechanisms. *EMBO Rep.* 17, 1221–1235. doi: 10.15252/embr.201642641

Dukowic-Schulze, S., Harris, A., Li, J., Sundararajan, A., Mudge, J., Retzel, E. F., et al. (2014). Comparative transcriptomics of early meiosis in *Arabidopsis* and maize. *J. Genet. Genom.* 41, 139–152. doi: 10.1016/j.jgg.2013.11.007

Durand, A. N., Inigo, S., Ritter, A., Iniesto, E., De Clercq, R., Staes, A., et al. (2016). The *Arabidopsis* iron-sulfur protein GRXS17 is a target of the ubiquitin E3 ligases RGLG3 and RGLG4. *Plant Cell Physiol.* 57, 1801–1813. doi: 10.1093/pcp/pcw122

Dye, B. T., and Schulman, B. A. (2007). Structural mechanisms underlying posttranslational modification by ubiquitin-like proteins. *Annu. Rev. Biophys. Biomol. Struct.* 36, 131–150. doi: 10.1146/annurev.biophys.36.040306.132820

Eloy, N. B., De Freitas Lima, M., Ferreira, P. C. G., and Inzé, D. (2015). The role of the anaphase-promoting complex/cyclosome in plant growth. *Crit. Rev. Plant Sci.* 34, 487–505. doi: 10.1080/07352689.2015.1078613

Emmerich, C. H., and Cohen, P. (2015). Optimising methods for the preservation, capture and identification of ubiquitin chains and ubiquitylated proteins by immunoblotting. *Biochem. Biophys. Res. Commun.* 466, 1–14. doi: 10.1016/j.bbrc.2015.08.109

Emms, D. M., and Kelly, S. (2015). OrthoFinder: solving fundamental biases in whole genome comparisons dramatically improves orthogroup inference accuracy. *Genome Biol.* 16:157. doi: 10.1186/s13059-015-0721-2

Franciosini, A., Lombardi, B., Iafrate, S., Pecce, V., Mele, G., Lupacchini, L., et al. (2013). The *Arabidopsis* COP9 SIGNALOSOME INTERACTING F-BOX KELCH 1 protein forms an SCF ubiquitin ligase and regulates hypocotyl elongation. *Mol. Plant* 6, 1616–1629. doi: 10.1093/mp/sst045

Franklin, A. E., Mcelver, J., Sunjevaric, I., Rothstein, R., Bowen, B., and Cande, W. Z. (1999). Three-dimensional microscopy of the Rad51 recombination protein during meiotic prophase. *Plant Cell* 11, 809–824. doi: 10.1105/tpc.11.5.809

Gagne, J. M., Downes, B. P., Shiu, S.-H., Durski, A. M., and Vierstra, R. D. (2002). The F-box subunit of the SCF E3 complex is encoded by a diverse superfamily of genes in *Arabidopsis*. *Proc. Natl. Acad. Sci.* 99, 11519–11524. doi: 10.1073/pnas.162339999

Glotzer, M., Murray, A. W., and Kirschner, M. W. (1991). Cyclin is degraded by the ubiquitin pathway. *Nature* 349, 132–138. doi: 10.1038/349132a0

Greer, E., Martín, A. C., Pendle, A., Colas, I., Jones, A. M., Moore, G., et al. (2012). The Ph1 locus suppresses Cdk2-type activity during premeiosis and meiosis in wheat. *Plant Cell* 24, 152–162. doi: 10.1105/tpc.111.094771

Grelon, M., Vezon, D., Gendrot, G., and Pelletier, G. (2001). AtSPO11-1 is necessary for efficient meiotic recombination in plants. *EMBO J.* 20, 589–600. doi: 10.1093/emboj/20.3.589

Grice, G. L., Lobb, I. T., Weekes, M. P., Gygi, S. P., Antrobus, R., and Nathan, J. A. (2015). The proteasome distinguishes between heterotypic and homotypic lysine-11-linked polyubiquitin chains. *Cell Rep.* 12, 545–553. doi: 10.1016/j.celrep.2015.06.061

Guan, Y., Leu, N. A., Ma, J., Chmátal, L., Ruthel, G., Bloom, J. C., et al. (2020). SKP1 drives the prophase I to metaphase I transition during male meiosis. *Sci. Adv.* 6:eaaz2129. doi: 10.1126/sciadv.aaz2129

Hansen, F. M., Tanzer, M. C., Bruning, F., Bludau, I., Stafford, C., Schulman, B. A., et al. (2021). Data-independent acquisition method for ubiquitinome analysis reveals regulation of circadian biology. *Nat. Commun.* 12:254. doi: 10.1038/s41467-020-20509-1

Harashima, H., and Schnittger, A. (2012). Robust reconstitution of active cell-cycle control complexes from co-expressed proteins in bacteria. *Plant Methods* 8:23. doi: 10.1186/1746-4811-8-23

Hatfield, P. M., Gosink, M. M., Carpenter, T. B., and Vierstra, R. D. (1997). The ubiquitin-activating enzyme (E1) gene family in *Arabidopsis thaliana*. *Plant J.* 11, 213–226. doi: 10.1046/j.1365-313X.1997.11020213.x

He, W., Rao, H., Tang, S., Bhagwat, N., Kulkarni, D. S., Ma, Y., et al. (2020). Regulated proteolysis of mutsgamma controls meiotic crossing over. *Mol. Cell* 78, 168–183 e165. doi: 10.1016/j.molcel.2020.02.001

He, Y., Wang, C., Higgins, J. D., Yu, J., Zong, J., Lu, P., et al. (2016). MEIOTIC F-BOX Is essential for male meiotic DNA double-strand break repair in rice. *Plant Cell* 28, 1879–1893. doi: 10.1105/tpc.16.00108

Hjerpe, R., Aillet, F., Lopitz-Otsoa, F., Lang, V., England, P., and Rodriguez, M. S. (2009). Efficient protection and isolation of ubiquitylated proteins using tandem ubiquitin-binding entities. *EMBO Rep.* 10, 1250–1258. doi: 10.1038/embor.2009.192

Hoppe, T. (2005). Multiubiquitylation by E4 enzymes: 'one size' doesn't fit all. *Trends Biochem. Sci.* 30, 183–187. doi: 10.1016/j.tibs.2005.02.004

Hristova, V., Sun, S., Zhang, H., and Chan, D. W. (2020). Proteomic analysis of degradation ubiquitin signaling by ubiquitin occupancy changes responding to 26S proteasome inhibition. *Clin. Proteomics* 17:2. doi: 10.1186/s12014-020-9265-x

Hsieh, P. H., He, S., Buttress, T., Gao, H., Couchman, M., Fischer, R. L., et al. (2016). *Arabidopsis* male sexual lineage exhibits more robust maintenance of CG methylation than somatic tissues. *Proc. Natl. Acad. Sci. U.S.A.* 113, 15132–15137. doi: 10.1073/pnas.1619074114

Hua, Z., Zou, C., Shiu, S. H., and Vierstra, R. D. (2011). Phylogenetic comparison of F-Box (FBX) gene superfamily within the plant kingdom reveals divergent evolutionary histories indicative of genomic drift. *PLoS One* 6:e16219. doi: 10.1371/journal.pone.0016219

Huang, M., and D'Andrea, A. D. (2010). A new nuclease member of the FAN club. *Nat. Struct. Mol. Biol.* 17, 926–928. doi: 10.1038/nsmb0810-926

Huang, Y., Minaker, S., Roth, C., Huang, S., Hieter, P., Lipka, V., et al. (2014). An E4 ligase facilitates polyubiquitination of plant immune receptor resistance proteins in *Arabidopsis*. *Plant Cell* 26, 485–496. doi: 10.1105/tpc.113.119057

Hughes, S. E., Hemenway, E., Guo, F., Yi, K., Yu, Z., and Hawley, R. S. (2019). The E3 ubiquitin ligase Sina regulates the assembly and disassembly of the synaptonemal complex in *Drosophila* females. *PLoS Genet.* 15:e1008161. doi: 10.1371/journal.pgen.1008161

Hunter, N., and Borts, R. H. (1997). Mlh1 is unique among mismatch repair proteins in its ability to promote crossing-over during meiosis. *Genes Dev.* 11, 1573–1582. doi: 10.1101/gad.11.12.1573

Iconomou, M., and Saunders, D. N. (2016). Systematic approaches to identify E3 ligase substrates. *Biochem. J.* 473, 4083–4101. doi: 10.1042/BCJ20160719

Iwata, E., Ikeda, S., Matsunaga, S., Kurata, M., Yoshioka, Y., Criqui, M. C., et al. (2011). GIGAS CELL1, a novel negative regulator of the anaphase-promoting complex/cyclosome, is required for proper mitotic progression and cell fate determination in *Arabidopsis*. *Plant Cell* 23, 4382–4393. doi: 10.1105/tpc.111.092049

Jahns, M. T., Vezon, D., Chambon, A., Pereira, L., Falque, M., Martin, O. C., et al. (2014). Crossover localisation is regulated by the neddylation posttranslational regulatory pathway. *PLoS Biol.* 12:e1001930. doi: 10.1371/journal.pbio.1001930

Jantsch, V., Pasierbek, P., Mueller, M. M., Schweizer, D., Jantsch, M., and Loidl, J. (2004). Targeted gene knockout reveals a role in meiotic recombination for ZHP-3, a Zip3-related protein in *Caenorhabditis elegans*. *Mol. Cell. Biol.* 24, 7998–8006. doi: 10.1128/MCB.24.18.7998-8006.2004

Jonak, K., Zagoriy, I., Oz, T., Graf, P., Rojas, J., Mengoli, V., et al. (2017). APC/C-Cdc20 mediates deprotection of centromeric cohesin at meiosis II in yeast. *Cell Cycle* 16, 1145–1152. doi: 10.1080/15384101.2017.1320628

Kamolsukyeunyong, W., Ruengphayak, S., Chumwong, P., Kusumawati, L., Chaichoompu, E., Jamboonsri, W., et al. (2019). Identification of spontaneous mutation for broad-spectrum brown planthopper resistance in a large, long-term fast neutron mutagenized rice population. *Rice (N. Y.)* 12:16. doi: 10.1186/s12284-019-0274-1

Katoh, K., and Standley, D. M. (2013). MAFFT multiple sequence alignment software version 7: improvements in performance and usability. *Mol. Biol. Evol.* 30, 772–780. doi: 10.1093/molbev/mst010

Keeney, S., Giroux, C. N., and Kleckner, N. (1997). Meiosis-specific DNA double-strand breaks are catalyzed by Spo11, a member of a widely conserved protein family. *Cell* 88, 375–384. doi: 10.1016/s0092-8674(00)81876-0

Kernan, J., Bonacci, T., and Emanuele, M. J. (2018). Who guards the guardian? Mechanisms that restrain APC/C during the cell cycle. *Biochim. Biophys. Acta Mol. Cell Res.* 1865, 1924–1933. doi: 10.1016/j.bbamcr.2018.09.011

Kevei, Z., Baloban, M., Da Ines, O., Tiricz, H., Kroll, A., Regulski, K., et al. (2011). Conserved CDC20 cell cycle functions are carried out by two of the five isoforms in *Arabidopsis thaliana*. *PLoS One* 6:e20618. doi: 10.1371/journal.pone.0020618

Khoo, K. H., Able, A. J., Chataway, T. K., and Able, J. A. (2012). Preliminary characterisation of two early meiotic wheat proteins after identification through 2D gel electrophoresis proteomics. *Funct. Plant Biol.* 39, 222–235. doi: 10.1071/FP11253

Kitajima, T. S., Kawashima, S. A., and Watanabe, Y. (2004). The conserved kinetochore protein shugoshin protects centromeric cohesion during meiosis. *Nature* 427, 510–517. doi: 10.1038/nature02312

Komander, D., Clague, M. J., and Urbe, S. (2009). Breaking the chains: structure and function of the deubiquitinases. *Nat. Rev. Mol. Cell Biol.* 10, 550–563. doi: 10.1038/nrm2731

Kong, H., Leebens-Mack, J., Ni, W., Depamphilis, C. W., and Ma, H. (2004). Highly heterogeneous rates of evolution in the SKP1 gene family in plants and animals: functional and evolutionary implications. *Mol. Biol. Evol.* 21, 117–128. doi: 10.1093/molbev/msh001

Kopanja, D., Roy, N., Stoyanova, T., Hess, R. A., Bagchi, S., and Raychaudhuri, P. (2011). Cul4A is essential for spermatogenesis and male fertility. *Dev. Biol.* 352, 278–287. doi: 10.1016/j.ydbio.2011.01.028

Kulathu, Y., and Komander, D. (2012). Atypical ubiquitylation—the unexplored world of polyubiquitin beyond Lys48 and Lys63 linkages. *Nat. Rev. Mol. Cell Biol.* 13, 508–523. doi: 10.1038/nrm3394

Lambing, C., and Heckmann, S. (2018). Tackling plant meiosis: from model research to crop improvement. *Front. Plant Sci.* 9:829. doi: 10.3389/fpls.2018.00829

Lambing, C., Osman, K., Nuntasoontorn, K., West, A., Higgins, J. D., Copenhaver, G. P., et al. (2015). *Arabidopsis* PCH2 mediates meiotic chromosome remodeling and maturation of crossovers. *PLoS Genet.* 11:e1005372. doi: 10.1371/journal.pgen.1005372

Lee, C. M., Feke, A., Li, M. W., Adamchek, C., Webb, K., Pruneda-Paz, J., et al. (2018). Decoys untangle complicated redundancy and reveal targets of circadian clock F-box proteins. *Plant Physiol.* 177, 1170–1186. doi: 10.1104/pp.18.00331

Lewandowska, D., Zhang, R., Colas, I., Uzrek, N., and Waugh, R. (2019). Application of a sensitive and reproducible label-free proteomic approach to explore the proteome of individual meiotic-phase Barley Anthers. *Front. Plant Sci.* 10:393. doi: 10.3389/fpls.2019.00393

Leyser, H., Lincoln, C., Timpte, C., Lammer, D., Turner, J., and Estelle, M. (1993). *Arabidopsis* auxin-resistance gene AXR1 encodes a protein related to ubiquitin-activating enzyme E1. *Nature* 364, 161–164. doi: 10.1038/364161a0

Li, C., Liang, Y., Chen, C., Li, J., Xu, Y., Xu, Z., et al. (2006). Cloning and expression analysis of TSK1, a wheat SKP1 homologue, and functional comparison with *Arabidopsis* ASK1 in male meiosis and auxin signalling. *Funct. Plant Biol.* 33, 381–390. doi: 10.1071/FP06026

Li, X., Ye, J., Ma, H., and Lu, P. (2018). Proteomic analysis of lysine acetylation provides strong evidence for involvement of acetylated proteins in plant meiosis and tapetum function. *Plant J.* 93, 142–154. doi: 10.1111/tpj.13766

Li, Y., Lan, Q., Gao, Y., Xu, C., Xu, Z., Wang, Y., et al. (2020). Ubiquitin linkage specificity of deubiquitinases determines cyclophilin nuclear localization and degradation. *iScience* 23:100984. doi: 10.1016/j.isci.2020.100984

Li, Y., Qin, B., Shen, Y., Zhang, F., Liu, C., You, H., et al. (2018). HEIP1 regulates crossover formation during meiosis in rice. *Proc. Natl. Acad. Sci. U.S.A.* 115, 10810–10815. doi: 10.1073/pnas.1807871115

Lin, D. Y., Huang, Y. S., Jeng, J. C., Kuo, H. Y., Chang, C. C., Chao, T. T., et al. (2006). Role of SUMO-interacting motif in Daxx SUMO modification, subnuclear localization, and repression of sumoylated transcription factors. *Mol. Cell* 24, 341–354. doi: 10.1016/j.molcel.2006.10.019

Ling, R., Colón, E., Dahmus, M. E., and Callis, J. (2000). Histidine-tagged ubiquitin substitutes for wild-type ubiquitin in *Saccharomyces cerevisiae* and facilitates isolation and identification of in vivo substrates of the ubiquitin pathway. *Anal. Biochem.* 282, 54–64. doi: 10.1006/abio.2000.4586

Littlepage, L. E., and Ruderman, J. V. (2002). Identification of a new APC/C recognition domain, the A box, which is required for the Cdh1-dependent destruction of the kinase Aurora-A during mitotic exit. *Genes Dev.* 16, 2274–2285. doi: 10.1101/gad.1007302

Liu, F., Ni, W., Griffith, M. E., Huang, Z., Chang, C., Peng, W., et al. (2004). The ASK1 and ASK2 genes are essential for *Arabidopsis* early development. *Plant Cell* 16, 5–20. doi: 10.1105/tpc.017772

Liu, M., Shi, S., Zhang, S., Xu, P., Lai, J., Liu, Y., et al. (2014). SUMO E3 ligase AtMMS21 is required for normal meiosis and gametophyte development in *Arabidopsis*. *BMC Plant Biol.* 14:153. doi: 10.1186/1471-2229-14-153

Liu, Y., Lai, J., Yu, M., Wang, F., Zhang, J., Jiang, J., et al. (2016). The *Arabidopsis* SUMO E3 ligase AtMMS21 dissociates the E2Fa/DPa complex in cell cycle regulation. *Plant Cell* 28, 2225–2237. doi: 10.1105/tpc.16.00439

López-Mosqueda, J., and Dikic, I. (2014). Deciphering functions of branched ubiquitin chains. *Cell* 157, 767–769. doi: 10.1016/j.cell.2014.04.026

Ludwig, C., Gillet, L., Rosenberger, G., Amon, S., Collins, B. C., and Aebersold, R. (2018). Data-independent acquisition-based SWATH−MS for quantitative proteomics: a tutorial. *Mol. Syst. Biol.* 14:e8126. doi: 10.15252/msb.20178126

March, E., and Farrona, S. (2018). Plant deubiquitinases and their role in the control of gene expression through modification of histones. *Front. Plant Sci.* 8:2274. doi: 10.3389/fpls.2017.02274

Mark, K. G., Loveless, T. B., and Toczyski, D. P. (2016). Isolation of ubiquitinated substrates by tandem affinity purification of E3 ligase-polyubiquitin-binding domain fusions (ligase traps). *Nat. Protoc.* 11, 291–301. doi: 10.1038/nprot.2016.008

Marrocco, K., Lecureuil, A., Nicolas, P., and Guerche, P. (2003). The *Arabidopsis* SKP1-like genes present a spectrum of expression profiles. *Plant Mol. Biol.* 52, 715–727. doi: 10.1023/A:1025056008926

Martinez-Garcia, M., Fernandez-Jimenez, N., Santos, J. L., and Pradillo, M. (2020). Duplication and divergence: new insights into AXR1 and AXL functions in DNA repair and meiosis. *Sci. Rep.* 10:8860. doi: 10.1038/s41598-020-65734-2

Matzke, M. A., and Mosher, R. A. (2014). RNA-directed DNA methylation: an epigenetic pathway of increasing complexity. *Nat. Rev. Genet.* 15, 394–408. doi: 10.1038/nrg3683

Mavrommati, I., Faedda, R., Galasso, G., Li, J., Burdova, K., Fischer, R., et al. (2018). beta-TrCP- and casein kinase II-mediated degradation of cyclin f controls timely mitotic progression. *Cell Rep.* 24, 3404–3412. doi: 10.1016/j.celrep.2018.08.076

McLoud, J. D., and Yang, M. (2012). The conserved function of skp1 in meiosis. *Front. Genet.* 3:179. doi: 10.3389/fgene.2012.00179

Mercier, R., Jolivet, S., Vezon, D., Huppe, E., Chelysheva, L., Giovanni, M., et al. (2005). Two meiotic crossover classes cohabit in *Arabidopsis*. *Curr. Biol.* 15, 692–701. doi: 10.1016/j.cub.2005.02.056

Mercier, R., Mezard, C., Jenczewski, E., Macaisne, N., and Grelon, M. (2015). The molecular biology of meiosis in plants. *Annu. Rev. Plant Biol.* 66, 297–327. doi: 10.1146/annurev-arplant-050213-035923

Metzger, M. B., Hristova, V. A., and Weissman, A. M. (2012). HECT and RING finger families of E3 ubiquitin ligases at a glance. *J. Cell Sci.* 125, 531–537. doi: 10.1242/jcs.091777

Meyer, H. J., and Rape, M. (2014). Enhanced protein degradation by branched ubiquitin chains. *Cell* 157, 910–921. doi: 10.1016/j.cell.2014.03.037

Miller, M. J., Barrett-Wilt, G. A., Hua, Z., and Vierstra, R. D. (2010). Proteomic analyses identify a diverse array of nuclear processes affected by small ubiquitin-like modifier conjugation in *Arabidopsis*. *Proc. Natl. Acad. Sci. U.S.A.* 107, 16512–16517. doi: 10.1073/pnas.1004181107

Min, M., Mevissen, T. E., De Luca, M., Komander, D., and Lindon, C. (2015). Efficient APC/C substrate degradation in cells undergoing mitotic exit depends on K11 ubiquitin linkages. *Mol. Biol. Cell* 26, 4325–4332. doi: 10.1091/mbc.E15-02-0102

Mocciaro, A., and Rape, M. (2012). Emerging regulatory mechanisms in ubiquitin-dependent cell cycle control. *J. Cell Sci.* 125, 255–263. doi: 10.1242/jcs.091199

Nguyen, L.-T., Schmidt, H. A., Von Haeseler, A., and Minh, B. Q. (2014). IQ-TREE: a fast and effective stochastic algorithm for estimating maximum-likelihood phylogenies. *Mol. Biol. Evol.* 32, 268–274. doi: 10.1093/molbev/msu300

Niu, B., Wang, L., Zhang, L., Ren, D., Ren, R., Copenhaver, G. P., et al. (2015). *Arabidopsis* cell division Cycle 20.1 is required for normal meiotic spindle assembly and chromosome segregation. *Plant Cell* 27, 3367–3382. doi: 10.1105/tpc.15.00834

Nowack, M. K., Harashima, H., Dissmeyer, N., Zhao, X., Bouyer, D., Weimer, A. K., et al. (2012). Genetic framework of cyclin-dependent kinase function in *Arabidopsis*. *Dev. Cell* 22, 1030–1040. doi: 10.1016/j.devcel.2012.02.015

O'Connor, H. F., Lyon, N., Leung, J. W., Agarwal, P., Swaim, C. D., Miller, K. M., et al. (2015). Ubiquitin-activated interaction traps (UBAITs) identify E3 ligase binding partners. *EMBO Rep.* 16, 1699–1712. doi: 10.15252/embr.201540620

Ogawa, D., Abe, K., Miyao, A., Kojima, M., Sakakibara, H., Mizutani, M., et al. (2011). RSS1 regulates the cell cycle and maintains meristematic activity under stress conditions in rice. *Nat. Commun.* 2:278. doi: 10.1038/ncomms1279

Osman, K., Higgins, J. D., Sanchez-Moran, E., Armstrong, S. J., and Franklin, F. C. H. (2011). Pathways to meiotic recombination in *Arabidopsis thaliana*. *New Phytol.* 190, 523–544. doi: 10.1111/j.1469-8137.2011.03665.x

Osman, K., Yang, J., Roitinger, E., Lambing, C., Heckmann, S., Howell, E., et al. (2018). Affinity proteomics reveals extensive phosphorylation of the Brassica chromosome axis protein ASY 1 and a network of associated proteins at prophase I of meiosis. *Plant J.* 93, 17–33. doi: 10.1111/tpj.13752

Pawlowski, W. P., Wang, C.-J. R., Golubovskaya, I. N., Szymaniak, J. M., Shi, L., Hamant, O., et al. (2009). Maize AMEIOTIC1 is essential for multiple early meiotic processes and likely required for the initiation of meiosis. *Proc. Natl. Acad. Sci. U.S.A.* 106, 3603–3608. doi: 10.1073/pnas.0810115106

Pfleger, C. M., and Kirschner, M. W. (2000). The KEN box: an APC recognition signal distinct from the D box targeted by Cdh1. *Genes Dev.* 14, 655–665. doi: 10.1101/gad.14.6.655

Pines, J. (1995). Cyclins and cyclin-dependent kinases: a biochemical view. *Biochem. J.* 308, 697–711. doi: 10.1042/bj3080697

Plafker, S. M., Plafker, K. S., Weissman, A. M., and Macara, I. G. (2004). Ubiquitin charging of human class III ubiquitin-conjugating enzymes triggers their nuclear import. *J. Cell Biol.* 167, 649–659. doi: 10.1083/jcb.200406001

Prusicki, M. A., Keizer, E. M., Van Rosmalen, R. P., Komaki, S., Seifert, F., Muller, K., et al. (2019). Live cell imaging of meiosis in *Arabidopsis thaliana*. *Elife* 8:e42834. doi: 10.7554/eLife.42834

Pyatnitskaya, A., Borde, V., and De Muyt, A. (2019). Crossing and zipping: molecular duties of the ZMM proteins in meiosis. *Chromosoma* 128, 181–198. doi: 10.1007/s00412-019-00714-8

Qiao, H., Prasada Rao, H. B., Yang, Y., Fong, J. H., Cloutier, J. M., Deacon, D. C., et al. (2014). Antagonistic roles of ubiquitin ligase HEI10 and SUMO ligase RNF212 regulate meiotic recombination. *Nat. Genet.* 46, 194–199. doi: 10.1038/ng.2858

Qiao, R., Weissmann, F., Yamaguchi, M., Brown, N. G., Vanderlinden, R., Imre, R., et al. (2016). Mechanism of APC/CCDC20 activation by mitotic phosphorylation. *Proc. Natl. Acad. Sci. U.S.A.* 113, E2570–E2578. doi: 10.1073/pnas.1604929113

Ramadan, A., Nemoto, K., Seki, M., Shinozaki, K., Takeda, H., Takahashi, H., et al. (2015). Wheat germ-based protein libraries for the functional characterisation of the *Arabidopsis* E2 ubiquitin conjugating enzymes and the RING-type E3 ubiquitin ligase enzymes. *BMC Plant Biol.* 15:275. doi: 10.1186/s12870-015-0660-9

Rao, H. B. D. P., Qiao, H., Bhatt, S. K., Bailey, L. R. J., Tran, H. D., Bourne, S. L., et al. (2017). A SUMO-ubiquitin relay recruits proteasomes to chromosome axes to regulate meiotic recombination. *Science* 355, 403–407. doi: 10.1126/science.aaf6407

Rayner, S. L., Morsch, M., Molloy, M. P., Shi, B., Chung, R., and Lee, A. (2019). Using proteomics to identify ubiquitin ligase-substrate pairs: how novel methods may unveil therapeutic targets for neurodegenerative diseases. *Cell. Mol. Life Sci.* 76, 2499–2510. doi: 10.1007/s00018-019-03082-9

Reynolds, A., Qiao, H., Yang, Y., Chen, J. K., Jackson, N., Biswas, K., et al. (2013). RNF212 is a dosage-sensitive regulator of crossing-over during mammalian meiosis. *Nat. Genet.* 45, 269–278. doi: 10.1038/ng.2541

Risseeuw, E. P., Daskalchuk, T. E., Banks, T. W., Liu, E., Cotelesage, J., Hellmann, H., et al. (2003). Protein interaction analysis of SCF ubiquitin E3 ligase subunits from *Arabidopsis*. *Plant J.* 34, 753–767. doi: 10.1046/j.1365-313X.2003.01768.x

Rodrigo-Brenni, M. C., and Morgan, D. O. (2007). Sequential E2s drive polyubiquitin chain assembly on APC targets. *Cell* 130, 127–139. doi: 10.1016/j.cell.2007.05.027

Rose, C. M., Isasa, M., Ordureau, A., Prado, M. A., Beausoleil, S. A., Jedrychowski, M. P., et al. (2016). Highly multiplexed quantitative mass spectrometry analysis of ubiquitylomes. *Cell Syst.* 3:e394. doi: 10.1016/j.cels.2016.08.009

Ross, P. L., Huang, Y. N., Marchese, J. N., Williamson, B., Parker, K., Hattan, S., et al. (2004). Multiplexed protein quantitation in *Saccharomyces cerevisiae* using amine-reactive isobaric tagging reagents. *Mol. Cell. Proteomics* 3, 1154–1169. doi: 10.1074/mcp.M400129-MCP200

Roux, K. J., Kim, D. I., Raida, M., and Burke, B. (2012). A promiscuous biotin ligase fusion protein identifies proximal and interacting proteins in mammalian cells. *J. Cell Biol.* 196, 801–810. doi: 10.1083/jcb.201112098

Roy, D., and Sadanandom, A. (2021). SUMO mediated regulation of transcription factors as a mechanism for transducing environmental cues into cellular signaling in plants. *Cell Mol. Life Sci.* doi: 10.1007/s00018-020-03723-4

Saracco, S. A., Hansson, M., Scalf, M., Walker, J. M., Smith, L. M., and Vierstra, R. D. (2009). Tandem affinity purification and mass spectrometric analysis of ubiquitylated proteins in *Arabidopsis*. *Plant J.* 59, 344–358. doi: 10.1111/j.1365-313X.2009.03862.x

Sawada, H., Mino, M., and Akasaka, M. (2014). "Sperm proteases and extracellular ubiquitin–proteasome system involved in fertilization of ascidians and sea urchins," in *Posttranslational Protein Modifications in the Reproductive System*, 1 Edn, ed. P. Sutovsky (New York, NY: Springer), 1–11. doi: 10.1007/978-1-4939-0817-2_1

Serra, H., Lambing, C., Griffin, C. H., Topp, S. D., Nageswaran, D. C., Underwood, C. J., et al. (2018). Massive crossover elevation via combination of HEI10 and recq4a recq4b during *Arabidopsis* meiosis. *Proc. Natl. Acad. Sci.* 115, 2437–2442. doi: 10.1073/pnas.1713071115

Shi, Y., Chan, W. K., Jung, S. Y., Malovannaya, A., Wang, Y., and Qin, J. (2011). A data set of human endogenous protein ubiquitination sites. *Mol. Cell. Proteomics* 10:M110.002089. doi: 10.1074/mcp.M110.002089

Shunmugam, A. S., Bollina, V., Dukowic-Schulze, S., Bhowmik, P. K., Ambrose, C., Higgins, J. D., et al. (2018). MeioCapture: an efficient method for staging and isolation of meiocytes in the prophase I sub-stages of meiosis in wheat. *BMC Plant Biol.* 18:293. doi: 10.1186/s12870-018-1514-z

Singh, M. K., Nicolas, E., Gherraby, W., Dadke, D., Lessin, S., and Golemis, E. A. (2007). HEI10 negatively regulates cell invasion by inhibiting cyclin B/Cdk1 and other promotility proteins. *Oncogene* 26, 4825–4832. doi: 10.1038/sj.onc.1210282

Skelly, M. J., Furniss, J. J., Grey, H., Wong, K. W., and Spoel, S. H. (2019). Dynamic ubiquitination determines transcriptional activity of the plant immune coactivator NPR1. *Elife* 8:e47005. doi: 10.7554/eLife.47005

Sofroni, K., Takatsuka, H., Yang, C., Dissmeyer, N., Komaki, S., Hamamura, Y., et al. (2020). CDKD-dependent activation of CDKA;1 controls microtubule dynamics and cytokinesis during meiosis. *J. Cell Biol.* 219:e201907016. doi: 10.1083/jcb.201907016

Song, M., Hakala, K., Weintraub, S. T., and Shiio, Y. (2011). Quantitative proteomic identification of the BRCA1 ubiquitination substrates. *J. Proteome Res.* 10, 5191–5198. doi: 10.1021/pr200662b

Sowa, M. E., Bennett, E. J., Gygi, S. P., and Harper, J. W. (2009). Defining the human deubiquitinating enzyme interaction landscape. *Cell* 138, 389–403. doi: 10.1016/j.cell.2009.04.042

Strong, E. R., and Schimenti, J. C. (2010). Evidence implicating CCNB1IP1, a RING domain-containing protein required for meiotic crossing over in mice, as an E3 SUMO ligase. *Genes (Basel)* 1, 440–451. doi: 10.3390/genes1030440

Swatek, K. N., and Komander, D. (2016). Ubiquitin modifications. *Cell Res* 26, 399–422. doi: 10.1038/cr.2016.39

Tagwerker, C., Flick, K., Cui, M., Guerrero, C., Dou, Y., Auer, B., et al. (2006). A tandem affinity tag for two-step purification under fully denaturing conditions: application in ubiquitin profiling and protein complex identification combined with in vivocross-linking. *Mol. Cell Proteomics* 5, 737–748. doi: 10.1074/mcp.M500368-MCP200

Takahashi, N., Kuroda, H., Kuromori, T., Hirayama, T., Seki, M., Shinozaki, K., et al. (2004). Expression and interaction analysis of *Arabidopsis* Skp1-related genes. *Plant Cell Physiol.* 45, 83–91. doi: 10.1093/pcp/pch009

Tan, M. K., Lim, H. J., Bennett, E. J., Shi, Y., and Harper, J. W. (2013). Parallel SCF adaptor capture proteomics reveals a role for SCFFBXL17 in NRF2 activation via BACH1 repressor turnover. *Mol. Cell* 52, 9–24. doi: 10.1016/j.molcel.2013.08.018

Tang, X., Zhang, Z. Y., Zhang, W. J., Zhao, X. M., Li, X., Zhang, D., et al. (2010). Global gene profiling of laser-captured pollen mother cells indicates molecular pathways and gene subfamilies involved in rice meiosis. *Plant Physiol.* 154, 1855–1870. doi: 10.1104/pp.110.161661

Thines, B., Katsir, L., Melotto, M., Niu, Y., Mandaokar, A., Liu, G., et al. (2007). JAZ repressor proteins are targets of the SCF(COI1) complex during jasmonate signalling. *Nature* 448, 661–665. doi: 10.1038/nature05960

Thrower, J. S., Hoffman, L., Rechsteiner, M., and Pickart, C. M. (2000). Recognition of the polyubiquitin proteolytic signal. *EMBO J.* 19, 94–102. doi: 10.1093/emboj/19.1.94

Udeshi, N. D., Mani, D. C., Satpathy, S., Fereshetian, S., Gasser, J. A., Svinkina, T., et al. (2020). Rapid and deep-scale ubiquitylation profiling for biology and translational research. *Nat. Commun.* 11:359. doi: 10.1038/s41467-019-14175-1

Vader, G. (2015). Pch2(TRIP13): controlling cell division through regulation of HORMA domains. *Chromosoma* 124, 333–339. doi: 10.1007/s00412-015-0516-y

van der Wal, L., Bezstarosti, K., Sap, K. A., Dekkers, D. H. W., Rijkers, E., Mientjes, E., et al. (2018). Improvement of ubiquitylation site detection by Orbitrap mass spectrometry. *J. Proteomics* 172, 49–56. doi: 10.1016/j.jprot.2017.10.014

Walker, J., Gao, H., Zhang, J., Aldridge, B., Vickers, M., Higgins, J. D., et al. (2018). Sexual-lineage-specific DNA methylation regulates meiosis in *Arabidopsis*. *Nat. Genet.* 50, 130–137. doi: 10.1038/s41588-017-0008-5

Walsh, C. K., and Sadanandom, A. (2014). Ubiquitin chain topology in plant cell signaling: a new facet to an evergreen story. *Front. Plant Sci.* 5:122. doi: 10.3389/fpls.2014.00122

Wang, K., Wang, M., Tang, D., Shen, Y., Miao, C., Hu, Q., et al. (2012). The role of rice HEI10 in the formation of meiotic crossovers. *PLoS Genet.* 8:e1002809. doi: 10.1371/journal.pgen.1002809

Wang, S., Cao, L., and Wang, H. (2016). *Arabidopsis* ubiquitin-conjugating enzyme UBC22 is required for female gametophyte development and likely involved in Lys11-linked ubiquitination. *J. Exp. Bot.* 67, 3277–3288. doi: 10.1093/jxb/erw142

Wang, Y., and Copenhaver, G. P. (2018). Meiotic recombination: mixing it up in plants. *Annu. Rev. Plant Biol.* 69, 577–609. doi: 10.1146/annurev-arplant-042817-040431

Wang, Y., Hou, Y., Gu, H., Kang, D., Chen, Z. L., Liu, J., et al. (2013). The *Arabidopsis* anaphase-promoting complex/cyclosome subunit 1 is critical for both female gametogenesis and embryogenesis(F). *J. Integr. Plant Biol.* 55, 64–74. doi: 10.1111/jipb.12018

Wang, Y., and Yang, M. (2006). The *ARABIDOPSIS* SKP1-LIKE1 (ASK1) protein acts predominately from leptotene to pachytene and represses homologous recombination in male meiosis. *Planta* 223, 613–617. doi: 10.1007/s00425-005-0154-3

Wang, Y. F., Chao, Q., Li, Z., Lu, T. C., Zheng, H. Y., Zhao, C. F., et al. (2019). Large-scale identification and time-course quantification of ubiquitylation events during maize seedling De-etiolation. *Genomics Proteomics Bioinformatics* 17, 603–622. doi: 10.1016/j.gpb.2018.05.005

Ward, J. O., Reinholdt, L. G., Motley, W. W., Niswander, L. M., Deacon, D. C., Griffin, L. B., et al. (2007). Mutation in mouse hei10, an e3 ubiquitin ligase, disrupts meiotic crossing over. *PLoS Genet.* 3:e139. doi: 10.1371/journal.pgen.0030139

Watanabe, M., Saeki, Y., Takahashi, H., Ohtake, F., Yoshida, Y., Kasuga, Y., et al. (2020). A substrate-trapping strategy to find E3 ubiquitin ligase substrates identifies Parkin and TRIM28 targets. *Commun. Biol.* 3:592. doi: 10.1038/s42003-020-01328-y

West, A. M. V., Rosenberg, S. C., Ur, S. N., Lehmer, M. K., Ye, Q., Hagemann, G., et al. (2019). A conserved filamentous assembly underlies the structure of the meiotic chromosome axis. *eLife* 8, e40372. doi: 10.7554/eLife.40372

Wickliffe, K. E., Lorenz, S., Wemmer, D. E., Kuriyan, J., and Rape, M. (2011). The mechanism of linkage-specific ubiquitin chain elongation by a single-subunit E2. *Cell* 144, 769–781. doi: 10.1016/j.cell.2011.01.035

Wijnker, E., Harashima, H., Muller, K., Parra-Nunez, P., De Snoo, C. B., Van De Belt, J., et al. (2019). The Cdk1/Cdk2 homolog CDKA;1 controls the recombination landscape in *Arabidopsis*. *Proc. Natl. Acad. Sci. U.S.A.* 116, 12534–12539. doi: 10.1073/pnas.1820753116

Wijnker, E., and Schnittger, A. (2013). Control of the meiotic cell division program in plants. *Plant Reprod.* 26, 143–158. doi: 10.1007/s00497-013-0223-x

Wu, Z., Tong, M., Tian, L., Zhu, C., Liu, X., Zhang, Y., et al. (2020). Plant E3 ligases SNIPER1 and SNIPER2 broadly regulate the homeostasis of sensor NLR immune receptors. *EMBO J.* 39:e104915. doi: 10.15252/embj.2020104915

Xie, D.-X., Feys, B. F., James, S., Nieto-Rostro, M., and Turner, J. G. (1998). *COI1*: an *Arabidopsis* gene required for jasmonate-regulated defense and fertility. *Science* 280, 1091–1094. doi: 10.1126/science.280.5366.1091

Xu, G., Paige, J. S., and Jaffrey, S. R. (2010). Global analysis of lysine ubiquitination by ubiquitin remnant immunoaffinity profiling. *Nat. Biotechnol.* 28, 868–873. doi: 10.1038/nbt.1654

Xu, M., Skaug, B., Zeng, W., and Chen, Z. J. (2009). A ubiquitin replacement strategy in human cells reveals distinct mechanisms of IKK activation by TNFα and IL-1β. *Mol. cell* 36, 302–314. doi: 10.1016/j.molcel.2009.10.002

Xu, R. Y., Xu, J., Wang, L., Niu, B., Copenhaver, G. P., Ma, H., et al. (2019). The *Arabidopsis* anaphase-promoting complex/cyclosome subunit 8 is required for male meiosis. *New Phytol.* 224, 229–241. doi: 10.1111/nph.16014

Yamano, H. (2019). APC/C: current understanding and future perspectives. *F1000Research* 8:F1000. doi: 10.12688/f1000research.18582.1

Yang, C., Hamamura, Y., Sofroni, K., Bower, F., Stolze, S. C., Nakagami, H., et al. (2019). SWITCH 1/DYAD is a WINGS APART-LIKE antagonist that maintains sister chromatid cohesion in meiosis. *Nat. Commun.* 10:1755. doi: 10.1038/s41467-019-09759-w

Yang, C., Sofroni, K., Wijnker, E., Hamamura, Y., Carstens, L., Harashima, H., et al. (2020). The *Arabidopsis* Cdk1/Cdk2 homolog CDKA;1 controls chromosome axis assembly during plant meiosis. *EMBO J.* 39:e101625. doi: 10.15252/embj.2019101625

Yang, H., Lu, P., Wang, Y., and Ma, H. (2011). The transcriptome landscape of *Arabidopsis* male meiocytes from high-throughput sequencing: the complexity and evolution of the meiotic process. *Plant J.* 65, 503–516. doi: 10.1111/j.1365-313X.2010.04439.x

Yang, M., Hu, Y., Lodhi, M., Mccombie, W. R., and Ma, H. (1999). The *Arabidopsis* SKP1-LIKE1 gene is essential for male meiosis and may control homologue separation. *Proc. Natl. Acad. Sci.* 96, 11416–11421. doi: 10.1073/pnas.96.20.11416

Yang, X., Timofejeva, L., Ma, H., and Makaroff, C. A. (2006). The *Arabidopsis* SKP1 homolog ASK1 controls meiotic chromosome remodeling and release of chromatin from the nuclear membrane and nucleolus. *J. Cell Sci.* 119, 3754–3763. doi: 10.1242/jcs.03155

Yao, X., Yang, H., Zhu, Y., Xue, J., Wang, T., Song, T., et al. (2018). The canonical E2Fs are required for Germline development in *Arabidopsis*. *Front. Plant Sci.* 9:638. doi: 10.3389/fpls.2018.00638

Ye, J., Zhang, Z., Long, H., Zhang, Z., Hong, Y., Zhang, X., et al. (2015). Proteomic and phosphoproteomic analyses reveal extensive phosphorylation of regulatory proteins in developing rice anthers. *Plant J.* 84, 527–544. doi: 10.1111/tpj.13019

Yin, Y., Lin, C., Kim, S. T., Roig, I., Chen, H., Liu, L., et al. (2011). The E3 ubiquitin ligase Cullin 4A regulates meiotic progression in mouse spermatogenesis. *Dev. Biol.* 356, 51–62. doi: 10.1016/j.ydbio.2011.05.661

Yoshida, Y., Saeki, Y., Murakami, A., Kawawaki, J., Tsuchiya, H., Yoshihara, H., et al. (2015). A comprehensive method for detecting ubiquitinated substrates using TR-TUBE. *Proc. Natl. Acad. Sci. U.S.A.* 112, 4630–4635. doi: 10.1073/pnas.1422313112

Yuan, D., Lai, J., Xu, P., Zhang, S., Zhang, J., Li, C., et al. (2014). AtMMS21 regulates DNA damage response and homologous recombination repair in *Arabidopsis*. *DNA Repair (Amst.)* 21, 140–147. doi: 10.1016/j.dnarep.2014.04.006

Yuan, T. L., Huang, W. J., He, J., Zhang, D., and Tang, W. H. (2018). Stage-specific gene profiling of germinal cells helps delineate the mitosis/meiosis transition. *Plant Physiol.* 176, 1610–1626. doi: 10.1104/pp.17.01483

Zhang, F., Tang, D., Shen, Y., Xue, Z., Shi, W., Ren, L., et al. (2017). The F-box protein ZYGO1 mediates bouquet formation to promote homologous pairing, synapsis, and recombination in rice meiosis. *Plant Cell* 29, 2597–2609. doi: 10.1105/tpc.17.00287

Zhang, J., Wang, C., Higgins, J. D., Kim, Y. J., Moon, S., Jung, K. H., et al. (2019). A Multiprotein complex regulates interference-sensitive crossover formation in rice. *Plant Physiol.* 181, 221–235. doi: 10.1104/pp.19.00082

Zhang, Y., Song, G., Lal, N. K., Nagalakshmi, U., Li, Y., Zheng, W., et al. (2019). TurboID-based proximity labeling reveals that UBR7 is a regulator of N NLR immune receptor-mediated immunity. *Nat. Commun.* 10:3252. doi: 10.1038/s41467-019-11202-z

Zheng, B., Chen, X., and Mccormick, S. (2011). The anaphase-promoting complex is a dual integrator that regulates both MicroRNA-mediated transcriptional

regulation of cyclin B1 and degradation of Cyclin B1 during *Arabidopsis* male gametophyte development. *Plant Cell* 23, 1033–1046. doi: 10.1105/tpc.111.083980

Zhu, L., Cheng, H., Peng, G., Wang, S., Zhang, Z., Ni, E., et al. (2020). Ubiquitinome profiling reveals the landscape of ubiquitination regulation in rice young panicles. *Genomics Proteomics Bioinformatics* 18, 305–320. doi: 10.1016/j.gpb.2019.01.005

Zhuang, M., Guan, S., Wang, H., Burlingame, A. L., and Wells, J. A. (2013). Substrates of IAP ubiquitin ligases identified with a designed orthogonal E3 ligase, the NEDDylator. *Mol. Cell* 49, 273–282. doi: 10.1016/j.molcel.2012.10.022

Ziolkowski, P. A., Underwood, C. J., Lambing, C., Martinez-Garcia, M., Lawrence, E. J., Ziolkowska, L., et al. (2017). Natural variation and dosage of the HEI10 meiotic E3 ligase control *Arabidopsis* crossover recombination. *Genes Dev.* 31, 306–317. doi: 10.1101/gad.295501.116

Zuin, A., Isasa, M., and Crosas, B. (2014). Ubiquitin signaling: extreme conservation as a source of diversity. *Cells* 3, 690–701. doi: 10.3390/cells3030690

Conflict of Interest: The authors declare that the research was conducted in the absence of any commercial or financial relationships that could be construed as a potential conflict of interest.

GLOSSARY

AGG11	ABERRANT GAMETOGENESIS 1
AM11	AMEIOTIC 1
ASKK	ARABIDOPSIS SKP1-LIKE
ASY11	ASYNAPTIC 1
ASY33	ASYNAPTIC 3
AXR11	AUXIN RESISTANT 1
ββ-TrCPP	BETA-TRANSDUCIN REPEATS-CONTAINING PROTEIN 1
BirAA	BIFUNCTIONAL LIGASE/REPRESSOR A
BRCA11	BREAST AND OVARIAN CANCER SUSCEPTIBILITY PROTEIN 1
CAP-D33	CONDENSIN-2 COMPLEX SUBUNIT D3
CCS522	CELL CYCLE SWITCH PROTEIN 52
CDC200	CELL DIVISION CYCLE 20
CFK11	COP9 SIGNALOSOME INTERACTING F_BOX KELCH 1
CDKK	CYCLIN DEPENDANT KINASE
COI11	CORONATINE INSENSITIVE 1
CUL11	CULLIN 1
DMC11	DISRUPTED MEIOTIC CDNA 1
DPaa	DIMERIZATION PARTNER A
DRM22	DOMAINS REARRANGED METHYLTRANSFERASE2
E2FF	E2 FACTOR
EST11	EVER SHORTER TELOMERES PROTEIN 1
HEI100	HUMAN ENHANCER OF INVASION 10
HEIP11	HEI10 INTERACTION PROTEIN
HPY22	HIGH PLOIDY 2
HR23AA	HOMOLOGUE OF RAD23 A
JMJ166	JMJC DOMAIN-CONTAINING PROTEIN 16
MER33	MEIOTIC RECOMBINATION 3
MLH33	MUTL HOMOLOG 3
MMD11	MALE MEIOCYTE DEATH 1
MMS211	METHYL METHANESULFONATE SENSITIVITY GENE 21
MOFF	MEIOTIC F-BOX
MSH44	MUTS HOMOLOG 4
MSH55	MUTS HOMOLOG 5
MUSE33	MUTANT, SNC1-ENHANCING 3
OSD11	OMISSION OF SECOND DIVISION 1
OSK11	ORYZA SATIVA SKP1-LIKE
PANS11	PATRONUS 1
PCH22	PACHYTENE CHECKPOINT PROTEIN 2
PDS55	PRECOCIOUS DISSOCIATION OF SISTER 5
PTDD	PARTING DANCERS
RAD511	RADIATION-SENSITIVE 51
RAD233	RADIATION-SENSITIVE 23
RNF2122	RING FINGER PROTEIN 212
RSS11	RICE SALT SENSITIVITY1
SGOO	SHUGOSHIN
SHOC11	SHORTAGE IN CHIASMATA 1
SINAA	SEVEN *IN ABSENTIA*
SMC11	STRUCTURAL MAINTENANCE OF CHROMOSOMES 1
SMC33	STRUCTURAL MAINTENANCE OF CHROMOSOMES 3
SMC55	STRUCTURAL MAINTENANCE OF CHROMOSOME 5
SMC66	STRUCTURAL MAINTENANCE OF CHROMOSOME 6
SMG77	SUPPRESSOR WITH MORPHOGENETIC EFFECTS ON GENITALIA 7
SNIPER 11	SNC1-INFLUENCING PLANT E3 LIGASE REVERSE 1
SNIPER 22	SNC1-INFLUENCING PLANT E3 LIGASE REVERSE 2
SUMOO	SMALL UBIQUITIN-LIKE MODIFIER
SWI11	SWITCH 1
SYCP22	SYNAPTONEMAL COMPLEX PROTEIN 2
SYP33	SYNAPTONEMAL COMPLEX PROTEIN 3
TAMM	TARDY ASYNCHRONUS MEIOSIS
TDM11	THREE DIVISION MUTANT 1
TEX111	TESTIS-EXPRESSED GENE 11
TOPIII	TOPOISOMERASE II
TRIP133	THYROID RECEPTOR-INTERACTING PROTEIN 13
UBC222	UBIQUITIN CONJUGATING ENZYME E2 22
UBE2SS	UBIQUITIN CONJUGATING ENZYME E2 S
UBE2CC	UBIQUITIN CONJUGATING ENZYME E2 C
UBE4AA	UBIQUITINATION FACTOR E4A
UBP3/44	UBIQUITIN SPECIFIC PROTEASE3/4
UFD-22	UBIQUITIN FUSION DEGRADATION-2
WAPLL	WINGS APART-LIKE
ZYGO11	ZYGOTENE1
ZYP11	MOLECULAR ZIPPER 1-LIKE PROTEIN
ZIP33	MOLECULAR ZIPPER PROTEIN 3
ZIP44	MOLECULAR ZIPPER PROTEIN 4

frontiers in Plant Science

REVIEW
published: 22 April 2021
doi: 10.3389/fpls.2021.658296

Meiosis Progression and Recombination in Holocentric Plants: What Is Known?

*Paulo G. Hofstatter, Gokilavani Thangavel, Marco Castellani and André Marques**

Department of Chromosome Biology, Max Planck Institute for Plant Breeding Research, Cologne, Germany

Differently from the common monocentric organization of eukaryotic chromosomes, the so-called holocentric chromosomes present many centromeric regions along their length. This chromosomal organization can be found in animal and plant lineages, whose distribution suggests that it has evolved independently several times. Holocentric chromosomes present an advantage: even broken chromosome parts can be correctly segregated upon cell division. However, the evolution of holocentricity brought about consequences to nuclear processes and several adaptations are necessary to cope with this new organization. Centromeres of monocentric chromosomes are involved in a two-step cohesion release during meiosis. To deal with that holocentric lineages developed different adaptations, like the chromosome remodeling strategy in *Caenorhabditis elegans* or the inverted meiosis in plants. Furthermore, the frequency of recombination at or around centromeres is normally very low and the presence of centromeric regions throughout the entire length of the chromosomes could potentially pose a problem for recombination in holocentric organisms. However, meiotic recombination happens, with exceptions, in those lineages in spite of their holocentric organization suggesting that the role of centromere as recombination suppressor might be altered in these lineages. Most of the available information about adaptations to meiosis in holocentric organisms is derived from the animal model *C. elegans.* As holocentricity evolved independently in different lineages, adaptations observed in *C. elegans* probably do not apply to other lineages and very limited research is available for holocentric plants. Currently, we still lack a holocentric model for plants, but good candidates may be found among Cyperaceae, a large angiosperm family. Besides holocentricity, chiasmatic and achiasmatic inverted meiosis are found in the family. Here, we introduce the main concepts of meiotic constraints and adaptations with special focus in meiosis progression and recombination in holocentric plants. Finally, we present the main challenges and perspectives for future research in the field of chromosome biology and meiosis in holocentric plants.

Keywords: holocentric chromosome, meiotic recombination, cohesion, centromere, inverted meiosis

OPEN ACCESS

Edited by:
Mónica Pradillo, Complutense University of Madrid, Spain

Reviewed by:
Scott Hawley, Stowers Institute for Medical Research, United States
Marcial Escudero, Sevilla University, Spain

****Correspondence:***
André Marques
amarques@mpipz.mpg.de

Specialty section:
This article was submitted to Plant Cell Biology, a section of the journal Frontiers in Plant Science

Received: *25 January 2021*
Accepted: *22 March 2021*
Published: *22 April 2021*

Citation:
Hofstatter PG, Thangavel G, Castellani M and Marques A (2021) Meiosis Progression and Recombination in Holocentric Plants: What Is Known? Front. Plant Sci. 12:658296. doi: 10.3389/fpls.2021.658296

INTRODUCTION

Meiosis, Conserved Mechanisms and Adaptations

Meiosis is a type of cell division responsible for reducing the number of chromosomes in diploid cells by half to produce haploid cells. It is a central step responsible for shuffling genetic information through meiotic recombination and produce genetic variation in eukaryotic life-cycles (Zickler and Kleckner, 2015). This is possible due to two rounds of cell division after a single DNA replication event with the participation of a specific and specialized meiotic machinery (Schurko and Logsdon, 2008).

Preliminary evidence suggests that meiosis is an ancestral feature of eukaryotes, what can robustly explain the patterns of pervasive occurrence of sexual processes in all eukaryotic diversity (Speijer et al., 2015). Despite the extreme conservation of the main meiotic steps even in the most distantly related groups, several lineages have specific meiotic adaptations. In *Drosophila*, several components of the core eukaryotic machinery playing roles in meiosis have been lost or even replaced: the meiosis-specific DMC1 recombinase was replaced by a distant homolog of it, spin-D/RAD51C (Abdu et al., 2003). *Schizosaccharomyces pombe* has lost the main meiotic pathway to resolve crossovers (COs) and heavily relies on a secondary pathway for the resolution of COs (which lacks interference) (Cromie et al., 2006). As a result, CO numbers are significantly higher in *S. pombe* compared to other model organisms, such as *Arabidopsis thaliana* (this plant presents around 1.5 CO per bivalent and both crossover resolution pathways are present) (Mercier et al., 2015). *S. pombe* has also lost the synaptonemal complex (Lorenz et al., 2004) and, thus, performs meiosis with a highly reduced machinery when compared to other well-characterized models. However, meiotic specializations are not restricted to the molecular machinery underpinning the main steps of the process. Some organisms exhibit morphological specializations as a consequence of structural peculiarities of chromosomal organization. For instance, homologous chromosomes (homologs) from some species of the genus *Oenothera* do not synapse upon meiosis rendering them functionally asexual even though they perform meiotic divisions (Johnson et al., 2009). This is due to large scale rearrangements inside the chromosomes, what leads to a state of permanent translocation heterozygosity. Another challenge to the regular progression of meiosis is the evolution of holocentric chromosomes in several lineages. In the main holocentric model, the nematode *C. elegans*, meiosis progresses in such a way that only a single chiasma is formed for each chromosome pair (Martinez-Perez et al., 2008; Martinez-Perez and Colaiacovo, 2009). In the case of holocentric plants of the families *Cyperaceae* (sedges) and Juncaceae (rushes), inverted meiosis evolved to cope with the holocentric chromosome structure: sister-chromatids are separated in the first meiotic division, while homologs are separated only upon the second division (Cabral et al., 2014; Heckmann et al., 2014; Marques et al., 2016). In an even more extreme case, *Rhynchospora tenuis* (Cyperaceae) presents achiasmatic inverted meiosis, whose viability seems to be possible due to the very small number of holocentric chromosomes inside the nucleus (just two pairs) so that even random segregation would produce some viable offspring (Cabral et al., 2014).

Meiosis Progression and Recombination in Monocentric Plants

The sequence of events associated with canonical (monocentric) meiosis is well-established (**Figure 1A**). The homologs pair and synapse by the formation of the synaptonemal complex. After the introduction of double-strand breaks onto DNA, a process of DNA repair based on inter-homolog recombination ensues (Zickler and Kleckner, 2015). The sister chromatids are held together by cohesion along the chromosome arms and centromeres. By the end of prophase I, the homologs have recombined, are physically connected by chiasmata, and meiotic cohesin REC8 along chromosome arms is released (Xu et al., 2005). This segregation scheme necessitates a two-step loss of sister chromatid cohesion. Cohesin is removed distally to chiasmata to allow homologs to segregate during meiosis I while being partially maintained to enable sister-chromatids to partition correctly during meiosis II. In organisms that are monocentric, this sequential loss of cohesion is regulated by shugoshin which is specifically associated to centromeres (Kitajima et al., 2004). Shugoshin protects cohesin at the centromere until meiosis II by recruiting the conserved phosphatase, PP2A, to antagonize the phosphorylation and removal of the cohesin complex (Kitajima et al., 2006; Riedel et al., 2006). At metaphase I, the bivalents align to the metaphase plate with the sister kinetochores being poleward mono-oriented. At anaphase I, homologous centromeres are bi-oriented, the bivalents are detached, as chiasmata are resolved, and the homologs migrate to opposite poles. The sisters are held together until metaphase II by centromeric cohesion. The sister kinetochores now face opposite poles during metaphase II, centromeric cohesion is lost, the sister-chromatids are released and migrate to opposite poles as well. At the end of the meiosis, each nucleus has a haploid number of chromosomes (Mercier et al., 2015).

Meiotic recombination is essential to sexual reproduction and the generation of genetic diversity and, thus, has a profound effect on patterns of genetic variation and is an important tool for crop breeding (Taagen et al., 2020). Variation in recombination rates is of particular interest due to efforts to increase the rate of genetic gain in agricultural crops by breaking up large linkage blocks containing both beneficial and detrimental alleles. Meiotic recombination events (crossovers, i.e., COs) are unevenly distributed throughout eukaryotic genomes, some regions exhibiting higher recombination rates (hotspots), while other exhibiting lower rates (cold spots) (Petes, 2001; Fernandes et al., 2019). The causes of this observed uneven distribution are currently not well-understood.

In most eukaryotes there is at least one CO per chromosome per meiotic event, which is normally required for faithful segregation of chromosomes. Additionally, the average number of COs is relatively low, typically from 1 to 3 events per chromosome (Mercier et al., 2015). In monocentric chromosomes, the density of COs is extremely heterogeneous

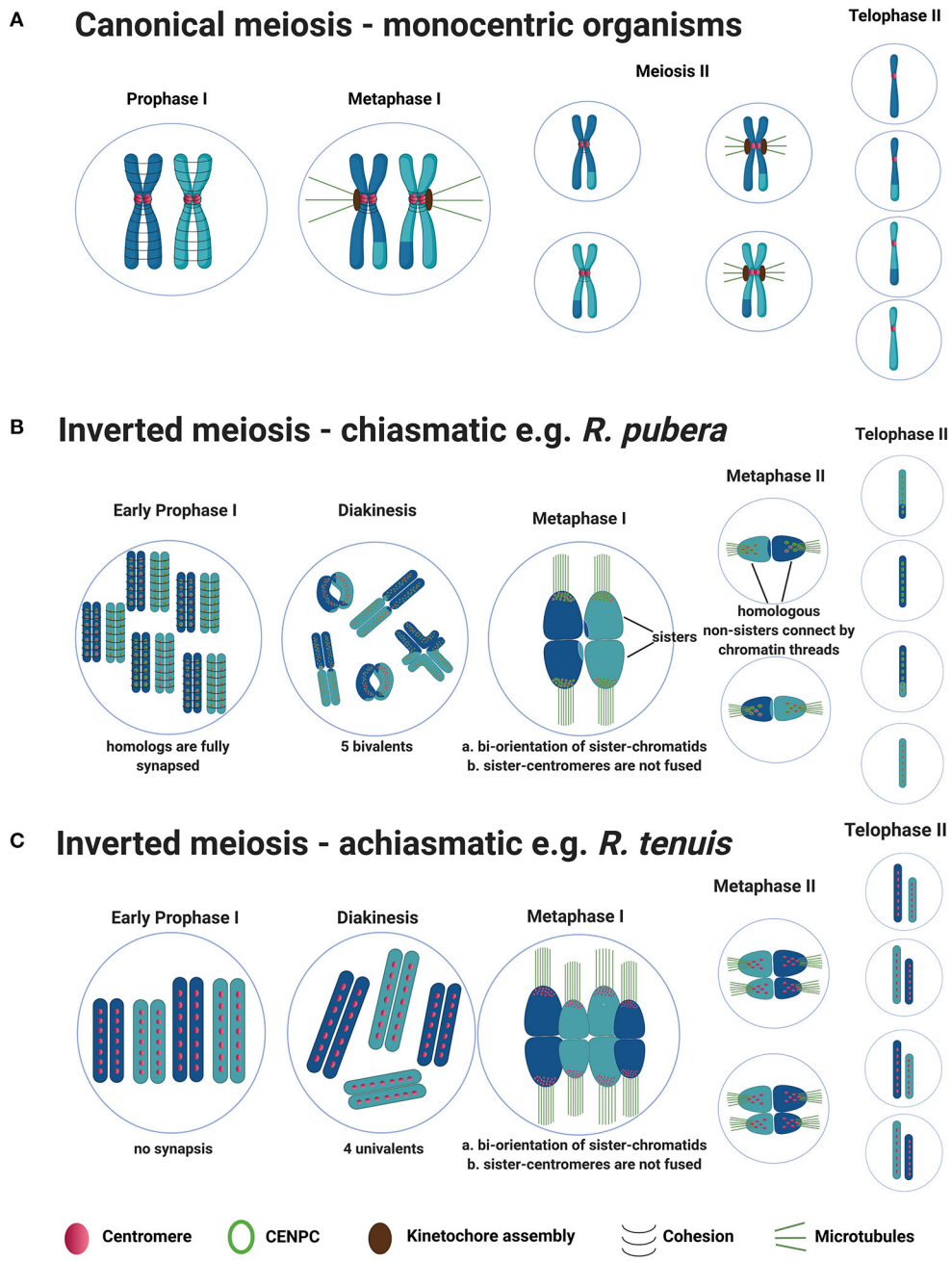

FIGURE 1 | General model for canonical meiosis in monocentric organisms vs. inverted meiosis (both chiasmatic and achiamatic) in holocentric plants. **(A)** Canonical meiosis: During meiosis I reciprocal genetic exchange between homologs (crossovers) occurs, sisters-chromatids mono-orient via fused sister-centromeres and segregate to the same poles. During meiosis II, sisters-chromatids bi-orient and segregate to the opposite poles, resulting in four haploid gametes at the end. **(B)** Schematic representation of chiasmatic inverted meiosis observed in *R. pubera* (from metaphase I only one bivalent is illustrated for better understanding). During meiosis I, COs take place but the difference is that, centromeres from sisters are not fused, sister chromatids bi-orient and segregate to the opposite poles already at anaphase I. During meiosis II homologous non-sisters align, bi-orient and segregate to the opposite poles, resulting in four haploid gametes similar to canonical meiosis. **(C)** Schematic representation of achiasmatic inverted meiosis observed in *R. tenuis*. The sequence of events during inverted meiosis observed in *R. tenuis* is similar to that of *R. pubera*, but meiosis in *R. tenuis* is reported to be achiasmatic i.e., crossover formation doesn't occur during prophase I. As a result, four univalents are observed during diakinesis instead of two bivalents.

at both large (chromosomal) and small scales (kb). Peri- and centromeric regions are largely depleted in COs (cold regions) (Petes, 2001; Fernandes et al., 2019). In some extreme cases, such as wheat, up to 80% of the genome hardly ever experience any COs (Choulet et al., 2014). These regions contain ∼30% of the genes which are thus out of reach for plant breeding.

To exchange DNA, the chromosomes must undergo double-strand breaks. This process of physiologically induced DNA fragmentation is conserved in the vast majority of eukaryotes and is carried out by the topoisomerase-like protein SPO11 (Keeney et al., 1997; Keeney, 2008). After SPO11 introduces double-strand breaks, the free 3′ ends left are targeted by the recombinases RAD51A and DMC1. These proteins help the 3′ ends to search for homologs as templates for repair. After the invasion of the single strand, a recombination intermediate structure is formed, the displacement loop (D-loop) (Brown and Bishop, 2014). DNA synthesis of both ends generate a new structure called double Holliday Junction (dHJ) (Wyatt and West, 2014). A CO is an outcome of the resolution of a dHJ, but other outcomes are possible (Allers and Lichten, 2001). In this case, the invading strand is ejected from the D-loop and anneal to the single-strand 3'end of the original double-strand break. Crossovers may be resolved in two main ways: the main pathway 1 (exhibiting interference) and a secondary pathway 2 (lacking interference). The pathway 1 is a meiosis-specific process with many associated proteins (the so-called ZMM proteins), namely MSH4, MSH5, MER3, HEI10, ZIP4, SHOC1, PTD (Mercier et al., 2015). This pathway is highly conserved among eukaryotes. The secondary pathway involves the protein MUS81. The existence of additional crossover pathways cannot be excluded (Mercier et al., 2015; Lambing et al., 2017).

Holocentric Chromosomes

Apart from the monocentric organization, another type of chromosomal organization, the holocentric (holokinetic) chromosomes, evolved independently in many lineages of unicellular eukaryotes, green plants, and metazoans (Melters et al., 2012; Escudero et al., 2016). Holocentric chromosomes have no distinct primary constriction visible while condensed, as they harbor multiple centromeric domains along their lengths (Heckmann et al., 2013; Steiner and Henikoff, 2014; Marques et al., 2015). Thus, spindle fibers attach along almost the entire poleward surface of the chromatids. As a result, sister-chromatids migrate to opposite poles parallel to each other during anaphase, while in the case of monocentric chromosomes microtubule spindles attach to a distinct kinetochore and the sister chromatids move together to opposite poles at anaphase with a clear attachment of microtubules onto the centromere.

Although organisms with holocentric chromosomes are considered relatively rare, clades possessing such chromosomal structure include more than 350,000 species (Kral et al., 2019). Between 1.5 and 2.0% of the flowering plants (∼5,500 species) are supposed to have holocentric chromosomes (Bures et al., 2013). Likely, due to the lack of chromosome studies, holocentricity should be even more common than reported.

A multiplication of centromeric sequences from one location to multiple sites along the chromosome arms has been proposed as a possible mechanism of holocentromere formation (Greilhuber, 1995). One common explanation for the evolution of holocentric chromosomes is their putative advantage over monocentric ones when it comes to chromosome breakages and consequent karyotypic variation (Zedek and Bures, 2018). The studies on artificial chromosomal rearrangements in various holocentric species showed that chromosome fragments retaining centromeric activity are stably transmitted during mitosis and meiosis (Heckmann et al., 2014; Jankowska et al., 2015).

Recent findings in holocentrics have brought back the discussion about the chromosome structure plasticity of holocentric lineages, including both CENH3-based and CENH3-less holocentromeres (Marques and Pedrosa-Harand, 2016; Drinnenberg and Akiyoshi, 2017). Such plasticity seems to be evolutionarily advantageous for it would increase the resistance of chromosomes against breaks and fusions. However, no difference in diversification rates between monocentrics and holocentrics seems to occur (Marquez-Corro et al., 2018).

Meiosis Progression in Holocentric Organisms

The best studied holocentric organism is the animal model *C. elegans*, and much of what we know about meiotic adaptations in organisms with this kind of chromosome structure derives from it (for additional information, see Wormbook (2005). However, due to the independent origin of holocentric organisms, adaptations in distantly related holocentric lineages are likely to be lineage-specific. In *C. elegans*, despite of its unique adaptations, meiosis progress resembles the process in monocentric organisms, in the way that homologs segregate at the end of meiosis I (Lui and Colaiacovo, 2013). During prophase I, chromosome remodeling processes occur, bivalents acquired a cruciform appearance with a long and a short arm and homologs are segregated to opposite poles l in a way similar to canonical meiosis. But the two-step loss of cohesion is accomplished through an alternate mechanism in a LAB-1 (a functional analog of shugoshin) dependent way (De Carvalho et al., 2008).

Meiotic Progression in Holocentric Plants Is Associated With Inverted Meiosis

Recently, several works have employed modern tools to better characterize the structure and function of holocentric centromeres (holocentromeres) during mitosis and meiosis in plants (Heckmann et al., 2013, 2014; Cabral et al., 2014; Marques et al., 2015, 2016; Oliveira et al., 2019; Neumann et al., 2020). However, the lack of genomic data and functional studies on holocentric plants hamper a better understanding of their cell-division-related adaptations. Upon mitosis, holocentricity does not affect sister chromosome segregation mechanisms, and a parallel migration of sister chromatids substitutes the typical V-shape migration of monocentric chromatids. In contrast, during meiosis several challenges appear because centromeres are not restricted to a single domain as in monocentrics, but rather dispersed across several domains genome-wide.

Thus, the stepwise cohesion release observed in monocentric chromosomes is not possible, since sister-holocentromeres are not associated in holocentric plants precluding their mono-orientation (Cabral et al., 2014; Heckmann et al., 2014; Marques et al., 2016). Additionally, the chromosome remodeling mechanism observed in *C. elegans* is unlike in holocentric plants, since they can have more than one CO per bivalent

and maintenance of holocentromeric activity during meiosis forces the bi-orientation of sister-holocentromeres. Therefore, holocentric plants have developed a different kind of meiosis called post-reductional or inverted meiosis to segregate their chromosomes. The phenomenon of inverted meiosis was first reported as early as 1940 in *Carex* (Wahl, 1940) and since then has been found in other holocentric plants of *Cuscuta*, *Luzula* and *Rhynchospora* (Malheiros et al., 1947; Pazy and Plitman, 1991; Cabral et al., 2014; Heckmann et al., 2014) but also in holocentric insects (Battaglia and Boyes, 1955; Nokkala et al., 2002; Viera et al., 2009). In this type of meiosis, the bivalents align themselves perpendicular to the equatorial plate during metaphase I with bi-orientation of sister-chromatids forcing them to separate to opposite poles during anaphase I (equational division during meiosis I) (**Figure 1B**). Thus, at the end of meiosis I, the daughter cells remain diploid. During meiosis II, thin chromatin threads are seen connecting the homologous non-sisters, which then separate to the opposite poles (reductional division during meiosis II). Although these chromatin threads are observed in both *Luzula* and *Rhynchospora*, it is not yet known what is the mechanism coordinating these connections (Cabral et al., 2014; Heckmann et al., 2014).

Furthermore, very little is known about the protein dynamics involved in the cohesion release and CO control during inverted meiosis in plants. Besides, in the plant genus *Rhynchospora* (beaksedge) both chiasmatic and achiasmatic inverted meiosis have been observed (Cabral et al., 2014). Apparently, meiotic recombination seems to occur in *R. pubera* (2n = 10), since chiasmata formation and the presence of meiosis-associated proteins (RAD51A, ASY1) have been observed, which represent the normal axis formation and occurrence and processing of DNA double strand breaks. In theory, inverted meiosis should be associated with a complete release of the meiotic cohesin REC8 between sister-chromatids already at end of meiosis I, allowing sisters to segregate at anaphase I (**Figure 1B**). However, sister-holocentromeres are not associated in holocentric plants, which could potentially interfere with the role of shugoshin. The behavior of cohesin or shugoshin in holocentric plants exhibiting inverted meiosis is unknown. Furthermore, the achiasmatic species *R. tenuis* ($2n = 4$) exhibits no chiasmata (**Figure 1C**). This species has the smallest reported number of chromosomes in the family and performs meiosis with the formation of four univalents, despite of RAD51 foci being observed, which suggests that DSBs are still occurring but being processed without crossovers (Cabral et al., 2014). Whether a defect in the meiotic machinery of this species is responsible for the achiasmy observed and whether the female meiosis is also achiasmatic is subject to current studies in our group. A similar phenomenon could be identified in a monocentric plant species, *Helianthemum squamatum*, which also exhibits a very small number of chromosomes when compared with close relatives (Aparicio et al., 2019).

The mechanisms behind the inverted meiosis have been further studied in *Luzula elegans* (Heckmann et al., 2014). Anti-CENH3 immunolabeling patterns appeared as linear lines during mitosis as well as meiosis. The authors propose that, a single linear functional centromere may be formed during meiosis and mitosis. Additionally, CENH3 signals from sisters-chromatids always remain separate. This may help, in the bi-polar orientation of the sisters. Each chromatid makes, end to end connection, by means of thin heterochromatin threads with its homologous partner which starts as early as pachytene. These connections are known to be established by satellite elements like LeSAT7, LeSAT11 and may represent chiasmata preserved at sub-telomeric regions (**Figure 2A**). A similar hypothesis was also proposed by Ris (1942) while researching on inverted meiosis in aphids. This connection may be involved in ensuring the correct segregation of homologous non-sister chromatids during the second meiotic division. In *Luzula elegans*, immunolocalization with anti-ASY1 and anti-ZYP1 signals were

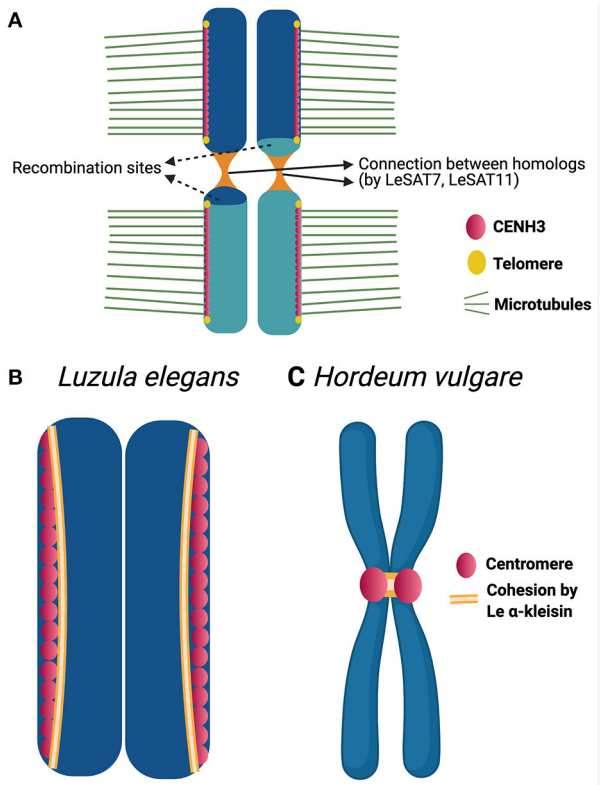

FIGURE 2 | Chromatin threads and cohesion in *Luzula* chromosomes. **(A)** Model highlighting the structural adaptations during inverted meiosis of *Luzula elegans* (see Heckmann et al., 2014) for further details). A rod bivalent with single crossover is illustrated in the model. CENH3 (centromeric protein) appears as a single linear line and centromeres of sisters are not fused. The sister chromatids bi-orient and attach to microtubules from opposite poles. Homologous non-sister chromatids associate with each other by end-to-end connections reported to be established by satellite elements, which maintain non-sister chromatids together up to meiosis II. **(B,C)** CENH3 and Le α-kleisin distribution during mitotic metaphase of *Luzula elegans* **(B)** and *Hordeum vulgare* **(C)** (see Ma et al., 2016) for further details). In the holocentric plant *Luzula*, CENH3(centromeric protein) appear as linear signals during mitotic metaphase. Le α-kleisin appears in the CENH3 regions and not between sister centromeric units. Whereas, in case of the monocentric plant *Hordeum vulgare*, the same Le α-kleisin is reported to present in the centromeric regions as well as establishing a connection between the sister centromeres.

observed as linear lines during early prophase I and telomere bouquet formation was also observed (Heckmann et al., 2014). Thus, early prophase events like DNA double strand break repair, pairing, synapsis and telomere bouquet formation appears the same as canonical meiosis.

Many questions remain a mystery with respect to inverted meiosis. What causes the sisters to separate during meiosis I? Is the cohesion mechanism, which plays a key role in holding the sisters together during meiosis I of canonical meiosis, evolved to enable inverted meiosis? How do the kinetochore proteins assemble and function during inverted meiosis? Monocentric organisms have mechanisms to prevent separase from degrading the cohesion in localized centromeric regions during anaphase I. This enables the sisters to be held together until anaphase II (Nasmyth, 2015). In holocentrics, which have diffuse centromeres, the mechanism of centromeric cohesion protection may be disabled. This may result in the loss of centromeric cohesion and allows the sisters to separate during meiosis I. Attempts to study cohesion mechanism during inverted meiosis were made in *Luzula elegans* (Ma et al., 2016). Signals of LeAlpha-kleisin-1 (cohesin ortholog of AtSYN4) appear during early prophase as reported for cohesin in monocentric meiosis, as demonstrated by immunolabeling. During both mitotic and meiotic metaphases I and II, these signals are observed in CENH3-positive regions but not between sister chromatids (**Figure 2B**). The authors also carried out the same experiment in the monocentric plant *Hordeum vulgare* (barley). In this experiment using the same antibody, the signals were observed in centromeric regions as well as in between the sister chromatids in mitotic metaphase (**Figure 2C**). Thus, the cohesion which connects the sister centromeres together in the monocentric species, barley, seems to not play the same role in the holocentric *Luzula*. This may be an early evidence that the function of a cohesin in monocentric may not be the same in a holocentric organism. It is speculated that LeAlpha-kleisin-1 may be involved in the centromere assembly but lost the function of establishing connection between sisters in *Luzula*. We cannot rule out the possibility of other cohesins involved in the connection between sisters. Thus, cohesins as potential candidates to be studied in future may give us more insights.

Anti-CENH3 immunolabeling patterns appeared as linear lines during mitosis in *R. pubera*. However, during meiosis centromeres form clusters (so-called cluster-holocentromeres) along the poleward side of the bivalents where the microtubules attach perpendicularly during meiosis I and the clusters are present in the middle of the chromatids during meiosis II (Marques et al., 2016). Additionally, CENPC, which represents the outer kinetochore protein, is also co-localized with CENH3 in meiosis which may refer to a conserved assembly of meiotic kinetochores on the holocentromeres (**Figure 1B**). This is the first report about kinetochore proteins in holocentric plants. But still, studies on kinetochore proteins like MIS12 (required for fusion of sister kinetochores), cohesion proteins like SMC1, SMC3, SCC3, REC8 (involved in centromeric cohesion during meiosis I) and shugoshin are necessary to provide more evidence to understand the observed phenomena during inverted meiosis.

The differences in the centromere organization during inverted meiosis of *Luzula* and *Rhynchopsora* show that the mechanisms differ in both cases and the regulation of inverted meiosis may be more complex. Regardless of the differences, in both cases the non-homologous chromatids appear to be connected by thin chromatin threads during meiosis II, as in case of *Luzula* specific tandem repeats were associated to such threads, but the nature of this connection is not yet identified in *Rhynchospora*. Heterochromatic threads seems to play an important role in the separation of achiasmate homologs during female meiosis in *Drosophila* (Hughes and Hawley, 2014). In this particular case the threads seem to be resolved by Topoisomerase II during meiosis I. However, chromatin threads in both *Luzula* and *Rhynchospora* are also observed in meiosis II, whether a similar mechanism occurs in the case of inverted meiosis in these holocentric plants is yet to be shown.

Meiotic Recombination in Holocentric Organisms

Being holocentric can have interesting implications for meiosis. In most eukaryotes and model plant species recombination is suppressed or highly reduced at centromeres (Copenhaver et al., 1998; Fernandes et al., 2019). Recombination at centromeres can disrupt their structural function, impair proper segregation and cause aneuploidy (Nambiar and Smith, 2016). Because of the meiotic recombination suppression at and near centromeres in monocentric organisms, it is of particular interest to understand how meiotic recombination works in organisms with holocentric chromosomes (**Figure 3A**). However, much of what we know about recombination in a holocentric organism comes from studies in *C. elegans*, wherein centromere proteins such as CENH3 and CENP-C are dispensable during meiosis (Monen et al., 2005) and likely do not affect meiotic recombination. In this case recombination rates broadly vary according to physical position in all six of its chromosomes. Each chromosome is comprised of three large domains: a low-recombining, gene-dense center, and two high-recombining arms (Barnes et al., 1995; Rockman and Kruglyak, 2009).

In Lepidoptera, the largest and most diverse holocentric lineage, meiotic recombination is restricted to male meiosis and frequent karyotype reorganization events are associated with wide variations in chromosome counts across species (Hill et al., 2019). Although high recombination densities were reported for some Lepidopteran insects (Wilfert et al., 2007), this does not seem to be linked to holocentricity.

Meiotic Recombination in Holocentric Plants

For the time being there are no detailed analysis about recombination frequencies in holocentric plants and all we know derive from basic cytological studies. Recently, the first linkage map for the presumed holocentric plant *Carex scoparia* (Escudero et al., 2018) has been reported, but without the physical map and holocentromere characterization the recombination landscape for a holocentric plant is still unknown. Understanding

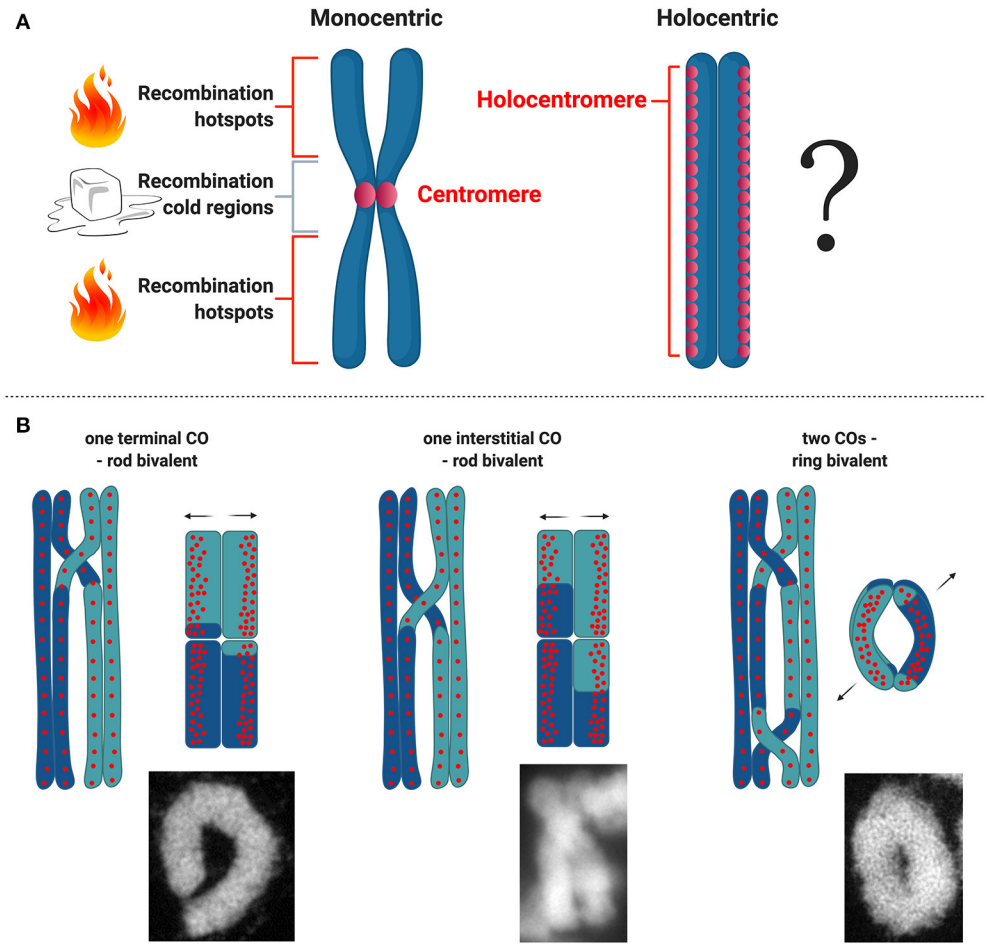

FIGURE 3 | Meiotic recombination in holocentric plants. **(A)** Scheme of what is known about distribution of hotspots for meiotic recombination with respect to centromere organization on monocentric and holocentric plant chromosomes. **(B)** Types of CO and bivalent formation and corresponding models with regard to centromeric units distribution in *R. pubera*. Bivalent microscopic images were made by *M. Castellani*.

how recombination is regulated in holocentric plants will potentially unveil new strategies to deal with this chromosome structure during meiosis. Specially in the case of holocentric plants where chromosomes maintain their holocentromere function during meiosis in contrast to *C. elegans* (Heckmann et al., 2014; Marques et al., 2016), which could potentially interfere with the designation of CO events. In the particular case of the plant *R. pubera*, holocentromeres of *R. pubera* extend linearly for the whole length of the chromosomes until their very ends (Cabral et al., 2014; Marques et al., 2015, 2016). Despite the observation that chiasmata frequently link homologs terminally, it seems that recombination in *R. pubera* also happens in internal regions (**Figure 3B**). Proximity of CO events to centromeric units cannot yet be quantified and recombination may happen in intervals where these units are not present. It is interesting though that centromeric units in *R. pubera* are associated with highly abundant repeats (Tyba repeats), which build short arrays of ∼15 kb long and are dispersed genome wide (Marques et al., 2015). In this sense the repeat-based holocentromeres of *R. pubera* seem to assemble in chromatin structures more similar to repeat-based monocentromes. It was estimated that each chromosome should have between 800 and 1,300 repeat-based centromere domains. Taking in account that RAD51 foci are found dispersed in early prophase I (Cabral et al., 2014) and that CENH3 does show similar signals (Marques et al., 2016), DSB sites could potentially occur very close or even within centromeric units.

Cytological observations in *R. pubera* show that at diakinesis five bivalents are present, and physically connected by chiasmata. In this species, ring-shaped bivalents are supposed to be connected by two chiasmata and rod-like bivalents to be connected by only one (Cabral et al., 2014). Observing the shapes of these bivalents, it seems that in *R. pubera* COs are happening mostly at the ends of the chromosomes, but, less frequent, internal COs are also observed. The occurrence of internal COs suggests that recombination events may take place in the vicinity of centromeric repeats (**Figure 3B**). Similar findings were observed in *Luzula* (Heckmann et al., 2014). Moreover,

this is an evidence that the final product of recombination, the crossover, is present at the end of prophase I and that CO interference is occurring as well as CO assurance. Considering the conservation level of the whole ZMM pathway, it seems that meiotic recombination in *R. pubera* is happening and that is not impaired by holocentromeres or inverted meiosis. These observations are quite interesting considering that the holocentromeres in *R. pubera* are repeat-based and distributed along the entire chromosomes in meiosis (Marques et al., 2016). It will be particularly interesting to study whether COs are somehow affected by such centromere distribution and where they are formed.

The molecular basis of recombination repression at centromeres is still not clear. Two possible ways are speculated to happen: either recombination is repressed at the DSB level by modulating the action or the binding of SPO11, or at the level of how DSBs are repaired and processed by the meiosis-specific DMC1 (Nambiar and Smith, 2016). Recent findings using budding and fission yeast has proposed a role for the kinetochore and cohesion as important regulators of DSBs formation within centromeres and surrounding regions (Vincenten et al., 2015; Kuhl and Vader, 2019). Considering the apparent proximity of recombination events and centromeres in *R. pubera*, it is still unclear whether these repression mechanisms exist and if so, how they are regulated. If we look at other well-studied model eukaryotes, the centromere effect appears to be highly conserved and also very efficient in avoiding COs in pericentromeric regions. In *Drosophila melanogaster* the DSB landscape appears to be flat along the chromosome arm, but downstream recombination is then affected by the centromere effect that eliminates pericentromeric recombination intermediates and models the recombination pattern (Hatkevich et al., 2017; Brady et al., 2018). In maize the centromeric effect seems to work with a different mechanism but with the same result. In centromeric regions of maize DSB can be detected, but COs are absent (He et al., 2017). In *Arabidopsis*, Spo11-oligos resulting from Chip-seq experiment are depleted at pericentromeric regions, where CO are also absent, indicating reduced levels of DSBs at these regions (Choi et al., 2018). In yeast, kinetochore complexes protect centromeric regions, reducing dramatically DSB and CO (Vincenten et al., 2015; Kuhl and Vader, 2019).

A similar question involves the presence of so-called hotspots and cold regions of recombination, regions on the chromosomes where recombination is more or less likely to take place. Multiple species, including plants, display hot and cold spots (e.g., centromeric regions) (Choi and Henderson, 2015). However, the presence of holocentromeres in *R. pubera* makes it difficult to predict the presence of hotspots or cold regions or to speculate about their location. Perhaps the situation is that there are no hotspots in *R. pubera* similar to *C. elegans*. A study in *C. elegans* has made a detailed analysis of recombination rate in a 2 Mb region, discovering that there are no clear hotspots, but recombination rates are constant, constrained only by the structural domain of the chromosome arm (Kaur and Rockman, 2014). This is a unique case similar only to S. *pombe*, which is not holocentric.

A different case is the one of the holocentric relative *Rhynchospora tenuis*. In this species chiasmata are not observed and at least male meiosis seems to be complete achiasmatic (**Figure 1C**). The further observation of RAD51 during early prophase I suggests, in principle, that DSBs are being formed (Cabral et al., 2014). The absence of recombination outcomes might be evidence of the disruption of the ZMM recombination pathway in one or more points. Mutations in the SC of *C. elegans* negatively affect recombination and crossover regulation (Colaiacovo et al., 2003). However, this behavior is not consistent among plant species. For instance, in barley it was reported that dramatic reduction of normal levels of ZYP1 by RNAi also drastically reduce CO formation (Barakate et al., 2014). However, in the case of *Arabidopsis* and rice a malfunctioning SC does not affect recombination and may even increase CO frequency and abolish CO interference (Wang et al., 2010; Capilla-Perez et al., 2021; France et al., 2021). In both holocentric *Rhynchospora* and *Luzula* it was shown that they apparently have conserved SC structures as immunostaining with SC proteins showed the conserved pattern for monocentric species (Cabral et al., 2014; Heckmann et al., 2014). Whether SC proteins are involved in CO regulation in holocentric plants is currently unknown and should be subject of future studies.

An interesting point in holocentric clades is that chromosome numbers tend to vary greatly within the group which could be a consequence of lack of centromere constrain. However, this may not be true for all holocentric clades (Ruckman et al., 2020). In the *Cyperaceae* family, which is the largest group of holocentric plants, chromosomes vary from $n = 2$ to $n = 108$ (Roalson, 2008). Although the lowest chromosome number in angiosperms is found in *Rhynchospora tenuis* ($n = 2$), we can also find extraordinarily very high chromosomes numbers in other genera within this family, for instance in *Carex* (Wieclaw et al., 2020) and *Cyperus* (Roalson, 2008). Since the number of chromosomes is proportional to recombination rates, high chromosome numbers would also impose higher recombination rates in holocentric plants, specially, in this case where the number of chiasmata tends to be typically low, with one or two CO per bivalent. However, a fitness balance must exist otherwise holocentric organisms would tend to have always high chromosome numbers, which is not the case. High chromosome numbers would potentially increase the complexity of the recombination process with likely more possibilities of mistakes in the segregation process.

Holokinetic Drive

Besides the occurrence of inverted meiosis, holocentric sedges (Cyperaceae) also exhibit another peculiar process: the formation of pseudomonads by the end of the microspore meiosis (Rocha et al., 2016, 2018). During this process, three microspores degenerate and only one proceeds with gametogenesis. Thus, only one pollen grain results from each meiotic event in these plants. This specific feature could relate the segregation process with the size of the chromosomes in a process called holokinetic drive, which was first introduced by Bures and Zedek (2014). According to this hypothesis, there would be a selection for chromosomal size upon meiosis. Either the smallest or the largest chromosomes would be favored depending on the case, and

formation of pseudomonads could accelerate this process. A negative correlation between chromosome number and total genome size observed in several holocentric groups seems to support this. For instance, this correlation has been recently reported for the genus *Rhynchospora* (Burchardt et al., 2020). Moreover, it has been recently proposed that centromere drive could occur in association with holokinetic drive in members of *Cyperaceae* and, thus, the meiotic asymmetry in both sexes of this family could increase the potential for selfish centromeres to gain an advantage in both male and female meiosis (Krátká et al., 2021). Alternatively, the selection of the survival cell could be related with the results of the recombination process, wherein the best combination of alleles resulting from the meiotic event would be selected.

PERSPECTIVES AND FUTURE AIMS

The mechanisms behind inverted meiosis in holocentric organisms are currently unknown. The occurrence of inverted meiosis demands modification in the conserved mechanisms of meiotic cohesion and chromosome segregation. New adaptations and differential regulation of meiotic cohesions such as REC8 and centromere cohesion guardians such as shugoshins are expected to have happened. Additionally, modification of the spindle attachment machinery also should be expected due to an alternative centromeric organization. Furthermore, the observed chiasmata formation between holocentric chromosomes demands adaptations of the mechanisms that prevent recombination at or around centromeres. The limited knowledge of holocentromeres and close relatives of *Cyperaceae* limits us to speculate about what to expect in terms of adaptations of the meiotic recombination machinery to holocentricity. Future studies aiming the molecular characterization of such mechanisms will be of interest for evolutionary and comparative biology studies.

AUTHOR CONTRIBUTIONS

PH drafted the section about the meiotic machinery in eukaryotes, incorporated the different contributions and reviewed the text. GT drafted the sections about meiosis progression and inverted meiosis in holocentrics. MC drafted the section about meiotic recombination. AM drafted the sections about holocentric plants, reviewed and supervised the production process of the manuscript. Figures were made by GT and AM. All authors contributed to the article and approved the submitted version.

FUNDING

PH, MC, and AM were funded by Max Planck Society. GT thanks to the DAAD/India Ph.D. fellowship.

ACKNOWLEDGMENTS

We thank both reviewers for the insightful comments and suggestions that helped the improvement of the manuscript. All figure illustrations were created with BioRender.com.

REFERENCES

Abdu, U., Gonzalez-Reyes, A., Ghabrial, A., and Schupbach, T. (2003). The *Drosophila* spn-D gene encodes a RAD51C-like protein that is required exclusively during meiosis. *Genetics* 165, 197–204.

Allers, T., and Lichten, M. (2001). Differential timing and control of noncrossover and crossover recombination during meiosis. *Cell* 106, 47–57. doi: 10.1016/S0092-8674(01)00416-0

Aparicio, A., Escudero, M., Valdes-Florido, A., Pachon, M., Rubio, E., Albaladejo, R. G., et al. (2019). Karyotype evolution in Helianthemum (Cistaceae): dysploidy, achiasmate meiosis and ecological specialization in *H. squamatum*, a true gypsophile. *Bot. J. Linn. Soc.*191, 484–501. doi: 10.1093/botlinnean/boz066

Barakate, A., Higgins, J. D., Vivera, S., Stephens, J., Perry, R. M., Ramsay, L., et al. (2014). The synaptonemal complex protein ZYP1 is required for imposition of meiotic crossovers in barley. *Plant Cell* 26, 729–740. doi: 10.1105/tpc.113.121269

Barnes, T. M., Kohara, Y., Coulson, A., and Hekimi, S. (1995). Meiotic recombination, noncoding DNA and genomic organization in *Caenorhabditis elegans*. *Genetics* 141, 159–179. doi: 10.1093/genetics/141.1.159

Battaglia, E., and Boyes, J. W. (1955). Post-reductional meiosis: its mechanismand causes. *Caryologia* 8, 87–134. doi: 10.1080/00087114.1955.10797554

Brady, M. M., Mcmahan, S., and Sekelsky, J. (2018). Loss of *Drosophila* Mei-41/ATR alters meiotic crossover patterning. *Genetics* 208, 579–588. doi: 10.1534/genetics.117.300634

Brown, M. S., and Bishop, D. K. (2014). DNA strand exchange and RecA homologs in meiosis. *Cold Spring Harb. Perspect. Biol.* 7:a016659. doi: 10.1101/cshperspect.a016659

Burchardt, P., Buddenhagen, C. E., Gaeta, M. L., Souza, M. D., Marques, A., and Vanzela, A. L. L. (2020). Holocentric karyotype evolution in rhynchospora is marked by intense numerical, structural, and genome size changes. *Front. Plant Sci.* 11:536507. doi: 10.3389/fpls.2020.536507

Bures, P., and Zedek, F. (2014). Holokinetic drive: centromere drive in chromosomes without centromeres. *Evolution* 68, 2412–2420. doi: 10.1111/evo.12437

Bures, P., Zedek, F., and Markova, M. (2013). "Holocentric chromosomes," in *Plant Genome Diversity,* eds J. Greilhuber, J. Dolezel, and J. F. Wendel (Vienna: Springer-Verlag Wien). doi: 10.1007/978-3-7091-1160-4_12

Cabral, G., Marques, A., Schubert, V., Pedrosa-Harand, A., and Schlogelhofer, P. (2014). Chiasmatic and achiasmatic inverted meiosis of plants with holocentric chromosomes. *Nat. Commun.* 5:5070. doi: 10.1038/ncomms6070

Capilla-Perez, L., Durand, S., Hurel, A., Lian, Q., Chambon, A., Taochy, C., Solier, V., Grelon, M., and Mercier, M. (2021). The synaptonemal complex imposes crossover interference and heterochiasmy in *Arabidopsis*. *Proc. Natl. Acad. Sci. U. S. A.* 118:e2023613118. doi: 10.1073/pnas.2023613118

Choi, K., and Henderson, I. R. (2015). Meiotic recombination hotspots - a comparative view. *Plant J.* 83, 52–61. doi: 10.1111/tpj.12870

Choi, K., Zhao, X. H., Tock, A. J., Lambing, C., Underwood, C. J., Hardcastle, T. J., et al. (2018). Nucleosomes and DNA methylation shape meiotic DSB frequency in *Arabidopsis thaliana* transposons and gene regulatory regions. *Genome Res.* 28, 532–546. doi: 10.1101/gr.225599.117

Choulet, F., Alberti, A., Theil, S., Glover, N., Barbe, V., Daron, J., et al. (2014). Structural and functional partitioning of bread wheat chromosome 3B. *Science* 345:1249721. doi: 10.1126/science.1249721

Colaiacovo, M. P., Macqueen, A. J., Martinez-Perez, E., Mcdonald, K., Adamo, A., La Volpe, A., et al. (2003). Synaptonemal complex assembly in *C. elegans* is dispensable for loading strand-exchange proteins but critical for proper completion of recombination. *Dev. Cell* 5, 463–474. doi: 10.1016/S1534-5807(03)00232-6

Copenhaver, G. P., Browne, W. E., and Preuss, D. (1998). Assaying genome-wide recombination and centromere functions with Arabidopsis tetrads. *Proc. Natl. Acad. Sci. U. S. A.* 95, 247–252. doi: 10.1073/pnas.95.1.247

Cromie, G. A., Hyppa, R. W., Taylor, A. F., Zakharyevich, K., Hunter, N., and Smith, G. R. (2006). Single holliday junctions are intermediates of meiotic recombination. *Cell* 127, 1167–1178. doi: 10.1016/j.cell.2006.09.050

De Carvalho, C. E., Zaaijer, S., Smolikov, S., Gu, Y., Schumacher, J. M., and Colaiacovo, M. P. (2008). LAB-1 antagonizes the aurora B kinase in *C. elegans*. *Genes Dev.* 22, 2869–2885. doi: 10.1101/gad.1691208

Drinnenberg, I. A., and Akiyoshi, B. (2017). Evolutionary lessons from species with unique kinetochores. *Prog. Mol. Subcell. Biol.* 56, 111–138. doi: 10.1007/978-3-319-58592-5_5

Escudero, M., Hahn, M., and Hipp, A. L. (2018). RAD-seq linkage mapping and patterns of segregation distortion in sedges: meiosis as a driver of karyotypic evolution in organisms with holocentric chromosomes. *J. Evol. Biol.* 31, 833–843. doi: 10.1111/jeb.13267

Escudero, M., Marquez-Corro, J. I., and Hipp, A. L. (2016). The phylogenetic origins and evolutionary history of holocentric chromosomes. *Syst. Bot.* 41, 580–585. doi: 10.1600/036364416X692442

Fernandes, J. B., Wlodzimierz, P., and Henderson, I. R. (2019). Meiotic recombination within plant centromeres. *Curr. Opin. Plant Biol.* 48, 26–35. doi: 10.1016/j.pbi.2019.02.008

France, M. G., Enderle, J., Röhrig, S., Puchta, H., Franklin, F. C. H., and Higgins, J. D. (2021). ZYP1 is required for obligate cross-over formation and cross-over interference in *Arabidopsis*. *PNAS*. 118:e2021671118. doi: 10.1073/pnas.2021671118

Greilhuber, J. (1995). "Chromosomes of the monocotyledons (general aspects)," in *Monocotyledons: Systematics and Evolution*, eds P. J. Rudall, P. J. Cribb, D. F. Cutler, and C. J. Humphries (Surrey: Kew Royal Botanic Gardens), 379–414.

Hatkevich, T., Kohl, K. P., Mcmahan, S., Hartmann, M. A., Williams, A. M., and Sekelsky, J. (2017). Bloom syndrome helicase promotes meiotic crossover patterning and homolog disjunction. *Curr. Biol.* 27, 96–102. doi: 10.1016/j.cub.2016.10.055

He, Y., Wang, M. H., Dukowic-Schulze, S., Zhou, A., Tiang, C. L., Shilo, S., et al. (2017). Genomic features shaping the landscape of meiotic double-strand-break hotspots in maize. *Proc. Natl. Acad. Sci. U. S. A.* 114, 12231–12236. doi: 10.1073/pnas.1713225114

Heckmann, S., Jankowska, M., Schubert, V., Kumke, K., Ma, W., and Houben, A. (2014). Alternative meiotic chromatid segregation in the holocentric plant *Luzula elegans*. *Nat. Commun.* 5:4979. doi: 10.1038/ncomms5979

Heckmann, S., Macas, J., Kumke, K., Fuchs, J., Schubert, V., Ma, L., et al. (2013). The holocentric species *Luzula elegans* shows interplay between centromere and large-scale genome organization. *Plant J.* 73, 555–565. doi: 10.1111/tpj.12054

Hill, J., Rastas, P., Hornett, E. A., Neethiraj, R., Clark, N., Morehouse, N., et al. (2019). Unprecedented reorganization of holocentric chromosomes provides insights into the enigma of lepidopteran chromosome evolution. *Sci. Adv.* 5:eaau3648. doi: 10.1126/sciadv.aau3648

Hughes, S. E., and Hawley, R. S. (2014). Topoisomerase II is required for the proper separation of heterochromatic regions during drosophila melanogaster female meiosis. *PLoS Genet.* 10:e1004650. doi: 10.1371/journal.pgen.1004650

Jankowska, M., Fuchs, J., Klocke, E., Fojtova, M., Polanska, P., Fajkus, J., et al. (2015). Holokinetic centromeres and efficient telomere healing enable rapid karyotype evolution. *Chromosoma* 124, 519–528. doi: 10.1007/s00412-015-0524-y

Johnson, M. T., Agrawal, A. A., Maron, J. L., and Salminen, J. P. (2009). Heritability, covariation and natural selection on 24 traits of common evening primrose (*Oenothera biennis*) from a field experiment. *J. Evol. Biol.* 22, 1295–1307. doi: 10.1111/j.1420-9101.2009.01747.x

Kaur, T., and Rockman, M. V. (2014). Crossover heterogeneity in the absence of hotspots in *Caenorhabditis elegans*. *Genetics* 196, 137–148. doi: 10.1534/genetics.113.158857

Keeney, S. (2008). Spo11 and the formation of DNA double-strand breaks in meiosis. *Genome Dyn. Stab.* 2, 81–123. doi: 10.1007/7050_2007_026

Keeney, S., Giroux, C. N., and Kleckner, N. (1997). Meiosis-specific DNA double-strand breaks are catalyzed by Spo11, a member of a widely conserved protein family. *Cell* 88, 375–384. doi: 10.1016/S0092-8674(00)81876-0

Kitajima, T. S., Kawashima, S. A., and Watanabe, Y. (2004). The conserved kinetochore protein shugoshin protects centromeric cohesion during meiosis. *Nature* 427, 510–517. doi: 10.1038/nature02312

Kitajima, T. S., Sakuno, T., Ishiguro, K., Iemura, S., Natsume, T., Kawashima, S. A., et al. (2006). Shugoshin collaborates with protein phosphatase 2A to protect cohesin. *Nature* 441, 46–52. doi: 10.1038/nature04663

Kral, J., Forman, M., Korinkova, T., Lerma, A. C. R., Haddad, C. R., Musilova, J., et al. (2019). Insights into the karyotype and genome evolution of haplogyne spiders indicate a polyploid origin of lineage with holokinetic chromosomes. *Sci. Rep.* 9:3001. doi: 10.1038/s41598-019-39034-3

Krátká, M., Šmerda, J., Lojdová, K., Bureš, P., and Zedek, F. (2021). Holocentric chromosomes probably do not prevent centromere drive in *Cyperaceae*. *Front. Plant Sci.* 12:642661. doi: 10.3389/fpls.2021.642661

Kuhl, L. M., and Vader, G. (2019). Kinetochores, cohesin, and DNA breaks: controlling meiotic recombination within pericentromeres. *Yeast* 36, 121–127. doi: 10.1002/yea.3366

Lambing, C., Franklin, F. C., and Wang, C. R. (2017). Understanding and manipulating meiotic recombination in plants. *Plant Physiol.* 173, 1530–1542. doi: 10.1104/pp.16.01530

Lorenz, A., Wells, J. L., Pryce, D. W., Novatchkova, M., Eisenhaber, F., Mcfarlane, R. J., et al. (2004). *S. pombe* meiotic linear elements contain proteins related to synaptonemal complex components. *J. Cell. Sci.* 117, 3343–3351. doi: 10.1242/jcs.01203

Lui, D. Y., and Colaiacovo, M. P. (2013). Meiotic development in *Caenorhabditis elegans*. *Adv. Exp. Med. Biol.* 757, 133–170. doi: 10.1007/978-1-4614-4015-4_6

Ma, W., Schubert, V., Martis, M. M., Hause, G., Liu, Z., Shen, Y., et al. (2016). The distribution of alpha-kleisin during meiosis in the holocentromeric plant *Luzula elegans*. *Chromosome Res.* 24, 393–405. doi: 10.1007/s10577-016-9529-5

Malheiros, N., Castro, D., and Câmara, A. (1947). Cromosomas sem centrómero localizado: O caso de *Luzula purpurea* link. *Agron. Lusitana* 9, 51–74.

Marques, A., and Pedrosa-Harand, A. (2016). Holocentromere identity: from the typical mitotic linear structure to the great plasticity of meiotic holocentromeres. *Chromosoma* 125, 669–681. doi: 10.1007/s00412-016-0612-7

Marques, A., Ribeiro, T., Neumann, P., Macas, J., Novak, P., Schubert, V., et al. (2015). Holocentromeres in *Rhynchospora* are associated with genome-wide centromere-specific repeat arrays interspersed among euchromatin. *Proc. Natl. Acad. Sci. U.S.A.* 112, 13633–13638. doi: 10.1073/pnas.1512255112

Marques, A., Schubert, V., Houben, A., and Pedrosa-Harand, A. (2016). Restructuring of holocentric centromeres during meiosis in the plant rhynchospora pubera. *Genetics* 204, 555–568. doi: 10.1534/genetics.116.191213

Marquez-Corro, J. I., Escudero, M., and Luceno, M. (2018). Do holocentric chromosomes represent an evolutionary advantage? A study of paired analyses of diversification rates of lineages with holocentric chromosomes and their monocentric closest relatives. *Chromosome Res.* 26, 139–152. doi: 10.1007/s10577-017-9566-8

Martinez-Perez, E., and Colaiacovo, M. P. (2009). Distribution of meiotic recombination events: talking to your neighbors. *Curr. Opin. Genet. Dev.* 19, 105–112. doi: 10.1016/j.gde.2009.02.005

Martinez-Perez, E., Schvarzstein, M., Barroso, C., Lightfoot, J., Dernburg, A. F., and Villeneuve, A. M. (2008). Crossovers trigger a remodeling of meiotic chromosome axis composition that is linked to two-step loss of sister chromatid cohesion. *Genes Dev.* 22, 2886–2901. doi: 10.1101/gad.1694108

Melters, D. P., Paliulis, L. V., Korf, I. F., and Chan, S. W. (2012). Holocentric chromosomes: convergent evolution, meiotic adaptations, and genomic analysis. *Chromosome Res.* 20, 579–593. doi: 10.1007/s10577-012-9292-1

Mercier, R., Mezard, C., Jenczewski, E., Macaisne, N., and Grelon, M. (2015). The molecular biology of meiosis in plants. *Annu. Rev. Plant Biol.* 66, 297–327. doi: 10.1146/annurev-arplant-050213-035923

Monen, J., Maddox, P. S., Hyndman, F., Oegema, K., and Desai, A. (2005). Differential role of CENP-A in the segregation of holocentric *C. elegans* chromosomes during meiosis and mitosis. *Nat. Cell Biol.* 7, 1248–1255. doi: 10.1038/ncb1331

Nambiar, M., and Smith, G. R. (2016). Repression of harmful meiotic recombination in centromeric regions. *Semin. Cell Dev. Biol.* 54, 188–197. doi: 10.1016/j.semcdb.2016.01.042

Nasmyth, K. (2015). A meiotic mystery: how sister kinetochores avoid being pulled in opposite directions during the first division. *Bioessays* 37, 657–665. doi: 10.1002/bies.201500006

Neumann, P., Oliveira, L., Cizkova, J., Jang, T. S., Klemme, S., Novak, P., et al. (2020). Impact of parasitic lifestyle and different types of centromere organization on chromosome and genome evolution in the plant genus *Cuscuta*. *New Phytol.* 229, 2365–2377. doi: 10.1111/nph.17003

Nokkala, S., Laukkanen, A., and Nokkala, C. (2002). Mitotic and meiotic chromosomes in *Somatochlora metallica* (Cordulidae, Odonata). The absence of localized centromeres and inverted meiosis. *Hereditas* 136, 7–12. doi: 10.1034/j.1601-5223.2002.1360102.x

Oliveira, L., Neumann, P., Jang, T. S., Klemme, S., Schubert, V., Koblizkova, A., et al. (2019). Mitotic spindle attachment to the holocentric chromosomes of *Cuscuta europaea* does not correlate with the distribution of CENH3 chromatin. *Front. Plant Sc.* 10:1799. doi: 10.3389/fpls.2019.01799

Pazy, B., and Plitman, U. (1991). Unusual chromosome separation in meiosis of *Cuscuta L. Genome* 34, 533–536. doi: 10.1139/g91-082

Petes, T. D. (2001). Meiotic recombination hot spots and cold spots. *Nat. Rev. Genet.* 2, 360–369. doi: 10.1038/35072078

Riedel, C. G., Katis, V. L., Katou, Y., Mori, S., Itoh, T., Helmhart, W., et al. (2006). Protein phosphatase 2A protects centromeric sister chromatid cohesion during meiosis I. *Nature* 441, 53–61. doi: 10.1038/nature04664

Ris, H. (1942). A cytological and experimental analysis of the meiotic behavior of the univalent X chromosome in the bearberry aphid Tamalia (==Phyllaphis) coweni (CkLL). *J. Exp. Zool.* 90, 267–330. doi: 10.1002/jez.1400900207

Roalson, E. H. (2008). A synopsis of chromosome number variation in the *Cyperaceae*. *Bot. Rev.* 74, 209–393. doi: 10.1007/s12229-008-9011-y

Rocha, D. M., Marques, A., Andrade, C. G. T. J., Guyot, R., Chaluvadi, S. R., Pedrosa-Harand, A., et al. (2016). Developmental programmed cell death during asymmetric microsporogenesis in holocentric species of *Rhynchospora* (*Cyperaceae*). *J. Exp. Bot.* 67, 5391–5401. doi: 10.1093/jxb/erw300

Rocha, D. M., Vanzela, A. L. L., and Mariath, J. E. A. (2018). Comparative study of microgametogenesis in members of *Cyperaceae* and *Juncaceae*: a shift from permanent pollen tetrads to pseudomonads. *Bot. J. Linn. Soc.* 188, 59–73. doi: 10.1093/botlinnean/boy041

Rockman, M. V., and Kruglyak, L. (2009). Recombinational landscape and population genomics of *Caenorhabditis elegans*. *PLoS Genet.* 5:e1000419. doi: 10.1371/journal.pgen.1000419

Ruckman, S. N., Jonika, M. M., Casola, C., and Blackmon, H. (2020). Chromosome number evolves at equal rates in holocentric and monocentric clades. *PLoS Genet.* 16:e1009076. doi: 10.1371/journal.pgen.1009076

Schurko, A. M., and Logsdon, J. M. Jr. (2008). Using a meiosis detection toolkit to investigate ancient asexual "scandals" and the evolution of sex. *Bioessays* 30, 579–589. doi: 10.1002/bies.20764

Speijer, D., Lukes, J., and Elias, M. (2015). Sex is a ubiquitous, ancient, and inherent attribute of eukaryotic life. *Proc. Natl. Acad. Sci. U. S. A.* 112, 8827–8834. doi: 10.1073/pnas.1501725112

Steiner, F. A., and Henikoff, S. (2014). Holocentromeres are dispersed point centromeres localized at transcription factor hotspots. *eLife* 3:e02025. doi: 10.7554/eLife.02025.025

Taagen, E., Bogdanove, A. J., and Sorrells, M. E. (2020). Counting on crossovers: controlled recombination for plant breeding. *Trends Plant Sci.* 25, 455–465. doi: 10.1016/j.tplants.2019.12.017

Viera, A., Page, J., and Rufas, J. S. (2009). Inverted meiosis: the true bugs as a model to study. *Genome Dyn.* 5, 137–156. doi: 10.1159/000166639

Vincenten, N., Kuhl, L. M., Lam, I., Oke, A., Kerr, A. R., Hochwagen, A., et al. (2015). The kinetochore prevents centromere-proximal crossover recombination during meiosis. *eLife* 4:e10850. doi: 10.7554/eLife.10850.036

Wahl, H. A. (1940). Chromosome numbers and meiosis in the genus Carex. *Am. J. Bot.* 27, 458–470. doi: 10.1002/j.1537-2197.1940.tb14707.x

Wang, M., Wang, K. J., Tang, D., Wei, C. X., Li, M., Shen, Y., et al. (2010). The central element protein ZEP1 of the synaptonemal complex regulates the number of crossovers during meiosis in rice. *Plant Cell* 22, 417–430. doi: 10.1105/tpc.109.070789

Wieclaw, H., Kalinka, A., and Koopman, J. (2020). Chromosome numbers of Carex (*Cyperaceae*) and their taxonomic implications. *PLoS ONE* 15:e0228353. doi: 10.1371/journal.pone.0228353

Wilfert, L., Gadau, J., and Schmid-Hempel, P. (2007). Variation in genomic recombination rates among animal taxa and the case of social insects. *Heredity* 98, 189–197. doi: 10.1038/sj.hdy.6800950

Wormbook (2005). *WormBook, The Online Review of C. elegans Biology*. T.C.E.R. Community. Available online at: http://www.wormbook.org (accessed March 20, 2021).

Wyatt, H. D., and West, S. C. (2014). Holliday junction resolvases. *Cold Spring Harb. Perspect. Biol.* 6:a023192. doi: 10.1101/cshperspect.a023192

Xu, H., Beasley, M. D., Warren, W. D., Van Der Horst, G. T., and Mckay, M. J. (2005). Absence of mouse REC8 cohesin promotes synapsis of sister chromatids in meiosis. *Dev. Cell* 8, 949–961. doi: 10.1016/j.devcel.2005.03.018

Zedek, F., and Bures, P. (2018). Holocentric chromosomes: from tolerance to fragmentation to colonization of the land. *Ann. Bot.* 121, 9–16. doi: 10.1093/aob/mcx118

Zickler, D., and Kleckner, N. (2015). Recombination, Pairing, and synapsis of homologs during meiosis. *Cold Spring Harb. Perspect. Biol.* 7. doi: 10.1101/cshperspect.a016626

Conflict of Interest: The authors declare that the research was conducted in the absence of any commercial or financial relationships that could be construed as a potential conflict of interest.

frontiers in Plant Science

REVIEW
published: 18 May 2021
doi: 10.3389/fpls.2021.672914

From Microscopy to Nanoscopy: Defining an *Arabidopsis thaliana* Meiotic Atlas at the Nanometer Scale

Jason Sims†, Peter Schlögelhofer† and Marie-Therese Kurzbauer*†*

Department of Chromosome Biology, Max Perutz Labs, University of Vienna, Vienna BioCenter, Vienna, Austria

OPEN ACCESS

Edited by:
Christophe Lambing, University of Cambridge, United Kingdom

Reviewed by:
Isabelle Colas, The James Hutton Institute, United Kingdom
Alice R. Darbyshire, University of Birmingham, United Kingdom

***Correspondence:**
Jason Sims
jason.sims@univie.ac.at
Marie-Therese Kurzbauer
marie-therese.kurzbauer@univie.ac.at

†ORCID:
Jason Sims
orcid.org/0000-0003-4235-2488
Peter Schlögelhofer
orcid.org/0000-0002-0909-3587
Marie-Therese Kurzbauer
orcid.org/0000-0003-3858-4497

Specialty section:
This article was submitted to Plant Cell Biology, a section of the journal Frontiers in Plant Science

Received: *26 February 2021*
Accepted: *27 April 2021*
Published: *18 May 2021*

Citation:
Sims J, Schlögelhofer P and Kurzbauer MT (2021) From Microscopy to Nanoscopy: Defining an Arabidopsis thaliana Meiotic Atlas at the Nanometer Scale. Front. Plant Sci. 12:672914. doi: 10.3389/fpls.2021.672914

Visualization of meiotic chromosomes and the proteins involved in meiotic recombination have become essential to study meiosis in many systems including the model plant *Arabidopsis thaliana*. Recent advances in super-resolution technologies changed how microscopic images are acquired and analyzed. New technologies enable observation of cells and nuclei at a nanometer scale and hold great promise to the field since they allow observing complex meiotic molecular processes with unprecedented detail. Here, we provide an overview of classical and advanced sample preparation and microscopy techniques with an updated *Arabidopsis* meiotic atlas based on super-resolution microscopy. We review different techniques, focusing on stimulated emission depletion (STED) nanoscopy, to offer researchers guidance for selecting the optimal protocol and equipment to address their scientific question.

Keywords: *Arabidopsis*, meiosis, cytology, super-resolution microscopy, immunofluorescence

MEIOSIS

Meiosis is a specialized cell division and the basis for genetic diversity through sexual reproduction. Understanding its molecular mechanisms and involved factors is therefore essential for human health and fertility and, importantly, for plant breeding and food security.

In contrast to somatic cells that give rise to identical daughter cells by mitotic (equational) cell division, germ cells divide meiotically to form haploid gametes, thereby ensuring constant karyotypes over generations. During the first meiotic division, after DNA replication, homologous chromosomes pair, recombine and are then separated to opposite poles of the cell. Thereafter, sister chromatids segregate during the second division. Meiosis is completed by the formation of four genetically different haploid precursor cells that develop into gametic cells.

The coordinated and tightly controlled formation of DNA double-strand breaks (DSBs) and their repair is a prerequisite for successful meiotic divisions: it ensures the pairing and segregation of homologous chromosomes as well as re-shuffling of genetic traits. Several proteins necessary for DSB formation have been identified in a variety of organisms, with the conserved topoisomerase-related protein SPO11 as the catalytically active factor within the DSB-forming complexes (reviewed in Keeney, 2001; Edlinger and Schlogelhofer, 2011; Lam and Keeney, 2014; Robert et al., 2016). SPO11-interacting proteins link sites of DSB-formation to the chromosome axis (Blat et al., 2002; Panizza et al., 2011; Acquaviva et al., 2013). The meiotic axis is formed by axial element proteins like ASY1/Hop1, ASY3/Red1, and ASY4 (Hollingsworth et al., 1990; Rockmill and Roeder, 1990; Armstrong et al., 2002; Ferdous et al., 2012; Chambon et al., 2018; West et al., 2019), together with cohesin proteins, among them SCC3 and

REC8 (Klein et al., 1999; Toth et al., 1999; Cai et al., 2003; Chelysheva et al., 2005), and it is required for several processes from DSB formation to recombinational repair. Once the DSB has been formed, SPO11 is released from the DNA by the MRE11/RAD50/Xrs2-NBS1 (MRX/N) complex stimulated by COM1/Sae2 (Neale et al., 2005; Uanschou et al., 2007; Milman et al., 2009; Cannavo et al., 2018). The break ends are resected and coated with the RecA-related recombinases RAD51 and DMC1, highly conserved proteins that facilitate strand invasion of homologous sequences (Bishop, 1994; Dresser et al., 1997; Doutriaux et al., 1998; Couteau et al., 1999; Li et al., 2004; Kurzbauer et al., 2012). Subsequent DNA repair results in either crossover (CO) or non-crossover (NCO) events (reviewed in Osman et al., 2011; Hunter, 2015; Mercier et al., 2015; Sansam and Pezza, 2015), according to the selected repair template and the resolution of repair intermediates. Most organisms including *Arabidopsis thaliana*, form a large number of DSBs but only a fraction is channeled into CO recombination (Buhler et al., 2007; Hunter, 2007; Sanchez-Moran et al., 2007; Vignard et al., 2007). COs are formed in the context of the meiotic axes and the synaptonemal complex (SC) and physically link homologous chromosomes to enable correct segregation. The SC is a protein structure that builds on the axes, tightly connects homologous chromosomes and is required for inter-homolog recombination and interference (Zickler and Kleckner, 1999; Kleckner, 2006; Mercier et al., 2015; Smith and Nambiar, 2020; Capilla-Perez et al., 2021; France et al., 2021). The repair of the residual breaks yields NCO products, possibly *via* synthesis-dependent strand-annealing, intersister recombination, or non-homologous end-joining (Higgins et al., 2004; Chen et al., 2008; Mancera et al., 2008; Sims et al., 2019). Recombined homologous chromosomes segregate during the first, reductional, division, and sister chromatids during the second, mitosis-like, division, yielding four haploid cells.

THE MODEL ORGANISM *ARABIDOPSIS THALIANA*

Arabidopsis thaliana, or thale cress, is a small flowering plant in the mustard family and has become a widely used model organism for diverse research fields over the last decades. The weed is a simple angiosperm and has been used as a convenient model for plant biology. It is also widely used for addressing fundamental questions regarding functions common to all eukaryotes (reviewed in Meinke et al., 1998), with many factors and processes being conserved from yeast to humans and also present in plants. *Arabidopsis* plants are small, easy to cultivate under lab conditions and have a rather short life cycle of approximately 8 weeks. They are self-fertilizing and produce thousands of seeds per individual, making them especially attractive for use in genetic research. With about 135 mega base pairs, *A. thaliana* has one of the smallest plant genomes, distributed to only five chromosomes. The genome is among the best-curated ones (Berardini et al., 2015) and its near-complete sequence is available since the year 2000 (Arabidopsis Genome, 2000). We recently contributed, using latest generation sequencing approaches, considerable portions of the highly repetitive rDNA units of the nucleolus organizing region 2 (Sims et al., 2021). One of the most important advantages for the study of meiosis and related research in general is that *Arabidopsis* is thought to have very "relaxed" DNA repair checkpoints, enabling researchers to follow phenotypes of various DNA repair mutants through meiosis. In contrast to most other higher model organisms, only very few mutants (e.g., *blap75/rmi1, top3a-1*; Chelysheva et al., 2008; Hartung et al., 2008) have been identified that arrest in meiosis I and never undergo a second division. Most *Arabidopsis* mutants grow normally and complete the meiotic program regardless of accumulating DNA damage or chromosome missegregation, enabling thorough (epistatic) analyses.

These features, together with good accessibility of meiotic tissue, make *Arabidopsis* an excellent model organism to study meiosis, particularly suited for cytological analysis. There are differences between male and female meiosis (e.g., CO number; Drouaud et al., 2007; Giraut et al., 2011) and both deserve attention, but male meiocytes are more accessible because of the anatomy of *Arabidopsis* flowers. Therefore, male meiosis is typically analyzed and the focus of this review.

MEIOTIC STAGES (OBSERVED UNDER THE WIDEFIELD MICROSCOPE)

During **leptotene**, the first stage of meiotic prophase I, chromosomes condense after DNA replication and become visible as thin threads organized along the emerging chromosome axis. At this early stage, DSBs are formed and resected and recombinases are loaded onto ssDNA-overhangs. Leptotene nuclei can be easily identified in spreads of pollen mother cells (PMCs): thin chromatin threads are dispersed over the nucleus and the nucleolus is often visible as a darker area (**Figure 1A**). Leptotene is usually indistinguishable between the wild-type and DSB-deficient mutants like *spo11-2-3*, where chromosomes segregate randomly, leading to a strong reduction of fertility (**Figure 1A1**; Hartung et al., 2007). Likewise, DNA repair mutants like *com1-1*, which are completely sterile because DSBs are not processed and repaired (Uanschou et al., 2007), form regular leptotene meiocytes (**Figure 1A2**). Immunohistochemical staining reveals that the axial element proteins ASY1 and ASY3 and cohesins, such as SCC3 and REC8, are loaded during leptotene to form the axis and both recombinases, RAD51 and DMC1, appear as foci at DSB sites (**Figure 2**; Chelysheva et al., 2005; Ferdous et al., 2012; Kurzbauer et al., 2012; Cromer et al., 2013).

Zygotene is marked by the completed establishment of the meiotic axis. Chromosomes search for their homologous partner as repair templates and the SC starts to polymerize. Recombinase foci usually peak during this stage, indicating that DNA repair is in full swing (Sanchez-Moran et al., 2007; Kurzbauer et al., 2012). In acid spreads, the chromatin now appears as thicker threads partially clustered to one side of the nucleus. It is still impossible to differentiate between wild-type and DSB-deficient (*spo11-2-3*) meiocytes or nuclei lacking DNA

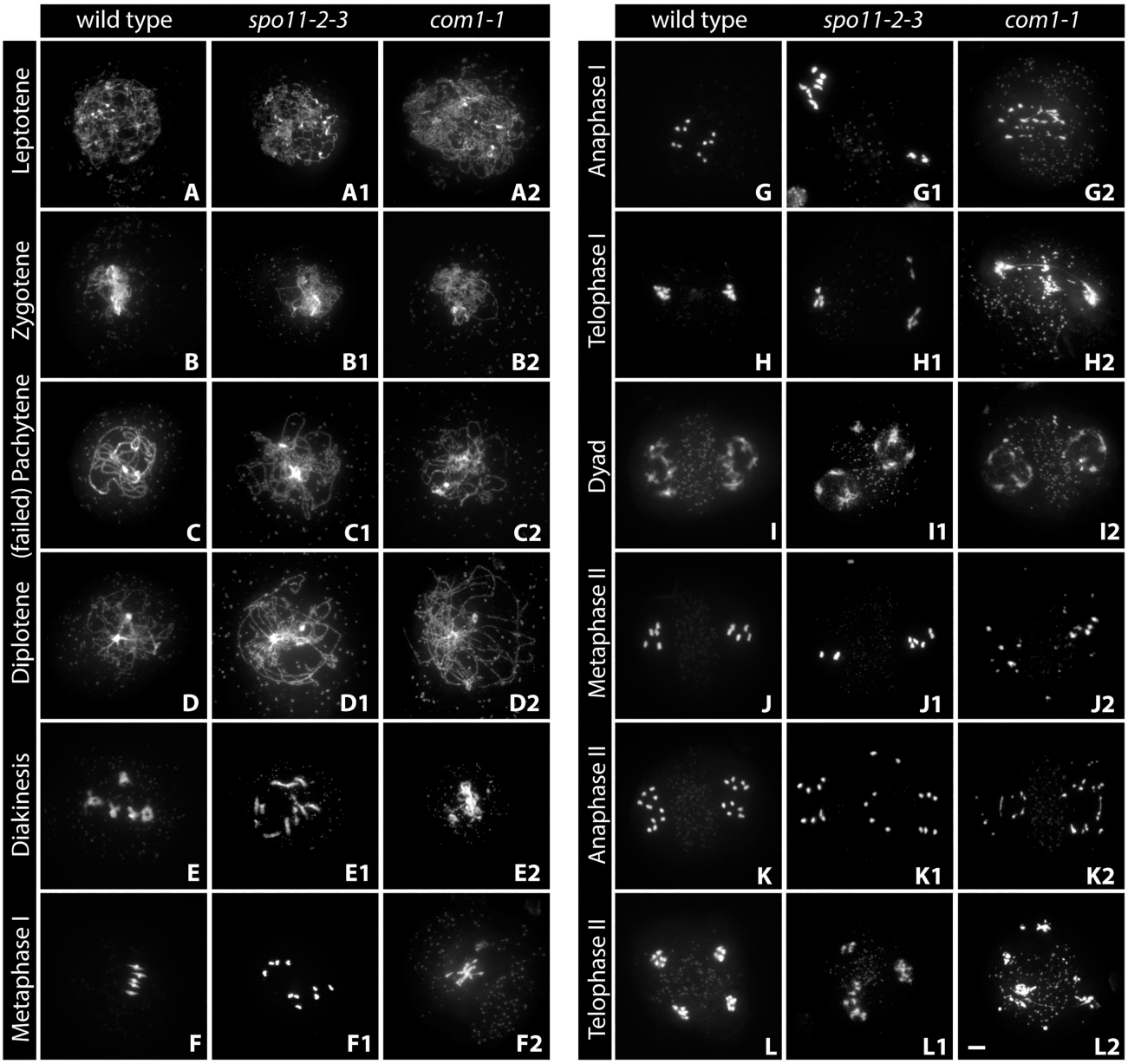

FIGURE 1 | Acid-spread nuclei from pollen mother cells (PMCs) depicting the meiotic progression in wild-type, double-strand break (DSB)-deficient (*spo11-2-3*) and DNA-repair-deficient (*com1-1*) male meiocytes. The spreads were stained with DAPI and imaged with an epifluorescence microscope. See text for details. Meiotic stages are indicated. Scale Bar: 5 μm.

repair factors like COM1 (**Figures 1A**–**A2**). The axial element proteins ASY1/3 appear as continuous threads over the entire length of all chromosomes in immunohistochemistry and cohesin staining is more pronounced. Staining for the SC protein ZYP1 reveals that some protein is already present on chromatin, but full polymerization will only be observed in pachytene (**Figure 2**). Pro-CO factors like the ZMM proteins MSH4/5 and HEI10, for example, are visible as numerous foci on chromatin (Chelysheva et al., 2012).

Complete synapsis is reached by polymerization of SC proteins from telomere to telomere and stable recombination intermediates are formed during **pachytene**. Synapsed chromosomes appear as thick, puffed up threads on acid spreads (**Figure 1C**) and staining for ZYP1 reveals full polymerization along chromosomes (**Figure 2**). ZYP1 is therefore an ideal marker when measuring total SC length within a nucleus (Drouaud et al., 2007; Lloyd et al., 2018; Kurzbauer et al., 2021). ASY1 can still be detected along pachytene chromosomes, but the staining is remarkably less bright apart from few brightly stained stretches (**Figure 2**) that mark the nucleolus organizer regions (NORs) containing the 45S rDNA genes (Fransz et al., 1998; Sims et al., 2019). The ASY3 signal, marking the axes now incorporated into the

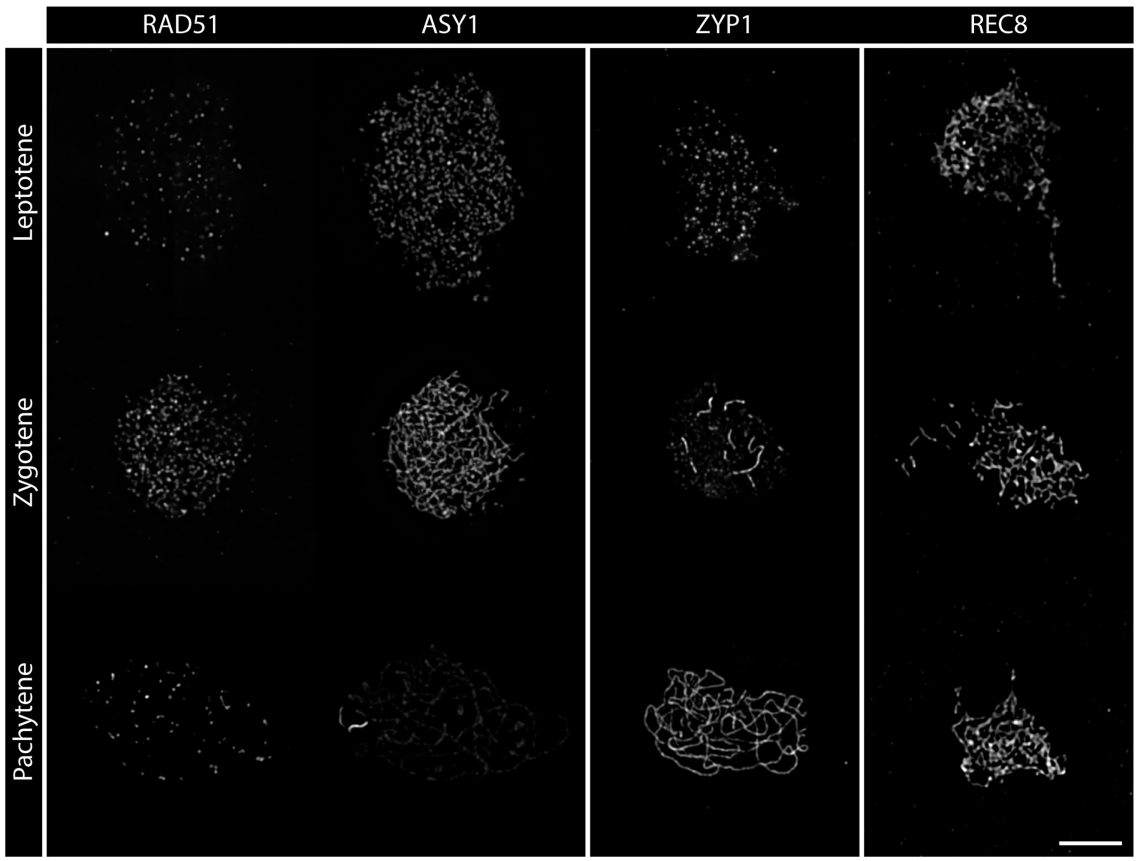

FIGURE 2 | Detergent-spread nuclei from PMCs depicting the meiotic progression from leptotene to pachytene in the wild-type. The spreads were stained for the recombinase RAD51, the axial element protein ASY1, the transverse filament protein ZYP1, or the meiosis-specific cohesin subunit REC8. Images were acquired with an epifluorescence microscope. Meiotic stages are indicated. Scale Bar: 5 μm.

SC, is intense and overlaps with ZYP1 staining. The axes can also be visualized by staining for the cohesin subunits REC8 and SCC3 that appear thread-like (**Figure 2**). In mutants deficient for DSB formation or repair, such as *spo11-2-3* and *com1-1*, axis formation often appears to be normal, but synapsis is never complete. Pachytene stages are not found and nuclei seem to directly progress from zygotene to diplotene (**Figures 1C1**, **2**). In these mutants, ZYP1 appears as foci or short stretches but does not fully polymerize, while axis staining is usually unaffected. Meiocytes of plants lacking axis proteins, such as ASY1 and ASY3, never fully synapse (Caryl et al., 2000; Ferdous et al., 2012) and full pachytene stages are also not observed in cohesion-deficient mutants like *scc3* and *rec8* (Bai et al., 1999; Chelysheva et al., 2005). Similarly, complete synapsis is not observed when the transverse filament ZYP1 proteins are depleted or absent (Higgins et al., 2005; Osman et al., 2006; Capilla-Perez et al., 2021; France et al., 2021). During wild-type pachytene (and up to diakinesis), ZMM proteins MSH4/5 and HEI10, as well as MLH1/3, localize to CO sites and form around 9–11 bright foci per nucleus, corresponding to the average number of chiasmata. Immunohistochemical staining for the mentioned proteins is often used to determine the number of interfering class I COs (Chelysheva et al., 2010, 2012).

Diplotene is the last stage of meiosis regularly amenable to analysis by detergent/surface spreading. The SC disassembles and homologous chromosomes remain linked by COs. Chromatin appears as thin, brittle, or fragmentary threads that usually occupy the whole nuclear area in acid spreads (**Figures 1D–D2**). Immunohistochemical images are characterized by weak axis staining.

Chromosomes condense during **diakinesis** and maximum condensation is reached during **metaphase I.** Pairs of homologous chromosomes, bivalents, align at the metaphase plate and COs are cytologically visible as so-called chiasmata (**Figures 1E**,**F**). Meiocytes are no longer compatible with detergent spreading, but acid spreading allows for further investigation of meiotic progression. Analysis of diakinesis and metaphase I chromosomes is among the first steps during the characterization of a newly found mutant, since a lot of information regarding defects can be gained. In case DSBs are not made, as in *spo11* mutants, bivalents cannot be formed and 10 univalents are observed (Grelon et al., 2001; Stacey et al., 2006; **Figures 1E1**,**F1**). The same phenotype is found in mutants deficient in interhomolog-recombination like plants lacking functional DMC1 (Couteau et al., 1999). When only a subset of interhomolog recombination events is affected, varying amounts of univalents and bivalents are observed (Higgins et al., 2004; Crismani et al., 2012;

Girard et al., 2014; Kurzbauer et al., 2018). Mutant plants deficient for DNA repair like *com1-1* display aberrant chromosome behavior in diakinesis and metaphase-chromosomes are often not visible as five distinct bivalents, but rather appear as an entangled mass of chromatin (**Figures 1E2**,**F2**). Chromosome fragments may be visible as well (Bleuyard et al., 2004; Bleuyard and White, 2004). Similar defects, together with univalent formation, are often observed in plants lacking functional cohesin proteins SCC3 or REC8 (Bai et al., 1999; Chelysheva et al., 2005). Immunohistochemical staining is possible but requires special slide treatment (see section "Fluorescence *in situ* Hybridization"). Metaphase I nuclei are also analyzed to determine the number of chiasmata formed in a meiotic nucleus. Individual chromosomes are identified by fluorescence *in situ* hybridization (FISH) staining for the 5S and 45S rDNA repeats (see section "Widefield Epifluorescence Microscopy") and the number of chiasmata per chromosome arm is deduced from bivalent shape (Sanchez Moran et al., 2001; Lopez et al., 2012).

Homologs segregate to opposite cell poles during **anaphase I** (**Figure 1G**) and start to decondense in **telophase I** at the end of the first meiotic division (**Figure 1H**). These two stages are highly informative, because chromosome fragments are visible when DNA repair is defective (as in *com1-1*, **Figures 1G2**,**H2**) and chromosome missegregation can be observed when homolog interactions are reduced or absent (as in *spo11-2-3*; **Figures 1G1**,**H1**; Grelon et al., 2001; Stacey et al., 2006). In addition, irregular repair might manifest in chromatin bridges, well visible during these (and subsequent) stages (**Figures 1H2**,**L2**; Uanschou et al., 2007; Kurzbauer et al., 2021) and cohesion-deficiencies may result in premature sister separation (Cai et al., 2003; Chelysheva et al., 2005).

The second, mitosis-like, division starts with the rather decondensed **dyad** stage (also called prophase II, **Figure 1I**) and chromosomes condense again during **metaphase II** (**Figure 1J**). Sister chromatids are then separated during **anaphase II** (**Figure 1K**), reach now four (or more/less in the case of missegregation as in *spo11-2-3*; **Figures 1L**,**L1**) poles in **telophase II** (**Figure 1L**) and finally decondense in the **tetrad** stage. Chromosome fragments and/or bridges usually persist and can be observed during all stages of meiosis II in DNA repair-deficient mutants like *com1-1* (**Figures 1I2**–**L2**).

At the end of wild-type meiosis, each originally diploid cell gives rise to four haploid gamete precursor cells (**Figure 1L**). Further mitotic divisions and development yield microspores (male gametes, pollen) or macrospores (female gametes, egg cells) that will reconstitute diploid organisms after nuclear fusion upon fertilization. DNA repair mutants often form polyads as a consequence of chromosome missegregation, and because chromosome fragments tend to stay highly condensed, they are visible up to the last stage of meiosis (**Figure 1L2**).

CLASSICAL SAMPLE PREPARATION TECHNIQUES

Male meiotic nuclei develop within anthers of small buds close to the center of *Arabidopsis* inflorescences. In order to subject them to cytological analysis to follow chromosomes through meiosis, several layers of tissue have to be removed mechanically and the syncytium-surrounding callose eliminated by digestion. Finally, remaining membranes and cytoplasm are cleared away by spreading and chromatin is spread and fixed to the slide. Two different sample preparation techniques – and several variations thereof – are used for most cytological studies, depending on the specific research question (see below).

Acid Spreads

Production of acetic acid spreads of PMCs followed by chromatin staining is a standard technique to analyze meiotic progression and assess chromosome structure and segregation in male *Arabidopsis* meiocytes since the 1990s (Ross et al., 1996). The technique has been refined over the years but the basic procedure (destaining and fixation in acetic acid/ethanol, enzymatic digestion of the cell wall and spreading with acetic acid/ethanol) is still the same (Fransz et al., 1998; Armstrong et al., 2001). The procedure is rather simple, required reagents and equipment are widely available. It is usually the starting point for studying mutant phenotypes related to meiosis. Preparation of acid spreads allows for a relatively quick assessment of which stage of meiosis is defective in a mutant of interest (see section "Classical Sample Preparation Techniques"). Several years ago, this spreading technique was developed further to allow for the staining of proteins constituting the axis and/or the SC as well as closely associated factors. Like the original, this refined method preserves chromosome structure by strong fixation and removes cytoplasm by acetic acid treatment. It includes additional microwave treatment to increase the accessibility of epitopes to antibodies, thereby allowing for immunostaining of nuclei in all stages of meiosis (Chelysheva et al., 2010, 2012, 2013).

Detergent Spreads

Detergent spreading followed by immunohistochemical staining with antibodies directed against meiotic proteins and fluorescently labeled secondary antibodies for visualization is used for a more detailed analysis of events during early-to-mid meiotic prophase. It enables investigation of the temporal expression and localization of proteins from leptotene to diplotene when antibodies are available. The technique for male plant meiocytes was originally developed for electron microscopic analyses in the Jones lab (Albini et al., 1984) and has been optimized over the years (for example, Armstrong et al., 2002; Chelysheva et al., 2005; Kurzbauer et al., 2012; Armstrong and Osman, 2013; Martinez-Garcia et al., 2018; Sims et al., 2020b). The original basic procedure involves preparation of anthers containing meiotic cells, enzymatic digestion (for example, with cytohelicase, adigestive enzyme from *Helix pomatia* containing several enzymatic activities required to digest the callose surrounding meiotic syncytia), chromatin spreading with a detergent (often Lipsol) and formaldehyde fixation on glass slides. The protocol yields

differing amounts of meiotic nuclei on slides, since the exact stage of meiocytes in the anthers is hard to predict and some material is lost during preparation. Additionally, the non-meiotic tissue of anthers present on the slides leads to high amounts of background staining. To overcome this, we previously took advantage of a technique developed by Chen et al. (2010). Meiotic nuclei develop within four elongated syncytia per anther (six anthers per flower) that can be separated from the surrounding tissue. Mechanical extraction and subsequent collection of those "columns" with a glass capillary allows for enrichment of meiotic nuclei in very small volumes and greatly improved the quality of microscopic preparations (Kurzbauer et al., 2012; Sims et al., 2020b). The preparation furthermore removes all non-meiotic cells, improving digestion and spreading efficiency, reducing background staining and increasing the amount of analyzable nuclei per microscopic slide. This reduces the time spent at the microscope considerably and enables more thorough analyses by super-resolution microscopy (see below).

ADVANCED SAMPLE PREPARATION TECHNIQUES

Specific research questions often demand a precise localization of molecular events to defined chromosomal locations, with respect to the entire genome or to its spatial position within the nucleus. Such analyses are enabled by the techniques presented below that were developed over the last decades with the contribution of many researchers.

Fluorescence *in situ* Hybridization

Fluorescence *in situ* hybridization or FISH is a cytological technique developed more than 35 years ago (Bauman et al., 1980) and widely used to specifically mark nucleic acid sequences in chromosome preparations. It has a wide range of applications from individualizing each chromosome to monitoring specific chromosomal regions. The principle of FISH has not changed since its first application but the protocols and techniques used to prepare the samples and the hybridization probes have improved over the years. In brief, the fixed spread chromosomes (see section "Fluorescence *in situ* Hybridization") are heat-denatured in order to allow fluorescently labeled nucleic acid probes to hybridize to their DNA target. The nucleic acid probes can be "self-made" by synthesizing DNA from template sequences and incorporating fluorescent base analogs, or by using custom-made, commercially available labeled locked nucleic acid (LNA) sequences (Paulasova and Pellestor, 2004). LNA probes have the great advantage to have a strong affinity to DNA (or RNA) and can bind to their target at lower temperatures than regular DNA-only probes. Recent techniques combine bioinformatic platforms and PCR-based oligonucleotide labeling to allow imaging of regions from tens of kilobases to megabases (Beliveau et al., 2012). In addition, pre-labeled oligomer probes (PLOPs) were used to mark repetitive regions of different plant species and have the potential of reducing the hybridization time from hours to minutes (Waminal et al., 2018). The FISH technique has been widely used within the meiotic plant community and is an essential tool to determine the chiasma frequency on individual chromosomes. To this end, bivalents are unequivocally identified by FISH labeling of the 5S and 45S rDNA regions and the number of chiasmata per chromosome arm is deduced from bivalent shape (Sanchez Moran et al., 2001; Lopez et al., 2012; Armstrong, 2013; Kurzbauer et al., 2018, 2021). Finally, single-molecule RNA-FISH has become increasingly popular to analyze transcription in plant tissues. It involves the use of fluorescently labeled DNA probes that bind multiple times within a single mRNA transcript (Femino et al., 1998; Duncan et al., 2016). This technique is routinely used on root meristems but, to our knowledge, has not yet been optimized for meiotic cells (Duncan and Rosa, 2018).

Targeted Analysis of Chromatin Events

The Targeted Analysis of Chromatin Events (TACE) is an advanced cytological method that combines an improved immunocytology protocol (detergent spreads; see section "Targeted Analysis of Chromatin Events") with the hybridization of FISH probes targeting large chromosomal regions (Sims et al., 2020b). Thereby, the localization and abundance of meiotic proteins can be determined at specific chromosomal loci of interest. Regular FISH on acid-spread chromosome preparations is used to visualize any desired chromosome locus but the harsh preparation followed by heat denaturation of the DNA/RNA can cause mis-folding or loss of proteins and failure of detection. It is therefore important to fine-tune the denaturation and hybridization steps to detect both the proteins of interest and the desired chromosomal loci. For this specific application, LNA probes are favorable due to their low hybridization temperatures. TACE has been used recently to determine the abundance of RAD51 DNA repair foci in defined regions with and without an ectopic rDNA insertion (Sims et al., 2019). It can be easily adapted to specific research questions by combining different sets of antibodies and nucleic acid probes.

Whole Mount Immuno FISH

Whole mount immunolocalization is a popular sample preparation technique when the proteins of interest are to be analyzed in 3D preserved tissues and nuclei and is especially recommended for visualizing female *Arabidopsis* meiocytes (Escobar-Guzman et al., 2015). Tissue clearing may be necessary to improve protein detection and has been implemented in studies of both female and male meiosis (Hedhly et al., 2018; Tofanelli et al., 2019). FISH is usually performed on spread samples (see previous sections). Specific questions, however, may require preserving the spatial organization of the cell and the relative position of genomic loci or protein complexes within the nucleus. Whole mount FISH protocols were developed that maintain the structural integrity of nuclei, cells and even tissues in 3D and let researchers address the

original spatial relations. Several protocols are currently available and have been optimized for different tissues: a necessity, since a caveat for whole mount preparations is the difference in cell wall composition and thickness affecting the penetrance of antibodies and probes (Bauwens et al., 1994; Bass et al., 1997; Costa and Shaw, 2006; Berr and Schubert, 2007; Bey et al., 2018). The special whole mount immuno FISH (Who-M-I-FISH) technique has been optimized for the simultaneous detection of meiotic proteins and genomic loci, while maintaining the 3D structure of meiotic nuclei within intact anthers (Sims et al., 2020a). It has been used recently to determine the 3D localization of the rDNA regions within the nucleus in relation to the localization of the HORMA domain protein ASY1 (Sims et al., 2019). The long duration of the protocol and the often incomplete penetrance of the primary antibodies through the plant cell wall make the Who-M-I-FISH a challenging technique that should only be considered when addressing specific questions.

MICROSCOPY TECHNIQUES

The wide range of microscopy technologies that were developed in the last decade, together with long approved techniques, offers a large choice of microscopes that can fit any lab requirement. In the meiotic field, cytological analysis is a necessary and widely used tool for all model organisms.

Widefield Epifluorescence Microscopy

Widefield epifluorescence microscopy uses a basic illumination principle that permanently illuminates the whole sample and detects emitted light with a digital camera. It can be considered as the "workhorse" technology that enables a first screen of the samples and a general overall assessment of sample quality and staining efficiency. Widefield microscopy is regularly used to analyze and image acid spreads, FISH preparations and detergent spreads with all of the previously described improvements. This technology is still the prime candidate for quantitative analysis due to its user-friendly set up and the affordable price. The X-Y resolution of this technology is limited by diffraction to ~200 nm, and the axial resolution to about 500–700 nm (Verdaasdonk et al., 2014; Kubalová et al., 2021). The possibility to deconvolve and further process the acquired images can improve resolution and image quality. For these reasons, widefield epifluorescence microscopy is still the system of choice for most applications.

In order to achieve higher resolutions some microscopy technologies make use of sophisticated optics and algorithms to surpass the physical ~200 nm diffraction limit (Biggs, 2010; Kubalová et al., 2021).

Confocal Laser Scanning-Airyscan Microscopy

Confocal Laser Scanning-Airyscan microscopy or LSM-Airyscan uses a new detector concept, developed by the company Zeiss, implemented on confocal laser-scanning microscopes. Canonical confocal microscopes scan specimens point-by-point, using point illumination and a pinhole at the detector level to eliminate out-of-focus light. In addition, the LSM-Airyscan has a 32-channel detector that collects 32 pinhole images with positional information at every scan point. This enables very light-effective imaging with improved resolution. According to the manufacturer, and based on imaging of fluorescent beads, the Airyscan detector system can reach a super-resolution of 120 nm in the x-y and 350 nm in the z plane even when scanning thick samples (Huff, 2015; Huff et al., 2017; Kubalová et al., 2021). This makes the LSM-Airyscan the microscopy technique of choice when imaging thick samples, such as whole mount preparations, although more complicated to operate. The LSM-Airyscan system relies on algorithms to reconstruct the image and achieve super-resolution, which can cause artifacts (Korobchevskaya et al., 2017). Image acquisition by confocal laser scanning microscopy is rather fast, particularly suited for live imaging of thick samples. In fact, it is one of the best-suited technologies for live imaging of meiotic cells in intact tissues (Prusicki et al., 2019). Alternatively, **light sheet fluorescence microscopy** may be employed to follow meiotic progression live (Valuchova et al., 2020). Here, the sample is excited with a thin sheet of laser light and optical sections are captured. Acquisition speed and low phototoxicity allow for extended imaging periods with a large field of view, but, being diffraction-limited, the resolution cannot compete with LSM-Airyscan systems.

Structured Illumination Microscopy

Structured Illumination Microscopy (SIM) illuminates the sample using patterned light at different focal planes. Multiple images of the different light patterns are combined by a computer algorithm to reconstruct a super-resolved image. SIM microscopy can reach a resolution of 100 nm in the x-y and 350 nm in the z plane and it is one the most widely used super-resolution techniques (Kubalová et al., 2021). SIM is generally easy to use and suitable for a wide variety of samples, although it is not optimal for thick samples; it is based on widefield microscopy and fails in the presence of excessive out-of-focus light (Cox, 2015). Furthermore, because it uses algorithms to reconstruct the image, there is a chance of generating artifacts in the final image. Hammer-stroke or honeycomb-like artifacts are most common and can be mistaken for biological structures (Schaefer et al., 2004; Komis et al., 2015; Lambert and Waters, 2017; Sivaguru et al., 2018; Kubalová et al., 2021).

In general, SIM is used for 3D reconstructions of completely or partially spread samples allowing a more detailed analysis of the localization of proteins. Many labs routinely use SIM and contributed to the optimization of the sample preparation for an optimal performance (for example, Schermelleh et al., 2008; Lambing et al., 2015; Hesse et al., 2019; Mittmann et al., 2019; Ku et al., 2020; Morgan and Wegel, 2020). SIM has been used to study many different aspects of meiotic cells from the structure of the axis/synaptonemal complex to the

architecture of centromeres (Lloyd et al., 2018; Morgan et al., 2020; Schubert et al., 2020).

Stimulated Emission Depletion Microscopy

Stimulated emission depletion or STED microscopy is a technology based on laser scanning confocal microscopy but uses a depletion laser, bearing a donut shape, in conjunction with the excitation laser beam. The depletion laser de-excites fluorophores, which are not at the center of the donut, thereby preventing a spontaneous emission and creating an extremely small photon-emitting spot. The fluorescence at the periphery of the excited spot is silenced, thereby improving the resolution far beyond the diffraction limit (Hell and Wichmann, 1994; Klar and Hell, 1999). STED nanoscopy has similar requirements as classical confocal microscopy but with some differences in sample preparation. Specific fluorophores are required to achieve the best resolution. These fluorophores need to withstand the power of the depletion laser and resist its bleaching capacity. Furthermore, the mounting medium used on the samples can severely alter imaging quality. Hence, extra caution must be taken when preparing the sample for STED imaging.

Fluorophores emitting in the far-red wavelength (700–800 nm) can reach up to 30 nm of resolution, in contrast to red wavelength emitters (620–750 nm), which can reach a maximum of 50–60 nm (in the X-Y plane, maximum axial resolution is around 90 nm; Kubalová et al., 2021). This discrepancy in the resolution between the two wavelengths needs to be taken into account when performing protein co-localization studies. A great advantage of STED nanoscopy, if compared to other super-resolution techniques, is that the final acquired imaged is not the result of algorithm-based image reconstruction, but rather of a purely physical improvement in resolution. This minimizes artifacts and maintains image fidelity (Lambert and Waters, 2017). STED nanoscopy is a recent technology and has not yet been widely adopted by the meiosis community but has been used to study the length of DNA loops, the width and structure of the synaptonemal complex and precise abundance of meiotic proteins at specific sites (Sims et al., 2019; Capilla-Perez et al., 2021; Kubalová et al., 2021; Kurzbauer et al., 2021).

The basic STED set-up is not well suited for live imaging owing to the requirement of the high-intensity depletion laser. This can result in a reduction of cell fitness, but new techniques are being developed that will improve super-resolution live cell imaging in the future (Sharma et al., 2020).

One of the great advantages of the STED technology, which allowed the system to jump into the microscopy market, is the capacity to upgrade existing microscopes to a STED system with an affordable basic version (Abberior STEDycon). This unfortunately comes with some limitations such as a restriction in the number of channels that can be imaged in super-resolution and only in 2D. Bigger and more costly setups overcome these limitations providing super-resolution in more channels and in 3D.

Certainly, there are very powerful other super-resolution technologies available, such as **photo-activated localization microscopy** (PALM) or **stochastic optical reconstruction microscopy** (STORM), which can reach a resolution of 10 nm (Komis et al., 2018). Both are widefield techniques and rely on the detection of individual fluorophore molecules to overcome the diffraction limit. In short, fluorophores are sparsely activated and forced into "blinking" by spontaneous photobleaching (PALM) or reversible On/Off switching (STORM). A large number of images are generated, where each contains signals emitted by a different set of fluorescent molecules, enabling their precise localization. The complexity of the sample preparation and the inherent post-acquisition processing, required to reconstruct the final image, can be prone to artifact generation (Whelan and Bell, 2015; Lambert and Waters, 2017). For these specific reasons, the STED technology is often preferable when analyzing meiotic spreads in super-resolution and with maximum image fidelity.

Overall, the possibility for every lab to upgrade any existing epifluorescence microscope with commercially available STED technology brings the possibility to use super-resolution imaging on a daily basis.

FROM MICROSCOPY TO NANOSCOPY: NEW VIEWS ON MEIOSIS

Super-Resolution Meiotic Atlas

The first complete "atlas" of meiosis in *A. thaliana* was published in 1996 and encompassed images of acid-spread pollen mother cells in all stages from pre-leptotene to telophase II. The idea of the authors was to provide a reference of normal chromosome behavior and appearance in wild-type meiosis against which mutant phenotypes could be compared, using "simple light microscopic techniques" (Ross et al., 1996). About 25 years later, we present an updated meiotic atlas, combining classical slide preparation by acid spreading (see section "Fluorescence *in situ* Hybridization") with the rather new chromatin dye SiR-Hoechst (SiR-DNA; Lukinavicius et al., 2015) and state-of-the-art STED nanoscopy (**Figure 3**; **Supplementary Material**). Acid spreading is extremely efficient and, together with the use of an optimized chromatin dye and a STED nanoscope, enables the observation of meiotic chromosomes at a nanometer scale, revealing fascinating details and opening possibilities for new analyses.

The size of chromatin loops, for example, can be measured in euchromatic and heterochromatic regions from leptotene to diakinesis (see **Figures 3A–E**; Kurzbauer et al., 2021) without the requirement for additional FISH labeling or electron microscopy, that had been used previously to measure the length of chromatin loops of meiotic chromosomes (Anderson et al., 1988; Moens and Pearlman, 1988; Heng et al., 1996; Novak et al., 2008). Synaptonemal complex length and loop size are inversely correlated through loop density (Kleckner, 2006), a parameter that can be determined fairly easily using the above described techniques. Pachytene nuclei are furthermore often spread well enough to distinguish chromatin from the two synapsed homologous chromosomes (**Figure 3C**), opening the

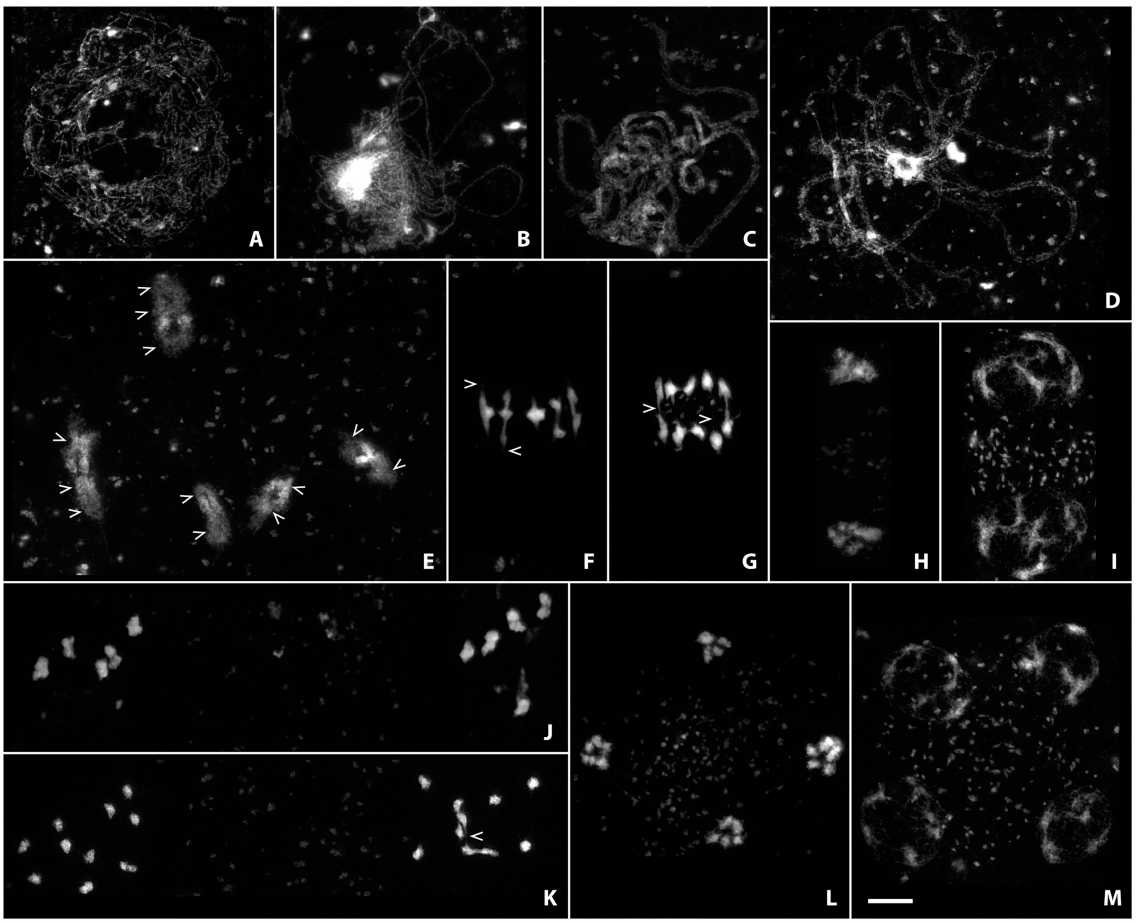

FIGURE 3 | Acid-spread nuclei from pollen mother cells depicting the meiotic progression in wild-type male meiocytes in super-resolution. Chromatin was stained with SiR DNA and imaged with a stimulated emission depletion (STED) nanoscope. The meiotic stages are: **(A)** Leptotene; **(B)** Zygotene; **(C)** Pachytene; **(D)** Diplotene; **(E)** Diakinesis; **(F)** Metaphase I; **(G)** Anaphase I; **(H)** Telophase I; **(I)** Dyad; **(J)** Metaphase II; **(K)** Anaphase II; **(L)** Telophase II; **(M)** Tetrad. Scale Bar: 5 μm.

possibility to screen for unpaired or mispaired regions that might be caused by translocations or other chromosomal aberrations. During diakinesis, chiasmata (the cytologically visible form of crossovers) can be directly observed and their number approximated without the use of further markers (**Figure 3E**; arrowheads). Delicate chromatin protrusions are visible during diakinesis and metaphase I (**Figures 3E,F**; examples marked by arrowheads), and connections between segregating chromosomes by crossover recombination can be seen well into anaphase I (**Figure 3G**; examples marked by arrowheads). Early on in meiosis II, before sister chromatids have really separated, they already become visible as discrete chromatin entities (**Figure 3J**). Fine connections may be observed in anaphase II (**Figure 3K**; arrowhead) before sisters finally segregate to separate poles, and chromosomes progressively decondense during telophase II and the tetrad stage (**Figures 3L,M**).

Imaging at such high resolution on classically prepared slides has only recently become available and will be very useful for future studies. Meiotic progression of mutant meiocytes can now be studied in greater detail, since very subtle defects are more obvious when imaged in super-resolution. Even small chromosomal fragments may be identified, premature sister separation can be observed, thin chromosome bridges become visible, and changes in loop size may be assessed.

The Meiotic Axis and the Synaptonemal Complex in Super-Resolution

Preparation of detergent-spread meiotic nuclei, together with immunofluorescence staining and imaging by STED nanoscopy, offers new possibilities to study basic chromosomal structures, especially important for model organisms with rather small chromosomes like *Arabidopsis*. The structure of the SC (mainly studied using electron microscopy) appears to be highly conserved with a width of around 100 nm in many organisms with vastly different genome and chromosome sizes (e.g., Zickler and Kleckner, 1999). With 100 nm or more being the resolution limit for other super-resolution techniques (see section"From Microscopy to Nanoscopy: New Views on Meiosis"), imaging substructures of the SC is an ideal case for STED nanoscopy: in pachytene, ASY3 staining is intense

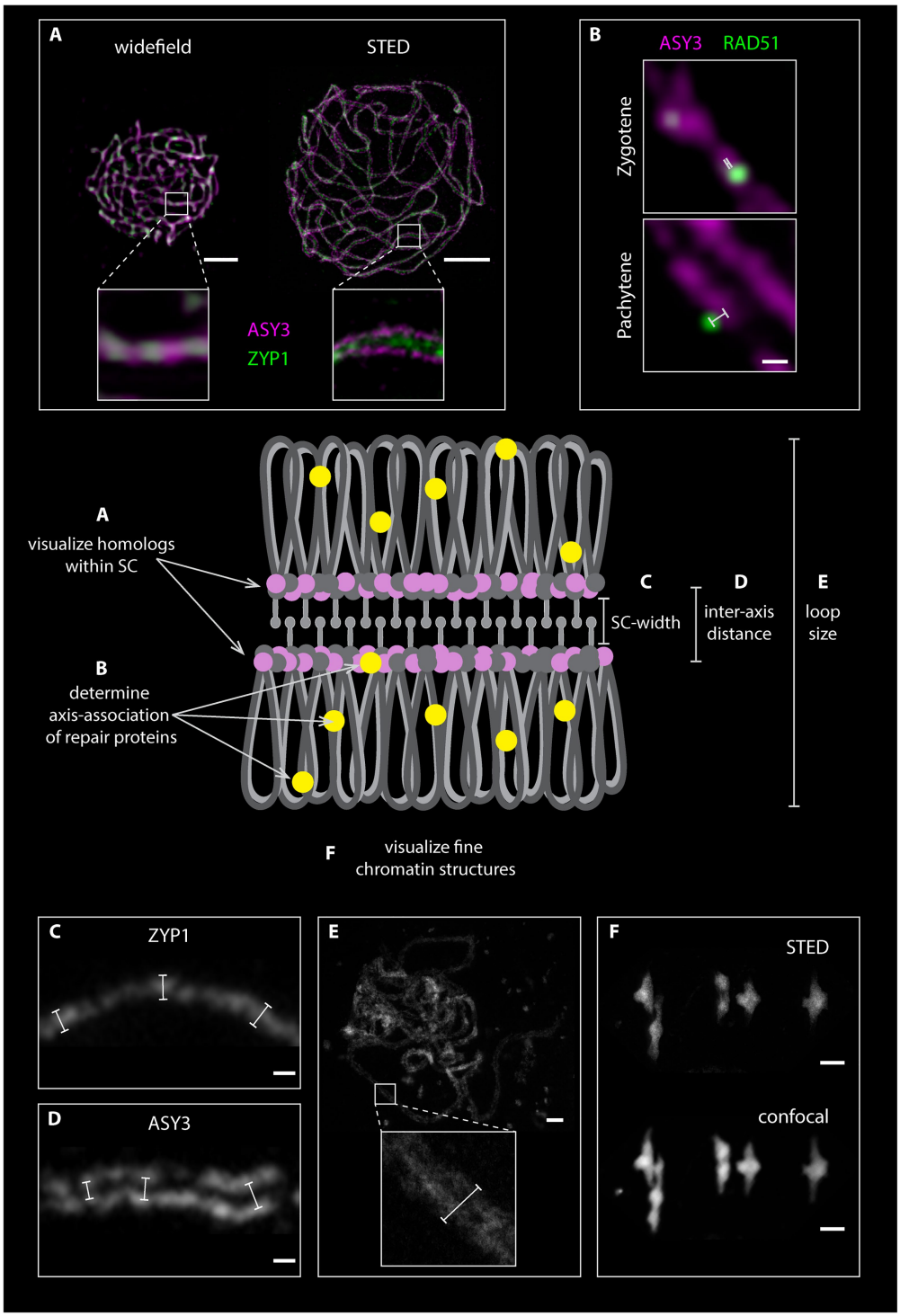

FIGURE 4 | Graphical representation of homologous chromosomes with a fully formed synaptonemal complex (SC). The loops of the homologous chromosomes are depicted in gray, the axial elements in pink and dark gray, the SC transverse filaments in light gray and repair proteins in yellow. Chromosomal features, which can be assessed by STED nanoscopy, are highlighted. **(A)**. Comparison between widefield and STED images of detergent-spread male meiotic nuclei, which were stained for the axis (ASY3) in magenta and the transverse filament (ZYP1) in green. **(B)**. Magnification of meiotic chromosomes in zygotene and pachytene stage stained for ASY3 (magenta) and the recombinase RAD51 (green). White bars indicate the distance measurements of each focus from the center for the axis. **(C)** and **(D)** Examples of measurements of SC width and inter-axis distance in nuclei stained for ZYP1 **(C)** and ASY3 **(D)**. **(E)** Measurement of DNA loop length on an acid spread pachytene nucleus. **(F)**. Comparison between STED and confocal microscopy of an acid-spread nucleus at metaphase I stained with SYBR green (confocal) and SiR DNA (STED). Scale Bars: **(A,E,F)** 2 μm; **(B,C,D)** 100 nm.

and appears as parallel threads around the ZYP1 signal, while the localization of both proteins appears almost identical in epifluorescence images (**Figure 4A**; **Supplementary Material**). It is therefore possible to not only visualize both axes embedded in the SC of synapsed homologs, but also to measure the distances between them, providing a novel parameter for defining meiotic chromosomes (**Figures 4C–E**; **Supplementary Material**). Such measurements only recently revealed that the *Arabidopsis* SC is roughly 125 nm wide, that axis midpoints are about 140 nm apart, and that those parameters depend on regulatory proteins (Kurzbauer et al., 2021). The homologous axes can also be distinguished when staining for cohesins like REC8 and SCC3 that appear as abundant, close-packed foci alongside transverse filaments, in contrast to thick lines observed with widefield microscopy (compare **Figures 2, 5**). STED imaging of *Arabidopsis* nuclei also reveals that extensive chromosome axis remodeling, in preparation for higher condensation during subsequent stages, results in axis structures highly similar to those observed in "tinsel-like" stages in the large genome cereals barley and wheat (Colas et al., 2017). Instead of the curved threads visible during zygotene or pachytene, the ASY3-stained axes appear as short, straight, and thicker stretches with kinks in between (**Figure 6A**; **Supplementary Material**). Nanoscopic analysis of *Arabidopsis* detergent spreads furthermore shows that the axis opens up around HEI10-labeled recombination sites, forming pocket-like substructures, in diplotene (**Figures 6B,C**; **Supplementary Material**), similar to previous observations in *Caenorhabditis elegans* (Woglar and Villeneuve, 2018). Since antibodies directed against numerous components of meiotic chromosomes are available, future nanoscopic studies will shed light on previously unknown (or rather unseen) substructures and protein (co-)localization and refine our understanding of basic meiotic processes.

Meiotic Repair Proteins and Co-localization of Complex Partners

The abundance and localization of meiotic repair proteins have been predominantly addressed using epifluorescence microscopy. More recently, SIM, and in some cases STORM, have been used to analyze the dynamics of proteins throughout meiotic prophase (Brown et al., 2015; Woglar and Villeneuve, 2018; Hinch et al., 2020; Morgan and Wegel, 2020; Slotman et al., 2020).

The nanoscale resolution of 30 nm in STED nanoscopy allows analyzing the position and dynamics of proteins with

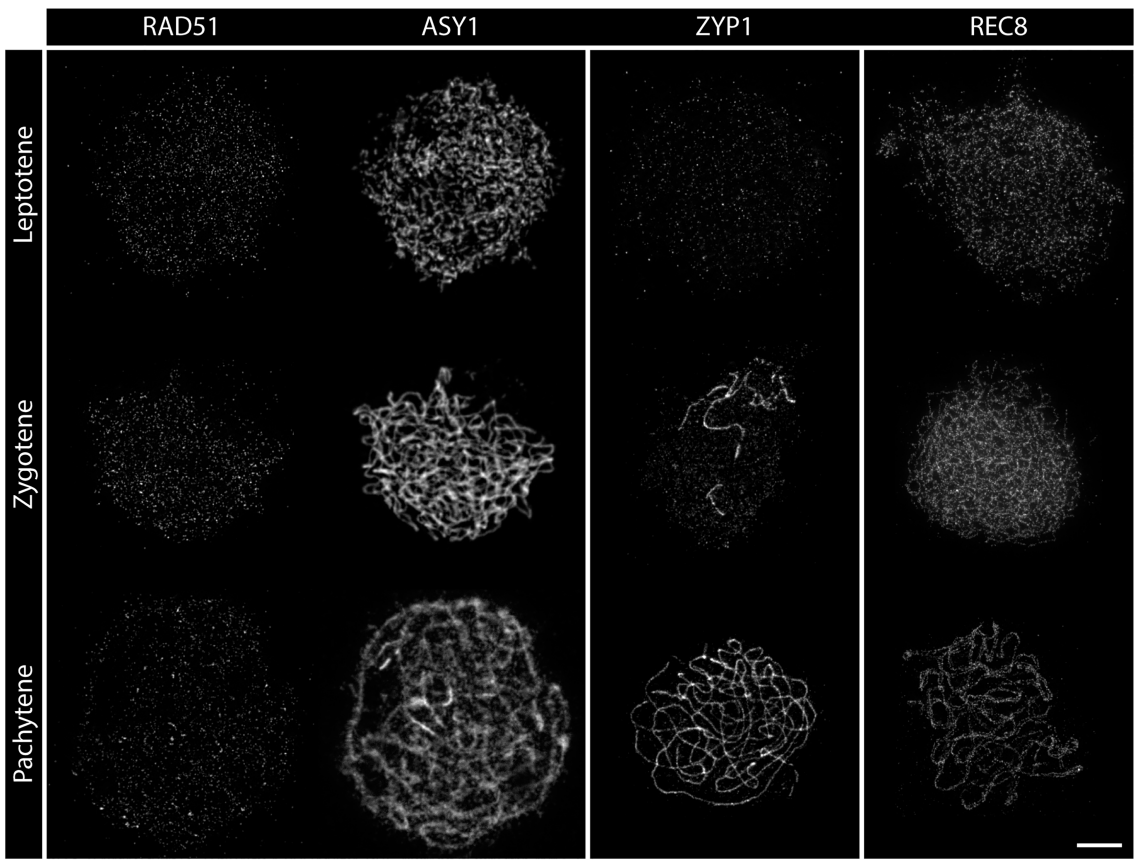

FIGURE 5 | Detergent-spread nuclei from pollen mother cells depicting the meiotic progression in the wild type. The spread nuclei were stained for the recombinase RAD51, the axial element protein ASY1, the transverse filament protein ZYP1, or the cohesin subunit REC8. Images were acquired with a STED nanoscope. Stages of meiotic prophase are indicated. Scale Bar: 2 μm.

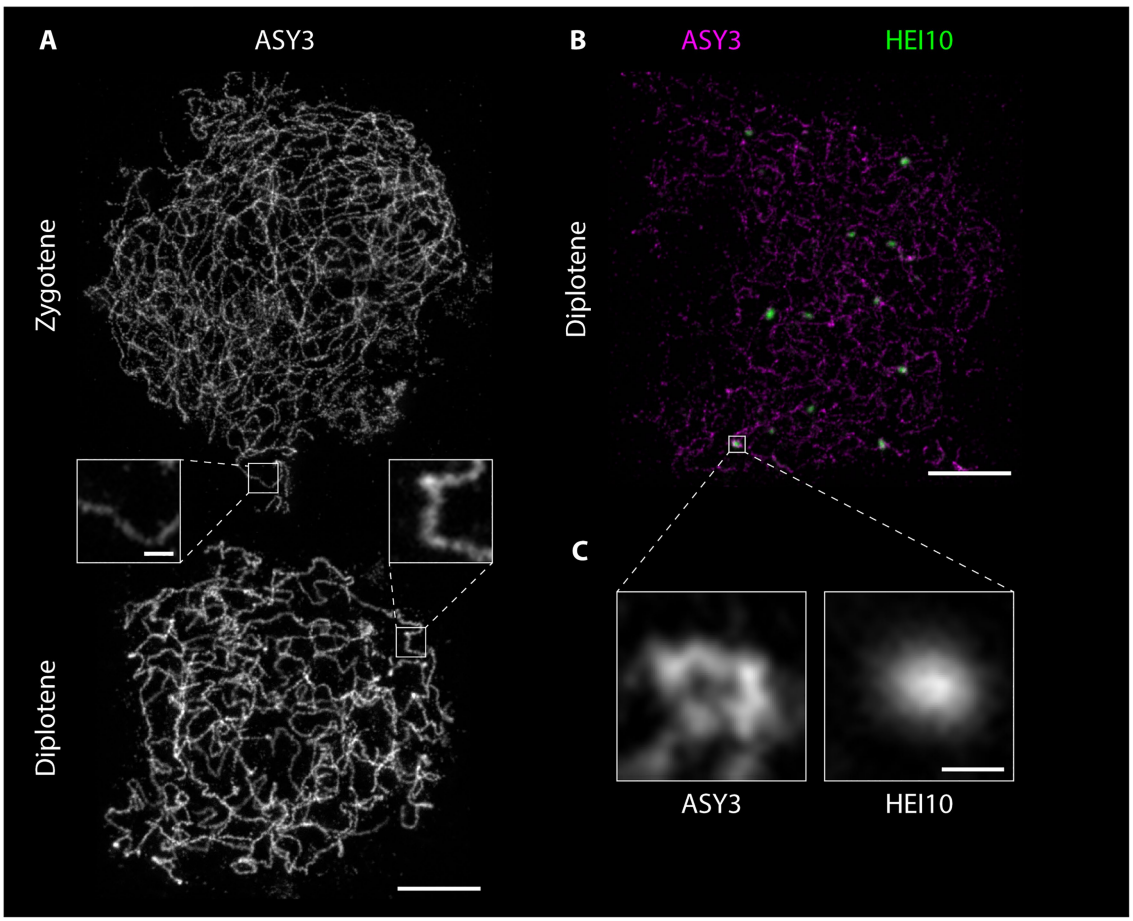

FIGURE 6 | Detergent-spread male meiotic nuclei were stained for the axial element protein ASY3 **(A)** or ASY3 and the ubiquitin ligase HEI10 **(B)** and imaged with a STED nanoscope. Scale Bar: 2 μm. Panel **(C)** shows a magnification of the highlighted region in panel **(B)**. Scale Bar: 200 nm.

nanometer precision in a qualitative and quantitative manner. Furthermore, the absence of image reconstruction alleviates the concern of generating artifacts. The most striking difference between the canonical epifluorescence microscopy and STED nanoscopy in terms of protein localization by immunofluorescence is in the number of detected proteins. Each single focus found at an epifluorescence microscope is composed of several smaller foci at the STED (compare RAD51 staining in **Figures 2, 5**). While RAD51 foci, for example, were found to be mainly circular and peak in zygotene at around 200 foci per nucleus in widefield images (Kumar et al., 2019; Sims et al., 2019; Kurzbauer et al., 2021), more than 1,000 foci are found in images acquired by STED nanoscopy (**Figure 5**). In addition, foci seem to assume different shapes over time, with few larger clusters forming in pachytene and likely representing different repair intermediates. In this sense, most of the measurements made in terms of numbers and shapes of proteins at the epifluorescence microscope need to be re-evaluated at the STED.

The nanoscale resolution provided by STED imaging furthermore allows precise localization of proteins within the meiotic nucleus and in relation to other proteins, the chromatin loops or other substructures. These new parameters should be taken into account in future studies and will help to characterize meiotic players and their function. New insights can be gained by observing the dynamics of specific proteins and their relation to the chromosome axis, where DSBs are thought to form. The axis association of RAD51, for example, changes throughout meiotic prophase (**Figures 5, 7**; **Supplementary Material**), with the recombinase being initially located on (or in close proximity of) the ASY3-labeled axis in leptotene/zygotene stages and then further apart in pachytene (**Figures 7B,C**; **Supplementary Material**), when homolog invasion is completed. Similar dynamics can be expected for further repair proteins.

Another interesting aspect amenable to analysis by STED nanoscopy is the possibility to address the co-localization of complex partners. At a spatial resolution of 30 nm, proteins that appear to cover the entire axis in widefield images appear as individual and defined foci (compare REC8 staining in **Figures 2, 5**) in STED-acquired images. This holds promise to reveal more complex relationships between proteins and requires a redefinition of co-localization for future studies. When measuring co-localization between

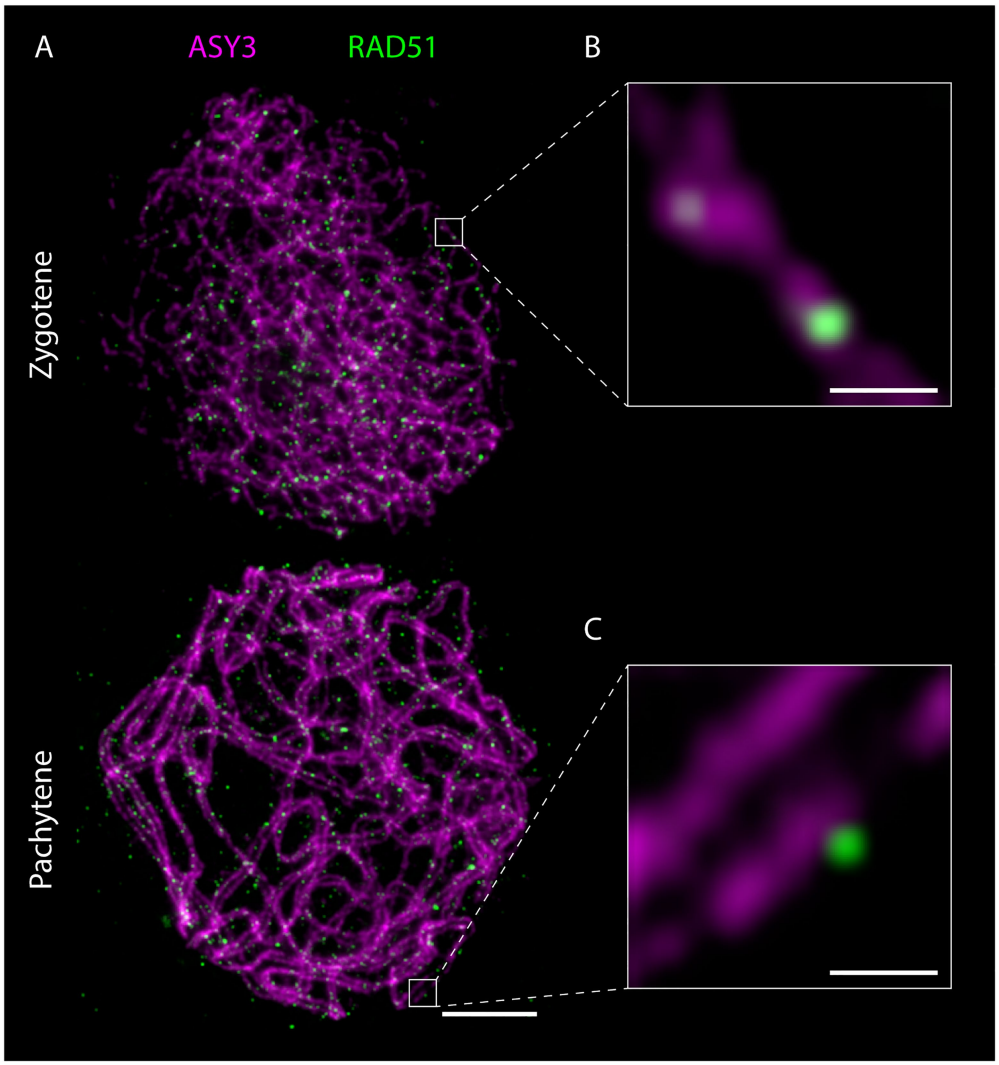

FIGURE 7 | Detergent-spread male meiotic nuclei were stained for the axial element protein ASY3 and the recombinase RAD51 and imaged with a STED nanoscope. Scale Bar: 2 μm. Panels **(B)** and **(C)** show magnifications of the highlighted regions in panel **(A)**. Scale Bars: 200 nm.

proteins one important caveat needs to be taken into consideration: the measurements could yield deviating results depending on the primary antibody used for the analysis. This is because each primary antibody might recognize different epitopes of the same protein, and this can be resolved at a resolution of 30 nm, as shown in a recent publication (Capilla-Perez et al., 2021). Furthermore, an additional variation is added to the measurements if the combination of primary and secondary antibodies, which is roughly 30 nm long, is taken into account.

CONCLUDING REMARKS

The advent of super-resolution microscopy has dramatically changed the way, we analyze and acquire our images. This has generated a new line-up of parameters to consider which in turn generate novel and unexpected results. The use of STED nanoscopy for acquiring qualitative and quantitative data will provide a portfolio of parameters to be analyzed: while the described technique certainly opens new possibilities for mutant analyses, it will also serve to better understand wild-type meiosis. In fact, with new technologies come new insights, which will shed new light on old problems. Without a doubt, the advancements in technology and the improvement of the different microscopy techniques will push the boundaries of our current knowledge and promote exciting new revelations.

AUTHOR CONTRIBUTIONS

JS, PS, and M-TK: conceptualization and writing. JS and M-TK: visualization. PS: funding acquisition. All authors contributed to the article and approved the submitted version.

FUNDING

We thank the University of Vienna (I031-B), the Austrian Science Fund FWF (SFB F34; DK W1238-B20; I 3685-B25), and the European Union (FP7-ITN 606956) for funding.

ACKNOWLEDGMENTS

We thank the Max Perutz Labs light microscopy facility and Abberior for technical support with the STEDYCON system and previous lab members Andrea Pedrosa-Harand, Tanja Siwiec, Mona Frey (von Harder), and Katja Schneider for contributing to the development of our cytological protocols.

SUPPLEMENTARY MATERIAL

The Supplementary Material for this article can be found online at: https://www.frontiersin.org/articles/10.3389/fpls.2021.672914/full#supplementary-material

Supplementary Material | Poster version of **Figures 3, 4, 6, 7**.

REFERENCES

Acquaviva, L., Szekvolgyi, L., Dichtl, B., Dichtl, B. S., de La Roche Saint Andre, C., Nicolas, A., et al. (2013). The COMPASS subunit Spp1 links histone methylation to initiation of meiotic recombination. *Science* 339, 215–218. doi: 10.1126/science.1225739

Albini, S. M., Jones, G. H., and Wallace, B. M. (1984). A method for preparing two-dimensional surface-spreads of synaptonemal complexes from plant meiocytes for light and electron microscopy. *Exp. Cell Res.* 152, 280–285. doi: 10.1016/0014-4827(84)90255-6

Anderson, L. K., Stack, S. M., and Sherman, J. D. (1988). Spreading synaptonemal complexes from *Zea mays*. I. No synaptic adjustment of inversion loops during pachytene. *Chromosoma* 96, 295–305. doi: 10.1007/BF00286917

Arabidopsis Genome, I. (2000). Analysis of the genome sequence of the flowering plant *Arabidopsis thaliana*. *Nature* 408, 796–815. doi: 10.1038/35048692

Armstrong, S. (2013). Spreading and fluorescence in situ hybridization of male and female Meiocyte chromosomes from *Arabidopsis thaliana* for cytogenetical analysis. *Methods Mol. Biol.* 990, 3–11. doi: 10.1007/978-1-62703-333-6_1

Armstrong, S. J., Caryl, A. P., Jones, G. H., and Franklin, F. C. (2002). Asy1, a protein required for meiotic chromosome synapsis, localizes to axis-associated chromatin in Arabidopsis and brassica. *J. Cell Sci.* 115, 3645–3655. doi: 10.1242/jcs.00048

Armstrong, S. J., Franklin, F. C., and Jones, G. H. (2001). Nucleolus-associated telomere clustering and pairing precede meiotic chromosome synapsis in *Arabidopsis thaliana*. *J. Cell Sci.* 114, 4207–4217. doi: 10.1242/jcs.114.23.4207

Armstrong, S., and Osman, K. (2013). Immunolocalization of meiotic proteins in *Arabidopsis thaliana*: method 2. *Methods Mol. Biol.* 990, 103–107. doi: 10.1007/978-1-62703-333-6_10

Bai, X., Peirson, B. N., Dong, F., Xue, C., and Makaroff, C. A. (1999). Isolation and characterization of SYN1, a RAD21-like gene essential for meiosis in Arabidopsis. *Plant Cell* 11, 417–430. doi: 10.1105/tpc.11.3.417

Bass, H. W., Marshall, W. F., Sedat, J. W., Agard, D. A., and Cande, W. Z. (1997). Telomeres cluster de novo before the initiation of synapsis: a three-dimensional spatial analysis of telomere positions before and during meiotic prophase. *J. Cell Biol.* 137, 5–18. doi: 10.1083/jcb.137.1.5

Bauman, J. G., Wiegant, J., Borst, P., and van Duijn, P. (1980). A new method for fluorescence microscopical localization of specific DNA sequences by in situ hybridization of fluorochromelabelled RNA. *Exp. Cell Res.* 128, 485–490. doi: 10.1016/0014-4827(80)90087-7

Bauwens, S., Katsanis, K., Van Montagu, M., Van Oostveldt, P., and Engler, G. (1994). Procedure for whole mount fluorescence in situ hybridization of interphase nuclei on *Arabidopsis thaliana*. *Plant J.* 6, 123–131. doi: 10.1046/j.1365-313X.1994.6010123.x

Beliveau, B. J., Joyce, E. F., Apostolopoulos, N., Yilmaz, F., Fonseka, C. Y., McCole, R. B., et al. (2012). Versatile design and synthesis platform for visualizing genomes with oligopaint FISH probes. *Proc. Natl. Acad. Sci. U. S. A.* 109, 21301–21306. doi: 10.1073/pnas.1213818110

Berardini, T. Z., Reiser, L., Li, D., Mezheritsky, Y., Muller, R., Strait, E., et al. (2015). The Arabidopsis information resource: making and mining the "gold standard" annotated reference plant genome. *Genesis* 53, 474–485. doi: 10.1002/dvg.22877

Berr, A., and Schubert, I. (2007). Interphase chromosome arrangement in *Arabidopsis thaliana* is similar in differentiated and meristematic tissues and shows a transient mirror symmetry after nuclear division. *Genetics* 176, 853–863. doi: 10.1534/genetics.107.073270

Bey, T. D., Koini, M., and Fransz, P. (2018). "Fluorescence in situ hybridization (FISH) and immunolabeling on 3D preserved nuclei" in *Plant Chromatin Dynamics: Methods and Protocols*. eds. M. Bemer and C. Baroux (New York, NY: Springer New York), 467–480.

Biggs, D. S. (2010). 3D deconvolution microscopy. *Curr. Protoc. Cytom.* 19, 11–20. doi: 10.1002/0471142956.cy1219s52

Bishop, D. K. (1994). RecA homologs Dmc1 and Rad51 interact to form multiple nuclear complexes prior to meiotic chromosome synapsis. *Cell* 79, 1081–1092. doi: 10.1016/0092-8674(94)90038-8

Blat, Y., Protacio, R. U., Hunter, N., and Kleckner, N. (2002). Physical and functional interactions among basic chromosome organizational features govern early steps of meiotic chiasma formation. *Cell* 111, 791–802. doi: 10.1016/S0092-8674(02)01167-4

Bleuyard, J. Y., Gallego, M. E., and White, C. I. (2004). Meiotic defects in the Arabidopsis rad50 mutant point to conservation of the MRX complex function in early stages of meiotic recombination. *Chromosoma* 113, 197–203. doi: 10.1007/s00412-004-0309-1

Bleuyard, J. Y., and White, C. I. (2004). The Arabidopsis homologue of Xrcc3 plays an essential role in meiosis. *EMBO J.* 23, 439–449. doi: 10.1038/sj.emboj.7600055

Brown, M. S., Grubb, J., Zhang, A., Rust, M. J., and Bishop, D. K. (2015). Small Rad51 and Dmc1 complexes often co-occupy both ends of a meiotic DNA double strand break. *PLoS Genet.* 11:e1005653. doi: 10.1371/journal.pgen.1005653

Buhler, C., Borde, V., and Lichten, M. (2007). Mapping meiotic single-strand dna reveals a new landscape of DNA double-strand breaks in *Saccharomyces cerevisiae*. *PLoS Biol.* 5:e324. doi: 10.1371/journal.pbio.0050324

Cai, X., Dong, F., Edelmann, R. E., and Makaroff, C. A. (2003). The Arabidopsis SYN1 cohesin protein is required for sister chromatid arm cohesion and homologous chromosome pairing. *J. Cell Sci.* 116, 2999–3007. doi: 10.1242/jcs.00601

Cannavo, E., Johnson, D., Andres, S. N., Kissling, V. M., Reinert, J. K., Garcia, V., et al. (2018). Regulatory control of DNA end resection by Sae2 phosphorylation. *Nat. Commun.* 9:4016. doi: 10.1038/s41467-018-06417-5

Capilla-Perez, L., Durand, S., Hurel, A., Lian, Q., Chambon, A., Taochy, C., et al. (2021). The synaptonemal complex imposes crossover interference and heterochiasmy in Arabidopsis. *Proc. Natl. Acad. Sci. U. S. A.* 118:e2023613118. doi: 10.1073/pnas.2023613118

Caryl, A. P., Armstrong, S. J., Jones, G. H., and Franklin, F. C. (2000). A homologue of the yeast HOP1 gene is inactivated in the Arabidopsis meiotic mutant asy1. *Chromosoma* 109, 62–71. doi: 10.1007/s004120050413

Chambon, A., West, A., Vezon, D., Horlow, C., De Muyt, A., Chelysheva, L., et al. (2018). Identification of ASYNAPTIC4, a component of the meiotic chromosome Axis. *Plant Physiol.* 178, 233–246. doi: 10.1104/pp.17.01725

Chelysheva, L., Diallo, S., Vezon, D., Gendrot, G., Vrielynck, N., Belcram, K., et al. (2005). AtREC8 and AtSCC3 are essential to the monopolar orientation of the kinetochores during meiosis. *J. Cell Sci.* 118, 4621–4632. doi: 10.1242/jcs.02583

Chelysheva, L. A., Grandont, L., and Grelon, M. (2013). Immunolocalization of meiotic proteins in brassicaceae: method 1. *Methods Mol. Biol.* 990, 93–101. doi: 10.1007/978-1-62703-333-6_9

Chelysheva, L., Grandont, L., Vrielynck, N., le Guin, S., Mercier, R., and Grelon, M. (2010). An easy protocol for studying chromatin and recombination protein dynamics during *Arabidopsis thaliana* meiosis: immunodetection of cohesins, histones and MLH1. *Cytogenet. Genome Res.* 129, 143–153. doi: 10.1159/000314096

Chelysheva, L., Vezon, D., Belcram, K., Gendrot, G., and Grelon, M. (2008). The Arabidopsis BLAP75/Rmi1 homologue plays crucial roles in meiotic double-strand break repair. *PLoS Genet.* 4:e1000309. doi: 10.1371/journal.pgen.1000309

Chelysheva, L., Vezon, D., Chambon, A., Gendrot, G., Pereira, L., Lemhemdi, A., et al. (2012). The Arabidopsis HEI10 is a new ZMM protein related to Zip3. *PLoS Genet.* 8:e1002799. doi: 10.1371/journal.pgen.1002799

Chen, C., Farmer, A. D., Langley, R. J., Mudge, J., Crow, J. A., May, G. D., et al. (2010). Meiosis-specific gene discovery in plants: RNA-Seq applied to isolated Arabidopsis male meiocytes. *BMC Plant Biol.* 10:280. doi: 10.1186/1471-2229-10-280

Chen, S. Y., Tsubouchi, T., Rockmill, B., Sandler, J. S., Richards, D. R., Vader, G., et al. (2008). Global analysis of the meiotic crossover landscape. *Dev. Cell* 15, 401–415. doi: 10.1016/j.devcel.2008.07.006

Colas, I., Darrier, B., Arrieta, M., Mittmann, S. U., Ramsay, L., Sourdille, P., et al. (2017). Observation of extensive chromosome axis remodeling during the "diffuse-phase" of meiosis in large genome cereals. *Front. Plant Sci.* 8:1235. doi: 10.3389/fpls.2017.01235

Costa, S., and Shaw, P. (2006). Chromatin organization and cell fate switch respond to positional information in Arabidopsis. *Nature* 439, 493–496. doi: 10.1038/nature04269

Couteau, F., Belzile, F., Horlow, C., Grandjean, O., Vezon, D., and Doutriaux, M. P. (1999). Random chromosome segregation without meiotic arrest in both male and female meiocytes of a dmc1 mutant of Arabidopsis. *Plant Cell* 11, 1623–1634. doi: 10.1105/tpc.11.9.1623

Cox, S. (2015). Super-resolution imaging in live cells. *Dev. Biol.* 401, 175–181. doi: 10.1016/j.ydbio.2014.11.025

Crismani, W., Girard, C., Froger, N., Pradillo, M., Santos, J. L., Chelysheva, L., et al. (2012). FANCM limits meiotic crossovers. *Science* 336, 1588–1590. doi: 10.1126/science.1220381

Cromer, L., Jolivet, S., Horlow, C., Chelysheva, L., Heyman, J., De Jaeger, G., et al. (2013). Centromeric cohesion is protected twice at meiosis, by SHUGOSHINs at anaphase I and by PATRONUS at interkinesis. *Curr. Biol.* 23, 2090–2099. doi: 10.1016/j.cub.2013.08.036

Doutriaux, M. P., Couteau, F., Bergounioux, C., and White, C. I. (1998). Isolation and characterisation of the RAD51 and DMC1 homologs from *Arabidopsis thaliana*. *Mol. Gen. Genet.* 257, 283–291. doi: 10.1007/s004380050649

Dresser, M. E., Ewing, D. J., Conrad, M. N., Dominguez, A. M., Barstead, R., Jiang, H., et al. (1997). DMC1 functions in a *Saccharomyces cerevisiae* meiotic pathway that is largely independent of the RAD51 pathway. *Genetics* 147, 533–544. doi: 10.1093/genetics/147.2.533

Drouaud, J., Mercier, R., Chelysheva, L., Berard, A., Falque, M., Martin, O., et al. (2007). Sex-specific crossover distributions and variations in interference level along *Arabidopsis thaliana* chromosome 4. *PLoS Genet.* 3:e106. doi: 10.1371/journal.pgen.0030106

Duncan, S., Olsson, T. S. G., Hartley, M., Dean, C., and Rosa, S. (2016). A method for detecting single mRNA molecules in *Arabidopsis thaliana*. *Plant Methods* 12:13. doi: 10.1186/s13007-016-0114-x

Duncan, S., and Rosa, S. (2018). Gaining insight into plant gene transcription using smFISH. *Transcription* 9, 166–170. doi: 10.1080/21541264.2017.1372043

Edlinger, B., and Schlogelhofer, P. (2011). Have a break: determinants of meiotic DNA double strand break (DSB) formation and processing in plants. *J. Exp. Bot.* 62, 1545–1563. doi: 10.1093/jxb/erq421

Escobar-Guzman, R., Rodriguez-Leal, D., Vielle-Calzada, J. P., and Ronceret, A. (2015). Whole-mount immunolocalization to study female meiosis in Arabidopsis. *Nat. Protoc.* 10, 1535–1542. doi: 10.1038/nprot.2015.098

Femino, A. M., Fay, F. S., Fogarty, K., and Singer, R. H. (1998). Visualization of single RNA transcripts in situ. *Science* 280, 585–590. doi: 10.1126/science.280.5363.585

Ferdous, M., Higgins, J. D., Osman, K., Lambing, C., Roitinger, E., Mechtler, K., et al. (2012). Inter-homolog crossing-over and synapsis in Arabidopsis meiosis are dependent on the chromosome axis protein AtASY3. *PLoS Genet.* 8:e1002507. doi: 10.1371/journal.pgen.1002507

France, M. G., Enderle, J., Rohrig, S., Puchta, H., Franklin, F. C. H., and Higgins, J. D. (2021). ZYP1 is required for obligate cross-over formation and cross-over interference in Arabidopsis. *Proc. Natl. Acad. Sci. U. S. A.* 118:e2021671118. doi: 10.1073/pnas.2021671118

Fransz, P., Armstrong, S. J., Alonso-Blanco, C., Fischer, T. C., Torres-Ruiz, R. A., and Jones, G. H. (1998). Cytogenetics for the model system *Arabidopsis thaliana*. *Plant J.* 13, 867–876.

Girard, C., Crismani, W., Froger, N., Mazel, J., Lemhemdi, A., Horlow, C., et al. (2014). FANCM-associated proteins MHF1 and MHF2, but not the other Fanconi anemia factors, limit meiotic crossovers. *Nucleic Acids Res.* 42, 9087–9095. doi: 10.1093/nar/gku614

Giraut, L., Falque, M., Drouaud, J., Pereira, L., Martin, O. C., and Mezard, C. (2011). Genome-wide crossover distribution in *Arabidopsis thaliana* meiosis reveals sex-specific patterns along chromosomes. *PLoS Genet.* 7:e1002354. doi: 10.1371/journal.pgen.1002354

Grelon, M., Vezon, D., Gendrot, G., and Pelletier, G. (2001). AtSPO11-1 is necessary for efficient meiotic recombination in plants. *EMBO J.* 20, 589–600. doi: 10.1093/emboj/20.3.589

Hartung, F., Suer, S., Knoll, A., Wurz-Wildersinn, R., and Puchta, H. (2008). Topoisomerase 3alpha and RMI1 suppress somatic crossovers and are essential for resolution of meiotic recombination intermediates in *Arabidopsis thaliana*. *PLoS Genet.* 4:e1000285. doi: 10.1371/journal.pgen.1000285

Hartung, F., Wurz-Wildersinn, R., Fuchs, J., Schubert, I., Suer, S., and Puchta, H. (2007). The catalytically active tyrosine residues of Both SPO11-1 and SPO11-2 are required for meiotic double-Strand break induction in Arabidopsis. *Plant Cell* 19, 3090–3099. doi: 10.1105/tpc.107.054817

Hedhly, A., Vogler, H., Eichenberger, C., and Grossniklaus, U. (2018). Whole-mount clearing and staining of Arabidopsis flower organs and Siliques. *J. Vis. Exp.* 12:56441. doi: 10.3791/56441

Hell, S. W., and Wichmann, J. (1994). Breaking the diffraction resolution limit by stimulated emission: stimulated-emission-depletion fluorescence microscopy. *Opt. Lett.* 19, 780–782. doi: 10.1364/OL.19.000780

Heng, H. H., Chamberlain, J. W., Shi, X. M., Spyropoulos, B., Tsui, L. C., and Moens, P. B. (1996). Regulation of meiotic chromatin loop size by chromosomal position. *Proc. Natl. Acad. Sci. U. S. A.* 93, 2795–2800. doi: 10.1073/pnas.93.7.2795

Hesse, S., Zelkowski, M., Mikhailova, E. I., Keijzer, C. J., Houben, A., and Schubert, V. (2019). Ultrastructure and dynamics of synaptonemal complex components during meiotic pairing and synapsis of standard (A) and accessory (B) Rye chromosomes. *Front. Plant Sci.* 10:773. doi: 10.3389/fpls.2019.00773

Higgins, J. D., Armstrong, S. J., Franklin, F. C., and Jones, G. H. (2004). The Arabidopsis MutS homolog AtMSH4 functions at an early step in recombination: evidence for two classes of recombination in Arabidopsis. *Genes Dev.* 18, 2557–2570. doi: 10.1101/gad.317504

Higgins, J. D., Sanchez-Moran, E., Armstrong, S. J., Jones, G. H., and Franklin, F. C. (2005). The Arabidopsis synaptonemal complex protein ZYP1 is required for chromosome synapsis and normal fidelity of crossing over. *Genes Dev.* 19, 2488–2500. doi: 10.1101/gad.354705

Hinch, A. G., Becker, P. W., Li, T., Moralli, D., Zhang, G., Bycroft, C., et al. (2020). The configuration of RPA, RAD51, and DMC1 binding in meiosis reveals the nature of critical recombination intermediates. *Mol. Cell* 79, 689–701.e610. doi: 10.1016/j.molcel.2020.06.015

Hollingsworth, N. M., Goetsch, L., and Byers, B. (1990). The HOP1 gene encodes a meiosis-specific component of yeast chromosomes. *Cell* 61, 73–84. doi: 10.1016/0092-8674(90)90216-2

Huff, J. (2015). The Airyscan detector from ZEISS: confocal imaging with improved signal-to-noise ratio and super-resolution. *Nat. Methods* 12, i–ii. doi: 10.1038/nmeth.f.388

Huff, J., Bergter, A., Birkenbeil, J., Kleppe, I., Engelmann, R., and Krzic, U. (2017). The new 2D Superresolution mode for ZEISS Airyscan. *Nat. Methods* 14:1223. doi: 10.1038/nmeth.f.404

Hunter, N. (2007). "Meiotic recombination" in *Molecular Genetics of Recombination*. eds. A. Aguilera and R. Rothstein (Berlin, Heidelberg: Springer Berlin Heidelberg), 381–442.

Hunter, N. (2015). Meiotic recombination: the essence of heredity. *Cold Spring Harb. Perspect. Biol.* 7:a016618. doi: 10.1101/cshperspect.a016618

Keeney, S. (2001). Mechanism and control of meiotic recombination initiation. *Curr. Top. Dev. Biol.* 52, 1–53. doi: 10.1016/s0070-2153(01)52008-6

Klar, T. A., and Hell, S. W. (1999). Subdiffraction resolution in far-field fluorescence microscopy. *Opt. Lett.* 24, 954–956. doi: 10.1364/OL.24.000954

Kleckner, N. (2006). Chiasma formation: chromatin/axis interplay and the role(s) of the synaptonemal complex. *Chromosoma* 115, 175–194. doi: 10.1007/s00412-006-0055-7

Klein, F., Mahr, P., Galova, M., Buonomo, S. B., Michaelis, C., Nairz, K., et al. (1999). A central role for cohesins in sister chromatid cohesion, formation of axial elements, and recombination during yeast meiosis. *Cell* 98, 91–103. doi: 10.1016/S0092-8674(00)80609-1

Komis, G., Mistrik, M., Samajova, O., Ovecka, M., Bartek, J., and Samaj, J. (2015). Superresolution live imaging of plant cells using structured illumination microscopy. *Nat. Protoc.* 10, 1248–1263. doi: 10.1038/nprot.2015.083

Komis, G., Novak, D., Ovecka, M., Samajova, O., and Samaj, J. (2018). Advances in imaging plant cell dynamics. *Plant Physiol.* 176, 80–93. doi: 10.1104/pp.17.00962

Korobchevskaya, K., Lagerholm, B. C., Colin-York, H., and Fritzsche, M. (2017). Exploring the potential of airyscan microscopy for live cell imaging. *Photo-Dermatology* 4:41. doi: 10.3390/photonics4030041

Ku, J. C., Ronceret, A., Golubovskaya, I., Lee, D. H., Wang, C., Timofejeva, L., et al. (2020). Dynamic localization of SPO11-1 and conformational changes of meiotic axial elements during recombination initiation of maize meiosis. *PLoS Genet.* 16:e1007881. doi: 10.1371/journal.pgen.1007881

Kubalová, I., Němečková, A., Weisshart, K., Hřibová, E., and Schubert, V. (2021). Comparing super-resolution microscopy techniques to analyze chromosomes. *Int. J. Mol. Sci.* 22:1903. doi: 10.3390/ijms22041903

Kumar, R., Duhamel, M., Coutant, E., Ben-Nahia, E., and Mercier, R. (2019). Antagonism between BRCA2 and FIGL1 regulates homologous recombination. *Nucleic Acids Res.* 47, 5170–5180. doi: 10.1093/nar/gkz225

Kurzbauer, M. T., Janisiw, M. P., Paulin, L. F., Prusen Mota, I., Tomanov, K., Krsicka, O., et al. (2021). ATM controls meiotic DNA double-strand break formation and recombination and affects synaptonemal complex organization in plants. *Plant Cell*. doi: 10.1093/plcell/koab045 [Epub ahead of print]

Kurzbauer, M. T., Pradillo, M., Kerzendorfer, C., Sims, J., Ladurner, R., Oliver, C., et al. (2018). *Arabidopsis thaliana* FANCD2 promotes meiotic crossover formation. *Plant Cell* 30, 415–428. doi: 10.1105/tpc.17.00745

Kurzbauer, M. T., Uanschou, C., Chen, D., and Schlogelhofer, P. (2012). The recombinases DMC1 and RAD51 are functionally and spatially separated during meiosis in Arabidopsis. *Plant Cell* 24, 2058–2070. doi: 10.1105/tpc.112.098459

Lam, I., and Keeney, S. (2014). Mechanism and regulation of meiotic recombination initiation. *Cold Spring Harb. Perspect. Biol.* 7:a016634. doi: 10.1101/cshperspect.a016634

Lambert, T. J., and Waters, J. C. (2017). Navigating challenges in the application of superresolution microscopy. *J. Cell Biol.* 216, 53–63. doi: 10.1083/jcb.201610011

Lambing, C., Osman, K., Nuntasoontorn, K., West, A., Higgins, J. D., Copenhaver, G. P., et al. (2015). Arabidopsis PCH2 mediates meiotic chromosome remodeling and maturation of crossovers. *PLoS Genet.* 11:e1005372. doi: 10.1371/journal.pgen.1005372

Li, W., Chen, C., Markmann-Mulisch, U., Timofejeva, L., Schmelzer, E., Ma, H., et al. (2004). The Arabidopsis AtRAD51 gene is dispensable for vegetative development but required for meiosis. *Proc. Natl. Acad. Sci. U. S. A.* 101, 10596–10601. doi: 10.1073/pnas.0404110101

Lloyd, A., Morgan, C., FC, H. F., and Bomblies, K. (2018). Plasticity of meiotic recombination rates in response to temperature in Arabidopsis. *Genetics* 208, 1409–1420. doi: 10.1534/genetics.117.300588

Lopez, E., Pradillo, M., Oliver, C., Romero, C., Cunado, N., and Santos, J. L. (2012). Looking for natural variation in chiasma frequency in *Arabidopsis thaliana*. *J. Exp. Bot.* 63, 887–894. doi: 10.1093/jxb/err319

Lukinavicius, G., Blaukopf, C., Pershagen, E., Schena, A., Reymond, L., Derivery, E., et al. (2015). SiR-Hoechst is a far-red DNA stain for live-cell nanoscopy. *Nat. Commun.* 6:8497. doi: 10.1038/ncomms9497

Mancera, E., Bourgon, R., Brozzi, A., Huber, W., and Steinmetz, L. M. (2008). High-resolution mapping of meiotic crossovers and non-crossovers in yeast. *Nature* 454, 479–485. doi: 10.1038/nature07135

Martinez-Garcia, M., Schubert, V., Osman, K., Darbyshire, A., Sanchez-Moran, E., and Franklin, F. C. H. (2018). TOPII and chromosome movement help remove interlocks between entangled chromosomes during meiosis. *J. Cell Biol.* 217, 4070–4079. doi: 10.1083/jcb.201803019

Meinke, D. W., Cherry, J. M., Dean, C., Rounsley, S. D., and Koornneef, M. (1998). *Arabidopsis thaliana*: a model plant for genome analysis. *Science* 282, 679–682.

Mercier, R., Mezard, C., Jenczewski, E., Macaisne, N., and Grelon, M. (2015). The molecular biology of meiosis in plants. *Annu. Rev. Plant Biol.* 66, 297–327. doi: 10.1146/annurev-arplant-050213-035923

Milman, N., Higuchi, E., and Smith, G. R. (2009). Meiotic DNA double-strand break repair requires two nucleases, MRN and Ctp1, to produce a single size class of Rec12 (Spo11)-oligonucleotide complexes. *Mol. Cell. Biol.* 29, 5998–6005. doi: 10.1128/MCB.01127-09

Mittmann, S., Arrieta, M., Ramsay, L., Waugh, R., and Colas, I. (2019). Preparation of barley pollen mother cells for confocal and super resolution microscopy. *Methods Mol. Biol.* 1900, 167–179. doi: 10.1007/978-1-4939-8944-7_11

Moens, P. B., and Pearlman, R. E. (1988). Chromatin organization at meiosis. *BioEssays* 9, 151–153. doi: 10.1002/bies.950090503

Morgan, C., and Wegel, E. (2020). Cytological characterization of *Arabidopsis arenosa* polyploids by SIM. *Methods Mol. Biol.* 2061, 37–46. doi: 10.1007/978-1-4939-9818-0_4

Morgan, C., Zhang, H., Henry, C. E., Franklin, F. C. H., and Bomblies, K. (2020). Derived alleles of two axis proteins affect meiotic traits in autotetraploid *Arabidopsis arenosa*. *Proc. Natl. Acad. Sci. U. S. A.* 117, 8980–8988. doi: 10.1073/pnas.1919459117

Neale, M. J., Pan, J., and Keeney, S. (2005). Endonucleolytic processing of covalent protein-linked DNA double-strand breaks. *Nature* 436, 1053–1057. doi: 10.1038/nature03872

Novak, I., Wang, H., Revenkova, E., Jessberger, R., Scherthan, H., and Höög, C. (2008). Cohesin Smc1beta determines meiotic chromatin axis loop organization. *J. Cell Biol.* 180, 83–90. doi: 10.1083/jcb.200706136

Osman, K., Higgins, J. D., Sanchez-Moran, E., Armstrong, S. J., and Franklin, F. C. (2011). Pathways to meiotic recombination in *Arabidopsis thaliana*. *New Phytol.* 190, 523–544. doi: 10.1111/j.1469-8137.2011.03665.x

Osman, K., Sanchez-Moran, E., Higgins, J. D., Jones, G. H., and Franklin, F. C. (2006). Chromosome synapsis in Arabidopsis: analysis of the transverse filament protein ZYP1 reveals novel functions for the synaptonemal complex. *Chromosoma* 115, 212–219. doi: 10.1007/s00412-005-0042-4

Panizza, S., Mendoza, M. A., Berlinger, M., Huang, L., Nicolas, A., Shirahige, K., et al. (2011). Spo11-accessory proteins link double-strand break sites to the chromosome axis in early meiotic recombination. *Cell* 146, 372–383. doi: 10.1016/j.cell.2011.07.003

Paulasova, P., and Pellestor, F. (2004). The peptide nucleic acids (PNAs): a new generation of probes for genetic and cytogenetic analyses. *Ann. Genet.* 47, 349–358. doi: 10.1016/j.anngen.2004.07.001

Prusicki, M. A., Keizer, E. M., van Rosmalen, R. P., Komaki, S., Seifert, F., Muller, K., et al. (2019). Live cell imaging of meiosis in *Arabidopsis thaliana*. *elife* 8:e42834. doi: 10.7554/eLife.42834

Robert, T., Vrielynck, N., Mezard, C., de Massy, B., and Grelon, M. (2016). A new light on the meiotic DSB catalytic complex. *Semin. Cell Dev. Biol.* 54, 165–176. doi: 10.1016/j.semcdb.2016.02.025

Rockmill, B., and Roeder, G. S. (1990). Meiosis in asynaptic yeast. *Genetics* 126, 563–574. doi: 10.1093/genetics/126.3.563

Ross, K. J., Fransz, P., and Jones, G. H. (1996). A light microscopic atlas of meiosis in *Arabidopsis thaliana*. *Chromosom. Res.* 4, 507–516. doi: 10.1007/BF02261778

Sanchez Moran, E., Armstrong, S. J., Santos, J. L., Franklin, F. C., and Jones, G. H. (2001). Chiasma formation in *Arabidopsis thaliana* accession Wassileskija and in two meiotic mutants. *Chromosom. Res.* 9, 121–128. doi: 10.1023/A:1009278902994

Sanchez-Moran, E., Santos, J. L., Jones, G. H., and Franklin, F. C. (2007). ASY1 mediates AtDMC1-dependent interhomolog recombination during meiosis in Arabidopsis. *Genes Dev.* 21, 2220–2233. doi: 10.1101/gad.439007

Sansam, C. L., and Pezza, R. J. (2015). Connecting by breaking and repairing: mechanisms of DNA strand exchange in meiotic recombination. *FEBS J.* 282, 2444–2457. doi: 10.1111/febs.13317

Schaefer, L. H., Schuster, D., and Schaffer, J. (2004). Structured illumination microscopy: artefact analysis and reduction utilizing a parameter optimization approach. *J. Microsc.* 216, 165–174. doi: 10.1111/j.0022-2720.2004.01411.x

Schermelleh, L., Carlton, P. M., Haase, S., Shao, L., Winoto, L., Kner, P., et al. (2008). Subdiffraction multicolor imaging of the nuclear periphery with 3D structured illumination microscopy. *Science* 320, 1332–1336. doi: 10.1126/science.1156947

Schubert, V., Neumann, P., Marques, A., Heckmann, S., Macas, J., Pedrosa-Harand, A., et al. (2020). Super-resolution microscopy reveals diversity

of plant centromere architecture. *Int. J. Mol. Sci.* 21:3488. doi: 10.3390/ijms21103488

Sharma, R., Singh, M., and Sharma, R. (2020). Recent advances in STED and RESOLFT super-resolution imaging techniques. *Spectrochim. Acta A Mol. Biomol. Spectrosc.* 231:117715. doi: 10.1016/j.saa.2019.117715

Sims, J., Chen, C., Schlogelhofer, P., and Kurzbauer, M. T. (2020b). Targeted analysis of chromatin events (TACE). *Methods Mol. Biol.* 2061, 47–58. doi: 10.1007/978-1-4939-9818-0_5

Sims, J., Chouaref, J., and Schlogelhofer, P. (2020a). Whole-mount Immuno-FISH on Arabidopsis Meiocytes (WhoMI-FISH). *Methods Mol. Biol.* 2061, 59–66. doi: 10.1007/978-1-4939-9818-0_6

Sims, J., Copenhaver, G. P., and Schlogelhofer, P. (2019). Meiotic DNA repair in the nucleolus employs a nonhomologous end-joining mechanism. *Plant Cell* 31, 2259–2275. doi: 10.1105/tpc.19.00367

Sims, J., Sestini, G., Elgert, C., von Haeseler, A., and Schlögelhofer, P. (2021). Sequencing of the Arabidopsis NOR2 reveals its distinct organization and tissue-specific rRNA ribosomal variants. *Nat. Commun.* 12:387. doi: 10.1038/s41467-020-20728-6

Sivaguru, M., Urban, M. A., Fried, G., Wesseln, C. J., Mander, L., and Punyasena, S. W. (2018). Comparative performance of airyscan and structured illumination superresolution microscopy in the study of the surface texture and 3D shape of pollen. *Microsc. Res. Tech.* 81, 101–114. doi: 10.1002/jemt.22732

Slotman, J. A., Paul, M. W., Carofiglio, F., de Gruiter, H. M., Vergroesen, T., Koornneef, L., et al. (2020). Super-resolution imaging of RAD51 and DMC1 in DNA repair foci reveals dynamic distribution patterns in meiotic prophase. *PLoS Genet.* 16:e1008595. doi: 10.1371/journal.pgen.1008595

Smith, G. R., and Nambiar, M. (2020). New solutions to old problems: molecular mechanisms of meiotic crossover control. *Trends Genet.* 36, 337–346. doi: 10.1016/j.tig.2020.02.002

Stacey, N. J., Kuromori, T., Azumi, Y., Roberts, G., Breuer, C., Wada, T., et al. (2006). Arabidopsis SPO11-2 functions with SPO11-1 in meiotic recombination. *Plant J.* 48, 206–216. doi: 10.1111/j.1365-313X.2006.02867.x

Tofanelli, R., Vijayan, A., Scholz, S., and Schneitz, K. (2019). Protocol for rapid clearing and staining of fixed Arabidopsis ovules for improved imaging by confocal laser scanning microscopy. *Plant Methods* 15:120. doi: 10.1186/s13007-019-0505-x

Toth, A., Ciosk, R., Uhlmann, F., Galova, M., Schleiffer, A., and Nasmyth, K. (1999). Yeast cohesin complex requires a conserved protein, Eco1p(Ctf7), to establish cohesion between sister chromatids during DNA replication. *Genes Dev.* 13, 320–333. doi: 10.1101/gad.13.3.320

Uanschou, C., Siwiec, T., Pedrosa-Harand, A., Kerzendorfer, C., Sanchez-Moran, E., Novatchkova, M., et al. (2007). A novel plant gene essential for meiosis is related to the human CtIP and the yeast COM1/SAE2 gene. *EMBO J.* 26, 5061–5070. doi: 10.1038/sj.emboj.7601913

Valuchova, S., Mikulkova, P., Pecinkova, J., Klimova, J., Krumnikl, M., Bainar, P., et al. (2020). Imaging plant germline differentiation within Arabidopsis flowers by light sheet microscopy. *elife* 9:e52546. doi: 10.7554/eLife.52546

Verdaasdonk, J. S., Stephens, A. D., Haase, J., and Bloom, K. (2014). Bending the rules: widefield microscopy and the Abbe limit of resolution. *J. Cell. Physiol.* 229, 132–138. doi: 10.1002/jcp.24439

Vignard, J., Siwiec, T., Chelysheva, L., Vrielynck, N., Gonord, F., Armstrong, S. J., et al. (2007). The interplay of RecA-related proteins and the MND1-HOP2 complex during meiosis in *Arabidopsis thaliana*. *PLoS Genet.* 3, 1894–1906. doi: 10.1371/journal.pgen.0030176

Waminal, N. E., Pellerin, R. J., Kim, N. S., Jayakodi, M., Park, J. Y., Yang, T. J., et al. (2018). Rapid and efficient FISH using pre-labeled oligomer probes. *Sci. Rep.* 8:8224. doi: 10.1038/s41598-018-26667-z

West, A. M., Rosenberg, S. C., Ur, S. N., Lehmer, M. K., Ye, Q., Hagemann, G., et al. (2019). A conserved filamentous assembly underlies the structure of the meiotic chromosome axis. *elife* 8:e40372. doi: 10.7554/eLife.40372

Whelan, D. R., and Bell, T. D. (2015). Image artifacts in single molecule localization microscopy: why optimization of sample preparation protocols matters. *Sci. Rep.* 5:7924. doi: 10.1038/srep07924

Woglar, A., and Villeneuve, A. M. (2018). Dynamic architecture of DNA repair complexes and the synaptonemal complex at sites of meiotic recombination. *Cell* 173, 1678–1691.e16. doi: 10.1016/j.cell.2018.03.066

Zickler, D., and Kleckner, N. (1999). Meiotic chromosomes: integrating structure and function. *Annu. Rev. Genet.* 33, 603–754. doi: 10.1146/annurev.genet.33.1.603

Conflict of Interest: The authors declare that the research was conducted in the absence of any commercial or financial relationships that could be construed as a potential conflict of interest.

frontiers in Plant Science

REVIEW
published: 04 June 2021
doi: 10.3389/fpls.2021.672489

Telomeres and Subtelomeres Dynamics in the Context of Early Chromosome Interactions During Meiosis and Their Implications in Plant Breeding

Miguel Aguilar[1] *and Pilar Prieto*[2]*

[1]*Área de Fisiología Vegetal, Universidad de Córdoba, Córdoba, Spain,* [2]*Plant Breeding Department, Institute for Sustainable Agriculture, Agencia Estatal Consejo Superior de Investigaciones Científicas (CSIC), Córdoba, Spain*

OPEN ACCESS

Edited by:
Christophe Lambing, University of Cambridge, United Kingdom

Reviewed by:
Changbin Chen, Arizona State University, United States
Zhukuan Cheng, University of Chinese Academy of Sciences, China

***Correspondence:**
Pilar Prieto
pilar.prieto@ias.csic.es
orcid.org/0000-0002-8160-808X

Specialty section:
This article was submitted to Plant Cell Biology, a section of the journal Frontiers in Plant Science

Received: *25 February 2021*
Accepted: *06 May 2021*
Published: *04 June 2021*

Citation:
Aguilar M and Prieto P (2021) Telomeres and Subtelomeres Dynamics in the Context of Early Chromosome Interactions During Meiosis and Their Implications in Plant Breeding. Front. Plant Sci. 12:672489. doi: 10.3389/fpls.2021.672489

Genomic architecture facilitates chromosome recognition, pairing, and recombination. Telomeres and subtelomeres play an important role at the beginning of meiosis in specific chromosome recognition and pairing, which are critical processes that allow chromosome recombination between homologs (equivalent chromosomes in the same genome) in later stages. In plant polyploids, these terminal regions are even more important in terms of homologous chromosome recognition, due to the presence of homoeologs (equivalent chromosomes from related genomes). Although telomeres interaction seems to assist homologous pairing and consequently, the progression of meiosis, other chromosome regions, such as subtelomeres, need to be considered, because the DNA sequence of telomeres is not chromosome-specific. In addition, recombination operates at subtelomeres and, as it happens in rye and wheat, homologous recognition and pairing is more often correlated with recombining regions than with crossover-poor regions. In a plant breeding context, the knowledge of how homologous chromosomes initiate pairing at the beginning of meiosis can contribute to chromosome manipulation in hybrids or interspecific genetic crosses. Thus, recombination in interspecific chromosome associations could be promoted with the aim of transferring desirable agronomic traits from related genetic donor species into crops. In this review, we summarize the importance of telomeres and subtelomeres on chromatin dynamics during early meiosis stages and their implications in recombination in a plant breeding framework.

Keywords: crops, wheat, terminal chromosome regions, chromosome recognition, homologous pairing, recombination, meiosis

FROM GENOME TO CHROMOSOMES

A genome is the genetic information of a living organism. In eukaryotic organisms, like plants, the genetic information is carried by chromosomes, within the cell nucleus. A chromosome is made up by a supramolecular structure, called chromatin, which is a complex of a linear DNA molecule associated with several different proteins. Chromatin structure

displays a multidimensional architecture. At its basic organizational level, a section of about 146 bp of the linear DNA molecule is wrapped around a canonical set of eight monomers (two copies of H2A, H2B, H3, and H4). The term nucleosome is used to describe the basic chromatin section (McGinty and Tan, 2015). Beyond the nucleosome scale, the chromatin fiber of around 10 nm diameter is further organized as an array of nucleosomes, with the participation of histone H1, a linker between adjacent nucleosomes, and packed in a higher order more compacted structure to form the so called 30 nm fiber that is in turn organized into folds of 150–200 kbp with an average diameter of 250 nm in interphase chromosomes, up to 850 nm in more compacted metaphase chromosomes (Dixon et al., 2016). Both the molecular composition and architecture of chromatin are not static but dynamic. Besides the intrinsic variable nature of the DNA sequence, chromatin molecular variations are the result of DNA methylation and demethylation, post-translational modifications of histones (including acetylation, methylation, phosphorylation, polyADP-ribosylation, and ubiquitination), replacing of canonical histone proteins by other non-canonical forms, and incorporation/elimination/modification of other non-histone proteins. This dynamical molecular composition of chromatin determines its organization and the state of compaction both at local and overall chromosome level, which is intimately related with its functionality around the whole cell cycle.

Microscopy observations of different intensity of chromatin staining allowed the distinction between darker and lighter stained regions of chromosomes, called heterochromatin and euchromatin, respectively (Heitz, 1928). Molecular analyses of chromatin revealed a correlation between the DNA sequence and the state of chromatin, being heterochromatin more densely packed, rich in repeat sequences and poor in genes, while euchromatin is all the way around, more loosely packed, poor in repeats and rich in genes.

Molecular differences of chromatin at the DNA level are also due to DNA modifications. Although adenine can also be modified by methylation, the most frequent DNA modification is cytosine methylation (5 mC). In plants, an RNA-directed DNA methylation machinery is responsible for *de novo* DNA methylation (Law and Jacobsen, 2010). DNA methylation status is the overall result of *de novo* methylation, maintenance of methylation, and active demethylation. Plants have a unique mechanism of DNA demethylation based on DNA glycosylases that excise and replace 5mC through a base excision repair pathway (Parrilla-Doblas et al., 2019). Regulation of transposon silencing, gene expression, and chromosome interactions is achieved by DNA methylation. This mechanism is particularly relevant in plant development, reproduction, and responses to biotic and abiotic stress conditions (Parrilla-Doblas et al., 2019).

The protein part of chromatin is also subject to important modifications. There are multiple isoforms of histones that can replace the canonical ones with a profound impact on chromatin functionality (Koyama and Kurumizaka, 2018). In plants, except for histone H4, all the core histones have several isoforms that eventually replace the canonical forms. These variant forms have properties that confer them different roles in DNA repair, gene switching, meiotic recombination, and chromosome segregation (Malik and Henikoff, 2003).

A thorough analysis of histone genes in the model plant *Arabidopsis thaliana* revealed a complex system of multiple gene families. While H4 is represented by a gene family that encodes an identical protein, the rest of histones gene families (H1, H2A, H2B, and H3) include genes that code for different isoforms. For histone H1, H2A, and H2B, each gene encodes a unique histone variant, while several genes encode H3.1 and H3.3 proteins. A total of 3 H1, 13 H2A, 11 H2B, 15 H3, and 8 H4 genes have been identified (Probst et al., 2020).

The main variants of H1, namely H1.1 and H1.2, are considered the canonical forms and their main function is related to chromatin compaction. H1.3, however, is necessary for adequate response to abiotic stress. Under non-stressed conditions, H1.3 expression is localized to a few cell types such as guard cells, but is strongly induced by abscisic acid, drought, and limited light (Rutowicz et al., 2015).

H2A.X is involved in DNA repair. H2A.W variants were initially believed to be exclusively involved with H3K9me2 and cytosine methylation, and with transposable element silencing. Today, an overall picture arises that plant H2A.W variants might play a role analogous to mammal KAP1 and HP1, with essential roles in cell differentiation and development (Lorković et al., 2017). H2A.Z variant has been related with metabolism (Yu et al., 2016) and with many physiological processes, including development (Jarillo and Piñeiro, 2015) or stress (Asensi-Fabado et al., 2017).

Several H2B variants are present in plants, as shown in *Arabidopsis*, where 11 different variants have been described (Probst et al., 2020). However, the genome distribution and possible functions remain unknown for most of them.

H3 histone is also present in multiple variants in plants. The *Arabidopsis* genome contains 15 genes coding for histone H3 representing H3.1, H3.3, CenH3, and other atypical variants. Five H3.1 genes are specifically expressed in S-phase and seem to be incorporated into nucleosomes during DNA synthesis (Okada et al., 2005; Jiang and Berger, 2017). There are three H3.3 genes and the protein deposition in nucleosomes seems to be independent of DNA-synthesis, since their expression is ubiquitous, even in non-proliferating cells (Okada et al., 2005). CenH3 is the third major H3 variant, coded by a single gene. It specifies the centromere and localizes to a specific subset of the centromeric 180 bp repeats (Nagaki et al., 2003).

Regarding their genome-wide distribution, H3.1 and H3.3 show important differences.

H3.1 is enriched in heterochromatic regions, while H3.3 is preferentially located at chromosome arms (Stroud et al., 2012). H3.3 accumulates in the 3' regions of transcribed genes and its distribution correlates well with transcriptional activity (Stroud et al., 2012), but it is also found in other regions, including telomeres (Vaquero-Sedas and Vega-Palas, 2013) and rDNA repeats (Duc et al., 2017).

In summary, the conformation of chromatin architecture at different levels seems to be greatly dependent on the substitution of core histones by replacement variants, and this,

in turns, have profound functional implications that affect the whole plant life cycle.

Histones have unstructured N-terminal domains that protrude from the nucleosome core. Both nucleosome core and N-terminal domains can be post-translationally modified (Cosgrove and Wolberger, 2005). Besides methylation, post-translational modifications (PTMs) include acetylation, phosphorylation, and others. Methylation can have either permissive or repressive effects, while acetylation is related with chromatin activation. After the histone code theory, gene expression is affected by specific histone modifications (Strahl and Allis, 2000). More recent studies have revealed a complex and dynamic landscape of histone posttranslational modifications (PTMs) with multiple modifications added and removed from the same histone tail of the same nucleosome (Lee et al., 2010). The overall PTMs state of histones has a deep impact in chromatin architecture, and in turn in metabolism, cell differentiation, development, and response to environmental changes and stress conditions (Leung and Gaudin, 2020).

Besides the modifications caused by histone exchanging or by PTMs, chromatin can be remodeled by nucleosome mobilization to diverse DNA locations or removed by ATP-dependent remodeling enzymes. These remodeling factors are important for gene expression since they control the access of the transcription machinery through common mechanisms that include DNA unwrapping from the nucleosome core and DNA loop translocation along the nucleosomes (Saha et al., 2006; Zofall et al., 2006).

Chromatin is a dynamic multimolecular complex that shows a variable level of compaction and condensation/relaxation around the cell cycle. Many non-histone proteins interact with chromatin in a dynamical way so that they can support or remodel chromatin architecture conferring specific properties to the resulting structure. These changes affect local chromatin architecture, chromosome organization, and chromosome packaging, as well as DNA functionality, and it obviously has an influence on chromosome pairing and recombination.

Structural maintenance class of proteins (SMC) are a group of non-histone proteins, some of them having ATP-binding sites and enzymatic properties, that are essential for chromosome condensation, sister chromatid cohesion and segregation. Cohesins form a ring-shaped complex that support cohesion of sister chromatids, a fundamental mechanism for chromosome segregation. The cohesin complex is a ring composed of SMC1, SMC3 (two SMC subunits), and an α-kleisin, which recruits a fourth SMC subunit (SCC3). To achieve cohesion, the cohesin complex entraps DNA molecules. This process is regulated by other cohesin-binding proteins and modifying enzymes around the cell cycle (Nishiyama, 2019). Condensins form complexes that support chromatin compaction and packaging into chromosomes. They are a heterodimer of SMC2 and SMC4, two structural maintenance proteins that associate with specific regulatory subunits (Mainiero and Pawlowski, 2014). Both condensins and cohesins play important roles in chromosome organization to ensure genome stability.

Genetic insulator proteins like CTCF (CCCTC-Binding Factor), which play a relevant role in gene regulation by establishing topologically active domains (TADs) in animals, seem to be absent in plants. Neither TAD structures that function as insulated genomic units nor TAD border-binding insulator proteins have been reported. In maize and tomato, however, there are reports of long-range chromatin loops separating active and inactive domains, and other evidences of the existence of TADs or TADs-like domains in plants with large genomes (Liu et al., 2017; Wang et al., 2018). The study of TAD borders in plants suggests that TAD formation could be determined by the binding of specific TCP transcription factors and bZip proteins (Stam et al., 2019).

Another important class of non-histone proteins is constituted by the high mobility group (HMG) proteins. HMGA proteins have 4 A/T-hook DNA-binding motifs, are structurally flexible and bind A/T-rich DNA stretches. They could form higher-order transcription factor complexes through multiple protein-protein and protein-DNA interactions. HMGB proteins present a single HMG-box DNA-binding domain. They recognize specific DNA structures with no sequence specificity to enhance the structural flexibility of DNA and enable the assembly of nucleoprotein structures that control transcription and recombination (Grasser, 2003).

As a group, non-histone proteins have a relevant role in chromatin compaction to achieve higher-order chromatin structures as well as regulating its dynamical architecture, which has deep consequences on gene expression. At a global scale, these chromatin interactions regulate several processes including DNA repair, cell cycle, reproduction, differentiation, and multiple aspects of plant development.

NUCLEAR ARCHITECTURE IN INTERPHASE AND MEIOSIS

The dynamic nature of chromatin and chromosomes is evidenced by the different changes that they experience around the cell cycle. These changes affect not only the molecular composition of chromosomes but also their local and global architecture, localization and arrangement within the nucleus, and their interactions with other nuclear and cellular structures. All these changes are relevant in the context of regulation of gene expression, cell differentiation, and development, response to environmental changes and stress conditions. And they are particularly relevant to understand the complex process of cell division, including mitosis and meiosis.

The studies on chromatin and chromosome dynamics, especially in meiosis, have been paid much more attention in the context of plant reproductive processes partly because the initial studies were based on visual observations through the light microscope, and the highly condensed chromatin during cell division is easier to visualize than in the interphase. The importance of plant breeding has also contributed to focus the study of chromosome dynamics during meiosis. However, during the last decades, newer and more powerful techniques have been developed such as fluorescence *in situ* hybridization (FISH), immunofluorescence-FISH, 3D FISH (Chaumeil et al., 2013), 3C, 4C, 5C, and Hi-C (high-throughput chromosome

conformation capture; Dekker, 2006; Shaw, 2010; De Wit and de Laat, 2012; Dekker et al., 2013), fluorescence recovery after photobleaching (FRAP; White and Stelzer, 1999; Phair and Misteli, 2001), Covalent Attachment of Tagged Histones to Capture and Identify Turnover (CATCH-IT; Deal et al., 2010), or Single-Particle Tracking (SPT; Straight et al., 1996; Belmont et al., 1999). With the aid of these techniques, the attention has been extended to the study of chromosomes around the cell cycle, particularly during the interphase, having in mind the idea that the knowledge of chromosome dynamics during the interphase will also help to understand chromosome dynamics during mitosis and meiosis.

Multiple studies conducted in the model plant *A. thaliana* and other species have allowed the elucidation of interphase chromatin organization. Chromatin is relatively relaxed and decondensed in interphase nuclei. However, its arrangement within the nucleus is far from being random. Each chromosome seems to occupy a specific region within the nucleus. This idea was initially suggested by Rabl (1885). Boveri (1909) introduced the concept of chromosome territory (CT). CTs were experimentally confirmed by FISH using chromosome-specific probes in human cells (Manuelidis and Borden, 1988). Chromosome territories were also demonstrated in the model plant *A. thaliana* by Lysak et al. (2001).

In *Arabidopsis*, chromosomes are organized in a way that all telomeres are clustered around the nucleolus and tend to associate with it, as an anticipation of homologous pairing in meiosis. Centromeres, however, are dispersed toward the periphery of the nucleus (Armstrong et al., 2001; Fransz et al., 2002). In this species, whose genome is very small (135 Mbp), heterochromatin around the centromeres shows dense bodies called chromocenters. These chromocenters are inactive chromatin regions, enriched in sequence repeats, from which euchromatic regions arise as loops that give a characteristic rosette structure to *Arabidopsis* chromosome territories (Fransz et al., 2002). The positioning of *Arabidopsis* chromosomes relative to each other seems to be random (De Nooijer et al., 2009), except for those chromosomes that carry nucleolar organizing regions (NORs), which contain multiple copies of rRNAs arranged in tandem (Pecinka et al., 2004). The association of NORs with the nucleolus must cause the clustering of all the chromosomes that contain NORs. Specific interchromosomal interactions and dynamics can be influenced by this configuration in *A. thaliana*. A recent study in autotetraploid *Arabidopsis* suggests that chromosome territories are somehow independent (Zhang et al., 2019).

In other plant species, some of them with large genomes such as wheat (14.5 Gbp), chromosomes display the so called Rabl configuration, where the chromosome is folded at the centromere so that both telomeres and subtelomeric regions are close together. Telomeres are grouped at one pole and centromeres are grouped at the opposite pole of the nucleus (Anamthawat-Jonsson and Heslop-Harrison, 1990; Cowan et al., 2001; Doğan and Liu, 2018). Beyond the existence of CTs, the study of polyploid organisms like wheat and *Brassica napus* has shown that chromosomes of the different subgenomes are not intermingled but segregated, so that all chromosomes of a subgenome occupy a kind of genome territory, being the interactions among chromosomes of the same subgenome more probable and intense. In the case of bread wheat, its genome includes three subgenomes (A, B, and D) that would occupy three different genome territories within the nucleus (Concia et al., 2020).

Interphase chromosomes are not just occupying a chromosome territory; they interact with other macromolecules and structures. The interactions of telomeres and centromeres with lamina nuclear envelope and nucleolus proteins allowed the definition of two broad chromosome domains that have profound functional implications. Lamina-associated domains (LADs) are extensive chromatin stretches that interact with a network of lamin fibers near the inner nuclear membrane (Guelen et al., 2008). Nucleolus-associated chromatin domains (NADs) are chromatin regions in contact with the nucleolus (van Koningsbruggen et al., 2010). Several studies during the last 20 years have allowed the identification of multiple factors that seem to be involved in the positional control of chromosomes, through their interaction with centromeres and telomeres during the interphase in plants. Besides the structural maintenance of chromosome (SMC) complexes, these factors include a few proteins of the nuclear membrane and the nucleolus (Oko et al., 2020) that have allowed the definition of LADs and NADs also in plants.

Plant LADs involve both telomeric and centromeric domains. Telomeres are localized at the nuclear periphery during the interphase (Dong and Jiang, 1998), with some exceptions, such as *Arabidopsis*, where the nucleolus interacts with telomeres (Roberts et al., 2009). As it is the case in yeasts, there must be a few membrane proteins playing an important function in the positioning of telomeres at the nuclear periphery, though none have been identified in plants yet (Ebrahimi and Cooper, 2016). In maize, ZmSUN2 seems to be involved in the localization of telomeres at the periphery of the nucleus in meiosis, but the function of ZmSUN2 during the interphase remains unknown (Murphy et al., 2014). In plants, as in other eukaryotes, centromeres are anchored at the periphery of the nucleus (Muller et al., 2019). Regardless of Rabl or non-Rabl configuration of plant chromosomes, the anchoring of centromeres at the periphery of the nucleus could fix their position in the interphase. The knowledge of the protein factors involved in centromere anchoring to the nuclear periphery is more extensive. In *Arabidopsis*, whose chromosomes show a non-Rabl configuration, SUN proteins seem to maintain the centromere position near the nuclear periphery (Poulet et al., 2017) and might function as a linker of Nucleoskeleton and Cytoskeleton complex (LINC). This complex, formed by proteins located at the inner and outer nuclear membranes, links the lamina with the cytoskeleton (Fernández-Álvarez et al., 2016). Also, in *Arabidopsis*, CROWDED NUCLEI 1, a putative SUN-interacting protein (Graumann, 2014), mediates the tethering of chromosome arms and centromeric heterochomatin at the periphery of the nucleus (Hu et al., 2019). Considering that *Schizosaccharomyces pombe* Lem2 protein is involved in the positioning of interphasic telomeres and centromeres (Barrales et al., 2016; Fernández-Álvarez et al., 2016), the possibility exists that the positioning of plant centromeres and telomeres could also be controlled

by CRWNs, condensin II and other proteins implicated in centromere positioning. As proposed by Oko et al. (2020), the fact that Lem2 prevents the loss of Rabl-type configuration in *S. pombe* during interphase suggests the existence of a mechanism that keeps centromere clustering in plants with Rabl configuration with telomeres at the opposite side (Hou et al., 2012; Barrales et al., 2016; Fernández-Álvarez et al., 2016).

Regarding plant NADs, it is known that *Arabidopsis* chromosomes are organized in a way that all telomeres are clustered around the nucleolus and tend to interact with it. NADs were identified in isolated nucleoli (Pontvianne et al., 2016). NADs are rich in transposable elements and poorly expressed genes, what agrees with the fact that interactions with the nucleolus occur through telomeric and subtelomeric regions. *Arabidopsis* NUCLEOLIN 1 (NUC1) is involved in telomere-nucleolus associations and seems to be essential to keep telomere length (Pontvianne et al., 2016). When compared to animals, our knowledge of plant LADs and NADs is still very limited. We do not know their precise limits, all the numerous factors involved in their organization and control, and how they evolve around the cell-cycle, and in the context of development and changing environmental conditions (Pontvianne and Liu, 2020).

In interphase nuclei, chromosomes not only interact with other macromolecules and nuclear structures within the nucleus, but they also interact among them either directly or through proteins or more complex structures. Besides its basic function as information storage, the whole genome should also be considered as a physical structure with internal forces being exerted and transmitted within chromosomes and among chromosomes, and also from and to the rest of the nucleus and the whole cell. The limited volume of the nucleus enables this interaction, which is already supported by the non-random distribution of chromatin, with a precise distribution of heterochromatic and euchromatic regions, TADs, LADs, NADS, and CTs. Transcription factories, trans-regulation of gene expression, replication machineries, and DNA repair mechanisms reveal the existence of interchromosomal interactions during the interphase and explain the connection between organization and function of the whole genome.

In a species with a small genome like *A. thaliana*, telomeres are clustered at the nucleolus during interphase (Armstrong et al., 2001). The interaction between NORs and nucleolus determines the nonrandom association of chromosomes and might have direct effects on interchromosomal interactions and dynamics. Associations were found to be basically random among chromosomes 1, 3, and 5, while the associations of NOR-bearing chromosomes 2 and 4 were more frequent. The association of NOR-bearing chromosomes would be due to the interaction of both homologs with a single nucleolus, as found in expanded leaves and root meristems (Cremer et al., 2001; Pecinka et al., 2004; Berr and Schubert, 2007). A similar picture of chromosome associations was found in *Arabidopsis lyrata*, another *Brassicaceae* with larger genome (Berr et al., 2006).

As mentioned before, a Hi-C study of autotetraploid *Arabidopsis* showed increased interchromosomal interactions and reduced intra-arm interactions in comparison with a diploid strain. These increased interchromosomal interactions were localized around centromeres, while decreased intertelomeric interactions were observed among all chromosomes in autotetraploid plants. The results of this study suggested that autotetraploid *Arabidopsis* had less compacted chromosome arms and that interchromosomal interactions presented higher strengths in the autotetraploid compared to the diploid strain. The increased interchromosomal interactions were unspecific and no preferential interactions were found between any given pair of heterologous chromosomes (Zhang et al., 2019).

A similar Hi-C study in rice (*Oryza sativa* L.) revealed that chromosomes occupy specific territories, and they interact preferentially with certain chromosomes (Dong et al., 2018). Two sets of chromosomes (1 through 5 and 10 through 12) interacted preferentially within the set, while the remaining chromosomes (6, 7, 8, and 9) did not show apparent associations at all. These observations suggest that chromosomes that show more frequent associations must be physically closer in space within the nucleus. The difference between rice and *Arabidopsis* could be explained because rice has a larger and more complex genome with a larger number of chromosomes (Dong et al., 2018).

The observed interactions among chromosomes could be at least partly explained because of the spontaneous Brownian motion within the constrained space of the nucleus. However, we must also consider the importance of other more intense forces that are delivered during the multiple active processes that concern chromatin and chromosomes at work. One of these processes is transcription. Chromatin conformation determines the access of the transcription machinery to the DNA (Kouzine et al., 2014). The arrangement of CTs that allows the approach of certain chromosome regions led to the idea of transcriptional factories, hundreds of sites with an especially high transcriptional activity (Sexton et al., 2007; Sutherland and Bickmore, 2009).

The distribution of transcriptional activity across chromosomes underlies many aspects of large-scale nuclear architecture including interchromosomal associations (Agrawal et al., 2020; Menon, 2020). *Arabidopsis* transcriptionally active genes do not associate in transcription factories (Liu et al., 2016). The picture is different in species with more complex genomes. In plants with large genomes like hexaploid wheat, transcription factories have been shown to allow both intra- and interchromosomal contacts associated to RNA polymerase involving multiple genes displaying similar expression levels (Concia et al., 2020).

Replication is another chromosomal process that seems to imply interchromosomal interactions. In plants, there is little information about chromosome interactions during replication. In *Arabidopsis*, however, they found a correlation between genomic regions that replicate during the interphase and genomic features, chromatin state, accessibility, and chromosomal interactions. They suggest that sequences that are close together tend to replicate at the same time (Concia et al., 2018). A similar picture was found in a larger study involving time and position parameters of DNA replication in several *Poaceae* including wheat, oat, rye, barley, *Brachypodium*, rice, and maize (Němečková et al., 2020).

DNA repair also implies both intra- and interchromosomal interactions. DNA repair is extremely important in plants, due to their sessile nature and their exposure to multiple mutagenic agents like ionizing radiation, heavy metals, and other types of biotic and biotic sources of stress, besides the endogenous processes that can result in DNA damage. Among all the types of damages that DNA can suffer, double strand break (DSB) is the most severe. The major mechanism of DSB repair in somatic plant cells is non-homologous end joining (NHEJ), but some DSBs are fixed by homologous recombination (HR). NHEJ may result in loss or change of information due to deletions, inversions, translocations, or insertion of sequences from elsewhere in the genome (Lieberman-Lazarovich and Levy, 2011; Knoll et al., 2014).

DNA repair by HR can follow two different mechanisms: single-strand annealing (SSA) and synthesis dependent strand annealing (SDSA). SDSA is the major mechanism of conservative HR repair in plant somatic cells (Knoll et al., 2014). Sister chromatids can be used as template in the S and G2 phases, and this is the most efficient kind of template. However, DNA repair by SDSA HR is also possible in interphase somatic cells between homologous chromosomes, or also between homoeologs (in the case of polyploid plants), and even between heterologous chromosomes, though it occurs at very low frequencies. In tomato, induced allele dependent DSB repair has been proposed (Gisler et al., 2002; Knoll et al., 2014).

In humans, it is known that during G_0-phase, as early as 5 min after DNA damage induced by ionizing radiation, homologous chromosomes interact at the DSB sites, what could be explained by the existence of a fast mechanism to localize homologous chromosomes where DSBs are generated (Gandhi et al., 2013). In plants, the precise mechanisms of chromosome approach and interaction to allow DSB repair by HR are not known. Recombination between homologs in somatic tissues is not well-documented because of intrinsic difficulties. In tobacco, it was shown that somatic HR is not frequent in the absence of DSB induction (Carlson, 2016). More recently, Filler-Hayut et al. (2017) showed that the induction of DSBs in tomato somatic cells *via* CRISPR-Cas9 increases the frequency of homologous contact and recombination between homologous chromosomes, demonstrating that the meiotic HR machinery is not necessary for DSB-induced homologous recombination. Even though there is not enough information, concerted chromatin modifications seem to determine DSBs repair through the repair machinery and repair factors. Chromatin changes are also correlated with the movement of repair sites to the periphery of the nucleus for HR repair of DSBs in heterochromatic DNA (Kim, 2019).

In plants, somatic homologous pairing and recombination is not frequent, though it is relevant in certain situations. The fact that multiple processes like transcription, genetic regulation, replication, and DNA repair allow interchromosomal contacts throughout the whole cell-cycle points to the relevance of all these processes to explain homologous chromosome pairing and recombination in the interphase, in somatic cells, as well as in reproductive cells and meiosis.

Transcription seems to be particularly relevant, since it could somehow set off somatic pairing of homologous chromosomes (Hiraoka, 2020). Homologous chromosomes, with identical chromosome architecture, display almost identical patterns of transcription factories and heterochromatin (Cook, 1997). Homologous chromosomes are thought to be joined at the transcriptional factories (Cook, 1997; Ding et al., 2010). Non-coding RNAs accumulate on their gene loci, and they could contribute to the association of homologous chromosomes through allelic loci (Ding et al., 2012).

In plants, though homologous chromosome pairing seems to be usually random and transient in somatic cells (Schubert and Shaw, 2011), there is evidence of constitutive homologous chromosome pairing at least in certain cell types. A study on the arrangement *Brachypodium distachyon* chromosomes in root cells interphase nuclei showed that the association of homologous chromosome arm CTs is more frequent than expected in a random arrangement of all chromosomes within the nucleus (Robaszkiewicz et al., 2016).

Although preceded by heterologous association through centromeres, homologous pairing along the entire chromosomes was also described in hexaploid wheat floral tissue prior to meiosis (Martínez-Pérez et al., 1999). The Rabl configuration of wheat chromosomes was observed in premeiotic cells (Naranjo, 2015a). This configuration is important for homologous recognition, since it facilitates homologs search and alignment (Pernickova et al., 2019). In rice, they found initial chromosome association between homologs in undifferentiated anther cells and xylem vessel cells. In wheat and related polyploids, however, initial association in undifferentiated anthers was found between non-homologous or related chromosomes, but not between homologs (Prieto et al., 2004b). All these observations support the concept that somatic homologous pairing might precede and contribute at least partially to meiotic homologous pairing and recombination, as already suggested (Gerton and Hawley, 2005).

THE STRUCTURE AND FUNCTION OF CHROMOSOME ENDS

Despite the evident relevance of multiple types of interchromosomal interactions occurring around the whole cell-cycle, chromosome ends (telomeres and subtelomeric regions) are known to be involved in specific homologous chromosome recognition and pairing during early meiosis, which are critical processes that allow chromosome recombination between homologs in later stages. In plant polyploid species, like wheat and maize, these terminal regions are even more important in terms of homologous chromosome recognition, due to the presence of homoeologs (equivalent chromosomes from related genomes) and the necessity to prevent pairing and recombination between non-homologous or homoeologous chromosomes.

The chromosomal reorganization that takes place at the beginning of meiosis seems to be rather ubiquitous in the process of homology searching in higher eukaryotes (Blokhina et al., 2019). Telomeric sequences are highly conserved.

Chromosome ends cluster near the nuclear membrane to form a "bouquet" structure. This process facilitates homologs preliminary interactions and further pairing and recombination (Naranjo, 2014). Although telomeres interaction seems to assist homologous pairing and consequently, the progression of meiosis, other chromosome regions such as subtelomeres need to be considered, because telomere sequences are not specific for any chromosome. In addition, recombination operates at subtelomeres and, in some crop species, there seems to be a correlation between recombination and homologous pairing. A complete characterization including the DNA sequence, as well as chromatin composition, modifications, and 3D architecture, together with the molecules (proteins, RNA, etc.) interacting with it, is needed to get insight into the function of telomeres and subtelomeres in pairing and recombination.

In most eucaryotes, the telomere sequence is typically constituted by short G/C-rich repeats organized in tandem, with the G-rich strand 3' end toward the chromosome end, which often has a G-overhang that forms a single strand protrusion (**Table 1**). Some plant species like *A. thaliana* and other angiosperms do not have this overhang or at least not in all chromosomes (Kazda et al., 2012). The model plant *A. thaliana* was the first multicellular organism whose telomere sequence was cloned and characterized (Richards and Ausubel, 1988). In the majority of plant species, telomeres sequences are formed by arrays of tandem repeats of variable length from less than 1 kbp to tens of kbp, depending upon species, variety, organism, and chromosome (Fajkus et al., 1995a,b). The TTTAGGG telomeric repeat first found in *Arabidopsis* was considered ubiquitous among most plant species (Kilian et al., 1995), with a few exceptions as the unicellular green alga *Chlamydomonas reinhardtii*, whose telomeric repeat is TTTTAGGG (Petracek et al., 1990), and a group of Asparagales, where it is TTAGGG (Sykorova et al., 2003b; Weiss-Schneeweiss et al., 2004). But more recently, a higher variability around the formula $(T_xA_yG_z)_n$ has been found in many species of *Solanaceae*, *Amaryllidaceae*, *Lentibulariaceae*, and many algae (Peska and Garcia, 2020). This variability seems to be the result of evolutionary divergence. In monocots, telomeric sequences evolved from (TTTAGGG)*n* and a change to (TTAGGG)*n* occurred in *Iridaceae*, while (CTCGGTTATGGG)*n* sequence is found in *Allium* (Fajkus et al., 2019).

The distal part of the telomere is changing continuously as a result of two opposing processes: a shortening due to the end-replication problem and exonucleolytic resection vs. an active elongation by the action of telomerase (Fitzgerald et al., 1999; Riha et al., 2001; Riha and Shippen, 2003). G-rich overhangs, besides other important functions, could act by invading the telomere contiguous duplex region so that a t-loop is formed. This would be a maintenance mechanism for the telomere protective cap (Cesare et al., 2003). Plant telomeres are maintained by telomerase, as it occurs in mammals (McClintock, 1939). Telomerase is expressed and active in meristematic cells of all growing tissues and organs such as apex, root tips, young leaves, inflorescences, flowers, and seedlings, while it is absent in completely differentiated and mature tissues (McClintock, 1941; Kilian et al., 1998). In most organisms, including plants, telomerase is formed by two elements: telomerase reverse transcriptase (TERT) and telomerase RNA (TR; Veldman et al., 2004; Hockemeyer et al., 2006). Telomerase also includes other proteins that are necessary for its function (Tommerup et al., 1994; Wu et al., 2006). TERTs are highly conserved (Sykorova and Fajkus, 2009), while TRs are very diverse both in sequence and length among most organisms. In plants, however, the TR gene is highly conserved (Fajkus et al., 2019). In plants, an HR-based telomerase maintenance mechanism (ALT) is probably active during early plant development (Bryan et al., 1997; Ruckova et al., 2008). ALT is dependent of t-loops, which resembles the first steps of HR (Griffith et al., 1999).

Chromosome ends are protected by proteins associated with telomeres. This protection implies the distinction between natural chromosome ends from accidental DNA breaks, avoiding the unwanted action of the repairing machinery on telomeres. In humans, this set of telomere-binding proteins, a complex known as shelterin, include TRF1, TRF2, POT1, and other proteins that interact with telomeres indirectly (De Lange, 2005, 2018). Besides its protective function, the shelterin complex also

TABLE 1 | General features of chromosome ends.

G-overhang	Telomere	Telomere-subtelomere junction	Subtelomere
Length = A few nucleotides 3'-G_n	Length = Up to hundreds of bp (TTTAGGG)*n*	Length = Up to a few kbp Variable number of telomere degenerate repeats close to telomere repeats.	Length = Up to hundreds of kbp Highly polymorphic set of transposons, retrotransposons, low complexity DNA, genes including tRNAs, transcription factors, and metabolic genes with functions that are required for adaptation to the environment.
Common, but absent in some chromosomes and species.	Common, but absent in some chromosomes and species.		
	(TTAGGG)*n* in Iridaceae	Tandem arrays of rRNA genes in some chromosomes of many species.	Highly variable pattern of multiple sequence features (rice).
	(TTTTAGGG)n in *Chlamydomonas reinhardtii.*	BAAAA (B = C, T, G) and a poly-G stretch of about 32 bp in *Arabidopsis.*	Sets of specific repeats (barley and wheat).
	(CTCGGTTATGGG)*n* in *Allium.*		Large blocks of heterochomatin (rye).
	(TxAyGz)*n* in Solanaceae, Amaryllidaceae, Lentibulariaceae, and many algae.		

contributes to the recruitment of telomerase, the movement of the replication fork or the creation of t-loops (Procházková-Schrumpfová et al., 2019). Plant telomeres also have a shelterin-like complex, though its characterization is still incomplete. As putative components of this shelterin-like complex, TRB proteins were identified in *A. thaliana* (Schrumpfova et al., 2014) and maize (Marian et al., 2003). These proteins bind telomere DNA specifically both *in vitro* and *in vivo* and interact with the TERT subunit of telomerase (Peska et al., 2011; Schrumpfova et al., 2014; Zhou et al., 2018).

Plant Ku and POT1b proteins associate with TER2, a TR that is not necessary for telomere maintenance (Cifuentes-Rojas et al., 2011). Ku70/80 heterodimer plays an important role in the protection of blunt-end telomeres. Plants conserve all orthologs of scaffold box H/ACA of small nucleolar RNAs. A CST protein complex seems to be relevant for an efficient replication of plant telomeres. RTEL also takes part in the maintenance of the homeostasis of telomeres (Procházková-Schrumpfová et al., 2019).

We should also have in mind that most of the telomere chromatin is tightly packed in nucleosomes, being the nucleosomal spacing in telomeres shorter than elsewhere in the chromatin (Fajkus et al., 1995a,b). In addition, other telomere heterochromatin features are possible, since nearby regions form large heterochromatin blocks in many plants (Louis and Vershinin, 2005). This could be particularly relevant when the long rack of regular telomere repeats is absent. Some *Alliaceae* and *Solanaceae* have lost G-rich telomeric repeats (Sykorova et al., 2003a, 2006). In *Allium cepa* (onion), chromosome ends were proposed to contain satellite repeats and transposons (Pich and Schubert, 1998). Thus, maintenance of telomere structure in *Alliaceae* could imply an epigenetic mechanism as in *Drosophila*. In *Arabidopsis*, they reported telomerase-deficient mutants that lacked telomeric DNA but partially retained the ability to end-cap their chromosomes, suggesting the existence of an adaptive mechanism to the loss of telomeric DNA based on the formation of terminal heterochromatin blocks (Watson et al., 2005).

Telomeres are also subject to epigenetic modifications. Methyl-Cytosines (mCs) were detected in telomeric repeats of *Arabidopsis* (Ogrocka et al., 2014), *Nicotiana tabacum* (Majerova et al., 2011), and other plants (Majerova et al., 2014). Telomere homeostasis was altered because of a reduction of genomic DNA methylation in *Arabidopsis* (Xie and Shippen, 2018) but not in tobacco (Majerova et al., 2011), which reveals significant differences in the regulation of telomere homeostasis by methylation. The plant telomeric chromatin displays a dual epigenetic character, since chromatin was associated with heterochromatin and euchromatic marks in telomeres (Majerova et al., 2014; Sovakova et al., 2018). A general conclusion on the epigenetic state of telomeric chromatin is not possible since it is very dynamic and variable with the physiology of the organism. Epigenetic modifications are responsible for the regulation of telomere functioning (Procházková-Schrumpfová et al., 2019; Achrem et al., 2020).

In all organisms with a complex genome, including *Homo sapiens*, *Arabidopsis*, and wheat, the region that is closed to the telomere, is usually characterized by the presence of a variable number of telomere degenerate repeats (Aguilar and Prieto, 2020). Though a clear functional or structural definition is not available, the subtelomere is usually considered as the region extending from the telomere up to the first chromosome-specific sequence (Louis, 2014). A common feature supposed to be shared by plant chromosome ends is a region of highly repetitive and reorganized DNA before the first active gene (Alkhimova et al., 2004; Aguilar and Prieto, 2020). *Arabidopsis* chromosomes, however, have short and simple subtelomeric regions. Except for two chromosome ends, where telomeric tandem repeats are right adjacent to tandem arrays of rRNA genes, subtelomeres contain a few repeats of the sequence BAAAA (B = C, T, G) and a poly-G stretch of about 32 bp (Kuo et al., 2006). A recent study in wheat chromosome ends, however, did not show any characteristic pattern among five different chromosomes whose telomere-subtelomere border regions were studied. The characteristic features found in *Arabidopsis* were absent in wheat, but many different elements (genes, retrotransposons, transposons, tandem repeats, and low complexity DNA) were found, as in other plants (**Table 1**; Aguilar and Prieto, 2020).

Subtelomeres are highly polymorphic and, as a matter of fact, they are less conserved than chromosome ends. Genes are very abundant, and recombination is more frequent in these regions (Emden et al., 2019). These characteristics make it more difficult to analyze the actual role of subtelomeres in genome stability, replication, and also in chromosome pairing and recombination (Emden et al., 2019). Chromosome subtelomeric distal regions seem to play important roles in other processes including transcription, chromosome dynamics during meiosis, and the regulation of the cell cycle cell (Blackburn, 2005).

In most species, the analysis of subtelomeres has been focused on a distal segment of around 500 kbp (Mizuno et al., 2008). These studies revealed many differences among species. In *A. thaliana*, probably due to its small genome, subtelomeres seem to be short and rather simple, and their sequences are very variable among non-homologous chromosomes (Kuo et al., 2006). Rice subtelomeres showed a highly variable pattern of multiple sequence features (Mizuno et al., 2014), while rye subtelomeres contain large blocks of heterochomatin (Evtushenko et al., 2016). Sets of specific repeats were found in subtelomeres of some species including barley and wheat (Prieto et al., 2004a; Salina et al., 2009). Due to this variability and diversity, the fine structure of subtelomeres remains undetermined (**Table 1**).

The sequence variability of subtelomeres has suggested various possible functions roles of these regions in the stability of chromosomes and their dynamics. Rice subtelomeres, for instance, were involved in transposon movement and recombination (Fan et al., 2008). As shown in rye and wheat, there seems to be a correlation between recombination and chromosome pairing between homologs (Valenzuela et al., 2013). Subtelomeres are frequently affected by recombination events in most systems studied, and these events occur more often in in non-coding regions (Aguilar and Prieto, 2020). The role of subtelomeres in recognition and pairing of homologous chromosomes during

meiosis is not well-understood yet. There are some evidences, however, that these regions might be very important, as suggested by a study in Zebra fish, where they found presynaptic subtelomeric chromosome alignment without a fully association of telomeres (Blokhina et al., 2019).

Except for rice and *A. thaliana* (Kuo et al., 2006), the knowledge of the role of subtelomeres in early meiosis is not abundant in plants. Some evidences were found in cereals. Rye subtelomeres showed large clusters of heterochromatic regions at the onset of meiosis (Mikhailova et al., 2001). Wheat has also provided evidences supporting the function of subtelomeres in chromosome pairing. FISH experiments showed that, in the absence of subtelomeric sequences, chromatin remodeling failed and homologous chromosomes would not recognize and pair (Calderón et al., 2014). The relevant function of subtelomeres in recombination was also shown in experiments using wheat lines with distal chromosome deletions (Naranjo, 2015b).

DNA folding and arrangement within the nucleus is also very important for the understanding of the role of subtelomeres in chromosome interactions and pairing. Some of the proteins that are relevant for chromosomes architecture could also be very important, as shown in the case of meiotic cohesins (Zhu and Wang, 2019). Ding et al. (2016) showed that the absence of meiotic cohesins implied a structural change of the chromosome axis, which provoked a failure of homologous chromosomes interaction and pairing. Despite these interesting evidences, further studies are required to demonstrate the actual relevance of the axis formation for homologous chromosome pairing.

A possible role of CTCF, Ying Yang 1, and similar proteins with a known function in chromosome arrangement, has also been suggested in the context of homologous chromosome pairing during meiosis (Beagan et al., 2017). Loop-forming CTCF and cohesins show a similar distribution throughout the chromosome (Wendt et al., 2008). Plant CTCFs, however, have not been identified, though there could be proteins with equivalent functions. Subirana and Messeguer (2011) already mentioned the possibility that HMG proteins could participate in chromosome interaction and homologous pairing.

A recent study of the sequence characteristics of bread wheat distal subtelomeres suggests that the high polymorphism of multiple sequence features, including transposons, retrotransposons, low complexity DNA, and gene-coding sequences, might be responsible for the specificity of interchromosomal interactions at early meiosis, something that is particularly important in a hexaploidy organism like wheat (Aguilar and Prieto, 2020). This study included many other sequence features like the distribution of CpG islands and binding sites of proteins that could play a relevant role in pairing and recombination events. The pattern distribution of all these features seems to be rather specific among heterologous and homoeologous chromosomes (Aguilar and Prieto, 2020).

A study of genes located the in rice subtelomeres revealed a density of 1 gene per 5.9 kbp (Fan et al., 2008). A similar analysis done in wheat showed an average density of 1 gene per 9.5 kbp with a high variability both in density and pattern of gene distribution among the chromosomes studied (Aguilar and Prieto, 2020). Some of these subtelomeric genes that have already been characterized are tRNAs, transcription factor, and metabolic genes. All of them share in common that they represent functions that are required for adaptation to the environment, as suggested by Brown et al. (2010).

The abundance and distribution of transposable elements (TEs) was also chromosome specific in wheat subtelomeres (Aguilar and Prieto, 2020). Several mechanisms could explain the abundance of TEs in subtelomeres, TEs are removed by recombination at a much lower rate in heterochromatic regions, because recombination occurs at a lower frequency in these compacted regions (Zamudio et al., 2015). Besides, TEs density and recombination rate seem to be inversely correlated (Daron et al., 2014). The differential pattern distribution of TEs could support the role of subtelomeres in the specific interactions and pairing of homologs during meiosis.

Plant subtelomeres also include many different repeat sequences, including satellites, simple repeats, and low complexity repeats (Heacock et al., 2004; Torres et al., 2011). In wheat, they account for more than 90% of the entire genome (Li et al., 2004). An analysis of wheat distal subtelomeric region revealed a specific pattern of distribution of these sequences in every chromosome (Aguilar and Prieto, 2020). In maize, tandem repeats are less abundant in the subtelomeric regions but more common across the rest of the chromosome, particularly concentrated in knob regions (Lamb et al., 2007). The abundance and distribution of repeats varies among cereals (Vershinin and Evtushenko, 2014).

In wheat, the overall distribution of repeats, TEs, and genes reveals the same complex and dynamic structure of distal subtelomeres found in all the organisms analyzed, what provides a specificity that could be determinant for homologous chromosome pairing during meiosis (Vershinin and Evtushenko, 2014; Aguilar and Prieto, 2020). However, none of the elements found in subtelomeres is specific of this region, what reinforces the idea that is the pattern of distribution of these elements what is really relevant. Many evidences suggest that subtelomeres play several relevant roles besides chromosome pairing. They could contribute to protect genes located near the chromosome ends and stabilize telomeric regions in the absence of telomeric repeats (Louis and Vershinin, 2005; Garrido-Ramos, 2015).

Other sequence features like GC content and the distribution of CpG islands could also help to understand the role of subtelomeres in chromosome pairing. In bread wheat, these two features showed a great variability among subtelomeres of different chromosomes. GC content is correlated with recombination frequency, which in turn is influenced by homologous chromosome pairing (Sundararajan et al., 2016; Aguilar and Prieto, 2020). A high density of GC content was also correlated with the occurrence of DSBs and crossovers in many organisms (Sundararajan et al., 2016). DSBs seem to be necessary for recombination to take place. The identification of several sequence motifs different organisms suggests that DSBs and crossovers seem to be determined by the presence of specific sequences that could be related to a more relaxed chromatin that facilitates the access of SPO11 and the production

of many DSBs (Choi et al., 2018). The analysis of wheat distal subtelomeric regions for the presence of DSB hotspot motifs revealed a good correlation between these sequence motifs and hot recombination spots, with clear differences among chromosomes. A good correlation was also found between density of DSB hot spots and TEs. The differences of sequence patterns among homoeologs subtelomeres in bread wheat point to the possibility that the determinants of chromosome pairing and recombination are related to the very sequence of subtelomeric DNA (Darrier et al., 2017; Aguilar and Prieto, 2020).

Pairing of homologous chromosomes might require the contribution of proteins during the initial stages when chromosomes approach and initiate their interaction (Ding et al., 2016). An analysis of wheat subtelomeres revealed the presence of putative binding sites of some of the proteins that are considered as candidates to play a relevant role in these initial stages of chromosome pairing. Wheat homologous to human SMC1β meiosis-specific cohesin, Ying Yang 1, and HMG were studied (Aguilar and Prieto, 2020). HMG proteins are particularly interesting, since they were suggested to be involved in initial interactions between homologous chromosomes through AT-rich sites (Subirana and Messeguer, 2011). The distribution of putative binding sites for all these proteins showed great differences among wheat chromosomes. An interesting differential pattern of HMG binding sites was revealed, what supports a possible role of HMG proteins during the initial interactions prior to homologous pairing (Aguilar and Prieto, 2020).

CHROMOSOME INTERACTIONS DURING PREMEIOSIS AND EARLY MEIOSIS

The spatial distribution of the genome within the three-dimensional nucleus is dynamic during meiosis and linked to regulation of gene expression. Chromosome movements and chromatin remodeling let homologous chromosomes find and associate each other in pairs (Scherthan, 2001; Prieto et al., 2004c; Naranjo, 2014). In most organisms and mainly in plants, chromosomes associate by centromeres at the onset of meiosis, but homologs physically begin interacting through the terminal regions of the chromosomes when the bouquet is formed (leptotene) while all telomeres remained attached to the nuclear envelope. Consequently, the benefit of this telomere cluster on the subtelomeric regions is clear. Subtelomeres have to occupy a very limited space within the nucleus which facilitates the interaction and progressive stabilization of unstable chromosome interactions.

During the process of meiosis, chromosomes need to reorganize and enormously condense, which is crucial for their correct pairing, recombination, and segregation. In mammalian cells, mitotic and meiotic chromosomes show a similar higher-order structure (Kleckner et al., 2013). The higher-order structure of chromosomes is critical in many species (including plants) for diverse cellular processes such as chromosome interactions during meiosis. In meiotic prophase, after DNA replication, chromosomes that are dispersed through the nucleus undergo substantial structural remodeling. When meiosis begins, chromosomes individualize and compact progressively, but pairing, synapsis, and recombination also occurred with their homologous partners. The organization of early meiotic chromosomes is connected with the progression of these interchromosomal interactions, indicating that chromosome morphology is essential for the events mentioned before (Yamada and Ohta, 2013). Chromatin remodeling at the beginning of meiosis is particularly decisive in plants because plant genomes are usually large and complex, carrying a huge number of repetitive DNA, which could allow non-homologous chromosome interactions resulting in chromosome miss-segregation. Chromosome dynamics has been recorded in live maize meiocytes inside intact anthers at the beginning of meiosis showing that chromosomes exhibited an extremely complex dynamic in zygotene and pachytene (Sheehan and Pawlowski, 2009). The observation of different types of chromosome movements at different stages of meiosis in maize meiocytes suggested the existence of multiple mechanisms affecting chromosome mobility, including telomeres attached to the nuclear envelope causing chromosome end movements. Chromosome movements during zygotene in maize illustrate a nice picture on how homologous loci could approach each other in complex genomes allowing chromosomes to search each other based on recombination-dependent homology. Consequently, the dynamic chromosome movements could permit different pairing combinations until correct homologous interactions are successful (Golubovskaya et al., 2002; Sheehan and Pawlowski, 2009).

Two conserved features of meiotic chromosome dynamics, telomeres attached to the nuclear membrane and the random telomeres motion, have been suggested to enable homologous pairing, although their specific functions in meiosis continue to be elucidated. The fact of telomeres being attached to the nuclear envelope might reduce the speed of pairing in contrast with the rates of non-attached chromosomes. Nevertheless, the arbitrarily directed vigorous forces applied to telomeres accelerate chromosome pairing enormously, based on the statistical properties of the telomere force oscillations (Marshall and Fung, 2016). The linker of nucleoskeleton and cytoskeleton (LINC) complexes are important during meiosis. Proteins AtSUN1 and AtSUN2,which are included in the LINC and situated in the internal part of the nuclear envelope, interact with the KASH protein located in the outer nuclear envelope and are implicated in tethering telomeres to the nuclear envelope. As stated before, this attachment contributes to chromosome movements as demonstrated in the double mutant *Atsun1* and *Atsun2* of *A. thaliana*, which showed a delay in prophase I meiotic progression, incomplete synapsis and deficiencies in recombination that result in unbalanced gametes and sterility (Varas et al., 2015). Recently, a partial redundant role of OsSUN1 and OsSUN2 in early meiosis has been also reported in rice (Zhang et al., 2020). *Ossun1* and *Ossun2* double mutants revealed drastic aberrations in telomere clustering, homologous pairing, and crossover formation. In rice, OsSUN2 seems to play a more critical role than OsSUN1 in meiosis, being essential for the telomere bouquet formation (Zhang et al., 2020). ZYGO1 also plays a role in bouquet formation during early meiosis in rice (Zhang et al., 2017). So far, the SUN/KASH protein complex that attach telomeres to the nuclear envelope have

not been discovered in wheat yet, but the presence of the *Ph1* locus affects the dynamics of telomere bouquet formation by delaying it, what might imply that chromosomes have more time to check potential pairing facilitating correct homologous chromosome pairing (Richards et al., 2012).

The increased rate of initial pairing at the distal chromosome regions does not only depend on chromosome elongation but instead seems to be also connected with irregular distribution of subtelomeric regions. Hence, active motion of telomeres drives optimal pairing in subtelomeric regions. The distribution is more irregular at the subtelomeres than at the telomeres themselves, according to the results showing that initial pairing rates are highest in subtelomeric sites (Marshall and Fung, 2016). These observations mean that cytoskeletal forces applied on telomeres can regulate abnormal diffusion of subtelomeric chromatin to increase the rate of collisions. Both the limitation of the irregular diffusion to subtelomeres and the initial pairing occurring most likely in subtelomeric regions, when telomeres undergo insistent random walks can describe why in some species, specific "pairing centers" that mediate homologous pairing tend to be located toward the chromosome ends (Marshall and Fung, 2016).

The molecular mechanism explaining how homologous chromosomes associate in pairs at the onset of meiosis as a prelude to recombination remains poorly understood although accurate homologous chromosome associations at the beginning of meiosis are prerequisite for successful recombination between homologs and ensure plant fertility. Chromosome remodeling in meiosis initiates in leptotene stage, when the DNA condenses and sister chromatids are firmly attached (Remeseiro and Losada, 2013). During leptotene, chromatin fibers are looped and anchored to axial elements at the core of the chromosomes (McNicoll et al., 2013). Recombination also begins at this stage. Thus, SPO11 produces DSBs into DNA (Keeney, 2008) and the ends contiguous to these breaks are bound by RAD51 and DMC1 (San Filippo et al., 2008). This process is supposed to be an important feature in homologous recognition in most species. Moreover, the pattern of meiotic recombination has been interpreted as evidence of premeiotic pairing.

Premeiotic homologous pairing has been described in higher eukaryotes such as *Drosophila melanogaster*, suggesting implications for DSB repair in premeiotic cells (Rong and Golic, 2003). In plants, premeiotic homologous pairing has been described in the cultivated rice *O. sativa* and a wild relative *Oryza punctata* (Prieto et al., 2004b). Multiple evidences suggest that chromosome pairing and crossing over are not totally codependent (Jordan, 2006; Zickler and Kleckner, 2015; Calderón et al., 2018). There must be a characteristic of the genomic architecture that could facilitate the processes of recognition and pairing between homologous chromosomes independently of recombination and DNA damage. HMG proteins could participate in these processes by interacting with AT-rich sites, which might be accessible in the expanded DNA loops (Subirana and Messeguer, 2011) and should be studied in the subtelomeric regions in detail. This theory could fit with a mechanism to stabilize the associations between homologs through pairing proteins that interact with AT-rich DNA regions accessible within the DNA protruding loops. Nevertheless, the initial interactions between homologs at the chromosome ends to recognize each other to pair and the molecular factors involved are still unclear, although several genes like HOP1, REC8, and RED1 have been suggested playing essential functions in chromosome associations (Coutou et al., 2004; Jordan, 2006; Ding et al., 2016). A recent mathematical model in polyploids supporting this hypothesis suggested that telomeres are engaged under active forces in a tug-of-war against zippering (Marshall and Fung, 2019). Thus, homologous chromosome regions are competing for zippering with homoeologous regions when telomeres are attached to the nuclear envelope and shaking. Zippering of true homologs is only allowed when the affinity between the distal chromosome regions is strong enough to oppose shaking. This hypothesis agrees with the observations that sequence specificity is essential for the pairing process, essentially in chromosome regions like subtelomeres where DNA sequences are exposed to rapid change (Calderón et al., 2014).

When prophase enters early zygotene, DNA fibers expand and chromatin surface becomes more complex (Dawe et al., 1994). Telomeres cluster at the nuclear envelope into the bouquet and heterochromatic knobs elongate (Scherthan, 2007). As stated earlier, the telomere bouquet has been observed in most plants, animals, and fungi, including budding and fission yeast, mouse, wheat, and maize, among others (Martínez-Pérez et al., 2003; Prieto et al., 2004c; Sheehan and Pawlowski, 2009). In wheat, telomeres are spread around the nucleus and at the onset of meiosis start associating in one side of the nucleus, opposite to centromeres, to form the bouquet (**Figure 1**; Martínez-Pérez et al., 2003). Although many cytogenetic analyses have clearly shown the formation of the bouquet during early meiosis, little evidence about the molecular mechanism to form the telomeres bouquet is available as mentioned before. In addition, though the bouquet itself is not a general characteristic in all organisms, chromosomes associate in most of them by specific regions (telomeres or pairing centers) in a small region of the nucleus (nuclear envelope or nucleolus). Moreover, these telomeres or pairing centers use cytoskeletal elements to perform chromosome movements around this region, and sometimes all telomeres gather within an even smaller bouquet region.

Cell live imaging has been used to visualize chromosome dynamics, but only a few works have been carried out in plants to observe meiosis in real time. The quantification of meiotic phases with high temporal resolution, the diverse chromosome movements during prophase I, as well as some information related to spindle dynamics and chromosome paring have been described in live meiocytes of maize (mentioned earlier) and *Arabidopsis* by visualizing whole chromosomes and microtubules (Sheehan and Pawlowski, 2009; Nannas et al., 2016; Prusicki et al., 2019). Cell live imaging to show telomeres dynamics using a novel CRISP-dCas9 system has been carried out in plant somatic tissues in *Nicothiana benthamiana*. This approach was also combined with fluorescence-labeled proteins and revealed long-range chromatin movements occurring during a short period of time in somatic cells (Dreissig et al., 2017).

In meiosis, how telomeres move along the nuclear envelope and associate in the bouquet, as well as the relative roles of

telomeres diffusion and direct movements have been studied using a combination of fluorescence microscopy with mathematical modeling in wheat as described earlier. Sister chromatid telomeres were always found associated to a randomly orientated hemisphere of the meiocytes nuclear envelope and associated in pairs before the telomere bouquet formation (Richards et al., 2012). Such initial telomere associations have also been described in rye (Carlton et al., 2003), maize (Golubovskaya et al., 2002), and rice (Prieto et al., 2004b). The mathematical model mentioned earlier, which incorporates the dynamic of telomere cluster moving along the nuclear envelope, did also include the study of the mechanism of telomeres bouquet formation (Marshall and Fung, 2019). It provides a natural explanation of the pure drift of telomeres to associate and form the bouquet. Although telomeres diffusion might occur, it would be negligible (Richards et al., 2012). In the simplest version of the model, telomere cluster moves with constant drift speed toward the bouquet site (**Figure 1**). Diffusion is not enough to explicate the deviation in the time of the bouquet formation and directed movements are also required (Carlton et al., 2003; Richards et al., 2012). Thus, a substantial organization of the cytoskeleton (or some other similar structure) is required, creating a grid along which telomeres can move toward the bouquet spot. It is unclear which structural elements are involved in these plant species because SUN/KASH proteins, which link telomeres through the nuclear envelope, have not been described in wheat and in most of plant species. Other possibilities include microtubules (as in animals), although the process in rye does not involve microtubules (Cowan and Cande, 2002), actin (as in *Saccharomyces cerevisiae*), nuclear envelope structural proteins (like the nuclear lamins in animals), or perhaps even the controversial idea of a nuclear matrix.

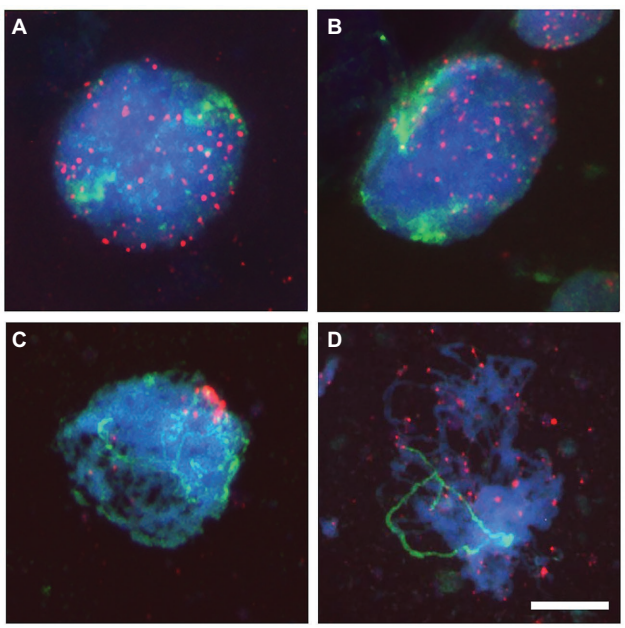

FIGURE 1 | Telomeres dynamic at the onset of meiosis in a wheat line carrying a pair of homologous chromosomes from the wild barley *Hordeum chilense*. Telomeres (red) and *H. chilense* chromosomes (green) were detected in fluorescence *in situ* hybridization (FISH) experiments in wheat meiocytes. Total genomic DNA was counterstained with DAPI (blue). **(A)** Early meiotic nucleus with all telomeres dispersed. Barley chromosomes are occupying different regions within the nucleus. **(B)** As meiosis progresses, telomeres start associating and physically located in one side of the nucleus. **(C)** Early meiotic nucleus with the telomeres clustered in a bouquet. Homologous barley chromosomes are intimately interacting and associating in pairs from the telomeric region. **(D)** Telomeres disperse from the bouquet and homologous chromosomes remained associated in pairs. Bar 10 μm.

Little information about the molecular mechanisms by which chromosomes specifically recognize a partner to correctly associate in pairs is available, although it has tremendous implications on chromosome dynamics (as described before) and homologous recombination. Recognition between homologous chromosomes must happen at the onset of meiosis and, especially in plant polyploids, it must be highly controlled, because each chromosome has to discriminate its homolog not only from other chromosomes but also from the homoeologous chromosomes of the related genomes. Experiments involving recognition and pairing processes between chromosomes during meiosis are still difficult because these processes are extremely dynamic, occur only among some chromosome regions and are not synchronized from one nucleus to the other (Zickler, 2006). In the context of meiosis, the term "pairing" denotes homologous associations occurring before the formation of the synaptonemal complex, which stabilizes homologs for synapsis and recombination. In fact, the pattern of meiotic recombination has been interpreted as evidence of premeiotic pairing, as it has mentioned before. There must be a feature of the genomic architecture that might facilitate chromosome recognition and pairing independently of recombination and DNA damage (**Figure 2**). As stated earlier, HMG proteins might participate in homologous chromosome (Subirana and Messeguer, 2011) and should be studied in the subtelomeric regions in detail.

During early meiosis, chromatin decondensation and chromosome movements allow homologs to find each other to associate in pairs (Scherthan, 2001; Prieto et al., 2004c; Naranjo, 2014). In most organisms, and particularly in plants, chromosomes start interacting physically at the bouquet stage, and telomeres being associated to the interior of the nuclear envelope (**Figures 1, 2**). DNA regions adjacent to telomeres (subtelomeres) might take advantage of this telomere cluster because they are obligated to be in a limited space meanwhile the instigation and progressive stabilization of chromosome interactions occur. The focus on subtelomeres, which are adjacent to telomeres, is an exciting area of study although the polymorphic nature of these regions represents a challenge from a technical perspective. Subtelomeres are less evolutionary conserved than telomeres and include recombination hot spots among other features that complicate the picture of the potential conserved functions of these high-polymorphic regions (Linardopoulou et al., 2005; Louis and Vershinin, 2005; Emden et al., 2019). These DNA segments and their associated proteins are essential for genome stability (Rietchman et al., 2005; Emden et al., 2019).

The implications of subtelomeric regions in chromosome recognition and pairing have been evaluated using wheat lines carrying a pair of homologous chromosomes with terminal deletions from wild barley (Calderón et al., 2014).

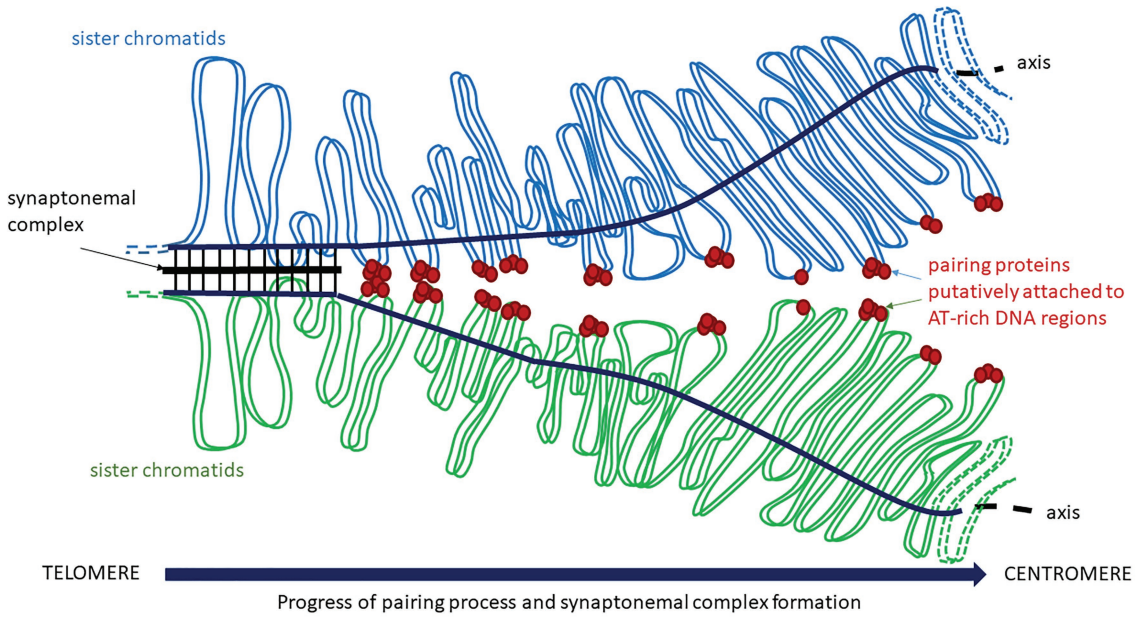

FIGURE 2 | Chromosome pairing and synaptonemal complex formation. Homologs approach and start their interaction putatively through pairing proteins attached to AT-rich regions on DNA loops before the assembly of the synaptonemal complex.

In situ hybridization experiments in these wheat lines clearly showed a function of subtelomeres in the initial processes of homologous recognition and pairing at the onset of meiosis. Although telomeres were present, in the absence of the subtelomeric sequences, chromosome recognition between homologs did not occur and consequently, chromosome pairing is not initiated (Calderón et al., 2014). In addition, in the chromosome arms without subtelomeres chromatin remodeling also failed, though the pairing signal could be conducted from the other chromosome end where subtelomeres were present and successfully initiated chromosome pairing. These observations also contributed to explain the lack of recombination in these terminal regions of the chromosomes (Calderón et al., 2014). According to this, the deficiency in recombination in the terminal region of chromosomes was also confirmed in wheat lines having a deletion at the distal region of any chromosome arm, which did not recover the level of chiasma frequency reached by the intact chromosome (Naranjo, 2015b), supporting the importance of the subtelomeric regions in recombination.

In some species, once homologous chromosomes have associated, the stabilization of both chromosomes depends on the formation of chromosome axis and the synaptonemal complex. In addition, DSB breaks, recombination, and crossover are also needed (Zickler and Kleckner, 2015; Barzel and Kupier, 2018). However, there are numerous indications suggesting that chromosome pairing and crossover are, at least, not completely co-dependent. Pairing can proceed without DSB creation and it can also occur, sometimes between homoeologs, without a subsequent crossover (Zickler and Kleckner, 2015; Barzel and Kupier, 2018; Calderón et al., 2018). This again means that there must be a characteristic on the chromosome architecture that might facilitate recognition, pairing, and recombination without DNA damage. For example, in the absence of homologous chromosomes in the wheat background, homoeologs can pair along their full length although crossing over does not occur in the presence of the *Ph1* locus but in its absence (Calderón et al., 2018; Calderón and Prieto, 2021).

In summary, when a chromosome finds a homolog to associate, their axial elements, now called lateral elements, are linked by the central element of the synaptonemal complex (Fraune et al., 2012). During zygotene, recombination is solved *via* crossovers or non-crossovers (Muyt et al., 2009). Chromosomes continue condensing through diplotene, the synaptonemal complex disappears and the homologs remain together as bivalents through crossovers, which are cytological visualized as chiasmata. It is clear that the importance of terminal chromosome regions including telomeres and subtelomeres, playing crucial roles on chromosome dynamics and interactions during early meiosis in plants.

IMPLICATIONS OF CHROMOSOME DYNAMICS IN PLANT BREEDING

Exploitation of the whole range of available genetic diversity in plant species could help plant breeders to develop new crop varieties that will be needed in the future to feed the increasing human population. The ability of one chromosome to specifically recognize and associate in pairs only with its homolog, as we have seen before, is a success of meiosis to ensure plant fertility but it is a tremendous barrier that plant breeders need to overcome. Breeders develop inter-specific genetic crosses between the cultivated variety and related species to introduce desirable genes from exotic germplasms into the crop. But in the case of wheat, for instance, sexual hybridization between wheat and related species usually

generates interspecific hybrids that contain a haploid set of each parental. This means that wheat and wild relative chromosomes do not usually associate and recombine in many such hybrids. In the context of breeding, it is necessary to shed more light on interspecific associations by the distal chromosome regions and recombination in hybrids or in interspecific genetic crosses, which are developed with the aim of introgressing necessary agronomic characters from related species into crops such as wheat.

Alien chromosome additions have a significant use both in breeding and in plant genetic studies. The specific genetic and cytogenetic properties of DNA introgressions into a crop make these plant materials useful tools for fundamental research, helping to explain the processes of interactions and associations at the distal chromosome regions during specific processes such as meiosis, homoeologous recombination, distribution of specific markers or repetitive DNA sequences, and regulation of gene expression (Chang and de Jong, 2005). For example, in hexaploid, wheat has been developed chromosome introgressions (additions) of both cultivated (*H. vulgare*) and wild (*H. chilense*) barley (Miller et al., 1982; Islam et al., 1978, 1981). These addition lines have a huge potential for plant meiosis studies. For instance, one specific chromosome pair or just a chromosome section can be studied in the wheat background using genomic *in situ* hybridization (GISH) and, consequently rearrangements and interactions can be also analyze uniquely at the distal chromosome regions in a pair of homologous chromosomes (Naranjo et al., 2010; Rey et al., 2015b).

The analysis of the terminal chromosome regions is greatly important in a breeding framework, as telomeres and subtelomeres drive chromosome movements facilitating chromosome interactions, homologous pairing, and consequently recombination. In addition, crossovers are usually located at the terminal region of the chromosomes, as we have described before. In the case of a plant polyploid species such as wheat, pairing and recombination between wheat chromosomes and those from related species carrying desirable traits are suppressed because of its big genome stability, which have adverse effects in a plant breeding framework. Thus, it is crucial to study the effect of terminal regions including telomeres and subtelomeres on chromosome recognition and pairing in the framework of plant breeding. In the polyploid wheat background, addition lines of an extra wild barley pair of homologous chromosomes with terminal deletions are also available (Said et al., 2012). *In situ* hybridization in meiocytes in early meiosis was carried out in these wheat lines to shed light on the subtelomeres effect on the initial processes of homologous recognition and pairing at the onset of meiosis. When subtelomeres are absent, homologous chromosomes are not able to recognize each other and cannot initiate chromosome pairing (Calderón et al., 2014). In addition, chromatin remodeling also fail in the arms without subtelomeres, which implies a delay in pairing, although the pairing signal can be conducted from the other chromosome end which carry subtelomeres and can initiate chromosome pairing. These observations also contribute to explain the lack of recombination in these terminal chromosome regions (Calderón et al., 2014). The absence of recombination in the terminal region of chromosomes was also confirmed in wheat lines with a distal deletion of any chromosome arm. As it was mentioned before, the level of chiasma frequency reached in these deleted chromosomes did not reach the one on the intact chromosomes (Naranjo, 2015b), supporting the importance of the subtelomeric regions in recombination.

Several approaches have been exploited to promote and increase chromosome interactions and recombination between non-homologous chromosomes in a breeding framework. The *Ph1* locus is the main wheat locus suppressing homoeologous recombination between alien and wheat chromosomes, limiting the introgression of desired traits from wheat relatives (Riley and Chapman, 1958; Sears, 1976). Pairing can occur between related chromosomes in lines carrying deletions encompassing the *Ph1* locus, but the chromosomes are heavily rearranged, making recombination between the wheat and related chromosomes difficult but possible. However, interspecific recombination between *Hordeum* species and wheat has been reported at the terminal chromosome regions when the *Ph1* locus was not present (Calderón and Prieto, 2021).

Other approaches have been used from the early fifties with the aim of transferring genes from one species to another. For example, Sears (1956) transferred resistance genes from *Aegilops umbellulata* into wheat. The gametocidal genes are also a tool to transfer chromosomal segments into wheat (Masoudi-Nejad et al., 2002). Unfortunately, these techniques create random breaks and fusion between chromosomes; consequently, most chromosome translocations happen between non-homologs, getting genetic duplications or deficiencies which are not genetically equilibrated. Thus, these random chromosome manipulations are not interesting in plant breeding to be used as genetic tools. It is necessary the development of chromosome manipulation methods that might affect homoeologous chromosome interactions and recombination. Thus, it would be possible to generate more stable genetic introgressions which could be genetically compensated and transmitted to the next generation. A better picture to allow the manipulation of chromosome associations and promote interspecific recombination for plant breeding purposes can be provided by improving our insights into the genetic factors controlling chromosome dynamics and associations at the terminal chromosome regions including telomeres and subtelomeres during meiosis in model plant species such as wheat.

AUTHOR CONTRIBUTIONS

MA and PP conceived and wrote this review. All authors contributed to the article and approved the submitted version.

FUNDING

This review has been funded by grant PID2019-103996RB-I00 from Spanish Ministerio de Ciencia e Innovación.

ACKNOWLEDGMENTS

The authors deeply appreciate reviewers' comments.

REFERENCES

Achrem, M., Szućko, I., and Kalinka, A. (2020). The epigenetic regulation of centromeres and telomeres in plants and animals. *Comp. Cytogenet.* 14, 265–311. doi: 10.3897/CompCytogen.v14i2.51895

Agrawal, A., Ganai, N., Sengupta, S., and Menon, G. I. (2020). Nonequilibrium biophysical processes influence the large-scale architecture of the cell nucleus. *Biophys. J.* 118, 2229–2244. doi: 10.1016/j.bpj.2019.11.017

Aguilar, M., and Prieto, P. (2020). Sequence analysis of wheat subtelomeres reveals a high polymorphism among homoeologous chromosomes. *Plant Genome* 13:e20065. doi: 10.1002/tpg2.20065

Alkhimova, O. G., Mazurok, N. A., Potapova, T. A., Zakian, S. M., Heslop-Harrison, J. S., and Vershinin, A. V. (2004). Diverse patterns of the tandem repeats organization in rye chromosomes. *Chromosoma* 113, 42–52. doi: 10.1007/s00412-004-0294-4

Anamthawat-Jonsson, K., and Heslop-Harrison, J. S. (1990). Centromeres, telomeres and chromatin in the interphase nucleus of cereals. *Caryologia* 43, 205–213. doi: 10.1080/00087114.1990.10796999

Armstrong, S. J., Franklin, F. C., and Jones, G. H. (2001). Nucleolus-associated telomere clustering and pairing precede meiotic chromosome synapsis in *Arabidopsis thaliana*. *J. Cell Sci.* 114, 4207–4217. doi: 10.1242/jcs.114.23.4207

Asensi-Fabado, M. A., Amtmann, A., and Perrella, G. (2017). Plant responses to abiotic stress: the chromatin context of transcriptional regulation. *Biochim. Biophys. Acta Gene Regul. Mech.* 1860, 106–122. doi: 10.1016/j.bbagrm.2016.07.015

Barrales, R. R., Forn, M., Georgescu, P. R., Sarkadi, Z., and Braun, S. (2016). Control of heterochromatin localization and silencing by the nuclear membrane protein Lem2. *Genes Dev.* 30, 133–148. doi: 10.1101/gad.271288.115

Barzel, A., and Kupier, M. (2018). Finding a match: how do homologous sequences get together for recombination? *Nat. Rev. Genet.* 9, 27–37. doi: 10.1038/nrg2224

Beagan, J. A., Duong, M. T., Titus, K. R., Zhou, L., Cao, Z., Ma, J., et al. (2017). YY1 and CTCF orchestrate a 3D chromatin looping switch during early neural lineage commitment. *Genome Res.* 27, 1139–1152. doi: 10.1101/gr.215160.116

Belmont, A. S., Li, G., Sudlow, G., and Robinett, C. (1999). Visualization of large-scale chromatin structure and dynamics using the lac operator/lac repressor reporter system. *Methods Cell Biol.* 58, 203–222. doi: 10.1016/s0091-679x(08)61957-3

Berr, A., Pecinka, A., Meister, A., Kreth, G., Fuchs, J., Blattner, F. R., et al. (2006). Chromosome arrangement and nuclear architecture but not centromeric sequences are conserved between *Arabidopsis thaliana* and *Arabidopsis lyrata*. *Plant J.* 48, 771–783. doi: 10.1111/j.1365-313X.2006.02912.x

Berr, A., and Schubert, I. (2007). Interphase chromosome arrangement in *Arabidopsis thaliana* is similar in differentiated and meristematic tissues and shows a transient mirror symmetry after nuclear division. *Genetics* 176, 853–863. doi: 10.1534/genetics.107.073270

Blackburn, E. H. (2005). Telomerase and cancer - Kirk A. Landon - AACR prize for basic cancer research lecture. *Mol. Cancer Res.* 3, 477–482. doi: 10.1158/1541-7786.MCR-05-0147

Blokhina, Y. P., Nguyen, A. D., Draper, B. W., and Burgess, S. M. (2019). The telomere bouquet is a hub where meiotic double-strand breaks, synapsis, and stable homolog juxtaposition are coordinated in the zebrafish, *Danio rerio*. *PLoS Genet.* 15:e1007730. doi: 10.1371/journal.pgen.1007730

Boveri, T. (1909). Die Blastomerenkerne von Ascaris megalocephala und die Theorie der Chromosomenindividualitat. *Arch. Zellforsch.* 3, 181–286.

Brown, C. A., Murray, A. W., and Verstrepen, K. J. (2010). Rapid expansion and functional divergence of subtelomeric gene families in yeasts. *Curr. Biol.* 20, 895–903. doi: 10.1016/j.cub.2010.04.027

Bryan, T. M., Englezou, A., DallaPozza, L., Dunham, M. A., and Reddel, R. R. (1997). Evidence for an alternative mechanism for maintaining telomere length in human tumors and tumor-derived cell lines. *Nat. Med.* 3, 1271–1274. doi: 10.1038/nm1197-1271

Calderón, M. C., and Prieto, P. (2021). Wild and cultivated homoeologous barley chromosomes can associate and recombine in wheat in the absence of the *Ph1* locus. *Agronomy* 11:147. doi: 10.3390/agronomy11010147

Calderón, M. C., Rey, M. D., Cabrera, A., and Prieto, P. (2014). The subtelomeric region is important for chromosome recognition and pairing during meiosis. *Sci. Rep.* 4:6488. doi: 10.1038/srep06488

Calderón, M. C., Rey, M. D., Martín, A., and Prieto, P. (2018). Homoeologous chromosomes from two Hordeum species can recognize and associate during meiosis in wheat in the presence of the *Ph1* locus. *Front. Plant Sci.* 9:585. doi: 10.3389/fpls.2018.00585

Carlson, P. S. (2016). Mitotic crossing-over in a higher plant. *Genet. Res.* 24, 109–112. doi: 10.1017/S0016672300015123

Carlton, P. M., Cowan, C. R., and Cande, W. Z. (2003). Directed motion of telomeres in the formation of the meiotic bouquet revealed by time course and simulation analysis. *Mol. Biol. Cell* 14, 2832–2843. doi: 10.1091/mbc.e02-11-0760

Cesare, A. J., Quinney, N., Willcox, S., Subramanian, D., and Griffith, J. D. (2003). Telomere looping in *P. sativum* (common garden pea). *Plant J.* 36, 271–279. doi: 10.1046/j.1365-313X.2003.01882.x

Chang, S. B., and de Jong, H. (2005). Production of alien chromosome additions and their utility in plant genetics. *Cytogenet. Genome Res.* 109, 335–343. doi: 10.1159/000082417

Chaumeil, J., Micsinai, M., and Skok, J. A. (2013). Combined immunofluorescence and DNA FISH on 3D-preserved interphase nuclei to study changes in 3D nuclear organization. *J. Vis. Exp.* 72:e50087. doi: 10.3791/50087

Choi, K., Zhao, X., Lambing, C., Underwood, C. J., Hardcastle, T. J., Serra, H., et al. (2018). Nucleosomes and DNA methylation shape meiotic DSB frequency in *Arabidopsis thaliana* transposons and gene regulatory regions. *Genome Res.* 28, 532–546. doi: 10.1101/gr.225599.117

Cifuentes-Rojas, C., Kannan, K., Tseng, L., and Shippen, D. E. (2011). Two RNA subunits and POT1a are components of *Arabidopsis* telomerase. *Proc. Natl. Acad. Sci. U. S. A.* 108, 73–78. doi: 10.1073/pnas.1013021107

Concia, L., Brooks, A. M., Wheeler, E., Zynda, G. J., Wear, E. E., LeBlanc, C., et al. (2018). Genome-wide analysis of the *Arabidopsis* replication timing program. *Plant Physiol.* 176, 2166–2185. doi: 10.1104/pp.17.01537

Concia, L., Veluchamy, A., Ramirez-Prado, J. S., Martin-Ramirez, A., Huang, Y., Perez, M., et al. (2020). Wheat chromatin architecture is organized in genome territories and transcription factories. *Genome Biol.* 21:104. doi: 10.1186/s13059-020-01998-1

Cook, P. R. (1997). The transcriptional basis of chromosome pairing. *J. Cell Sci.* 110, 1033–1040. doi: 10.1242/jcs.110.9.1033

Cosgrove, M. S., and Wolberger, C. (2005). How does the histone code work? *Biochem. Cell Biol.* 83, 468–476. doi: 10.1139/o05-137

Coutou, F., Goodyer, W., and Zetka, M. (2004). Finding and keeping your partner during meiosis. *Cell Cycle* 3, 1014–1016. doi: 10.4161/cc.3.8.1077

Cowan, C. R., and Cande, W. Z. (2002). Meiotic telomere clustering is inhibited by colchicine but does not require cytoplasmic microtubules. *J. Cell Sci.* 115, 3747–3756. doi: 10.1242/jcs.00055

Cowan, C. R., Carlton, P. M., and Cande, W. Z. (2001). The polar arrangement of telomeres in interphase and meiosis: Rabl organization and the bouquet. *Plant Physiol.* 125, 532–538. doi: 10.1104/pp.125.2.532

Cremer, M., von Hase, J., Volm, T., Brero, A., Kreth, G., Walter, J., et al. (2001). Non-random radial higher-order chromatin arrangements in nuclei of diploid human cells. *Chromosom. Res.* 9, 41–567. doi: 10.1023/a:1012495201697

Daron, J., Glover, N., Pingault, L., Theil, S., Jamilloux, V., Paux, E., et al. (2014). Organization and evolution of transposable elements along the bread wheat chromosome 3B. *Genome Biol.* 15:46. doi: 10.1186/s13059-014-0546-4

Darrier, B., Rimbert, H., Balfourier, F., Pingault, L., Josselin, A. A., Servin, B., et al. (2017). High-resolution mapping of crossover events in the hexaploid wheat genome suggests a universal recombination mechanism. *Genetics* 206, 1373–1388. doi: 10.1534/genetics.116.196014

Dawe, K. R., Sedat, J. W., Agard, D. A., and Cande, W. Z. (1994). Meiotic chromosome pairing in maize is associated with a novel chromosome structure. *Cell* 76, 901–912. doi: 10.1016/0092-8674(94)90364-6

De Lange, T. (2005). Shelterin: The protein complex that shapes and safeguards human telomeres. *Genes Dev.* 19, 2100–2110. doi: 10.1101/gad.1346005

De Lange, T. (2018). What I got wrong about shelterin. *J. Biol. Chem.* 293, 10453–10456. doi: 10.1074/jbc.AW118.003234

De Nooijer, S., Wellink, J., Mulder, B., and Bisseling, T. (2009). Non-specific interactions are sufficient to explain the position of heterochromatic chromocenters and nucleoli in interphase nuclei. *Nucleic Acids Res.* 37, 3558–3568. doi: 10.1093/nar/gkp219

De Wit, E., and de Laat, W. (2012). A decade of 3C technologies: insights into nuclear organization. *Genes Dev.* 26, 11–24. doi: 10.1101/gad.179804.111

Deal, R. B., Henikoff, J. G., and Henikoff, S. (2010). Genome-wide kinetics of nucleosome turnover determined by metabolic labeling of histones. *Science* 328, 1161–1164. doi: 10.1126/science.1186777

Dekker, J. (2006). The three 'C' s of chromosome conformation capture: controls, controls, controls. *Nat. Methods* 3, 17–21. doi: 10.1038/nmeth823

Dekker, J., Marti-Renom, M. A., and Mirny, L. A. (2013). Exploring the three-dimensional organization of genomes: interpreting chromatin interaction data. *Nat. Rev. Genet.* 14, 390–403. doi: 10.1038/nrg3454

Ding, D. Q., Haraguchi, T., and Hiraoka, Y. (2010). From meiosis to postmeiotic events: alignment and recognition of homologous chromosomes in meiosis. *FEBS J.* 277, 565–570. doi: 10.1111/j.1742-4658.2009.07501.x

Ding, D. Q., Haraguchi, T., and Hiraoka, Y. (2012). Chromosomally-retained RNA mediates homologous pairing. *Nucleus* 3, 516–519. doi: 10.4161/nucl.22732

Ding, D. Q., Matsuda, A., Okamasa, K., Nagahama, Y., Haraguchi, T., and Hiraoka, Y. (2016). Meiotic cohesin-based chromosome structure is essential for homologous chromosome pairing in *Schizosaccharomyces pombe*. *Chromosoma* 125, 205–214. doi: 10.1007/s00412-015-0551-8

Dixon, J. R., Gorkin, D. U., and Ren, B. (2016). Chromatin domains: the unit of chromosome organization. *Mol. Cell* 62, 668–680. doi: 10.1016/j.molcel.2016.05.018

Doğan, E. S., and Liu, C. (2018). Three-dimensional chromatin packing and positioning of plant genomes. *Nat. Plants* 4, 521–529. doi: 10.1038/s41477-018-0199-5

Dong, F., and Jiang, J. (1998). Non-Rabl patterns of centromere and telomere distribution in the interphase nuclei of plant cells. *Chromosom. Res.* 6, 551–558. doi: 10.1023/A:1009280425125

Dong, Q., Li, N., Li, X., Yuan, Z., Xie, D., Wang, X., et al. (2018). Genome-wide Hi-C analysis reveals extensive hierarchical chromatin interactions in rice. *Plant J.* 94, 1141–1156. doi: 10.1111/tpj.13925

Dreissig, S., Schiml, S., Schindele, P., Weiss, O., Rutten, T., Schubert, V., et al. (2017). Live-cell imaging in plants reveals dynamic telomere movements. *Plant J.* 91, 565–573. doi: 10.1111/tpj.13601

Duc, C., Benoit, M., Détourné, G., Simon, L., Poulet, A., Jung, M., et al. (2017). *Arabidopsis* ATRX modulates H3.3 occupancy and fine-tunes gene expression. *Plant Cell* 29, 1773–1793. doi: 10.1105/tpc.16.00877

Ebrahimi, H., and Cooper, J. P. (2016). Finding a place in the SUN: telomere maintenance in a diverse nuclear landscape. *Curr. Opin. Cell Biol.* 40, 145–152. doi: 10.1016/j.ceb.2016.03.011

Emden, T. S., Forn, M., Forné, I., Sarkadi, Z., Capella, M., Martín-Caballero, L., et al. (2019). Shelterin and subtelomeric DNA sequences control nucleosome maintenance and genome stability. *EMBO Rep.* 20:e47181. doi: 10.15252/embr.201847181

Evtushenko, E. V., Levitsky, V. G., Elisafenko, E. A., Gunbin, K. V., Belousov, A. I., Šafář, J., et al. (2016). The expansion of heterochromatin blocks in rye reflects the co-amplification of tandem repeats and adjacent transposable elements. *BMC Genomics* 17:337. doi: 10.1186/s12864-016-2667-5

Fajkus, J., Kovarik, A., Kralovics, R., and Bezdek, M. (1995a). Organization of telomeric and subtelomeric chromatin in the higher plant *Nicotiana tabacum*. *Mol. Gen. Genet.* 247, 633–638. doi: 10.1007/BF00290355

Fajkus, J., Kralovics, R., Kovarik, A., and Fajkusova, L. (1995b). The telomeric sequence is directly attached to the HRS60 subtelomeric tandem repeat in tobacco chromosomes. *FEBS Lett.* 364, 33–35. doi: 10.1016/0014-5793(95)00347-C

Fajkus, P., Peška, V., Závodník, M., Fojtová, M., Fulnečková, J., Dobias, S., et al. (2019). Telomerase RNAs in land plants. *Nucleic Acids Res.* 47, 9842–9856. doi: 10.1093/nar/gkz695

Fan, C., Zhang, Y., Yu, Y., Rounsley, S., Long, M., and Wing, R. A. (2008). The subtelomere of *Oryza sativa* chromosome 3 short arm as a hot bed of new gene origination in rice. *Mol. Plant* 1, 839–850. doi: 10.1093/mp/ssn050

Fernández-Álvarez, A., Bez, C., O'Toole, E. T., Morphew, M., and Cooper, J. P. (2016). Mitotic nuclear envelope breakdown and spindle nucleation are controlled by interphase contacts between centromeres and the nuclear envelope. *Dev. Cell* 39, 544–559. doi: 10.1016/j.devcel.2016.10.021

Filler-Hayut, S., Melamed-Bessudo, C., and Levy, A. A. (2017). Targeted recombination between homologous chromosomes for precise breeding in tomato. *Nat. Commun.* 8:15605. doi: 10.1038/ncomms15605

Fitzgerald, M. S., Riha, K., Gao, F., Ren, S., McKnight, T. D., and Shippen, D. E. (1999). Disruption of the telomerase catalytic subunit gene from *Arabidopsis* inactivates telomerase and leads to a slow loss of telomeric DNA. *Proc. Natl. Acad. Sci. U. S. A.* 96, 14813–14818.

Fransz, P., De Jong, J. H., Lysak, M., Castiglione, M. R., and Schubert, I. (2002). Interphase chromosomes in *Arabidopsis* are organized as well defined chromocenters from which euchromatin loops emanate. *Proc. Natl. Acad. Sci. U. S. A.* 99, 14584–14589. doi: 10.1073/pnas.212325299

Fraune, J., Schramm, S., Alsheimer, M., and Benavente, R. (2012). The mammalian synaptonemal complex: protein components, assembly and role in meiotic recombination. *Exp. Cell Res.* 318, 1340–1346. doi: 10.1016/j.yexcr.2012.02.018

Gandhi, M., Evdokimova, V. N., Cuenco, K. T., Bakkenist, C. J., and Nikiforov, Y. E. (2013). Homologous chromosomes move and rapidly initiate contact at the sites of double-strand breaks in genes in G_0-phase human cells. *Cell Cycle* 12, 547–552. doi: 10.4161/cc.23754

Garrido-Ramos, M. A. (2015). Satellite DNA in plants: more than just rubbish. *Cytogenet. Genome Res.* 146, 153–170. doi: 10.1159/000437008

Gerton, J. L., and Hawley, R. S. (2005). Homologous chromosome interactions in meiosis: diversity amidst conservation. *Nat. Rev. Genet.* 6, 477–487. doi: 10.1038/nrg1614

Gisler, B., Solomon, S., and Puchta, H. (2002). The role of double-strand break-induced allelic homologous recombination in somatic plant cells. *Plant J.* 32, 277–284. doi: 10.1046/j.1365-313X.2002.01421.x

Golubovskaya, I. N., Harper, L. C., Pawlowski, W. P., Schichnes, D., and Cande, W. Z. (2002). The pam1 gene is required for meiotic bouquet formation and efficient homologous synapsis in maize (*Zea mays* L.). *Genetics* 162, 1979–1993. doi: 10.1093/genetics/162.4.1979

Grasser, K. D. (2003). Chromatin-associated HMGA and HMGB proteins: versatile co-regulators of DNA-dependent processes. *Plant Mol. Biol.* 53, 281–295. doi: 10.1023/B:PLAN.0000007002.99408.ba

Graumann, K. (2014). Evidence for LINC1-SUN associations at the plant nuclear periphery. *PLoS One* 9:7. doi: 10.1371/journal.pone.0093406

Griffith, J. D., Comeau, L., Rosenfield, S., Stansel, R. M., Bianchi, A., Moss, H., et al. (1999). Mammalian telomeres end in a large duplex loop. *Cell* 97, 503–514. doi: 10.1016/S0092-8674(00)80760-6

Guelen, L., Pagie, L., Brasset, E., Meuleman, W., Faza, M. B., Talhout, W., et al. (2008). Domain organization of human chromosomes revealed by mapping of nuclear lamina interactions. *Nature* 453, 948–951. doi: 10.1038/nature06947

Heacock, M., Spangler, E., Riha, K., Puizina, J., and Shippen, D. E. (2004). Molecular analysis of telomere fusions in *Arabidopsis*: multiple pathways for chromosome end-joining. *EMBO J.* 23, 2304–2313. doi: 10.1038/sj.emboj.7600236

Heitz, E. (1928). Das Heterochromatin der Moose. *Jahrb. Wiss. Bot.* 69, 762–818.

Hiraoka, Y. (2020). Phase separation drives pairing of homologous chromosomes. *Curr. Genet.* 66, 881–887. doi: 10.1007/s00294-020-01077-9

Hockemeyer, D., Daniels, J. P., Takai, H., and de Lange, T. (2006). Recent expansion of the telomeric complex in rodents: two distinct POT1 proteins protect mouse telomeres. *Cell* 126, 63–77. doi: 10.1016/j.cell.2006.04.044

Hou, H. T., Zhou, Z., Wang, Y., Wang, J. Y., Kallgren, S. P., Kurchuk, T., et al. (2012). Csi1 links centromeres to the nuclear envelope for centromere clustering. *J. Cell Biol.* 199, 735–744. doi: 10.1083/jcb.201208001

Hu, B., Wang, N., Bi, X. L., Karaaslan, E. S., Weber, A. L., Zhu, W. S., et al. (2019). Plant Lamin-like proteins mediate chromatin tethering at the nuclear periphery. *Genome Biol.* 20:87. doi: 10.1186/s13059-019-1694-3

Jarillo, J. A., and Piñeiro, M. (2015). H2A.Z mediates different aspects of chromatin function and modulates flowering responses in *Arabidopsis*. *Plant J.* 83, 96–109. doi: 10.1111/tpj.12873

Jiang, D., and Berger, F. (2017). DNA replication-coupled histone modification maintains Polycomb gene silencing in plants. *Science* 357, 1146–1149. doi: 10.1126/science.aan4965

Jordan, P. (2006). Initiation of homologous chromosome pairing during meiosis. *Biochem. Soc. Trans.* 34, 545–549. doi: 10.1042/BST0340545

Islam, A. K. M. R., Shepherd, K. W., and Sparrow, D. H. B. (1978). "Production and characterization of wheat–barley addition lines," in *Proceedings of the 5th International Wheat Genetics Symposium*. ed. S. Ramanujam (Science Publishers Inc., India), 356–371.

Islam, A. K. M. R., Shepherd, K. W., and Sparrow, D. H. B. (1981). Isolation and characterization of euplasmic wheat–barley chromosome addition lines. *Heredity* 46, 160–174. doi: 10.1038/hdy.1981.24

Kazda, A., Zellinger, B., Rossler, M., Derboven, E., Kusenda, B., and Riha, K. (2012). Chromosome end protection by blunt-ended telomeres. *Genes Dev.* 26, 1703–1713. doi: 10.1101/gad.194944.112

Keeney, S. (2008). Spo11 and the formation of DNA double-strand breaks in meiosis. *Genome Dyn. Stab.* 2, 81–123. doi: 10.1007/7050_2007_026

Kilian, A., Heller, K., and Kleinhofs, A. (1998). Development patterns of telomerase activity in barley and maize. *Plant Mol. Biol.* 37, 621–628. doi: 10.1023/A:1005994629814

Kilian, A., Stiff, C., and Kleinhofs, A. (1995). Barley telomeres shorten during differentiation but grow in callus culture. *Proc. Natl. Acad. Sci. U. S. A.* 92, 9555–9559.

Kim, J. H. (2019). Chromatin remodeling and epigenetic regulation in plant DNA damage repair. *Int. J. Mol. Sci.* 20:4093. doi: 10.3390/ijms20174093

Kleckner, N., Zickler, D., and Guillaume, W. (2013). Chromosome capture brings it all together. *Science* 342, 940–941. doi: 10.1126/science.1247514

Knoll, A., Fauser, F., and Puchta, H. (2014). DNA recombination in somatic plant cells: mechanisms and evolutionary consequences. *Chromosom. Res.* 22, 191–201. doi: 10.1007/s10577-014-9415-y

Kouzine, F., Levens, D., and Baranello, L. (2014). DNA topology and transcription. *Nucleus* 5, 195–202. doi: 10.4161/nucl.28909

Koyama, M., and Kurumizaka, H. (2018). Structural diversity of the nucleosome. *J. Biochem.* 163, 85–95. doi: 10.1093/jb/mvx081

Kuo, F., Olsen, K. M., and Richards, E. J. (2006). Natural variation in a subtelomeric region of *Arabidopsis*: implications for the genomic dynamics of a chromosome end. *Genetics* 173, 401–417. doi: 10.1534/genetics.105.055202

Lamb, J. C., Meyer, J. M., Corcoran, B., Kato, A., Han, F., and Birchler, J. A. (2007). Distinct chromosomal distribution of highly repetitive sequences in maize. *Chromosom. Res.* 15, 33–49. doi: 10.1007/s10577-006-1102-1

Law, J. A., and Jacobsen, S. E. (2010). Establishing, maintaining and modifying DNA methylation patterns in plants and animals. *Nat. Rev. Genet.* 11, 204–220. doi: 10.1038/nrg2719

Lee, J. S., Smith, E., and Shilatifard, A. (2010). The language of histone crosstalk. *Cell* 142, 682–685. doi: 10.1016/j.cell.2010.08.011

Leung, J., and Gaudin, V. (2020). Who rules the cell? An Epi-tale of histone, DNA, RNA, and the metabolic deep state. *Front. Plant Sci.* 11:181. doi: 10.3389/fpls.2020.00181

Li, W., Zhang, P., Fellers, J. P., Friebe, B., and Gill, B. S. (2004). Sequence composition, organization, and evolution of the core Triticeae genome. *Plant J.* 40, 500–511. doi: 10.1111/j.1365-313X.2004.02228.x

Lieberman-Lazarovich, M., and Levy, A. (2011). Homologous recombination in plants: an antireview. *Methods Mol. Biol.* 701, 51–65. doi: 10.1007/978-1-61737-957-4_3

Linardopoulou, E. V., Williams, E. M., Fan, Y. X., Friedman, C., Young, J. M., and Trask, B. J. (2005). Human subtelomeres are hotspots of interchromosomal recombination and segmental duplication. *Nature* 437, 94–100. doi: 10.1038/nature04029

Liu, C., Cheng, Y. J., Wang, J. W., and Weigel, D. (2017). Prominent topologically associated domains differentiate global chromatin packing in rice from Arabidopsis. *Nat. Plants* 3, 742–748. doi: 10.1038/s41477-017-0005-9

Liu, C., Wang, C., Wang, G., Becker, C., Zaidem, M., and Weigel, D. (2016). Genome-wide analysis of chromatin packing in *Arabidopsis thaliana* at single-gene resolution. *Genome Res.* 26, 1057–1068. doi: 10.1101/gr.204032.116

Lorković, Z. J., Park, C., Goiser, M., Jiang, D., Kurzbauer, M. T., Schlögelhofer, P., et al. (2017). Compartmentalization of DNA damage response between heterochromatin and euchromatin is mediated by distinct H2A histone variants. *Curr. Biol.* 27, 1192–1199. doi: 10.1016/j.cub.2017.03.002

Louis, E. J. (2014). "Introduction," in *Subtelomeres*. eds. E. J. Louis and M. M. Becker (Berlin: Springer), 1–12.

Louis, E. J., and Vershinin, A. V. (2005). Chromosome ends: different sequences may provide conserved functions. *BioEssays* 27, 685–697. doi: 10.1002/bies.20259

Lysak, M. A., Fransz, P. F., Ali, H. B., and Schubert, I. (2001). Chromosome painting in *Arabidopsis thaliana*. *Plant J.* 28, 689–697. doi: 10.1046/j.1365-313x.2001.01194.x

Mainiero, S., and Pawlowski, W. P. (2014). Meiotic chromosome structure and function in plants. *Cytogenet. Genome Res.* 143, 6–17. doi: 10.1159/000365260

Majerova, E., Fojtova, M., Mozgova, I., Bittova, M., and Fajkus, J. (2011). Hypomethylating drugs efficiently decrease cytosine methylation in telomeric DNA and activate telomerase without affecting telomere lengths in tobacco cells. *Plant Mol. Biol.* 77, 371–380. doi: 10.1007/s11103-011-9816-7

Majerova, E., Mandakova, T., Vu, G. T. H., Fajkus, J., Lysak, M. A., and Fojtova, M. (2014). Chromatin features of plant telomeric sequences at terminal vs. internal positions. *Front. Plant Sci.* 5:593. doi: 10.3389/fpls.2014.00593

Malik, H. S., and Henikoff, S. (2003). Phylogenomics of the nucleosome. *Nat. Struct. Biol.* 10, 882–891. doi: 10.1038/nsb996

Manuelidis, L., and Borden, J. (1988). Reproducible compartmentalization of individual chromosome domains in human CNS cells revealed by *in situ* hybridization and three-dimensional reconstruction. *Chromosoma* 96, 397–410. doi: 10.1007/BF00303033

Marian, C. O., Bordoli, S. J., Goltz, M., Santarella, R. A., Jackson, L. P., Danilevskaya, O., et al. (2003). The maize single myb histone 1 gene, Smh1, belongs to a novel gene family and encodes a protein that binds telomere DNA repeats in vitro. *Plant Physiol.* 133, 1336–1350. doi: 10.1104/pp.103.026856

Marshall, W. F., and Fung, J. C. (2016). Modeling meiotic chromosome pairing: nuclear envelope attachment, telomere-led active random motion, and anomalous diffusion. *Phys. Biol.* 13:026003. doi: 10.1088/1478-3975/13/2/026003

Marshall, W. F., and Fung, J. C. (2019). Modeling meiotic chromosome pairing: A tug of war between telomere forces and a pairing-based Brownian ratchet leads to increased pairing fidelity. *Phys. Biol.* 16:046005. doi: 10.1088/1478-3975/ab15a7

Martínez-Pérez, E., Shaw, P., Aragón-Alcaide, L., and Moore, G. (2003). Chromosomes form into seven groups in hexaploid and tetraploid wheat as a prelude to meiosis. *Plant J.* 36, 21–29. doi: 10.1046/j.1365-313X.2003.01853.x

Martínez-Pérez, E., Shaw, P., Reader, S., Aragón-Alcaide, L., Miller, T., and Moore, G. (1999). Homologous chromosome pairing in wheat. *J. Cell Sci.* 112, 1761–1769. doi: 10.1242/jcs.112.11.1761

Masoudi-Nejad, A., Nasuda, S., Mcintosh, R. A., and Endo, T. R. (2002). Transfer of rye chromosome segments to wheat by a gametocidal system. *Chromosom. Res.* 10, 349–357. doi: 10.1023/A:1016845200960

McClintock, B. (1939). The behavior in successive nuclear divisions of a chromosome broken at meiosis. *Proc. Natl. Acad. Sci. U. S. A.* 25, 405–416.

McClintock, B. (1941). The stability of broken ends of chromosomes in *Zea mays*. *Genetics* 26, 234–282. doi: 10.1093/genetics/26.2.234

McGinty, R. K., and Tan, S. (2015). Nucleosome structure and function. *Chem. Rev.* 115, 2255–2273. doi: 10.1021/cr500373h

McNicoll, F., Stevense, M., and Jessberger, R. (2013). Cohesin in gametogenesis. *Curr. Top. Dev. Biol.* 102, 1–34. doi: 10.1016/B978-0-12-416024-8.00001-5

Menon, G. I. (2020). Chromatin as an active polymeric material. *Emerg. Top. Life Sci.* 4, 111–118. doi: 10.1042/ETLS20200010

Mikhailova, E. I., Sosnikhina, S. P., Kirillova, G. A., Tikholiz, O. A., Smirnov, V. G., Jones, N., et al. (2001). Nuclear dispositions of subtelomeric and pericentromeric chromosomal domains during meiosis in asynaptic mutants of rye (*Secale cereale* L.). *J. Cell Sci.* 114, 1875–1882. doi: 10.1242/jcs.114.10.1875

Miller, T. E., Hutchinson, J., and Chapman, V. (1982). Investigation of a preferentially transmitted *Aegilops sharonensis* chromosome in wheat. *Theor. Appl. Genet.* 61, 27–33. doi: 10.1007/BF00261506

Mizuno, H., Wu, J., Katayose, Y., Kanamori, H., Sasaki, T., and Matsumoto, T. (2008). Characterization of chromosome ends on the basis of the structure of TrsA subtelomeric repeats in rice (*Oryza sativa* L.). *Mol. Gen. Genomics.* 280, 19–24. doi: 10.1007/s00438-008-0341-6

Mizuno, H., Wu, J., and Matsumoto, T. (2014). "Characterization of chromosomal ends on the basis of chromosome specific telomere variants and subtelomeric repeats in rice (*Oryza sativa* L.)," in *Subtelomeres*. eds. E. J. Louis and M. M. Becker (Berlin: Springer), 187–194.

Muller, H., Gil, J., and Drinnenberg, I. A. (2019). The impact of centromeres on spatial genome architecture. *Trends Genet.* 35, 565–578. doi: 10.1016/j.tig.2019.05.003

Murphy, S. P., Gumber, H. K., Mao, Y., and Bass, H. W. (2014). A dynamic meiotic SUN belt includes the zygotene-stage telomere bouquet and is disrupted in chromosome segregation mutants of maize (*Zea mays* L.). *Front. Plant Sci.* 5:314. doi: 10.3389/fpls.2014.00314

Muyt, A. D., Mercier, R., Mézard, C., and Grelon, M. (2009). Meiotic recombination and crossovers in plants. *Genome Dyn.* 5, 14–25. doi: 10.1159/000166616

Nagaki, K., Talbert, P. B., Zhong, C. X., Dawe, R. K., Henikoff, S., and Jiang, J. (2003). Chromatin immunoprecipitation reveals that the 180-bp satellite repeat is the key functional DNA element of *Arabidopsis thaliana* centromeres. *Genetics* 163, 1221–1225. doi: 10.1093/genetics/163.3.1221

Nannas, N. J., Higgins, D. M., and Dawe, R. K. (2016). Anaphase asymmetry and dynamic repositioning of the division plane during maize meiosis. *J. Cell Sci.* 129, 4014–4024. doi: 10.1242/jcs.194860

Naranjo, T. (2014). Dynamics of rye telomeres in a wheat background during early meiosis. *Cytogenet. Genome Res.* 143, 60–68. doi: 10.1159/000363524

Naranjo, T. (2015a). Contribution of structural chromosome mutants to the study of meiosis in plants. *Cytogenet. Genome Res.* 147, 55–69. doi: 10.1159/000442219

Naranjo, T. (2015b). Forcing the shift of the crossover site to proximal regions in wheat chromosomes. *Theor. Appl. Genet.* 128, 1855–1863. doi: 10.1007/s00122-015-2552-7

Naranjo, T., Valenzuela, N. T., and Perera, E. (2010). Chiasma frequency is region specific and chromosome conformation dependent in a rye chromosome added to wheat. *Cytogenet. Genome Res.* 129, 33–142. doi: 10.1159/000314029

Němečková, A., Koláčková, V., Vrána, J., Doležel, J., and Hřibová, E. (2020). DNA replication and chromosome positioning throughout the interphase in three dimensional space of plant nuclei. *J. Exp. Bot.* 71, 6262–6272. doi: 10.1093/jxb/eraa370

Nishiyama, T. (2019). Cohesion and cohesin-dependent chromatin organization. *Curr. Opin. Cell Biol.* 58, 8–14. doi: 10.1016/j.ceb.2018.11.006

Ogrocka, A., Polanska, P., Majerova, E., Janeba, Z., Fajkus, J., and Fojtova, M. (2014). Compromised telomere maintenance in hypomethylated *Arabidopsis thaliana* plants. *Nucleic Acids Res.* 42, 2919–2931. doi: 10.1093/nar/gkt1285

Okada, T., Endo, M., Singh, M. B., and Bhalla, P. L. (2005). Analysis of the histone H3 gene family in *Arabidopsis* and identification of the male-gamete-specific variant AtMGH3. *Plant J.* 44, 557–568. doi: 10.1111/j.1365-313X.2005.02554.x

Oko, Y., Ito, N., and Sakamoto, T. (2020). The mechanisms and signifcance of the positional control of centromeres and telomeres in plants. *J. Plant Res.* 133, 471–478. doi: 10.1007/s10265-020-01202-2

Parrilla-Doblas, J. T., Roldán-Arjona, T., Ariza, R. R., and Córdoba-Cañero, D. (2019). Active DNA Demethylation in plants. *Int. J. Mol. Sci.* 20:4683. doi: 10.3390/ijms20194683

Pecinka, A., Schubert, V., Meister, A., Kreth, G., Klatte, M., Lysak, M. A., et al. (2004). Chromosome territory arrangement and homologous pairing in nuclei of *Arabidopsis thaliana* are predominantly random except for NOR bearing chromosomes. *Chromosoma* 113, 258–269. doi: 10.1007/s00412-004-0316-2

Pernickova, K., Linc, G., Gaal, E., Kopecký, D., Šamajová, O., and Lukaszewski, A. (2019). Out-of-position telomeres in meiotic leptotene appear responsible for chiasmata pairing in an inversion heterozygote in wheat (*Triticum aestivum* L.). *Chromosoma* 128, 31–39. doi: 10.1007/s00412-018-0686-5

Peska, V., and Garcia, S. (2020). Origin, diversity, and evolution of telomere sequences in plants. *Front. Plant Sci.* 11:117. doi: 10.3389/fpls.2020.00117

Peska, V., Schrumpova, P. P., and Fajkus, J. (2011). Using the telobox to search for plant telomere binding proteins. *Curr. Protein Pept. Sci.* 12, 75–83. doi: 10.2174/138920311795684968

Petracek, M. E., Lefebvre, P. A., Silflow, C. D., and Berman, J. (1990). Chlamydomonas telomere sequences are A+T-rich but contain three consecutive G–C base pairs. *Proc. Natl. Acad. Sci. U. S. A.* 87, 8222–8226.

Phair, R. D., and Misteli, T. (2001). Kinetic modelling approaches to in vivo imaging. *Nat. Rev. Mol. Cell Biol.* 2, 898–907. doi: 10.1038/35103000

Pich, U., and Schubert, I. (1998). Terminal heterochromatin and alternative telomeric sequences in *Allium cepa*. *Chromosom. Res.* 6, 315–321. doi: 10.1023/A:1009227009121

Pontvianne, F., Carpentier, M. C., Durut, N., Pavlištová, V., Jaške, K., Schořová, S., et al. (2016). Identification of nucleolus-associated chromatin domains reveals a role for the nucleolus in 3D Organization of the *A. thaliana* genome. *Cell Rep.* 16, 1574–1587. doi: 10.1016/j.celrep.2016.07.016

Pontvianne, F., and Liu, C. (2020). Chromatin domains in space and their functional implications. *Curr. Opin. Plant Biol.* 54, 1–10. doi: 10.1016/j.pbi.2019.11.005

Poulet, A., Duc, C., Voisin, M., Desset, S., Tutois, S., Vanrobays, E., et al. (2017). The LINC complex contributes to heterochromatin organisation and transcriptional gene silencing in plants. *J. Cell Sci.* 130, 590–601. doi: 10.1242/jcs.194712

Prieto, P., Martin, A., and Cabrera, A. (2004a). Chromosomal distribution of telomeric and telomeric-associated sequences in *Hordeum chilense* by *in situ* hybridization. *Hereditas* 141, 122–127. doi: 10.1111/j.1601-5223.2004.01825.x

Prieto, P., Santos, A. P., Moore, G., and Shaw, P. (2004b). Chromosomes associate premeiotically and in xylem vessel cells via their telomeres and centromeres in diploid rice (*Oryza sativa*). *Chromosoma* 112, 300–307. doi: 10.1007/s00412-004-0274-8

Prieto, P., Shaw, P., and Moore, G. (2004c). Homologue recognition during meiosis is associated with a change in chromatin conformation. *Nat. Cell Biol.* 6, 906–908. doi: 10.1038/ncb1168

Probst, A. V., Desvoyes, B., and Gutiérrez, C. (2020). Similar yet critically different: the distribution, dynamics and function of histone variants. *J. Exp. Bot.* 71, 5191–5204. doi: 10.1093/jxb/eraa230

Procházková-Schrumpfová, P., Fojtová, M., and Fajkus, J. (2019). Telomeres in plants and humans: not so different, not so similar. *Cell* 8:58. doi: 10.3390/cells8010058

Prusicki, M. A., Keizer, E. M., van Rosmalen, R. P., Komaki, S., Seifert, F., Müller, K., et al. (2019). Live cell imaging of meiosis in *Arabidopsis thaliana*—a landmark system. *elife* 8:e42834. doi: 10.7554/eLife.42834

Rabl, C. (1885). Uber Zelltheilung. *Morphol. Jahrb.* 10, 214–330.

Remeseiro, S., and Losada, A. (2013). Cohesin, a chromatin engagement ring. *Curr. Opin. Cell Biol.* 25, 63–71. doi: 10.1016/j.ceb.2012.10.013

Rey, M. D., Calderón, M. C., and Prieto, P. (2015b). The use of the ph1b mutant to induce recombination between the chromosomes of wheat and barley. *Front. Plant Sci.* 6:160. doi: 10.3389/fpls.2015.00160

Richards, E. J., and Ausubel, F. M. (1988). Isolation of a higher eukaryotic telomere from *Arabidopsis thaliana*. *Cell* 53, 127–136. doi: 10.1016/0092-8674(88)90494-1

Richards, D. M., Greer, E., Martin, A. C., Moore, G., Shaw, P. J., and Howard, M. (2012). Quantitative dynamics of telomere bouquet formation. *PLoS Comput. Biol.* 8:e1002812. doi: 10.1371/journal.pcbi.1002812

Rietchman, H., Ambrosini, A., and Paul, S. (2005). Human subtelomere structure and variation. *Chromosom. Res.* 13, 505–515. doi: 10.1007/s10577-005-0998-1

Riha, K., McKnight, T. D., Griffing, L. R., and Shippen, D. E. (2001). Living with genome instability: plant responses to telomere dysfunction. *Science* 291, 1797–1800. doi: 10.1126/science.1057110

Riha, K., and Shippen, D. E. (2003). Ku is required for telomeric C-rich strand maintenance but not for end-to-end chromosome fusions in *Arabidopsis*. *Proc. Natl. Acad. Sci. U. S. A.* 100, 611–615. doi: 10.1073/pnas.0236128100

Riley, R., and Chapman, V. (1958). Genetic control of the cytologically diploid behaviour of hexaploid wheat. *Nature* 182, 713–715. doi: 10.1038/182713a0

Robaszkiewicz, E., Idziak-Helmcke, D., Tkacz, M. A., Chrominski, K., and Hasterok, R. (2016). The arrangement of *Brachypodium distachyon* chromosomes in interphase nuclei. *J. Exp. Bot.* 67, 5571–5583. doi: 10.1093/jxb/erw325

Roberts, N. Y., Osman, K., and Armstrong, S. J. (2009). Telomere distribution and dynamics in somatic and meiotic nuclei of *Arabidopsis thaliana*. *Cytogenet. Genome Res.* 124, 193–201. doi: 10.1159/000218125

Rong, Y. S., and Golic, K. G. (2003). The homologous chromosome is an effective template for the repair of mitotic DNA doulble-strand breaks in *Drosophila*. *Genetics* 165, 1831–1842. doi: 10.1093/genetics/165.4.1831

Ruckova, E., Friml, J., Schrumpfova, P. P., and Fajkus, J. (2008). Role of alternative telomere lengthening unmasked in telomerase knock-out mutant plants. *Plant Mol. Biol.* 66, 637–646. doi: 10.1007/s11103-008-9295-7

Rutowicz, K., Puzio, M., Halibart-Puzio, J., Lirski, M., Kotliński, M., Kroteń, M. A., et al. (2015). A specialized histone H1 variant is required for adaptive responses to complex abiotic stress and related DNA methylation in *Arabidopsis*. *Plant Physiol.* 169, 2080–2101. doi: 10.1104/pp.15.00493

Saha, A., Wittmeyer, J., and Cairns, B. R. (2006). Chromatin remodelling: The industrial revolution of DNA around histones. *Nat. Rev. Mol. Cell Biol.* 7, 437–447. doi: 10.1038/nrm1945

Said, M., Recio, R., and Cabrera, A. (2012). Development and characterization of structural changes in chromosome 3Hch from *Hordeum chilense* in common wheat and their use in physical mapping. *Euphytica* 188, 429–440. doi: 10.1007/s10681-012-0712-2

Salina, E. A., Sergeeva, E. M., Adonina, I. G., Shcherban, A. B., Afonnikov, D. A., Belcram, H., et al. (2009). Isolation and sequence analysis of the wheat B genome subtelomeric DNA. *BMC Genomics* 10:414. doi: 10.1186/1471-2164-10-414

San Filippo, J., Sung, P., and Klein, H. (2008). Mechanism of eukaryotic homologous recombination. *Annu. Rev. Biochem.* 77, 229–257. doi: 10.1146/annurev.biochem.77.061306.125255

Scherthan, H. (2001). A bouquet makes ends meet. *Nat. Rev. Mol. Cell Biol.* 2, 621–627. doi: 10.1038/35085086

Scherthan, H. (2007). Telomere attachment and clustering during meiosis. *Cell. Mol. Life Sci.* 64, 117–124. doi: 10.1007/s00018-006-6463-2

Schrumpfova, P. P., Vychodilova, I., Dvorackova, M., Majerska, J., Dokladal, L., Schorova, S., et al. (2014). Telomere repeat binding proteins are functional components of *Arabidopsis* telomeres and interact with telomerase. *Plant J.* 77, 770–781. doi: 10.1111/tpj.12428

Schubert, I., and Shaw, P. (2011). Organization and dynamics of plant interphase chromosomes. *Trends Plant Sci.* 16, 273–281. doi: 10.1016/j.tplants.2011.02.002

Sears, E. R. (1956). Transfer of leaf-rust resistance from *Aegilops umbellulata* to wheat. *Brookhaven Symp. Biol.* 9, 1–21.

Sears, E. R. (1976). Genetic control of chromosome pairing in wheat. *Annu. Rev. Genet.* 10, 31–51. doi: 10.1146/annurev.ge.10.120176.000335

Sexton, T., Umlauf, D., Kurukuti, S., and Fraser, P. (2007). The role of transcription factories in large-scale structure and dynamics of interphase chromatin. *Semin. Cell Dev. Biol.* 18, 691–697. doi: 10.1016/j.semcdb.2007.08.008

Shaw, P. J. (2010). Mapping chromatin conformation. *F1000 Biol. Rep.* 2:18. doi: 10.3410/B2-18

Sheehan, M. J., and Pawlowski, W. P. (2009). Live imaging of rapid chromosome movements in meiotic prophase I in maize. *Proc. Natl. Acad. Sci. U. S. A.* 106, 20989–20994. doi: 10.1073/pnas.0906498106

Sovakova, P. P., Magdolenova, A., Konecna, K., Rajecka, V., Fajkus, J., and Fojtova, M. (2018). Telomere elongation upon transfer to callus culture reflects the reprogramming of telomere stability control in *Arabidopsis*. *Plant Mol. Biol.* 98, 81–99. doi: 10.1007/s11103-018-0765-2

Stam, M., Tark-Dame, M., and Fransz, P. (2019). 3D genome organization: a role for phase separation and loop extrusion? *Curr. Opin. Plant Biol.* 48, 36–46. doi: 10.1016/j.pbi.2019.03.008

Strahl, B. D., and Allis, C. D. (2000). The language of covalent histone modifications. *Nature* 403, 41–45. doi: 10.1038/47412

Straight, A. F., Belmont, A. S., Robinett, C. C., and Murray, A. W. (1996). GFP tagging of budding yeast chromosomes reveals that protein-protein interactions can mediate sister chromatid cohesion. *Curr. Biol.* 6, 1599–1608. doi: 10.1016/S0960-9822(02)70783-5

Stroud, H., Otero, S., Desvoyes, B., Ramírez-Parra, E., Jacobsen, S. E., and Gutierrez, C. (2012). Genome-wide analysis of histone H3.1 and H3.3 variants in *Arabidopsis thaliana*. *Proc. Natl. Acad. Sci. U. S. A.* 109, 5370–5375. doi: 10.1073/pnas.1203145109

Subirana, J. A., and Messeguer, X. (2011). The distribution of alternating AT sequences in eukaryotic genomes suggests a role in homologous chromosome recognition in meiosis. *J. Theor. Biol.* 283, 28–34. doi: 10.1016/j.jtbi.2011.05.025

Sundararajan, A., Dukowic-Schulze, S., Kwicklis, M., Engstrom, K., Garcia, N., Oviedo, O. J., et al. (2016). Gene evolutionary trajectories and GC patterns driven by recombination in *Zea mays*. *Front. Plant Sci.* 7:1433. doi: 10.3389/fpls.2016.01433

Sutherland, H., and Bickmore, W. A. (2009). Transcription factories: gene expression in unions? *Nat. Rev. Genet.* 10, 457–466. doi: 10.1038/nrg2592

Sykorova, E., and Fajkus, J. (2009). Structure-function relationships in telomerase genes. *Biol. Cell.* 101, 375–392. doi: 10.1042/BC20080205

Sykorova, E., Fajkus, J., Meznikova, M., Lim, K. Y., Neplechova, K., Blattner, F. R., et al. (2006). Minisatellite telomeres occur in the family Alliaceae but are lost in *Allium*. *Am. J. Bot.* 93, 814–823. doi: 10.3732/ajb.93.6.814

Sykorova, E., Lim, K. Y., Chase, M. W., Knap, S., Leitch, I. J., Leitch, A. R., et al. (2003a). The absence of *Arabidopsis*-type telomeres in *Cestrum* and closely related genera *Vestia* and *Sessea* (Solanaceae): first evidence from eudicots. *Plant J.* 34, 283–291. doi: 10.1046/j.1365-313x.2003.01731.x

Sykorova, E., Lim, K. Y., Kunicka, Z., Chase, M. W., Bennett, M. D., Fajkus, J., et al. (2003b). Telomere variability in the monocotyledonous plant order Asparagales. *Proc. R. Soc. Lond. B Biol. Sci.* 270, 1893–1904. doi: 10.1098/rspb.2003.2446

Tommerup, H., Dousmanis, A., and de Lange, T. (1994). Unusual chromatin in human telomeres. *Mol. Cell. Biol.* 14, 5777–5785. doi: 10.1128/MCB.14.9.5777

Torres, G. A., Gong, Z., Iovene, M., Hirsch, C. D., Buell, C. R., Bryan, G. J., et al. (2011). Organization and evolution of subtelomeric satellite repeats in the potato genome. *G3* 1, 85–92. doi: 10.1534/g3.111.000125

Valenzuela, N. T., Perera, E., and Naranjo, T. (2013). Identifying crossover-rich regions and their effect on meiotic homologous interactions by partitioning chromosome arms of wheat and rye. *Chromosom. Res.* 21, 433–445. doi: 10.1007/s10577-013-9372-x

van Koningsbruggen, S., Gierlinski, M., Schofield, P., Martin, D., Barton, G. J., Ariyurek, Y., et al. (2010). High-resolution whole-genome sequencing reveals that specific chromatin domains from most human chromosomes associate with nucleoli. *Mol. Biol. Cell* 21, 3735–3748. doi: 10.1091/mbc.E10-06-0508

Vaquero-Sedas, M. I., and Vega-Palas, M. A. (2013). Differential association of *Arabidopsis* telomeres and centromeres with histone H3 variants. *Sci. Rep.* 3:1202. doi: 10.1038/srep01202

Varas, J., Graumann, K., Osman, K., Pradillo, M., Evans, D., Santos, J., et al. (2015). Absence of SUN1 and SUN2 proteins in *Arabidopsis thaliana* leads to a delay in meiotic progression and defects in synapsis and recombination. *Plant J.* 81, 329–346. doi: 10.1111/tpj.12730

Veldman, T., Etheridge, K. T., and Counter, C. M. (2004). Loss of hPot1 function leads to telomere instability and a cut-like phenotype. *Curr. Biol.* 14, 2264–2270. doi: 10.1016/j.cub.2004.12.031

Vershinin, A. V., and Evtushenko, E. V. (2014). "What is the specificity of plant subtelomeres?," in *Subtelomeres*. eds. E. J. Louis and M. M. Becker (Berlin: Springer), 195–211.

Wang, M., Wang, P., Lin, M., Ye, Z., Li, G., Tu, L., et al. (2018). Evolutionary dynamics of 3D genome architecture following polyploidization in cotton. *Nat. Plants* 4, 90–97. doi: 10.1038/s41477-017-0096-3

Watson, M., Bulankova, P., Riha, K., Shippen, D. E., and Vyskot, B. (2005). Telomerase independent cell survival in *Arabidopsis thaliana*. *Plant J.* 43, 662–674. doi: 10.1111/j.1365-313X.2005.02479.x

Weiss-Schneeweiss, H., Riha, K., Jang, C. G., Puizina, J., Scherthan, H., and Schweizer, D. (2004). Chromosome termini of the monocot plant *Othocallis sibericaare* maintained by telomerase, which specifically synthesizes vertebrate-type telomere sequences. *Plant J.* 37, 484–493. doi: 10.1046/j.1365-313X.2003.01974.x

Wendt, K. S., Yoshida, K., Itoh, T., Bando, M., Koch, B., Schirghuber, E., et al. (2008). Cohesin mediates transcriptional insulation by CCCTC-binding factor. *Nature* 451, 796–801. doi: 10.1038/nature06634

White, J., and Stelzer, E. (1999). Photobleaching GFP reveals protein dynamics inside live cells. *Trends Cell Biol.* 9, 61–65. doi: 10.1016/S0962-8924(98)01433-0

Wu, I., Multani, A. S., He, H., Cosme-Blanco, W., Deng, Y., Deng, J. M., et al. (2006). Pot1 deficiency initiates DNA damage checkpoint activation and aberrant homologous recombination at telomeres. *Cell* 126, 49–62. doi: 10.1016/j.cell.2006.05.037

Xie, X. Y., and Shippen, D. E. (2018). DDM1 guards against telomere truncation in *Arabidopsis*. *Plant Cell Rep.* 37, 501–513. doi: 10.1007/s00299-017-2245-6

Yamada, T., and Ohta, K. (2013). Initiation of meiotic recombination in chromatin structure. *J. Biochem.* 154, 107–114. doi: 10.1093/jb/mvt054

Yu, N., Nützmann, H. W., MacDonald, J. T., Moore, B., Field, B., Berriri, S., et al. (2016). Delineation of metabolic gene clusters in plant genomes by chromatin signatures. *Nucleic Acids Res.* 44, 2255–2265. doi: 10.1093/nar/gkw100

Zamudio, N., Barau, J., Teissandier, A., Walter, M., Borsos, M., Servant, N., et al. (2015). DNA methylation restrains transposons from adopting a chromatin signature permissive for meiotic recombination. *Genes Dev.* 29, 1256–1270. doi: 10.1101/gad.257840.114

Zhang, F., Ma, L., Zhang, C., Du, G., Shen, Y., Tang, D., et al. (2020). The SUN domain proteins OsSUN1 and OsSUN2 play critical but partially redundant roles in meiosis. *Plant Physiol.* 183, 1517–1530. doi: 10.1104/pp.20.00140

Zhang, F., Tang, D., Shen, Y., Xue, Z., Shi, W., Ren, L., et al. (2017). The F-box protein ZYGO1 mediates bouquet formation to promote homologous pairing, synapsis, and recombination in rice meiosis. *Plant Cell* 29, 2597–2609. doi: 10.1105/tpc.17.00287

Zhang, H., Zheng, R., Wang, Y., Zhang, Y., Hong, P., Fang, Y., et al. (2019). The effects of *Arabidopsis* genome duplication on the chromatin organization and transcriptional regulation. *Nucleic Acids Res.* 47, 7857–7869. doi: 10.1093/nar/gkz511

Zhou, Y., Wang, Y. J., Krause, K., Yang, T. T., Dongus, J. A., Zhang, Y. J., et al. (2018). Telobox motifs recruit CLF/SWN-PRC2 for H3K27me3 deposition via TRB factors in *Arabidopsis*. *Nat. Genet.* 50:638. doi: 10.1038/s41588-018-0109-9

Zhu, Z., and Wang, X. (2019). Roles of cohesin in chromosome architecture and gene expression. *Semin. Cell Dev. Biol.* 90, 187–193. doi: 10.1016/j.semcdb.2018.08.004

Zickler, D. (2006). From early homologue recognition to synaptonemal complex formation. *Chromosoma* 115, 158–174. doi: 10.1007/s00412-006-0048-6

Zickler, D., and Kleckner, N. (2015). Recombination, pairing, and synapsis of homologs during meiosis. *Cold Spring Harb. Perspect. Biol.* 7:a016626. doi: 10.1101/cshperspect.a016626

Zofall, M., Persinger, J., Kassabov, S. R., and Bartholomew, B. (2006). Chromatin remodelling by ISW2 and SWI/SNF requires DNA translocation inside the nucleosome. *Nat. Struct. Mol. Biol.* 13, 339–346. doi: 10.1038/nsmb1071

Conflict of Interest: The authors declare that the research was conducted in the absence of any commercial or financial relationships that could be construed as a potential conflict of interest.

frontiers in Plant Science

REVIEW
published: 19 July 2021
doi: 10.3389/fpls.2021.708948

Rewiring Meiosis for Crop Improvement

*Pallas Kuo[1], Olivier Da Ines[2] and Christophe Lambing[1]**

[1]Department of Plant Sciences, University of Cambridge, Cambridge, United Kingdom, [2]Institut Génétique Reproduction et Développement (iGReD), Université Clermont Auvergne, UMR 6293 CNRS, U1103 INSERM, Clermont-Ferrand, France

Meiosis is a specialized cell division that contributes to halve the genome content and reshuffle allelic combinations between generations in sexually reproducing eukaryotes. During meiosis, a large number of programmed DNA double-strand breaks (DSBs) are formed throughout the genome. Repair of meiotic DSBs facilitates the pairing of homologs and forms crossovers which are the reciprocal exchange of genetic information between chromosomes. Meiotic recombination also influences centromere organization and is essential for proper chromosome segregation. Accordingly, meiotic recombination drives genome evolution and is a powerful tool for breeders to create new varieties important to food security. Modifying meiotic recombination has the potential to accelerate plant breeding but it can also have detrimental effects on plant performance by breaking beneficial genetic linkages. Therefore, it is essential to gain a better understanding of these processes in order to develop novel strategies to facilitate plant breeding. Recent progress in targeted recombination technologies, chromosome engineering, and an increasing knowledge in the control of meiotic chromosome segregation has significantly increased our ability to manipulate meiosis. In this review, we summarize the latest findings and technologies on meiosis in plants. We also highlight recent attempts and future directions to manipulate crossover events and control the meiotic division process in a breeding perspective.

Keywords: meiosis, meiotic recombination, centromere, telomere, plant, chromatin, epigenetic, ploidy

OPEN ACCESS

Edited by:
Chang Liu,
University of Hohenheim, Germany

Reviewed by:
Raphael Mercier,
Max Planck Institute for Plant Breeding Research, Germany
Stefan Heckmann,
Leibniz Institute of Plant Genetics and Crop Plant Research (IPK), Germany

***Correspondence:**
Christophe Lambing
cal66@cam.ac.uk

Specialty section:
This article was submitted to Plant Cell Biology, a section of the journal Frontiers in Plant Science

Received: *12 May 2021*
Accepted: *17 June 2021*
Published: *19 July 2021*

Citation:
Kuo P, Da Ines O and Lambing C (2021) Rewiring Meiosis for Crop Improvement. Front. Plant Sci. 12:708948. doi: 10.3389/fpls.2021.708948

CHROMATIN AND RECOMBINATION IN MEIOSIS

Meiotic Recombination

Meiosis is a specialized cell division taking place in sexually reproducing organisms during which a cell undergoes two rounds of chromosome segregation to form four daughter cells of halved ploidy. Each daughter cell contains a set of chromosomes with varying genetic contents to the others due to genetic exchanges and random assortment of homologous chromosomes and sister chromatids. The first meiotic segregation faces a unique situation whereby chromosomes undergo recombination events leading to reciprocal exchanges between homologs, also called crossovers (COs; Mercier et al., 2015). COs are important to create novel genetic diversity, and this natural process is utilized during breeding strategies to break the linkage between genes, facilitating the removal of unfavorable genetic elements or improving the mapping of quantitative trait locus (Mercier et al., 2015).

Meiotic recombination initiates with the formation of programmed DNA double-strand breaks (DSBs) induced by a topoisomerase-like complex related to the archaeal TopoVI DNA topoisomerase (Topo VI). Topo VI is an heterotetrameric enzymatic complex comprising two A and two B subunits and catalyzing DNA strand breakages (Bergerat et al., 1997). In meiosis, SPO11 and MTOPVIB form a complex with topoisomerase-like activity to create a DSB onto which SPO11 remains covalently bound to the DSB end *via* a phosphotyrosyl bond (Robert et al., 2016; Vrielynck et al., 2016). SPO11 forms meiotic DSBs as a homodimer in animals and fungi, and as a SPO11-1/SPO11-2 heterodimer in plants (Mercier et al., 2015). Studies of SPO11 proteins between plant species reveal that the number of orthologs varies greatly (Sprink and Hartung, 2014; Da Ines et al., 2020). In *Arabidopsis thaliana*, three SPO11 paralogs are identified but only SPO11-1 and SPO11-2 are involved in meiotic DSB formation (Hartung et al., 2007). Rice has five SPO11 paralogs and only SPO11-1 and SPO11-2 have a confirmed role in meiosis while loss of *spo11-4* has no meiotic defects (Yu et al., 2010; Fayos et al., 2020). The high number of SPO11 paralogs in plants makes genetic engineering to control meiotic recombination more challenging. However, SPO11 orthologs are sufficiently conserved between plant species as to complement each other's loss of function mutations. For instance, expression of bread wheat SPO11-2 restores fertility in Arabidopsis *spo11-2* (Benyahya et al., 2020; Da Ines et al., 2020) while expression of bread wheat SPO11-1-5D restores fertility in both rice and Arabidopsis *spo11-1* (Da Ines et al., 2020). Additional proteins are required for DSB formation and appear conserved between plants (Jing et al., 2019). For example, Arabidopsis PRD1 (De Muyt et al., 2007), PRD2 and PRD3 (De Muyt et al., 2009), and DFO (Zhang et al., 2012) are all essential for the formations of meiotic DSB. Similarly, rice *prd1* (Shi et al., 2021), *mtopVIb* (Fu et al., 2016; Xue et al., 2016) and *prd3/pair1* (Nonomura et al., 2004), and maize *mtopVIb* (Jing et al., 2020) are defective in DSB formation.

Cytological studies using DNA damage markers, such as γ-H2AX and RAD51, revealed the formation of a large number of DSBs in early meiosis. It is estimated that between 150 and 200 meiotic DSBs are formed in Arabidopsis and between ~200 and 2,000 in crops with larger genome (Ferdous et al., 2012; Higgins et al., 2012; Sidhu et al., 2015; Gardiner et al., 2019; Benyahya et al., 2020). DSBs are formed on the chromatin which is organized in arrays of loops anchored to a proteinaceous linear structure called the chromosome axis (Zickler and Kleckner, 1999; Kleckner, 2006). In plants, components of the chromosome axis include meiotic cohesin REC8 (Chelysheva et al., 2005; Golubovskaya et al., 2006), HORMA-domain-containing proteins ASY1/PAIR2 (Armstrong et al., 2002; Nonomura et al., 2006), and coiled-coil proteins ASY3/PAIR3/DSY2 (Wang et al., 2011; Ferdous et al., 2012; Lee et al., 2015) and ASY4 (Chambon et al., 2018; Osman et al., 2018). The axis proteins ASY3/DSY2/Red1 are essential for DSB formation (Panizza et al., 2011; Ferdous et al., 2012; Lee et al., 2015), and chromosome axis length covaries with the number of DSB markers on a per-nucleus basis in Arabidopsis and budding yeast, highlighting the important regulatory functions of the axis on recombination initiation (Wang et al., 2019b; Lambing et al., 2020b).

Following DSB formation, DSB ends are resected by the MRN/COM1 complex to form 3' overhang single-stranded DNA (ssDNA) onto which RPA, RAD51, and DMC1 are recruited to form nucleoprotein filaments (Mercier et al., 2015). Multiple strand invasions of the chromosome filaments favor homologous chromosome alignment and are critical for chromosome pairing in most species (Cloud et al., 2012; Hong et al., 2013). Successful pairing leads to installation of a tripartite structure called the synaptonemal complex (SC) which consists of a transverse filament formed with ZYP1 and connecting the two homologous axes (Mercier et al., 2015). The SC initiates at recombination sites (Zhang et al., 2014a; Lambing et al., 2015), and several lines of evidence suggest that SC components regulate CO formation (Higgins et al., 2005; Barakate et al., 2014; Chen et al., 2015; Voelkel-Meiman et al., 2015; Capilla-Perez et al., 2021; France et al., 2021). Meiotic DSB repair results in a CO or a non-CO, with a possibility of gene conversion in either case (Berchowitz and Copenhaver, 2010). Gene conversions are short unidirectional exchanges (few hundreds base pairs) of genetic information between chromosomes. Gene conversion events are rare, and the control over gene conversion is not well understood. The frequency of gene conversion per meiosis on a given locus is estimated between ~10^{-4} and 10^{-6} (Sun et al., 2012; Drouaud et al., 2013; Wijnker et al., 2013). Gene conversion frequency is associated with MSH4, a protein required for CO formation (Drouaud et al., 2013), and can be detected on the heterochromatin regions where COs are repressed (Shi et al., 2010).

How a DSB's fate is determined is still not fully understood, but it is thought that pro- and anti-CO pathways influence the repair outcome at DSB sites (Mercier et al., 2015). For example, a set of proteins collectively named "ZMM" (SHOC1, PTD, HEI10, ZIP4, MER3, MSH4, and MSH5 in Arabidopsis) stabilizes inter-homolog joint molecules and promotes CO formation (Mercier et al., 2015). In contrast, anti-CO proteins, such as FANCM, BLM/RECQ4, TOP3α, FIGL1, disengage joint molecules *via* helicase or topoisomerase activities, and repress CO formation (Crismani et al., 2012; Mercier et al., 2015; Seguela-Arnaud et al., 2015). During meiotic DSB repair, the ssDNA ends elongate *via* DNA synthesis using the homologous chromosome as a template. If heterozygosity is shared between the homologous template and the ssDNA end, disengagement of this ssDNA and repair by an anti-CO pathway could lead to a non-CO associated with a gene conversion (Berchowitz and Copenhaver, 2010). Recent studies in budding yeast indicate that complex partner switches may be common during meiosis, creating chromatids with mosaic allelic patterns (Mcmahill et al., 2007; Marsolier-Kergoat et al., 2018).

Each bivalent chromosome must form at least one CO, termed an obligate CO, to form the physical link between chromosomes which is essential to ensure proper chromosome segregation in meiosis. In most species, CO formation is limited to 1–3 per chromosome pair (Jones and Franklin, 2006; Mercier et al., 2015). Several factors have been reported to contribute

to these phenomena: CO homeostasis (Henderson and Keeney, 2004), CO interference (Kleckner et al., 2004), limited amount of pro-CO factors (Ziolkowski et al., 2017), and the presence of anti-CO factors (Crismani et al., 2012; Girard et al., 2015; Seguela-Arnaud et al., 2015). CO homeostasis is a phenomenon buffering changes in DSB number for the maintenance of total COs. In this context, an elevation or a decrease in DSBs does not impact CO number. While CO homeostasis is observed in budding yeast (Martini et al., 2006), it may be different in plants (Sidhu et al., 2015; Xue et al., 2018). In contrast, CO interference is a phenomenon resulting in the non-random distribution of COs whereby the formation of one CO inhibits the formation of additional COs in adjacent regions, thus preventing clustering of COs (Wang et al., 2015). Although factors involved in this phenomenon are unclear, it has been suggested that a combination of physical stresses generated from the expansion and contraction of chromatin compressing the chromosome axis during prophase I, combined with the diffusion of proteins along the axis, contribute to the establishment of an interfering signal (Wang et al., 2015; Zhang et al., 2018). In accordance with this model, components of the chromosome axis have been implicated in CO interference in budding yeast (Zhang et al., 2014b), *Caenorhabditis elegans* (Libuda et al., 2013; Zhang et al., 2018), and Arabidopsis (Lambing et al., 2020a; Capilla-Perez et al., 2021; France et al., 2021). However, the chromosome axis in itself may not be sufficient to impose CO interference since axis is formed in *asy1* and *zyp1* mutant lines in which interference is lost (Lambing et al., 2020a; Capilla-Perez et al., 2021; France et al., 2021).

Chromatin and DSB Hotspots

DSBs are not randomly formed on the genome. Instead, they are enriched in nucleosome-depleted regions (Pan et al., 2011; Lam and Keeney, 2015; Choi et al., 2018). It appears that regions with high nucleosome occupancy prevent SPO11 accessibility and thus restrict DSB formation. DSB formation also takes place in the context of chromatin loops anchored to a chromosome axis. Counterintuitively, certain components of the DSB machinery are found associated with the chromosome axis while DSBs are located in the chromatin loops, away from the axial sites in budding yeast (Panizza et al., 2011; Stanzione et al., 2016). To reconcile the two observations, it was proposed that chromatin loops are tethered to the axis prior to DSB formation. In support of this model, Spp1, a PHD finger-domain protein, was found to interact with H3K4me3 modifications located on the chromatin loop, and with Mer2 protein, a component of the DSB machinery located on the axis in budding yeast (Acquaviva et al., 2013; Sommermeyer et al., 2013). This observation indicates a complex interaction between chromatin loop organization, epigenetics marks, and recombination. Interestingly, DSB hotspots are enriched at the 5' end of genes, and axis components are enriched at the 3' end of genes and are influenced by transcriptional activity in budding yeast (Pan et al., 2011; Lam and Keeney, 2015; Medhi et al., 2016). Arabidopsis DSB maps show enrichment of DSBs at the 5' and 3' end of genes, in regions of low nucleosome occupancy and with markers of open chromatin (e.g., H3K4me3). DSBs are correspondingly depleted in heterochromatic regions that are enriched in transposons, GC content, and DNA methylation (Choi et al., 2018). Consistent with budding yeast, ChIP-seq of Arabidopsis axis protein revealed that REC8 and DSBs occupy distinct sites. REC8 also shows a preferential polarization toward the end of genes that is influenced by transcriptional activity (Lambing et al., 2020b). Comparing genome-wide Arabidopsis axis and DSB profiles revealed no correlation between the enrichment of SPO11-1-oligos and REC8 or ASY1 over genes, indicating that although the chromosome axis is important for DSB formation, the amount of axis protein does not specify the frequency of DSBs locally (Lambing et al., 2020a,b). Additional factors likely influence the local frequency of DSB formation.

Influence of Heterochromatin and Centromeres on Meiosis

Although COs are suppressed over the heterochromatin, a substantial number of DSBs has been detected over the pericentromeric heterochromatic regions, including at transposons, in Arabidopsis (Choi et al., 2018; Underwood et al., 2018) and maize (He et al., 2017). The maize genome is ~85% transposons, and comparative analysis shows that DSBs are distributed along the entire chromosomes without specific polarization, while COs are skewed toward the end of the chromosomes (He et al., 2017). Few COs were reported in the heterochromatic knob regions in maize but at much lower frequency than its DSB frequency (Stack et al., 2017). Thus, an interesting possibility is that recombination may not be fully suppressed on the heterochromatin and centromeres but rather channeled to favor non-CO outcomes, such as inter-sister repair. Indeed, gene conversions were detected in maize centromeric regions (Shi et al., 2010).

CO suppression over the centromeric heterochromatin is widely conserved (Ellermeier et al., 2010; Li et al., 2015; Phillips et al., 2015). The molecular mechanisms allowing this suppression are not clear, but appear instrumental since centromeric COs have been associated with increased rates of mis-segregation and aneuploidy in multiple species (Fernandes et al., 2019). On the other hand, understanding suppression of CO at or close to the centromeres is of particular importance for breeding, given that lack of meiotic CO in pericentromeric regions is a major bottleneck in varietal development of crop plants.

Centromeres are the sites of kinetochore assembly which enable microtubule fiber attachment and thus faithful segregation of chromosomes during mitotic and meiotic division. The structure and organization of the centromeres vary considerably between species with centromeres occupying a short sequence, a region or even the entire chromosome (Steiner and Henikoff, 2015; Talbert and Henikoff, 2020). Point centromeres are typical in budding yeast (Prosee et al., 2020) while *C. elegans* and some plants display holocentric chromosomes where the whole chromosome acts as a centromere (Melters et al., 2012). Holocentric chromosomes impose a specific problem to meiosis and how meiosis is remodeled in holocentric plants is being

extensively investigated (Marques and Pedrosa-Harand, 2016). Most plants and mammals, however, exhibit regional centromeres. In plants, regional centromeres are largely composed of centromeric satellite repeats and centromeric retrotransposon arrays that can be several megabases long (Lamb et al., 2007; Ma et al., 2007; Fernandes et al., 2019). Yet, a centromere is generally not defined by a specific DNA sequence but rather by the presence of the specific histone H3 variant CenH3 (mammalian CENP-A), which acts as a particular epigenetic mark that establishes functional centromeres. CenH3 is present at all functional centromeres independently of their DNA sequence, and this epigenetic specification of centromere identity is broadly conserved in eukaryotes (Steiner and Henikoff, 2015; Fernandes et al., 2019; Talbert and Henikoff, 2020).

How centromeres function during meiosis in plants is still poorly understood but a number of studies have described the essential role of early centromere associations in homologous chromosome recognition, pairing, and subsequent synapsis during meiosis (reviewed in Da Ines and White, 2015; Sepsi and Schwarzacher, 2020). Remarkably, early centromere associations seem not directly mediated by DSB formation and recombination but rather by local chromatin homology, although stabilization of centromere pairing appears to be partially dependent on recombination initiation (Da Ines et al., 2012; Da Ines and White, 2015; Sepsi and Schwarzacher, 2020). Centromere association requires active centromeres and the presence of functional CENH3 variants (Zhang et al., 2013). Thus, despite high-DNA sequence homology, initial centromere interactions are driven by specific chromatin structure and centromeric proteins. In particular, early centromere associations are strongly dependent on the REC8 cohesin enrichment as well as DNA repeats organization at centromeres. In wheat, recent work has revealed that centromere satellite organization has diverged in the different wheat sub-genomes and these rearrangements of CENH3 nucleosomes likely influence centromere interaction and further homologous chromosome pairing (Su et al., 2019).

It is possible that early centromere association may impede access of the recombination machinery and thereby may play a key role in suppressing CO at centromeres. This is supported by the recent demonstration that REC8 enrichment is strongly correlated with suppression of meiotic DSBs and crossovers in Arabidopsis (Lambing et al., 2020b). Given that REC8 cohesin protein is highly enriched at centromeric sites from early meiosis I up to meiosis II and that centromere coupling and pairing also require the presence of REC8 (Cai et al., 2003; Zhang et al., 2013), it is conceivable that early centromere associations are intricately linked to suppression of recombination at centromeres.

ENGINEERING MEIOTIC RECOMBINATION

Increasing Meiotic Recombination Genome Wide

In most plants, only few COs are formed on each chromosome per meiosis and this phenomenon limits the potential to create novel genetic diversity (Mercier et al., 2015). This is caused in part by a limited amount of pro-CO factors, the repressive activity of anti-CO factors and the action of CO interference. The majority of COs is formed by the ZMM pathway. Among actors of this pathway, the E3 ligase HEI10 is dosage-dependent for recombination, with an increase in *HEI10* expression being sufficient to increase the total genetic map length by 2-fold in hybrid Arabidopsis, but with limited effect on the CO rate over the heterochromatic regions (Ziolkowski et al., 2017). Overexpression of *HEI10* in Arabidopsis is also found to decrease CO interference although it is unclear how HEI10 impacts this process (Serra et al., 2018). The regulation of HEI10 dosage is a promising avenue to increase CO number in crops by stabilizing the recombination events maturing into class I COs and reducing the strength of CO interference. Recent studies identified protein phosphatase X1 and ZYP1/ZEP1 as additional factors limiting class I CO formation suggesting that other strategies may be possible to increase class I CO rate (Wang et al., 2010, 2015; Capilla-Perez et al., 2021; France et al., 2021; Nageswaran et al., 2021).

Several anti-CO factors affecting class II COs have been identified with non-functional redundancy (Mercier et al., 2015; Wang and Copenhaver, 2018). For instance, mutations in *fancm* helicase and *recq4* helicase or *recq4* and *figl1/flip* AAA-ATPase complex cause a 10-fold elevation in the CO rate across several genetic intervals in inbred Arabidopsis (Fernandes et al., 2018). This strategy was successfully transferred into crops with *recq4* mutant showing a significant increase in crossover frequency in rice, tomato, and pea (Mieulet et al., 2018; De Maagd et al., 2020). Surprisingly, the extra COs formed in anti-class II CO mutants are present in regions with low degree of polymorphism (Fernandes et al., 2018; Blackwell et al., 2020). In particular, *fancm* recombination phenotype seems to be sensitive to the hybrid context as it can be detected in brassica, pea, and rice but not in Arabidopsis, tomato and wheat hybrid lines. It was postulated that a high degree of polymorphism in the hybrid lines could interfere with *fancm*-dependent CO formation (Blary et al., 2018; Mieulet et al., 2018; De Maagd et al., 2020; Raz et al., 2020).

The effect of combining HEI10 over-expressor with the repression of *recq4* was tested, and the study showed a cumulative effect on CO frequency in hybrid Arabidopsis transgenic lines. However, heterochromatin recombination was not substantially increased in these lines and this strategy may have a more limited effect on crop genomes with large heterochromatin composition (Serra et al., 2018).

Modulation of the Recombination Landscape

Meiotic recombination is not uniformly distributed along plant genomes which restricts the potential for crop improvement during breeding. In maize and barley, about 20% of all genes are located in heterochromatin, where recombination cold spot regions reside (Taagen et al., 2020), and a remodeling of the recombination landscape toward these regions could facilitate the introduction of genetic diversity. A striking negative correlation exists between CO rate, transposon content, and DNA methylation in plants (Lambing et al., 2017). In non-CG DNA methylation and H3K9me2 Arabidopsis mutant lines,

the recombination landscape is altered with increased COs in centromere-proximal regions. Although DSBs are also increased, a significant deficit in DSB yield remains visible on the heterochromatin in H3K9me2-deficient mutant line, and this may be an important limiting factor for CO formation in Arabidopsis heterochromatin (Underwood et al., 2018). A direct translation of these findings to economically important crops is challenging. Epigenetic mutants in plants with larger genomes show alterations in vegetative development and fertility defects (Li et al., 2014; Tan et al., 2016; Corem et al., 2018). Alternative strategies could overcome these limitations. For example, transient silencing of epigenetic genes in reproductive tissues using virus-induced gene silencing (VIGS) could have an effect on the recombination landscape while preserving plant development.

Meiotic-specific factors closely associated with recombination molecules are likely more promising targets for the control of CO landscape. For example, components of the chromosome axis are involved in the decision between inter-sister and inter-homolog recombination and Arabidopsis ASY1 and ASY3 promote CO formation (Lambing et al., 2020a). Arabidopsis ASY1 ChIP sequencing revealed that ASY1 is enriched over the centromere-proximal regions, and a gradual reduction of ASY1 is associated with a remodeling of the COs from the centromere-proximal to the distal regions (Lambing et al., 2020a). It is speculated that the distal regions are crossover prone regions due to the early homologous pairing of the telomeres while the proximal regions are crossover prone due to the enrichment of ASY1 (Armstrong et al., 2001; Lambing et al., 2020a; **Figure 1C**).

The CO landscape in cereals is distinct from Arabidopsis and COs are exclusively formed in distal ends of the chromosomes (**Figure 1**; Phillips et al., 2015; Osman et al., 2021). Moreover, the spatio-temporal formation of the chromosome axis which is observed from immunostaining of ASY1, the deposition of ZYP1 which marks synapsis between homologous chromosomes, and the formation of DSBs differ significantly between cereals and Arabidopsis (**Figures 1A,C**). For example, axis, synapsis, and DSB formation are initiated on the distal regions before being detected on the interstitial and centromere-proximal regions in barley and wheat (Higgins et al., 2012; Lambing et al., 2017; Desjardins et al., 2020; Osman et al., 2021). In contrast, no polarization of axis formation or DSB formation is detected in Arabidopsis (Lambing et al., 2017; **Figure 1A**). It is conceivable that COs are exclusively distal in cereals because the distal regions experience first the formation of DSBs and the pro-CO activity of ASY1 (**Figures 1B,C**). In this context, it is important to remodel ASY1 ons the chromosomes to achieve a remodeling of the CO landscape in cereals. Indeed, this can be achieved by increasing the temperature in barley (Higgins et al., 2012). The change of temperature reduces the polarization of axis formation, and ASY1 is detected more evenly on the chromosomes which is associated with an elevation of interstitial and centromere-proximal chiasmata (Higgins et al., 2012). However, this strategy may not be applicable to every crops, as seen in the observation that wheat recombination is only slightly and locally altered at high temperature (Coulton et al., 2020).

Targeted Recombination

Targeting recombination is potentially a preferred strategy compared to a genome-wide change in CO frequency, because it allows precise positioning of recombination events on the genome. This could be achieved by targeting recombination proteins to a specific locus or to locally alter the epigenome. DSBs are generally enriched in promoters, introns, and terminators of genes (Choi et al., 2018) and are depleted in exonic regions that are enriched in nucleosome and axis REC8 cohesin (**Figure 2B**; Choi et al., 2018; Lambing et al., 2020b). Electron microscopy studies show that the chromosome axis forms an electron dense structure (Kleckner, 2006) and the compact structure of the axis could inherently prevent DSB formation even if SPO11 is targeted to this region. Therefore, a fine analysis of the chromatin landscape appears important for the design of targeted recombination to maximize the efficiency of DSB formation.

CO cold spots have generally low DSB frequency and are enriched in nucleosome density, DNA methylation, and epigenetic silencing marks (Yelina et al., 2015; Choi et al., 2018; Underwood et al., 2018). Loss of DNA methylation is associated with a gain of DSBs in Arabidopsis (Choi et al., 2018; Underwood et al., 2018) and represents an interesting strategy for targeted recombination. In Arabidopsis, DNA is actively demethylated by ROS1 and related glycosylase enzymes through a base excision-repair process (Gong et al., 2002; Penterman et al., 2007; Zhu et al., 2007; Zhang and Zhu, 2012). An alternative pathway dependent on Ten-eleven translocation methylcytosine dioxygenase 1 (TET1) exists in human that biochemically removes DNA methylation. TET1 catalyzes the oxidation of 5-methylcytosine (5mC) to 5-hydroxymethylcytosine which is the initial step for DNA demethylation (Wu and Zhang, 2017). Fusion of human TET1 to an artificial zing finger or to CRISPR/dCas9 effectively demethylates DNA at targeted loci in Arabidopsis (**Figure 2A**; Gallego-Bartolome et al., 2018). This method could in theory be used in conjunction with CRISPR/dCAS9 fused with SPO11 or a component of the DSB machinery to promote DSB formation in an otherwise cold region (**Figure 2A**).

The recruitment of SPO11 protein to a specific locus does not necessary ensure the formation of a DSB (even less so a CO-prone DSB). To form a DSB, SPO11 requires not only to be part of a protein complex but also to be functionally active (Robine et al., 2007; Sarno et al., 2017). Studies from budding yeast revealed that not every locus bound by SPO11-GAL4 is proficient to form DSBs, and the establishment of a DSB is determined by local factors (Robine et al., 2007; Sarno et al., 2017). In plants, a recent study suggests that expression of a MTOPVIB-dCas9 fusion protein to induce targeted meiotic DSB within a CO hotspot located in a subtelomeric region of chromosome 3 is not sufficient to affect CO frequency (Yelina et al., 2021). In budding yeast, it is estimated that around 40% of the DSBs are converted to COs (Mancera et al., 2008). In contrasts, in Arabidopsis (Ferdous et al., 2012), maize (Sidhu et al., 2015), and barley (Higgins et al., 2012) only about 2–5% of the DSB rate accounts for the total CO number and it is likely that the targeted DSBs will convert to COs at low frequency. In addition, a budding yeast study showed that expression of

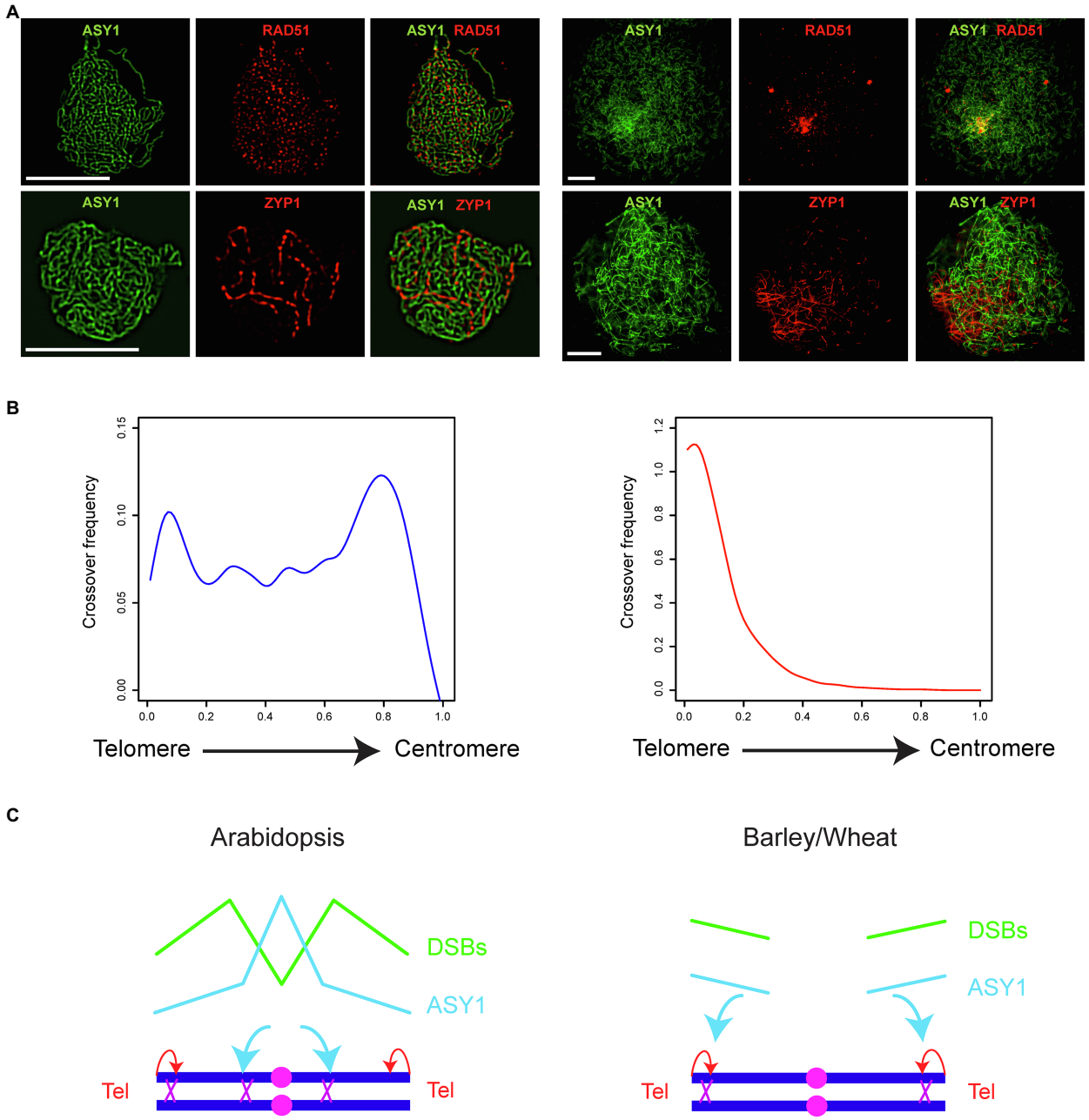

FIGURE 1 | Crossover patterning in Arabidopsis and cereals. **(A)** Co-immunostaining of ASY1 (green) and RAD51 (red) at leptotene or ASY1 (green) and ZYP1 (red) at zygotene in Arabidopsis (left panel) and hexaploid bread wheat *Triticum aestivum* cv. *Cadenza* (right panel; provided by Kim Osman, University of Birmingham, United Kingdom). Scale bar = 10 μm. **(B)** Crossover frequency along an axis from telomere to centromere in Arabidopsis (blue, left panel; replotted using the CO data of all chromosomes from Serra et al., 2018) and barley (red, right panel; CO data of all chromosomes provided by Mikel Arrieta, The James Hutton Institute, United Kingdom). **(C)** Two forces influence the crossover landscape: telomere-led recombination (red arrows) and ASY1 (cyan arrows). In leptotene, axis and DSBs are formed along the chromosomes at a similar time but in distinct levels in Arabidopsis (left panel). In contrast, axis and DSBs are formed first toward the distal end of the chromosomes in barley and wheat at leptotene (right panel). This difference in the spatio-temporal formation of axis and DSBs is associated with a different landscape of crossovers between Arabidopsis and barley/wheat. Pink filled circles represent centromeres, dark blue lines represent homologous chromosomes, and purple crosses represent crossovers. The landscape of ASY1 enrichment (cyan) and DSB frequency (green) in early prophase I are represented with solid lines.

SPO11-GAL4 in a *spo11* null mutant forms DSBs at GAL4 sites but also at natural sites (Pecina et al., 2002). If conserved in plants, this propensity of SPO11 may further reduce the targeted effect. Moreover, barley and wheat chromosome axes initiate first in distal regions in early prophase (Higgins et al., 2012; Osman et al., 2021). It is unknown whether SPO11 is functionally active to form a DSB without a chromosome axis when recruited in centromere-proximal regions at an early stage of meiosis.

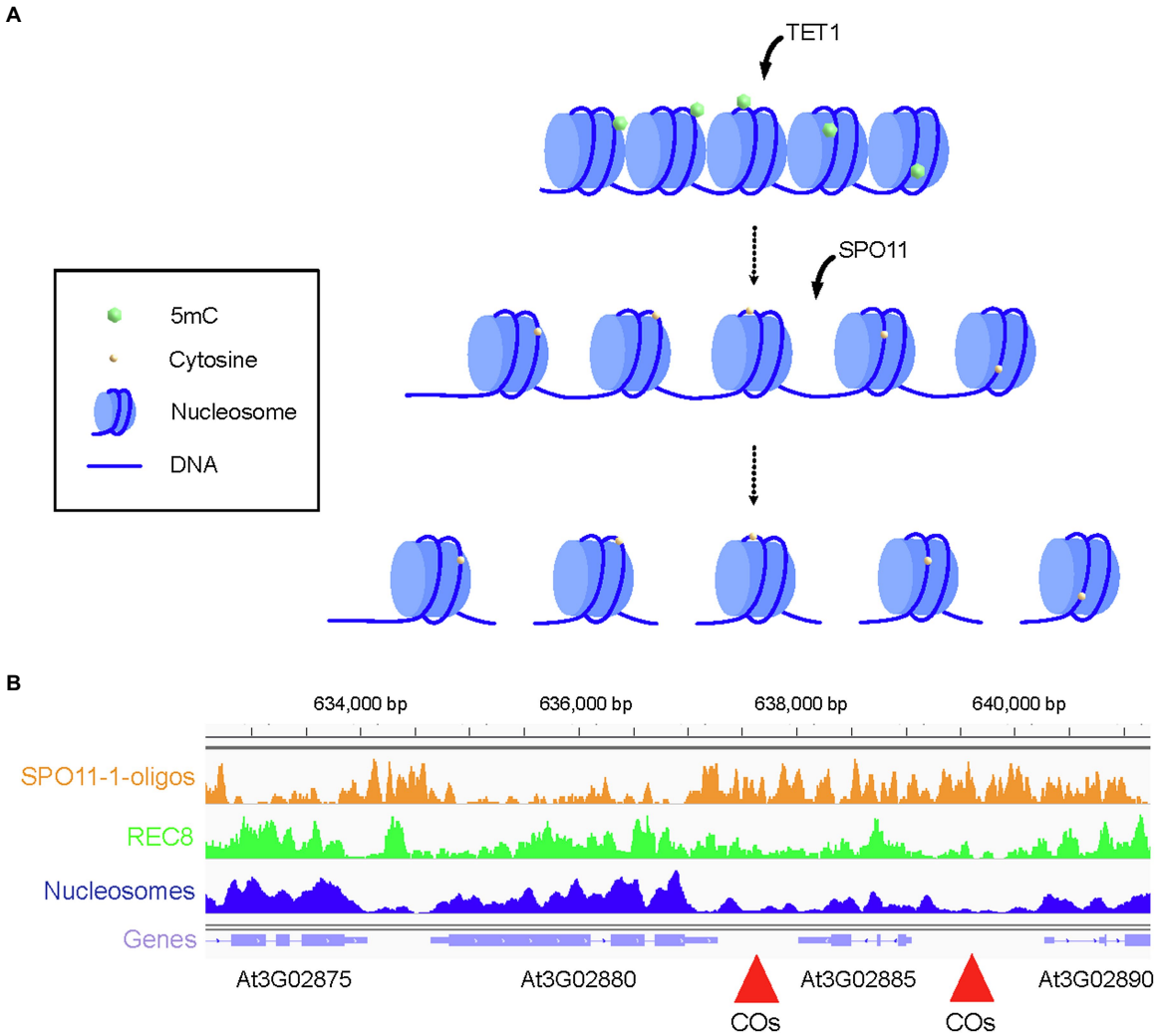

FIGURE 2 | Strategies to remodel the crossover rate locally. **(A)** Representation of a cold spot region enriched in nucleosome and silencing epigenetic marks, such as DNA methylation in all three contexts (CG, CHG, and CHH). Chromatin is methylated on 5mCs. Targeted recruitment of TET1 catalyzes the removal of silencing epigenetic marks and decompaction of chromatin while the targeted recruitment of SPO11 catalyzes formation of DSBs. Meiotic DSBs are repaired by the homologous recombination pathway leading to the formation of NCO, NCO with gene conversion, or CO. **(B)** Genome browser view of the crossover hotspot *3a* on chromosome 3 of Arabidopsis. SPO11-1-oligo (orange), REC8 ChIP-seq (green), and nucleosome (MNase, dark blue) profiles are shown alongside the gene organization (purple). Regions with high crossover rate are indicated with red arrowheads. Coordinates on the chromosome 3 are shown above the genome browser view.

The induction of targeted recombination can have undesirable effects on recombination elsewhere in the genome. For example, the formation of DSBs at targeted sites inhibits the formation of DSBs in adjacent natural sites in budding yeast (Robine et al., 2007). Moreover, if the targeted DSB is converted to a CO this will inhibit the formation of a second CO in the adjacent regions *via* a phenomenon called CO interference (Berchowitz and Copenhaver, 2010). In Arabidopsis, the effect of CO interference is detected over 8–10 Mb of DNA and the formation of a targeted CO will likely remodel the recombination landscape on that chromosome (Serra et al., 2018). Unlike COs, gene conversions have relatively short length (<2 kb) and are detected in most parts of the genome including across centromeric regions in plants (Shi et al., 2010). This type of recombination events is interesting because it only modifies the DNA sequence locally and does not seem to be under the same controls as COs (Shi et al., 2010). Moreover, targeted gene conversion events are unlikely to modify the broad CO landscape (Berchowitz and Copenhaver, 2010). This outcome is particularly interesting for plant breeding where targeted recombination is required to increase allelic diversity locally, such as in heterochromatic regions.

CHROMOSOME ENGINEERING TO INFLUENCE MEIOTIC RECOMBINATION

Chromosome Structure and Crossovers

Chromosome structure is also a strong determinant of CO formation and localization (Rowan et al., 2019). Chromosomal rearrangements,

such as inversions or translocations, usually suppress recombination, and this is particularly challenging for breeding since they may inhibit the transfer of important traits between different plant cultivars. Indeed, a number of inversions and translocations can be detected by comparing the genomic sequences between accessions (Zapata et al., 2016). Recently, somatic chromosomal engineering using CRISPR/Cas9 has proven useful for restoring recombination in naturally rearranged chromosomal regions in Arabidopsis (Schmidt et al., 2020). A particularly well-known case of inversion in Arabidopsis is the heterochromatic knob on chromosome 4 (Fransz et al., 2000). When an Arabidopsis accession carrying this inversion is crossed with an accession without inverted knob, CO formation within the entire rearranged region is suppressed (Schmidt et al., 2020). The authors developed an egg cell-specific expression system of the Cas9 nuclease that allows rearranging the structure of plant chromosomes in a targeted and heritable manner (Beying et al., 2020; Schmidt et al., 2020). Remarkably, reversion of the 1.1 Mb heterochromatic knob on chromosome 4 fully restored CO formation in this region (Schmidt et al., 2020). This is a particularly promising achievement for breeding given that many crop plants have experienced substantial chromosomal rearrangements that strongly affect CO formation.

Effect of Ploidy Manipulation on Crossovers

Interestingly, a link between increased ploidy level and crossover formation has been demonstrated in a number of plants (reviewed in Pele et al., 2017). For instance, in Arabidopsis, analyses of CO formation in one genetic interval show that both male and female CO frequencies are significantly higher in newly formed auto- and allopolyploids compared to their diploid progenitors (Pecinka et al., 2011). Additionally, studies in Brassica demonstrated that Brassica allotriploid hybrids exhibit a significant crossover increase compare to their progenitors (Leflon et al., 2010; Suay et al., 2014; Pele et al., 2017). This increase occurs genome wide and affects both male and female meiosis, although stronger increase is observed in female and is associated with a significant remodeling of the CO landscape with the presence of COs in the vicinity of centromeres. Remarkably, this increase is also accompanied by a strong decrease in CO interference (Suay et al., 2014; Pele et al., 2017). Although the underlying mechanism remains to be demonstrated, it appears that the link between ploidy level and CO increase is associated with genetic content. Indeed, further work in Brassica has shown that the addition of one specific chromosome (C genome chromosome 9) is sufficient to increase CO in polyploid hybrids while addition of other chromosomes had no effect (Suay et al., 2014). Altogether, these results suggest that manipulating ploidy level and/or chromosome composition may be a promising alternative for plant breeders to modulate CO formation and ultimately increase genetic diversity of crop plants.

HOW CAN WE REMODEL MEIOSIS FOR CROP IMPROVEMENT?

The manipulation of meiotic recombination gives the breeders a tool to create a new and desirable allele of gene that could be incorporated to a germ line and, unlike the product of mitotic recombination, this trait will be carried to the whole plant as it develops. However, such trait can be removed/modified as meiotic recombination continuously occurs in the following generations. Moreover, the process of meiosis maintains the ploidy of the progeny and limits cross-breeding between accessions or related species containing different ploidy. To overcome these constraints for crop breeding, the meiotic division processes could be engineered to adapt the need of a breeding program.

Diploid Gametes

An important application for remodeling the meiotic division process is to allow formation of unreduced gametes (**Figure 3**). Indeed, a major function of meiosis is to reduce the chromosome complement by half with two successive divisions following a single round of DNA replication. Consequently, circumvention of one division allows formation of unreduced gametes which have proved useful for breeding. Specifically, unreduced gametes are used by breeders to engineer sexual polyploidization (Brownfield and Kohler, 2011; Crismani and Mercier, 2012; De Storme and Geelen, 2013; Ronceret and Vielle-Calzada, 2015). They can facilitate crosses between plants with different ploidy levels or to be utilized to create new polyploid species exhibiting increased genetic diversity and hybrid vigor. It has long been considered that formation of diploid gametes is, at least in part, genetically controlled. Accordingly, a number of mutants producing diploid gametes have been identified in various plants (for reviews see Brownfield and Kohler, 2011; Crismani and Mercier, 2012; De Storme and Geelen, 2013; Ronceret and Vielle-Calzada, 2015). These mutants are usually classified as first division restitution (FDR) or second division restitution (SDR) depending on whether the mutations affect the first or second division, respectively (**Figures 3A–C**). In Arabidopsis, notable examples of these are mutations in *parallel-spindle 1* or *Jason* that both lead to FDR through disturbance of spindle orientation and positioning (D'Erfurth et al., 2008; De Storme and Geelen, 2011). On the contrary, SDR has been obtained by mutating genes controlling entry into second division, such as OMISSION OF DIVISION 1 (*OSD1*) a key regulator of the anaphase promoting complex, or the cyclin *CYCA1;2*/TARDY ASYNCHRONOUS MEIOSIS (*TAM1*; D'Erfurth et al., 2009, 2010). A key difference between FDR and SDR is that they lead to different genetic outcomes. FDR-influenced chromosomes are non-sister chromatids, and therefore, FDR is often considered to produce unreduced gametes with enriched heterozygous marker genotypes (from centromeres to first crossover sites). On the contrary, in SDR, affected chromosomes are sister chromatids (second division not occurring) and the unreduced gametes exhibit homozygous marker genotypes from the centromeres to the first crossover site. Hence, it is important to take into account the desired level of heterozygosity when considering FDR or SDR for a breeding strategy. Interestingly, diploid gametes may also be obtained by applying external stimuli. For example, a high number of diploid gametes are produced when haploid Arabidopsis plants are treated with a 4°C cold shock for several

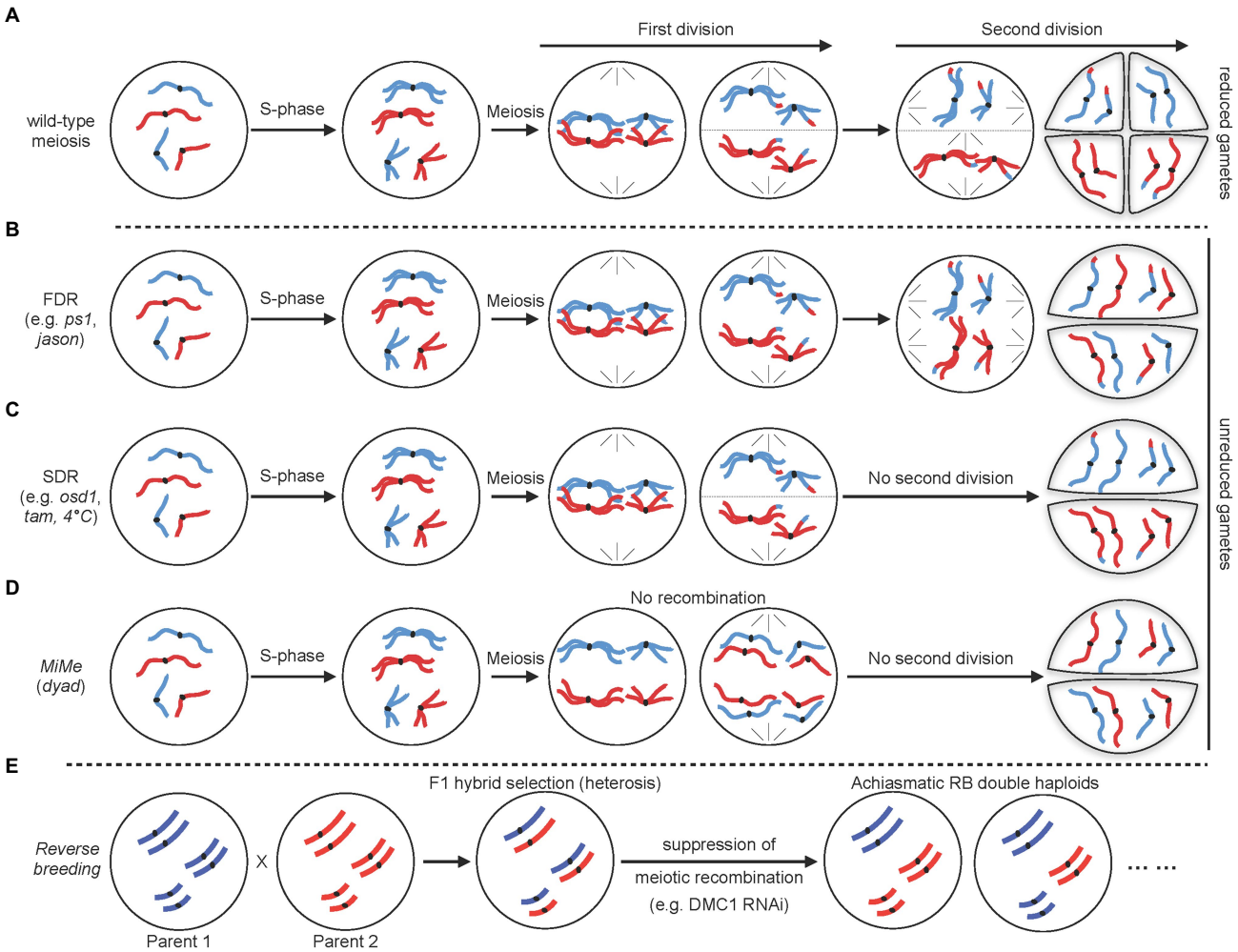

FIGURE 3 | Schematic representation of different strategies to remodel the meiotic division. **(A)** Normal meiotic division resulting in haploid (n) gametes. **(B,C)** Non-reductional meiotic divisions resulting in unreduced (2n) meiotic products. First division restitution (FDR; **B**) and second division restitution (SDR; **C**) lead to different levels of heterozygosity (see text for details). **(D)** Schematic diagram of apomeiosis obtained through MiMe strategy. **(E)** Reverse breeding strategy. For simplification, in each case, a diploid cell with only two chromosome pairs is shown with maternal and paternal chromosomes in red and blue, respectively.

hours during flowering stage and this process primarily undergoes SDR (De Storme and Geelen, 2011). Whether this strategy is effective in crops and if other stimuli may trigger similar effects are not yet known. Nevertheless, such approach may be highly relevant for breeding since it would be classified as non-transgenic.

Apomeiosis

Both FDR and SDR result in unreduced gametes which contains chromosomes that were recombined *via* meiotic recombination. However, regarding to breeding strategies, unreduced gametes that have retained parental genome are more useful. Apomixis, in particular, is a form of asexual reproduction allowing clonal reproduction through seeds (Spillane et al., 2004). Apomixis produces progenies that are genetically identical to the maternal genome. This is especially beneficial on the breeding of hybrid varieties since it allows fixation of an elite hybrid genome and its clonal propagation through seeds. Although apomixis naturally occurs in a number of angiosperms, it is absent in most important crops (Spillane et al., 2004). Its success relies on the circumvention of both meiosis and fertilization. A cornerstone of apomixis is thus apomeiosis, a deregulated form of meiosis resulting in a mitotic-like division that prevents recombination and ploidy reduction. Several single mutants disrupting the meiotic process and leading to apomeiosis have been identified in Arabidopsis, rice, and maize (Ronceret and Vielle-Calzada, 2015; **Figure 3D**). However, these mutants are usually sterile and form apomeiotic gametes at an extremely low frequency. The best example of these is the Arabidopsis *DYAD/SWITCH1* gene, a regulator of meiotic chromosome organizations essential for meiotic entry (Ravi et al., 2008). Artificial apomeiosis has been successfully achieved through mutation of this single gene (Ravi et al., 2008). In the *dyad* allele, alteration of the meiotic process into a mitotic-like division leads to the formation of unreduced female gametes that retain parental heterozygosity, representative of apomeiosis. However, although this appeared

promising at first sight, it is hardly amenable to crops since *dyad* plants are nearly sterile and less than 1% of the *dyad* ovules generate viable gametes (Ravi et al., 2008).

Rather than mutating a single gene, a major success in engineering apomeiosis was later obtained by combining several mutations that disrupt the key steps of the meiotic division (D'Erfurth et al., 2009; **Figure 3D**). This was accomplished by simultaneously disrupting three key steps of meiosis: (1) bypassing of the second meiotic division to allow production of functional diploid gametes; this can be achieved through mutating and removing the function of the key regulator *OSD1*, (2) suppression of meiotic recombination to prevent formation of recombined gametes. This can be achieved through mutation of genes involved in meiotic DSB formation. For example, using a null allele of *SPO11-1* to eliminate the initiation of meiotic DSB formation, and (3) allowing segregation of sister chromatids at the first division through loss-of-function of the meiotic-specific cohesin REC8. In Arabidopsis, plants with this genotype undergo meiosis that is replaced by mitosis and they are called *MiMe* (for Mitosis instead of Meiosis). This remodeling of meiosis gives rise to functional diploid gametes with genetically identical genomes (D'Erfurth et al., 2009; **Figure 3D**). The practicability of this technology was further demonstrated by alternatively targeting other genes disrupting the key steps of meiosis. For instance, the use of *osd1* mutation to bypass the second meiotic segregation has been successfully replaced by mutation of the cyclin *CYCA1; 2/TAM1* or use of a *tdm1* dominant mutation (D'Erfurth et al., 2010; Cifuentes et al., 2016). Similarly, suppression of meiotic recombination can be obtained by mutating various components of the meiotic DSB complex (e.g., *PRD1*, *PRD2*, or *PRD3*; Mieulet et al., 2016). This artificial engineering of apomeiosis is a particularly ground-breaking achievement since *MiMe* plants are fertile and produce near wild-type levels of viable apomeiotic gametes. Remarkably, this technology has also recently been translated to rice (Mieulet et al., 2016). Through mutation of rice *OSD1*, *PAIR1* (rice homolog of *PRD3*), and *REC8*, the authors could reproduce the *MiMe* genotype and, importantly, showed that rice *MiMe* plants remained fertile. Altogether these data demonstrate the potential of the *MiMe* technology for engineering apomeiosis in plants. Yet, it remains unclear whether this technology is applicable to other crops and, in particular, polyploid species, such as bread wheat. Another obstacle of this technology is that since gametes are diploid and normal fertilization continues to occur, ploidy is expected to double at each generation. To overcome this problem, *MiMe* technology has been combined with genome elimination strategies that allow removal of a complete set of chromosome from one parent after fertilization (Ishii et al., 2016; Jacquier et al., 2020). Such genome elimination is usually accomplished by using haploid inducer lines which can be obtained through manipulation of the centromeric histone 3 variant (CENH3; Ravi et al., 2008; Marimuthu et al., 2011), or the *MATRILINEAL*/*NOT-LIKE DAD*/*PHOSPHOLIPASE A1* gene (Wang et al., 2019a). Haploid inducer lines do not directly affect meiosis and will thus not be described here. For detailed description of haploid inducer lines and genome elimination, readers are directed to several excellent recent reviews (Ishii et al., 2016; Jacquier et al., 2020). Alternatively, creation of haploid plants can also be obtained by misexpression in egg cell of the *BABY BOOM 1* (*BBM1*) gene (Khanday et al., 2019). *BBM1* is a male-expressed gene essential to initiate embryogenesis after fertilization and misexpression of *BBM1* in egg cell is sufficient to trigger parthenogenesis and the production of haploid plants (Khanday et al., 2019). Remarkably, combining one of these strategies with MiMe technology has allowed engineering clonal reproduction in both Arabidopsis and rice (Marimuthu et al., 2011; Khanday et al., 2019; Wang et al., 2019a; Khanday and Sundaresan, 2021). Yet, frequencies of clonal embryo remain low (haploid inducer lines are not fully penetrant) and overall seed production is also strongly decreased. This means that broad implementation of apomixis in a sustainable way in crops will require further research to unravel new factors and mechanisms controlling apomeiosis and haploid induction. However, to achieve this will also require a better understanding of the interplay between these two components of apomixis.

Reverse Breeding

Heterozygous hybrids have the tendency to outperform their homozygous parents in fitness (Chen, 2010; Labroo et al., 2021). This phenomenon, known as hybrid vigor or heterosis, is widely used by breeders to produce elite varieties with improved field quality. Creation of these elite heterozygous hybrids is achieved by crossing two selected homozygous parents. However, such favorable hybrids cannot be stably maintained because allele combinations are reshuffled by genetic recombination during meiosis before being transmitted to the progeny. This means that offspring lose the heterosis effect and breeders must continuously recreate favorable hybrids. Different strategies have been proposed to preserve transmission of heterozygous genotypes. Reverse breeding, which is an alternative to apomixis, has emerged as a promising strategy to fix hybrid genomes (Dirks et al., 2009; **Figure 3E**). Reverse breeding generates homozygous parental lines from a heterozygous hybrid. When applied to hybrids with known parents, the approach can also be used to generate chromosome substitution lines, in which the chromosome of one line is replaced by the chromosome of another line (Dirks et al., 2009). The method relies on suppression of meiotic crossovers in the hybrid followed by the production of doubled haploids from non-recombinant gametes (Dirks et al., 2009; **Figure 3E**). The practicability of the method was originally demonstrated in Arabidopsis by silencing the meiotic-specific recombinase DMC1 using RNA interference (Wijnker et al., 2012, 2014). Non-recombinant gametes were converted into haploid adult plants using centromere-mediated genome elimination and fertile diploids (double haploids) and were eventually obtained by self-pollination of those haploids (Wijnker et al., 2012). The main limitation of the method lies in the fact that suppression of meiotic recombination leads to achiasmatic chromosomes which segregate randomly. Production of balanced non-recombinant gametes thus relies on fortuitous balanced

segregation, whose frequency strongly depends on chromosome number. The method is thus limited to species with low chromosome number (less than 12; Dirks et al., 2009). An alternative to the solution would be to reduce, but not completely suppress, CO formation. Having one or a few CO would still lead to low production of CO-free gametes but will also increase the production of gametes with low CO numbers, which would prove useful for reverse breeding. This strategy was recently validated by downregulating Arabidopsis *MSH5* gene expression through VIGS (Calvo-Baltanas et al., 2020). Furthermore, VIGS has the additional advantage of allowing transient downregulation and thus avoids integration of a stable transgene in the genome, which is a strong concern for breeders. Altogether, these data suggest that reverse breeding could be effectively applied to many crops. However, unlike apomixis, this strategy has not yet been demonstrated in crops.

CONCLUDING REMARKS

Several novel insights on meiosis have emerged in recent years and form a framework to develop innovative technologies to accelerate pre-breeding strategies. However, most of our understanding of meiosis is based on Arabidopsis research and it is of particular importance to pivot toward the translational potential of these discoveries and the study of other plant species. It is likely that future studies will identify significant differences in the regulation of meiosis between Arabidopsis and crops which may occlude a direct transfer of certain strategies between plants. Comparative studies of meiosis across a broad range of species will address this gap in our knowledge and have the potential to identify new functional pathways and to provide a deeper understanding of the evolution of meiotic gene function.

AUTHOR CONTRIBUTIONS

All authors listed have made a substantial, direct and intellectual contribution to the work, and approved it for publication.

ACKNOWLEDGMENTS

We would like to thank Dr. Kim Osman for providing the images of wheat chromosome staining and Dr. Mikel Arrieta and the James Hutton Institute for providing the crossover frequency data in Barley. We would also like to thank Dr. Charles White and Dr. Alexander Blackwell for their comments on the manuscript.

REFERENCES

Acquaviva, L., Szekvolgyi, L., Dichtl, B., Dichtl, B. S., De La Roche Saint Andre, C., Nicolas, A., et al. (2013). The COMPASS subunit Spp1 links histone methylation to initiation of meiotic recombination. *Science* 339, 215–218. doi: 10.1126/science.1225739

Armstrong, S. J., Caryl, A. P., Jones, G. H., and Franklin, F. C. (2002). Asy1, a protein required for meiotic chromosome synapsis, localizes to axis-associated chromatin in Arabidopsis and brassica. *J. Cell Sci.* 115, 3645–3655. doi: 10.1242/jcs.00048

Armstrong, S. J., Franklin, F. C., and Jones, G. H. (2001). Nucleolus-associated telomere clustering and pairing precede meiotic chromosome synapsis in *Arabidopsis thaliana*. *J. Cell Sci.* 114, 4207–4217. doi: 10.1242/jcs.114.23.4207

Barakate, A., Higgins, J. D., Vivera, S., Stephens, J., Perry, R. M., Ramsay, L., et al. (2014). The synaptonemal complex protein ZYP1 is required for imposition of meiotic crossovers in barley. *Plant Cell* 26, 729–740. doi: 10.1105/tpc.113.121269

Benyahya, F., Nadaud, I., Da Ines, O., Rimbert, H., White, C., and Sourdille, P. (2020). SPO11.2 is essential for programmed double-strand break formation during meiosis in bread wheat (*Triticum aestivum* L.). *Plant J.* 104, 30–43. doi: 10.1111/tpj.14903

Berchowitz, L. E., and Copenhaver, G. P. (2010). Genetic interference: don't stand so close to me. *Curr. Genomics* 11, 91–102. doi: 10.2174/138920210790886835

Bergerat, A., De Massy, B., Gadelle, D., Varoutas, P. C., Nicolas, A., and Forterre, P. (1997). An atypical topoisomerase II from archaea with implications for meiotic recombination. *Nature* 386, 414–417. doi: 10.1038/386414a0

Beying, N., Schmidt, C., Pacher, M., Houben, A., and Puchta, H. (2020). CRISPR-Cas9-mediated induction of heritable chromosomal translocations in Arabidopsis. *Nat. Plants* 6, 638–645. doi: 10.1038/s41477-020-0663-x

Blackwell, A. R., Dluzewska, J., Szymanska-Lejman, M., Desjardins, S., Tock, A. J., Kbiri, N., et al. (2020). MSH2 shapes the meiotic crossover landscape in relation to interhomolog polymorphism in Arabidopsis. *EMBO J.* 39:e104858. doi: 10.15252/embj.2020104858

Blary, A., Gonzalo, A., Eber, F., Berard, A., Berges, H., Bessoltane, N., et al. (2018). FANCM limits meiotic crossovers in brassica crops. *Front. Plant Sci.* 9:368. doi: 10.3389/fpls.2018.00368

Brownfield, L., and Kohler, C. (2011). Unreduced gamete formation in plants: mechanisms and prospects. *J. Exp. Bot.* 62, 1659–1668. doi: 10.1093/jxb/erq371

Cai, X., Dong, F., Edelmann, R. E., and Makaroff, C. A. (2003). The Arabidopsis SYN1 cohesin protein is required for sister chromatid arm cohesion and homologous chromosome pairing. *J. Cell Sci.* 116, 2999–3007. doi: 10.1242/jcs.00601

Calvo-Baltanas, V., Wijnen, C. L., Yang, C., Lukhovitskaya, N., De Snoo, C. B., Hohenwarter, L., et al. (2020). Meiotic crossover reduction by virus-induced gene silencing enables the efficient generation of chromosome substitution lines and reverse breeding in *Arabidopsis thaliana*. *Plant J.* 104, 1437–1452. doi: 10.1111/tpj.14990

Capilla-Perez, L., Durand, S., Hurel, A., Lian, Q., Chambon, A., Taochy, C., et al. (2021). The synaptonemal complex imposes crossover interference and heterochiasmy in Arabidopsis. *Proc. Natl. Acad. Sci. U. S. A.* 118:e2023613118. doi: 10.1073/pnas.2023613118

Chambon, A., West, A., Vezon, D., Horlow, C., De Muyt, A., Chelysheva, L., et al. (2018). Identification of ASYNAPTIC4, a component of the meiotic chromosome axis. *Plant Physiol.* 178, 233–246. doi: 10.1104/pp.17.01725

Chelysheva, L., Diallo, S., Vezon, D., Gendrot, G., Vrielynck, N., Belcram, K., et al. (2005). AtREC8 and AtSCC3 are essential to the monopolar orientation of the kinetochores during meiosis. *J. Cell Sci.* 118, 4621–4632. doi: 10.1242/jcs.02583

Chen, Z. J. (2010). Molecular mechanisms of polyploidy and hybrid vigor. *Trends Plant Sci.* 15, 57–71. doi: 10.1016/j.tplants.2009.12.003

Chen, X., Suhandynata, R. T., Sandhu, R., Rockmill, B., Mohibullah, N., Niu, H., et al. (2015). Phosphorylation of the synaptonemal complex protein zip1 regulates the crossover/noncrossover decision during yeast meiosis. *PLoS Biol.* 13:e1002329. doi: 10.1371/journal.pbio.1002329

Choi, K., Zhao, X., Tock, A. J., Lambing, C., Underwood, C. J., Hardcastle, T. J., et al. (2018). Nucleosomes and DNA methylation shape meiotic DSB frequency in *Arabidopsis thaliana* transposons and gene regulatory regions. *Genome Res.* 28, 532–546. doi: 10.1101/gr.225599.117

Cifuentes, M., Jolivet, S., Cromer, L., Harashima, H., Bulankova, P., Renne, C., et al. (2016). TDM1 regulation determines the number of meiotic divisions. *PLoS Genet.* 12:e1005856. doi: 10.1371/journal.pgen.1005856

Cloud, V., Chan, Y. L., Grubb, J., Budke, B., and Bishop, D. K. (2012). Rad51 is an accessory factor for Dmc1-mediated joint molecule formation during meiosis. *Science* 337, 1222–1225. doi: 10.1126/science.1219379

Corem, S., Doron-Faigenboim, A., Jouffroy, O., Maumus, F., Arazi, T., and Bouche, N. (2018). Redistribution of CHH methylation and small interfering RNAs across the genome of tomato ddm1 mutants. *Plant Cell* 30, 1628–1644. doi: 10.1105/tpc.18.00167

Coulton, A., Burridge, A. J., and Edwards, K. J. (2020). Examining the effects of temperature on recombination in wheat. *Front. Plant Sci.* 11:230. doi: 10.3389/fpls.2020.00230

Crismani, W., Girard, C., Froger, N., Pradillo, M., Santos, J. L., Chelysheva, L., et al. (2012). FANCM limits meiotic crossovers. *Science* 336, 1588–1590. doi: 10.1126/science.1220381

Crismani, W., and Mercier, R. (2012). What limits meiotic crossovers? *Cell Cycle* 11, 3527–3528. doi: 10.4161/cc.21963

Da Ines, O., Abe, K., Goubely, C., Gallego, M. E., and White, C. I. (2012). Differing requirements for RAD51 and DMC1 in meiotic pairing of centromeres and chromosome arms in *Arabidopsis thaliana*. *PLoS Genet.* 8:e1002636. doi: 10.1371/journal.pgen.1002636

Da Ines, O., Michard, R., Fayos, I., Bastianelli, G., Nicolas, A., Guiderdoni, E., et al. (2020). Bread wheat TaSPO11-1 exhibits evolutionarily conserved function in meiotic recombination across distant plant species. *Plant J.* 103, 2052–2068. doi: 10.1111/tpj.14882

Da Ines, O., and White, C. I. (2015). Centromere associations in meiotic chromosome pairing. *Annu. Rev. Genet.* 49, 95–114. doi: 10.1146/annurev-genet-112414-055107

De Maagd, R. A., Loonen, A., Chouaref, J., Pele, A., Meijer-Dekens, F., Fransz, P., et al. (2020). CRISPR/Cas inactivation of RECQ4 increases homeologous crossovers in an interspecific tomato hybrid. *Plant Biotechnol. J.* 18, 805–813. doi: 10.1111/pbi.13248

De Muyt, A., Pereira, L., Vezon, D., Chelysheva, L., Gendrot, G., Chambon, A., et al. (2009). A high throughput genetic screen identifies new early meiotic recombination functions in *Arabidopsis thaliana*. *PLoS Gent.* 5:e1000654. doi: 10.1371/journal.pgen.1000654

De Muyt, A., Vezon, D., Gendrot, G., Gallois, J.-L., Stevens, R., and Grelon, M. (2007). AtPRD1 is required for meiotic double strand break formation in *Arabidopsis thaliana*. *EMBO J.* 26, 4126–4137. doi: 10.1038/sj.emboj.7601815

De Storme, N., and Geelen, D. (2011). The Arabidopsis mutant jason produces unreduced first division restitution male gametes through a parallel/fused spindle mechanism in meiosis II. *Plant Physiol.* 155, 1403–1415. doi: 10.1104/pp.110.170415

De Storme, N., and Geelen, D. (2013). Sexual polyploidization in plants––cytological mechanisms and molecular regulation. *New Phytol.* 198, 670–684. doi: 10.1111/nph.12184

D'Erfurth, I., Cromer, L., Jolivet, S., Girard, C., Horlow, C., Sun, Y., et al. (2010). The cyclin-A CYCA1;2/TAM is required for the meiosis I to meiosis II transition and cooperates with OSD1 for the prophase to first meiotic division transition. *PLoS Genet.* 6:e1000989. doi: 10.1371/journal.pgen.1000989

D'Erfurth, I., Jolivet, S., Froger, N., Catrice, O., Novatchkova, M., and Mercier, R. (2009). Turning meiosis into mitosis. *PLoS Biol.* 7:e1000124. doi: 10.1371/journal.pbio.1000124

D'Erfurth, I., Jolivet, S., Froger, N., Catrice, O., Novatchkova, M., Simon, M., et al. (2008). Mutations in AtPS1 (*Arabidopsis thaliana* parallel spindle 1) lead to the production of diploid pollen grains. *PLoS Genet.* 4:e1000274. doi: 10.1371/journal.pgen.1000274

Desjardins, S. D., Ogle, D. E., Ayoub, M. A., Heckmann, S., Henderson, I. R., Edwards, K. J., et al. (2020). MutS homologue 4 and MutS homologue 5 maintain the obligate crossover in wheat despite stepwise gene loss following polyploidization. *Plant Physiol.* 183, 1545–1558. doi: 10.1104/pp.20.00534

Dirks, R., Van Dun, K., De Snoo, C. B., Van Den Berg, M., Lelivelt, C. L., Voermans, W., et al. (2009). Reverse breeding: a novel breeding approach based on engineered meiosis. *Plant Biotechnol. J.* 7, 837–845. doi: 10.1111/j.1467-7652.2009.00450.x

Drouaud, J., Khademian, H., Giraut, L., Zanni, V., Bellalou, S., Henderson, I. R., et al. (2013). Contrasted patterns of crossover and non-crossover at *Arabidopsis thaliana* meiotic recombination hotspots. *PLoS Genet.* 9:e1003922. doi: 10.1371/journal.pgen.1003922

Ellermeier, C., Higuchi, E. C., Phadnis, N., Holm, L., Geelhood, J. L., Thon, G., et al. (2010). RNAi and heterochromatin repress centromeric meiotic recombination. *Proc. Natl. Acad. Sci. U. S. A.* 107, 8701–8705. doi: 10.1073/pnas.0914160107

Fayos, I., Meunier, A. C., Vernet, A., Navarro-Sanz, S., Portefaix, M., Lartaud, M., et al. (2020). Assessment of the roles of SPO11-2 and SPO11-4 in meiosis in rice using CRISPR/Cas9 mutagenesis. *J. Exp. Bot.* 71, 7046–7058. doi: 10.1093/jxb/eraa391

Ferdous, M., Higgins, J. D., Osman, K., Lambing, C., Roitinger, E., Mechtler, K., et al. (2012). Inter-homolog crossing-over and synapsis in Arabidopsis meiosis are dependent on the chromosome axis protein AtASY3. *PLoS Genet.* 8:e1002507. doi: 10.1371/journal.pgen.1002507

Fernandes, J. B., Seguela-Arnaud, M., Larcheveque, C., Lloyd, A. H., and Mercier, R. (2018). Unleashing meiotic crossovers in hybrid plants. *Proc. Natl. Acad. Sci. U. S. A.* 115, 2431–2436. doi: 10.1073/pnas.1713078114

Fernandes, J. B., Wlodzimierz, P., and Henderson, I. R. (2019). Meiotic recombination within plant centromeres. *Curr. Opin. Plant Biol.* 48, 26–35. doi: 10.1016/j.pbi.2019.02.008

France, M. G., Enderle, J., Rohrig, S., Puchta, H., Franklin, F. C. H., and Higgins, J. D. (2021). ZYP1 is required for obligate cross-over formation and cross-over interference in Arabidopsis. *Proc. Natl. Acad. Sci. U. S. A.* 118:2021671118. doi: 10.1073/pnas.2021671118

Fransz, P. F., Armstrong, S., De Jong, J. H., Parnell, L. D., Van Drunen, C., Dean, C., et al. (2000). Integrated cytogenetic map of chromosome arm 4S of *A. thaliana*: structural organization of heterochromatic knob and centromere region. *Cell* 100, 367–376. doi: 10.1016/S0092-8674(00)80672-8

Fu, M., Wang, C., Xue, F., Higgins, J., Chen, M., Zhang, D., et al. (2016). The DNA topoisomerase VI-B subunit OsMTOPVIB is essential for meiotic recombination initiation in rice. *Mol. Plant* 9, 1539–1541. doi: 10.1016/j.molp.2016.07.006

Gallego-Bartolome, J., Gardiner, J., Liu, W., Papikian, A., Ghoshal, B., Kuo, H. Y., et al. (2018). Targeted DNA demethylation of the Arabidopsis genome using the human TET1 catalytic domain. *Proc. Natl. Acad. Sci. U. S. A.* 115, E2125–E2134. doi: 10.1073/pnas.1716945115

Gardiner, L. J., Wingen, L. U., Bailey, P., Joynson, R., Brabbs, T., Wright, J., et al. (2019). Analysis of the recombination landscape of hexaploid bread wheat reveals genes controlling recombination and gene conversion frequency. *Genome Biol.* 20:69. doi: 10.1186/s13059-019-1675-6

Girard, C., Chelysheva, L., Choinard, S., Froger, N., Macaisne, N., Lemhemdi, A., et al. (2015). AAA-ATPase FIDGETIN-LIKE 1 and helicase FANCM antagonize meiotic crossovers by distinct mechanisms. *PLoS Genet.* 11:e1005369. doi: 10.1371/journal.pgen.1005448

Golubovskaya, I. N., Hamant, O., Timofejeva, L., Wang, C. J., Braun, D., Meeley, R., et al. (2006). Alleles of afd1 dissect REC8 functions during meiotic prophase I. *J. Cell Sci.* 119, 3306–3315. doi: 10.1242/jcs.03054

Gong, Z., Morales-Ruiz, T., Ariza, R. R., Roldan-Arjona, T., David, L., and Zhu, J. K. (2002). ROS1, a repressor of transcriptional gene silencing in Arabidopsis, encodes a DNA glycosylase/lyase. *Cell* 111, 803–814. doi: 10.1016/S0092-8674(02)01133-9

Hartung, F., Wurz-Wildersinn, R., Fuchs, J., Schubert, I., Suer, S., and Puchta, H. (2007). The catalytically active tyrosine residues of both SPO11-1 and SPO11-2 are required for meiotic double-strand break induction in Arabidopsis. *Plant Cell* 19, 3090–3099. doi: 10.1105/tpc.107.054817

He, Y., Wang, M., Dukowic-Schulze, S., Zhou, A., Tiang, C. L., Shilo, S., et al. (2017). Genomic features shaping the landscape of meiotic double-strand-break hotspots in maize. *Proc. Natl. Acad. Sci. U. S. A.* 114, 12231–12236. doi: 10.1073/pnas.1713225114

Henderson, K. A., and Keeney, S. (2004). Tying synaptonemal complex initiation to the formation and programmed repair of DNA double-strand breaks. *Proc. Natl. Acad. Sci. U. S. A.* 101, 4519–4524. doi: 10.1073/pnas.0400843101

Higgins, J. D., Perry, R. M., Barakate, A., Ramsay, L., Waugh, R., Halpin, C., et al. (2012). Spatiotemporal asymmetry of the meiotic program underlies the predominantly distal distribution of meiotic crossovers in barley. *Plant Cell* 24, 4096–4109. doi: 10.1105/tpc.112.102483

Higgins, J. D., Sanchez-Moran, E., Armstrong, S. J., Jones, G. H., and Franklin, F. C. (2005). The Arabidopsis synaptonemal complex protein ZYP1 is required for chromosome synapsis and normal fidelity of crossing over. *Genes Dev.* 19, 2488–2500. doi: 10.1101/gad.354705

Hong, S., Sung, Y., Yu, M., Lee, M., Kleckner, N., and Kim, K. P. (2013). The logic and mechanism of homologous recombination partner choice. *Mol. Cell* 51, 440–453. doi: 10.1016/j.molcel.2013.08.008

Ishii, T., Karimi-Ashtiyani, R., and Houben, A. (2016). Haploidization via chromosome elimination: means and mechanisms. *Annu. Rev. Plant Biol.* 67, 421–438. doi: 10.1146/annurev-arplant-043014-114714

Jacquier, N. M. A., Gilles, L. M., Pyott, D. E., Martinant, J. P., Rogowsky, P. M., and Widiez, T. (2020). Puzzling out plant reproduction by haploid induction for innovations in plant breeding. *Nat. Plants* 6, 610–619. doi: 10.1038/s41477-020-0664-9

Jing, J.-L., Zhang, T., Kao, Y.-H., Huang, T.-H., Wang, C. J. R., and He, Y. (2020). *ZmMTOPVIB* enables DNA double-strand break formation and bipolar spindle assembly during maize meiosis. *Plant Physiol.* 184, 1811–1822. doi: 10.1104/pp.20.00933

Jing, J.-L., Zhang, T., Wang, Y. Z., and He, Y. (2019). Advances towards how meiotic recombination is initiated: a coparative view and perspectives for plant meiosis research. *Int. J. Mol. Sci.* 20:4718. doi: 10.3390/ijms20194718

Jones, G. H., and Franklin, F. C. (2006). Meiotic crossing-over: obligation and interference. *Cell* 126, 246–248. doi: 10.1016/j.cell.2006.07.010

Khanday, I., Skinner, D., Yang, B., Mercier, R., and Sundaresan, V. (2019). A male-expressed rice embryogenic trigger redirected for asexual propagation through seeds. *Nature* 565, 91–95. doi: 10.1038/s41586-018-0785-8

Khanday, I., and Sundaresan, V. (2021). Plant zygote development: recent insights and applications to clonal seeds. *Curr. Opin. Plant Biol.* 59:101993. doi: 10.1016/j.pbi.2020.101993

Kleckner, N. (2006). Chiasma formation: chromatin/axis interplay and the role(s) of the synaptonemal complex. *Chromosoma* 115, 175–194. doi: 10.1007/s00412-006-0055-7

Kleckner, N., Zickler, D., Jones, G. H., Dekker, J., Padmore, R., Henle, J., et al. (2004). A mechanical basis for chromosome function. *Proc. Natl. Acad. Sci. U. S. A.* 101, 12592–12597. doi: 10.10732/Fpnas.0402724101

Labroo, M. R., Studer, A. J., and Rutkoski, J. E. (2021). Heterosis and hybrid crop breeding: a multidisciplinary review. *Front. Genet.* 24:643761. doi: 10.3389/fgene.2021.643761

Lam, I., and Keeney, S. (2015). Nonparadoxical evolutionary stability of the recombination initiation landscape in yeast. *Science* 350, 932–937. doi: 10.1126/science.aad0814

Lamb, J. C., Yu, W., Han, F., and Birchler, J. A. (2007). Plant chromosomes from end to end: telomeres, heterochromatin and centromeres. *Curr. Opin. Plant Biol.* 10, 116–122. doi: 10.1016/j.pbi.2007.01.008

Lambing, C., Franklin, F. C., and Wang, C. R. (2017). Understanding and manipulating meiotic recombination in plants. *Plant Physiol.* 173, 1530–1542. doi: 10.1104/pp.16.01530

Lambing, C., Kuo, P. C., Tock, A. J., Topp, S. D., and Henderson, I. R. (2020a). ASY1 acts as a dosage-dependent antagonist of telomere-led recombination and mediates crossover interference in Arabidopsis. *Proc. Natl. Acad. Sci. U. S. A.* 117, 13647–13658. doi: 10.1073/pnas.1921055117

Lambing, C., Osman, K., Nuntasoontorn, K., West, A., Higgins, J. D., Copenhaver, G. P., et al. (2015). Arabidopsis PCH2 mediates meiotic chromosome remodeling and maturation of crossovers. *PLoS Genet.* 11:e1005372. doi: 10.1371/journal.pgen.1005372

Lambing, C., Tock, A. J., Topp, S. D., Choi, K., Kuo, P. C., Zhao, X., et al. (2020b). Interacting genomic landscapes of rec8-cohesin, chromatin, and meiotic recombination in Arabidopsis. *Plant Cell* 32, 1218–1239. doi: 10.1105/tpc.19.00866

Lee, D. H., Kao, Y. H., Ku, J. C., Lin, C. Y., Meeley, R., Jan, Y. S., et al. (2015). The axial element protein desynaptic2 mediates meiotic double-strand break formation and synaptonemal complex assembly in maize. *Plant Cell* 27, 2516–2529. doi: 10.1105/tpc.15.00434

Leflon, M., Grandont, L., Eber, F., Huteau, V., Coriton, O., Chelysheva, L., et al. (2010). Crossovers get a boost in brassica allotriploid and allotetraploid hybrids. *Plant Cell* 22, 2253–2264. doi: 10.1105/tpc.110.075986

Li, Q., Eichten, S. R., Hermanson, P. J., Zaunbrecher, V. M., Song, J., Wendt, J., et al. (2014). Genetic perturbation of the maize methylome. *Plant Cell* 26, 4602–4616. doi: 10.1105/tpc.114.133140

Li, X., Li, L., and Yan, J. (2015). Dissecting meiotic recombination based on tetrad analysis by single-microspore sequencing in maize. *Nat. Commun.* 6:6648. doi: 10.1038/ncomms7648

Libuda, D. E., Uzawa, S., Meyer, B. J., and Villeneuve, A. M. (2013). Meiotic chromosome structures constrain and respond to designation of crossover sites. *Nature* 502, 703–706. doi: 10.1038/nature12577

Ma, J., Wing, R. A., Bennetzen, J. L., and Jackson, S. A. (2007). Plant centromere organization: a dynamic structure with conserved functions. *Trends Genet.* 23, 134–139. doi: 10.1016/j.tig.2007.01.004

Mancera, E., Bourgon, R., Brozzi, A., Huber, W., and Steinmetz, L. M. (2008). High-resolution mapping of meiotic crossovers and non-crossovers in yeast. *Nature* 454, 479–485. doi: 10.1038/nature07135

Marimuthu, M. P., Jolivet, S., Ravi, M., Pereira, L., Davda, J. N., Cromer, L., et al. (2011). Synthetic clonal reproduction through seeds. *Science* 331:876. doi: 10.1126/science.1199682

Marques, A., and Pedrosa-Harand, A. (2016). Holocentromere identity: from the typical mitotic linear structure to the great plasticity of meiotic holocentromeres. *Chromosoma* 125, 669–681. doi: 10.1007/s00412-016-0612-7

Marsolier-Kergoat, M. C., Khan, M. M., Schott, J., Zhu, X., and Llorente, B. (2018). Mechanistic view and genetic control of dna recombination during meiosis. *Mol. Cell* 70, 9–20. doi: 10.1016/j.molcel.2018.02.032

Martini, E., Diaz, R. L., Hunter, N., and Keeney, S. (2006). Crossover homeostasis in yeast meiosis. *Cell* 126, 285–295. doi: 10.1016/j.cell.2006.05.044

Mcmahill, M. S., Sham, C. W., and Bishop, D. K. (2007). Synthesis-dependent strand annealing in meiosis. *PLoS Biol.* 5:e299. doi: 10.1371/journal.pbio.0050299

Medhi, D., Goldman, A. S., and Lichten, M. (2016). Local chromosome context is a major determinant of crossover pathway biochemistry during budding yeast meiosis. *eLife* 5:e19669. doi: 10.7554/eLife.19669

Melters, D. P., Paliulis, L. V., Korf, I. F., and Chan, S. W. (2012). Holocentric chromosomes: convergent evolution, meiotic adaptations, and genomic analysis. *Chromosom. Res.* 20, 579–593. doi: 10.1007/s10577-012-9292-1

Mercier, R., Mezard, C., Jenczewski, E., Macaisne, N., and Grelon, M. (2015). The molecular biology of meiosis in plants. *Annu. Rev. Plant Biol.* 66, 297–327. doi: 10.1146/annurev-arplant-050213-035923

Mieulet, D., Aubert, G., Bres, C., Klein, A., Droc, G., Vieille, E., et al. (2018). Unleashing meiotic crossovers in crops. *Nat. Plants* 4, 1010–1016. doi: 10.1038/s41477-018-0311-x

Mieulet, D., Jolivet, S., Rivard, M., Cromer, L., Vernet, A., Mayonove, P., et al. (2016). Turning rice meiosis into mitosis. *Cell Res.* 26, 1242–1254. doi: 10.1038/cr.2016.117

Nageswaran, D. C., Kim, J., Lambing, C., Kim, J., Park, J., Kim, E.-J., et al. (2021). HIGH CROSSOVER RATE1 encodes PROTEIN PHOSPHATASE X1 and restricts meiotic crossovers in Arabidopsis. *Nat. Plants* 7, 452–467. doi: 10.1038/s41477-021-00889-y

Nonomura, K., Nakano, F. T., Eiguchi, M., Miyao, A., Hirochika, H., and Kurata, N. (2004). The novel gene HOMOLOGOUS PAIRING ABERRATION IN RICE MEIOSIS1 of rice encodes a putative coiled-coil protein required for homologous chromosome pairing in MEIOSIS. *Plant Cell* 16, 1008–1020. doi: 10.1105/tpc.020701

Nonomura, K., Nakano, M., Eiguchi, M., Suzuki, T., and Kurata, N. (2006). PAIR2 is essential for homologous chromosome synapsis in rice meiosis I. *J. Cell Sci.* 119, 217–225. doi: 10.1242/jcs.02736

Osman, K., Algopishi, U., Higgins, J. D., Henderson, I. R., Edwards, K. J., Franklin, F. C. H., et al. (2021). Distal bias of meiotic crossovers in hexaploid bread wheat reflects spatio-temporal asymmetry of the meiotic program. *Front. Plant Sci.* 12:631323. doi: 10.33892/Ffpls.2021.631323

Osman, K., Yang, J., Roitinger, E., Lambing, C., Heckmann, S., Howell, E., et al. (2018). Affinity proteomics reveals extensive phosphorylation of the brassica chromosome axis protein ASY1 and a network of associated proteins at prophase I of meiosis. *Plant J.* 93, 17–33. doi: 10.1111/tpj.13752

Pan, J., Sasaki, M., Kniewel, R., Murakami, H., Blitzblau, H. G., Tischfield, S. E., et al. (2011). A hierarchical combination of factors shapes the genome-wide topography of yeast meiotic recombination initiation. *Cell* 144, 719–731. doi: 10.1016/j.cell.2011.02.009

Panizza, S., Mendoza, M. A., Berlinger, M., Huang, L., Nicolas, A., Shirahige, K., et al. (2011). Spo11-accessory proteins link double-strand break sites to the chromosome axis in early meiotic recombination. *Cell* 146, 372–383. doi: 10.1016/j.cell.2011.07.003

Pecina, A., Smith, K. N., Mezard, C., Murakami, H., Ohta, K., and Nicolas, A. (2002). Targeted stimulation of meiotic recombination. *Cell* 111, 173–184. doi: 10.1016/S0092-8674(02)01002-4

Pecinka, A., Fang, W., Rehmsmeier, M., Levy, A. A., and Mittelsten Scheid, O. (2011). Polyploidization increases meiotic recombination frequency in Arabidopsis. *BMC Biol.* 9:24. doi: 10.11862/F1741-7007-9-24

Pele, A., Falque, M., Trotoux, G., Eber, F., Negre, S., Gilet, M., et al. (2017). Amplifying recombination genome-wide and reshaping crossover landscapes in brassicas. *PLoS Genet.* 13:e1006794. doi: 10.1371/journal.pgen.1006794

Penterman, J., Zilberman, D., Huh, J. H., Ballinger, T., Henikoff, S., and Fischer, R. L. (2007). DNA demethylation in the Arabidopsis genome. *Proc. Natl. Acad. Sci. U. S. A.* 104, 6752–6757. doi: 10.1073/pnas.0701861104

Phillips, D., Jenkins, G., Macaulay, M., Nibau, C., Wnetrzak, J., Fallding, D., et al. (2015). The effect of temperature on the male and female recombination landscape of barley. *New Phytol.* 208, 421–429. doi: 10.1111/nph.13548

Prosee, R. F., Wenda, J. M., and Steiner, F. A. (2020). Adaptations for centromere function in meiosis. *Essays Biochem.* 64, 193–203. doi: 10.1042/EBC20190076

Ravi, M., Marimuthu, M. P., and Siddiqi, I. (2008). Gamete formation without meiosis in Arabidopsis. *Nature* 451, 1121–1124. doi: 10.1038/nature06557

Raz, A., Dahan-Meir, T., Melamed-Bessudo, C., Leshkowitz, D., and Levy, A. A. (2020). Redistribution of meiotic crossovers along wheat chromosomes by virus-induced gene silencing. *Front. Plant Sci.* 11:635139. doi: 10.3389/fpls.2020.635139

Robert, T., Nore, A., Brun, C., Maffre, C., Crimi, B., Bourbon, H. M., et al. (2016). The TopoVIB-like protein family is required for meiotic DNA double-strand break formation. *Science* 351, 943–949. doi: 10.1126/science.aad5309

Robine, N., Uematsu, N., Amiot, F., Gidrol, X., Barillot, E., Nicolas, A., et al. (2007). Genome-wide redistribution of meiotic double-strand breaks in *Saccharomyces cerevisiae*. *Mol. Cell. Biol.* 27, 1868–1880. doi: 10.1128/MCB.02063-06

Ronceret, A., and Vielle-Calzada, J. P. (2015). Meiosis, unreduced gametes, and parthenogenesis: implications for engineering clonal seed formation in crops. *Plant Reprod.* 28, 91–102. doi: 10.1007/s00497-015-0262-6

Rowan, B. A., Heavens, D., Feuerborn, T. R., Tock, A. J., Henderson, I. R., and Weigel, D. (2019). An ultra high-density *Arabidopsis thaliana* crossover map that refines the influences of structural variation and epigenetic features. *Genetics* 213, 771–787. doi: 10.1534/genetics.119.302406

Sarno, R., Vicq, Y., Uematsu, N., Luka, M., Lapierre, C., Carroll, D., et al. (2017). Programming sites of meiotic crossovers using Spo11 fusion proteins. *Nucleic Acids Res.* 45:e164. doi: 10.1093/nar/gkx739

Schmidt, C., Fransz, P., Ronspies, M., Dreissig, S., Fuchs, J., Heckmann, S., et al. (2020). Changing local recombination patterns in Arabidopsis by CRISPR/Cas mediated chromosome engineering. *Nat. Commun.* 11:4418. doi: 10.10382/Fs41467-020-18277-z

Seguela-Arnaud, M., Crismani, W., Larcheveque, C., Mazel, J., Froger, N., Choinard, S., et al. (2015). Multiple mechanisms limit meiotic crossovers: top3alpha and two BLM homologs antagonize crossovers in parallel to FANCM. *Proc. Natl. Acad. Sci. U. S. A.* 112, 4713–4718. doi: 10.1073/pnas.1423107112

Sepsi, A., and Schwarzacher, T. (2020). Chromosome-nuclear envelope tethering - a process that orchestrates homologue pairing during plant meiosis? *J. Cell Sci.* 133:jcs243667. doi: 10.1242/jcs.243667

Serra, H., Lambing, C., Griffin, C. H., Topp, S. D., Nageswaran, D. C., Underwood, C. J., et al. (2018). Massive crossover elevation via combination of HEI10 and recq4a recq4b during Arabidopsis meiosis. *Proc. Natl. Acad. Sci. U. S. A.* 115, 2437–2442. doi: 10.1073/pnas.1713071115

Shi, W., Ji, J., Xue, Z., Zhang, F., Miao, Y., Yang, H., et al. (2021). PRD1, a homologous recombination initiation factor, is involved in spindle assembly in rice meiosis. *New Phytol.* 230, 585–600. doi: 10.1111/nph.17178

Shi, J., Wolf, S. E., Burke, J. M., Presting, G. G., Ross-Ibarra, J., and Dawe, R. K. (2010). Widespread gene conversion in centromere cores. *PLoS Biol.* 8:e1000327. doi: 10.1371/journal.pbio.1000327

Sidhu, G. K., Fang, C., Olson, M. A., Falque, M., Martin, O. C., and Pawlowski, W. P. (2015). Recombination patterns in maize reveal limits to crossover homeostasis. *Proc. Natl. Acad. Sci. U. S. A.* 112, 15982–15987. doi: 10.1073/pnas.1514265112

Sommermeyer, V., Beneut, C., Chaplais, E., Serrentino, M. E., and Borde, V. (2013). Spp1, a member of the Set1 complex, promotes meiotic DSB formation in promoters by tethering histone H3K4 methylation sites to chromosome axes. *Mol. Cell* 49, 43–54. doi: 10.1016/j.molcel.2012.11.008

Spillane, C., Curtis, M. D., and Grossniklaus, U. (2004). Apomixis technology development-virgin births in farmers' fields? *Nat. Biotechnol.* 22, 687–691. doi: 10.1038/nbt976

Sprink, T., and Hartung, F. (2014). The splicing fate of plant SPO11 genes. *Front. Plant Sci.* 5:214. doi: 10.3389/fpls.2014.00214

Stack, S. M., Shearer, L. A., Lohmiller, L., and Anderson, L. K. (2017). Meiotic crossing over in maize knob heterochromatin. *Genetics* 205, 1101–1112. doi: 10.1534/genetics.116.196089

Stanzione, M., Baumann, M., Papanikos, F., Dereli, I., Lange, J., Ramlal, A., et al. (2016). Meiotic DNA break formation requires the unsynapsed chromosome axis-binding protein IHO1 (CCDC36) in mice. *Nat. Cell Biol.* 18, 1208–1220. doi: 10.1038/ncb3417

Steiner, F. A., and Henikoff, S. (2015). Diversity in the organization of centromeric chromatin. *Curr. Opin. Genet. Dev.* 31, 28–35. doi: 10.1016/j.gde.2015.03.010

Su, H., Liu, Y., Liu, C., Shi, Q., Huang, Y., and Han, F. (2019). Centromere satellite repeats have undergone rapid changes in polyploid wheat subgenomes. *Plant Cell* 31, 2035–2051. doi: 10.1105/tpc.19.00133

Suay, L., Zhang, D., Eber, F., Jouy, H., Lode, M., Huteau, V., et al. (2014). Crossover rate between homologous chromosomes and interference are regulated by the addition of specific unpaired chromosomes in brassica. *New Phytol.* 201, 645–656. doi: 10.1111/nph.12534

Sun, Y., Ambrose, J. H., Haughey, B. S., Webster, T. D., Pierrie, S. N., Munoz, D. F., et al. (2012). Deep genome-wide measurement of meiotic gene conversion using tetrad analysis in *Arabidopsis thaliana*. *PLoS Genet.* 8:e1002968. doi: 10.1371/journal.pgen.1002968

Taagen, E., Bogdanove, A. J., and Sorrells, M. E. (2020). Counting on crossovers: controlled recombination for plant breeding. *Trends Plant Sci.* 25, 455–465. doi: 10.1016/j.tplants.2019.12.017

Talbert, P. B., and Henikoff, S. (2020). What makes a centromere? *Exp. Cell Res.* 389:111895. doi: 10.1016/j.yexcr.2020.111895

Tan, F., Zhou, C., Zhou, Q., Zhou, S., Yang, W., Zhao, Y., et al. (2016). Analysis of chromatin regulators reveals specific features of rice DNA methylation pathways. *Plant Physiol.* 171, 2041–2054. doi: 10.1104/pp.16.00393

Underwood, C. J., Choi, K., Lambing, C., Zhao, X., Serra, H., Borges, F., et al. (2018). Epigenetic activation of meiotic recombination near *Arabidopsis thaliana* centromeres via loss of H3K9me2 and non-CG DNA methylation. *Genome Res.* 28, 519–531. doi: 10.1101/gr.227116.117

Voelkel-Meiman, K., Johnston, C., Thappeta, Y., Subramanian, V. V., Hochwagen, A., and Macqueen, A. J. (2015). Separable crossover-promoting and crossover-constraining aspects of zip1 activity during budding yeast meiosis. *PLoS Genet.* 11:e1005335. doi: 10.1371/journal.pgen.1005335

Vrielynck, N., Chambon, A., Vezon, D., Pereira, L., Chelysheva, L., De Muyt, A., et al. (2016). A DNA topoisomerase VI-like complex initiates meiotic recombination. *Science* 351, 939–943. doi: 10.1126/science.aad5196

Wang, Y., and Copenhaver, G. P. (2018). Meiotic recombination: mixing it up in plants. *Annu. Rev. Plant Biol.* 29, 577–609. doi: 10.1146/annurev-arplant-042817-040431

Wang, C., Liu, Q., Shen, Y., Hua, Y., Wang, J., Lin, J., et al. (2019a). Clonal seeds from hybrid rice by simultaneous genome engineering of meiosis and fertilization genes. *Nat. Biotechnol.* 37, 283–286. doi: 10.1038/s41587-018-0003-0

Wang, S., Veller, C., Sun, F., Ruiz-Herrera, A., Shang, Y., Liu, H., et al. (2019b). Per-nucleus crossover covariation and implications for evolution. *Cell* 177, 326–338. doi: 10.1016/j.cell.2019.02.021

Wang, K., Wang, C., Liu, Q., Liu, W., and Fu, Y. (2015). Increasing the genetic recombination frequency by partial loss of function of the synaptonemal complex in rice. *Mol. Plant* 8, 1295–1298. doi: 10.1016/j.molp.2015.04.011

Wang, K., Wang, M., Tang, D., Shen, Y., Qin, B., Li, M., et al. (2011). PAIR3, an axis-associated protein, is essential for the recruitment of recombination elements onto meiotic chromosomes in rice. *Mol. Biol. Cell* 22, 12–19. doi: 10.1091/mbc.e10-08-0667

Wang, M., Wang, K., Tang, D., Wei, C., Li, M., Shen, Y., et al. (2010). The central element protein ZEP1 of the synaptonemal complex regulates the number of crossovers during meiosis in rice. *Plant Cell* 22, 417–430. doi: 10.1105/tpc.109.070789

Wang, S., Zickler, D., Kleckner, N., and Zhang, L. (2015). Meiotic crossover patterns: obligatory crossover, interference and homeostasis in a single process. *Cell Cycle* 14, 305–314. doi: 10.4161/15384101.2014.991185

Wijnker, E., Deurhof, L., Van De Belt, J., De Snoo, C. B., Blankestijn, H., Becker, F., et al. (2014). Hybrid recreation by reverse breeding in *Arabidopsis thaliana*. *Nat. Protoc.* 9, 761–772. doi: 10.1038/nprot.2014.049

Wijnker, E., James, G. V., Ding, J., Becker, F., Klasen, J. R., Rawat, V., et al. (2013). The genomic landscape of meiotic crossovers and gene conversions in *Arabidopsis thaliana*. *eLife* 2:e01426. doi: 10.7554/eLife.01426

Wijnker, E., Van Dun, K., De Snoo, C. B., Lelivelt, C. L., Keurentjes, J. J., Naharudin, N. S., et al. (2012). Reverse breeding in *Arabidopsis thaliana* generates homozygous parental lines from a heterozygous plant. *Nat. Genet.* 44, 467–470. doi: 10.1038/ng.2203

Wu, X., and Zhang, Y. (2017). TET-mediated active DNA demethylation: mechanism, function and beyond. *Nat. Rev. Genet.* 18, 517–534. doi: 10.1038/nrg.2017.33

Xue, Z., Li, Y., Zhang, L., Shi, W., Zhang, C., Feng, M., et al. (2016). OsMTOPVIB promotes meiotic DNA double-strand break formation in rice. *Mol. Plant* 9, 1535–1538. doi: 10.1016/j.molp.2016.07.005

Xue, M., Wang, J., Jiang, L., Wang, M., Wolfe, S., Pawlowski, W. P., et al. (2018). The number of meiotic double-strand breaks influences crossover distribution in Arabidopsis. *Plant Cell* 30, 2628–2638. doi: 10.1105/tpc.18.00531

Yelina, N. E., Gonzalez-Jorge, S., Hirsz, D., Yang, Z., and Henderson, I. R. (2021). CRISPR targeting of MEIOTIC-TOPOISOMERASE VIB-dCas9 to a recombination hotspot is insufficient to increase crossover frequency in Arabidopsis. bioRxiv [Preprint]. doi: 10.1101/2021.02.01.429210

Yelina, N. E., Lambing, C., Hardcastle, T. J., Zhao, X., Santos, B., and Henderson, I. R. (2015). DNA methylation epigenetically silences crossover hot spots and controls chromosomal domains of meiotic recombination in Arabidopsis. *Genes Dev.* 29, 2183–2202. doi: 10.1101/gad.270876.115

Yu, H., Wang, M., Tang, D., Wang, K., Chen, F., Gong, Z., et al. (2010). OsSPO11-1 is essential for both homologous chromosome pairing and crossover formation in rice. *Chromosoma* 119, 625–636. doi: 10.1007/s00412-010-0284-7

Zapata, L., Ding, J., Willing, E. M., Hartwig, B., Bezdan, D., Jiao, W. B., et al. (2016). Chromosome-level assembly of *Arabidopsis thaliana* Ler reveals the extent of translocation and inversion polymorphisms. *Proc. Natl. Acad. Sci. U. S. A.* 113, E4052–E4060. doi: 10.1073/pnas.1607532113

Zhang, L., Espagne, E., De Muyt, A., Zickler, D., and Kleckner, N. E. (2014a). Interference-mediated synaptonemal complex formation with embedded crossover designation. *Proc. Natl. Acad. Sci. U. S. A.* 111, E5059–E5068. doi: 10.1073/pnas.1416411111

Zhang, L., Kohler, S., Rillo-Bohn, R., and Dernburg, A. F. (2018). A compartmentalized signaling network mediates crossover control in meiosis. *elife* 7:e30789. doi: 10.7554/eLife.30789.001

Zhang, J., Pawlowski, W. P., and Han, F. (2013). Centromere pairing in early meiotic prophase requires active centromeres and precedes installation of the synaptonemal complex in maize. *Plant Cell* 25, 3900–3909. doi: 10.1105/tpc.113.117846

Zhang, C., Song, Y., Cheng, Z. H., Wang, Y.-X., Zhu, J., Ma, H., et al. (2012). The *Arabidopsis thaliana* DSB formation (AtDFO) gene is required for meiotic double-strand break formation. *Plant J.* 72, 271–281. doi: 10.1111/j.1365-313X.2012.05075.x

Zhang, L., Wang, S., Yin, S., Hong, S., Kim, K. P., and Kleckner, N. (2014b). Topoisomerase II mediates meiotic crossover interference. *Nature* 511, 551–556. doi: 10.1038/nature13442

Zhang, H., and Zhu, J. K. (2012). Active DNA demethylation in plants and animals. *Cold Spring Harb. Symp. Quant. Biol.* 77, 161–173. doi: 10.1101/sqb.2012.77.014936

Zhu, J., Kapoor, A., Sridhar, V. V., Agius, F., and Zhu, J. K. (2007). The DNA glycosylase/lyase ROS1 functions in pruning DNA methylation patterns in Arabidopsis. *Curr. Biol.* 17, 54–59. doi: 10.1016/j.cub.2006.10.059

Zickler, D., and Kleckner, N. (1999). Meiotic chromosomes: integrating structure and function. *Annu. Rev. Genet.* 33, 603–754. doi: 10.1146/annurev.genet.33.1.603

Ziolkowski, P. A., Underwood, C. J., Lambing, C., Martinez-Garcia, M., Lawrence, E. J., Ziolkowska, L., et al. (2017). Natural variation and dosage of the HEI10 meiotic E3 ligase control Arabidopsis crossover recombination. *Genes Dev.* 31, 306–317. doi: 10.1101/gad.295501.116

Conflict of Interest: The authors declare that the research was conducted in the absence of any commercial or financial relationships that could be construed as a potential conflict of interest.

The reviewer SH declared a past co-authorship with one of the authors CL to the handling editor.

frontiers in Plant Science

REVIEW
published: 20 August 2021
doi: 10.3389/fpls.2021.662185

License to Regulate: Noncoding RNA Special Agents in Plant Meiosis and Reproduction

*Wojciech Dziegielewski and Piotr A. Ziolkowski**

Laboratory of Genome Biology, Institute of Molecular Biology and Biotechnology, Adam Mickiewicz University, Poznan, Poland

The complexity of the subcellular processes that take place during meiosis requires a significant remodeling of cellular metabolism and dynamic changes in the organization of chromosomes and the cytoskeleton. Recently, investigations of meiotic transcriptomes have revealed additional noncoding RNA factors (ncRNAs) that directly or indirectly influence the course of meiosis. Plant meiosis is the point at which almost all known noncoding RNA-dependent regulatory pathways meet to influence diverse processes related to cell functioning and division. ncRNAs have been shown to prevent transposon reactivation, create germline-specific DNA methylation patterns, and affect the expression of meiosis-specific genes. They can also influence chromosome-level processes, including the stimulation of chromosome condensation, the definition of centromeric chromatin, and perhaps even the regulation of meiotic recombination. In many cases, our understanding of the mechanisms underlying these processes remains limited. In this review, we will examine how the different functions of each type of ncRNA have been adopted in plants, devoting attention to both well-studied examples and other possible functions about which we can only speculate for now. We will also briefly discuss the most important challenges in the investigation of ncRNAs in plant meiosis.

Keywords: meiosis, noncoding RNA, RNA interference, RNA-dependent DNA methylation, small RNA, plants

OPEN ACCESS

Edited by:
Olivier Da Ines,
Université Clermont Auvergne, France

Reviewed by:
Chloe Girard,
UMR9198 Institut de Biologie Intégrative de la Cellule (I2BC), France
Qian Du,
Cornell University, United States

***Correspondence:**
Piotr A. Ziolkowski
pzio@amu.edu.pl

Specialty section:
This article was submitted to Plant Cell Biology, a section of the journal Frontiers in Plant Science

Received: *31 January 2021*
Accepted: *07 June 2021*
Published: *20 August 2021*

Citation:
Dziegielewski W and Ziolkowski PA (2021) License to Regulate: Noncoding RNA Special Agents in Plant Meiosis and Reproduction. Front. Plant Sci. 12:662185. doi: 10.3389/fpls.2021.662185

INTRODUCTION

The basis of sexual reproduction is the fusion of two haploid cells called gametes to form a diploid cell that is the beginning of a new individual (Villeneuve and Hillers, 2001). For this to be possible, the genetic material from both parents has to be shuffled, and the chromosome number is reduced by half during the production of gametes or the spores that will later form gametes. Reduction of ploidy occurs during a type of cell division specific for all eukaryotes called meiosis (Villeneuve and Hillers, 2001). During meiosis, the cell undergoes profound functional and structural changes, including chromosome condensation, formation of programmed DNA double-strand breaks (DSBs), homologous chromosome pairing, and reciprocal exchanges of genetic information (crossovers) between paired chromosomes (Hunter, 2015; Mercier et al., 2015). At the same time, genetic information must be specially protected against damage that could occur, for example, as a result of the activity of transposable elements (TEs). Due to the uniqueness and complexity of meiosis, as well as its special importance for the preservation

of genetic variability, it is very strictly controlled (Hunter, 2015; Mercier et al., 2015).

After initiation of the meiotic pathway, a massive transcription switch has been observed to activate in many eukaryotes, including yeasts, plants, and mammals (Primig et al., 2000; Zhou and Pawlowski, 2014; da Cruz et al., 2016). Although the number of genes expressed during meiosis differs among species, transcriptomic studies have revealed recurring patterns of coexpressed genes, which can be grouped into clusters associated with specific stages of meiosis. The early wave of meiosis-related genes is expressed during S phase and is connected with recombination and homologous chromosome pairing, while the mid- and late waves are expressed during metaphase and the onset of anaphase (Winter, 2012; Margolin et al., 2014; Flórez-Zapata et al., 2016). Recent RNA-seq studies and genetic approaches have revealed that a large number of different noncoding RNAs (ncRNAs) are involved in the onset and progression of meiosis, performing diverse molecular functions (Lardenois et al., 2011; Atkinson et al., 2018).

Noncoding RNAs can be classified as small RNAs (sRNAs; up to 30 nt), medium-size ncRNAs (mncRNAs; 31–200 nt), and long ncRNAs (lncRNAs; over 200 nt). This partly reflects their biogenesis and mode of action, especially with regard to sRNAs vs. lncRNAs. However, the division into sRNAs, mncRNAs, and lncRNAs is somewhat arbitrary, as the boundaries between the different classes are not strict. To our knowledge, there is no information on the specific role of mncRNAs in meiosis; therefore, this group of ncRNAs will not be included in this review. Both sRNAs and lncRNAs have been found in meiotic transcriptomes.

Small RNAs are associated with a number of gene and transposon silencing phenomena, which are collectively known as RNA interference (RNAi; Castel and Martienssen, 2013). RNAi has been described in many eukaryotes, including animals, plants, and yeast, although it has been lost in the *Saccharomyces cerevisiae* lineage (Drinnenberg et al., 2009). Two types of sRNA molecules are central for RNAi: microRNAs (miRNAs), which are derived from genome-encoded single-stranded RNAs, and small interfering RNAs (siRNAs), which originate from the processing of double-stranded RNA (dsRNA) precursors, usually transposable elements (Castel and Martienssen, 2013). In the context of meiosis, it is worth distinguishing one additional group of sRNAs, that is, phased small interfering RNAs (phasiRNAs). phasiRNAs are secondary siRNAs generated from miRNA target transcripts by their processing and controlled degradation. All sRNAs are single-stranded noncoding RNAs that function as gene/transposon repressors, which can operate *via* the cleavage of target transcripts, inhibition of mRNA translation, or repression of chromatin modification (Castel and Martienssen, 2013).

All types of sRNAs have been found to be highly expressed in plant generative tissues and especially important in plant sexual reproduction (Song et al., 2012). The role of long ncRNAs in meiosis is much less studied, but it seems important, especially for the organization of chromosomes and definition of centromere chromatin (Topp et al., 2004). In this review, we attempted to present the current knowledge and understanding of the role of noncoding RNA-dependent processes in plant meiosis, often referring to similarities with other eukaryotes. We did not aim to thoroughly analyze the biogenesis of particular types of ncRNAs or the mechanisms of their action, as the complexity of the pathways related to ncRNAs is beyond the scope of this review. Therefore, we decided to include only the most basic information on ncRNA biogenesis, which is necessary for understanding their function. Instead, we focused on discussing the research and experimental work addressing processes for which the influence of ncRNA on the initiation and course of meiosis is known or could be deduced.

miRNAs REGULATE DEVELOPMENTAL CHANGES IN PLANTS BY AFFECTING THE EXPRESSION OF TRANSCRIPTION FACTORS

Plant miRNA-encoding genes are transcribed by Pol II into hairpin-structured pre-miRNAs, which are then sequentially processed by a Dicer-like endonuclease (DCL) to generate mature miRNAs. Next, miRNAs are loaded onto Argonaute (AGO) effector proteins and usually transported to the cytoplasm to regulate their target gene expression (Voinnet, 2009). miRNAs recognize transcripts of their target genes based on sequence complementarity and repress their expression by transcript cleavage, which dominates in plants, or translational repression, which is common in animals (Voinnet, 2009). This pathway of gene silencing is often referred to as posttranscriptional gene silencing (PTGS; Hamilton and Baulcombe, 1999). miRNAs frequently target transcription factors (TFs); for example, it is estimated that approximately 66% of experimentally verified targets in crops are TFs (Tang and Chu, 2017). Of the miRNA-targeted TFs, many are involved in the control of stage transition in plant development, and blocking miRNA expression often leads to visible developmental defects (Mallory and Vaucheret, 2006).

As miRNAs are relatively short (usually 21-nt), and some level of mismatch between the miRNA and transcript is allowed, a single miRNA is capable of targeting different members of a gene family. For example, a single miR167 eliminates transcripts of ARF6 and ARF8, two TFs essential for correct gynoecium and stamen development in *Arabidopsis thaliana* (Wu et al., 2006). miR172 regulates floral transition and flower development by repressing the *AP2* TF gene family in *A. thaliana* (Aukerman and Sakai, 2003). This function is evolutionarily conserved, as it has been reported even in distantly related species, including soybean, maize, rice, and barley (Tang and Chu, 2017). Similarly, miR159 controls floral development by negatively regulating *GAMYB* genes belonging to MYB transcription factors (Tsuji et al., 2006). The absence of miR159 results in the degeneration of the tapetum, which is required for anther post-meiotic development (Papini et al., 1999). Consequently, a lack of miR159 results in male sterility (Millar and Gubler, 2005). The

miR159-*GAMYB* pathway is conserved in higher plants and is present in both monocots, such as rice and barley (Tsuji et al., 2006), and dicots, such as *Arabidopsis* (Palatnik et al., 2007) and strawberry (Csukasi et al., 2012).

MicroRNAs in Regulation of Gene Expression in Meiosis

Yang et al. (2011) sequenced the *Arabidopsis* male meiocyte transcriptome and identified the expression of several miRNA genes. Among the miRNAs identified was miR163, which is known to target five SAM-dependent methyltransferase genes; indeed, the expression of these genes was not detected in meiocytes, suggesting that they are suppressed by miR163 (Yang et al., 2011). It should be noted that only immature miRNAs were able to be detected by the authors due to the method applied. A recent study focusing on sRNAs in *Arabidopsis*, soybean, and cucumber meiocyte transcriptomes provided a more comprehensive picture (Huang et al., 2020). Although miRNAs were less abundant in meiocytes than in leaves in all three species, 10 to 29% of the miRNAs showed preferential expression during meiosis. One of them was miR167, which is upregulated in meiocytes of all three species and, as previously mentioned, targets genes encoding ARF transcription factors (Huang et al., 2020).

It has also been shown that mutations in genes encoding proteins involved in miRNA biogenesis and function can affect the expression of genes important for meiosis initiation and meiotic recombination in *A. thaliana* (Oliver et al., 2017). Mutants of *DCL*, *HYL1*, *HEN1*, *HST*, and *AGO1* showed increased expression of *SPO11-1*, a topoisomerase responsible for meiotic DSB formation; *DMC1* and *RAD51*, recombinases involved in the strand invasion step; *MSH4*, a component of the Class I crossover pathway; or *MUS81*, a structure-specific endonuclease acting in the Class II crossover pathway, among others (Oliver et al., 2017). These results, however, must be interpreted with caution because the tested mutants do not participate exclusively in miRNA pathways and the research material consisted of flower buds and not pure meiocytes.

Potential Roles of miRNAs in Chromosome Condensation

Control of chromosome condensation that occurs in meiosis may depend on miRNAs, and indirect evidence for this relationship has been described. In *Arabidopsis*, mutations in miRNA machinery genes, such as *DCL1*, *HYL1*, *HEN1*, *HST*, *AGO1*, and *AGO4*, have been found to impair the fertility and morphology of reproductive organs (Oliver et al., 2016, 2017). The numbers of viable pollen mother cells (PMCs) and megaspore mother cells (MMCs) were significantly reduced in all the investigated mutants compared to wild-type plants (Oliver et al., 2017). Interestingly, the sterility effect was stronger for PMCs than MMCs, which is consistent with observations in rice and maize showing the much greater importance of RNAi in male rather than female sporogenesis (Liu et al., 2020c). Apart from *hst*, partial chromatin decondensation was observed in chromosomes in pachytene in all mutants tested. This was not associated with an observable alteration in the histone modification pattern (H3K9me2, H3K4me2/3, and H3K27me3), although the limited resolution of cytology-based techniques does not allow exclusion of the possibility that such changes have occurred (Oliver et al., 2016, 2017). This may suggest that miRNAs regulate chromatin remodeling factors that influence DNA accessibility (Oliver et al., 2014, 2017; Pradillo and Santos, 2018).

In addition to the abovementioned functions, some miRNAs have been shown to play an indirect role in meiosis by triggering phasiRNA processing (see below).

SMALL INTERFERING RNAs ARE CRUCIAL FOR TRANSPOSON SILENCING AND HIGH MEIOTIC DNA METHYLATION LEVELS AND ARE INVOLVED IN THE CONTROL OF GENE EXPRESSION IN MEIOSIS

Transposon Inactivation *via* Two siRNA-Dependent Pathways

siRNAs, typically 21 or 24-nt in length, are formed by cleaving longer dsRNAs that are produced from single-stranded RNAs by the action of RNA-dependent RNA polymerases (RDRs) or by annealing with *cis*-antisense RNAs (Castel and Martienssen, 2013). Like miRNAs, siRNAs can induce PTGS when loaded onto AGO proteins, resulting in transposon silencing. This group of siRNAs is usually called natural antisense transcript siRNAs (NAT-siRNAs; Axtell, 2013; Fei et al., 2013). In plant reproduction, this role of siRNAs has been extensively studied in relation to the male and female gametophytes of *A. thaliana* (Slotkin et al., 2009; Olmedo-Monfil et al., 2010). In response to the transcriptional reactivation of the subset of retrotransposons, siRNAs are produced in large quantities, preventing retrotransposition. There are indications that this phenomenon takes place in a cell-nonautonomous manner, and siRNAs are produced in one cell (central cell) and then transported to other cells (egg cells). Interestingly, the production of siRNAs and AGO9 is essential for the proper development of female gametophytes, determining cell fate in *Arabidopsis* ovules (Olmedo-Monfil et al., 2010).

In addition to PTGS, a related mechanism exists in plants by which RNA molecules direct the DNA methylation of their target DNA sequences, called RNA-dependent DNA methylation (RdDM; Matzke and Mosher, 2014; Erdmann and Picard, 2020). In RdDM, siRNAs, typically 24-nt long, guide DRM methyltransferases to specific target loci in the DNA. Since these siRNAs lead to the deposition of repressive chromatin marks, they are often referred to as heterochromatic siRNAs (Axtell, 2013; Fei et al., 2013). siRNAs are generally produced from transposable elements (TEs) and repeats and are transcribed by plant-specific RNA polymerase IV (Pol IV) with the second strand synthesized by RNA-dependent RNA polymerase 2 (RDR2), which is cleaved into mature siRNA by Dicer enzymes (Matzke et al., 2015). This mainly occurs as a consequence

of extensive heterochromatin decondensation during male gametogenesis in vegetative cells and female gametogenesis in central cells (Slotkin et al., 2009; Ibarra et al., 2012). Thus, the major role of RdDM includes silencing new transposon insertions by DNA methylation and constant reinforcement of DNA methylation patterns in existing TEs to prevent their transposition (Matzke and Mosher, 2014; Erdmann and Picard, 2020). Examples of the role of RdDM in the regulation of development-related genes include especially floral transition (*FWA*; Soppe et al., 2000), imprinted expression in endosperm (Vu et al., 2013), seed dormancy (Iwasaki et al., 2019), and fruit ripening (Cheng et al., 2018). However, recent data show that RdDM targeting of both TEs and genes is also directly active during meiosis (see below).

Effects of siRNA-Guided RdDM on DNA Methylation in Meiosis

Reports based on whole-genome bisulfite sequencing have revealed changes in DNA methylation levels during sexual reproduction, which provides evidence for the extensive role of RdDM in *Arabidopsis* meiosis (Calarco et al., 2012; Walker et al., 2017). Unlike mammalian germ cells, the plant germline retains most DNA methylation, preventing transposon expression. It should be noted that in addition to canonical CG methylation, plants can also methylate DNA in the sequence contexts CHG and CHH, which does not occur in mammals. CHG methylation is also preserved in the plant germline, while asymmetric CHH methylation is lost from retrotransposons in meiocytes (Calarco et al., 2012; Walker et al., 2017). This CHH methylation is restored after fertilization by RdDM guided by 24-bp siRNAs (Jullien et al., 2012). Interestingly, nearly 1,300 loci were found to be hypermethylated in *Arabidopsis* meiocytes when compared to somatic tissues, and this DNA methylation was shown to be RdDM dependent (Walker et al., 2017). Hypermethylated loci occur not only in TEs (approximately 800 loci) but also in genes (nearly 500 loci; Long et al., 2021). In both cases, methylation is triggered by germline-specific 24-nt siRNAs, which are transcribed from TEs; however, genic methylation is established with imperfect sequence homology (Long et al., 2021). These siRNAs are produced in tapetum cells (nurse cells for PMCs; hence called nurse cell-derived siRNAs, niRNAs) with the help of the generative tissue-specific chromatin remodeler CLASSY3 (Zhou et al., 2021) and further transported to meiocytes *via* plasmodesmata (**Figure 1**; Long et al., 2021).

Most of the newly established genic methylation is germline-specific and results in corresponding gene repression in meiocytes (Walker et al., 2017). Sex lineage-specific hypermethylation has been observed for 84 pre-tRNA loci, the function of which remains unknown (Walker et al., 2017). One of the new targets is located within the last intron of *MPS1*, a gene involved in chromosome segregation during meiosis (Walker et al., 2017). Mutation in *MPS1* results in frequent occurrence of triads or polyads instead of tetrads (Jiang et al., 2009). In RdDM, the loss of DNA methylation in mutants disrupts the splicing of this intron, which creates a premature stop codon and, as a consequence, a nonfunctional protein (Walker et al., 2017).

The fact that tapetum-derived siRNAs arise from transposons and show only imperfect matches with genic sequences suggests that this type of regulation of meiotic gene expression evolved from the original RdDM task of preventing transposon expansion (Long et al., 2021). Although classical RdDM in somatic cells is sufficient to silence most transposons in *Arabidopsis*, some groups of transposons, e.g., those from the *Gypsy* family, are expressed specifically in the germline (Long et al., 2021). This explains why new targets of RdDM need to be established in meiocytes that establish germline lineages. However, it is not entirely clear why the RdDM pathway, which precisely targets DNA methylation in somatic cells based on a perfect siRNA target match, shows a relatively large number of off-targets in meiocytes. It is speculated that the activity of RNA polymerase V (Pol V), an important RdDM component, is elevated in meiosis, which can result in a higher number of off-targets (Long et al., 2021).

Impact on Centromere Organization During Meiotic Division

Small RNAs, likely belonging to the siRNA class, play a role in the functioning of centromeres in plants (Gutbrod and Martienssen, 2020). Mutants of the rice meiosis-specific AGO gene *MEIOSIS ARRESTED AT LEPTOTENE1 (MEL1)* have been found to show impaired chromosome condensation in meiosis associated with major disruption of histone 3 lysine 9 methylation (H3K9me) at pericentromeres (Nonomura et al., 2007; Komiya et al., 2014; Fan et al., 2016). In addition, mutants of the AGO homologue AGO104 in maize have been found to show abnormal chromosome condensation, spindle defects, and aberrant chromosome segregation, leading to the presence of micronuclei in the later stages of meiosis (Singh et al., 2011). In both of these mutants, a disruption of centromeric and pericentromeric chromatin modification was observed, manifested by a significant decrease in DNA methylation in non-CG sequence contexts (Singh et al., 2011). The *Arabidopsis* AGO104 counterpart AGO4 also shows defects in chromosome segregation in mitosis and meiosis (Oliver et al., 2016). These effects are similar to the well-studied phenomenon of transcriptional gene silencing in fission yeasts: Transcription from repeated elements located in pericentromeric regions generates lncRNAs, which are then used to create siRNAs. siRNAs are loaded onto Ago1, which directs the RNA-induced transcriptional silencing complex (RITS) to the pericentromere through interaction with nascent lncRNAs. RITS in turn recruits the histone methyltransferase complex, which is responsible for H3K4me. The heterochromatin protein Swi6 binds to H3K9me and reinforces the heterochromatin state. Swi6 also participates in the recruitment of the cohesin complex, which holds sister chromatids together (Ellermeier et al., 2010; Gutbrod and Martienssen, 2020). While the exact process for forming centromeric heterochromatin with RNAi support is arguably different in plants than in yeasts, the functional similarities are striking together (Gutbrod and Martienssen, 2020).

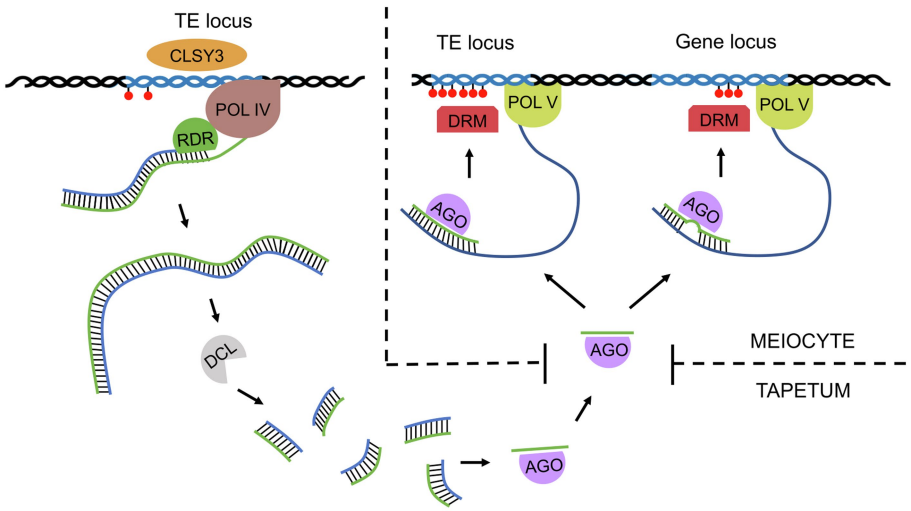

FIGURE 1 | A simplified model of siRNA function in male *Arabidopsis* meiosis. The reproductive tissue-specific chromatin remodeler CLASSY3 (CLSY3) recruits Pol IV to some transposons in tapetum cells. The resulting transcripts are converted into double-stranded RNA (dsRNA) by RDR polymerase and then sliced by Dicer-like endonuclease (DCL) into 24-nt siRNAs. Single-stranded siRNAs are then loaded onto an Argonaute (AGO) and transported to meiocytes. There, siRNAs bind to nascent Pol V products, inducing local DNA methylation (red circles) *via* DRM methyltransferase. siRNAs perfectly match the transcripts of transposons from which they derive; however, in the case of genes, siRNAs usually pair imperfectly, allowing mismatches. Such gene methylation is germline specific, which indicates an increased sensitivity of RdDM machinery in meiocytes compared to somatic cells.

SECONDARY siRNAs PLAY MULTIPLE AND DIVERSE ROLES IN MALE MEIOSIS

In addition to primary siRNAs, whose precursor dsRNA is created by hybridization of independently transcribed RNAs, secondary siRNAs, whose precursor dsRNA synthesis is induced by an upstream sRNA trigger, also play an important role in plants (Axtell, 2013; Fei et al., 2013). PhasiRNAs are a recently discovered group of secondary siRNAs that seem to be of key importance in sporogenesis and male meiosis in numerous plants (Fei et al., 2013; Liu et al., 2020c). They are 21-nt or 24-nt secondary siRNAs generated by the processing of precursor transcripts triggered by miRNAs. Cleavage of the precursor transcript occurs at regular intervals; thus, phasiRNAs exhibit a distinctive, phased configuration (**Figure 2**; Johnson et al., 2009; Song et al., 2012). Reproductive phasiRNAs have been primarily identified in grasses but have more recently been confirmed to be widespread in flowering plants (Dukowic-Schulze et al., 2016; Kakrana et al., 2018; Huang et al., 2019; Yu et al., 2019; Huang et al., 2020). Recent work has reported the presence of reproductive phasiRNAs in dicots, although they are absent in legumes and *Arabidopsis* (Xia et al., 2019). In many plants, including *Arabidopsis*, rice, and maize, trans-acting siRNAs (tasiRNAs) have been described, whose name derives from their ability to target transcripts different than their source transcript, i.e., in *trans* (Vazquez et al., 2004; Allen et al., 2005; Adenot et al., 2006; Chen et al., 2010a). However, as many phasiRNAs can act in *trans* as well, tasiRNAs can be considered a subclass of phasiRNAs in which *trans*-targets have been identified (Axtell, 2013; Fei et al., 2013).

21-nt Reproductive phasiRNAs in Meiosis Progression

The 21-nt reproductive phasiRNAs are enriched mainly in early stage anthers and therefore are called premeiotic reproductive phasiRNAs (Zhai et al., 2015). This group of phasiRNAs is triggered by miR2118 (Johnson et al., 2009), and their production probably takes place in tapetum cells, from which phasiRNAs are transported to meiocytes (Zhai et al., 2015). Similar to other sRNAs, phasiRNAs function when loaded on AGO proteins. Research in rice and maize has revealed that 21-nt phasiRNAs in germ cells are bound by a specific AGO called MEL1 (known as AGO5c in maize; Nonomura et al., 2007; Komiya et al., 2014). Indeed, knockouts of *MEL1* show meiotic arrest in the early stages of prophase I and suggest that 21-nt premeiotic phasiRNAs directly or indirectly affect steps in meiotic progression, including chromosome compaction, presynaptic chromosome association, DSB formation, synapsis, and recombination (Nonomura et al., 2007; Komiya et al., 2014; Liu and Nonomura, 2016). Defects in chromatin condensation result from the limitation of prophase I histone modifications, in particular H3K9me2 (Nonomura et al., 2007; Liu and Nonomura, 2016). In centromeric regions, this leads to a partial mislocalization of centromere-specific histone 3 variant (Liu and Nonomura, 2016). It is currently unclear what causes the asynaptic phenotype observed in the *mel1* mutant. In this mutant, the distribution of PAIR2, a rice HORMA-domain protein, is no different from that in wild-type plants. On the other hand, the ZEP1 protein, a central transverse element of the rice synaptonemal complex, does not load properly onto chromosomes (Komiya et al., 2014).

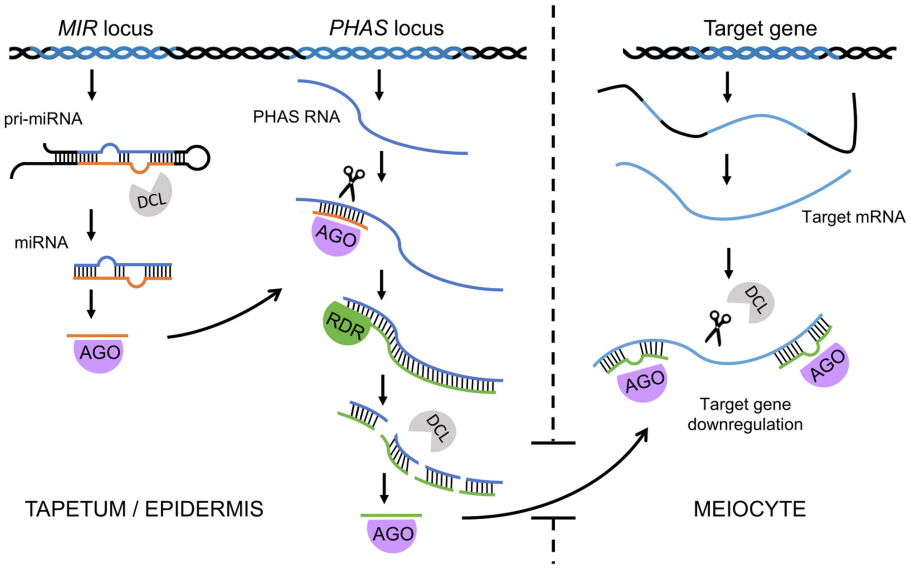

FIGURE 2 | A simplified model for phased small interfering RNA biogenesis and function in male meiosis in grasses. miRNAs are transcribed from *MIR* loci, and after processing by Dicer (DCL), one miRNA strand is loaded onto the AGO protein. The miRNA-AGO complex binds to a *PHAS* transcript based on sequence complementarity, cleaves it at the binding site, and triggers synthesis of the second strand. dsRNA is then sliced by DCL starting from the cleavage site in a phased manner. The resulting phasiRNAs are then loaded onto another AGO protein (e.g., MEL1) and transported from the tapetum (21-nt phasiRNAs) or epidermis (24-nt phasiRNAs) to meiocytes. Finally, the phasiRNA-AGO complexes bind target transcripts of genes or transposable elements and, with the help of DCL, trigger their degradation.

Rice shows recombination-dependent chromosome pairing, so one possibility is that the lack of synapses in the *mel1* mutant is a consequence of an almost complete absence of DSBs. Two additional AGO proteins, MAGO1 and MAGO2, have been recently identified in maize; these proteins are involved in the 21-nt reproductive phasiRNA pathway and accumulate mostly in anther epidermal cells and in developing meiocytes (Lee et al., 2020).

In rice, two loci encoding miR2118-dependent phasiRNA transcript precursors, *PMS1* and *PMS3*, have been isolated from a line used for hybrid rice production *via* photoperiod-induced male sterility (Ding et al., 2012a; Zhou et al., 2012; Fan et al., 2016). These loci were linked to DNA polymorphism that affects 21-nt phasiRNA production and results in male sterility (Fan et al., 2016). In the photoperiod-sensitive mutant line, male sterility is caused by premature degeneration of tapetum cells (Shi et al., 2009), suggesting that phasiRNAs affect the development of these cells. However, phasiRNA target identification is much more difficult than for other sRNA classes; targets therefore remain unknown in many cases. A recent study in rice revealed that 21-nt MEL1-dependent phasiRNAs bind and posttranscriptionally reduce the translation of nearly 2,300 proteins classified as adenyl ribonucleotide-binding proteins, kinases and hydrolases (Zhang et al., 2020a). These targets belong to genes rapidly downregulated in the transition steps observed during prophase I (Nelms and Walbot, 2019). Therefore, the function of 21-nt premeiotic phasiRNAs may be to eliminate the expression of specific gene categories at the onset of meiosis (**Figure 2**; Zhang et al., 2020a). On the other hand, a subclass of 21-nt miR2118-dependent phasiRNAs in maize was shown to be involved in male germline retrotransposon silencing under heat stress conditions (Lee et al., 2020). Inactivation of this pathway leads to male sterility at elevated temperatures, which is due to extensive transposon activation. This shows that 21-nt phasiRNAs may adopt different functions in male meiosis.

Effects of 24-nt phasiRNAs on DNA Methylation

The 24-nt phasiRNAs are also highly enriched in anthers; however, at a later stage, coincident with meiosis, they are often referred to as meiotic phasiRNAs (Zhai et al., 2015). Their production is triggered mainly by miR2275 (Johnson et al., 2009), and they are likely to be loaded on the AGO18 effector protein (Fei et al., 2016). Several lines of evidence suggest that 24-nt phasiRNAs are produced in epidermis and tapetum cells and, to some extent, transported to meiocytes (Zhai et al., 2015; Dukowic-Schulze et al., 2016; Nan et al., 2017; Ono et al., 2018; Xia et al., 2019). Thus, as with *Arabidopsis* siRNAs and 21-nt phasiRNAs, 24-nt phasiRNAs must be delivered to meiocytes from nurse cells. Supplying the elements of individual RNAi systems from nurse cells appears to be a universal means of ncRNA-dependent meiocyte control (Lei and Liu, 2020).

Since the components of the phasiRNA biogenesis pathway are shared with other sRNAs, their mutants cannot be used to characterize the role of phasiRNAs in meiosis (Liu et al., 2020c).

Fortunately for 24-nt phasiRNA research, the expression of their precursors in anthers depends on specific bHLH transcription factors, including rice ETERNAL TAPETUM1 (EAT1; Ono et al., 2018) and maize MS23 (Nan et al., 2017). Mutants of the genes encoding these TFs exhibit a male-sterile phenotype with delayed and asynchronous meiosis. Moreover, decondensed chromosomes were frequently observed in diakinesis and metaphase I in the *eat1* mutant (Ono et al., 2018). Mutation of DCL5, the Dicer protein responsible for miR2275 processing, has been found to result in almost complete loss of 24-nt phasiRNAs in maize (Teng et al., 2020). The maize *dcl5* mutants were male sterile, which was likely due to delayed development of the tapetum cells; the progression of meiosis was, however, not investigated in this contribution (Teng et al., 2020). Recent studies of both mutants in maize showed that 24-nt phasiRNAs can increase CHH methylation in most *PHAS* loci (Zhang et al., 2020b). As this latter study was performed in meiotic anthers and not in meiocytes, this DNA methylation profile is likely to correspond to abundant somatic tapetum cells (Zhang et al., 2020b). If we assume that in maize, as in *Arabidopsis*, the RdDM pathway is hyperactive in meiocytes (Long et al., 2021), it can be speculated that 24-nt phasiRNAs are capable of creating a germline-specific DNA methylation pattern in *trans*, providing a specific control for genes important in meiosis and additional silencing of transposable elements.

Epigenetically Activated siRNAs in Triploid Block

Apart from phasiRNA, the plant germline contains another type of secondary siRNA – epigenetically activated siRNAs (easiRNAs; McCue et al., 2012; Creasey et al., 2014; Borges et al., 2018; Martinez et al., 2018). The formation of these siRNAs is related to the fact that in the germline, there is a significant decrease in DNA methylation in the CHH context, which in turn causes transient activation of retrotransposons (Creasey et al., 2014). easiRNAs arise from miRNA-dependent degradation of these retrotransposon transcripts shortly after meiosis (Borges et al., 2018). Interestingly, easiRNAs act as a quantitative signal for paternal genome dosage and are thus required for postfertilization genome stability and seed viability (Martinez et al., 2018). In the presence of easiRNAs, triploid seeds abort due to gene dysregulation, a phenomenon known as a triploid block. Depletion of easiRNAs bypasses the triploid block in response to elevated paternal ploidy, although it remains unclear how easiRNAs mediate this process (Borges et al., 2018; Martinez et al., 2018).

UNCLASSIFIED MEIOCYTE-SPECIFIC SMALL RNAs MAY BE ASSOCIATED WITH MEIOTIC DSBs

Recent advances in the development of techniques for the isolation of pure PMC fractions in *Arabidopsis* have allowed for a more detailed analysis of sRNAs in meiosis. A group of approximately two thousand meiocyte-specific sRNAs (ms-sRNAs) of 23–24 nucleotides has been characterized based on comparison with the sRNAs present in leaves (Huang et al., 2019). Although ms-sRNAs require components of the RNAi machinery, including RNA Pol IV and DICER, for their formation, their origin remains unclear. Intriguingly, many of them map to genes that are upregulated in meiocytes and do not show meiosis-specific DNA methylation. Therefore, the authors hypothesized that this group of ms-sRNAs plays a role in the suppression of meiosis-specific genes in successive developmental stages (Huang et al., 2019). Even more interesting is the fact that approximately two-thirds of ms-sRNAs are not formed in the *spo11* mutant, which is defective for meiotic DSB formation, and this group is associated with common crossover hotspot motifs (CTT-repeat and A-rich) and open chromatin (Huang et al., 2019).

Recently, Liu et al. (2020a) characterized a new rice mutant allele for RNA-dependent RNA polymerase 6 (RDR6), which is necessary for dsRNA synthesis (Kumakura et al., 2009). The mutant showed a dramatic reduction in meiotic DSB formation, which resulted in the lack of chromosome pairing, lack of synapsis and pachytene arrest (Liu et al., 2020a). In this mutant, a significant increase in 24-nt sRNAs was reported, which is associated with a large number of downregulated genes, including some involved in DSB formation. Whether observations made by Huang et al. (2019) and Liu et al. (2020a) are related to each other currently remains unknown.

Although the function of these sRNAs in DSB repair needs to be further elucidated, they show similarities to qiRNAs in the filamentous fungus *Neurospora crassa* (Lee et al., 2009). qiRNAs arise in response to DNA damage in somatic cells and are also dependent on RNAi components, such as AGO and Dicer proteins as well as an RDR. Mutants of the genes involved in the production of qiRNA are sensitive to DNA damaging factors, suggesting that qiRNAs may be involved in DNA repair (Lee et al., 2009). In turn, in mammalian cells, a particular class of sRNAs is induced by DSBs (DSB-induced RNAs, diRNAs; Wei et al., 2012; Gao et al., 2014). In the Ago2 and Dicer mutants, which do not generate diRNAs, recruitment of RAD51 to DSBs is blocked. In contrast, proteins involved in DSB end processing, such as MRE11 and RPA, are normally loaded onto chromatin. This indicates the involvement of diRNAs in repair by homologous recombination (Gao et al., 2014).

LONG ncRNAs PROVIDE SUBSTRATES FOR sRNA FORMATION, SUPPORT THE FORMATION OF CENTROMERIC CHROMATIN, AND CAN POTENTIALLY BE INVOLVED IN THE REGULATION OF MEIOTIC GENE EXPRESSION

Long ncRNAs are transcripts longer than 200 bp that are not translated into proteins (Chekanova, 2015). Similar to mRNAs, many are transcribed by RNA polymerase II and undergo similar processing, including 5'-end capping, splicing, and the addition of a polyA tail. In plants, however, there are two

additional RNA polymerases that can lead to the formation of lncRNAs, i.e., polymerase IV and Pol V (Wierzbicki et al., 2008). As a rule, the transcripts of these polymerases do not undergo the usual mRNA processing and are therefore not stable. The resulting lncRNAs are usually substrates for the production of siRNAs involved in RdDM (Matzke and Mosher, 2014). The direct role of lncRNAs is widely known in yeast meiosis, where lncRNAs play a key role in the regulation of the meiotic switch and meiotic gene expression and in fission yeast even facilitate chromosome pairing (Van Werven et al., 2012; Ding et al., 2012b). Much less is known in plants than in yeasts about the importance of lncRNAs in meiosis. One of the reasons may be the very low expression level of long noncoding RNAs in plants, which makes them difficult to detect using the standard sequencing depth (Golicz et al., 2018).

Potential Regulatory Roles of lncRNAs

The role of lncRNAs in developmental processes is well characterized in the context of floral transition. For instance, epigenetic regulation by three vernalization-dependent lncRNAs, *COLDAIR*, *COOLAIR*, and *COLDWRAP,* is important for inducing floral transition in *A. thaliana* by influencing the expression of *FLC*, the gene encoding a major repressor of flowering (Liu et al., 2010; Heo and Sung, 2011; Kim and Sung, 2017). Examples of lncRNAs acting in sexual reproduction are limited. One of them is *LDMAR* (long-day-specific male-fertility-associated RNA), which controls programmed cell death in developing anthers (Ding et al., 2012a). A certain amount of the *LDMAR* transcript is required for the normal development of pollen in rice grown under long-day conditions. Reduction of *LDMAR* transcripts leads to premature programmed cell death, resulting in photoperiod-sensitive male sterility (Ding et al., 2012a). Another example is *osa-eTM160*, which acts as an *miR160* sponge, an RNA containing complementary binding sites to miRNA. Expression of *osa-eTM160* at early anther developmental stages attenuates the repression of ARF mRNAs by *osa-miR160* and therefore regulates flower development (Wang et al., 2017).

Two recent studies have reported meiosis-specific lncRNAs isolated from plant meiocytes. Comparison of genes differentially expressed between sunflower meiocytes and somatic tissues allowed the identification of almost 7,000 lncRNAs that were exclusively expressed in meiocytes (Flórez-Zapata et al., 2016). At least 40% of these meiotically expressed lncRNAs showed sequence similarity with different sRNAs. In many cases, the identified lncRNAs are sRNA precursors or may mimic sRNA targets, thus acting like *osa-eTM160* as a miRNA sponge. Similarly, many of the nearly 5,000 lncRNAs specific for autotetraploid rice PMCs and MMCs were associated with miRNA and phasiRNA levels (Li et al., 2020). However, it seems very likely that some of these lncRNAs have additional regulatory functions, similar to those in yeast or in the regulation of developmental gene expression in *Arabidopsis*.

Formation of the Centromeric Chromatin

In many eukaryotes, including plants, ncRNAs have been shown to influence the organization of chromatin in centromeres and appear to play a direct role in their function. Plant centromeres consist of the central core, containing satellite repeats, and the flanking pericentromeric heterochromatin. Centromeres have a dual function in cell division; they (1) enable the attachment of the CENH3 (equivalent to human CENP-A), which is required for kinetochore binding and karyokinetic spindle function, and (2) are essential for sister chromosome cohesion. In humans, loading of the CENP-A histone on the centromere has been shown to be dependent on the presence of centromere transcripts (Quénet and Dalal, 2014). Noncoding RNAs transcribed from human alpha satellites form complexes with CENP-A and CENP-C, and switching off their expression leads to the reduction of these proteins (McNulty et al., 2017). Similarly, the expression of centromeric retrotransposons and satellite repeats has been observed in maize (Topp et al., 2004). Nearly half of the resulting 40–200-nt noncoding RNAs are tightly bound to CENH3, suggesting that, as in humans, ncRNAs may play a key role in the formation of centromeric chromatin (Topp et al., 2004). More recent work indicates that among the ncRNAs linked to centromeric chromatin are also circular RNAs formed by back-splicing of some centromeric retrotransposons (Liu et al., 2020b). These circular RNAs bind to the centromere *via* RNA-DNA hybrids (the so-called R-loops) and give rise to chromatin loops and increase CENH3 accumulation. Although these observations were made based on the formation of centromeres in somatic cells, the convergent function of centromeres in mitosis and meiosis suggests at least partial universality of the processes.

The best-studied role of lncRNAs in plant meiosis is that of a substrate for the production of phasiRNAs. In this case, the lncRNA is transcribed from loci termed *PHAS* loci (*TAS* loci for tasiRNAs). Interestingly, not all *PHAS* loci are noncoding: A comprehensive study by Zheng et al. (2015) found that nearly half of the 3,300 *PHAS* loci identified in 23 plant species were protein coding. However, *PHAS* lncRNAs are only intermediates lacking biological functions separate from those of the phasiRNAs that form from them (Liu et al., 2020c).

CONCLUDING REMARKS AND FUTURE DIRECTIONS

The ncRNA-dependent mechanisms involved in the regulation of meiosis in plants are diverse and complex (**Table 1** and **Figure 3**). This is mainly due to the existence of extensive and diverse regulatory pathways involving short RNAs, primary PTGS and RdDM, which are involved in RNAi (**Figure 3**). It is generally accepted that the primary function of the RNAi system is immune defense against exogenous genetic elements, such as transposons and viruses (Cerutti and Casas-Mollano, 2006). The role of RNAi in the regulation of gene expression, for example, through the miRNA pathway, appeared later in the course of evolution (Cerutti and Casas-Mollano, 2006). Since most functions of noncoding RNAs in meiosis can be classified as: (1) preventing mobile element activity, (2) regulating gene expression, and (3) controlling chromosome condensation, the high complexity of ncRNA-based mechanisms

TABLE 1 | Role of ncRNAs in plant meiosis and reproduction.

Stage of sexual development	Type of ncRNA	Organism	Function	Described in:
Transcription control	miRNA	Flowering plants	miRNAs bind to targeted transcript and mediate its cleavage. Many different transcriptional factors, responsible for development of generative organs, are controlled by miRNAs. Moreover, some meiosis-specific genes are upregulated in *A. thaliana* mutants of miRNA machinery, suggesting their potential role in meiosis transcriptional control.	Tsuji et al., 2006; Oliver et al., 2017; Tang and Chu, 2017
	siRNA	Flowering plants	siRNAs prevent TE expansion in two pathways: (1) *via* PTGS by binding to TE transcripts to induce their cleavage and (2) *via* RdDM by guiding DRM methyltransferases to specific TE loci to establish CHG or CHH DNA methylation, which prevents new transposon insertions and transpositions. Moreover, siRNAs are responsible for restoring the CHH methylation after the fertilization.	Calarco et al., 2012; Walker et al., 2017; Erdmann and Picard, 2020
Meiotic double-strand break formation	SPO11-1-dependent sRNAs	*A. thaliana*	SPO11-1-dependent small RNAs are enriched with CO-associated DNA motifs and are related to CO hotspots and genes that lack DNA methylation. The exact function remains unknown.	Huang et al., 2019
Centromere organization	mncRNAs and lncRNA	*Z. mays*	mncRNAs and lncRNAs bind to CENH3 histone variant facilitating formation of centromeric chromatin, which is required for proper karyokinetic spindle function and for sister chromosome cohesion.	Topp et al., 2004
	siRNAs/phasiRNAs	*O. sativa* *Z. mays*	siRNAs/phasiRNAs loaded onto MEL1 (rice) or AGO104 (maize) are responsible for RNA-mediated chromosome condensation in pericentromeres resulting from H3K9me and non-CG DNA methylation. Mutants of *MEL1/AGO104* exhibit meiocyte arrest, because of spindle defects and abnormal chromosome condensation.	Singh et al., 2011; Komiya et al., 2014
DNA methylation and silencing	meiocyte-specific sRNAs (ms-sRNAs)	*A. thaliana*	ms-sRNAs produced from meiotically expressed genes *via* RNA processing machinery are guided toward gene promoters to establish CHH methylation. High abundance of ms-sRNA is observed at Helitrons – a DNA transposon family known to overlap with DSB hotspots.	Huang et al., 2020
	siRNAs (niRNAs)	*A. thaliana*	niRNAs expressed in the tapetum from TE loci and subsequently transported to meiocytes trigger RdDM of transposons and genes.	Walker et al., 2017; Long et al., 2021
Floral transition	lncRNA	*A. thaliana*	Vernalization-dependent lncRNAs, *COLDAIR*, *COOLAIR*, and *COLDWRAP*, regulate the H3K27me3 levels by recruiting PRC2 at the *FLOWERING LOCUS C*, a major negative regulator of flowering.	Liu et al., 2010; Heo and Sung, 2011; Kim and Sung, 2017; Tian et al., 2019
Parental genome dosage	easiRNAs	*A. thaliana*	Pol IV is responsible for biogenesis of epigenetically activated siRNAs in the male gametophyte. easiRNAs mediate hybridization barriers between diploid seed and tetraploid pollen, by forming a quantitative signal for paternal chromosome number. easiRNAs target transcripts produced by Pol II or Pol V and interfere with DNA methylation establishment.	Borges et al., 2018; Martinez et al., 2018; Wang et al., 2020

(Continued)

TABLE 1 | Continued

Stage of sexual development	Type of ncRNA	Organism	Function	Described in:
Tapetum development	21-nt phasiRNAs	*O. sativa* *Z. mays*	Expression of 21-nt phasiRNAs is triggered by miR2118 in the tapetum from *PHAS* loci. 21-nt phasiRNAs accumulate in anther epidermal cells and developing meiocytes, suggesting potential role of premeiotic phasiRNAs in the male meiosis initiation by affecting the expression of meiotic genes and contributing to retrotransposon silencing.	Johnson et al., 2009; Ding et al., 2012a; Zhou et al., 2012; Zhai et al., 2015; Lee et al., 2020; Fan et al., 2016
	24-nt phasiRNAs		Expression of 24-nt phasiRNAs is triggered by miR2275. Most likely, phasiRNAs are loaded on AGO18 effector protein and are responsible for proper tapetum development, by maintaining CHH DNA methylation levels.	Johnson et al., 2009; Zhai et al., 2015; Dukowic-Schulze et al., 2016; Fei et al., 2016; Xia et al., 2019; Zhang et al., 2020b
Anther development	lncRNA and siRNA	*O. sativa*	Long-day-specific male-fertility-associated RNA (*LDMAR*) is necessary for anther and pollen development. A specific siRNA named *Psi-LDMAR* has been associated with regulating levels of *LDMAR* transcript by targeting RdDM to its promoter region.	Ding et al., 2012a,b
	lncRNA and miRNA		A lncRNA *osa-eTM160* can mimic the target of osa-miR160 in order to release the repression of *osa-ARF18* gene, which is important in anther development.	Wang et al., 2017

in plants may be due to the high level of transposons in their genomes. Consistent with this view, it appears that species with large genomes rich in transposable elements, such as maize, show a greater variety of ncRNA-based control mechanisms than do plants with small and simple genomes, such as *Arabidopsis*. One example of this is the reproductive tissue-specific phasiRNA, which is absolutely crucial for the fertility of many plants with complex, TE-rich genomes (Fei et al., 2013; Liu et al., 2020c).

TEs can integrate into genic sequences, rendering them inactive; therefore, they are dangerous to genome integrity (Ernst et al., 2017; Erdmann and Picard, 2020). Control of transposon activity is of particular importance in sexual lineages because new transposon insertions could be passed on to subsequent generations. Recent studies suggest that cells entering meiosis show increased activity of some RNAi components (Long et al., 2021), which may translate into increased off-target activity. Until now, it was widely accepted that mismatches are allowed in the case of sRNA acting in PTGS (Voinnet, 2009; Castel and Martienssen, 2013). However, recent studies have also shown that in the case of RdDM, a complete match between sRNA and the target is not required (Fei et al., 2021; Long et al., 2021). The biological significance of this fact is probably related to the rapid evolution of transposable elements: By allowing sRNA target mismatches in the PTGS and TGS RdDM pathways, it is possible to prevent the expansion of TEs that accumulate mutations rapidly. However, the consequence is a greater influence of sRNA-mediated processes on gene activity in meiosis. Hence, we propose that meiosis-specific regulation of gene expression through siRNA-related pathways (siRNA and phasiRNA) evolved as a side effect of the increasing activity and flexibility of these pathways in meiocytes in the fight against TE expansion.

In plants, we are just beginning to understand the importance of noncoding RNAs in meiosis. There are several reasons for such a situation. One of them is the parallel occurrence of many different ncRNA-mediated pathways, which can be difficult to differentiate. Especially, in the case of sRNAs, machinery required for sRNA biogenesis and functioning, including Dicer and AGO proteins, is often shared between individual pathways. It should also be taken into account that each pathway leads to the production of many different sRNAs having different targets. Therefore, the use of mutants for genes encoding components of these pathways is often not informative. Certain aspects of ncRNA functioning, however, can be solved using conditional mutants, where the expression of a given ncRNA synthesis component is limited to a selected tissue only. For example, Long et al. (2021) used an *rdr2* mutant into which they introduced a functional RDR2 under a tapetum-specific promoter. Thanks to this experiment, it was possible to establish that siRNAs directing DNA methylation in meiocytes are produced in tapetum cells and then transported to meiocytes.

Currently, the most frequently used approach is based on the identification of sRNAs by sequencing and their successive characterization. This is possible thanks to the rapid improvement in the efficiency of high-throughput sequencing techniques, often utilizing single-cell protocols and techniques for the isolation of super-pure meiocyte fractions (Chen et al., 2010b; Dukowic-Schulze et al., 2020). New techniques for isolating PMCs are based on microdissection (Chen and Retzel, 2013); however, in the case of grasses, flow cytometry is also successfully used, which significantly improves the throughput (Chang et al., 2018).

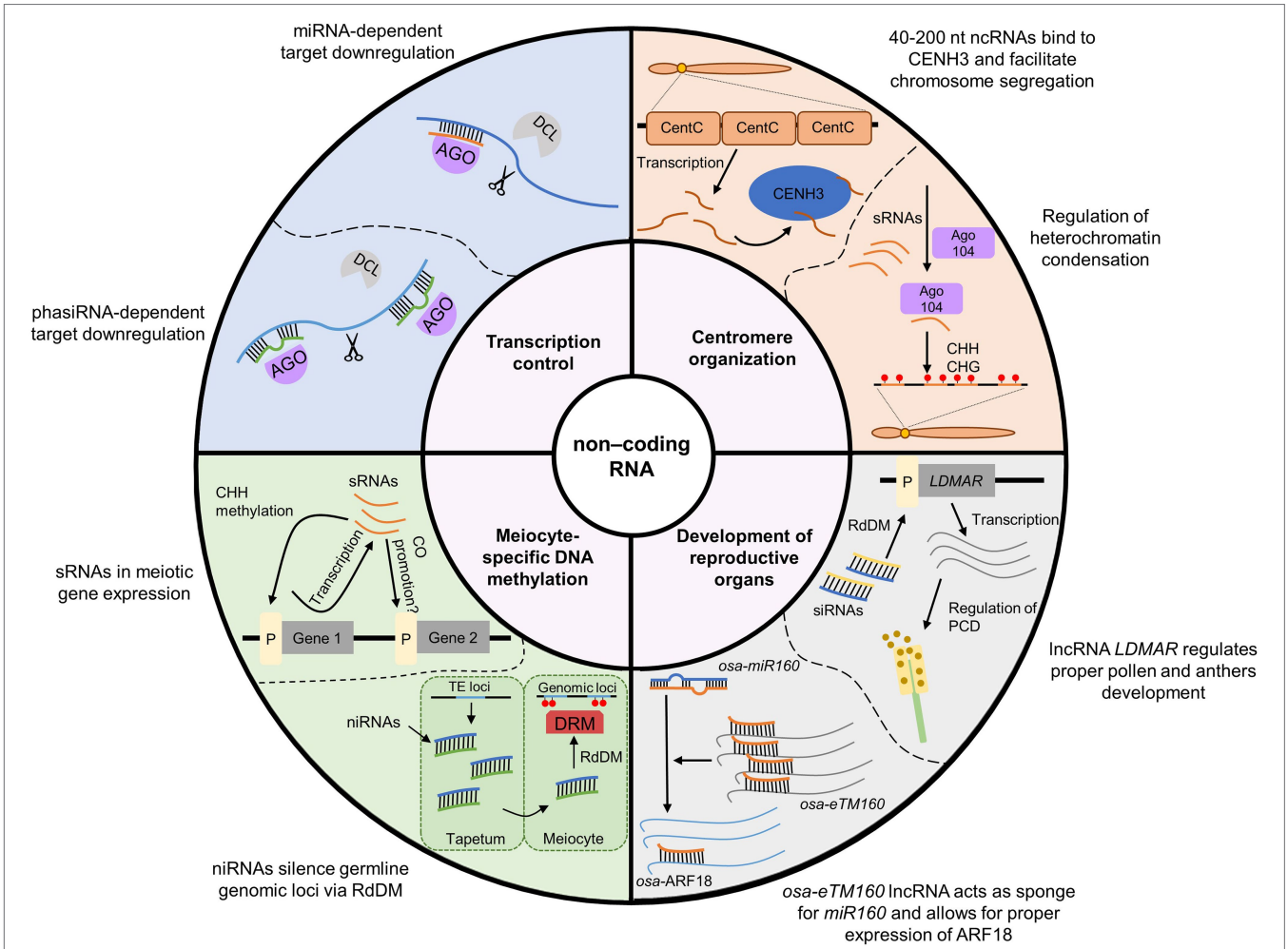

FIGURE 3 | Summary of the most important functions of ncRNAs in meiosis in plants. For the sake of simplicity, only the most characteristic examples of individual processes are presented. A more detailed explanation is provided in **Table 1**.

It is, however, worth noting that while we have overcome the technical issues with PMC isolation in many plant species, we still do not have efficient methods for isolating MMCs. Therefore, in many cases, it is not possible to confirm to what extent the findings on male meiosis will be reflected in the formation of female gametophytes. In the genome-editing era, the development of new methods, such as CUT&RUN and CUT&Tag (Skene et al., 2018; Kaya-Okur et al., 2019), superresolution microscopy (Sydor et al., 2015), and systems enabling living-cell imaging for plant meiosis (Prusicki et al., 2019), should significantly expand our research capabilities.

AUTHOR CONTRIBUTIONS

WD and PAZ wrote the review. All authors contributed to the article and approved the submitted version.

FUNDING

We appreciate financial support from the Polish National Science Centre (grant no. 2016/22/E/NZ2/00455) and the Foundation for Polish Science (grant no. POIR.04.04.00–00-5C0F/17-00).

REFERENCES

Adenot, X., Elmayan, T., Lauressergues, D., Boutet, S., Bouché, N., Gasciolli, V., et al. (2006). DRB4-dependent TAS3 trans-acting siRNAs control leaf morphology through AGO7. *Curr. Biol.* 16, 927–932. doi: 10.1016/j.cub.2006.03.035

Allen, E., Xie, Z., Gustafson, A. M., and Carrington, J. C. (2005). microRNA-directed phasing during trans-acting siRNA biogenesis in plants. *Cell* 121, 207–221. doi: 10.1016/j.cell.2005.04.004

Atkinson, S. R., Marguerat, S., Bitton, D. A., Rodríguez-López, M., Rallis, C., Lemay, J. F., et al. (2018). Long noncoding RNA repertoire and targeting by nuclear exosome, cytoplasmic exonuclease, and RNAi in fission yeast. *RNA* 24, 1195–1213. doi: 10.1261/rna.065524.118

Aukerman, M. J., and Sakai, H. (2003). Regulation of flowering time and floral organ identity by a microRNA and its Apetala2-Like target genes. *Plant Cell* 15, 2730–2741. doi: 10.1105/tpc.016238

Axtell, M. J. (2013). Classification and comparison of small RNAs from plants. *Annu. Rev. Plant Biol.* 64, 137–159. doi: 10.1146/annurev-arplant-050312-120043

Borges, F., Parent, J.-S., van Ex, F., Wolff, P., Martínez, G., Köhler, C., et al. (2018). Transposon-derived small RNAs triggered by miR845 mediate genome dosage response in *Arabidopsis*. *Nat. Genet.* 50, 186–192. doi: 10.1038/s41588-017-0032-5

Calarco, J. P., Borges, F., Donoghue, M. T. A., Van Ex, F., Jullien, P. E., Lopes, T., et al. (2012). Reprogramming of DNA methylation in pollen guides epigenetic inheritance via small RNA. *Cell* 151, 194–205. doi: 10.1016/j.cell.2012.09.001

Castel, S. E., and Martienssen, R. A. (2013). RNA interference in the nucleus: roles for small RNAs in transcription, epigenetics and beyond. *Nat. Rev. Genet.* 14, 100–112. doi: 10.1038/nrg3355

Cerutti, H., and Casas-Mollano, J. A. (2006). On the origin and functions of RNA-mediated silencing: from protists to man. *Curr. Genet.* 50, 81–99. doi: 10.1007/s00294-006-0078-x

Chang, P., Tseng, Y., Chen, P., and Wang, C. R. (2018). Using flow cytometry to isolate maize Meiocytes for next generation sequencing: a time and labor efficient method. *Curr. Protoc. Plant Biol.* 3:e20068. doi: 10.1002/cppb.20068

Chekanova, J. A. (2015). Long non-coding RNAs and their functions in plants. *Curr. Opin. Plant Biol.* 27, 207–216. doi: 10.1016/j.pbi.2015.08.003

Chen, H. M., Chen, L. T., Patel, K., Li, Y. H., Baulcombe, D. C., and Wu, S. H. (2010a). 22-nucleotide RNAs trigger secondary siRNA biogenesis in plants. *Proc. Natl. Acad. Sci. U. S. A.* 107, 15269–15274. doi: 10.1073/pnas.1001738107

Chen, C., Farmer, A. D., Langley, R. J., Mudge, J., Crow, J. A., May, G. D., et al. (2010b). Meiosis-specific gene discovery in plants: RNA-Seq applied to isolated *Arabidopsis* male meiocytes. *BMC Plant Biol.* 10:280. doi: 10.1186/1471-2229-10-280

Chen, C., and Retzel, E. F. (2013). Analyzing the meiotic transcriptome using isolated meiocytes of *Arabidopsis thaliana*. *Methods Mol. Biol.* 990, 203–213. doi: 10.1007/978-1-62703-333-6_20

Cheng, J., Niu, Q., Zhang, B., Chen, K., Yang, R., Zhu, J.-K., et al. (2018). Downregulation of RdDM during strawberry fruit ripening. *Genome Biol.* 19:212. doi: 10.1186/s13059-018-1587-x

Creasey, K. M., Zhai, J., Borges, F., Van Ex, F., Regulski, M., Meyers, B. C., et al. (2014). MiRNAs trigger widespread epigenetically activated siRNAs from transposons in *Arabidopsis*. *Nature* 508, 411–415. doi: 10.1038/nature13069

Csukasi, F., Donaire, L., Casañal, A., Martínez-Priego, L., Botella, M. A., Medina-Escobar, N., et al. (2012). Two strawberry miR159 family members display developmental-specific expression patterns in the fruit receptacle and cooperatively regulate fa-GAMYB. *New Phytol.* 195, 47–57. doi: 10.1111/j.1469-8137.2012.04134.x

da Cruz, I., Rodríguez-Casuriaga, R., Santiñaque, F. F., Farías, J., Curti, G., Capoano, C. A., et al. (2016). Transcriptome analysis of highly purified mouse spermatogenic cell populations: gene expression signatures switch from meiotic-to postmeiotic-related processes at pachytene stage. *BMC Genomics* 17:294. doi: 10.1186/s12864-016-2618-1

Ding, J., Lu, Q., Ouyang, Y., Mao, H., Zhang, P., Yao, J., et al. (2012a). A long noncoding RNA regulates photoperiod-sensitive male sterility, an essential component of hybrid rice. *Proc. Natl. Acad. Sci. U. S. A.* 109, 2654–2659. doi: 10.1073/pnas.1121374109

Ding, J., Shen, J., Mao, H., Xie, W., Li, X., and Zhang, Q. (2012b). RNA-directed DNA methylation is involved in regulating photoperiod- sensitive male sterility in rice. *Mol. Plant* 5, 1210–1216. doi: 10.1093/mp/sss095

Drinnenberg, I. A., Weinberg, D. E., Xie, K. T., Mower, J. P., Wolfe, K. H., Fink, G. R., et al. (2009). RNAi in budding yeast. *Science* 326, 544–550. doi: 10.1126/science.1176945

Dukowic-Schulze, S., Garcia, N., Shunmugam, A. S. K., Kagale, S., and Chen, C. (2020). Isolating male meiocytes from maize and wheat for "-omics" analyses. *Methods Mol. Biol.* 2061, 237–258. doi: 10.1007/978-1-4939-9818-0_17

Dukowic-Schulze, S., Sundararajan, A., Ramaraj, T., Kianian, S., Pawlowski, W. P., Mudge, J., et al. (2016). Novel meiotic miRNAs and indications for a role of phasiRNAs in meiosis. *Front. Plant Sci.* 7:762. doi: 10.3389/fpls.2016.00762

Ellermeier, C., Higuchi, E. C., Phadnis, N., Holm, L., Geelhood, J. L., Thon, G., et al. (2010). RNAi and heterochromatin repress centromeric meiotic recombination. *Proc. Natl. Acad. Sci. U. S. A.* 107, 8701–8705. doi: 10.1073/pnas.0914160107

Erdmann, R. M., and Picard, C. L. (2020). RNA-directed DNA methylation. *PLoS Genet.* 16:e1009034. doi: 10.1371/journal.pgen.1009034

Ernst, C., Odom, D. T., and Kutter, C. (2017). The emergence of piRNAs against transposon invasion to preserve mammalian genome integrity. *Nat. Commun.* 8:1411. doi: 10.1038/s41467-017-01049-7

Fan, Y., Yang, J., Mathioni, S. M., Yu, J., Shen, J., Yang, X., et al. (2016). PMS1T, producing phased small-interfering RNAs, regulates photoperiod-sensitive male sterility in rice. *Proc. Natl. Acad. Sci. U. S. A.* 113, 15144–15149. doi: 10.1073/pnas.1619159114

Fei, Y., Nyikó, T., and Molnar, A. (2021). Non-perfectly matching small RNAs can induce stable and heritable epigenetic modifications and can be used as molecular markers to trace the origin and fate of silencing RNAs. *Nucleic Acids Res.* 49, 1900–1913. doi: 10.1093/nar/gkab023

Fei, Q., Xia, R., and Meyers, B. C. (2013). Phased, secondary, small interfering RNAs in posttranscriptional regulatory networks. *Plant Cell* 25, 2400–2415. doi: 10.1105/tpc.113.114652

Fei, Q., Yang, L., Liang, W., Zhang, D., and Meyers, B. C. (2016). Dynamic changes of small RNAs in rice spikelet development reveal specialized reproductive phasiRNA pathways. *J. Exp. Bot.* 67, 6037–6049. doi: 10.1093/jxb/erw361

Flórez-Zapata, N. M. V., Reyes-Valdés, M. H., and Martínez, O. (2016). Long non-coding RNAs are major contributors to transcriptome changes in sunflower meiocytes with different recombination rates. *BMC Genomics* 17:490. doi: 10.1186/s12864-016-2776-1

Gao, M., Wei, W., Li, M. M., Wu, Y. S., Ba, Z., Jin, K. X., et al. (2014). Ago2 facilitates Rad51 recruitment and DNA double-strand break repair by homologous recombination. *Cell Res.* 24, 532–541. doi: 10.1038/cr.2014.36

Golicz, A. A., Bhalla, P. L., and Singh, M. B. (2018). lncRNAs in plant and animal sexual reproduction. *Trends Plant Sci.* 23, 195–205. doi: 10.1016/j.tplants.2017.12.009

Gutbrod, M. J., and Martienssen, R. A. (2020). Conserved chromosomal functions of RNA interference. *Nat. Rev. Genet.* 21, 311–331. doi: 10.1038/s41576-019-0203-6

Hamilton, A. J., and Baulcombe, D. C. (1999). A species of small antisense RNA in posttranscriptional gene silencing in plants. *Science* 286, 950–952. doi: 10.1126/science.286.5441.950

Heo, J. B., and Sung, S. (2011). Vernalization-mediated epigenetic silencing by a long intronic noncoding RNA. *Science* 331, 76–79. doi: 10.1126/science.1197349

Huang, J., Wang, C., Li, X., Fang, X., Huang, N., Wang, Y., et al. (2020). Conservation and divergence in the Meiocyte sRNAomes of *Arabidopsis*, soybean, and cucumber. *Plant Physiol.* 182, 301–317. doi: 10.1104/pp.19.00807

Huang, J., Wang, C., Wang, H., Lu, P., Zheng, B., Ma, H., et al. (2019). Meiocyte-specific and at SPO11-1-dependent small RNAs and their association with meiotic gene expression and recombination. *Plant Cell* 31, 444–464. doi: 10.1105/tpc.18.00511

Hunter, N. (2015). Meiotic recombination: the essence of heredity. *Cold Spring Harb. Perspect. Biol.* 7:a016618. doi: 10.1101/cshperspect.a016618

Ibarra, C. A., Feng, X., Schoft, V. K., Hsieh, T. F., Uzawa, R., Rodrigues, J. A., et al. (2012). Active DNA demethylation in plant companion cells reinforces transposon methylation in gametes. *Science* 337, 1360–1364. doi: 10.1126/science.1224839

Iwasaki, M., Hyvärinen, L., Piskurewicz, U., and Lopez-Molina, L. (2019). Non-canonical RNA-directed DNA methylation participates in maternal and environmental control of seed dormancy. *eLife* 8:e37434. doi: 10.7554/eLife.37434

Jiang, H., Wang, F. F., Wu, Y. T., Zhou, X., Huang, X. Y., Zhu, J., et al. (2009). Multipolar spindle 1 (mps1), a novel coiled-coil protein of *Arabidopsis thaliana*, is required for meiotic spindle organization. *Plant J.* 59, 1001–1010. doi: 10.1111/j.1365-313X.2009.03929.x

Johnson, C., Kasprzewska, A., Tennessen, K., Fernandes, J., Nan, G. L., Walbot, V., et al. (2009). Clusters and superclusters of phased small RNAs in the developing inflorescence of rice. *Genome Res.* 19, 1429–1440. doi: 10.1101/gr.089854.108

Jullien, P. E., Susaki, D., Yelagandula, R., Higashiyama, T., and Berger, F. (2012). DNA methylation dynamics during sexual reproduction in *Arabidopsis thaliana*. *Curr. Biol.* 22, 1825–1830. doi: 10.1016/j.cub.2012.07.061

Kakrana, A., Mathioni, S. M., Huang, K., Hammond, R., Vandivier, L., Patel, P., et al. (2018). Plant 24-nt reproductive phasiRNAs from intramolecular duplex mRNAs in diverse monocots. *Genome Res.* 28, 1333–1344. doi: 10.1101/gr.228163.117

Kaya-Okur, H. S., Wu, S. J., Codomo, C. A., Pledger, E. S., Bryson, T. D., Henikoff, J. G., et al. (2019). CUT&tag for efficient epigenomic profiling

of small samples and single cells. *Nat. Commun.* 10:1930. doi: 10.1038/s41467-019-09982-5

Kim, D.-H., and Sung, S. (2017). Vernalization-triggered intragenic chromatin loop formation by long noncoding RNAs. *Dev. Cell* 40, 302.e4–312.e4. doi: 10.1016/j.devcel.2016.12.021

Komiya, R., Ohyanagi, H., Niihama, M., Watanabe, T., Nakano, M., Kurata, N., et al. (2014). Rice germline-specific Argonaute MEL1 protein binds to phasiRNAs generated from more than 700 lincRNAs. *Plant J.* 78, 385–397. doi: 10.1111/tpj.12483

Kumakura, N., Takeda, A., Fujioka, Y., Motose, H., Takano, R., and Watanabe, Y. (2009). SGS3 and RDR6 interact and colocalize in cytoplasmic SGS3/RDR6-bodies. *FEBS Lett.* 583, 1261–1266. doi: 10.1016/j.febslet.2009.03.055

Lardenois, A., Liu, Y., Walther, T., Chalmel, F., Evrard, B., Granovskaia, M., et al. (2011). Execution of the meiotic noncoding RNA expression program and the onset of gametogenesis in yeast require the conserved exosome subunit Rrp6. *Proc. Natl. Acad. Sci. U. S. A.* 108, 1058–1063. doi: 10.1073/pnas.1016459108

Lee, H. C., Chang, S. S., Choudhary, S., Aalto, A. P., Maiti, M., Bamford, D. H., et al. (2009). QiRNA is a new type of small interfering RNA induced by DNA damage. *Nature* 459, 274–277. doi: 10.1038/nature08041

Lee, Y.-S., Maple, R., Dürr, J., Dawson, A., Tamim, S., Del Genio, C., et al. (2020). A transposon surveillance mechanism that safeguards plant male fertility during stress. *Nat. Plants* 7, 34–41. doi: 10.1038/s41477-020-00818-5

Lei, X., and Liu, B. (2020). Tapetum-dependent male meiosis progression in plants: increasing evidence emerges. *Front. Plant Sci.* 10:1667. doi: 10.3389/fpls.2019.01667

Li, X., Shahid, M. Q., Wen, M., Chen, S., Yu, H., Jiao, Y., et al. (2020). Global identification and analysis revealed differentially expressed lncRNAs associated with meiosis and low fertility in autotetraploid rice. *BMC Plant Biol.* 20:82. doi: 10.1186/s12870-020-2290-0

Liu, F., Marquardt, S., Lister, C., Swiezewski, S., and Dean, C. (2010). Targeted 3' processing of antisense transcripts triggers *Arabidopsis* FLC chromatin silencing. *Science* 327, 94–97. doi: 10.1126/science.1180278

Liu, H., and Nonomura, K. I. (2016). A wide reprogramming of histone H3 modifications during male meiosis I in rice is dependent on the Argonaute protein MEL1. *J. Cell Sci.* 129, 3553–3561. doi: 10.1242/jcs.184937

Liu, C., Shen, Y., Qin, B., Wen, H., Cheng, J., Mao, F., et al. (2020a). *Oryza sativa* RNA-dependent RNA polymerase 6 contributes to double-strand break formation in meiosis. *Plant Cell* 32, 3273–3289. doi: 10.1105/tpc.20.00213

Liu, Y., Su, H., Zhang, J., Liu, Y., Feng, C., and Han, F. (2020b). Back-spliced RNA from retrotransposon binds to centromere and regulates centromeric chromatin loops in maize. *PLoS Biol.* 18:e3000582. doi: 10.1371/journal.pbio.3000582

Liu, Y., Teng, C., Xia, R., and Meyers, B. C. (2020c). PhasiRNAs in plants: their biogenesis, genic sources, and roles in stress responses, development, and reproduction. *Plant Cell* 32, 3059–3080. doi: 10.1105/tpc.20.00335

Long, J., Walker, J., She, W., Aldridge, B., Gao, H., and Feng, X. (2021). Nurse cell-derived small RNAs define paternal epigenetic inheritance in *Arabidopsis*. bioRxiv [Preprint]. doi:10.1101/2021.01.25.428150

Mallory, A. C., and Vaucheret, H. (2006). Functions of microRNAs and related small RNAs in plants. *Nat. Genet.* 38, S31–S36. doi: 10.1038/ng1791

Margolin, G., Khil, P. P., Kim, J., Bellani, M. A., and Camerini-Otero, R. D. (2014). Integrated transcriptome analysis of mouse spermatogenesis. *BMC Genomics* 15:39. doi: 10.1186/1471-2164-15-39

Martinez, G., Wolff, P., Wang, Z., Moreno-Romero, J., Santos-González, J., Conze, L. L., et al. (2018). Paternal easiRNAs regulate parental genome dosage in *Arabidopsis*. *Nat. Genet.* 50, 193–198. doi: 10.1038/s41588-017-0033-4

Matzke, M. A., Kanno, T., and Matzke, A. J. M. (2015). RNA-directed DNA methylation: the evolution of a complex epigenetic pathway in flowering plants. *Annu. Rev. Plant Biol.* 66, 243–267. doi: 10.1146/annurev-arplant-043014-114633

Matzke, M. A., and Mosher, R. A. (2014). RNA-directed DNA methylation: an epigenetic pathway of increasing complexity. *Nat. Rev. Genet.* 15, 394–408. doi: 10.1038/nrg3683

McCue, A. D., Nuthikattu, S., Reeder, S. H., and Slotkin, R. K. (2012). Gene expression and stress response mediated by the epigenetic regulation of a transposable element small RNA. *PLoS Genet.* 8:e1002474. doi: 10.1371/journal.pgen.1002474

McNulty, S. M., Sullivan, L. L., and Sullivan, B. A. (2017). Human centromeres produce chromosome-specific and array-specific alpha satellite transcripts that are complexed with CENP-A and CENP-C. *Dev. Cell* 42, 226.e6–240.e6. doi: 10.1016/j.devcel.2017.07.001

Mercier, R., Mézard, C., Jenczewski, E., Macaisne, N., and Grelon, M. (2015). The molecular biology of meiosis in plants. *Annu. Rev. Plant Biol.* 66, 297–327. doi: 10.1146/annurev-arplant-050213-035923

Millar, A. A., and Gubler, F. (2005). The *Arabidopsis* GAMYB-like genes, MYB33 and MYB65, are microRNA-regulated genes that redundantly facilitate anther development. *Plant Cell* 17, 705–721. doi: 10.1105/tpc.104.027920

Nan, G. L., Zhai, J., Arikit, S., Morrow, D., Fernandes, J., Mai, L., et al. (2017). MS23, a master basic helix-loop-helix factor, regulates the specification and development of the tapetum in maize. *Development* 144, 163–172. doi: 10.1242/dev.140673

Nelms, B., and Walbot, V. (2019). Defining the developmental program leading to meiosis in maize. *Science* 364, 52–56. doi: 10.1126/science.aav6428

Nonomura, K. I., Morohoshi, A., Nakano, M., Eiguchi, M., Miyao, A., Hirochika, H., et al. (2007). A germ cell-specific gene of the ARGONAUTE family is essential for the progression of premeiotic mitosis and meiosis during sporogenesis in rice. *Plant Cell* 19, 2583–2594. doi: 10.1105/tpc.107.053199

Oliver, C., Pradillo, M., Jover-Gil, S., Cuñado, N., Ponce, M. R., and Santos, J. L. (2017). Loss of function of *Arabidopsis* microRNA-machinery genes impairs fertility, and has effects on homologous recombination and meiotic chromatin dynamics. *Sci. Rep.* 7:9280. doi: 10.1038/s41598-017-07702-x

Oliver, C., Santos, J. L., and Pradillo, M. (2014). On the role of some ARGONAUTE proteins in meiosis and DNA repair in *Arabidopsis thaliana*. *Front. Plant Sci.* 5:177. doi: 10.3389/fpls.2014.00177

Oliver, C., Santos, J. L., and Pradillo, M. (2016). Accurate chromosome segregation at first meiotic division requires AGO4, a protein involved in RNA-dependent DNA methylation in *Arabidopsis thaliana*. *Genetics* 204, 543–553. doi: 10.1534/genetics.116.189217

Olmedo-Monfil, V., Durán-Figueroa, N., Arteaga-Vázquez, M., Demesa-Arévalo, E., Autran, D., Grimanelli, D., et al. (2010). Control of female gamete formation by a small RNA pathway in *Arabidopsis*. *Nature* 464, 628–632. doi: 10.1038/nature08828

Ono, S., Liu, H., Tsuda, K., Fukai, E., Tanaka, K., Sasaki, T., et al. (2018). EAT1 transcription factor, a non-cell-autonomous regulator of pollen production, activates meiotic small RNA biogenesis in rice anther tapetum. *PLoS Genet.* 14:e1007238. doi: 10.1371/journal.pgen.1007238

Palatnik, J. F., Wollmann, H., Schommer, C., Schwab, R., Boisbouvier, J., Rodriguez, R., et al. (2007). Sequence and expression differences underlie functional specialization of *Arabidopsis* MicroRNAs miR159 and miR319. *Dev. Cell* 13, 115–125. doi: 10.1016/j.devcel.2007.04.012

Papini, A., Mosti, S., and Brighigna, L. (1999). Programmed-cell-death events during tapetum development of angiosperms. *Protoplasma* 207, 213–221. doi: 10.1007/BF01283002

Pradillo, M., and Santos, J. L. (2018). Genes involved in miRNA biogenesis affect meiosis and fertility. *Chromosom. Res.* 26, 233–241. doi: 10.1007/s10577-018-9588-x

Primig, M., Williams, R. M., Winzeler, E. A., Tevzadze, G. G., Conway, A. R., Hwang, S. Y., et al. (2000). The core meiotic transcriptome in budding yeasts. *Nat. Genet.* 26, 415–423. doi: 10.1038/82539

Prusicki, M. A., Keizer, E. M., van Rosmalen, R. P., Komaki, S., Seifert, F., Müller, K., et al. (2019). Live cell imaging of meiosis in *Arabidopsis thaliana*. *eLife* 8:e42834. doi: 10.7554/eLife.42834

Quénet, D., and Dalal, Y. (2014). A long non-coding RNA is required for targeting centromeric protein A to the human centromere. *eLife* 3:e03254. doi: 10.7554/eLife.03254

Shi, Y., Zhao, S., and Yao, J. (2009). Premature tapetum degeneration: a major cause of abortive pollen development in photoperiod sensitive genic male sterility in rice. *J. Integr. Plant Biol.* 51, 774–781. doi: 10.1111/j.1744-7909.2009.00849.x

Singh, M., Goel, S., Meeley, R. B., Dantec, C., Parrinello, H., Michaud, C., et al. (2011). Production of viable gametes without meiosis in maize deficient for an ARGONAUTE protein. *Plant Cell* 23, 443–458. doi: 10.1105/tpc.110.079020

Skene, P. J., Henikoff, J. G., and Henikoff, S. (2018). Targeted in situ genome-wide profiling with high efficiency for low cell numbers. *Nat. Protoc.* 13, 1006–1019. doi: 10.1038/nprot.2018.015

Slotkin, R. K., Vaughn, M., Borges, F., Tanurdžić, M., Becker, J. D., Feijó, J. A., et al. (2009). Epigenetic reprogramming and small RNA silencing of transposable elements in pollen. *Cell* 136, 461–472. doi: 10.1016/j.cell.2008.12.038

Song, X., Li, P., Zhai, J., Zhou, M., Ma, L., Liu, B., et al. (2012). Roles of DCL4 and DCL3b in rice phased small RNA biogenesis. *Plant J.* 69, 462–474. doi: 10.1111/j.1365-313X.2011.04805.x

Soppe, W. J. J., Jacobsen, S. E., Alonso-Blanco, C., Jackson, J. P., Kakutani, T., Koornneef, M., et al. (2000). The late flowering phenotype of fwa mutants is caused by gain-of-function epigenetic alleles of a homeodomain gene. *Mol. Cell* 6, 791–802. doi: 10.1016/S1097-2765(05)00090-0

Sydor, A. M., Czymmek, K. J., Puchner, E. M., and Mennella, V. (2015). Super-resolution microscopy: from single molecules to supramolecular assemblies. *Trends Cell Biol.* 25, 730–748. doi: 10.1016/j.tcb.2015.10.004

Tang, J., and Chu, C. (2017). MicroRNAs in crop improvement: fine-tuners for complex traits. *Nat. Plants* 3:17077. doi: 10.1038/nplants.2017.77

Teng, C., Zhang, H., Hammond, R., Huang, K., Meyers, B. C., and Walbot, V. (2020). Dicer-like 5 deficiency confers temperature-sensitive male sterility in maize. *Nat. Commun.* 11:2912. doi: 10.1038/s41467-020-16634-6

Tian, Y., Zheng, H., Zhang, F., Wang, S., Ji, X., Xu, C., et al. (2019). PRC2 recruitment and H3K27me3 deposition at FLC require FCA binding of COOLAIR. *Sci. Adv.* 5:eaau7246. doi: 10.1126/sciadv.aau7246

Topp, C. N., Zhong, C. X., and Dawe, R. K. (2004). Centromere-encoded RNAs are integral components of the maize kinetochore. *Proc. Natl. Acad. Sci. U. S. A.* 101, 15986–15991. doi: 10.1073/pnas.0407154101

Tsuji, H., Aya, K., Ueguchi-Tanaka, M., Shimada, Y., Nakazono, M., Watanabe, R., et al. (2006). GAMYB controls different sets of genes and is differentially regulated by microRNA in aleurone cells and anthers. *Plant J.* 47, 427–444. doi: 10.1111/j.1365-313X.2006.02795.x

Van Werven, F. J., Neuert, G., Hendrick, N., Lardenois, A., Buratowski, S., Van Oudenaarden, A., et al. (2012). Transcription of two long noncoding RNAs mediates mating-type control of gametogenesis in budding yeast. *Cell* 150, 1170–1181. doi: 10.1016/j.cell.2012.06.049

Vazquez, F., Vaucheret, H., Rajagopalan, R., Lepers, C., Gasciolli, V., Mallory, A. C., et al. (2004). Endogenous trans-acting siRNAs regulate the accumulation of arabidopsis mRNAs. *Mol. Cell* 16, 69–79. doi: 10.1016/j.molcel.2004.09.028

Villeneuve, A. M., and Hillers, K. J. (2001). Whence meiosis? *Cell* 106, 647–650. doi: 10.1016/S0092-8674(01)00500-1

Voinnet, O. (2009). Origin, biogenesis, and activity of plant MicroRNAs. *Cell* 136, 669–687. doi: 10.1016/j.cell.2009.01.046

Vu, T. M., Nakamura, M., Calarco, J. P., Susaki, D., Lim, P. Q., Kinoshita, T., et al. (2013). RNA-directed DNA methylation regulates parental genomic imprinting at several loci in *Arabidopsis*. *Development* 140, 2953–2960. doi: 10.1242/dev.092981

Walker, J., Gao, H., Zhang, J., Aldridge, B., Vickers, M., Higgins, J. D., et al. (2017). Sexual-lineage-specific DNA methylation regulates meiosis in *Arabidopsis*. *Nat. Genet.* 50, 130–137. doi: 10.1038/s41588-017-0008-5

Wang, Z., Butel, N., Santos-González, J., Borges, F., Yi, J., Martienssen, R. A., et al. (2020). Polymerase IV plays a crucial role in pollen development in Capsella. *Plant Cell* 32, 950–966. doi: 10.1105/tpc.19.00938

Wang, M., Wu, H. J., Fang, J., Chu, C., and Wang, X. J. (2017). A long noncoding RNA involved in rice reproductive development by negatively regulating osa-miR160. *Sci. Bull.* 62, 470–475. doi: 10.1016/j.scib.2017.03.013

Wei, W., Ba, Z., Gao, M., Wu, Y., Ma, Y., Amiard, S., et al. (2012). A role for small RNAs in DNA double-strand break repair. *Cell* 149, 101–112. doi: 10.1016/j.cell.2012.03.002

Wierzbicki, A. T., Haag, J. R., and Pikaard, C. S. (2008). Noncoding transcription by RNA polymerase pol IVb/pol V mediates transcriptional silencing of overlapping and adjacent genes. *Cell* 135, 635–648. doi: 10.1016/j.cell.2008.09.035

Winter, E. (2012). The Sum1/Ndt80 transcriptional switch and commitment to meiosis in *Saccharomyces cerevisiae*. *Microbiol. Mol. Biol. Rev.* 76, 1–15. doi: 10.1128/MMBR.05010-11

Wu, M. F., Tian, Q., and Reed, J. W. (2006). Arabidopis microRNA 167 controls patterns of ARF6 and ARF8 expression, and regulates both female and male reproduction. *Development* 133, 4211–4218. doi: 10.1242/dev.02602

Xia, R., Chen, C., Pokhrel, S., Ma, W., Huang, K., Patel, P., et al. (2019). 24-nt reproductive phasiRNAs are broadly present in angiosperms. *Nat. Commun.* 10:627. doi: 10.1038/s41467-019-08543-0

Yang, H., Lu, P., Wang, Y., and Ma, H. (2011). The transcriptome landscape of *Arabidopsis* male meiocytes from high-throughput sequencing: the complexity and evolution of the meiotic process. *Plant J.* 65, 503–516. doi: 10.1111/j.1365-313X.2010.04439.x

Yu, L., Guo, R., Jiang, Y., Ye, X., Yang, Z., Meng, Y., et al. (2019). Identification of novel phasiRNAs loci on long non-coding RNAs in *Arabidopsis thaliana*. *Genomics* 111, 1668–1675. doi: 10.1016/j.ygeno.2018.11.017

Zhai, J., Zhang, H., Arikit, S., Huang, K., Nan, G. L., Walbot, V., et al. (2015). Spatiotemporally dynamic, cell-type-dependent premeiotic and meiotic phasiRNAs in maize anthers. *Proc. Natl. Acad. Sci. U. S. A.* 112, 3146–3151. doi: 10.1073/pnas.1418918112

Zhang, Y. C., Lei, M. Q., Zhou, Y. F., Yang, Y. W., Lian, J. P., Yu, Y., et al. (2020a). Reproductive phasiRNAs regulate reprogramming of gene expression and meiotic progression in rice. *Nat. Commun.* 11:6031. doi: 10.1038/s41467-020-19922-3

Zhang, M., Ma, X., Wang, C., Li, Q., Meyers, B. C., Springer, N. M., et al. (2020b). CHH DNA methylation increases at 24-PHAS loci depend on 24-nt phased small interfering RNAs in maize meiotic anthers. *New Phytol.* 229, 2984–2997. doi: 10.1111/nph.17060

Zheng, Y., Wang, Y., Wu, J., Ding, B., and Fei, Z. (2015). A dynamic evolutionary and functional landscape of plant phased small interfering RNAs. *BMC Biol.* 13:32. doi: 10.1186/s12915-015-0142-4

Zhou, M., Coruh, C., Xu, G., Bourbousse, C., Lambolez, A., and Law, J. A. (2021). The CLASSY family controls tissue-specific DNA methylation patterns in *Arabidopsis*. bioRxiv [Preprint]. doi:10.1101/2021.01.23.427869

Zhou, H., Liu, Q., Li, J., Jiang, D., Zhou, L., Wu, P., et al. (2012). Photoperiod- and thermo-sensitive genic male sterility in rice are caused by a point mutation in a novel noncoding RNA that produces a small RNA. *Cell Res.* 22, 649–660. doi: 10.1038/cr.2012.28

Zhou, A., and Pawlowski, W. P. (2014). Regulation of meiotic gene expression in plants. *Front. Plant Sci.* 5:413. doi: 10.3389/fpls.2014.00413

Conflict of Interest: The authors declare that the research was conducted in the absence of any commercial or financial relationships that could be construed as a potential conflict of interest.

Publisher's Note: All claims expressed in this article are solely those of the authors and do not necessarily represent those of their affiliated organizations, or those of the publisher, the editors and the reviewers. Any product that may be evaluated in this article, or claim that may be made by its manufacturer, is not guaranteed or endorsed by the publisher.

frontiers in Plant Science

REVIEW
published: 07 September 2021
doi: 10.3389/fpls.2021.717423

The Formation of Bivalents and the Control of Plant Meiotic Recombination

*Yared Gutiérrez Pinzón, José Kenyi González Kise, Patricia Rueda and Arnaud Ronceret**

Laboratory of Cytogenomics of Meiosis, Instituto de Biotecnología, Departamento de Biología Molecular de Plantas, National Autonomous University of Mexico (UNAM), Cuernavaca, Mexico

During the first meiotic division, the segregation of homologous chromosomes depends on the physical association of the recombined homologous DNA molecules. The physical tension due to the sites of crossing-overs (COs) is essential for the meiotic spindle to segregate the connected homologous chromosomes to the opposite poles of the cell. This equilibrated partition of homologous chromosomes allows the first meiotic reductional division. Thus, the segregation of homologous chromosomes is dependent on their recombination. In this review, we will detail the recent advances in the knowledge of the mechanisms of recombination and bivalent formation in plants. In plants, the absence of meiotic checkpoints allows observation of subsequent meiotic events in absence of meiotic recombination or defective meiotic chromosomal axis formation such as univalent formation instead of bivalents. Recent discoveries, mainly made in Arabidopsis, rice, and maize, have highlighted the link between the machinery of double-strand break (DSB) formation and elements of the chromosomal axis. We will also discuss the implications of what we know about the mechanisms regulating the number and spacing of COs (obligate CO, CO homeostasis, and interference) in model and crop plants.

Keywords: Meiosis, recombination, synapsis, obligate crossing-over, interference, CO homeostasis, heterochiasmy

OPEN ACCESS

Edited by:
Mónica Pradillo, Complutense University of Madrid, Spain

Reviewed by:
Jason Sims, Max F. Perutz Laboratories GmbH, Austria
Charles Underwood, Max Planck Institute for Plant Breeding Research, Germany
Heïdi Serra, Centre National de la Recherche Scientifique (CNRS), France

****Correspondence:***
Arnaud Ronceret
arnaud.ronceret@ibt.unam.mx

Specialty section:
This article was submitted to Plant Cell Biology, a section of the journal Frontiers in Plant Science

Received: *30 May 2021*
Accepted: *13 August 2021*
Published: *07 September 2021*

Citation:
Gutiérrez Pinzón Y, González Kise JK, Rueda P and Ronceret A (2021) The Formation of Bivalents and the Control of Plant Meiotic Recombination. Front. Plant Sci. 12:717423. doi: 10.3389/fpls.2021.717423

INTRODUCTION

Meiosis is one of the most dynamic processes for a plant genome (Ronceret and Pawlowski, 2010; Prusicki et al., 2019). To achieve a reductional division, the meiotic cell goes through one round of DNA replication followed by two cell divisions (Mercier et al., 2015). The meiotic divisions have evolved from the machinery toolkit used by the regular mitotic division with additional regulatory functions allowing the reductional division (Wilkins and Holliday, 2009). Several differences between meiosis and mitosis are discernible already at prophase I with the introduction of meiotic-specific processes such as meiotic recombination, pairing, and synapsis of homologs. During the whole meiotic prophase I, the nuclear chromosome content is duplicated and each homolog is constituted by two sister chromatids. Bivalents are defined as connected homologous chromosomes, forming a unit of four DNA molecules, essential for the equilibrated segregation of the chromosome pool. The formation of bivalents occurs during the prophase I of meiosis and involves the coordination between homologous recombination, pairing, and synapsis (Mercier et al., 2015). During meiotic metaphase I, a specific bipolar conformation of the meiotic spindle attachment to centromeres allows the segregation of these recombined bivalents.

In plants, male and female meiosis occur in different organs. Though most meiotic mechanisms are shared between sexes, some differences have long been observed between male and female meiotic recombination rates. After the two successive meiotic divisions, haploid spores, which contain only one set of each chromosome, are formed. These separated male or female spores undergo the gametophytic phase giving rise to distinct male and female gametes. Fertilization between gametes restores the diploid state crucial for the sexual life cycle and the genome maintenance of the species.

Understanding the formation of how new meiotic DNA molecules are formed is of special value for breeding since it is a fundamental basis for genetics, evolution, and genomic crop improvement (Melamed-Bessudo et al., 2016; Lambing et al., 2017; Blary and Jenczewski, 2019; Bolaños-Villegas and Argüello-Miranda, 2019; Taagen et al., 2020; Kuo et al., 2021).

This review will focus on the recent advances in the understanding of the genetic control of meiotic recombination and bivalent formation in diploid plant species, mainly Arabidopsis, rice, and maize. For the more complex bivalent and multivalent formation in polyploid plants [Refer the reviews of Cifuentes et al. (2010), Mason and Wendel (2020), and Svačina et al. (2020)]. Several important discoveries have been made in these last few years concerning the mechanisms of crossing-over (CO) interference (impeding the formation of adjacent COs), non-crossing-over (NCO) pathways, obligate CO (to maintain at least one CO by bivalent), CO homeostasis [the buffering of CO numbers despite the reduction in double-strand breaks (DSBs) number], and heterochiasmy (difference in male and female CO frequencies). For an overview of the plant meiotic genes and mechanisms discovered before 2018, see the excellent reviews of Luo et al. (2014), Mercier et al. (2015), and Wang and Copenhaver (2018). An overview of the proteins regulating bivalent formation grouped by functional modules is listed in **Figure 1**.

REGULATION OF THE MEIOTIC CELL FATE AND MEIOTIC TRANSCRIPTOME

In plants, the germline fate acquisition where meiosis will occur involves the specific transcription factor SPOROCYTELESS also known as NOZZLE in Arabidopsis (Yang et al., 1999; Wei et al., 2015) and rice (Ren et al., 2018). In rice, the ARGONAUTE protein MEL1 plays an essential role in male and female meiotic cell fate (Nonomura et al., 2007; Komiya et al., 2014; Liu and Nonomura, 2016). The rice MEL2 is an RNA recognition motif protein binding the 3′-UTRs and involved in the translational regulation of key meiotic genes (Nonomura et al., 2011; Miyazaki et al., 2015). In Arabidopsis, no MEL orthologs have been described but AGO9 and AGO4 are involved in female gamete specification (Olmedo-Monfil et al., 2010), while small interfering RNA inhibits retrotranspositions in the male germline (Long et al., 2021). Argonautes are the key players in distinct small RNAs (sRNAs) pathways involved in transcriptome regulation (Oliver et al., 2014). Transcriptomic analysis of different steps of germline cells and meiocytes has revealed dramatic transcriptomic changes during prophase I in various plant species. In maize, single-cell RNA sequencing reveals a profound two steps reorganization of the transcriptome at the leptotene stage when meiotic recombination initiate (Nelms and Walbot, 2019). The sRNAs (micro-RNA and phased secondary small interfering RNA) are particular dynamics during prophase in rice, maize, sunflower, soybean, and cucumber (Dukowic-Schulze et al., 2016; Flórez-Zapata et al., 2016; Huang et al., 2020; Zhang et al., 2021) and, at least in Arabidopsis male meiocytes, play a critical role in meiotic recombination potentially *via* the AGO4 pathway (Oliver et al., 2016, 2017; Pradillo and Santos, 2018).

Though sex-specific transcriptomes have been obtained in various plant species (Dukowic-Schulze et al., 2020; Liu et al., 2020; Barakate et al., 2021), a systematic comparison between male and female meiotic transcriptomes has not yet been performed.

In maize, hypoxia arising naturally within growing anther tissue was reported to act as a positional cue to set male germ cell fate (Kelliher and Walbot, 2012). The cytology of plant female meiosis has been historically more challenging but is now prone to analysis due to new techniques of the whole immunolocalization of plant ovules (Escobar-Guzman et al., 2015; Gordillo et al., 2020). In Arabidopsis, the specification of only one germ cell line per ovule has been analyzed and involved complex positional clues and identify RBR1 as a central hub for female meiocyte differentiation (Zhao et al., 2017). RBR1 is also required for the recombinase RAD51 localization to DNA lesions (Biedermann et al., 2017). *SWITCH1/AMEIOTIC* is an essential gene allowing the entry in male and female meiosis. SWI1 was recently identified as a functional Sororin-like antagonist (Yang et al., 2019) of the WINGS APART-LIKE (WAPL) that removes cohesin from chromosome *via* the prophase pathway before the action of separase at anaphase onset (De et al., 2014). Accordingly, SWI1/AM1 is a nuclear protein installed on the whole chromatin from premeiotic replication and is only maintained in centromere regions during pachytene in maize (Pawlowski et al., 2009). However, this remaining centromeric localization was not observed in rice (Che et al., 2011) suggesting plant-specific variations for this regulation.

FORMATION OF THE MEIOTIC COHESIN COMPLEX

DNA replication is followed by the appearance of meiotic-specific components of the cohesin complex (formed by SMC1, SMC3, SCC2, SCC3, and REC8) (Cai et al., 2003; Chelysheva et al., 2005; Wang et al., 2020). Cohesin turnover and localization on chromatin are mediated by WAPL (De et al., 2014), PDS5 (Pradillo et al., 2015), and CTF7 (Singh et al., 2013). REC8 is a meiotic-specific kleisin that replaces the mitotic SCC1 subunit in this complex. It was shown in tomato that the four subunits of the meiotic cohesin complex are discontinuously distributed along the chromosome length from leptotene through early diplotene (Qiao et al., 2011). In maize, SMC3 is essential for sister chromatid cohesion and facilitates centromere coupling (Zhang et al., 2020d), a peculiar configuration associating the centromeres before pairing commences along chromosome

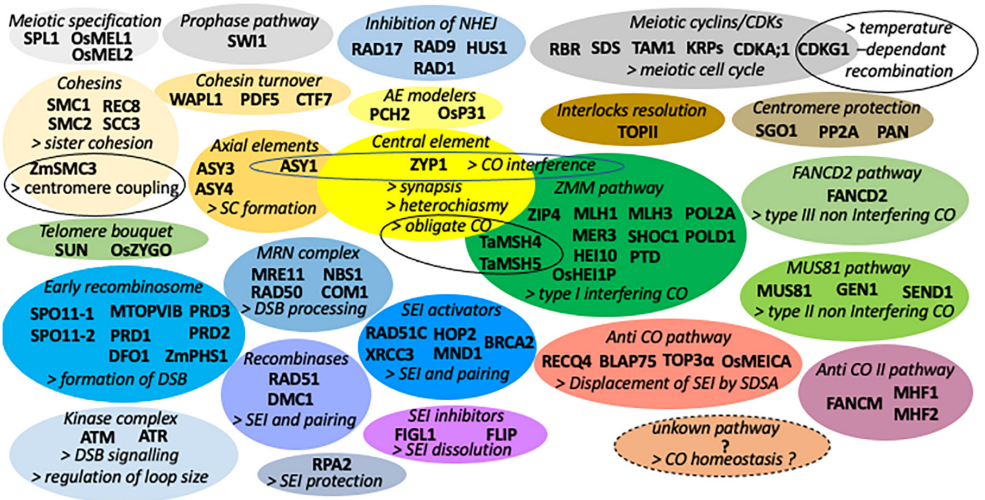

FIGURE 1 | List of proteins regulating bivalent formation grouped by functional modules under a different colored bubble. For simplification, the list only gives the name of Arabidopsis proteins unless the two-letter symbol of the species is specified before the protein name (Os rice, Ta durum wheat, and Zm maize).

arms (Ronceret et al., 2009). The current working models of chromatin organization suppose that the meiotic cohesin complex forms a ring attaching the two replicated sister chromatids and organizes the chromatin by forming the base of chromatin loops (Zickler and Kleckner, 2015; Kim and Choi, 2019; Grey and de Massy, 2021). Chromosome conformation capture (HiC) experiments have not yet been performed on plant meiotic genomes to analyze their chromosomal loop domain organization (Golicz et al., 2020). In Arabidopsis, ChIP-seq experiments have shown that REC8 is associated with repetitive centromeric and pericentromeric regions of high nucleosome occupancy, the opposite of where meiotic DSBs and crossovers are found at the chromosome and fine scales (Lambing et al., 2020b). REC8 containing cohesin complex is largely protected by the Shugoshin (SGO)-PP2A complex around centromeres during meiosis I (Zamariola et al., 2014; Yuan et al., 2018; Zhang et al., 2019) and by PAN during interkinesis (Cromer et al., 2019). These protections allow the coordinated separation of the homologous chromosomes during meiosis I and the release of the sister chromatin only during meiosis II *via* a separase-dependent proteolytic cleavage of the centromeric kleisin subunit REC8 (Cromer et al., 2019).

FORMATION OF THE AXIAL ELEMENT OF THE SYNAPTONEMAL COMPLEX

The synaptonemal complex (SC) is a proteinaceous ultrastructure formed of two axial elements (AEs) and a central element. Elements of the AEs are installed on chromatin during leptotene before synapsis occurs. In plants, several components of the AEs have been identified: the HORMA domain ASY1/PAIR2 (Armstrong et al., 2002; Nonomura et al., 2004a), the associated coiled-coiled proteins ASY3/DSY2/PAIR3 (Yuan et al., 2009; Ferdous et al., 2012; Lee et al., 2015; Osman et al., 2018) and ASY4 (Chambon et al., 2018). The cohesin REC8 is supposed to anchor chromatin to the AEs of the SC *via* PAIR3/ASY3 (Wang et al., 2011) though a direct interaction between REC8 and any AE protein is yet unknown. However, in Arabidopsis, ASY1 and REC8 ChiP-seq strongly correlate suggesting that both proteins associate with similar regions of the genome at global and fine scales (Lambing et al., 2020b). In maize, DSY2 (homolog of ASY3 and PAIR3) forms an alternative pattern with ASY1 on AE and can interact with ZYP1 while ASY1 cannot (Lee et al., 2015). In addition, the AAA^{+} ATPase PACHYTENE CHECKPOINT 2 (PCH2)/CRC1 is essential for the ASY1 depletion before synapsis (Lambing et al., 2015). Its interacting partner $P31^{comet}$ participates in ASY1 import in the nucleus and the removal of non-phosphorylated ASY1 from the chromosomal axis (Balboni et al., 2020). In rice, CRC1/PCH2 can directly interact with ZEP1/ZYP1 while P31 cannot (Ji et al., 2016). In addition, the role of some SC proteins in the initiation of meiotic recombination such as DSY2/ASY3 in maize (Lee et al., 2015), CRC1/PCH2 (Miao et al., 2013) and P31 in rice (Ji et al., 2016) pinpoints to the essential role of AE elements on the initiation of meiotic recombination.

FORMATION OF THE EARLY RECOMBINOSOME

During meiosis, two homologous DNA molecules can form new recombined ones using the general mechanics of the error-proof DNA damage repair pathways (Mercier et al., 2015; Wang and Copenhaver, 2018; Zelkowski et al., 2019). The initiation of meiotic recombination starts with the introduction of DNA DSBs. The DSBs are formed by the SPO11 complex composed of the catalytical A subunits, SPO11-1 (Grelon et al., 2001; Edlinger and Schlögelhofer, 2011; Da Ines et al., 2020) and SPO11-2 (Stacey et al., 2006;

Hartung et al., 2007b; Benyahya et al., 2020), associated with two B subunits, called MTOPVIB of the class II topoisomerase type VI (Fu et al., 2016; Vrielynck et al., 2016; Xue et al., 2016). The Arabidopsis *spo11-1* mutant has an interesting distinctive 23 and 24 nt sRNA profile than wild type in male meiocytes. These SPO11-1-dependent sRNAs are mapped to bind coding sequences and some CO feature motifs, while some sRNAs can target some meiotic genes such as RAD51 or ASK1 (Huang et al., 2019). Whether or not these sRNAs are produced at or near the site of DSBs and represent a signaling mode for repairing the DSB requires further work.

Though every CO is derived from a DSB event, not all DSBs are repaired as COs, and a vast majority of DSBs result in NCOs (Mercier et al., 2015). In maize, the CML228 inbred line that has naturally less DSBs (evaluated by the RAD51 number) has a correlated decreased CO number compare to B73 and other inbreds, indicating that the level of CO homeostasis is limited (Sidhu et al., 2015). In Arabidopsis, hypomorphic *spo11-1* mutants that reduce the DSB number also diminish the CO number but interestingly also alter the pattern of CO toward the telomeres (Xue et al., 2018). These data suggest that, at least in these two model plant species, CO homeostasis is not observed or limited.

In maize, using superresolution microscopy, it was observed that only a subset of SPO11-1 foci, the one closely associated with the AEs, correspond to the number of DSBs formed in leptotene (Ku et al., 2020). This suggests that the topoisomerase II-like nuclease function of the SPO11-1 complex occurs only when it is associate with the AE (Ku et al., 2020). Whether or not this particular configuration allows the nuclease activity of only one of the two attached sister chromatids is not known. The SPO11-1 "early recombinosome" complex also contains various accessory proteins that might participate in the tethering between the chromatin loop and the axis where DSBs are formed. SPO11-1 and MTOPVIB can interact with PRD1 (Vrielynck et al., 2016; Tang et al., 2017). In addition, rice and maize MTOPVIB, rice PRD1, and Arabidopsis PRD2/MPS1 are required for the assembly of the meiotic bipolar spindle (Ji et al., 2016; Xue et al., 2019; Jing et al., 2020; Shi et al., 2021). It was long recognized in maize that the meiotic spindle can associate around chromatin independently of the formation of the bivalent (Chan and Cande, 1998; Nannas et al., 2016) suggesting that the multipolar spindle observed in the meiotic recombination mutants might be a consequence of the formation of univalents instead of bivalents. The rice PRD1 initially forms numerous foci during leptotene, progressively restricted to few foci colocalizing with centromeric CENH3 and other kinetochore proteins (MIS12, NDC80, and CENP-C) at pachytene (Shi et al., 2021). PRD1 can directly interact with REC8 and SGO1 (Shi et al., 2021) suggesting a mechanism for early coordination between DSB formation and meiotic spindle organization. Other SPO11-associated factors such as DFO1, PRD1, PRD2, and PRD3/PAIR1 have also been identified as essential for DSB formation (Nonomura et al., 2004b; De Muyt et al., 2007, 2009; Zhang et al., 2012) but their relationship, specific function, and potential interaction with the cohesin and AE proteins still need to be explored (Mercier et al., 2015; Kim and Choi, 2019). PHS1, discovered in maize (Pawlowski et al., 2004), is poorly conserved with the rec114 yeast DSB factor but has a divergent function in plants. It is involved in the nuclear localization of the RAD50 protein into the nucleus in maize and Arabidopsis (Ronceret et al., 2009). SKI8 is also not conserved between yeast and Arabidopsis (Jolivet et al., 2006). Interestingly, the PRD2/MPS1 can form different splicing isoforms depending on the methylation status of its intron 9, dependent on the RNA-directed DNA methylation pathway (Walker et al., 2018).

GENOMIC MAPPING OF DSBs AND RECOMBINATION MOTIFS

Several studies using ChIP or SPO11 oligonucleotide sequencing have now revealed the genomic pattern of DSBs in maize and Arabidopsis. As previously well-known, genomes contain hotspots of COs, that are now correlated with genomic hotspots regions more prone to form DSBs (He et al., 2017; Choi et al., 2018; Tock and Henderson, 2018). In these two diploid species, DSBs are associated with specific active chromosome features such as transcriptional start sites that are depleted of nucleosomes. In Arabidopsis, several motifs associated with recombination have been defined. The A-rich motif is preferentially associated with promoters, while the CCN repeat and the CTT repeat motifs are preferentially associated with genes (Shilo et al., 2015). The motifs correlating with COs are not necessarily identical to motifs correlating with sites of DSB. This suggests that several genomic contexts required for the different steps of recombination progressively shape the choice of chromosomal exchange sites. The presence of a similar but not identical 20-bp-long GC-rich degenerate DNA sequence motif was correlated with DSB formation in maize and Arabidopsis (He et al., 2017; Choi et al., 2018). Interestingly, while DSBs are also formed in regions that will not form CO such as centromeric regions and repetitive DNA (especially RNA transposons), it was found that only DSBs formed in genic regions will form CO in maize (He et al., 2017). In Arabidopsis, mutants affecting the methylation of H3K9me2 and DNA CG and non-CG in the transposon-rich pericentromeric heterochromatin also increase the formation of DSB near centromeres (Underwood et al., 2018; Fernandes et al., 2019). In maize, the *mop1* mutation (homolog of RDR2) that removes CHH methylation adjacent to hotspots also affects the recombination landscape, increasing it in the chromosome arm but decreasing it in pericentromeric regions (Zhao et al., 2021). These data indicate that though the molecular bases are distinct in species of different genome sizes, and with relative repetitive element contents, a strong effect of epigenetic and chromatin state controls the fate of the early meiotic recombinosome.

SIGNALING AND PROCESSING OF THE DSBs

The programmed DSBs are identified by the signaling pathway of DNA damages *via* the ATM and ATR kinases (Kim and Choi, 2019; Zhang et al., 2020a). In budding yeast, ATM/ATR can phosphorylate REC8 and other chromosome

axis proteins and, therefore, modulate CO homeostasis (Kim and Choi, 2019). It is not clear, however, if this is also the case in plants. The meiocyte nuclei use prepared recombination machinery to repair the numerous endogenous DSBs using a preferential homologous recombination pathway. The somatically preferred non-homologous end joining (NHEJ) is suppressed by the exonuclease (RAD9-RAD1-HUS1) 9-1-1 complex system (Che et al., 2014; Hu et al., 2016). This 9-1-1 complex itself is possibly recruited by the DNA damage sensor RAD17 (Hu et al., 2018). This inhibition is essential to avoid inaccurate interactions between non-homologous chromosomes during meiosis (Che et al., 2014). The DSBs are rapidly associated with the phosphorylation of histone H2AX and processed by endonuclease and exonucleases activities of the MRN complex composed of MRE11, RAD50, NBS1, and COM1 (Bleuyard et al., 2004; Puizina et al., 2004; Uanschou et al., 2007; Waterworth et al., 2007; Lohmiller et al., 2008; Šamanić et al., 2013; Wang Y. et al., 2018) creating 5′ overhang sequences. These sequences are recognized by specialized single DNA strand affine replication protein A (RPA) types such as RPA1a in Arabidopsis (Osman et al., 2009) or RPA1C and RPA2C in rice (Li et al., 2013). RPAs are generally involved in telomere-length maintenance (Aklilu et al., 2020) suggesting a functionalization of this single DNA strand capping for the processing of meiotic DSBs.

SINGLE-END INVASIONS AND PAIRING

These single ends can invade homologous sequences (process called single-end invasion or SEI) thanks to the recombinase activities of RAD51 and DMC1 (Couteau et al., 1999; Li et al., 2004). These recombinases have the properties to form a strong homology-based DNA triple helix called a displacement loop (D-loop) (Kurzbauer et al., 2012; Wang et al., 2016; Singh et al., 2017; Colas et al., 2019; Draeger et al., 2020). The RAD51 and DMC1 are part of the same recombinase protein family also containing RAD51C and XRCC3 that derive from the same ancestor but have undergone subfunctionalization (Bleuyard et al., 2004; Da Ines et al., 2013; Pradillo et al., 2014). RAD51C and XRCC3 facilitate the RAD51 chromosome localization (Su et al., 2017; Jing et al., 2019; Zhang et al., 2020c). RAD51 and DMC1 also associate with other proteins modulating their activities such as BRCA2 (Siaud et al., 2004; Dray et al., 2006; Seeliger et al., 2012; Fu et al., 2020), FIGL1 and FLIP (Zhang P. et al., 2017; Fernandes et al., 2018a; Kumar et al., 2019), or MND1, and HOP2 (Vignard et al., 2007; Uanschou et al., 2013; Aklilu et al., 2020). Rice MND1/MSF1 can interact with RPA2b and HOP2 (Lu et al., 2020), while OsHOP2 can directly interact with the SC central element ZEP1/ZYP1 suggesting a second mechanism for the link observed between early recombination and synapsis (Shi et al., 2019) at the SEI step. The excess number of SEI creating several interconnections between homologous chromosomes (also called interhomolog joint molecules) were proposed to be involved in the pairing process (Pawlowski et al., 2003). Pairing allows the recognition between accurate homologs before its stabilization by the polymerization and lateral extension of the SC during zygotene.

ANTICROSSOVER PATHWAYS

The number of DSB and SEI is far greater than the number of COs and the vast majority of DSBs [around 85% in Arabidopsis (Higgins et al., 2004) and 97.7% in durum wheat (Desjardins et al., 2020)] are resolved as NCOs. NCOs are formed when the SEI occurs on the sister chromatid but also when a D-loop formed on the homologous chromosome is resolved in a configuration that only involves the exchange of genetic material in a short sequence called conversion tracts (Mercier et al., 2015; Wang and Copenhaver, 2018). Three parallel anti-CO pathways have been discovered using suppressor genetic screens of *zmm* meiotic recombination mutants in Arabidopsis (Séguéla-Arnaud et al., 2015).

The first NCO pathway involves the SGS1/BLM helicases homologs RECQ4A and RECQB (Hartung et al., 2007a; Higgins et al., 2011) and the topoisomerases TOP3α (Hartung et al., 2008) associated with BLAP75/RMI (Chelysheva et al., 2008), which unwinds D-loops leading to a sixfold CO number increase in Arabidopsis (Séguéla-Arnaud et al., 2015). In rice, the MEICA protein that interacts with TOP3a also has an anticrossover activity (Hu et al., 2017).

The anti-CO pathway that involves the FANCM helicase possibly displaces the invading strand through the synthesis-dependent strand annealing (SDSA) process (Crismani et al., 2012). SDSA can form NCOs by annealing the SEI with the other end of the DSB, repairing the DSB using the original DNA molecules. FANCM has two binding cofactors MHF1 and MHF2 that also limit the number of COs formed *via* the type II non-interfering pathway (Dangel et al., 2014; Girard et al., 2014). Interestingly, the anti-CO effect due to FANCM is more pronounced in inbred than in hybrids backgrounds (Girard et al., 2015). The FANCM pathway also affects COs in a *Brassica rapa* pure line (Blary et al., 2018). In lettuce, the *fancm* mutant shows a univalent phenotype not observed in other species (Li et al., 2021) indicating possible divergence in the regulation of this pathway or different consequences between species of different genome sizes.

Another cumulative NCO pathway involves the FIDGETIN AAA-ATPase FIGL1 (Girard et al., 2015; Zhang P. et al., 2017) and its partner FLIP (Fernandes et al., 2018a). FIGL1 directly interacts with RAD51 and DMC1 and is proposed to limit SEI and CO number (Fernandes et al., 2018a). Using the mutants of these different pathways or combining them together or with elevated expression of the procrossover factors HEI10 (Serra et al., 2018) are particularly interesting for agronomy since it allows to unleash the number of CO by several folds in various plant species and potentially speed up new breeding strategies (Fernandes et al., 2018b; Mieulet et al., 2018). Interestingly, these CO increase do not cause problems in chromosome segregation. The relative role of these different pathways in male vs. female plant meiosis requires further analysis.

SYNAPSIS AND ROLE OF THE SC IN THE REGULATION OF RECOMBINATION

The central element ZYP1 of the SC starts polymerizing during zygotene to form a protein complex resembling a zipper structure connecting the two meiotic homologous chromosomes from telomere to telomere at pachytene. The two AEs are called lateral elements once they form this tripartite structure (Higgins et al., 2005; West et al., 2019; Darrier et al., 2020; Kurzbauer et al., 2021). Although two redundant ZYP1 proteins sharing 87% identity are present in Arabidopsis; their relative role is still unknown. The SC can regulate the number and spacing of CO. While barley *zyp1* mutants show limited CO numbers (Barakate et al., 2014), the homolog rice *zep1* mutants have the opposite effect (Wang et al., 2010). The SC components have diverged rapidly among eukaryotes but the general SC structure is conserved (West et al., 2019). These results might reflect divergent modes of regulation of the SC on CO between different species. ZYP1 was also recently reported as required for CO interference and the obligate CO (France et al., 2021). In Arabidopsis *zyp1a/b* null mutant, heterochiasmy is abolished (Capilla-Pérez et al., 2021). These recent data suggest that the SC coordinates the regulation of obligate CO, interference, and heterochiasmy. Arabidopsis *asy1* mutants also abolish CO interference (Lambing et al., 2020a). ASY1 acts as an antagonist of telomere-led recombination in a gene dosage-sensitive manner (Lambing et al., 2020a). The ASY1 immunolocalization signal disappears concomitantly with the loading of the central element ZYP1 (Lee et al., 2015). This suggests that obligate CO, heterochiasmy, and interference mechanisms are not directly mediated by either ASY1 or ZYP1 but rather involve the regulation of the SC length. ASY1 can be phosphorylated by CDKA;1 counteracting the ASY1 disassembly activity of PCH2 and P31 (Yang et al., 2020), which suggests a dynamic control of SC length regulation. The phosphorylation of the ASY1 protein increases its binding affinity with the chromatin-anchoring ASY3/DSY2 protein (Yang et al., 2020). ATM is another meiotic protein kinase essential to limit DSB number; it regulates chromatin loop size and affects SC length and width (Kurzbauer et al., 2021). The relative role of ATM and CDKA1;1 in the phosphorylation of SC components or other meiotic proteins is still unknown.

FORMATION OF THE LATE RECOMBINOSOME AND CROSSOVER PATHWAYS

The DNA repair of the damaged molecules involves the formation of double Holliday junctions (dHJs) that are resolved by resolvases leading to CO or NCO. Two pathways of CO formation have been described in plants.

The interfering pathway (CO type I) positions CO with non-random spacing between each CO event. In general, the CO type I accounts for the majority (80–95%) of all COs in plant species (Mercier et al., 2015). It involves the ZMM pathway, namely, MER3 (Chen et al., 2005; Mercier et al., 2005), ZIP4 (Chelysheva et al., 2007), the DNA mismatch repair mutS/mutL homologs MSH/MLH (MSH4, MSH5, MSH7, MLH1, and MLH3) (Higgins et al., 2004, 2008b; Chelysheva et al., 2010; Colas et al., 2016) and HEI10 (Chelysheva et al., 2012; Ziolkowski et al., 2017). In rice, a new member of the ZMM pathway was discovered through its interaction with HEI10, MSH4, and ZIP4 and named HEI1P1 (Li et al., 2018). SHOC1 and PTD, which were described in Arabidopsis as involved in the type I CO pathway (Macaisne et al., 2008, 2011), are conserved and play similar roles in rice (Ren et al., 2019). Interestingly, it was found that the obligate COs (that ensure the correct chromosome segregation during anaphase I) are maintained by MSH4 and MSH5 in durum wheat (Desjardins et al., 2020). In the allotetraploid *Brassica napus*, reducing the MSH4 copy number prevents non-homologous CO (Gonzalo et al., 2019). The analysis of hypomorph mutants of two essential B-class DNA polymerases (the delta POLD1 supposed to be involved in DNA lagging strand synthesis and the Epsilon POL2A thought to be involved in DNA leading strand synthesis) has shown that they are also involved in the formation of type I COs (Huang et al., 2015; Wang C. et al., 2018). It was first hypothesized that elongation activity of these polymerases is required for the process of meiotic recombination but the multifunctionality of these POL proteins, containing exonuclease proofreading domains (Ronceret et al., 2005), could complicate the interpretation of the activity required during meiotic recombination. In addition, DNA polymerases are involved in the deposition of the H3K4me3 transcriptionally active epigenetic marks linked to DSB formation and participate in DNA repair (Yin et al., 2009; Iglesias et al., 2015) suggesting other possibilities for the role of DNA POL in the formation of type I COs. However, since most of the *pol* mutants have embryo-lethality phenotypes (Ronceret et al., 2005; Wang et al., 2019) this is a difficult topic to study.

The second minor CO pathway (type II or non-interfering) can form closely spaced COs. In plants, it involves the dHJ resolvases (structure-specific endonuclease) MUS81 (Higgins et al., 2008a), GEN1 (Wang et al., 2017), and SEND1, which is also essential for telomere stability (Geuting et al., 2009; Olivier et al., 2015).

Though it was found to be involved in the mechanism of interference in yeast, the topoisomerase TOPII was not found to have an effect on CO interference in Arabidopsis but to facilitate interlocks resolution (remove interlacement of different bivalents at the time of synapsis) (Martinez-Garcia et al., 2018) that are normally all resolved by pachytene (Wang et al., 2009). Interestingly, TOPII is associated with the chromosome axis and accumulates in entangled regions during the zygotene stage (Martinez-Garcia et al., 2018). In Arabidopsis, a second non-interfering pathway of CO (called type III non-interfering CO in **Figure 1**), parallel to the MUS81 (type II) CO pathway, depends on FANCD2 and contributes to the formation of some non-interfering COs (Kurzbauer et al., 2018). The hotspots and coldspots of recombination are supposably due to the combined effects of chromatin features and the different anticrossover and crossover pathways. The relative mechanisms by which the CO rate is modulated at these sites still require further exploration.

EFFECTS OF GENOMIC REGIONS, CENTROMERE PAIRING, TELOMERE BOUQUET, AND REPEATED DNA RECOMBINATION

Various genomic regions are known to have variable recombination rates in various plant species. New whole genome sequencing techniques have now given us a clear vision of the recombination maps at a fine scale in several plant species (Hellsten et al., 2013; Luo et al., 2019; Rowan et al., 2019). It is known that the genomic recombination rate is influenced by epigenetic marks, the genetic background (Sidhu et al., 2015; Ziolkowski et al., 2017; Dreissig et al., 2019; Lawrence et al., 2019), and the level of heterozygosity (Ziolkowski et al., 2015). It also greatly depends on chromatin structural variation where large inversion and translocations can suppress recombination (Rowan et al., 2019; Termolino et al., 2019). The molecular basis of this suppression is still unclear but probably involves the abnormal SC installation on unpaired chromatin loop domains.

Chromosome conformation changes are highly dynamic during meiotic prophase, involving active mechanisms to gather telomeres at the nuclear envelope (called telomere bouquet), centromere coupling, and chromosome pairing and synapsis (Sepsi and Schwarzacher, 2020; Lenykó-Thegze et al., 2021).

In maize and rice, the SUN proteins are involved in telomere bouquet formation (Murphy et al., 2014), synapsis, and CO formation (Zhang et al., 2020b). SUN1 and SUN2 Arabidopsis mutants delay the progression of meiosis, affect synapsis, and reduce the chiasma number (Varas et al., 2015). The role of AtSUN1 and AtSUN2 on the bouquet has not yet been analyzed since the Arabidopsis telomere bouquet was only recently defined using techniques that maintain the 3D structure of the nucleus intact (Hurel et al., 2018). In rice, the bouquet is dependent on the PAIR3/ASY3 AE element (Wang et al., 2011) and on the F-Box ZYGO protein that also affects the initiation of homologous pairing (Zhang F. et al., 2017). In maize, SPO11-1 foci are transiently observed on the nuclear periphery and seem excluded from the nucleolus (Ku et al., 2020) suggesting a potential gathering of the DSBs machinery at the nuclear envelope and that its chromatin localization is not homogenous on the genome. Interestingly in Arabidopsis, the repetitive nucleolus organizing regions (NORs) acquired distinct chromatin characteristics during meiosis with strong ASY1 signals and the absence of the synaptic ZYP1 protein. The nucleolus employs an NHEJ mechanism requiring LIG4 (instead of the homologous recombination pathway dependent on RAD51) to repair the few DSBs produced in NORs and avoid unequal recombination in the repetitive recombinant DNA clusters (Sims et al., 2019). The presence of fewer COs in the heterochromatic repetitive knob region was observed cytogenetically in maize male meiocytes (Stack et al., 2017). However, by contrast to the nucleolus, knob meiotic recombination still uses the homologous recombination pathway as observed by the presence of MLH1 foci. This indicates that the diminution of meiotic recombination in distinctive heterochromatin regions probably uses several distinct mechanisms.

EFFECTS OF AGE AND SEX ON MEIOTIC RECOMBINATION

A moderate effect of the age of the shoot apical meristem on the number of CO was reported in Arabidopsis (Francis et al., 2007; Toyota et al., 2011; Li et al., 2017; Saini et al., 2020). Whether or not these age effects also occur in other plants is still unknown.

Sex difference in CO frequency is called heterochiasmy. In Arabidopsis, the CO number is higher in male meiocytes than in female meiocytes (Drouaud et al., 2007; Giraut et al., 2011; Saini et al., 2020). By sequencing Arabidopsis male and female backcrossed plants, 4.58 crossovers were found in male backcrossed compared to 3.08 in female backcrosses (Capilla-Pérez et al., 2021), noting that only half of the true CO number can be identified since gametes inherit a single chromatid and CO involves only two of the four chromatids of a bivalent. In Arabidopsis and maize, the difference is attributed to the length of the SC and the distribution of CO is also different in male and female meiocytes (Giraut et al., 2011; Kianian et al., 2018; Lloyd and Jenczewski, 2019; Luo et al., 2019). It was recently demonstrated that heterochiasmy is enforced in Arabidopsis by the SC central element ZYP1 (Capilla-Pérez et al., 2021). This suggests that heterochiasmy and SC length differences in male and female meiocytes are regulated by a common molecular pathway.

EFFECT OF ENVIRONMENTAL CONDITIONS ON MEIOSIS

In plants, meiosis occurs in flowers whose development was initiated *via* various past and present environmental clues (Antoniou-Kourounioti et al., 2021). The temperature variation is also known to modify the meiotic and somatic recombination rate using fluorescent-tagged lines (Francis et al., 2007; Li et al., 2017; Saini et al., 2017) correlated with cytological MLH1 foci counting (Lloyd et al., 2018). In Arabidopsis, both high (28°C) and low (8°C) temperature conditions increase meiotic recombination compared to medium temperature (18°C). Interestingly, external temperatures are negatively correlated with the SC length that is itself correlated with the CO number. A correlation between SC length and CO number per chromosome was found (von Wettstein et al., 1984). Consequently, the longer SC length observed at low temperatures can explain the higher number of CO but not the increase of CO number observed at the higher temperatures. This increase in CO due to high temperature is not due to an increase in DSB formation as observed with γH2A.X and RAD51 foci. These extra COs are class I (ZMM) pathway as evidenced by increased MLH1 and HEI10 focus numbers in male meiocytes (Blary et al., 2018). Using mutants of different CO pathways in Arabidopsis, it was confirmed that the extra COs are derived from the interfering type I CO pathways and not to the type II (Modliszewski et al., 2018; De Storme and Geelen, 2020). The response of CO number to external temperature is not a universal stress response since saline stress does not affect it. Though the effect of temperature on COs was also observed and analyzed

in barley, it seems that the mechanism of action is distinct. In contrast to Arabidopsis, the SC length in barley male meiocytes increases with higher temperature. The number of CO type I is not altered but their position shifted toward more internal non-telomeric regions as observed with cytologically mapped MLH3 foci (Phillips et al., 2015). The same effect of the position shifting from distal to more internal CO is also observed for some chromosome arms in wheat (Coulton et al., 2020). Though it seems an attractive and easy parameter that could modulate CO in crops, it appears that extremal temperatures have also other deleterious effects on the progression of meiosis such as defects of secondary division and wall formation reducing euploidy and seed set (De Storme et al., 2012; Draeger and Moore, 2017; De Storme and Geelen, 2020).

The presence of the histone H2A.Z was determined as the marker of the thermosensory response in Arabidopsis, with H2A.Z deposition decreasing with increasing temperatures (Kumar and Wigge, 2010). In addition, the CO sites overlap with the presence of H2A.Z nucleosome at gene promoters (Choi et al., 2013). Arabidopsis mutants of the H2A.Z placement show lower CO frequency. The correlation between H2A.Z and CO frequencies could explain the part of the effect of lower temperatures increasing CO frequency but not the effects of higher temperatures. Indeed, the higher CO frequency of Arabidopsis plants grown at 12°C compared to plants grown at 21°C disappears in mutants defective for H2A.Z deposition (Kumar and Wigge, 2010). The relation between the deposition of H2A.Z and the phosphorylation of γH2AX associated with the formation of DSB is currently unknown.

Another key factor of this regulation of the meiotic recombination by temperature is the cyclin-dependent kinase CDKG1. Arabidopsis *cdkg1* mutants show temperature-sensitive meiotic defect at 23°C but not at 12°C with abnormally formed SC, lower CO frequency, and reduce the bivalent number (Zheng et al., 2014; Nibau et al., 2020b). There are temperature-dependent isoforms of CDKG1 (Nibau et al., 2020a). These isoforms can interact with the spliceosome and can regulate the splicing of other spliceosome components and the Callose synthase5 forming the pollen wall (Huang et al., 2013; Cavallari et al., 2018). It is still not known that whether or not the CDKG1-dependent temperature-sensitive regulation affects the production of different splicing variants of meiotic genes or affects H2A.Z deposition.

Another meiotic cyclin CDKA;1 has an important role in the regulation of the recombination landscape (Wijnker et al., 2019). CDKA;1 is also involved earlier in the germline fate decision *via* the inactivation of RBR1 (Chen et al., 2011; Zhao et al., 2017) pointing out the coordinating role of a peculiar meiotic CDK as a key factor for the meiotic fate and the regulation of meiotic recombination. What are the relative roles of the meiotic CDKs, the associated meiotic cyclins (such as SDS and TAM), and CDK inhibitors (KRPs) in the coordinated control of meiotic recombination in different temperature conditions remain to be analyzed.

Other factors such as climate, agrochemicals, heavy metals, combustible gasses, pharmaceuticals, and pathogens are known to modify meiosis in plants (Modliszewski and Copenhaver, 2017; Fuchs et al., 2018; Dreissig et al., 2019) but their mechanistic modes of action still need to be explored.

CONCLUSION

The understanding of several fundamental meiotic processes has strongly advanced during the past few years thanks to many studies in model and non-model plant species. **Figure 1** summarizes the different proteins and functional modules known to be involved in the formation of bivalents.

The new techniques of isolated cell high throughput sequencing will revolutionize the questions we can ask about the dynamic meiotic chromosome conformation through prophase I.

Though controversial for many years, the divergence of several basic molecular meiotic mechanisms is now clear between different plant species. Achiasmatic inverted meiosis has also been reported in few non-model plants (Cabral et al., 2014; Heckmann et al., 2014; Hofstatter et al., 2021) underlining the extreme diversity of the plant meiotic programs. It contradicts the predictive expected assumptions based on phylogenetic relationships between plant species. In this perspective, one of the future challenges will be to identify the actual biochemical functions of the meiotic proteins not only based on the putative function supposed by the homology of conserved protein families. These interspecific differences are probably the real essence of the meiotic process that has evolved to bring genomic diversity. Even in the same species, there are known sex and cell to cell variability (Wang et al., 2019). It underlines the importance of studying directly meiosis in crops to manipulate it properly. Increasing our meiotic manipulation tools for improving plant breeding strategies is essential to cope with the challenge of feeding 10 billon humans by 2050.

AUTHOR CONTRIBUTIONS

YGP and AR prepared and wrote the manuscript. JKGK and PR contributed to the survey of bibliographic references. All authors read and approved the final manuscript.

FUNDING

Relevant research in the Ronceret lab was supported by a grant from the Mexican SEP-CONACYT Ciencia Básica CB-2017-2018-A1-S-8496 to AR.

ACKNOWLEDGMENTS

We would like to thank Mathilde Grelon (INRAE, Versailles, France) and Wojtek Pawlowski (Cornell University, United States) for the critical reading of the manuscript. We would also like to thank the constructive suggestions of the three reviewers. We would like to apologize for the colleagues that have not been cited due to limitations of manuscript length.

REFERENCES

Aklilu, B. B., Peurois, F., Saintomé, C., Culligan, K. M., Kobbe, D., Leasure, C., et al. (2020). Functional diversification of replication protein a paralogs and telomere length maintenance in *Arabidopsis*. *Genetics* 215, 989–1002. doi: 10.1534/genetics.120.303222

Antoniou-Kourounioti, R. L., Zhao, Y., Dean, C., and Howard, M. (2021). Feeling every bit of winter – distributed temperature sensitivity in vernalization. *Front. Plant Sci.* 12:628726. doi: 10.3389/fpls.2021.628726

Armstrong, S. J., Caryl, A. P., Jones, G. H., and Franklin, F. C. (2002). Asy1, a protein required for meiotic chromosome synapsis, localizes to axis-associated chromatin in *Arabidopsis* and *Brassica*. *J. Cell Sci.* 115, 3645–3655. doi: 10.1242/jcs.00048

Balboni, M., Yang, C., Komaki, S., Brun, J., and Schnittger, A. (2020). COMET functions as a PCH2 Cofactor in regulating the HORMA domain Protein ASY1. *Curr. Biol.* 30, 4113–4127. doi: 10.1016/j.cub.2020.07.089

Barakate, A., Higgins, J. D., Vivera, S., Stephens, J., Perry, R. M., Ramsay, L., et al. (2014). The synaptonemal complex protein ZYP1 is required for imposition of meiotic crossovers in barley. *Plant Cell.* 26, 729–740. doi: 10.1105/tpc.113.121269

Barakate, A., Orr, J., Schreiber, M., Colas, I., Lewandowska, D., McCallum, N., et al. (2021). Barley anther and meiocyte transcriptome dynamics in meiotic prophase I. *Front. Plant Sci.* 11:619404. doi: 10.3389/fpls.2020.619404

Benyahya, F., Nadaud, I., Da Ines, O., Rimbert, H., White, C., and Sourdille, P. (2020). SPO11.2 is essential for programmed double-strand break formation during meiosis in bread wheat (*Triticum aestivum* L.). *Plant J.* 104, 30–43. doi: 10.1111/tpj.14903

Biedermann, S., Harashima, H., Chen, P., Heese, M., Bouyer, D., Sofroni, K., et al. (2017). The retinoblastoma homolog RBR1 mediates localization of the repair protein RAD51 to DNA lesions in *Arabidopsis*. *EMBO J.* 36, 1279–1297. doi: 10.15252/embj.201694571

Blary, A., Gonzalo, A., Eber, F., Bérard, A., Bergès, H., Bessoltane, N., et al. (2018). FANCM limits meiotic crossovers in *Brassica* Crops. *Front. Plant Sci.* 9:368. doi: 10.3389/fpls.2018.00368

Blary, A., and Jenczewski, E. (2019). Manipulation of crossover frequency and distribution for plant breeding. *Theor. Appl. Genet.* 132, 575–592. doi: 10.1007/s00122-018-3240-1

Bleuyard, J. Y., Gallego, M. E., and White, C. I. (2004). Meiotic defects in the *Arabidopsis* rad50 mutant point to conservation of the MRX complex function in early stages of meiotic recombination. *Chromosoma* 113, 197–203. doi: 10.1007/s00412-004-0309-1

Bolaños-Villegas, P., and Argüello-Miranda, O. (2019). Meiosis research in orphan and non-orphan tropical crops. *Front. Plant Sci.* 10:74. doi: 10.3389/fpls.2019.00074

Cabral, G., Marques, A., Schubert, V., Pedrosa-Harand, A., and Schlogelhofer, P. (2014). Chiasmatic and achiasmatic inverted meiosis of plants with holocentric chromosomes. *Nat. Commun.* 5:5070. doi: 10.1038/ncomms6070

Cai, X., Dong, F., Edelmann, R. E., and Makaroff, C. A. (2003). The *Arabidopsis* SYN1 cohesin protein is required for sister chromatid arm cohesion and homologous chromosome pairing. *J. Cell Sci.* 116, 2999–3007. doi: 10.1242/jcs.00601

Capilla-Pérez, L., Durand, S., Hurel, A., Lian, Q., Chambon, A., Taochy, C., et al. (2021). The synaptonemal complex imposes crossover interference and heterochiasmy in *Arabidopsis*. *Proc. Natl. Acad. Sci. U.S.A.* 118, e2023613118. doi: 10.1073/pnas.2023613118

Cavallari, N., Nibau, C., Fuchs, A., Dadarou, D., Barta, A., and Doonan, J. H. (2018). The cyclin-dependent kinase G group defines a thermosensitive alternative splicing circuit modulating the expression of Arabidopsis ATU2AF65A. *Plant J.* 94, 1010–1022. doi: 10.1111/tpj.13914

Chambon, A., West, A., Vezon, D., Horlow, C., De Muyt, A., Chelysheva, L., et al. (2018). Identification of ASYNAPTIC4, a component of the meiotic chromosome axis. *Plant Physiol.* 178, 233–246. doi: 10.1104/pp.17.01725

Chan, A., and Cande, W. Z. (1998). Maize meiotic spindles assemble around chromatin and do not require paired chromosomes. *J. Cell Sci.* 111, 3507–3515. doi: 10.1242/jcs.111.23.3507

Che, L., Tang, D., Wang, K., Wang, M., Zhu, K., Yu, H., et al. (2011). OsAM1 is required for leptotene-zygotene transition in rice. *Cell Res.* 21, 654–665. doi: 10.1038/cr.2011.7

Che, L., Wang, K., Tang, D., Liu, Q., Chen, X., Li, Y., et al. (2014). OsHUS1 Facilitates Accurate Meiotic Recombination in Rice. *PLoS Genetics.* 10:e1004405. doi: 10.1371/journal.pgen.1004405

Chelysheva, L., Diallo, S., Vezon, D., Gendrot, G., Vrielynck, N., Belcram, K., et al. (2005). AtREC8 and AtSCC3 are essential to the monopolar orientation of the kinetochores during meiosis. *J. Cell Sci.* 118, 4621–4632. doi: 10.1242/jcs.02583

Chelysheva, L., Grandont, L., Vrielynck, N., le Guin, S., Mercier, R., and Grelon, M. (2010). An easy protocol for studying chromatin and recombination protein dynamics during Arabidopsis thaliana meiosis: immunodetection of cohesins, histones and MLH1. *Cytogenet. Genome Res.* 129, 143–153. doi: 10.1159/000314096

Chelysheva, L., Vezon, D., Belcram, K., Gendrot, G., and Grelon, M. (2008). The *Arabidopsis* BLAP75/Rmi homologue plays crucial roles in meiotic double-strand break repair. *PLoS Genet.* 4:e1000309. doi: 10.1371/journal.pgen.1000309

Chelysheva, L., Vezon, D., Chambon, A., Gendrot, G., Pereira, L., Lemhemdi, A., et al. (2012). The *Arabidopsis* HEI10 is a new ZMM protein related to Zip3. *PLoS Genet.* 8:e1002799. doi: 10.1371/journal.pgen.1002799

Chelysheva, L. A., Gendrot, G., Vezon, D., Doutriaux, M. P., Mercier, R., and Grelon, M. (2007). Zip4/Spo22 is required for class I CO formation but not for synapsis completion in *Arabidopsis thaliana*. *PLoS Genet.* 3:e83. doi: 10.1371/journal.pgen.0030083

Chen, Z., Higgins, J. D., Hui, J. T. L., Li, J., Franklin, F. C. H., and Berger, F. (2011). Retinoblastoma protein is essential for early meiotic events in *Arabidopsis*. *EMBO J.* 30, 744–755. doi: 10.1038/emboj.2010.344

Chen, Z., Zhangh, W., Timofejeva, L., Gerardin, Y., and Ma, H. (2005). The *Arabidopsis* ROCK-N-ROLLERS gene encodes a homolog of the yeast ATP-dependent DNA helicase MER3 and is required for normal meiotic crossover formation. *Plant J.* 43, 321–334. doi: 10.1111/j.1365-313x.2005.02461.x

Choi, K., Zhao, X., Kelly, K. A., Venn, O., Higgins, J. D., Yelina, N. E., et al. (2013). *Arabidopsis* meiotic crossover hot spots overlap with H2A.Z nucleosomes at gene promoters. *Nat. Genet.* 45, 1327–1336.

Choi, K., Zhao, X., Tock, A. J., Lambing, C., Underwood, C. J., Hardcastle, T. J., et al. (2018). Nucleosomes and DNA methylation shape meiotic DSB frequency in Arabidopsis thaliana transposons and gene regulatory regions. *Genome Res.* 28, 532–546. doi: 10.1101/gr.225599.117

Cifuentes, M., Eber, F., Lucas, M.-O., Lode, M., Chèvre, A.-M., and Jenczewski, E. (2010). Repeated polyploidy drove different levels of crossover suppression between homoeologous chromosomes in Brassica napus allohaploids. *Plant Cell* 22, 2265–2276.

Colas, I., Barakate, A., Macaulay, M., Schreiber, M., Stephens, J., Vivera, S., et al. (2019). desynaptic5 carries a spontaneous semi-dominant mutation affecting Disrupted Meiotic cDNA 1 in barley. *J. Exp. Bot.* 70, 2683–2698. doi: 10.1093/jxb/erz080

Colas, I., Macaulay, M., Higgins, J. D., Phillips, D., Barakate, A., Posch, M., et al. (2016). A spontaneous mutation in MutL-Homolog 3 (HvMLH3) affects synapsis and crossover resolution in the barley desynaptic mutant *des10*. *New Phytol.* 212, 693–707. doi: 10.1111/nph.14061

Coulton, A., Burridge, A. J., and Edwards, K. J. (2020). Examining the effects of temperature on recombination in wheat. *Front. Plant Sci.* 11:230. doi: 10.3389/fpls.2020.00230

Couteau, F., Belzile, F., Horlow, C., Grandjean, O., Vezon, D., and Doutriaux, M. P. (1999). Random chromosome segregation without meiotic arrest in both male and female meiocytes of a dmc1 mutant of *Arabidopsis*. *Plant Cell* 11, 1623–1634. doi: 10.1105/tpc.11.9.1623

Crismani, W., Girard, C., Froger, N., Pradillo, M., Santos, J. L., Chelysheva, L., et al. (2012). FANCM limits meiotic crossovers. *Science* 336, 1588–1590. doi: 10.1126/science.1220381

Cromer, L., Jolivet, S., Singh, D. K., Berthier, F., De Winne, N., De Jaeger, G., et al. (2019). Patronus is the elusive plant securin, preventing chromosome separation by antagonizing separase. *Proc. Natl. Acad. Sci. U.S.A.* 116, 16018–16027. doi: 10.1073/pnas.1906237116

Da Ines, O., Degroote, F., Goubely, C., Amiard, S., Gallego, M. E., and White, C. I. (2013). Meiotic recombination in *Arabidopsis* is catalysed by DMC1, with RAD51 playing a supporting role. *PLoS Genet.* 9:e1003787. doi: 10.1371/journal.pgen.1003787

Da Ines, O., Michard, R., Fayos, I., Bastianelli, G., Nicolas, A., Guiderdoni, E., et al. (2020). Bread wheat TaSPO11-1 exhibits evolutionarily conserved function in meiotic recombination across distant plant species. *Plant J.* 103, 2052–2068. doi: 10.1111/tpj.14882

Dangel, N. J., Knoll, A., and Puchta, H. (2014). MHF1 plays Fanconi anaemia complementation group M protein (FANCM)-dependent and FANCM-independent roles in DNA repair and homologous recombination in plants. *Plant J.* 78, 822–833. doi: 10.1111/tpj.12507

Darrier, B., Arrieta, M., Mittmann, S. U., Sourdille, P., Ramsay, L., Waugh, R., et al. (2020). "Following the formation of synaptonemal complex formation in wheat and barley by high-resolution microscopy," in *Plant Meiosis: Methods and Protocols*, eds M. Pradillo and S. Heckmann (New York, NY: Springer New York), 207–215. doi: 10.1007/978-1-4939-9818-0_15

De, K., Sterle, L., Krueger, L., Yang, X., and Makaroff, C. A. (2014). *Arabidopsis thaliana* WAPL Is essential for the prophase removal of cohesin during meiosis. *PLoS Genet.* 10:e1004497. doi: 10.1371/journal.pgen.1004497

De Muyt, A., Pereira, L., Vezon, D., Chelysheva, L., Gendrot, G., Chambon, A., et al. (2009). A high throughput genetic screen identifies new early meiotic recombination functions in *Arabidopsis thaliana*. *PLoS Genet.* 5:e1000654. doi: 10.1371/journal.pgen.1000654

De Muyt, A., Vezon, D., Gendrot, G., Gallois, J. L., Stevens, R., and Grelon, M. (2007). AtPRD1 is required for meiotic double strand break formation in *Arabidopsis thaliana*. *EMBO J.* 26, 4126–4137. doi: 10.1038/sj.emboj.7601815

De Storme, N., Copenhaver, G. P., and Geelen, D. (2012). Production of diploid male gametes in *Arabidopsis* by cold-induced destabilization of postmeiotic radial microtubule arrays. *Plant Physiol.* 160, 1808–1826. doi: 10.1104/pp.112.208611

De Storme, N., and Geelen, D. (2020). High temperatures alter cross-over distribution and induce male meiotic restitution in *Arabidopsis thaliana*. *Commun. Biol.* 3, 187–187.

Desjardins, S. D., Ogle, D. E., Ayoub, M. A., Heckmann, S., Henderson, I. R., Edwards, K. J., et al. (2020). MutS homologue 4 and MutS homologue 5 maintain the obligate crossover in wheat despite stepwise gene loss following polyploidization. *Plant Physiol.* 183, 1545–1558. doi: 10.1104/pp.20.00534

Draeger, T., Martin, C. A., Alabdullah, A. K., Pendle, A., Rey, M.-D., Shaw, P., et al. (2020). Dmc1 is a candidate for temperature tolerance during wheat meiosis. *Theor. Appl. Genet.* 133, 809–828. doi: 10.1007/s00122-019-03508-9

Draeger, T., and Moore, G. (2017). Short periods of high temperature during meiosis prevent normal meiotic progression and reduce grain number in hexaploid wheat (*Triticum aestivum* L.). *Theor. Appl. Genet.* 130, 1785–1800. doi: 10.1007/s00122-017-2925-1

Dray, E., Siaud, N., Dubois, E., and Doutriaux, M. P. (2006). Interaction between *Arabidopsis* Brca2 and its partners Rad51, Dmc1, and Dss1. *Plant Physiol.* 140, 1059–1069. doi: 10.1104/pp.105.075838

Dreissig, S., Mascher, M., and Heckmann, S. (2019). Variation in recombination rate is shaped by domestication and environmental conditions in barley. *Mol. Biol. Evol.* 36, 2029–2039. doi: 10.1093/molbev/msz141

Drouaud, J., Mercier, R., Chelycheva, L., Bérard, A., Falque, A., Martin, O., et al. (2007). Sex-specific crossover distributions and variations in interference level along *Arabidopsis thaliana* chromosome 4. *PLoS Genet.* 3:e106. doi: 10.1371/journal.pgen.0030106

Dukowic-Schulze, S., Garcia, N., Shunmugam, A. S. K., Kagale, S., and Chen, C. (2020). "Isolating male meiocytes from maize and wheat for "-Omics" analyses," in *Plant Meiosis: Methods and Protocols*, eds M. Pradillo and S. Heckmann (New York, NY: Springer New York), 237–258. doi: 10.1007/978-1-4939-9818-0_17

Dukowic-Schulze, S., Sundararajan, A., Ramaraj, T., Kianian, S., Pawlowski, W. P., Mudge, J., et al. (2016). Novel meiotic miRNAs and indications for a role of PhasiRNAs in meiosis. *Front. Plant Sci.* 7:762. doi: 10.3389/fpls.2016.00762

Edlinger, B., and Schlögelhofer, P. (2011). Have a break: determinants of meiotic DNA double strand break (DSB) formation and processing in plants. *J. Exp. Bot.* 62, 1545–1563. doi: 10.1093/jxb/erq421

Escobar-Guzman, R., Rodriguez-Leal, D., Vielle-Calzada, J.-P., and Ronceret, A. (2015). Whole-mount immunolocalization to study female meiosis in *Arabidopsis*. *Nat. Protocols* 10, 1535–1542. doi: 10.1038/nprot.2015.098

Ferdous, M., Higgins, J. D., Osman, K., Lambing, C., Roitinger, E., Mechtler, K., et al. (2012). Inter-homolog crossing-over and synapsis in *Arabidopsis* meiosis are dependent on the chromosome axis protein AtASY3. *PLoS Genet.* 8:e1002507. doi: 10.1371/journal.pgen.1002507

Fernandes, J. B., Duhamel, M., Seguéla-Arnaud, M., Froger, N., Girard, C., Choinard, S., et al. (2018a). FIGL1 and its novel partner FLIP form a conserved complex that regulates homologous recombination. *PLoS Genet.* 14:e1007317. doi: 10.1371/journal.pgen.1007317

Fernandes, J. B., Séguéla-Arnaud, M., Larchevêque, C., Lloyd, A. H., and Mercier, R. (2018b). Unleashing meiotic crossovers in hybrid plants. *Proc. Natl. Acad. Sci. U.S.A.* 115, 2431–2436.

Fernandes, J. B., Wlodzimierz, P., and Henderson, I. R. (2019). Meiotic recombination within plant centromeres. *Curr. Opin. Plant Biol.* 48, 26–35. doi: 10.1016/j.pbi.2019.02.008

Flórez-Zapata, N. M. V., Reyes-Valdés, M. H., and Martínez, O. (2016). Long non-coding RNAs are major contributors to transcriptome changes in sunflower meiocytes with different recombination rates. *BMC Genomics* 17:490. doi: 10.1186/s12864-016-2776-1

France, M. G., Enderle, J., Röhrig, S., Puchta, H., Franklin, F. C. H., and Higgins, J. D. (2021). ZYP1 is required for obligate cross-over formation and cross-over interference in *Arabidopsis*. *Proc. Natl. Acad Sci. U.S.A.* 118:e2021671118. doi: 10.1073/pnas.2021671118

Francis, K. E., Lam, S. Y., Harrison, B. D., Bey, A. L., Berchowitz, L. E., and Copenhaver, G. P. (2007). Pollen tetrad-based visual assay for meiotic recombination in *Arabidopsis*. *Proc. Natl. Acad Sci. U.S.A.* 104, 3913–3918. doi: 10.1073/pnas.0608936104

Fu, M., Wang, C., Xue, F., Higgins, J., Chen, M., Zhang, D., et al. (2016). The DNA topoisomerase VIB Subunit OsMTOPVIB is essential for meiotic recombination initiation in rice. *Mol. Plant* 9, 1539–1541. doi: 10.1016/j.molp.2016.07.006

Fu, R., Wang, C., Shen, H., Zhang, J., Higgins, J. D., and Liang, W. (2020). Rice OsBRCA2 is required for DNA double-strand break repair in meiotic cells. *Front. Plant Sci.* 11:600820. doi: 10.3389/fpls.2020.600820

Fuchs, L. K., Jenkins, G., and Phillips, D. W. (2018). Anthropogenic impacts on meiosis in plants. *Front. Plant Sci.* 9:1429. doi: 10.3389/fpls.2018.01429

Geuting, V., Kobbe, D., Hartung, F., Dürr, J., Focke, M., and Puchta, H. (2009). Two distinct MUS81-EME1 complexes from *Arabidopsis* process holliday junctions. *Plant Physiol.* 150, 1062–1071. doi: 10.1104/pp.109.136846

Girard, C., Chelysheva, L., Choinard, S., Froger, N., Macaisne, N., Lehmemdi, A., et al. (2015). AAA-ATPase FIDGETIN-LIKE 1 and helicase FANCM antagonize meiotic crossovers by distinct mechanisms. *PLoS Genet.* 11:e1005369. doi: 10.1371/journal.pgen.1005369

Girard, C., Crismani, W., Froger, N., Mazel, J., Lemhemdi, A., Horlow, C., et al. (2014). FANCM-associated proteins MHF1 and MHF2, but not the other Fanconi anemia factors, limit meiotic crossovers. *Nucleic Acids Res.* 42, 9087–9095. doi: 10.1093/nar/gku614

Giraut, L., Falque, M., Drouaud, J., Pereira, L., Martin, O. C., and Mézard, C. (2011). Genome-wide crossover distribution in *Arabidopsis thaliana* meiosis reveals sex-specific patterns along chromosomes. *PLoS Genet.* 7:e1002354. doi: 10.1371/journal.pgen.1002354

Golicz, A. A., Bhalla, P. L., Edwards, D., and Singh, M. B. (2020). Rice 3D chromatin structure correlates with sequence variation and meiotic recombination rate. *Commun. Biol.* 3:235.

Gonzalo, A., Lucas, M.-O., Charpentier, C., Sandmann, G., Lloyd, A., and Jenczewski, E. (2019). Reducing MSH4 copy number prevents meiotic crossovers between non-homologous chromosomes in Brassica napus. *Nat. Commun.* 10:2354.

Gordillo, S. V. G., Escobar-Guzman, R., Rodriguez-Leal, D., Vielle-Calzada, J.-P., and Ronceret, A. (2020). "Whole-mount immunolocalization procedure for plant female meiocytes," in *Plant Meiosis: Methods and Protocols*, eds M. Pradillo and S. Heckmann (New York, NY: Springer New York), 13–24. doi: 10.1007/978-1-4939-9818-0_2

Grelon, M., Vezon, D., Gendrot, G., and Pelletier, G. (2001). *AtSPO11-1* is necessary for efficient meiotic recombination in plants. *EMBO J.* 20, 589–600. doi: 10.1093/emboj/20.3.589

Grey, C., and de Massy, B. (2021). Chromosome organization in early meiotic prophase. *Front. Cell Dev. Biol.* 9:688878. doi: 10.3389/fcell.2021.688878

Hartung, F., Suer, S., Knoll, A., Wurz-Wildersinn, R., and Puchta, H. (2008). Topoisomerase 3 alpha and RMI1 suppress somatic crossovers and are essential

for resolution of meiotic recombination intermediates in *Arabidopsis thaliana*. *PLoS Genet.* 4:e1000285. doi: 10.1371/journal.pgen.1000285

Hartung, F., Suer, S., and Puchta, H. (2007a). Two closely related RecQ helicases have antagonistic roles in homologous recombination and DNA repair in *Arabidopsis thaliana*. *Proc. Natl. Acad. Sci. U.S.A.* 104, 18836–18841. doi: 10.1073/pnas.0705998104

Hartung, F., Wurz-Wildersinn, R., Fuchs, J., Schubert, I., Suer, S., and Puchta, H. (2007b). The catalytically active tyrosine residues of both SPO11-1 and SPO11-2 are required for meiotic double-strand break induction in *Arabidopsis*. *Plant Cell* 19, 3090–3099. doi: 10.1105/tpc.107.054817

He, Y., Wang, M., Dukowic-Schulze, S., Zhou, A., Tiang, C.-L., Shilo, S., et al. (2017). Genomic features shaping the landscape of meiotic double-strand-break hotspots in maize. *Proc. Natl. Acad. Sci. U.S.A.* 114, 12231–12236. doi: 10.1073/pnas.1713225114

Heckmann, S., Jankowska, M., Schubert, V., Kumke, K., Ma, W., and Houben, A. (2014). Alternative meiotic chromatid segregation in the holocentric plant *Luzula elegans*. *Nat. Commun.* 5:4979.

Hellsten, U., Wright, K. M., Jenkins, J., Shu, S., Yuan, Y., Wessler, S. R., et al. (2013). Fine-scale variation in meiotic recombination in Mimulus inferred from population shotgun sequencing. *Proc. Natl. Acad. Sci. U.S.A.* 110, 19478–19482. doi: 10.1073/pnas.1319032110

Higgins, J. D., Armstrong, S. J., Franklin, F. C., and Jones, G. H. (2004). The *Arabidopsis* MutS homolog AtMSH4 functions at an early step in recombination: Evidence for two classes of recombination in *Arabidopsis*. *Genes Dev.* 18, 2557–2570. doi: 10.1101/gad.317504

Higgins, J. D., Buckling, E. F., Franklin, F. C., and Jones, G. H. (2008a). Expression and functional analysis of AtMUS81 in *Arabidopsis* meiosis reveals a role in the second pathway of crossing-over. *Plant J.* 54, 152–162. doi: 10.1111/j.1365-313x.2008.03403.x

Higgins, J. D., Ferdous, M., Osman, K., and Franklin, F. C. (2011). The RecQ helicase AtRECQ4A is required to remove inter-chromosomal telomeric connections that arise during meiotic recombination in *Arabidopsis*. *Plant J.* 65, 492–502. doi: 10.1111/j.1365-313X.2010.04438.x

Higgins, J. D., Sanchez-Moran, E., Armstrong, S. J., Jones, G. H., and Franklin, F. C. H. (2005). The *Arabidopsis* synaptonemal complex protein ZYP1 is required for chromosome synapsis and normal fidelity of crossing over. *Genes Dev.* 19, 2488–2500. doi: 10.1101/gad.354705

Higgins, J. D., Vignard, J., Mercier, R., Pugh, A. G., Franklin, F. C., and Jones, G. H. (2008b). AtMSH5 partners AtMSH4 in the class I meiotic crossover pathway in Arabidopsis thaliana, but is not required for synapsis. *Plant J.* 55, 28–39. doi: 10.1111/j.1365-313x.2008.03470.x

Hofstatter, P. G., Thangavel, G., Castellani, M., and Marques, A. (2021). Meiosis progression and recombination in holocentric plants: what is known? *Front. Plant Sci.* 12:658296. doi: 10.3389/fpls.2021.658296

Hu, Q., Li, Y., Wang, H., Shen, Y., Zhang, C., Du, G., et al. (2017). Meiotic chromosome association 1 interacts with TOP3α and regulates meiotic recombination in rice. *Plant Cell* 29, 1697–1708. doi: 10.1105/tpc.17.00241

Hu, Q., Tang, D., Wang, H., Shen, Y., Chen, X., Ji, J., et al. (2016). The exonuclease homolog OsRAD1 promotes accurate meiotic double-strand break repair by suppressing nonhomologous end joining. *Plant Physiol.* 172, 1105–1116.

Hu, Q., Zhang, C., Xue, Z., Ma, L., Liu, W., Shen, Y., et al. (2018). OsRAD17 is required for meiotic double-strand break repair and plays a redundant role with OsZIP4 in synaptonemal complex assembly. *Front. Plant Sci.* 9:1236. doi: 10.3389/fpls.2018.01236

Huang, J., Cheng, Z., Wang, C., Hong, Y., Su, H., Wang, J., et al. (2015). Formation of interference-sensitive meiotic cross-overs requires sufficient DNA leading-strand elongation. *Proc. Natl. Acad. Sci. U.S.A.* 112, 12534–12539. doi: 10.1073/pnas.1507165112

Huang, J., Wang, C., Li, X., Fang, X., Huang, N., Wang, Y., et al. (2020). Conservation and divergence in the meiocyte sRNAomes of *Arabidopsis*, soybean, and cucumber. *Plant Physiol.* 182, 301–317. doi: 10.1104/pp.19.00807

Huang, J., Wang, C., Wang, H., Lu, P., Zheng, B., Ma, H., et al. (2019). Meiocyte-specific and AtSPO11-1–dependent small RNAs and their association with meiotic gene expression and recombination. *Plant Cell* 31, 444–464. doi: 10.1105/tpc.18.00511

Huang, X.-Y., Niu, J., Sun, M.-X., Zhu, J., Gao, J.-F., Yang, J., et al. (2013). CYCLIN-DEPENDENT KINASE G1 Is *Associated* with the spliceosome to Regulate CALLOSE SYNTHASE5 splicing and pollen wall formation in *Arabidopsis*. *Plant Cell* 25, 637–648. doi: 10.1105/tpc.112.107896

Hurel, A., Phillips, D., Vrielynck, N., Mézard, C., Grelon, M., and Christophorou, N. (2018). A cytological approach to studying meiotic recombination and chromosome dynamics in Arabidopsis thaliana male meiocytes in three dimensions. *Plant J.* 95, 385–396. doi: 10.1111/tpj.13942

Iglesias, F. M., Bruera, N. A., Dergan-Dylon, S., Marino-Buslje, C., Lorenzi, H., Mateos, J. L., et al. (2015). The *Arabidopsis* DNA polymerase δ has a role in the deposition of transcriptionally active epigenetic marks, development and flowering. *PLoS Genet.* 11:e1004975. doi: 10.1371/journal.pgen.1004975

Ji, J., Tang, D., Shen, Y., Xue, Z., Wang, H., Shi, W., et al. (2016). P31comet, a member of the synaptonemal complex, participates in meiotic DSB formation in rice. *Proc. Natl. Acad. Sci. U.S.A.* 113, 10577–10582. doi: 10.1073/pnas.1607334113

Jing, J., Zhang, T., Wang, Y., Cui, Z., and He, Y. (2019). ZmRAD51C is essential for double-strand break repair and homologous recombination in maize meiosis. *Int. J. Mol. Sci.* 20:5513. doi: 10.3390/ijms20215513

Jing, J.-L., Zhang, T., Kao, Y.-H., Huang, T.-H., Wang, C.-J. R., and He, Y. (2020). ZmMTOPVIB enables DNA double-strand break formation and bipolar spindle assembly during maize meiosis. *Plant Physiol.* 184, 1811–1822. doi: 10.1104/pp.20.00933

Jolivet, S., Vezon, D., Froger, N., and Mercier, R. (2006). Non conservation of the meiotic function of the Ski8/Rec103 homolog in *Arabidopsis*. *Genes Cells* 11, 615–622. doi: 10.1111/j.1365-2443.2006.00972.x

Kelliher, T., and Walbot, V. (2012). Hypoxia triggers meiotic fate acquisition in maize. *Science* 337, 345–348. doi: 10.1126/science.1220080

Kianian, P. M. A., Wang, M., Simons, K., Ghavami, F., He, Y., Dukowic-Schulze, S., et al. (2018). High-resolution crossover mapping reveals similarities and differences of male and female recombination in maize. *Nat. Commun.* 9:2370.

Kim, J., and Choi, K. (2019). Signaling-mediated meiotic recombination in plants. *Curr. Opin. Plant Biol.* 51, 44–50. doi: 10.1016/j.pbi.2019.04.001

Komiya, R., Ohyanagi, H., Niihama, M., Watanabe, T., Nakano, M., Kurata, N., et al. (2014). Rice germline-specific Argonaute *MEL1* protein binds to phasiRNAs generated from more than 700 lincRNAs. *Plant J.* 78, 385–397. doi: 10.1111/tpj.1248

Ku, J.-C., Ronceret, A., Golubovskaya, I., Lee, D. H., Wang, C., Timofejeva, L., et al. (2020). Dynamic localization of SPO11-1 and conformational changes of meiotic axial elements during recombination initiation of maize meiosis. *PLoS Genet.* 16:e1007881. doi: 10.1371/journal.pgen.1007881

Kumar, R., Duhamel, M., Coutant, E., Ben-Nahia, E., and Mercier, R. (2019). Antagonism between BRCA2 and FIGL1 regulates homologous recombination. *Nucleic Acids Res.* 47, 5170–5180. doi: 10.1093/nar/gkz225

Kumar, S. V., and Wigge, P. A. (2010). H2A.Z-containing nucleosomes mediate the thermosensory response in *Arabidopsis*. *Cell* 140, 136–147. doi: 10.1016/j.cell.2009.11.006

Kuo, P., Da Ines, O., and Lambing, C. (2021). Rewiring meiosis for crop improvement. *Front. Plant Sci.* 12:708948. doi: 10.3389/fpls.2021.708948

Kurzbauer, M. T., Janisiw, M. P., Paulin, L. F., Prusén Mota, I., Tomanov, K., Krsicka, O., et al. (2021). ATM controls meiotic DNA double-strand break formation and recombination and affects synaptonemal complex organization in plants. *Plant Cell* 33, 1633–1656. doi: 10.1093/plcell/koab045

Kurzbauer, M.-T., Pradillo, M., Kerzendorfer, C., Sims, J., Ladurner, R., Oliver, C., et al. (2018). *Arabidopsis thaliana* FANCD2 promotes meiotic crossover formation. *Plant Cell* 30, 415–428. doi: 10.1105/tpc.17.00745

Kurzbauer, M. T., Uanschou, C., Chen, D., and Schlogelhofer, P. (2012). The recombinases DMC1 and RAD51 are functionally and spatially separated during meiosis in *Arabidopsis*. *Plant Cell* 24, 2058–2070. doi: 10.1105/tpc.112.098459

Lambing, C., Franklin, F. C. H., and Wang, C.-J. R. (2017). Understanding and manipulating meiotic recombination in plants. *Plant Physiol.* 173, 1530–1542. doi: 10.1104/pp.16.01530

Lambing, C., Kuo, P. C., Tock, A. J., Topp, S. D., and Henderson, I. R. (2020a). ASY1 acts as a dosage-dependent antagonist of telomere-led recombination and mediates crossover interference in Arabidopsis. *Proc. Natl. Acad. Sci. U.S.A.* 117, 13647–13658. doi: 10.1073/pnas.1921055117

Lambing, C., Osman, K., Nuntasoontorn, K., West, A., Higgins, J. D., Copenhaver, G. P., et al. (2015). *Arabidopsis* PCH2 mediates meiotic chromosome

remodeling and maturation of crossovers. *PLoS Genet.* 11:e1005372. doi: 10.1371/journal.pgen.1005372

Lambing, C., Tock, A. J., Topp, S. D., Choi, K., Kuo, P. C., Zhao, X., et al. (2020b). Interacting genomic landscapes of REC8-cohesin, chromatin, and meiotic recombination in *Arabidopsis*. *Plant Cell* 32, 1218–1239. doi: 10.1105/tpc.19.00866

Lawrence, E. J., Gao, H., Tock, A. J., Lambing, C., Blackwell, A. R., Feng, X., et al. (2019). Natural variation in TBP-ASSOCIATED FACTOR 4b controls meiotic crossover and germline transcription in *Arabidopsis*. *Curr. Biol.* 29, 2676–2686. doi: 10.1016/j.cub.2019.06.084

Lee, D. H., Kao, Y.-H., Ku, J.-C., Lin, C.-Y., Meeley, R., Jan, Y.-S., et al. (2015). The axial element protein DESYNAPTIC2 mediates meiotic double-strand break formation and synaptonemal complex assembly in maize. *Plant Cell* 27, 2516–2529. doi: 10.1105/tpc.15.00434

Lenykó-Thegze, A., Fábian, A., Mihók, E., Makai, D., and Cseh, A. (2021). Pericentromeric chromatin reorganisation follows the initiation of recombination and coincides with early events of synapsis in cereals. *Plant J.* doi: 10.1111/tpj.15391 [Epub ahead of print].

Li, F., De Storme, N., and Geelen, D. (2017). Dynamics of male meiotic recombination frequency during plant development using fluorescent tagged lines in *Arabidopsis thaliana*. *Sci. Rep*. 7:42535.

Li, W., Chen, C., Markmann-Mulisch, U., Timofejeva, L., Schmelzer, E., Ma, H., et al. (2004). The *Arabidopsis* AtRAD51 gene is dispensable for vegetative development but required for meiosis. *Proc. Natl. Acad. Sci. U.S.A.* 101, 10596–10601. doi: 10.1073/pnas.0404110101

Li, X., Chang, Y., Xin, X., Zhu, C., Li, X., Higgins, J. D., et al. (2013). Replication protein A2c coupled with replication protein A1c regulates crossover formation during meiosis in rice. *Plant Cell* 25, 3885–3899. doi: 10.1105/tpc.113.118042

Li, X., Yu, M., Bolaños-Villegas, P., Zhang, J., Ni, D., Ma, H., et al. (2021). Fanconi anemia ortholog FANCM regulates meiotic crossover distribution in plants. *Plant Physiol.* 186, 344–360. doi: 10.1093/plphys/kiab061

Li, Y., Qin, B., Shen, Y., Zhang, F., Liu, C., You, H., et al. (2018). HEIP1 regulates crossover formation during meiosis in rice. *Proc. Natl. Acad. Sci. U.S.A.* 115, 10810–10815. doi: 10.1073/pnas.1807871115

Liu, H., Cao, A., Yang, L., and Wang, J. (2020). "Rice female meiosis: genome-wide mRNA, small RNA, and DNA methylation analysis during ovule development," in *Plant Meiosis: Methods and Protocols*, eds M. Pradillo and S. Heckmann (New York, NY: Springer New York), 267–280. doi: 10.1007/978-1-4939-9818-0_19

Liu, H., and Nonomura, K. I. (2016). A wide reprogramming of histone H3 modifications during male meiosis I in rice is dependent on the Argonaute protein *MEL1*. *J. Cell Sci.* 129, 3553–3561. doi: 10.1242/jcs.184937

Lloyd, A., and Jenczewski, E. (2019). Modelling sex-specific crossover patterning in *Arabidopsis*. *Genetics* 211, 847–859. doi: 10.1534/genetics.118.301838

Lloyd, A., Morgan, C., Franklin, C., and Bomblies, K. (2018). Plasticity of meiotic recombination rates in response to temperature in *Arabidopsis*. *Genetics* 208, 1409–1420. doi: 10.1534/genetics.117.300588

Lohmiller, L. D., de Muyt, A., Howard, B., Offenberg, H. H., Heyting, C., Grelon, M., et al. (2008). Cytological analysis of MRE11 protein during early meiotic prophase I in Arabidopsis and tomato. *Chromosoma* 117, 277–288. doi: 10.1007/s00412-007-0147-z

Long, J., Walker, J., She, W., Aldridge, B., Gao, H., Deans, S., et al. (2021). Nurse cell–derived small RNAs define paternal epigenetic inheritance in *Arabidopsis*. *Science* 373:eabh0556. doi: 10.1126/science.abh0556

Lu, J., Wang, C., Wang, H., Zheng, H., Bai, W., Lei, D., et al. (2020). OsMFS1/OsHOP2 complex participates in rice male and female development. *Front. Plant Sci.* 11:518. doi: 10.3389/fpls.2020.00518

Luo, C., Li, X., Zhang, Q., and Yan, J. (2019). Single gametophyte sequencing reveals that crossover events differ between sexes in maize. *Nat. Commun.* 10:785.

Luo, Q., Li, Y., Shen, Y., and Cheng, Z. (2014). Ten years of gene discovery for meiotic event control in rice. *J. Genet. Genomics* 41, 125–137. doi: 10.1016/j.jgg.2014.02.002

Macaisne, N., Novatchkova, M., Peirera, L., Vezon, D., Jolivet, S., Froger, N., et al. (2008). SHOC1, an XPF endonuclease-related protein, is essential for the formation of class I meiotic crossovers. *Curr. Biol*. 18, 1432–1437. doi: 10.1016/j.cub.2008.08.041

Macaisne, N., Vignard, J., and Mercier, R. (2011). SHOC1 and PTD form an XPF-ERCC1-like complex that is required for formation of class I crossovers. *J. Cell Sci*. 124, 2687–2691. doi: 10.1242/jcs.088229

Martinez-Garcia, M., Schubert, V., Osman, K., Darbyshire, A., Sanchez-Moran, E., and Franklin, F. C. H. (2018). TOPII and chromosome movement help remove interlocks between entangled chromosomes during meiosis. *J. Cell Biol.* 217, 4070–4079. doi: 10.1083/jcb.201803019

Mason, A. S., and Wendel, J. F. (2020). Homoeologous exchanges, segmental allopolyploidy, and polyploid genome evolution. *Front. Genet.* 11:1014. doi: 10.3389/fgene.2020.01014

Melamed-Bessudo, C., Shilo, S., and Levy, A. A. (2016). Meiotic recombination and genome evolution in plants. *Curr. Opin. Plant Biol.* 30, 82–87. doi: 10.1016/j.pbi.2016.02.003

Mercier, R., Jolivet, S., Vezon, D., Huppe, E., Chelysheva, L., Giovanni, M., et al. (2005). Two meiotic crossover classes cohabit in *Arabidopsis*: one is dependent on *MER3*, whereas the other one is not. *Curr. Biol.* 15, 692–701.

Mercier, R., Mezard, C., Jenczewski, E., Macaisne, N., and Grelon, M. (2015). The molecular biology of meiosis in plants. *Ann. Rev. Plant Biol.* 66, 297–327. doi: 10.1146/annurev-arplant-050213-035923

Miao, C. B., Tang, D., Zhang, H. G., Wang, M., Li, Y. F., Tang, S. Z., et al. (2013). CENTRAL REGION COMPONENT1, a novel synaptonemal complex component, is essential for meiotic recombination initiation in rice. *Plant Cell* 25, 2998–3009. doi: 10.1105/tpc.113.113175

Mieulet, D., Aubert, G., Bres, C., Klein, A., Droc, G., Vieille, E., et al. (2018). Unleashing meiotic crossovers in crops. *Nat. Plants* 4, 1010–1016. doi: 10.1038/s41477-018-0311-x

Miyazaki, M., Sato, Y., Asano, T., Nagamura, Y., and Nonomura, K. I. (2015). Rice MEL2, the RNA recognition motif (RRM) protein, binds *in vitro* to meiosis-expressed genes containing U-rich RNA consensus sequences in the 3'-UTR. *Plant Mol. Biol.* 89, 293–307. doi10.1007/s11103-015-0369-z

Modliszewski, J. L., and Copenhaver, G. P. (2017). Meiotic recombination gets stressed out: CO frequency is plastic under pressure. *Curr. Opin. Plant Biol.* 36, 95–102. doi: 10.1016/j.pbi.2016.11.019

Modliszewski, J. L., Wang, H., Albright, A. R., Lewis, S. M., Bennett, A. R., Huang, J., et al. (2018). Elevated temperature increases meiotic crossover frequency via the interfering (Type I) pathway in *Arabidopsis thaliana*. *PLoS Genet.* 14:e1007384. doi: 10.1371/journal.pgen.1007384

Murphy, S. P., Gumber, H. K., Mao, Y., and Bass, H. W. (2014). A dynamic meiotic SUN belt includes the zygotene-stage telomere bouquet and is disrupted in chromosome segregation mutants of maize (Zea mays L.). *Front. Plant Sci.* 5:314. doi: 10.3389/fpls.2014.00314

Nannas, N. J., Higgins, D. M., and Dawe, R. K. (2016). Anaphase asymmetry and dynamic repositioning of the division plane during maize meiosis. *J. Cell Sci.* 129, 4014–4024.

Nelms, B., and Walbot, V. (2019). Defining the developmental program leading to meiosis in maize. *Science* 364, 52–56. doi: 10.1126/science.aav6428

Nibau, C., Dadarou, D., Kargios, N., Mallioura, A., Fernandez-Fuentes, N., Cavallari, N., et al. (2020a). A functional kinase is necessary for cyclin-dependent kinase G1 (CDKG1) to maintain fertility at high ambient temperature in *Arabidopsis*. *Front. Plant Sci.* 11:586870. doi: 10.3389/fpls.2020.586870

Nibau, C., Lloyd, A., Dadarou, D., Betekhtin, A., Tsilimigka, F., Phillips, D. W., et al. (2020b). CDKG1 is required for meiotic and somatic recombination intermediate processing in *Arabidopsis*. *Plant Cell* 32, 1308–1322. doi: 10.1105/tpc.19.00942

Nonomura, K. I., Eiguchi, M., Nakano, M., Takashima, K., Komeda, N., Fukuchi, S., et al. (2011). A novel RNA-recognition-motif protein is required for premeiotic G1/S-phase transition in rice (*Oryza sativa* L.). *PLoS Genet.* 7:e1001265. doi: 10.1371/journal.pgen.1001265

Nonomura, K. I., Morohoshi, A., Nakano, M., Eiguchi, M., Miyao, A., Hirochika, H., et al. (2007). A germ cell specific gene of the ARGONAUTE family is essential for the progression of premeiotic mitosis and meiosis during sporogenesis in rice. *Plant Cell* 19, 2583–2594. doi: 10.1105/tpc.107.053199

Nonomura, K. I., Nakano, M., Eiguchi, M., Suzuki, T., and Kurata, N. (2004a). *PAIR2* is essential for homologous chromosome synapsis in rice meiosis I. *J. Cell Sci.* 119, 217–225. doi: 10.1242/jcs.02736

Nonomura, K. I., Nakano, M., Fukuda, T., Eiguchi, M., Miyao, A., Hirochika, H., et al. (2004b). The novel gene *HOMOLOGOUS PAIRING ABERRATION*

IN RICE MEIOSIS1 of rice encodes a putative coiled–coil protein required for homologous chromosome pairing in meiosis. *Plant Cell* 16, 1008–1020. doi: 10.1105/tpc.020701

Oliver, C., Pradillo, M., Jover-Gil, S., Cuñado, N., Ponce, M. R., and Santos, J. L. (2017). Loss of function of *Arabidopsis* microRNA-machinery genes impairs fertility, and has effects on homologous recombination and meiotic chromatin dynamics. *Sci. Rep.* 7:9280.

Oliver, C., Santos, J. L., and Pradillo, M. (2014). On the role of some ARGONAUTE proteins in meiosis and DNA repair in *Arabidopsis thaliana*. *Front. Plant Sci.* 5:177. doi: 10.3389/fpls.2014.00177

Oliver, C., Santos, J. L., and Pradillo, M. (2016). Accurate chromosome segregation at first meiotic division requires AGO4, a protein involved in RNA-dependent dna methylation in *Arabidopsis thaliana*. *Genetics* 204, 543–553. doi: 10.1534/genetics.116.189217

Olivier, M., Da Ines, O., Amiard, S., Serra, H., Goubely, C., White, C. I., et al. (2015). The structure-specific endonucleases MUS81 and SEND1 are essential for telomere stability in *Arabidopsis*. *Plant Cell.* 28, 74–86. doi: 10.1105/tpc.15.00898

Olmedo-Monfil, V., Durán-Figueroa, N., Arteaga-Vázquez, M., Demesa-Arévalo, E., Autran, D., Grimanelli, D., et al. (2010). Control of female gamete formation by a small RNA pathway in *Arabidopsis*. *Nature* 464, 628–632. doi: 10.1038/nature08828

Osman, K., Sanchez-Moran, E., Mann, S. C., Jones, G. H., and Franklin, F. C. H. (2009). Replication protein A (AtRPA1a) is required for class I crossover formation but is dispensable for meiotic DNA break repair. *EMBO J.* 28, 394–404. doi: 10.1038/emboj.2008.295

Osman, K., Yang, J., Roitinger, E., Lambing, C., Heckmann, S., Howell, E., et al. (2018). Affinity proteomics reveals extensive phosphorylation of the *Brassica* chromosome axis protein ASY1 and a network of associated proteins at prophase I of meiosis. *Plant J.* 93, 17–33. doi: 10.1111/tpj.13752

Pawlowski, W. P., Golubovskaya, I. N., and Cande, W. Z. (2003). Altered nuclear distribution of recombination protein RAD51 in maize mutants suggests the involvement of RAD51 in meiotic homology recognition. *Plant Cell* 15, 1807–1816. doi: 10.1105/tpc.012898

Pawlowski, W. P., Golubovskaya, I. N., Timofejevva, L., Meeley, R. B., Sheridan, W. F., and Cande, W. Z. (2004). Coordination of meiotic recombination, pairing and synapsis by PHS1. *Science* 303, 89–92. doi: 10.1126/science.1091110

Pawlowski, W. P., Wang, C.-J. R., Golubovskaya, I. N., Szymaniak, J. M., Shi, L., Hamant, O., et al. (2009). Maize AMEIOTIC1 is essential for multiple early meiotic processes and likely required for the initiation of meiosis. *Proc. Natl. Acad. Sci. U.S.A.* 106, 3603–3608. doi: 10.1073/pnas.0810115106

Phillips, D., Jenkins, G., Macaulay, M., Nibau, C., Wnetrzak, J., Fallding, D., et al. (2015). The effect of temperature on the male and female recombination landscape of barley. *New Phytol.* 208, 421–429. doi: 10.1111/nph.13548

Pradillo, M., Knoll, A., Oliver, C., Varas, J., Corredor, E., Puchta, H., et al. (2015). Involvement of the Cohesin Cofactor PDS5 (SPO76) during meiosis and DNA repair in *Arabidopsis thaliana*. *Front. Plant Sci.* 6:1034. doi: 10.3389/fpls.2015.01034

Pradillo, M., and Santos, J. L. (2018). Genes involved in miRNA biogenesis affect meiosis and fertility. *Chromosome Res.* 26, 233–241. doi: 10.1007/s10577-018-9588-x

Pradillo, M., Varas, J., Oliver, C., and Santos, J. L. (2014). On the role of AtDMC1, AtRAD51 and its paralogs during *Arabidopsis* meiosis. *Front. Plant Sci.* 5:23. doi: 10.3389/fpls.2014.00023

Prusicki, M. A., Keizer, E. M., van Rosmalen, R. P., Komaki, S., Seifert, F., Müller, K., et al. (2019). Live cell imaging of meiosis in *Arabidopsis thaliana*. *eLife* 8:e42834.

Puizina, J., Siroky, J., Mokros, P., Schweizer, D., and Riha, K. (2004). Mre11 deficiency in *Arabidopsis* is associated with chromosomal instability in somatic cells and Spo11-dependent genome fragmentation during meiosis. *Plant Cell* 16, 1968–1978. doi: 10.1105/tpc.104.022749

Qiao, H., Lohmiller, L. D., and Anderson, L. K. (2011). Cohesin proteins load sequentially during prophase I in tomato primary microsporocytes. *Chromosome Res.* 19, 193–207. doi: 10.1007/s10577-010-9184-1

Ren, L., Tang, D., Zhao, T., Zhang, F., Liu, C., Xue, Z., et al. (2018). OsSPL regulates meiotic fate acquisition in rice. *New Phytol.* 218, 789–803. doi: 10.1111/nph.15017

Ren, Y., Chen, D., Li, W., Zhou, D., Luo, T., Yuan, G., et al. (2019). OsSHOC1 and OsPTD1 are essential for crossover formation during rice meiosis. *Plant J.* 98, 315–328.

Ronceret, A., Doutriaux, M.-P., Golubovskaya, I. N., and Pawlowski, W. P. (2009). PHS1 regulates meiotic recombination and homologous chromosome pairing by controlling the transport of RAD50 to the nucleus. *Proc. Natl. Acad. Sci. U.S.A.* 106, 20121–20126. doi: 10.1073/pnas.0906273106

Ronceret, A., Guilleminot, J., Lincker, F., Gadea-Vacas, J., Delorme, V., Bechtold, N., et al. (2005). Genetic analysis of two *Arabidopsis* DNA polymerase epsilon subunits during early embryogenesis. *Plant J.* 44, 223–236. doi: 10.1111/j.1365-313x.2005.02521.x

Ronceret, A., and Pawlowski, W. P. (2010). Chromosome dynamics in meiotic prophase I in plants. *Cytogenet. Genome Res.* 129, 173–183. doi: 10.1159/000313656

Rowan, B. A., Heavens, D., Feuerborn, T. R., Tock, A. J., Henderson, I. R., and Weigel, D. (2019). An ultra high-density *Arabidopsis thaliana* crossover map that refines the influences of structural variation and epigenetic features. *Genetics* 213, 771–787. doi: 10.1534/genetics.119.302406

Saini, R., Singh, A. K., Dhanapal, S., Saeed, T. H., Hyde, G. J., and Baskar, R. (2017). Brief temperature stress during reproductive stages alters meiotic recombination and somatic mutation rates in the progeny of *Arabidopsis*. *BMC Plant Biol.* 17:103. doi: 10.1186/s12870-017-1051-1

Saini, R., Singh, A. K., Hyde, G. J., and Baskar, R. (2020). Levels of heterochiasmy during *Arabidopsis* development as reported by fluorescent tagged lines. *G3* 10, 2103–2110. doi: 10.1534/g3.120.401296

Šamanić, I., Simunić, J., Riha, K., and Puizina, J. (2013). Evidence for distinct functions of MRE11 in *Arabidopsis* meiosis. *PLoS One* 8:e78760. doi: 10.1371/journal.pone.0078760

Seeliger, K., Dukowic-Schulze, S., Wurz-Wildersinn, R., Pacher, M., and Puchta, H. (2012). BRCA2 is a mediator of RAD51- and DMC1-facilitated homologous recombination in *Arabidopsis thaliana*. *New Phytol.* 193, 364–375. doi: 10.1111/j.1469-8137.2011.03947.x

Séguéla-Arnaud, M., Crismani, W., Larchevêque, C., Mazel, J., Froger, N., Choinard, S., et al. (2015). Multiple mechanisms limit meiotic crossovers: TOP3α and two BLM homologs antagonize crossovers in parallel to FANCM. *Proc. Natl. Acad. Sci. U.S.A.* 112, 4713–4718. doi: 10.1073/pnas.1423107112

Sepsi, A., and Schwarzacher, T. (2020). Chromosome–nuclear envelope tethering – a process that orchestrates homologue pairing during plant meiosis? *J. Cell Sci.* 133:jcs243667.

Serra, H., Lambing, C., Griffin, C. H., Topp, S. D., Nageswaran, D. C., Underwood, C. J., et al. (2018). Massive crossover elevation via combination of HEI10 and recq4a recq4b during Arabidopsis meiosis. *Proc. Natl. Acad. Sci. U.S.A.* 115, 2437–2442. doi: 10.1073/pnas.1713071115

Shi, W., Ji, J., Xue, Z., Zhang, F., Miao, Y., Yang, H., et al. (2021). PRD1, a homologous recombination initiation factor, is involved in spindle assembly in rice meiosis. *New Phytol.* 230, 585–600. doi: 10.1111/nph.17178

Shi, W., Tang, D., Shen, Y., Xue, Z., Zhang, F., Zhang, C., et al. (2019). OsHOP2 regulates the maturation of crossovers by promoting homologous pairing and synapsis in rice meiosis. *New Phytol.* 222, 805–819. doi: 10.1111/nph.15664

Shilo, S., Melamed-Bessudo, C., Dorone, Y., Barkai, N., and Levy, A. A. (2015). DNA crossover motifs associated with epigenetic modifications delineate open chromatin regions in *Arabidopsis*. *Plant Cell* 27, 2427–2436. doi: 10.1105/tpc.15.00391

Siaud, N., Dray, E., Gy, I., Gerard, E., Takvorian, N., and Doutriaux, M. P. (2004). Brca2 is involved in meiosis in *Arabidopsis thaliana* as suggested by its interaction with Dmc1. *EMBO J.* 23, 1392–1401. doi: 10.1038/sj.emboj.7600146

Sidhu, G. K., Fang, C., Olson, M. A., Falque, M., Martin, O. C., and Pawlowski, W. P. (2015). Recombination patterns in maize reveal limits to crossover homeostasis. *Proc. Natl. Acad. Sci. U.S.A.* 112, 15982–15987. doi: 10.1073/pnas.1514265112

Sims, J., Copenhaver, G. P., and Schlögelhofer, P. (2019). Meiotic DNA repair in the nucleolus employs a nonhomologous end-joining mechanism. *Plant Cell* 31, 2259–2275. doi: 10.1105/tpc.19.00367

Singh, D. K., Andreuzza, S., Panoli, A. P., and Siddiqi, I. (2013). AtCTF7 is required for establishment of sister chromatid cohesion and association of cohesin with chromatin during meiosis in *Arabidopsis*. *BMC Plant Biol.* 13:117. doi: 10.1186/1471-2229-13-117

Singh, G., Da Ines, O., Gallego, M. E., and White, C. I. (2017). Analysis of the impact of the absence of RAD51 strand exchange activity in *Arabidopsis* meiosis. *PLoS One* 12:e0183006. doi: 10.1371/journal.pone.0183006

Stacey, N. J., Kuromori, T., Azumi, Y., Roberts, G., Breuer, C., Wada, T., et al. (2006). Arabidopsis SPO11-2 functions with SPO11-1 in meiotic recombination. *Plant J.* 48, 206–216. doi: 10.1111/j.1365-313x.2006.02867.x

Stack, S. M., Shearer, L. A., Lohmiller, L., and Anderson, L. K. (2017). Meiotic crossing over in maize knob heterochromatin. *Genetics* 205, 1101–1112. doi: 10.1534/genetics.116.196089

Su, H., Cheng, Z., Huang, J., Lin, J., Copenhaver, G. P., Ma, H., et al. (2017). Arabidopsis RAD51, RAD51C and XRCC3 proteins form a complex and facilitate RAD51 localization on chromosomes for meiotic recombination. *PLoS Genet.* 13:e1006827. doi: 10.1371/journal.pgen.1006827

Svačina, R., Sourdille, P., Kopecký, D., and Bartoš, J. (2020). Chromosome pairing in polyploid grasses. *Front. Plant Sci.* 11:1056. doi: 10.3389/fpls.2020.01056

Taagen, E., Bogdanove, A. J., and Sorrells, M. E. (2020). Counting on crossovers: controlled recombination for plant breeding. *Trends Plant Sci.* 25, 455–465. doi: 10.1016/j.tplants.2019.12.017

Tang, Y., Yin, Z., Zeng, Y., Zhang, Q., Chen, L., He, Y., et al. (2017). MTOPVIB interacts with AtPRD1 and plays important roles in formation of meiotic DNA double-strand breaks in *Arabidopsis*. *Sci Rep.* 7:10007.

Termolino, P., Falque, M., Aiese Cigliano, R., Cremona, G., Paparo, R., Ederveen, A., et al. (2019). Recombination suppression in heterozygotes for a pericentric inversion induces the interchromosomal effect on crossovers in *Arabidopsis*. *Plant J.* 100, 1163–1175. doi: 10.1111/tpj.14505

Tock, A. J., and Henderson, I. R. (2018). Hotspots for initiation of meiotic recombination. *Front. Genet.* 9:521. doi: 10.3389/fgene.2018.00521

Toyota, M., Matsuda, K., Kakutani, T., Terao Morita, M., and Tasaka, M. (2011). Developmental changes in crossover frequency in *Arabidopsis*. *Plant J.* 65, 589–599. doi: 10.1111/j.1365-313x.2010.04440.x

Uanschou, C., Ronceret, A., Von Harder, M., De Muyt, A., Vezon, D., Pereira, L., et al. (2013). Sufficient amounts of functional HOP2/MND1 complex promote interhomolog DNA repair but are dispensable for intersister dna repair during meiosis in *Arabidopsis*. *Plant Cell* 25, 4924–4940. doi: 10.1105/tpc.113.118521

Uanschou, C., Siwiec, T., Pedrosa-Harand, A., Kerzendorfer, C., Sanchez-Moran, E., Novatchkova, M., et al. (2007). A novel plant gene essential for meiosis is related to the human *CtIP* and the yeast *COM1/SAE2* gene. *EMBO J.* 26, 5061–5070. doi: 10.1038/sj.emboj.7601913

Underwood, C. J., Choi, K., Lambing, C., Zhao, X., Serra, H., Borges, F., et al. (2018). Epigenetic activation of meiotic recombination near *Arabidopsis thaliana* centromeres via loss of H3K9me2 and non-CG DNA methylation. *Genome Res.* 28, 519–531. doi: 10.1101/gr.227116.117

Varas, J., Graumann, K., Osman, K., Pradillo, M., Evans, D. E., Santos, J. L., et al. (2015). Absence of SUN1 and SUN2 proteins in *Arabidopsis thaliana* leads to a delay in meiotic progression and defects in synapsis and recombination. *Plant J.* 81, 329–346. doi: 10.1111/tpj.12730

Vignard, J., Siwiec, T., Chelysheva, L., Vrielynck, N., Gonord, F., Armstrong, S. J., et al. (2007). The interplay of RecA-related proteins and the MND1-HOP2 complex during meiosis in *Arabidopsis thaliana*. *PLoS Genet.* 3:1894–1906. doi: 10.1371/journal.pgen.0030176

von Wettstein, D., Rasmussen, S. W., and Holm, P. B. (1984). The synaptonemal complex in genetic segregation. *Annu. Rev. Genet.* 18, 331–413. doi: 10.1146/annurev.ge.18.120184.001555

Vrielynck, N., Chambon, A., Vezon, D., Pereira, L., Chelysheva, L., De Muyt, A., et al. (2016). A DNA topoisomerase VI–like complex initiates meiotic recombination. *Science* 351, 939–943. doi: 10.1126/science.aad5196

Walker, J., Gao, H., Zhang, J., Aldridge, B., Vickers, M., Higgins, J. D., et al. (2018). Sexual-lineage-specific DNA methylation regulates meiosis in *Arabidopsis*. *Nat. Genet.* 50, 130–137. doi: 10.1038/s41588-017-0008-5

Wang, C., Higgins, J. D., He, Y., Lu, P., Zhang, D., and Liang, W. (2017). Resolvase OsGEN1 mediates DNA repair by homologous recombination. *Plant Physiol.* 173, 1316–1329. doi: 10.1104/pp.16.01726

Wang, C., Huang, J., Zhang, J., Wang, H., Han, Y., Copenhaver, G. P., et al. (2018). The largest subunit of DNA polymerase delta is required for normal formation of meiotic type I crossovers. *Plant Physiol.* 179, 446–459. doi: 10.1104/pp.18.00861

Wang, C.-J. R., Carlton, P. M., Golubovskaya, I. N., and Cande, W. Z. (2009). Interlock formation and coiling of meiotic chromosome axes during synapsis. *Genetics* 183, 905–915. doi: 10.1534/genetics.109.108688

Wang, H., Hu, Q., Tang, D., Liu, X., Du, G., Shen, Y., et al. (2016). OsDMC1 is not required for homologous pairing in rice meiosis. *Plant Physiol.* 171, 230–241. doi: 10.1104/pp.16.00167

Wang, H., Xu, W., Sun, Y., Lian, Q., Wang, C., Yu, C., et al. (2020). The cohesin loader SCC2 contains a PHD finger that is required for meiosis in land plants. *PLoS Genet.* 16:e1008849. doi: 10.1371/journal.pgen.1008849

Wang, K., Wang, M., Tang, D., Shen, Y., Qin, B., Li, M., et al. (2011). PAIR3, an axis-associated protein, is essential for the recruitment of recombination elements onto meiotic chromosomes in rice. *Mol. Biol. Cell.* 22, 12–19. doi: 10.1091/mbc.e10-08-0667

Wang, M., Wang, K., Tang, D., Wei, C., Li, M., Shen, Y., et al. (2010). The central element protein ZEP1 of the synaptonemal complex regulates the number of crossovers during meiosis in rice. *Plant Cell* 22, 417–430. doi: 10.1105/tpc.109.070789

Wang, S., Veller, C., Sun, F., Ruiz-Herrera, A., Shang, Y., Liu, H., et al. (2019). Per-nucleus crossover covariation and implications for evolution. *Cell* 177, 326–338. doi: 10.1016/j.cell.2019.02.021

Wang, Y., and Copenhaver, G. P. (2018). Meiotic recombination: mixing it up in plants. *Ann. Rev. Plant Biol.* 69, 577–609. doi: 10.1146/annurev-arplant-042817-040431

Wang, Y., Jiang, L., Zhang, T., Jing, J., and He, Y. (2018). ZmCom1 is required for both mitotic and meiotic recombination in maize. *Front. Plant Sci.* 9:1005. doi: 10.3389/fpls.2018.01005

Waterworth, W. M., Altun, C., Armstrong, S. J., Roberts, N., Dean, P. J., Young, K., et al. (2007). NBS1 is involved in DNA repair and plays a synergistic role with ATM in mediating meiotic homologous recombination in plants. *Plant J.* 52, 41–52. doi: 10.1111/j.1365-313X.2007.03220.x

Wei, B., Zhang, J., Pang, C., Yu, H., Guo, D., Jiang, H., et al. (2015). The molecular mechanism of SPOROCYTELESS/NOZZLE in controlling *Arabidopsis* ovule development. *Cell Res.* 25, 121–134. doi: 10.1038/cr.2014.145

West, A. M. V., Rosenberg, S. C., Ur, S. N., Lehmer, M. K., Ye, Q., Hagemann, G., et al. (2019). A conserved filamentous assembly underlies the structure of the meiotic chromosome axis. *eLife* 8:e40372.

Wijnker, E., Harashima, H., Müller, K., Parra-Nuñez, P., de Snoo, C. B., van de Belt, J., et al. (2019). The Cdk1/Cdk2 homolog CDKA;1 controls the recombination landscape in *Arabidopsis*. *Proc. Natl. Acad Sci. U.S.A.* 116, 12534–12539. doi: 10.1073/pnas.1820753116

Wilkins, A. S., and Holliday, R. (2009). The evolution of meiosis from mitosis. *Genetics* 181, 3–12. doi: 10.1534/genetics.108.099762

Xue, M., Wang, J., Jiang, L., Wang, M., Wolfe, S., Pawlowski, W. P., et al. (2018). The number of meiotic double-strand breaks influences crossover distribution in *Arabidopsis*. *Plant Cell* 30, 2628–2638. doi: 10.1105/tpc.18.00531

Xue, Z., Li, Y., Zhang, L., Shi, W., Zhang, C., Feng, M., et al. (2016). OsMTOPVIB promotes meiotic DNA double-strand break formation in rice. *Mol. Plant* 9, 1535–1538. doi: 10.1016/j.molp.2016.07.005

Xue, Z., Liu, C., Shi, W., Miao, Y., Shen, Y., Tang, D., et al. (2019). OsMTOPVIB is required for meiotic bipolar spindle assembly. *Proc. Natl. Acad. Sci. U.S.A.* 116, 15967–15972. doi: 10.1073/pnas.1821315116

Yang, C., Hamamura, Y., Sofroni, K., Böwer, F., Stolze, S. C., Nakagami, H., et al. (2019). SWITCH 1/DYAD is a WINGS APART-LIKE antagonist that maintains sister chromatid cohesion in meiosis. *Nat. Commun.* 10:1755.

Yang, C., Sofroni, K., Wijnker, E., Hamamura, Y., Carstens, L., Harashima, H., et al. (2020). The *Arabidopsis* Cdk1/Cdk2 homolog CDKA;1 controls chromosome axis assembly during plant meiosis. *EMBO J.* 39:e101625.

Yang, W. C., Ye, D., Xu, J., and Sundaresan, V. (1999). The *SPOROCYTELESS* gene of *Arabidopsis* is required for initiation of sporogenesis and encodes a novel nuclear protein. *Genes Dev.* 13, 2108–2117. doi: 10.1101/gad.13.16.2108

Yin, H., Zhang, X., Liu, J., Wang, Y., He, J., Yang, T., et al. (2009). Epigenetic regulation, somatic homologous recombination, and abscisic acid signaling are influenced by DNA polymerase {epsilon} mutation in *Arabidopsis*. *Plant Cell* 21, 386–402. doi: 10.1105/tpc.108.061549

Yuan, G., Ahootapeh, B. H., Komaki, S., Schnittger, A., Lillo, C., De Storme, N., et al. (2018). PROTEIN PHOSHATASE 2A B' α and β maintain centromeric sister chromatid cohesion during meiosis in *Arabidopsis*. *Plant Physiol.* 178, 317–328. doi: 10.1104/pp.18.00281

Yuan, W. Y., Li, X. W., Chang, Y. X., Wen, R. Y., Chen, G. X., Zhang, Q. F., et al. (2009). Mutation of the rice gene *PAIR3* results in lack of bivalent formation in meiosis. *Plant J.* 59, 303–315. doi: 10.1111/j.1365-313X.2009.03870.x

Zamariola, L., De Storme, N., Vannerum, K., Vandepoele, K., Armstrong, S. J., Franklin, F. C. H., et al. (2014). SHUGOSHINs and PATRONUS protect meiotic centromere cohesion in *Arabidopsis thaliana*. *Plant J.* 77, 782–794. doi: 10.1111/tpj.12432

Zelkowski, M., Olson, M. A., Wang, M., and Pawlowski, W. (2019). Diversity and determinants of meiotic recombination landscapes. *Trends Genet.* 35, 359–370. doi: 10.1016/j.tig.2019.02.002

Zhang, C., Song, Y., Cheng, Z. H., Wang, Y. X., Zhu, J., Ma, H., et al. (2012). The *Arabidopsis thaliana* DSB formation (AtDFO) gene is required for meiotic double-strand break formation. *Plant J.* 72, 271–281. doi: 10.1111/j.1365-313x.2012.05075.x

Zhang, C., Zhang, F., Cheng, X., Liu, K., Tang, J., Li, Y., et al. (2020a). OsATM safeguards accurate repair of meiotic double-strand breaks in rice. *Plant Physiol.* 183, 1047–1057. doi: 10.1104/pp.20.00053

Zhang, F., Ma, L., Zhang, C., Du, G., Shen, Y., Tang, D., et al. (2020b). The SUN domain proteins OsSUN1 and OsSUN2 play critical but partially redundant roles in meiosis. *Plant Physiol.* 183, 1517–1530. doi: 10.1104/pp.20.00140

Zhang, F., Shen, Y., Miao, C., Cao, Y., Shi, W., Du, G., et al. (2020c). OsRAD51D promotes homologous pairing and recombination by preventing nonhomologous interactions in rice meiosis. *New Phytol.* 227, 824–839. doi: 10.1111/nph.16595

Zhang, F., Tang, D., Shen, Y., Xue, Z., Shi, W., Ren, L., et al. (2017). The F-box protein ZYGO1 mediates bouquet formation to promote homologous pairing, synapsis, and recombination in rice meiosis. *Plant Cell* 29, 2597–2609. doi: 10.1105/tpc.17.00287

Zhang, J., Feng, C., Su, H., Liu, Y., Liu, Y., and Han, F. (2020d). The cohesin complex subunit ZmSMC3 participates in meiotic centromere pairing in maize. *Plant Cell* 32, 1323–1336. doi: 10.1105/tpc.19.00834

Zhang, M., Ma, X., Wang, C., Li, Q., Meyers, B. C., Springer, N. M., et al. (2021). CHH DNA methylation increases at 24-PHAS loci depend on 24-nt phased small interfering RNAs in maize meiotic anthers. *New Phytol.* 229, 2984–2997. doi: 10.1111/nph.17060

Zhang, P., Zhang, Y., Sun, L., Sinumporn, S., Yang, Z., Sun, B., et al. (2017). The Rice AAA-ATPase OsFIGNL1 Is essential for male meiosis. *Front Plant Sci.* 8:1639. doi: 10.3389/fpls.2017.01639

Zhang, Y.-L., Zhang, H., Gao, Y.-J., Yan, L.-L., Yu, X.-Y., Yang, Y.-H., et al. (2019). Protein Phosphatase 2A B'α and B'β protect centromeric cohesion during meiosis I. *Plant Physiol.* 179, 1556–1568. doi: 10.1104/pp.18.01320

Zhao, M., Ku, J.-C., Liu, B., Yang, D., Yin, L., Ferrell, T. J., et al. (2021). The *mop1* mutation affects the recombination landscape in maize. *Proc. Natl. Acad. Sci. U.S.A.* 118:e2009475118. doi: 10.1073/pnas.2009475118

Zhao, X. A., Bramsiepe, J., Van Durme, M., Komaki, S., Prusicki, M. A., Maruyama, D., et al. (2017). RETINOBLASTOMA RELATED1 mediates germline entry in *Arabidopsis*. *Science* 356:eaaf6532. doi: 10.1126/science.aaf6532

Zheng, T., Nibau, C., Phillips, D. W., Jenkins, G., Armstrong, S. J., and Doonan, J. H. (2014). CDKG1 protein kinase is essential for synapsis and male meiosis at high ambient temperature in *Arabidopsis thaliana*. *Proc. Natl. Acad Sci. U.S.A.* 111, 2182–2187. doi: 10.1073/pnas.1318460111

Zickler, D., and Kleckner, N. (2015). Recombination, pairing, and synapsis of homologs during meiosis. *Cold Spring Harb. Perspect. Biol.* 7:a016626. doi: 10.1101/cshperspect.a016626

Ziolkowski, P. A., Berchowitz, L. E., Lambing, C., Yelina, N. E., Zhao, X., Kelly, K. A., et al. (2015). Juxtaposition of heterozygous and homozygous regions causes reciprocal crossover remodelling via interference during *Arabidopsis* meiosis. *Elife* 4:e03708.

Ziolkowski, P. A., Underwood, C. J., Lambing, C., Martinez-Garcia, M., Lawrence, E. J., Ziolkowska, L., et al. (2017). Natural variation and dosage of the HEI10 meiotic E3 ligase control *Arabidopsis* crossover recombination. *Genes Dev.* 31, 306–317. doi: 10.1101/gad.295501.116

Conflict of Interest: The authors declare that the research was conducted in the absence of any commercial or financial relationships that could be construed as a potential conflict of interest.

Publisher's Note: All claims expressed in this article are solely those of the authors and do not necessarily represent those of their affiliated organizations, or those of the publisher, the editors and the reviewers. Any product that may be evaluated in this article, or claim that may be made by its manufacturer, is not guaranteed or endorsed by the publisher.

frontiers in Plant Science

ORIGINAL RESEARCH
published: 05 October 2021
doi: 10.3389/fpls.2021.748252

Structural Maintenance of Chromosomes 5/6 Complex Is Necessary for Tetraploid Genome Stability in *Arabidopsis thaliana*

*Fen Yang[1,2], Nadia Fernández Jiménez[3], Joanna Majka[1,4], Mónica Pradillo[3] and Ales Pecinka[1]**

[1] Institute of Experimental Botany, Czech Academy of Sciences, Centre of the Region Haná for Biotechnological and Agricultural Research, Olomouc, Czechia, [2] Department of Cell Biology and Genetics, Faculty of Natural Sciences, Palacký University, Olomouc, Czechia, [3] Department of Genetics, Physiology and Microbiology, Faculty of Biology, Universidad Complutense de Madrid, Madrid, Spain, [4] Institute of Plant Genetics, Polish Academy of Sciences, Poznań, Poland

OPEN ACCESS

Edited by:
Jean Molinier,
UPR 2357 Institut de Biologie Moléculaire des Plantes (IBMP), France

Reviewed by:
Isabelle Colas,
The James Hutton Institute, United Kingdom
Luca Comai,
University of California, Davis, United States

***Correspondence:**
Ales Pecinka
pecinka@ueb.cas.cz

Specialty section:
This article was submitted to Plant Cell Biology, a section of the journal Frontiers in Plant Science

Received: 27 July 2021
Accepted: 06 September 2021
Published: 05 October 2021

Citation:
Yang F, Fernández Jiménez N, Majka J, Pradillo M and Pecinka A (2021) Structural Maintenance of Chromosomes 5/6 Complex Is Necessary for Tetraploid Genome Stability in Arabidopsis thaliana. Front. Plant Sci. 12:748252. doi: 10.3389/fpls.2021.748252

Polyploidization is a common phenomenon in the evolution of flowering plants. However, only a few genes controlling polyploid genome stability, fitness, and reproductive success are known. Here, we studied the effects of loss-of-function mutations in NSE2 and NSE4A subunits of the Structural Maintenance of Chromosomes 5/6 (SMC5/6) complex in autotetraploid *Arabidopsis thaliana* plants. The diploid *nse2* and *nse4a* plants show partially reduced fertility and produce about 10% triploid offspring with two paternal and one maternal genome copies. In contrast, the autotetraploid *nse2* and *nse4a* plants were almost sterile and produced hexaploid and aneuploid progeny with the extra genome copies or chromosomes coming from both parents. In addition, tetraploid mutants had more severe meiotic defects, possibly due to the presence of four homologous chromosomes instead of two. Overall, our study suggests that the SMC5/6 complex is an important player in the maintenance of tetraploid genome stability and that autotetraploid Arabidopsis plants have a generally higher frequency of but also higher tolerance for aneuploidy compared to diploids.

Keywords: SMC5/6 complex, polyploidy, seed development, meiosis, *NSE2*, genome stability

INTRODUCTION

Maintenance of genome stability is essential for ensuring plant growth, fertility, and proper genomic constitution of the offspring (Roy, 2014; Hu et al., 2016). The family of Structural Maintenance of Chromosomes (SMC) complexes includes ATP-dependent molecular machines with a unique ability to process chromosome-scale DNA molecules (Uhlmann, 2016). The SMC5/6 complex is an evolutionarily conserved member of the SMC family that is involved in DNA damage repair, DNA replication, and cell divisions (Kegel and Sjögren, 2010; Aragón, 2018). The core part of the complex consists of SMC5 and SMC6 protein heterodimer, where the subunits are attached via their hinge domains. SMC6 has two partially functionally redundant paralogs in Arabidopsis. Both play roles under ambient conditions, but only SMC6B takes place in DNA damage repair (Watanabe et al., 2009; Yan et al., 2013; Zou et al., 2021). Opposite to the hinge domains are the head domains,

where the NON-SMC ELEMENT (NSE) NSE1-NSE3-NSE4 subcomplex bridges the SMC heterodimer. Here, the kleisin type protein NSE4 closes the SMC ring by interacting with both SMC5 and SMC6 subunits (Palecek and Gruber, 2015). The NSE1 and NSE3 subunits regulate the conformation of NSE4. While *NSE1* and *NSE3* are single-copy genes in Arabidopsis, there are two NSE4 paralogs (NSE4A and NSE4B) that show distinct expression patterns and functions (Díaz et al., 2019). The NSE2 subunit is attached to the coiled-coil region of SMC5 and is one of the two E3 SUMO ligases in Arabidopsis (Ishida et al., 2012). Additionally, plant-specific SMC5/6 subunits ARABIDOPSIS SNI1 ASSOCIATED PROTEIN 1 (ASAP1) and SUPPRESSOR OF NPR1-1; INDUCIBLE 1 (SNI1) have been described (Yan et al., 2013). ASAP1 and SNI1 were proposed to be functionally homologous to the yeast SMC5/6 complex chromatin-loader subunits NSE5 and NSE6.

SMC5/6 complex controls multiple biological processes in plants. There is solid evidence that the SMC5/6 complex is important for the repair of specific types of DNA damage in Arabidopsis (Mengiste et al., 1999; Watanabe et al., 2009; Yuan et al., 2014; Díaz et al., 2019). This may be mainly due to its essential role in homologous recombination (HR) where the loss of function from SMC6B results in reduced HR levels (Mengiste et al., 1999; Watanabe et al., 2009). NSE2 function is not essential for Arabidopsis survival, but the plants are strongly affected in their vegetative and generative development including poor growth of roots, earlier flowering, reduced height, and decreased fertility (Huang et al., 2009; Ishida et al., 2009; Xu et al., 2013; Liu et al., 2014; Kwak et al., 2016). Recently, several studies pointed toward the importance of the SMC5/6 complex during plant sexual reproduction, including meiosis, pollen viability, and seed development (Liu et al., 2014; Díaz et al., 2019; Yang et al., 2021; Zou et al., 2021). NSE2, NSE4, and SNI1 were found to play an important role in meiosis. NSE4A was localized to the synaptonemal complex and the mutants showed chromosome fragmentation and frequent meiotic irregularities (Zelkowski et al., 2019). At least part of this trait seems due to the role of SMC5/6 in the regulation of meiotic recombination. Here, RAD51 directly suppresses the SMC5/6 complex to promote DMC1-based recombination (Chen et al., 2021). Another role of the SMC5/6 complex is to secure the development of properly reduced haploid gametes in meiotic recombination independent manner (Yang et al., 2021). The NSE2, NSE4A, and SNI1 mutants show recombination-independent problems in chromosome segregation and produce unreduced microspores. Fertilization with diploid pollen leads to abnormal seed development in these mutants. This is most likely due to an unbalanced parental dosage with two maternal and two paternal genome copies in the endosperm (Jullien and Berger, 2010). An excess of paternal genetic information leads to seed overgrowth and the absence of cellularization, which frequently results in seed abortion (Köhler et al., 2012). Some of such abnormal seeds still survive and produce polyploid (triploid) offspring.

Polyploidization, i.e., whole genome duplication, is a common phenomenon in higher plants, and both autopolyploids and allopolyploids often occur in nature. Polyploidization plays a significant role in the evolution of Angiosperms as the major mechanism providing raw material for gene sub- and neofunctionalization (Van De Peer et al., 2009). However, newly established polyploids can experience genomic shock represented by changes at genomic, chromosome, and gene levels (reviewed in Comai, 2005). This includes genome downsizing, structural chromosome rearrangements, amplification and/or reactivation of repetitive elements, modifications of the gene expression patterns, and rapid sequence changes in multigene families, such as rDNAs. Polyploidization often leads to altered morphology compared to the ancestral lines and in autotetraploid occasionally also to developmental abnormalities and/or reduced fertility. One of the major challenges in tetraploids is thought to be the more complex meiosis due to the presence of the four nearly identical (homologous chromosomes, autopolyploids) or similar (homeologous chromosomes, allopolyploids) copies of chromosomes. In both types of polyploids, natural selection should favor strategies to control pairing preferences that result in disomic inheritance and proper segregation of genetic material during meiosis. This is true in Arabidopsis, where auto- and allotetraploids show strict homologous chromosome pairing (Pecinka et al., 2011). The elimination of certain sequences, chromosome rearrangements, and dysploidy seem to contribute to the meiotic cytological diploidization (Mandáková and Lysak, 2018). Since it is a long process, intermediate situations with different chromosomes showing different rates of bivalent formation (tetrasomic inheritance for some chromosomes and disomic inheritance for others) are possible (Santos et al., 2003). Recently, it has been found that particular alleles of the meiotic chromosome pairing genes *ASY1* and *ASY3* lead to a reduced number of quadrivalents compared to bivalents in tetraploid *Arabidopsis arenosa* (Morgan et al., 2020; Seear et al., 2020), indicating an evolutionary selection toward specific tetraploid meiotic phenotypes.

Despite these findings, it remains largely unknown whether tetraploid mutants of meiotic genes show diploid-like or new phenotypes. This may contribute to a better understanding of their role in meiosis. Here, we analyzed the consequences of polyploidy in the SMC5/6 complex mutants and show that autotetraploid plants of two SMC5/6 complex mutants *nse2* and *nse4a* display several characteristics that differ from their diploid cytotypes.

MATERIALS AND METHODS

Plant Materials and Growth Conditions

All strains used in this study were in Columbia-0 (Col-0) background. We used following mutants (diploid): *nse2-1/hpy2-1*, *nse4a-2* (GK-768H08), and *qrt1-4* (SALK_024104C). *nse2-1* is an ethyl methanesulfonate (EMS) mutant allele that was isolated in the laboratory of Prof. Keiko Sugimoto, RIKEN Center for Sustainable Resource Science, Japan. Other T-DNA insertion mutants were collected from the Salk Institute Genomic Analysis Laboratory (SiGnAL[1]; Alonso et al., 2003),

[1]http://signal.salk.edu/cgi-bin/tdnaexpress

and provided by the Nottingham Arabidopsis Stock Centre (NASC). Genotyping of T-DNA mutant was performed by PCR with a combination of three primers, T-DNA specific primers: LBb1.3 (5′-ATTTTGCCGATTTCGGAAC-3′) for *qrt1-4*; o84747_m (5′-ATAATAACGCTGCGGACATCTAC-3′) for *nse4a-2*, and two specific primers for the corresponding gene: LPNSE4A-2 (5′-GCTCAACAGGCGGTCATTTG-3′) and RPNSE4A-2 (5′-ACAAAAGCCACTTAACTGCTACA-3′); LPQRT1-4 (5′-TCTCTTCCCAGAAAAGGCTTC-3′) and RPQ RT1-4 (5′-CGTGGGTCTCAAGAATCTTTG-3′); *nse2-1* plants were selected based on the mutant features (Ishida et al., 2009). Double mutants were generated by crossing and selection in F_2 and F_3 generations. All lines were used as homozygotes unless stated otherwise.

Data related to diploid controls were published in a separate study (Yang et al., 2021). Both diploid and tetraploid plants were cultivated under the same growth conditions. Tetraploid *A. thaliana* plants were generated by submerging 2 weeks old *in vitro* grown diploid plants in 0.1% (w/v) colchicine (Sigma-Aldrich) in dark at room temperature for 1 h. Subsequently, plants were gently washed with copious amounts of tap water, transplanted to soil, and grown until maturity. Seeds were collected from individual plants, 20–30 biggest seeds were manually selected and propagated into plants for ploidy measurements (see below).

For *in vitro* growth, Arabidopsis seeds were surface sterilized (70% ethanol with 0.5% TritonX-100 v/v) for 10 min and washed three times with sterile water. Dried seeds were sown on 0.5 × Murashige and Skoog (MS) agar medium, stratified in dark for 2 days at 4°C and then cultivated in a climatic chamber (Percival) under 16 h light/8 h dark cycle, 21°C day and 19°C night temperature. For cultivation in soil, 2-week-old diploid or tetraploid seedlings were transplanted to the moist soil after ploidy measurements, then the pots were moved to an air-conditioned chamber with controlled long-day conditions (16 h light/8 h dark cycle, 21°C day and 19°C night temperature, 150 μmol photons m^{-2} s^{-1} light intensity provided by white-light tubes).

Ploidy Measurements and Flow Cytometry

For tetraploid selection, plants grown from the big seeds produced by colchicine-treated plants were used. To determine the somatic ploidy levels, 1–2 young leaves were chopped with a razor blade in 500 μL Otto I solution (0.1M citric acid, 0.5% Tween 20 v/v). The nuclear suspension was filtered through 50 μm nylon mesh and stained with 1 mL of Otto II solution (0.4M $Na_2HPO_4{\cdot}12H_2O$) containing 2 μg DAPI (4′,6-diamidino-2-phenylindole). The ploidy was analyzed on a Partec PAS I flow cytometer with diploid WT plants used as an external standard. For the offspring ploidy measurements, seeds were collected per silique and all seeds per silique were sown (this avoids selection bias occurring when seed are collected per whole plant and the shrunk seeds are typically lighter and less round – thus often coming late during standard sowing procedures) and analyzed as described above.

Hoyer's Clearing

Flowers with green or white closed anthers were manually emasculated. Two days later, ovules were dissected and cleared by Hoyer's solution as described (Liu and Meinke, 1998) with modifications. Dissolve 25 g Arabic gum in 25 mL distilled water in a glass beaker by heating to 60°C and stirring with a magnetic stirrer for about 1 h under a fume hood. Add 100 g chloral hydrate and keep dissolving until the solution will be clear and have an amber color. Subsequently add 10 mL glycerol, mix and keep the solution in dark at room temperature. Dissect ovules on a clear microscopic slide, add 20 μl Hoyer's solution and mount with a 24 × 40 mm coverslip without applying a pressure. The slides were kept at 4°C overnight (or longer) and examined with an inverted microscope Olympus IX 83 using differential interference contrast (DIC) optics.

Pollen Viability Assays

Fluorescein diacetate (FDA)-buffer mixture was prepared as described: 1 μL FDA (Sigma-Aldrich) stock solution (2 mg/mL in acetone) was added to 1 mL of BK buffer [0.127 mM Ca(NO3)2·4H2O, 0.081 mM MgSO4·7H2O, 0.1 mM KNO3, 15% Sucrose w/v and 10 mM MOPS, pH 7.5]. 20 μL FDA-buffer mixture was dripped to a microscopic slide then one opened flower was dropped into the FDA-buffer mixture and covered with 24 × 40 mm coverslip carefully. Data for pollen viability analysis were collected from at least three plants per genotype. The fluorescein fluorescence was observed after 20 min of staining using an inverted microscope Olympus IX 83: at 543/620 nm excitation/emission wavelengths and the same region was photographed with DIC optics to get the number of all pollen grains. ImageJ was used to merge the DIC and fluorescein channels.

Cytological Experiments

The fixation of flower buds and chromosome spreads were carried out as described (Sánchez Moran et al., 2001), including minor modifications to adapt the protocol for the study of autopolyploids (Parra-Nunez et al., 2020). Data for cytological analyses were collected from at least three plants per genotype. Meiocytes were analyzed with an Olympus BX-61 epifluorescent microscope and images were captured with an Olympus DP-71 digital camera (Olympus, Germany). Using x100 magnification oil immersion objective resulted in an ultra-high image resolution of 4080 × 3072 and 46.40 pixels/μm. Manual mode was selected to allow the preferred image brightness to be set by clicking and dragging the slider positioned in the exposure time. The images were captured in grayscale and edited in Adobe Photoshop.

For mitotic chromosome number counting, fresh inflorescences were fixed in ethanol: chloroform: acetic acid (6:3:1) solution overnight at room temperature then enzymatically digested in 0.3% (w/v) cellulase Onozuka R-10 (Serva, Germany, catalog no. 1641903), cytohelicase from *Helix pomatia* (Sigma-Aldrich, St. Louis, catalog no. C8274) and pectolyase from *Aspergillus japonicus* (Sigma-Aldrich, St. Louis, catalog no. P3026) for 3 h at 37°C. After the enzymatic digestion, single flower buds were dissected and chopped

in 60% acetic acid and slides were placed on the heating block for 2 min at 50°C. Then, cells on slides were fixed in Carnoy's fixative. Chromosomes were counterstained with DAPI 1.5 μg/mL (Vector Laboratories, United States). All slides were examined with Axio Imager Z.2 Zeiss microscope (Zeiss, Germany) equipped with Cool Cube 1 camera (Metasystems, Germany). We used ×60 and ×100 objectives and filter for DAPI (emission spectrum '405 nm). Scale bars were adjusted to the objective that was applied. Image processing was carried out using ISIS software 5.4.7 (Metasystems, Germany) and Adobe Photoshop software (CS5).

Software

Microsoft Office Excel 2016, PowerPoint 2016, GraphPad Prism 8.2.1, ImageJ 1.52p, Adobe Photoshop CS5 and Illustrator were used for graph and image composition.

RESULTS

Tetraploidy Enhances Fertility Defects in *nse2-1* and *nse4a-2* Plants

The diploid (2x) Arabidopsis *nse2* mutant plants have a significantly reduced fertility (Liu et al., 2014; Yang et al., 2021). To analyze the dosage-dependent role of *NSE2*, we produced autotetraploid wild-type (4x WT) and *nse2-1* (4x *nse2-1*) plants (Yang et al., 2021). With these lines, we noticed that 4x *nse2-1* plants had a reduced root length in the juvenile stage and a lower plant height at the adult stage compared with 4x WT (**Figures 1A,B**). The same differences were observed also between 2x *nse2-1* and 2x WT plants (**Figures 1A,B**), but both 4x WT and 4x *nse2-1* plants were bigger and had longer roots. In contrast, the siliques from 4x *nse2-1* were thicker but shorter than those of 2x *nse2*-1, possibly indicating that the autotetraploidy increases the seed size but enhances fertility defects of *nse2-1*, respectively (**Figure 1C**).

To further explore this observation, we analyzed the seed traits of 4x WT and mutant plants. We included also tetraploid *nse4a-2* (4x *nse4a-2*) because *NSE4A* is another subunit of SMC5/6 complex whose loss-of-function plants have fertility defects (Díaz et al., 2019). Dry seeds from 4x WT plants were larger than those from diploid WT (2x WT), but both were regular in shape and had a normal light brown color (**Figure 2A**). In contrast, both 2x and 4x mutants produced seeds with a variable shape, size, and color, including very large or little seeds, shrunk, and colored from normal to dark brown (**Figure 2A**). Analysis of siliques 13 days after self-pollination (DAP) revealed that 4x WT produced 84.3% normal seeds, 10.2% aborted ovules and 5.5% abnormal seeds (plants/siliques/seeds = 3/15/899, **Figures 2B,C** and **Table 1**). Equally old 4x *nse2-1* and 4x *nse4a-2* plants showed 11.6 and 51.8% normal seeds, 72.6 and 31.1% aborted ovules, and 15.8 and 17.1% abnormal seeds (plants/siliques/seeds = 3/15/739 and 3/15/843, respectively; **Figures 2B–D** and **Table 1**). Hence, the frequencies of both aborted ovules and abnormal seeds were significantly increased in 4x mutants compared to 4x WT (Fisher's exact test, $P < 0.00001$; **Figures 2C,D** and **Supplementary Table 1**). In addition, the comparison of the traits in 4x mutants relative to the 2x mutants (data from Yang et al., 2021) revealed that the ovule abortion and seed abnormality were statistically significantly more pronounced in the 4x *nse2-1* compared to the 2x mutant plants (Fisher's exact test, $P < 0.001$, **Supplementary Table 2**). This suggested ploidy-dependent fertility defects in tetraploid *nse2-1* mutants. However, no significant difference in the frequency of abnormal seeds was found for the 4x and 2x *nse4a-2* plants (Fisher's exact test, $P = 0.4299$; **Supplementary Table 2**). It may be because *nse4a-2* is a partial loss-of-function allele (Díaz et al., 2019).

To test for the contribution of the parents to the abnormal seeds, we performed reciprocal crosses between 4x WT and 4x mutant plants. When 4x WT plants were fertilized by either 4x *nse2-1* or 4x *nse4a*-2, we observed 11.0 and 15.1% abnormal seeds 13 DAP (plants/siliques/seeds = 3/15/691 and 3/14/802, respectively; **Figures 2B–D** and **Table 1**). On contrary, when 4x WT was used to pollinate 4x *nse2-1* or 4x *nse4a-2,* there were only 6.9 and 3.5% abnormal seeds found (plants/siliques/seeds = 3/15/607 and 3/15/722, respectively). This generally matched 5.5% such seeds in self-pollinated 4x WT (plants/siliques/seeds = 3/15/899; **Figures 2B–D** and **Table 1**) and was significantly less than in the above mentioned reciprocal crosses (Fisher's exact test, $P < 0.05$; **Supplementary Table 1**). This suggests that the abnormal seed development is caused predominantly paternally, and to a minor extent also maternally, in 4x *nse2-1* and 4x *nse4a-2* mutants.

Tetraploid *nse2* Leads to Defects in Both Male and Female Gametophytes

Previously, we showed that 2x *nse2-2* mutations cause ovule lethal defects (Yang et al., 2021). In contrast, the genetic material of the diploid microspores was at least partially transmissible and resulted in abnormal seed development. Here, we analyzed the female and male gametophyte development in the context of 4x *nse2-1* mutant plants.

First, we inspected the female gametophyte development (**Table 1**). In crosses where 4x *nse2-1* was used as a mother, we found 42.5% aborted ovules. This suggests that 4x *nse2* has a pre-zygotic maternal dysfunction. To determine a possible source of this defect, we analyzed the morphology of 54 embryo sacs in 2x and 104 in 4x *nse2-1* plants, respectively. In 2x *nse2-1*, there were 13.0% (7 out of 54) WT-like embryo sacs, 38.9% (21 out of 54) ovules without embryo sacs, 22.2% (12 out of 54) embryo sacs without nucleus and 25.9% embryo sacs with three nuclei (14 out of 54). In 4x *nse2-1*, only 4.8% of ovules (5 out of 104) carried WT-like embryo sacs (with a smaller egg cell nucleus and larger central cell nucleus positioned closer and more distant to the micropylar pole, respectively) and the majority of the ovules (95.2%; 99 out of 104) showed diverse defects (**Figure 3**). In total, 72.1% (75 out of 104) ovules fully lacked an embryo sac or it was without detectable nuclei (**Figures 3B,C**). In 23.1% (24 out of 104) of the ovules, embryo sacs contained nuclei, but they deviated from the WT parameters. There was only one nucleus, three nuclei, or occasionally also two nuclei that were abnormally positioned (**Figures 3D–G**). This suggests that tetraploidy in combination with *nse2-1* mutation results in severe female pre-zygotic sterility,

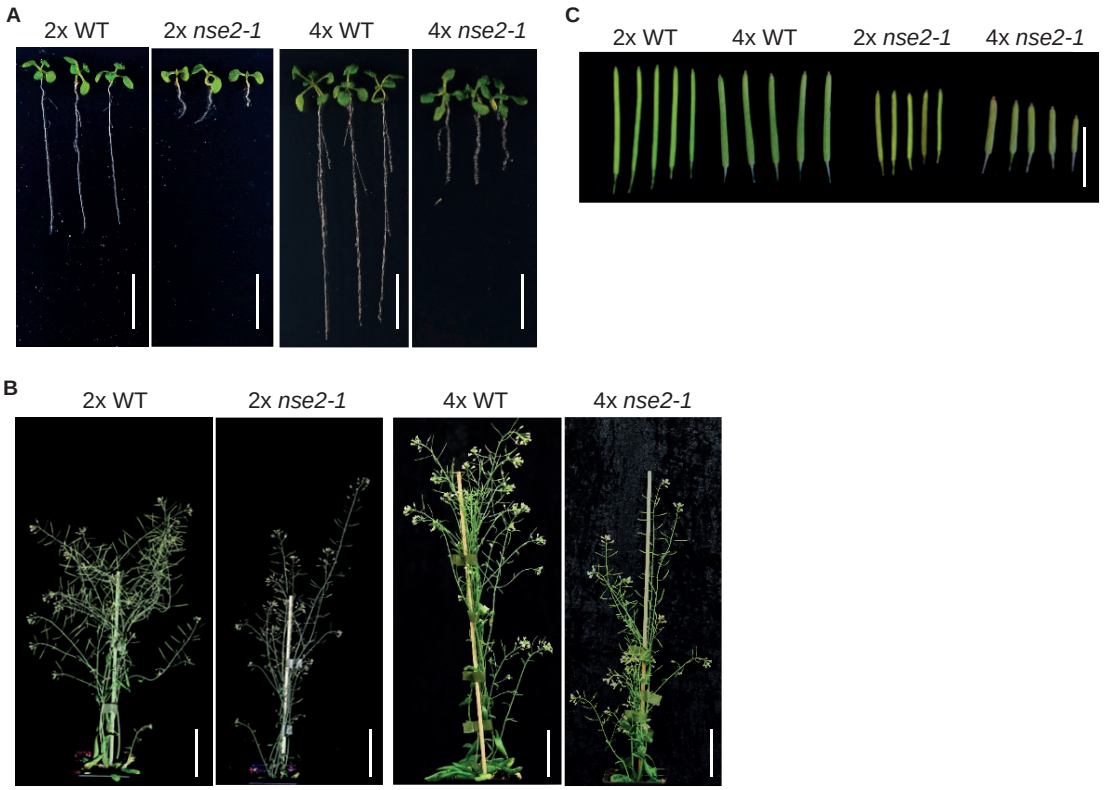

FIGURE 1 | Developmental phenotype of diploid (2x) and tetraploid (4x) WT and *nse2-1* plants. **(A)** The phenotype of 2-weeks-old *in vitro* grown seedlings. Scale bar = 1 cm. **(B)** The whole plant phenotype of 5-week-old plants. Scale bars = 5 cm. **(C)** Representative siliques of the analyzed genotypes. Scale bar = 1 cm.

but at least some of the embryo sacs with abnormal nuclei can be fertilized.

Second, we assessed several male gametophyte traits. Using fluorescein diacetate (FDA) assay, we quantified the microspore viability. This revealed 29.4% (375 out of 1275) viable pollen in 4x *nse2-1* which was significantly less than 62.2% (941 out of 1512, Fisher's exact test, $P < 0.00001$) of such pollen in 4x WT plants (**Figures 4A,B**). It has to be noted that both 4x WT and *nse2-1* had also significantly less viable pollen compared to 2x WT and 2x *nse2-1* (95.3 and 65.0%, respectively; based on published data of Yang et al. (2021); Fisher's exact test, $P < 0.00001$) grown under the same cultivation conditions (**Supplementary Table 3**).

The 4x WT and 4x *nse2-1* genotypes used in this study were produced in the *qrt1-4* mutant background and were representing 4x WT *qrt1-4* single and 4x *nse2-1 qrt1-4* double mutants. The *qrt1* mutations cause a stable association of the microspores arising from one meiosis which allows scoring for a constitution of the male meiotic products and also for abnormally developed (small and shrunk) microspores (Preuss et al., 1994). In 4x *nse2-1 qrt1-4*, we found 32.5% (414 out of 1275) shrunk microspores (**Figure 4A**, arrows), which is similar with the 27% in 2x *nse2-1 qrt1-4* plants (**Figure 4C**). However, both 4x and 2x WT *qrt1-4* plants showed much lower frequencies (5.0 and 0.7%, **Figure 4C**) of shrunken microspores in our experiments (75 out of 1512 and 4 out of 575, respectively; **Figure 4A**, arrows; **Supplementary Table 4**). This suggests that 4x WT plants have a seven-fold higher frequency of pollen abortion compared to the 2x WT and the pollen abortion rate remained similarly high in the mutants irrespective of their ploidy. Finally, we scored how many microspores were produced from one meiotic division (irrespective of their viability and shape). All meiotic products were tetrads in 4x WT *qrt1-4*, indicating that these plants undergo normal reductional division. On contrary, 4x *nse2-1* plants produced less than half (40.4%) of microspores in tetrads (**Figure 4D**). The remaining meiotic products were monads (9.6%), dyads (37.8%), triads (11.2%), and rarely even pentads (1.1%). This suggests abnormal meiosis in 4x *nse2* with the possible absence of the reductional divisions (monads to triads) or multipolar spindle (pentads).

Taken together, our results showed that 4x *nse2* plants produce a high number of abnormal male and female gametes.

Defective Male Meiosis Leads to Unreduced and Aneuploid Microspores in 4x *nse2-1* Plants

Meiotic progression in 2x *nse2* pollen mother cells takes place normally at prophase I. During metaphase I five bivalents are formed, but they are more stretched and elongated than in 2x WT. At anaphase I, chromosome fragments are present in most cells. During second meiotic division different problems are revealed such as non-reduced nuclei, extensive

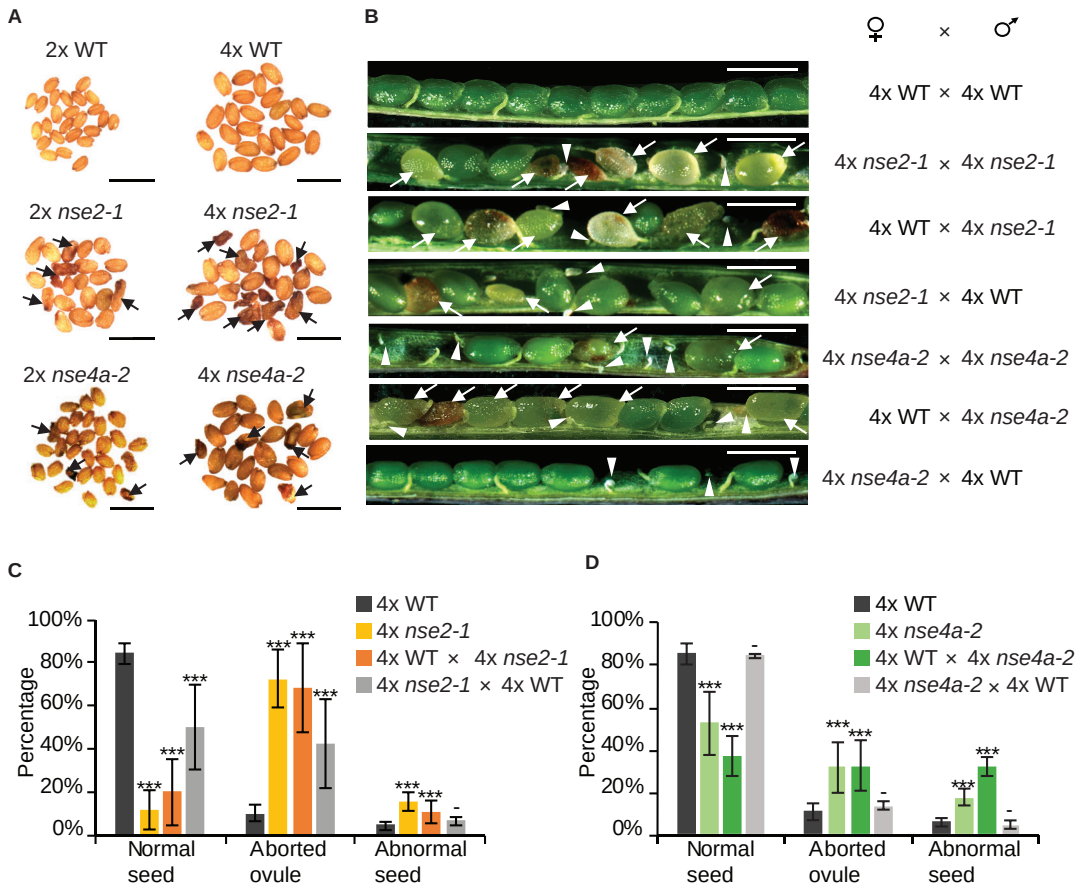

FIGURE 2 | Reduced fertility of tetraploid *nse2-1* and *nse4a-2* plants. **(A)** Representative dry seeds of diploid (2x) and tetraploid (4x) WT, *nse2-1*, and *nse4a-2* plants. Arrows indicate examples of shrunken seeds. Scale bars = 1 mm. **(B)** Opened siliques 13 days after pollination (DAP). Aborted ovules are marked with arrowheads and abnormal seeds (typically shrunk, brown/pale, or partially transparent) with arrows. Scale bar = 1 mm. **(C,D)** Frequencies of normal seeds (NS), aborted ovules (AO) and abnormal seeds (AS) in manually pollinated 4x WT, 4x *nse2-1*, and 4x *nse4a-2* plants and their F1 reciprocal crosses. Error bars represent standard deviation among the means of three individual plants. Significance in Fisher's exact test relative to 4x WT in the given group (NS, AO, AS): – = $P > 0.05$, * = $P < 0.05$, ** = $P < 0.01$, and *** = $P < 0.001$. Source values and basic counts are provided in **Supplementary Table 1**.

chromosome fragmentation, and chromosome bridges, among others (Yang et al., 2021).

Similar to the situation in 2x *nse2*, we found no apparent differences between 4x *nse2-1* and 4x WT plants at prophase I. In both genetic backgrounds, we observed nearly complete synapsis at pachynema with some unsynapsed regions due to the presence of synaptic partner switches produced by multivalent associations involving three or even four chromosomes (**Figures 5A,B**, arrowheads). At metaphase I, the different multivalent associations in tetraploids depend on the pattern of CO formation among the four homologous chromosomes. In 4x WT plants, we observed bivalents and quadrivalents, but occasionally also trivalents and univalents (**Figure 5A**, arrowheads). In 4x *nse2-1* plants, we did not detect apparent differences in chromosome associations from WT, with bivalent and quadrivalent associations also being the majority (**Figure 5B**). Nevertheless, the frequency of cells with univalents was twice (14.81%, 4 out of 27) that of the WT (7.30%, 6 out of 82). Chromatin did not appear normal either, due to the frequent presence of constrictions and even fragments, which was similar to the observations in 2x *nse2* plants (Yang et al., 2021). During anaphase I and telophase I, chromosomal fragmentation increased, spanning the region between the segregating chromosomes, being evidenced in all 45 cells analyzed (**Figure 5B**). During these stages, we did not observe fragmentation in 4x WT plants in any case and we only detected chromosome laggards in one of the cells analyzed (6.25%, 1 out of 16) (**Figure 5A**, bottom row, arrows).

In the second meiotic division, the defects in 4x *nse2-1* plants were more drastic than in the first meiotic division, as a result of an accumulation of errors (**Figures 5B,C**). Meiotic irregularities were detected in almost all analyzed cells (93.0%, 40 out of 43), namely: (i) chromosome fragmentation (27.9%), (ii) chromatin bridges (23.3%), (iii) abnormal segregation (13.9%), (iv) meiocytes with several problems including chromosomal bridges and fragments (16.3%), and (v) non-reduced meiocytes (11.6%). In contrary, only 68.75% of the meiocytes have second meiotic division defect in 2x *nse2* pollen mother cells (Yang et al.,

TABLE 1 | Seed phenotype of self-pollinated and reciprocally crossed between tetraploid (4x) WT, *nse2-1*, and *nse4a-2* plants.

Mother	Father	Events (n)	Trait (%)		
			Normal seeds	Aborted ovules	Abnormal seeds
4x WT	4x WT	899	84.3	10.2	5.5
4x *nse2-1*	4x *nse2-1*	739	11.6	72.5	15.8
4x WT	4x *nse2-1*	691	20.3	68.7	11.0
4x *nse2-1*	4x WT	607	50.6	42.5	6.9
4x *nse4a-2*	4x *nse4a-2*	843	51.8	31.1	17.1
4x WT	4x *nse4a-2*	802	53.2	31.7	15.1
4x *nse4a-2*	4x WT	722	83.4	13.2	3.5

TABLE 2 | Flow cytometry-based ploidy levels of F1 offspring plants from tetraploid (4x) WT, *nse2-1*, and *nse4a-2* parents.

Genotype		Germination rate (%)	Events (n)	Ploidy (%)				
Mother	Father			Euploid		Aneuploid		
				4x	6x	Total	+	−
4x WT	4x WT	72.7%	120	96.7	0.0	3.3	100.0	0.0
4x *nse2-1*	4x *nse2-1*	48.7%	92	32.6	19.6	47.8	70.5	29.5
4x WT	4x *nse2-1*	66.3%	163	75.4	8.6	16.0	88.5	11.5
4x *nse2-1*	4x WT	84.9%	247	84.2	1.2	14.6	69.4	30.6
4x *nse4a-2*	4x *nse4a-2*	89.1%	196	85.2	6.6	8.2	68.8	31.2
4x WT	4x *nse4a-2*	55.8%	91	91.2	4.4	4.4	100.0	0.0
4x *nse4a-2*	4x WT	88.6%	124	93.5	0.0	6.5	75.0	25.0

4x = tetraploid, 6x = hexaploid. + = DNA gain, − = DNA loss.

2021). In 4x WT plants, the irregularities were also detected in a low percentage of meiocytes (8.6%, 13 out of 150) during the second meiotic division (**Figure 5C**). On contrary to 4x *nse2-1*, chromosomal bridges or fragments were never observed in 4x WT plants. However, they displayed incorrect segregation of one or two chromosomes (possibly due to the formation of univalents and multivalents in metaphase I).

At the end of the meiotic division, only tetrads (n = 134) with apparently balanced nuclei were observed in 4x WT plants (**Figures 5A,D**), although we cannot exclude occasional aneuploidies (as a consequence of improper segregation during the second meiotic division). These aneuploidies would only affect one or two chromosomes. In 4x *nse2-1* plants, we observed dyads (54.3%, 44 out of 81), triads (3.7%, 3 out of 81), tetrads (35.8%, 29 out of 81), and even tetrads with micronuclei (6.17%, 5 out of 81) (**Figures 5B,D**). In 2x *nse2* plants the tetrads represented 49.2% and no micronuclei were observed (Yang et al., 2021). In summary, analysis of meiosis in 4x *nse2-1* plants revealed that the defects during later stages of meiosis were enhanced compared to 2x *nse2-1* plants.

Tetraploid *nse2-1* and *nse4a-2* Plants Produce Aneuploid Offspring

The spectrum of meiotic defects in 4x *nse2-1* plants prompted us to analyze the ploidy levels of their progeny by flow cytometry. Among the offspring from self-pollinated 4x WT plants (n = 120), we found 96.7% tetraploids (117 out of 120) and 3.3% (3 out of 120) putative aneuploids (**Table 2**). The three putative aneuploid WT plants showed minimal shifts of the flow cytometry peaks relative to the known tetraploid control. This is in contrast with an earlier study which showed that natural and synthetic 4x WT Arabidopsis plants produced about 30% aneuploid progeny (Henry et al., 2006). Since Henry and colleagues used more sensitive detection methods and also pointed to a lower sensitivity of flow cytometry to detect single chromosome addition/loss genotypes, our frequencies are most likely an underestimation.

Among 92 plants derived from self-pollinated 4x *nse2-1*, we found 32.6% tetraploids (30 out of 92), 47.8% putative aneuploids (44 out of 92), and 19.6% hexaploids (18 out of 92) (**Table 2** and **Figure 6**). The hexaploids were most likely a product of a fusion of one reduced and one unreduced gamete. The flow cytometry analysis of the aneuploid mutant plants indicated that 70.5% (31 out of 44) gained and 29.5% (13 out of 44) lost one or more chromosomes (**Table 2**). In the self-pollinated 4x *nse4a-2* (n = 196), we found 85.2% tetraploids (167 out of 196), 8.2% putative aneuploids (16 out of 196), and 6.6% hexaploids (13 out of 196) (**Table 2**). Similar to 4x *nse2-1*, about two-thirds (68.7%) of the putative aneuploids gained and one-third (31.3%) lost one or more chromosomes (**Table 2**).

To confirm the aneuploidy, we performed cytology analysis on the selected candidates that appeared to have either extra or missing chromosomes (**Figure 5C**). To address the parental contribution to the ploidy changes in the progeny, we performed reciprocal crosses between 4x WT and 4x *nse2* plants and analyzed the ploidy of the resulting plants (**Table 2**). The

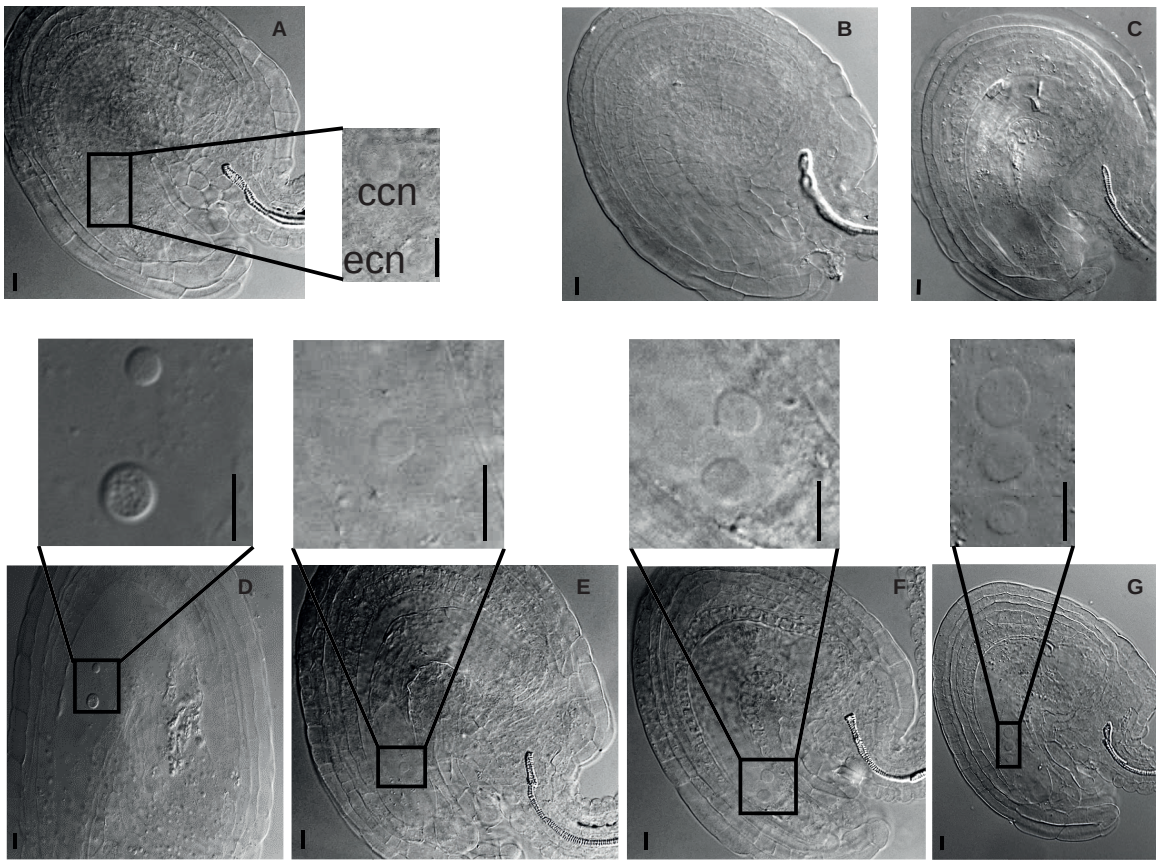

FIGURE 3 | Developmental defects in female gametophyte of tetraploid *nse2-1*. Cleared ovules from 4x *nse2-1* were observed under a differential interference contrast microscope. The nuclei are marked with dashed circles and arrows. Scale bars = 10 μm. **(A)** A typical 4x WT-like embryo sac showing one egg cell nucleus (ecn) and one central cell nucleus (ccn). **(B–G)** 4x *nse2-1* ovules displaying specific defects: **(B)** absence of embryo sac and **(C)** embryo sacs **(C)** without nuclei, **(D)** with two nuclei at the abnormal position, **(E)** only one nucleus, **(F)** two equally size nuclei, and **(G)** one smaller nucleus and two bigger nuclei.

hexaploidy was caused 7.2-fold more frequently by the unreduced paternal over the maternal 4x *nse2-1* gametes (8.6 versus 1.2%, respectively; **Table 2**). In contrast, the aneuploidy was caused equally by the paternal (15.3%) and the maternal (14.2%) 4x *nse2-1* gametes (**Table 2**). We found similar trends for the induction of hexaploidy and aneuploidy in the progeny of 4x *nse4a-2*. There were 4.0% hexaploids in 4x WT × 4x *nse4a-2* crosses versus 0% hexaploids in reciprocal crossing direction (**Table 2**). The aneuploid offspring arose almost equally from both paternal and maternal gametes (4.4 and 6.5%, respectively; **Table 2**).

Hence, the 4x SMC5/6 complex mutants produce higher-polyploid and also aneuploid offspring from both parents.

DISCUSSION

Here, we analyzed the effects of polyploidy on the genome stability and reproductive success in the background of autotetraploid Arabidopsis SMC5/6 complex deficient mutants. Most of our experiments focused on *NSE2*, which encodes an important, but in Arabidopsis non-essential, E3 SUMO ligase subunit of the SMC5/6 complex (Ishida et al., 2009). For a subset of experiments, we analyzed also *NSE4A*, as the kleisin subunit of the SMC5/6 complex that is active in both somatic and reproductive tissues and is essential for plant survival (Díaz et al., 2019). The strong loss-of-function alleles of *NSE4A* are lethal in Arabidopsis and the *nse4a-2* allele used here is a partial loss-of-function mutant. This is in agreement with our observations that the defects of both mutants are similar, but those of *nse4a-2* plants are generally weaker.

The SMC5/6 complex has multiple functions during meiosis. It is required for the repair of SPO11-induced DNA double-strand breaks and its absence produces a severe chromosome fragmentation due to the presence of entanglements and concatenations generated as a consequence of an accumulation of joint molecules (JM) (Copsey et al., 2013; Xaver et al., 2013; Menolfi et al., 2015). A recent study from Arabidopsis also suggested that RAD51 restrains the SMC5/6 complex from inhibiting the activity of meiotic recombinase DMC1 (Chen et al., 2021). In addition, *nse2* mutants generate diplogametes (Yang et al., 2021). The non-reduced nuclei result from cells with an abnormal spindle organization in which organelles are not organized in a defined band after telophase I. Interestingly, this trait is recombination-independent. In this study, we analyzed

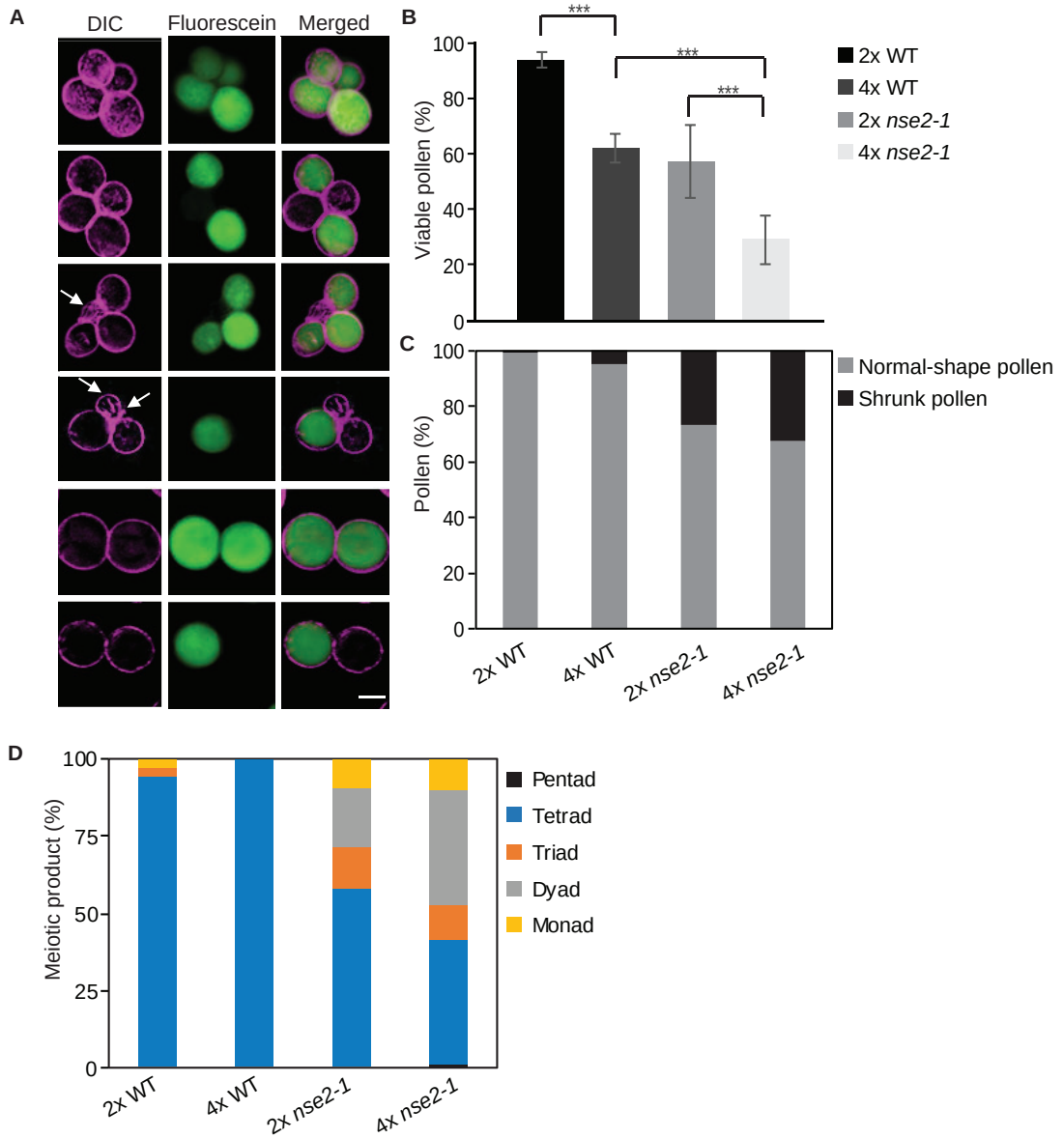

FIGURE 4 | Microspore phenotype of tetraploid (4x) *nse2-1* plants. **(A)** Representative mature pollen stained by fluorescein diacetate from 4x *nse2-1 qrt1-4* plants. Differential interference contrast (DIC) images were pseudocolored in violet. Viable microspores are indicated by fluorescein signals (green). Shrunk microspores are indicated by arrows. Scale bar = 20 μm. **(B)** Frequencies of viable pollen from 2x WT, 4x WT, 2x *nse2-1*, and 4x *nse2-1* (all in *qrt1-4* background). Error bars represent standard deviations among the means of two or three individual plants. Significance in Fisher's exact test: – = $P > 0.05$, * = $P < 0.05$, ** = $P < 0.01$, and *** = $P < 0.001$. Source values and basic counts are provided in **Supplementary Table 3**. **(C)** Quantification of normal-shape and shrunken pollen observed in 2x WT, 4x WT, 2x *nse2-1*, and 4x *nse2-1* in *qrt1-4* background. **(D)** Quantification of meiotic products with different numbers of microspores as observed in 2x WT, 4x WT, 2x *nse2-1*, and 4x *nse2-1* in *qrt1-4* background.

the consequences of polyploidy in the SMC5/6 complex mutants to find whether the duplication of the entire genome will buffer or enhance the defects present in the diploid mutant and whether there will be new features compared to WT plants. We observed a higher frequency of univalents in 4x *nse2* compared to the 4x WT plants. However, in the diploid mutant, five bivalents are invariably formed, as in the diploid control (Yang et al., 2021). The defects of the tetraploid mutant were more drastic in the second meiotic division. A higher percentage of meiocytes with abnormalities was observed with respect to the diploid mutant (93 *vs.* 69%, see also Yang et al., 2021). This could be explained by the role of the SMC5/6 complex in the HR process (Chen et al., 2021), which may be more important in the autotetraploid context as suggested by our data. The accumulation of JMs would be higher in a situation in which the chances of finding homologous sequences to recombine are

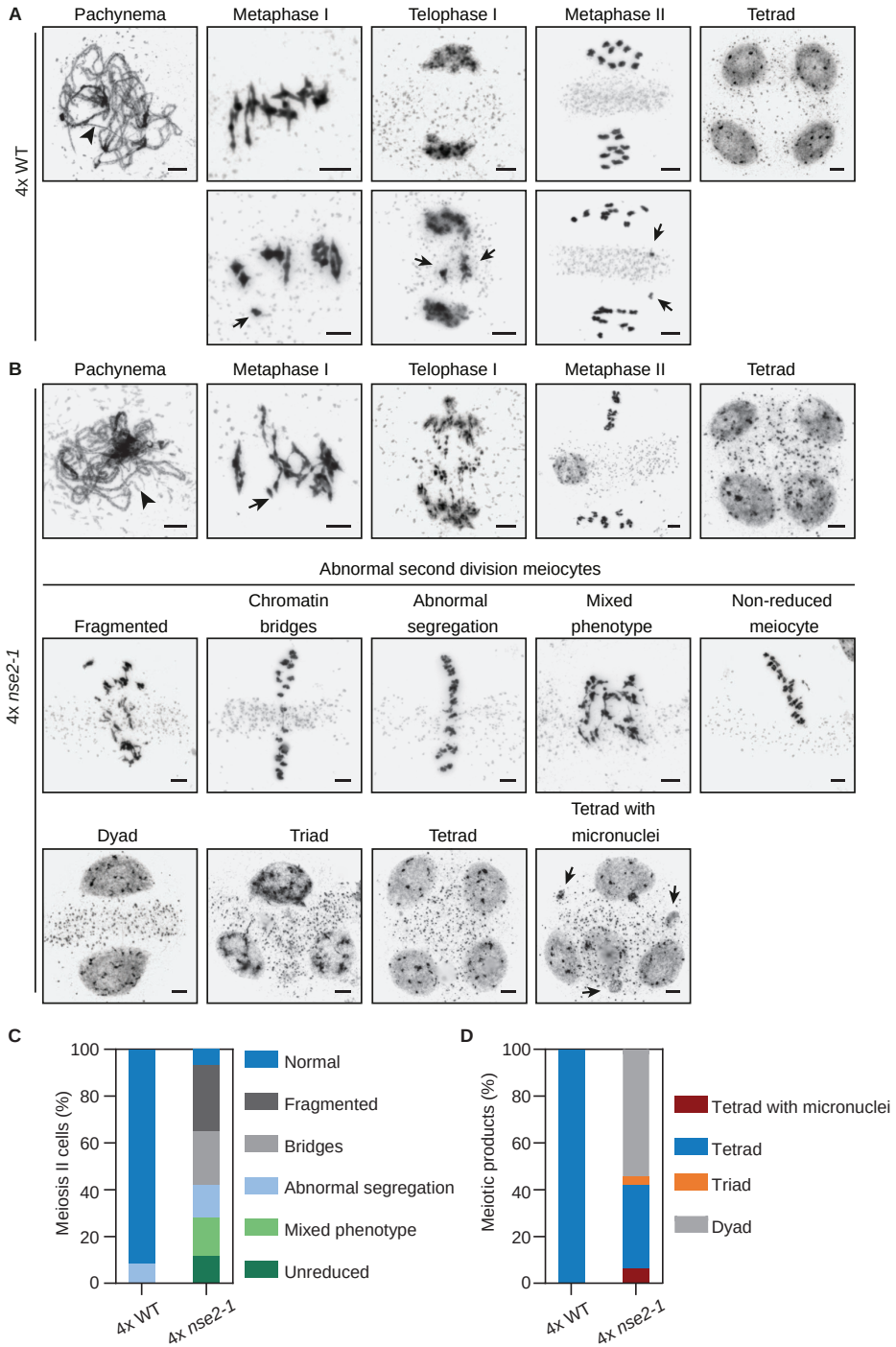

FIGURE 5 | Analysis of male meiosis in 4x *nse2-1* plants. **(A)** Representative images of selected meiotic stages in 4x WT plants. Top row: Unsynapsed regions are detected in pachynema (arrowhead). At metaphase I, the chromosome associations are mostly bivalents and quadrivalents. In most meiocytes, chromosome segregation is correct, both in the first and second meiotic division, resulting in the formation of tetrads with balanced nuclei. Bottom row: Examples of metaphase I with a univalent, telophase I with a delay in chromosome segregation, and a metaphase II with chromatids resulting from the equational segregation of anaphase I univalent. **(B)** Representative images of the phenotype observed in 4x *nse2-1* plants. As well as in WT plants, there were some unsynapsed regions at pachynema (arrowhead). At metaphase I, an increase in the frequency of univalents (arrow) was detected with respect to the WT. Complex entanglements were also frequent at this stage. Telophases I displayed a high frequency of chromosome fragments. Meiotic problems were also evident during the second meiotic division in almost all cells analyzed, including chromosome fragmentation, chromatin bridges and/or abnormal chromosome segregation, and non-reduced meiocytes. At the end of the meiotic division, dyads, triads, tetrads, and tetrads with micronuclei were formed (bottom row). See the text for more details. Scale bars = 5 μm. **(C)** Quantification of the different phenotype observed in 4x *nse2-1* plants during second meiotic division. **(D)** Quantification of division products at the end of meiosis. Note: The data for 2x WT and 2x *nse2* plants were published previously (Yang et al., 2021; **Figures 3**, **4**).

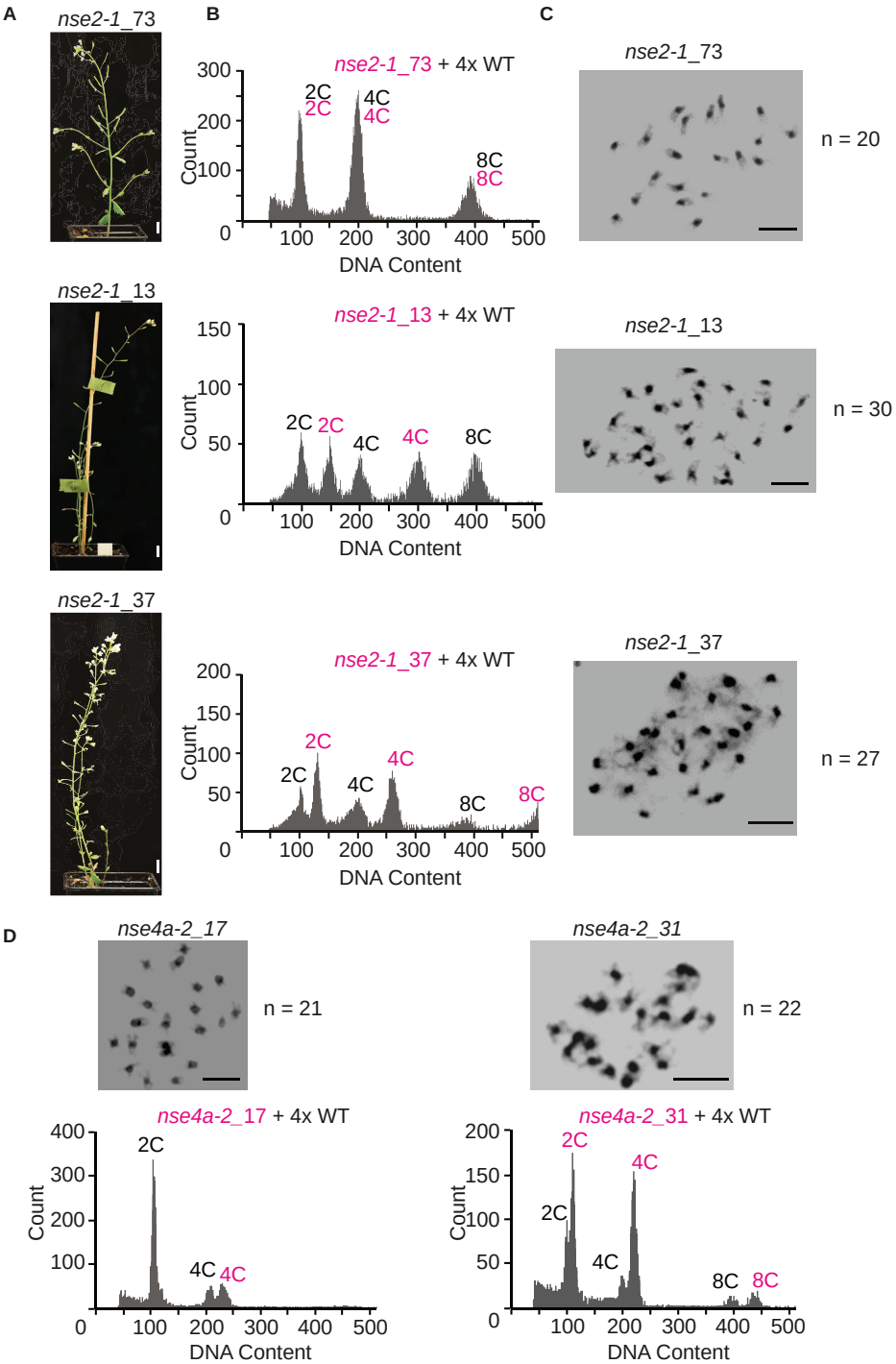

FIGURE 6 | Flow-cytometry ploidy determination in offspring of 4x *nse2-1* and 4x *nse4a-2* plants. **(A)** Phenotype of selected 4-weeks-old plants of *nse2-1_73*, *nse2-1_13*, and *nse2-1_37*. Scale bars = 1 cm. **(B)** Flow-cytometry histograms of plants shown in panel **(A)**, indicating that *nse2-1_73* is tetraploid, *nse2-1_13* hexaploid, and *nse2-1_37* aneuploid. For the ploidy measurements, the nuclei suspension was prepared by mixing leaves from tested *nse2-1* plants and 4x WT control. Multiple peaks correspond to nuclei of different C content as indicated. **(C)** Mitotic figures of *nse2-1_73*, *nse2-1_13*, and *nse2-1_37* plants. The number of chromosomes is given next to the figures. Scale bars = 5 μm. **(D)** Mitotic metaphase plates and flow-cytometry histograms of the ploidy level of two selected aneuploid *nse4-2* plants. Chromosome numbers are given right of the figures. Scale bars = 5 μm. The ploidy levels were measured by preparing the nuclei suspension from a mix of the leaves the *nse4a-2* candidate plant and 4x WT control. Note that an addition of a single or two chromosomes is clearer visible at 4C peaks (or 8C peaks if visible).

increased (Voorrips and Maliepaard, 2012). On the other hand, in 4x *nse2* plants we detected a lower percentage (nearly half) of second division meiocytes displaying all chromosomes on one side of the organelle band (non-reduced) compared to 2x *nse2* plants (11.63 *vs.* 19.40%, see also Yang et al., 2021). Although the percentage of dyads was similar in the tetraploid and the diploid *nse2-1* plants, a lower percentage of tetrads was detected in 4x *nse2* plants. In the 4x mutant, we also observed tetrads with micronuclei, which were not formed in the case of the 2x mutant. As mentioned above, non-reduced meiocytes appear as a consequence of recombination-independent problems generated by the absence of the SMC5/6 complex. In our recent study focusing on the meiosis of 2x *nse2* plants, we showed that this may be related to the organization of the spindle, to the interaction of the kinetochores and the spindle or to delays in chromosome segregation (Yang et al., 2021). In this context, the improper localization of a defined organelle band prevents the formation of two defined nuclei with five chromosomes each (2x *nse2*) or ten chromosomes each (4x *nse2*). The fact that the frequency of non-reduced meiocytes is lower in the 4x relative to the 2x mutant can be explained by the increase in the number of chromosomes. The location of all twenty chromosomes in a single nucleus is less likely than the location of the ten chromosomes. This would also explain why there are more aneuploidies in the tetraploid mutant and a greater reduction in fertility.

The meiotic irregularities in SMC5/6 complex mutants have also profound effects on the seed development and offspring genomic constitution. The 4x *nse2* plants are almost sterile, with less than 10% normal seeds, compared to about 35% such seeds in the 2x mutant. This is due to a strongly affected ovule development leaving only about 30% of ovules capable of seed development in 4x *nse2-1*. Many of the developing seeds are aneuploid, represented mostly by addition of one or two chromosomes. Importantly, the aneuploidy was caused equally from both maternal and paternal sides. Rarely, also unreduced female gametes of tetraploid *nse2* plants gave rise to the hexaploid offspring. These are tetraploidy-associated characters because we observed neither the aneuploidy offspring nor the viable unreduced female gametes in 2x *nse2* plants.

The analysis of polyploids makes it possible to explore some aspects of meiosis more in depth compared to diploids, since in a polyploid condition the chances of pairing and finding homologous sequences to recombine increase. Altogether, our results highlight that the mutations in the SMC5/6 complex cause partially common, but also some unique characters when comparing the phenotypes of diploid and the tetraploid plants. A similar situation has been described in other mutants, for example, those affecting suppressors of recombination like *FANCONI ANEMIA COMPLEMENTATION GROUP M* (*FANCM*). The *fancm* mutants produce a significant increase in HR in diploid plants (Crismani et al., 2012; Li et al., 2021). However, silencing FANCM in tetraploid plants has less or no effect on recombination (Blary et al., 2018; Raz et al., 2021). This indicates that due to the specificities of tetraploid meiosis, the importance of certain molecular factors and complexes may increase or decrease. In summary, the described defects highlight the importance of studying the consequences of mutations in genes affecting meiosis and reproductive development in diploid versus polyploid conditions, especially in the crop species, where polyploids could provide the potential to increase agriculturally important traits.

DATA AVAILABILITY STATEMENT

The original contributions presented in the study are included in the article/**Supplementary Material**, further inquiries can be directed to the corresponding author.

AUTHOR CONTRIBUTIONS

AP, FY, and MP designed the project. FY performed plant phenotypic characterization, crosses, analysis of pollen, and ploidy measurements. NF prepared and analyzed meiocytes. JM counted mitotic chromosome numbers. AP and FY wrote the manuscript with help of other authors. All authors approved the submitted version.

FUNDING

This work was supported by Purkyně Fellowship from the Czech Academy of Sciences, GAČR grant 19-13848S, INTER-COST grant LTC18026 from the Ministry of Education Youth and Sports, Czechia (all to AP), China Scholarship Council Fellowship (File No. 201604910685), and the Fisher Scholarship from the Palacký University in Olomouc (both to FY). AP was also supported by the European Regional Development Fund project "Plants as a tool for sustainable global development" (No. CZ.02.1.01/0.0/0.0/16_019/0000827). NF was a Ph.D. fellow funded by the FPU program of the Spanish Ministry of Education (FPU16/02772). MP acknowledges the support of the European Union (Marie Curie ITN, MEICOM 765212). AP and MP were part of the International Plant Nucleus Consortium (IPNC, https://radar.brookes.ac.uk) and COST Action CA 16212 "INDEPTH" (https://www.cost.eu/actions/CA16212/).

ACKNOWLEDGMENTS

We thank D. Kopecký for a critical reading of the manuscript and E. Jahnová, H. Tvardíková, and Z. Bursová for excellent technical assistance.

SUPPLEMENTARY MATERIAL

The Supplementary Material for this article can be found online at: https://www.frontiersin.org/articles/10.3389/fpls.2021.748252/full#supplementary-material

REFERENCES

Alonso, J. M., Stepanova, A. N., Leisse, T. J., Kim, C. J., Chen, H., Shinn, P., et al. (2003). Genome-wide insertional mutagenesis of Arabidopsis thaliana. *Science.* 301, 653–657. doi: 10.1126/science.1086391

Aragón, L. (2018). The Smc5/6 complex: new and old functions of the enigmatic long-distance relative. *Annu. Rev. Genet.* 52, 89–107. doi: 10.1146/annurev-genet-120417-031353

Blary, A., Gonzalo, A., Eber, F., Bérard, A., Bergès, H., Bessoltane, N., et al. (2018). FANCM limits meiotic crossovers in brassica crops. *Front. Plant Sci.* 9:368. doi: 10.3389/fpls.2018.00368

Chen, H., He, C., Wang, C., Wang, X., Ruan, F., Yan, J., et al. (2021). RAD51 supports DMC1 by inhibiting the SMC5/6 complex during meiosis. *Plant Cell* 33, 2869–2882. doi: 10.1093/plcell/koab136

Comai, L. (2005). The advantages and disadvantages of being polyploid. *Nat. Rev. Genet.* 6, 836–846. doi: 10.1038/nrg1711

Copsey, A., Tang, S., Jordan, P. W., Blitzblau, H. G., Newcombe, S., Chan, A. C., et al. (2013). Smc5/6 coordinates formation and resolution of joint molecules with chromosome morphology to ensure meiotic divisions. *PLoS Genet.* 9:e1004071. doi: 10.1371/journal.pgen.1004071

Crismani, W., Girard, C., Froger, N., Pradillo, M., Santos, J. L., Chelysheva, L., et al. (2012). FANCM limits meiotic crossovers. *Science* 336, 1588–1590. doi: 10.1126/science.1220381

Díaz, M., Pečinková, P., Nowicka, A., Baroux, C., Sakamoto, T., Gandha, P. Y., et al. (2019). The SMC5/6 complex subunit NSE4A is involved in DNA damage repair and seed development. *Plant Cell* 31, 1579–1597. doi: 10.1105/tpc.18.00043

Henry, I. M., Dilkes, B. P., and Comai, L. (2006). Molecular karyotyping and aneuploidy detection in *Arabidopsis thaliana* using quantitative fluorescent polymerase chain reaction. *Plant J.* 48, 307–319. doi: 10.1111/j.1365-313X.2006.02871.x

Hu, Z., Cools, T., and De Veylder, L. (2016). Mechanisms used by plants to cope with DNA damage. *Annu. Rev. Plant Biol.* 67, 439–462. doi: 10.1146/annurev-arplant-043015-111902

Huang, L., Yang, S., Zhang, S., Liu, M., Lai, J., Qi, Y., et al. (2009). The Arabidopsis SUMO E3 ligase AtMMS21, a homologue of NSE2/MMS21, regulates cell proliferation in the root. *Plant J.* 60, 666–678. doi: 10.1111/j.1365-313X.2009.03992.x

Ishida, T., Fujiwara, S., Miura, K., Stacey, N., Yoshimura, M., Schneider, K., et al. (2009). SUMO E3 ligase HIGH PLOIDY2 regulates endocycle onset and meristem maintenance in Arabidopsis. *Plant Cell* 21, 2284–2297. doi: 10.1105/tpc.109.068072

Ishida, T., Yoshimura, M., Miura, K., and Sugimoto, K. (2012). MMS21/HPY2 and SIZ1, Two Arabidopsis SUMO E3 Ligases, Have Distinct Functions in Development. *PLoS One* 7:e46897. doi: 10.1371/journal.pone.0046897

Jullien, P. E., and Berger, F. (2010). Parental Genome Dosage Imbalance Deregulates Imprinting in Arabidopsis. *PLoS Genet.* 6:e1000885. doi: 10.1371/journal.pgen.1000885

Kegel, A., and Sjögren, C. (2010). The Smc5 / 6 Complex: more than repair? *Cold Spring Harb. Symp. Quant. Biol.* 75, 179–187. doi: 10.1101/sqb.2010.75.047

Köhler, C., Wolff, P., and Spillane, C. (2012). Epigenetic mechanisms underlying genomic imprinting in plants. *Annu. Rev. Plant Biol.* 63, 331–352. doi: 10.1146/annurev-arplant-042811-105514

Kwak, J. S., Son, G. H., Kim, S. I., Song, J. T., and Seo, H. S. (2016). Arabidopsis HIGH PLOIDY2 Sumoylates and stabilizes flowering locus C through Its E3 ligase activity. *Front. Plant Sci.* 7:530. doi: 10.3389/fpls.2016.00530

Li, X., Yu, M., Bolaños-Villegas, P., Zhang, J., Ni, D., Ma, H., et al. (2021). Fanconi anemia ortholog FANCM regulates meiotic crossover distribution in plants. *Plant Physiol.* 186, 344–360. doi: 10.1093/plphys/kiab061

Liu, C. M., and Meinke, D. W. (1998). The titan mutants of Arabidopsis are disrupted in mitosis and cell cycle control during seed development. *Plant J.* 16, 21–31. doi: 10.1046/j.1365-313x.1998.00268.x

Liu, M., Shi, S., Zhang, S., Xu, P., Lai, J., Liu, Y., et al. (2014). SUMO E3 ligase AtMMS21 is required for normal meiosis and gametophyte development in Arabidopsis. *BMC Plant Biol.* 14:153. doi: 10.1186/1471-2229-14-153

Mandáková, T., and Lysak, M. A. (2018). Post-polyploid diploidization and diversification through dysploid changes. *Curr. Opin. Plant Biol.* 42, 55–65. doi: 10.1016/j.pbi.2018.03.001

Mengiste, T., Revenkova, E., Bechtold, N., and Paszkowski, J. (1999). An SMC-like protein is required for efficient homologous recombination in arabidopsis. *EMBO J.* 18, 4505–4512. doi: 10.1093/emboj/18.16.4505

Menolfi, D., Delamarre, A., Lengronne, A., Pasero, P., and Branzei, D. (2015). Essential Roles of the Smc5/6 Complex in replication through natural pausing sites and endogenous DNA damage tolerance. *Mol. Cell* 60, 835–846. doi: 10.1016/j.molcel.2015.10.023

Morgan, C., Zhang, H., Henry, C. E., Franklin, F. C. H., and Bomblies, K. (2020). Derived alleles of two axis proteins affect meiotic traits in autotetraploid Arabidopsis arenosa. *Proc. Natl. Acad. Sci. U. S. A.* 117, 8980–8988. doi: 10.1073/pnas.1919459117

Palecek, J. J., and Gruber, S. (2015). Kite Proteins: a superfamily of SMC/Kleisin partners conserved across bacteria, archaea, and eukaryotes. *Structure* 23, 2183–2190. doi: 10.1016/j.str.2015.10.004

Parra-Nunez, P., Pradillo, M., and Santos, J. L. (2020). "How to Perform an Accurate Analysis of Metaphase I Chromosome Configurations in Autopolyploids of *Arabidopsis thaliana*," in *Plant Meiosis: Methods and Protocols*, eds M. Pradillo and S. Heckmann (New York: Springer), 25–36. doi: 10.1007/978-1-4939-9818-0_3

Pecinka, A., Fang, W., Rehmsmeier, M., Levy, A. A., and Mittelsten Scheid, O. (2011). Polyploidization increases meiotic recombination frequency in Arabidopsis. *BMC Biol.* 9:24. doi: 10.1186/1741-7007-9-24

Preuss, D., Rhee, S. Y., and Davis, R. W. (1994). Tetrad analysis possible in Arabidopsis with mutation of the QUARTET (QRT) genes. *Science* 264, 1458–1460. doi: 10.1126/science.8197459

Raz, A., Dahan-Meir, T., Melamed-Bessudo, C., Leshkowitz, D., and Levy, A. A. (2021). Redistribution of meiotic crossovers along wheat chromosomes by virus-induced gene silencing. *Front. Plant Sci.* 11:635139. doi: 10.3389/fpls.2020.635139

Roy, S. (2014). Maintenance of genome stability in plants: repairing DNA double strand breaks and chromatin structure stability. *Front. Plant Sci.* 5:487. doi: 10.3389/fpls.2014.00487

Sánchez Moran, E., Armstrong, S. J., Santos, J. L., Franklin, F. C. H., and Jones, G. H. (2001). Chiasma formation in *Arabidopsis thaliana* accession Wassileskija and in two meiotic mutants. *Chromosome Res.* 9, 121–128. doi: 10.1023/A:1009278902994

Santos, J. L., Alfaro, D., Armstrong, S. J., Franklin, F. C. H., and Jones, G. H. (2003). Partial diploidization of meiosis in autotetraploid *Arabidopsis thaliana*. *Genetics* 165, 1533–1540. doi: 10.1093/genetics/165.3.1533

Seear, P. J., France, M. G., Gregory, C. L., Heavens, D., Schmickl, R., Yant, L., et al. (2020). A novel allele of ASY3 is associated with greater meiotic stability in autotetraploid Arabidopsis lyrata. *PLoS Genet.* 16:e1008900. doi: 10.1371/journal.pgen.1008900

Uhlmann, F. (2016). SMC complexes: from DNA to chromosomes. *Nat. Rev. Mol. Cell Biol.* 17, 399–412. doi: 10.1038/nrm.2016.30

Van De Peer, Y., Fawcett, J. A., Proost, S., Sterck, L., and Vandepoele, K. (2009). The flowering world: a tale of duplications. *Trends Plant Sci.* 14, 680–688. doi: 10.1016/j.tplants.2009.09.001

Voorrips, R. E., and Maliepaard, C. A. (2012). The simulation of meiosis in diploid and tetraploid organisms using various genetic models. *BMC Bioinformatics* 13:248. doi: 10.1186/1471-2105-13-248

Watanabe, K., Pacher, M., Dukowic, S., Schubert, V., Puchta, H., and Schubert, I. (2009). The Structural maintenance of chromosomes 5/6 complex promotes sister chromatid alignment and homologous recombination after DNA damage in *Arabidopsis thaliana*. *Plant Cell* 21, 2688–2699. doi: 10.1105/tpc.108.060525

Xaver, M., Huang, L., Chen, D., and Klein, F. (2013). Smc5/6-Mms21 prevents and eliminates inappropriate recombination intermediates in meiosis. *PLoS Genet.* 9:e1004067. doi: 10.1371/journal.pgen.1004067

Xu, P., Yuan, D., Liu, M., Li, C., Liu, Y., Zhang, S., et al. (2013). AtMMS21, an SMC5/6 complex subunit, is involved in stem cell niche maintenance and DNA damage responses in Arabidopsis roots. *Plant Physiol.* 161, 1755–1768. doi: 10.1104/pp.112.208942

Yan, S., Wang, W., Marqués, J., Mohan, R., Saleh, A., Durrant, W. E., et al. (2013). Salicylic acid activates DNA damage responses to potentiate plant immunity. *Mol. Cell* 52, 602–610. doi: 10.1016/j.molcel.2013.09.019

Yang, F., Fernández-Jiménez, N., Tučková, M., Vrána, J., Cápal, P., Díaz, M., et al. (2021). Defects in meiotic chromosome segregation lead to unreduced male gametes in Arabidopsis SMC5/6 complex mutants. *Plant Cell* 33, 3104–3119. doi: 10.1093/plcell/koab178

Yuan, D., Lai, J., Xu, P., Zhang, S., Zhang, J., Li, C., et al. (2014). AtMMS21 regulates DNA damage response and homologous recombination repair in Arabidopsis. *DNA Repair (Amst).* 21, 140–147. doi: 10.1016/j.dnarep.2014.04.006

Zelkowski, M., Zelkowska, K., Conrad, U., Hesse, S., Lermontova, I., Marzec, M., et al. (2019). Arabidopsis NSE4 proteins act in somatic nuclei and meiosis to ensure plant viability and fertility. *Front. Plant Sci.* 10:774. doi: 10.3389/fpls.2019.00774

Zou, W., Li, G., Jian, L., Qian, J., Liu, Y., and Zhao, J. (2021). Arabidopsis SMC6A and SMC6B have redundant function in seed and gametophyte development. *J. Exp. Bot.* 72, 4871–4887. doi: 10.1093/jxb/erab181

Conflict of Interest: The authors declare that the research was conducted in the absence of any commercial or financial relationships that could be construed as a potential conflict of interest.

Publisher's Note: All claims expressed in this article are solely those of the authors and do not necessarily represent those of their affiliated organizations, or those of the publisher, the editors and the reviewers. Any product that may be evaluated in this article, or claim that may be made by its manufacturer, is not guaranteed or endorsed by the publisher.

frontiers in Plant Science

ORIGINAL RESEARCH
published: 12 November 2021
doi: 10.3389/fpls.2021.706560

An Induced Mutation in *HvRECQL4* Increases the Overall Recombination and Restores Fertility in a Barley *HvMLH3* Mutant Background

Mikel Arrieta[1†], Malcolm Macaulay[1†], Isabelle Colas[1], Miriam Schreiber[1], Paul D. Shaw[2], Robbie Waugh[1,3] and Luke Ramsay[1*]*

[1] Cell and Molecular Sciences, The James Hutton Institute, Dundee, United Kingdom, [2] Information and Computational Sciences, The James Hutton Institute, Dundee, United Kingdom, [3] Division of Plant Sciences, The University of Dundee at The James Hutton Institute, Dundee, United Kingdom

OPEN ACCESS

Edited by:
Christophe Lambing,
University of Cambridge,
United Kingdom

Reviewed by:
Chloe Girard,
UMR9198 Institut de Biologie Intégrative de la Cellule (I2BC), France
Nico De Storme,
KU Leuven, Belgium

***Correspondence:**
Robbie Waugh
robbie.waugh@hutton.ac.uk
Luke Ramsay
luke.ramsay@hutton.ac.uk

[†] These authors have contributed equally to this work

Specialty section:
This article was submitted to Plant Cell Biology, a section of the journal Frontiers in Plant Science

Received: 07 May 2021
Accepted: 28 September 2021
Published: 12 November 2021

Citation:
Arrieta M, Macaulay M, Colas I, Schreiber M, Shaw PD, Waugh R and Ramsay L (2021) An Induced Mutation in HvRECQL4 Increases the Overall Recombination and Restores Fertility in a Barley HvMLH3 Mutant Background.
Front. Plant Sci. 12:706560.
doi: 10.3389/fpls.2021.706560

Plant breeding relies on the meiotic recombination or crossing over to generate the new combinations of the alleles along and among the chromosomes. However, crossing over is constrained in the crops such as barley by a combination of the low frequency and biased distribution. In this study, we attempted to identify the genes that limit the recombination by performing a suppressor screen for the restoration of fertility to the semi-fertile barley mutant *desynaptic10* (*des10*), carrying a mutation in the barley ortholog of *MutL-Homolog 3* (*HvMLH3*), a member of the MutL-homolog (MLH) family of DNA mismatch repair genes. *des10* mutants exhibit reduced recombination and fewer chiasmata, resulting in the loss of obligate crossovers (COs) leading to chromosome mis-segregation. We identified several candidate suppressor lines and confirmed their restored fertility in an *Hvmlh3* background in the subsequent generations. We focus on one of the candidate suppressor lines, *SuppLine2099*, which showed the most complete restoration of fertility. We characterized this line by using a target-sequence enrichment and sequencing (TENSEQ) capture array representing barley orthologs of 46 meiotic genes. We found that *SuppLine2099* contained a C/T change in the anti-CO gene *RecQ-like helicase 4 (RECQL4)* resulting in the substitution of a non-polar glycine to a polar aspartic acid (G700D) amino acid in the conserved helicase domain. Single nucleotide polymorphism (SNP) genotyping of F_3 populations revealed a significant increase in the recombination frequency in lines with *Hvrecql4* in the *Hvmlh3* background that was associated with the restoration of fertility. The genotyping also indicated that there was nearly double the recombination levels in homozygous *Hvrecql4* lines compared to the wild type (WT). However, we did not observe any significant change in the distribution of CO events. Our results confirm the anti-CO role of *RECQL4* in a large genome cereal and establish the possibility of testing the utility of increasing recombination in the context of traditional crop improvement.

Keywords: meiosis, suppressor screen, recombination, barley, desynaptic mutant, crossover

INTRODUCTION

The crossing over that occurs during meiosis generates new combinations of the alleles that subsequently become the substrate for the selection either *via* the natural evolution or by human-driven selection during the traditional plant breeding. When crossing over occurs in a hybrid plant, genetic materials are physically exchanged among the homologous chromosomes with the resulting progeny containing a genotypic mosaic of the original hybrid genome. In an inbreeding crop plant such as barley, subsequent generations of the self-fertilization and selection return the plants to near homozygosity and it is these genotypes that are further multiplied and commercially marketed as the fixed inbred lines or cultivars. Barley has a large genome of around 5 Gb (Mascher et al., 2017; Jayakodi et al., 2020; Schreiber et al., 2020) and similar to the other crops, the number and distribution of crossovers (COs) are limited (Blary and Jenczewski, 2019). In particular, CO position is highly skewed to the distal regions of the chromosomes, which creates recombination-poor regions of the genome that contain a considerable number of genes (Mayer et al., 2012; Darrier et al., 2017; Mascher et al., 2017). This lack of recombination impacts genetic variation, constrains breeding progress and the introgression of the novel traits, and reduces the efficiency of molecular cloning and the discrimination of quantitative trait locus (QTL) (Darrier et al., 2017; Blary and Jenczewski, 2019). It has been proposed that positively increasing recombination could improve the speed and accuracy of plant breeding and genetic programs (Wijnker and de Jong, 2008).

Crossovers arise from the repair of double-strand breaks (DSBs) in DNA (Wang and Copenhaver, 2018) via two alternative pathways. Class I is the predominant pathway that results in homologous recombination (HR). It is considered to be sensitive to interference, i.e., the existence of one CO limits the formation of another one close by each other (Berchowitz and Copenhaver, 2010). Class I repairs are dependent upon the well-studied ZMM (ZYP, MSH, and MER-3) protein complexes and the pro-CO E3 ligase HEI10 and involve the DNA mismatch repair proteins such as MutL-homologs (MLH1 and MLH3) (Mercier et al., 2015; Wang and Copenhaver, 2018). Class II COs are generated by the CO junction endonuclease MUS81-dependent pathway (Higgins et al., 2008; Wang and Copenhaver, 2018). These are believed to be mostly insensitive to interference and, thus, class II COs may occur relatively independently from each other. The frequency of class II COs has been estimated to be in the range of 15–25% of the total COs in *Arabidopsis* (Copenhaver, 2003; Mercier et al., 2005; Higgins et al., 2012) and 5–10% in barley (Barakate et al., 2014).

Genetic suppressor screens of *Arabidopsis* mutants (ZIP1, MSH4/5, MER3, SCHO1, and Hei10) with reduced CO and associated semi-sterility have identified genes repressing CO number by the restoration of fertility in the mutants such as anti-CO genes including the orthologs of *Fanconi anemia group M* (*FANCM)* (Crismani et al., 2012), *Fidgetin-like 1* (*FIGL1)* (Girard et al., 2015; Fernandes et al., 2018), *DNA topoisomerase 3α* (*TOP3α*) (Séguéla-Arnaud et al., 2015), and *RecQ-like helicase 4* (*RECQL4*) (Séguéla-Arnaud et al., 2015).

Following the principles of these *Arabidopsis* studies, we performed a suppressor screen by mutagenizing the semi-sterile barley mutant *desynaptic10* (*des10)* and then examining the individual progenies in the M_4 generation for the restoration of fertility. *des10* (Lundqvist et al., 1997) was previously characterized as a 159-bp deletion in the mismatch repair gene *MutL-Homolog 3* (*HvMlh3*) and shows a much reduced number of COs, abnormal synapsis progression, chromosome mis-segregation, and a subsequent reduction of fertility (Colas et al., 2016). To the best of our knowledge, a suppressor screen of *MLH3* mutants has not been performed before in *Arabidopsis* perhaps because the phenotype is less severe compared to the ZMM mutants used (Crismani et al., 2012; Girard et al., 2015; Séguéla-Arnaud et al., 2015). Our phenotypic screen identified several candidate suppressor lines that improve fertility in the *Hvmlh3* genetic background. We focus on the phenotypic, molecular, and cytological characterization of the single line, *SuppLine2099*, which exhibited the most complete restoration of fertility.

MATERIALS AND METHODS

DNA Extraction

Leaf tissue was collected from the seedlings ∼2 weeks after sowing at the two-leaf stage of development. DNA extractions were carried out by using the QIAamp 96 DNA QIAcube HT Kit (Qiagen, Venlo, Netherlands) from ∼100 mg of young leaf tissue as per the instructions of the suppliers on the QIAcube HT nucleic acid purification platform (Qiagen, Venlo, Netherlands).

Suppressor Screen on *desynaptic10*

The suppressor screen used the Bc_5F_5 near-isogenic line BW230 *des10* (syn. *HvMlh3*) in the *cv*. Bowman background (Druka et al., 2010; Colas et al., 2016). BW230 *des10* plants were multiplied in a polytunnel and glasshouse to finally generate around 18,000 seeds. These seeds were divided into three separate lots and were mutagenized with Ethyl methanesulfonate (EMS) at 20, 25, and 30 mM concentrations, respectively, as described previously (Caldwell et al., 2004; Schreiber et al., 2019). M_1 seeds were grown in summer 2016 in the soil in a polytunnel in Dundee (UK), harvested, and bulked by treatment (EMS concentration). This process was repeated for M_2 and M_3 generations (outline of the process in **Supplementary Figure 1**). Finally, 10 plants that showed increased fertility relative to the semi-sterile BW230 *des10* were selected from the M_4 generation. These were genotyped with a custom Kompetitive allele-specific PCR (KASP) marker diagnostic for the presence/absence of the 159 bp deletion in *Hvmlh3* to confirm the presence of the *des10* mutation (Colas et al., 2016). A custom target enrichment MyBaits Array (Daicel Arbor Biosciences, Ann Arbor, Michigan, USA) comprising 46 meiotic genes was then used to screen for mutations, exactly as described previously (Schreiber et al., 2019).

Plant Material

Plants (*Hordeum vulgare* L.) were grown in 6-inch pots in a glasshouse under 16 h of light at 18–20°C and 8 h of dark at 16°C. A general-purpose mix compost containing peat, sand,

limestone, Perlite, Celcote, Osmocote®, and Exemptor® was used in all the experiments.

Crossing and F_1 Population Development

Crosses were made in the glasshouse with pollen from the barley *cv*. Barke used to pollinate the emasculated spikes of the suppressor line *SuppLine2099* (*cv*. Bowman background). F_1 seeds were harvested and sown in 96 well single seed descent (SSD) trays in the glasshouse, where leaf tissue was collected and DNA extracted as described above. The success of the cross was confirmed by checking F_1 plant heterozygosity by genotyping the plants with a series of custom made KASP (LGC) markers (**Supplementary Material 1A**) and subsequent sequencing of the alleles. Confirmed F_1 plants were moved to 6-inch pots and grown in the glasshouse (bagged at flowering) to produce a large number of self-fertilized F_2 seeds forming a segregating F_2 population. An outline of the experiment is illustrated in **Supplementary Figure 2**.

F_2 Population Development

F_2 seeds from a single F_1 line were sown in 96 well SSD trays in the glasshouse. After DNA extraction, a total of 267 F_2 plants from the suppressor line cross were genotyped for the mutations in the two target genes by KASP markers (**Supplementary Material 1B**). Genotyping allowed the identification of the four groups of F_2 plants that were homozygous at both the loci for either mutant or the wild type (WT) allele (**Supplementary Figure 2**). A total of 52 plants were selected and those plants were moved to bigger 6-inch pots in the glasshouse conditions to produce the F_3 seeds to be genotyped with the 50K iSelect single nucleotide polymorphism (SNP) array (Bayer et al., 2017).

F_2 Fertility Assessment

The fertility of the selected F_2 plants was assessed by counting the fertile seeds and total florets on three random ears per mature plant and by threshing all ears of each plant with a single ear thresher (Haldrup GmbH, Ilshofen, Germany) and calculating the thousand grain weight (TGW), grain weight per ear, and seeds per ear with a Marvin Digital Seed Analyser (GTA Sensorik GmbH, Neubrandenburg, Germany). Fertility comparisons were carried out by using a *t*-test with the *ggplot2* (https://CRAN.R-project.org/package=ggplot2) and *ggpubr* (https://CRAN.R-project.org/package=ggpubr) packages in R software (version 3.6.1, R Foundation, Vienna, Austria).

F_3 Population Development

The 52 selected F_2s were genotyped by using the 50K iSelect SNP array and 10 individuals from each of the four homozygous allele groups were chosen to maximize the informative heterozygous genome coverage in the final F_3 populations to be used for the genetic analysis. F_3 seeds from chosen F_2 family were sown in 96 well SSD trays in the glasshouse, aiming to grow 10 F_3 plants per chosen F_2 family (one family would remain smaller). DNA was extracted from these plants (for 50k genotyping and recombination analysis) and once mature, F_4 seeds were harvested for the cytological analysis.

Kompetitive Allele-Specific PCR Genotyping

Diagnostic KASP assays were designed for each of the two target mutations segregating in the F_2 families (**Supplementary Material 1B**). DNA sequence containing 70 bp on each side of the mutations was used to design two allele-specific and a common primer for each KASP assay with a web-based allele-specific primer (WASP) design tool (https://bioinfo.biotec.or.th/WASP). Primers were synthesized by Sigma (Sigma-Aldrich Co Ltd (Merck), Kenilworth, NJ, USA). Eight μl reactions were prepared in the MicroAmp Fast optical 96-well-plates (Thermo Fisher Scientific, Waltham, MA, USA) by using $<$ 3 ng of DNA, 4 μl of 2 $\times$ KASP reagent (LGC, Middlesex, UK), two allele-specific primers at 0.16 μM each, and a conserved primer at 0.4 μM. PCR and genotyping were completed by using a StepOne Plus real-time PCR machine (Applied Biosystems, Thermo Fisher Scientific, Waltham, MA, USA). Sample fluorescence was measured at 20°C for 2 min; then, DNA was denatured for 15 min at 94 C followed by 10 cycles of 20 s at 94 C and 1 min at 62 C (decreasing by 0.7 C per cycle). This was followed by 32 cycles of 20 s at 94 C and 1 min at 55 C. Samples were then cooled to 20 C for 2 min to allow the fluorescence measurement. Alleles were scored by using the StepOnePlus Software (Applied Biosystems, Thermo Fisher Scientific, Waltham, MA, USA).

50K Genotyping and Scoring

DNA was quantified and quality checked by using a spectrometer (NanoDrop Technologies LLC, DE, USA). DNA with absorbance ratios at both 260/280 nm and 260/230 nm of $>$ 1.8 was used and the DNA concentration was adjusted by dilution to 20 ng/μl. A total amount of 300 ng DNA per sample was lyophilized and sent to the Geneseek (Neogen Europe, Ltd., Auchincruive, UK) for Illumina high-throughput screening by using the Infinium HTS assay and the HiScan array imaging (Illumina, San Diego, California, USA) by using the Barley 50K iSelect SNP array (Bayer et al., 2017). R and Theta scores were extracted from the resulting idat files by using the GenomeStudio Genotyping Module version 2.0.2 (Illumina, San Diego, California, USA) and the allele scores were created by using the paRsnps (an in-house software package for clustering, visualizing, and comparing the Illumina SNP genotyping data).

50K Data Cleaning and Recombination Analysis

For the preliminary 50K data cleaning, a custom R script was used to remove the monomorphic and ambiguous markers showing highly skewed allele frequencies. The latter SNP data were characterized by intercalated isolated heterozygous calls which falsely inflated the number of the COs, so individuals with an abundance of such calls leading to CO number higher than 35 were discarded from the analysis. Markers with $>$ 5% missing data were also removed. The nucleotide calls were then changed to A/B/H format with A being the homozygous allele call for the *SuppLine2099* parent B for *cv*. Barke parent and H for a heterozygous allele call.

The physical order of the markers and their respective physical position on the barley genome was obtained from the current physical assembly (MorexV2, Monat et al., 2019). Prior to CO scoring, for each F_3 family (sharing the same F_2 origin), markers that were homozygous in the parental F_2 individual were removed from the analysis, so that only recombination in the F_2 would be assessed. CO events were scored as an allele change between the two consecutive markers; a single CO was considered when either the homozygous allele call of any of the two parental alleles changed to a heterozygous call or vice versa. Changes from either the parental homozygous call to the other were considered as a double CO. In order to consider any CO as validated, the allele change needed to be maintained in the following three markers to the position of the switch. This rather conservative approach may underestimate the number of COs, but avoided the inflation of the CO counts by the isolated false allele calls. The effect of missing data in the three-marker window on CO calling was corrected manually.

Recombination fraction (r) was calculated by dividing the number of COs between the two markers and the number of the individuals that had no missing data for those two markers. The recombination distance was then calculated by using the Kosambi map function:

$$Kosambi\ distance\ (cM) = \frac{ln[(1 + 2 * (\frac{r}{2}))/(1 - 2 * (\frac{r}{2}))]}{4} * 100$$

The mid-physical point between the two markers was used as the physical position of a CO for binning recombination events in the physical intervals and *ggplot* and *ggpubr* R packages were used to plot the recombination frequency and distribution graphs.

Differences in recombination between the four homozygous allele groups for entire chromosomes and for the three chromosomal zones described in Mascher et al. (2017) were compared using the Wilcoxon's signed rank test (as in Devaux et al., 1995) using the R *ggpubr* package. The comparison of the relative proportion of recombination was carried out with the contingency table and the chi-squared test.

Cytology

F_4 seeds from randomly chosen F_3 families were grown under controlled standard conditions (16 h light at 18°C, 8 h dark at 14°C) in 6-inch pots. Spikes of between 1.8 and 2.2 cm (at metaphase stage) were harvested from the plants and fixed in 1:3 acetic acid/EtOH for at least 24 h at 4–6°C. Anther dissection was carried out under a stereo microscope (Leica Microsystems, Wetzlar, Germany) and squashed on a microscope slide in a drop of 0.5% acetocarmine. Meiotic stages were determined by checking the slides under light microscope (Olympus K2, Olympus Corporation, Tokyo, Japan) and chromosome spreads were prepared according to Colas et al. (2016) with slight modification. Slides were mounted in Fluoroshield containing 0.0002% 4′,6-diamidino-2-phenylindole (DAPI) (Abcam, ab104139, Cambridge, UK), and the coverslips were sealed with nail polish. Three-dimensional (3D) stack images (512 × 512, 12 bits, optimal sectioning) were taken with a confocal Zeiss LSM 710 microscope equipped with the W Plan-Apochromat 63X/1.0 M27 objective (laser light 405 nm, 4 lines averaging). Raw images were processed with the Imaris Deconvolution ClearView 9.5 (Imaris, Zurich, Switzerland) (parameters in **Supplementary Material 2**). Chiasmata were manually counted by using the Imaris 9.5.1 (Imaris, Zurich, Switzerland) Spot module from the stack images. Projections of 3D pictures, Gaussian smoothing, and light brightness/contrast/color adjustments were performed with the Imaris 9.5.1 (Imaris, Zurich, Switzerland) (Bitplane).

RESULTS

Suppressor Screen of BW230 *desynaptic10*

18,000 seeds of BW230 *des10* (syn. *Hvmlh3*) (Colas et al., 2016) were mutagenized with 20, 25, and 30 mM EMS and grown in a polytunnel in 2016. M_2 plants and M_3 families were grown again in the same facility in 2017 and 2018, respectively, and screened for increased fertility when compared to BW230 *des10*. 10 M_4 plants were identified and 3 M_5 plants from each were grown in the glasshouse to confirm the fertility levels (**Supplementary Figure 3**). To explore whether the suppressor lines contained mutations in any previously characterized meiotic genes, we conducted a sequence-based screen by using a hybridization-capture MyBaits probe pool (Schreiber et al., 2019). The capture contained probes covering the exonic regions of the barley orthologs of 46 known meiotic genes including the anti-CO genes discovered previously in *Arabidopsis* (Schreiber et al., 2019) with some intronic and untranslated region (UTR) sequences also captured due to gene structure and the length of reads (Schreiber et al., 2019). Hybridization capture followed by sequencing on an Illumina MiSeq instrument revealed that nine of the fertility-restored plants contained mutations in the different meiotic genes (**Supplementary Table 1**). In this study, we focus on one line, *SuppLine2099*, which showed the highest level of the restored fertility compared to BW230 *des10* (**Supplementary Figure 3**).

Mapping the Illumina reads against the genomic sequence of the 46 meiotic genes used in the probe pool (Schreiber et al., 2019) revealed that *SuppLine2099* contained a non-synonymous C/T point mutation (**Figure 1**) in the coding sequence of *HvRECQL4* (CDS included in **Supplementary Material 3**); the C/T change in exon 13 resulted in a predicted amino acid change from a non-polar glycine to a polar aspartic acid (G700D) amino acid in the conserved helicase domain. Analysis of the likely impact of this substitution using the Protein Variation Effect Analyzer (PROVEAN) (Choi et al., 2012) revealed a score of 6.851, which is predicted as deleterious.

A Mutation in *RecQ-Like Helicase 4* Restores Fertility to BW230 *desynaptic10*

To confirm that the G700D substitution in HvREQL4 was responsible for the restoration of fertility, *SuppLine2099* was crossed onto *cv*. Barke and F_1 plants grown to generate F_2 seed (outline of the experiment shown in **Supplementary Figure 2**). F_2 plants were then selected based on their genotype at *HvRECQL4* and *HvMLH3*, with the seed of the following four

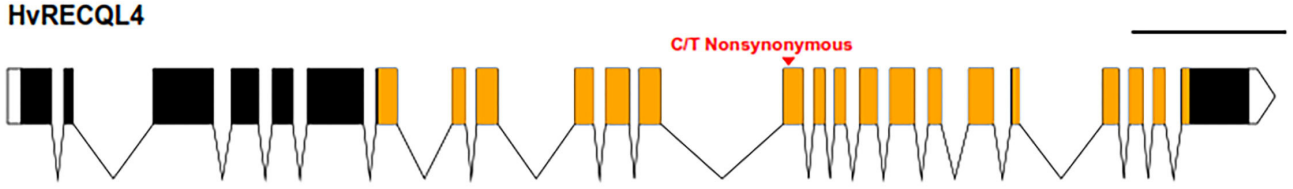

FIGURE 1 | Graphical representation of *HvRECQl4*. The 24 exons are represented by the boxes joined by the introns with untranslated regions (UTRs) unfilled and the conserved helicase domain in orange. The position of the mutation is marked by the red arrow. Scale bar: 1 kb. Diagram produced with the exon-intron graphic maker (wormweb.org/exonintron).

possible homozygous classes identified and selected: *RECQL4 MLH3*, *recql4*$_{G700D}$ *MLH3*, *RECQL4 mlh3*$_{des10}$, or *recql4*$_{G700D}$ *mlh3*$_{des10}$, which will be referred to as the WT, *recql4*, *mlh3*, and *RECQL4 MLH3* (double mutant), respectively. The number of plants in each class was 20, 11, 9, and 13, respectively. The fertility of the F_2s was assessed in the glasshouse by using three ears of each plant. A significant ($p < 0.0001$) reduction of fertility (**Figure 2**) was observed in the *mlh3* plants, which had an average of 22.3% of fertile seeds/ears compared to the WT with 72.2%, while the *recql4* and *RECQL4 MLH3* classes showed no significant difference to the WT (65.2 and 71.1%). The restitution of fertility in the *RECQL4 MLH3* class was clear with similar fertility to the *recql4* class, despite slight differences in the number of seeds and number of florets (**Supplementary Figure 4**). No differences were found between the four F_2 subpopulations for TGW suggesting that once seed had set neither mutations individually nor together had a significant impact on the seed development (**Supplementary Figure 4**).

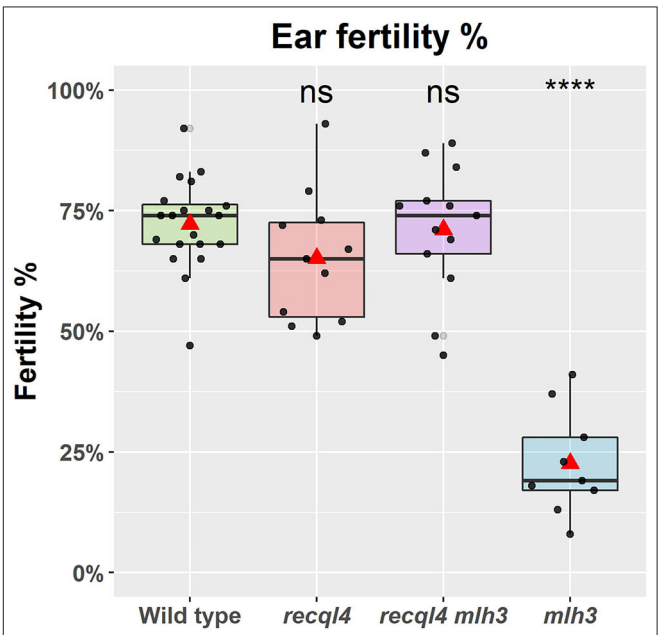

FIGURE 2 | Fertility of the selected F_2 plants as a percentage of fertile florets per ear (%). The statistical comparison with the wild type (WT) was done with the *t*-test where "ns" is not significant, ****$p < 0.0001$. The red triangle shows the mean per genotype. Each dot in the graph represents the average three ears of one plant.

Hvrecql4$_{G700D}$ Mutation Restores and Increases the Number of Chiasmata in a *Hvmlh3*$_{des10}$ Background

Given the WT levels of fertility in the *recql4* and *recql4mlh3* classes, we examined metaphase spreads of the male meiocytes to investigate whether parallel differences could also be detected cytologically. We grew F_4 plants from randomly selected and genotyped F_3s that were representative of the four population classes (**Figure 3**). At metaphase I, the WT population was characterized by the expected seven doughnut-shaped ring bivalents (**Figure 3A**; **Supplementary Figures 5A,E**) that relate to the expected presence of two distal chiasmata in the barley chromosomes at meiosis (Higgins et al., 2012; Barakate et al., 2014; Ramsay et al., 2014). Occasional rod bivalents (**Supplementary Figure 5E**) and ring bivalents with three chiasmata (**Figure 3A**, marked with an arrow) could also be observed as previously described (Colas et al., 2016) with an average of 16.5 chiasmata per cell ($n = 16$, **Figure 3E**). In stark contrast, individuals from the *mlh3* population were characterized by a clear abundance of rod bivalents and univalents (**Figure 3B**), as observed previously on BW230 *des10* (Colas et al., 2016). The reduction of chiasmata compared to WT was significant with an average of 9.1 chiasmata/cell ($n = 11$, **Figure 3E**). Consistent with the restoration of fertility, both populations containing the *recql4*$_{G700D}$ mutation (**Figures 3C,D**) showed seven ring bivalents. Some of these appeared to have more than two chiasmata, characterized by the presence of a knob or bump in the ring (**Figures 3A,C,D**, arrow). Other bivalents, particularly in the double mutant, exhibited a diamond shape (asterisk in **Figures 3C,D**), which may indicate the presence of multiple chiasmata at the distal ends of a single bivalent. The average number of chiasmata per cell was higher compared to WT with 18.3 ($n = 6$) and 19.3 ($n = 24$) chiasmata/cell for *recql4* and double mutant, respectively, which was due to the presence of the triple and quadruple chiasmata bivalents, though this increase was only significant for the double mutant (**Figure 3E**). No significant

differences were found between the two *recql4* containing families. The results of a more conservative scoring with all the ring bivalents being viewed as representing only two chiasmata are shown in **Supplementary Table 2**. The scoring of the metaphase spreads was complicated by the "stickiness" observed in the *recql4* containing lines with occasional chromosome bridges being also observed especially in the double mutants (**Supplementary Figures 5D,H**; **Supplementary Figure 6**).

Optimizing Genetic Analysis in the F_3

Genetic markers are only informative in F_3 families if they are heterozygous in the parental F_2 plants. To optimize the subsequent genetic analysis, heterozygous coverage of the genome was optimized by selecting a combination of the 10 most informative F_2s from the WT and each *mlh3 recql4* mutant class, and up to 10 F_3 plants per family were genotyped using the barley 50K SNP array (Bayer et al., 2017). After cleaning the data, 11,965 polymorphic markers remained in population sizes of 95, 86, 93, and 95 individuals for WT, *recql4*, *mlh3*, and *RECQL4 MLH3* populations, respectively (all the genotyping data is included in **Supplementary Material 4**). Marker coverage in the distal regions was estimated based on the position of the first and last polymorphic marker for each chromosome on the barley physical map, which was used to determine the percentage of the distal chromosome regions missing from the analysis. Missing coverage in the distal extremities was <0.5% for all the chromosomes, except chromosome 3H, which missed ∼0.96% in both the arms, and chromosome 6H, which had 2.74% of missed distal regions, mainly from the long arm (**Supplementary Table 3**). We then partitioned the markers into the three zones described in Mascher et al. (2017) and in **Figure 4**. The largest number of the markers was located in interstitial zone 2 followed by the most distal zone 1 though the density of the markers was higher in zone 1. The pericentromeric zone 3 had the lowest number of markers and the lowest density. The number of genetically informative individuals in each population varied along with the genome according to the location of heterozygosity of the parental F_2s, varying from 10 individuals in the least covered area to 85 individuals in the best. As expected, the number of polymorphic individuals dropped to zero around the position of *MLH3* and *RECQL4*. *RECQL4* was inherited in a large linkage block covering the entire pericentromeric region (part of zone 2 and all of zone 3) of chromosome 2H, while *MLH3* was inherited in a short linkage block in zone 2 of chromosome 5H (gene and introgression are located in **Figure 4**).

Assessing Recombination Frequency

Crossover events on the F_2 generation were estimated as the allele changes between the consecutive markers and were translated into genetic distance (cM) by using the Kosambi mapping function. Both the overall genome wide recombination frequency and total for each chromosome were assessed (**Figure 5A**; **Supplementary Figure 7A**). **Figure 5** revealed that the population containing only the *recql4*$_{G700D}$ mutation had the highest number of recombination events with a total map length of 1924.5 cM (equivalent to 38.5 COs) followed by the double mutant with 1686.1 cM (33.7 COs), the WT with 985.9 cM (19.7 COs), and finally the *mlh3*$_{des10}$ population with 354.3 cM (7.1 COs). This order was maintained for all the chromosomes except for 7H where the double mutant showed the highest recombination (**Supplementary Figure 7A**). Differences in total recombination between each of the three mutant populations with the WT were significant (the Wilcoxon signed-rank test, **Figure 5A**). In the case of the *mlh3* population, we observed a significant reduction ($p < 0.05$) in recombination of 63.15% compared to the WT. In contrast, the *recql4* single mutant nearly doubled the WT recombination (95.2% increase, $p < 0.05$), while the increase in the double mutant was slightly less (71% increase, $p < 0.05$) compared to the WT. Comparing the double mutant and *MLH3* populations, indicated an increase of 476% ($p < 0.05$) associated with the presence of *recql4*$_{G700D}$. Finally, in the comparisons between the three mutant populations, significant differences ($p < 0.05$) were found between the two *recql4*$_{G700D}$ containing populations compared with *mlh3*, but not between each other ($p > 0.05$).

Recombination Distribution

Correlations between the genetic (cM) and physical maps (Mbp) (**Figure 4**) clearly show the well-described skewed patterns of recombination in barley for each chromosome (Mascher et al., 2017). To quantify and compare the distribution of recombination along the chromosomes and between the populations, we plotted recombination frequency in each of the three previously designated genomic zones (**Figure 5B**) with the short distal zone 1 being gene dense and relatively recombinogenic, the interstitial zone 2 displaying less recombination, and the large pericentromeric zone 3 showing no or very little recombination despite containing a considerable proportion of the gene complement (Mascher et al., 2017). The *recql4* population showed the highest overall levels followed by the double mutant, WT then *mlh3* populations. Chromosome-wise (**Supplementary Figure 7B**) this order was conserved except for interstitial zone 2 of chromosome 2H where the WT had more recombination compared to double mutant, and chromosome 7H where the double mutant had higher recombination compared to *recql4*$_{G700D}$. The Wilcoxon signed-rank test showed a significant increase of recombination ($p < 0.05$) in both zones 1 and 2 of the *recql4* and double mutant populations and significantly ($p < 0.05$) less recombination in the *mlh3* population compared to the WT. The pericentromeric zone 3 did not show any significant differences in recombination between any of the populations. The difference in the relative distribution of recombination between the zones among the populations was compared by using the contingency table and the chi-squared test (**Supplementary Table 4**). Interestingly, the WT and *mlh3* populations showed no significant differences between their relative proportions of recombination in zone 1/zone 2, but both the *recql4*$_{G700D}$-containing populations had significantly ($p < 0.05$) more proportional recombination (around 4%) skewed from zone 2 to zone 1. Finally, to

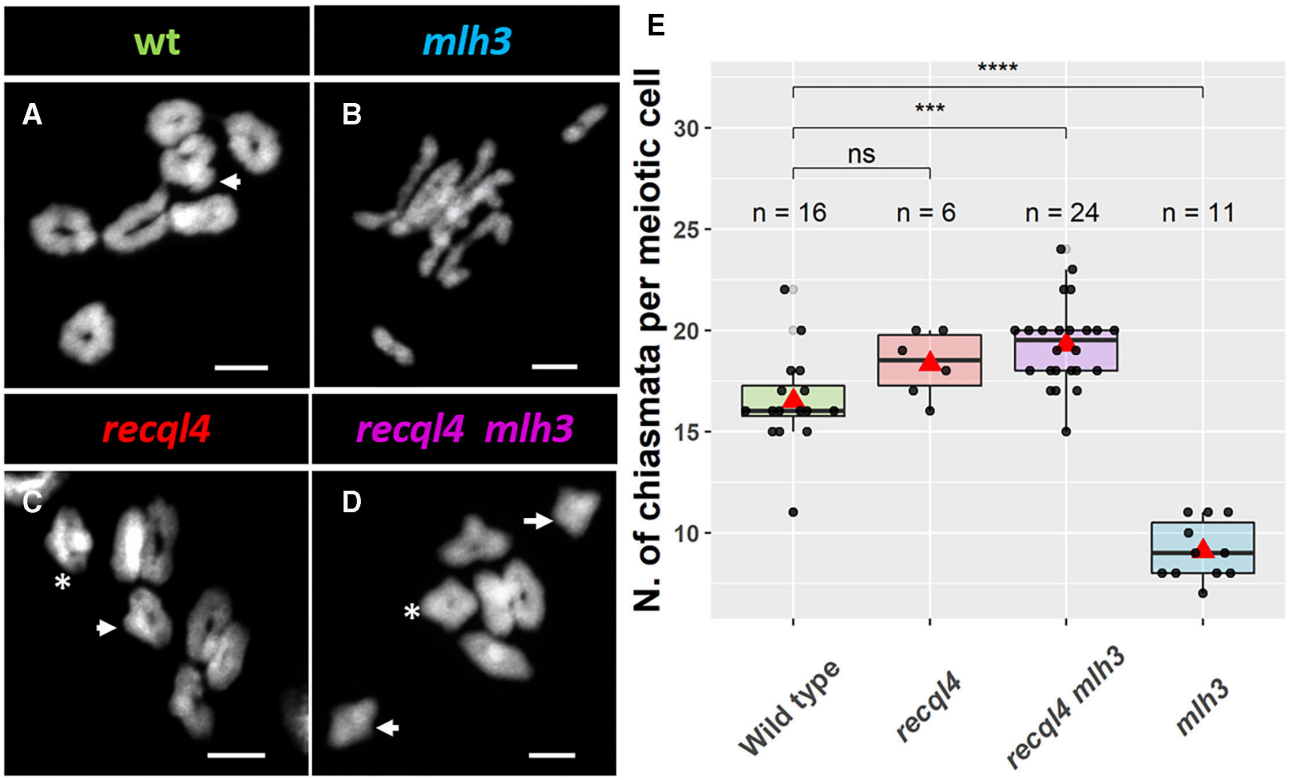

FIGURE 3 | Cytology of male meiosis on F_4 plants of the different populations: **(A)** WT, **(B)** *mlh3,* **(C)** *recql4*, and **(D)** *recql4 mlh3*. White arrows indicate the bivalents counted with three crossovers and asterisks refer to the bivalents with four crossovers. **(E)** Total chiasmata count per cell and population. The statistical comparison with the WT was carried out with the *t*-test where "ns" is not significant, ***$p < 0.001$, ****$p < 0.0001$. The red triangle shows the mean per genotype. Bar size: 10 μm.

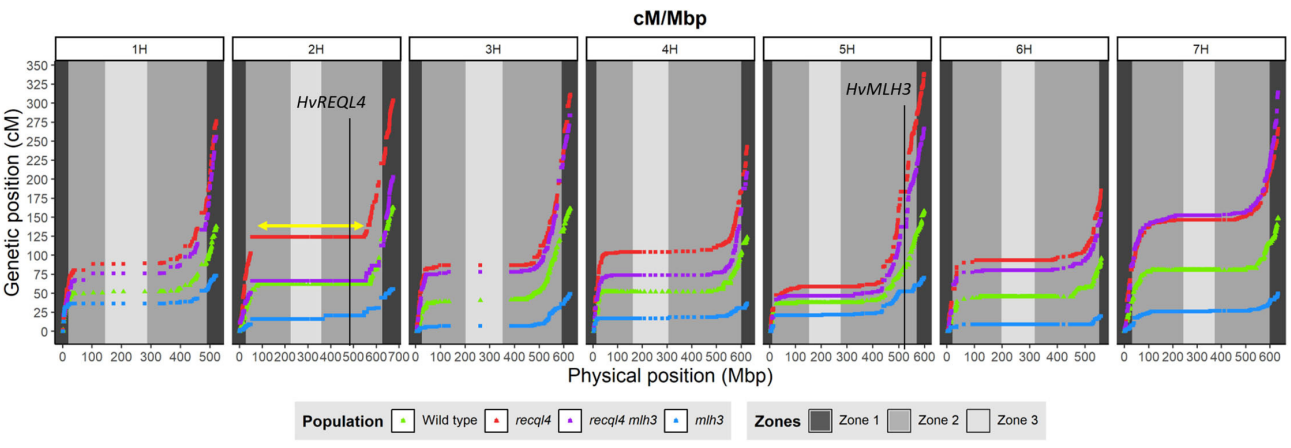

FIGURE 4 | Comparison of the genetic map (cM) and the physical map (Mbp) for each population (WT in green, *mlh3* in blue, *recql4* in red, and the double mutants in purple). The physical positions of *HvRECQL4* and *HvMLH3* are marked with a vertical line in 2H and 5H chromosomes, respectively. The yellow arrow marked in the 2H chromosome indicates the block introgressed together with *HvRECQL4*.

provide a higher resolution overview of the distribution of recombination in all the populations, we divided each chromosome into 50 bins, each representing ∼2% of the physical length of each chromosome, and combined the amount of recombination (cM) observed in each bin across all seven barley chromosomes into a single measure. **Figure 6** shows the resulting recombination landscape for each of the four populations and clearly illustrates the significant increase in both *recql4*$_{G700D}$-containing populations in the first 8% and last 8% of the genome.

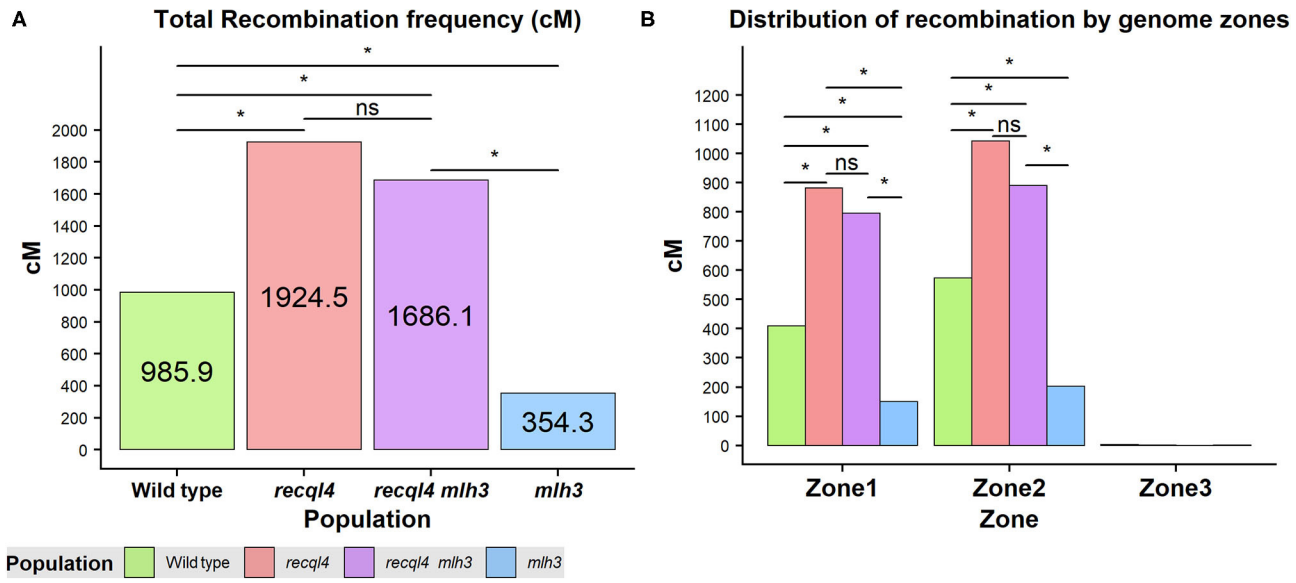

FIGURE 5 | (A) Total recombination frequency (cM) for each population. **(B)** Distribution of recombination by the three genomic zones for each population genome-wise. The differences between populations genome wide were tested by the Wilcoxon signed-rank test where *ns* = not significant, $^*p < 0.05$.

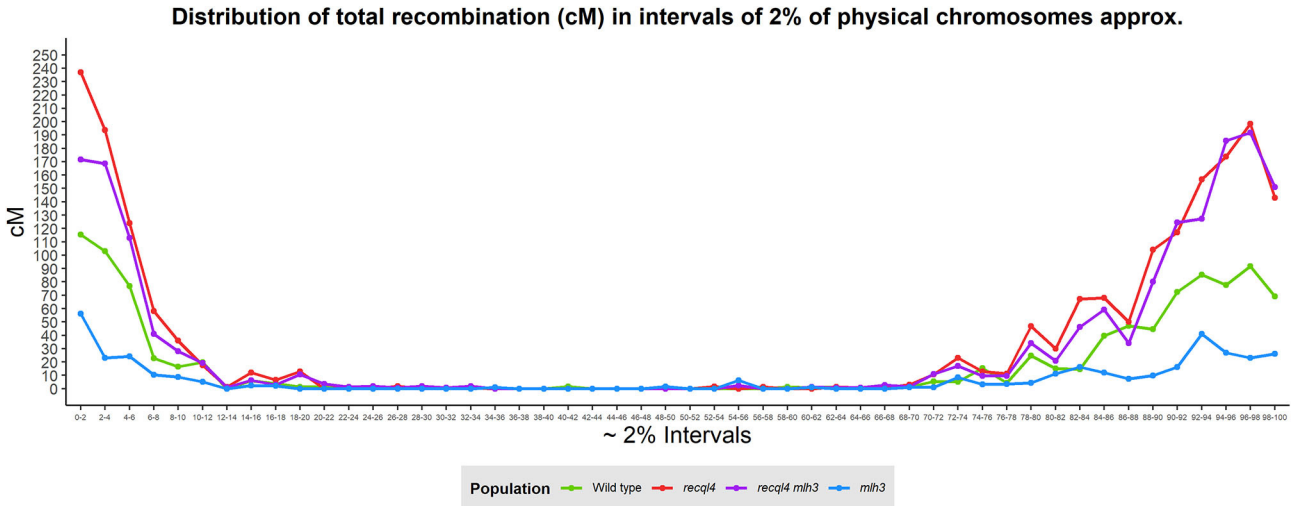

FIGURE 6 | Genome-wide distribution of recombination based on the division of the physical chromosomes in 2% intervals.

DISCUSSION

In this study, we show that the presence of a single C/T nucleotide change that generates a G700D non-synonymous substitution in *RECQL4* is able to restore fertility to the previously described semi-sterile BW230 *des10* mutant of barley that had shown to contain a 159-bp deletion in *HvMLH3* (Colas et al., 2016). Restoration of fertility in *SuppLine2099* is associated with a restoration of a full-ring bivalent complement at metaphase with a clear indication of additional chiasmata in plants in the *recql4* and *recql4mlh3* classes (**Figure 3**). Genetic mapping showed that the *recql4* mutation in *SuppLine2099* displayed an unprecedented increase in meiotic recombination frequency to nearly double compared to the WT and over four times higher compared to the $mlh3_{des10}$ mutant. The increase in recombination associated with mutations in *RECQL4* (*ca.*2.0-fold) is similar to that has been observed in other species, albeit at a slightly lower level. Mieulet et al. (2018) reported that *recql4* driven increases in recombination in a range of species including rice (3.2-fold), pea (4.7-fold), and tomato (2.7-fold), while Serra et al. (2018) and Fernandes et al. (2017) reported an increase of 3.3- and 3.8-fold, respectively, in *Arabidopsis*. However, recombination rates

are species-specific and affected by the genomic features (Tiley and Burleigh, 2015) and barley, with a large genome of about 5 Gb, exhibits pronounced, distally skewed recombination (Mayer et al., 2012; Mascher et al., 2017; Schreiber et al., 2020), so it may not be entirely legitimate to compare that had been observed in barley to these other species. Moreover, the comparisons are complicated by the fact that the *RECQL4* mutant studied is potentially not as strong as the exonic T-DNA insertion mutants (Fernandes et al., 2017; Mieulet et al., 2018; Serra et al., 2018) or nonsense-induced TILLING mutants (Mieulet et al., 2018) utilized in the other studies.

The recombination data reported indicates that a non-synonymous G700D amino acid substitution in the conserved helicase domain of *HvRECQL4* results in an increase in recombination exclusively across zones 1 and 2 in the barley genome (Mascher et al., 2017), i.e., the increase occurs in the regions of the barley genome that already undergo recombination in the WT. This is similar to the results for rice shown by Mieulet et al. (2018). The recombination cold pericentromeric zone 3 showed no increase in recombination indicating that the induced increase in recombination frequency was not accompanied by any fundamental change in CO distribution (Mieulet et al., 2018). The relative recombination patterns among the four populations studied in our limited population sizes indicate that in the *recql4*-containing populations, recombination was further skewed toward distal zone 1 with a concomitant reduction in interstitial zone 2. This difference potentially relates to the fundamental constraints on the distribution of recombination in large genome cereals that is driven by the spatial and temporal progression of synapsis from the telomeres to the centromeres and the associated positioning and fate of DSBs and CO intermediates (Higgins et al., 2012).

It is of interest that $recql4_{G700D}$ was identified in our suppressor screen of *BW230 des10,* a genotype that we previously demonstrated contains a deletion in *HvMLH3* (Colas et al., 2016). A mutation in *RECQL4* was previously identified in a suppressor screen in *Arabidopsis* Landsberg erecta by using the class I CO meiotic mutant *msh4* (Séguéla-Arnaud et al., 2015). Intriguingly, suppressor mutations in *RECQL4* were not identified in the earlier screens conducted by using the *Columbia* ecotype due to the gene being duplicated in the *Arabidopsis* genome and *Columbia* containing two functional variants of the gene compared to only one in Landsberg erecta. To the best of our knowledge, a suppressor screen in an *MLH3* mutant background has not been carried out in *Arabidopsis* where the focus has been on the use of ZMM mutants and CO formation with the clearer phenotype that brings. However, it is reassuring that this screen in barley identified a mutant in the helicase domain of *RECQL4* as did the suppressor screen in *msh4* in *Arabidopsis* (Séguéla-Arnaud et al., 2015) highlighting the potential of suppressor screens of non-ZMM mutants to identify the relevant genetic factors and the potential of studies in the non-model species.

Rather than following a traditional and extended positional cloning route to characterize the nature of the mutation in *SuppLine2099*, we used target sequence enrichment of the known meiotic genes combined with the Illumina sequencing to highlight the causal mutation (Schreiber et al., 2019). The restoration of fertility was confirmed in the F_2 populations (**Figure 2**) where the percentage of fertile florets in the double $recql4_{G700D}$ *mlh3* mutant plants reached the WT levels. Interestingly, the total number of florets per ear was lower than the WT and *mlh3* in both $recql4_{G700D}$-containing mutant populations. Both populations containing the $recql4_{G700D}$ allele inherited the mutation in a large linkage block (approximately sized 450 Mbp) covering the whole of zone 3 and much of zone 2 on chromosome 2H. Given that *cv*. Bowman, the recurrent parent of BW320 *des10* has a reduced number of florets compared to *cv*. Barke (data not shown) and it is possible that the associated changes found in the floret number (**Supplementary Figure 4**) could be a background effect inherited with the $recql4_{G700D}$ mutation via linkage drag. Alternatively, the phenotype observed could potentially be a direct result of the disrupted function of RECQL4 with an effect on the multiple interactions controlling fertility and inflorescence development in barley. Use of the barley 50K iSelect SNP array allowed robust genome wide genotyping and the length of the WT population genetic map of 985.9 cM is close compared to observed in the previous studies (Li et al., 2010; Zhou et al., 2015; Bayer et al., 2017), despite the reduced mapping power inherent in the use of F_3 material. It is possible that the recombination observed in our populations may be somewhat underestimated due to marker monomorphism and, in particular, this may explain the lower overall recombination found on chromosome 6H (**Supplementary Figure 7A**). Nevertheless, the strong reduction of total genetic map length of 63.1% detected in the *mlh3* population in this study was similar though slightly more severe than the 54.1% reported in Colas et al. (2016), though each study used a different cross and the latter used a previous lower density 9K genotyping array.

Metaphase spreads on the $mlh3_{des10}$mutation-containing F_4 plants revealed fewer chiasmata compared to the WT with a predominance of rod bivalents (**Figure 3**) and occasional univalents. This metaphase I phenotype and the comparison to the seven ring bivalents in the WT are entirely congruent with that previously reported for the BW230 *des10* mutant and the WT (Colas et al., 2016). The cytological appearance of bivalents in plants with the $recql4_{G700D}$ mutation was suggestive of multiple distal chiasmata—though detailed counts were impossible to determine. Similar observations have been found previously in the cytological studies in the anti-CO mutants in *Arabidopsis* (Crismani et al., 2012; Séguéla-Arnaud et al., 2015) and reflect the general difficulty in estimating CO numbers from chiasmata counts (Colas et al., 2016). Furthermore, the number of COs estimated from the metaphase spreads is lower compared to those estimated by the genetic maps as observed previously in barley (Ramsay et al., 2014) and these differences are even higher (nearly double) for the $recql4_{G700D}$-containing populations, underlining the difficulties of this approach to discern between the closely neighboring chiasmata. The difficulty in assessing CO numbers in the double mutant was potentially exacerbated by the presence of the chromosome bridges at metaphase, which potentially indicates specific issues in the resolution of the repair intermediates.

Both cytological characterization and genetic segregation analysis indicated that the *recql4* single and *RECQL4 MLH3* double mutant had a broadly similar CO phenotype. Both mutants displayed ring bivalents and bivalents with more than two COs with some showing evidence of the chromosome bridges in the double mutant (**Supplementary Figure 6**). An increase in the average chiasmata/cell counts (**Figure 3E**) was only found significant for the double mutant (compared to WT), but the number of available cells for the *recql4* population was unfortunately much more limited ($n = 6$). This population was also not significantly different from the double mutant, suggesting the increased trend of *recql4* could be more consistent if more pictures/cells were available. The observations in the double mutant are particularly striking given the severely disrupted phenotype of genotypes containing $mlh3_{des10}$ alone and are consistent with the genetic data indicating a 4.75-fold increase in recombination in *RECQL4 MLH3*. This level of increase in the recombination mirrors found in the suppressor screens in *Arabidopsis* by using ZMM mutants (Crismani et al., 2012) and corresponds to the restoration of fertility found in *SuppLine2099*. Further studies are needed to confirm whether the increase in CO numbers in the double (and single mutant) is through non-interfering class II COs as reported by Séguéla-Arnaud et al. (2015) and whether the temporal delay in repair events in an *mlh3* background (Colas et al., 2016; Toledo et al., 2019) alters the balance of class I/II CO resulting from the resolution of the repair intermediates.

As shown in the other systems, combining $recql4_{G700D}$ with additional mutations may establish the possibility of inducing even more recombination in barley. Serra et al. (2018) increased recombination levels of a *recql4a recql4b* double mutant of *Arabidopsis* from 3.3- to 3.7-fold by increasing the dosage of the pro-CO E3 ligase *HEI10* via genetic transformation. In the case of anti-CO genes, although it has been reported that they act independently (Séguéla-Arnaud et al., 2015), double mutants do not necessarily result in a further CO increase. Thus, *fancm* on its own induced an increase in recombination in *Arabidopsis*, rice, and pea, but not in the subsequent studies in *Arabidopsis* F_1 hybrids (Crismani et al., 2012; Mieulet et al., 2018) or wheat (Raz et al., 2021). Moreover, the combination of *fancm* and *recql4* did not show a further increase over *recql4* in *Arabidopsis* or pea (Mieulet et al., 2018). The highest levels of recombination in hybrid *Arabidopsis* were found by combining *recql4* and *figl1* (Fernandes et al., 2017). However, mutating *figl1* induced sterility in rice (Zhang et al., 2017), pea, and tomato (Mieulet et al., 2018). While such undesired and species-specific effects necessitate further study, the use of the mutant alleles in the early stages of a breeding program as suggested by Mieulet et al. (2018) may have the potential to speed up the breeding process.

To conclude, we provide evidence that a mutation in *RECQL4*, as demonstrated in the other species, significantly boosts recombination in a large genome cereal such as barley. The scale of the increase is greater compared to the other approaches that have so far been shown to increase recombination in barley such as temperature (Phillips et al., 2015). The availability of a demonstrated effective non-GM anti-CO allele of *RECQL4* in barley opens the possibility of testing whether increasing recombination will, or will not, have an enabling role in general or specific aspects of crop improvement such as introgression breeding. Given the limits to the plasticity of recombination remain unknown, intriguing options remain to be explored, such as combining $recql4_{G700D}$ in barley with other mutations or combining genetic variants with "treatments" such as temperature (Phillips et al., 2015; Modliszewski et al., 2018), chemicals (Rey et al., 2018), or speed breeding conditions (Ghosh et al., 2018). While we have underlined the potentially important role of *RECQL4* as an anti-CO factor in barley, a major challenge remains in assessing if and how $recql4_{G700D}$ can be used effectively to improve the rate of genetic gain in barley crop improvement.

CONCLUSION

By screening for the restoration of fertility of a semi-sterile *HvMLH3* mutant, we identified a non-synonymous suppressor G700D mutation in the anti-CO gene *HvRECQL4*. We show that in both the WT and *Hvmlh3* genetic backgrounds, the G700D mutation increases recombination frequency significantly (ca. 2- and >4-fold, respectively) with the CO distribution showing a stronger skew toward the telomeric regions compared to the WT and no change in the lack of recombination in the pericentromeric regions of the chromosomes. The availability of germplasm containing the $recql4_{G700D}$ mutation will allow us to test the hypothesis that increasing recombination can increase the rate of genetic gain or rapidly reduce the size of introgressed genomic segments from the wild or alien species in the plant breeding programs.

DATA AVAILABILITY STATEMENT

The original contributions presented in the study are included in the article/**Supplementary Materials**, further inquiries can be directed to the corresponding author/s.

AUTHOR CONTRIBUTIONS

RW and LR conceptualized and supervised the research experiment. MM conducted the experiment to generate the suppressor lines and MS identified the meiotic mutations. MA conducted the experiment work by creating populations to be genotyped and for cytology and drafted the manuscript. Genotype data were processed by MM and PS and analyzed by MA. Cytological samples were prepared by MA and analyzed by IC. LR, RW, IC, MS, and MM reviewed and contributed to improving the manuscript. RW, LR, MA, and IC reviewed last version of the manuscript. All authors contributed to the article and approved the submitted version.

FUNDING

This research was funded by the European Community's Seventh Framework Programme FP7/2007–2013 under Grant Agreement

No. 222883 MeioSys and by the ERC advanced grant Shuffle (Project ID: 669182). LR and RW were funded from the Scottish Government's Rural and Environment Science and Analytical Services Division Theme 2 Work Program 2.1 and IC was funded by the BBSRC BB/T008636/1.

ACKNOWLEDGMENTS

We would like to acknowledge Philip Smith for proofreading and Colin Alexander from Biomathematics & Statistics Scotland (BIOSS) for help and advice.

SUPPLEMENTARY MATERIAL

The Supplementary Material for this article can be found online at: https://www.frontiersin.org/articles/10.3389/fpls.2021.706560/full#supplementary-material

Supplementary Material 1 | Kompetitive allele-specific PCR (KASP) primer oligos (Excel).

Supplementary Material 2 | Parameters in the raw images processed with Imaris (Excel).

Supplementary Material 3 | *HvRECQL4* genomic and protein sequence (pdf).

Supplementary Material 4 | 50K genotyping data (Excel).

Supplementary Figure 1 | Suppressor screening population development and process summary.

Supplementary Figure 2 | (A) Outline of the development of F_3 populations to be genotyped. **(B)** Selection of the genotypes across the generations to create F_3 populations. *SuppLine2099* was crossed with *cv*. Barke background to generate heterozygous F_1s, which were grown to produce F_2 seed. F_2 plants were grown and selected by using Kompetitive allele-specific PCR (KASP) genotyping for targeting the segregating mutations. Only the four homozygous combinations were selected to be grown as F_2 families and produce F_3 seeds. These were later grown and genotyped with the 50K assay to study the effect of the mutation in F_2 recombination. The alleles in the mutated genes are indicated by the square box color, being green for the wild type (WT)-like allele, dark red for the $recql4_{G700D}$ mutation, and light blue for the $mlh3_{des10}$ mutation. The gray area in the chromosomes indicates different recombinant backgrounds among the populations.

Supplementary Figure 3 | Barchart showing the average fertility of the three plants per selected line in the suppressor screening. *SuppLine2099* was chosen for the present study It is marked in purple and *desynaptic10 (des10)* in blue.

Supplementary Figure 4 | Different fertility phenotypes of the selected F_2 plants. **(A)** Total seeds per ear, **(B)** the Total number of florets per ear, **(C)** Total grams per ear, **(D)** Thousand grain weight (TGW). The statistical comparisons were done with the *t*-test where "ns" is not significant, $^{*}p < 0.05$, $^{**}p < 0.01$, $^{***}P < 0.001$, $^{****}p < 0.0001$. All the comparisons are done by using the WT as a reference. The red triangle shows the mean per genotype. Each dot in the graph represents the average of 3 years of one plant, except for grams per year and TGW, where all the ears of the plants were used.

Supplementary Figure 5 | Cytology of male meiosis on the F_4 plants of different populations: **(A,E)** WT, **(B,F)** *mlh3,* **(C,G)** *recql4*, and **(D,H)** *recql4mlh3*. Chiasmata counts are pointed with the gray dots (when discernible) and the chromosome bridges marked with white arrows. Bar size: 5 μm.

Supplementary Figure 6 | Quantitative scoring of the chromosome bridges per meiotic cell. The statistical comparisons are done with the *t*-test where "ns" is not significant, $^{****}p < 0.0001$. All the comparisons are done by using the WT as a reference.

Supplementary Figure 7 | (A) Genetic chromosome length (cM) of every chromosome for each population. **(B)** Distribution of recombination by the genomic zones for each population chromosome-wise.

Supplementary Table 1 | Exome capture output and mutation details of the lines selected in the suppressor screening. *SuppLine2099* (first row) was selected for this study.

Supplementary Table 2 | Rescoring of chiasmata counts by using a more conservative approach of counting only the ring bivalents.

Supplementary Table 3 | Polymorphic marker summary. Details of distal regions not covered by polymorphic markers.

Supplementary Table 4 | Relative percentage of recombination contained in each genomic zone for each population. The significance is calculated by the contingency table and the chi-squared test of the proportions of recombination in each population compared to the WT control (ns = not significant, $^{*}p < 0.05$, $^{**}p < 0.001$).

REFERENCES

Barakate, A., Higgins, J. D., Vivera, S., Stephens, J., Perry, R. M., Ramsay, L., et al. (2014). The synaptonemal complex protein ZYP1 is required for imposition of meiotic crossovers in barley. *Plant Cell* 26, 729–740. doi: 10.1105/tpc.113.121269

Bayer, M. M., Rapazote-Flores, P., Ganal, M., Hedley, P. E., Macaulay, M., Plieske, J., et al. (2017). Development and evaluation of a barley 50k iSelect SNP array. *Front. Plant Sci.* 8:1792. doi: 10.3389/fpls.2017.01792

Berchowitz, L. E., and Copenhaver, G. P. (2010). Genetic interference: don't stand so close to me. *Curr. Genomics* 11, 91–102. doi: 10.2174/138920210790886835

Blary, A., and Jenczewski, E. (2019). Manipulation of crossover frequency and distribution for plant breeding. *Theor. Appl. Genet.* 132, 575–592. doi: 10.1007/s00122-018-3240-1

Caldwell, D. G., McCallum, N., Shaw, P., Muehlbauer, G. J., Marshall, D. F., and Waugh, R. (2004). A structured mutant population for forward and reverse genetics in Barley (*Hordeum vulgare* L.). *Plant J.* 40, 143–150. doi: 10.1111/j.1365-313X.2004.02190.x

Choi, Y., Sims, G. E., Murphy, S., Miller, J. R., and Chan, A. P. (2012). Predicting the functional effect of amino acid substitutions and indels. *PLoS ONE* 7:e46688. doi: 10.1371/journal.pone.0046688

Colas, I., Macaulay, M., Higgins, J. D., Phillips, D., Barakate, A., Posch, M., et al. (2016). A spontaneous mutation in MutL-Homolog 3 (HvMLH3) affects synapsis and crossover resolution in the barley desynaptic mutant des10. *New Phytol.* 212, 693–707. doi: 10.1111/nph.14061

Copenhaver, G. P. (2003). Crossover interference in *Arabidopsis*. *Am. J. Hum. Genet.* 73, 188–197. doi: 10.1086/376610

Crismani, W., Girard, C., Froger, N., Pradillo, M., Santos, J. L., Chelysheva, L., et al. (2012). FANCM limits meiotic crossovers. *Science* 336, 1588–1590. doi: 10.1126/science.1220381

Darrier, B., Rimbert, H., Balfourier, F., Pingault, L., Josselin, A. A., Servin, B., et al. (2017). High-resolution mapping of crossover events in the hexaploid wheat genome suggests a universal recombination mechanism. *Genetics* 206, 1373–1388. doi: 10.1534/genetics.116.196014

Devaux, P., Kilian, A., and Kleinhofs, A. (1995). Comparative mapping of the barley genome with male and female recombination-derived, doubled haploid populations. *Mol. Gen. Genet.* 249, 600–608. doi: 10.1007/BF00418029

Druka, A., Potokina, E., Luo, Z., Jiang, N., Chen, X., Kearsey, M., et al. (2010). Expression quantitative trait locianalysis in plants. *Plant Biotechnol. J.* 8, 10–27. doi: 10.1111/j.1467-7652.2009.00460.x

Fernandes, J. B., Duhamel, M., Seguéla-Arnaud, M., Froger, N., Girard, C., Choinard, S., et al. (2018). FIGL1 and its novel partner FLIP form a conserved complex that regulates homologous recombination. *PLoS Genet.* 14:e1007317. doi: 10.1371/journal.pgen.1007317

Fernandes, J. B., Seguéla-Arnaud, M., Larchevêque, C., Lloyd, A. H., and Mercier, R. (2017). Unleashing meiotic crossovers in hybrid plants. *Proc. Natl. Acad. Sci. U.S.A.* 2017:13078. doi: 10.1101/159640

Ghosh, S., Ramirez-Gonzalez, R. H., Simmonds, J., Wells, R., Rayner, T., Hafeez, A., et al. (2018). Speed breeding in growth chambers and glasshouses for crop breeding and model plant research. *Nat. Protoc.* 13, 2944–2963. doi: 10.1038/s41596-018-0072-z

Girard, C., Chelysheva, L., Choinard, S., and Froger, N., Macaisne, N., Lehmemdi, A., et al. (2015). AAA-ATPase FIDGETIN-LIKE 1 and helicase FANCM antagonize meiotic crossovers by distinct mechanisms. *PLoS Genet.* 11:e1005369. doi: 10.1371/journal.pgen.1005369

Higgins, J. D., Buckling, E. F., Franklin, F. C. H., and Jones, G. H. (2008). Expression and functional analysis of *AtMUS81* in *Arabidopsis* meiosis reveals a role in the second pathway of crossing-over. *Plant J.* 54, 152–162. doi: 10.1111/j.1365-313X.2008.03403.x

Higgins, J. D., Perry, R. M., Barakate, A., Ramsay, L., Waugh, R., Halpin, C., et al. (2012). Spatiotemporal asymmetry of the meiotic program underlies the predominantly distal distribution of meiotic crossovers in barley. *Plant Cell* 24, 4096–4109. doi: 10.1105/tpc.112.102483

Jayakodi, M., Padmarasu, S., Haberer, G., Bonthala, V. S., Gundlach, H., Monat, C., et al. (2020). The barley pan-genome reveals the hidden legacy of mutation breeding. *Nature* 588, 284–289. doi: 10.1038/s41586-020-2947-8

Li, H., Kilian, A., Zhou, M., Wenzl, P., Huttner, E., Mendham, N., et al. (2010). Construction of a high-density composite map and comparative mapping of segregation distortion regions in barley. *Mol. Genet. Genomics* 284, 319–331. doi: 10.1007/s00438-010-0570-3

Lundqvist, U., Franckowiak, J., and Konishi, T. (1997). New and revised descriptions of barley genes. *Barley Genet. Newsl. Med. Sci. Hist. Soc.* 26. 22–516.

Mascher, M., Gundlach, H., Himmelbach, A., Beier, S., Twardziok, S. O., Wicker, T., et al. (2017). A chromosome conformation capture ordered sequence of the barley genome. *Nature* 544, 427–433. doi: 10.1038/nature22043

Mayer, K. F. X., Waugh, R., Langridge, P., Close, T. J., Wise, R. P., Graner, A., et al. (2012). A physical, genetic and functional sequence assembly of the barley genome. *Nature* 491, 711–716. doi: 10.1038/nature11543

Mercier, R., Jolivet, S., Vezon, D., Huppe, E., Chelysheva, L., Giovanni, M., et al. (2005). Two meiotic crossover classes cohabit in *Arabidopsis*: One is dependent on *MER3*, whereas the other one is not. *Curr. Biol.* 15, 692–701. doi: 10.1016/j.cub.2005.02.056

Mercier, R., Mézard, C., Jenczewski, E., Macaisne, N., and Grelon, M. (2015). The molecular biology of meiosis in plants. *Annu. Rev. Plant Biol.* 66, 297–327. doi: 10.1146/annurev-arplant-050213-035923

Mieulet, D., Aubert, G., Bres, C., Klein, A., Droc, G., Vieille, E., et al. (2018). Unleashing meiotic crossovers in crops. *Nat. Plants* 4, 1010–1016. doi: 10.1038/s41477-018-0311-x

Modliszewski, J. L., Wang, H., Albright, A. R., Lewis, S. M., Bennett, A. R., Huang, J., et al. (2018). Elevated temperature increases meiotic crossover frequency via the interfering (Type I) pathway in *Arabidopsis thaliana*. *PLoS Genet.* 14:e1007384. doi: 10.1371/journal.pgen.1007384

Monat, C., Padmarasu, S., Lux, T., Wicker, T., Gundlach, H., Himmelbach, A., et al. (2019). TRITEX: chromosome-scale sequence assembly of Triticeae genomes with open-source tools. *Genome Biol.* 20:284. doi: 10.1186/s13059-019-1899-5

Phillips, D., Jenkins, G., Macaulay, M., Nibau, C., Wnetrzak, J., Fallding, D., et al. (2015). The effect of temperature on the male and female recombination landscape of barley. *New Phytol.* 208, 421–429. doi: 10.1111/nph.13548

Ramsay, L., Colas, I., and Waugh, R. (2014). "Modulation of meiotic recombination," in *Biotechnological Approaches to Barley Improvement*, eds J. Kumlehn and N. Stein (Berlin; Heidelberg: Springer), 311–329. doi: 10.1007/978-3-662-44406-1_16

Raz, A., Dahan-Meir, T., Melamed-Bessudo, C., Leshkowitz, D., and Levy, A. A. (2021). Redistribution of meiotic crossovers along wheat chromosomes by virus-induced gene silencing. *Front. Plant Sci.* 11:635139. doi: 10.3389/fpls.2020.635139

Rey, M., Martín, A. C., Smedley, M., Hayta, S., Harwood, W., Shaw, P., et al. (2018). Magnesium increases homoeologous crossover frequency in *ZIP4* (*Ph1*) mutant wheat-wild relative hybrids. *Front. Plant Sci.* 9:509. doi: 10.1101/278341

Schreiber, M., Barakate, A., Uzrek, N., Macaulay, M., Sourdille, A., Morris, J., et al. (2019). A highly mutagenised barley (*cv*. Golden Promise) TILLING population coupled with strategies for screening - by - sequencing. *Plant Methods* 15:99. doi: 10.1186/s13007-019-0486-9

Schreiber, M., Mascher, M., Wright, J., Padmarasu, S., Himmelbach, A., Heavens, D., et al. (2020). A genome assembly of the barley 'transformation reference' cultivar golden promise. *G3 Genes Genomes Genet.* 10, 1823–1827. doi: 10.1101/2020.02.12.945550

Séguéla-Arnaud, M., Crismani, W., Larchevêque, C., Mazel, J., Froger, N., Choinard, S., et al. (2015). Multiple mechanisms limit meiotic crossovers: TOP3α and two BLM homologs antagonize crossovers in parallel to FANCM. *Proc. Natl. Acad. Sci. U.S.A.* 112, 4713–4718. doi: 10.1073/pnas.1423107112

Serra, H., Lambing, C., Griffin, C. H., Topp, S. D., Nageswaran, D. C., Underwood, C. J., et al. (2018). Massive crossover elevation via combination of *HEI10* and *recq4a recq4b* during *Arabidopsis* meiosis. *Proc. Natl. Acad. Sci. U.S.A.* 115, 2437–2442. doi: 10.1073/pnas.1713071115

Tiley, G. P., and Burleigh, J. G. (2015). The relationship of recombination rate, genome structure, and patterns of molecular evolution across angiosperms. *BMC Evol. Biol.* 15:194. doi: 10.1186/s12862-015-0473-3

Toledo, M., Sun, X., Brieño-Enríquez, M. A., Raghavan, V., Gray, S., Pea, J., et al. (2019). A mutation in the endonuclease domain of mouse MLH3 reveals novel roles for MutLγ during crossover formation in meiotic prophase I. *PLoS Genet.* 15:e1008177. doi: 10.1371/journal.pgen.1008177

Wang, Y., and Copenhaver, G. P. (2018). Meiotic recombination : mixing it up in plants. *Annu. Rev. Plant Biol.* 69, 577–609. doi: 10.1146/annurev-arplant-042817-040431

Wijnker, E., and de Jong, H. (2008). Managing meiotic recombination in plant breeding. *Trends Plant Sci.* 13, 640–646. doi: 10.1016/j.tplants.2008.09.004

Zhang, P., Zhang, Y., Sun, L., Sinumporn, S., and Yang, Z. (2017). The Rice AAA-ATPase OsFIGNL1 is essential for male meiosis. *Front. Plant Sci.* 8:1639. doi: 10.3389/fpls.2017.01639

Zhou, G., Zhang, Q., Zhang, X., Tan, C., and Li, C. (2015). Construction of high-density genetic map in barley through restriction-site associated DNA sequencing. *PLoS ONE* 10:e0133161. doi: 10.1371/journal.pone.0133161

Conflict of Interest: The authors declare that the research was conducted in the absence of any commercial or financial relationships that could be construed as a potential conflict of interest.

Publisher's Note: All claims expressed in this article are solely those of the authors and do not necessarily represent those of their affiliated organizations, or those of the publisher, the editors and the reviewers. Any product that may be evaluated in this article, or claim that may be made by its manufacturer, is not guaranteed or endorsed by the publisher.

frontiers in Plant Science

REVIEW
published: 21 December 2021
doi: 10.3389/fpls.2021.718346

Caught in the Act: Live-Cell Imaging of Plant Meiosis

*Maria Ada Prusicki, Martina Balboni, Kostika Sofroni†, Yuki Hamamura and Arp Schnittger**

Department of Developmental Biology, Institute for Plant Science and Microbiology, University of Hamburg, Hamburg, Germany

Live-cell imaging is a powerful method to obtain insights into cellular processes, particularly with respect to their dynamics. This is especially true for meiosis, where chromosomes and other cellular components such as the cytoskeleton follow an elaborate choreography over a relatively short period of time. Making these dynamics visible expands understanding of the regulation of meiosis and its underlying molecular forces. However, the analysis of meiosis by live-cell imaging is challenging; specifically in plants, a temporally resolved understanding of chromosome segregation and recombination events is lacking. Recent advances in live-cell imaging now allow the analysis of meiotic events in plants in real time. These new microscopy methods rely on the generation of reporter lines for meiotic regulators and on the establishment of *ex vivo* culture and imaging conditions, which stabilize the specimen and keep it alive for several hours or even days. In this review, we combine an overview of the technical aspects of live-cell imaging in plants with a summary of outstanding questions that can now be addressed to promote live-cell imaging in Arabidopsis and other plant species and stimulate ideas on the topics that can be addressed in the context of plant meiotic recombination.

Keywords: chromosome, recombination, microscopy, cell division, culture media, fluorescent reporter, time course

OPEN ACCESS

Edited by:
Christophe Lambing, University of Cambridge, United Kingdom

Reviewed by:
André Marques, Max Planck Institute for Plant Breeding Research, Germany
Olivier Da Ines, Université Clermont Auvergne, France

***Correspondence:**
Arp Schnittger
arp.schnittger@uni-hamburg.de

†Present address:
Kostika Sofroni, Department of Meiosis, Max Planck Institute for Biophysical Chemistry, Göttingen, Germany

Specialty section:
This article was submitted to Plant Cell Biology, a section of the journal Frontiers in Plant Science

Received: *31 May 2021*
Accepted: *29 November 2021*
Published: *21 December 2021*

Citation:
Prusicki MA, Balboni M, Sofroni K, Hamamura Y and Schnittger A (2021) Caught in the Act: Live-Cell Imaging of Plant Meiosis. Front. Plant Sci. 12:718346. doi: 10.3389/fpls.2021.718346

INTRODUCTION

Meiosis is a specialized cell division process required for sexual reproduction. It consists of one round of DNA replication followed by two consecutive events of chromosome segregation that result in four genetically different cells with half the DNA content of the mother cell (e.g., haploid meiotic products are formed in diploid organisms). In animals, meiosis directly produces the gametes. By contrast, the meiotic products of plants, called spores, undergo several cell divisions, from just a few in vascular plants such as Arabidopsis (*Arabidopsis thaliana*) and maize (*Zea mays*) to many in non-vascular plants such as the moss *Physcomitrium* (*Physcomitrella*) *patens* and the genus *Marchantia*, to produce a gametophyte. The mature gametophyte harbors the actual gametes. In the case of flowering plants, including Arabidopsis and maize, the female gametophyte holds an egg cell and a central cell embedded in the embryo sac; the male gametophyte contains two sperm cells encapsulated in a pollen grain (Hater et al., 2020; Hafidh and Honys, 2021).

Some of the first observations of meiosis, dating from the late 19th century, were made by Oscar Hertwig, who studied sea urchins, and Eduard Van Beneden, who investigated the nematode *Ascaris megalocephala* (Hertwig, 1876; Van Beneden, 1883). Since then, microscopy has

become a vital approach to investigate meiosis. In particular, cell spreads, immunostaining, and fluorescence *in situ* hybridization (FISH) analyses have been used to assemble the current extensive knowledge of meiosis (Keeney, 2009; Pradillo and Heckmann, 2020). These methods offer excellent spatial resolution, especially when subjected to super-resolution microscopy such as structured illumination microscopy (SIM), stimulated emission depletion (STED), and stochastic optical reconstruction microscopy (STORM), which have revealed the organization of the cohesin and synaptonemal complex (SC) in, for example, fruit fly (*Drosophila melanogaster*), the nematode *Caenorhabditis elegans*, mouse (*Mus musculus*), and recently Arabidopsis (Cahoon et al., 2017; Hernandez et al., 2018; Yoon et al., 2018; Xu et al., 2019; Sims et al., 2021).

However, as these techniques rely on fixed meiocytes, they give only a snapshot of the dynamic events taking place during the two cell divisions. Specifically, it is difficult to analyze meiotic progression in a heterogeneous population in which some cells behave differently from others: e.g., proceeding through meiosis at different paces and adopting different cellular configurations. Moreover, chromosome spreading procedures inherently rely on disrupting a higher-order three-dimensional structure and collapsing it onto a two-dimensional surface to make local chromatin details visible, such as the co-localization pattern of the recombinases DISRUPTED MEIOTIC cDNA1 (DMC1) and RADIATION51 (RAD51) (Reitz et al., 2019). In addition, the washing steps of immunolocalization experiments can also affect the pattern and abundance of biological structures and molecules, especially when they localize to the cytoplasm or nucleoplasm. On one hand, these washing steps can help enhance or reveal a specific localization pattern; for instance, the association of CYCLIN-DEPENDENT KINASE A;1 (CDKA;1) with chromatin in male meiotic cells in Arabidopsis only became visible after the nucleoplasmic fraction of CDKA;1 was reduced by the washing steps during immunolocalization experiments (Bulankova et al., 2010; Zhao et al., 2012; Yang et al., 2020). On the other hand, by changing the relative distribution of antigens, immunolocalization data deliver only a limited perspective of the situation found in nature. For instance, the above-mentioned nucleoplasmic localization of CDKA;1 might in fact be biologically relevant. Moreover, not all epitopes are always accessible to an antibody, further decreasing the levels or aspects of the detected proteins.

Recent advances in microscopy, such as the improved light-gathering and detection sensitivity of laser scanning and spinning disk confocal microscope systems and the development of (lattice) light sheet microscopy, have made it possible to obtain cytological data in three and even four dimensions and to follow the course of meiosis in real time with little perturbation.

Early live-cell imaging studies of meiosis were conducted in fission yeast (*Schizosaccharomyces pombe*), budding yeast (*Saccharomyces cerevisiae*), and Drosophila in the 1990s (Chikashige et al., 1994; Smith et al., 1995; Matthies et al., 1996). The work in fission and budding yeasts was based on wide-field and fluorescence microscopy. Chikashige et al. (1994) monitored nuclear movements in fission yeast, attributing a leading function to the telomeres during the horse-tail configuration, which is a specific prophase stage characterized by parallel chromosome threads that extend longitudinally from one side of the nucleus to the other. Matthies et al. (1996) used a laser confocal scanning microscope (LCSM) to follow the dynamics of spindle assembly in Drosophila oocytes, which revealed that meiotic spindle formation in this organism does not depend on the presence of microtubule organizing centers, but rather is organized by the chromosomes.

Key questions in meiotic research regarding the mechanism, function, and regulation of chromosome pairing, telomere bouquet formation, CO formation, and spindle formation have since then been assessed by live-cell imaging, which has provided new insights. These studies included further analyses in fission yeast (Tomita and Cooper, 2007), budding yeast (Conrad et al., 2008; Koszul and Kleckner, 2009; Lee et al., 2012, 2020), and Drosophila (Hughes et al., 2011; Colombié et al., 2013; Christophorou et al., 2015), as well as *C. elegans* (Vargas et al., 2019), and mammalian cells (Schuh and Ellenberg, 2007; Kitajima et al., 2011; Holubcová et al., 2013; Lee et al., 2015; Pfender et al., 2015; Kyogoku and Kitajima, 2017; Mogessie and Schuh, 2017; Enguita-Marruedo et al., 2018; Nikalayevich et al., 2018; Silva et al., 2020; Wang et al., 2020).

An extensive discussion of the use of live-cell imaging of animal and yeast meiosis goes beyond the scope of this review. Therefore, we only highlight a few examples here that opened new research directions in meiosis and should stimulate equivalent lines of research in plants, as illustrated by the work of Kyogoku and Kitajima (2017) and Wang et al. (2020), in which the authors studied the biophysical regulation of meiosis, which is normally not accessible in fixed material. To this end, Kyogoku and Kitajima combined micromanipulation of cell size and cell shape with live-cell imaging. This work revealed that the large size of the oocyte correlates with errors in chromosome bi-orientation and with a less stringent spindle assembly checkpoint due to a low nucleus-to-cytoplasm ratio and therefore to the frequent aneuploidy of mammal oocytes (Kyogoku and Kitajima, 2017). Wang et al. (2020) succeeded in measuring the cytoplasmic stream and the underlying hydrodynamic forces generated, which correlated with the correct extrusion of the second polar body after meiosis II in mammalian oocytes.

Finally, live-cell imaging has been instrumental in performing new genetic screens (Pfender et al., 2015). Pfender et al. (2015) studied the function of 774 genes involved in meiosis using small interfering RNA (siRNA)–mediated silencing coupled with live-cell imaging. Groups of 12 siRNAs were injected into early-stage oocytes, which were still embedded into follicles, to induce knock-down phenotypes. Once the oocytes were fully grown, they were extruded and injected with mRNAs for *GFP-a-tubulin* (a-tubulin fused to the green fluorescent protein [GFP]) and *H2B-mRFP* (histone H2B fused to the red fluorescent protein [RFP]) and incubated for 2–3 h to allow the translation of the fluorescent proteins before observation on a LCSM. Multiple cells were imaged in parallel, in four dimensions, as previously described (Schuh and Ellenberg, 2007). A manual evaluation of the phenotypes led to the description of 50 meiotic disturbances, including presence of lagging chromosomes, spindle length, or absence of nuclear envelope breakdown (NEB), which

each corresponded to malfunctions of single genes, including previously unknown genes.

LIVE-CELL IMAGING OF MEIOSIS IN PLANTS: TECHNICAL ASPECTS

In contrast to animal and yeast systems, live-cell imaging in plants has not been a prominent technique to study meiosis in the past, with only a few articles presenting live-cell imaging data until recently (Yu et al., 1997; Sheehan and Pawlowski, 2009; Higgins et al., 2016; Nannas et al., 2016; Ingouff et al., 2017). This fact is surprising for several reasons. First, live-cell imaging is extensively used to analyze various aspects of plant development and physiology, e.g., plant reproduction and the sensing of metabolites (Higashiyama et al., 2001; Okuda et al., 2009; Jones et al., 2014). Second, due to their large chromosomes and, hence, exquisite cell biology, many plant species (for instance, lily [*Lilium* sp.] and maize) are often used as model systems to study cell division, reaching as far back as one of the first optical description of mitosis by Strasburger (1888). One possible explanation for the lag in applying live-cell imaging to plant meiosis may stem from the challenges associated with directly observing plant meiocytes, as they are buried deep within reproductive tissues (**Figure 1**).

Recently, complementary experimental setups have been developed to overcome these shortcomings for the imaging of plant germ cells (Cromer et al., 2019; Prusicki et al., 2019; Valuchova et al., 2020). As these techniques are straightforward, they have the potential to be widely adopted in the plant meiosis field. One crucial consideration is to carefully evaluate how meiocytes can be reached and how they can be kept alive for long-term analyses spanning several hours.

Sample Mounting and Medium Selection

Plants are sensitive to environmental conditions, including temperature, osmolarity, and humidity (Buchanan et al., 2015). Therefore, it is crucial to apply proper environmental conditions when performing a live-cell imaging experiment and to choose an appropriate culture medium to maintain tissue viability without altering its development.

Isolated Meiocytes

Male meiocytes, or pollen mother cells (PMCs), develop within the anthers, are sustained by a layer of tapetum cells, and are protected by the middle layer, the endothecium, and the epidermis (**Figure 1**). Direct observations of isolated meiocytes require that immature flower buds to be collected and opened, and their anthers removed and excised at one end. Meiocytes are then extruded by gentle squeezing from the end distal from the cut and finally transferred onto the appropriate medium.

Early attempts to culture meiocytes were published in 1967 (Ito and Stern, 1967) studying meiotic division *in vitro*. Lily microsporocytes were cultured in a culture medium whose composition was based on White's solution (White, 1964) from zygotene through the meiotic progression (Ito and Stern, 1967; **Table 1**). Several challenges emerged from this first study in culturing isolated meiocytes. First, damage inflicted during meiocyte extraction severely affected the survival of the cells *in vitro*. Second, the success rate of meiocyte cell culture depended on the starting meiotic stage; meiocytes at early meiosis were delicate and suffered damage much more easily than older cells (Ito and Stern, 1967). This higher sensitivity might be related to intracellular connections among meiocytes and between meiocytes and tapetal cells, which appear to be very tight at early stages (Heslop-Harrison, 1966), resulting in rupture during dissection.

Nonetheless, meiocytes from various species of liliaceous plants have been successfully cultured since then (Stern and Hotta, 1970; Takegami et al., 1981; Ryan, 1983). Modifications to the composition of the original medium, such as the addition of microelements, known to increase cell survival, allowed the culturing of isolated meiocytes from rye (*Secale cereale*) (De La Peña, 1986; Rueda and Vázquez, 1988; **Table 1**).

However, while these plants have large enough chromosomes to be viewed using transmission light microscopy, none of these species is easily genetically tractable. Hence, adapting the methods implemented for the culture of lily and rye meiocytes to a system more amenable to genetic manipulation, such as maize, was an important advance to study the molecular mechanisms underlying meiosis in plants. Living maize meiocytes were successfully cultured and remained viable from pachytene to telophase II, and progression of meiosis and chromosome segregation was monitored for 24 h by epifluorescence microscopy (Chan and Zacheus Cande, 2000).

In addition to the specific composition of the culture medium, two environmental factors are crucial for culturing maize meiocytes: (1) the osmolarity of the medium, with an emphasis on sucrose concentration [the concentration range is very narrow for maize (0.28–0.34 M) (Chan and Zacheus Cande, 2000) but varies from plant to plant (Takegami et al., 1981)]; and (2) the temperature: maize meiocytes cannot be cultured at temperatures below 25°C without causing abnormal chromosome segregation (Yu et al., 1997).

Further experiments on isolated meiocytes have only been conducted in maize, following the same culturing principles based on White's solution (White, 1964), with a few adjustments (**Table 1**). For example, the sucrose concentration was lowered to 0.1 M and the medium was supplemented with 0.1 M maltose, 1% (v/v) Guillard's antibiotic concentrated solution, and 0.25 mM *n*-propyl gallate, known to increase the longevity of maize protoplasts in culture (Yu et al., 1997). Meiocytes extruded into this medium were viable for 9 h or longer and were observed undergoing meiosis II (Yu et al., 1997). The same medium was used to support growth of maize male meiocytes while imaging live meiosis I and meiosis II by fluorescence microscopy (Higgins et al., 2016; Nannas et al., 2016; **Table 1**).

Dissected Anthers

The first microscopy study of meiosis in intact and living plant anthers was performed in African lily (*Agapanthus umbelatus*) (Feijó and Cox, 2001). Freshly isolated anthers were incubated on a minimal medium (artificial pond water [APW]) that supported tissue viability without inducing major alterations in size or

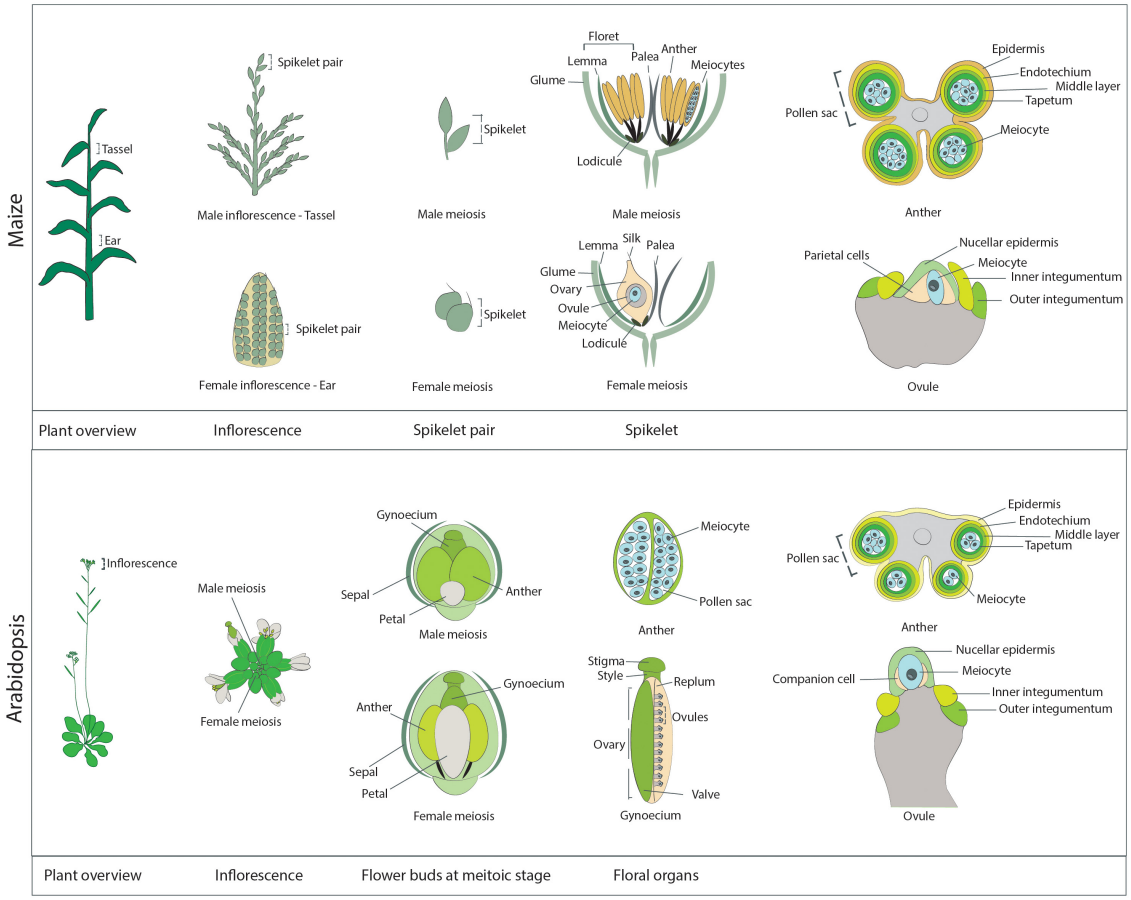

FIGURE 1 | Schematic overview of the reproductive structures harboring meiocytes in maize **(upper panel)** and Arabidopsis **(lower panel)**. Maize: A maize plant at the meiotic stage. The immature male inflorescence, the tassel, is located at the last internode, while the immature female inflorescence, the ear, is positioned at the base of leaves in the midsection of the plant. The individual reproductive units of each inflorescence are the spikelets, which occur in pairs. Each spikelet comprises two florets, subtended by a pair of glumes. On the tassel, each floret contains a lemma, a palea, and three anthers, which harbor the male meiocytes. The maize anther at the meiotic stage is approximately 4 mm in length. As seen from the transverse section of an anther (right-most diagram), the meiocytes occupy the inner part of each of the four pollen sacs forming the anther and are surrounded by four cell layers: the tapetum, the middle layer, the endothecium, and the epidermis. A meiotic ear is approximately 20 mm in length. In each ear, only one of the two florets is functional, while the other floret degenerates. Each functional floret harbors the ovary, which contains one ovule enclosing the meiocyte and the parietal cells. The ovule structure at the meiotic stage is characterized by the presence of the inner and outer integuments, which elongate on each side of the nucellus. Arabidopsis: An Arabidopsis plant at the meiotic stage. Each inflorescence consists of multiple flower buds at different developmental stages. Each flower bud contains the male floral organs (six anthers) and the female floral organ (the gynoecium). These reproductive organs are surrounded by four petals and four sepals. Male meiosis takes place in flower buds when they are approximately 0.8 mm in length, are round in shape (not elongated), and contain very small petals that do not cover the anthers, which are approximately 0.2 mm in length. The transverse section of an Arabidopsis anther reveals a structure similar to that of maize anthers: The meiocytes occupy the inner part of each of the four pollen sacs, surrounded by the tapetum, the middle layer, the endothecium, and the epidermis. Female meiosis takes place in elongated flower buds that are approximately 1.2 mm in length (hence slightly later than male meiosis; at this stage anthers are elongated and start to get a yellow shade). The gynoecium, or pistil, reaches approximately 0.9 mm in length at the meiotic stage. It is composed of the stigma, the style, and the ovary, which contains multiple ovules, connected to the replum and protected by valves. As with maize, at the meiotic stage, primordia of the inner and outer integuments are visible rising on the side of the nucellus, while inside the nucellus it is possible to identify a single meiocyte and a pair of companion cells.

morphology for up to 3 days in culture (Feijó and Cox, 2001). APW is also an optically clear isotonic solution that causes minimal light scattering; moreover, APW is a minimal medium, i.e., without sugar, and is thus less likely to become contaminated with bacteria over long time-course experiments (Sheehan and Pawlowski, 2009; **Table 1**).

A similar approach was successfully implemented for imaging maize meiocytes; culturing them in a microscope slide chamber containing APW to examine chromosome dynamics during meiosis prophase I ensured a viability of over 30 h (Sheehan and Pawlowski, 2009). This approach allowed the application of chemicals, agents, or drugs such as cytoskeleton-disrupting drugs (latrunculin and colchicine) and the observation of the resulting effects in living microspore mother cells (Sheehan and Pawlowski, 2009).

Imaging entire anthers offers the advantage of maintaining the developmental context of meiocytes, at least to some extent, thus limiting the influence of *in vitro* culturing on

TABLE 1 | Composition of media used for live cell imaging of isolated meiocytes, dissected anthers and flower buds + depicts addition of, * modified concentration compared to the original medium cited, – depletion of.

	Specimen	Plant species	Medium		Comments/ Description	Microscope	Publication
1	Isolated meiocytes	*Lilium*	Modified White's solution		Temperature 20 ± 1°C	Transmitted light microscope	Ito and Stern, 1967
			Component	g/L			
			$Ca(NO_3)_2$*$4H_2O$	0.3			
			K NO_3	0.08			
			KCl	0.065			
			$MgSO_4$*$7H_2O$	0.75			
			Na_2SO_4	0.2			
			NaH_2PO_4*H_2O	0.019			
			$MnSO_4$*$4H_2O$	5×10^{-3}			
			$ZnSO_4$*$7H_2O$	3×10^{-3}			
			H_3BO_3	15×10^{-4}			
			KI	75×10^{-5}			
			$CuSO_4$	1×10^{-5}			
			Na_2MoO_4	1×10^{-6}			
			$Fe_2(SO_4)_3$	0.001			
			Glycine	0.003			
			Nicotinic acid	5×10^{-4}			
			Thyamine	1×10^{-4}			
			Pyridoxine	1×10^{-4}			
			Sucrose	0.3 M	pH 5.6–5.8		
2	Isolated meiocytes	*Secale cereale* cultivar JNK	Based on 1		Temperature 21 ± 1°C	Transmitted light microscope	De La Peña, 1986
			+ MoO 3	1×10^{-5}			
			+ Mesoinositol	0.1			
			+ Nicotinic acid	5×10^{-4}			
			* $MnSO_4$*$4H_2O$	3.9×10^{-3}			
			* KI	7.5×10^{-5}			
			+ $AlCl_3$	1×10^{-4}			
			+ $NiCl_2$*$6H_2O$	1×10^{-4}			
			* Glycine	0.051			
			+ Valine	0.05			
			+ Glutamine	0.05			
			+ Lysine	0.05			
			+ Methionine	0.05			
			+ Threonine	0.05			
			+ L-isoleucine	0.05	pH 5.8–5.9		
3	Isolated meiocytes	*Zea mays,* line W23	Based on 2		Traces elements such as Mo, Ni, and Al were not required for culturing maize meiocytes	Polarized microscope, differential interference contrast (DIC) microscope and epifluorescence microscope	Chan and Zacheus Cande, 2000
			*Sucrose	0.28–0.34 M			
			– MoO3, $AlCl_3$, $NiCl_2$*$6H_2O$		Temperature not lower than 25°C		
4	Isolated meiocytes	*Zea mays,* line W23	Based on 2		Temperature 25 ± 1°C	Epifluorescence microscope	Yu et al., 1997
			* Sucrose	0.1 M			Nannas et al., 2016
			+ Maltose	0.1M			
			+ Guillard's antibiotic concentrated solution	1%			
			+ *n*-propyl gallate	0.25 mM			
5	Anthers	*Agapanthus umbelatus*	Artificial Pond Water (APW)			Two-photon excitation microscope	Feijó and Cox, 2001
		Zea mays	NaCl	0.1 M		Two-photon excitation microscope	Sheehan and Pawlowski, 2009
			$CaCl_2$	0.1 M			
			KCl	0.1 M			

(Continued)

TABLE 1 | (Continued)

	Specimen	Plant species	Medium		Comments/ Description	Microscope	Publication
6	Flower buds	*Arabidopsis thaliana*	Apex growth medium			Confocal laser scanning microscope	Prunet et al., 2016
			Murashige and Skoog basal salt mixture without vitamins	0.5 x			
			Sucrose	1%			
			Agarose	0.80%			
			Myo-inositol	0.01%			
			Nicotinic acid	0.0001%			
			Pyridoxine hydrochloride	0.0001%			
			Thiamine hydrochloride	0.001%			
			Glycine	0.0002%			
			Cytokinins (*N6*-benzyladenine)	500 nM	pH 5.8		
7	Flower buds	*Arabidopsis thaliana*	*In vitro* culture medium (Nitsch medium)			Two-photon excitation microscope	Ingouff et al., 2017
			Trehalose	5% [w/v]			
			MES-KOH at pH 5.8	0.05% [w/v]			
			Gamborg's vitamin solution	1x			
			Agarose	8%			
8	Flower buds	*Arabidopsis thaliana*	Apex Culture Medium (ACM)		Temperature 21°C	Confocal laser scanning microscope	Prusicki et al., 2019
			Murashige and Skoog basal salt	0.5x			
			Sucrose	1%			
			Agarose	0.80%			
			Myo-inositol	0.01%			
			Nicotinic acid	0.0001%			
			Pyridoxine hydrochloride	0.0001%			
			Thiamine hydrochloride	0.001%			
			Glycine	0.0002%	pH 5.8		
9	Flower buds	*Arabidopsis thaliana*	Murashige and Skoog basal salt	0.5x	Temperature 21°C	Light sheet fluorescence microscope	Valuchova et al., 2020
			Sucrose	5%			
			Agarose	1%	pH 5.8		

isolated meiocytes. Recently, this isolation method was applied to Arabidopsis; time-lapse movies of isolated anthers were recorded by a LCSM for over 4 h (Cromer et al., 2019). Flower buds were dissected, and undamaged anthers were transferred onto a slide topped by a spacer (0.12 mm deep) and filled with water as culturing medium. However, isolated anthers are fragile, especially at early stages when they contain meiocytes, and the dissection itself can easily stress and damage them, limiting the time span of live-cell imaging and raising the possibility that any observation reflects a stress reaction instead.

Flower Buds

As an alternative to isolated anthers, entire flower buds can be imaged, as recently established in Arabidopsis (Prusicki et al., 2019). Using entire flower buds is the least invasive *ex vivo* technique and thus further reduces the potential influence of sample handling before and during imaging. In the case of Arabidopsis, movies of living meiocytes of up to 30 h have been obtained (Prusicki et al., 2019).

This method is derived from the procedure previously applied for the observation of the development of emerging floral buds (Prunet et al., 2016; **Table 1**). Inflorescences are harvested, and all but one young flower primordium, which contains cells undergoing meiosis, are removed. The upper sepal is then removed to reveal two of the six anthers. Finally, the bud along with the pedicel and a few millimeters of the stem is embedded in Arabidopsis apex culture medium (ACM) (**Table 1**), kept in place with a drop of agarose, submerged in water, and imaged with an upright LCSM equipped with a water immersion objective (Prusicki et al., 2019, 2020a,b). Samples remain alive for up to 2 days with this method, allowing the analysis of the entire meiosis progression (Prusicki et al., 2019). This method also allows the addition of drugs

such as oryzalin to the imaging medium; in the case of oryzalin, the effects induced by microtubule depolymerization can then be monitored in living meiocytes (Sofroni et al., 2020). Moreover, this imaging setup was also used to follow meiotic progression under heat stress, which was induced by using a heated incubation chamber surrounding the microscopic stage (De Jaeger-Braet et al., 2021).

Flower buds are also the starting material for an alternative approach of live-cell imaging for both the male and female germ cell lineage by light sheet fluorescence microscopy (LSFM) (Valuchova et al., 2020). The flower buds at a stage of interest are detached from inflorescences, and their sepals and petals are removed. To observe female meiosis, the anthers are excised, the stigma is cut off, and the valves are opened to expose the ovules attached to the septum. The dissected specimen is then embedded into capillaries containing medium with 1% (w/v) low-melting-point agarose (Valuchova et al., 2020; **Table 1**). Exploiting the fast image acquisition speed and the low phototoxicity and photobleaching of LSFM, long-term imaging sessions of up to 5 days are possible; three-dimensional images can also be acquired over time, allowing the introduction of a fourth dimension in the data.

While imaging entire flower buds is the method with the greatest potential, this approach is also limited in terms of specimen size. Imaging larger and/or more complex flower primordia than those of Arabidopsis, like maize, will require the development of other setups. Possible alternatives include a technique pioneered for live-cell imaging of methylation changes during Arabidopsis sporogenesis and gametogenesis. Here, the inflorescences are embedded in a solid *in vitro* culture medium (Nitsch medium), dissected with a vibratome, and observed by two-photon microscopy (Ingouff et al., 2017; **Table 1**).

Reporter Lines

A prerequisite for the study of cellular dynamics during meiosis is the labeling of cellular components (organelles, chromatin, microtubules, and others) so they can be visualized by chemical staining or by fluorescently labeled fusion proteins.

Chemical staining with the nucleic acid stains SYTO 12 and DAPI (4′,6-diamidino-2-phenylindole) has been used to visualize isolated meiocytes or anthers in maize (Sheehan and Pawlowski, 2009; Higgins et al., 2016; Nannas et al., 2016). Chemical staining can be achieved on non-transgenic materials, which can be an advantage for plant species that cannot be transformed easily. However, the chemicals need to cross multiple cell layers before reaching and entering the meiocytes, making them more suited for imaging isolated cells. Protein chimeras, or fluorescent reporters, offer another route. They consist of a fusion between a fluorescent protein (FP) such as enhanced green fluorescent protein (EGFP), mVenus, or mCherry and the protein of interest. The transgenes encoding these fusions may be driven by the promoter of the gene of interest to minimize the potential for overexpression artifacts (Bastiaens and Pepperkok, 2000; DeBlasio et al., 2010). However, proteins with lower abundance might not be easily detectable during live-cell imaging; in these cases, highly active promoters like *UBIQUITIN10* (*UBQ10*) or *RIBOSOMAL PROTEIN S5A* (*RPS5A*) (Weijers et al., 2001) are sometimes preferred choices. Alternatively, tissue-specific promoters, like that of *DMC1*, are employed when the promoter of interest is too weak or not well defined (Zhao et al., 2017). Typically, the FPs are added to the N or C terminus of the protein of interest; however, inserting the fluorescent tags along the protein might be necessary if a fusion to either terminus interferes with protein function, as it does in ZIPPER1 (ZYP1) (Yang et al., 2019).

Choosing the right FP is the first step in designing any live-cell imaging assay. New FPs are constantly developed, and it is well advised to browse the literature for the latest advances in the field or check databases such as *I love GFP*[1]. Ideal FPs for live-cell imaging are as bright and as photostable as possible. However, photostability will hinder fluorescence recovery after photobleaching (FRAP) experiments. Multimeric FPs, such as the tetrameric DsRed, are brighter but are likely to produce artifacts and/or interfere with protein function through forced dimerization or multimerization of the target protein. FPs should also be selected to allow the concomitant visualization of two or even three proteins at the same time. Often a GFP or yellow fluorescent protein (YFP) variant is combined with an RFP variant due to the adequate spectral separation of their excitation and emission spectra. When selecting the right FP, another consideration is that some proteins are excited with shorter wavelengths; for example, blue light is more toxic to the cell than longer wavelengths. However, the shorter the wavelength, the higher will be the spatial resolution due to the diffraction limit of microscopy. Another challenge in plant applications is the notorious autofluorescence of plant cells from chlorophyll, lignin, and flavonoids that may interfere with the detection of the fluorescent reporter of interest.

Photo-switchable and photo-activatable FPs have recently been applied to live-cell imaging in plants, expanding the palette of available reporters. One example is the monomeric fluorescent reporter EosFP, which is irreversibly converted from a green-emitting to a red-emitting protein upon exposure to ultraviolet light. When fused to proteins with multiple subcellular localizations, EosFP allows for a color-based differentiation between individual cells and organelle subpopulations and can be adapted to tracking subcellular structures and their interactions (Mathur et al., 2012). For instance, the *35Spro:H2B-mEosFP* reporter, expressing a fusion construct between *histone H2B* and *EosFP* driven by the cauliflower mosaic virus (CaMV) 35S promoter, was transformed into tobacco (*Nicotiana tabacum*) and Arabidopsis plants to study endoreplication and changes in DNA content in living cells (Wozny et al., 2012). A second example is the photo-convertible monomeric protein Kikume Green-Red (mKikGR) variant, which was fused to HISTONE THREE RELATED10 (HTR10, with the reporter construct *HTR10pro:HTR10-mKikGR*) to study the dynamics of two identical sperm cells during fertilization in Arabidopsis (Hamamura et al., 2011).

Fluorescent reporters are not only useful as fusion proteins that inform on protein localization; they can also be designed to

[1]https://t1p.de/ypjk

visualize and quantify the transcriptional response to a chemical stimulus, such as with the auxin reporter *DR5:N7-mVenus* (**Table 2**), used to indirectly visualize the distribution of the phytohormone during flower development (Valuchova et al., 2020). In this case, the fluorescent tag is not fused to another protein, but instead provides a visual read-out of the transcriptional activation of the synthetic *DR5* promoter by auxin (Valuchova et al., 2020).

Chromosome and Chromatin Markers

Meiosis-specific events including pairing, recombination, assembly, and disassembly of the SC take place in the nucleus. Dissecting their dynamics requires nuclear markers (reviewed in Wozny et al., 2012) and histone markers such as the histone H2A HTA10 and the histone H2B HTB9 (Valuchova et al., 2020) to highlight chromatin, as they are present throughout meiosis (**Figure 2** and **Table 2**). The development of reporters encoding meiosis-specific proteins may also be needed. To date, several functional meiosis-specific reporter lines have been generated and used in live-cell imaging experiments or *in vivo* localization studies: markers for the cohesin complex (REC8 [RECOMBINATION8], SWI1 [SWITCHING DEFICIENT1], and WAPL [WINGS APART-LIKE]) (**Figure 2** and **Table 2**; Prusicki et al., 2019; Yang et al., 2019) and markers for the chromosome axis, synaptonemal complex components, and their regulators ASYNAPTIC1 (ASY1), ASY3, ASY4, ZYP1b, PACHYTENE CHECKPOINT2 (PCH2), and COMET (**Figure 2** and **Table 2**; Chambon et al., 2018; Yang et al., 2019, 2020; Balboni et al., 2020; Valuchova et al., 2020). These reporters have been instrumental in unraveling the dynamics of chromosomes in meiotic cells and in elucidating more complex cellular mechanisms, such as the prophase pathway of cohesin removal in plants and the regulation of the meiotic chromosome axis (Cromer et al., 2019; Yang et al., 2019, 2020; Balboni et al., 2020).

Centromeres are typically fluorescently tagged using CENTROMERIC HISTONE H3 (CENH3) and constitute a visual marker to determine gametophytic and somatic ploidy in Arabidopsis (De Storme et al., 2016; Liu et al., 2017). A maize YFP-tagged centromere line derived from the *ZmCENH3* cDNA sequence (35S*pro:CenH3:YFP*) has been reported, but it has yet to be used in meiotic studies (Jin et al., 2008; **Table 2**). With respect to telomeres, live-cell CRISPR-Cas9-based imaging using EGFP or mRuby2 fused to the CRISPR-associated nuclease Cas9 allowed the visualization of telomeric regions *in vivo* in *Nicotiana benthamiana* leaves by harnessing the intrinsic ability of the nuclease to recognize palindromic repeats (Dreissig et al., 2017; Khosravi et al., 2020; **Table 2**). However, to date telomeres have not been successfully observed by live-cell imaging in any plant during meiosis.

Finally, levels and changes in DNA methylation during meiosis and gametophyte development in Arabidopsis are accessible via live-cell imaging of specific reporters for CG or non-CG methylation marks, such as *HTR5pro:MBD-Venus* (a fusion between a methyl-CpG-binding domain [MBD] and Venus under the control of the histone H3 *HTR5* promoter) and *HTR5pro:SUVH9-Venus* (a fusion between SU(VAR)3-9 HOMOLOG 9 and Venus), respectively (**Table 2**; Ingouff et al., 2017).

Cytoskeletal Markers

The microtubule cytoskeleton plays an essential role during cell divisions and undergoes dramatic changes over the course of meiosis. Therefore, fluorescent reporters for cytoskeletal elements provide important information on meiotic progression. A maize reporter line consisting of a fusion protein between the cyan fluorescent protein (CFP) and TUBULIN BETA, *ECFP-TUB* (**Table 2**), was used to study spindle assembly (Higgins et al., 2016) and the positioning of the division plane during metaphase I and II (Nannas et al., 2016). Similar reporters were developed in Arabidopsis with TUBULIN alpha (TUA5) and TUBULIN beta (TUB4) fused to TagRFP (*RPS5Apro:TagRFP-TUB4* and *RPS5Apro:TagRFP-TUA5*) and driven by the *RPS5A* promoter (**Figure 2** and **Table 2**). These reporters made it possible to describe the spatiotemporal dynamics of microtubule configurations during meiosis (Prusicki et al., 2019) and revealed microtubule dynamics anomalies in mutants with lower CDK activity such as *tam* (*tardy asynchronous meiosis*) or the *cdka;1 cdkd;3* double mutant (Prusicki et al., 2019; Sofroni et al., 2020).

A GFP-tagged tubulin reporter driven by the *UBIQUITIN14* promoter (*UBQ14pro:GFP-TUA6*) (**Table 2**) allowed the visualization of tubulin in fixed Arabidopsis anthers (Brownfield et al., 2015). Furthermore, motor proteins such as microtubule-associated proteins (MAPs) are emerging as powerful reporters to characterize meiotic cytokinesis, as is the case of the reporter *MAP65-3pro:GFP-MAP65-3* (**Figure 2** and **Table 2**; Sofroni et al., 2020).

In contrast to microtubules, the regulation of actin filaments has not been extensively studied in plants, even though their relevance during cell division is well known (Rasmussen et al., 2013). FP-tagged Lifeact (Era et al., 2009), a yeast-derived actin-binding peptide, has provided a means to visualize actin filaments during pollen tube growth (Vogler and Sprunck, 2015; Liao and Weijers, 2018) and cell division (Wu and Bezanilla, 2014; Kimata et al., 2016). Of the naturally accumulating actin-binding proteins, only ACTIN RELATED PROTEIN6 (ARP6) fused to YFP was observed during meiosis, with a focus on ovules undergoing megasporogenesis (Qin et al., 2014; **Table 2**).

Cell Cycle Reporters

Markers able to differentiate phases of the cell cycle are very powerful tools when studying cell division and cell cycle progression (Echevarría et al., 2021). For example, reporters based on *PROLIFERATING CELL NUCLEAR ANTIGEN1* (*PCNA1*) (*PCNA1pro:PCNA1-sGFP* and *PCNA1pro:PCNA1-TagRFP*) allow distinction between pre-meiotic and early meiotic stages, as PCNA;1 accumulates in small speckles during early S-phase and in large foci in late S-phase, while it shows a diffuse localization throughout the nucleoplasm after S-phase (**Figure 2** and **Table 2**; Yokoyama et al., 2016; Valuchova et al., 2020).

CDKs (in particular CDKA;1) and cyclins are among the main regulators of meiosis (Harashima et al., 2013, 2016; Wijnker and Schnittger, 2013), and several fluorescent reporters

TABLE 2 | Fluorescent reporters expressed, or potentially expressed, in meiosis.

Cell compartment	Plant species	Construct	Meiotic specific	Meiotic phase	Publication
Chromosome and chromatin markers					
Histones	*Arabidopsis thaliana*	PRO_{HTA10}:HTA10:RFP	No	All meiosis	Valuchova et al., 2020
		PRO_{H2B}:H2B:mRuby2	No	All meiosis	Valuchova et al., 2020
		PRO_{35S}:H2B:mEosFP	No	Not observed during meiosis	Wozny et al., 2012
		PRO_{HTR10}:HTR10:mKikGR	No	Not observed during meiosis	Hamamura et al., 2011
Centromeric histones	*Zea mays*	PRO_{35S}:CenH3:YFP	No	All meiosis	Jin et al., 2008
Telomeres	*Nicotiana Benthamiana*	PRO_{PcUbi4}:Sp/Sa-dCas9:eGFP/mRuby2	No	Not observed during meiosis	Dreissig et al., 2017
		PRO_{UBQ6}:sgRNA-telomere	No	Not observed during meiosis	Dreissig et al., 2017
		PRO_{Ubi}:dCas9:2xMS2:GFP	No	Not observed during meiosis	Khosravi et al., 2020
		PRO_{35S}:dCas9:2xMS2:GFP	No	Not observed during meiosis	Khosravi et al., 2020
		PRO_{RPS5A}:dCas9:2xMS2:GFP	No	Not observed during meiosis	Khosravi et al., 2020
		PRO_{Ubi}:dCas9:3xPP7:GFP	No	Not observed during meiosis	Khosravi et al., 2020
		PRO_{35S}:dCas9:3xPP7:GFP	No	Not observed during meiosis	Khosravi et al., 2020
		PRO_{RPS5A}:dCas9:3xPP7:GFP	No	Not observed during meiosis	Khosravi et al., 2020
DNA Methylation: CG type	*Arabidopsis thaliana*	PRO_{HTR5}:MBD:Venus	No	All meiosis	Ingouff et al., 2017
DNA Methylation: CHH type	*Arabidopsis thaliana*	PRO_{HTR5}:SUVH9:Venus	No	All meiosis	Ingouff et al., 2017
DNA replication	*Arabidopsis thaliana*	PRO_{PCNA1}:PCNA1:GFP	No	Not observed during meiosis	Yokoyama et al., 2016
		PRO_{PCNA1}:PCNA1:TagRFP	No	All meiosis, specific dots and speckles in S-phase	Valuchova et al., 2020
Cohesion	*Arabidopsis thaliana*	PRO_{REC8}:REC8:GFP	Yes	Prophase, metaphase I	Prusicki et al., 2019
		PRO_{SWI1}:SWI1:GFP/RFP	Yes	Leptotene	Yang et al., 2019
		PRO_{WAPL1}:WAPL1:GFP	No	All meiosis	Yang et al., 2019
Chromosome axis and synaptonemal complex	*Arabidopsis thaliana*	PRO_{ASY1}:ASY1:GFP/RFP	Yes	Prophase	Yang et al., 2020
		PRO_{ASY1}:ASY1:eYFP	Yes	Prophase	Valuchova et al., 2020
		PRO_{ASY3}:ASY3:RFP	Yes	Prophase	Yang et al., 2020
		PRO_{ASY4}:ASY4:eYFP	Yes	Prophase	Chambon et al., 2018
		PRO_{ZYP1b}:ZYP1b:GFP	Yes	Zygotene, pachytene	Yang et al., 2020
		PRO_{PCH2}:PCH2:GFP	No	Prophase	Yang et al., 2020
		PRO_{COMET}:COMET:GFP	No	Prophase	Balboni et al., 2020
Cytoskeletal markers					
Microtubules	*Zea mays*	CFP:TUB1	No	All meiosis	Higgins et al., 2016; Nannas et al., 2016
	Arabidopsis thaliana	PRO_{UBQ14}:GFP:TUA6	No	All meiosis	Brownfield et al., 2015
		PRO_{RPS5A}:TagRFP:TUB4	No	All meiosis	Prusicki et al., 2019
		PRO_{RPS5A}:TagRFP:TUA5	No	All meiosis	Prusicki et al., 2019
Phragmoplast	*Arabidopsis thaliana*	$PRO_{MAP65-3}$:GFP:MAP65-3	No	Cytokinesis	Sofroni et al., 2020
Actin	*Arabidopsis thaliana*	PRO_{35S}:Lifeact:Venus	No	Not observed during meiosis	Era et al., 2009
Actin related protein	*Arabidopsis thaliana*	PRO_{ARP6}:ARP6:YFP	No	Prophase, female meiosis	Qin et al., 2014
Organelle reporters					
Golgi	*Arabidopsis thaliana*	PRO_{JAS}: JAS:GFP	No	All meiosis, organeller band	Brownfield et al., 2015
		PRO_{UBQ14}:JAS:GFP	No	All meiosis, organeller band	Brownfield et al., 2015
Nucelar envelope	*Arabidopsis thaliana*	PRO_{SUN1}:SUN1:GFP	No	All meiosis	Varas et al., 2015
		PRO_{SUN2}:SUN2:GFP.	No	All meiosis	Varas et al., 2015
Plasma membrane	*Arabidopsis thaliana*	PRO_{SYP132}:GFP:SYP132	No	All meiosis	Sofroni et al., 2020
Cell cycle reporters					
CDKs	*Arabidopsis thaliana*	$PRO_{CDKA;1}$:CDKA;1:mVenus	No	All meiosis	Sofroni et al., 2020
		$PRO_{CDKA;1}$:CDKA;1:mTurquoise	No	All meiosis	Sofroni et al., 2020
		$PRO_{CDKD;1}$:CDKD;1:mVenus	No	All meiosis	Sofroni et al., 2020
		$PRO_{CDKD;2}$:CDKD;2:mVenus	No	All meiosis	Sofroni et al., 2020
		$PRO_{CDKD;3}$:CDKD;3:mVenus	No	All meiosis	Sofroni et al., 2020
Cyclin	*Arabidopsis thaliana*	$PRO_{CYB3;1}$:CYCB3;1:GFP	No	Prophase, metaphase I	Sofroni et al., 2020
Checkpoints	*Arabidopsis thaliana*	PRO_{BORR}:BORR:GFP	No	Anaphase I, II and cytokinesis	Komaki et al., 2020
		PRO_{INCENP}:GFP:INCENP	No	Anaphase I, II and cytokinesis	Komaki et al., 2020
Homologous recombination reporters					
Double strand breaks	*Arabidopsis thaliana*	PRO_{RAD51}.RAD51:GFP	No	Not observed during meiosis	Da Ines et al., 2013
	Arabidopsis thaliana	PRO_{RBR}:mCherry:RBR	No	Not observed during meiosis	Biedermann et al., 2017

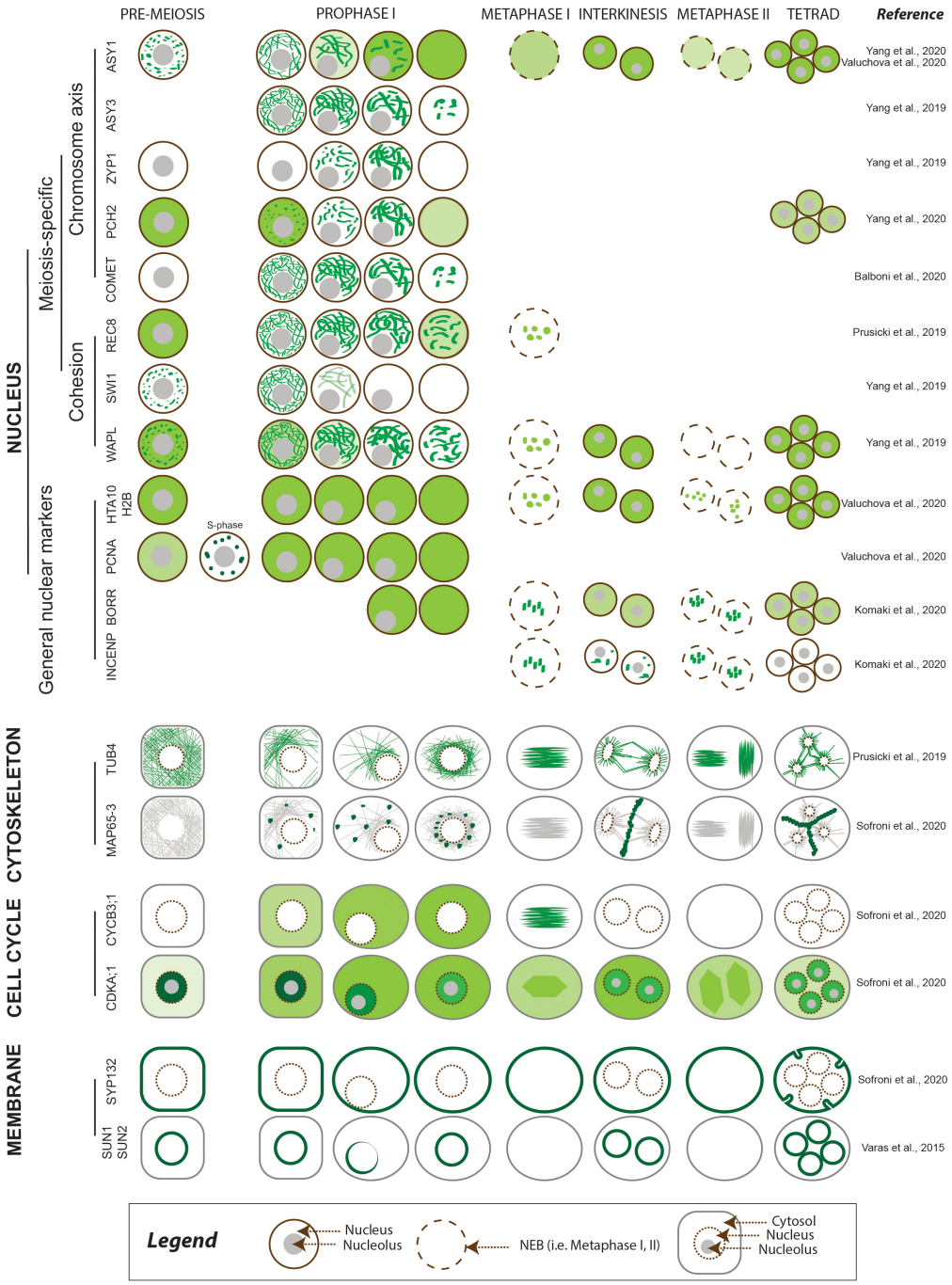

FIGURE 2 | Meiotic localization patterns of meiosis-specific and non-meiosis-specific plant proteins reported to date. The abundance of the protein of interest is depicted using different shades of green, corresponding to the relative intensity of the signal. The nucleus is outlined in brown, with other cellular compartments shown in gray.

have already been developed to explore their dynamics. For example, the reporters *CDKA1;1pro:CDKA;1-mVenus* and *CDKA1;1pro:CDKA;1-mTurquoise* revealed the accumulation pattern of CDKA;1, which shows high abundance in the nucleus at early prophase, followed by a decrease at mid and late prophase, as reflected by the observed increase in fluorescence from the cytosol (**Figure 2** and **Table 2**; Sofroni et al., 2020; Yang et al., 2020). Furthermore, the dynamics of CDKA;1 accumulation have been analyzed concomitantly with those of its regulators, such as CDK-activating kinases, which in Arabidopsis consist of cyclins like CYCB3;1 and D-type CDKs. CYCB3;1 exhibited a distinct association with the first meiotic spindle at

metaphase I, making it a good reporter for the spindle (Sofroni et al., 2020; **Figure 2** and **Table 2**).

Other cell cycle reporters are based on kinetochore components: the chromosome passenger complex (CPC) proteins *BORRpro:BORR-GFP* (encoding a fusion between the plant Borealin-like protein BOREALIN-RELATED and GFP) and *INCENPpro:GFP-INCENP* (for INNER CENTROMERE PROTEIN) are characterized by a highly dynamic localization pattern from nuclear envelope breakdown until the onset of anaphase (Komaki et al., 2020; **Figure 2** and **Table 2**). Additional reporters for kinetochore components such as spindle assembly checkpoint (SAC) proteins are available and awaiting analysis during meiosis (Komaki and Schnittger, 2017). These reporters can also be used to study chromosome dynamics (see above).

Membrane and Organellar Markers

During meiotic progression, membranes and other compartments, e.g., the nuclear envelope, organelles, and phragmoplast components, play pivotal roles in chromosome pairing, spindle positioning, and successful cytokinesis (Murphy et al., 2014; Brownfield et al., 2015; Varas et al., 2015). Tracking membrane and organelle behavior *in vivo* thus has the potential to reveal interesting aspects of their function and regulation. To date, published work in this area of research is limited (Brownfield et al., 2015; Varas et al., 2015). Varas et al. (2015) visualized the nuclear envelope in Arabidopsis anthers using the fluorescent reporters *SUN1pro:SUN1-GFP* and *SUN2pro:SUN2-GFP* (**Figure 2** and **Table 2**). SUN1 and SUN2 (for Sad1/UNC-84) are two components of the protein complex that form a bridge over the nuclear membrane and link elements from the nucleoplasm to the cytoskeleton (Varas et al., 2015). Brownfield et al. (2015) used the reporters *JASpro:JAS-GFP* and *UBQ14pro:JAS-GFP* (encoding a fusion protein between the unknown protein JASON [JAS] and GFP) (**Table 2**) to study the behavior of the organellar band, which forms after the first meiotic division. JAS was reported to localize to endomembrane vesicles involved in Golgi trafficking (Brownfield et al., 2015). Various FP-based reporters for the Golgi apparatus, the endoplasmic reticulum, peroxisomes, mitochondria, the plasma membrane, and the tonoplast have been introduced in Arabidopsis, tobacco, and rice but have yet to be analyzed during meiosis (Brownfield et al., 2015; Dangol et al., 2017; Ito et al., 2018). Finally, the *SYP132pro:GFP-SYP132* reporter line (encoding GFP fused to SYNTAXIN OF PLANTS132 [SYP132]) was used to fluorescently label the plasma membrane in male meiocytes and revealed an outside–in direction of membrane invagination during male meiosis, whether cytokinesis was simultaneous or successive (**Figure 2** and **Table 2**; Sofroni et al., 2020).

Recombination Markers

So far, very few reporters have been generated in plants to monitor recombination. The above-mentioned chromosome axis markers and reporters for the SC allow a broad temporal assignment of recombination processes based on previous annotation of each stage with immunolocalization techniques, for instance, labeling double-strand break (DSB) formation and localizing ASY1 to the axis roughly within a similar time window (Sanchez-Moran et al., 2007). Likewise, the reduction of HOMOLOG OF HUMAN HEI 10 (HEI10) foci from about 100 to around 10 in male meiosis is indicative of crossover (CO) formation and corresponds to the duration of the complete decoration of the chromosome axis by ASY1 to its partial removal from chromosome arms (Chelysheva et al., 2012). Moreover, the presence of the SC coincides with CO maturation, as visualized by the incorporation of the transverse filament component ZYP1.

However, a direct visualization of components of the recombination machinery has seldom been achieved. There is a lag in generating recombination reporters for proteins directly involved in DSB and CO formation and resolution such as SPORULATION11 (SPO11), DMCI1, HEI10, MutL HOMOLOG1 (MLH1), MutS HOMOLOG4 (MSH4), and MMS and UV SENSITIVE81 (MUS81); these proteins are instead extensively used in immunolocalization experiments in fixed samples. Although functional reporters for the Arabidopsis homologous recombination repair components RETINOBLASTOMA RELATED1 (RBR1) and RAD51 (*RBR1pro:mCherry-RBR1* and *RAD51pro:RAD51-GFP*) are available (Chen et al., 2011; Da Ines et al., 2013; Biedermann et al., 2017), they have not yet been characterized or assessed for progression of meiotic recombination.

ASPECTS OF PLANT MEIOSIS STUDIED BY LIVE-CELL IMAGING

Time Courses

A change in meiotic duration, or in the duration of specific meiotic stages, is one of the main phenotypic alterations of plants exposed to suboptimal environmental conditions, such as high or low temperatures (reviewed in Bennett, 1971, 1977; Bomblies et al., 2015). Furthermore, the chronology of meiotic stages is often altered in meiotic mutants, such as in the maize mutant *pam1* (*plural abnormalities in meiosis1*) (Golubovskaya et al., 2002) and the Arabidopsis *tam* (Magnard et al., 2001; Prusicki et al., 2019), *msh4* (Higgins et al., 2004), *mlh3* (Jackson et al., 2006), and *pans1ΔD* (*patronus1*) mutants (Cromer et al., 2019) as well as plants expressing a dominant negative version of RAD51 (Singh et al., 2017). Accordingly, time courses of plant meiosis have been performed since the late 1960s using methods based on DNA labeling first with radioactive compounds (Ekberg and Eriksson, 1965; Lindgren et al., 1969; works from Bennett, reviewed in Bennett, 1971, 1977) and later with the modified thymine analogs 5-bromo-2′-deoxyuridine (BrdU) (Armstrong et al., 2003; Higgins et al., 2004; Jackson et al., 2006; Sanchez-Moran et al., 2007) and 5-ethynyl-2′-deoxyuridine (EdU) (Higgins et al., 2012; Stronghill et al., 2014; Varas et al., 2015; Singh et al., 2017) (an overview of time courses for plant meiosis in wild-type backgrounds is presented in **Table 3**).

In time-course experiments, the length of meiotic phases is determined by measuring the time between the labeling pulse (meiotic S-phase) and the appearance of marked chromosomes at specific stages. For instance, labeled chromosomes with a zygotene conformation are detected in Arabidopsis starting from

TABLE 3 | Duration of meiosis in plants.

MONOCOT																		
Plant species	**Publication**	**Method**	**Temperature**	**Overall duration of male meiosis**	***S-phase/G2***	***Leptotene***	***Zygotene***	***Pachytene***	***Diplotene***	***Diakinesis***	***Metaphase I***	***Anaphase I***	***Telophase I***	***Interkinesis***	***Prophase II***	***Metaphase II***	***Anaphase II***	***Telophase II***	***Tetrads***
Allium cepa	Vasil, 1959	Aceto-carmine staining	NOT GIVEN	96 h	//	//	//	//	//	//	//	//	//	//	//	//	//	//	//
Convallaria majalis	Reported in Bennett, 1977	Not available	20°C	72 h	//	//	//	//	//	//	//	//	//	//	//	//	//	//	//
Dasypyrum villosum	Stefani and Colonna, 1996	Aceto-orcein staining	Field in May	35 ± 1.7 h	//			15.5 h						10.5 h				8 h	//
			Field in July	22 ± 2 h	//			12 h						6 h				3.5 h	//
			5°C	136 ± 14.4 h	//			69.5 h						46 h				22 h	//
			10°C	88 ± 5.3 h	//			48 h						20.5 h				20 h	//
			20°C	29 h	//			14 h						10 h				5 h	//
			28°C	21 ± 0.7 h	//			12.5 h						5.5 h				4.5 h	//
			35°C	17 ± 0.7 h	//			10 h						5 h				3 h	//
Endymion nonscriptus	Wilson, 1959	Aceto-carmine staining	0°C	864 h	//	//	//	//	//	//	//	//	//	//	//	//	//	//	//
			5°C	360 h	//	//	//	//	//	//	//	//	//	//	//	//	//	//	//
			10°C	168 h	//	//	//	//	//	//	//	//	//	//	//	//	//	//	//
			15°C	84 h	//	//	//	//	//	//	//	//	//	//	//	//	//	//	//
			20°C	48 h	//	//	//	//	//	//	//	//	//	//	//	//	//	//	//
			25°C	30 h	//	//	//	//	//	//	//	//	//	//	//	//	//	//	//
			30°C	20 h	//	//	//	//	//	//	//	//	//	//	//	//	//	//	//
			15–21°C	66 h	//	//	//	//	//	//	//	//	//	//	//	//	//	//	//
Fritillaria meleagris	Barber, 1942	Acetocarmine staining	12–15°C	400 h APPROXIMATE	//	//	//	//	//	//	//	//	//	//	//	//	//	//	//
Hordeum vulgare: unspecified variety	Lindgren et al., 1969	Aceto-orcein staining	NOT GIVEN	//		5.30%		32.60%						19.90%					23.70%
				//	//	//	//	//	19.50%	8%	24.80%	2.40%	4.60%	13.00%	1.50%	7.20%	5.40%	13.60%	
				//	//	//	//	//	17.90%	7.50%	24.10%	2.50%	4.70%	13.40%	1.60%	7.60%	5.80%	14.90%	
				//	3 days after the first anaylsed material all the anthers had microspores → all meiocytes terminated meiosis. One "spikelet unit" see Ekberg and Eriksson (1965), is less than 16 h → shorter stages less than 1 h														
Hordeum vulgare: Sultan	Bennett and Finch, 1971	Feulgen staining	20°C	39.4 h	//	12 h	9 h	8.8 h	2.2 h	36 min	1.6 h	30 min	30 min	dyad stage: 2 h		1.2 h	30 min	30 min	8 h
Hordeum vulgare: Ymer	Finch and Bennett, 1972	Thymidine pulse + autoradiography	20°C	39 h	//	11.5 h	9 h	9.3 h	1.9 h	36 min	1.6 h	30 min	30 min	dyad stage: 1.7 h		1.5 h	30 min	30 min	>7 h
Hordeum vulgare: Ymer 4X	Finch and Bennett, 1972	Thymidine pulse + autoradiography	20°C	31 h	//	9 h	7 h	7 h	1.8 h	30 min	1.5 h	24 min	24 min	dyad stage: 1.5 h		1 h	24 min	24 min	>6 h
Hordeum vulgare: Morex	Higgins et al., 2012	BrdU and EdU labeling	22°C	43 h	13 h							43 h							
			30°C	43 h	9 h							43 h							
Lilium candidum	Reported in Bennett, 1977	Not available	NOT GIVEN	168 h	//	//	//	//	//	//	//	//	//	//	//	//	//	//	//
Lilium henryi	Reported in Bennett, 1977	Not available	NOT GIVEN	170 h	//	//	//	//	//	//	//	//	//	//	//	//	//	//	//
Lilium hybrid: Black Beuty	Bennett et al., 1975	Fuchsin staining	20°C	264 h	//	//	//	//	//	//	//	//	//	//	//	//	//	//	//
Lilium hybrid: Sonata	Bennett et al., 1975	Fuchsin staining	20°C	180 h	//	//	//	//	//	//	//	//	//	//	//	//	//	//	//
Lilium longiflorum: variety unspecified	Marquardt, 1937	Aceto-carmine staining	NOT GIVEN	96 h	//	//	//	//	//	//	//	//	//	//	//	//	//	//	//
Lilium longiflorum: Nellie White	Ito and Stern, 1967	Autoradiography	22°C	ca192 h	//	//	//	//	//	//	//	//	//	//	//	//	//	//	//
Lilium longiflorum: Croft	Taylor and McMaster, 1953	Autoradiography	23°C	ca192 h	//	//	//	//	//	//	//	//	//	//	//	//	//	//	//
Lilium longiflorum: Floridii	Erickson, 1948	Aceto-orcein staining	NOT GIVEN	ca240h	//	//	//	//	//	//	//	//	//	//	//	//	//	//	//
Ornithogalum virens	Church and Wimber, 1969	Thymidine pulse + autoradiography	18°C	72 h - APPROXIMATE	//	//	//	//	//	//	//	//	//	//	//	//	//	//	//
Secale cereale	Bennett et al., 1971, 1972; Bennett and Smith, 1972	Feulgen staining	15°C	88 h	//	//	//	//	//	//	//	//	//	//	//	//	//	//	//
			20°C	51 h	//	20 h	11.4 h	8 h	1 h	36 min	2 h	1 h	1 h	dyads: 2.5 h		1.7 h	1 h	1 h	//
			25°C	39 h	//	//	//	//	//	//	//	//	//	//	//	//	//	//	//
Secale cereale 4X	Bennett and Smith, 1972	Feulgen staining	20°C	38 h	//	13 h	9 h	6.4 h	1 h	36 min	1.8 h	42 min	42 min	dyad stage: 2 h		1.4 h	42 min	42 min	//
Tradescantia paludosa	Reported in Bennett, 1977	Not available	NOT GIVEN	126 h	//	//	//	//	//	//	//	//	//	//	//	//	//	//	//
Tradescantia reflexa	Reported in Bennett, 1977	Not available	NOT GIVEN	144 hs	//	//	//	//	//	//	//	//	//	//	//	//	//	//	//
Trillium erectum	Hotta and Stern, 1963	Autoradiography	1°C	2160 h	//	//	//	//	//	//	//	//	//	//	//	//	//	//	//
	Hotta and Stern, 1963	Autoradiography	2°C	1680 h	//	//	//	//	//	//	//	//	//	//	//	//	//	//	//
	Kemp, 1964	Propronio-carmine	5°C	960 h	//	//	//	//	//	//	//	//	//	//	//	//	//	//	//
	Ito and Stern, 1967	Autoradiography	15°C	288 h	//	//	//	//	//	//	//	//	//	//	//	//	//	//	//

(Continued)

TABLE 3 | (Continued)

MONOCOT																			
Plant species	**Publication**	**Method**	**Temperature**	**Overall duration of male meiosis**	***S-phase/G2***	***Leptotene***	***Zygotene***	***Pachytene***	***Diplotene***	***Diakinesis***	***Metaphase I***	***Anaphase I***	***Telophase I***	***Interkinesis***	***Prophase II***	***Metaphase II***	***Anaphase II***	***Telophase II***	***Tetrads***
Triticale turgidum: durum	Bennett and Kaltsikes, 1973	Feulgen/aceto-carmine staining	20°C	31 h	//			23.7 h						7.5 h					//
Triticale: genotype A (CS/K-TA)	Bennett and Smith, 1972	Feulgen/aceto-carmine staining	20°C	21 h	//	7.5 h	3 h	2.25 h	1 h	30 min	1.75 h	30 min	30 min	dyad stage: 1.5 h		1.25 h	30 min	30 min	//
Triticale: genotype B (CS/Pet-TA)	Bennett and Smith, 1972	Feulgen/aceto-carmine staining	20°C	22 h	//			15.5 h						6.5 h					//
Triticale: Rosner	Bennett and Smith, 1972	Feulgen/aceto-carmine staining	20°C	34 h	//			26.5 h						7.5 h					//
Triticum diococcum 4X	Bennett and Smith, 1972	Feulgen/aceto-carmine staining	20°C	30 h	//			22.5 h						7.5 h					//
Triticum aestivum x Secale cereale	Bennett et al., 1974	Feulgen/aceto-carmine staining	20°C	35.5 h	//			28 h						7.5 h					10 h
Triticum aestivum: Chinese Spring	Bennett et al., 1971, 1972	Thymidine pulse + autoradiography	15°C	43 h	//	//	//	//	//	//	//	//	//	//	//	//	//	//	//
			20°C	24 h	//	10.4 h	3.4 h	2.2 h	36 min	24 min	1.6 h	30 min	30 min	dyad stage: 2 h		1.4 h	30 min	30 min	//
			25°C	18 h	//	//	//	//	//	//	//	//	//	//	//	//	//	//	//
Triticum aestivum: Holdfast	Reported in Bennett, 1977	Not available	15°C	45 h	//	//	//	//	//	//	//	//	//	//	//	//	//	//	//
			20°C	24 or 25 h	//	//	//	//	//	//	//	//	//	//	//	//	//	//	//
Triticum monococcum	Bennett and Smith, 1972	Feulgen/aceto-carmine staining	20°C	42 h	//			34 h						8 h					//
Tulbaghia violacea	Reported in Bennett, 1977	Not available	20°C	130 h	//	//	//	//	//	//	//	//	//	//	//	//	//	//	//
Zea mays	Hsu et al., 1988	Aceto-carmine staining	NOT GIVEN	119.1 h	//	43 h	31 h	12.2 h	7.1 h	7.2 h	4.4 h	1.6 h	1.6 h	1.8 h	0.4 h	3.9 h	2.1 h	2.8 h	//
	Yu et al., 1997	Live cell imaging	25 ±1°C	Meiosis II: 5 h	//	//	//	//	//	//	//	//	//	2.5 h	1.5 h		1 h		//
	Nannas et al., 2016	Live cell imaging	NOT GIVEN	Anaphases: 12 min	//	//	//	//	//	//	//	12.7 ± 3.2 min	//	//	//	//	11 ± 3.7 min	//	//
DICOTS																			
Plant species	**Publication**	**Method**	**Temperature**	**Meiosis duration overall**	***S-phase/G2***	***Leptotene***	***Zygotene***	***Pachytene***	***Diplotene***	***Diakinesis***	***Metaphase I***	***Anaphase I***	***Telophase I***	***Interkinesis***	***Prophase II***	***Metaphase II***	***Anaphase II***	***Telophase II***	***Tetrads***
Alliaria petiolata	Reported in Bennett, 1977	Not available	NOT GIVEN	24 h	//	//	//	//	//	//	//	//	//	//	//	//	//	//	//
Anthirrium majus	Reported in Bennett, 1977	Not available	NOT GIVEN	24 to 34 h	//	//	//	//	//	//	//	//	//	//	//	//	//	//	//
Arabidopsis thaliana: Ws WT	Armstrong et al., 2003	BrdU labeling	18.5°–20°C	33 h	9 h	6 h		15.3 h						2.7 h					//
Arabidopsis thaliana: Ler WT	Stronghill et al., 2014	EdU labeling	21°C	29 h	7 h	5 h	6 h	10 h	1 h	//	//	//	//	//	//	//	//	//	//
Arabidopsis thaliana: Col-0 WT	Sanchez-Moran et al., 2007	BrdU labeling	NOT GIVEN	32 h	10 h	7 h		12 h	//					3 h					//
	Prusicki et al., 2019	Live cell imaging	21°C	26 h (from late leptotene)	//	>1.5 h	6 h	9.5 h	3 h		1 h		1 h			4 h			//
	Valuchova et al., 2020	Live cell imaging	21°C	47 h	90 min/ 3.5 h		//				1 h			//		50–90 min			//
	De Jaeger-Braet et al., 2021	Live cell imaging	21°C	21.2 h (from late leptotene to anaphase II)	//	14 h*			6 h**		47 min			52 min		46 min		3.6 h	//
			30°C/ 1 week	18.1 h (from late leptotene to anaphase II)	//	10.1 h*			6.3 h**		39 min			45 min		37 min		4.2 h	//
			30°C heat-shock	16.1 h (from late leptotene to anaphase II)	//	9.3 h*			6.1 h**		32 min			47 min		29 min		3.5 h	//
			34°C heat-shock	18.1 h (from late leptotene to anaphase II)	//	7.1 h*			8.7 h**		34 min			59 min		24 min		//	//

(Continued)

TABLE 3 | (Continued)

DICOTS																			
Plant species	**Publication**	**Method**	**Temperature**	**Overall duration of male meiosis**	***S-phase/G2***	***Leptotene***	***Zygotene***	***Pachytene***	***Diplotene***	***Diakinesis***	***Metaphase I***	***Anaphase I***	***Telophase I***	***Interkinesis***	***Prophase II***	***Metaphase II***	***Anaphase II***	***Telophase II***	***Tetrads***
Beta vulgaris	Reported in Bennett, 1977	Not available	20°C	24 h	//	//	//	//	//	//	//	//	//	//	//	//	//	//	//
Capsella bursa-pastoris	Reported in Bennett, 1977	Not available	NOT GIVEN	18 h	//	//	//	//	//	//	//	//	//	//	//	//	//	//	//
Haplopappus gracilis	Reported in Bennett, 1977	Not available	NOT GIVEN	24–36 h	//	//	//	//	//	//	//	//	//	//	//	//	//	//	//
Lycopersicum esculentum (Solanum lycopersicum)	Reported in Bennett, 1977	Not available	20°C	24–30 h	//	//	//	//	//	//	//	//	//	//	//	//	//	//	//
Lycopersicum peruvianum	Pacini and Cresti, 1978	Uranyl acetate staining	NOT GIVEN	Prophase 12 h	//			12 h			//	//	//	//	//	//	//	//	//
Petunia hybrida	Izhar and Frankel, 1973	Fixed anthers/ staining not specified	15–17°C night /25–30°C day	16 h		4 h		2 h	2 h	1 h		2 h		1 h		1 h		3 h	12 h
Pisum sativum	Reported in Bennett, 1977	Not available	20°C	30 h	//	//	//	//	//	//	//	//	//	//	//	//	//	//	//
Veronica chamaedrys	Reported in Bennett, 1977	Not available	NOT GIVEN	20 h	//	//	//	//	//	//	//	//	//	//	//	//	//	//	//
Vicia faba	Reported in Bennett, 1977	Not available	NOT GIVEN	72 to 96 h	//	//	//	//	//	//	//	//	//	//	//	//	//	//	//
Vicia sativa	Reported in Bennett, 1977	Not available	20°C	24 h	//	//	//	//	//	//	//	//	//	//	//	//	//	//	//
GYMNOSPERM																			
Pinus laricio	Chamberlain, 1935 (Reported in Izhar and Frankel, 1973)	Not available	NOT GIVEN	3 months	//	//	//	//	//	//	//	//	//	//	//	//	//	//	//

// depicts not calculated or not specified data,
** inlcudes early pachytene,*
*** includes only late pachytene - diplotene.*

18 h after a pulse, while it takes 30 h after a pulse to label chromosomes from diakinesis to telophase II, indicating that the zygotene–pachytene interval lasts for about 12 h in Arabidopsis (Sanchez-Moran et al., 2007).

However, this method is laborious and relies on the efficiency of chromosome spreads in combination with immunocytochemistry. Thus, sample sizes are typically small and preclude a quantitative analysis of the resulting data. For the same reason, it is also difficult to obtain reliable estimates for heterogeneous cell populations, as for example in the *tam* mutant background. Likewise, short phases, such a meiosis II, which lasts approximately 3 h in Arabidopsis, are difficult to analyze with this method (Armstrong et al., 2003; Sanchez-Moran et al., 2007; Stronghill et al., 2014).

By contrast, live-cell imaging techniques allow the direct observation of individual cells while they undergo meiosis. Moreover, at least in the case of male meiocytes, several samples can be analyzed in one scan, making it possible, though still tedious, to obtain statistically robust sample sizes by scanning several anthers. The first dataset to temporally resolve meiotic phases by live-cell imaging was collected on maize meiocytes observed from metaphase I to telophase II (prometaphase I–metaphase I, up to 60 min; anaphase I, up to 30 min; interkinesis, up to 150 min; prometaphase II–metaphase II, up to 90 min; anaphase II/telophase II, up to 60 min) (**Table 3**; Yu et al., 1997, 1999). Likewise, it was possible to determine the duration of these phases in Arabidopsis from zygotene onward (zygotene, 6 h; pachytene, 9.5 h; diplotene and diakinesis, 3 h; metaphase I and anaphase I, 1 h; telophase and interkinesis, 1 h; second meiotic division, 4 h) (**Table 3**; Prusicki et al., 2019).

In Arabidopsis, meiotic time courses measured by live-cell imaging recapitulate the results obtained by pulse labeling experiments for an overall duration of meiosis of about 26 h (**Table 3**; Prusicki et al., 2019). Live-cell imaging revealed then that an increase of the ambient temperature to 30°C resulted in an acceleration of most but not all meiotic phases in Arabidopsis (De Jaeger-Braet et al., 2021). For instance, the duration of metaphase I to anaphase I was shortened from nearly 1 h to approximately 0.5 h at 30°C. An additional temperature raise to 34°C sped up specific phases of meiosis even further, e.g., late leptotene to early pachytene lasted approximately 14 h at 21°C, 9 h at 30°C and only 7 h at 34°C. At 34°C, however, pachytene to diakinesis was considerably delayed from 6 h at 21°C and 30°C to almost 9 h at 34°C. This delay, together with genetic and cell biological data, indicated the presence of a recombination checkpoint in plants (see below) (De Jaeger-Braet et al., 2021).

Obviously, the choice of reporters will limit the amount of information retrieved. In the case of the time course published by Prusicki et al. (2019), the use of REC8 and TUBULIN as cellular markers offered sufficient cellular criteria (morphological resolution) to dissect meiosis from prophase I until telophase II, although it was not possible to calculate the timing of S-phase or G2 phase, or the exact moment of meiosis onset. To obtain information on these early phases, Valuchova et al. (2020) used the *PCNA-TagRFP* reporter, which allowed the determination of the lengths of late S-phase and G2 phase to be 90 min

and 3.5 h, respectively, much shorter durations than previously estimated (**Table 3**).

Live-cell imaging can also help analyze mutants or situations in which not all meiocytes behave similarly: to distinguish between populations of meiocytes whose progression is arrested, or with a population of meiocytes that progress at various rates through meiosis and will eventually exit meiosis after a prolonged time, as exemplified by *tam* and the weak loss-of-function allele *smg7-1* of *SUPPRESSOR WITH MORPHOGENETIC EFFECTS ON GENITALIA7*, which encodes a factor involved in RNA decay. In the case of *tam* mutants, defective in a CDKA;1 cyclin cofactor, meiocytes show prolonged late-pachytene/diplotene stages, lasting 3–5 h longer than in the wild type. Notably, different populations of meiocytes were identified with distinct microtubules structures (Prusicki et al., 2019). Live-cell imaging of *smg7-1* revealed that the previously described arrest at anaphase II occasionally results from a regression of cells that already entered telophase II. Such a regression was not observed in fixed material, where it would likely have been misinterpreted as slower progression of a sub-population of meiocytes (Valuchova et al., 2020). These examples underscore the power of live-cell imaging.

Microtubule Rearrangements and Regulation

The cytoskeleton undergoes major rearrangements during meiosis, as illustrated in Arabidopsis. Microtubules are evenly distributed across the cytoplasm at the onset of meiosis but take on an arc-like structure resembling a half-moon during early prophase. Similar to mitosis, a full-moon-like microtubule structure surrounds the nucleus later in prophase; when the nuclear envelope breaks down, microtubules rapidly rearrange to form the first spindle in metaphase I and the second spindle in metaphase II (Prusicki et al., 2019). These different arrangements offer visible native markers for the identification of meiotic stages in the absence of a specific meiotic marker and in an imaging setup that does not reach the same level of chromosomal resolution achieved by cell spreads (Prusicki et al., 2019).

Altered microtubule dynamics can have a strong effect on the meiotic outcome, as seen in the maize mutant *dv1* (*divergent spindle1*), which carries a mutation in *ZmKin6*, a member of the kinesin-14A subfamily of minus end–directed microtubule motor proteins. The *dv1* mutant shows an aberrant spindle shape at metaphase I, ultimately resulting in lagging chromosomes at anaphase I. This phenotype was validated by movies of metaphase I of isolated maize meiocytes (Higgins et al., 2016).

Moreover, microtubules are affected in mutants with lower CDK activity, for example, in *tam*, in which phragmoplast-like structures are observed prior to nuclear envelope breakdown (Prusicki et al., 2019). Similarly, ectopic phragmoplasts were observed when a weak loss-of-function allele of *cdka;1* was combined with mutants of *CDKD;3*, a *CDK-ACTIVATING KINASE* (*cdka;1^{VF} cdkd;3*). Moreover, meiocytes of *cdka;1^{VF} cdkd;3* plants also displayed loss of the half-moon and full-moon structures and premature cytokinesis after the first male meiotic division (Sofroni et al., 2020).

Chromosome Movements and Segregation

Chromosome trajectories during prophase in maize were described by Sheehan and Pawlowski (2009) as following three types of movement: rotational movement of the entire chromatin, rapid short-distance oscillations of extruded chromosome segments, and slower paced movements of chromosome segments located inside the chromatin mass. Moreover, these movements vary considerably between different meiotic phases; zygotene chromosomes move rapidly in a short-range pattern, while chromosome arms move more slowly and cover longer distances in pachytene. Chromosome movements disappear when the anthers are treated with drugs that affect cytoskeleton polymerization (latrunculin B and colchicine), demonstrating that they depend on both actin and tubulin.

The shape of the nuclear envelope (NE) also changes during prophase, not as a consequence of chromosome movements, but due to the force of chromosome movements itself (Sheehan and Pawlowski, 2009). Chromosomes move rapidly in Arabidopsis. In addition, the nucleus and the nucleolus show a characteristic movement pattern during Arabidopsis prophase, with the nucleus moving from a central position during premeiotic stages to a lateral position during early prophase, only to then return to a central position at late pachytene–diplotene. Similarly, the nucleolus is located at the periphery of the nucleus at the onset of leptotene and stays there until diakinesis. Moreover, both the nucleus (chromatin mass) and the nucleolus appear to spin at different speeds during the entire prophase I (Prusicki et al., 2019). The dynamics of prophase chromosomes have been linked to homologous chromosome pairing (Sheehan and Pawlowski, 2009). However, the functional relevance of chromosome movements is not yet fully understood, although it is hoped that live-cell imaging will help reveal their role and regulation.

At later stages of meiosis, chromosomes are highly condensed and are distributed to opposite cell poles during anaphase I and II. These movements are mediated by spindle microtubules attached to kinetochores, multi-protein structures that connect chromosomes to the microtubule fibers of the spindle. The speed of chromosome segregation was accurately measured in maize meiocytes by Yu et al. (1997). Maize chromosomal architecture is characterized by the presence of knobs, also called neocentromeres, which offer a second anchoring point between chromatin and the cytoskeleton besides centromeres or kinetochores. Knobs and kinetochores promoted movements with different kinetics, with speeds of 1.08 and 0.78 mm/min, respectively. However, the faster movements of knobs did not appear to influence the speed of the kinetochore of the same chromosome, ultimately causing a stretching of chromosome arms during anaphase, but not an overall faster chromosome movement, demonstrating that the predominant force during meiotic anaphase was dependent on kinetochore movements (Yu et al., 1997). Furthermore, live-cell imaging revealed that the two pools of homologous chromosomes segregate toward the cell poles following an asymmetric motion: The chromosome mass that is furthest from the edge of the cell moves faster and farther to reestablish the lost symmetry

necessary to achieve a balanced cytokinesis. The phragmoplast forms at the half-point between the chromosome masses and not at the spindle zone, as previously hypothesized (Nannas et al., 2016).

Protein Turnover and Regulation of Meiosis

Live-cell imaging is also a powerful tool to monitor protein abundance and, thus, the regulation of meiotic progression. Examples include the above-mentioned quantitative dissection of CDKA;1 localization (Yang et al., 2020).

Live-cell imaging offered a clear and quantitative picture of the gradual loss of REC8 from chromosomes mediated by WAPL, which provided evidence for the prophase pathway of cohesion removal during meiosis (Yang et al., 2019). Likewise, the molecular mechanisms underpinning the protection of centromeric cohesion at anaphase I were assessed by the imaging of plants expressing *REC8pro:REC8-GFP*. The plant homolog of securin, PANS1, prevents the cleavage of centromeric cohesin by the separase protease. REC8 removal at chromosome arms requires the degradation of PANS1 to release the repression imposed on separase, ultimately promoting the segregation of the chromosome homologs. The direct microscopy observations of REC8-GFP behavior in meiocytes expressing a variant of PANS1 that can no longer be degraded (*DMC1pro:PANS1ΔD*) demonstrated that PANS1 degradation is necessary to remove the remaining REC8 from chromosome arms at anaphase I and to promote homolog segregation (Cromer et al., 2019).

MEIOTIC RECOMBINATION OBSERVATIONS BY LIVE-CELL IMAGING

Recombination is a key event during meiosis; therefore, understanding its underlying mechanisms and regulatory principles is important in many fundamental and applied aspects of plant life: to obtain insights into genome evolution, biodiversity, and breeding (Grelon, 2016; Lambing et al., 2017; Wang and Copenhaver, 2018).

Several techniques have been adopted to investigate recombination, ranging from immunolocalization on cell spreads and *in situ* hybridization (among many: Schwarzacher, 2003; Kurzbauer et al., 2018; Martinez-Garcia et al., 2018; Sims et al., 2019) to three-dimensional immunolocalization (Hurel et al., 2018), fluorescent transgenic lines (FTLs) to visualize segregation (Francis et al., 2007), and genotyping by sequencing or chromatin immunoprecipitation followed by sequencing (ChIP-seq) methods to explore the role of epigenetic modifications on recombination cold and hot spots (Pawlowski et al., 2013; Lambing and Heckmann, 2018; Pradillo and Heckmann, 2020).

Being able to follow recombination in real time will open the door to a new level of understanding of this central aspect of meiosis. A first example comes from live-cell imaging of meiosis in Arabidopsis under heat stress (34°C) that uncovered the presence of a long-doubted recombination checkpoint, also known as pachytene checkpoint (De Jaeger-Braet et al., 2021). In animals and yeast, aberrant recombination structures and the complete loss of recombination cause a delay of pachytene (Bishop et al., 1992; Rockmill et al., 1995; Barchi et al., 2005). This arrest is controlled by the checkpoint kinase ATAXIA TELANGIECTASIA MUTATED (ATM). Since in Arabidopsis and other plants the loss of recombination, as for instance seen in *dmc1* mutants, does not cause meiotic arrest, it was concluded that plants do not possess a pachytene checkpoint (Couteau et al., 1999; Grelon et al., 2001; Caryl et al., 2003; Higgins et al., 2004; Li et al., 2004, 2009; Jones and Franklin, 2008; Wijnker and Schnittger, 2013). However, imaging *dmc1* and other mutants in which recombination is abolished such as *spo11-1* at 34°C revealed that the duration of pachytene reverted to almost the level seen in the wildtype at 21°C indicating that the pachytene delay is recombination dependent. Importantly, the pachytene delay in Arabidopsis is also absent in *atm* mutants exposed to 34°C (De Jaeger-Braet et al., 2021). Thus, it appears that there is a pachytene checkpoint in plants. However, this checkpoint likely monitors aberrant recombination structures rather than the absence of COs.

Now, it will be very interesting to further zoom into these defective recombination structures knowing that heat stress and other environmental conditions can modify the position and number of COs (Phillips et al., 2015; Morgan et al., 2017; De Storme and Geelen, 2020). To this end, it will be very informative to follow the recombination machinery itself. However, live-cell imaging of recombination is challenging and is largely limited by three important factors: the current achievable resolution, the movement of chromosomes, and the availability of reporter lines to label proteins of the recombination machinery and to highlight specific chromosomal regions such as the 45S rDNA region and telomeres *in vivo*.

As outlined above, the dynamics of the meiotic chromosome axis, which is key for recombination, is well established by following components such as ASY1, ASY3, and REC8. New reporter lines and live-cell imaging assays now need to be established for the analysis of DSB formation, strand invasion, and CO resolution. These new tools will make it possible to study the appearance and disappearance of each component of the recombination machinery to determine their relative order and how the recombination machinery is affected in various mutant backgrounds.

These studies may explain how a defined DSB site is resolved as a CO, how a CO is assigned to class I or class II, or how CO interference is established, which is far from being fully understood. As recently shown by immuno-cytochemistry, the E3 ligase HEI10, which is a crucial determinant of type I COs and CO interference, is present along the chromosome axis in early pachytene. It then accumulates in growing foci, which are evenly distributed at the expense of smaller, closely spaced peaks in mid and late pachytene (Morgan et al., 2021). It will be now very interesting to follow these foci in real time and correlate their dynamics with other type I CO components by live-cell imaging.

This work may also be extendable to studying recombination during female meiosis, which is differently regulated in both Arabidopsis and crop species (Giraut et al., 2011; Qin et al., 2014; Zhao et al., 2014; Kianian et al., 2018). Furthermore,

live-cell imaging has also the great potential to contribute to an understanding of species-specific difference in meiosis. For instance, the duration of leptotene and early pachytene was extended in *spo11-1* mutants in Arabidopsis while in yeast, the corresponding mutants progress faster through meiosis than the wildtype (Klapholz et al., 1985; Jiao et al., 1999; Cha et al., 2000; De Jaeger-Braet et al., 2021). Thus, the era of live-cell imaging for meiosis has just begun, with many exciting discoveries ahead of us.

AUTHOR CONTRIBUTIONS

MP, MB, KS, YH, and AS selected the content and the references, contributed to define the content structure and revised and approved the article. MP, MB and KS designed the figures and the tables. MP, MB and AS wrote the article. All authors contributed to the article and approved the submitted version.

FUNDING

This work was supported by a grant from the Human Frontier Science Program (RGP0023) and a grant from the BMBF to AS (MeioCheck).

ACKNOWLEDGMENTS

We are grateful to Joke de Jaeger-Braet (University of Hamburg) and Konstantinos Lampou (University of Hamburg) for helpful discussion of the manuscript. We thank the Plant Editors for editing this manuscript.

REFERENCES

Armstrong, S. J., Franklin, F. C. H., and Jones, G. H. (2003). A meiotic time-course for *Arabidopsis thaliana*. *Sex Plant Reprod.* 16, 141–149. doi: 10.1007/s00497-003-0186-4

Balboni, M., Yang, C., Komaki, S., Brun, J., and Schnittger, A. (2020). COMET functions as a PCH2 cofactor in regulating the HORMA domain protein ASY1. *Curr. Biol.* 30, 4113–4127.e6. doi: 10.1016/j.cub.2020.07.089

Barber, H. N. (1942). The experimental control of chromosome pairing in Fritillaria. *J. Genet.* 43, 359–374. doi: 10.1007/BF02982908

Barchi, M., Mahadevaiah, S., Di Giacomo, M., Baudat, F., de Rooij, D. G., Burgoyne, P. S., et al. (2005). Surveillance of different recombination defects in mouse spermatocytes yields distinct responses despite elimination at an identical developmental stage. *Mol. Cell. Biol.* 25, 7203–7215. doi: 10.1128/MCB.25.16.7203-7215.2005

Bastiaens, P. I., and Pepperkok, R. (2000). Observing proteins in their natural habitat: the living cell. *Trends Biochem. Sci.* 25, 631–637. doi: 10.1016/s0968-0004(00)01714-x

Bennett, M. D. (1971). The duration of meiosis. *Proc. R. Soc. Lond. B* 178, 277–299. doi: 10.1098/rspb.1971.0066

Bennett, M. D. (1977). The time and duration of meiosis. *Philos. Trans. R. Soc. Lond. B* 277, 201–226. doi: 10.1098/rstb.1977.0012

Bennett, M. D., and Finch, R. A. (1971). Duration of meiosis in barley. *Genet. Res.* 17, 209–214. doi: 10.1017/S0016672300012234

Bennett, M. D., and Kaltsikes, P. J. (1973). The duration of meiosis in a diploid rye, a tetraploid wheat and the hexaploid triticale derived from them. *Can. J. Genet. Cytol.* 15, 671–679. doi: 10.1139/g73-080

Bennett, M. D., and Smith, J. B. (1972). The effects of polyploidy on meiotic duration and pollen development in cereal anthers. *Proc. R. Soc. Lond. B* 181, 81–107.

Bennett, M. D., Chapman, V., and Riley, R. (1971). The duration of meiosis in pollen mother cells of wheat, rye and Triticale. *Proc. R. Soc. Lond. Ser. B. Biol. Sci.* 178, 259–275. doi: 10.1098/rspb.1971.0065

Bennett, M. D., Dover, G. A., and Riley, R. (1974). Meiotic duration in wheat genotypes with or without homoeologous meiotic chromosome pairing. *Proc. R. Soc. Lond. Ser. B. Biol. Sci.* 187, 191–207. doi: 10.1098/rspb.1974.0069

Bennett, M. D., Smith, J. B., and Kemble, R. (1972). The effect of temperature on meiosis and pollen development in wheat and rye. *Can. J. Genet. Cytol.* 14, 615–624. doi: 10.1139/g72-076

Bennett, M. D., Stern, H., and Riley, R. (1975). The time and duration of female meiosis in Lilium. *Proc. R. Soc. Lond. Ser. B. Biol. Sci.* 188, 459–475. doi: 10.1098/rspb.1975.0031

Biedermann, S., Harashima, H., Chen, P., Heese, M., Bouyer, D., Sofroni, K., et al. (2017). The retinoblastoma homolog RBR1 mediates localization of the repair protein RAD51 to DNA lesions in *Arabidopsis*. *EMBO J.* 36, 1279–1297. doi: 10.15252/embj.201694571

Bishop, D. K., Park, D., Xu, L., and Kleckner, N. (1992). DMC1: a meiosis-specific yeast homolog of E. coli recA required for recombination, synaptonemal complex formation, and cell cycle progression. *Cell* 69, 439–456. doi: 10.1016/0092-8674(92)90446-J

Bomblies, K., Higgins, J. D., and Yant, L. (2015). Meiosis evolves: adaptation to external and internal environments. *New Phytol.* 208, 306–323. doi: 10.1111/nph.13499

Brownfield, L., Yi, J., Jiang, H., Minina, E. A., Twell, D., and Köhler, C. (2015). Organelles maintain spindle position in plant meiosis. *Nat. Commun.* 6:6492. doi: 10.1038/ncomms7492

Buchanan, B. B., Gruissem, W., and Jones, R. L. (2015). *Biochemistry and Molecular Biology of Plants*. Hoboken, NJ: John Wiley & Sons.

Bulankova, P., Riehs-Kearnan, N., Nowack, M. K., Schnittger, A., and Riha, K. (2010). Meiotic progression in *Arabidopsis* is governed by complex regulatory interactions between SMG7, TDM1, and the meiosis I-specific cyclin TAM. *Plant Cell* 22, 3791–3803. doi: 10.1105/tpc.110.078378

Cahoon, C. K., Yu, Z., Wang, Y., Guo, F., Unruh, J. R., Slaughter, B. D., et al. (2017). Superresolution expansion microscopy reveals the three-dimensional organization of the *Drosophila* synaptonemal complex. *Proc. Natl. Acad. Sci. U.S.A.* 114, E6857–E6866. doi: 10.1073/pnas.1705623114

Caryl, A. P., Jones, G. H., and Franklin, F. C. (2003). Dissecting plant meiosis using *Arabidopsis thaliana* mutants. *J. Exp. Bot.* 54, 25–38. doi: 10.1093/jxb/erg041

Cha, R. S., Weiner, B. M., Keeney, S., Dekker, J., and Kleckner, N. (2000). Progression of meiotic DNA replication is modulated by interchromosomal interaction proteins, negatively by Spo11p and positively by Rec8p. *Genes Dev.* 14, 493–503. doi: 10.1101/gad.14.4.493

Chambon, A., West, A., Vezon, D., Horlow, C., Muyt, A. D., Chelysheva, L., et al. (2018). Identification of ASYNAPTIC4, a component of the meiotic chromosome axis. *Plant Physiol.* 178, 233–246. doi: 10.1104/pp.17.01725

Chamberlain, C. J. (1935). *Gymnosperms, Structure and Evolution*. Chicago: Chicago University Press, 286–287.

Chan, A., and Zacheus Cande, W. (2000). Maize meiocytes in culture. *Plant Cell Tissue Organ Cult.* 60:187. doi: 10.1023/A:1006420425525

Chelysheva, L., Vezon, D., Chambon, A., Gendrot, G., Pereira, L., Lemhemdi, A., et al. (2012). The *Arabidopsis* HEI10 is a new ZMM protein related to Zip3. *PLoS Genet.* 8:e1002799. doi: 10.1371/journal.pgen.1002799

Chen, Z., Higgins, J. D., Hui, J. T. L., Li, J., Franklin, F. C. H., and Berger, F. (2011). Retinoblastoma protein is essential for early meiotic events in *Arabidopsis*. *EMBO J.* 30, 744–755. doi: 10.1038/emboj.2010.344

Chikashige, Y., Ding, D. Q., Funabiki, H., Haraguchi, T., Mashiko, S., Yanagida, M., et al. (1994). Telomere-led premeiotic chromosome movement in fission yeast. *Science* 264, 270–273. doi: 10.1126/science.8146661

Christophorou, N., Rubin, T., Bonnet, I., Piolot, T., Arnaud, M., and Huynh, J.-R. (2015). Microtubule-driven nuclear rotations promote meiotic chromosome dynamics. *Nat. Cell Biol.* 17, 1388–1400. doi: 10.1038/ncb3249

Church, K., and Wimber, D. E. (1969). Meiosis in the grasshopper: chiasma frequency after elevated temperature and x-rays. *Can. J. Genet. Cytol.* 11, 209–216. doi: 10.1139/g69-025

Colombié, N., Głuszek, A. A., Meireles, A. M., and Ohkura, H. (2013). Meiosis-Specific stable binding of augmin to acentrosomal spindle poles promotes biased microtubule assembly in oocytes. *PLoS Genet.* 9:e1003562. doi: 10.1371/journal.pgen.1003562

Conrad, M. N., Lee, C.-Y., Chao, G., Shinohara, M., Kosaka, H., Shinohara, A., et al. (2008). Rapid telomere movement in meiotic prophase is promoted by NDJ1, MPS3, and CSM4 and is modulated by recombination. *Cell* 133, 1175–1187. doi: 10.1016/j.cell.2008.04.047

Couteau, F., Belzile, F., Horlow, C., Grandjean, O., Vezon, D., and Doutriaux, M. P. (1999). Random chromosome segregation without meiotic ar-rest in both male and female meiocytes of a dmc1 mutant of *Arabidopsis*. *Plant Cell* 11, 1623–1634. doi: 10.1105/tpc.11.9.1623

Cromer, L., Jolivet, S., Singh, D. K., Berthier, F., Winne, N. D., Jaeger, G. D., et al. (2019). Patronus is the elusive plant securin, preventing chromosome separation by antagonizing separase. *Proc. Natl. Acad. Sci. U.S.A.* 116, 16018–16027. doi: 10.1073/pnas.1906237116

Da Ines, O., Degroote, F., Goubely, C., Amiard, S., Gallego, M. E., and White, C. I. (2013). Meiotic recombination in *Arabidopsis* is catalysed by DMC1, with RAD51 playing a supporting role. *PLoS Genet.* 9:e1003787. doi: 10.1371/journal.pgen.1003787

Dangol, S., Singh, R., Chen, Y., and Jwa, N.-S. (2017). Visualization of multicolored in vivo organelle markers for co-localization studies in *Oryza sativa*. *Mol. Cells* 40, 828–836. doi: 10.14348/molcells.2017.0045

De Jaeger-Braet, J., Krause, L., Buchholz, A., and Schnittger, A. (2021). Heat stress reveals a specialized variant of the pachytene checkpoint in meiosis of *Arabidopsis thaliana*. *Plant Cell* koab257. doi: 10.1093/plcell/koab257

De La Peña, A. (1986). 'In vitro' culture of isolated meiocytes of rye, Secale cereale L. *Environ. Exp. Bot.* 26, 17–23. doi: 10.1016/0098-8472(86)90048-1

De Storme, N., and Geelen, D. (2020). High temperatures alter cross-over distribution and induce male meiotic restitution in *Arabidopsis thaliana*. *Commun. Biol.* 3, 1–15. doi: 10.1038/s42003-020-0897-1

De Storme, N., Keçeli, B. N., Zamariola, L., Angenon, G., and Geelen, D. (2016). CENH3-GFP: a visual marker for gametophytic and somatic ploidy determination in *Arabidopsis thaliana*. *BMC Plant Biol.* 16:1. doi: 10.1186/s12870-015-0700-5

DeBlasio, S. L., Sylvester, A. W., and Jackson, D. (2010). Illuminating plant biology: using fluorescent proteins for high-throughput analysis of protein localization and function in plants. *Brief. Funct. Genomics* 9, 129–138. doi: 10.1093/bfgp/elp060

Dreissig, S., Schiml, S., Schindele, P., Weiss, O., Rutten, T., Schubert, V., et al. (2017). Live-cell CRISPR imaging in plants reveals dynamic telomere movements. *Plant J.* 91, 565–573. doi: 10.1111/tpj.13601

Echevarría, C., Gutierrez, C., and Desvoyes, B. (2021). Tools for assessing cell cycle progression in plants. *Plant Cell Physiol.* 62, 1231–1238. doi: 10.1093/pcp/pcab066

Ekberg, I., and Eriksson, G. (1965). Demonstration of meiosis and pollen mitosis by photomicrograps and the distribution of meiotic stages in barley spikes. *Hereditas* 53, 127–136. doi: 10.1111/j.1601-5223.1965.tb01985.x

Enguita-Marruedo, A., Cappellen, W. A. V., Hoogerbrugge, J. W., Carofiglio, F., Wassenaar, E., Slotman, J. A., et al. (2018). Live cell analyses of synaptonemal complex dynamics and chromosome movements in cultured mouse testis tubules and embryonic ovaries. *Chromosoma* 127, 341–359. doi: 10.1007/s00412-018-0668-7

Era, A., Tominaga, M., Ebine, K., Awai, C., Saito, C., Ishizaki, K., et al. (2009). Application of lifeact reveals F-actin dynamics in *Arabidopsis thaliana* and the liverwort, marchantia polymorpha. *Plant Cell Physiol.* 50, 1041–1048. doi: 10.1093/pcp/pcp055

Erickson, R. O. (1948). Cytological and growth correlations in the flower bud and anther of *Lilium longiflorum*. *Am. J. Bot.* 35, 729–739. doi: 10.1002/j.1537-2197.1948.tb08143.x

Feijó, J. A., and Cox, G. (2001). Visualization of meiotic events in intact living anthers by means of two-photon microscopy. *Micron* 32, 679–684. doi: 10.1016/S0968-4328(00)00097-4

Finch, R. A., and Bennett, M. D. (1972). The duration of meiosis in diploid and autotetraploid barley. *Can. J. Genet. Cytol.* 14, 507–515. doi: 10.1139/g72-063

Francis, K. E., Lam, S. Y., Harrison, B. D., Bey, A. L., Berchowitz, L. E., and Copenhaver, G. P. (2007). Pollen tetrad-based visual assay for meiotic recombination in *Arabidopsis*. *Proc. Natl. Acad. Sci. U.S.A.* 104, 3913–3918. doi: 10.1073/pnas.0608936104

Giraut, L., Falque, M., Drouaud, J., Pereira, L., Martin, O. C., and Mézard, C. (2011). Genome-Wide crossover distribution in *Arabidopsis thaliana* meiosis reveals sex-specific patterns along chromosomes. *PLoS Genet.* 7:e1002354. doi: 10.1371/journal.pgen.1002354

Golubovskaya, I. N., Harper, L. C., Pawlowski, W. P., Schichnes, D., and Cande, W. Z. (2002). The pam1 gene is required for meiotic bouquet formation and efficient homologous synapsis in maize (*Zea mays* L.). *Genetics* 162, 1979–1993. doi: 10.1093/genetics/162.4.1979

Grelon, M. (2016). Meiotic recombination mechanisms. *C. R. Biol.* 339, 247–251. doi: 10.1016/j.crvi.2016.04.003

Grelon, M., Vezon, D., Gendrot, G., and Pelletier, G. (2001). AtSPO11-1 is necessary for efficient meiotic recombination in plants. *EMBO J.* 20, 589–600. doi: 10.1093/emboj/20.3.589

Hafidh, S., and Honys, D. (2021). Reproduction multitasking: the male gametophyte. *Annu. Rev. Plant Biol.* 72, 581–614. doi: 10.1146/annurev-arplant-080620-021907

Hamamura, Y., Saito, C., Awai, C., Kurihara, D., Miyawaki, A., Nakagawa, T., et al. (2011). Live-Cell imaging reveals the dynamics of two sperm cells during double fertilization in *Arabidopsis thaliana*. *Curr. Biol.* 21, 497–502. doi: 10.1016/j.cub.2011.02.013

Harashima, H., Dissmeyer, N., and Schnittger, A. (2013). Cell cycle control across the eukaryotic kingdom. *Trends Cell Biol.* 23, 345–356. doi: 10.1016/j.tcb.2013.03.002

Harashima, H., Dissmeyer, N., Hammann, P., Nomura, Y., Kramer, K., Nakagami, H., et al. (2016). Modulation of plant growth in vivo and identification of kinase substrates using an analog-sensitive variant of CYCLIN-DEPENDENT KINASE A;1. *BMC Plant Biol.* 16:209. doi: 10.1186/s12870-016-0900-7

Hater, F., Nakel, T., and Groß-Hardt, R. (2020). Reproductive multitasking: the female gametophyte. *Annu. Rev. Plant Biol.* 71, 517–546. doi: 10.1146/annurev-arplant-081519-035943

Hernandez, M. R., Davis, M. B., Jiang, J., Brouhard, E. A., Severson, A. F., and Csankovszki, G. (2018). Condensin I protects meiotic cohesin from WAPL-1 mediated removal. *PLoS Genetics* 14:e1007382. doi: 10.1371/journal.pgen.1007382

Hertwig, W. A. O. (1876). Beiträge zur kenntniss der bildung, befruchtung und theilung des thierischen eies. *Morphol. Jahrbuch* 1, 347–434.

Heslop-Harrison, J. (1966). Cytoplasmic connexions between angiosperm meiocytes. *Ann. Bot.* 30, 221–222. doi: 10.1093/oxfordjournals.aob.a084069

Higashiyama, T., Yabe, S., Sasaki, N., Nishimura, Y., Miyagishima, S., Kuroiwa, H., et al. (2001). Pollen tube attraction by the synergid cell. *Science* 293, 1480–1483. doi: 10.1126/science.1062429

Higgins, D. M., Nannas, N. J., and Dawe, R. K. (2016). The maize divergent spindle-1 (dv1) gene encodes a Kinesin-14A motor protein required for meiotic spindle pole organization. *Front. Plant Sci.* 7:1277. doi: 10.3389/fpls.2016.01277

Higgins, J. D., Armstrong, S. J., Franklin, F. C. H., and Jones, G. H. (2004). The Arabidopsis MutS homolog AtMSH4 functions at an early step in recombination: evidence for two classes of recombination in *Arabidopsis*. *Genes Dev.* 18, 2557–2570. doi: 10.1101/gad.317504

Higgins, J. D., Perry, R. M., Barakate, A., Ramsay, L., Waugh, R., Halpin, C., et al. (2012). Spatiotemporal asymmetry of the meiotic program underlies the predominantly distal distribution of meiotic crossovers in barley. *Plant Cell* 24, 4096–4109. doi: 10.1105/tpc.112.102483

Holubcová, Z., Howard, G., and Schuh, M. (2013). Vesicles modulate an actin network for asymmetric spindle positioning. *Nat. Cell Biol.* 15:937. doi: 10.1038/ncb2802

Hotta, Y., and Stern, H. (1963). Synthesis of messenger-like ribonucleic acid and protein during meiosis in isolated cells of trillium erectum. *J. Cell Biol.* 19, 45–58. doi: 10.1083/jcb.19.1.45

Hsu, S.-Y., Huang, Y.-C., and Peerson, P. A. (1988). Development pattern of microspores in *Zea mays* L. the maturation of upper and lower florets of spikelets among an assortment of genotypes. *Madyca* 33, 77–98.

Hughes, S. E., Beeler, J. S., Seat, A., Slaughter, B. D., Unruh, J. R., Bauerly, E., et al. (2011). Gamma-Tubulin is required for bipolar spindle assembly and for proper kinetochore microtubule attachments during prometaphase I

in *Drosophila* oocytes. *PLoS Genet.* 7:e1002209. doi: 10.1371/journal.pgen.1002209

Hurel, A., Phillips, D., Vrielynck, N., Mézard, C., Grelon, M., and Christophorou, N. (2018). A cytological approach to studying meiotic recombination and chromosome dynamics in *Arabidopsis thaliana* male meiocytes in three dimensions. *Plant J.* 95, 385–396. doi: 10.1111/tpj.13942

Ingouff, M., Selles, B., Michaud, C., Vu, T. M., Berger, F., Schorn, A. J., et al. (2017). Live-cell analysis of DNA methylation during sexual reproduction in Arabidopsis reveals context and sex-specific dynamics controlled by noncanonical RdDM. *Genes Dev.* 31, 72–83. doi: 10.1101/gad.289397.116

Ito, M., and Stern, H. (1967). Studies of meiosis in vitro: I. In vitro culture of meiotic cells. *Dev. Biol.* 16, 36–53. doi: 10.1016/0012-1606(67)90016-4

Ito, Y., Uemura, T., and Nakano, A. (2018). The Golgi entry core compartment functions as a COPII-independent scaffold for ER-to-Golgi transport in plant cells. *J. Cell Sci.* 131:jcs203893. doi: 10.1242/jcs.203893

Izhar, S., and Frankel, R. (1973). Duration of meiosis in Petunia anthers in vivo and in floral bud culture. *Acta Bot. Neerl.* 22, 14–22.

Jackson, N., Sanchez-Moran, E., Buckling, E., Armstrong, S. J., Jones, G. H., and Franklin, F. C. H. (2006). Reduced meiotic crossovers and delayed prophase I progression in AtMLH3-deficient *Arabidopsis*. *EMBO J.* 25, 1315–1323. doi: 10.1038/sj.emboj.7600992

Jiao, K., Bullard, S. A., Salem, L., and Malone, R. E. (1999). Coordination of the initiation of recombination and the reductional division in meiosis in *Saccharomyces cerevisiae*. *Genetics* 152, 117–128. doi: 10.1093/genetics/152.1.117

Jin, W., Lamb, J. C., Zhang, W., Kolano, B., Birchler, J. A., and Jiang, J. (2008). Histone modifications associated with both A and B chromosomes of maize. *Chromosome Res.* 16, 1203–1214. doi: 10.1007/s10577-008-1269-8

Jones, A. M., Danielson, J. Å, ManojKumar, S. N., Lanquar, V., Grossmann, G., and Frommer, W. B. (2014). Abscisic acid dynamics in roots detected with genetically encoded FRET sensors. *eLife* 3:e01741. doi: 10.7554/eLife.01741

Jones, G. H., and Franklin, F. C. (2008). "Meiosis in *Arabidopsis thaliana*: recombination, chromosome organization and meiotic progression," in *Recombination and Meiosis: Crossing-Over and Disjunction*, eds R. Egel and D. H. Lankenau (Berlin: Springer), 279–306. doi: 10.1023/a:1022831724990

Keeney, S. ed. (2009). *Meiosis: Cytological Methods*, Vol. 2. Totowa, NJ: Humana Press. doi: 10.1007/978-1-60761-103-5

Kemp, C. L. (1964). The effects of inhibitors of RNA and protein synthesis on cytological development during meiosis. *Chromosoma* 15, 652–665. doi: 10.1007/BF00319997

Khosravi, S., Schidele, P., Gladilin, E., Dunemann, F., Rutten, T., Putcha, H., et al. (2020). Application of aptamers improves CRISPR-based live imaging of plant telomeres. *Front. Plant Sci.* 11:1254. doi: 10.3389/fpls.2020.01254

Kianian, P. M. A., Wang, M., Simons, K., Ghavami, F., He, Y., Dukowic-Schulze, S., et al. (2018). High-resolution crossover mapping reveals similarities and differences of male and female recombination in maize. *Nat. Commun.* 9:2370. doi: 10.1038/s41467-018-04562-5

Kimata, Y., Higaki, T., Kawashima, T., Kurihara, D., Sato, Y., Yamada, T., et al. (2016). Cytoskeleton dynamics control the first asymmetric cell division in Arabidopsis zygote. *Proc. Natl. Acad. Sci. U.S.A.* 113, 14157–14162. doi: 10.1073/pnas.1613979113

Kitajima, T. S., Ohsugi, M., and Ellenberg, J. (2011). Complete kinetochore tracking reveals error-prone homologous chromosome biorientation in mammalian oocytes. *Cell* 146, 568–581. doi: 10.1016/j.cell.2011.07.031

Klapholz, S., Waddell, C. S., and Esposito, R. E. (1985). The role of the SPO11 gene in meiotic recombination in yeast. *Genetics* 110, 187–216. doi: 10.1093/genetics/110.2.187

Komaki, S., and Schnittger, A. (2017). The spindle assembly checkpoint in *Arabidopsis* is rapidly shut off during severe stress. *Dev. Cell* 43, 172–185.e5. doi: 10.1016/j.devcel.2017.09.017

Komaki, S., Takeuchi, H., Hamamura, Y., Heese, M., Hashimoto, T., and Schnittger, A. (2020). Functional analysis of the plant chromosomal passenger complex. *Plant Physiol.* 183, 1586–1599. doi: 10.1104/pp.20.00344

Koszul, R., and Kleckner, N. (2009). Dynamic chromosome movements during meiosis: a way to eliminate unwanted connections? *Trends Cell Biol.* 19, 716–724. doi: 10.1016/j.tcb.2009.09.007

Kurzbauer, M.-T., Pradillo, M., Kerzendorfer, C., Sims, J., Ladurner, R., Oliver, C., et al. (2018). *Arabidopsis thaliana* FANCD2 promotes meiotic crossover formation. *Plant Cell* 30, 415–428. doi: 10.1105/tpc.17.00745

Kyogoku, H., and Kitajima, T. S. (2017). Large cytoplasm is linked to the error-prone nature of oocytes. *Dev. Cell* 41, 287–298.e4. doi: 10.1016/j.devcel.2017.04.009

Lambing, C., and Heckmann, S. (2018). Tackling plant meiosis: from model research to crop improvement., tackling plant meiosis: from model research to crop improvement. *Front. Plant Sci.* 9:829. doi: 10.3389/fpls.2018.00829

Lambing, C., Franklin, F. C. H., and Wang, C.-J. R. (2017). Understanding and manipulating meiotic recombination in plants[OPEN]. *Plant Physiol.* 173, 1530–1542. doi: 10.1104/pp.16.01530

Lee, C.-Y., Bisig, C. G., Conrad, M. N., Ditamo, Y., Previato de Almeida, L., Dresser, M. E., et al. (2020). Telomere-led meiotic chromosome movements: recent update in structure and function. *Nucleus* 11, 111–116. doi: 10.1080/19491034.2020.1769456

Lee, C.-Y., Conrad, M. N., and Dresser, M. E. (2012). Meiotic chromosome pairing is promoted by telomere-led chromosome movements independent of bouquet formation. *PLoS Genet.* 9:e1002730. doi: 10.1371/journal.pgen.1002730

Lee, C.-Y., Horn, H. F., Stewart, C. L., Burke, B., Bolcun-Filas, E., Schimenti, J. C., et al. (2015). Mechanism and regulation of rapid telomere prophase movements in mouse meiotic chromosomes. *Cell Rep.* 11, 551–563. doi: 10.1016/j.celrep.2015.03.045

Li, W., Chen, C., Markmann-Mulisch, U., Timofejeva, L., Schmelzer, E., Ma, H., et al. (2004). The *Arabidopsis* AtRAD51 gene is dispensable for vegetative development but required for meiosis. *Proc. Natl. Acad. Sci. U.S.A.* 101, 10596–10601. doi: 10.1073/pnas.0404110101

Li, X. C., Barringer, B. C., and Barbash, D. A. (2009). The pachytene check- point and its relationship to evolutionary patterns of polyploidiza-tion and hybrid sterility. *Heredity* 102, 24–30. doi: 10.1038/hdy.2008.84

Liao, C.-Y., and Weijers, D. (2018). A toolkit for studying cellular reorganization during early embryogenesis in *Arabidopsis thaliana*. *Plant J.* 93, 963–976. doi: 10.1111/tpj.13841

Lindgren, D., Eriksson, G., and Ekberg, I. (1969). The relative duration of the meiotic stages in pollen mother cells of barley. *Hereditas* 63, 205–212. doi: 10.1111/j.1601-5223.1969.tb02262.x

Liu, B., Storme, N. D., and Geelen, D. (2017). Gibberellin induces diploid pollen formation by interfering with meiotic cytokinesis. *Plant Physiol.* 173, 338–353. doi: 10.1104/pp.16.00480

Magnard, J.-L., Yang, M., Chen, Y.-C. S., Leary, M., and McCormick, S. (2001). The Arabidopsis gene tardy asynchronous meiosis is required for the normal pace and synchrony of cell division during male meiosis. *Plant Physiol.* 127, 1157–1166. doi: 10.1104/pp.010473

Marquardt, H. (1937). Die meiosis von oenothera I. *Z. Zellforsch.* 27, 159–210. doi: 10.1007/BF01880081

Martinez-Garcia, M., Schubert, V., Osman, K., Darbyshire, A., Sanchez-Moran, E., and Franklin, F. C. H. (2018). TOPII and chromosome movement help remove interlocks between entangled chromosomes during meiosis. *J. Cell Biol.* 217, 4070–4079. doi: 10.1083/jcb.201803019

Mathur, J., Griffiths, S., Barton, K., and Schattat, M. H. (2012). "Chapter eight – green-to-Red photoconvertible mEosFP-aided live imaging in plants," in *Methods in Enzymology Imaging and Spectroscopic Analysis of Living Cells*, ed. P. M. Conn (Cambridge, MA: Academic Press), 163–181. doi: 10.1016/B978-0-12-391857-4.00008-2

Matthies, H. J., McDonald, H. B., Goldstein, L. S., and Theurkauf, W. E. (1996). Anastral meiotic spindle morphogenesis: role of the non-claret disjunctional kinesin-like protein. *J. Cell Biol.* 134, 455–464. doi: 10.1083/jcb.134.2.455

Mogessie, B., and Schuh, M. (2017). Actin protects mammalian eggs against chromosome segregation errors. *Science* 357:eaal1647. doi: 10.1126/science.aal1647

Morgan, C. H., Zhang, H., and Bomblies, K. (2017). Are the effects of elevated temperature on meiotic recombination and thermotolerance linked via the axis and synaptonemal complex? *Philos. Trans. R. Soc. Lond. B Biol. Sci.* 372:20160470. doi: 10.1098/rstb.2016.0470

Morgan, C., Fozard, J. A., Hartley, M., Henderson, I. R., Bomblies, K., and Howard, M. (2021). Diffusion-mediated HEI10 coarsening can explain meiotic crossover

positioning in *Arabidopsis*. *Nat. Commun.* 12:4674. doi: 10.1038/s41467-021-24827-w

Murphy, S. P., Gumber, H. K., Mao, Y., and Bass, H. W. (2014). A dynamic meiotic SUN belt includes the zygotene-stage telomere bouquet and is disrupted in chromosome segregation mutants of maize (*Zea mays* L.). *Front. Plant Sci.* 5:314. doi: 10.3389/fpls.2014.00314

Nannas, N. J., Higgins, D. M., and Dawe, R. K. (2016). Anaphase asymmetry and dynamic repositioning of the division plane during maize meiosis. *J. Cell Sci.* 129, 4014–4024. doi: 10.1242/jcs.194860

Nikalayevich, E., Bouftas, N., and Wassmann, K. (2018). "Detection of separase activity using a cleavage sensor in live mouse oocytes," in *Mouse Oocyte Development: Methods and Protocols Methods in Molecular Biology*, eds M.-H. Verlhac and M.-E. Terret (New York, NY: Springer), 99–112. doi: 10.1007/978-1-4939-8603-3_11

Okuda, S., Tsutsui, H., Shiina, K., Sprunck, S., Takeuchi, H., Yui, R., et al. (2009). Defensin-like polypeptide LUREs are pollen tube attractants secreted from synergid cells. *Nature* 458, 357–361. doi: 10.1038/nature07882

Pacini, E., and Cresti, M. (1978). Ultrastructural characteristics of the tapetum and microspore mother cells in *Lycopersicum peruvianum* during meiotic prophase. *Bull. Soc. Bot. Fr. Actual. Bot.* 125, 121–128.

Pawlowski, W. P., Grelon, M., and Armstrong, S. (2013). Analyzing meiosis in Barley. *Methods Mol. Biol.* 990, 135–144. doi: 10.1007/978-1-62703-333-6_14

Pfender, S., Kuznetsov, V., Pasternak, M., Tischer, T., Santhanam, B., and Schuh, M. (2015). Live imaging RNAi screen reveals genes essential for meiosis in mammalian oocytes. *Nature* 524, 239–242. doi: 10.1038/nature14568

Phillips, D., Jenkins, G., Macaulay, M., Nibau, C., Wnetrzak, J., Fallding, D., et al. (2015). The effect of temperature on the male and female recombination landscape of barley. *New Phytol.* 208, 421–429. doi: 10.1111/nph.13548

Pradillo, M., and Heckmann, S. eds (2020). *Plant Meiosis: Methods and Protocols*. New York, NY: Humana Press. doi: 10.1007/978-1-4939-9818-0

Prunet, N., Jack, T. P., and Meyerowitz, E. M. (2016). Live confocal imaging of Arabidopsis flower buds. *Dev. Biol.* 419, 114–120. doi: 10.1016/j.ydbio.2016.03.018

Prusicki, M. A., Hamamura, Y., and Schnittger, A. (2020a). "A practical guide to live-cell imaging of meiosis in *Arabidopsis*," in *Plant Meiosis: Methods and Protocols Methods in Molecular Biology*, eds M. Pradillo and S. Heckmann (New York, NY: Springer), 3–12. doi: 10.1007/978-1-4939-9818-0_1

Prusicki, M. A., Keizer, E. M., van Rosmalen, R. P., Komaki, S., Seifert, F., Müller, K., et al. (2019). Live cell imaging of meiosis in *Arabidopsis thaliana*. *eLife* 8:e42834. doi: 10.7554/eLife.42834

Prusicki, M., Keizer, E., van Rosmalen, R., Fleck, C., and Schnittger, A. (2020b). Live cell imaging of male meiosis in *Arabidopsis* by a landmark-based system. *Bio Protoc.* 10:e3611. doi: 10.21769/BioProtoc.3611

Qin, Y., Zhao, L., Skaggs, M. I., Andreuzza, S., Tsukamoto, T., Panoli, A., et al. (2014). ACTIN-RELATED PROTEIN6 regulates female meiosis by modulating meiotic gene expression in *Arabidopsis*. *Plant Cell* 26, 1612–1628. doi: 10.1105/tpc.113.120576

Rasmussen, C. G., Wright, A. J., and Müller, S. (2013). The role of the cytoskeleton and associated proteins in determination of the plant cell division plane. *Plant J.* 75, 258–269. doi: 10.1111/tpj.12177

Reitz, D., Grubb, J., and Bishop, D. K. (2019). A mutant form of Dmc1 that bypasses the requirement for accessory protein Mei5-Sae3 reveals independent activities of Mei5-Sae3 and Rad51 in Dmc1 filament stability. *PLoS Genet.* 15:e1008217. doi: 10.1371/journal.pgen.1008217

Rockmill, B., Sym, M., Scherthan, H., and Roeder, G. S. (1995). Roles for two RecA homologs in promoting meiotic chromosome synapsis. *Genes Dev.* 9, 2684–2695. doi: 10.1101/gad.9.21.2684

Rueda, J., and Vázquez, A. M. (1988). Meiotic behaviour of the pollen mother cells in cultured anthers of rye excised at early meiotic prophase. *Genome* 30, 161–165. doi: 10.1139/g88-028

Ryan, K. (1983). Chromosome movements in pollen mother cells: techniques for living cell cine-microscopy and for electron microscopy. *Mikroskopie* 40, 67–78.

Sanchez-Moran, E., Santos, J.-L., Jones, G. H., and Franklin, F. C. H. (2007). ASY1 mediates AtDMC1-dependent interhomolog recombination during meiosis in *Arabidopsis*. *Genes Dev.* 21, 2220–2233. doi: 10.1101/gad.439007

Schuh, M., and Ellenberg, J. (2007). Self-Organization of MTOCs replaces centrosome function during Acentrosomal spindle assembly in live mouse oocytes. *Cell* 130, 484–498. doi: 10.1016/j.cell.2007.06.025

Schwarzacher, T. (2003). Meiosis, recombination and chromosomes: a review of gene isolation and fluorescent in situ hybridization data in plants. *J. Exp. Bot.* 54, 11–23. doi: 10.1093/jxb/erg042

Sheehan, M. J., and Pawlowski, W. P. (2009). Live imaging of rapid chromosome movements in meiotic prophase I in maize. *Proc. Natl. Acad. Sci. U.S.A.* 106, 20989–20994. doi: 10.1073/pnas.0906498106

Silva, M. C. C., Powell, S., Ladstätter, S., Gassler, J., Stocsits, R., Tedeschi, A., et al. (2020). Wapl releases Scc1-cohesin and regulates chromosome structure and segregation in mouse oocytes. *J. Cell Biol.* 219:e201906100. doi: 10.1083/jcb.201906100

Sims, J., Copenhaver, G. P., and Schlögelhofer, P. (2019). Meiotic DNA repair in the nucleolus employs a nonhomologous end-joining mechanism. *Plant Cell* 31, 2259–2275. doi: 10.1105/tpc.19.00367

Sims, J., Schlögelhofer, P., and Kurzbauer, M.-T. (2021). From microscopy to nanoscopy: defining an *Arabidopsis thaliana* meiotic atlas at the nanometer scale. *Front. Plant Sci.* 12:672914. doi: 10.3389/fpls.2021.672914

Singh, G., Da Ines, O., Gallego, M. E., and White, C. I. (2017). Analysis of the impact of the absence of RAD51 strand exchange activity in *Arabidopsis meiosis*. *PLoS One* 12:e0183006. doi: 10.1371/journal.pone.0183006

Smith, M. G., Simon, V. R., O'Sullivan, H., and Pon, L. A. (1995). Organelle-cytoskeletal interactions: actin mutations inhibit meiosis-dependent mitochondrial rearrangement in the budding yeast *Saccharomyces cerevisiae*. *Mol. Biol. Cell* 6, 1381–1396. doi: 10.1091/mbc.6.10.1381

Sofroni, K., Takatsuka, H., Yang, C., Dissmeyer, N., Komaki, S., Hamamura, Y., et al. (2020). CDKD-dependent activation of CDKA;1 controls microtubule dynamics and cytokinesis during meiosis. *J. Cell Biol.* 219:e201907016. doi: 10.1083/jcb.201907016

Stefani, A., and Colonna, N. (1996). The influence of temperature on meiosis and microspores development in *Dasypyrum villosum* (L.) P. Candargy. *Cytologia* 61, 277–283. doi: 10.1508/cytologia.61.277

Stern, H., and Hotta, Y. (1970). "Chapter 15 culture of meiotic cells for biochemical studies11this work was supported by a grant from the national science foundation (NSF-GB-5173x) and by supplementary assistance from the Institute for Studies in Developmental Biology (USPHS-HD03015 and NSF-GB-6476)," in *Methods in Cell Biology*, ed. D. M. Prescott (Cambridge, MA: Academic Press), 497–513. doi: 10.1016/S0091-679X(08)61761-6

Strasburger, E. (1888). *Über Kern-und Zelltheilungen im Pflanzenreiche, nebst einem Anhang über Befruchtung*. Jena: Fisher.

Stronghill, P. E., Azimi, W., and Hasenkampf, C. A. (2014). A novel method to follow meiotic progression in Arabidopsis using confocal microscopy and 5-ethynyl-2'-deoxyuridine labeling. *Plant Methods* 10:33. doi: 10.1186/1746-4811-10-33

Takegami, M. H., Yoshioka, M., Tanaka, I., and Ito, M. (1981). Characteristics of isolated microsporocytes from Liliaceous plants for studies of the meiotic cell cycle in vitro. *Plant Cell Physiol.* 22, 1–10. doi: 10.1093/oxfordjournals.pcp.a076135

Taylor, J. H., and McMaster, R. D. (1953). Autoradiographic and microphotometric studies of desoxyribose nucleic acid during microgametogenesis in *Lilium longiflorum*. *Chromosoma* 6, 489–521. doi: 10.1007/BF01259951

Tomita, K., and Cooper, J. P. (2007). The telomere bouquet controls the meiotic spindle. *Cell* 130, 113–126. doi: 10.1016/j.cell.2007.05.024

Valuchova, S., Mikulkova, P., Pecinkova, J., Klimova, J., Krumnikl, M., Bainar, P., et al. (2020). Imaging plant germline differentiation within *Arabidopsis* flowers by light sheet microscopy. *eLife* 9:e52546. doi: 10.7554/eLife.52546

Van Beneden, E. (1883). *Recherches sur la maturation de l'oeuf, la fecondation et la division cellulaire /par Éduard Van Beneden*. *Libraire Clemm and G.Massonéditeur*. Available online at: https://gallica.bnf.fr/ark:/12148/bpt6k97385454 (accessed May 27, 2021).

Varas, J., Graumann, K., Osman, K., Pradillo, M., Evans, D. E., Santos, J. L., et al. (2015). Absence of SUN1 and SUN2 proteins in *Arabidopsis thaliana* leads to a delay in meiotic progression and defects in synapsis and recombination. *Plant J.* 81, 329–346. doi: 10.1111/tpj.12730

Vargas, E., McNally, K. P., Cortes, D. B., Panzica, M. T., Danlasky, B. M., Li, Q., et al. (2019). Spherical spindle shape promotes perpendicular cortical orientation by preventing isometric cortical pulling on both spindle poles during C.

elegans female meiosis. *Development* 146:dev178863. doi: 10.1242/dev.178863

Vasil, I. K. (1959). Cultivation of excised anthers in vitro —effect of nucleic acids. *J. Exp. Bot.* 10, 399–408. doi: 10.1093/jxb/10.3.399

Vogler, F., and Sprunck, S. (2015). F-actin forms mobile and unwinding ring-shaped structures in germinating *Arabidopsis* pollen expressing Lifeact. *Plant Signal. Behav.* 10:e1075684. doi: 10.1080/15592324.2015.1075684

Wang, H., Li, Y., Yang, J., Duan, X., Kalab, P., Sun, S. X., et al. (2020). Symmetry breaking in hydrodynamic forces drives meiotic spindle rotation in mammalian oocytes. *Sci. Adv.* 6:eaaz5004. doi: 10.1126/sciadv.aaz5004

Wang, Y., and Copenhaver, G. P. (2018). Meiotic recombination: mixing it up in plants. *Annu. Rev. Plant Biol.* 69, 577–609. doi: 10.1146/annurev-arplant-042817-040431

Weijers, D., Dijk, M. F., Vencken, R.-J., Quint, A., Hooykaas, P., and Offringa, R. (2001). An *Arabidopsis* minute-like phenotype caused by a semi-dominant mutation in a RIBOSOMAL PROTEIN S5 gene. *Development* 128, 4289–4299.

White, P. R. (1964). *The Cultivation of Animal and Plant Cells*, 1954th Edn. New York, NY: The Ronald Press Company.

Wijnker, E., and Schnittger, A. (2013). Control of the meiotic cell division program in plants. *Plant Reprod.* 26, 143–158. doi: 10.1007/s00497-013-0223-x

Wilson, J. Y. (1959). Duration of meiosis in relation to temperature. *Heredity* 13, 263–267. doi: 10.1038/hdy.1959.29

Wozny, M., Schattat, M. H., Mathur, N., Barton, K., and Mathur, J. (2012). Color recovery after photoconversion of H2B::mEosFP allows detection of increased nuclear DNA content in developing plant cells. *Plant Physiol.* 158, 95–106. doi: 10.1104/pp.111.187062

Wu, S.-Z., and Bezanilla, M. (2014). Myosin VIII associates with microtubule ends and together with actin plays a role in guiding plant cell division. *eLife* 3:e03498. doi: 10.7554/eLife.03498

Xu, H., Tong, Z., Ye, Q., Sun, T., Hong, Z., Zhang, L., et al. (2019). Molecular organization of mammalian meiotic chromosome axis revealed by expansion STORM microscopy. *Proc. Natl. Acad. Sci. U.S.A.* 116, 18423–18428. doi: 10.1073/pnas.1902440116

Yang, C., Hamamura, Y., Sofroni, K., Böwer, F., Stolze, S. C., Nakagami, H., et al. (2019). SWITCH 1/DYAD is a WINGS APART-LIKE antagonist that maintains sister chromatid cohesion in meiosis. *Nat. Commun.* 10:1755. doi: 10.1038/s41467-019-09759-w

Yang, C., Sofroni, K., Wijnker, E., Hamamura, Y., Carstens, L., Harashima, H., et al. (2020). The Arabidopsis Cdk1/Cdk2 homolog CDKA;1 controls chromosome axis assembly during plant meiosis. *EMBO J.* 39:e101625. doi: 10.15252/embj.2019101625

Yokoyama, R., Hirakawa, T., Hayashi, S., Sakamoto, T., and Matsunaga, S. (2016). Dynamics of plant DNA replication based on PCNA visualization. *Sci. Rep.* 6:29657. doi: 10.1038/srep29657

Yoon, S., Choi, E.-H., Kim, J.-W., and Kim, K. P. (2018). Structured illumination microscopy imaging reveals localization of replication protein A between chromosome lateral elements during mammalian meiosis. *Exp. Mol. Med.* 50, 1–12. doi: 10.1038/s12276-018-0139-5

Yu, H.-G., Hiatt, E. N., Chan, A., Sweeney, M., and Dawe, R. K. (1997). Neocentromere-mediated chromosome movement in maize. *J. Cell Biol.* 139, 831–840.

Yu, H.-G., Muszynski, M. G., and Kelly Dawe, R. (1999). The maize homologue of the cell cycle checkpoint protein MAD2 reveals kinetochore substructure and contrasting mitotic and meiotic localization patterns. *J. Cell Biol.* 145, 425–435.

Zhao, L., He, J., Cai, H., Lin, H., Li, Y., Liu, R., et al. (2014). Comparative expression profiling reveals gene functions in female meiosis and gametophyte development in *Arabidopsis*. *Plant J.* 80, 615–628. doi: 10.1111/tpj.12657

Zhao, X., Bramsiepe, J., Durme, M. V., Komaki, S., Prusicki, M. A., Maruyama, D., et al. (2017). RETINOBLASTOMA RELATED1 mediates germline entry in *Arabidopsis*. *Science* 356:eaaf6532. doi: 10.1126/science.aaf6532

Zhao, X., Harashima, H., Dissmeyer, N., Pusch, S., Weimer, A. K., Bramsiepe, J., et al. (2012). A general G1/S-Phase cell-cycle control module in the flowering plant *Arabidopsis thaliana*. *PLoS Genet.* 8:e1002847. doi: 10.1371/journal.pgen.1002847

Conflict of Interest: The authors declare that the research was conducted in the absence of any commercial or financial relationships that could be construed as a potential conflict of interest.

Publisher's Note: All claims expressed in this article are solely those of the authors and do not necessarily represent those of their affiliated organizations, or those of the publisher, the editors and the reviewers. Any product that may be evaluated in this article, or claim that may be made by its manufacturer, is not guaranteed or endorsed by the publisher.

Advantages of publishing in Frontiers

OPEN ACCESS
Articles are free to read for greatest visibility and readership

FAST PUBLICATION
Around 90 days from submission to decision

HIGH QUALITY PEER-REVIEW
Rigorous, collaborative, and constructive peer-review

TRANSPARENT PEER-REVIEW
Editors and reviewers acknowledged by name on published articles

Frontiers
Avenue du Tribunal-Fédéral 34
1005 Lausanne | Switzerland

Visit us: www.frontiersin.org
Contact us: frontiersin.org/about/contact

REPRODUCIBILITY OF RESEARCH
Support open data and methods to enhance research reproducibility

DIGITAL PUBLISHING
Articles designed for optimal readership across devices

FOLLOW US
@frontiersin

IMPACT METRICS
Advanced article metrics track visibility across digital media

EXTENSIVE PROMOTION
Marketing and promotion of impactful research

LOOP RESEARCH NETWORK
Our network increases your article's readership